

Special Issue Reprint

---

# Recent Advances in the Synthesis, Functionalization and Applications of Pyrazole-Type Compounds II

---

Edited by  
Vera L. M. Silva and Artur M. S. Silva

[mdpi.com/journal/molecules](https://mdpi.com/journal/molecules)

# **Recent Advances in the Synthesis, Functionalization and Applications of Pyrazole-Type Compounds II**



# Recent Advances in the Synthesis, Functionalization and Applications of Pyrazole-Type Compounds II

Editors

**Vera L. M. Silva**

**Artur M. S. Silva**



Basel • Beijing • Wuhan • Barcelona • Belgrade • Novi Sad • Cluj • Manchester

*Editors*

Vera L. M. Silva

Department of Chemistry

University of Aveiro

Aveiro

Portugal

Artur M. S. Silva

Department of Chemistry

University of Aveiro

Aveiro

Portugal

*Editorial Office*

MDPI

St. Alban-Anlage 66

4052 Basel, Switzerland

This is a reprint of articles from the Special Issue published online in the open access journal *Molecules* (ISSN 1420-3049) (available at: [www.mdpi.com/journal/molecules/special\\_issues/pyrazole.type\\_compounds.II](http://www.mdpi.com/journal/molecules/special_issues/pyrazole.type_compounds.II)).

For citation purposes, cite each article independently as indicated on the article page online and as indicated below:

Lastname, A.A.; Lastname, B.B. Article Title. *Journal Name* **Year**, *Volume Number*, Page Range.

**ISBN 978-3-0365-8791-2 (Hbk)**

**ISBN 978-3-0365-8790-5 (PDF)**

[doi.org/10.3390/books978-3-0365-8790-5](https://doi.org/10.3390/books978-3-0365-8790-5)

© 2023 by the authors. Articles in this book are Open Access and distributed under the Creative Commons Attribution (CC BY) license. The book as a whole is distributed by MDPI under the terms and conditions of the Creative Commons Attribution-NonCommercial-NoDerivs (CC BY-NC-ND) license.

# Contents

About the Editors . . . . . vii

**Vera L. M. Silva and Artur M. S. Silva**

Special Issue "Recent Advances in the Synthesis, Functionalization and Applications of Pyrazole-Type Compounds II"

Reprinted from: *Molecules* **2023**, *28*, 5873, doi:10.3390/molecules28155873 . . . . . 1

**Karolina Dzedulionytė, Melita Veikšaitė, Vít Morávek, Vida Malinauskienė, Greta Račkauskienė and Algirdas Šačkus et al.**

Convenient Synthesis of *N*-Heterocycle-Fused Tetrahydro-1,4-diazepinones

Reprinted from: *Molecules* **2022**, *27*, 8666, doi:10.3390/molecules27248666 . . . . . 5

**Greta Utecht-Jarzyńska, Anna Kowalczyk and Marcin Jasiński**

Fluorinated and Non-Fluorinated 1,4-Diarylpyrazoles via MnO<sub>2</sub>-Mediated Mechanochemical Deacylative Oxidation of 5-Acylpyrazolines †

Reprinted from: *Molecules* **2022**, *27*, 8446, doi:10.3390/molecules27238446 . . . . . 33

**Karolina Kula, Agnieszka Łapczuk, Mikołaj Sadowski, Jowita Kras, Karolina Zawadzińska and Oleg M. Demchuk et al.**

On the Question of the Formation of Nitro-Functionalized 2,4-Pyrazole Analogs on the Basis of Nitrylimine Molecular Systems and 3,3,3-Trichloro-1-Nitroprop-1-Ene

Reprinted from: *Molecules* **2022**, *27*, 8409, doi:10.3390/molecules27238409 . . . . . 49

**Matteo Lusardi, Aldo Profumo, Chiara Rotolo, Erika Iervasi, Camillo Rosano and Andrea Spallarossa et al.**

Regioselective Synthesis, Structural Characterization, and Antiproliferative Activity of Novel Tetra-Substituted Phenylaminopyrazole Derivatives

Reprinted from: *Molecules* **2022**, *27*, 5814, doi:10.3390/molecules27185814 . . . . . 61

**Lyudmila Kayukova, Anna Vologzhanina, Pavel Dorovatovskii, Gulnur Baitursynova, Elmira Yergaliyeva and Ayazhan Kurmangaliyeva et al.**

Reaction Products of  $\beta$ -Aminopropioamidoximes Nitrobenzenesulfochlorination: Linear and Rearranged to Spiropyrazolinium Salts with Antidiabetic Activity

Reprinted from: *Molecules* **2022**, *27*, 2181, doi:10.3390/molecules27072181 . . . . . 77

**Arturo Gamonal Ruiz-Crespo, Laura Galán-Fernández, Paloma Martínez-Martín and Juan Carlos Rodríguez-Ubis**

An Orthogonal Synthetic Approach to Nonsymmetrical Bisazolyl 2,4,6-Trisubstituted Pyridines

Reprinted from: *Molecules* **2022**, *27*, 1746, doi:10.3390/molecules27051746 . . . . . 93

**Joungmo Cho, Venkata Subbaiah Sadu, Yohan Han, Yunsoo Bae, Hwajeong Lee and Kee-In Lee**

Structural Requirements of 1-(2-Pyridinyl)-5-pyrazolones for Disproportionation of Boronic Acids

Reprinted from: *Molecules* **2021**, *26*, 6814, doi:10.3390/molecules26226814 . . . . . 105

**Beatričė Razmienė, Eva Řezníčková, Vaida Dambrauskienė, Radek Ostruszka, Martin Kubala and Asta Žukauskaitė et al.**

Synthesis and Antiproliferative Activity of 2,4,6,7-Tetrasubstituted-2*H*-pyrazolo[4,3-*c*]pyridines

Reprinted from: *Molecules* **2021**, *26*, 6747, doi:10.3390/molecules26216747 . . . . . 115

|   |            |
|---|------------|
| <b>Vaida Milišiūnaitė, Elena Plytninkienė, Roberta Bakšienė, Aurimas Bieliauskas, Sonata Krikštolaitytė and Greta Račkauskienė et al.</b><br>Convenient Synthesis of Pyrazolo[4',3':5,6]pyrano[4,3-c][1,2] oxazoles via Intramolecular Nitrile Oxide Cycloaddition<br>Reprinted from: <i>Molecules</i> <b>2021</b> , <i>26</i> , 5604, doi:10.3390/molecules26185604 . . . . .  | <b>143</b> |
| <b>Abdulrhman Alsayari, Abdullatif Bin Muhsinah, Yahya I. Asiri, Faiz A. Al-aizari, Nabila A. Kheder and Zainab M. Almarhoon et al.</b><br>Synthesis, Characterization, and Biological Evaluation of Some Novel Pyrazolo[5,1- <i>b</i> ]thiazole Derivatives as Potential Antimicrobial and Anticancer Agents<br>Reprinted from: <i>Molecules</i> <b>2021</b> , <i>26</i> , 5383, doi:10.3390/molecules26175383 . . . . . | <b>161</b> |
| <b>Wei-Syuan Lin and Shigeki Kuwata</b><br>Recent Developments in Reactions and Catalysis of Protic Pyrazole Complexes<br>Reprinted from: <i>Molecules</i> <b>2023</b> , <i>28</i> , 3529, doi:10.3390/molecules28083529 . . . . .  | <b>174</b> |
| <b>Diana Becerra, Rodrigo Abonia and Juan-Carlos Castillo</b><br>Recent Applications of the Multicomponent Synthesis for Bioactive Pyrazole Derivatives<br>Reprinted from: <i>Molecules</i> <b>2022</b> , <i>27</i> , 4723, doi:10.3390/molecules27154723 . . . . .   | <b>211</b> |
| <b>Vera L. M. Silva and Artur M. S. Silva</b><br>Revisiting the Chemistry of Vinylpyrazoles: Properties, Synthesis, and Reactivity<br>Reprinted from: <i>Molecules</i> <b>2022</b> , <i>27</i> , 3493, doi:10.3390/molecules27113493 . . . . .  | <b>293</b> |
| <b>Andrzej Danel, Ewa Gondek, Mateusz Kucharek, Paweł Szlachcic and Arkadiusz Gut</b><br><i>1H</i> -Pyrazolo[3,4- <i>b</i> ]quinolines: Synthesis and Properties over 100 Years of Research<br>Reprinted from: <i>Molecules</i> <b>2022</b> , <i>27</i> , 2775, doi:10.3390/molecules27092775 . . . . .   | <b>313</b> |
| <b>Ana Donaire-Arias, Ana Maria Montagut, Raimon Puig de la Bellacasa, Roger Estrada-Tejedor, Jordi Teixidó and José I. Borrell</b><br><i>1H</i> -Pyrazolo[3,4- <i>b</i> ]pyridines: Synthesis and Biomedical Applications<br>Reprinted from: <i>Molecules</i> <b>2022</b> , <i>27</i> , 2237, doi:10.3390/molecules27072237 . . . . .  | <b>376</b> |

# About the Editors

## **Vera L. M. Silva**

Vera L. M. Silva is currently an Assistant Professor in the Chemistry Department of the University of Aveiro and a Researcher at the REQUIMTE–Associated Laboratory for Green Chemistry–Clean Technologies and Processes. She obtained a BSc in Analytical Chemistry (1998), a master's in Chemistry of Natural Products and Food Stuffs (2002) and a PhD in Chemistry (2006) from the University of Aveiro. She is an Organic Chemist and a member of the Molecular Synthesis group of REQUIMTE. Her main research interests comprise the synthesis and structural characterization of novel compounds for medicinal applications and the development of sustainable organic synthesis methodologies, based on more contemporary tools such as ohmic heating. As part of her research activity, she has published 3 book chapters, 1 e-book, around 70 SCI papers, and 2 papers in national scientific journals with peer review, and she is the co-author of 1 patent. Her activities also include the supervision and co-supervision of 6 PhD (2 concluded) and 11 MSc students, 25 Bachelor students (third-year graduation projects), and 5 Erasmus students. She has participated in several national research projects and one international research project, and she has presented several oral and poster communications at national and international scientific meetings. In 2011 and 2013, she was awarded the prize for Best Poster Communication both in national scientific meetings.

## **Artur M. S. Silva**

Artur M. S. Silva is currently a full professor in the Chemistry Department and vice-rector for research and innovation at the University of Aveiro (UA). He is a Board Member of the European Chemical Society and a Fellow of the European Academy of Sciences and of Chemistry Europe. He was the President of the Portuguese Chemical Society from 2016 to 2023.

He obtained both a BSc (1987) and a PhD in Organic Chemistry (1993) at the UA. He joined the Department of Chemistry of the same university in 1987 as an Assistant and was appointed as an Auxiliary Professor in 1996, Associate Professor in 1999, and Full Professor in 2001. He has published more than 840 SCI papers, 2 e-books, and 54 book chapters, has delivered more than 64 lectures in scientific meetings, and is the co-author of 5 patents. His publications have been cited more than 21400 times, and his Hirsch-index is 65. He has supervised 19 post-doctoral fellows, 41 PhD students, and 43 MSc students; he has also participated in 33 financed Portuguese and European projects and in 8 bilateral financed projects with European Research Groups.





Editorial

# Special Issue “Recent Advances in the Synthesis, Functionalization and Applications of Pyrazole-Type Compounds II”

Vera L. M. Silva \*  and Artur M. S. Silva \* 

LAQV-REQUIMTE, Department of Chemistry, University of Aveiro, 3810-193 Aveiro, Portugal

\* Correspondence: verasilva@ua.pt (V.L.M.S.); artur.silva@ua.pt (A.M.S.S.); Tel.: +351-234-370704 (V.L.M.S.); +351-234-370714 (A.M.S.S.)

Pyrazole and its derivatives are considered privileged *N*-heterocycles with immense therapeutic potential. In current medicinal chemistry, the incorporation of a pyrazole nucleus is a common practice by which to develop new drug-like molecules with different bioactivities, such as anti-cancer, anti-diabetic, anti-inflammatory, anti-neurodegenerative, anti-bacterial, among others, giving rise to a great number of approved therapeutics. Pyrazoles are also found within a variety of agrochemicals (fungicides, insecticides, and herbicides) and are versatile scaffolds for synthetic manipulations. The structural features of pyrazoles—mainly tautomerism, with possible implications for their reactivity, their dyeing and fluorescence properties, as well as their diverse applications—have stimulated the work of several research groups towards the synthesis and functionalization of pyrazole-type compounds and the study of their properties.

After the success of the first edition of this Special Issue, this second edition has the same goal—that is, to provide a broad survey of the most recent advances in pyrazole’s chemistry.

In this second edition, ten original research articles and five reviews covering some of the most recent advances in the synthesis, transformation, properties, and relevant applications of pyrazoles are reported. A. Žukauskaitė, E. Arbačiauskienė and their coworkers reported a regioselective strategy for synthesizing ethyl 1-(oxiran-2-ylmethyl)-3-aryl-1*H*-pyrazole-5-carboxylates from easily accessible 3(5)-aryl-1*H*-pyrazole-5(3)-carboxylates. By using different bases, reaction media, and temperatures, regioselective alkylation was achieved, and the established conditions were applied to the synthesis of novel pyrazolo[1,5-*a*][1,4]diazepin-4-ones via the ring-opening of the oxirane with amines and a direct cyclization sequence. They further applied this synthetic strategy to investigate the reactivity of ethyl 1*H*-indole-2-carboxylate and ethyl benzo[*d*]imidazole-2-carboxylate scaffolds, which led to the formation of additional fused tetrahydro[1,4]diazepino[1,2-*a*]indol-1-one and tetrahydro-1*H*-benzo[4,5]imidazo[1,2-*a*][1,4]diazepin-1-one derivatives [1]. Polyfunctionalized pyrazoles, of general interest in medicine and material sciences, were the subject studied by M. Jasiński and coworkers, who described a solvent-free two-step mechanochemical synthesis of trifluoromethylated and non-fluorinated polysubstituted pyrazoles in moderate-to-high regioselectivity and fair yields, starting from simple substrates, chalcones, and hydrazonoyl halides. The protocol comprises [3 + 2]-cycloaddition of in situ-generated nitrile imines and chalcones, followed by the oxidation of the initially formed 5-acylpyrazolines with activated MnO<sub>2</sub>. The second step proceeds via an exclusive deacylative pathway to give a series of 1,4-diarylpyrazoles functionalized with a fluorinated (CF<sub>3</sub>) or non-fluorinated (Ph, COOEt, Ac) substituent at C-3 of the heterocyclic ring. They have also shown that, in contrast, the MnO<sub>2</sub>-mediated oxidation of a model isomeric 4-acylpyrazoline proceeded with low chemoselectivity, leading to fully substituted pyrazole as a major product formed via dehydrogenative aromatization. This work also

**Citation:** Silva, V.L.M.; Silva, A.M.S. Special Issue “Recent Advances in the Synthesis, Functionalization and Applications of Pyrazole-Type Compounds II”. *Molecules* **2023**, *28*, 5873. <https://doi.org/10.3390/molecules28155873>

Received: 31 July 2023

Accepted: 2 August 2023

Published: 4 August 2023



**Copyright:** © 2023 by the authors. Licensee MDPI, Basel, Switzerland. This article is an open access article distributed under the terms and conditions of the Creative Commons Attribution (CC BY) license (<https://creativecommons.org/licenses/by/4.0/>).

evidenced the application of nitrile imines as building blocks for organic synthesis [2]. R. Jasiński and coworkers used molecular electron density theory (MEDT) to explain the unexpected formation of 1-(4-bromophenyl)-3-phenyl-5-nitropyrazole in the reaction between (*E*)-3,3,3-trichloro-1-nitroprop-1-ene and *N*-(4-bromophenyl)-*C*-arylnitrylimine. Although the theoretical MEDT studies showed that both possible [3 + 2]-cycloaddition pathways may occur from a kinetic point of view, of which the formation of 1-(4-bromophenyl)-3-aryl-4-trichloromethyl-5-nitro- $\Delta^2$ -pyrazoline was more probable, the experimental results showed that this reaction occurred with full regioselectivity. However, the extremely unstable obtained products were spontaneously converted through a unique  $\text{CHCl}_3$ -elimination process to give the unexpected pyrazole systems [3]. A. Spallarossa and coworkers reported the regio- and chemoselective one-pot synthesis of a small library of highly functionalized phenylaminopyrazoles by the one-pot condensation of active methylene reagents, phenylisothiocyanate, and substituted hydrazine. Preliminary cell-based assays performed via the MTT method on a panel of eight tumor cell lines (namely, breast cancer: MCF7, MDA-MB231, SK-Br3; melanoma: SKMEL-28; ovarian cancer: SKOV-3; liver cancer: Hep-G2; cervical cancer: HeLa; and lung cancer: A549) and one normal human fibroblasts cell line (GM-6114) showed that these phenylaminopyrazoles are poorly cytotoxic against both the selected cell lines [4]. L. Kayukova, A. Vologzhanina, and their coworkers demonstrated that the reaction products of the nitrobenzenesulfochlorination of  $\beta$ -aminopropioamidoximes strongly depend on the structure of the initial substrates and temperature. In addition, the authors reported the results of the in vitro screening of the library of nitrobenzenesulfochlorination products for anti-diabetic activity. Two distinct compounds, obtained in the *p*-nitrobenzenesulfochlorination of  $\beta$ -(thiomorpholin-1-yl)- and  $\beta$ -(benzimidazol-1-yl)propioamidoximes showed high  $\alpha$ -glucosidase activity superior to the activity of the acarbose standard [5]. J.-C. Rodríguez-Ubis and coworkers reported an orthogonal synthetic approach to non-symmetrical bisazolyl 2,4,6-trisubstituted pyridines, important ligands in a variety of transition and lanthanide ions complexes, starting from the readily available 4-bromo-2,6-difluoropyridine. Both fluorine atoms allow for easy selective stepwise substitution, and the bromine atom provides easy access to additional functionalities through both Suzuki and Sonogashira Pd(0) cross-coupling reactions. This strategy gives access to pyridines with different substituents on the pyrazole, indazole, and pyridine heterocycles, it being possible to tune the electronic  $\pi$  character of these trisheterocyclic units to obtain the best candidates for ligands [6]. On the basis of the formation of four-coordinate boron(III) complexes in the reaction of 1-(2-pyridinyl)pyrazol-5-one derivatives with arylboronic acids in basic media, K.-I. Lee and coworkers revealed the key structural requirements of 1-(2-pyridinyl)pyrazol-5-ones for disproportionation of boronic acids, which are the use of unprotected acid and the presence of a [N,O]-bidentate ligand. Although the exact mechanism of this disproportionation is not clear, the reported method is particularly important for the synthesis of four-coordinate organoboron species to ensure a completely efficient assembly of multi-component structures in a single operation [7]. Pyrazolopyridines are among the most studied condensed pyrazole systems in medicinal chemistry. E. Arbačiauskienė and coworkers reported the synthesis of a library of 2,4,6,7-tetrasubstituted-2*H*-pyrazolo[4,3-*c*]pyridines and the evaluation of their anti-proliferative activity against K562, MV4-11, and MCF-7 cancer cell lines. Out of the tested compounds, 4-(2,6-diphenyl-2*H*-pyrazolo[4,3-*c*]pyridin-7-yl)phenol proved to be the most active. Further experiments carried out by these authors revealed that it blocks proliferation and induces cell death in K562 cells. They also examined and discussed the influence of an additional substituent at the 7-position on the biological and optical properties of the compounds [8]. A. Šačkus, E. Arbačiauskienė and coworkers developed a simple and efficient synthetic route for the preparation of 3*a*,4-dihydro-3*H*,7*H*- and 4*H*,7*H*-pyrazolo[4',3':5,6]pyrano[4,3-*c*][1,2]oxazoles from easily obtainable 3-(prop-2-en-1-yloxy)- or 3-(prop-2-yn-1-yloxy)-1*H*-pyrazole-4-carbaldehydes via the intramolecular nitrile oxide cycloaddition (INOC) reaction of intermediate oximes. The key step is the nitrile oxide preparation from the corresponding aldoximes, which was carried out via

oxidation with sodium hypochlorite. Pyrazolo[4',3':5,6]pyrano[4,3-*c*][1,2]oxazoles with various substituents at C-3 or C-7 were synthesized. Through extensive NMR spectroscopic studies carried out using standard and advanced methods, the authors unambiguously confirmed the predomination of the *syn*-isomer of intermediate aldoximes [9]. Bearing in mind the remarkable biological activities of both pyrazole and thiazole scaffolds, Y. N. Mabkhot and coworkers developed a convenient synthesis of novel pyrazolo[5,1-*b*]thiazole-based heterocycles. They also selected some examples of these compounds which were screened and evaluated for their anti-microbial and anti-cancer activities. Due to the promising results found, these compounds can be regarded as leading compounds in the future design of new drug molecules [10]. *N*-unsubstituted pyrazoles are considered versatile ligands in various fields, such as materials chemistry and homogeneous catalysis, owing to their proton-responsive nature. S. Kuwata and coworker provided an overview of the reactivities of protic pyrazole complexes. The coordination chemistry of pincer-type 2,6-bis(1*H*-pyrazol-3-yl)pyridines is first reviewed as a class of compounds for which significant advances have been made in the last decade. They described the stoichiometric reactivities of protic pyrazole complexes with inorganic nitrogenous compounds, which possibly relates to the inorganic nitrogen cycle in nature. They also outlined the catalytic application of protic pyrazole complexes, emphasizing mechanistic aspects. Moreover, they discussed the role of the NH group in the protic pyrazole ligand and the resulting metal–ligand cooperation [11]. The recent developments of multicomponent reactions for the synthesis of biologically active molecules containing the pyrazole moiety were reviewed by J.-C. Castillo and coworkers. They analyzed the articles published from 2015 to date related to anti-bacterial, anti-cancer, anti-fungal, anti-oxidant, anti-inflammatory, anti-mycobacterial, anti-malarial,  $\alpha$ -glucosidase and  $\alpha$ -amylase inhibitory activity, and miscellaneous activities of pyrazole derivatives obtained exclusively via a multicomponent reaction. Various plausible synthetic mechanisms and molecular docking studies were presented and discussed. This work is an important contribution for the development of more biologically active molecules and marketed drugs containing the pyrazole moiety using one-pot, atom economic synthetic strategies [12]. Vinylpyrazoles (pyrazolyl olefins) are interesting motifs in organic chemistry but have been overlooked. A. Silva and V. Silva revisited the chemistry of this type of pyrazoles. They described the properties and synthetic routes of vinylpyrazoles and highlighted their versatility as building blocks for the construction of more complex organic molecules via different organic reactions. They also gave some prospects regarding the future development of the chemistry of these interesting compounds [13]. A. Danel and coworkers summarized a little over 100 years (1911–2021) of research on the synthesis and the photophysical and biological properties of 1*H*-pyrazolo[3,4-*b*]quinolines. They reported on the main methods of synthesis, which include Friedländer condensation, synthesis from anthranilic acid derivatives, multicomponent synthesis, and others, and the use of this class of compounds as potential fluorescent sensors and biologically active compounds. This work can serve as a kind of guide for researchers who are involved in the synthesis of nitrogen-condensed heterocycles [14]. J. I. Borrell and coworkers analyzed the diversity of substituents present in the important group of heterocyclic compounds, the pyrazolo[3,4-*b*]pyridines, at N-1, C-3, C-4, C-5, and C-6. They also reported synthetic methods used for their synthesis, starting from a pre-formed pyrazole or pyridine, as well as the biomedical applications of such compounds. They summarized the most important biological targets and molecules developed, showing the high versatility of these structures [15].

In conclusion, pyrazoles' chemistry is undoubtedly a current and relevant topic of investigation. Several research groups have contributed to the advancement of this topic by designing novel compounds and developing synthetic strategies for the preparation and post-functionalization of pyrazoles, or by studying their structures, properties, and potential applications. Herein, important advances in pyrazoles' chemistry have been revealed. We thank all the authors for their valuable contributions to this Special Issue and offer them our immense gratitude for having chosen this Special Issue in which to

publish their research works, thus placing this Special Issue in the top-ten Special Issues that collected the most papers in 2022. We are also deeply grateful to the staff members of MDPI for their editorial support.

**Conflicts of Interest:** The authors declare no conflict of interest.

## References

1. Dzedulionytė, K.; Veikšaitė, M.; Morávek, V.; Malinauskienė, V.; Račkauskienė, G.; Šačkus, A.; Žukauskaitė, A.; Arbačiauskienė, E. Convenient Synthesis of *N*-Heterocycle-Fused Tetrahydro-1,4-diazepinones. *Molecules* **2022**, *27*, 8666. [CrossRef] [PubMed]
2. Utecht-Jarzyńska, G.; Kowalczyk, A.; Jasiński, M. Fluorinated and Non-Fluorinated 1,4-Diarylpyrazoles via MnO<sub>2</sub>-Mediated Mechanochemical Deacylative Oxidation of 5-Acylpyrazolines. *Molecules* **2022**, *27*, 8446. [CrossRef] [PubMed]
3. Kula, K.; Łapczuk, A.; Sadowski, M.; Kras, J.; Zawadzińska, K.; Demchuk, O.M.; Gaurav, G.K.; Wróblewska, A.; Jasiński, R. On the Question of the Formation of Nitro-Functionalized 2,4-Pyrazole Analogs on the Basis of Nitylimine Molecular Systems and 3,3,3-Trichloro-1-Nitroprop-1-Ene. *Molecules* **2022**, *27*, 8409. [CrossRef] [PubMed]
4. Lusardi, M.; Profumo, A.; Rotolo, C.; Iervasi, E.; Rosano, C.; Spallarossa, A.; Ponassi, M. Regioselective Synthesis, Structural Characterization, and Antiproliferative Activity of Novel Tetra-Substituted Phenylaminopyrazole Derivatives. *Molecules* **2022**, *27*, 5814. [CrossRef] [PubMed]
5. Kayukova, L.; Vologzhanina, A.; Dorovatovskii, P.; Baitursynova, G.; Yergaliyeva, E.; Kurmangaliyeva, A.; Shulgau, Z.; Adekenov, S.; Shaimerdenova, Z.; Akatan, K. Reaction Products of β-Aminopropioamidoximes Nitrobenzenesulfochlorination: Linear and Rearranged to Spiropyrazolinium Salts with Antidiabetic Activity. *Molecules* **2022**, *27*, 2181. [CrossRef] [PubMed]
6. Gamonal Ruiz-Crespo, A.; Galán-Fernández, L.; Martínez-Martín, P.; Rodríguez-Ubis, J.C. An Orthogonal Synthetic Approach to Nonsymmetrical Bisazoly 2,4,6-Trisubstituted Pyridines. *Molecules* **2022**, *27*, 1746. [CrossRef] [PubMed]
7. Cho, J.; Sadu, V.S.; Han, Y.; Bae, Y.; Lee, H.; Lee, K.-I. Structural Requirements of 1-(2-Pyridinyl)-5-pyrazolones for Disproportionation of Boronic Acids. *Molecules* **2021**, *26*, 6814. [CrossRef] [PubMed]
8. Razmienė, B.; Řezníčková, E.; Dambrauskienė, V.; Ostruszka, R.; Kubala, M.; Žukauskaitė, A.; Kryštof, V.; Šačkus, A.; Arbačiauskienė, E. Synthesis and Antiproliferative Activity of 2,4,6,7-Tetrasubstituted-2*H*-pyrazolo[4,3-*c*]pyridines. *Molecules* **2021**, *26*, 6747. [CrossRef] [PubMed]
9. Milišiūnaitė, V.; Plytninkienė, E.; Bakšienė, R.; Bieliauskas, A.; Krikštolaitytė, S.; Račkauskienė, G.; Arbačiauskienė, E.; Šačkus, A. Convenient Synthesis of Pyrazolo[4',3':5,6]pyrano[4,3-*c*][1,2]oxazoles via Intramolecular Nitrile Oxide Cycloaddition. *Molecules* **2021**, *26*, 5604. [CrossRef] [PubMed]
10. Alsayari, A.; Muhsinah, A.B.; Asiri, Y.I.; Al-aizari, F.A.; Kheder, N.A.; Almarhoon, Z.M.; Ghabbour, H.A.; Mabkhot, Y.N. Synthesis, Characterization, and Biological Evaluation of Some Novel Pyrazolo[5,1-*b*]thiazole Derivatives as Potential Antimicrobial and Anticancer Agents. *Molecules* **2021**, *26*, 5383. [CrossRef] [PubMed]
11. Lin, W.-S.; Kuwata, S. Recent Developments in Reactions and Catalysis of Protic Pyrazole Complexes. *Molecules* **2023**, *28*, 3529. [CrossRef] [PubMed]
12. Becerra, D.; Abonia, R.; Castillo, J.-C. Recent Applications of the Multicomponent Synthesis for Bioactive Pyrazole Derivatives. *Molecules* **2022**, *27*, 4723. [CrossRef] [PubMed]
13. Silva, V.L.M.; Silva, A.M.S. Revisiting the Chemistry of Vinylpyrazoles: Properties, Synthesis, and Reactivity. *Molecules* **2022**, *27*, 3493. [CrossRef] [PubMed]
14. Danel, A.; Gondek, E.; Kucharek, M.; Szlachcic, P.; Gut, A. 1*H*-Pyrazolo[3,4-*b*]quinolines: Synthesis and Properties over 100 Years of Research. *Molecules* **2022**, *27*, 2775. [CrossRef] [PubMed]
15. Donaire-Arias, A.; Montagut, A.M.; Puig de la Bellacasa, R.; Estrada-Tejedor, R.; Teixidó, J.; Borrell, J.I. 1*H*-Pyrazolo[3,4-*b*]pyridines: Synthesis and Biomedical Applications. *Molecules* **2022**, *27*, 2237. [CrossRef] [PubMed]

**Disclaimer/Publisher's Note:** The statements, opinions and data contained in all publications are solely those of the individual author(s) and contributor(s) and not of MDPI and/or the editor(s). MDPI and/or the editor(s) disclaim responsibility for any injury to people or property resulting from any ideas, methods, instructions or products referred to in the content.

Article

# Convenient Synthesis of *N*-Heterocycle-Fused Tetrahydro-1,4-diazepinones

 Karolina Dzedulionytė <sup>1</sup>, Melita Veikšaitė <sup>1</sup>, Vít Morávek <sup>2</sup>, Vida Malinauskienė <sup>1</sup>, Greta Račkauskienė <sup>3</sup>, Algirdas Šačkus <sup>1,3</sup>, Asta Žukauskaitė <sup>1,2,\*</sup> and Eglė Arbačiauskienė <sup>1,\*</sup>
<sup>1</sup> Department of Organic Chemistry, Kaunas University of Technology, Radvilėnu pl. 19A, LT-50254 Kaunas, Lithuania

<sup>2</sup> Department of Chemical Biology, Palacký University, Šlechtitelů 27, CZ-78371 Olomouc, Czech Republic

<sup>3</sup> Institute of Synthetic Chemistry, Kaunas University of Technology, K. Baršausko g. 59, LT-51423 Kaunas, Lithuania

\* Correspondence: asta.zukauskaite@upol.cz (A.Ž.); egle.arbaciauskiene@ktu.lt (E.A.)

**Abstract:** A general approach towards the synthesis of tetrahydro-4*H*-pyrazolo[1,5-*a*][1,4]diazepin-4-one, tetrahydro[1,4]diazepino[1,2-*a*]indol-1-one and tetrahydro-1*H*-benzo[4,5]imidazo[1,2-*a*][1,4]diazepin-1-one derivatives was introduced. A regioselective strategy was developed for synthesizing ethyl 1-(oxiran-2-ylmethyl)-1*H*-pyrazole-5-carboxylates from easily accessible 3(5)-aryl- or methyl-1*H*-pyrazole-5(3)-carboxylates. Obtained intermediates were further treated with amines resulting in oxirane ring-opening and direct cyclisation—yielding target pyrazolo[1,5-*a*][1,4]diazepin-4-ones. A straightforward two-step synthetic approach was applied to expand the current study and successfully functionalize ethyl 1*H*-indole- and ethyl 1*H*-benzo[*d*]imidazole-2-carboxylates. The structures of fused heterocyclic compounds were confirmed by <sup>1</sup>H, <sup>13</sup>C, and <sup>15</sup>N-NMR spectroscopy and HRMS investigation.

**Keywords:** pyrazole; indole; benzimidazole; fused *N*-heterocycles; regioselective *N*-alkylation; oxirane ring-opening; cyclisation

**Citation:** Dzedulionytė, K.; Veikšaitė, M.; Morávek, V.; Malinauskienė, V.; Račkauskienė, G.; Šačkus, A.; Žukauskaitė, A.; Arbačiauskienė, E. Convenient Synthesis of *N*-Heterocycle-Fused Tetrahydro-1,4-diazepinones.

*Molecules* **2022**, *27*, 8666.

<https://doi.org/10.3390/molecules27248666>

Academic Editors: Vera L. M. Silva and Artur M. S. Silva

Received: 15 November 2022

Accepted: 6 December 2022

Published: 7 December 2022

**Publisher's Note:** MDPI stays neutral with regard to jurisdictional claims in published maps and institutional affiliations.

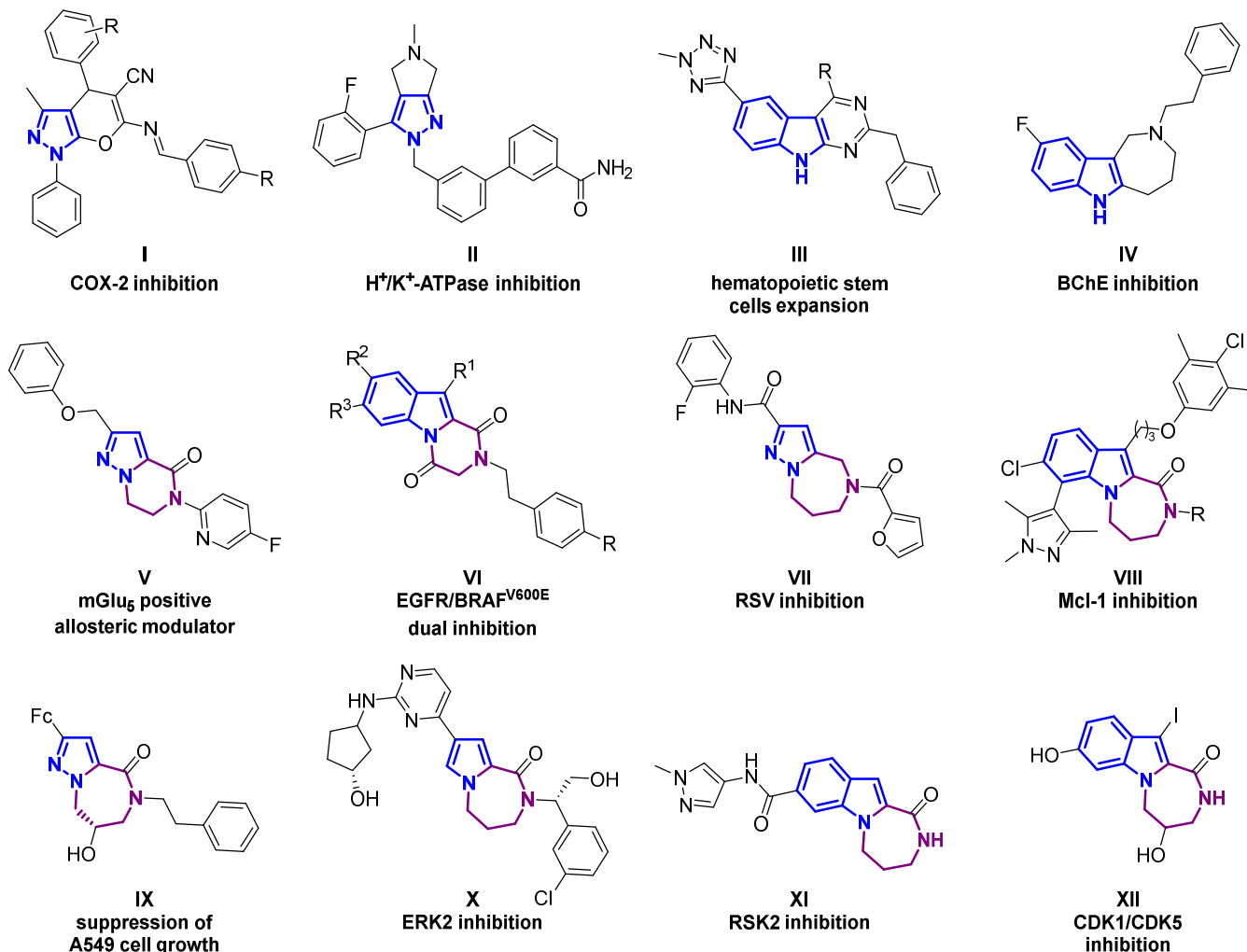


**Copyright:** © 2022 by the authors. Licensee MDPI, Basel, Switzerland. This article is an open access article distributed under the terms and conditions of the Creative Commons Attribution (CC BY) license (<https://creativecommons.org/licenses/by/4.0/>).

## 1. Introduction

Nitrogen-based heterocyclic compounds are integrated into everyday life, including pharmaceuticals [1–3], agrochemicals [4,5], various plastics [6,7], dyes [8,9], and other functional materials [10–13]. When it comes to drug discovery, the development of effective and inexpensive active ingredients is one of the main goals of researchers in the field of medicinal chemistry. Over the years, great attention has been paid to fused heterocyclic derivatives, which are versatile molecules, exhibiting a wide variety of biological properties including antioxidant, antimicrobial, antiproliferative and other activities [14–17]. For example, fused pyrano[2,3-*c*]pyrazole derivatives **I** were designed, synthesized and have been identified as prospective COX-2 inhibitors (Figure 1) [18]. A more recent study by Wang et al. encompasses a discovery of novel pyrrolo[3,4-*c*]pyrazol-3-carboxamides, where lead compound **II** exhibited potent inhibition towards H<sup>+</sup>/K<sup>+</sup>-ATPase and in vivo histamine-stimulated gastric acid secretion [19]. In the field of indole-based chemistry, Feng et al. reported 9*H*-pyrimido[4,5-*b*]indol-4-amines **III** as promising non-toxic hematopoietic stem cells ex vivo expansion agents [20]. In the study of Purgatorio and co-workers, azepino[4,3-*b*]indole **IV** was found to be a useful and versatile scaffold for developing new small molecules inhibiting BChE, which is a promising drug target in severe Alzheimer's disease [21]. Fused systems with two 1,4-distanced nitrogen atoms encompass a variety of biological activities. For instance, Conde-Ceide et al. reported series of 6,7-dihydropyrazolo[1,5-*a*]pyrazin-4-one derivatives, such as **V**, as mGlu<sub>5</sub> receptor-positive allosteric modulators with efficacy in preclinical models of schizophrenia [22], whereas 2,3-dihydropyrazino[1,2-*a*]indole-1,4-dione derivatives **VI** were reported to act as dual EGFR/BRAF<sup>V600E</sup> inhibitors [23]. Among

a variety of condensed systems, fusion of diazepine with selected heterocycles is important as it represents the most significant class of compounds in terms of clinical use [24]. Another notable example includes 5,6,7,8-tetrahydro-4*H*-pyrazolo[1,5-*a*][1,4]diazepine-2-carboxamide **VII** as a non-nucleoside inhibitor of the respiratory syncytial virus (RSV) polymerase complex [25] (Figure 1).



**Figure 1.** Biologically relevant fused heterocyclic derivatives.

Combining the azaheterocycle scaffold into one structure with the diazepinone motif has been shown to result in biologically active compounds. However, to date examples of biologically active pyrazole-, pyrrole-, indole- and benzo[*d*]imidazole-fused diazepinone derivatives are limited. For example, tricyclic indole-diazepinones **VIII** inhibit induced myeloid leukaemia cell differentiation protein (Mcl-1) [26,27]. Chiral ferrocenylpyrazolo[1,5-*a*][1,4]diazepin-4-one **IX** was reported to suppress the growth of A549 lung cancer cells through cell cycle arrest, and H322 together with H1299 lung cancer cells by inducing apoptosis [28]. On the other hand, pyrrole or indole-fused diazepinones **X–XII** demonstrated inhibitory activity of various kinases, namely, extracellular signal-regulated kinase 2 (ERK2) [29], ribosomal S6 kinase (RSK) [30,31], cyclin-dependent kinase 1 (CDK1), and cyclin-dependent kinase 5 (CDK5) [32]. The abovementioned fused systems are not very widely investigated; therefore, it may be a promising entry in the field of synthetic and medicinal chemistry.

In our previous studies, we investigated the synthesis and biological activity of various annulated pyrazole systems such as substituted 2*H*-pyrazolo[4,3-*c*]pyridines [33–35],

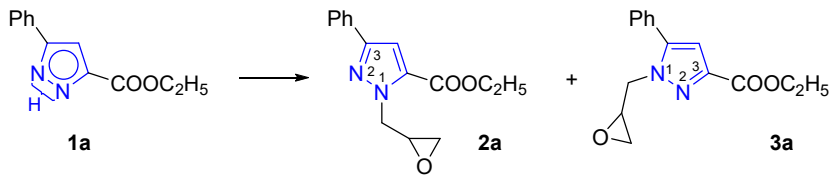
benzopyrano[2,3-*c*]pyrazol-4(2*H*)-ones [36], 2*H*-furo[2,3-*c*]pyrazole ring systems [37], and others. In continuation of our previous research on fused heterocycles, herein we report an efficient two-step synthesis of tetrahydro-4*H*-pyrazolo[1,5-*a*][1,4]diazepin-4-ones, tetrahydro[1,4]diazepino[1,2-*a*]indol-1-ones and tetrahydro-1*H*-benzo[4,5]imidazo[1,2-*a*][1,4]-diazepin-1-ones.

## 2. Results and Discussion

It is known that NH-pyrazoles usually exhibit annular *N,N*-prototropy [38,39]. *N*-Alkylation of asymmetrically ring-substituted 1*H*-pyrazoles generally results in the formation of a mixture of regioisomeric *N*-substituted products [40–43] and therefore regioselective *N*-alkylation requires optimization of reaction conditions [44]. Wright et al. has reported that alkylation of ethyl 1*H*-pyrazole-3(5)-carboxylate in the presence of  $K_2CO_3$  was found to favor the formation of ethyl 1-substituted pyrazole-3-carboxylates while the formation of 1-substituted-1*H*-pyrazole-5-carboxylates could be sterically redirected by alkylating ethyl 3-(triphenylsilyl)-1*H*-pyrazole-5-carboxylate and removing the triphenylsilyl group with  $Bu_4NF$  [45]. In another study implemented by Xu et al., regioselective *N*-alkylation of NH-pyrazoles was accessed by using  $MgBr_2$  and *i*- $Pr_2NEt$  or  $K_2CO_3$  and leading to the formation of different regioisomers [46,47].

In this work, the formation of the desired 1-(oxiran-2-ylmethyl)-3-aryl-1*H*-pyrazole-5-carboxylates by alkylation of easily accessible NH-pyrazoles [48] with 2-(chloromethyl)oxirane was optimized using **1a** as a model compound. As shown in Table 1, reaction outcome is highly dependent on the choice of the base and the solvent. First, application of different bases in solvent-free conditions was investigated. When ethyl 3-phenyl-1*H*-pyrazole-5-carboxylate **1a** was treated with 2-(chloromethyl)oxirane in the presence of  $K_2CO_3$  at 70 °C (Entry 1) [49], a full conversion of **1a** was only achieved after 16 h affording regioisomer **2a** in 24% yield. Reaction using  $Cs_2CO_3$  as a base at lower temperature (Entry 2) [50] proceeded giving isomers **2a** and **3a** in 3:2 ratio. Interestingly, when reaction was conducted using NaH (Entry 3), it proved to proceed in high regioselectivity. However, as the major product the undesired 5-phenyl-1*H*-pyrazole-3-carboxylate **3a** was obtained. Reaction with KOH in the presence of a catalytic amount of TBAB [51] also did not provide an increase in the yield of desired regioisomer **2a** (Entry 4).

**Table 1.** Optimization of reaction conditions to access **2a**.



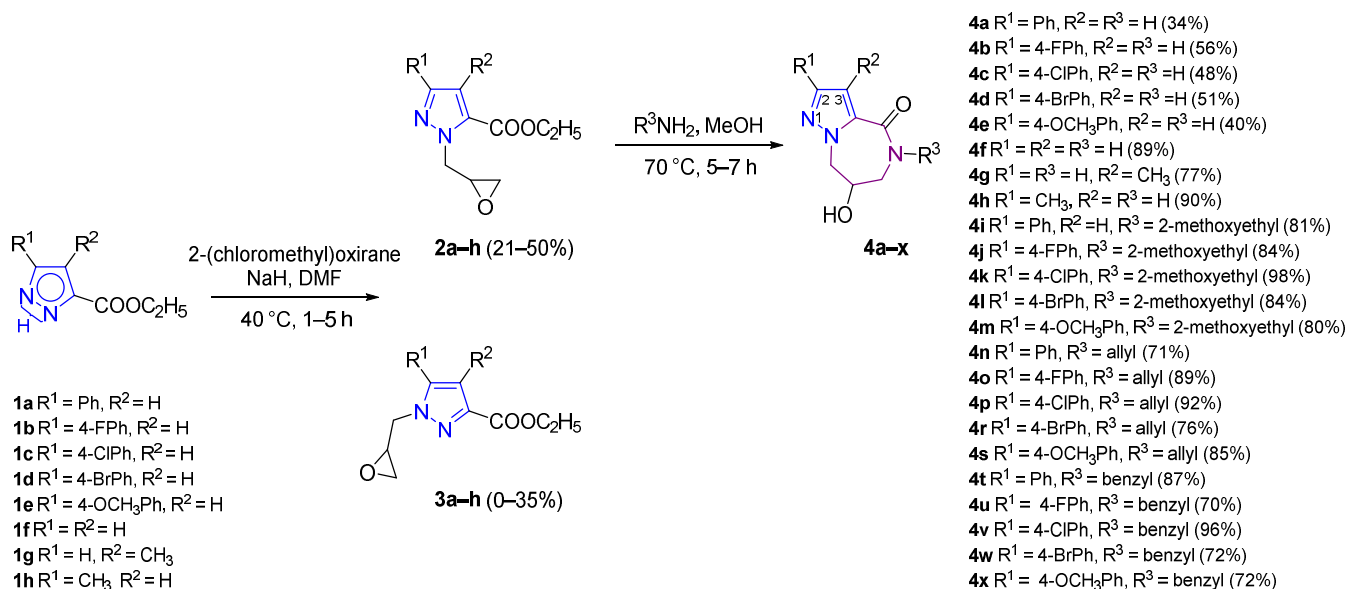
| Entry          | 2-(Chloromethyl)oxirane | Base              | Solvent | Temp.  | Time | Yield |     |
|----------------|-------------------------|-------------------|---------|--------|------|-------|-----|
|                |                         |                   |         |        |      | 2a    | 3a  |
| 1              | 15 eq                   | 1.5 eq $K_2CO_3$  | neat    | 70 °C  | 16 h | 24%   | -   |
| 2              | 10 eq                   | 1.1 eq $Cs_2CO_3$ | neat    | 40 °C  | 5 h  | 30%   | 20% |
| 3              | 10 eq                   | 1.3 eq NaH        | neat    | 40 °C  | 5 h  | -     | 50% |
| 4 <sup>a</sup> | 11.5 eq                 | 2.0 eq KOH        | neat    | 40 °C  | 6 h  | 7%    | 33% |
| 5              | 5 eq                    | 3.0 eq $Cs_2CO_3$ | DMF     | 50 °C  | 24 h | 49%   | 6%  |
| 6              | 1.5 eq                  | 1.5 eq NaH        | DMF     | 40 °C  | 5 h  | 50%   | -   |
| 7              | 2.6 eq                  | 1.4 eq $Cs_2CO_3$ | ACN     | reflux | 5 h  | 45%   | -   |

<sup>a</sup> TBAB was used as a phase transfer catalyst.

Subsequently, alkylation reaction conditions were investigated in the presence of solvent. To our satisfaction, both  $Cs_2CO_3$  (Entry 5) [52] and NaH (Entry 6) in DMF [53] provided desired isomer **2a** as the major product in high regioselectivity. An attempt to perform reaction in refluxing ACN using  $Cs_2CO_3$  as a base [54] gave similar results (Entry 7). Interestingly, we noticed that alkylation using NaH proved to be highly regioselective

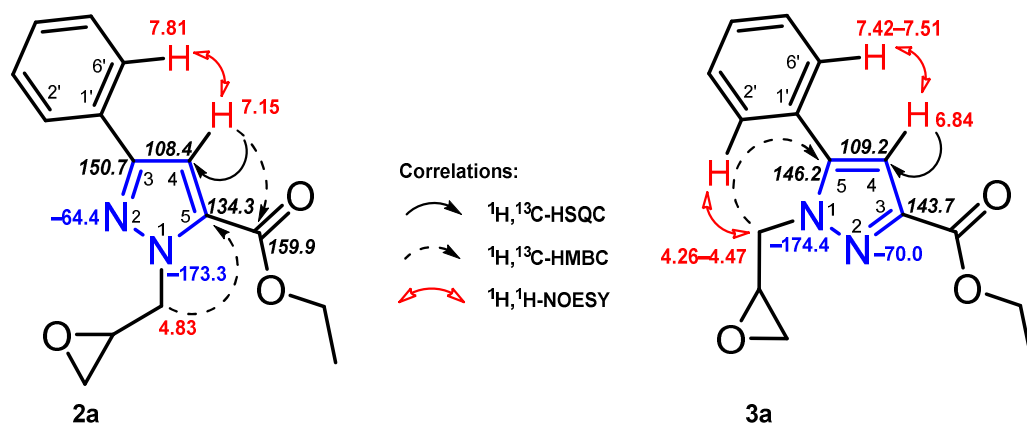


the ratio of obtained products was drastically shifted by changing the reaction media. The use of DMF as a solvent in the presence of NaH was selected as the most suitable approach to synthesize ethyl 1-(oxiran-2-ylmethyl)-3-phenyl-1*H*-pyrazole-5-carboxylates **2a–h** as it required overall reduced reaction time and temperature for full conversion of pyrazoles **1a–h** (Scheme 1). Although the reactions exhibit high regioselectivity, obtained yields did not exceed 53–61% due to instability of products **2a–e** during the purification process.



**Scheme 1.** Synthesis of tetrahydro-4*H*-pyrazolo[1,5-*a*][1,4]diazepin-4-ones **4a–x** via *N*-alkylation and subsequent cyclisation reactions.

Differentiation between major **2a** and minor **3a** isomers was implemented based on <sup>1</sup>H,<sup>13</sup>C-HSQC, <sup>1</sup>H,<sup>13</sup>C-NOESY, <sup>1</sup>H,<sup>13</sup>C- and <sup>1</sup>H,<sup>15</sup>N-HMBC experimental data. For example, <sup>1</sup>H,<sup>13</sup>C-HMBC experiment of regioisomer **2a** revealed 3-bond correlation between NCH<sub>2</sub> protons at δ 4.83 ppm and C-5 of pyrazole ring at δ 134.3 ppm (Figure 2). In the <sup>1</sup>H,<sup>15</sup>N-HMBC spectrum, the same NCH<sub>2</sub> protons exhibited 2-bond correlation with N-1 pyrrole-like (δ −173.3 ppm) and 3-bond correlation with N-2 pyridine-like (δ −64.4 ppm) nitrogen atoms. The <sup>1</sup>H,<sup>1</sup>H-NOESY spectrum indicated close-in-space proton interaction between phenyl ring 2'(*6'*)-protons (δ 7.81 ppm) and pyrazole 4-H proton at δ 7.15 ppm.



**Figure 2.** Relevant <sup>1</sup>H,<sup>13</sup>C-HSQC, <sup>1</sup>H,<sup>13</sup>C-HMBC, <sup>1</sup>H,<sup>15</sup>N-HMBC correlations and <sup>1</sup>H NMR (red), <sup>13</sup>C NMR (italic), <sup>15</sup>N NMR (blue) chemical shifts of regioisomers **2a** and **3a**.

The structure of minor regioisomer **3a** was elucidated in a similar manner. The <sup>1</sup>H,<sup>13</sup>C-HMBC spectrum indicated that NCH<sub>2</sub> protons correlate with pyrazole C-5 carbon

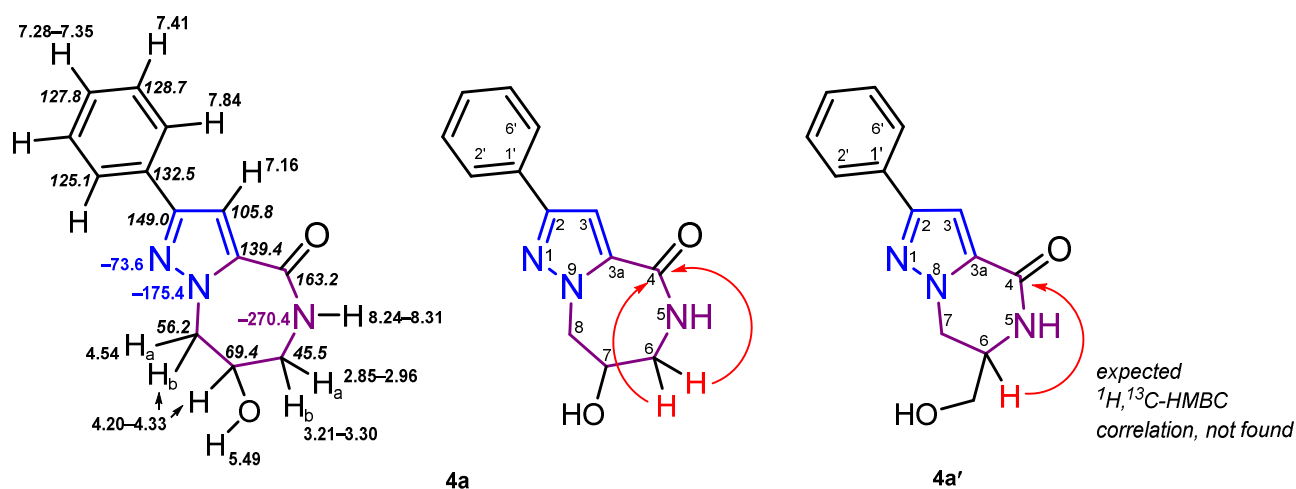
at  $-146.2$  ppm. Unambiguous distinction amongst both regioisomers can be determined using the  $^1\text{H}, ^1\text{H}$ -NOESY experiment. Close-in-space proton interaction was observed between phenyl ring 2'(6')-H protons and pyrazole 4-H proton at  $\delta$  6.84 ppm, whereas regioisomer **3a** additionally exhibited NOEs between aromatic phenyl ring 2'(6')-protons and  $\text{NCH}_2$  protons at  $\delta$  4.26–4.47 ppm.

According to the synthetic strategy, ethyl 1-(oxiran-2-ylmethyl)-3-aryl-1*H*-pyrazole-5-carboxylates **2a–h** were further used to obtain novel fused pyrazole-diazepinone systems via oxirane ring-opening. Due to high ring-strain, epoxides are prone to undergoing ring-opening reactions upon treatment with various nucleophiles [55] alone, or under the use of transition metal or organocatalysts [56–58]. On the other side, small heterocycles are also able to react with diverse electrophiles, affording a variety of functionalized molecules. Unlike the nucleophilic ring-opening reactions, the electrophilic ring-opening of small heterocycles cannot proceed by itself [59]. Methods reported in the literature for the epoxide ring-opening with amines are mainly focused on reactions mediated by a range of catalysts, activators, and promoters, in either solvent or solvent-free media [55,60–63]. In our study, intermediates **2a–h** were treated with various primary amines or ammonia in methanol (Scheme 1). Reaction monitoring indicated that ring closure proceeds rapidly to form a 1,4-diazepinone ring fused to pyrazole as no intermediate or side products have been observed, as opposed to the study reported by Shen et al. [28]. Reactions with primary amines, such as 2-methoxyethyl-, allyl- and benzylamines, afforded pyrazole-diazepinones **4i–x** in good to excellent yields (70–98%), while reactions with ammonia gave derivatives **4a–e** in substantially lower yields of 34–56%. Interestingly, tetrahydro-4*H*-pyrazolo[1,5-*a*][1,4]diazepin-4-ones **4g,h** bearing a methyl substituent in either 2- or 3-position as well as 2,3-unsubstituted pyrazole **4f** were obtained in higher yields (70–91%) compared to their phenyl-substituted counterparts **4a–e**.

A possible pyrazole-fused 1,4-diazepinone formation mechanism involves an amine-induced  $\text{S}_{\text{N}}2$  ring-opening at the less sterically hindered site of the oxirane ring [64]. Formed primary or secondary amine rapidly reacts with carbonyl carbon of an ester group, resulting in fused intermediate which further undergoes deprotonation and alkoxy group elimination to form final tetrahydro-4*H*-pyrazolo[1,5-*a*][1,4]diazepin-4-ones **4a–x**.

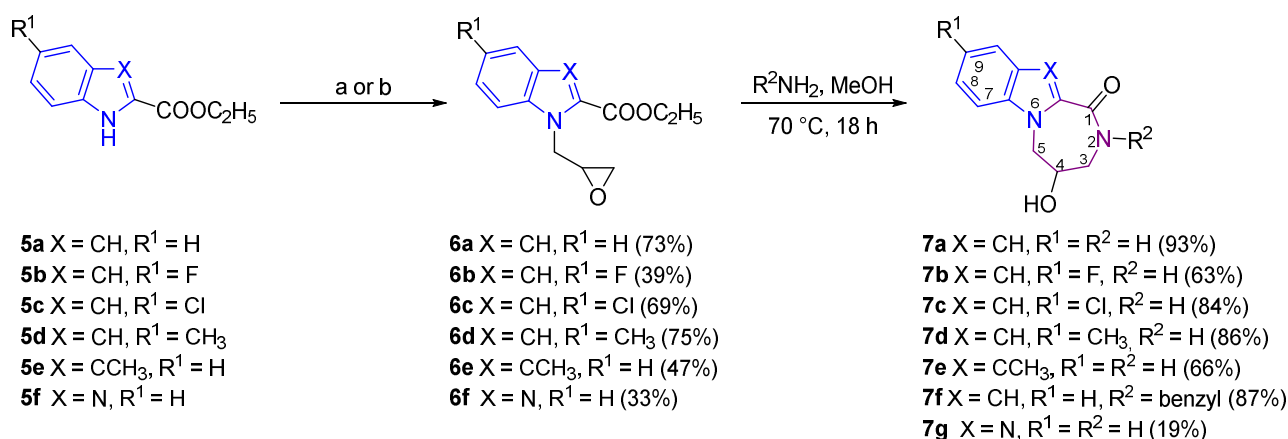
To substantiate the structures of novel compounds, an unambiguous assignment of chemical shifts was carried out by investigating combined NMR spectroscopic data, i.e.,  $^1\text{H}, ^{13}\text{C}$ -HSQC,  $^1\text{H}, ^{13}\text{C}$ -HMBC,  $^1\text{H}, ^{15}\text{N}$ -HMBC and  $^1\text{H}, ^1\text{H}$ -NOESY. In principle, cyclisation of ethyl 1-(oxiran-2-ylmethyl)-1*H*-pyrazole-5-carboxylate **2a** with ammonia could form two different isomers **4a** and **4a'** (Figure 3). The  $^1\text{H}, ^{13}\text{C}$ -HMBC experiment revealed a three-bond correlation between NH proton at  $\delta$  8.24–8.31 ppm and C-3a carbon at  $\delta$  139.4 ppm. Moreover, the same NH proton exhibited strong three-bond connectivity with tertiary C-7 carbon at 69.4 ppm. Interactions between C-4 carbon and 3-H at  $\delta$  7.16 ppm as well as 6- $\text{H}_a\text{H}_b$  protons were observed. Strong three-bond connectivity was observed in the  $^1\text{H}, ^{15}\text{N}$ -HMBC spectrum between 7-H proton and pyrrole-like nitrogen atom N-9 at  $\delta$   $-175.4$  ppm. In case of putative isomer **4a'**, the heteronuclear multiple bond correlations between NH proton and secondary aliphatic carbons should be observed. Furthermore, C-4 carbon would not exhibit three-bond correlation with aliphatic protons connected to a secondary carbon atom.

A brief experiment was performed with minor regioisomer **3a** in order to investigate if cyclisation reaction is possible when carboxylate and oxirane fragments are distanced via an additional nitrogen atom. Ethyl 1*H*-pyrazole-3-carboxylate **3a** was treated with either ammonia or benzyl amine; however, analysis of LC/MS and NMR data indicated that both reactions resulted in the oxirane ring opening without subsequent cyclisation.

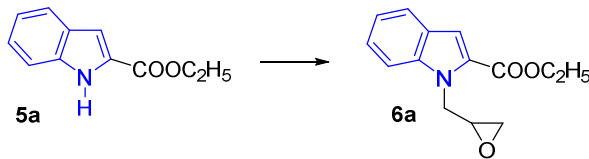


**Figure 3.** Determination of possible isomeric structures **4a** and **4a'**. Relevant <sup>1</sup>H, <sup>13</sup>C-HMBC correlations and <sup>1</sup>H NMR, <sup>13</sup>C NMR (italic), <sup>15</sup>N NMR (in blue) chemical shifts of compound **4a**.

Subsequently, we sought to investigate the reactivity of ethyl 1*H*-indole-2-carboxylate **5a–e** and benzo[*d*]imidazole-2-carboxylate **5f** scaffolds and derive target tetrahydro[1,4]diazepino[1,2-*a*]indol-1-ones and tetrahydro-1*H*-benzo[4,5]imidazo[1,2-*a*][1,4]diazepin-1-one utilizing the same straightforward 2-step approach (Scheme 2). *N*-Alkylation of **5a** with 2-(chloromethyl)oxirane using NaH in DMF at 40 °C provided ethyl 1-(oxiran-2-ylmethyl)-1*H*-indole-2-carboxylate **6a** in 54% yield. To increase the yield of target intermediate, several attempts to optimize reaction conditions were undertaken (Table 2). Unfortunately, neither elevation of reaction temperature, nor change of base or solvent have significant impact on the reaction outcome (Entries 2–5). Finally, the use of KOH base in DMF resulted not only in higher reactivity of starting 1*H*-indole-2-carboxylate **5a** (Entry 5) but also suppressed the formation of side products. Conditions utilizing the KOH-DMF system were applied to obtain ethyl 1-(oxiran-2-ylmethyl)-1*H*-indole-2-carboxylates **6a–e** in 39–75% yields (Scheme 2).



**Scheme 2.** Synthesis of 4-hydroxy-2,3,4,5-tetrahydro-1*H*-[1,4]diazepino[1,2-*a*]indol-1-ones **7a–f** and 4-hydroxy-2,3,4,5-tetrahydro-1*H*-benzo[4,5]imidazo[1,2-*a*][1,4]diazepin-1-one **7g** via 2-step approach. *N*-Alkylation conditions: (a) 2-(chloromethyl)oxirane, KOH, DMF, 40 °C, 1 h (for **5a–e**); (b) 2-(chloromethyl)oxirane, NaH, DMF, 60 °C, 4 h (for **5f**).

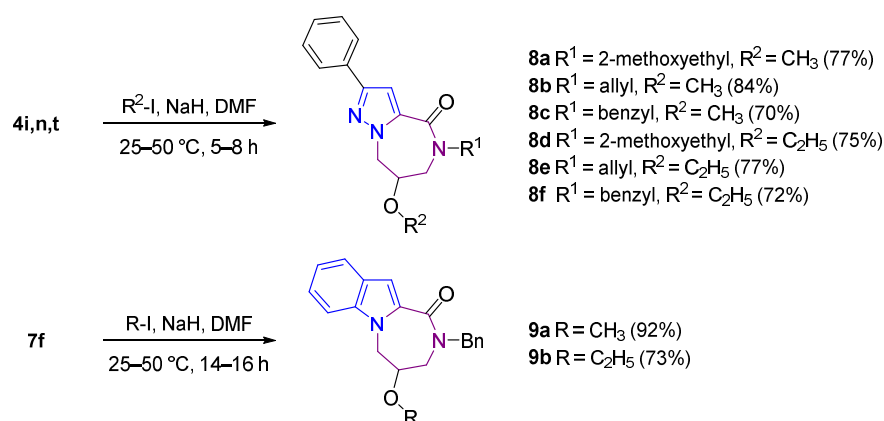
**Table 2.** Optimization of reaction conditions between 5a and 2-(chloromethyl)oxirane.


| Entry | 2-(Chloromethyl)oxirane | Base                                  | Solvent | Temp. | Time | Yield |
|-------|-------------------------|---------------------------------------|---------|-------|------|-------|
| 1     | 1.5 eq                  | 1.0 eq NaH                            | DMF     | 40 °C | 5 h  | 54%   |
| 2     | 1.5 eq                  | 1.0 eq NaH                            | DMF     | 60 °C | 4 h  | 48%   |
| 3     | 1.2 eq                  | 2.0 eq K <sub>2</sub> CO <sub>3</sub> | DMF     | 90 °C | 4 h  | 40%   |
| 4     | 1.5 eq                  | 2.0 eq K <sub>2</sub> CO <sub>3</sub> | DMF     | 90 °C | 4 h  | 63%   |
| 5     | 1.5 eq                  | 1.0 eq NaH                            | DMSO    | 40 °C | 6 h  | 59%   |
| 6     | 1.5 eq                  | 3.0 eq KOH                            | DMF     | 40 °C | 1 h  | 73%   |

Interestingly, in the case benzo[*d*]imidazole-2-carboxylate **5f**, optimized conditions using KOH were not efficient as alkylation product was not obtained, suggesting lower reactivity of the NH group of this compound. Fortunately, *N*-alkylation of benzo[*d*]imidazole-2-carboxylate **5f** was accomplished under primary optimized conditions utilizing NaH-DMF at 60 °C, giving rise to target intermediate **6f** in 33% yield as other alkylation conditions did not provide a better result.

In the next step, applicability of direct ring opening-cyclisation reaction was investigated. Ethyl 1-(oxiran-2-ylmethyl)-1*H*-indole-2-carboxylates **6a–e** and ethyl 1-(oxiran-2-ylmethyl)-1*H*-benzo[*d*]imidazole-2-carboxylate (**6f**) were treated with either ammonia or benzylamine in methanol. Reactions proceeded in the same manner as using pyrazole counterparts and yielded 4-hydroxy-2,3,4,5-tetrahydro-1*H*-[1,4]diazepino[1,2-*a*]indol-1-ones and 4-hydroxy-2,3,4,5-tetrahydro-1*H*-benzo[4,5]imidazo[1,2-*a*][1,4]diazepin-1-one **7a–f** in fair to excellent (63–98%) yields, with an exception of **7g** which was isolated in a mere 19% yield. In comparison, Putey et al. [32] assessed synthesis of 2,3,4,5-tetrahydro[1,4]diazepino[1,2-*a*]indol-1-ones in a 4-step procedure.

To expand the structural diversity and compound library of fused tetrahydro-4*H*-pyrazolo[1,5-*a*][1,4]diazepin-4-ones and tetrahydro[1,4]diazepino[1,2-*a*]indol-1-ones, 5-substituted 7-hydroxy-2-phenyl-5,6,7,8-tetrahydro-4*H*-pyrazolo[1,5-*a*][1,4]diazepin-4-ones **4i,n,t** and 2-benzyl-4-hydroxy-2,3,4,5-tetrahydro-1*H*-[1,4]diazepino[1,2-*a*]indol-1-one **7f** were further modified using methyl- and ethyl iodides as *O*-alkylating agents (Scheme 3). Reactions were carried out involving NaH as a base in DMF, where reaction temperature and time were substituent dependent, i.e., compounds bearing benzyl group at 5-position required longer reaction times and higher temperatures. Compounds **8a–f** and **9a,b** were obtained in 70–92% yields.

**Scheme 3.** *O*-Alkylation of 5-substituted 7-hydroxy-2-phenyl-5,6,7,8-tetrahydro-4*H*-pyrazolo[1,5-*a*][1,4]diazepin-4-ones **4i,n,t** and 2-benzyl-4-hydroxy-2,3,4,5-tetrahydro-1*H*-[1,4]diazepino[1,2-*a*]indol-1-one **7f** using methyl and ethyl iodides.

### 3. Materials and Methods

#### 3.1. General

The reagents and solvents were purchased from commercial suppliers and used without further purification unless otherwise indicated. Reaction progress was monitored by thin-layer chromatography (TLC) on pre-coated ALUGRAM<sup>®</sup>Xtra SIL G/UV<sub>254</sub> plates (Macherey—Nagel<sup>™</sup>, Düren, Germany). The purification of the reaction mixtures was performed using flash chromatography on a glass column, stationary phase—silica gel (high-purity grade 9385, pore size 60 Å, particle size 230–400 mesh, Merck KGaA, Darmstadt, Germany). The <sup>1</sup>H, <sup>13</sup>C and <sup>15</sup>N-NMR spectra were recorded in chloroform-D (CDCl<sub>3</sub>) or dimethyl sulfoxide-*d*<sub>6</sub> (DMSO-*d*<sub>6</sub>) at 25 °C on either Jeol ECA-500 (500 MHz—<sup>1</sup>H NMR, 126 MHz—<sup>13</sup>C NMR) or Jeol EC2 400R (400 MHz—<sup>1</sup>H NMR, 101 MHz—<sup>13</sup>C NMR) spectrometer equipped with a 5 mm Royal probe (JEOL USA, Inc., Peabody, MA, USA), or Bruker Avance III 400 spectrometer (400 MHz—<sup>1</sup>H NMR, 101 MHz—<sup>13</sup>C NMR, 40 MHz—<sup>15</sup>N NMR) using a 5 mm directly detecting BBO probe (Bruker BioSpin AG, Fallanden, Switzerland). Residual solvent signals were used as internal standards, i.e., for DMSO-*d*<sub>6</sub>  $\delta^1_H = 2.50$  and  $\delta^{13}_C = 39.52$ , for CDCl<sub>3</sub>  $\delta^1_H = 7.26$  and  $\delta^{13}_C = 77.16$ . <sup>15</sup>N chemical shifts were recalculated using a reference of neat external nitromethane standard (coaxial capillary). <sup>19</sup>F NMR spectra (376 MHz) were obtained on a Bruker Avance III 400 instrument; here absolute referencing via  $\delta$  ratio was used. The full and unambiguous assignments of the <sup>1</sup>H, <sup>13</sup>C, <sup>15</sup>N-NMR resonances were achieved using a combination of standard NMR spectroscopic techniques. The following abbreviations are used in reporting NMR data: Ph, phenyl; Ox, oxirane. Melting points were determined using the apparatus DigiMelt MPA160 (Stanford Research Systems Inc., Sunnyvale, CA, USA) or Büchi B-540 (Büchi Labortechnik AG, Flawil, Switzerland) and are provided uncorrected. The IR spectra were recorded on a Bruker TENSOR 27 (Bruker Optik GmbH, Ettlingen, Germany) or Nicolet Impact 410 (SpectraLab Scientific Inc., Markham, ON, Canada) FTIR spectrometer using pressured KBr pellets. HRMS spectra were recorded on a micrOTOF-Q III Bruker (Bruker Daltonik GmbH, Bremen, Germany) or Agilent 6230 TOF LC/MS (Agilent Technologies Inc., Santa Clara, CA, United States) spectrometer in electrospray ionization (ESI) mode. <sup>1</sup>H, <sup>13</sup>C, <sup>19</sup>F, and <sup>1</sup>H,<sup>15</sup>N-HMBC NMR spectra, as well as HRMS data of new compounds, are provided in Figures S1–S229 of the Supplementary Materials.

#### 3.2. Synthetic Procedures

##### 3.2.1. General Procedure for Synthesis of Starting 3(5)-Aryl-1H-pyrazole-5(3)-carboxylates (**1a–h**) [48,65]

To a 0.5 M solution of sodium ethoxide (1.1 eq) in ethanol, appropriate acetophenone (1 eq) and diethyl oxalate (1 eq) were added, and the resulting mixture was stirred at room temperature for 16 h in an inert atmosphere. Upon completion, the reaction mixture was quenched with 1 M HCl solution until neutral pH and extracted with ethyl acetate. Organic layer was washed with brine, dried over anhydrous Na<sub>2</sub>SO<sub>4</sub>, filtered, and concentrated under reduced pressure. The residue was purified by column chromatography on silica gel (*n*-hexane/ethyl acetate 15/1, *v/v*). Obtained ketoester (1 eq) was dissolved in a mixture of ethanol and acetic acid (7/3, *v/v*, 0.2 M), 55% aqueous hydrazine hydrate solution (1.1 eq) was added, and the reaction mixture was stirred at room temperature for 16 h. Subsequently, solvents were evaporated, and residue was dissolved in ethyl acetate and washed with 10% aqueous NaHCO<sub>3</sub> solution. Organic layer was washed again with brine, dried over anhydrous Na<sub>2</sub>SO<sub>4</sub>, filtered, and concentrated under reduced pressure. The residue was purified by column chromatography on silica gel (*n*-hexane/ethyl acetate/methanol gradient from 8/1/0.1 to 1/1/0.1, *v/v/v*) to give corresponding pyrazoles **1a–h** in good yields (75–87%).

### 3.2.2. Synthesis of Ethyl 1-(oxiran-2-ylmethyl)-1H-pyrazole-3(5)-carboxylates (**2a–h** and **3a,f–h**)

Appropriate pyrazole **1a–h** (1 eq) was dissolved in dry dimethyl formamide (0.4 M) and NaH (1.5 eq; 60% dispersion in mineral oil) was added followed by 2-(chloromethyl)oxirane (1.5 eq). The reaction mixture was stirred at 40 °C for 1–5 h. Upon completion, the reaction mixture was concentrated to approximately 1/3 volume, diluted with ethyl acetate, and washed with brine. Organic layer was separated, dried over anhydrous Na<sub>2</sub>SO<sub>4</sub>, filtered, and concentrated under reduced pressure. The residue was purified by column chromatography.

#### Ethyl 1-(oxiran-2-ylmethyl)-3-phenyl-1H-pyrazole-5-carboxylate **2a**

Purified by column chromatography on silica gel (*n*-hexane/ethyl acetate gradient from 10/1 to 8/1, *v/v*). White solid, mp 53–54 °C, 60% (3.13 g). *R<sub>f</sub>* = 0.72 (*n*-hexane/ethyl acetate 7/3, *v/v*). IR (KBr)  $\nu_{\max}$ , cm<sup>-1</sup>: 2981, 1721 (C=O), 1261, 1086, 1073, 764, 758, 693, 436. <sup>1</sup>H NMR (400 MHz, CDCl<sub>3</sub>)  $\delta_{\text{H}}$  ppm: 1.41 (t, *J* = 7.1 Hz, 3H, CH<sub>3</sub>), 2.58–2.63 (m, 1H, Ox CH<sub>a</sub>H<sub>b</sub>), 2.81 (t, *J* = 4.4 Hz, 1H, CH<sub>a</sub>H<sub>b</sub>), 3.40–3.47 (m, Ox 1H, CH), 4.38 (q, *J* = 7.1 Hz, 2H, CH<sub>2</sub>CH<sub>3</sub>), 4.83 (qd, *J* = 14.2, 4.6 Hz, 2H, NCH<sub>2</sub>), 7.15 (s, 1H, 4-H), 7.29–7.37 (m, 1H, Ph 4-H), 7.38–7.44 (m, 2H, Ph 3,5-H), 7.78–7.84 (m, 2H, Ph 2,6-H). <sup>13</sup>C NMR (101 MHz, CDCl<sub>3</sub>)  $\delta_{\text{C}}$  ppm: 14.4 (CH<sub>3</sub>), 45.8 (Ox CH<sub>2</sub>), 50.7 (Ox CH), 53.0 (NCH<sub>2</sub>), 61.4 (CH<sub>2</sub>CH<sub>3</sub>), 108.4 (C-4), 125.8 (Ph C-2,6), 128.3 (Ph C-4), 128.8 (Ph C-3,5), 132.5 (Ph C-1), 134.3 (C-5), 150.7 (C-3), 159.9 (C=O). <sup>15</sup>N NMR (40 MHz, CDCl<sub>3</sub>)  $\delta_{\text{N}}$  ppm: −175.6 (N-1), −66.2 (N-2). HRMS (ESI) for C<sub>15</sub>H<sub>16</sub>N<sub>2</sub>NaO<sub>3</sub> ([M+Na]<sup>+</sup>): calcd *m/z* 295.1053, found *m/z* 295.1053.

#### Ethyl 3-(4-fluorophenyl)-1-(oxiran-2-ylmethyl)-1H-pyrazole-5-carboxylate **2b**

Purified by column chromatography on silica gel (*n*-hexane/ethyl acetate 8/1, *v/v*). White solid, mp 98–99 °C, 59% (2.04 g). *R<sub>f</sub>* = 0.56 (*n*-hexane/ethyl acetate 7/3, *v/v*). IR (KBr)  $\nu_{\max}$ , cm<sup>-1</sup>: 3140, 3061, 2979, 1730 (C=O), 1445, 1263, 1214, 1086, 849, 761. <sup>1</sup>H NMR (400 MHz, DMSO-*d*<sub>6</sub>)  $\delta_{\text{H}}$  ppm: 1.33 (t, *J* = 7.1 Hz, 3H, CH<sub>3</sub>), 2.48–2.51 (m, 1H, Ox CH<sub>a</sub>H<sub>b</sub>), 2.72 (t, *J* = 4.5 Hz, 1H, Ox CH<sub>a</sub>H<sub>b</sub>), 3.36–3.42 (m, 1H, Ox CH), 4.33 (q, *J* = 7.1 Hz, 2H, CH<sub>2</sub>CH<sub>3</sub>), 4.60 (dd, *J* = 14.5, 5.5 Hz, 1H, NCH<sub>a</sub>), 4.85 (dd, *J* = 14.5, 3.6 Hz, 1H, NCH<sub>b</sub>), 7.21–7.29 (m, 2H, Ph 3,5-H), 7.38 (s, 1H, 4-H), 7.86–7.95 (m, 2H, Ph 2,6-H). <sup>13</sup>C NMR (101 MHz, DMSO-*d*<sub>6</sub>)  $\delta_{\text{C}}$  ppm: 14.0 (CH<sub>3</sub>), 44.8 (Ox CH<sub>2</sub>), 50.2 (Ox CH), 52.8 (NCH<sub>2</sub>), 61.1 (CH<sub>2</sub>CH<sub>3</sub>), 108.0 (C-4), 115.65 (d, <sup>2</sup>*J*<sub>CF</sub> = 21.6 Hz, Ph C-3,5), 127.35 (d, <sup>3</sup>*J*<sub>CF</sub> = 8.3 Hz, Ph C-2,6), 128.54 (d, <sup>4</sup>*J*<sub>CF</sub> = 3.0 Hz, Ph C-1), 134.1 (C-5), 148.6 (C-3), 159.0 (C=O), 162.07 (d, *J*<sub>CF</sub> = 244.8 Hz, Ph C-4). <sup>15</sup>N NMR (40 MHz, DMSO-*d*<sub>6</sub>)  $\delta_{\text{N}}$  ppm: −173.3 (N-1), −65.1 (N-2). <sup>19</sup>F NMR (376 MHz, DMSO-*d*<sub>6</sub>)  $\delta_{\text{F}}$  ppm: −113.8 (Ph 6-F). HRMS (ESI) for C<sub>15</sub>H<sub>15</sub>FN<sub>2</sub>NaO<sub>3</sub> ([M+Na]<sup>+</sup>): calcd *m/z* 313.0959, found *m/z* 313.0959.

#### Ethyl 3-(4-chlorophenyl)-1-(oxiran-2-ylmethyl)-1H-pyrazole-5-carboxylate **2c**

Purified by column chromatography on silica gel (*n*-hexane/ethyl acetate gradient from 8/1 to 7/1, *v/v*). Pale yellow solid, mp 110–111 °C, 53% (551 mg). *R<sub>f</sub>* = 0.57 (*n*-hexane/ethyl acetate 7/3, *v/v*). IR (KBr)  $\nu_{\max}$ , cm<sup>-1</sup>: 3127, 2982, 2960, 1715 (C=O), 1460, 1266, 1123, 1088, 835, 766. <sup>1</sup>H NMR (400 MHz, DMSO-*d*<sub>6</sub>)  $\delta_{\text{H}}$  ppm: 1.34 (t, *J* = 7.1 Hz, 3H, CH<sub>3</sub>), 2.51–2.53 (m, 1H, Ox CH<sub>a</sub>CH<sub>b</sub>), 2.79 (t, *J* = 4.5 Hz, 1H, Ox CH<sub>a</sub>H<sub>b</sub>), 3.37–3.43 (m, 1H, Ox CH), 4.34 (q, *J* = 7.1 Hz, 2H, CH<sub>2</sub>CH<sub>3</sub>), 4.61 (dd, *J* = 14.5, 5.6 Hz, 1H, NCH<sub>a</sub>), 4.86 (dd, *J* = 14.4, 3.6 Hz, 1H, NCH<sub>b</sub>), 7.42 (s, 1H, 4-H), 7.45–7.51 (m, 2H, Ph 3,5-H), 7.86–7.93 (m, 2H, Ph 2,6-H). <sup>13</sup>C NMR (101 MHz, DMSO-*d*<sub>6</sub>)  $\delta_{\text{C}}$  ppm: 14.0 (CH<sub>3</sub>), 44.8 (Ox CH<sub>2</sub>), 50.1 (Ox CH), 52.9 (NCH<sub>2</sub>), 61.1 (CH<sub>2</sub>CH<sub>3</sub>), 108.3 (C-4), 127.0 (Ph C-2,6), 128.8 (Ph C-3,5), 130.8 (Ph C-1), 132.7 (Ph C-4), 134.2 (C-5), 148.3 (C-3), 159.0 (C=O). <sup>15</sup>N NMR (40 MHz, DMSO-*d*<sub>6</sub>)  $\delta_{\text{N}}$  ppm: −172.3 (N-1), −65.2 (N-2). HRMS (ESI) for C<sub>15</sub>H<sub>15</sub>ClN<sub>2</sub>NaO<sub>3</sub> ([M+Na]<sup>+</sup>): calcd *m/z* 329.0663, found *m/z* 329.0663.

Ethyl 3-(4-bromophenyl)-1-(oxiran-2-ylmethyl)-1H-pyrazole-5-carboxylate **2d**

Purified by column chromatography on silica gel (*n*-hexane/ethyl acetate gradient from 10/1 to 8/1, *v/v*). White solid, mp 120–121 °C, 58% (1.88 g).  $R_f = 0.60$  (*n*-hexane/ethyl acetate 7/3, *v/v*). IR (KBr)  $\nu_{\max}$ ,  $\text{cm}^{-1}$ : 3127, 2979, 1716 (C=O), 1459, 1436, 1267, 1123, 1092, 832, 766.  $^1\text{H}$  NMR (400 MHz, DMSO- $d_6$ )  $\delta_{\text{H}}$  ppm: 1.33 (t,  $J = 7.1$  Hz, 3H, CH<sub>3</sub>), 2.48–2.52 (m, 1H, Ox CH<sub>a</sub>H<sub>b</sub>), 2.78 (t,  $J = 4.5$  Hz, 1H, Ox CH<sub>a</sub>H<sub>b</sub>), 3.37–3.42 (m, 1H, Ox CH), 4.33 (q,  $J = 7.1$  Hz, 2H, CH<sub>2</sub>CH<sub>3</sub>), 4.60 (dd,  $J = 14.5, 5.6$  Hz, 1H, NCH<sub>a</sub>), 4.86 (dd,  $J = 14.5, 3.6$  Hz, 1H, NCH<sub>b</sub>), 7.43 (s, 1H, 4-H), 7.58–7.64 (m, 2H, Ph 3,5-H), 7.79–7.86 (m, 2H, Ph 2,6-H).  $^{13}\text{C}$  NMR (101 MHz, DMSO- $d_6$ )  $\delta_{\text{C}}$  ppm: 14.0 (CH<sub>3</sub>), 44.8 (Ox CH<sub>2</sub>), 50.1 (Ox CH), 52.9 (NCH<sub>2</sub>), 61.1 (CH<sub>2</sub>CH<sub>3</sub>), 108.3 (C-4), 121.3 (Ph C-4), 127.3 (Ph C-2,6), 131.2 (Ph C-3,5), 131.7 (Ph C-1), 134.2 (C-5), 148.4 (C-3), 159.0 (C=O).  $^{15}\text{N}$  NMR (40 MHz, DMSO- $d_6$ )  $\delta_{\text{N}}$  ppm: –172.3 (N-1), –64.8 (N-2). HRMS (ESI) for C<sub>15</sub>H<sub>15</sub>BrN<sub>2</sub>NaO<sub>3</sub> ([M+Na]<sup>+</sup>): calcd  $m/z$  373.0158, found  $m/z$  373.0158 and 375.0136.

Ethyl 3-(4-methoxyphenyl)-1-(oxiran-2-ylmethyl)-1H-pyrazole-5-carboxylate **2e**

Purified by column chromatography on silica gel (*n*-hexane/ethyl acetate 8/1, *v/v*). White solid, mp 75–76 °C, 61% (1.9 g).  $R_f = 0.49$  (*n*-hexane/ethyl acetate 7/2 *v/v*). IR (KBr)  $\nu_{\max}$ ,  $\text{cm}^{-1}$ : 3139, 2975, 2938, 2836, 1726 (C=O), 1447, 1086, 1029, 846, 758.  $^1\text{H}$  NMR (400 MHz, DMSO- $d_6$ )  $\delta_{\text{H}}$  ppm: 1.33 (t,  $J = 7.1$  Hz, 3H, CH<sub>3</sub>), 2.47–2.50 (m, 1H, Ox CH<sub>a</sub>CH<sub>b</sub>), 2.78 (t,  $J = 4.5$  Hz, 1H, Ox CH<sub>a</sub>H<sub>b</sub>), 3.35–3.42 (m, 1H, Ox CH), 3.79 (s, 3H, OCH<sub>3</sub>), 4.33 (q,  $J = 7.1$  Hz, 2H, CH<sub>2</sub>CH<sub>3</sub>), 4.59 (dd,  $J = 14.5, 5.5$  Hz, 1H, NCH<sub>a</sub>), 4.84 (dd,  $J = 14.4, 3.5$  Hz, 1H, NCH<sub>b</sub>), 6.93–7.02 (m, 2H, Ph 3,5-H), 7.30 (s, 1H, 4-H), 7.75–7.83 (m, 2H, Ph 2,6-H).  $^{13}\text{C}$  NMR (101 MHz, DMSO- $d_6$ )  $\delta_{\text{C}}$  ppm: 14.1 (CH<sub>3</sub>), 44.8 (Ox CH<sub>2</sub>), 50.2 (Ox CH), 52.7 (NCH<sub>2</sub>), 55.2 (OCH<sub>3</sub>), 61.0 (CH<sub>2</sub>CH<sub>3</sub>), 107.5 (C-4), 114.2 (Ph C-3,5), 124.6 (Ph C-1), 126.6 (Ph C-2,6), 133.9 (C-5), 149.4 (C-3), 159.1 (C=O), 159.3 (Ph C-4).  $^{15}\text{N}$  NMR (40 MHz, DMSO- $d_6$ )  $\delta_{\text{N}}$  ppm: –174.5 (N-1) –67.0 (N-2). HRMS (ESI) for C<sub>16</sub>H<sub>18</sub>N<sub>2</sub>NaO<sub>4</sub> ([M+Na]<sup>+</sup>): calcd  $m/z$  325.1159, found  $m/z$  325.1159.

Ethyl 1-(oxiran-2-ylmethyl)-1H-pyrazole-5-carboxylate **2f**

Purified by column chromatography on silica gel (*n*-hexane/ethyl acetate 4/1, *v/v*). Colorless liquid, 21% (30 mg).  $R_f = 0.57$  (*n*-hexane/ethyl acetate 2/1, *v/v*). IR (KBr)  $\nu_{\max}$ ,  $\text{cm}^{-1}$ : 2985, 1722 (C=O), 1518, 1312, 1254, 1121, 1105, 1039, 765.  $^1\text{H}$  NMR (400 MHz, CDCl<sub>3</sub>)  $\delta_{\text{H}}$  ppm: 1.39 (t,  $J = 7.1$  Hz, 3H, CH<sub>3</sub>), 2.54–2.56 (m, 1H, Ox CH<sub>a</sub>H<sub>b</sub>), 2.80 (t,  $J = 4.4$  Hz, 1H, Ox CH<sub>a</sub>H<sub>b</sub>), 3.37–3.40 (m, 1H, Ox CH), 4.36 (q,  $J = 7.1$  Hz, 2H, CH<sub>2</sub>CH<sub>3</sub>), 4.73 (dd,  $J = 14.2, 5.2$  Hz, 1H, NCH<sub>a</sub>H<sub>b</sub>), 4.86 (dd,  $J = 14.2, 4.2$  Hz, 1H, NCH<sub>a</sub>H<sub>b</sub>), 6.86 (d,  $J = 1.5$  Hz, 1H, 4-H), 7.53 (d,  $J = 1.4$  Hz, 1H, 3-H).  $^{13}\text{C}$  NMR (101 MHz, CDCl<sub>3</sub>)  $\delta_{\text{C}}$  ppm: 14.3 (CH<sub>3</sub>), 45.8 (Ox CH<sub>2</sub>), 50.7 (Ox CH), 53.0 (NCH<sub>2</sub>), 61.3 (CH<sub>2</sub>CH<sub>3</sub>), 111.6 (C-4), 133.0 (C-5), 138.8 (C-3), 159.9 (COO).  $^{15}\text{N}$  NMR (40 MHz, CDCl<sub>3</sub>)  $\delta_{\text{N}}$  ppm: –173.5 (N-1), –60.2 (N-2). HRMS (ESI) for C<sub>9</sub>H<sub>13</sub>N<sub>2</sub>O<sub>3</sub> ([M+H]<sup>+</sup>): calcd  $m/z$  197.0921, found  $m/z$  197.0916.

Ethyl 4-methyl-1-(oxiran-2-ylmethyl)-1H-pyrazole-5-carboxylate **2g**

Purified by column chromatography on silica gel (*n*-hexane/ethyl acetate 4/1, *v/v*). Colorless liquid, 26% (36 mg).  $R_f = 0.47$  (*n*-hexane/ethyl acetate 2/1, *v/v*). IR (KBr)  $\nu_{\max}$ ,  $\text{cm}^{-1}$ : 2983, 1716 (C=O), 1449, 1277, 1113, 1042.  $^1\text{H}$  NMR (400 MHz, CDCl<sub>3</sub>)  $\delta_{\text{H}}$  ppm: 1.40 (t,  $J = 7.1$  Hz, 3H, CH<sub>2</sub>CH<sub>3</sub>), 2.26 (s, 3H, 4-CH<sub>3</sub>), 2.52–2.54 (m, 1H, Ox CH<sub>a</sub>H<sub>b</sub>), 2.78 (t,  $J = 4.4$  Hz, 1H, Ox CH<sub>a</sub>H<sub>b</sub>), 3.34–3.37 (m, 1H, Ox CH), 4.38 (q,  $J = 7.1$  Hz, 2H, CH<sub>2</sub>CH<sub>3</sub>), 4.68 (dd,  $J = 14.3, 5.1$  Hz, 1H, NCH<sub>a</sub>H<sub>b</sub>), 4.80 (dd,  $J = 14.3, 4.1$  Hz, 1H, NCH<sub>a</sub>H<sub>b</sub>), 7.36 (s, 1H, 3-H).  $^{13}\text{C}$  NMR (101 MHz, CDCl<sub>3</sub>)  $\delta_{\text{C}}$  ppm: 10.9 (4-CH<sub>3</sub>), 14.3 (CH<sub>2</sub>CH<sub>3</sub>), 45.7 (Ox CH<sub>2</sub>), 50.8 (Ox CH), 53.5 (NCH<sub>2</sub>), 61.0 (CH<sub>2</sub>CH<sub>3</sub>), 123.1 (C-4), 130.1 (C-5), 140.2 (C-3), 160.7 (COO).  $^{15}\text{N}$  NMR (40 MHz, CDCl<sub>3</sub>)  $\delta_{\text{N}}$  ppm: –174.6 (N-1), –63.9 (N-2). HRMS (ESI) for C<sub>10</sub>H<sub>15</sub>N<sub>2</sub>O<sub>3</sub> ([M+H]<sup>+</sup>): calcd  $m/z$  211.1077, found  $m/z$  211.1067.

**Ethyl 3-methyl-1-(oxiran-2-ylmethyl)-1H-pyrazole-5-carboxylate 2h**

Purified by column chromatography on silica gel (*n*-hexane/ethyl acetate 4/1, *v/v*). Colorless liquid, 24% (32 mg).  $R_f = 0.42$  (*n*-hexane/ethyl acetate 2/1, *v/v*). IR (KBr)  $\nu_{\max}$ ,  $\text{cm}^{-1}$ : 2962, 2909, 1722 (C=O), 1461, 1262, 1085, 767.  $^1\text{H}$  NMR (400 MHz,  $\text{CDCl}_3$ )  $\delta_{\text{H}}$  ppm: 1.37 (t,  $J = 7.1$  Hz, 3H,  $\text{CH}_2\text{CH}_3$ ), 2.28 (s, 3H, 3- $\text{CH}_3$ ), 2.55–2.57 (m, 1H, Ox  $\text{CH}_a\text{H}_b$ ), 2.79 (t,  $J = 4.4$  Hz, 1H, Ox  $\text{CH}_a\text{H}_b$ ), 3.34–3.38 (m, 1H, Ox CH), 4.33 (q,  $J = 7.1$  Hz, 2H,  $\text{CH}_2\text{CH}_3$ ), 4.63 (dd,  $J = 14.3, 5.2$  Hz, 1H,  $\text{NCH}_a\text{H}_b$ ), 4.78 (dd,  $J = 14.3, 4.1$  Hz, 1H,  $\text{NCH}_a\text{H}_b$ ), 6.64 (s, 1H, 4-H).  $^{13}\text{C}$  NMR (101 MHz,  $\text{CDCl}_3$ )  $\delta_{\text{C}}$  ppm: 13.5 (3- $\text{CH}_3$ ), 14.4 ( $\text{CH}_2\text{CH}_3$ ), 45.8 (Ox  $\text{CH}_2$ ), 50.8 (Ox CH), 52.7 ( $\text{NCH}_2$ ), 61.2 ( $\text{CH}_2\text{CH}_3$ ), 111.0 (C-4), 133.4 (C-5), 148.0 (C-3), 160.0 (COO).  $^{15}\text{N}$  NMR (40 MHz,  $\text{CDCl}_3$ )  $\delta_{\text{N}}$  ppm: –178.6 (N-1), –64.1 (N-2). HRMS (ESI) for  $\text{C}_{10}\text{H}_{15}\text{N}_2\text{O}_3$  ( $[\text{M}+\text{H}]^+$ ): calcd  $m/z$  211.1077, found  $m/z$  211.1075.

**Ethyl 1-(oxiran-2-ylmethyl)-5-phenyl-1H-pyrazole-3-carboxylate 3a**

Purified by column chromatography on silica gel (*n*-hexane/ethyl acetate gradient from 8/1 to 1/1, *v/v*). Colorless resin, 56% (20 mg).  $R_f = 0.37$  (*n*-hexane/ethyl acetate 1/1, *v/v*). IR (KBr)  $\nu_{\max}$ ,  $\text{cm}^{-1}$ : 2986, 1729 (C=O), 1214, 765, 701.  $^1\text{H}$  NMR (400 MHz,  $\text{CDCl}_3$ )  $\delta_{\text{H}}$  ppm: 1.41 (t,  $J = 7.1$  Hz, 3H,  $\text{CH}_3$ ), 2.49–2.53 (m, 1H, Ox  $\text{CH}_a\text{H}_b$ ), 2.81 (t,  $J = 4.3$  Hz, 1H, Ox  $\text{CH}_a\text{H}_b$ ), 3.40–3.45 (m, 1H, Ox CH), 4.26–4.47 (m, 4H,  $\text{CH}_2\text{CH}_3$ ,  $\text{NCH}_2$ ), 6.84 (s, 1H, 4-H), 7.42–7.51 (m, 5H, Ph 2,3,4,5,6-H).  $^{13}\text{C}$  NMR (101 MHz,  $\text{CDCl}_3$ )  $\delta_{\text{C}}$  ppm: 14.6 ( $\text{CH}_3$ ), 46.0 (Ox  $\text{CH}_2$ ), 50.7 (Ox CH), 51.6 ( $\text{NCH}_2$ ), 61.2 ( $\text{CH}_2\text{CH}_3$ ), 109.2 (C-4), 129.0 (Ph C-1,2,6), 129.4 (Ph C-4), 129.5 (Ph C-3,5), 143.7 (C-3), 146.2 (C-5), 162.5 (C=O).  $^{15}\text{N}$  NMR (40 MHz,  $\text{CDCl}_3$ )  $\delta_{\text{N}}$  ppm: –174.4 (N-1), –70.0 (N-2). HRMS (ESI) for  $\text{C}_{15}\text{H}_{16}\text{N}_2\text{NaO}_3$  ( $[\text{M}+\text{Na}]^+$ ): calcd  $m/z$  295.1053, found  $m/z$  295.1051.

**Ethyl 1-(oxiran-2-ylmethyl)-1H-pyrazole-3-carboxylate 3f**

Purified by column chromatography on silica gel (*n*-hexane/ethyl acetate gradient from 4/1 to 2/1, *v/v*). Colorless liquid, 28% (39 mg).  $R_f = 0.49$  (*n*-hexane/ethyl acetate 1/2, *v/v*). IR (KBr)  $\nu_{\max}$ ,  $\text{cm}^{-1}$ : 2986, 1721 (C=O), 1375, 1237, 1173, 1154, 1027, 765.  $^1\text{H}$  NMR (400 MHz,  $\text{CDCl}_3$ )  $\delta_{\text{H}}$  ppm: 1.40 (t,  $J = 7.1$ , 3H,  $\text{CH}_3$ ), 2.49–2.51 (m, 1H, Ox  $\text{CH}_a\text{H}_b$ ), 2.87 (t,  $J = 4.2$  Hz, 1H, Ox  $\text{CH}_a\text{H}_b$ ), 3.36–3.38 (m, 1H, Ox CH), 4.21 (dd,  $J = 14.7, 6.0$  Hz, 1H,  $\text{NCH}_a\text{H}_b$ ), 4.41 (q,  $J = 7.1$  Hz, 2H,  $\text{CH}_2\text{CH}_3$ ), 4.62 (dd,  $J = 14.7, 2.6$  Hz, 1H,  $\text{NCH}_a\text{H}_b$ ), 6.84 (d,  $J = 2.1$  Hz, 1H, 4-H), 7.53 (d,  $J = 2.1$  Hz, 1H, 5-H).  $^{13}\text{C}$  NMR (101 MHz,  $\text{CDCl}_3$ )  $\delta_{\text{C}}$  ppm: 14.5 ( $\text{CH}_3$ ), 45.5 (Ox  $\text{CH}_2$ ), 50.4 (Ox CH), 54.6 ( $\text{NCH}_2$ ), 61.2 ( $\text{CH}_2\text{CH}_3$ ), 109.5 (C-4), 131.7 (C-5), 144.2 (C-3), 162.4 (COO).  $^{15}\text{N}$  NMR (40 MHz,  $\text{CDCl}_3$ )  $\delta_{\text{N}}$  ppm: –171.8 (N-1), –68.9 (N-2). HRMS (ESI) for  $\text{C}_9\text{H}_{13}\text{N}_2\text{O}_3$  ( $[\text{M}+\text{H}]^+$ ): calcd  $m/z$  197.0921, found  $m/z$  197.0915.

**Ethyl 4-methyl-1-(oxiran-2-ylmethyl)-1H-pyrazole-3-carboxylate 3g**

Purified by column chromatography on silica gel (*n*-hexane/ethyl acetate gradient from 4/1 to 2/1, *v/v*). Colorless liquid, 35% (48 mg).  $R_f = 0.47$  (*n*-hexane/ethyl acetate 1/2, *v/v*). IR (KBr)  $\nu_{\max}$ ,  $\text{cm}^{-1}$ : 2983, 2932, 1716 (C=O), 1448, 1367, 1254, 1108.  $^1\text{H}$  NMR (400 MHz,  $\text{CDCl}_3$ )  $\delta_{\text{H}}$  ppm: 1.41 (t,  $J = 7.1$  Hz, 3H,  $\text{CH}_2\text{CH}_3$ ), 2.29 (s, 3H, 4- $\text{CH}_3$ ), 2.49–2.51 (m, 1H, Ox  $\text{CH}_a\text{H}_b$ ), 2.86 (t,  $J = 4.2$  Hz, 1H, Ox  $\text{CH}_a\text{H}_b$ ), 3.33–3.35 (m, 1H, Ox CH), 4.13 (dd,  $J = 14.7, 6.0$  Hz, 1H,  $\text{NCH}_a\text{H}_b$ ), 4.41 (q,  $J = 7.1$  Hz, 2H,  $\text{CH}_2\text{CH}_3$ ), 4.55 (dd,  $J = 14.7, 2.5$  Hz, 1H,  $\text{NCH}_a\text{H}_b$ ), 7.33 (s, 1H, 5-H).  $^{13}\text{C}$  NMR (101 MHz,  $\text{CDCl}_3$ )  $\delta_{\text{C}}$  ppm: 9.9 (4- $\text{CH}_3$ ), 14.5 ( $\text{CH}_2\text{CH}_3$ ), 45.4 (Ox  $\text{CH}_2$ ), 50.5 (Ox CH), 54.5 ( $\text{NCH}_2$ ), 60.8 ( $\text{CH}_2\text{CH}_3$ ), 121.5 (C-4), 131.0 (C-5), 141.4 (C-3), 163.0 (COO).  $^{15}\text{N}$  NMR (40 MHz,  $\text{CDCl}_3$ )  $\delta_{\text{N}}$  ppm: –175.7 (N-1), –69.2 (N-2). HRMS (ESI) for  $\text{C}_{10}\text{H}_{15}\text{N}_2\text{O}_3$  ( $[\text{M}+\text{H}]^+$ ): calcd  $m/z$  211.1077, found  $m/z$  211.1072.

**Ethyl 5-methyl-1-(oxiran-2-ylmethyl)-1H-pyrazole-3-carboxylate 3h**

Purified by column chromatography on silica gel (*n*-hexane/ethyl acetate gradient from 4/1 to 2/1, *v/v*). White solid, mp 31–33 °C, 29% (40 mg).  $R_f = 0.47$  (*n*-hexane/ethyl acetate 1/2, *v/v*). IR (KBr)  $\nu_{\max}$ ,  $\text{cm}^{-1}$ : 2985, 1721 (C=O), 1446, 1386, 1228, 1032, 780.  $^1\text{H}$  NMR (400 MHz,  $\text{CDCl}_3$ )  $\delta_{\text{H}}$  ppm: 1.39 (t,  $J = 7.1$  Hz, 3H,  $\text{CH}_2\text{CH}_3$ ), 2.34 (s, 3H, 5- $\text{CH}_3$ ),



2.47–2.49 (m, 1H, Ox CH<sub>a</sub>H<sub>b</sub>), 2.82 (t,  $J = 4.3$  Hz, 1H, Ox CH<sub>a</sub>H<sub>b</sub>), 3.33–3.37 (m, 1H, Ox CH), 4.21 (dd,  $J = 15.0, 5.2$  Hz, 1H, NCH<sub>a</sub>H<sub>b</sub>), 4.39 (q,  $J = 7.1$  Hz, 2H, CH<sub>2</sub>CH<sub>3</sub>) 4.53 (dd,  $J = 15.0, 2.4$  Hz, 1H, NCH<sub>a</sub>H<sub>b</sub>), 6.57 (s, 1H, 4-H). <sup>13</sup>C NMR (101 MHz, CDCl<sub>3</sub>) δ<sub>C</sub> ppm: 11.4 (5-CH<sub>3</sub>), 14.5 (CH<sub>2</sub>CH<sub>3</sub>), 45.3 (Ox CH<sub>2</sub>), 50.9 (Ox CH), 51.4 (NCH<sub>2</sub>), 61.0 (CH<sub>2</sub>CH<sub>3</sub>), 108.6 (C-4), 141.3 (C-5), 143.1 (C-3), 162.6 (COO). <sup>15</sup>N NMR (40 MHz, CDCl<sub>3</sub>) δ<sub>N</sub> ppm: −173.3 (N-1), −70.8 (N-2). HRMS (ESI) for C<sub>10</sub>H<sub>15</sub>N<sub>2</sub>O<sub>3</sub> ([M+H]<sup>+</sup>): calcd  $m/z$  211.1077, found  $m/z$  211.1070.

### 3.2.3. Synthesis of 7-Hydroxy-5,6,7,8-tetrahydro-4H-pyrazolo[1,5-*a*][1,4]diazepin-4-ones (4a–x)

**Procedure a.** Carboxylate **2a–h** (1 eq) was dissolved in 2M ammonia (30 eq) solution in methanol, sealed in a pressure tube and stirred at 70 °C for 5–18 h. After completion, excess of ammonia in methanol was evaporated under reduced pressure. The residue was purified by column chromatography.

**Procedure b.** To a solution of carboxylate **2a–e** (1 eq) in methanol (5 M), appropriate primary amine (3 eq) was added, the reaction mixture was sealed in a pressure tube and was stirred at 70 °C for 7 h. After completion, the reaction mixture was poured into water and extracted with ethyl acetate. Combined organic layers were washed with brine, dried over anhydrous Na<sub>2</sub>SO<sub>4</sub>, filtered, and concentrated under reduced pressure. The residue was purified by column chromatography.

#### 7-Hydroxy-2-phenyl-5,6,7,8-tetrahydro-4H-pyrazolo[1,5-*a*][1,4]diazepin-4-one **4a**

Purified by column chromatography on silica gel (gradient from *n*-hexane/ethyl acetate/methanol gradient from 1/9/0 to 1/15/0.5, *v/v*). White solid, decomp. 246 °C, procedure a –34% (27 mg).  $R_f = 0.40$  (dichloromethane/methanol 100/5, *v/v*). IR (KBr)  $\nu_{\max}$ , cm<sup>−1</sup>: 3270, 3196, 3074, 2925, 1681 (C=O), 1460, 1440, 771, 752, 685. <sup>1</sup>H NMR (400 MHz, DMSO-*d*<sub>6</sub>) δ<sub>H</sub> ppm: 2.85–2.96 (m, 1H, 6-H<sub>a</sub>), 3.21–3.30 (m, 1H, 6-H<sub>b</sub>), 4.20–4.33 (m, 2H, 7-H, 8-H<sub>a</sub>), 4.54 (dd,  $J = 13.8, 4.8$  Hz, 1H, 8-H<sub>b</sub>), 5.49 (d,  $J = 3.8$  Hz, 1H, OH), 7.16 (s, 1H, 3-H), 7.28–7.35 (m, 1H, Ph 4-H), 7.36–7.45 (m, 2H, Ph 3,5-H), 7.80–7.88 (m, 2H, Ph 2,6-H), 8.24–8.31 (m, 1H, NH). <sup>13</sup>C NMR (101 MHz, DMSO-*d*<sub>6</sub>) δ<sub>C</sub> ppm: 45.5 (C-6), 56.2 (C-8), 69.4 (C-7), 105.8 (C-3), 125.1 (Ph C-2,6), 127.8 (Ph C-4), 128.7 (Ph C-3,5), 132.5 (Ph C-1), 139.4 (C-3a), 149.0 (C-2), 163.2 (C-4). <sup>15</sup>N NMR (40 MHz, DMSO-*d*<sub>6</sub>) δ<sub>N</sub> ppm: −270.4 (N-5), −175.4 (N-9), −73.6 (N-1). HRMS (ESI) for C<sub>13</sub>H<sub>13</sub>N<sub>3</sub>NaO<sub>2</sub> ([M+Na]<sup>+</sup>): calcd  $m/z$  266.0900, found  $m/z$  266.0900.

#### 2-(4-Fluorophenyl)-7-hydroxy-5,6,7,8-tetrahydro-4H-pyrazolo[1,5-*a*][1,4]diazepin-4-one **4b**

Purified by column chromatography on silica gel (*n*-hexane/ethyl acetate/methanol gradient from 1/9/0 to 1/15/0.5, *v/v*). Pale yellow solid, decomp. 216 °C, procedure a –56% (86 mg).  $R_f = 0.38$  (dichloromethane/methanol 100/5, *v/v*). IR (KBr)  $\nu_{\max}$ , cm<sup>−1</sup>: 3305, 3206, 3071, 2947, 2923, 1681, 1457, 1442, 841, 809. <sup>1</sup>H NMR (400 MHz, DMSO-*d*<sub>6</sub>) δ<sub>H</sub> ppm: 3.74 (dt,  $J = 12.2, 5.8$  Hz, 1H, 6-H<sub>a</sub>), 4.09 (dt,  $J = 14.5, 5.4$  Hz, 1H, 6-H<sub>b</sub>), 5.02–5.15 (m, 2H, 7-H, 8-H<sub>a</sub>), 5.36 (dd,  $J = 13.9, 5.0$  Hz, 1H, 8-H<sub>b</sub>), 8.00 (s, 1H, 3-H), 8.04–8.11 (m, 2H, Ph 3,5-H), 8.67–8.75 (m, 2H, Ph 2,6-H), 9.12–9.18 (m, 1H, NH). <sup>13</sup>C NMR (101 MHz, DMSO-*d*<sub>6</sub>) δ<sub>C</sub> ppm: 45.5 (C-6), 56.2 (C-8), 69.3 (C-7), 105.8 (C-3), 115.59 (d, <sup>2</sup> $J_{CF} = 21.5$  Hz, Ph C-3,5), 127.12 (d, <sup>3</sup> $J_{CF} = 8.2$  Hz, Ph C-2,6), 129.10 (d, <sup>4</sup> $J_{CF} = 3.0$  Hz, Ph C-1), 139.6 (C-3a), 148.2 (C-2), 161.83 (d,  $J_{CF} = 244.3$  Hz, Ph C-4), 163.1 (C-4). <sup>15</sup>N NMR (40 MHz, DMSO-*d*<sub>6</sub>) δ<sub>N</sub> ppm: −270.5 (N-5), −175.3 (N-9), −73.8 (N-1). <sup>19</sup>F NMR (376 MHz, DMSO-*d*<sub>6</sub>) δ<sub>F</sub> ppm: −114.4 (Ph 6-F). HRMS (ESI) for C<sub>13</sub>H<sub>12</sub>FN<sub>3</sub>NaO<sub>2</sub> ([M+Na]<sup>+</sup>): calcd  $m/z$  284.0806, found  $m/z$  284.0806.

#### 2-(4-Chlorophenyl)-7-hydroxy-5,6,7,8-tetrahydro-4H-pyrazolo[1,5-*a*][1,4]diazepin-4-one **4c**

Purified by column chromatography on silica gel (*n*-hexane/ethyl acetate/methanol gradient from 1/9/0 to 1/20/0.5, *v/v*). White solid, decomp. 249 °C, procedure a –48% (59 mg).  $R_f = 0.38$  (dichloromethane/methanol 100/5, *v/v*). IR (KBr)  $\nu_{\max}$ , cm<sup>−1</sup>: 3297,

3210, 3080, 2917, 1683 (C=O), 1451, 1435, 1089, 834, 809.  $^1\text{H}$  NMR (400 MHz, DMSO- $d_6$ )  $\delta_{\text{H}}$  ppm: 2.86–2.95 (m, 1H, 6- $\text{H}_a$ ), 3.21–3.30 (m, 1H, 6- $\text{H}_b$ ), 4.19–4.31 (m, 2H, 7-H, 8- $\text{H}_a$ ), 4.54 (dd,  $J = 13.9, 4.9$  Hz, 1H, 8- $\text{H}_b$ ), 5.53 (br s, 1H, OH), 7.20 (s, 1H, 3-H), 7.43–7.50 (m, 2H, Ph 3,5-H), 7.82–7.91 (m, 2H, Ph 2,6-H), 8.28–8.33 (m, 1H, NH).  $^{13}\text{C}$  NMR (101 MHz, DMSO- $d_6$ )  $\delta_{\text{C}}$  ppm: 45.5 (C-6), 56.3 (C-8), 69.3 (C-7), 106.0 (C-3), 126.8 (Ph C-2,6), 128.8 (Ph C-3,5), 131.4 (Ph C-1), 132.3 (Ph C-4), 139.6 (C-3a), 147.9 (C-2), 163.0 (C-4).  $^{15}\text{N}$  NMR (40 MHz, DMSO- $d_6$ )  $\delta_{\text{N}}$  ppm: –270.4 (N-5), –174.0 (N-9), –69.7 (N-1). HRMS (ESI) for  $\text{C}_{13}\text{H}_{12}\text{ClN}_3\text{NaO}_2$  ( $[\text{M}+\text{Na}]^+$ ): calcd  $m/z$  300.0510, found  $m/z$  300.0510.

#### 2-(4-Bromophenyl)-7-hydroxy-5,6,7,8-tetrahydro-4H-pyrazolo[1,5-a][1,4]diazepin-4-one **4d**

Purified by column chromatography on silica gel (*n*-hexane/ethyl acetate/methanol gradient from 1/9/0 to 1/12/0.5, *v/v*). White solid, decomp. 230 °C, procedure a –51% (50 mg).  $R_f = 0.40$  (dichloromethane/methanol 100/5, *v/v*). IR (KBr)  $\nu_{\text{max}}$ ,  $\text{cm}^{-1}$ : 3292, 3214, 3079, 1680 (C=O), 1455 and 1434 (doublet), 1071, 991, 922, 816 and 807 (doublet).  $^1\text{H}$  NMR (400 MHz, DMSO- $d_6$ )  $\delta_{\text{H}}$  ppm: 2.90 (dt,  $J = 12.2, 5.8$  Hz, 1H, 6- $\text{H}_a$ ), 3.26 (dt,  $J = 14.4, 5.3$  Hz, 1H, 6- $\text{H}_b$ ), 4.19–4.33 (m, 2H, 7-H, 8- $\text{H}_a$ ), 4.54 (dd,  $J = 13.9, 4.9$  Hz, 1H, 8- $\text{H}_b$ ), 5.49 (d,  $J = 41$  Hz, 1H, OH), 7.20 (s, 1H, 3-H), 7.57–7.64 (m, 2H, Ph 3,5-H), 7.76–7.84 (m, 2H, Ph 2,6-H), 8.29 (t,  $J = 5.1$  Hz, 1H, NH).  $^{13}\text{C}$  NMR (101 MHz, DMSO- $d_6$ )  $\delta_{\text{C}}$  ppm: 45.5 (C-6), 56.3 (C-8), 69.3 (C-7), 106.0 (C-3), 120.8 (Ph C-4), 127.1 (Ph C-2,6), 131.7 (Ph C-3,5), 131.8 (Ph C-1), 139.6 (C-3a), 148.0 (C-2), 163.0 (C-4).  $^{15}\text{N}$  NMR (40 MHz, DMSO- $d_6$ )  $\delta_{\text{N}}$  ppm: –173.4 (N-9), –72.7 (N-1). HRMS (ESI) for  $\text{C}_{13}\text{H}_{12}\text{BrN}_3\text{NaO}_2$  ( $[\text{M}+\text{Na}]^+$ ): calcd  $m/z$  344.0005, found  $m/z$  344.0005 and 345.9983.

#### 7-Hydroxy-2-(4-methoxyphenyl)-5,6,7,8-tetrahydro-4H-pyrazolo[1,5-a][1,4]diazepin-4-one **4e**

Purified by column chromatography on silica gel (*n*-hexane/ethyl acetate/methanol gradient from 1/9/0 to 1/10/0.5, *v/v*). White solid, decomp. 239 °C, procedure a –40% (38 mg).  $R_f = 0.41$  (dichloromethane/methanol 100/5, *v/v*). IR (KBr)  $\nu_{\text{max}}$ ,  $\text{cm}^{-1}$ : 3200, 3078, 2928, 1681 (C=O), 1463, 1447, 1251, 1176, 1027, 821.  $^1\text{H}$  NMR (400 MHz, DMSO- $d_6$ )  $\delta_{\text{H}}$  ppm: 2.91 (dt,  $J = 11.9, 5.7$  Hz, 1H, 6- $\text{H}_a$ ), 3.25 (dt,  $J = 14.6, 5.4$  Hz, 1H, 6- $\text{H}_b$ ), 3.78 (s, 3H,  $\text{OCH}_3$ ), 4.18–4.32 (m, 2H, 7-H, 8- $\text{H}_a$ ), 4.51 (dd,  $J = 14.1, 5.1$  Hz, 1H, 8- $\text{H}_b$ ), 5.48 (d,  $J = 4.2$  Hz, 1H, OH), 6.94–7.00 (m, 2H, Ph 3,5-H), 7.07 (s, 1H, 3-H), 7.73–7.79 (m, 2H, Ph 2,6-H), 8.22–8.27 (m, 1H, NH).  $^{13}\text{C}$  NMR (101 MHz, DMSO- $d_6$ )  $\delta_{\text{C}}$  ppm: 45.6 (C-6), 55.1 ( $\text{CH}_3$ ), 56.1 (C-8), 69.4 (C-7), 105.2 (C-3), 114.1 (Ph C-3,5), 125.2 (Ph C-1), 126.4 (Ph C-2,6), 139.3 (C-3a), 149.0 (C-3), 156.0 (Ph C-4), 163.2 (C-4).  $^{15}\text{N}$  NMR (40 MHz, DMSO- $d_6$ )  $\delta_{\text{N}}$  ppm: –270.1 (N-5), –176.5 (N-9), –74.9 (N-1). HRMS (ESI) for  $\text{C}_{14}\text{H}_{15}\text{N}_3\text{NaO}_3$  ( $[\text{M}+\text{Na}]^+$ ): calcd  $m/z$  296.1006, found  $m/z$  296.1006.

#### 7-Hydroxy-5,6,7,8-tetrahydro-4H-pyrazolo[1,5-a][1,4]diazepin-4-one **4f**

Purified by column chromatography on silica gel (dichloromethane/methanol 100/5, *v/v*). White solid, decomp. 195 °C, procedure a –89% (76 mg).  $R_f = 0.41$  (dichloromethane/methanol 9/1, *v/v*). IR (KBr)  $\nu_{\text{max}}$ ,  $\text{cm}^{-1}$ : 3210, 3127, 3081, 2933, 1685 (C=O), 1387, 1351, 1182, 825.  $^1\text{H}$  NMR (400 MHz, DMSO- $d_6$ )  $\delta_{\text{H}}$  ppm: 2.81–2.87 (m, 1H, 6- $\text{H}_a$ ), 3.16–3.22 (m, 1H, 6- $\text{H}_b$ ), 4.18 (dd,  $J = 14.0, 4.3$  Hz, 1H, 8- $\text{H}_a$ ), 4.21–4.27 (m, 1H, 7-H), 4.48 (dd,  $J = 14.0, 5.1$  Hz, 1H, 8- $\text{H}_b$ ), 5.44 (d,  $J = 4.0$  Hz, 1H, OH), 6.66 (d,  $J = 0.7$  Hz, 1H, 3-H), 7.47 (d,  $J = 0.6$  Hz, 1H, 2-H), 8.22 (s, 1H, NH).  $^{13}\text{C}$  NMR (101 MHz, DMSO- $d_6$ )  $\delta_{\text{C}}$  ppm: 45.6 (C-6), 55.9 (C-8), 69.4 (C-7), 108.8 (C-3), 137.79 (C-3a), 137.83 (C-2), 163.4 (C-4).  $^{15}\text{N}$  NMR (40 MHz, DMSO- $d_6$ )  $\delta_{\text{N}}$  ppm: –271.1 (N-5), –173.3 (N-9), –66.0 (N-1). HRMS (ESI) for  $\text{C}_7\text{H}_{10}\text{N}_3\text{O}_2$  ( $[\text{M}+\text{H}]^+$ ): calcd  $m/z$  168.0768, found  $m/z$  168.0763.

#### 7-Hydroxy-3-methyl-5,6,7,8-tetrahydro-4H-pyrazolo[1,5-a][1,4]diazepin-4-one **4g**

Purified by column chromatography on silica gel (dichloromethane/methanol 100/5, *v/v*). White solid, decomp. 213 °C, procedure a –77% (67 mg).  $R_f = 0.45$  (dichloromethane/methanol 9/1, *v/v*). IR (KBr)  $\nu_{\text{max}}$ ,  $\text{cm}^{-1}$ : 3301, 3203, 3078, 2932, 1678 (C=O), 1382, 1320,

1247, 1099, 922.  $^1\text{H}$  NMR (400 MHz,  $\text{DMSO-}d_6$ )  $\delta_{\text{H}}$  ppm: 2.10 (s, 3H,  $\text{CH}_3$ ), 2.77–2.84 (m, 1H, 6- $\text{H}_a$ ), 3.12–3.19 (m, 1H, 6- $\text{H}_b$ ), 4.09 (dd,  $J = 14.2, 4.2$  Hz, 1H, 8- $\text{H}_a$ ), 4.17–4.23 (m, 1H, 7-H), 4.40 (dd,  $J = 14.1, 5.4$  Hz, 1H, 8- $\text{H}_b$ ), 5.39 (d,  $J = 4.1$  Hz, 1H, OH), 7.29 (s, 1H, 2-H), 8.14 (s, 1H, NH).  $^{13}\text{C}$  NMR (101 MHz,  $\text{DMSO-}d_6$ )  $\delta_{\text{C}}$  ppm: 8.7 ( $\text{CH}_3$ ), 45.5 (C-6), 55.7 (C-8), 69.7 (C-7), 119.4 (C-3), 133.8 (C-3a), 138.4 (C-2), 164.0 (COO).  $^{15}\text{N}$  NMR (40 MHz,  $\text{DMSO-}d_6$ )  $\delta_{\text{N}}$  ppm: –270.3 (N-5), –176.2 (N-9), –69.1 (N-1). HRMS (ESI) for  $\text{C}_8\text{H}_{12}\text{N}_3\text{O}_2$  ( $[\text{M}+\text{H}]^+$ ): calcd  $m/z$  182.0924, found  $m/z$  182.0923.

#### 7-Hydroxy-2-methyl-5,6,7,8-tetrahydro-4H-pyrazolo[1,5-*a*][1,4]diazepin-4-one **4h**

Purified by column chromatography on silica gel (dichloromethane/methanol 100/5, *v/v*). White solid, decomp. 232 °C, procedure a –90% (78 mg).  $R_f = 0.44$  (dichloromethane/methanol 9/1, *v/v*). IR (KBr)  $\nu_{\text{max}}$ ,  $\text{cm}^{-1}$ : 3254, 3144, 2936, 1689 (C=O), 1635, 1464, 1453, 1135, 1054, 758.  $^1\text{H}$  NMR (400 MHz,  $\text{DMSO-}d_6$ )  $\delta_{\text{H}}$  ppm: 2.16 (s, 1H,  $\text{CH}_3$ ), 2.82–2.89 (m, 1H, 6- $\text{H}_a$ ), 3.15–3.21 (m, 1H, 6- $\text{H}_b$ ), 4.08 (dd,  $J = 14.2, 4.4$  Hz, 1H, 8- $\text{H}_a$ ), 4.17–4.24 (m, 1H, 7-H), 4.38 (dd,  $J = 14.2, 5.4$  Hz, 1H, 8- $\text{H}_b$ ), 5.40 (d,  $J = 4.1$  Hz, 1H, OH), 6.43 (s, 1H, 3-H), 8.15 (s, 1H, NH).  $^{13}\text{C}$  NMR (101 MHz,  $\text{DMSO-}d_6$ )  $\delta_{\text{C}}$  ppm: 13.0 ( $\text{CH}_3$ ), 45.6 (C-6), 55.5 (C-8), 69.5 (C-7), 108.1 (C-3), 138.4 (C-3a), 146.1 (C-2), 163.4 (COO).  $^{15}\text{N}$  NMR (40 MHz,  $\text{DMSO-}d_6$ )  $\delta_{\text{N}}$  ppm: –271.6 (N-5), –178.8 (N-9), –68.9 (N-1). HRMS (ESI) for  $\text{C}_8\text{H}_{12}\text{N}_3\text{O}_2$  ( $[\text{M}+\text{H}]^+$ ): calcd  $m/z$  182.0924, found  $m/z$  182.0923.

#### 7-Hydroxy-5-(2-methoxyethyl)-2-phenyl-5,6,7,8-tetrahydro-4H-pyrazolo[1,5-*a*][1,4]diazepin-4-one **4i**

Purified by column chromatography on silica gel (*n*-hexane/ethyl acetate 1/9, *v/v*). White solid, mp 134–135 °C, procedure b –81% (99 mg).  $R_f = 0.40$  (ethyl acetate). IR (KBr)  $\nu_{\text{max}}$ ,  $\text{cm}^{-1}$ : 3274, 3135, 2932, 1651 (C=O), 1435, 1296, 1177, 1113, 764, 691.  $^1\text{H}$  NMR (400 MHz,  $\text{DMSO-}d_6$ )  $\delta_{\text{H}}$  ppm: 3.15 (dd,  $J = 15.0, 7.5$  Hz, 1H, 5- $\text{CH}_a$ ), 3.29 (s, 3H,  $\text{CH}_3$ ), 3.41–3.56 (m, 4H, 5- $\text{CH}_b$ ,  $\text{CH}_2\text{O}$ , 6- $\text{H}_a$ ), 3.89 (dt,  $J = 13.5, 5.2$  Hz, 1H, 6- $\text{H}_b$ ), 4.24 (dd,  $J = 14.1, 3.2$  Hz, 1H, 8- $\text{H}_a$ ), 4.35–4.42 (m, 1H, 7-H), 4.47 (dd,  $J = 14.1, 5.1$  Hz, 1H, 8- $\text{H}_b$ ), 5.52 (d,  $J = 4.3$  Hz, 1H, OH), 7.17 (s, 1H, 3-H), 7.28–7.34 (m, 1H, Ph 4-H), 7.37–7.45 (m, 2H, Ph 3,5-H), 7.81–7.86 (m, 2H, Ph 2,6-H).  $^{13}\text{C}$  NMR (101 MHz,  $\text{DMSO-}d_6$ )  $\delta_{\text{C}}$  ppm: 46.8 (C-6), 52.8 (5- $\text{CH}_2$ ), 55.9 (C-8), 58.0 ( $\text{CH}_3$ ), 69.5 (C-7), 69.9 ( $\text{CH}_2\text{O}$ ), 105.4 (C-3), 125.1 (Ph C-2,6), 127.8 (Ph C-4), 128.7 (Ph C-3,5), 132.5 (Ph C-1), 139.3 (C-3a), 149.0 (C-2), 161.6 (C-4).  $^{15}\text{N}$  NMR (40 MHz,  $\text{DMSO-}d_6$ )  $\delta_{\text{N}}$  ppm: –264.8 (N-5), –175.6 (N-9), –73.7 (N-1). HRMS (ESI) for  $\text{C}_{16}\text{H}_{19}\text{N}_3\text{NaO}_3$  ( $[\text{M}+\text{Na}]^+$ ): calcd  $m/z$  324.1319, found  $m/z$  324.1319.

#### 2-(4-Fluorophenyl)-7-hydroxy-5-(2-methoxyethyl)-5,6,7,8-tetrahydro-4H-pyrazolo[1,5-*a*][1,4]diazepin-4-one **4j**

Purified by column chromatography on silica gel (*n*-hexane/ethyl acetate gradient from 4/1 to 1/5, *v/v*). White solid, mp 133–134 °C, procedure b –84% (285 mg).  $R_f = 0.46$  (ethyl acetate). IR (KBr)  $\nu_{\text{max}}$ ,  $\text{cm}^{-1}$ : 3299, 2941, 2903, 2819, 1620, 1471, 1215, 1113, 827, 806.  $^1\text{H}$  NMR (400 MHz,  $\text{DMSO-}d_6$ )  $\delta_{\text{H}}$  ppm: 3.14 (dd,  $J = 15.0, 7.5$  Hz, 1H, 6- $\text{H}_a$ ), 3.28 (s, 3H,  $\text{CH}_3$ ), 3.39–3.57 (m, 4H, 5- $\text{CH}_a$ , 6- $\text{H}_b$ ,  $\text{CH}_2\text{O}$ ), 3.89 (dt,  $J = 10.6, 5.0$  Hz, 1H, 5- $\text{CH}_b$ ), 4.23 (dd,  $J = 14.1, 2.6$  Hz, 1H, 8- $\text{H}_a$ ), 4.34–4.50 (m, 2H, 7-H, 8- $\text{H}_b$ ), 5.52 (d,  $J = 3.9$  Hz, 1H, OH), 7.17 (s, 1H, 3-H), 7.20–7.28 (m, 2H, Ph 3,5-H), 7.84–7.92 (m, 5.9 Hz, 2H, Ph 2,6-H).  $^{13}\text{C}$  NMR (101 MHz,  $\text{DMSO-}d_6$ )  $\delta_{\text{C}}$  ppm: 46.8 (5- $\text{CH}_2$ ), 52.8 (C-6), 55.9 (C-8), 58.0 ( $\text{CH}_3$ ), 69.5 (C-7), 69.9 ( $\text{CH}_2\text{O}$ ), 105.4 (C-3), 115.59 (d,  $^2J_{\text{CF}} = 21.5$  Hz, Ph C-3,5), 127.09 (d,  $^3J_{\text{CF}} = 8.2$  Hz, Ph C-2,6), 129.1 (d,  $^4J_{\text{CF}} = 3.0$  Hz, Ph C-1), 139.4 (C-3a), 148.1 (C-2), 161.5 (C-4), 161.82 (d,  $J_{\text{CF}} = 244.3$  Hz, Ph C-4).  $^{15}\text{N}$  NMR (40 MHz,  $\text{DMSO-}d_6$ )  $\delta_{\text{N}}$  ppm: –264.6 (N-5), –175.6 (N-9), –75.2 (N-1).  $^{19}\text{F}$  NMR (376 MHz,  $\text{DMSO-}d_6$ )  $\delta_{\text{F}}$  ppm: –114.4 (1F, m, Ph 6-F). HRMS (ESI) for  $\text{C}_{16}\text{H}_{18}\text{FN}_3\text{NaO}_3$  ( $[\text{M}+\text{Na}]^+$ ): calcd  $m/z$  342.1224, found  $m/z$  342.1224.

2-(4-Chlorophenyl)-7-hydroxy-5-(2-methoxyethyl)-5,6,7,8-tetrahydro-4H-pyrazolo[1,5-a][1,4]diazepin-4-one **4k**

Purified by column chromatography on silica gel (*n*-hexane/ethyl acetate gradient from 4/1 to 1/9, *v/v*). Pale pink solid, mp 148–149 °C, procedure b –98% (221 mg).  $R_f = 0.41$  (ethyl acetate). IR (KBr)  $\nu_{\max}$ ,  $\text{cm}^{-1}$ : 3300, 2941, 2877, 1623 (C=O), 1469, 1400, 1111, 1068, 826, 756.  $^1\text{H}$  NMR (400 MHz, DMSO- $d_6$ )  $\delta_{\text{H}}$  ppm: 3.14 (dd,  $J = 14.9, 7.4$  Hz, 1H, 6- $\text{H}_a$ ), 3.29 (s, 3H,  $\text{CH}_3$ ), 3.40–3.58 (m, 4H, 5- $\text{CH}_a$ , 6- $\text{H}_b$ ,  $\text{CH}_2\text{O}$ ), 3.84–3.94 (m, 1H, 5- $\text{CH}_b$ ), 4.24 (dd,  $J = 14.1, 2.5$  Hz, 1H, 8- $\text{H}_a$ ), 4.35–4.51 (m, 2H, 7-H, 8- $\text{H}_b$ ), 5.53 (d,  $J = 3.8$  Hz, 1H, OH), 7.21 (s, 1H, 3-H), 7.37–7.54 (m, 2H, Ph 3,5-H), 7.77–7.95 (m, 2H, Ph 2,6-H).  $^{13}\text{C}$  NMR (101 MHz, DMSO- $d_6$ )  $\delta_{\text{C}}$  ppm: 46.8 (5- $\text{CH}_2$ ), 52.8 (C-6), 56.0 (C-8), 58.0 ( $\text{CH}_3$ ), 69.5 (C-7), 69.9 ( $\text{CH}_2\text{O}$ ), 105.7 (C-3), 126.8 (Ph C-2,6), 128.8 (Ph C-3,5), 131.4 (Ph C-1), 132.3 (Ph C-4), 139.5 (C-3a), 147.9 (C-2), 161.4 (C-4).  $^{15}\text{N}$  NMR (40 MHz, DMSO- $d_6$ )  $\delta_{\text{N}}$  ppm: –264.3 (N-5), –174.7 (N-9), –74.3 (N-1). HRMS (ESI) for  $\text{C}_{16}\text{H}_{18}\text{ClN}_3\text{NaO}_3$  ( $[\text{M}+\text{Na}]^+$ ): calcd  $m/z$  358.0929, found  $m/z$  358.0929.

2-(4-Bromophenyl)-7-hydroxy-5-(2-methoxyethyl)-5,6,7,8-tetrahydro-4H-pyrazolo[1,5-a][1,4]diazepin-4-one **4l**

Purified by column chromatography on silica gel (*n*-hexane/ethyl acetate gradient from 3/1 to 1/9, *v/v*). White solid, mp 143–144 °C, procedure b –84% (339 mg).  $R_f = 0.43$  (ethyl acetate). IR (KBr)  $\nu_{\max}$ ,  $\text{cm}^{-1}$ : 3292, 2943, 2876, 1621 (C=O), 1545, 1467, 1107, 1070, 1007, 812.  $^1\text{H}$  NMR (400 MHz, DMSO- $d_6$ )  $\delta_{\text{H}}$  ppm: 3.14 (dd,  $J = 15.0, 7.6$  Hz, 1H, 6- $\text{H}_a$ ), 3.28 (s, 3H,  $\text{CH}_3$ ), 3.40–3.57 (m, 4H, 6- $\text{H}_b$ ,  $\text{NCH}_a$ ,  $\text{CH}_2\text{O}$ ), 3.89 (dt,  $J = 10.6, 5.1$  Hz, 1H,  $\text{NCH}_b$ ), 4.23 (dd,  $J = 14.1, 2.9$  Hz, 1H, 8- $\text{H}_a$ ), 4.35–4.42 (m, 1H, 7-H), 4.47 (dd,  $J = 14.1, 5.0$  Hz, 1H, 8- $\text{H}_b$ ), 5.53 (d,  $J = 3.2$  Hz, 1H, OH), 7.21 (s, 1H, 3-H), 7.56–7.63 (m, 2H, Ph 3,5-H), 7.76–7.83 (m, 2H, Ph 2,6-H).  $^{13}\text{C}$  NMR (101 MHz, DMSO- $d_6$ )  $\delta_{\text{C}}$  ppm: 46.8 ( $\text{NCH}_2$ ), 52.8 (C-6), 56.0 (C-8), 58.0 ( $\text{CH}_3$ ), 69.5 (7-H), 69.9 ( $\text{CH}_2\text{O}$ ), 105.6 (C-3), 120.8 (Ph C-4), 127.1 (Ph C-2,6), 131.7 (Ph C-3,5), 131.8 (Ph C-1), 139.5 (C-3a), 147.9 (C-2), 161.4 (C-4).  $^{15}\text{N}$  NMR (40 MHz, DMSO- $d_6$ )  $\delta_{\text{N}}$  ppm: –264.5 (N-5), –174.5 (N-9), –73.9 (N-1). HRMS (ESI) for  $\text{C}_{16}\text{H}_{18}\text{BrN}_3\text{NaO}_3$  ( $[\text{M}+\text{Na}]^+$ ): calcd  $m/z$  402.0424, found  $m/z$  402.0424 and 404.0409.

7-Hydroxy-5-(2-methoxyethyl)-2-(4-methoxyphenyl)-5,6,7,8-tetrahydro-4H-pyrazolo[1,5-a][1,4]diazepin-4-one **4m**

Purified by column chromatography on silica gel (*n*-hexane/ethyl acetate gradient from 3.5/1 to 1/9, *v/v*). White solid, mp 147–148 °C, procedure b –80% (274 mg).  $R_f = 0.38$  (ethyl acetate). IR (KBr)  $\nu_{\max}$ ,  $\text{cm}^{-1}$ : 3212, 2982, 2943, 2882, 2838, 1651 (C=O), 1448, 1249, 1020, 834.  $^1\text{H}$  NMR (400 MHz, DMSO- $d_6$ )  $\delta_{\text{H}}$  ppm: 3.15 (dd,  $J = 15.0, 7.4$  Hz, 1H, 6- $\text{H}_a$ ), 3.28 (s, 3H,  $\text{OCH}_3$ ), 3.39–3.57 (m, 4H, 5- $\text{CH}_a$ ,  $\text{CH}_2\text{O}$ , 6- $\text{H}_b$ ), 3.78 (s, 3H, Ph 4- $\text{OCH}_3$ ), 3.89 (dt,  $J = 13.6, 5.2$  Hz, 1H, 5- $\text{CH}_b$ ), 4.21 (dd,  $J = 14.0, 3.1$  Hz, 1H, 8- $\text{H}_a$ ), 4.34–4.47 (m, 2H, 7-H, 8- $\text{H}_b$ ), 5.52 (d,  $J = 4.2$  Hz, 1H, OH), 6.93–6.99 (m, 2H, Ph 3,5-H), 7.07 (s, 1H, 3-H), 7.73–7.80 (m, 2H, Ph 2,6-H).  $^{13}\text{C}$  NMR (101 MHz, DMSO- $d_6$ )  $\delta_{\text{C}}$  ppm: 46.8 (5- $\text{CH}_2$ ), 52.9 (C-6), 55.1 ( $\text{CH}_3$ ), 55.8 (C-8), 58.1 ( $\text{OCH}_3$ ), 69.6 (C-7), 70.0 ( $\text{CH}_2\text{O}$ ), 104.9 (C-3), 114.1 (Ph C-3,5), 125.2 (Ph C-1), 126.4 (Ph C-2,6), 139.2 (C-3a), 148.9 (C-2), 159.0 (Ph C-4), 161.7 (C-4).  $^{15}\text{N}$  NMR (40 MHz, DMSO- $d_6$ )  $\delta_{\text{N}}$  ppm: –264.5 (N-5), –176.2 (N-9), –77.0 (N-1). HRMS (ESI) for  $\text{C}_{17}\text{H}_{21}\text{N}_3\text{NaO}_4$  ( $[\text{M}+\text{Na}]^+$ ): calcd  $m/z$  354.1424, found  $m/z$  354.1424.

5-Allyl-7-hydroxy-2-phenyl-5,6,7,8-tetrahydro-4H-pyrazolo[1,5-a][1,4]diazepin-4-one **4n**

Purified by column chromatography on silica gel (*n*-hexane/ethyl acetate 1/9, *v/v*). White solid, mp 126–127 °C, procedure b –71% (231 mg).  $R_f = 0.42$  (*n*-hexane/ethyl acetate 3/7, *v/v*). IR (KBr)  $\nu_{\max}$ ,  $\text{cm}^{-1}$ : 3346, 2939, 1619 (C=O), 1470, 1431, 1286, 1055, 942, 749, 690.  $^1\text{H}$  NMR (400 MHz, DMSO- $d_6$ )  $\delta_{\text{H}}$  ppm: 3.09 (dd,  $J = 15.0, 7.3$  Hz, 1H, 6- $\text{H}_a$ ), 3.38 (dd,  $J = 15.0, 5.1$  Hz, 1H, 6- $\text{H}_b$ ), 3.94 (dd,  $J = 15.1, 6.4$  Hz, 1H, 5- $\text{CH}_a$ ), 4.20–4.31 (m, 2H, 5- $\text{CH}_b$ , 8- $\text{H}_a$ ), 4.34–4.42 (m, 1H, 7-H), 4.55 (dd,  $J = 14.4, 5.4$  Hz, 1H, 8- $\text{H}_b$ ), 5.18–5.29 (m, 2H,  $\text{CH}_2\text{-CH=CH}_2$ ), 5.55 (d,  $J = 4.2$  Hz, 1H, OH), 5.87 (ddd,  $J = 22.5, 10.8, 5.9$  Hz, 1H,  $\text{CH}_2\text{-CH=CH}_2$ ), 7.19 (s, 1H, 3-H), 7.29–7.35 (m, 1H, Ph 4-H), 7.37–7.44 (m, 2H, Ph 3,5-H),

7.81–7.88 (m, 2H, Ph 2,6-H).  $^{13}\text{C}$  NMR (101 MHz, DMSO- $d_6$ )  $\delta_{\text{C}}$  ppm: 49.6 (5-CH<sub>2</sub>), 51.3 (C-6), 55.9 (C-8), 69.3 (C-7), 105.8 (C-3), 117.8 (CH<sub>2</sub>-CH=CH<sub>2</sub>), 125.1 (Ph C-2,6), 127.8 (Ph C-4), 128.7 (Ph C-3,5), 132.5 (Ph C-1), 133.5 (CH<sub>2</sub>-CH=CH<sub>2</sub>), 139.2 (C-3a), 149.0 (C-2), 161.3 (C-4).  $^{15}\text{N}$  NMR (40 MHz, DMSO- $d_6$ )  $\delta_{\text{N}}$  ppm: −263.8 (N-5), −175.4 (N-9), −73.8 (N-1). HRMS (ESI) for C<sub>16</sub>H<sub>17</sub>N<sub>3</sub>NaO<sub>2</sub> ([M+Na]<sup>+</sup>): calcd  $m/z$  306.1213, found  $m/z$  306.1213.

5-Allyl-2-(4-fluorophenyl)-7-hydroxy-5,6,7,8-tetrahydro-4H-pyrazolo[1,5-a][1,4]diazepin-4-one **4o**

Purified by column chromatography on silica gel (*n*-hexane/ethyl acetate gradient from 7/2 to 1/9, *v/v*). White solid, mp 143–144 °C, procedure b −89% (175 mg).  $R_f$  = 0.39 (*n*-hexane/ethyl acetate 3/7, *v/v*). IR (KBr)  $\nu_{\text{max}}$ , cm<sup>−1</sup>: 3230, 2951, 2892, 1651, 1461, 1440, 933, 837, 816, 756.  $^1\text{H}$  NMR (400 MHz, DMSO- $d_6$ )  $\delta_{\text{H}}$  ppm: 3.08 (dd,  $J$  = 15.0, 7.3 Hz, 1H, 6-H<sub>a</sub>), 3.38 (dd,  $J$  = 15.0, 5.1 Hz, 1H, 6-H<sub>b</sub>), 3.94 (dd,  $J$  = 15.2, 6.3 Hz, 1H, 5-CH<sub>a</sub>), 4.19–4.32 (m, 2H, 5-CH<sub>b</sub>, 8-H<sub>a</sub>), 4.34–4.42 (m, 1H, 7-H), 4.54 (dd,  $J$  = 14.3, 5.3 Hz, 1H, 8-H<sub>b</sub>), 5.18–5.28 (m,  $J$  = 14.0 Hz, 2H, CH<sub>2</sub>-CH=CH<sub>2</sub>), 5.55 (d,  $J$  = 4.1 Hz, 1H, OH), 5.87 (dq,  $J$  = 10.9, 5.8 Hz, 1H, CH<sub>2</sub>-CH=CH<sub>2</sub>), 7.20 (s, 1H, 3-H), 7.21–7.29 (m, 2H, Ph 3,5-H), 7.84–7.92 (m, 2H, Ph 2,6-H).  $^{13}\text{C}$  NMR (101 MHz, DMSO- $d_6$ )  $\delta_{\text{C}}$  ppm: 49.6 (5-CH<sub>2</sub>), 51.3 (C-6), 55.9 (C-8), 69.3 (C-7), 105.7 (C-3), 115.59 (d,  $^2J_{\text{CF}}$  = 21.5 Hz, Ph C-3,5), 117.8 (CH<sub>2</sub>-CH=CH<sub>2</sub>), 127.10 (d,  $^3J_{\text{CF}}$  = 8.2 Hz, Ph C-2,6), 129.07 (d,  $^4J_{\text{CF}}$  = 3.0 Hz, Ph C-1), 133.5 (CH<sub>2</sub>-CH=CH<sub>2</sub>), 139.2 (C-3a), 148.1 (C-2), 161.3 (C-4), 161.83 (d,  $J_{\text{CF}}$  = 244.3 Hz, Ph C-4).  $^{15}\text{N}$  NMR (40 MHz, DMSO- $d_6$ )  $\delta_{\text{N}}$  ppm: −264.0 (N-5), −175.1 (N-9), −74.3 (N-1).  $^{19}\text{F}$  NMR (376 MHz, DMSO- $d_6$ )  $\delta_{\text{F}}$  ppm: −114.4 (Ph 6-F). HRMS (ESI) for C<sub>16</sub>H<sub>16</sub>FN<sub>3</sub>NaO<sub>2</sub> ([M+Na]<sup>+</sup>): calcd  $m/z$  324.1119, found  $m/z$  324.1119.

5-Allyl-2-(4-chlorophenyl)-7-hydroxy-5,6,7,8-tetrahydro-4H-pyrazolo[1,5-a][1,4]diazepin-4-one **4p**

Purified by column chromatography on silica gel (*n*-hexane/ethyl acetate gradient from 7/2 to 1/9, *v/v*). White solid, mp 179–180 °C, procedure b −92% (188 mg).  $R_f$  = 0.42 (*n*-hexane/ethyl acetate 3/7, *v/v*). IR (KBr)  $\nu_{\text{max}}$ , cm<sup>−1</sup>: 3363, 2939, 2891, 1620, 1470, 1091, 1053, 939, 812, 753.  $^1\text{H}$  NMR (400 MHz, DMSO- $d_6$ )  $\delta_{\text{H}}$  ppm: 3.08 (dd,  $J$  = 15.0, 7.3 Hz, 1H, 6-H<sub>a</sub>), 3.38 (dd,  $J$  = 15.0, 5.1 Hz, 1H, 6-H<sub>b</sub>), 3.94 (dd,  $J$  = 15.1, 6.3 Hz, 1H, 5-H<sub>a</sub>), 4.19–4.42 (m, 3H, 5-CH<sub>b</sub>, 7-H, 8-H<sub>a</sub>), 4.55 (dd,  $J$  = 14.4, 5.4 Hz, 1H, 8-H<sub>b</sub>), 5.19–5.29 (m, 2H, CH<sub>2</sub>-CH=CH<sub>2</sub>), 5.55 (d,  $J$  = 4.2 Hz, 1H, OH), 5.86 (ddd,  $J$  = 22.5, 10.8, 5.9 Hz, 1H, CH<sub>2</sub>-CH=CH<sub>2</sub>), 7.23 (s, 1H, 3-H), 7.43–7.51 (m, 2H, Ph 3,5-H), 7.83–7.91 (m, 2H, Ph 2,6-H).  $^{13}\text{C}$  NMR (101 MHz, DMSO- $d_6$ )  $\delta_{\text{C}}$  ppm: 49.6 (5-CH<sub>2</sub>), 51.2 (C-6), 56.0 (C-8), 69.3 (C-7), 106.0 (C-3), 117.8 (CH<sub>2</sub>-CH=CH<sub>2</sub>), 126.8 (Ph C-2,6), 128.8 (Ph C-3,5), 131.4 (Ph C-1), 132.3 (Ph C-4), 133.4 (CH<sub>2</sub>-CH=CH<sub>2</sub>), 139.3 (C-3a), 147.9 (C-2), 161.2 (C-4).  $^{15}\text{N}$  NMR (40 MHz, DMSO- $d_6$ )  $\delta_{\text{N}}$  ppm: −264.1 (N-5), −174.4 (N-9), −73.7 (N-1). HRMS (ESI) for C<sub>16</sub>H<sub>16</sub>ClN<sub>3</sub>NaO<sub>2</sub> ([M+Na]<sup>+</sup>): calcd  $m/z$  340.0823, found  $m/z$  340.0823.

5-Allyl-2-(4-bromophenyl)-7-hydroxy-5,6,7,8-tetrahydro-4H-pyrazolo[1,5-a][1,4]diazepin-4-one **4r**

Purified by column chromatography on silica gel (*n*-hexane/ethyl acetate gradient 1/9, *v/v*). White solid, mp 186–187 °C, procedure b −76% (277 mg).  $R_f$  = 0.43 (*n*-hexane/ethyl acetate 3/7, *v/v*). IR (KBr)  $\nu_{\text{max}}$ , cm<sup>−1</sup>: 3366, 2938, 1621 (C=O), 1469, 1434, 1052, 1006, 933, 811, 752.  $^1\text{H}$  NMR (400 MHz, DMSO- $d_6$ )  $\delta_{\text{H}}$  ppm: 3.08 (dd,  $J$  = 14.9, 7.3 Hz, 1H, 6-H<sub>a</sub>), 3.35–3.42 (m, 1H, 6-H<sub>b</sub>), 3.94 (dd,  $J$  = 15.1, 6.2 Hz, 1H, 5-CH<sub>a</sub>), 4.19–4.32 (m, 2H, 5-CH<sub>b</sub>, 8-H<sub>a</sub>), 4.34–4.41 (m, 1H, 7-H), 4.55 (dd,  $J$  = 14.3, 5.3 Hz, 1H, 8-H<sub>b</sub>), 5.18–5.28 (m, 2H, CH<sub>2</sub>-CH=CH<sub>2</sub>), 5.56 (d,  $J$  = 4.0 Hz, 1H, OH), 5.81–5.92 (m, 1H, CH<sub>2</sub>-CH=CH<sub>2</sub>), 7.23 (s, 1H, 3-H), 7.57–7.63 (m, 2H, Ph 3,5-H), 7.78–7.84 (m, 2H, Ph 2,6-H).  $^{13}\text{C}$  NMR (101 MHz, DMSO- $d_6$ )  $\delta_{\text{C}}$  ppm: 49.6 (5-CH<sub>2</sub>), 51.2 (C-6), 56.0 (C-8), 69.3 (C-7), 106.0 (C-3), 117.8 (CH<sub>2</sub>-CH=CH<sub>2</sub>), 120.9 (Ph C-4), 127.1 (Ph C-2,6), 131.67 (Ph C-3,5), 131.73 (Ph C-1), 133.4 (CH<sub>2</sub>-CH=CH<sub>2</sub>), 139.3 (C-3a), 147.9 (C-2), 161.2 (C-4).  $^{15}\text{N}$  NMR (40 MHz, DMSO- $d_6$ )  $\delta_{\text{N}}$  ppm: −263.2

(N-5),  $-173.1$  (N-9),  $-74.0$  (N-1). HRMS (ESI) for  $C_{16}H_{16}BrN_3NaO_2$  ( $[M+Na]^+$ ): calcd  $m/z$  384.0318, found  $m/z$  384.0318 and 386.0303.

5-Allyl-7-hydroxy-2-(4-methoxyphenyl)-5,6,7,8-tetrahydro-4H-pyrazolo[1,5-a][1,4]diazepin-4-one **4s**

Purified by column chromatography on silica gel (*n*-hexane/ethyl acetate gradient from 4/1 to 1/9, *v/v*). White solid, mp 134–135 °C, procedure b –85% (301 mg).  $R_f = 0.35$  (*n*-hexane/ethyl acetate 1.5/3.5, *v/v*). IR (KBr)  $\nu_{max}$ ,  $cm^{-1}$ : 3284, 2932, 2835, 1624 (C=O), 1467, 1285, 1061, 1026, 935, 828.  $^1H$  NMR (400 MHz, DMSO- $d_6$ )  $\delta_H$  ppm: 3.08 (dd,  $J = 15.0$ , 7.2 Hz, 1H, 6- $H_a$ ), 3.37 (dd,  $J = 14.8$ , 4.9 Hz, 1H, 6- $H_b$ ), 3.78 (s, 3H, Ph 4-OCH<sub>3</sub>), 3.94 (dd,  $J = 15.1$ , 6.4 Hz, 1H, 5-CH<sub>a</sub>), 4.20 (dd,  $J = 14.3$ , 3.8 Hz, 1H, 8- $H_a$ ), 4.28 (dd,  $J = 15.1$ , 5.3 Hz, 1H, 5-CH<sub>b</sub>), 4.33–4.40 (m, 1H, 7-H), 4.51 (dd,  $J = 14.3$ , 5.4 Hz, 1H, 8- $H_b$ ), 5.17–5.28 (m, 2H, CH<sub>2</sub>-CH=CH<sub>2</sub>), 5.54 (d,  $J = 4.2$  Hz, 1H, OH), 5.86 (ddd,  $J = 22.5$ , 10.3, 5.9 Hz, 1H, CH<sub>2</sub>-CH=CH<sub>2</sub>), 6.93–7.00 (m, 2H, Ph 3,5-H), 7.10 (s, 1H, 3-H), 7.72–7.80 (m, 2H, Ph 2,6-H).  $^{13}C$  NMR (101 MHz, DMSO- $d_6$ )  $\delta_C$  ppm: 49.6 (5-CH<sub>2</sub>), 51.3 (C-6), 55.1 (Ph 4-OCH<sub>3</sub>), 55.8 (C-8), 69.4 (C-7), 105.2 (C-3), 114.1 (Ph C-3,5), 117.8 (CH<sub>2</sub>-CH=CH<sub>2</sub>), 125.2 (Ph C-1), 126.4 (Ph C-2,6), 133.5 (CH<sub>2</sub>-CH=CH<sub>2</sub>), 139.0 (C-3a), 148.9 (C-2), 159.0 (Ph C-4), 161.4 (C-4).  $^{15}N$  NMR (40 MHz, DMSO- $d_6$ )  $\delta_N$  ppm:  $-176.8$  (N-9),  $-75.9$  (N-1). HRMS (ESI) for  $C_{17}H_{19}N_3NaO_3$  ( $[M+Na]^+$ ): calcd  $m/z$  336.1319, found  $m/z$  336.1319.

5-Benzyl-7-hydroxy-2-phenyl-5,6,7,8-tetrahydro-4H-pyrazolo[1,5-a][1,4]diazepin-4-one **4t**

Purified by column chromatography on silica gel (*n*-hexane/ethyl acetate 1/9, *v/v*). Pale yellow solid, mp 167–168 °C, procedure b –87% (138 mg).  $R_f = 0.55$  (*n*-hexane/ethyl acetate 3/7, *v/v*). IR (KBr)  $\nu_{max}$ ,  $cm^{-1}$ : 3257, 3143, 2892, 1649 (C=O), 1451, 1235, 765 and 754 (doublet), 705 and 692 (doublet).  $^1H$  NMR (400 MHz, DMSO- $d_6$ )  $\delta_H$  ppm: 3.08 (dd,  $J = 14.9$ , 7.5 Hz, 1H, 6- $H_a$ ), 3.37 (dd,  $J = 15.0$ , 5.2 Hz, 1H, 6- $H_b$ ), 4.12–4.19 (m, 1H, 7-H), 4.24 (dd,  $J = 14.4$ , 3.5 Hz, 1H, 8- $H_a$ ), 4.43–4.56 (m, 2H, 5-CH<sub>a</sub>, 8- $H_b$ ), 4.96 (d,  $J = 14.7$  Hz, 1H, 5-CH<sub>b</sub>), 5.51 (d,  $J = 4.1$  Hz, 1H, OH), 7.25 (s, 1H, 3-H), 7.29–7.35 (m, 2H, CPh 4-H, CH<sub>2</sub>Ph 4-H), 7.36–7.44 (m, 6H, CPh 3,5-H, CH<sub>2</sub>Ph 2,3,5,6-H), 7.82–7.88 (m, 2H, CPh 2,6-H).  $^{13}C$  NMR (101 MHz, DMSO- $d_6$ )  $\delta_C$  ppm: 50.3 (5-CH<sub>2</sub>), 51.3 (C-6), 55.9 (C-8), 69.3 (C-7), 105.9 (C-3), 125.1 (CPh C-2,6), 127.5 (CH<sub>2</sub>Ph C-4), 127.8 (CPh C-4), 128.1 (CH<sub>2</sub>Ph C-2,6), 128.6 (CH<sub>2</sub>Ph C-3,5), 128.7 (CPh C-3,5), 132.5 (CPh C-1), 137.5 (CH<sub>2</sub>Ph C-1), 139.0 (C-3a), 149.0 (C-2), 161.7 (C-4).  $^{15}N$  NMR (40 MHz, DMSO- $d_6$ )  $\delta_N$  ppm:  $-259.1$  (N-5),  $-176.3$  (N-9),  $-73.3$  (N-1). HRMS (ESI) for  $C_{20}H_{19}N_3NaO_2$  ( $[M+Na]^+$ ): calcd  $m/z$  356.1369, found  $m/z$  356.1370.

5-Benzyl-2-(4-fluorophenyl)-7-hydroxy-5,6,7,8-tetrahydro-4H-pyrazolo[1,5-a][1,4]diazepin-4-one **4u**

Purified by column chromatography on silica gel (*n*-hexane/ethyl acetate gradient from 4/1 to 1/9, *v/v*). Pale yellow solid, mp 192–193 °C, procedure b –70% (301 mg).  $R_f = 0.52$  (*n*-hexane/ethyl acetate 1.5/3.5, *v/v*). IR (KBr)  $\nu_{max}$ ,  $cm^{-1}$ : 3291, 3144, 2945, 1617 (C=O), 1470, 1442, 1230, 839, 701, 639.  $^1H$  NMR (400 MHz, DMSO- $d_6$ )  $\delta_H$  ppm: 3.07 (dd,  $J = 14.9$ , 7.5 Hz, 1H, 6- $H_a$ ), 3.34–3.40 (m, 1H, 6- $H_b$ ), 4.11–4.26 (m, 2H, 7-H, 8- $H_a$ ), 4.43–4.55 (m, 2H, 5-CH<sub>a</sub>, 8- $H_b$ ), 4.96 (d,  $J = 14.7$  Hz, 1H, 5-CH<sub>b</sub>), 5.50 (d,  $J = 4.0$  Hz, 1H, OH), 7.20–7.41 (m, 8H, 3-H, CPh 3,5-H, CH<sub>2</sub>Ph 2,3,4,5,6-H), 7.85–7.93 (m, 2H, CPh 2,6-H).  $^{13}C$  NMR (101 MHz, DMSO- $d_6$ )  $\delta_C$  ppm: 50.3 (5-CH<sub>2</sub>), 51.3 (C-6), 55.9 (C-8), 69.2 (C-7), 105.9 (C-3), 115.61 (d,  $^2J_{CF} = 21.5$  Hz, CPh C-3,5), 127.10 (d,  $^3J_{CF} = 8.2$  Hz, CPh C-2,6), 127.5 (CH<sub>2</sub>Ph C-4), 128.1 (CH<sub>2</sub>Ph C-2,6), 128.6 (CH<sub>2</sub>Ph C-3,5), 129.06 (d,  $^4J_{CF} = 2.8$  Hz, CPh C-1), 137.5 (CH<sub>2</sub>Ph C-1), 139.1 (C-3a), 148.2 (C-2), 161.6 (C-4), 161.84 (d,  $J_{CF} = 244.3$  Hz, CPh C-4).  $^{15}N$  NMR (40 MHz, DMSO- $d_6$ )  $\delta_N$  ppm:  $-259.9$  (N-5),  $-175.3$  (N-9),  $-74.4$  (N-1).  $^{19}F$  NMR (376 MHz, DMSO- $d_6$ )  $\delta_F$  ppm:  $-114.3$  (CPh 6-F). HRMS (ESI) for  $C_{20}H_{18}FN_3NaO_2$  ( $[M+Na]^+$ ): calcd  $m/z$  374.1275, found  $m/z$  374.1275.

5-Benzyl-2-(4-chlorophenyl)-7-hydroxy-5,6,7,8-tetrahydro-4H-pyrazolo[1,5-a]  
[1,4]diazepin-4-one **4v**

Purified by column chromatography on silica gel (*n*-hexane/ethyl acetate gradient from 7/2 to 1/9, *v/v*). White solid, mp 181–182 °C, procedure b –96% (419 mg).  $R_f = 0.57$  (*n*-hexane/ethyl acetate 3/7, *v/v*). IR (KBr)  $\nu_{\max}$ ,  $\text{cm}^{-1}$ : 3246, 2939, 1619 (C=O), 1455, 1434, 1091, 830 and 819 (doublet), 757, 699.  $^1\text{H}$  NMR (400 MHz, DMSO- $d_6$ )  $\delta_{\text{H}}$  ppm: 3.08 (dd,  $J = 14.9, 7.5$  Hz, 1H, 6- $\text{H}_a$ ), 3.37 (dd,  $J = 15.0, 5.0$  Hz, 1H, 6- $\text{H}_b$ ), 4.11–4.27 (m, 2H, 7-H, 8- $\text{H}_a$ ), 4.43–4.57 (m, 2H, 5- $\text{CH}_a$ , 8- $\text{H}_b$ ), 4.96 (d,  $J = 14.7$  Hz, 1H, 5- $\text{CH}_b$ ), 5.51 (d,  $J = 3.6$  Hz, 1H, OH), 7.28–7.41 (m, 6H, 3-H,  $\text{CH}_2\text{Ph}$  2,3,4,5,6-H), 7.44–7.50 (m, 2H, CPh 3,5-H), 7.84–7.91 (m, 2H, CPh 2,6-H).  $^{13}\text{C}$  NMR (101 MHz, DMSO- $d_6$ )  $\delta_{\text{C}}$  ppm: 50.3 (5- $\text{CH}_2$ ), 51.3 (C-6), 56.0 (C-8), 69.2 (C-7), 106.1 (C-3), 126.8 (CPh C-2,6), 127.5 ( $\text{CH}_2\text{Ph}$  C-4), 128.1 ( $\text{CH}_2\text{Ph}$  C-2,6), 128.6 ( $\text{CH}_2\text{Ph}$  C-3,5), 128.8 (CPh C-3,5), 131.4 (CPh C-1), 132.3 (CPh C-4), 137.5 ( $\text{CH}_2\text{Ph}$  C-1), 139.2 (C-3a), 147.9 (C-2), 161.6 (C-4).  $^{15}\text{N}$  NMR (40 MHz, DMSO- $d_6$ )  $\delta_{\text{N}}$  ppm: –259.6 (N-5), –174.8 (N-9), –73.4 (N-1). HRMS (ESI) for  $\text{C}_{20}\text{H}_{18}\text{ClN}_3\text{NaO}_2$  ( $[\text{M}+\text{Na}]^+$ ): calcd  $m/z$  390.0980, found  $m/z$  390.0980.

5-Benzyl-2-(4-bromophenyl)-7-hydroxy-5,6,7,8-tetrahydro-4H-pyrazolo[1,5-a]  
[1,4]diazepin-4-one **4w**

Purified by column chromatography on silica gel (*n*-hexane/ethyl acetate 1/9, *v/v*). Pale yellow solid, mp 157–158 °C, procedure b –72% (287 mg).  $R_f = 0.57$  (*n*-hexane/ethyl acetate 3/7, *v/v*). IR (KBr)  $\nu_{\max}$ ,  $\text{cm}^{-1}$ : 3270, 1619 (C=O), 1460, 1429, 1247, 1068, 1009, 816, 756, 701.  $^1\text{H}$  NMR (400 MHz, DMSO- $d_6$ )  $\delta_{\text{H}}$  ppm: 3.08 (dd,  $J = 14.9, 7.6$  Hz, 1H, 6- $\text{H}_a$ ), 3.34–3.41 (m, 1H, 6- $\text{H}_b$ ), 4.12–4.18 (m, 1H, 7-H), 4.20–4.27 (m, 1H, 8- $\text{H}_a$ ), 4.46 (d,  $J = 14.7$  Hz, 1H, 5- $\text{CH}_a$ ), 4.52 (dd,  $J = 14.4, 5.3$  Hz, 1H, 8- $\text{H}_b$ ), 4.96 (d,  $J = 14.7$  Hz, 1H, 5- $\text{CH}_b$ ), 5.51 (d,  $J = 4.1$  Hz, 1H, OH), 7.28–7.34 (m, 2H, 3-H,  $\text{CH}_2\text{Ph}$  4-H), 7.35–7.39 (m, 4H,  $\text{CH}_2\text{Ph}$  2,3,5,6-H), 7.56–7.64 (m, 2H, CPh 3,5-H), 7.78–7.85 (m, 2H, CPh 2,6-H).  $^{13}\text{C}$  NMR (101 MHz, DMSO- $d_6$ )  $\delta_{\text{C}}$  ppm: 50.4 (5- $\text{CH}_2$ ), 51.3 (C-6), 56.0 (C-8), 69.2 (C-7), 106.1 (C-3), 120.9 (CPh C-4), 127.1 (CPh C-2,6), 127.5 ( $\text{CH}_2\text{Ph}$  C-4), 128.2 ( $\text{CH}_2\text{Ph}$  C-3,5), 128.6 ( $\text{CH}_2\text{Ph}$  C-2,6), 131.68 (CPh C-3,5), 131.72 (CPh C-1), 137.5 ( $\text{CH}_2\text{Ph}$  C-1), 139.2 (C-3a), 148.0 (C-2), 161.6 (C-4).  $^{15}\text{N}$  NMR (40 MHz, DMSO- $d_6$ )  $\delta_{\text{N}}$  ppm: –259.5 (N-5), –174.5 (N-9), –73.7 (N-1). HRMS (ESI) for  $\text{C}_{20}\text{H}_{18}\text{BrN}_3\text{NaO}_2$  ( $[\text{M}+\text{Na}]^+$ ): calcd  $m/z$  434.0475, found  $m/z$  434.0475 and 436.0445.

5-Benzyl-7-hydroxy-2-(4-methoxyphenyl)-5,6,7,8-tetrahydro-4H-pyrazolo[1,5-a]  
[1,4]diazepin-4-one **4x**

Purified by column chromatography on silica gel (*n*-hexane/ethyl acetate gradient from 3.5/1 to 1/9, *v/v*). White solid, mp 179–180 °C, procedure b –72% (313 mg).  $R_f = 0.46$  (*n*-hexane/ethyl acetate 1.5/3.5, *v/v*). IR (KBr)  $\nu_{\max}$ ,  $\text{cm}^{-1}$ : 3204, 1651 (C=O), 1462, 1436, 1250, 1180, 1029, 833, 753, 705.  $^1\text{H}$  NMR (400 MHz, DMSO- $d_6$ )  $\delta_{\text{H}}$  ppm: 3.07 (dd,  $J = 14.9, 7.5$  Hz, 1H, 6- $\text{H}_a$ ), 3.36–3.40 (m, 1H, 6- $\text{H}_b$ ), 3.78 (s, 3H, - $\text{OCH}_3$ ), 4.11–4.24 (m, 2H, 7-H, 8- $\text{H}_a$ ), 4.42–4.53 (m, 2H, 5- $\text{CH}_a$ , 8- $\text{H}_b$ ), 4.96 (d,  $J = 14.7$  Hz, 1H, 5- $\text{CH}_b$ ), 5.50 (s, 1H, OH), 6.94–7.00 (m, 2H, CPh 3,5-H), 7.15 (s, 1H, 3-H), 7.28–7.34 (m, 1H,  $\text{CH}_2\text{Ph}$  4-H), 7.35–7.41 (m, 4H,  $\text{CH}_2\text{Ph}$  2,3,5,6-H), 7.74–7.81 (m, 2H, CPh 2,6-H).  $^{13}\text{C}$  NMR (101 MHz, DMSO- $d_6$ )  $\delta_{\text{C}}$  ppm: 50.4 (5- $\text{CH}_2$ ), 51.4 (C-6), 55.1 ( $\text{OCH}_3$ ), 55.8 (C-8), 69.3 (C-7), 105.3 (C-3), 114.1 (CPh C-3,5), 125.1 (CPh C-1), 126.4 (CPh C-2,6), 127.5 ( $\text{CH}_2\text{Ph}$  C-4), 128.1 ( $\text{CH}_2\text{Ph}$  C-2,6), 128.6 ( $\text{CH}_2\text{Ph}$  C-3,5), 137.6 ( $\text{CH}_2\text{Ph}$  C-1), 138.9 (C-3a), 149.0 (C-2), 159.0 (CPh C-4), 161.8 (C-4).  $^{15}\text{N}$  NMR (40 MHz, DMSO- $d_6$ )  $\delta_{\text{N}}$  ppm: –258.9 (N-5), –176.9 (N-9), –75.4 (N-1). HRMS (ESI) for  $\text{C}_{21}\text{H}_{21}\text{N}_3\text{NaO}_3$  ( $[\text{M}+\text{Na}]^+$ ): calcd  $m/z$  386.1475, found  $m/z$  386.1475.

3.2.4. Synthesis of Ethyl 1-(oxiran-2-ylmethyl)-1H-indole-2-carboxylates (**6a–e**) and Ethyl 1-(oxiran-2-ylmethyl)-1H-benzo[*d*]imidazole-2-carboxylate (**6f**)

**Procedure a.** Indole-2-carboxylate **5a–e** (1 eq) was dissolved in dry dimethyl formamide (0.2 M) and KOH (3 eq; flakes) was added followed by 2-(chloromethyl)oxirane (1.5 eq). The reaction mixture was stirred at 40 °C for 1 h under argon atmosphere. Upon completion, the mixture was concentrated to approximately 1/3 volume, diluted with

ethyl acetate, and washed with brine. Organic layer was separated, dried over anhydrous  $\text{Na}_2\text{SO}_4$ , filtered, and concentrated under reduced pressure. The residue was purified by column chromatography.

**Procedure b.** Benzimidazole-2-carboxylate **5f** (1 eq) was dissolved in dry dimethyl formamide (0.3 M) and NaH (1.5 eq; 60% dispersion in mineral oil) was added followed by 2-(chloromethyl)oxirane (1.5 eq). The reaction mixture was stirred at 60 °C for 4 h. Upon completion, the reaction mixture was cooled to 0 °C, quenched with water and extracted with ethyl acetate. The combined organic phases were washed with brine, dried over anhydrous  $\text{Na}_2\text{SO}_4$ , filtered, and concentrated under reduced pressure. The residue was purified by column chromatography.

#### Ethyl 1-(oxiran-2-ylmethyl)-1*H*-indole-2-carboxylate **6a**

Purified by column chromatography on silica gel (*n*-hexane/ethyl acetate 8/1, *v/v*). White solid, mp 47–49 °C, procedure a –73% (94 mg).  $R_f = 0.29$  (*n*-hexane/ethyl acetate 6/1, *v/v*). IR (KBr)  $\nu_{\text{max}}$ ,  $\text{cm}^{-1}$ : 3064, 2974, 2928, 1713 (C=O), 1408, 1265, 1205, 1140, 1096, 744.  $^1\text{H}$  NMR (400 MHz,  $\text{CDCl}_3$ )  $\delta_{\text{H}}$  ppm: 1.41 (t,  $J = 7.1$  Hz, 3H,  $\text{CH}_3$ ), 2.49–2.53 (m, 1H, Ox  $\text{CH}_a\text{H}_b$ ), 2.77 (t,  $J = 4.2$  Hz, 1H, Ox  $\text{CH}_a\text{H}_b$ ), 3.33–3.39 (m, 1H, Ox CH), 4.38 (q,  $J = 7.1$  Hz, 2H,  $\text{CH}_2\text{CH}_3$ ), 4.56 (dd,  $J = 15.1, 5.0$  Hz, 1H,  $\text{NCH}_a\text{H}_b$ ), 5.03 (dd,  $J = 15.1, 2.4$  Hz, 1H,  $\text{NCH}_a\text{H}_b$ ), 7.14–7.18 (m, 1H, 5-H), 7.34–7.37 (m, 2H, 3-H, 6-H), 7.45–7.47 (m, 1H, 7-H), 7.66–7.68 (m, 1H, 4-H).  $^{13}\text{C}$  NMR (101 MHz,  $\text{CDCl}_3$ )  $\delta_{\text{C}}$  ppm: 14.5 ( $\text{CH}_3$ ), 45.5 (Ox  $\text{CH}_a\text{H}_b$ ), 46.2 ( $\text{NCH}_a\text{H}_b$ ), 51.6 (Ox CH), 60.8 ( $\text{CH}_2\text{CH}_3$ ), 110.9 (C-7), 111.1 (C-3), 121.1 (C-5), 122.7 (C-4), 125.5 (C-6), 126.1 (C-3a), 127.7 (C-2), 140.0 (C-7a), 162.3 (COO).  $^{15}\text{N}$  NMR (40 MHz,  $\text{CDCl}_3$ )  $\delta_{\text{N}}$  ppm: –250.9 (N). HRMS (ESI) for  $\text{C}_{14}\text{H}_{16}\text{NO}_3$  ( $[\text{M}+\text{H}]^+$ ): calcd  $m/z$  246.1125, found  $m/z$  246.1119.

#### Ethyl 5-fluoro-1-(oxiran-2-ylmethyl)-1*H*-indole-2-carboxylate **6b**

Purified by column chromatography on silica gel (*n*-hexane/ethyl acetate 8/1, *v/v*). White solid, mp 65–66 °C, procedure a –39% (50 mg).  $R_f = 0.19$  (*n*-hexane/ethyl acetate 6/1, *v/v*). IR (KBr)  $\nu_{\text{max}}$ ,  $\text{cm}^{-1}$ : 2974, 2930, 1713 (C=O), 1527, 1266, 1246, 1177, 1091, 756.  $^1\text{H}$  NMR (400 MHz,  $\text{CDCl}_3$ )  $\delta_{\text{H}}$  ppm: 1.41 (t,  $J = 7.1$  Hz, 3H,  $\text{CH}_3$ ), 2.45–2.53 (m, 1H, Ox  $\text{CH}_a\text{H}_b$ ), 2.79 (t,  $J = 4.2$  Hz, 1H, Ox  $\text{CH}_a\text{H}_b$ ), 3.32–3.40 (m, 1H, Ox CH), 4.38 (q,  $J = 7.1$  Hz, 2H,  $\text{CH}_2\text{CH}_3$ ), 4.47 (dd,  $J = 15.2, 5.3$  Hz, 1H,  $\text{NCH}_a\text{H}_b$ ), 5.08 (dd,  $J = 15.2, 2.4$  Hz, 1H,  $\text{NCH}_a\text{H}_b$ ), 7.07–7.15 (m, 1H, 6-H), 7.24–7.33 (m, 2H, 3-H, 7-H), 7.38–7.45 (m, 1H, 4-H).  $^{13}\text{C}$  NMR (101 MHz,  $\text{CDCl}_3$ )  $\delta_{\text{C}}$  ppm: 14.5 ( $\text{CH}_3$ ), 45.3 (Ox  $\text{CH}_a\text{H}_b$ ), 46.6 ( $\text{NCH}_a\text{H}_b$ ), 51.7 (Ox CH), 61.0 ( $\text{CH}_2\text{CH}_3$ ), 106.7 (d,  $J = 23.2$  Hz, C-7), 110.7 (d,  $J = 5.1$  Hz, C-3), 112.1 (d,  $J = 10.1$  Hz, C-4), 114.6 (d,  $J = 27.3$  Hz, C-6), 126.1 (d,  $J = 11.1$  Hz, C-3a), 129.0 (C-2), 136.7 (C-7a), 158.4 (d,  $J = 238.4$  Hz, C-5), 162.0 (COO).  $^{15}\text{N}$  NMR (40 MHz,  $\text{CDCl}_3$ )  $\delta_{\text{N}}$  ppm: –250.9 (N).  $^{19}\text{F}$  NMR (376 MHz,  $\text{DMSO}-d_6$ )  $\delta_{\text{F}}$  ppm: –127.7 (F). HRMS (ESI) for  $\text{C}_{14}\text{H}_{15}\text{FNO}_3$  ( $[\text{M}+\text{H}]^+$ ): calcd  $m/z$  264.1030, found  $m/z$  264.1031.

#### Ethyl 5-chloro-1-(oxiran-2-ylmethyl)-1*H*-indole-2-carboxylate **6c**

Purified by column chromatography on silica gel (*n*-hexane/ethyl acetate 8/1, *v/v*). White solid, mp 79–80 °C, procedure a –69% (72 mg).  $R_f = 0.23$  (*n*-hexane/ethyl acetate 6/1, *v/v*). IR (KBr)  $\nu_{\text{max}}$ ,  $\text{cm}^{-1}$ : 2984, 2928, 1703 (C=O), 1517, 1457, 1252, 1199, 763.  $^1\text{H}$  NMR (400 MHz,  $\text{CDCl}_3$ )  $\delta_{\text{H}}$  ppm: 1.42 (t,  $J = 7.1$  Hz, 3H,  $\text{CH}_3$ ), 2.48 (dd,  $J = 4.4, 2.6$  Hz, 1H, Ox  $\text{CH}_a\text{H}_b$ ), 2.78 (t,  $J = 4.3$  Hz, 1H, Ox  $\text{CH}_a\text{H}_b$ ), 3.32–3.38 (m, 1H, Ox CH), 4.38 (q,  $J = 7.1$  Hz, 2H,  $\text{CH}_2\text{CH}_3$ ), 4.47 (dd,  $J = 15.2, 5.4$  Hz, 1H,  $\text{NCH}_a\text{H}_b$ ), 5.07 (dd,  $J = 15.2, 2.6$  Hz, 1H,  $\text{NCH}_a\text{H}_b$ ), 7.25–7.26 (m, 1H, 3-H), 7.28–7.30 (m, 1H, 6-H), 7.39–7.41 (m, 1H, 7-H), 7.62–7.63 (m, 1H, 4-H).  $^{13}\text{C}$  NMR (101 MHz,  $\text{CDCl}_3$ )  $\delta_{\text{C}}$  ppm: 14.5 ( $\text{CH}_3$ ), 45.3 (Ox  $\text{CH}_a\text{H}_b$ ), 46.5 ( $\text{NCH}_a\text{H}_b$ ), 51.6 (Ox CH), 61.1 ( $\text{CH}_2\text{CH}_3$ ), 110.3 (C-3), 112.3 (C-7), 121.7 (C-4), 125.9 (C-6), 126.8 (C-5), 126.9 (C-3a), 128.8 (C-2), 138.3 (C-7a), 162.0 (COO).  $^{15}\text{N}$  NMR (40 MHz,  $\text{CDCl}_3$ )  $\delta_{\text{N}}$  ppm: –250.0 (N). HRMS (ESI) for  $\text{C}_{14}\text{H}_{15}\text{ClNO}_3$  ( $[\text{M}+\text{H}]^+$ ): calcd  $m/z$  280.0735, found  $m/z$  280.0733.



Ethyl 5-methyl-1-(oxiran-2-ylmethyl)-1H-indole-2-carboxylate **6d**

Purified by column chromatography on silica gel (*n*-hexane/ethyl acetate 8/1, *v/v*). White solid, mp 72–74 °C, procedure a –75% (96 mg).  $R_f = 0.27$  (*n*-hexane/ethyl acetate 6/1, *v/v*). IR (KBr)  $\nu_{\max}$ ,  $\text{cm}^{-1}$ : 2976, 1706 (C=O), 1408, 1263, 1211, 1128, 1096, 763.  $^1\text{H}$  NMR (400 MHz,  $\text{CDCl}_3$ )  $\delta_{\text{H}}$  ppm: 1.41 (t,  $J = 7.1$  Hz, 3H,  $\text{CH}_2\text{CH}_3$ ), 2.44 (s, 3H, 5- $\text{CH}_3$ ), 2.49 (dd,  $J = 4.4, 2.6$  Hz, 1H, Ox  $\text{CH}_a\text{H}_b$ ), 2.76 (t,  $J = 4.4$  Hz, 1H, Ox  $\text{CH}_a\text{H}_b$ ), 3.32–3.37 (m, 1H, Ox CH), 4.37 (q,  $J = 7.1$  Hz, 2H,  $\text{CH}_2\text{CH}_3$ ), 4.55 (dd,  $J = 15.1, 5.0$  Hz, 1H,  $\text{NCH}_a\text{H}_b$ ), 4.99 (dd,  $J = 15.1, 3.2$  Hz, 1H,  $\text{NCH}_a\text{H}_b$ ), 7.16–7.20 (m, 1H, 6-H), 7.22–7.27 (m, 1H, 3-H), 7.33–7.37 (m, 1H, 7-H), 7.42–7.48 (m, 1H, 4-H).  $^{13}\text{C}$  NMR (101 MHz,  $\text{CDCl}_3$ )  $\delta_{\text{C}}$  ppm: 14.5 ( $\text{CH}_2\text{CH}_3$ ), 21.5 (5- $\text{CH}_3$ ), 45.5 (Ox  $\text{CH}_a\text{H}_b$ ), 46.2 ( $\text{NCH}_a\text{H}_b$ ), 51.7 (Ox CH), 60.7 ( $\text{CH}_2\text{CH}_3$ ), 110.59 (C-7), 110.62 (C-3), 121.9 (C-4), 126.3 (C-3a), 127.5 (C-6), 127.6 (C-2), 130.4 (C-5), 138.5 (C-7a), 162.3 (COO).  $^{15}\text{N}$  NMR (40 MHz,  $\text{CDCl}_3$ )  $\delta_{\text{N}}$  ppm: –251.8 (N). HRMS (ESI) for  $\text{C}_{15}\text{H}_{18}\text{NO}_3$  ( $[\text{M}+\text{H}]^+$ ): calcd  $m/z$  260.1281, found  $m/z$  260.1277.

Ethyl 3-methyl-1-(oxiran-2-ylmethyl)-1H-indole-2-carboxylate **6e**

Purified by column chromatography on silica gel (petroleum ether/ethyl acetate gradient from 9/1 to 8/1, *v/v*). Colorless liquid, procedure a –47% (60 mg).  $R_f = 0.14$  (petroleum ether/ethyl acetate 10/1, *v/v*). IR (KBr)  $\nu_{\max}$ ,  $\text{cm}^{-1}$ : 1698 (C=O), 1273, 1250, 1208, 1129, 1111, 741.  $^1\text{H}$  NMR (500 MHz,  $\text{CDCl}_3$ )  $\delta_{\text{H}}$  ppm: 1.44 (t,  $J = 7.2$  Hz, 3H,  $\text{CH}_2\text{CH}_3$ ), 2.49 (dd,  $J = 4.9, 2.8$  Hz, 1H, Ox  $\text{CH}_a\text{H}_b$ ), 2.59 (s, 3H, 5- $\text{CH}_3$ ), 2.74–2.77 (m, 1H, Ox  $\text{CH}_a\text{H}_b$ ), 3.33–3.37 (m, 1H, Ox CH), 4.42 (q,  $J = 7.1$  Hz, 2H,  $\text{CH}_2\text{CH}_3$ ), 4.50 (dd,  $J = 15.3, 5.2$  Hz, 1H,  $\text{NCH}_a\text{H}_b$ ), 4.94 (dd,  $J = 15.3, 3.4$  Hz,  $\text{NCH}_a\text{H}_b$ ), 7.13–7.17 (m, 1H, 5-H), 7.33–7.37 (m, 1H, 6-H), 7.39–7.43 (m, 1H, 7-H), 7.64–7.69 (m, 1H, 4-H).  $^{13}\text{C}$  NMR (125 MHz,  $\text{CDCl}_3$ )  $\delta_{\text{C}}$  ppm: 11.0 (3- $\text{CH}_3$ ), 14.5 ( $\text{CH}_2\text{CH}_3$ ), 45.4 (Ox  $\text{CH}_a\text{H}_b$ ), 46.4 ( $\text{NCH}_a\text{H}_b$ ), 51.8 (Ox CH), 60.6 ( $\text{CH}_2\text{CH}_3$ ), 110.6 (C-7), 120.2 (C-5), 120.8 (C-4), 121.5 (C<sub>q</sub>), 124.6 (C<sub>q</sub>), 125.7 (C-6), 127.4 (C<sub>q</sub>), 139.1 (C<sub>q</sub>), 163.2 (COO).  $^{15}\text{N}$  NMR (40 MHz,  $\text{CDCl}_3$ )  $\delta_{\text{N}}$  ppm: –254.7 (N). HRMS (ESI) for  $\text{C}_{15}\text{H}_{18}\text{NO}_3$  ( $[\text{M}+\text{H}]^+$ ): calcd  $m/z$  260.1281, found  $m/z$  260.1276.

Ethyl 1-(oxiran-2-ylmethyl)-1H-benzo[d]imidazole-2-carboxylate **6f**

Purified by column chromatography on silica gel (petroleum ether/ethyl acetate gradient from 1/1 to 2/3, *v/v*). White solid, mp 49–52 °C, procedure b –33% (86 mg).  $R_f = 0.37$  (petroleum ether/ethyl acetate 1/1, *v/v*). IR (KBr)  $\nu_{\max}$ ,  $\text{cm}^{-1}$ : 2360, 2341, 1709 (C=O), 1494, 1457, 1410, 1338, 1283, 1202, 1138, 743.  $^1\text{H}$  NMR (500 MHz,  $\text{DMSO}-d_6$ )  $\delta_{\text{H}}$  ppm: 1.34 (t,  $J = 7.2$  Hz, 3H,  $\text{CH}_3$ ), 2.42–2.45 (m, 1H, Ox  $\text{CH}_a\text{H}_b$ ), 2.72 (t,  $J = 4.4$  Hz, Ox  $\text{CH}_a\text{H}_b$ ), 3.33–3.38 (m, 1H, Ox CH), 4.37 (q,  $J = 7.1$  Hz, 2H,  $\text{CH}_2\text{CH}_3$ ), 4.58 (dd,  $J = 15.1, 8.7$  Hz, 1H,  $\text{NCH}_a\text{H}_b$ ), 5.03 (dd,  $J = 15.3, 3.1$  Hz,  $\text{NCH}_a\text{H}_b$ ), 7.29–7.34 (m, 1H, 5-H), 7.37–7.42 (m, 1H, 6-H), 7.69–7.72 (m, 1H, 7-H), 7.74–7.78 (m, 1H, 4-H).  $^{13}\text{C}$  NMR (125 MHz,  $\text{DMSO}-d_6$ )  $\delta_{\text{C}}$  ppm: 14.5 ( $\text{CH}_3$ ), 45.2 (Ox  $\text{CH}_a\text{H}_b$ ), 46.8 ( $\text{NCH}_a\text{H}_b$ ), 50.9 (Ox CH), 62.2 ( $\text{CH}_2\text{CH}_3$ ), 112.5 (C-7), 121.4 (C-4), 124.0 (C-5), 125.7 (C-6), 136.8 (C<sub>q</sub>), 141.5 (C<sub>q</sub>), 141.6 (C<sub>q</sub>), 160.1 (COO).  $^{15}\text{N}$  NMR (40 MHz,  $\text{DMSO}-d_6$ )  $\delta_{\text{N}}$  ppm: –229.8 (N). HRMS (ESI) for  $\text{C}_{13}\text{H}_{14}\text{N}_2\text{O}_3$  ( $[\text{M}+\text{H}]^+$ ): calcd  $m/z$  247.1077, found  $m/z$  247.1071.

3.2.5. Synthesis of 4-Hydroxy-2,3,4,5-tetrahydro-1H-[1,4]diazepino[1,2-*a*]indol-1-ones (**7a–f**) and 4-Hydroxy-2,3,4,5-tetrahydro-1H-benzo[4,5]imidazo[1,2-*a*][1,4]diazepin-1-one (**7g**)

**Procedure a.** Ethyl 1-(oxiran-2-ylmethyl)-1H-indole-2-carboxylate **6a–e** or ethyl 1-(oxiran-2-ylmethyl)-1H-benzo[*d*]imidazole-2-carboxylate **6f** (1 eq) was dissolved in 7M ammonia (100 eq) solution in methanol, sealed in a pressure tube and stirred at 70 °C for 18 h. After completion, the reaction mixture was cooled to 0 °C, quenched with water and extracted with ethyl acetate. The combined organic phases were washed with brine, dried over anhydrous  $\text{Na}_2\text{SO}_4$ , filtered, and concentrated under reduced pressure. The residue was purified by column chromatography.

**Procedure b.** To a solution of ethyl 1-(oxiran-2-ylmethyl)-1H-indole-2-carboxylate **7a** (1eq) in methanol (5 M) benzylamine (3 eq) was added, the reaction mixture was sealed in a pressure tube and stirred at 70 °C for 18 h. After completion, the reaction mixture

was poured into water and extracted with ethyl acetate. The combined organic phases were washed with brine, dried over anhydrous  $\text{Na}_2\text{SO}_4$ , filtered, and concentrated under reduced pressure. The residue was purified by column chromatography.

#### 4-Hydroxy-2,3,4,5-tetrahydro-1*H*-[1,4]diazepino[1,2-*a*]indol-1-one **7a**

Purified by column chromatography on silica gel (dichloromethane/methanol 100/5, *v/v*). White solid, decomp. 216 °C, procedure a –93% (82 mg).  $R_f = 0.45$  (dichloromethane/methanol 9/1, *v/v*). IR (KBr)  $\nu_{\text{max}}$ ,  $\text{cm}^{-1}$ : 3318, 3194, 3049, 2895, 1660 (C=O), 1643 (C=O), 1549, 1461, 1407, 740.  $^1\text{H}$  NMR (400 MHz,  $\text{DMSO-}d_6$ )  $\delta_{\text{H}}$  ppm: 2.83 (dt,  $J = 12.0, 5.6$  Hz, 1H, 3- $\text{H}_a$ ), 3.21 (dt,  $J = 11.3, 5.4$  Hz, 1H, 3- $\text{H}_b$ ), 4.18–4.28 (m, 2H, 5- $\text{H}_a$ , 4-H), 4.42 (dd,  $J = 13.9, 4.1$  Hz, 1H, 5- $\text{H}_b$ ), 5.37 (d,  $J = 3.8$  Hz, 1H, OH), 6.93 (s, 1H, 11-H), 7.06–7.10 (m, 1H, 9-H), 7.25–7.29 (m, 1H, 8-H), 7.55–7.57 (m, 1H, 7-H), 7.62–7.64 (m, 1H, 10-H), 8.08–8.10 (m, 1H, NH).  $^{13}\text{C}$  NMR (101 MHz,  $\text{DMSO-}d_6$ )  $\delta_{\text{C}}$  ppm: 45.6 (C-3), 48.2 (C-5), 69.5 (C-4), 105.3 (C-11), 110.5 (C-7), 119.9 (C-9), 121.6 (C-10), 123.5 (C-8), 126.0 (C-10a), 134.7 (C-11a), 137.5 (C-6a), 165.5 (C-1).  $^{15}\text{N}$  NMR (40 MHz,  $\text{DMSO-}d_6$ )  $\delta_{\text{N}}$  ppm: –272.6 (N-2), –249.8 (N-6). HRMS (ESI) for  $\text{C}_{12}\text{H}_{13}\text{N}_2\text{O}_2$  ( $[\text{M}+\text{H}]^+$ ): calcd  $m/z$  217.0972, found  $m/z$  217.0969.

#### 9-Fluoro-4-hydroxy-2,3,4,5-tetrahydro-1*H*-[1,4]diazepino[1,2-*a*]indol-1-one **7b**

Purified by column chromatography on silica gel (dichloromethane/methanol 100/5, *v/v*). White solid, decomp. 220 °C, procedure a –63% (56 mg).  $R_f = 0.55$  (dichloromethane/methanol 9/1, *v/v*). IR (KBr)  $\nu_{\text{max}}$ ,  $\text{cm}^{-1}$ : 3335, 3283, 3200, 3047, 1647 (C=O), 1548, 1408, 1203, 796.  $^1\text{H}$  NMR (400 MHz,  $\text{DMSO-}d_6$ )  $\delta_{\text{H}}$  ppm: 2.78–2.87 (m, 1H, 3- $\text{H}_a$ ), 3.16–3.26 (m, 1H, 3- $\text{H}_b$ ), 4.16–4.30 (m, 2H, 5- $\text{H}_a$ , 4-H), 4.43 (dd,  $J = 14.0, 4.2$  Hz, 1H, 5- $\text{H}_b$ ), 5.38 (d,  $J = 4.0$  Hz, 1H, OH), 6.91 (s, 1H, 11-H), 7.08–7.19 (m, 1H, 8-H), 7.36–7.43 (m, 1H, 10-H), 7.56–7.63 (m, 1H, 7-H), 8.12–8.20 (m, 1H, NH).  $^{13}\text{C}$  NMR (101 MHz,  $\text{DMSO-}d_6$ )  $\delta_{\text{C}}$  ppm: 45.6 (C-3), 48.5 (C-5), 69.5 (C-4), 105.0 (d,  $^4J_{\text{CF}} = 5.1$  Hz, C-11), 105.8 (d,  $^2J_{\text{CF}} = 23.3$  Hz, C-10), 111.9 (d,  $^3J_{\text{CF}} = 9.8$  Hz, C-7), 112.1 (d,  $^2J_{\text{CF}} = 26.6$  Hz, C-8), 126.1 (d,  $^3J_{\text{CF}} = 10.6$  Hz, C-10a), 134.2 (C-6a), 136.3 (C-11a), 157.2 (d,  $J_{\text{CF}} = 233.1$  Hz, C-9), 165.2 (C-1).  $^{15}\text{N}$  NMR (40 MHz,  $\text{DMSO-}d_6$ )  $\delta_{\text{N}}$  ppm: –271.8 (N-2), –250.1 (N-6). HRMS (ESI) for  $\text{C}_{12}\text{H}_{12}\text{FN}_2\text{O}_2$  ( $[\text{M}+\text{H}]^+$ ): calcd  $m/z$  235.0877, found  $m/z$  235.0876.

#### 9-Chloro-4-hydroxy-2,3,4,5-tetrahydro-1*H*-[1,4]diazepino[1,2-*a*]indol-1-one **7c**

Purified by column chromatography on silica gel (dichloromethane/methanol 100/5, *v/v*). White solid, decomp. 210 °C, procedure a –84% (75 mg).  $R_f = 0.52$  (dichloromethane/methanol 9/1, *v/v*). IR (KBr)  $\nu_{\text{max}}$ ,  $\text{cm}^{-1}$ : 3325, 3275, 3191, 3046, 1660 (C=O), 1643 (C=O), 1545, 1408, 797.  $^1\text{H}$  NMR (400 MHz,  $\text{DMSO-}d_6$ )  $\delta_{\text{H}}$  ppm: 2.86–2.75 (m, 1H, 3- $\text{H}_a$ ), 3.27–3.14 (m, 1H, 3- $\text{H}_b$ ), 4.29–4.16 (m, 2H, 4-H, 5- $\text{H}_a$ ), 4.43 (dd,  $J = 13.8, 3.9$  Hz, 1H, 5- $\text{H}_b$ ), 5.39 (d,  $J = 3.8$  Hz, 1H, OH), 6.91 (s, 1H, 11-H), 7.24–7.31 (m, 1H, 8-H), 7.57–7.65 (m, 1H, 7-H), 7.68–7.73 (m, 1H, 10-H), 8.14–8.22 (m, 1H, NH).  $^{13}\text{C}$  NMR (101 MHz,  $\text{DMSO-}d_6$ )  $\delta_{\text{C}}$  ppm: 45.5 (C-3), 48.5 (C-5), 69.4 (C-4), 104.7 (C-11), 112.3 (7-C), 120.6 (C-10), 123.5 (C-8), 124.4 (C-9), 127.0 (C-10a), 135.9 (C-6a), 136.1 (C-11a), 165.1 (C-1).  $^{15}\text{N}$  NMR (40 MHz,  $\text{DMSO-}d_6$ )  $\delta_{\text{N}}$  ppm: –271.5 (N-2), –248.7 (N-6). HRMS (ESI) for  $\text{C}_{12}\text{H}_{12}\text{ClN}_2\text{O}_2$  ( $[\text{M}+\text{H}]^+$ ): calcd  $m/z$  251.0582, found  $m/z$  251.0580.

#### 4-Hydroxy-9-methyl-2,3,4,5-tetrahydro-1*H*-[1,4]diazepino[1,2-*a*]indol-1-one **7d**

Purified by column chromatography on silica gel (dichloromethane/methanol 100/5, *v/v*). White solid, decomp. 225 °C, procedure a –86% (76 mg).  $R_f = 0.66$  (dichloromethane/methanol 9/1, *v/v*). IR (KBr)  $\nu_{\text{max}}$ ,  $\text{cm}^{-1}$ : 3319, 3194, 3046, 1659 (C=O), 1640 (C=O), 1552, 1463, 1407, 790.  $^1\text{H}$  NMR (400 MHz,  $\text{DMSO-}d_6$ )  $\delta_{\text{H}}$  ppm: 2.38 (s, 3H,  $\text{CH}_3$ ), 2.78–2.87 (m, 1H, 3- $\text{H}_a$ ), 3.15–3.24 (m, 1H, 3- $\text{H}_b$ ), 4.16 (dd,  $J = 14.3, 4.3$  Hz, 1H, 5- $\text{H}_a$ ), 4.20–4.27 (m, 1H, 4-H), 4.38 (dd,  $J = 14.2, 4.7$  Hz, 1H, 5- $\text{H}_b$ ), 5.35 (d,  $J = 4.1$  Hz, 1H, OH), 6.83 (s, 1H, 11-H), 7.06–7.14 (m, 1H, 8-H), 7.37–7.42 (m, 1H, 10-H), 7.41–7.47 (m, 1H, 7-H), 8.02–8.09 (m, 1H, NH).  $^{13}\text{C}$  NMR (101 MHz,  $\text{DMSO-}d_6$ )  $\delta_{\text{C}}$  ppm: 21.0 ( $\text{CH}_3$ ), 45.7 (C-3), 48.3 (C-5), 69.6 (C-4), 104.8 (C-11), 110.2 (C-7), 120.9 (C-10), 125.3 (C-8), 126.2 (C-9), 128.5 (C-10a), 134.6 (C-11a),

136.0 (C-6a), 165.6 (C-1).  $^{15}\text{N}$  NMR (40 MHz, DMSO- $d_6$ )  $\delta_{\text{N}}$  ppm: -273.1 (N-2), -250.9 (N-6).  $^{19}\text{F}$  NMR (376 MHz, DMSO- $d_6$ )  $\delta_{\text{F}}$  ppm: -123.9 (F). HRMS (ESI) for  $\text{C}_{13}\text{H}_{15}\text{N}_2\text{O}_2$  ( $[\text{M}+\text{H}]^+$ ): calcd  $m/z$  231.1128, found  $m/z$  231.1124.

#### 4-Hydroxy-11-methyl-2,3,4,5-tetrahydro-1H-[1,4]diazepino[1,2-a]indol-1-one **7e**

Purified by column chromatography on silica gel (petroleum ether/ethyl acetate/methanol gradient from 1/3/0 to 5/20/1,  $v/v/v$ ). White solid, decomp. 218 °C, procedure a -66% (66 mg).  $R_f = 0.42$  (ethyl acetate/methanol 10/1,  $v/v$ ). IR (KBr)  $\nu_{\text{max}}$ ,  $\text{cm}^{-1}$ : 3308, 1631 (C=O), 1556, 1461, 1418, 1383, 1362, 1341, 1329, 1259, 1066, 733.  $^1\text{H}$  NMR (500 MHz, DMSO- $d_6$ )  $\delta_{\text{H}}$  ppm: 2.36 (s, 3H, CH<sub>3</sub>), 2.76 (dt,  $J = 14.4, 6.0$  Hz, 1H, 3-H<sub>a</sub>), 3.13 (dt,  $J = 14.4, 5.8$  Hz, 1H, 3-H<sub>b</sub>), 4.10 (dd,  $J = 14.2, 4.4$  Hz, 1H, 5-H<sub>a</sub>), 4.12–4.19 (m, 1H, 4-H), 4.32 (dd,  $J = 14.4, 4.9$  Hz, 1H, 5-H<sub>b</sub>), 5.30 (d,  $J = 4.0$  Hz, 1H, OH), 7.02–7.10 (m, 1H, 9-H), 7.22–7.29 (m, 1H, 8-H), 7.47–7.52 (m, 1H, 7-H), 7.57–7.62 (m, 1H, 10-H), 7.97–8.02 (m, 1H, NH).  $^{13}\text{C}$  NMR (125 MHz, DMSO- $d_6$ )  $\delta_{\text{C}}$  ppm: 9.6 (CH<sub>3</sub>), 46.1 (C-3), 48.6 (C-5), 69.4 (C-4), 110.6 (C-7), 115.5 (C<sub>q</sub>), 119.6 (C-9), 120.3 (C-10), 124.3 (C-8), 127.4 (C<sub>q</sub>), 130.3 (C<sub>q</sub>), 137.0 (C<sub>q</sub>), 166.3 (C-1).  $^{15}\text{N}$  NMR (40 MHz, DMSO- $d_6$ )  $\delta_{\text{N}}$  ppm: -271.4 (N-2), -254.4 (N-6). HRMS (ESI) for  $\text{C}_{13}\text{H}_{15}\text{N}_2\text{O}_2$  ( $[\text{M}+\text{H}]^+$ ): calcd  $m/z$  231.1128, found  $m/z$  231.1126.

#### 2-Benzyl-4-hydroxy-2,3,4,5-tetrahydro-1H-[1,4]diazepino[1,2-a]indol-1-one **7f**

Purified by column chromatography on silica gel (petroleum ether/ethyl acetate gradient from 7/1 to 1/6,  $v/v$ ). White solid, mp 183–184 °C, procedure b -87% (142.1 mg).  $R_f = 0.53$  (petroleum ether/ethyl acetate 3/1,  $v/v$ ). IR (KBr)  $\nu_{\text{max}}$ ,  $\text{cm}^{-1}$ : 3313 (OH), 2360, 2341, 1610 (C=O), 1541, 1421, 1079, 740.  $^1\text{H}$  NMR (400 MHz, DMSO- $d_6$ )  $\delta_{\text{H}}$  ppm: 3.01 (dd,  $J = 14.8, 7.4$  Hz, 1H, 3-H<sub>a</sub>), 3.31 (dd,  $J = 14.8, 5.2$  Hz, 1H, 3-H<sub>b</sub>), 4.06–4.14 (m, 1H, 4-H), 4.23 (dd,  $J = 14.6, 3.8$  Hz, 1H, 5-H<sub>a</sub>), 4.38 (dd,  $J = 14.6, 4.9$  Hz, 1H, 5-H<sub>b</sub>), 4.46 (d,  $J = 14.6$  Hz, 1H, 2-CH<sub>a</sub>), 5.00 (d,  $J = 14.6$  Hz, 1H, 2-CH<sub>b</sub>), 5.40 (d,  $J = 4.0$  Hz, 1H, OH), 6.99–7.01 (m, 1H, 11-H), 7.05–7.11 (m, 1H, 9-H), 7.23–7.35 (m, 2H, 8-H, CH<sub>2</sub>Ph 4-H), 7.36–7.41 (m, 4H, CH<sub>2</sub>Ph 2,3,5,6-H), 7.50–7.57 (m, 1H, 7-H), 7.61–7.67 (m, 1H, 10-H).  $^{13}\text{C}$  NMR (101 MHz, DMSO- $d_6$ )  $\delta_{\text{C}}$  ppm: 48.1 (C-5), 50.4 (CH<sub>2</sub>Ph), 51.4 (C-3), 69.1 (C-4), 105.5 (C-11), 110.4 (C-7), 120.0 (C-9), 121.6 (C-10), 123.6 (C-8), 126.0 (C-10a), 127.4 (CH<sub>2</sub>Ph C-4), 128.2 (CH<sub>2</sub>Ph C-3,5), 128.7 (CH<sub>2</sub>Ph C-2,6), 134.3 (C-11a), 137.3 (C-6a), 137.9 (CH<sub>2</sub>Ph C-1), 163.9 (C-1).  $^{15}\text{N}$  NMR (40 MHz, DMSO- $d_6$ )  $\delta_{\text{N}}$  ppm: -255.0 (N-6), -265.7 (N-2). HRMS (ESI) for  $\text{C}_{19}\text{H}_{19}\text{N}_2\text{O}_2$  ( $[\text{M}+\text{H}]^+$ ): calcd  $m/z$  307.1441, found  $m/z$  307.1388.

#### 4-Hydroxy-2,3,4,5-tetrahydro-1H-benzo[4,5]imidazo[1,2-a][1,4]diazepin-1-one **7g**

Purified by column chromatography on silica gel (petroleum ether/ethyl acetate/methanol gradient from 1/5/0 to 1/12/1,  $v/v/v$ ). White solid, decomp. 190 °C, procedure a -19% (18 mg).  $R_f = 0.21$  (ethyl acetate/methanol 9/1,  $v/v$ ). IR (KBr)  $\nu_{\text{max}}$ ,  $\text{cm}^{-1}$ : 3379, 3220, 1676 (C=O), 1522, 1466, 1458, 1418, 1336, 1079, 741.  $^1\text{H}$  NMR (500 MHz, DMSO- $d_6$ )  $\delta_{\text{H}}$  ppm: 2.75 (dt,  $J = 15.0$  Hz, 6.1 Hz, 1H, 3-H<sub>a</sub>), 3.21 (dt,  $J = 14.7$  Hz, 5.8 Hz, 1H, 3-H<sub>b</sub>), 4.22–4.31 (m, 2H, 5-H<sub>a</sub>, 4-H), 4.49 (dd,  $J = 14.1$  Hz, 4.3 Hz, 1H, 5-H<sub>b</sub>), 5.35–5.55 (br s, 1H, OH), 7.23–7.28 (m, 1H, 9-H), 7.31–7.37 (m, 1H, 8-H), 7.63–7.73 (m, 2H, 7-H, 10-H), 8.56–8.63 (m, 1H, NH).  $^{13}\text{C}$  NMR (125 MHz, DMSO- $d_6$ )  $\delta_{\text{C}}$  ppm: 45.4 (C-3), 48.2 (C-5), 69.9 (C-4), 111.5 (C-7), 120.7 (C-10), 123.1 (C-9), 124.6 (C-8), 135.2 (C<sub>q</sub>), 142.0 (C<sub>q</sub>), 147.4 (C<sub>q</sub>), 163.2 (C-1). HRMS (ESI) for  $\text{C}_{11}\text{H}_{12}\text{N}_3\text{O}_2$  ( $[\text{M}+\text{H}]^+$ ): calcd  $m/z$  218.0924, found  $m/z$  218.0918.

#### 3.2.6. Synthesis of O-Alkylated 5-Substituted

7-Hydroxy-2-phenyl-5,6,7,8-tetrahydro-4H-pyrazolo[1,5-a][1,4]diazepin-4-ones (**8a–f**) and 2-Benzyl-4-hydroxy-2,3,4,5-tetrahydro-1H-[1,4]diazepino[1,2-a]indol-1-one (**9a,b**)

Pyrazolo-diazepinone **4i,n,t** or indole-diazepinone **7f** (1 eq) was dissolved in dimethyl formamide (0.1 M) and NaH (1.5 eq; 60% dispersion in mineral oil) was added followed by appropriate alkylating agent (1.5 eq). The reaction mixture was stirred at 25–50 °C for 5–8 h. Upon completion, the mixture was concentrated to approximately 1/3 volume, diluted with ethyl acetate, and washed with brine. Organic layer was dried over anhydrous

Na<sub>2</sub>SO<sub>4</sub>, filtered, and concentrated under reduced pressure. The residue was purified by column chromatography.

7-Methoxy-5-(2-methoxyethyl)-2-phenyl-5,6,7,8-tetrahydro-4H-pyrazolo[1,5-a][1,4]diazepin-4-one **8a**

Purified by column chromatography on silica gel (*n*-hexane/ethyl acetate 1/1, *v/v*). White solid, mp 88–89 °C, 77% (104 mg). *R*<sub>f</sub> = 0.41 (*n*-hexane/ethyl acetate 1/4, *v/v*). IR (KBr)  $\nu_{\max}$ , cm<sup>-1</sup>: 3120, 2933, 2890, 2828, 1638 (C=O), 1470, 1354, 1016, 771, 700. <sup>1</sup>H NMR (400 MHz, DMSO-*d*<sub>6</sub>)  $\delta_{\text{H}}$  ppm: 3.23 (dd, *J* = 15.2, 7.6 Hz, 1H, 5-CH<sub>a</sub>), 3.29 (s, 3H, CH<sub>2</sub>OCH<sub>3</sub>), 3.37 (s, 3H, 7-OCH<sub>3</sub>), 3.39–3.47 (m, 1H, 6-H<sub>a</sub>), 3.51–3.62 (m, 3H, 5-CH<sub>b</sub>, CH<sub>2</sub>O), 3.90 (dt, *J* = 13.6, 5.2 Hz, 1H, 6-H<sub>b</sub>), 4.05–4.12 (m, 1H, 7-H), 4.46 (qd, *J* = 14.7, 4.3 Hz, 2H, 8-H<sub>a</sub>H<sub>b</sub>), 7.18 (s, 1H, 3-H), 7.29–7.35 (m, 1H, Ph 4-H), 7.38–7.45 (m, 2H, Ph 3,5-H), 7.8–7.87 (m, 2H, Ph 2,6-H). <sup>13</sup>C NMR (101 MHz, DMSO-*d*<sub>6</sub>)  $\delta_{\text{C}}$  ppm: 46.6 (C-6), 50.0 (5-CH<sub>2</sub>), 52.1 (C-8), 56.3 (7-OCH<sub>3</sub>), 58.0 (CH<sub>2</sub>OCH<sub>3</sub>), 69.8 (CH<sub>2</sub>O), 79.2 (C-7), 105.5 (C-3), 125.2 (Ph C-2,6), 127.8 (Ph C-4), 128.7 (Ph C-3,5), 132.4 (Ph C-1), 139.3 (C-3a), 149.1 (C-2), 161.6 (C-4). <sup>15</sup>N NMR (40 MHz, DMSO-*d*<sub>6</sub>)  $\delta_{\text{N}}$  ppm: -266.0 (N-5), -176.2 (N-9), -74.1 (N-1). HRMS (ESI) for C<sub>17</sub>H<sub>21</sub>N<sub>3</sub>NaO<sub>3</sub> ([M+Na]<sup>+</sup>): calcd *m/z* 338.1475, found *m/z* 338.1475.

5-Allyl-7-methoxy-2-phenyl-5,6,7,8-tetrahydro-4H-pyrazolo[1,5-a][1,4]diazepin-4-one **8b**

Purified by column chromatography on silica gel (*n*-hexane/ethyl acetate 3.5/1, *v/v*). White solid, mp 89–90 °C, 84% (78 mg). *R*<sub>f</sub> = 0.47 (*n*-hexane/ethyl acetate 1/1, *v/v*). IR (KBr)  $\nu_{\max}$ , cm<sup>-1</sup>: 2984, 2929, 2826, 1657 (C=O), 1461, 1243, 1206, 1089, 770, 697. <sup>1</sup>H NMR (400 MHz, DMSO-*d*<sub>6</sub>)  $\delta_{\text{H}}$  ppm: 3.19 (dd, *J* = 15.2, 6.9 Hz, 1H, 6-H<sub>a</sub>), 3.36 (s, 3H, CH<sub>3</sub>), 3.46 (dd, *J* = 15.2, 5.0 Hz, 1H, 6-H<sub>b</sub>), 3.97 (dd, *J* = 15.1, 6.2 Hz, 1H, 5-CH<sub>a</sub>), 4.09 (dt, *J* = 10.4, 5.1 Hz, 1H, 7-H), 4.23 (dd, *J* = 15.1, 5.5 Hz, 1H, 5-CH<sub>b</sub>), 4.40 (dd, *J* = 14.7, 4.0 Hz, 1H, 8-H<sub>a</sub>), 4.58 (dd, *J* = 14.7, 5.4 Hz, 1H, 8-H<sub>b</sub>), 5.18–5.31 (m, 2H, CH<sub>2</sub>-CH=CH<sub>2</sub>), 5.81–5.92 (m, 1H, CH<sub>2</sub>-CH=CH<sub>2</sub>), 7.20 (s, 1H, 3-H), 7.29–7.36 (m, 1H, Ph 4-H), 7.37–7.45 (m, 2H, Ph 3,5-H), 7.81–7.88 (m, 2H, Ph 2,6-H). <sup>13</sup>C NMR (101 MHz, DMSO-*d*<sub>6</sub>)  $\delta_{\text{C}}$  ppm: 48.4 (C-6), 49.6 (5-CH<sub>2</sub>), 52.3 (C-8), 56.3 (CH<sub>3</sub>), 78.9 (C-7), 105.8 (C-3), 117.9 (CH<sub>2</sub>-CH=CH<sub>2</sub>), 125.1 (Ph C-2,6), 127.9 (Ph C-4), 128.7 (Ph C-3,5), 132.4 (Ph C-1), 133.4 (CH<sub>2</sub>-CH=CH<sub>2</sub>), 139.1 (C-3a), 149.1 (C-2), 161.3 (C-4). <sup>15</sup>N NMR (40 MHz, DMSO-*d*<sub>6</sub>)  $\delta_{\text{N}}$  ppm: -176.0 (N-9), -73.9 (N-1). HRMS (ESI) for C<sub>17</sub>H<sub>19</sub>N<sub>3</sub>NaO<sub>2</sub> ([M+Na]<sup>+</sup>): calcd *m/z* 320.1369, found *m/z* 320.1370.

5-Benzyl-7-methoxy-2-phenyl-5,6,7,8-tetrahydro-4H-pyrazolo[1,5-a][1,4]diazepin-4-one **8c**

Purified by column chromatography on silica gel (*n*-hexane/ethyl acetate 7/2, *v/v*). Pale yellow solid, mp 176–177 °C, 70% (57 mg). *R*<sub>f</sub> = 0.41 (*n*-hexane/ethyl acetate 3/2, *v/v*). IR (KBr)  $\nu_{\max}$ , cm<sup>-1</sup>: 3146, 2988, 2928, 2871, 1651 (C=O), 1449, 1241, 1101, 764, 695. <sup>1</sup>H NMR (400 MHz, DMSO-*d*<sub>6</sub>)  $\delta_{\text{H}}$  ppm: 3.19 (dd, *J* = 15.2, 7.1 Hz, 1H, 6-H<sub>a</sub>), 3.28 (s, 3H, CH<sub>3</sub>), 3.48 (dd, *J* = 15.2, 5.0 Hz, 1H, 6-H<sub>b</sub>), 3.86–3.93 (m, 1H, 7-H), 4.42 (dd, *J* = 14.8, 3.8 Hz, 1H, 8-H<sub>a</sub>), 4.48–4.59 (m, 2H, 8-H<sub>b</sub>, 5-CH<sub>a</sub>), 4.88 (d, *J* = 14.7 Hz, 1H, 5-CH<sub>b</sub>), 7.26 (s, 1H, 3-H), 7.30–7.35 (m, 2H, CPh 4-H, CH<sub>2</sub>Ph 4-H), 7.36–7.44 (m, 6H, CPh 3,5-H, CH<sub>2</sub>Ph 2,3,5,6-H), 7.82–7.87 (m, 2H, CPh 2,6-H). <sup>13</sup>C NMR (101 MHz, DMSO-*d*<sub>6</sub>)  $\delta_{\text{C}}$  ppm: 48.6 (C-6), 50.4 (5-CH<sub>2</sub>), 52.3 (C-8), 56.3 (CH<sub>3</sub>), 78.8 (C-7), 106.0 (C-3), 125.1 (CPh C-2,6), 127.5 (CH<sub>2</sub>Ph C-4), 127.9 (CPh C-4), 128.1 (CH<sub>2</sub>Ph C-2,6), 128.6 (CH<sub>2</sub>Ph C-3,5), 128.7 (CPh C-3,5), 132.4 (CPh C-1), 137.4 (CH<sub>2</sub>Ph C-1), 139.0 (C-3a), 149.2 (C-2), 161.7 (C-4). <sup>15</sup>N NMR (40 MHz, DMSO-*d*<sub>6</sub>)  $\delta_{\text{N}}$  ppm: -261.2 (N-5), -176.7 (N-9), -74.1 (N-1). HRMS (ESI) for C<sub>21</sub>H<sub>21</sub>N<sub>3</sub>NaO<sub>2</sub> ([M+Na]<sup>+</sup>): calcd *m/z* 370.1526, found *m/z* 370.1526.

7-Ethoxy-5-(2-methoxyethyl)-2-phenyl-5,6,7,8-tetrahydro-4H-pyrazolo[1,5-a][1,4]diazepin-4-one **8d**

Purified by column chromatography on silica gel (*n*-hexane/ethyl acetate/methanol 1/1/0.05, *v/v/v*). Yellowish resin, 75% (118 mg). *R*<sub>f</sub> = 0.54 (*n*-hexane/ethyl acetate 1/4, *v/v*). IR (KBr)  $\nu_{\max}$ , cm<sup>-1</sup>: 2977, 2931, 2893, 1647 (C=O), 1461, 1440, 1104, 1077, 769, 695. <sup>1</sup>H NMR (400 MHz, DMSO-*d*<sub>6</sub>)  $\delta_{\text{H}}$  ppm: 1.14 (t, *J* = 7.0 Hz, 3H, 7-OCH<sub>2</sub>CH<sub>3</sub>), 3.24 (dd, *J* = 15.3,

7.4 Hz, 1H, 5-CH<sub>a</sub>), 3.29 (s, 3H, CH<sub>2</sub>OCH<sub>3</sub>), 3.41–3.49 (m, 1H, 6-H<sub>a</sub>), 3.51–3.68 (m, 5H, 5-CH<sub>b</sub>, CH<sub>2</sub>OCH<sub>3</sub>, 7-OCH<sub>2</sub>), 3.88 (dt, *J* = 13.5, 5.0 Hz, 1H, 6-H<sub>b</sub>), 4.15–4.22 (m, 1H, 7-H), 4.44 (ddd, *J* = 18.2, 14.6, 4.4 Hz, 2H, 8-H<sub>a</sub>H<sub>b</sub>), 7.18 (s, 1H, 3-H), 7.29–7.36 (m, 1H, Ph 4-H), 7.38–7.45 (m, 2H, Ph 3,5-H), 7.81–7.87 (m, 2H, Ph 2,6-H). <sup>13</sup>C NMR (101 MHz, DMSO-*d*<sub>6</sub>) δ<sub>C</sub> ppm: 15.3 (7-OCH<sub>2</sub>CH<sub>3</sub>), 46.6 (C-6), 50.4 (5-CH<sub>2</sub>), 52.7 (C-8), 58.0 (CH<sub>2</sub>OCH<sub>3</sub>), 63.9 (7-OCH<sub>2</sub>), 69.8 (CH<sub>2</sub>OCH<sub>3</sub>), 77.4 (C-7), 105.5 (C-3), 125.1 (Ph C-2,6), 127.8 (Ph C-4), 128.7 (Ph C-3,5), 132.4 (Ph C-1), 139.3 (C-3a), 149.1 (C-2), 161.5 (C-4). <sup>15</sup>N NMR (40 MHz, DMSO-*d*<sub>6</sub>) δ<sub>N</sub> ppm: −265.2 (N-5), −175.8 (N-9), −74.2 (N-1). HRMS (ESI) for C<sub>18</sub>H<sub>23</sub>N<sub>3</sub>NaO<sub>3</sub> ([M+Na]<sup>+</sup>): calcd *m/z* 352.1632, found *m/z* 352.1632.

#### 5-Allyl-7-ethoxy-2-phenyl-5,6,7,8-tetrahydro-4H-pyrazolo[1,5-*a*][1,4]diazepin-4-one **8e**

Purified by column chromatography on silica gel (*n*-hexane/ethyl acetate 7/2, *v/v*). Pale yellow solid, mp 113–144 °C, 77% (116 mg). *R*<sub>f</sub> = 0.59 (*n*-hexane/ethyl acetate 1/1, *v/v*). IR (KBr) ν<sub>max</sub>, cm<sup>−1</sup>: 3118, 2980, 1645 (C=O), 1460, 1438, 1396, 1248, 1101, 770, 696. <sup>1</sup>H NMR (400 MHz, DMSO-*d*<sub>6</sub>) δ<sub>H</sub> ppm: 1.13 (t, *J* = 6.9 Hz, 3H, CH<sub>3</sub>), 3.20 (dd, *J* = 15.1, 6.8 Hz, 1H, 6-H<sub>a</sub>), 3.44 (dd, *J* = 15.1, 4.7 Hz, 1H, 6-H<sub>b</sub>), 3.50–3.65 (m, 2H, OCH<sub>2</sub>), 3.98 (dd, *J* = 15.1, 6.0 Hz, 1H, 5-CH<sub>a</sub>), 4.15–4.27 (m, 2H, 5-CH<sub>b</sub>, 7-H), 4.37 (dd, *J* = 14.6, 3.8 Hz, 1H, 8-H<sub>a</sub>), 4.58 (dd, *J* = 14.6, 5.4 Hz, 1H, 8-H<sub>b</sub>), 5.18–5.31 (m, 2H, CH<sub>2</sub>-CH=CH<sub>2</sub>), 5.81–5.93 (m, 1H, CH<sub>2</sub>-CH=CH<sub>2</sub>), 7.20 (s, 1H, 3-H), 7.29–7.36 (m, 1H, Ph 4-H), 7.38–7.45 (m, 2H, Ph 3,5-H), 7.81–7.87 (m, 2H, Ph 2,6-H). <sup>13</sup>C NMR (101 MHz, DMSO-*d*<sub>6</sub>) δ<sub>C</sub> ppm: 15.3 (CH<sub>3</sub>), 48.8 (C-6), 49.6 (5-CH<sub>2</sub>), 52.9 (C-8), 63.9 (OCH<sub>2</sub>), 77.1 (C-7), 105.8 (C-3), 117.8 (CH<sub>2</sub>-CH=CH<sub>2</sub>), 125.1 (Ph C-2,6), 127.9 (Ph C-4), 128.7 (Ph C-3,5), 132.4 (Ph C-1), 133.4 (CH<sub>2</sub>-CH=CH<sub>2</sub>), 139.1 (C-3a), 149.1 (C-2), 161.3 (C-4). <sup>15</sup>N NMR (40 MHz, DMSO-*d*<sub>6</sub>) δ<sub>N</sub> ppm: −265.6 (N-5), −176.4 (N-9), −73.9 (N-1). HRMS (ESI) for C<sub>18</sub>H<sub>21</sub>N<sub>3</sub>NaO<sub>2</sub> ([M+Na]<sup>+</sup>): calcd *m/z* 334.1526, found *m/z* 334.1526.

#### 5-Benzyl-7-ethoxy-2-phenyl-5,6,7,8-tetrahydro-4H-pyrazolo[1,5-*a*][1,4]diazepin-4-one **8f**

Purified by column chromatography on silica gel (*n*-hexane/ethyl acetate 3.5/1, *v/v*). Pale yellow solid, mp 115–116 °C, 72% (92 mg). *R*<sub>f</sub> = 0.55 (*n*-hexane/ethyl acetate 3/2, *v/v*). IR (KBr) ν<sub>max</sub>, cm<sup>−1</sup>: 3121, 2982, 2871, 1658 (C=O), 1460 and 1440 (doublet), 1239, 1105, 771, 693. <sup>1</sup>H NMR (400 MHz, DMSO-*d*<sub>6</sub>) δ<sub>H</sub> ppm: 1.06 (t, *J* = 7.0 Hz, 3H, CH<sub>3</sub>), 3.20 (dd, *J* = 15.2, 7.1 Hz, 1H, 6-H<sub>a</sub>), 3.39–3.58 (m, 3H, 6-H<sub>b</sub>, OCH<sub>2</sub>), 3.95–4.02 (m, 1H, 7-H), 4.38 (dd, *J* = 14.7, 3.8 Hz, 1H, 8-H<sub>a</sub>), 4.48–4.59 (m, 2H, 8-H<sub>b</sub>, 5-CH<sub>a</sub>), 4.88 (d, *J* = 14.7 Hz, 1H, 5-CH<sub>b</sub>), 7.26 (s, 1H, 3-H), 7.29–7.35 (m, 2H, CPh 4-H, CH<sub>2</sub>Ph 4-H), 7.36–7.44 (m, 6H, CPh 3,5-H, CH<sub>2</sub>Ph 2,3,5,6-H), 7.81–7.88 (m, 2H, CPh 2,6-H). <sup>13</sup>C NMR (101 MHz, DMSO-*d*<sub>6</sub>) δ<sub>C</sub> ppm: 15.2 (CH<sub>3</sub>), 49.0 (C-6), 50.4 (5-CH<sub>2</sub>), 52.9 (C-8), 63.8 (OCH<sub>2</sub>), 77.0 (C-7), 106.0 (C-3), 125.1 (CPh C-2,6), 127.4 (CH<sub>2</sub>Ph C-4), 127.9 (CPh C-4), 128.1 (CH<sub>2</sub>Ph C-2,6), 128.6 (CH<sub>2</sub>Ph C-3,5), 128.7 (CPh C-3,5), 132.4 (CPh C-1), 137.4 (CH<sub>2</sub>Ph C-1), 149.2 (C-2), 161.7 (C-4). <sup>15</sup>N NMR (40 MHz, DMSO-*d*<sub>6</sub>) δ<sub>N</sub> ppm: −261.6 (N-5), −176.1 (N-9), −73.5 (N-1). HRMS (ESI) for C<sub>22</sub>H<sub>23</sub>N<sub>3</sub>NaO<sub>2</sub> ([M+Na]<sup>+</sup>): calcd *m/z* 384.1682, found *m/z* 384.1682.

#### 2-Benzyl-4-methoxy-2,3,4,5-tetrahydro-1H-[1,4]diazepino[1,2-*a*]indol-1-one **9a**

Purified by column chromatography on silica gel (petroleum ether/ethyl acetate gradient from 5/1 to 2/1, *v/v*). White solid, mp 97–98 °C, 92% (50 mg). *R*<sub>f</sub> = 0.63 (petroleum ether/ethyl acetate 2/1, *v/v*). IR (KBr) ν<sub>max</sub>, cm<sup>−1</sup>: 1642 (C=O), 1541, 1457, 1421, 1099, 741. <sup>1</sup>H NMR (400 MHz, CDCl<sub>3</sub>) δ<sub>H</sub> ppm: 3.31–3.37 (m, 5H, CH<sub>3</sub>, 3-H<sub>a</sub>H<sub>b</sub>), 3.68 (p, *J* = 5.2 Hz, 1H, 4-H), 4.27 (dd, *J* = 14.7, 5.2 Hz, 1H, 5-H<sub>a</sub>), 4.33–4.41 (m, 2H, 2-CH<sub>a</sub>, 5-H<sub>b</sub>), 5.26 (d, *J* = 14.6 Hz, 1H, 2-CH<sub>b</sub>), 7.11–7.16 (m, 1H, 9-H), 7.19 (s, 1H, 11-H), 7.28–7.41 (m, 7H, 7-H, 8-H, CH<sub>2</sub>Ph 2,3,4,5,6-H), 7.66–7.71 (m, 1H, 10-H). <sup>13</sup>C NMR (101 MHz, CDCl<sub>3</sub>) δ<sub>C</sub> ppm: 45.1 (C-5), 48.5 (C-3), 51.5 (2-CH<sub>2</sub>), 57.0 (CH<sub>3</sub>), 79.7 (C-4), 107.5 (C-11), 109.4 (C-7), 120.5 (C-9), 122.5 (C-10), 124.4 (C-8), 126.9 (C-10a), 127.9 (CH<sub>2</sub>Ph C-4), 128.7 (CH<sub>2</sub>Ph C-3,5), 128.9 (CH<sub>2</sub>Ph C-2,6), 134.0 (C-11a), 137.4 (C-6a), 137.6 (CH<sub>2</sub>Ph C-1), 165.0 (C=O). <sup>15</sup>N NMR (40 MHz, CDCl<sub>3</sub>): δ<sub>N</sub> ppm: −259.5 (N-6), −267.8 (N-2). HRMS (ESI) for C<sub>20</sub>H<sub>21</sub>N<sub>2</sub>O<sub>2</sub> ([M+H]<sup>+</sup>): calcd *m/z* 321.1598, found *m/z* 321.1596.

### 2-Benzyl-4-ethoxy-2,3,4,5-tetrahydro-1*H*-[1,4]diazepino[1,2-*a*]indol-1-one 9b

Purified by column chromatography on silica gel (petroleum ether/ethyl acetate gradient from 5/1 to 4/1, *v/v*). Colorless resin, 73% (45 mg).  $R_f = 0.57$  (petroleum ether/ethyl acetate 2/1, *v/v*). IR (KBr)  $\nu_{\max}$ ,  $\text{cm}^{-1}$ : 2360, 2341, 1641 (C=O), 1540, 1417, 1100, 741.  $^1\text{H}$  NMR (400 MHz,  $\text{CDCl}_3$ )  $\delta_{\text{H}}$  ppm: 1.14–1.20 (m, 3H,  $\text{CH}_3$ ), 3.29–3.35 (m, 2H, 3- $\text{H}_a\text{H}_b$ ), 3.43–3.59 (m, 2H,  $\text{OCH}_2$ ), 3.73–3.81 (m, 1H, 4-H), 4.23–4.31 (m, 1H, 5- $\text{H}_a$ ), 4.33–4.42 (m, 2H, 2- $\text{CH}_a$ , 5- $\text{H}_b$ ), 5.22–5.30 (m, 1H, 2- $\text{CH}_b$ ), 7.10–7.21 (m, 2H, 9-H, 11-H), 7.27–7.41 (m, 7H, 7-H, 8-H,  $\text{CH}_2\text{Ph}$  2,3,4,5,6-H), 7.66–7.72 (m, 1H, 10-H).  $^{13}\text{C}$  NMR (101 MHz,  $\text{CDCl}_3$ )  $\delta_{\text{C}}$  ppm: 15.5 ( $\text{CH}_3$ ), 45.5 (C-5), 49.0 (C-3), 51.5 (2- $\text{CH}_2$ ), 64.8 ( $\text{OCH}_2$ ), 77.9 (C-4), 107.4 (C-11), 109.4 (C-7), 120.4 (C-9), 122.5 (C-10), 124.3 (C-8), 126.9 (C-10a), 127.90 ( $\text{CH}_2\text{Ph}$  C-4), 128.7 ( $\text{CH}_2\text{Ph}$  C-3,5), 128.9 ( $\text{CH}_2\text{Ph}$  C-2,6), 134.1 (C-11a), 137.5 (C-6a), 137.6 ( $\text{CH}_2\text{Ph}$  C-1), 165.1 (C-1).  $^{15}\text{N}$  NMR (40 MHz,  $\text{CDCl}_3$ ):  $\delta_{\text{N}}$  ppm: –259.8 (N-6), –268.6 (N-2). HRMS (ESI) for  $\text{C}_{21}\text{H}_{23}\text{N}_2\text{O}_2$  ( $[\text{M}+\text{H}]^+$ ): calcd  $m/z$  335,1781, found  $m/z$  335.1798.

## 4. Conclusions

To summarize, a regioselective strategy was developed for synthesizing ethyl 1-(oxiran-2-ylmethyl)-3-aryl-1*H*-pyrazole-5-carboxylates from easily accessible 3(5)-aryl-1*H*-pyrazole-5(3)-carboxylates. Regioselective alkylation was achieved via optimization using different bases, reaction media and temperatures. Established conditions were applied to the synthesis of novel pyrazolo[1,5-*a*][1,4]diazepin-4-one compound series via ring-opening of the oxirane with amines, and direct cyclisation sequence. Furthermore, the synthetic strategy was further applied to investigate the reactivity of ethyl 1*H*-indole-2-carboxylate and ethyl benzo[*d*]imidazole-2-carboxylate scaffolds which led to the formation of additional fused tetrahydro[1,4]diazepino[1,2-*a*]indol-1-one and tetrahydro-1*H*-benzo[4,5]imidazo[1,2-*a*][1,4]diazepin-1-one derivatives. The structures of all synthesized compounds were confirmed by detailed NMR spectroscopy and HRMS investigations.

**Supplementary Materials:** The following supporting information, containing  $^1\text{H}$ ,  $^{13}\text{C}$ ,  $^1\text{H}$ - $^{15}\text{N}$ -HMBC,  $^{19}\text{F}$  NMR and HRMS data, can be downloaded at: <https://www.mdpi.com/article/10.3390/molecules27248666/s1>.

**Author Contributions:** Conceptualization, A.Š., A.Ž. and E.A.; Data curation, G.R., A.Ž. and E.A.; Formal analysis, K.D., M.V. and V.M. (Vít Morávek); Funding acquisition, E.A.; Investigation, K.D., M.V., V.M. (Vít Morávek) and V.M. (Vida Malinauskienė); Methodology, A.Ž.; Resources, A.Ž. and E.A.; Supervision, A.Ž. and E.A.; Validation, A.Ž. and E.A.; Writing—original draft, K.D.; Writing—review and editing, A.Š., A.Ž. and E.A. All authors have read and agreed to the published version of the manuscript.

**Funding:** This work was supported by the Research Council of Lithuania (agreement No. S-MIP-20-60) and by the Internal Grant Agency of Palacký University (IGA\_PrF\_2022\_012).

**Institutional Review Board Statement:** Not applicable.

**Informed Consent Statement:** Not applicable.

**Data Availability Statement:** The data that support the findings of this study are available upon request.

**Conflicts of Interest:** The authors declare no conflict of interest. The funders had no role in the design of the study; in the collection, analyses, or interpretation of data; in the writing of the manuscript, or in the decision to publish the results.

**Sample Availability:** Not available.

## References

1. Taylor, R.D.; MacCoss, M.; Lawson, A.D.G. Rings in Drugs. *J. Med. Chem.* **2014**, *57*, 5845–5859. [CrossRef] [PubMed]
2. Vitaku, E.; Smith, D.T.; Njardarson, J.T. Analysis of the Structural Diversity, Substitution Patterns, and Frequency of Nitrogen Heterocycles among U.S. FDA Approved Pharmaceuticals. *J. Med. Chem.* **2014**, *57*, 10257–10274. [CrossRef] [PubMed]

3. McGrath, N.A.; Brichacek, M.; Njardarson, J.T. A Graphical Journey of Innovative Organic Architectures That Have Improved Our Lives. *J. Chem Educ* **2010**, *87*, 1348–1349. [CrossRef]
4. Liu, X.-H.; Yu, W.; Min, L.-J.; Wedge, D.E.; Tan, C.-X.; Weng, J.-Q.; Wu, H.-K.; Cantrell, C.L.; Bajsa-Hirschel, J.; Hua, X.-W.; et al. Synthesis and Pesticidal Activities of New Quinoxalines. *J. Agric. Food Chem* **2020**, *68*, 7324–7332. [CrossRef]
5. Schilling, W.; Zhang, Y.; Riemer, D.; Das, S. Visible-Light-Mediated Dearomatisation of Indoles and Pyrroles to Pharmaceuticals and Pesticides. *Chem. A Eur. J.* **2020**, *26*, 390–395. [CrossRef]
6. Qi, Y.; Wang, J.; Kou, Y.; Pang, H.; Zhang, S.; Li, N.; Liu, C.; Weng, Z.; Jian, X. Synthesis of an Aromatic N-Heterocycle Derived from Biomass and Its Use as a Polymer Feedstock. *Nat. Commun.* **2019**, *10*, 2107. [CrossRef]
7. Allard, N.; Aïch, R.B.; Gendron, D.; Boudreault, P.-L.T.; Tessier, C.; Alem, S.; Tse, S.-C.; Tao, Y.; Leclerc, M. Germafluorenes: New Heterocycles for Plastic Electronics. *Macromolecules* **2010**, *43*, 2328–2333. [CrossRef]
8. Al-Etaibi, A.; El-Asasery, M.; Ibrahim, M.; Al-Awadi, N. A Facile Synthesis of New Monoazo Disperse Dyes Derived from 4-Hydroxyphenylazopyrazole-5-Amines: Evaluation of Microwave Assisted Dyeing Behavior. *Molecules* **2012**, *17*, 13891–13909. [CrossRef]
9. Shams, H.Z.; Mohareb, R.M.; Helal, M.H.; Mahmoud, A.E.S. Design and Synthesis of Novel Antimicrobial Acyclic and Heterocyclic Dyes and Their Precursors for Dyeing and/or Textile Finishing Based on 2-n-Acylamino-4,5,6,7-Tetrahydrobenzo[b]Thiophene Systems. *Molecules* **2011**, *16*, 6271–6305. [CrossRef]
10. Mindt, M.; Beyraghdar Kashkooli, A.; Suarez-Diez, M.; Ferrer, L.; Jilg, T.; Bosch, D.; Martins dos Santos, V.; Wendisch, V.F.; Cankar, K. Production of Indole by *Corynebacterium Glutamicum* Microbial Cell Factories for Flavor and Fragrance Applications. *Microb. Cell Fact.* **2022**, *21*, 45. [CrossRef]
11. Yun, B.-S.; Kim, S.-Y.; Kim, J.-H.; Choi, S.; Lee, S.; Son, H.-J.; Kang, S.O. Synthesis and Characterization of Blue Phosphorescent NHC-Ir(III) Complexes with Annulated Heterocyclic 1,2,4-Triazolophenanthridine Derivatives for Highly Efficient PhOLEDs. *ACS Appl Electron. Mater.* **2022**, *4*, 2699–2710. [CrossRef]
12. Elie, M.; Renaud, J.-L.; Gaillard, S. N-Heterocyclic Carbene Transition Metal Complexes in Light Emitting Devices. *Polyhedron* **2018**, *140*, 158–168. [CrossRef]
13. Kerru, N.; Gummidi, L.; Maddila, S.; Gangu, K.K.; Jonnalagadda, S.B. A Review on Recent Advances in Nitrogen-Containing Molecules and Their Biological Applications. *Molecules* **2020**, *25*, 1909. [CrossRef]
14. Costa, R.F.; Turones, L.C.; Cavalcante, K.V.N.; Rosa Júnior, I.A.; Xavier, C.H.; Rosseto, L.P.; Napolitano, H.B.; da Castro, P.F.S.; Neto, M.L.F.; Galvão, G.M.; et al. Heterocyclic Compounds: Pharmacology of Pyrazole Analogs from Rational Structural Considerations. *Front. Pharm.* **2021**, *12*, 666725. [CrossRef]
15. Karrouchi, K.; Radi, S.; Ramli, Y.; Taoufik, J.; Mabkhot, Y.; Al-aizari, F.; Ansar, M. Synthesis and Pharmacological Activities of Pyrazole Derivatives: A Review. *Molecules* **2018**, *23*, 134. [CrossRef]
16. George, N.; Jawaid Akhtar, M.; Al Balushi, K.A.; Alam Khan, S. Rational Drug Design Strategies for the Development of Promising Multi-Target Directed Indole Hybrids as Anti-Alzheimer Agents. *Bioorg. Chem.* **2022**, *127*, 105941. [CrossRef]
17. Dhuguru, J.; Skouta, R. Role of Indole Scaffolds as Pharmacophores in the Development of Anti-Lung Cancer Agents. *Molecules* **2020**, *25*, 1615. [CrossRef]
18. Murahari, M.; Mahajan, V.; Neeladri, S.; Kumar, M.S.; Mayur, Y.C. Ligand Based Design and Synthesis of Pyrazole Based Derivatives as Selective COX-2 Inhibitors. *Bioorg. Chem.* **2019**, *86*, 583–597. [CrossRef]
19. Wang, X.; Xu, Y.; Zong, Z.; Cai, J.; Chen, C.; Zhang, Q.; Sun, X.; Li, J. Design, Synthesis and Biological Evaluation of Novel 5-Methyl-2,4,5,6-Tetrahydropyrrolo[3,4-c]Pyrazole Derivatives as Potent Potassium-Competitive Acid Blockers. *Bioorg. Med. Chem.* **2022**, *64*, 116765. [CrossRef]
20. Feng, Y.; Xie, X.-Y.; Yang, Y.-Q.; Sun, Y.-T.; Ma, W.-H.; Zhou, P.-J.; Li, Z.-Y.; Liu, H.-Q.; Wang, Y.-F.; Huang, Y.-S. Synthesis and Evaluation of Pyrimidoindole Analogs in Umbilical Cord Blood Ex Vivo Expansion. *Eur. J. Med. Chem.* **2019**, *174*, 181–197. [CrossRef]
21. Purgatorio, R.; de Candia, M.; Catto, M.; Carrieri, A.; Pisani, L.; De Palma, A.; Toma, M.; Ivanova, O.A.; Voskressensky, L.G.; Altomare, C.D. Investigating 1,2,3,4,5,6-Hexahydroazepino[4,3-b]Indole as Scaffold of Butyrylcholinesterase-Selective Inhibitors with Additional Neuroprotective Activities for Alzheimer's Disease. *Eur. J. Med. Chem.* **2019**, *177*, 414–424. [CrossRef] [PubMed]
22. Conde-Ceide, S.; Alcázar, J.; Alonso de Diego, S.A.; López, S.; Martín-Martín, M.L.; Martínez-Vituro, C.M.; Pena, M.-A.; Tong, H.M.; Lavreysen, H.; Mackie, C.; et al. Preliminary Investigation of 6,7-Dihydropyrazolo[1,5-a]Pyrazin-4-One Derivatives as a Novel Series of MGlU 5 Receptor Positive Allosteric Modulators with Efficacy in Preclinical Models of Schizophrenia. *Bioorg. Med. Chem. Lett.* **2016**, *26*, 429–434. [CrossRef] [PubMed]
23. Al-Wahaibi, L.H.; Gouda, A.M.; Abou-Ghadir, O.F.; Salem, O.I.A.; Ali, A.T.; Farghaly, H.S.; Abdelrahman, M.H.; Trembleau, L.; Abdu-Allah, H.H.M.; Youssif, B.G.M. Design and Synthesis of Novel 2,3-Dihydropyrazino[1,2-a]Indole-1,4-Dione Derivatives as Antiproliferative EGFR and BRAFV600E Dual Inhibitors. *Bioorg. Chem.* **2020**, *104*, 104260. [CrossRef] [PubMed]
24. Rashid, M.A.; Ashraf, A.; Rehman, S.S.; Shahid, S.A.; Mahmood, A.; Faruq, M. 1,4-Diazepines: A Review on Synthesis, Reactions and Biological Significance. *Curr. Org. Synth.* **2019**, *16*, 709–729. [CrossRef] [PubMed]
25. Jiménez-Somarribas, A.; Mao, S.; Yoon, J.-J.; Weisshaar, M.; Cox, R.M.; Marengo, J.R.; Mitchell, D.G.; Morehouse, Z.P.; Yan, D.; Solis, I.; et al. Identification of Non-Nucleoside Inhibitors of the Respiratory Syncytial Virus Polymerase Complex. *J. Med. Chem.* **2017**, *60*, 2305–2325. [CrossRef]

26. Shaw, S.; Bian, Z.; Zhao, B.; Tarr, J.C.; Veerasamy, N.; Jeon, K.O.; Belmar, J.; Arnold, A.L.; Fogarty, S.A.; Perry, E.; et al. Optimization of Potent and Selective Tricyclic Indole Diazepinone Myeloid Cell Leukemia-1 Inhibitors Using Structure-Based Design. *J. Med. Chem.* **2018**, *61*, 2410–2421. [CrossRef]
27. Lee, T.; Christov, P.P.; Shaw, S.; Tarr, J.C.; Zhao, B.; Veerasamy, N.; Jeon, K.O.; Mills, J.J.; Bian, Z.; Sensintaffar, J.L.; et al. Discovery of Potent Myeloid Cell Leukemia-1 (Mcl-1) Inhibitors That Demonstrate in Vivo Activity in Mouse Xenograft Models of Human Cancer. *J. Med. Chem.* **2019**, *62*, 3971–3988. [CrossRef]
28. Shen, S.L.; Shao, J.H.; Luo, J.Z.; Liu, J.T.; Miao, J.Y.; Zhao, B.X. Novel Chiral Ferrocenylpyrazolo[1,5-a][1,4]Diazepin-4-One Derivatives-Synthesis, Characterization and Inhibition against Lung Cancer Cells. *Eur. J. Med. Chem.* **2013**, *63*, 256–268. [CrossRef]
29. Bagdanoff, J.T.; Jain, R.; Han, W.; Zhu, S.; Madiera, A.M.; Lee, P.S.; Ma, X.; Poon, D. Tetrahydropyrrolo-Diazepinones as Inhibitors of ERK2 Kinase. *Bioorg. Med. Chem. Lett.* **2015**, *25*, 3788–3792. [CrossRef]
30. Boyer, S.J.; Burke, J.; Guo, X.; Kirrane, T.M.; Snow, R.J.; Zhang, Y.; Sarko, C.; Soleymanzadeh, L.; Swinamer, A.; Westbrook, J.; et al. Indole RSK Inhibitors. Part 1: Discovery and Initial SAR. *Bioorg. Med. Chem. Lett.* **2012**, *22*, 733–737. [CrossRef]
31. Kirrane, T.M.; Boyer, S.J.; Burke, J.; Guo, X.; Snow, R.J.; Soleymanzadeh, L.; Swinamer, A.; Zhang, Y.; Madwed, J.B.; Kashem, M.; et al. Indole RSK Inhibitors. Part 2: Optimization of Cell Potency and Kinase Selectivity. *Bioorg. Med. Chem. Lett.* **2012**, *22*, 738–742. [CrossRef]
32. Putey, A.; Fournet, G.; Lozach, O.; Perrin, L.; Meijer, L.; Joseph, B. Synthesis and Biological Evaluation of Tetrahydro[1,4]Diazepino[1,2-a]Indol-1-Ones as Cyclin-Dependent Kinase Inhibitors. *Eur. J. Med. Chem.* **2014**, *83*, 617–629. [CrossRef]
33. Razmienė, B.; Rezníčková, E.; Dambrauskienė, V.; Ostruszka, R.; Kubala, M.; Žukauskaitė, A.; Kryštof, V.; Šačkus, A.; Arbačiauskienė, E. Synthesis and Antiproliferative Activity of 2,4,6,7-Tetrasubstituted-2H-Pyrazolo[4,3-c]Pyridines. *Molecules* **2021**, *26*, 6747. [CrossRef]
34. Milišiūnaitė, V.; Arbačiauskienė, E.; Rezníčková, E.; Jorda, R.; Malínková, V.; Žukauskaitė, A.; Holzer, W.; Šačkus, A.; Kryštof, V. Synthesis and Anti-Mitotic Activity of 2,4- or 2,6-Disubstituted- and 2,4,6-Trisubstituted-2H-Pyrazolo[4,3-c]Pyridines. *Eur. J. Med. Chem.* **2018**, *150*, 908–919. [CrossRef]
35. Razmienė, B.; Vojáčková, V.; Rezníčková, E.; Malina, L.; Dambrauskienė, V.; Kubala, M.; Bajgar, R.; Kolářová, H.; Žukauskaitė, A.; Arbačiauskienė, E.; et al. Synthesis of N-Aryl-2,6-Diphenyl-2H-Pyrazolo[4,3-c]Pyridin-7-Amines and Their Photodynamic Properties in the Human Skin Melanoma Cell Line G361. *Bioorg. Chem.* **2022**, *119*, 105570. [CrossRef]
36. Milišiūnaitė, V.; Kadlecová, A.; Žukauskaitė, A.; Doležal, K.; Strnad, M.; Voller, J.; Arbačiauskienė, E.; Holzer, W.; Šačkus, A. Synthesis and Anthelmintic Activity of Benzopyrano[2,3-c]Pyrazolo-4(2H)-One Derivatives. *Mol. Divers.* **2020**, *24*, 1025–1042. [CrossRef]
37. Milišiūnaitė, V.; Paulavičiūtė, R.; Arbačiauskienė, E.; Martynaitis, V.; Holzer, W.; Šačkus, A. Synthesis of 2H-Furo[2,3-c]Pyrazole Ring Systems through Silver(I) Ion-Mediated Ring-Closure Reaction. *Beilstein J. Org. Chem.* **2019**, *15*, 679–684. [CrossRef]
38. Secieru, A.; O'Neill, P.M.; Cristiano, M.L.S. Revisiting the Structure and Chemistry of 3(5)-Substituted Pyrazoles. *Molecules* **2020**, *25*, 42. [CrossRef]
39. Kusakiewicz-Dawid, A.; Porada, M.; Dziuk, B.; Siodlak, D. Annular Tautomerism of 3(5)-Disubstituted-1H-Pyrazoles with Ester and Amide Groups. *Molecules* **2019**, *24*, 2632. [CrossRef]
40. Lin, R.; Chiu, G.; Yu, Y.; Connolly, P.J.; Li, S.; Lu, Y.; Adams, M.; Fuentes-Pesquera, A.R.; Emanuel, S.L.; Greenberger, L.M. Design, Synthesis, and Evaluation of 3,4-Disubstituted Pyrazole Analogues as Anti-Tumor CDK Inhibitors. *Bioorg. Med. Chem. Lett.* **2007**, *17*, 4557–4561. [CrossRef]
41. Guerrero, M.; Pérez, J.; Ros, J.; Branchadell, V.; Pellicer, E.; Sort, J.; Pons, J. Design of New N-Polyether Pyrazole Derived Ligands: Synthesis, Characterization and Regioselectivity. *Curr. Org. Synth.* **2013**, *11*, 149–155. [CrossRef]
42. Iškauskienė, M.; Ragaitė, G.; Sløk, F.A.; Šačkus, A. Facile Synthesis of Novel Amino Acid-like Building Blocks by N-Alkylation of Heterocyclic Carboxylates with N-Boc-3-Iodoazetidone. *Mol. Divers.* **2020**, *24*, 1235–1251. [CrossRef] [PubMed]
43. Matulevičiūtė, G.; Arbačiauskienė, E.; Kleizienė, N.; Kederienė, V.; Ragaitė, G.; Dagilienė, M.; Bieliauskas, A.; Milišiūnaitė, V.; Sløk, F.A.; Šačkus, A. Synthesis and Characterization of Novel Methyl (3)5-(N-Boc-Piperidinyl)-1H-Pyrazole-4-Carboxylates. *Molecules* **2021**, *26*, 3808. [CrossRef]
44. Huang, A.; Wo, K.; Lee, S.Y.C.; Kneitschel, N.; Chang, J.; Zhu, K.; Mello, T.; Bancroft, L.; Norman, N.J.; Zheng, S.L. Regioselective Synthesis, NMR, and Crystallographic Analysis of N1-Substituted Pyrazoles. *J. Org. Chem.* **2017**, *82*, 8864–8872. [CrossRef] [PubMed]
45. Wright, S.W.; Arnold, E.P.; Yang, X. Steric Redirection of Alkylation in 1H-Pyrazole-3-Carboxylate Esters. *Tetrahedron. Lett.* **2018**, *59*, 402–405. [CrossRef]
46. Xu, D.; Frank, L.; Nguyen, T.; Stumpf, A.; Russell, D.; Angelaud, R.; Gosselin, F. Magnesium-Catalyzed N2-Regioselective Alkylation of 3-Substituted Pyrazoles. *Synlett* **2020**, *31*, 595–599. [CrossRef]
47. Shen, S.L.; Zhu, J.; Li, M.; Zhao, B.X.; Miao, J.Y. Synthesis of Ferrocenyl Pyrazole-Containing Chiral Aminoethanol Derivatives and Their Inhibition against A549 and H322 Lung Cancer Cells. *Eur. J. Med. Chem.* **2012**, *54*, 287–294. [CrossRef]
48. Xiong, B.; Chen, S.; Zhu, P.; Huang, M.; Gao, W.; Zhu, R.; Qian, J.; Peng, Y.; Zhang, Y.; Dai, H.; et al. Design, Synthesis, and Biological Evaluation of Novel Thiazolyl Substituted Bis-Pyrazole Oxime Derivatives with Potent Antitumor Activities by Selectively Inducing Apoptosis and ROS in Cancer Cells. *Med. Chem.* **2019**, *15*, 743–754. [CrossRef]
49. Hafez, H.N.; El-Gazzar, A.R.B.A. Synthesis and Biological Evaluation of N- Pyrazolyl Derivatives and Pyrazolopyrimidine Bearing a Biologically Active Sulfonamide Moiety as Potential Antimicrobial Agent. *Molecules* **2016**, *21*, 1156. [CrossRef]



50. Thurmond, R.L.; Beavers, M.P.; Cai, H.; Meduna, S.P.; Gustin, D.J.; Sun, S.; Almond, H.J.; Karlsson, L.; Edwards, J.P. Nonpeptidic, Noncovalent Inhibitors of the Cysteine Protease Cathepsin S. *J. Med. Chem.* **2004**, *47*, 4799–4801. [CrossRef]
51. Schwarzkopf, J.; Sundermann, T.; Arnsmann, M.; Hanekamp, W.; Fabian, J.; Heidemann, J.; Pott, A.F.; Bettenworth, D.; Lehr, M. Inhibitors of Cytosolic Phospholipase A2 $\alpha$  with Carbamate Structure: Synthesis, Biological Activity, Metabolic Stability, and Bioavailability. *Med. Chem. Res.* **2014**, *23*, 5250–5262. [CrossRef]
52. Sundermann, T.; Arnsmann, M.; Schwarzkopf, J.; Hanekamp, W.; Lehr, M. Convergent and Enantioselective Syntheses of Cytosolic Phospholipase A 2 $\alpha$  Inhibiting N-(1-Indazol-1-Yl)propan-2-Yl)Carbamates. *Org. Biomol. Chem.* **2014**, *12*, 4021–4030. [CrossRef]
53. Kimura, T.; Hosokawa-Muto, J.; Asami, K.; Murai, T.; Kuwata, K. Synthesis of 9-Substituted 2,3,4,9-Tetrahydro-1H-Carbazole Derivatives and Evaluation of Their Anti-Prion Activity in TSE-Infected Cells. *Eur. J. Med. Chem.* **2011**, *46*, 5675–5679. [CrossRef]
54. Althaus, J.; Hake, T.; Hanekamp, W.; Lehr, M. 1-(5-Carboxyindazol-1-Yl)Propan-2-Ones as Dual Inhibitors of Cytosolic Phospholipase A2 $\alpha$  and Fatty Acid Amide Hydrolase: Bioisosteric Replacement of the Carboxylic Acid Moiety. *J. Enzym. Inhib. Med. Chem.* **2016**, *31*, 131–140. [CrossRef]
55. Saddique, F.A.; Zahoor, A.F.; Faiz, S.; Naqvi, S.A.R.; Usman, M.; Ahmad, M. Recent Trends in Ring Opening of Epoxides by Amines as Nucleophiles. *Synth. Commun.* **2016**, *46*, 831–868. [CrossRef]
56. Meninno, S.; Lattanzi, A. Epoxides: Small Rings to Play with under Asymmetric Organocatalysis. *ACS Org. Inorg. Au* **2022**, *2*, 289–305. [CrossRef]
57. Wang, C.; Luo, L.; Yamamoto, H. Metal-Catalyzed Directed Regio- and Enantioselective Ring-Opening of Epoxides. *Acc. Chem. Res.* **2016**, *49*, 193–204. [CrossRef]
58. Meninno, S.; Lattanzi, A. Organocatalytic Asymmetric Reactions of Epoxides: Recent Progress. *Chem.-A Eur. J.* **2016**, *22*, 3632–3642. [CrossRef]
59. Wang, C. Electrophilic Ring Opening of Small Heterocycles. *Synthesis* **2017**, *49*, 5307–5319. [CrossRef]
60. Li, D.; Wang, J.; Yu, S.; Ye, S.; Zou, W.; Zhang, H.; Chen, J. Highly Regioselective Ring-Opening of Epoxides with Amines: A Metal- A Nd Solvent-Free Protocol for the Synthesis of  $\beta$ -Amino Alcohols. *Chem. Commun.* **2020**, *56*, 2256–2259. [CrossRef]
61. Tan, N.; Yin, S.; Li, Y.; Qiu, R.; Meng, Z.; Song, X.; Luo, S.; Au, C.-T.; Wong, W.-Y. Synthesis and Structure of an Air-Stable Organobismuth Triflate Complex and Its Use as a High-Efficiency Catalyst for the Ring Opening of Epoxides in Aqueous Media with Aromatic Amines. *J. Organomet. Chem.* **2011**, *696*, 1579–1583. [CrossRef]
62. Hattori, G.; Yoshida, A.; Miyake, Y.; Nishibayashi, Y. Enantioselective Ring-Opening Reactions of Racemic Ethynyl Epoxides via Copper–Allenylidene Intermediates: Efficient Approach to Chiral  $\beta$ -Amino Alcohols. *J. Org. Chem.* **2009**, *74*, 7603–7607. [CrossRef] [PubMed]
63. Malhotra, S.V.; Andal, R.P.; Kumar, V. Aminolysis of Epoxides in Ionic Liquid 1-Ethylpyridinium Trifluoroacetate as Green and Efficient Reaction Medium. *Synth. Commun.* **2008**, *38*, 4160–4169. [CrossRef]
64. Hansen, T.; Vermeeren, P.; Haim, A.; van Dorp, M.J.H.; Codée, J.D.C.; Bickelhaupt, F.M.; Hamlin, T.A. Regioselectivity of Epoxide Ring-Openings via S N 2 Reactions Under Basic and Acidic Conditions. *Eur. J. Org. Chem* **2020**, *2020*, 3822–3828. [CrossRef]
65. Wu, Y.; Tang, C.; Rui, R.; Yang, L.; Ding, W.; Wang, J.; Li, Y.; Lai, C.C.; Wang, Y.; Luo, R.; et al. Synthesis and Biological Evaluation of a Series of 2-(((5-Akly / Aryl-1H-Pyrazol-3-Yl)Methyl)Thio)-5-Alkyl-6-(Cyclohexylmethyl)-Pyrimidin-4(3H)-Ones as Potential HIV-1 Inhibitors. *Acta Pharm Sin. B* **2020**, *10*, 512–528. [CrossRef]

Article

# Fluorinated and Non-Fluorinated 1,4-Diarylpyrazoles via MnO<sub>2</sub>-Mediated Mechanochemical Deacylative Oxidation of 5-Acylpyrazolines †

 Greta Utecht-Jarzyńska <sup>1</sup>, Anna Kowalczyk <sup>1,2</sup> and Marcin Jasiński <sup>1,\*</sup>
<sup>1</sup> Department of Organic and Applied Chemistry, Faculty of Chemistry, University of Lodz, Tamka 12, 91403 Lodz, Poland

<sup>2</sup> Doctoral School of Exact and Natural Sciences, University of Lodz, Banacha 12/16, 90237 Lodz, Poland

\* Correspondence: mjasinski@uni.lodz.pl; Tel.: +48-42-635-5766

† Dedicated to Professor Stanisław Leśniak (University of Lodz) on the occasion of his 70th birthday.

**Abstract:** A solvent-free two-step synthesis of polyfunctionalized pyrazoles under ball-milling mechanochemical conditions was developed. The protocol comprises (3 + 2)-cycloaddition of in situ generated nitrile imines and chalcones, followed by oxidation of the initially formed 5-acylpyrazolines with activated MnO<sub>2</sub>. The second step proceeds via an exclusive deacylative pathway, to give a series of 1,4-diarylpyrazoles functionalized with a fluorinated (CF<sub>3</sub>) or non-fluorinated (Ph, COOEt, Ac) substituent at C(3) of the heterocyclic ring. In contrast, MnO<sub>2</sub>-mediated oxidation of a model isomeric 4-acylpyrazoline proceeded with low chemoselectivity, leading to fully substituted pyrazole as a major product formed via dehydrogenative aromatization. The presented approach extends the scope of the known methods carried out in organic solvents and enables the preparation of polyfunctionalized pyrazoles, which are of general interest in medicine and material sciences.

**Keywords:** pyrazole; nitrile imine; mechanochemistry; (3 + 2)-cycloaddition; deacylation; oxidation

**Citation:** Utecht-Jarzyńska, G.; Kowalczyk, A.; Jasiński, M. Fluorinated and Non-Fluorinated 1,4-Diarylpyrazoles via MnO<sub>2</sub>-Mediated Mechanochemical Deacylative Oxidation of 5-Acylpyrazolines. *Molecules* **2022**, *27*, 8446. <https://doi.org/10.3390/molecules27238446>

Academic Editors: Vera L. M. Silva and Artur M. S. Silva

Received: 4 November 2022

Accepted: 29 November 2022

Published: 2 December 2022

**Publisher's Note:** MDPI stays neutral with regard to jurisdictional claims in published maps and institutional affiliations.



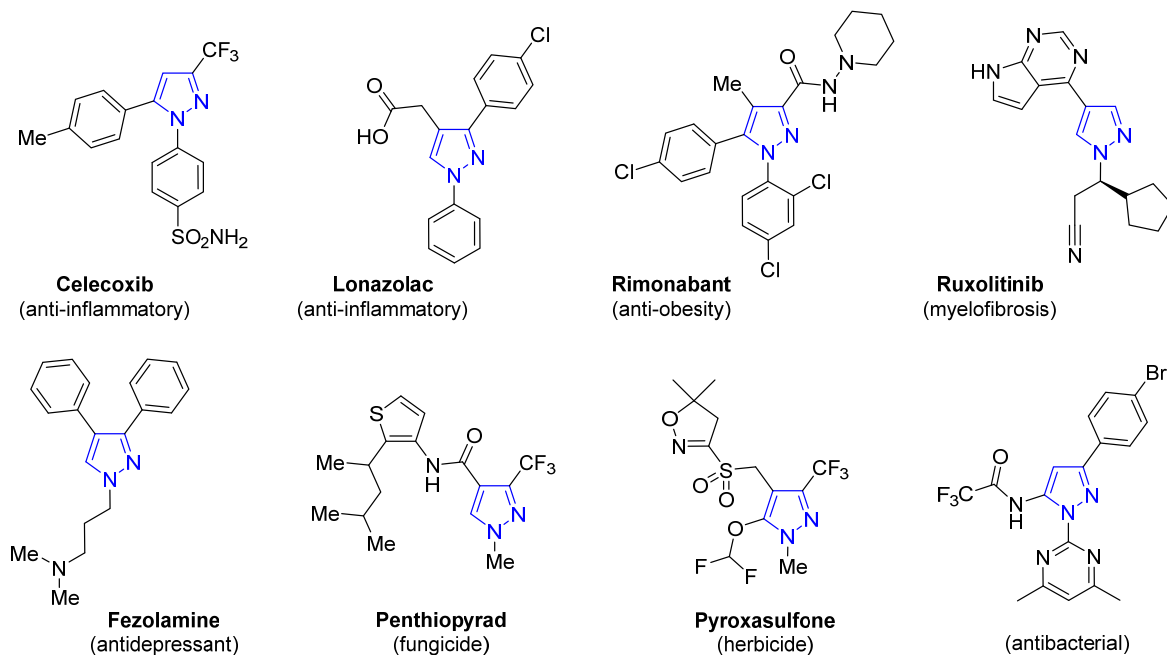
**Copyright:** © 2022 by the authors. Licensee MDPI, Basel, Switzerland. This article is an open access article distributed under the terms and conditions of the Creative Commons Attribution (CC BY) license (<https://creativecommons.org/licenses/by/4.0/>).

## 1. Introduction

Due to the discovery of a number of practical applications, there is increasing interest in the chemistry of pyrazole-based compounds, and fluorinated analogues are of special significance in medicine, crop protection, as well as material sciences [1–4]. The title heterocycle constitutes a key structural element of pharmaceuticals and agrochemicals; they exhibit a variety of biological activities such as being anti-inflammatory (e.g., Celecoxib, Lonazolac), antibacterial, anticancer (e.g., Crizotinib), anti-obesity (e.g., Rimonabant), antidepressant (e.g., Fezolamine), antiviral (e.g., Lenacapavir), and antifungal (e.g., Penthiopyrad), and have been widely applied as pesticides (Figure 1) [5–13]. In addition, some pyrazoles have been successfully applied in polymer chemistry, as well as for the preparation of advanced liquid crystalline materials [14,15]. Furthermore, polyfunctionalized pyrazoles can efficiently act as ligands in transition metal-catalyzed reactions [1,2,16]. Taking into account the general significance of this class of *N*-heterocycles, the development of new synthetic protocols to access pyrazoles with the desired substitution patterns is of great interest.

Out of the various synthetic methodologies for the preparation of pyrazole derivatives available thus far, condensation of 1,3-dielectrophilic agents (typically 1,3-diketones or their synthetic equivalents) with hydrazines is considered the most versatile and commonly applied strategy [1,2,4,5]. However, this classical method often suffers from regioselectivity issues and leads to isomeric pyrazoles, along with other by-products, which require tedious separation, e.g., using chromatography techniques. Hence, (3 + 2)-cycloaddition processes are an attractive alternative and enable straightforward access to the pyrazole skeleton through simultaneous formation of new carbon–carbon and carbon–nitrogen bonds. In

this context, diazoalkanes, and particularly nitrile imines, have been recognized as readily available and powerful 1,3-dipoles for the construction of the pyrazole ring [1,2,17].

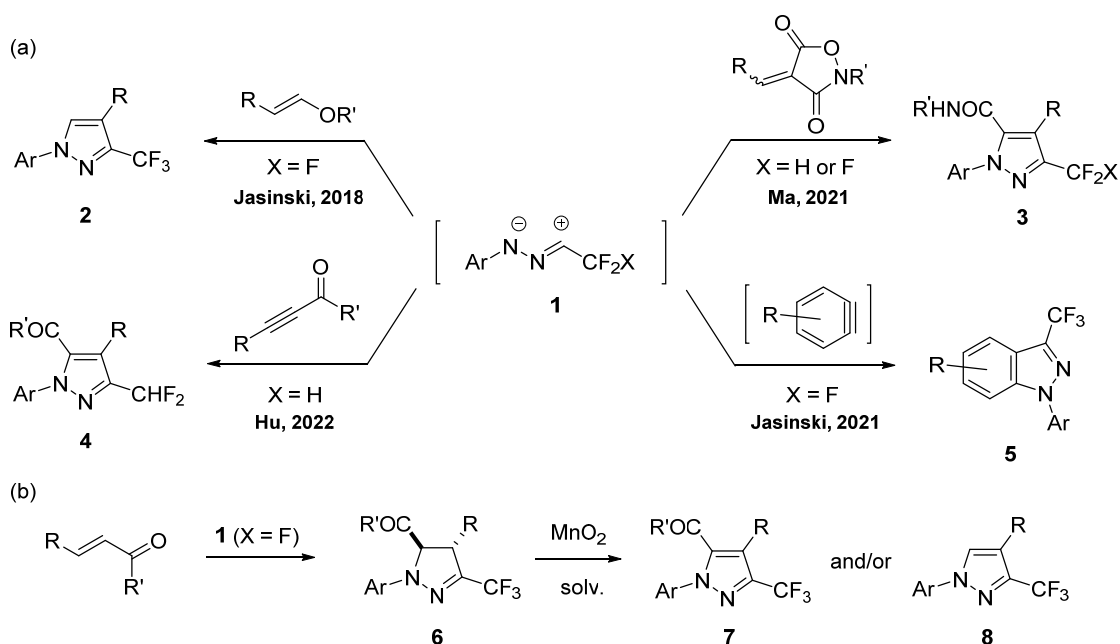


**Figure 1.** Structures of selected fluorinated and non-fluorinated pyrazole-based pharmaceuticals and agrochemicals.

On the other hand, the negative impacts on the environment and public health caused by the large amount of waste solvents produced during classical organic synthesis have to be taken into account. Recently, there has been a rapid development of green and sustainable synthetic protocols based on mechanochemical approaches, in which the reaction is activated by the absorption of mechanical energy originating from collisions of milling balls [18–21]. More importantly, these reactions can be performed either without any solvent or require only small amounts of so-called “liquid assisted grinding solvent” (LAGs), and in many instances the chemo- and regio-selectivity switch, leading to rather unexpected products being observed upon mechanochemical activation. Several interesting applications of mechanochemistry in the synthesis of pharmaceutically-relevant *N*-containing compounds, such as Dantrolene (muscle relaxant), Tolbutamide (antidiabetic), and Axitinib (anticancer), have been reported [22–24]. Furthermore, the presented technique has been successfully applied for preparation of pyrazoles, mainly via condensation reactions starting with 1,3-dicarbonyls [25–30], chalcones [31], or enaminones [32], and appropriate hydrazine derivatives. Notably, to the best of our knowledge, no mechanochemical nitrile imine (3 + 2)-cycloadditions leading to pyrazoles have been reported.

In a series of recent works, we and other groups have demonstrated fluorinated nitrile imines of type **1** and C=C or C≡C dipolarophiles as superior reaction partners for the efficient preparation of fluoroalkylated pyrazole and pyrazoline derivatives. For example, electron-rich enamines [33], vinyl ethers [34], alkoxyallenes [35], and benzynes [36], as well as electron-deficient nitro- [37] and cyanoalkenes [38], isoxazolidinediones [39], quinones [40], and ynone derivatives [41] have served as dipolarophilic agents. Exemplary reactions leading to polysubstituted pyrazoles **2–4** and bicyclic analogues **5** (indazoles) are depicted in Scheme 1a. More recently, we disclosed a general two-step protocol for two types of multi-substituted 3-trifluoromethylpyrazoles comprising (3 + 2)-cycloaddition of in situ generated nitrile imines **1** with chalcones, followed by MnO<sub>2</sub>-mediated aromatization of the first 5-acylpyrazolines **6** formed [42]. Remarkably, depending on the solvent used, the oxidation step preferentially afforded fully substituted pyrazoles **7** (in polar solvents such as DMF or DMSO) or proceeded via a deacylative pathway (in non-polar solvents, e.g., in

hexane), leading to 1,3,4-trisubstituted pyrazoles **8** as major products (Scheme 1b). Taking into account the well-documented significance of both fluorinated and non-fluorinated pyrazoles in medicine and material sciences, the solvent-free mechanochemical protocols of the above (3 + 2)-cycloaddition reaction and subsequent oxidation step should be examined. Furthermore, the scope of the studied processes, towards non-fluorinated analogues, should also be checked. Here, we report our recent results on a two-step synthesis of 1,4-diarylpyrazoles functionalized with CF<sub>3</sub>, COOEt, Ac, or Ph groups at C(3) of the heterocyclic ring, under solvent-free ball-milling mechanochemical conditions.

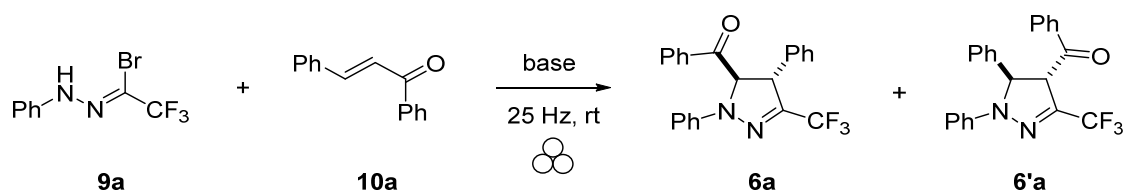


**Scheme 1.** Synthesis of fluoroalkylated pyrazoles through: (a) (3 + 2)-cycloadditions of nitrile imines **1** with selected C=C or C≡C dipolarophiles, leading to monocyclic (**2–4**) [34,39,41] and bicyclic (**5**) [36] derivatives and (b) trapping of **1** with enones, followed by MnO<sub>2</sub>-mediated oxidation of the first 5-acylpyrazolines **6** formed, leading to polysubstituted 3-trifluoromethylpyrazoles **7** and/or **8**.

## 2. Results and Discussion

The required CF<sub>3</sub>-nitrile imines of type **1** are readily available propargyl-type 1,3-dipoles, which can be generated in situ via base-induced dehydrohalogenation of the respective hydrazoneyl halides (or pseudohalides) [17,43]. A series of key precursors, namely hydrazoneyl bromides **9**, were prepared according to the general literature protocols, starting with commercially available substrates, i.e., fluoral hydrate and arylhydrazines [43–46]. According to our previous observations, the reversible generation of trifluoroacetonitrile imines **1** from the corresponding bromide **9** proceeds smoothly upon treatment with excess Et<sub>3</sub>N, at room temperature, in anhydrous THF as the solvent of choice. For this reason, initial mechanochemical experiments (steel balls,  $\varnothing$  7 mm; 25 Hz) were carried out using the known *C*-trifluoromethyl-*N*-phenyl nitrile imine (**1a**) and chalcone (**10a**) selected as model substrates, in the presence of Et<sub>3</sub>N (Scheme 2). As evidenced by TLC monitoring, a rapid (3 + 2)-cycloaddition reaction was observed, and after 1 h the expected 3-trifluoromethylpyrazoline **6a** was identified as a major component of the crude reaction mixture, along with small amounts of regioisomeric derivative **6'a** (in ca. 7:1 ratio, respectively), however, in moderate yield (56% conversion estimated based on <sup>1</sup>H NMR spectrum of crude mixture), as unconsumed chalcone **10a** accompanied by unidentified decomposition products of bromide **9a** were also detected. Then, the influence of a series of inorganic bases on the reaction course was briefly checked (Table 1). Whereas application of K<sub>2</sub>CO<sub>3</sub> as a base enhanced the conversion significantly (82%), further optimization with respect to the amount of nitrile imine precursor **9a** (1.2 equiv.) and with the volume of the

vessel used (5 mL) provided the (3 + 2)-cycloadducts in an excellent 93% yield. Subsequent separation by column chromatography provided spectroscopically pure samples of two pyrazolines, **6a** (75%) and **6'a** (13%). The relative orientation of substituents along the C(4)-C(5) bond in **6a** and **6'a** was established based on the  $^1\text{H}$  NMR spectra and by comparison with the literature data on other *trans*-configured 5-acylpyrazolines [42,47]. For example, in the case of compound **6a**, the diagnostic protons appeared as doublet of quartets ( $J_{\text{H-H}} = 5.6$  Hz,  $^4J_{\text{H-F}} \approx 0.9$  Hz) at  $\delta$  4.37 (4-H) and as doublet ( $J_{\text{H-H}} = 5.6$  Hz) at  $\delta$  5.76 (5-H), thereby confirming the fully diastereoselective addition of 1,3-dipole **1a** onto the C=C bond of the conjugated system of **10a**. The structure of minor isomer **6'a** was elucidated on the basis of  $^1\text{H}$  and  $^{13}\text{C}$  NMR supplemented with 2D NMR measurements (HMQC, HMBC). For example, in the  $^1\text{H}$  NMR spectrum of **6'a**, along with the characteristic set of signals attributed to phenyl groups, two additional absorptions, i.e., broadened doublet ( $J = 7.3$  Hz) located at  $\delta$  5.04 (4-H) and doublet ( $J_{\text{H-H}} = 7.3$  Hz) at  $\delta$  5.65 (5-H) nicely matched the proposed structure of **6'a**. Furthermore, in the  $^{13}\text{C}$  NMR spectrum of **6'a**, two diagnostic quartets found at  $\delta$  120.9 ( $^1J_{\text{C-F}} = 269.8$  Hz) and  $\delta$  133.5 ( $^2J_{\text{C-F}} = 38.0$  Hz), attributed to the  $\text{CF}_3$  group and C-3 atom, respectively, as well as a low intensity absorption (s) at  $\delta$  194.5 attributed to the C=O group, were found.



**Scheme 2.** Base-catalyzed mechanochemical (3 + 2)-cycloaddition of trifluoromethylated nitrile imine **1a** derived from hydrazonoyl bromide **9a** and chalcone (**10a**), leading to the isomeric benzoylpyrazolines **6a** (major) and **6'a** (minor).

**Table 1.** Optimization of (3 + 2)-cycloaddition reaction of **9a** and **10a**.

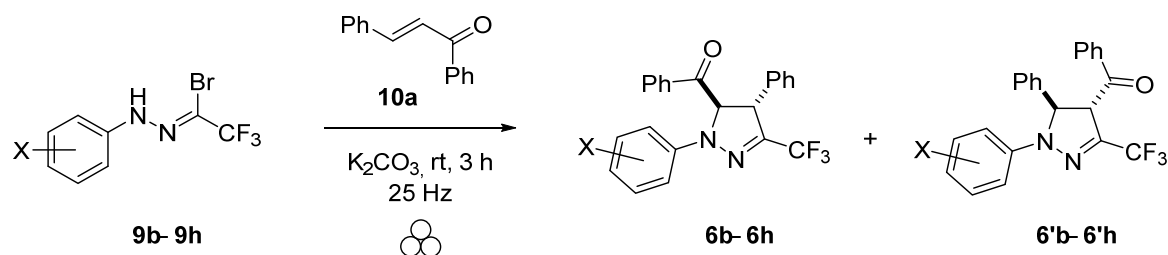
| Entry | Base                     | 9a:10a:Base<br>(Ratio) | Time<br>(min) | $V_{\text{jar}}$<br>(mL) | Conversion <sup>1</sup> (%) | Ratio (%) <sup>1</sup> (Isolated Yield) |         |
|-------|--------------------------|------------------------|---------------|--------------------------|-----------------------------|---|---------|
|       |                          |                        |               |                          |                             | 6a                                      | 6'a     |
| 1     | $\text{Et}_3\text{N}$    | 1.1:1.0:1.2            | 60            | 1.5                      | 56 <sup>2</sup>             | 87                                      | 13      |
| 2     | CsF                      | 1.1:1.0:1.2            | 60            | 1.5                      | 27 <sup>2</sup>             | 72                                      | 28      |
| 3     | KF                       | 1.1:1.0:1.2            | 60            | 1.5                      | 60 <sup>2</sup>             | 84                                      | 16      |
| 4     | $\text{Cs}_2\text{CO}_3$ | 1.1:1.0:1.2            | 60            | 1.5                      | 45 <sup>2</sup>             | 79                                      | 21      |
| 5     | $\text{K}_2\text{CO}_3$  | 1.1:1.0:1.2            | 60            | 1.5                      | 82                          | 81                                      | 19      |
| 6     | $\text{K}_2\text{CO}_3$  | 1.1:1.0:1.2            | 90            | 1.5                      | 84                          | 82                                      | 18      |
| 7     | $\text{K}_2\text{CO}_3$  | 1.2:1.0:1.3            | 90            | 5                        | 93                          | 80 (73)                                 | 20 (13) |
| 8     | $\text{K}_2\text{CO}_3$  | 1.2:1.0:1.3            | 180           | 5                        | 93                          | 82 (75)                                 | 18 (13) |

<sup>1</sup> Estimated based on  $^1\text{H}$  NMR spectra of crude reaction mixtures; <sup>2</sup> Partial decomposition of starting bromide **9a**.

It should be noted that the reaction of **9a** with **10a** carried out under classical conditions, i.e., in THF solution at room temperature, leads to pyrazoline **6a** (79%) exclusively, although after a rather long reaction time (4 days) [42]. In contrast, the mechanochemical activation of the studied (3 + 2)-cycloaddition provided the desired material **6a** in a comparable yield (75%) after a remarkably shorter reaction time of 3 h, but the competitive formation of small amounts of isomeric product **6'a** was observed.

With the optimized conditions in hand, we next turned our attention to the scope and limitations of the developed mechanochemical 1,3-dipolar cycloaddition. A series of nitrile imine precursors of type **9**, bearing either electron-donating (**9b–9d**) or electron-withdrawing (**9e**, **9g**, and **9h**) groups X located at *para* position of the phenyl ring, as well as disubstituted derivative **9f** (2,4- $\text{Cl}_2$ ), were examined in (3 + 2)-cycloadditions with a model chalcone (**10a**) (Scheme 3). As shown in Table 2, higher chemical yields were observed for reactions carried out with nitrile imine precursors **9b–9d**, i.e., bearing groups increasing the electron density at the negatively charged *N*-termini of the in situ generated dipole

**1**, and the expected products **6b–6d** (58–71%) were obtained after 3 h of only ball-milling. In contrast, in experiments performed with bromides functionalized with a strong EWG group (NO<sub>2</sub>, **9g**), and also with a PhCOO moiety (**9h**), complete consumption of the starting materials was observed after remarkably longer time (up to 24 h). In the latter cases, the formation of complex reaction mixtures also made the chromatographic isolation of the desired 5-benzoylpyrazolines **6** more difficult. Interestingly, despite the above differences, no remarkable impact of the electronic character of groups X on the regioselectivity of the studied (3 + 2)-cycloaddition could be observed. In all the cases, a mixture of isomeric products **6a–6h** and **6'a–6'h** in comparable ratios of ca. 4:1, respectively, were formed.



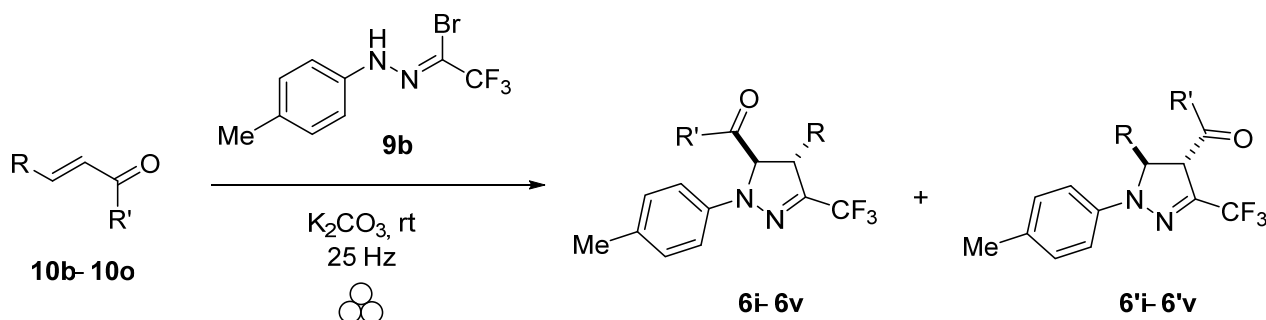
**Scheme 3.** Mechanochemical synthesis of 5-benzoyl-4-phenyl-3-trifluoromethylpyrazolines **6b–6h** derived from chalcone (**10a**); scope of hydrazonoyl bromides **9**.

**Table 2.** Ball-milling (3 + 2)-cycloadditions of **9b–9h** with model chalcone (**10a**).

| Entry          | Substrate | X                   | 6:6' Ratio <sup>1</sup> | Yield of <b>6</b> (%) <sup>2</sup> |
|----------------|-----------|---------------------|-------------------------|------------------------------------|
| 1              | <b>9b</b> | 4-Me                | 81:19                   | <b>6b</b> (70)                     |
| 2              | <b>9c</b> | 4- <i>i</i> -Pr     | 81:19                   | <b>6c</b> (71)                     |
| 3              | <b>9d</b> | 4-OBn               | 83:17                   | <b>6d</b> (58)                     |
| 4              | <b>9e</b> | 4-Cl                | 81:19                   | <b>6e</b> (53)                     |
| 5              | <b>9f</b> | 2,4-Cl <sub>2</sub> | 77:23                   | <b>6f</b> (54)                     |
| 6              | <b>9g</b> | 4-NO <sub>2</sub>   | 74:26                   | <b>6g</b> (10)                     |
| 7 <sup>3</sup> | <b>9g</b> | 4-NO <sub>2</sub>   | 79:21                   | <b>6g</b> (22)                     |
| 8 <sup>3</sup> | <b>9h</b> | 4-PhCOO             | 79:21                   | <b>6h</b> (17)                     |

<sup>1</sup> Estimated on the basis of <sup>1</sup>H NMR spectra of crude reaction mixtures; <sup>2</sup> Isolated yield; <sup>3</sup> Grinding time 24 h.

Next, to check the scope of chalcones and to test the functional group tolerance of mechanochemical (3 + 2)-cycloaddition, a series of aryl- and ferrocenyl-functionalized enones **10b–10o** were also added to the study and examined in reaction with *N*-(*p*-tolyl) nitrile imine **1b**, selected as a handful <sup>1</sup>H NMR-diagnostic representative (Scheme 4). In general, the expected 5-acylpyrazolines **6i–6v** were obtained in moderate to high yields, although longer reaction times were required to lead the reaction to completion in most cases (Table 3). Thus, apart from halogens (Cl, Br) and haloalkyl units (additional CF<sub>3</sub> group at phenyl ring), alkylamino and alkoxy substituents, as well as a ferrocenyl moiety, could be introduced.



**Scheme 4.** Synthesis of 5-acyl-3-trifluoromethylpyrazolines **6i–6v** using *N*-(*p*-tolyl) nitrile imine **1b** generated in situ from hydrazonoyl bromide **9b**; scope of chalcones **10**.

**Table 3.** Mechanochemical (3 + 2)-cycloadditions of **10b–10o** with model nitrile imine **1b**.

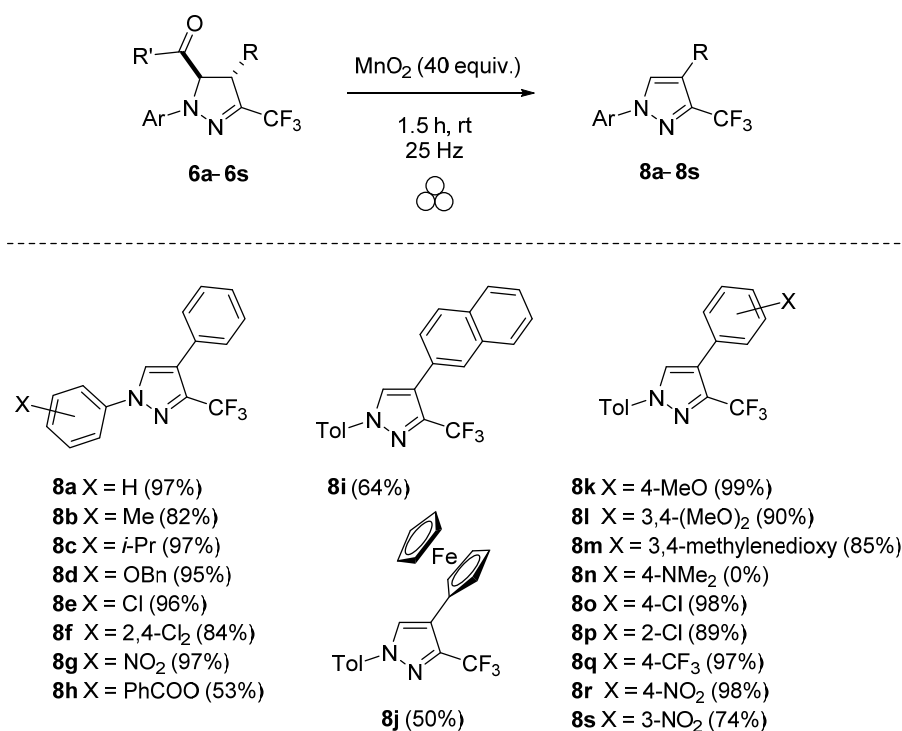
| Entry | Substrate  | R  | R'                                | Milling Time (h) | 6:6' Ratio (%) <sup>1</sup> | Yield of 6 (%) <sup>2</sup> |
|-------|------------|--|-----------------------------------|------------------|-----------------------------|-----------------------------|
| 1     | <b>10b</b> | 2-Nph <sup>3</sup>                                   | Ph                                | 9                | 77:23                       | <b>6i</b> (74)              |
| 2     | <b>10c</b> | Fc <sup>3</sup>                                      | Ph                                | 24               | 85:15                       | <b>6j</b> (38)              |
| 3     | <b>10d</b> | 4-MeOC <sub>6</sub> H <sub>4</sub>                   | Ph                                | 20               | 76:24                       | <b>6k</b> (59)              |
| 4     | <b>10e</b> | 3,4-(MeO) <sub>2</sub> C <sub>6</sub> H <sub>3</sub> | Ph                                | 18               | 100:0                       | <b>6l</b> (74)              |
| 5     | <b>10f</b> | 3,4-methylenedioxyphenyl                             | Ph                                | 12               | 88:12                       | <b>6m</b> (68)              |
| 6     | <b>10g</b> | 4-(Me <sub>2</sub> N)C <sub>6</sub> H <sub>4</sub>   | Ph                                | 36               | 65:35                       | <b>6n</b> (46)              |
| 7     | <b>10h</b> | 4-ClC <sub>6</sub> H <sub>4</sub>                    | Ph                                | 9                | 79:21                       | <b>6o</b> (70)              |
| 8     | <b>10i</b> | 2-ClC <sub>6</sub> H <sub>4</sub>                    | Ph                                | 10               | 77:23                       | <b>6p</b> (57)              |
| 9     | <b>10j</b> | 4-CF <sub>3</sub> C <sub>6</sub> H <sub>4</sub>      | Ph                                | 9                | 71:29                       | <b>6q</b> (28)              |
| 10    | <b>10k</b> | 4-NO <sub>2</sub> C <sub>6</sub> H <sub>4</sub>      | Ph                                | 28               | 73:27                       | <b>6r</b> (26)              |
| 11    | <b>10l</b> | 3-NO <sub>2</sub> C <sub>6</sub> H <sub>4</sub>      | Ph                                | 72               | 79:21                       | <b>6s</b> (65)              |
| 12    | <b>10m</b> | Ph   | Fc <sup>3</sup>                   | 24               | 71:29                       | <b>6t</b> (39)              |
| 13    | <b>10n</b> | Ph   | 4-BrC <sub>6</sub> H <sub>4</sub> | 16               | 85:15                       | <b>6u</b> (68)              |
| 14    | <b>10o</b> | Ph   | 3,4-methylenedioxyphenyl          | 20               | 82:18                       | <b>6v</b> (81)              |

<sup>1</sup> Estimated based on <sup>1</sup>H NMR spectra of crude reaction mixtures; <sup>2</sup> Isolated yield; <sup>3</sup> 2-Nph = naphth-2-yl; Fc = ferrocenyl.

Similarly to the results collected for series **6/6'a–6/6'h** (Schemes 2 and 3, Table 2), (3 + 2)-cycloadditions of **1b** with selected chalcones **10b–10o** proceeded in a comparable regioselectivity of ca. 4:1 in favor of 5-acylpyrazolines **6**. Again, only *trans*-configured products could be detected in the mother liquors. Interestingly, in the case of 3,4-methylenedioxy-functionalized chalcone (**10f**) and 3,4-dimethoxy analogue (**10e**), exceptionally high selectivity (ca. 9:1) or exclusive formation of target 5-acylpyrazolines **6m** and **6l**, respectively, was observed. On the other hand, the reaction of **1b** with another electron-rich chalcone, namely 4-(dimethylamino)chalcone (**10g**), provided only the expected (3 + 2)-cycloadducts **6n** and **6'n** as a ca. 2:1 mixture. Possibly, the observed decrease of selectivity resulted from the presence of the basic Me<sub>2</sub>N group in **10g**, which can compete with K<sub>2</sub>CO<sub>3</sub> in dehydrohalogenation of **9b**, thereby changing the electronic properties of chalcone **10g**, due to protonation. The observed moderate yield in cycloadditions of **1b** with chalcones **10c** and **10m**, leading to pyrazolines **6j** (38%) and **6t** (39%), also deserves a brief comment. Seemingly, the presence of the redox-active Fc group alters the reaction outcome and leads to complex mixtures, irrespective of the substitution pattern in chalcone.

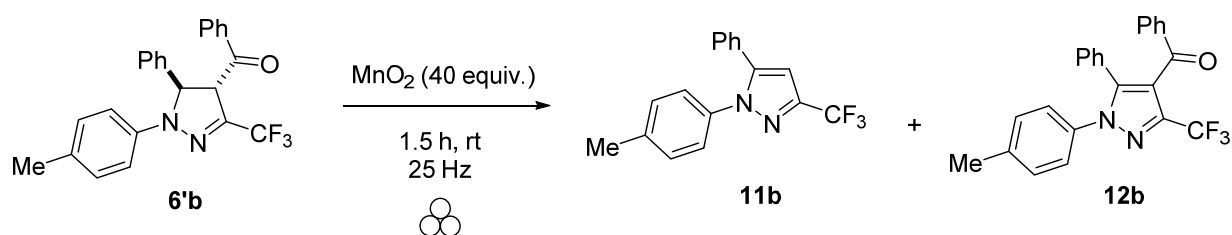
Prompted by the results disclosed in our recent work on the solvent-dependent oxidation of 5-benzoylpyrazolines [42], a series of 3-trifluoromethylated cycloadducts of type **6** were oxidized with an excess of activated MnO<sub>2</sub> under mechanochemical conditions. In a typical experiment, pyrazoline **6a** (1.0 mmol) was reacted with oxidant (activated MnO<sub>2</sub>, ca. 85%, <10 μm, 40 equiv.) using zirconium oxide ball-milling equipment (ball, ø 10 mm; jar, 10 mL), at 25 Hz. After the reaction was complete (1.5 h), the resulting material was washed with AcOEt and filtered through a short silica gel pad, to give 1,5-diphenyl-3-trifluoromethylpyrazole (**8a**), isolated as a sole product in excellent purity and a yield of 97% (Scheme 5). The observed result for MnO<sub>2</sub>-mediated mechanochemical deacylative oxidation nicely correspond to the recently reported aromatizative debenzoylation of **6a** carried out in non-polar solvents (i.e., hexane solutions). However, the latter protocol provided the final product **8a** after 2 days, by heating the reactants in organic medium at 60 °C [42].

Unfortunately, an attempted one-pot two-step synthesis of pyrazole **8a** was in vain. In the mentioned experiment, hydrazoneyl bromide **9a** and chalcone **10a** were mechanochemically reacted under the developed conditions (in the presence of K<sub>2</sub>CO<sub>3</sub>), followed by treatment of the resulting crude reaction mixture with excess activated MnO<sub>2</sub>. To our surprise, none of the expected pyrazole **8a** was detected in the mixture, thus indicating the necessity of (at least partial) pre-purification of the intermediate 5-benzoylpyrazoline **6a**. Indeed, simple filtration of crude **6a** through a short silica gel pad enabled fast synthesis of desired material **8a**, which was isolated in a high 66% overall yield (for two steps).



**Scheme 5.** Mechanochemical MnO<sub>2</sub>-mediated deacylative oxidation of 5-acylpyrazolines **6a–6s**, leading to 1,4-diaryl-3-trifluoromethylpyrazoles **8a–8s**.

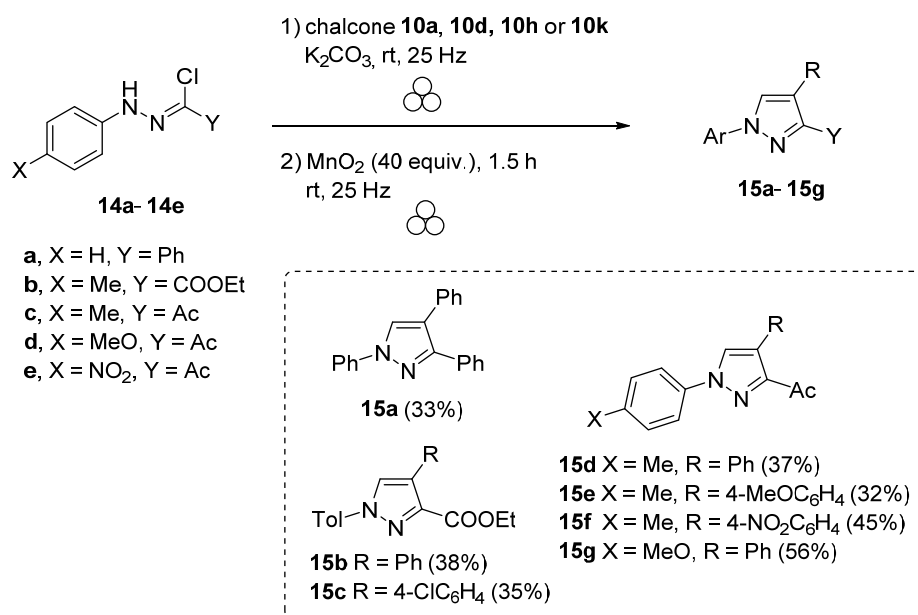
In continuation, a series of pyrazolines **6b–6s** was examined in reaction with MnO<sub>2</sub> under mechanochemical activation to afford the expected 1,4-diaryl-3-trifluoromethylpyrazoles **8b–8s** identified as the exclusive aromatization products, which were generally isolated in excellent yields. Only in the case of 4-benzoyloxy derivative (**6h**) and ferrocenyl-functionalized analogue (**6j**), either partial decomposition of the starting material or competitive dehydrogenative oxidation, leading to a fully substituted analogue (**7j**), respectively, was observed, and moderate amounts of the final pyrazoles **8h** (53%) and **8j** (50%) were isolated. Surprisingly, the attempted oxidation of pyrazoline **6n** bearing Me<sub>2</sub>N group resulted in complete decomposition of the starting material under the applied conditions. In order to check the reaction outcome in mechanochemical oxidation of isomeric 4-acylpyrazolines of type **6'**, available as minor products in (3 + 2)-cycloaddition of nitrile imines **1** and chalcones **10**, a model *trans*-4-benzoyl-5-phenyl-1-*p*-tolyl-3-trifluoromethylpyrazoline (**6'b**) was also examined under analogous reaction conditions. As shown in Scheme 6, treatment of the starting material **6'b** with excess MnO<sub>2</sub> provided, after 1.5 h of milling, a mixture of two pyrazole-based products in ca. 2:3 ratio, and they were identified as 5-phenyl-1-*p*-tolyl-3-trifluoromethylpyrazole (**11b**, 38%) and its 4-benzoylated analogue **12b** (56%). This result indicates that, in contrast to 5-acylpyrazoline **6b**, ball-milling oxidation of its structural isomer 4-acylpyrazoline **6'b** proceeds in low chemoselectivity and leads to dehydrogenative oxidation of product **12b** as a major component of the mixture.



**Scheme 6.** Synthesis of pyrazoles **11b** and **12b** formed via competitive deacylative vs. dehydrogenative aromatization of 4-benzoylpyrazoline **6'b**.

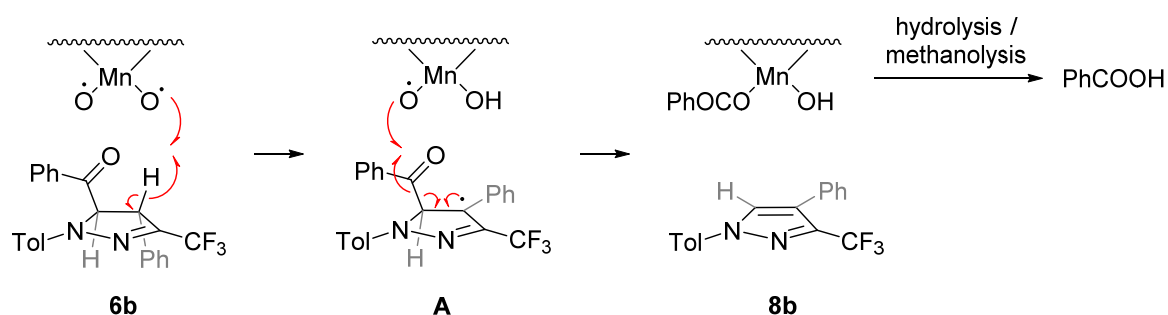


Finally, to further check the scope, a series of non-fluorinated pyrazolines **13a–13g** were prepared and examined in a mechanochemical oxidation reaction with activated  $\text{MnO}_2$ . Following the general protocol, five nitrile imine precursors **14a–14e** bearing either phenyl group or selected electron-withdrawing substituents ( $\text{COOEt}$ ,  $\text{Ac}$ ) located at the C-termini were reacted with a set of representative chalcones: **10a** ( $X = \text{H}$ ), **10d** ( $\text{OMe}$ ), **10h** ( $\text{Cl}$ ), and **10k** ( $X = \text{NO}_2$ ) (Scheme 7). The first formed 5-acylpyrazoline derivatives **13** were pre-purified by filtration through a short silica gel pad and subsequently reacted with  $\text{MnO}_2$  to provide the expected 1,3,4-trisubstituted pyrazoles **15a–15g** in an acceptable overall yield of 32–56% (for two steps). However, in the case of the highly electron-deficient nitrile imine **1e** functionalized with  $\text{O}_2\text{NC}_6\text{H}_4$ - and  $\text{Ac}$  groups, the (3 + 2)-cycloaddition step with chalcone **10a** afforded a complex mixture in which trace amounts of the expected pyrazoline **13h** (<5%) were detected. The presented results indicate that, along with trifluoromethylated nitrile imines, analogues bearing aryl, ester or acyl groups can also be applied in the developed two-step synthesis of 1,3,4-trisubstituted pyrazoles.



**Scheme 7.** Two-step synthesis of pyrazoles **15a–15g** using non-fluorinated nitrile imine precursors of type **14**.

It should be pointed out that all the presented deacylative oxidations of benzoylpyrazolines were performed using activated  $\text{MnO}_2$  ( $\approx 85\%$  purity,  $<10\ \mu\text{m}$ , Sigma Aldrich, St. Louis, MO, USA), which was used as received. In order to gain a greater insight about the studied transformation, non-activated manganese dioxide (Reagent Plus<sup>®</sup>,  $>99\%$ , Sigma Aldrich) was also tested, but in this case no deacylative aromatization could be observed when using 5-benzoylpyrazoline **6b** as a model compound. To test if hydroxyl radicals were involved in deacylative aromatization of **6b**, the latter experiment was repeated in the presence of trace amounts of water, but the reaction was not triggered. Finally, treatment of the resulting insoluble material formed in deacylative oxidation of **6b** with aqueous methanol released a colorless byproduct identified as benzoic acid. Based on these observations, the mechanism of the studied reaction is tentatively proposed. As depicted in Scheme 8, oxidation of **6b** proceeds preferentially at C(4), leading to fairly stable benzyl-type radical **A**. Then, the acyl group is transferred [48] from **A** onto the activated surface of the heterogeneous oxidant to give the aromatized product **8b** [49]. On the other hand, the presence of the benzoyl group at C(4) in isomeric pyrazoline **6'b** enhances the acidity of this position; and thus, the oxidation may possibly be initiated either at C(4) or at C(5), leading to a mixture of products formed via competitive dehydrogenation vs. deacylative aromatization processes.



**Scheme 8.** Proposed mechanism of deacylative oxidation of 5-acylpyrazolines.

### 3. Materials and Methods

#### 3.1. Chemical Synthesis General Methods

**Experimental procedures:** The ball-milling apparatus used was a Retsch MM 400 mixer mill (Retsch GmbH, Haan, Germany). Mechanochemical (3 + 2)-cycloadditions were performed in 5 mL stainless steel jars, with three stainless steel balls (7 mm diameter); oxidation reactions were conducted in 10 mL zirconium oxide jars, with one zirconium oxide ball (10 mm diameter). Solvents (hexane, CH<sub>2</sub>Cl<sub>2</sub>, AcOEt) were purchased and used as received. Products were purified by filtration through a short silica gel plug or by standard column chromatography (CC) on silica gel (230–400 mesh; Merck, Kenilworth, NJ, USA). The NMR spectra were taken on a Bruker AVIII instrument (<sup>1</sup>H at 600 MHz, <sup>13</sup>C at 151 MHz, and <sup>19</sup>F at 565 MHz) (Bruker BioSpin AG, Fällanden, Switzerland). Chemical shifts are reported relative to solvent residual peaks; for CDCl<sub>3</sub>: <sup>1</sup>H NMR: δ = 7.26, <sup>13</sup>C NMR: δ = 77.16, or to CFCl<sub>3</sub> (<sup>19</sup>F NMR: δ = 0.00) used as an external standard. Multiplicity of the signals in <sup>13</sup>C NMR spectra were deduced based on supplementary 2D measurements (HMQC, HMBC). The IR spectra were measured with an Agilent Cary 630 FTIR spectrometer (Agilent Technologies, Santa Clara, CA, USA), in neat. MS (ESI) were performed with a Varian 500-MS LC Ion Trap (Varian, Inc., Walnut Creek, CA, USA), while high resolution MS (ESI-TOF) measurements were taken with a Waters Synapt G2-Si mass spectrometer (Waters Corporation, Milford, MA, USA). Elemental analyses were performed with a Vario EL III (Elementar Analysensysteme GmbH, Langensfeld, Germany) instrument. Melting points were determined in capillaries with a MEL-TEMP apparatus (Laboratory Devices, Holliston, MA, USA) and are uncorrected. <sup>1</sup>H, <sup>13</sup>C, and <sup>19</sup>F NMR spectra of all new compounds can be found at Supplementary Materials file.

**Starting materials:** The CF<sub>3</sub>-nitrile imine precursors of type **9** were prepared by bromination of the corresponding trifluoroacetaldehyde arylhydrazones with NBS, according to the general protocol [43]. The required fluoral hydrazones were synthesized following the general literature procedure by condensation of aqueous fluoral hydrate (~75% in H<sub>2</sub>O) with commercial arylhydrazines [46]. Non-fluorinated hydrazonoyl chlorides **14a–14e** were prepared as previously reported [44,45]. Chalcones **10** were purchased or prepared via classical Claisen–Schmidt condensation, starting with appropriate aldehydes and methyl ketones, in ethanol. Activated MnO<sub>2</sub> (ca. 85%, <10 μm, Sigma-Aldrich, product no. 217646-100G), as well as the other commercially available solvents and starting materials, were purchased and used as received.

##### 3.1.1. General Procedure for Mechanochemical Synthesis of Pyrazolines **6**, **6'**, and **13**

Hydrazonoyl halide **9** or **14** (1.2 mmol), chalcone **10** (1.0 mmol), and solid K<sub>2</sub>CO<sub>3</sub> (1.3 mmol, 179 mg) were placed in a 5 mL stainless steel grinding jar with three stainless steel balls (7 mm diameter). The jar was closed and ball-milled at 25 Hz until the starting chalcone was fully consumed. Then, CH<sub>2</sub>Cl<sub>2</sub> (10 mL) was added, the precipitate was filtered off, washed with CH<sub>2</sub>Cl<sub>2</sub> (2 × 10 mL), and the solvent was removed under vacuum. The crude product of type **6** or **13** was purified by standard column chromatography (CC) or pre-purified by flash column chromatography (FCC) on silica. The structures of known pyrazolines **6c–6k**, **6o**, **6q**, **6r**, **6t–6v** were confirmed based on <sup>1</sup>H NMR spectra

supplemented by ESI-MS measurements and by comparison with original samples [42]; the byproducts **6'c–6'v** were not isolated. In the case of non-fluorinated analogues, crude pyrazolines **13a,13d–13g** were pre-purified by FCC and used for the next step, without further purification.

*trans*-5-Benzoyl-1,4-diphenyl-3-trifluoromethyl-4,5-dihydro-1H-pyrazole (**6a**) [50]: light yellow solid, 296 mg (75%), mp 159–161 °C. <sup>1</sup>H NMR (600 MHz, CDCl<sub>3</sub>) δ 4.37 (dq, <sup>4</sup>J<sub>H-F</sub> ≈ 0.9 Hz, J<sub>H-H</sub> = 5.6 Hz, 1H, 4-H), 5.76 (d, J<sub>H-H</sub> = 5.6 Hz, 1H, 5-H), 6.94–7.06, 7.19–7.29, 7.39–7.44, 7.48–7.52, 7.65–7.68, 7.87–7.89 (6m, 3H, 4H, 3H, 2H, 1H, 2H). <sup>13</sup>C NMR (151 MHz, CDCl<sub>3</sub>) δ 55.6, 74.3, 113.8, 120.9 (q, <sup>1</sup>J<sub>C-F</sub> = 270.6 Hz, CF<sub>3</sub>), 121.6, 127.7, 128.9, 129.2, 129.3, 129.5, 129.7, 133.1, 134.7, 137.5, 138.1 (q, <sup>2</sup>J<sub>C-F</sub> = 37.0 Hz, C-3), 142.7, 192.1. <sup>19</sup>F NMR (565 MHz, CDCl<sub>3</sub>) δ –63.0 (s<sub>br</sub>, CF<sub>3</sub>). ESI-MS (*m/z*) 417.2 (100, [M + Na]<sup>+</sup>).

*trans*-4-Benzoyl-1,5-diphenyl-3-trifluoromethyl-4,5-dihydro-1H-pyrazole (**6'a**): obtained as a minor product in the reaction of **9a** with **10a**; yellow solid, 51 mg (13%), mp 125–126 °C. <sup>1</sup>H NMR (600 MHz, CDCl<sub>3</sub>) δ 5.04 (d<sub>br</sub>, J<sub>H-H</sub> ≈ 7.3 Hz, 1H, 4-H), 5.65 (d, J<sub>H-H</sub> = 7.3 Hz, 1H, 5-H), 6.88–6.91, 7.03–7.06, 7.17–7.20, 7.23–7.25, 7.33–7.40, 7.48–7.51, 7.63–7.66, 7.88–7.90 (8m, 1H, 2H, 2H, 2H, 3H, 2H, 1H, 2H). <sup>13</sup>C NMR (151 MHz, CDCl<sub>3</sub>) δ 61.2, 71.0, 114.8, 120.9 (q, <sup>1</sup>J<sub>C-F</sub> = 269.8 Hz, CF<sub>3</sub>), 121.7, 126.0, 128.9, 129.14, 129.15, 129.16, 129.8, 133.5 (q, <sup>2</sup>J<sub>C-F</sub> = 38.0 Hz, C-3), 134.5, 135.5, 139.6, 142.6, 194.5. <sup>19</sup>F NMR (565 MHz, CDCl<sub>3</sub>) δ –63.1 (s, CF<sub>3</sub>). IR (neat) *v* 1677, 1595, 1577, 1301, 1264, 1208, 1148, 1118, 1066 cm<sup>−1</sup>. ESI-MS (*m/z*) 417.1 (31, [M + Na]<sup>+</sup>), 395.2 (100, [M + H]<sup>+</sup>).

*trans*-5-Benzoyl-1-(*p*-tolyl)-4-phenyl-3-trifluoromethyl-4,5-dihydro-1H-pyrazole (**6b**) [51]: light yellow solid, 286 mg (70%), mp 145–147 °C. <sup>1</sup>H NMR (600 MHz, CDCl<sub>3</sub>) δ 2.30 (s, 3H, Me), 4.38 (dq, <sup>4</sup>J<sub>H-F</sub> ≈ 1.0 Hz, J<sub>H-H</sub> ≈ 5.7 Hz, 1H, 4-H), 5.78 (d<sub>br</sub>, J ≈ 5.7 Hz, 1H, 5-H), 6.97, 7.09 (2d, J = 8.6 Hz, 2H each), 7.21–7.25, 7.40–7.52, 7.66–7.69, 7.88–7.91 (4m, 2H, 5H, 1H, 2H). <sup>13</sup>C NMR (151 MHz, CDCl<sub>3</sub>) δ 20.7, 55.6, 74.6, 113.9, 121.0 (q, <sup>1</sup>J<sub>C-F</sub> = 270.3 Hz, CF<sub>3</sub>), 127.5, 129.0, 129.1, 129.3, 129.7, 130.0, 130.9, 133.2, 134.6, 137.4 (q, <sup>2</sup>J<sub>C-F</sub> = 36.8 Hz, C-3), 137.6, 140.5, 192.3. <sup>19</sup>F NMR (565 MHz, CDCl<sub>3</sub>) δ –63.1 (s, CF<sub>3</sub>). ESI-MS (*m/z*) 431.2 (100, [M + Na]<sup>+</sup>).

*trans*-4-Benzoyl-1-(*p*-tolyl)-5-phenyl-3-trifluoromethyl-4,5-dihydro-1H-pyrazole (**6'b**): obtained as a minor product in the reaction of **9b** with **10a**; thick yellow oil, 53 mg (13%). <sup>1</sup>H NMR (600 MHz, CDCl<sub>3</sub>) δ 2.23 (s, 3H, Me), 5.04 (dq<sub>br</sub>, <sup>4</sup>J<sub>H-F</sub> ≈ 1.6 Hz, J<sub>H-H</sub> ≈ 7.5 Hz, 1H, 4-H), 5.64 (d, J<sub>H-H</sub> ≈ 7.5 Hz, 1H, 5-H), 6.93–7.00, 7.22–7.25, 7.32–7.39, 7.47–7.50, 7.63–7.66, 7.87–7.90 (6m, 4H, 2H, 3H, 2H, 1H, 2H). <sup>13</sup>C NMR (151 MHz, CDCl<sub>3</sub>) δ 20.7, 61.1, 71.2, 114.8, 121.0 (q, <sup>1</sup>J<sub>C-F</sub> = 269.5 Hz, CF<sub>3</sub>), 126.1, 128.8, 129.12, 129.14, 129.7, 129.8, 131.2, 132.8 (q, <sup>2</sup>J<sub>C-F</sub> = 37.9 Hz, C-3), 134.5, 135.4, 139.7, 140.3, 194.6. <sup>19</sup>F NMR (565 MHz, CDCl<sub>3</sub>) δ –63.0 (s, CF<sub>3</sub>). IR (neat) *v* 1752, 1662, 1495, 1446, 1260, 1219, 1163, 1133 cm<sup>−1</sup>. ESI-MS (*m/z*) 431.4 (100, [M + Na]<sup>+</sup>), 409.5 (39, [M + H]<sup>+</sup>). Anal. Calcd for C<sub>24</sub>H<sub>19</sub>F<sub>3</sub>N<sub>2</sub>O (408.1): C 70.58, H 4.69, N 6.86; found: C 70.49, H 4.69, N 6.89.

*trans*-5-Benzoyl-4-(3',4'-dimethoxyphenyl)-1-(*p*-tolyl)-3-trifluoromethyl-4,5-dihydro-1H-pyrazole (**6l**): light yellow solid, 347 mg (74%), mp 122–123 °C. <sup>1</sup>H NMR (600 MHz, CDCl<sub>3</sub>) δ 2.27 (s, 3H, Me), 3.81, 3.91 (2s, 3H each, 2OMe), 4.33 (d<sub>br</sub>, J ≈ 5.9 Hz, 1H, 4-H), 5.73 (d, J = 5.9 Hz, 1H, 5-H), 6.65 (d, J = 2.1 Hz, 1H), 6.76 (dd, J = 2.1, 8.2 Hz, 1H), 6.88 (d, J = 8.2 Hz, 1H), 6.91–6.93, 7.05–7.08, 7.48–7.51, 7.64–7.68, 7.87–7.90 (5m, 2H, 2H, 2H, 1H, 2H). <sup>13</sup>C NMR (151 MHz, CDCl<sub>3</sub>) δ 20.7, 55.4, 56.1, 56.2, 74.5, 110.4, 111.8, 113.9, 120.2, 121.0 (q, <sup>1</sup>J<sub>C-F</sub> = 270.4 Hz, CF<sub>3</sub>), 129.3 \*, 129.8, 130.0, 131.0, 133.2, 134.6, 137.4 (q, <sup>2</sup>J<sub>C-F</sub> = 36.6 Hz, C-3), 140.5, 149.5, 149.8, 192.4; \* higher intensity. <sup>19</sup>F NMR (565 MHz, CDCl<sub>3</sub>) δ –62.2 (s, CF<sub>3</sub>). IR (neat) *v* 1695, 1595, 1513, 1450, 1293, 1230, 1118 cm<sup>−1</sup>. HRMS (ESI-TOF) *m/z*: [M + H]<sup>+</sup> calcd for C<sub>26</sub>H<sub>24</sub>F<sub>3</sub>N<sub>2</sub>O<sub>3</sub> 469.1739, found 469.1743.

*trans*-5-Benzoyl-4-(3',4'-methylenedioxyphenyl)-1-(*p*-tolyl)-3-trifluoromethyl-4,5-dihydro-1H-pyrazole (**6m**): pale yellow solid, 307 mg (68%), mp 125–126 °C. <sup>1</sup>H NMR (600 MHz, CDCl<sub>3</sub>) δ 2.28 (s, 3H, Me), 4.31 (d<sub>br</sub>, J ≈ 5.5 Hz, 1H, 4-H), 5.73 (d, J = 5.5 Hz, 1H, 5-H), 6.01 (AB system, J = 4.8 Hz, 2H, OCH<sub>2</sub>O), 6.66–6.69 (m, 2H), 6.82 (d, J = 7.8 Hz, 1H), 6.92–6.94, 7.07–7.09, 7.50–7.54, 7.66–7.69, 7.90–7.92 (5m, 2H, 2H, 2H, 1H, 2H). <sup>13</sup>C NMR (151 MHz, CDCl<sub>3</sub>) δ 20.7, 55.3, 74.4, 101.7, 107.6, 109.0, 113.8, 121.0 (q, <sup>1</sup>J<sub>C-F</sub> = 270.3 Hz, CF<sub>3</sub>), 121.9, 129.2, 129.3, 130.0, 131.0, 131.2, 133.1, 134.6, 137.5 (q, <sup>2</sup>J<sub>C-F</sub> = 36.7 Hz, C-3), 140.4, 148.2,

148.9, 192.2.  $^{19}\text{F}$  NMR (565 MHz,  $\text{CDCl}_3$ )  $\delta$   $-62.3$  (s,  $\text{CF}_3$ ). IR (neat)  $\nu$  1685, 1595, 1517, 1446, 1245, 1118  $\text{cm}^{-1}$ . HRMS (ESI-TOF)  $m/z$ :  $[\text{M} + \text{H}]^+$  calcd for  $\text{C}_{25}\text{H}_{20}\text{F}_3\text{N}_2\text{O}_3$  453.1426, found 453.1427.

*trans*-5-Benzoyl-4-(4'-dimethylaminophenyl)-1-(*p*-tolyl)-3-trifluoromethyl-4,5-dihydro-1H-pyrazole (**6n**): orange solid, 208 mg (46%), mp 163–165 °C.  $^1\text{H}$  NMR (600 MHz,  $\text{CDCl}_3$ )  $\delta$  2.27 (s, 3H, Me), 2.99 (s, 6H, 2Me), 4.30 (d<sub>br</sub>,  $J \approx 5.5$  Hz, 1H, 4-H), 5.69 (d,  $J = 5.5$  Hz, 1H, 5-H), 6.69–6.72, 6.90–6.92, 7.03–7.07, 7.47–7.51, 7.64–7.66, 7.89–7.91 (6m, 2H, 2H, 4H, 2H, 1H, 2H).  $^{13}\text{C}$  NMR (151 MHz,  $\text{CDCl}_3$ )  $\delta$  20.7, 40.5, 55.1, 74.7, 112.9, 113.7, 121.1 (q,  $^1J_{\text{C-F}} = 270.5$  Hz,  $\text{CF}_3$ ), 124.6, 128.5, 129.22, 129.25, 130.0, 130.6, 133.3, 134.4, 138.1 (q,  $^2J_{\text{C-F}} = 36.2$  Hz, C-3), 140.7, 150.7, 192.5.  $^{19}\text{F}$  NMR (565 MHz,  $\text{CDCl}_3$ )  $\delta$   $-62.3$  (s,  $\text{CF}_3$ ). IR (neat)  $\nu$  1696, 1595, 1517, 1297, 1230, 1185, 1118, 1066  $\text{cm}^{-1}$ . ESI-MS ( $m/z$ ) 474.4 (100,  $[\text{M} + \text{Na}]^+$ ), 452.4 (97,  $[\text{M} + \text{H}]^+$ ). Anal. Calcd for  $\text{C}_{26}\text{H}_{24}\text{F}_3\text{N}_3\text{O}$  (451.2): C 69.17, H 5.36, N 9.31; found: C 69.11, H 5.26, N 9.30.

*trans*-5-Benzoyl-4-(2'-chlorophenyl)-1-(*p*-tolyl)-3-trifluoromethyl-4,5-dihydro-1H-pyrazole (**6p**): thick light orange oil, 252 mg (57%).  $^1\text{H}$  NMR (600 MHz,  $\text{CDCl}_3$ )  $\delta$  2.28 (s, 3H, Me), 5.10 (s<sub>br</sub>, 1H, 4-H), 5.76 (s<sub>br</sub>, 1H, 5-H), 6.93–6.95, 7.06–7.09, 7.25–7.36, 7.43–7.50, 7.64–7.67, 7.84–7.88 (6m, 2H, 2H, 3H, 3H, 1H, 2H).  $^{13}\text{C}$  NMR (151 MHz,  $\text{CDCl}_3$ )  $\delta$  20.7, 50.9(br), 74.0(br), 113.9, 120.8 (q,  $^1J_{\text{C-F}} = 270.3$  Hz,  $\text{CF}_3$ ), 128.4(br), 129.1, 129.2 \*, 130.0, 130.2, 130.4(br), 131.2, 133.2(br), 136.6, 135.3(br), 136.8 (q<sub>br</sub>,  $^2J_{\text{C-F}} \approx 37.0$  Hz, C-3), 140.4, 192.6; \*higher intensity.  $^{19}\text{F}$  NMR (565 MHz,  $\text{CDCl}_3$ )  $\delta$   $-62.6$  (s,  $\text{CF}_3$ ). IR (neat)  $\nu$  1692, 1599, 1517, 1297, 1230, 1118, 1066  $\text{cm}^{-1}$ . ESI-MS ( $m/z$ ) 465.4 (100,  $[\text{M} + \text{Na}]^+$ ), 443.5 (83,  $[\text{M} + \text{H}]^+$ ). Anal. Calcd for  $\text{C}_{24}\text{H}_{18}\text{F}_3\text{N}_2\text{O}$  (442.1): C 65.09, H 4.10, N 6.33; found: C 65.00, H 4.02, N 6.14.

*trans*-5-Benzoyl-4-(3'-nitrophenyl)-1-(*p*-tolyl)-3-trifluoromethyl-4,5-dihydro-1H-pyrazole (**6s**): light yellow solid, 295 mg (65%), mp 170–172 °C.  $^1\text{H}$  NMR (600 MHz,  $\text{CDCl}_3$ )  $\delta$  2.28 (s, 3H, Me), 4.50 (d<sub>br</sub>,  $J \approx 5.6$  Hz, 1H, 4-H), 5.75 (d,  $J = 5.6$  Hz, 1H, 5-H), 6.93–6.95, 7.07–7.09, 7.50–7.54 (3m, 2H, 2H, 2H), 7.55 (dt,  $J = 1.4, 7.8$  Hz, 1H), 7.62–7.65, 7.68–7.71, 7.85–7.87 (3m, 1H, 1H, 2H), 8.07 (pseudo-t,  $J \approx 2.0$  Hz, 1H), 8.28 (ddd,  $J = 1.1, 2.2, 8.2$  Hz, 1H).  $^{13}\text{C}$  NMR (151 MHz,  $\text{CDCl}_3$ )  $\delta$  20.7, 54.8, 74.1, 114.1, 120.8 (q,  $^1J_{\text{C-F}} = 270.2$  Hz,  $\text{CF}_3$ ), 122.7, 124.1, 129.1, 129.6, 130.1, 131.0, 131.7, 132.9, 133.6, 135.0, 136.1 (q,  $^2J_{\text{C-F}} = 37.3$  Hz, C-3), 139.5, 140.0, 149.0, 191.6.  $^{19}\text{F}$  NMR (565 MHz,  $\text{CDCl}_3$ )  $\delta$   $-62.2$  (s,  $\text{CF}_3$ ). IR (neat)  $\nu$  1689, 1595, 1536, 1353, 1297, 1230, 1152, 1122, 1070  $\text{cm}^{-1}$ . ESI-MS ( $m/z$ ) 476.4 (100,  $[\text{M} + \text{Na}]^+$ ), 454.4 (50,  $[\text{M} + \text{H}]^+$ ). Anal. Calcd for  $\text{C}_{24}\text{H}_{18}\text{F}_3\text{N}_3\text{O}_3$  (453.1): C 63.58, H 4.00, N 9.27; found: C 63.49, H 4.04, N 9.29.

Ethyl *trans*-5-benzoyl-4-phenyl-1-(*p*-tolyl)-4,5-dihydro-1H-pyrazole-3-carboxylate (**13b**): light yellow solid, 234 mg (57%), mp 133–134 °C.  $^1\text{H}$  NMR (600 MHz,  $\text{CDCl}_3$ )  $\delta$  1.20 (t,  $J = 7.1$  Hz, 3H, Et), 2.28 (s, 3H, Me), 4.13 (dq,  $J = 7.1, 10.9$  Hz, 1H, Et), 4.20 (dq,  $J = 7.1, 10.9$  Hz, 1H, Et), 4.46 (d,  $J = 4.9$  Hz, 1H, 4-H), 5.79 (d,  $J = 4.9$  Hz, 1H, 5-H), 7.02–7.09, 7.21–7.23, 7.34–7.40, 7.49–7.52, 7.65–7.67, 7.90–7.92 (6m, 4H, 2H, 3H, 2H, 1H, 2H).  $^{13}\text{C}$  NMR (151 MHz,  $\text{CDCl}_3$ )  $\delta$  14.2, 20.7, 55.4, 61.2, 74.3, 114.4, 127.5, 128.4, 129.2, 129.3, 129.5, 130.0, 131.4, 133.1, 134.5, 139.4, 139.98, 139.99, 161.8, 192.1. IR (neat)  $\nu$  1696, 1513, 1279, 1219, 1152, 1100, 1014  $\text{cm}^{-1}$ . ESI-MS ( $m/z$ ) 435.4 (100,  $[\text{M} + \text{Na}]^+$ ), 413.4 (31,  $[\text{M} + \text{H}]^+$ ). Anal. Calcd for  $\text{C}_{26}\text{H}_{24}\text{N}_2\text{O}_3$  (412.2): C 75.71, H 5.86, N 6.79; found: C 75.71, H 6.04, N 6.80.

Ethyl *trans*-5-benzoyl-4-(4'-chlorophenyl)-1-(*p*-tolyl)-4,5-dihydro-1H-pyrazole-3-carboxylate (**13c**): yellow solid, 245 mg (55%), mp 157–159 °C.  $^1\text{H}$  NMR (600 MHz,  $\text{CDCl}_3$ )  $\delta$  1.22 (t,  $J = 7.1$  Hz, 3H, Et), 2.27 (s, 3H, Me), 4.14 (dq,  $J = 7.1, 10.9$  Hz, 1H, Et), 4.21 (dq,  $J = 7.1, 10.9$  Hz, 1H, Et), 4.42 (d,  $J = 5.0$  Hz, 1H, 4-H), 5.74 (d,  $J = 5.0$  Hz, 1H, 5-H), 7.00–7.03, 7.07–7.09, 7.14–7.16, 7.34–7.36, 7.49–7.53, 7.66–7.69, 7.87–7.89 (7m, 2H, 2H 2H, 2H, 2H, 1H, 2H).  $^{13}\text{C}$  NMR (151 MHz,  $\text{CDCl}_3$ )  $\delta$  14.3, 20.8, 54.8, 61.3, 74.1, 114.4, 128.9, 129.1, 129.4, 129.7, 130.0, 131.7, 133.0, 134.4, 134.7, 138.0, 139.5, 139.8, 161.7, 191.8. ESI-MS ( $m/z$ ) 469.4 (100,  $[\text{M} + \text{Na}]^+$ ), 447.4 (63,  $[\text{M} + \text{H}]^+$ ). Anal. Calcd for  $\text{C}_{26}\text{H}_{23}\text{ClN}_2\text{O}_3$  (446.1): C 69.87, H 5.19, N 6.27; found: C 69.72, H 5.04, N 6.01.

### 3.1.2. General Procedure for Oxidation Reactions with Activated Manganese Dioxide

5-Acylpyrazoline of type **6** or **13** (1.0 mmol) and activated  $\text{MnO}_2$  (40 mmol, 4.09 g) were placed in a 10 mL zirconium oxide grinding jar with one zirconium oxide ball (10 mm

diameter). The jar was closed and subjected to grinding for 1.5 h in a vibratory ball-mill operated at 25 Hz. After AcOEt (20 mL) was added, the resulting mixture was filtered through a thin pad of silica gel and the solvent was evaporated to give pyrazole **8** or **15**. In the case of 4-benzoylpyrazoline **6'b**, the resulting products **11b** and **12b** were purified using standard column chromatography (SiO<sub>2</sub>). The structure of known fluorinated pyrazoles, i.e., **8a–8k**, **8n**, **8q**, and **8r** were confirmed based on <sup>1</sup>H NMR spectra and by comparison with the original samples [42].

**4-(3',4'-Dimethoxyphenyl)-1-(p-tolyl)-3-trifluoromethylpyrazole (8l)**: colorless solid, 326 mg (90%), mp 129–130 °C. <sup>1</sup>H NMR (600 MHz, CDCl<sub>3</sub>) δ 2.38 (s, 3H, Me), 3.898, 3.901 (2s, 3H each, 2OMe), 6.88–6.91, 6.99–7.03, 7.25–7.27, 7.58–7.60 (4m, 1H, 2H, 2H, 2H), 7.93 (s, 1H, 5-H). <sup>13</sup>C NMR (151 MHz, CDCl<sub>3</sub>) δ 21.0, 55.90, 55.91, 111.3, 112.0, 119.6, 120.9, 121.8 (q, <sup>1</sup>J<sub>C-F</sub> = 269.7 Hz, CF<sub>3</sub>), 122.9, 123.5(br), 127.3, 130.2, 137.0, 137.8, 139.9 (q, <sup>2</sup>J<sub>C-F</sub> = 36.4 Hz, C-3), 148.9\*; \*higher intensity. <sup>19</sup>F NMR (565 MHz, CDCl<sub>3</sub>) δ −59.3 (s, CF<sub>3</sub>). IR (neat)  $\nu$  1491, 1241, 1163, 1118 cm<sup>−1</sup>. (−)-ESI-MS (*m/z*) 361.4 (100, [M−H]<sup>−</sup>). Anal. Calcd for C<sub>19</sub>H<sub>17</sub>F<sub>3</sub>N<sub>2</sub>O<sub>2</sub> (362.1): C 62.98, H 4.73, N 7.73; found: C 63.00, H 4.69, N 7.44.

**4-(3',4'-Methylenedioxyphenyl)-1-(p-tolyl)-3-trifluoromethylpyrazole (8m)**: colorless solid, 294 mg (85%), mp 99–100 °C. <sup>1</sup>H NMR (600 MHz, CDCl<sub>3</sub>) δ 2.40 (s, 3H, Me), 6.00 (s, 2H, OCH<sub>2</sub>O), 6.85–6.87, 6.93–6.95, 7.27–7.29, 7.59–7.61 (4m, 1H, 2H, 2H, 2H), 7.90 (s<sub>br</sub>, 1H, 5-H). <sup>13</sup>C NMR (151 MHz, CDCl<sub>3</sub>) δ 21.1, 101.4, 108.5, 109.3, 119.7, 121.7 (q, <sup>1</sup>J<sub>C-F</sub> = 269.8 Hz, CF<sub>3</sub>), 122.4(br), 123.4(br), 127.5, 130.2, 137.1, 137.9, 140.0 (q, <sup>2</sup>J<sub>C-F</sub> = 36.5 Hz, C-3), 147.6, 147.9. <sup>19</sup>F NMR (565 MHz, CDCl<sub>3</sub>) δ −59.4 (s, CF<sub>3</sub>). IR (neat)  $\nu$  1480, 1223, 1167, 1118, 1036 cm<sup>−1</sup>. ESI-MS (*m/z*) 369.4 (100, [M + Na]<sup>+</sup>), 347.4 (76, [M + H]<sup>+</sup>). Anal. Calcd for C<sub>18</sub>H<sub>13</sub>F<sub>3</sub>N<sub>2</sub>O<sub>2</sub> (346.1): C 62.43, H 3.78, N 8.09; found: C 62.60, H 3.92, N 8.08.

**4-(2'-Chlorophenyl)-1-(p-tolyl)-3-trifluoromethylpyrazole (8p)**: thick light yellow oil, 299 mg (89%). <sup>1</sup>H NMR (600 MHz, CDCl<sub>3</sub>) δ 2.42 (s, 3H, Me), 7.29–7.36, 7.40–7.42, 7.48–7.51, 7.62–7.65 (4m, 4H, 1H, 1H, 2H), 7.99 (s, 1H, 5-H). <sup>13</sup>C NMR (151 MHz, CDCl<sub>3</sub>) δ 21.1, 119.7(br), 119.8, 121.4 (q, <sup>1</sup>J<sub>C-F</sub> = 270.1 Hz, CF<sub>3</sub>), 126.7, 128.8, 129.5, 129.7, 129.8, 130.3, 132.2(br), 134.1, 137.1, 138.0, 141.3 (q, <sup>2</sup>J<sub>C-F</sub> = 36.6 Hz, C-3). <sup>19</sup>F NMR (565 MHz, CDCl<sub>3</sub>) δ −60.0 (s, CF<sub>3</sub>). IR (neat)  $\nu$  1521, 1495, 1290, 1223, 1170, 1116, 1062 cm<sup>−1</sup>. ESI-MS (*m/z*) 359.3 (23, [M + Na]<sup>+</sup>), 337.3 (100, [M + H]<sup>+</sup>). Anal. Calcd for C<sub>17</sub>H<sub>12</sub>ClF<sub>3</sub>N<sub>2</sub> (336.1): C 60.64, H 3.59, N 8.32; found: C 60.51, H 3.39, N 8.47.

**4-(3'-Nitrophenyl)-1-(p-tolyl)-3-trifluoromethylpyrazole (8s)**: colorless solid, 257 mg (74%), mp 147–148 °C. <sup>1</sup>H NMR (600 MHz, CDCl<sub>3</sub>) δ 2.43 (s, 3H, Me), 7.31–7.33, 7.61–7.64, 7.82–7.84 (3m, 2H, 3H, 1H), 8.08 (s, 1H, 5-H), 8.24 (ddd, *J* = 1.0, 2.3, 8.2 Hz, 1H), 8.34 (pseudo-t, *J* ≈ 2.0 Hz, 1H). <sup>13</sup>C NMR (151 MHz, CDCl<sub>3</sub>) δ 21.2, 119.9, 121.3(br), 121.5 (q, <sup>1</sup>J<sub>C-F</sub> = 269.8 Hz, CF<sub>3</sub>), 122.9, 123.6, 128.0, 129.8, 130.4, 132.2, 134.8(br), 136.8, 138.5, 140.2 (q, <sup>2</sup>J<sub>C-F</sub> = 37.1 Hz, C-3), 148.5. <sup>19</sup>F NMR (565 MHz, CDCl<sub>3</sub>) δ −59.4 (s, CF<sub>3</sub>). IR (neat)  $\nu$  1521, 1349, 1282, 1226, 1170, 1118, 1074 cm<sup>−1</sup>. ESI-MS (*m/z*) 370.3 (100, [M + Na]<sup>+</sup>), 348.3 (70, [M + H]<sup>+</sup>). Anal. Calcd for C<sub>17</sub>H<sub>12</sub>F<sub>3</sub>N<sub>3</sub>O<sub>2</sub> (347.1): C 58.79, H 3.48, N 12.10; found: C 58.85, H 3.51, N 12.08.

**5-Phenyl-1-(p-tolyl)-3-trifluoromethylpyrazole (11b)** [34]: obtained as a minor product in oxidation of **6'b**; light yellow solid, 114 mg (38%), mp 74–76 °C. <sup>1</sup>H NMR (600 MHz, CDCl<sub>3</sub>) δ 2.37 (s, 3H, Me), 6.74 (s<sub>br</sub>, 1H, 4-H), 7.14–7.24, 7.30–7.36 (2m, 6H, 3H). <sup>13</sup>C NMR (151 MHz, CDCl<sub>3</sub>) δ 21.3, 105.5, 121.5 (q, <sup>1</sup>J<sub>C-F</sub> = 268.8 Hz, CF<sub>3</sub>), 125.5, 128.8, 128.95, 129.02, 129.5(br), 129.8, 137.0, 138.6, 143.2 (q, <sup>2</sup>J<sub>C-F</sub> = 38.3 Hz, C-3), 144.7. <sup>19</sup>F NMR (565 MHz, CDCl<sub>3</sub>) δ −62.2 (s, CF<sub>3</sub>). IR (neat)  $\nu$  1454, 1230, 1129, 1073 cm<sup>−1</sup>. HRMS (ESI-TOF) *m/z*: [M + H]<sup>+</sup> calcd for C<sub>17</sub>H<sub>14</sub>F<sub>3</sub>N<sub>2</sub> 303.1109, found 303.1104.

**4-Benzoyl-5-phenyl-1-(p-tolyl)-3-trifluoromethylpyrazole (12b)**: colorless solid, 228 mg (56%), mp 139–140 °C. <sup>1</sup>H NMR (600 MHz, CDCl<sub>3</sub>) δ 2.35 (s, 3H, Me), 7.07–7.10, 7.13–7.21, 7.28–7.32, 7.43–7.46, 7.72–7.74 (5m, 2H, 7H, 2H, 1H, 2H). <sup>13</sup>C NMR (151 MHz, CDCl<sub>3</sub>) δ 21.3, 119.8(br), 121.0 (q, <sup>1</sup>J<sub>C-F</sub> = 270.4 Hz, CF<sub>3</sub>), 125.4, 127.9, 128.4, 128.7, 129.5, 129.8, 129.9, 130.1, 133.5, 136.3, 137.5, 139.0, 141.5 (q, <sup>2</sup>J<sub>C-F</sub> = 37.9 Hz, C-3), 144.4. <sup>19</sup>F NMR (565 MHz, CDCl<sub>3</sub>) δ −60.3 (s, CF<sub>3</sub>). IR (neat)  $\nu$  1659, 1484, 1443, 1223, 1156, 1129, 1059 cm<sup>−1</sup>. HRMS (ESI-TOF) *m/z*: [M + H]<sup>+</sup> calcd for C<sub>24</sub>H<sub>18</sub>F<sub>3</sub>N<sub>2</sub>O 407.1371, found 407.1369.

**1,3,4-Triphenylpyrazole (15a)** [52]: light yellow solid, 97 mg (33%; for two steps, starting with 1.0 mmol of chalcone **10a** and chloride **14a**), mp 96–98 °C. <sup>1</sup>H NMR (600 MHz, CDCl<sub>3</sub>) δ 7.29–7.37, 7.47–7.50, 7.60–7.62, 7.80–7.82 (4m, 9H, 2H, 2H, 2H), 8.03 (s, 1H, 5-H). <sup>13</sup>C NMR (151 MHz, CDCl<sub>3</sub>) δ 119.1, 123.1, 126.6, 126.8, 127.1, 128.1, 128.5, 128.6, 128.7, 128.9, 129.6, 133.0, 133.3, 140.1, 150.6. IR (neat)  $\nu$  1722, 1599, 1502, 1401, 1215, 1059 cm<sup>-1</sup>. ESI-MS (*m/z*) 297.3 (100, [M + H]<sup>+</sup>).

**Ethyl 4-phenyl-1-(p-tolyl)-pyrazole-3-carboxylate (15b)**: colorless solid, 205 mg (67%), mp 99–102 °C. <sup>1</sup>H NMR (600 MHz, CDCl<sub>3</sub>) δ 1.32 (t, *J* = 7.1 Hz, 3H, Et), 2.41 (s, 3H, Me), 4.37 (q, *J* = 7.1 Hz, 2H, Et), 7.27–7.29, 7.33–7.37, 7.39–7.42, 7.51–7.53, 7.64–7.66 (5m, 2H, 1H, 2H, 2H, 2H), 7.93 (s, 1H, 5-H). <sup>13</sup>C NMR (151 MHz, CDCl<sub>3</sub>) δ 14.3, 21.2, 61.2, 120.1, 127.5, 127.7, 127.8, 128.2, 129.5, 130.2, 131.7, 137.4, 137.8, 141.2, 162.7. IR (neat)  $\nu$  1722, 1610, 1517, 1465, 1279, 1226, 1141 cm<sup>-1</sup>. ESI-MS (*m/z*) 329.2 (25, [M + Na]<sup>+</sup>), 307.2 (100, [M + H]<sup>+</sup>). Anal. Calcd for C<sub>19</sub>H<sub>18</sub>N<sub>2</sub>O<sub>2</sub> (306.1): C 74.49, H 5.92, N 9.14; found: C 74.47, H 6.00, N 9.21.

**Ethyl 4-(4'-chlorophenyl)-1-(p-tolyl)-pyrazole-3-carboxylate (15c)**: colorless solid, 218 mg (64%), mp 136–137 °C. <sup>1</sup>H NMR (600 MHz, CDCl<sub>3</sub>) δ 1.34 (t, *J* = 7.1 Hz, 3H, Et), 2.41 (s, 3H, Me), 4.38 (q, *J* = 7.1 Hz, 2H, Et), 7.27–7.29, 7.36–7.38, 7.45–7.47, 7.63–7.66 (4m, 2H, 2H, 2H, 2H), 7.92 (s, 1H, 5-H). <sup>13</sup>C NMR (151 MHz, CDCl<sub>3</sub>) δ 14.4, 21.2, 61.3, 120.1, 126.4, 127.8, 128.4, 130.18, 130.20, 133.7, 137.2, 138.0, 141.1, 162.5. IR (neat)  $\nu$  1707, 1476, 1442, 1349, 1282, 1226, 1156, 1107, 1077, 1033 cm<sup>-1</sup>. HRMS (ESI-TOF) *m/z*: [M + H]<sup>+</sup> calcd for C<sub>19</sub>H<sub>18</sub>ClN<sub>2</sub>O<sub>2</sub> 341.1057, found 341.1063.

**3-Acetyl-4-phenyl-1-(p-tolyl)-pyrazole (15d)**: colorless solid, 102 mg (37%; for two steps, starting with 1.0 mmol of chalcone **10a** and chloride **14c**), mp 137–139 °C. <sup>1</sup>H NMR (600 MHz, CDCl<sub>3</sub>) δ 2.42 (s, 3H, Me), 2.69 (s, 3H, Ac), 7.29–7.35, 7.38–7.41, 7.55–7.57, 7.65–7.67 (4m, 3H, 2H, 2H, 2H), 7.94 (s, 1H, 5-H). <sup>13</sup>C NMR (151 MHz, CDCl<sub>3</sub>) δ 21.2, 28.1, 119.6, 126.4, 127.7, 127.9, 128.3, 129.4, 130.3, 131.7, 137.4, 137.8, 137.6, 194.8. IR (neat)  $\nu$  1681, 1517, 1349, 1219, 1111 cm<sup>-1</sup>. ESI-MS (*m/z*) 299.3 (100, [M + Na]<sup>+</sup>), 277.3 (87, [M + H]<sup>+</sup>). Anal. Calcd for C<sub>18</sub>H<sub>16</sub>N<sub>2</sub>O (276.1): C 78.24, H 5.84, N 10.14; found: C 78.01, H 5.82, N 10.00.

**3-Acetyl-4-(4'-methoxyphenyl)-1-(p-tolyl)-pyrazole (15e)**: light brown solid, 98 mg (32%; for two steps, starting with 1.0 mmol of chalcone **10d** and chloride **14c**), mp 108–109 °C. <sup>1</sup>H NMR (600 MHz, CDCl<sub>3</sub>) δ 2.42 (s, 3H, Me), 2.68 (s, 3H, Ac), 3.84 (s, 3H, OMe), 6.92–6.95, 7.29–7.32, 7.49–7.52, 7.64–7.67 (4m, 2H each), 7.89 (s, 1H, 5-H). <sup>13</sup>C NMR (151 MHz, CDCl<sub>3</sub>) δ 21.2, 28.1, 55.5, 113.8, 119.6, 124.1, 126.1, 127.5, 130.3, 130.6, 137.5, 137.7, 147.6, 159.3, 194.8. IR (neat)  $\nu$  1692, 1551, 1498, 1450, 1387, 1346, 1249, 1182, 1107, 1029 cm<sup>-1</sup>. ESI-MS (*m/z*) 329.1 (100, [M + Na]<sup>+</sup>), 307.2 (71, [M + H]<sup>+</sup>). HRMS (ESI-TOF) *m/z*: [M + H]<sup>+</sup> calcd for C<sub>19</sub>H<sub>19</sub>N<sub>2</sub>O<sub>2</sub> 307.1447, found 307.1445.

**3-Acetyl-4-(4'-nitrophenyl)-1-(p-tolyl)-pyrazole (15f)**: light yellow solid, 144 mg (45%; for two steps, starting with 1.0 mmol of chalcone **10h** and chloride **14c**), mp 191–192 °C. <sup>1</sup>H NMR (600 MHz, CDCl<sub>3</sub>) δ 2.44 (s, 3H, Me), 2.72 (s, 3H, Ac), 7.32–7.34, 7.65–7.67, 7.73–7.75 (3m, 2H each), 8.02 (s, 1H, 5-H), 8.23–8.25 (m, 2H). <sup>13</sup>C NMR (151 MHz, CDCl<sub>3</sub>) δ 21.2, 27.9, 119.8, 123.5, 124.2, 128.4, 130.1, 130.4, 137.1, 138.4, 138.7, 147.2, 147.6, 194.7. IR (neat)  $\nu$  1692, 1603, 1502, 1334, 1215, 1103, 1073 cm<sup>-1</sup>. ESI-MS (*m/z*) 344.9 (100, [M + Na]<sup>+</sup>). Anal. Calcd for C<sub>18</sub>H<sub>15</sub>N<sub>3</sub>O<sub>3</sub> (321.1): C 67.28, H 4.71, N 13.08; found: C 67.35, H 4.93, N 12.95.

**3-Acetyl-1-(4'-methoxyphenyl)-4-phenylpyrazole (15g)**: orange solid, 163 mg (56%; for two steps, starting with 1.0 mmol of chalcone **10a** and chloride **14d**), mp 109–111 °C. <sup>1</sup>H NMR (600 MHz, CDCl<sub>3</sub>) δ 2.69 (s, 3H, Ac), 3.87 (s, 3H, OMe), 7.00–7.03, 7.32–7.35, 7.38–7.41, 7.55–7.57, 7.67–7.70 (5m, 2H, 1H, 2H, 2H, 2H), 7.88 (s, 1H, 5-H). <sup>13</sup>C NMR (151 MHz, CDCl<sub>3</sub>) δ 28.0, 55.7, 114.8, 121.3, 126.3, 127.6, 128.0, 128.2, 129.3, 131.7, 133.3, 147.5, 159.2, 194.6. IR (neat)  $\nu$  1685, 1513, 1466, 1353, 1260, 1221, 1174, 1118, 1029 cm<sup>-1</sup>. ESI-MS (*m/z*) 315.1 (92, [M + Na]<sup>+</sup>), 293.2 (100, [M + H]<sup>+</sup>). Anal. Calcd for C<sub>18</sub>H<sub>16</sub>N<sub>2</sub>O<sub>2</sub> (292.1): C 73.95, H 5.52, N 9.58; found: C 73.99, H 5.74, N 9.49.

#### 4. Conclusions

In summary, a solvent-free two-step mechanochemical synthesis of trifluoromethylated and non-fluorinated polysubstituted pyrazoles was developed, starting with simple substrates, i.e., chalcones and hydrazonoyl halides. The latter served as precursors for the  $K_2CO_3$ -induced in situ generation of nitrile imines, which were efficiently trapped with chalcones, to give the respective (3 + 2)-cycloadducts in moderate to high regioselectivity and fair yields. The first formed *trans*-configured 5-acylpyrazolines were oxidized with activated manganese dioxide under ball-milling to afford pyrazoles, formed through exclusive deacylative aromatization of the ring. Based on additional experiments, a mechanistic scenario comprising acyl-transfer onto the surface of heterogeneous oxidant was proposed. The presented results extend the scope of the previously reported method for the synthesis of the title compounds in organic solvents [42] and supplements recent developments, both in the synthesis of pyrazoles [2,53–55] and the application of nitrile imines as building blocks for organic synthesis [17,34–45,56–59].

**Supplementary Materials:** The following supporting information can be downloaded at: <https://www.mdpi.com/article/10.3390/molecules27238446/s1>: Copies of  $^1H$ ,  $^{13}C$ , and  $^{19}F$  NMR spectra of all new compounds.

**Author Contributions:** Conceptualization and methodology, M.J. and G.U.-J.; investigation, G.U.-J. and A.K.; writing—original draft preparation, G.U.-J.; writing—review and editing, M.J.; supervision, M.J.; project administration, M.J.; funding acquisition, M.J. All authors have read and agreed to the published version of the manuscript.

**Funding:** This research was funded by the University of Lodz within the framework of IDUB grant (M.J.; Grant No. 3/IDUB/DOS/2021).

**Data Availability Statement:** All the electronic experimental data and samples of new materials are available from the authors.

**Conflicts of Interest:** The authors declare no conflict of interest. The funders had no role in the design of the study; in the collection, analyses, or interpretation of data; in the writing of the manuscript; or in the decision to publish the results.

#### References

1. Fustero, S.; Sánchez-Roselló, M.; Barrio, P.; Simón-Fuentes, A. From 2000 to mid-2010: A fruitful decade for the synthesis of pyrazoles. *Chem. Rev.* **2011**, *111*, 6984–7034. [CrossRef] [PubMed]
2. Mykhailiuk, P.K. Fluorinated pyrazoles: From synthesis to applications. *Chem. Rev.* **2021**, *121*, 1670–1715. [CrossRef] [PubMed]
3. Raffa, D.; Maggio, B.; Raimondi, M.V.; Cascioferro, S.; Plescia, F.; Cancemi, G.; Daidone, G. Recent advanced in bioactive systems containing pyrazole fused with a five membered heterocycle. *Eur. J. Med. Chem.* **2015**, *97*, 732–746. [CrossRef]
4. Janin, Y.L. Preparation and chemistry of 3/5-halogenopyrazoles. *Chem. Rev.* **2012**, *112*, 3924–3958. [CrossRef]
5. Li, M.; Zhao, B.X. Progress of the synthesis of condensed pyrazole derivatives (from 2010 to mid-2013). *Eur. J. Med. Chem.* **2014**, *85*, 311–340. [CrossRef]
6. Abrigach, F.; Touzani, R. Pyrazole derivatives with NCN junction and their biological activity: A review. *Med. Chem.* **2016**, *6*, 292–298. [CrossRef]
7. Faria, J.V.; Vegi, P.F.; Migueta, A.G.C.; Silva dos Santos, M.; Bochat, N.; Bernardino, A.M.R. Recently reported biological activities of pyrazole compounds. *Bioorg. Med. Chem.* **2017**, *25*, 5891–5903. [CrossRef]
8. Kumar, V.; Kaur, K.; Gupta, G.K.; Sharma, A.K. Pyrazole containing natural products: Synthetic preview and biological significance. *Eur. J. Med. Chem.* **2013**, *69*, 735–753. [CrossRef]
9. El-Gamal, M.; Zareai, S.-O.; Madkour, M.M.; Anbar, H.S. Evaluation of substituted pyrazole-based kinase inhibitors in one decade (2011–2020): Current status and future prospects. *Molecules* **2022**, *27*, 330. [CrossRef]
10. Li, X.; Yu, Y.; Tu, Z. Pyrazole scaffold synthesis, functionalization, and applications in Alzheimer's disease and Parkinson's disease treatment (2011–2020). *Molecules* **2021**, *26*, 1202. [CrossRef]
11. Asproni, B.; Murineddu, G.; Corona, P.; Pinna, G.A. Tricyclic pyrazole-based compounds as useful scaffolds for cannabinoid CB1/CB2 receptor interaction. *Molecules* **2021**, *26*, 2126. [CrossRef] [PubMed]
12. Santos, N.E.; Carreira, A.R.F.; Silva, V.L.M.; Braga, S.S. Natural and biomimetic antitumor pyrazoles, a perspective. *Molecules* **2020**, *25*, 1364. [CrossRef] [PubMed]
13. Gomes, P.M.O.; Silva, A.M.S.; Silva, V.L.M. Pyrazoles as key scaffolds for the development of fluorine-18-labeled radiotracers for positron emission tomography (PET). *Molecules* **2020**, *25*, 1722. [CrossRef] [PubMed]

14. Elnagdy, H.M.F.; Chetia, T.; Dehingia, N.; Chetia, B.; Dutta, P.; Sarma, D. Sensing and optical activities of new pyrazole containing polymeric analogues. *Bull. Mater. Sci.* **2022**, *45*, 86. [CrossRef]
15. Cavero, E.; Uriel, S.; Romero, P.; Serrano, J.L.; Giménez, R. Tetrahedral zinc complexes with liquid crystalline and luminescent properties: Interplay between nonconventional molecular shapes and supramolecular mesomorphic order. *J. Am. Chem. Soc.* **2007**, *129*, 11608–11618. [CrossRef] [PubMed]
16. Trofimenko, S. Coordination chemistry of pyrazole-derived ligands. *Chem. Rev.* **1972**, *72*, 497–509. [CrossRef]
17. Jamieson, C.; Livingstone, K. *The Nitrile Imine 1,3-dipole; Properties, Reactivity and Applications*; Springer Nature: Cham, Switzerland, 2020.
18. Howard, J.L.; Cao, Q.; Browne, D.L. Mechanochemistry as an emerging tool for molecular synthesis: What can it offer? *Chem. Sci.* **2018**, *9*, 3080–3094. [CrossRef]
19. Tan, D.; Garcia, F. Main group mechanochemistry: From curiosity to established protocols. *Chem. Soc. Rev.* **2019**, *48*, 2274–2292. [CrossRef]
20. Pickhardt, W.; Grätz, S.; Borhardt, L. Direct mechanocatalysis: Using milling balls as catalysts. *Chem. Eur. J.* **2020**, *26*, 12903–12911. [CrossRef]
21. Leonardi, M.; Villacampa, M.; Menéndez, J.C. Multicomponent mechanochemical synthesis. *Chem. Sci.* **2018**, *9*, 2042–2064. [CrossRef]
22. Pérez-Venegas, M.; Juaristi, E. Mechanochemical and mechanoenzymatic synthesis of pharmacologically active compounds: A green perspective. *ACS Sustain. Chem. Eng.* **2020**, *8*, 8881–8893. [CrossRef]
23. Porcheddu, A.; Delogu, F.; De Luca, L.; Colacino, E. From lossen transposition to solventless “Medicinal Mechanochemistry”. *ACS Sustain. Chem. Eng.* **2019**, *7*, 12044–12051. [CrossRef]
24. Yu, J.; Hong, Z.; Yang, X.; Jiang, Y.; Jiang, Z.; Su, W. Bromide-assisted chemoselective Heck reaction of 3-bromoindazoles under high-speed ball-milling conditions: Synthesis of axitinib. *Beilstein J. Org. Chem.* **2018**, *14*, 786–795. [CrossRef]
25. El-Sayed, T.; Aboelnaga, A.; El-Atawy, M.A.; Hagar, M. Ball milling promoted N-heterocycles synthesis. *Molecules* **2018**, *23*, 1348. [CrossRef]
26. Singh, P.; Nath, M. A concise account on eco-friendly synthetic strategies for pyrazole heterocycles. *Curr. Green Chem.* **2019**, *6*, 198–209. [CrossRef]
27. Saeed, A.; Channar, P.A. A green mechanochemical synthesis of new 3,5-dimethyl-4-(arylsulfanyl)pyrazoles. *J. Heterocycl. Chem.* **2017**, *54*, 780–783. [CrossRef]
28. Chowhan, B.; Kour, J.; Gupta, M.; Paul, S. Green synthesis of bis(pyrazol-5-ole) and pyrazolopyranopyrimidine derivatives through mechanochemistry using chitosan as a biodegradable catalyst. *ChemistrySelect* **2021**, *6*, 7922–7930. [CrossRef]
29. Gomes, P.M.O.; Ouro, P.M.S.; Silva, A.M.S.; Silva, V.L.M. Styrylpyrazoles: Properties, synthesis and transformations. *Molecules* **2020**, *25*, 5886. [CrossRef]
30. Howard, J.L.; Nicholson, W.; Sagatov, Y.; Browne, D.L. One-pot multistep mechanochemical synthesis of fluorinated pyrazolone. *Beilstein J. Org. Chem.* **2017**, *13*, 1950–1956. [CrossRef]
31. Zhang, Z.; Tan, Y.-J.; Wang, C.-S.; Wu, H.-H. One-pot synthesis of 3,5-diphenyl-1H-pyrazoles from chalcones and hydrazine under mechanochemical ball milling. *Heterocycles* **2014**, *89*, 103–112. [CrossRef]
32. Paveglio, G.C.; Longhi, K.; Moreira, D.N.; München, T.S.; Tier, A.Z.; Gindri, I.M.; Bender, C.R.; Frizzo, C.P.; Zanatta, N.; Bonacorso, H.G.; et al. How mechanical and chemical features affect the green synthesis of 1H-pyrazoles in a ball mill. *ACS Sustain. Chem. Eng.* **2014**, *2*, 1895–1901. [CrossRef]
33. Oh, L.M. Synthesis of celecoxib via 1,3-dipolar cycloaddition. *Tetrahedron Lett.* **2006**, *47*, 7943–7946. [CrossRef]
34. Utecht, G.; Fruziński, A.; Jasiński, M. Polysubstituted 3-trifluoromethylpyrazoles: Regioselective (3+2)-cycloaddition of trifluoroacetonitrile imines with enol ethers and functional group transformations. *Org. Biomol. Chem.* **2018**, *16*, 1252–1257. [CrossRef] [PubMed]
35. Utecht, G.; Mlostoń, G.; Jasiński, M. A straightforward access to trifluoromethylated spirobipyrazolines through a double (3+2)-cycloaddition of fluorinated nitrile imines with alkoxyallenes. *Synlett* **2018**, *29*, 1753–1758. [CrossRef]
36. Kowalczyk, A.; Utecht-Jarzyńska, G.; Mlostoń, G.; Jasiński, M. A straightforward access to 3-trifluoromethyl-1H-indazoles via (3+2)-cycloaddition of arynes with nitrile imines derived from trifluoroacetonitrile. *J. Fluorine Chem.* **2021**, *241*, 109691. [CrossRef]
37. Wang, K.-H.; Liu, H.; Liu, X.; Bian, C.; Wang, J.; Su, Y.; Huang, D.; Hu, Y. Regioselective synthesis of 3-trifluoromethyl 4-substituted pyrazoles by [3+2]-cycloaddition of trifluoroacetonitrile imines and nitroalkenes. *Asian J. Org. Chem.* **2022**, *11*, e202200103-10. [CrossRef]
38. Zhou, Y.; Gao, C.-F.; Ma, H.; Nie, J.; Ma, J.-A.; Zhang, F.-G. Quadruple functionalized pyrazole pharmacophores by one-pot regioselective [3+2]-cycloaddition of fluorinated nitrile imines and dicyanoalkenes. *Chem Asian J.* **2022**, *17*, e202200436. [CrossRef]
39. Tian, Y.-C.; Li, J.-K.; Zhang, F.-G.; Ma, J.-A. Regioselective decarboxylative cycloaddition route to fully substituted 3-CF<sub>3</sub>-pyrazoles from nitrilimines and isoxazolidinediones. *Adv. Synth. Catal.* **2021**, *363*, 2093–2097. [CrossRef]
40. Utecht-Jarzyńska, G.; Nagła, K.; Mlostoń, G.; Heimgartner, H.; Palusiak, M.; Jasiński, M. A straightforward conversion of 1,4-quinones into polycyclic pyrazoles via [3+2]-cycloaddition with fluorinated nitrile imines. *Beilstein J. Org. Chem.* **2021**, *17*, 1509–1517. [CrossRef]
41. Han, T.; Wang, K.-H.; Yang, M.; Zhao, P.; Wang, F.; Wang, J.; Huang, D.; Hu, Y. Synthesis of difluoromethylated pyrazoles by the [3+2]-cycloaddition reaction of difluoroacetohydrazoneyl bromides. *J. Org. Chem.* **2022**, *87*, 498–511. [CrossRef]



42. Kowalczyk, A.; Utecht-Jarzyńska, G.; Mlostoń, G.; Jasiński, M. Trifluoromethylated pyrazoles via sequential (3+2)-cycloaddition of fluorinated nitrile imines with chalcones and solvent-dependent deacylative oxidation reactions. *Org. Lett.* **2022**, *24*, 2499–2503. [CrossRef] [PubMed]
43. Mlostoń, G.; Urbaniak, K.; Utecht, G.; Lentz, D.; Jasiński, M. Trifluoromethylated 2,3-dihydro-1,3,4-thiadiazoles via the regioselective [3+2]-cycloadditions of fluorinated nitrile imines with aryl, hetaryl, and ferrocenyl thioketones. *J. Fluorine Chem.* **2016**, *192*, 147–154. [CrossRef]
44. Al-Hussain, S.A.; Alshehrei, F.; Zaki, M.E.A.; Harras, M.F.; Farghaly, T.A.; Muhammad, Z.A. Fluorinated hydrazonoyl chlorides as precursors for synthesis of antimicrobial azoles. *J. Heterocyclic Chem.* **2021**, *58*, 589–602. [CrossRef]
45. Du, S.; Yang, Z.; Tang, J.; Chen, Z.; Wu, X.-F. Synthesis of 3H-1,2,4-triazol-3-ones via NiCl<sub>2</sub>-promoted cascade annulation of hydrazonoyl chlorides and sodium cyanate. *Org. Lett.* **2021**, *23*, 2359–2363. [CrossRef] [PubMed]
46. Wojciechowska, A.; Jasiński, M.; Kaszyński, P. Tautomeric equilibrium in trifluoroacetaldehyde arylhydrazones. *Tetrahedron* **2015**, *71*, 2349–2356. [CrossRef]
47. Shawali, A.S.; Ezmirly, S.T.; Bukhari, A.M. Nuclear magnetic resonance spectroscopy and the structures of the regioisomeric products of the cycloaddition of C-ethoxycarbonyl-N-arylnitrilimines to  $\alpha,\beta$ -unsaturated ketones. *Spectrochim. Acta Part A* **1992**, *48*, 1165–1171. [CrossRef]
48. Ortega-Martínez, A.; Molina, C.; Moreno-Cabrero, C.; Sansano, J.M.; Nájera, C. Deacylative reactions: Synthetic applications. *Eur. J. Org. Chem.* **2018**, 2394–2405. [CrossRef]
49. Fatiadi, A.J. Active manganese dioxide oxidation in organic chemistry—Part I. *Synthesis* **1976**, *1976*, 65–104. [CrossRef]
50. Xie, H.; Zhu, J.; Chen, Z.; Li, S.; Wu, Y. Reaction of a trifluoromethylated N-monosubstituted hydrazone with  $\alpha,\beta$ -ethenyl ketones: A novel synthesis of substituted pyrazolidines and pyrazolines. *Synthesis* **2011**, *17*, 2767–2774. [CrossRef]
51. Grzelak, P.; Utecht, G.; Jasiński, M.; Mlostoń, G. First (3+2)-cycloadditions of thiochalcones as C=S dipolarophiles: Efficient synthesis of 1,3,4-thiadiazoles via reactions with fluorinated nitrile imines. *Synthesis* **2017**, *49*, 2129–2137. [CrossRef]
52. Shi, C.; Ma, C.; Ma, H.; Zhou, X.; Cao, J.; Fan, Y.; Huang, G. Copper-catalyzed synthesis of 1,3,4-trisubstituted and 1,3,4,5-tetrasubstituted pyrazoles via [3+2] cycloadditions of hydrazones and nitroolefins. *Tetrahedron* **2016**, *72*, 4055–4058. [CrossRef]
53. Castillo, J.-C.; Portilla, J. Recent advances in the synthesis of new pyrazole derivatives. In *Targets in Heterocyclic Systems*; Italian Society of Chemistry: Rome, Italy, 2018; Chapter 9; pp. 194–223. [CrossRef]
54. Yet, L. Five-membered ring systems: With more than one N atom (chapter 5.4). In *Progress in Heterocyclic Chemistry*; Elsevier: Amsterdam, The Netherlands, 2020; Volume 31, pp. 325–361. [CrossRef]
55. Ríos, M.-C.; Portilla, J. Recent advances in synthesis and properties of pyrazoles. *Chemistry* **2022**, *4*, 940–968. [CrossRef]
56. Deepthi, A.; Acharjee, N.; Sruthi, S.L.; Meenakshy, C.B. An overview of nitrile imine based [3+2]-cycloadditions over half a decade. *Tetrahedron* **2022**, *116*, 132812. [CrossRef]
57. Utecht-Jarzyńska, G.; Michalak, A.; Banaś, J.; Mlostoń, G.; Jasiński, M. Trapping of trifluoroacetonitrile imines with mercaptoacetaldehyde and mercaptocarboxylic acids: An access to fluorinated 1,3,4-thiadiazine derivatives via (3+3)-annulation. *J. Fluorine Chem.* **2019**, *222–223*, 8–14. [CrossRef]
58. Zhang, Y.; Zeng, J.-L.; Chen, Z.; Wang, R. Base-promoted (3+2)-cycloaddition of trifluoroacetylhydrazonoyl chlorides with imidates en route to trifluoromethyl-1,2,4-triazoles. *J. Org. Chem.* **2022**, *87*, 14514–14522. [CrossRef]
59. Ren, Y.; Ma, R.; Feng, Y.; Wang, K.-H.; Wang, J.; Huang, D.; Lv, X.; Hu, Y. Synthesis of difluoroethyl pyrazolines and pyrazoles by [3+2] cycloaddition reaction of difluoroacetylhydrazonoyl bromides with electron-deficient olefins. *Asian J. Org. Chem.* **2022**, *11*, e202200438. [CrossRef]

## Article

# On the Question of the Formation of Nitro-Functionalized 2,4-Pyrazole Analogs on the Basis of Nitrylimine Molecular Systems and 3,3,3-Trichloro-1-Nitroprop-1-Ene

Karolina Kula <sup>1,\*</sup>, Agnieszka Łapczuk <sup>1,\*</sup>, Mikołaj Sadowski <sup>1</sup>, Jowita Kras <sup>1</sup>, Karolina Zawadzińska <sup>1</sup>, Oleg M. Demchuk <sup>2</sup>, Gajendra Kumar Gaurav <sup>3</sup>, Aneta Wróblewska <sup>4</sup> and Radomir Jasiński <sup>1,\*</sup>

<sup>1</sup> Department of Organic Chemistry and Technology, Cracow University of Technology, Warszawska 24, 31-155 Krakow, Poland

<sup>2</sup> Faculty of Medicine, The John Paul II Catholic University of Lublin, Konstantynow 1J, 20-708 Lublin, Poland

<sup>3</sup> Sustainable Process Integration Laboratory—SPIL, NETME Centre, Faculty of Mechanical Engineering, Brno University of Technology—VUT Brno, Technická 2896/2, 616-69 Brno, Czech Republic

<sup>4</sup> Centre of Molecular and Macromolecular Studies, Polish Academy of Sciences, Sienkiewicza 112, 90-363 Lodz, Poland

\* Correspondence: karolina.kula@pk.edu.pl (K.K.); agnieszka.lapczuk@pk.edu.pl (A.Ł.); radomir.jasinski@pk.edu.pl (R.J.)

**Abstract:** Experimental and theoretical studies on the reaction between (*E*)-3,3,3-trichloro-1-nitroprop-1-ene and *N*-(4-bromophenyl)-*C*-arylnitrylimine were performed. It was found that the title process unexpectedly led to 1-(4-bromophenyl)-3-phenyl-5-nitropyrazole instead of the expected  $\Delta^2$ -pyrazoline molecular system. This was the result of a unique  $\text{CHCl}_3$  elimination process. The observed mechanism of transformation was explained in the framework of the molecular electron density theory (MEDT). The theoretical results showed that both of the possible channels of [3 + 2] cycloaddition were favorable from a kinetic point of view, due to which the creation of 1-(4-bromophenyl)-3-aryl-4-tricholomethyl-5-nitro- $\Delta^2$ -pyrazoline was more probable. On the other hand, according to the experimental data, the presented reactions occurred with full regioselectivity.

**Keywords:** pyrazoline; pyrazole; nitrocompound; nitrylimine; cycloaddition reaction; molecular electron density theory; synthesis

**Citation:** Kula, K.; Łapczuk, A.; Sadowski, M.; Kras, J.; Zawadzińska, K.; Demchuk, O.M.; Gaurav, G.K.; Wróblewska, A.; Jasiński, R. On the Question of the Formation of Nitro-Functionalized 2,4-Pyrazole Analogs on the Basis of Nitrylimine Molecular Systems and 3,3,3-Trichloro-1-Nitroprop-1-Ene. *Molecules* **2022**, *27*, 8409. <https://doi.org/10.3390/molecules27238409>

Academic Editors: Vera L. M. Silva and Artur M. S. Silva

Received: 17 November 2022

Accepted: 24 November 2022

Published: 1 December 2022

**Publisher's Note:** MDPI stays neutral with regard to jurisdictional claims in published maps and institutional affiliations.



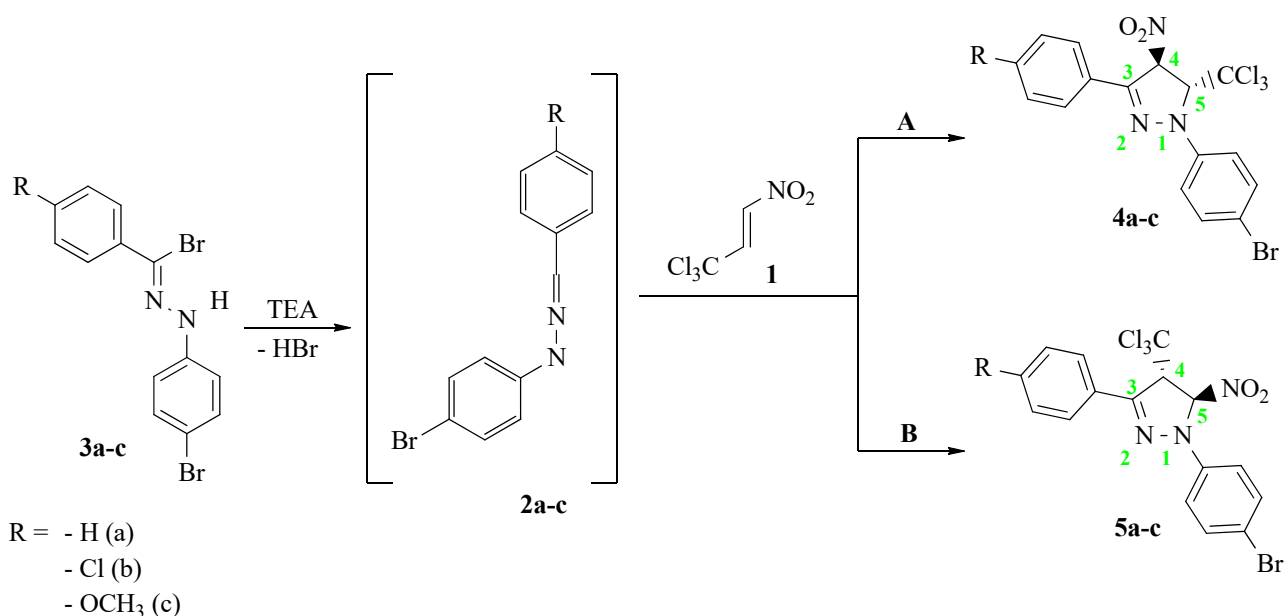
**Copyright:** © 2022 by the authors. Licensee MDPI, Basel, Switzerland. This article is an open access article distributed under the terms and conditions of the Creative Commons Attribution (CC BY) license (<https://creativecommons.org/licenses/by/4.0/>).

## 1. Introduction

Pyrazolines are heterocyclic systems containing nitrogen in their structure. They are significant organic compounds with many applications, not only as components for further organic synthesis but also as complete products. Pyrazolines and their analogs are five-membered heterocyclic compounds with one unsaturated double bond and two adjacent nitrogen atoms [1–3], which make them readily undergo various transformations. Due to the presence of the unsaturated bond and nitrogen atoms, pyrazolines have great biological activity and have many properties related to this. Many of these compounds are widely used in medicine as well as in other departments of industry. In particular, pyrazoline analogs show anticancer [4], anti-inflammatory [5], antiobesity, analgesic and antidepressant properties [6,7]. These compounds are also effective in treating Alzheimer's disease [8]. What is more, there are many drugs based on pyrazoline's structure, e.g., celecoxib [9], rimonabant, difenamizole and fezolamine. In industry, pyrazolines have been known since the early 1970s [10–12]. They were successfully applied as insecticides but also as inhibitors that control sodium channel functions [13,14]. Furthermore, the pyrazoline ring can be found in a variety of pesticides, mainly in fungicides [15,16], insecticides [17] and herbicides, including patented products such as fenpyroximate [18], fipronil [19,20], tebufenpyrad [21] and tolfenpyrad [20].

At this moment, several methods of pyrazoline preparation are known. The most common include the cyclocondensation of  $\alpha,\beta$ -unsaturated carbonyl compounds with hydrazine; the 1,3-alkylation reaction of hydrazines with 1,3-dihalopropanes; the intramolecular cyclization of hydrazones; as well as [3 + 2] the cycloaddition reaction (32CA) of alkene with diazocompounds, nitrylimines and also azomethine imines [22].

In the framework of this paper, we decided to shed a light on the possibility of the synthesis of new nitro-substituted analogs of pyrazoline on the basis of a 32CA reaction [23]. For the model of nitroalkene, we selected (*E*)-3,3,3-trichloro-1-nitroprop-1-ene (TNP) (**1**). TNP can be characterized by a very reactive structure for organic synthesis and the ability to insert different CX<sub>3</sub> and NO<sub>2</sub> groups into the main product, which additionally stimulates many important biologically active functions [24–28]. Moreover, this nitroalkene was successfully tested in 32CA reactions with many organic compounds, such as nitrones [29–31], nitrile *N*-oxides [32,33], diazocompounds [2,3,34] and *N*-azomethine ylides [35–37], and in other reactions [38–40]. In turn, to model the three-atom component (TAC) [23], we decided to use *N*-(4-bromophenyl)-*C*-phenylnitrylimine (NI) (**2a**). For such defined addends, reactions can be theoretically realized with two regioisomeric paths, leading to cycloadducts with a nitro group at the fourth (**4a**) or fifth (**5a**) position of a ring (Scheme 1).



**Scheme 1.** Theoretically possible reaction paths of 32CA between TNP (**1**) and NIs (**2a–c**).

## 2. Result and Discussion

In the first part of our research, we decided to shed a light on the nature of the interactions between (*E*)-3,3,3-trichloro-1-nitroprop-1-ene (**1**) and *N*-(4-bromophenyl)-*C*-phenylnitryl-imine (**2a**) and (on the margins of the main stream of the research) its substituted analogs (**2b,c**) (Scheme 1). For this purpose, the approach in the framework of the molecular electron density theory (MEDT) [41] was applied. Therefore, we calculated the respective global and local electronic properties of the model reaction components using conceptual density functional theory (CDFT) [42,43] methodologies. The CDFT is known as a strong implement that helps predict the reactivity of the components in polar processes such as cycloaddition. According to Domingo recommendations, all of the indices were determined via calculations based at the B3LYP/6-31G(d) level of theory in the gas phase [42–44]. The global reactivity indices, namely the electronic chemical potential  $\mu$ , chemical hardness  $\eta$ , global electrophilicity  $\omega$  and global nucleophilicity  $N$ , were determined and given in Table 1.

**Table 1.** Global electronic properties (electronic chemical potential  $\mu$ , chemical hardness  $\eta$ , global electrophilicity  $\omega$  and nucleophilicity  $N$ ; all in eV) for the studied reagents.

| Reagent   | $\mu$ | $\eta$ | $\omega$ | $N$  |
|-----------|-------|--------|----------|------|
| <b>1</b>  | −5.84 | 5.22   | 3.27     | 0.66 |
| <b>2a</b> | −3.32 | 3.84   | 1.66     | 3.76 |
| <b>2b</b> | −3.51 | 3.70   | 1.84     | 3.86 |
| <b>2c</b> | −3.55 | 3.42   | 1.43     | 3.88 |

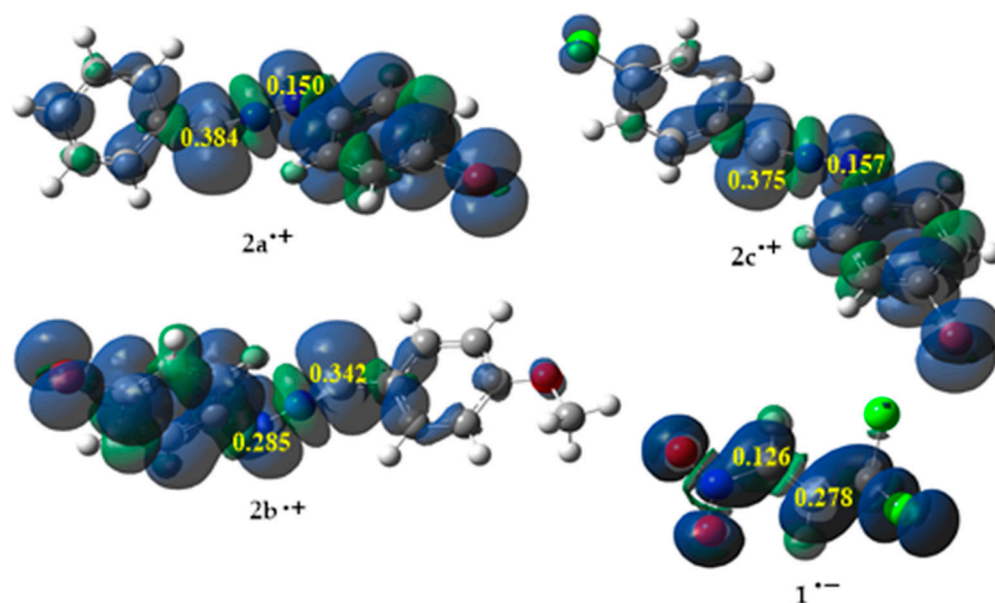
The value of the electronic chemical potential [42]  $\mu$  can estimate the direction of the electron density flux between reagents in the determined path of the reaction. In the case of the reaction between (*E*)-3,3,3-trichloro-1-nitroprop-1-ene (**1**) and *N*-(4-bromophenyl)-*C*-phenylnitryl-imine (**2a**), the electronic chemical potentials  $\mu$  were equal to −5.84 eV and −3.32 eV, respectively (Table 1). This indicated that in the course of this reaction, the flux of the electron density would take place in the conversion from nitrylimine (**2a**) to nitroalkene (**1**). Analogously, equal results could be observed for the other reagent systems, as, in all cases, nitrylimine (**2b–c**) was characterized by a higher value of the electronic chemical potential than nitroalkene (**1**). To sum up, all presented cycloaddition reactions should be classified as forward electron density fluxes (FEDF) in agreement with the CDFT analysis [45–48].

Next, the calculated values were global indices of the electrophilicity [44]  $\omega$  and nucleophilicity [49]  $N$  of the reagents. The electrophilicity  $\omega$  indices of nitrylimines (**2a–c**) fell within a range from 1.43 eV to 1.84 eV (Table 1), which allowed the conclusion that these compounds act like moderate electrophiles in a polar reaction due to the electrophilicity scale [42,50]. In turn, the nucleophilicity  $N$  indices of nitrylimines **2a–c** equaled from 3.88 eV to 3.86 eV, respectively (Table 1), which allowed the characterization of nitrylimines (**2a–c**) as rather strong nucleophiles in polar reactions, which was in agreement with the nucleophilicity scale [42,50].

Both the presence of an ER group, such as  $-\text{OCH}_3$ , or an EW group, such as  $-\text{Cl}$ , at the fourth position of the phenyl ring in nitrylimines (**2a–c**) insignificantly changed the global electronic properties of these TAC. On the other hand, (*E*)-3,3,3-trichloro-1-nitroprop-1-ene (**1**) was characterized by an electrophilicity index  $\omega$  of 3.27 eV and a nucleophilicity index  $N$  of 0.66 eV (Table 1). These values allowed the categorization of nitroalkene (**1**) as a super-strong electrophile and as a marginal nucleophile in polar reactions within the electrophilicity and nucleophilicity scales [42,50].

To be able to consider this reaction as a polar process, the character of the components need to be determined. Polar processes occur between good electrophiles and good nucleophiles. According to CDFT calculations (Table 1), the analyzed reactions between (*E*)-3,3,3-trichloro-1-nitroprop-1-ene (**1**) and nitrylimines (**2a–c**) are characterized by the major difference in their electrophilicity index ( $\Delta\omega > 1$  eV) [51,52]. According to this, the presented reactions should be classified as polar processes.

The regioselectivity of the polar process in which nonsymmetric reagents take part can be easily determined by measuring the interactions between the most electrophilic center, located in the electrophile, and the most nucleophilic center, located in the nucleophile. The most exact way to describe local reactivity is through electrophilic (radical-anionic) Parr functions  $P_k^+$  and nucleophilic (radical-cationic) Parr functions  $P_k^-$  [52–55]. To determine the abovementioned centers of the components, the Parr functions for the reagents were calculated and given in Figure 1.



**Figure 1.** The local electronic properties of substrates **1** and **2a–c** as three-dimensional representations (3D) of Mulliken atomic spin densities for the nitroalkene  $1^{\bullet-}$  radical anion and the nitylimines  $2a-c^{\bullet+}$  radical cations, together with values of the electrophilic ( $P_k^+$ ) Parr function of **1** and the nucleophilic ( $P_k^-$ ) Parr functions of **2a–c**.

The analysis of the electrophilic Parr function  $P_k^+$  of (*E*)-3,3,3-trichloro-1-nitroprop-1-ene (**1**) showed that the most electrophilic center was located on the  $C\beta$  carbon atom,  $P_{C\beta}^+ = 0.278$ , which means that this center should react with the most nucleophilic center of substituted nitylimines. In turn, the results of the nucleophilic Parr functions  $P_k^-$  for nitylimines (**2a–c**) showed that the most nucleophilic center was located on the carbon atom of the  $-N=N=C$ -structure fragment. Both of the presented centers determined the most favorable path of the considered reactions to be path **B**, leading to the products **5a–c** (Scheme 1) [52,55].

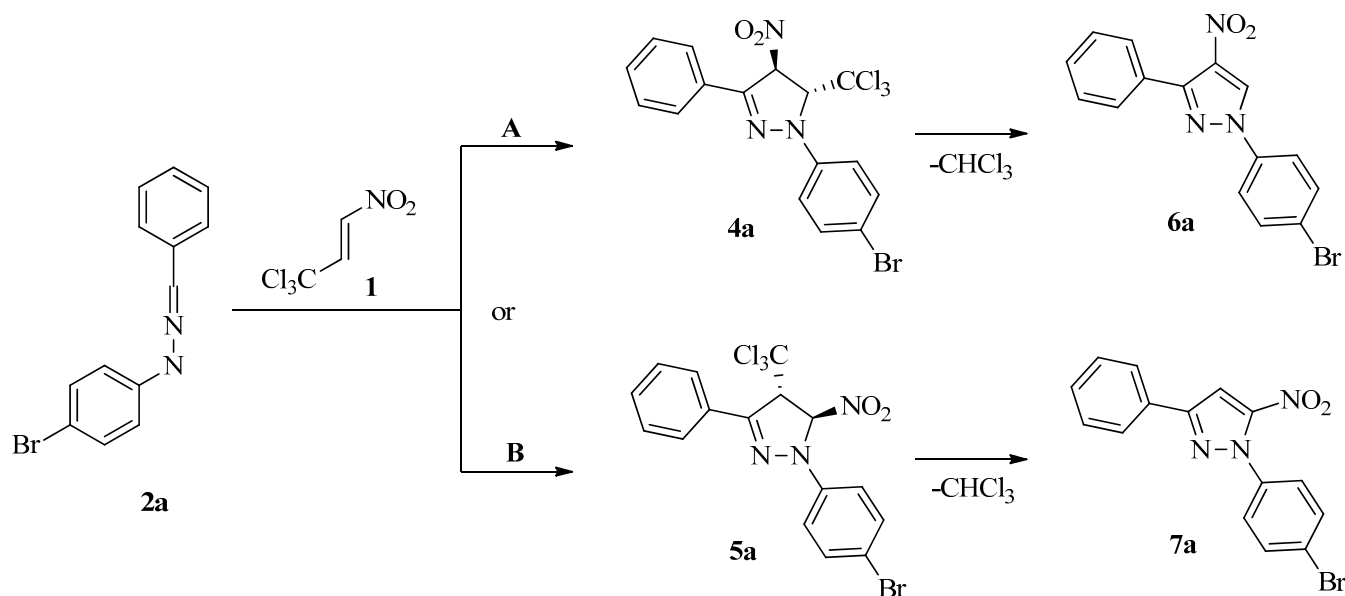
Next, we searched for good conditions for the reaction involving (*E*)-3,3,3-trichloro-1-nitroprop-1-ene (**1**) and *N*-(4-bromophenyl)-*C*-phenylnitylimine (**2a**). For this purpose, we conducted several tests using different reaction conditions, solvents and temperatures (Table 2). It was found that the analyzed process proceeded easily in benzene solution at room temperature. The TLC and HPLC examination of the postreaction mixture showed, without any doubts, the presence of only one reaction product ( $R_f = 0.56$  and  $R_t = 6.1$  min, respectively). It was easily isolated through column chromatography (see experimental part), and a solid material characterized by its adequate purity for analysis was obtained.

**Table 2.** Selected examples of reactions between TNP (**1**) and NI (**2a**) under different conditions.

| Temperature [°C] | Solvent | Reaction Time [h] | Catalyst                    | Yield [%] |
|------------------|---------|-------------------|-----------------------------|-----------|
| 25               | Benzene | 6                 | -                           | -         |
| 25               | Benzene | 24                | -                           | -         |
| 25               | Benzene | 6                 | Et <sub>3</sub> N           | 93        |
| 80               | Benzene | 6                 | Et <sub>3</sub> N           | 65        |
| 25               | Benzene | 6                 | <i>n</i> -PrNH <sub>2</sub> | 70        |
| 25               | Benzene | 6                 | CsCO <sub>3</sub>           | Trace     |
| 80               | Benzene | 6                 | CsCO <sub>3</sub>           | Trace     |

The IR spectrum of the isolated compound confirmed the presence of  $=N-N<$  and  $>C=N-$  moieties as well as the NO<sub>2</sub> group [56]. Unexpectedly, no bands connected with the expected existence of C-Cl bonds were detected. Next, based on HRMS analysis,

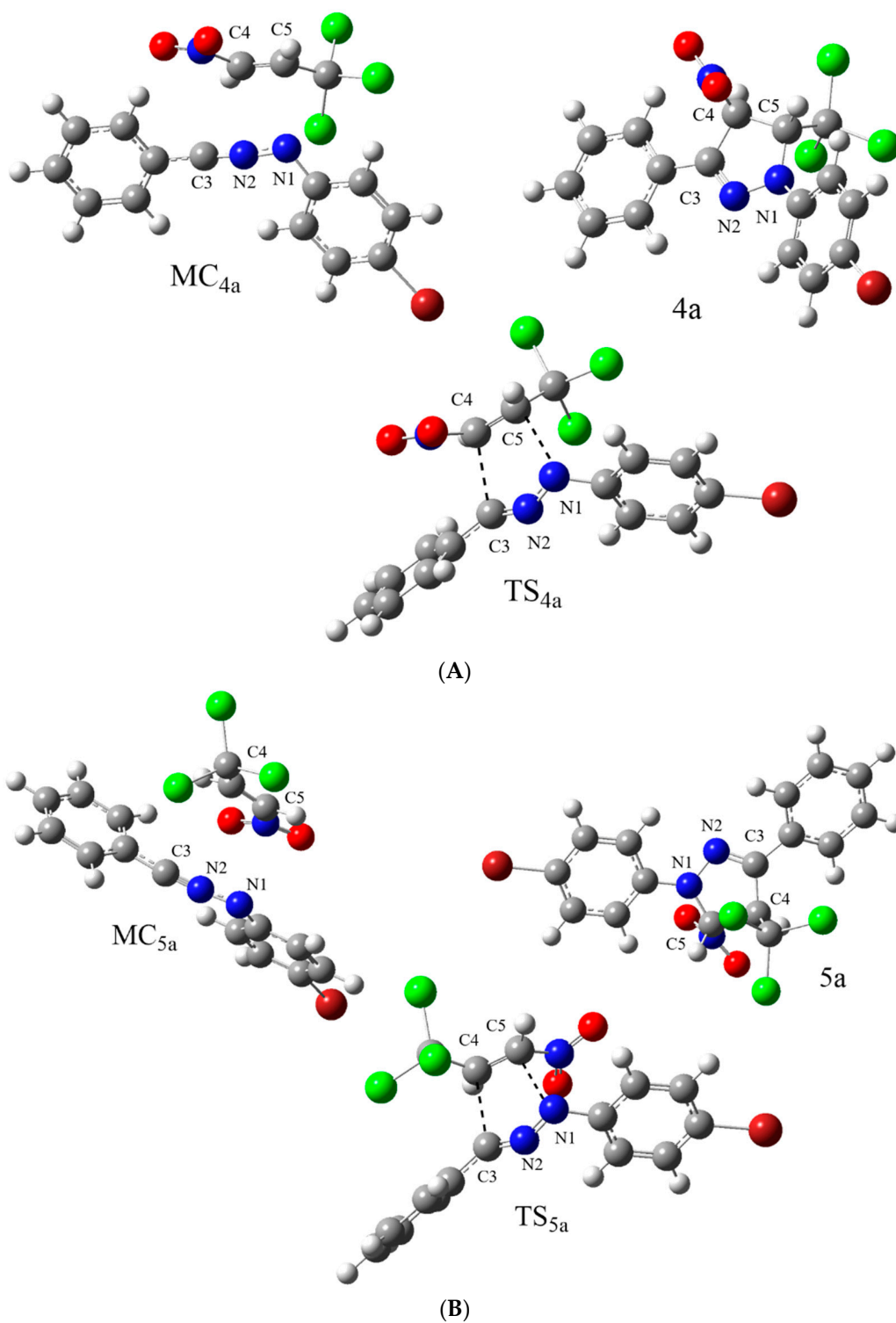
the compound was assigned the molecular formula of  $C_{15}H_{10}N_3O_2Br$ . The molecular weight of its molecular ion ( $[M + H]^+ = 344.0029$ ) was about 119.5 lower than those of the expected [3 + 2] cycloadducts. Lastly, in the  $^1H$ -NMR spectrum, the pair of expected doublets connected with the protons in the  $NO_2-C(H)-C(H)-CCl_3$  moiety was not detected. Due to the facts mentioned above, the isolated compound was not the expected pyrazoline (4a or 5a) but a product (6a or 7a) of the chloroform extrusion of the primary cycloadduct (4a or 5a) (Scheme 2).



**Scheme 2.** Competitive paths for the formation of regioisomeric pyrazoles (6a or 7a).

Unfortunately, the regioisomerism of the obtained pyrazole system was disputable because all the attempts to obtain a crystal form for RTG structural analysis were not successful. On the other hand, some valuable information regarding adduct regiochemistry can be derived from the NMR experiments. In particular, independently of the signal of the proton in the heterocyclic ring in the  $^1H$  NMR spectrum, we precisely identified signals from two different substituted benzene rings on the  $^1H$  and  $^{13}C$  NMR spectra (see Supplementary Materials). Using the HMBC experiment (see Supplementary Materials), we detected a clear correlation between the signal derived from the carbon atom of the benzene ring at the third position of the pyrazole molecular system and the signal derived from the proton connected directly to the pyrazole molecular system. On the other hand, similar correlations between the same proton and carbon atoms from the 4-bromophenyl moiety were not observed. This confirmed that the nitro group must be located at the C5 position of heterocyclic ring and, as a consequence, clearly showed that the isolated product exhibited the constitution of 1-(4-bromophenyl)-3-phenyl-5-nitropyrazole 7a. Therefore, as the primary [3 + 2] cycloaddition product, the adduct 5a should be exclusively considered.

In the next step, we decided to shed some light on the 1 + 2a cycloaddition process course using the DFT exploration of theoretically possible reaction channels (Scheme 2). It was found that both possible reaction channels were very similar in their nature. In particular, the first stage was the formation of a molecular complex (MC) (Figure 2). This was accompanied by the decrease of the enthalpy of the reaction system by a few kcal/mol. Due to the entropic factor, the Gibbs free energies of the formation of MCs were positive. This excluded the possibility of the existence of MCs as stable intermediates. Within MCs, no new chemical bonds were formed. Similar-type intermediates have been identified recently regarding many bimolecular processes, such as 32CAs [32,57–59], Diels–Alder reactions [54,60,61] and others [62–64]. Independent of the considered cycloaddition channel, the second reaction stage was a formation of the transition-state structure (TS) (Figure 2). The energetic barriers connected to the existence of TSs were relatively low (Table 3).



**Figure 2.** Views of critical structures of 32CA reaction of TNP (1) with NI (2a) in benzene solution according to WB97XD/6-311G(d,p)(PCM) calculations, for pathways (A) and (B) (Scheme 1).

**Table 3.** Kinetic and thermodynamic parameters of 32CA reaction of TNP (**1**) with NI (**2a**) according to WB97XD/6-311G(d,p)(PCM) calculations ( $\Delta H$  and  $\Delta G$  are given in kcal·mol<sup>-1</sup>;  $\Delta S$  is given in cal·mol<sup>-1</sup> K<sup>-1</sup>).

| Path | Transition                                     | $\Delta H$ | $\Delta G$ | $\Delta S$ |
|------|--|------------|------------|------------|
| A    | <b>1</b> + <b>2a</b> → <b>MC</b> <sub>4a</sub> | −6.61      | 3.32       | −42.41     |
|      | <b>1</b> + <b>2a</b> → <b>TS</b> <sub>4a</sub> | −0.74      | 11.52      | −50.26     |
|      | <b>1</b> + <b>2a</b> → <b>4a</b>               | −64.91     | −50.90     | −56.14     |
| B    | <b>1</b> + <b>2a</b> → <b>MC</b> <sub>5a</sub> | −8.80      | 0.69       | −40.97     |
|      | <b>1</b> + <b>2a</b> → <b>TS</b> <sub>5a</sub> | −2.25      | 10.50      | −51.90     |
|      | <b>1</b> + <b>2a</b> → <b>5a</b>               | −67.06     | −53.01     | −56.26     |

It was found interesting that the formation of pyrazoline **5a** was evidently favored from a kinetic point of view. This observation correlated well with the regiochemistry observed experimentally. Within TSs, the key interatomic distances were substantially reduced (Table 4). The synchronicity of the new bond formations was similar regarding both of the analyzed TSs. Next, the global electron density transfer (GEDT) [65] values suggested that optimized TSs should be treated as polar structures. However, this polarity was not sufficient in enforcing the stepwise, zwitterionic mechanism [66]. In a similar manner, we also theoretically explored 32CAs involving other nitrilimines (**2b,c**) (see Supplementary Materials). Our research suggested similar reaction regioselectivities and molecular mechanisms as well as the similar nature of their critical structures. Therefore, the suggested protocol for the preparation of nitro-substituted pyrazole analogs can be treated as a general protocol in some range.

**Table 4.** The key parameters of the critical structure parameters of 32CA reaction of TNP (**1**) with NI (**2a**) according to WB97XD/6-311G(d,p)(PCM) calculations.

|                         | C3-C4 r [Å] | $I_{C3-C4}$ | C5-N1 r [Å] | $I_{C5-N1}$ | $\Delta I$ | GEDT [e] |
|-------------------------|-------------|-------------|-------------|-------------|------------|----------|
| <b>MC</b> <sub>4a</sub> | 3.260       |             | 3.033       |             |            | 0.03     |
| <b>TS</b> <sub>4a</sub> | 2.242       | 0.521       | 2.355       | 0.378       | 0.14       | 0.17     |
| <b>4a</b>               | 1.516       |             | 1.452       |             |            |          |
| <b>MC</b> <sub>5a</sub> | 3.333       |             | 3.033       |             |            | 0.03     |
| <b>TS</b> <sub>5a</sub> | 2.275       | 0.509       | 2.383       | 0.309       | 0.20       | 0.20     |
| <b>5a</b>               | 1.526       |             | 1.409       |             |            |          |

### 3. Materials and Methods

#### 3.1. Materials

Commercially available (Sigma–Aldrich, Szelągowska 30, 61-626 Poznań, Poland) reagents and solvents were used. All solvents were tested with high pressure liquid chromatography before use. (*E*)-3,3,3-trichloro-1-nitroprop-1-ene (**1**) and *N*-(4-bromophenyl)-*C*-phenylnitrylimine (**2a**) were prepared in reactions described in literature [67–69].

#### 3.2. General Procedure for Cycloaddition Reactions

A mixture of 10 mmol of *N*-(4-bromophenyl)-*N'*-benzylidenehydrazine bromide (**1a**); 20 mmol of (*E*)-3,3,3-trichloro-1-nitroprop-1-ene (**3**); and 10 mmol of triethylamine in 5 mL of dry benzene was stirred in the dark at room temperature for 6 h. After that, the post-reaction mixture was washed with water, and solvent was evaporated in vacuo. The obtained semisolid mass was washed with cold petroleum ether, purified using column chromatography (stationary phase: SiO<sub>2</sub>, mobile phase: C-hex:AcOEt 9:1) and crystallized from ethanol. A white amorphous solid was obtained.

1-(4-bromophenyl)-3-phenyl-5-nitropyrazole (**7a**) was obtained as C<sub>15</sub>H<sub>10</sub>N<sub>3</sub>O<sub>2</sub>Br. Its yield was 93%, and its m.p. was 189–194 °C (EtOH). IR (KBr) results were as follows:  $\nu$  was 1617 (>C=C<), 1545 and 1351 (NO<sub>2</sub>), 1402 (=N–N<) and 1280 (–N=C<) cm<sup>-1</sup>. UV-Vis



(MeOH) results were as follows:  $\lambda$  was 262 nm.  $^1\text{H}$  NMR (500 MHz,  $\text{CDCl}_3$ ) results were as follows:  $\delta$  was 8.76 (s, 1H,  $\text{CH}=\text{C}-\text{NO}_2$ ), 7.80–7.77 (m, 2H,  $\text{CH}_{\text{Ar}}$ ), 7.70–7.66 (m, 4H,  $\text{CH}_{\text{Ar}}$ ) and 7.52–7.49 (m, 3H,  $\text{CH}_{\text{Ar}}$ ).  $^{13}\text{C}$  NMR (125 MHz,  $\text{CDCl}_3$ ) results were as follows:  $\delta$  was 148.53; 144.59; 137.46; 132.95; 129.78; 129.45; 128.26; 128.11; 122.24; 121.04; and 100.30. HR-MS (ESI, 200 °C) results calculated for  $\text{C}_{15}\text{H}_{10}\text{N}_3\text{O}_2\text{Br}$   $[\text{M} + \text{H}]^+ = 344.0019$  with a found value of 344.0029.

### 3.3. Analytical Techniques

For reaction progress testing, liquid chromatography (HPLC) was performed using a KNAUER apparatus equipped with a UV-Vis detector with application of the standard procedure [70–72]. LiChrospher RP-18 10  $\mu\text{m}$  column (4  $\times$  250 mm) was applied and methanol–water  $\text{MeOH}:\text{H}_2\text{O}$  (70:30  $v/v$ ) was used as eluent at a flow rate of 1.5  $\text{cm}^3 \text{min}^{-1}$ . Melting points were determined with the Boetius PHMK 05 apparatus and were not corrected. IR spectra (KBr pellets) were registered on a Thermo Nicolet 6700 FT-IR apparatus.  $^1\text{H}$  NMR (500 MHz) and  $^{13}\text{C}$  NMR (125 MHz) spectra were recorded with a Bruker AVANCE NMR spectrometer using  $\text{CDCl}_3$  as a solvent. TMS was used as an internal standard. UV-Vis spectra were determined for the 200–500 nm range through usage of spectrometer UV-5100 Biosens. HR-MS spectra were performed on a Shimadzu LCMS-IT-TOF instrument with ES ionization (heat block and CDL temperatures of 200 °C, nebulizing gas flow of 1.5 mL/min) connected to a Shimadzu Prominence two LC-20AD pump chromatograph equipped with Phenomenex Kinetex 2.6  $\mu\text{m}$  C18 100A column (acetonitrile–water mixtures,  $\text{ACN}:\text{H}_2\text{O}$ , 65:35  $v/v$ , were used as the eluent).

### 3.4. Computational Details

All computations were performed using the Gaussian 09 package [73] in the Prometheus computer cluster of the CYFRONET regional computer center in Cracow. DFT calculations were performed using the WB97XD/6-311G(d,p) [74,75] level of theory. A similar computational level has already been successfully used for the exploration of mechanistic aspects of other cycloaddition processes [45–47,76]. Calculations of all critical structures were performed at temperature  $T = 298 \text{ K}$  and pressure  $p = 1 \text{ atm}$ . All localized stationary points were characterized using vibrational analysis. It was found that starting molecules as well as products had positive Hessian matrices. On the other hand, all transition states showed only one negative eigenvalue in their Hessian matrices.

For all optimized transition states, intrinsic reaction coordinate (IRC) [77] computations were performed to verify that the located TSs were connected to the corresponding minimum stationary points associated with reactants and products. The solvent effects were simulated using a standard-procedure self-consistent reaction field (SCRF) [78,79] based on the polarizable continuum model (PCM) [80].

The global electron density transfer (GEDT) [68] values were designated based on the formula  $\text{GEDT} = |\sum q_A|$ , where  $q_A$  is the net Mulliken charge and where the sum is performed over all the atoms of (*E*)-3,3,3-trichloro-1-nitroprop-1-ene (3). In turn, the  $\sigma$ -bond development (*l*) indices were designated based on the formula [51,54]:

$$l_{X-Y} = 1 - \frac{r_{X-Y}^{\text{TS}} - r_{X-Y}^{\text{P}}}{r_{X-Y}^{\text{P}}}$$

where  $r_{X-Y}^{\text{TS}}$  is the distance between the reaction centers *X* and *Y* in the transition structure and where  $r_{X-Y}^{\text{P}}$  is the same distance in the corresponding product.

Global electronic properties of reactants, according to Domingo recommendations, were performed at B3LYP/6-31G(d) level of theory in the gas phase [42–44]. Electrophilic Parr functions  $\text{P}_k^+$  and nucleophilic Parr functions  $\text{P}_k^-$  were obtained from the changes in atomic spin density (ASD) of the reagents [52,55].

GaussView program [81] was used to visualize molecular geometries of all the systems as well as to show 3D representations of the radical anion and the radical cation.

#### 4. Conclusions

The reaction between (*E*)-3,3,3-trichloro-1-nitroprop-1-ene and *N*-(4-bromophenyl)-*C*-arylnitrylimines was examined using experimental and theoretical methods. The theoretical results showed that both of the considered 32CA channels are possible from a kinetic point of view of which the formation of 1-(4-bromophenyl)-3-aryl-4-tricholomethyl-5-nitro- $\Delta^2$ -pyrazoline is more probable. This conclusion was compatible with the presented MEDT study, where interactions between the  $C\beta$  atom of electrophilic (*E*)-3,3,3-trichloro-1-nitroprop-1-ene and the carbon atom of the  $-N=N=C-$  fragment of nucleophilic nitrilimine determine a more probable reaction path.

In turn, the experimental results of the 32CA reaction between (*E*)-3,3,3-trichloro-1-nitroprop-1-ene and *N*-(4-bromophenyl)-*C*-phenylnitrylimine showed that the presented reaction occurred with full regioselectivity. The obtained products were extremely unstable and spontaneously converted through  $CHCl_3$ -elimination to pyrazole systems. As a result, 1-(4-bromophenyl)-3-phenyl-5-nitropyrazole was obtained.

**Supplementary Materials:** The following supporting information can be downloaded at: <https://www.mdpi.com/article/10.3390/molecules27238409/s1>, pp. S2–S6. Computational data, pp. S7–S14.

**Author Contributions:** Conceptualization, K.K., A.Ł. and R.J.; methodology, K.K. and R.J.; investigation, K.K., M.S., O.M.D., G.K.G. and A.W.; resources, A.Ł.; data curation, K.K., A.Ł. and M.S.; writing—original draft preparation, K.K., A.Ł., K.Z. and R.J.; writing—review and editing, K.K., A.Ł. and R.J.; visualization, K.Z., M.S., G.K.G. and J.K.; software, K.Z., M.S. and J.K.; formal analysis, K.K., A.Ł., M.S., J.K., K.Z., A.W. and R.J.; supervision, R.J.; project administration, K.K., A.Ł. and R.J. All authors have read and agreed to the published version of the manuscript.

**Funding:** This research received no external funding.

**Institutional Review Board Statement:** Not applicable.

**Informed Consent Statement:** Not applicable.

**Data Availability Statement:** The data presented in this study are available on request from the corresponding author.

**Acknowledgments:** This research was supported in part by PL-Grid Infrastructure. All calculations reported in this paper were performed on the “Prometheus” supercomputer cluster in the CYFRONET computational center in Cracow.

**Conflicts of Interest:** The authors declare no conflict of interest.

**Sample Availability:** Samples of the compounds are available from the corresponding authors.

#### References

- Elkanzi, N.A.A. Review on Synthesis of prazole and pyrazolines. *Intent. J. Res. Pharm. Biomed. Sci.* **2013**, *4*, 17–26. [CrossRef]
- Kula, K.; Dobosz, J.; Jasiński, R.; Kačka-Zych, A.; Łapczuk-Krygier, A.; Mirosław, B.; Demchuk, O.M. [3+2] Cycloaddition of Diaryldiazomethanes with (*E*)-3,3,3-Trichloro-1-Nitroprop-1-Ene: An Experimental, Theoretical and Structural Study. *J. Mol. Struct.* **2020**, *1203*, 127473. [CrossRef]
- Kula, K.; Kačka-Zych, A.; Łapczuk-Krygier, A.; Wzorek, Z.; Nowak, A.K.; Jasiński, R. Experimental and Theoretical Mechanistic Study on the Thermal Decomposition of 3,3-Diphenyl-4-(Trichloromethyl)-5-Nitropyrazoline. *Molecules* **2021**, *26*, 1364. [CrossRef] [PubMed]
- Johnson, M.; Younglove, B.; Lee, L.; LeBlanc, R.; Holt, H.; Hills, P.; Mackay, H.; Brown, T.; Mooberry, S.L.; Lee, M. Design, Synthesis, and Biological Testing of Pyrazoline Derivatives of Combretastatin-A4. *Bioorg. Med. Chem. Lett.* **2007**, *17*, 5897–5901. [CrossRef] [PubMed]
- Amir, M.; Kumar, H.; Khan, S.A. Synthesis and Pharmacological Evaluation of Pyrazoline Derivatives as New Anti-Inflammatory and Analgesic Agents. *Bioorg. Med. Chem. Lett.* **2008**, *18*, 918–922. [CrossRef] [PubMed]
- Kerru, N.; Gummidi, L.; Maddila, S.; Gangu, K.K.; Jonnalagadda, S.B. A Review on Recent Advances in Nitrogen-Containing Molecules and Their Biological Applications. *Molecules* **2020**, *25*, 1909. [CrossRef]
- Sapnakumari, M.; Narayana, B.; Gurubasavarajswamy, P.M.; Sarojini, B.K. Design, Synthesis, and Pharmacological Evaluation of New Pyrazoline Derivatives. *Monatsh. Chem.* **2015**, *146*, 1015–1024. [CrossRef]

8. Bhandari, S.; Tripathi, A.C.; Saraf, S.K. Novel 2-Pyrazoline Derivatives as Potential Anticonvulsant Agents. *Med. Chem. Res.* **2013**, *22*, 5290–5296. [CrossRef]
9. Oh, L.M. Synthesis of Celecoxib via 1,3-Dipolar Cycloaddition. *Tetrahedron Lett.* **2006**, *47*, 7943–7946. [CrossRef]
10. Wellinga, K.; Grosscurt, A.C.; Van Hes, R. 1-Phenylcarbamoyl-2-Pyrazolines: A New Class of Insecticides. 1. Synthesis and Insecticidal Properties of 3-Phenyl-1-Phenylcarbamoyl-2-Pyrazolines. *J. Agric. Food Chem.* **1977**, *25*, 987–992. [CrossRef]
11. Van Hes, R.; Wellinga, K.; Grosscurt, A.C. 1-Phenylcarbamoyl-2-Pyrazolines: A New Class of Insecticides. 2. Synthesis and Insecticidal Properties of 3,5-Diphenyl-1-Phenylcarbamoyl-2-Pyrazolines. *J. Agric. Food Chem.* **1978**, *26*, 915–918. [CrossRef]
12. Yang, R.; Lv, M.; Xu, H. Synthesis of Piperine Analogs Containing Isoxazoline/Pyrazoline Scaffold and Their Pesticidal Bioactivities. *J. Agric. Food Chem.* **2018**, *66*, 11254–11264. [CrossRef] [PubMed]
13. McCann, S.F.; Annis, G.D.; Shapiro, R.; Piotrowski, D.W.; Lahm, G.P.; Long, J.K.; Lee, K.C.; Hughes, M.M.; Myers, B.J.; Griswold, S.M.; et al. The Discovery of Indoxacarb: Oxadiazines as a New Class of Pyrazoline-Type Insecticides. *Pest Manag. Sci.* **2001**, *57*, 153–164. [CrossRef] [PubMed]
14. von Stein, R.T.; Silver, K.S.; Soderlund, D.M. Indoxacarb, Metaflumizone, and Other Sodium Channel Inhibitor Insecticides: Mechanism and Site of Action on Mammalian Voltage-Gated Sodium Channels. *Pestic. Biochem. Physiol.* **2013**, *106*, 101–112. [CrossRef]
15. Rudolf, M.; Kobus, W. Insecticidal 1-(Phenylcarbamoyl)-2-Pyrazolines. *Chem. Abstr.* **1973**, *79*, 584.
16. Dong, C.; Gao, W.; Li, X.; Sun, S.; Huo, J.; Wang, Y.; Ren, D.; Zhang, J.; Chen, L. Synthesis of Pyrazole-4-Carboxamides as Potential Fungicide Candidates. *Mol. Divers.* **2021**, *25*, 2379–2388. [CrossRef]
17. Zhao, P.L.; Fu, W.; Zhang, M.Z.; Liu, Z.M.; Wei, H.; Yang, G.F. Synthesis, Fungicidal, and Insecticidal Activities of  $\beta$ -Methoxyacrylate-Containing N-Acetyl Pyrazoline Derivatives. *J. Agric. Food Chem.* **2008**, *56*, 10767–10773. [CrossRef]
18. Saber, M. Acute and Population Level Toxicity of Imidacloprid and Fenpyroximate on an Important Egg Parasitoid, *Trichogramma Cacoeciae* (Hymenoptera: Trichogrammatidae). *Ecotoxicology* **2011**, *20*, 1476–1484. [CrossRef]
19. Gunasekara, A.S.; Truong, T.; Goh, K.S.; Spurlock, F.; Tjeerdema, R.S. Environmental Fate and Toxicology of Fipronil. *J. Pestic. Sci.* **2007**, *32*, 189–199. [CrossRef]
20. Khan, M.A.; Ruberson, J.R. Lethal Effects of Selected Novel Pesticides on Immature Stages of *Trichogramma Pretiosum* (Hymenoptera: Trichogrammatidae). *Pest Manag. Sci.* **2017**, *73*, 2465–2472. [CrossRef]
21. Charli, A.; Jin, H.; Anantharam, V.; Kanthasamy, A.; Kanthasamy, A.G. Alterations in Mitochondrial Dynamics Induced by Tebufenpyrad and Pyridaben in a Dopaminergic Neuronal Cell Culture Model. *Neurotoxicology* **2016**, *53*, 302–313. [CrossRef] [PubMed]
22. Łapczuk-Krygier, A.; Kačka-Zych, A.; Kula, K. Recent Progress in the Field of Cycloaddition Reactions Involving Conjugated Nitroalkenes. *Curr. Chem. Lett.* **2019**, *8*, 13–38. [CrossRef]
23. Ríos-Gutiérrez, M.; Domingo, L.R. Unravelling the Mysteries of the [3+2] Cycloaddition Reactions. *Eur. J. Org. Chem.* **2019**, *2019*, 267–282. [CrossRef]
24. Verhaeghe, P.; Azas, N.; Hutter, S.; Castera-Ducros, C.; Laget, M.; Dumètre, A.; Gasquet, M.; Reboul, J.-P.; Rault, S.; Rathelot, P.; et al. Synthesis and in Vitro Antiplasmodial Evaluation of 4-Anilino-2-Trichloromethylquinazolines. *Bioorg. Med. Chem.* **2009**, *17*, 4313–4322. [CrossRef] [PubMed]
25. Boguszewska-Czubarra, A.; Kula, K.; Wnorowski, A.; Biernasiuk, A.; Popiołek, Ł.; Miodowski, D.; Demchuk, O.M.; Jasiński, R. Novel functionalized  $\beta$ -nitrostyrenes: Promising candidates for new antibacterial drugs. *Saudi Pharm. J.* **2019**, *27*, 593–601. [CrossRef] [PubMed]
26. Alston, T.A.; Porter, D.J.T.; Bright, H.J. The Bioorganic Chemistry of the Nitroalkyl Group. *Bioorg. Chem.* **1985**, *13*, 375–403. [CrossRef]
27. Winkler, R.; Hertweck, C. Biosynthesis of Nitro Compounds. *ChemBioChem* **2007**, *8*, 973–977. [CrossRef]
28. Raether, W.; Hänel, H. Nitroheterocyclic Drugs with Broad Spectrum Activity. *Parasitol. Res.* **2003**, *90*, 19–39. [CrossRef]
29. Fryźlewicz, A.; Łapczuk-Krygier, A.; Kula, K.; Demchuk, O.M.; Dresler, E.; Jasiński, R. Regio- and Stereoselective Synthesis of Nitrofunctionalized 1,2-Oxazolidine Analogs of Nicotine. *Chem. Heterocycl. Compd.* **2020**, *56*, 120–122. [CrossRef]
30. Jasiński, R.; Mróz, K.; Kačka, A. Experimental and Theoretical DFT Study on Synthesis of Sterically Crowded 2,3,3,(4)5-Tetrasubstituted-4-Nitroisoxazolidines via 1,3-Dipolar Cycloaddition Reactions Between Ketonitrone and Conjugated Nitroalkenes. *J. Heterocycl. Chem.* **2016**, *53*, 1424–1429. [CrossRef]
31. Jasiński, R.; Mróz, K. Kinetic Aspects of [3+2] Cycloaddition Reactions between (E)-3,3,3-Trichloro-1-Nitroprop-1-Ene and Ketonitrone. *React. Kinet. Mech. Catal.* **2015**, *116*, 35–41. [CrossRef]
32. Zawadzińska, K.; Ríos-Gutiérrez, M.; Kula, K.; Woliński, P.; Mirosław, B.; Krawczyk, T.; Jasiński, R. The Participation of 3,3,3-Trichloro-1-Nitroprop-1-Ene in the [3+2] Cycloaddition Reaction with Selected Nitrile N-Oxides in the Light of the Experimental and MEDT Quantum Chemical Study. *Molecules* **2021**, *26*, 6774. [CrossRef] [PubMed]
33. Kula, K.; Zawadzińska, K. Local Nucleophile-Electrophile Interactions in [3+2] Cycloaddition Reactions between Benzonitrile N-Oxide and Selected Conjugated Nitroalkenes in the Light of MEDT Computational Study. *Curr. Chem. Lett.* **2021**, *10*, 9–16. [CrossRef]
34. Jasiński, R. One-Step versus Two-Step Mechanism of Diels-Alder Reaction of 1-Chloro-1-Nitroethene with Cyclopentadiene and Furan. *J. Mol. Graph. Model.* **2017**, *75*, 55–61. [CrossRef]

35. Żmigrodzka, M.; Sadowski, M.; Dresler, E.; Demchuk, O.M.; Kula, K. Polar [3+2] Cycloaddition between N-Methyl Azomethine Ylide and Trans-3,3,3-Trichloro-1-Nitroprop-1-Ene. *Sci. Rad.* **2022**, *1*, 26–35. [CrossRef]
36. Żmigrodzka, M.; Dresler, E.; Hordyjewicz-Baran, Z.; Kulesza, R.; Jasiński, R. A Unique Example of Noncatalyzed [3+2] Cycloaddition involving (2E)-3-Aryl-2-Nitroprop-2-Enenitriles. *Chem. Heterocycl. Compd.* **2017**, *53*, 1161–1162. [CrossRef]
37. Barkov, A.; Zimnitskiy, N.; Korotaev, V.; Kutyashev, I.; Moshkin, V.; Sosnovskikh, V. Highly regio- and stereoselective 1,3-dipolar cycloaddition of stabilised azomethine ylides to 3,3,3-trihalogeno-1-nitropropenes: Synthesis of trihalomethylated spiro[indoline-3,2'-pyrrolidin]-2-ones and spiro[indoline-3,3'-pyrrolizin]-2-ones. *Tetrahedron* **2016**, *72*, 6825–6836. [CrossRef]
38. Korotaev, V.Y.; Sosnovskikh, V.Y.; Kutyashev, I.B.; Barkov, A.Y.; Matochkina, E.G.; Kodess, M.I. A simple and convenient synthesis of 4-methyl-3-nitro-2-trihalomethyl-2H-chromenes from N-unsubstituted imines of 2-hydroxyacetophenones and trichloro (trifluoro) ethylidene nitromethanes. *Tetrahedron* **2008**, *64*, 5055–5060. [CrossRef]
39. Golushko, A.A.; Sandzhieva, M.A.; Ivanov, A.Y.; Boyarskaya, I.A.; Khoroshilova, O.V.; Barkov, A.Y.; Vasilyev, A.V. Reactions of 3,3,3-Trihalogeno-1-nitropropenes with Arenes in the Supercacid CF<sub>3</sub>SO<sub>3</sub>H: Synthesis of (Z)-3, 3, 3-Trihalogeno-1,2-diarylpropan-1-one Oximes and Study on the Reaction Mechanism. *J. Org. Chem.* **2018**, *83*, 10142–10157. [CrossRef]
40. Golushko, A.A.; Khoroshilova, O.V.; Vasilyev, A.V. Synthesis of 1, 2, 4-oxadiazoles by tandem reaction of nitroalkenes with arenes and nitriles in the superacid TfOH. *J. Org. Chem.* **2019**, *84*, 7495–7500. [CrossRef]
41. Domingo, L.R. Molecular Electron Density Theory: A Modern View of Reactivity in Organic Chemistry. *Molecules* **2016**, *21*, 1319. [CrossRef] [PubMed]
42. Domingo, L.R.; Ríos-Gutiérrez, M.; Pérez, P. Applications of the Conceptual Density Functional Theory Indices to Organic Chemistry Reactivity. *Molecules* **2016**, *21*, 748. [CrossRef]
43. Parr, R.G.; Yang, W. *Density Functional Theory of Atoms and Molecules*, 1st ed.; Oxford University Press: New York, NY, USA, 1989.
44. Parr, R.G.; Szentpály, L.v.; Liu, S. Electrophilicity Index. *J. Am. Chem. Soc.* **1999**, *121*, 1922–1924. [CrossRef]
45. Domingo, L.R.; Kula, K.; Ríos-Gutiérrez, M. Unveiling the Reactivity of Cyclic Azomethine Ylides in [3+2] Cycloaddition Reactions within the Molecular Electron Density Theory. *Eur. J. Org. Chem.* **2020**, *2020*, 5938–5948. [CrossRef]
46. Mlostoń, G.; Kula, K.; Jasiński, R. A DFT Study on the Molecular Mechanism of Additions of Electrophilic and Nucleophilic Carbenes to Non-Enolizable Cycloaliphatic Thioketones. *Molecules* **2021**, *26*, 5562. [CrossRef] [PubMed]
47. Domingo, L.R.; Kula, K.; Ríos-Gutiérrez, M.; Jasiński, R. Understanding the Participation of Fluorinated Azomethine Ylides in Carbenoid-Type [3 + 2] Cycloaddition Reactions with Ynal Systems: A Molecular Electron Density Theory Study. *J. Org. Chem.* **2021**, *86*, 12644–12653. [CrossRef]
48. Domingo, L.R.; Ríos-Gutiérrez, M.; Silvi, B.; Pérez, P. The Mysticism of Pericyclic Reactions: A Contemporary Rationalisation of Organic Reactivity Based on Electron Density Analysis. *Eur. J. Org. Chem.* **2018**, *2018*, 1107–1120. [CrossRef]
49. Domingo, L.R.; Chamorro, E.; Pérez, P. Understanding the reactivity of captodative ethylenes in polar cycloaddition reactions. A theoretical study. *J. Org. Chem.* **2008**, *73*, 4615–4624. [CrossRef]
50. Domingo, L.R.; Ríos-Gutiérrez, M. *Conceptual Density Functional Theory*; Liu, S., Ed.; Wiley VCH GmbH: Weinheim, Germany, 2022; Chapter 24.
51. Fryźlewicz, A.; Olszewska, A.; Zawadzińska, K.; Woliński, P.; Kula, K.; Kačka-Zych, A.; Łapczuk-Krygier, A.; Jasiński, R. On the Mechanism of the Synthesis of Nitrofunctionalised  $\Delta^2$ -Pyrazolines via [3+2] Cycloaddition Reactions between  $\alpha$ -EWG-Activated Nitroethenes and Nitrylimine TAC Systems. *Organics* **2022**, *3*, 59–76. [CrossRef]
52. Aurell, M.J.; Domingo, L.R.; Pérez, P.; Contreras, R. A theoretical study on the regioselectivity of 1,3-dipolar cycloadditions using DFT-based reactivity indexes. *Tetrahedron* **2004**, *60*, 11503–11509. [CrossRef]
53. Mlostoń, G.; Jasiński, R.; Kula, K.; Heimgartner, H. A DFT Study on the Barton-Kellogg Reaction—The Molecular Mechanism of the Formation of Thiiranes in the Reaction between Diphenyldiazomethane and Diaryl Thioketones. *Eur. J. Org. Chem.* **2020**, *2020*, 176–182. [CrossRef]
54. Kula, K.; Kačka-Zych, A.; Łapczuk-Krygier, A.; Jasiński, R. Analysis of the Possibility and Molecular Mechanism of Carbon Dioxide Consumption in the Diels-Alder Processes. *Pure Appl. Chem.* **2021**, *93*, 427–446. [CrossRef]
55. Domingo, L.R.; Pérez, P.; Sáez, J.A. Understanding the Local Reactivity in Polar Organic Reactions through Electrophilic and Nucleophilic Parr Functions. *RSC Adv.* **2013**, *3*, 1486–1494. [CrossRef]
56. Ioffe, B.V. Characteristic Frequencies in the Infrared Spectra of Pyrazolines. *Chem. Heterocycl. Compd.* **1971**, *4*, 791–793. [CrossRef]
57. Jasiński, R. In the Searching for Zwitterionic Intermediates on Reaction Paths of [3 + 2] Cycloaddition Reactions between 2,2,4,4-Tetramethyl-3-Thiocyclobutanone S-Methylide and Polymerizable Olefins. *RSC Adv.* **2015**, *5*, 101045–101048. [CrossRef]
58. Jasiński, R. A Stepwise, Zwitterionic Mechanism for the 1,3-Dipolar Cycloaddition between (Z)-C-4-Methoxyphenyl-N-Phenylnitron and Gem-Chloronitroethene Catalysed by 1-Butyl-3-Methylimidazolium Ionic Liquid Cations. *Tetrahedron Lett.* **2015**, *56*, 532–535. [CrossRef]
59. Kula, K.; Łapczuk-Krygier, A. A DFT computational study on the [3+2] cycloaddition between parent thionitron and nitroethene. *Curr. Chem. Lett.* **2018**, *7*, 27–34. [CrossRef]
60. Kačka-Zych, A.; Pérez, P. Perfluorobicyclo[2.2.0]Hex-1(4)-Ene as Unique Partner for Diels–Alder Reactions with Benzene: A Density Functional Theory Study. *Theor. Chem. Acc.* **2021**, *140*, 17. [CrossRef]
61. Kačka-Zych, A.; Jasiński, R. Molecular Mechanism of Hetero Diels-Alder Reactions between (E)-1,1,1-Trifluoro-3-Nitrobut-2-Enes and Enamine Systems in the Light of Molecular Electron Density Theory. *J. Mol. Graph. Model.* **2020**, *101*, 107714. [CrossRef]

62. Demchuk, O.M.; Jasiński, R.; Pietrusiewicz, K.M. New Insights into the Mechanism of Reduction of Tertiary Phosphine Oxides by Means of Phenylsilane. *Heteroat. Chem.* **2015**, *26*, 441–448. [CrossRef]
63. Alnajjar, R.A.; Jasiński, R. Competition between [2+1]- and [4+1]-Cycloaddition Mechanisms in Reactions of Conjugated Nitroalkenes with Dichlorocarbene in the Light of a DFT Computational Study. *J. Mol. Model.* **2019**, *25*, 157. [CrossRef] [PubMed]
64. Kačka-Zych, A.; Jasiński, R. Mechanistic Aspects of the Synthesis of Seven-membered Internal Nitronates via Stepwise [4 + 3] Cycloaddition Involving Conjugated Nitroalkenes: Molecular Electron Density Theory Computational Study. *J. Comput. Chem.* **2022**, *43*, 1221–1228. [CrossRef] [PubMed]
65. Domingo, L.R. A New C–C Bond Formation Model Based on the Quantum Chemical Topology of Electron Density. *RSC Adv.* **2014**, *4*, 32415–32428. [CrossRef]
66. Jasiński, R.; Dresler, E. On the Question of Zwitterionic Intermediates in the [3+2] Cycloaddition Reactions: A Critical Review. *Organics* **2020**, *1*, 49–69. [CrossRef]
67. Shawali, A.S.; Farghaly, T.A.; Hussein, S.M.; Abdalla, M.M. Site-Selective Reactions of Hydrazonoyl Chlorides with Cyanoacetic Hydrazide and Its N-Arylidene Derivatives and Anti-Aggressive Activity of Prepared Products. *Arch. Pharm. Res.* **2013**, *36*, 694–701. [CrossRef]
68. Zhang, Y.; Liu, W.; Zhao, Z. Nucleophilic Trapping Nitrilimine Generated by Photolysis of Diaryltetrazole in Aqueous Phase. *Molecules* **2013**, *19*, 306–315. [CrossRef] [PubMed]
69. Perekalin, W.; Lipina, E.S.; Berestovitskaya, V.; Efremov, D.A. *Nitroalkenes: Conjugated Nitro Compounds*; Wiley: New York, NY, USA, 1994; ISBN 0471943185.
70. Beheshti, A.; Kamalzadeha, Z.; Haj-Maleka, M.; Payaba, M.; Rezvanfar, M.A.; Siadati, S.A. Development and Validation of a Reversed-Phase HPLC Method for Determination of Assay Content of Teriflunomide by the Aid of BOMD Simulations. *Curr. Chem. Lett.* **2021**, *10*, 281–294. [CrossRef]
71. Siadati, S.A.; Rezvanfar, M.A.; Payab, M.; Beheshti, A. Development and Validation of a Short Runtime Method for Separation of Trace Amounts of 4-Aminophenol, Phenol, 3-Nitrosalicylic Acid and Mesalamine by Using HPLC System. *Curr. Chem. Lett.* **2021**, *10*, 151–160. [CrossRef]
72. Demchuk, O.M.; Jasiński, R.; Strzelecka, D.; Dziuba, K.; Kula, K.; Chrzanowski, J.; Krasowska, D. A clean and simple method for deprotection of phosphines from borane complexes. *Pure Appl. Chem.* **2018**, *90*, 49–62. [CrossRef]
73. Frisch, M.J.; Trucks, G.W.; Schlegel, H.B.; Scuseria, G.E.; Robb, M.A.; Cheeseman, J.R.; Scalmani, G.; Barone, V.; Mennucci, B. *GAUSSIAN 09, Revision, C.01*; Gaussian, Inc.: Wallingford, CT, USA, 2009.
74. Hehre, M.J.; Radom, L.; Schleyer, P.v.R.; Pople, J. *Ab Initio Molecular Orbital Theory*; Wiley: New York, NY, USA, 1986.
75. Grimme, S.; Antony, J.; Ehrlich, S.; Krieg, H. A Consistent and Accurate Ab Initio Parametrization of Density Functional Dispersion Correction (DFT-D) for the 94 Elements H–Pu. *J. Chem. Phys.* **2010**, *132*, 154104. [CrossRef]
76. Zawadzińska, K.; Kula, K. Application of  $\beta$ -Phosphorylated Nitroethenes in [3+2] Cycloaddition Reactions Involving Benzonitrile N-Oxide in the Light of a DFT Computational Study. *Organics* **2021**, *2*, 26–37. [CrossRef]
77. Fukui, K. Formulation of the Reaction Coordinate. *J. Phys. Chem.* **1970**, *74*, 4161–4163. [CrossRef]
78. Tapia, O. Solvent Effect Theories: Quantum and Classical Formalisms and Their Applications in Chemistry and Biochemistry. *J. Math. Chem.* **1992**, *10*, 139–181. [CrossRef]
79. Tomasi, J.; Persico, M. Molecular Interactions in Solution: An Overview of Methods Based on Continuous Distributions of the Solvent. *Chem. Rev.* **1994**, *94*, 2027–2094. [CrossRef]
80. Cossi, M.; Barone, V.; Cammi, R.; Tomasi, J. Ab Initio Study of Solvated Molecules: A New Implementation of the Polarizable Continuum Model. *Chem. Phys. Lett.* **1996**, *255*, 327–335. [CrossRef]
81. Dennington, R.; Keith, T.A.; Millam, J.M. *GaussView, Version 6.0*; Semichem Inc.: Shawnee Mission, KS, USA, 2016.

Article

# Regioselective Synthesis, Structural Characterization, and Antiproliferative Activity of Novel Tetra-Substituted Phenylaminopyrazole Derivatives

Matteo Lusardi <sup>1,†</sup> , Aldo Profumo <sup>2,†</sup> , Chiara Rotolo <sup>1</sup>, Erika Iervasi <sup>2</sup>, Camillo Rosano <sup>2</sup> ,  
Andrea Spallarossa <sup>1,\*</sup>  and Marco Ponassi <sup>2</sup>

<sup>1</sup> Department of Pharmacy, University of Genova, Viale Benedetto XV, 3, 16132 Genova, Italy

<sup>2</sup> Proteomics and Mass Spectrometry Unit, IRCCS Ospedale Policlinico San Martino, Largo R. Benzi 10, 16132 Genova, Italy

\* Correspondence: andrea.spallarossa@unige.it

† These authors contributed equally to this work.

**Abstract:** A small library of highly functionalized phenylaminopyrazoles, bearing different substituents at position 1, 3, and 4 of the pyrazole ring, was prepared by the one-pot condensation of active methylene reagents, phenylisothiocyanate, and substituted hydrazine (namely, methyl- and benzyl-hydrazine). The identified reaction conditions proved to be versatile and efficient. Furthermore, the evaluation of alternative stepwise protocols affected the chemo- and regio-selectivity outcome of the one-pot procedure. The chemical identities of two *N*-methyl pyrazole isomers, selected as prototypes of the whole series, were unambiguously identified by means of NMR and mass spectrometry studies. Additionally, semiempirical calculations provided a structural rationale for the different chromatographic behavior of the two isomers. The prepared tetra-substituted phenylaminopyrazoles were tested in cell-based assays on a panel of cancer and normal cell lines. The tested compounds did not show any cytotoxic effect on the selected cell lines, thus supporting their pharmaceutical potentials.

**Keywords:** tetra-substituted pyrazoles; mass-spectrometry; antiproliferative activity; computational simulations

**Citation:** Lusardi, M.; Profumo, A.; Rotolo, C.; Iervasi, E.; Rosano, C.; Spallarossa, A.; Ponassi, M. Regioselective Synthesis, Structural Characterization, and Antiproliferative Activity of Novel Tetra-Substituted Phenylaminopyrazole Derivatives. *Molecules* **2022**, *27*, 5814. <https://doi.org/10.3390/molecules27185814>

Academic Editors: Vera L. M. Silva and Artur M. S. Silva

Received: 12 August 2022

Accepted: 5 September 2022

Published: 8 September 2022

**Publisher's Note:** MDPI stays neutral with regard to jurisdictional claims in published maps and institutional affiliations.



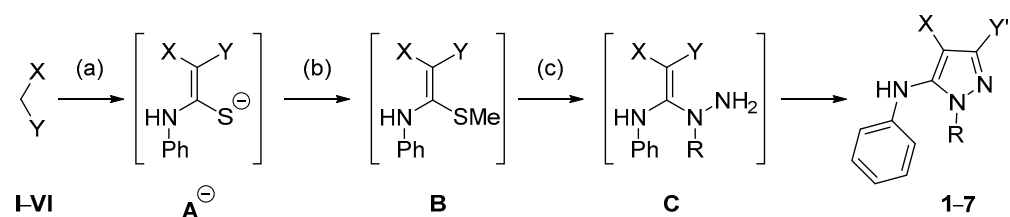
**Copyright:** © 2022 by the authors. Licensee MDPI, Basel, Switzerland. This article is an open access article distributed under the terms and conditions of the Creative Commons Attribution (CC BY) license (<https://creativecommons.org/licenses/by/4.0/>).

## 1. Introduction

Pyrazole represents a distinctive scaffold in medicinal chemistry [1–9] as pyrazole-containing compounds showed a wide spectrum of biological properties. As recently reviewed by Ebenezer and coworkers [10], pyrazoles showed anti-inflammatory activity [11,12] which was able to reduce the level of TNF $\alpha$  and/or the release of NO [13,14]. Furthermore, some pyrazole derivatives proved to be more potent COX-2 inhibitors than celecoxib with minimal ulcerogenic effect associated [15–17]. Some derivatives showed anti-inflammatory/analgesic dual activity [18,19], whereas other pyrazole compounds proved to interfere with the cannabinoid system and exert an analgesic effect [20]. Pyrazole derivatives proved also to be efficient antibacterial agents [21] able to block the proliferation of Gram-positive and Gram-negative pathogens through different mechanisms (e.g., inhibition of DNA-gyrase or DHFR enzymes) [22,23]. Additionally, a number of pyrazole derivatives showed anticancer activities [24,25] on different tumor cell lines. The molecular mechanism behind the antiproliferative activity of pyrazole compounds include the inhibition of the VEGFR-2 kinase [26], the dual blocking of cyclin-dependent kinase and histone deacetylase [27], or the targeting different signaling pathways, including ERK/MAPK and phosphatases [28]. Finally, pyrazole derivatives showed antifungal, hypoglycemic, antileishmanial, antimalaria, antituberculosis, and antioxidant properties thus supporting the pharmaceutical relevance of this heterocyclic nucleus [10].

In particular, functionalized phenylamino-substituted pyrazole derivatives proved to be effective agrochemical fungicides [29–31], hypoglycemic [32–34], and antiproliferative (Bruton’s kinase inhibitors or necroptosis-based cancer agents) [35–37] compounds. Interestingly, recent patents reported combination of fungicidal phenylamino pyrazoles with other compounds as novel insecticide and antibacterial agents [38,39].

According to the literature, phenylamino-substituted pyrazoles can be prepared by either the cyclization with hydrazine of a *N,S*-thioacetal intermediate [40] or the functionalization of a thiomethyl pyrazole with a suitable aniline [41]. These protocols allowed the preparation of tri- and tetra-substituted phenylamino pyrazoles in good yields though relying on stepwise protocols. Recently, we reported the chemo-selective, one-pot synthesis of highly substituted pyrazole compounds through the condensation of an active methylene reagent (AMR), isothiocyanate, and hydrazine [42]. Among the prepared tri-substituted pyrazoles, selected derivatives showed interesting antiproliferative activity being able to selectively inhibit the growth of SkMel28 and HeLa cells without affecting the proliferation of human fibroblasts [42]. To further evaluate the versatility of the developed procedure and identify unreported synthetic strategies for the preparation of pharmaceutically attractive phenylamino pyrazoles [29–39], we studied the condensation of phenylisothiocyanate, AMRs, and substituted hydrazines (namely, methylhydrazine and benzylhydrazine) to afford tetra-functionalized phenylamino-substituted pyrazole derivatives **1–7** (Scheme 1, Table 1). Eventually, the antiproliferative/cytotoxic activities of the synthesized molecules were evaluated against a panel of eight tumor and one normal fibroblast cell lines for preliminary biological characterization.

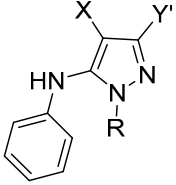


**Scheme 1.** One-pot synthesis of *N*-substituted pyrazoles **1–7**. Reaction conditions: (a) DMFdry, NaH, PhNCS, rt, 1 h; (b) MeI, rt, 3 h; (c) methylhydrazine or benzylhydrazine, 100 °C, 4 h. The structures of AMRs I–VI are reported in Table 1.

## 2. Results and Discussion

### 2.1. Chemistry

AMRs I–VI (Table 1) were sequentially reacted with phenylisothiocyanate, methyl iodide, and the proper substituted hydrazine under the previously reported one-pot, three-step conditions (Scheme 1) [42]. Briefly, the reaction in basic condition of AMRs with the phenylisothiocyanate led to the formation of thioamide intermediates **A**<sup>−</sup> that were *S*-methylated in situ with iodomethane. The so obtained *N,S*-thioacetal intermediates **B** were then condensed with substituted hydrazine to afford ring-opened intermediates **C** that led to the final pyrazole compounds **1–7** in moderate-to-good yields (Table 1).

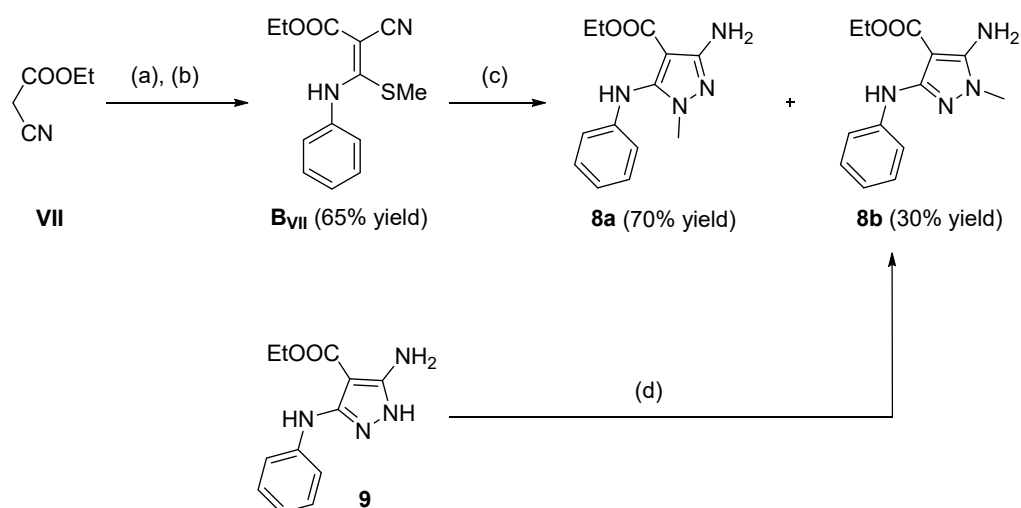
**Table 1.** Synthesized pyrazoles and active methylene reagents employed in the synthesis.


| AMR | X                  | Y                    | Cpd    | Y'              | R                  | Yield (%) |
|-----|--------------------|----------------------|--------|-----------------|--------------------|-----------|
| I   | CN                 | CN                   | 1 [43] | NH <sub>2</sub> | Me                 | 56        |
| II  | CN                 | COC(Me) <sub>3</sub> | 2      | t-Bu            | Me                 | 61        |
| III | CN                 | COPh                 | 3      | Ph              | Me                 | 60        |
| III | CN                 | COPh                 | 4      | Ph              | CH <sub>2</sub> Ph | 27        |
| IV  | COPh               | COPh                 | 5      | Ph              | Me                 | 50        |
| V   | COOMe              | CN                   | 6      | NH <sub>2</sub> | Me                 | 12        |
| VI  | SO <sub>2</sub> Ph | CN                   | 7      | NH <sub>2</sub> | Me                 | 61        |

Intriguingly, the tested conditions proved to be highly regio- and chemo-selective, allowing the isolation of a single *N*<sup>1</sup>-substituted pyrazole derivative. In particular, out of the two nucleophilic centres of methyl- or benzyl-hydrazine, the substituted nitrogen atom would selectively displace the SMe group of intermediates **B** leading to the formation of intermediate **C** (Scheme 1). As previously observed for unsubstituted hydrazine [42], the reactivity of hydrazinic NH<sub>2</sub> group in intermediates **C** is selectively oriented toward X or Y group, leading to the formation of a unique *N*<sup>1</sup>-substituted pyrazole. Thus, when X = COOMe and Y = CN, the hydrazinic amine group attacked the nitrile group, leading to the unique isolation of the 3-aminopyrazole derivative (compound **6**, Table 1) whereas when X = CN and Y = COR, the cyclization reaction occurs on the ketone even in the presence of a relevant steric hindrance (e.g., t-Bu; compound **2**, Table 1). The chemical identities of the pyrazole derivatives were assessed by NMR analysis and the NOESY spectrum of derivative **1** showed signals at {3.40; 6.80} ppm and {3.40; 8.50} ppm, thus indicating a spatial proximity between *N*-methyl groups and phenyl and NH hydrogens, respectively.

To further investigate the regioselectivity of the reaction, the synthesis of pyrazole **8** (closely related to derivative **6**) was carried out in a stepwise fashion (Scheme 2). Thus, ethyl cyanoacetate **VII** was condensed with phenyl isothiocyanate in the presence of NaH and then S-methylated. The so-obtained *N,S*-thioether **B<sub>VII</sub>** (yield: 65%) is a push–pull alkene bearing two electron withdrawing groups at one end of the double bond (i.e., COOEt and CN) and two electron donating substituents at the other end (i.e., NHPH and SMe). This arrangement promotes the  $\pi$  delocalization from the electron-donating groups ('push' terminus) to the electron-withdrawing groups ('pull' terminus) thus lowering the energetic barrier to C=C rotation [44–49] and enhancing the reactivity of push–pull alkenes with nucleophilic and electrophilic species. For these reasons, push–pull alkenes are versatile synthons used for the preparation of various chemical heterocyclic derivatives [49–51]. Differently from the one-pot procedure, the reaction between **B<sub>VI</sub>** and methylhydrazine in solvent free conditions led to the formation of a mixture of the two *N*-methyl pyrazole isomers **8a** and **8b** that were isolated in 30% and 70% quantitative yield, respectively. The two pyrazole compounds were separated by column chromatography and their chemical identity was unambiguously identified by NMR and mass spectrometry analyses.



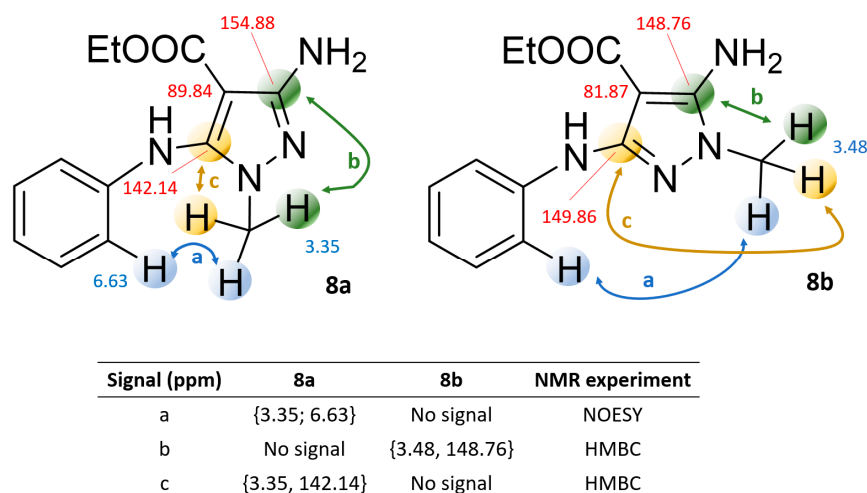


**Scheme 2.** Stepwise synthesis of *N*-methylpyrazoles **8a** and **8b**. Reaction conditions: (a) DMF<sub>dry</sub>, NaH, PhNCS, rt, 2 h; (b) MeI, rt, 16 h; (c) MeNHNH<sub>2</sub>, 80 °C, 1.5 h; (d) DMF<sub>dry</sub>, K<sub>2</sub>CO<sub>3</sub>, MeI, rt, 16 h.

Additionally, the methylation of pyrazole **9** (obtained as previously reported [42]) in the presence of K<sub>2</sub>CO<sub>3</sub> has been evaluated as an alternative procedure to afford compounds **8** (Scheme 2). Surprisingly, in the adopted conditions only compound **8b** has been isolated, thus highlighting the effect of the reaction conditions on the regioselective outcome of the procedure.

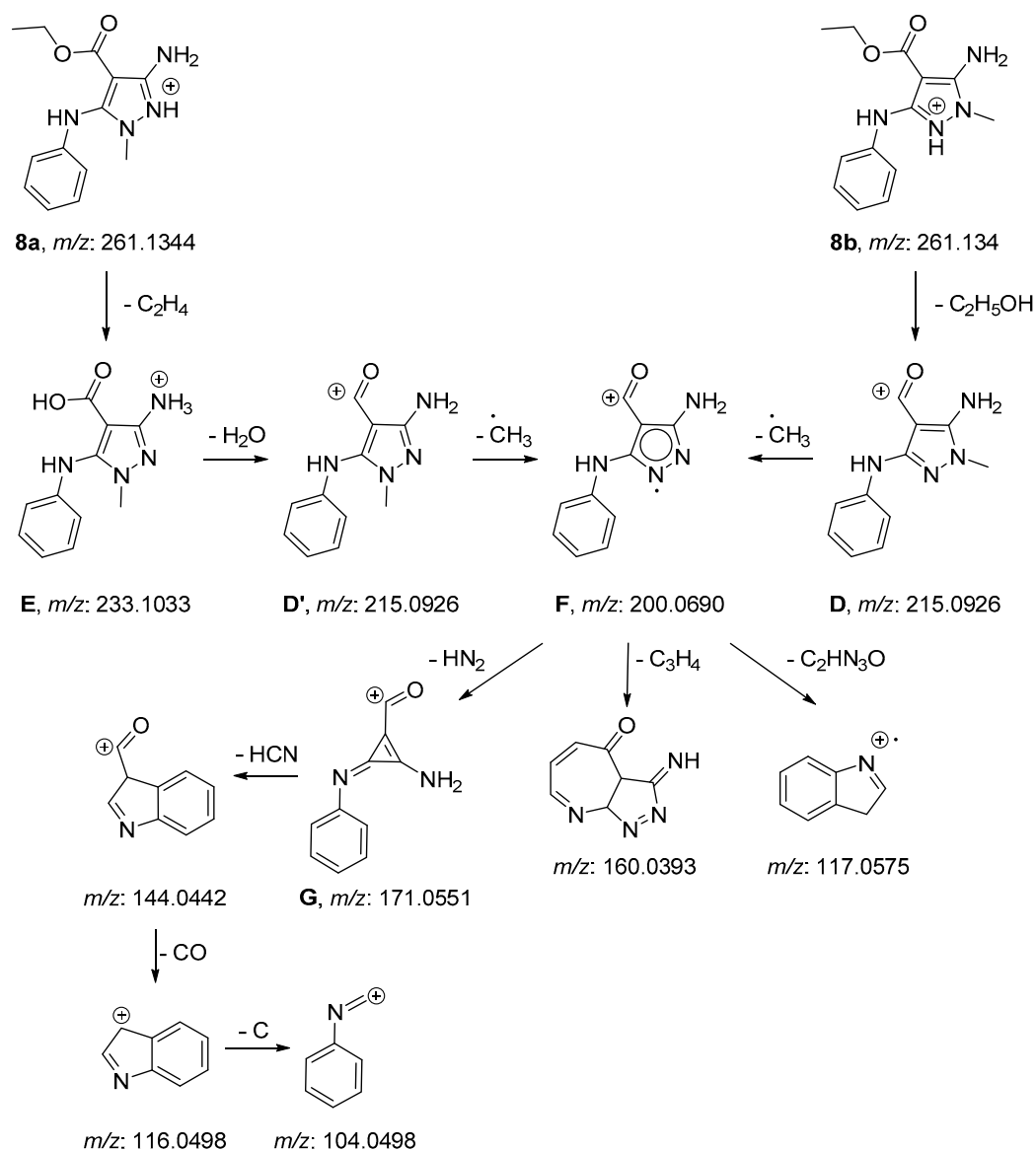
## 2.2. NMR and Mass Spectrometry Analyses of Derivatives **8a** and **8b**

The comparative analysis of the 2D-NMR spectra collected for **8a** and **8b** allowed the unambiguous assignment of the chemical structure of two pyrazole regioisomers. In particular, derivative **8a** displayed a signal at {3.35; 6.63} ppm in the NOESY spectrum related to the interaction between the spatially closed *N*-methyl and phenyl hydrogens (signal a, Figure 1). This signal is absent in the spectrum of **8b**, given the different relative position of the two groups. Furthermore, the interaction between the *N*-methyl hydrogens and the pyrazole carbon through a  $J^3_{C-H}$  coupling constant observed in the HMBC spectra further supported the identification of the two isomers (signals b and c, Figure 1). In particular, the peak observed at {3.35, 142.14} ppm refers to the heteronuclear coupling between the *N*-methyl hydrogens and the pyrazole carbon atom substituted with the *N*-phenyl group (i.e., compound **8a**) whereas the signal at {3.48, 148.76} ppm is related to the coupling between the methyl hydrogens and the pyrazole atom bearing the amine group (i.e., compound **8b**).



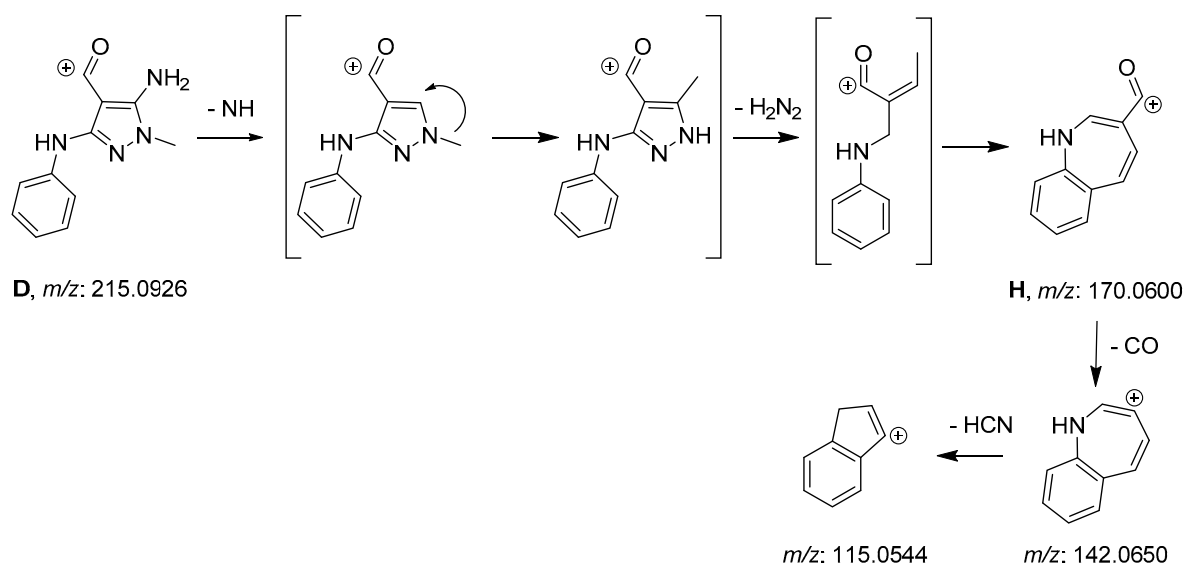
**Figure 1.** Relevant NMR couplings observed in NOESY and HMBC spectra of **8** regio-isomers. The interacting nuclei are differently colored, and the different interactions are indicated by double-headed arrows. The relevant chemical shift values are reported in red (carbon atom) and blue (proton atom).

In order to confirm the different structure of the two isomers **8a** and **8b** (Scheme 2), a complete flow injection analysis (FIA) mass spectrometry characterization was carried out. The protonated molecule ions  $[M + H]^+$  of both analytes were identified in the full scan spectra at  $m/z$  261.1344 (Figure S32, Supplementary Material); then, each molecule ion was subjected to collision-induced dissociation (CID) separately to produce fragment ions. The main fragment generated at the collision energy of 60 eV was  $m/z$  215.0926 for both species (**D** and **D'**, Scheme 3). Interestingly, the two isomers showed a different behavior in the  $MS^2$  spectrum as **8a** (and not its isomer **8b**) led to the formation of the transient intermediate species at  $m/z$  233.1033 (Figure S33, Supplementary Material). This observation highlighted a different susceptibility to the collision energy between the two compounds. In particular, the fragmentation of **8b** C(O)-O ester bond would directly afford the pyrazole acyl ion **D** (Scheme 3) and ethanol. Conversely, **8a** would form **D'** by a two-step fragmentation pattern that involved the initial cleavage of the ethyl group (and the consequent formation of the carboxylic acid intermediate **E**; Scheme 3) followed by the elimination of a water molecule. Q-Exactive plus does not allow us to run canonical  $MS^n$  experiments. However, we can set up a 'non-specific' in source fragmentation step able to ascertain, in the full scan analysis, the characteristic fragment ion identified during the first  $MS^2$  experiments. Thus, we selected  $m/z$  215.0926 ion as the progenitor fragment and a  $MS^3$  experiment was carried out. This protocol has been repeated for both isomers and for all of the successive  $MS^n$  analyses. This new fragmentation generates a main product ion at  $m/z$  200.0690 (fragment **F**, Scheme 3), compatible with the loss of the pyrazole methyl group. It is worth noting that **8a** and **8b** led to the formation of this common fragment that yielded the same ion panel, comprising  $m/z$  117.0575,  $m/z$  160.0393 and  $m/z$  171.0551. The latter fragment would be probably due to the rearrangement of pyrazole ring to obtain a cyclopropenyl ring after the loss of two nitrogen atoms (fragment **G**, Scheme 3) [52]. Further fragmentation of ion **G** led to the formation of fragments  $m/z$  144.0442,  $m/z$  116.0497, and  $m/z$  104.0498 possibly as the sequential loss of HCN, CO, and a carbon atom (Scheme 3).



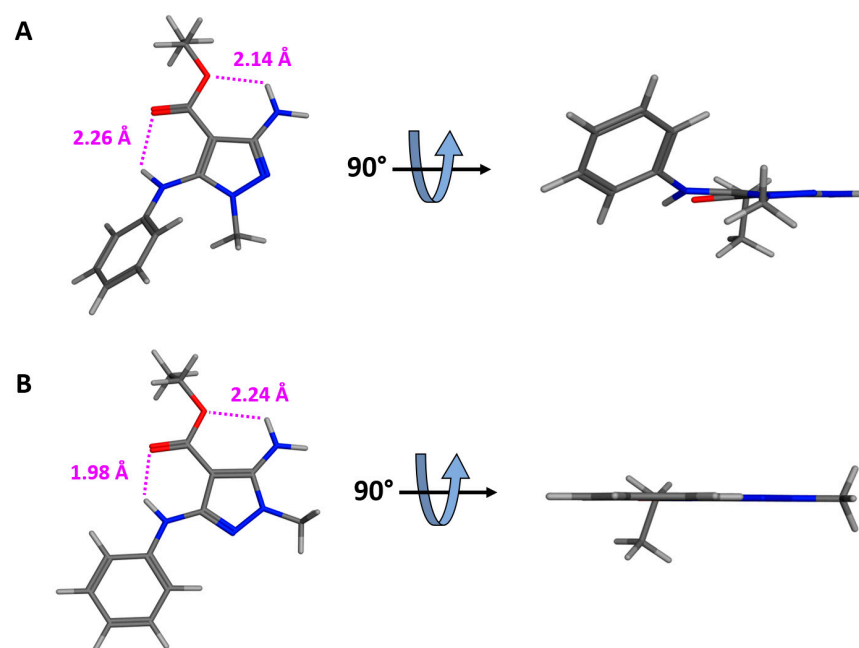
**Scheme 3.** Proposed fragmentation of isomers **8a** and **8b**.

Moreover, the MS<sup>3</sup> analysis of the  $m/z$  215.0926 ions evidenced that **8b**-derived molecules (namely ion **D**, Scheme 3) can undergo to an alternative fragmentation, generating an ion fragment at  $m/z$  170.0600 which was not observed in the case of the **8a** (Figure S34, Supplementary Material). This further difference in the behavior between the MS<sup>2</sup> products of the two isomers can be explained by the partial elimination of the amino-group from the pyrazole ring, followed by the N-C transposition of the methyl group (Scheme 4). The C-methylated intermediate was not identified in our study, but it has been reported in the literature for other pyrazole compounds structurally related to derivatives **8a** and **8b** [52]. The elimination of N<sub>2</sub>H<sub>2</sub> would generate an unstable intermediate that cyclizes to form the benzoazepine fragment **H** (Scheme 4). On the basis of the collected data, we can speculate that the rearrangement of molecule **D** ( $m/z$  215.0926) to afford fragment **H** (Scheme 4) can only occur if the *N*-methyl and amino groups are in close proximity, thus confirming the chemical identity of **8b**. The same transposition would be disadvantaged when these two groups are not in adjacent positions, as with compound **8a**.



**Scheme 4.** Proposed fragmentation of ion **D**.

The different chemical identity of compounds **8a** and **8b** would also affect the retention times of the two isomers ( $t(r)_{8a} = 13.70$  min;  $t(r)_{8b} = 20.03$  min) during the reverse phase (RP) HPLC analysis. In fact, in compound **8a** the pyrazole *N*-methyl group would prevent the adjacent phenyl ring to lay on the same plane of the pyrazole nucleus thus reducing the compound's affinity for the RP stationary phase. Conversely, in derivative **8b** the pyrazole *N*-methyl group would not influence the geometry of the *N*-phenyl ring that therefore would be co-planar to the heterocyclic portion. To further support this observation, semiempirical computational simulations (MOE software) were carried out on the two isomers (Figure 2). In the minimum energy conformers of **8a** and **8b**, the phenyl and pyrazole rings would assume different reciprocal orientations being co-planar in compound **8b** and laying on two different planes in derivative **8a**. The methyl-induced distortion of the phenyl ring would also affect the intramolecular hydrogen-bonding in the two conformers, as indicated by the different  $C=O \cdots HN$  distances and geometries in the two conformers (Figure 2).



**Figure 2.** Low energy conformers of **8a** (panel (A)) and **8b** (panel (B)). The intramolecular hydrogen bonds are represented as purple dotted lines. The O-H distances are also reported.

### 2.3. Antiproliferative Activity

To evaluate their effect on cell proliferation, phenylamino-pyrazole derivatives **1–8** were preliminarily tested using the MTT assay. A panel of eight tumor cell lines (namely, breast cancer: MCF7, MDA-MB231, SK-Br3; melanoma: SKMEL-28; ovarian cancer: SKOV-3; liver cancer: Hep-G2; cervical cancer: HeLa; lung cancer: A549) and one normal human fibroblasts cell line (GM-6114) was considered. The mean growth percentage values were determined at the fixed concentration of 10  $\mu\text{M}$ . Cisplatin was used as reference drug.

The results showed in Table 2 demonstrated that all tested compounds did not exhibit significant antiproliferative activity (grow inhibition percentage values higher than 68.36%) against the considered cancer cell lines. Moreover, all compounds proved to be non-cytotoxic against the human fibroblasts GM-6114 cell line at the concentration of 10  $\mu\text{M}$  (mean growth percentage range: 84.57–109.73%). Interestingly, derivatives **1–8** showed similar mean growth percentage values with previously synthesized *N*-unsubstituted analogs [42], thus highlighting that *N*-alkylation of the pyrazole nucleus marginally affected the antiproliferative/cytotoxic properties of the series.

Table 2. Antiproliferative activity of pyrazoles 1–8 <sup>a</sup>.

| Cpd       | Mean Growth Percentage $\pm$ SD |              |              |              |              |              |              |              |              |
|-----------|---------------------------------|--------------|--------------|--------------|--------------|--------------|--------------|--------------|--------------|
|           | MCF7                            | MDA-MB231    | Sk-Br3       | SKMEL28      | SKOV3        | Hep-G2       | HeLa         | A549         | GM-6114      |
| 1         | 108.43 $\pm$                    | 113.77 $\pm$ | 92.72 $\pm$  | 91.62 $\pm$  | 107.78 $\pm$ | 105.55 $\pm$ | 97.39 $\pm$  | 111.66 $\pm$ | 89.08 $\pm$  |
|           | 7.38                            | 4.39         | 2.94         | 3.38         | 3.35         | 7.40         | 10.47        | 3.77         | 11.38        |
| 2         | 107.37 $\pm$                    | 112.16 $\pm$ | 85.66 $\pm$  | 92.87 $\pm$  | 107.12 $\pm$ | 94.15 $\pm$  | 96.42 $\pm$  | 113.10 $\pm$ | 90.65 $\pm$  |
|           | 10.99                           | 6.85         | 3.28         | 4.06         | 5.64         | 3.81         | 7.05         | 5.64         | 3.32         |
| 3         | 118.46 $\pm$                    | 115.98 $\pm$ | 83.05 $\pm$  | 92.97 $\pm$  | 115.25 $\pm$ | 112.20 $\pm$ | 110.40 $\pm$ | 115.25 $\pm$ | 109.73 $\pm$ |
|           | 6.19                            | 2.45         | 2.41         | 3.68         | 3.37         | 7.47         | 2.49         | 5.96         | 8.12         |
| 4         | 92.21 $\pm$                     | 89.69 $\pm$  | 84.72 $\pm$  | 68.36 $\pm$  | 80.45 $\pm$  | 105.51 $\pm$ | 73.77 $\pm$  | 71.00 $\pm$  | 83.00 $\pm$  |
|           | 5.41                            | 2.90         | 4.38         | 3.13         | 3.38         | 8.80         | 6.86         | 3.40         | 6.51         |
| 5         | 111.88 $\pm$                    | 111.89 $\pm$ | 101.95 $\pm$ | 119.57 $\pm$ | 105.35 $\pm$ | 110.03 $\pm$ | 115.87 $\pm$ | 112.22 $\pm$ | 102.18 $\pm$ |
|           | 5.19                            | 2.95         | 3.18         | 1.57         | 6.08         | 2.11         | 9.17         | 4.10         | 8.31         |
| 6         | 105.46 $\pm$                    | 109.32 $\pm$ | 81.74 $\pm$  | 105.04 $\pm$ | 109.12 $\pm$ | 102.04 $\pm$ | 92.32 $\pm$  | 121.90 $\pm$ | 84.57 $\pm$  |
|           | 5.68                            | 6.43         | 4.92         | 2.76         | 5.64         | 4.42         | 2.62         | 5.92         | 4.03         |
| 7         | 104.20 $\pm$                    | 110.14 $\pm$ | 89.26 $\pm$  | 109.99 $\pm$ | 106.54 $\pm$ | 107.16 $\pm$ | 85.42 $\pm$  | 115.77 $\pm$ | 87.45 $\pm$  |
|           | 3.10                            | 4.88         | 3.54         | 3.30         | 4.47         | 12.07        | 6.98         | 3.02         | 7.73         |
| 8a        | 98.06 $\pm$                     | 87.02 $\pm$  | 94.76 $\pm$  | 82.21 $\pm$  | 106.46 $\pm$ | 101.20 $\pm$ | 103.26 $\pm$ | 99.70 $\pm$  | 107.65 $\pm$ |
|           | 3.31                            | 5.76         | 4.00         | 4.00         | 6.18         | 9.16         | 9.57         | 9.20         | 3.92         |
| 8b        | 100.13 $\pm$                    | 89.99 $\pm$  | 100.28 $\pm$ | 81.21 $\pm$  | 102.97 $\pm$ | 98.37 $\pm$  | 110.61 $\pm$ | 86.65 $\pm$  | 118.99 $\pm$ |
|           | 6.20                            | 5.16         | 4.10         | 4.31         | 4.37         | 8.17         | 7.72         | 9.83         | 9.70         |
| cisplatin | 72.74 $\pm$                     | 86.07 $\pm$  | 70.59 $\pm$  | 44.40 $\pm$  | 36.83 $\pm$  | 38.07 $\pm$  | 29.33 $\pm$  | 59.09 $\pm$  | 39.52 $\pm$  |
|           | 5.48                            | 7.04         | 3.83         | 2.53         | 4.35         | 2.22         | 2.23         | 6.03         | 2.74         |

<sup>a</sup> Data mean values for three separate experiments.

### 3. Materials and Methods

#### 3.1. Chemistry

Commercially available active methylene reagents, phenyl isothiocyanate, substituted hydrazine and reagents (55% sodium hydride dispersion in mineral oil, iodomethane) were purchased by Alfa-Aesar and Sigma-Aldrich. DMF was reagent grade and was dried on molecular sieves (5 Å 1/16" inch pellets). Unless otherwise stated, all commercial reagents were used without further purification. Organic solutions were dried over anhydrous sodium sulphate. A thin layer chromatography (TLC) system for routine monitoring the course of reactions and confirming the purity of analytical samples employed aluminium-backed silica gel plates (Merck DC-Alufolien Kieselgel 60 F254). DCM or DCM/2% methanol were used as a developing solvent and detection of spots was made by UV light and/or by iodine vapors. Melting points were determined on a Fisher-Johns apparatus and are uncorrected. <sup>1</sup>H NMR and <sup>13</sup>C NMR spectra were recorded on a Varian Gemini (Palo Alto, CA, USA) or JEOL JNM-ECZR (Tokyo, Japan) instrument; chemical shifts were reported in  $\delta$  (ppm) units relative to the internal reference tetramethylsilane, and the splitting patterns were described as follows: s (singlet), bs (broad singlet), d (doublet), t (triplet), q (quartet), and m (multiplet). The first order values reported for coupling constants J were given in Hz. Elemental analyses were performed by an EA1110 Analyzer, Fison Instruments (Milan, Italy).

#### 3.2. General Synthetic Procedure for the Preparation of Pyrazoles 1–7

To a dry DMF (10 mL) solution of the proper active methylene reagent (10 mmol), 55% sodium hydride dispersion in mineral oil (0.44 g, 10 mmol) was added under stirring at rt. After 45 min phenylisothiocyanate (1221  $\mu$ L, 10 mmol) was added in a single portion. The reaction mixture was stirred for 1 h at rt, then iodomethane (629  $\mu$ L, 10 mmol) was added. After 3 h, the reaction mixture was treated with the proper substituted hydrazine (25 mmol) at rt and was heated at 95–100 °C for 4 h. The reaction mixture was diluted with water (150 mL) and extracted with dichloromethane (3  $\times$  30 mL). The combined extracts were washed with water (5  $\times$  30 mL), dried with anhydrous Na<sub>2</sub>SO<sub>4</sub>, and filtered. Evaporating in vacuo gave a residue that was purified by crystallization from the suitable solvent or solvent mixture.

*3-amino-1-methyl-5-(pheylamino)-1H-pyrazole-4-carbonitrile (1)*. White solid. Mp 210–212 °C (DCM-MeOH); Yield: 56%. <sup>1</sup>H NMR (400 MHz, DMSO-*d*<sub>6</sub>): δ 3.40 (s, 3H, CH<sub>3</sub>N); 5.42 (bs, 2H, NH<sub>2</sub>); 6.77–6.82 (m, 2H, arom. H); 6.83–6.89 (m, 1H, arom. H); 7.20–7.26 (m, 2H, arom. H); 8.50 (bs, 1H, NH phenyl). <sup>13</sup>C NMR (101 MHz, DMSO-*d*<sub>6</sub>) δ 34.80, 69.74, 114.44, 115.69, 120.38, 129.25, 142.52, 144.40, 155.68. HRMS (ESI/APCI) *m/z* [M + H]<sup>+</sup> for C<sub>11</sub>H<sub>11</sub>N<sub>5</sub> calcd 214.1087, found 214.1089. Calcd for C<sub>11</sub>H<sub>11</sub>N<sub>5</sub>: C = 61.96; H = 5.20; N = 32.84. Found: C = 61.60; H = 5.50; N = 32.96.

*3-(tert-butyl)-1-methyl-5-(pheylamino)-1H-pyrazole-4-carbonitrile (2)*. White solid. Mp 157–159 °C (DCM); Yield: 61%. <sup>1</sup>H NMR (400 MHz, DMSO-*d*<sub>6</sub>): δ 1.33 (s, 9H, t-Bu); 3.59 (s, 3H, CH<sub>3</sub>N); 6.80–6.90 and 7.23–7.27 (m, 5H, arom. H); 8.62 (bs, 1H, NH, exchangeable). <sup>13</sup>C NMR (101 MHz, DMSO-*d*<sub>6</sub>) δ 160.46; 146.95; 142.23; 129.25; 120.66; 115.87; 114.80; 79.16; 35.44; 33.17; 28.88. HRMS (ESI/APCI) *m/z* [M + H]<sup>+</sup> for C<sub>15</sub>H<sub>18</sub>N<sub>4</sub> calcd 255.1604, found 255.1606. Calcd for C<sub>15</sub>H<sub>18</sub>N<sub>4</sub>: C = 70.84; H = 7.13; N = 22.03. Found: C = 70.96; H = 7.45; N = 22.06.

*1-methyl-3-phenyl-5-(phenylamino)-1H-pyrazole-4-carbonitrile (3)*. Yellow solid. Mp 229–231 °C (Ether-DCM); Yield: 60%. <sup>1</sup>H NMR (400 MHz, DMSO-*d*<sub>6</sub>): δ 3.74 (s, 3H, CH<sub>3</sub>N); 6.92–6.96 (m, 3H, arom. H); 7.26–7.32 (m, 2H, arom. H); 7.41–7.53 (m, 3H, arom. H); 7.83–7.87 (m, 2H, arom. H); 8.86 (bs, 1H, NH, exchangeable). <sup>13</sup>C NMR (101 MHz, DMSO-*d*<sub>6</sub>) δ 35.36, 72.30, 115.81, 117.88, 122.48, 127.52, 128.87, 129.19, 129.47, 131.06, 140.90, 146.96, 147.94. HRMS (ESI/APCI) *m/z* [M + H]<sup>+</sup> for C<sub>17</sub>H<sub>14</sub>N<sub>4</sub> calcd 275.1291, found 275.1293. Calcd for C<sub>17</sub>H<sub>14</sub>N<sub>4</sub>: C = 74.43; H = 5.14; N = 20.42. Found: C = 74.38; H = 5.47; N = 20.38.

*1-benzyl-3-phenyl-5-(phenylamino)-1H-pyrazole-4-carbonitrile (4)*. White solid. Mp 167–169 °C (Ether-DCM); Yield: 27%. <sup>1</sup>H NMR (400 MHz, DMSO-*d*<sub>6</sub>): δ 5.26 (s, 2H, CH<sub>2</sub>Ph); 6.82–6.86 and 7.06–7.08 and 7.20–7.34 and 7.52–7.59 (m, 15H, arom. H); 8.98 (bs, 1H, NH, exchangeable). <sup>13</sup>C NMR (101 MHz, DMSO-*d*<sub>6</sub>) δ 152.23; 148.43; 141.89; 136.49; 130.44; 129.26; 128.98; 128.69; 128.66; 127.66; 126.81; 126.58; 120.02; 116.49; 114.12; 80.51; 52.86. HRMS (ESI/APCI) *m/z* [M + H]<sup>+</sup> for C<sub>23</sub>H<sub>18</sub>N<sub>4</sub> calcd 351.1604, found 351.1603. Calcd for C<sub>23</sub>H<sub>18</sub>N<sub>4</sub>: C = 78.83; H = 5.18; N = 15.99. Found: C = 78.62; H = 4.94; N = 15.79.

*(1-methyl-3-phenyl-5-(phenylamino)-1H-pyrazol-4-yl)(phenyl)methanone (5)*. White solid. Mp 140–142 °C (DCM-MeOH); Yield: 50%. <sup>1</sup>H NMR (400 MHz, DMSO-*d*<sub>6</sub>): δ 3.66 (s, 3H, CH<sub>3</sub>N); 6.90–7.02 and 7.15–7.34 and 7.68–7.70 (m, 15H, arom. H); 9.22 (bs, 1H, NH, exchangeable). <sup>13</sup>C NMR (101 MHz, DMSO-*d*<sub>6</sub>) δ 191.81; 152.84; 145.60; 141.10; 138.70; 130.49; 130.20; 128.99; 128.89; 128.00; 127.98; 127.25; 120.23; 116.82; 106.23; 37.16. HRMS (ESI/APCI) *m/z* [M + H]<sup>+</sup> for C<sub>23</sub>H<sub>19</sub>N<sub>3</sub>O calcd 354.1601, found 354.1601. Calcd for C<sub>23</sub>H<sub>19</sub>N<sub>3</sub>O: C = 78.16; H = 5.42; N = 11.89. Found: C = 78.06; H = 5.76; N = 11.86.

*Methyl 3-amino-1-methyl-5-(phenylamino)-1H-pyrazole-4-carboxylate (6)*. White solid. Mp 151–153 °C (DCM-MeOH); Yield: 12%. <sup>1</sup>H NMR (400 MHz, DMSO-*d*<sub>6</sub>): δ 3.32 (s, 3H, NCH<sub>3</sub>); 3.56 (s, 3H, CH<sub>3</sub>O); 5.32 (bs, 2H, NH<sub>2</sub>, exchangeable); 6.62–6.68 (m, 2H, arom. H); 6.76–6.72 (m, 1H, arom. H); 7.15–7.21 (m, 2H, arom. H); 7.91 (bs, 1H, NH, exchangeable). <sup>13</sup>C NMR (101 MHz, DMSO-*d*<sub>6</sub>) δ 34.86, 50.28, 89.62, 115.02, 119.54, 129.08, 142.21, 144.40, 154.97, 163.72. HRMS (ESI/APCI) *m/z* [M + H]<sup>+</sup> for C<sub>12</sub>H<sub>14</sub>N<sub>4</sub>O<sub>2</sub> calcd 247.1190, found 247.1190. Calcd for C<sub>12</sub>H<sub>14</sub>N<sub>4</sub>O<sub>2</sub>: C = 58.53; H = 5.73; N = 22.75. Found: C = 58.84; H = 5.42; N = 22.43.

*1-methyl-N<sup>5</sup>-phenyl-4-(phenylsulfonyl)-1H-pyrazole-3,5-diamine (7)*. White solid. Mp 203–205 °C (DCM); Yield: 60%. <sup>1</sup>H NMR (400 MHz, DMSO-*d*<sub>6</sub>): δ 3.27 (s, 3H, CH<sub>3</sub>N); 5.38 (bs, 2H, NH<sub>2</sub>, exchangeable); 6.45–6.47 and 6.75–6.78 and 7.07–7.11 and 7.37–7.40 and 7.51–7.55 and 7.69–7.72 (m, 10H, arom. H); 7.95 (bs, 1H, NH, exchangeable). <sup>13</sup>C NMR (101 MHz, DMSO-*d*<sub>6</sub>): δ 152.19; 144.13; 143.21; 140.29; 132.69; 129.12; 128.90; 125.82; 119.51; 114.52; 98.12; 34.82. HRMS (ESI/APCI) *m/z* [M + H]<sup>+</sup> for C<sub>16</sub>H<sub>16</sub>N<sub>4</sub>O<sub>2</sub>S calcd 329.1067, found 329.1064. Calcd for C<sub>16</sub>H<sub>16</sub>N<sub>4</sub>O<sub>2</sub>S: C = 58.52; H = 4.91; N = 17.06; S = 9.76. Found: C = 58.64; H = 4.92; N = 17.13; S = 9.37.

### 3.3. Synthesis of Ethyl 2-Cyano-3-(methylthio)-3-(phenylamino)acrylate (B<sub>VI</sub>)

To a dry DMF (15 mL) solution of ethyl cyanoacetate (1085  $\mu$ L, 10 mmol) cooled at 0 °C, 55% sodium hydride dispersion in mineral oil (0.44 g, 10 mmol) was added in a single portion. The reaction mixture is stirred for 10 min at 0 °C and phenylisothiocyanate (1221  $\mu$ L, 10 mmol) was added and stirring was prolonged for 2h. Methyl iodide (629  $\mu$ L, 10 mmol) was added and the mixture was stirred at rt for 16h. The reaction mixture was diluted with water (50 mL) and a yellow solid precipitated. The crude material was collected by filtration, dried, and used without further purification.

Mp 83–85 °C (water) (litt [53]: 82 °C); Yield: 65%. <sup>1</sup>H NMR (200 MHz, CDCl<sub>3</sub>):  $\delta$  1.34 (t, 3H, J = 7.2 Hz, CH<sub>3</sub>); 2.23 (s, 3H, SCH<sub>3</sub>); 4.27 (q, 2H, J = 7.2 Hz, CH<sub>2</sub>O); 7.21–7.49 (m, 5H, arom. H); 11.51 (bs, 1H, NH, exchangeable). Calcd for C<sub>13</sub>H<sub>14</sub>N<sub>2</sub>O<sub>2</sub>S: C = 59.52; H = 5.38; N = 10.68; S = 12.22. Found: C = 59.82; H = 5.42; N = 10.60; S = 11.37.

### 3.4. Synthesis of Compounds 8a and 8b

A mixture of B<sub>VI</sub> (2.67 g, 10 mmol) and methylhydrazine (590  $\mu$ L, 11 mmol) was heated in a sealed tube at 80 °C for 1.5 h. The mixture was cooled at rt and water (10 mL) was added. A white solid precipitated and was collected by filtration. TLC analysis (eluent DCM/2% methanol mixture) revealed two spots with R<sub>f</sub> values of 0.11 (compound 8a) and 0.30 (compound 8b). The solid was dissolved in DCM and the two compounds were separated by column chromatography (silica gel, eluent: DCM-DCM/20% MeOH).

*Ethyl 3-amino-1-methyl-5-(phenylamino)-1H-pyrazole-4-carboxylate (8a)*. White solid. Mp 138–140 °C (EtOH); Yield: 70%. <sup>1</sup>H NMR (400 MHz, DMSO-*d*<sub>6</sub>):  $\delta$  0.94 (t, 3H, J = 7.1 Hz, CH<sub>3</sub>-C); 3.35 (s, 3H, CH<sub>3</sub>N); 3.96 (q, 2H, J = 7.1 Hz, CH<sub>2</sub>O); 4.71 (bs, 2H, NH<sub>2</sub>, exchangeable); 6.61–6.69 (m, 2H, arom. H); 6.74–6.85 (m, 1H, arom. H); 7.12–7.22 (m, 2H, arom. H); 7.93 (bs, 1H, NH, exchangeable). <sup>13</sup>C NMR (101 MHz, DMSO-*d*<sub>6</sub>)  $\delta$  13.91, 34.73, 58.71, 89.84, 114.91, 119.42, 129.02, 142.14, 144.62, 154.88, 163.33. HRMS (ESI/APCI) *m/z* [M + H]<sup>+</sup> for C<sub>13</sub>H<sub>16</sub>N<sub>4</sub>O<sub>2</sub> calcd 261.1346, found 261.1344. Calcd for C<sub>13</sub>H<sub>16</sub>N<sub>4</sub>O<sub>2</sub>: C = 59.99; H = 6.20; N = 21.52. Found: C = 60.20; H = 6.10; N = 21.86.

*Ethyl 5-amino-1-methyl-3-(phenylamino)-1H-pyrazole-4-carboxylate (8b)*. White solid. Mp 144–145 °C (EtOH); Yield: 30%. <sup>1</sup>H NMR (400 MHz, DMSO-*d*<sub>6</sub>):  $\delta$  1.30 (t, 3H, J = 7.1 Hz, CH<sub>3</sub>-C); 3.48 (s, 3H, CH<sub>3</sub>N); 4.25 (q, 2H, J = 7.1 Hz, CH<sub>2</sub>O); 6.23 (bs, 2H, NH<sub>2</sub>, exchangeable); 6.78–6.87 (m, 1H, arom. H); 7.18–7.28 (m, 2H, arom. H); 7.50–7.55 (m, 2H, arom. H); 8.05 (bs, 1H, NH, exchangeable). <sup>13</sup>C NMR (101 MHz, DMSO-*d*<sub>6</sub>)  $\delta$  14.56, 33.95, 58.91, 81.87, 116.27, 119.59, 128.81, 141.36, 148.76, 149.86, 163.95. HRMS (ESI/APCI) *m/z* [M + H]<sup>+</sup> for C<sub>13</sub>H<sub>16</sub>N<sub>4</sub>O<sub>2</sub> calcd 261.1346, found 261.1344. Calcd for C<sub>13</sub>H<sub>16</sub>N<sub>4</sub>O<sub>2</sub>: C = 59.99; H = 6.20; N = 21.52. Found: C = 60.18; H = 6.15; N = 21.32.

### 3.5. Synthesis of Compound 8b via Pyrazole Methylation

A dry DMF solution (5 mL) of pyrazole 9 [26] (377 mg, 1.5 mmol) and anhydrous K<sub>2</sub>CO<sub>3</sub> (251 mg, 1.8 mmol) was stirred at rt for 10 min. Methyl iodide (94  $\mu$ L, 1.5 mmol) was added and the suspension was stirred at rt for 16h. The sequential addition of water (10 mL) and solid ammonium chloride (pH = 7) led to the isolation of a white solid. Purification by crystallization from DCM/EtOH mixture afforded 118 mg (30% yield) of compound 8b.

### 3.6. Mass Spectrometry Analysis

#### 3.6.1. LC-HRMS

The two isomers were analyzed by high pressure liquid chromatography conducted using a Vanquish (Thermo Fisher Scientific, San Jose, CA, USA) UHPLC system composed of binary pump, autosampler, and column oven. In details, 10  $\mu$ L of a 1:1 mixture of the two isomers (concentration 1  $\mu$ M each) was injected onto a Simmetry 300 C18 column (150  $\times$  1 mm, 3.5  $\mu$ m particle size) (Waters) maintained at 25 °C. The eluents were 0.1% formic acid (eluent A) and acetonitrile (eluent B). Flow rate was 100  $\mu$ L/min. The mobile phase was a binary linear gradient in the following sequence: isocratic 20% B for five min, a linear gradient over the course of 60 min to 100% B, maintained at 100% B for



10 min and finally a linear gradient to 20% B in one min. The re-equilibration time in 20% B was 15 min. After HPLC separation, the eluent was directly sent to a Q Exactive Plus Orbitrap mass spectrometer (ThermoScientific, San Jose, CA, USA) equipped with a heated electrospray ionization source (HESI-II). Before analyses, the mass spectrometer was externally calibrated with the positive ion calibration solution (Thermo Fisher Scientific). Positive full-scan mass spectra were recorded in the mass range  $m/z$  100–400, at resolution 35,000. The following operating parameters were applied: sheath and auxiliary gas flow rate were 35 and 10 respectively; spray voltage 3.5 kV; S-lens RF level 100; capillary temperature 250 °C. The autogain control (AGC) was optimized at  $10^6$  with a maximum injection time (maxIT) of 250 ms. Software used for operating the UHPLC/HR-MS was Xcalibur (version 4.1). The full scan data were processed and the identity of the isomers was confirmed by comparing the high-resolution experimental data with their theoretical molecular weight.

### 3.6.2. FIA MS/MS

For MS/MS spectra collection, each sample was dissolved in DMSO (final concentration: 10 mM) and, after further dilution in acetonitrile (final concentration 100 nM), it was analyzed by flow injection mass spectrometry (FIA-MS). Briefly, five microliters of sample were injected into an eluent flow containing 0.1% formic acid in acetonitrile, generated by a Vanquish UHPLC system (Thermo Fisher Scientific, San Jose, CA, USA). The flow rate was 100  $\mu\text{L}/\text{min}$ . The eluent was directly sent to a Q Exactive™ Plus Hybrid Quadrupole-Orbitrap™ Mass Spectrometer (Thermo Fisher Scientific, San Jose, CA, USA) equipped with a heated electrospray ion source (HESI-II). Prior to each series of acquisitions, the mass spectrometer was externally calibrated with Positive Ion Calibration Solution (Thermo Fisher Scientific, San Jose, CA, USA). The same MS operating parameters as LC-MS analysis were applied. Full scan data were processed with Xcalibur version 4.1 (Thermo Fisher Scientific, San Jose, CA, USA). High-resolution mass spectra, ranging from 100 to 600  $m/z$ , were acquired in positive ion mode.

### 3.6.3. Biology

MTT assay was accomplished on a group of eight tumor cell lines: SKOV-3 (ovarian adenocarcinoma, ATCC, Manassas, VA, USA); MCF-7 (breast adenocarcinoma, Biologic Bank and Cell Factory, IRCCS Policlinico San Martino, Genoa, Italy); Hep-G2 (hepatocellular carcinoma, ATCC, Manassas, VA, USA); SK-Mel28 (skin melanoma, Biologic Bank and Cell Factory, IRCCS Policlinico San Martino, Genoa, Italy); MDA-MB231 (breast adenocarcinoma, Biologic Bank and Cell Factory, IRCCS Policlinico San Martino, Genoa, Italy); HeLa (cervical adenocarcinoma, Biologic Bank and Cell Factory, IRCCS Policlinico San Martino, Genoa, Italy); SK-BR3 (breast adenocarcinoma, Biologic Bank and Cell Factory, IRCCS Policlinico San Martino, Genoa, Italy); A549 (lung carcinoma, Biologic Bank and Cell Factory, IRCCS Policlinico San Martino, Genoa, Italy) and one normal cell line: Gm-6114 (embryonic human fibroblast, ATCC, Manassas, VA, USA). All cell lines were grown in DMEM (with 10% FBS, 2 mM Glutamine and 1% penstrep. All reagents were purchased from EuroClone (Milan, Italy), incubated at 37 °C with 5% CO<sub>2</sub> and humidified environment. Briefly, the nine cell lines were plated in 96 well plates at a proper cell density to achieve about 85% of confluence at the end of the protocol. The next day, the chemical compounds were dissolved in DMSO at a concentration of 10 mM. This stock solution was diluted using the complete growth medium and added to the wells to obtain the final working concentration of 10  $\mu\text{M}$ . After an incubation of 48 h, we add 30  $\mu\text{L}$  of MTT (3-(4,5-dimethyl-2-thiazolyl)-2,5-diphenyl-2H-tetrazolium bromide) diluted at 2 mg/mL with  $1 \times$  PBS. After 4 h of incubation, the supernatant was eliminated and 100  $\mu\text{L}/\text{well}$  of DMSO were used to solubilize the formazan precipitate. Then, subsequent to a 20 min incubation, the OD were measured at 570 nm using a plate reader. The results are expressed as a percentage of the control samples (100%) in which the cell lines were incubated with the same amount of solvent but without any chemical compounds. The assay was repeated

three times. In each set, every single compound was tested six times. Means and standard deviations were calculated.

### 3.7. Computational Calculations

The chemical structures of compounds **8a** and **8b** were drawn with MOE2009.10 (builder module) and energy minimization was carried out according to AM1, as implemented in MOE software version 2009.10. The calculations were run on a Linux PC (Intel® processor Core™ i7-2600 CPU@3.40 GHz).

## 4. Conclusions

A series of novel tetrasubstituted phenylamino pyrazoles has been prepared by the one-pot condensation of AMR, phenyl isothiocyanate, and substituted hydrazines. The adopted synthetic procedure proved to be versatile and efficient as demonstrated by the various properties of the AMR groups and the different steric hindrance of the substituted hydrazine compounds. Additionally, the developed protocol proved to be regio- and chemo-selective, allowing the isolation of compounds **1–7** as single *N*-substituted pyrazole isomer. The regioselectivity of the one-pot procedure was further studied by adopting a stepwise protocol. The condensation of the *N,S*-thioether **B<sub>VI</sub>** with methylhydrazine led to the formation of the two *N*-methyl pyrazole isomers **8a** and **8b** which were separated and fully characterized by NMR and mass spectrometry analyses. Conversely, the methylation of *N*-unsubstituted pyrazole **9** allowed the isolation of a single *N*-methyl derivative (namely, compound **8b**). In preliminary cell-based assays, the prepared compounds proved to be poorly cytotoxic against both a panel of mutated cell lines and normal human fibroblasts. Overall, the results of the current study further extend the applicability of the previously developed one-pot procedure and provided alternative synthetic routes for the regioselective synthesis of pharmaceutically attractive phenylaminopyrazole compounds.

**Supplementary Materials:** The following supporting information can be downloaded at: <https://www.mdpi.com/article/10.3390/molecules27185814/s1>, Figure S1: <sup>1</sup>H-NMR (400 MHz, *d*<sub>6</sub>-DMSO) spectrum of compound **1**; Figure S2: <sup>13</sup>C-NMR (101 MHz, *d*<sub>6</sub>-DMSO) spectrum of compound **1**; Figure S3: 2D NOESY (*d*<sub>6</sub>-DMSO) spectrum of compound **1**; Figure S4: 2D HMBC (*d*<sub>6</sub>-DMSO) spectrum of compound **1**; Figure S5: Fullscan analysis of compound **1**; Figure S6: <sup>1</sup>H-NMR (400 MHz, *d*<sub>6</sub>-DMSO) spectrum of compound **2**; Figure S7: <sup>13</sup>C-NMR (101 MHz, *d*<sub>6</sub>-DMSO) spectrum of compound **2**; Figure S8: Fullscan analysis of compound **2**; Figure S9: <sup>1</sup>H-NMR (400 MHz, *d*<sub>6</sub>-DMSO) spectrum of compound **3**; Figure S10: <sup>13</sup>C-NMR (101 MHz, *d*<sub>6</sub>-DMSO) spectrum of compound **3**; Figure S11: Fullscan analysis of compound **3**; Figure S12: <sup>1</sup>H-NMR (400 MHz, *d*<sub>6</sub>-DMSO) spectrum of compound **4**; Figure S13: <sup>13</sup>C-NMR (101 MHz, *d*<sub>6</sub>-DMSO) spectrum of compound **4**; Figure S14: Fullscan analysis of compound **4**; Figure S15: <sup>1</sup>H-NMR (400 MHz, *d*<sub>6</sub>-DMSO) spectrum of compound **5**; Figure S16: <sup>13</sup>C-NMR (101 MHz, *d*<sub>6</sub>-DMSO) spectrum of compound **5**; Figure S17: Fullscan analysis of compound **5**; Figure S18: <sup>1</sup>H-NMR (400 MHz, *d*<sub>6</sub>-DMSO) spectrum of compound **6**; Figure S19: <sup>13</sup>C-NMR (101 MHz, *d*<sub>6</sub>-DMSO) spectrum of compound **6**; Figure S20: Fullscan analysis of compound **6**; Figure S21: <sup>1</sup>H-NMR (400 MHz, *d*<sub>6</sub>-DMSO) spectrum of compound **7**; Figure S22: <sup>13</sup>C-NMR (101 MHz, *d*<sub>6</sub>-DMSO) spectrum of compound **7**; Figure S23: Fullscan analysis of compound **7**; Figure S24: <sup>1</sup>H-NMR (400 MHz, *d*<sub>6</sub>-DMSO) spectrum of compound **8a**; Figure S25: <sup>13</sup>C-NMR (101 MHz, *d*<sub>6</sub>-DMSO) spectrum of compound **8a**; Figure S26: 2D NOESY (*d*<sub>6</sub>-DMSO) spectrum of compound **8a**; Figure S27: 2D HMBC (*d*<sub>6</sub>-DMSO) spectrum of compound **8a**; Figure S28: <sup>1</sup>H-NMR (400 MHz, *d*<sub>6</sub>-DMSO) spectrum of compound **8b**; Figure S29: <sup>13</sup>C-NMR (101 MHz, *d*<sub>6</sub>-DMSO) spectrum of compound **8b**; Figure S30: 2D NOESY (*d*<sub>6</sub>-DMSO) spectrum of compound **8b**; Figure S31: 2D HMBC (*d*<sub>6</sub>-DMSO) spectrum of compound **8b**; Figure S32: Fullscan analysis of isomers **8a** and **8b**; Figure S33: Fragmentation spectra of precursor ion *m/z* 261.1344 for isomers **8a** and **8b**; Figure S34: Fragmentation spectra of precursor ion *m/z* 215.0926 for isomers **8a** and **8b**.

**Author Contributions:** Conceptualization, A.S., M.L., M.P. and A.P.; Methodology, A.S., M.L., M.P. and A.P.; Compound synthesis, A.S., C.R. (Chiara Rotolo) and M.L.; Mass-spectrometry analysis, A.P., M.P. and E.I.; Biological assay, M.P., E.I. and C.R. (Camillo Rosano); Writing—original draft

preparation, A.S.; Writing—review and editing, M.L., M.P., A.P., C.R. (Camillo Rosano), C.R. (Chiara Rotolo) and E.I. All authors have read and agreed to the published version of the manuscript.

**Funding:** This research was funded by University of Genova, grant “Fondo di Ricerca d’Ateneo (FRA)”. The work of Camillo Rosano, M.P., and A.P. was supported by the Italian Ministry of Health (Ricerca Corrente 2021).

**Institutional Review Board Statement:** Not applicable.

**Informed Consent Statement:** Not applicable.

**Data Availability Statement:** Not applicable.

**Acknowledgments:** The authors acknowledge Riccardo Raggio and Maria Anzaldi for technical support in NMR spectra acquisition and elemental analysis determinations.

**Conflicts of Interest:** The authors declare no conflict of interest.

**Sample Availability:** Samples of the compounds 1–8 are available from the authors.

## References

1. Kuo, T.-H.; Lin, T.-H.; Yang, R.-S.; Kuo, S.-C.; Fu, W.-M.; Hung, H.-Y. Novel pyrazole derivatives effectively inhibit osteoclastogenesis, a potential target for treating osteoporosis. *J. Med. Chem.* **2015**, *58*, 4954–4963. [CrossRef] [PubMed]
2. Tanitame, A.; Oyamada, Y.; Ofuji, K.; Fujimoto, M.; Iwai, N.; Hiyama, Y.; Suzuki, K.; Ito, H.; Terauchi, H.; Kawasaki, M.; et al. Synthesis and antibacterial activity of a novel series of potent DNA gyrase inhibitors. pyrazole derivatives. *J. Med. Chem.* **2004**, *47*, 3693–3696. [CrossRef] [PubMed]
3. Khunt, R.C.; Khedkar, V.M.; Chawda, R.S.; Chauhan, N.A.; Parikh, A.R.; Coutinho, E.C. Synthesis, antitubercular evaluation and 3D-QSAR study of N-phenyl-3-(4-fluorophenyl)-4-substituted pyrazole derivatives. *Bioorg. Med. Chem. Lett.* **2012**, *22*, 666–678. [CrossRef] [PubMed]
4. Takate, S.J.; Shinde, A.D.; Karale, B.K.; Akolkar, H.; Nawale, L.; Sarkar, D.; Mhaske, P.C. Thiazolyl-pyrazole derivatives as potential antimycobacterial agents. *Bioorg. Med. Chem. Lett.* **2019**, *29*, 1199–1202. [CrossRef] [PubMed]
5. Kumar, V.; Kaur, K.; Gupta, G.K.; Sharma, A.K. Pyrazole containing natural products: Synthetic preview and biological significance. *Eur. J. Med. Chem.* **2013**, *69*, 735–753. [CrossRef]
6. Ojwach, S.O.; Darkwa, J. Pyrazole and (pyrazol-1-yl)metal complexes as carbon–carbon coupling catalysts. *Inorg. Chim. Acta* **2010**, *363*, 1947–1964. [CrossRef]
7. Singer, R.A.; Caron, S.; McDermott, R.E.; Arpin, P.; Do, N.M. Alternative biarylphosphines for use in the palladium-catalyzed amination of aryl halides. *Synthesis* **2003**, *11*, 1727–1731. [CrossRef]
8. Singer, R.A.; Dore, M.; Sieser, J.E.; Berliner, M.A. Development of nonproprietary phosphine ligands for the Pd-catalyzed amination reaction. *Tetrahedron Lett.* **2006**, *47*, 3727–3731. [CrossRef]
9. Kowalczyk, R.; Skarzewski, J. Regioselective synthesis of optically active (pyrazolyl)pyridines with adjacent quaternary carbon stereocenter: Chiral N,N-donating ligands. *Tetrahedron* **2005**, *61*, 623–628. [CrossRef]
10. Ebenezer, O.; Shapi, M.; Tuszynski, J.A. A Review of the recent development in the synthesis and biological evaluations of pyrazole derivatives. *Biomedicines* **2022**, *10*, 1124. [CrossRef]
11. Sui, Z.; Guan, J.; Ferro, M.P.; McCoy, K.; Wachter, M.P.; Murray, W.V.; Singer, M.; Steber, M.; Ritchie, D.M.; Argentieri, D.C. 1,3-Diarylcycloalkanopyrazoles and diphenyl hydrazides as selective inhibitors of cyclooxygenase-2. *Bioorg. Med. Chem. Lett.* **2000**, *10*, 601–604. [CrossRef]
12. Bekhit, A.A.; Abdel-Aziem, T. Design, synthesis and biological evaluation of some pyrazole derivatives as anti-inflammatory-antimicrobial agents. *Bioorg. Med. Chem.* **2004**, *12*, 1935–1945. [CrossRef]
13. Abd El-Karim, S.S.; Mohamed, H.S.; Abdelhameed, M.F.; Amr, A.E.; Almehezia, A.A.; Nossier, E.S. Design, synthesis and molecular docking of new pyrazole-thiazolidinones as potent anti-inflammatory and analgesic agents with TNF-alpha inhibitory activity. *Bioorg. Chem.* **2021**, *111*, 104827. [CrossRef]
14. Shi, J.B.; Chen, L.Z.; Wang, B.S.; Huang, X.; Jiao, M.M.; Liu, M.M.; Tang, W.J.; Liu, X.H. Novel Pyrazolo [4,3-d] pyrimidine as Potent and Orally Active Inducible Nitric Oxide Synthase (iNOS) Dimerization Inhibitor with Efficacy in Rheumatoid Arthritis Mouse Model. *J. Med. Chem.* **2019**, *62*, 4013–4031. [CrossRef]
15. Abdellatif, K.R.A.; Abdelall, E.K.A.; Elshemy, H.A.H.; El-Nahass, E.; Abdel-Fattah, M.M.; Abdelgawad, Y.Y.M. New indomethacin analogs as selective COX-2 inhibitors: Synthesis, COX-1/2 inhibitory activity, anti-inflammatory, ulcerogenicity, histopathological, and docking studies. *Arch. Pharm.* **2021**, *354*, 2000328. [CrossRef]
16. Harras, M.F.; Sabour, R.; Alkamali, O.M. Discovery of new non-acidic lonazolac analogues with COX-2 selectivity as potent anti-inflammatory agents. *MedChemComm* **2019**, *10*, 1775–1788. [CrossRef]
17. Abdellatif, K.R.A.; El-Saadi, M.T.; Elzayat, S.G.; Amin, N.H. New substituted pyrazole derivatives targeting COXs as potential safe anti-inflammatory agents. *Future Med. Chem.* **2019**, *11*, 1871–1887. [CrossRef]

18. Taher, A.T.; Sarg, M.T.M.; Ali, N.R.E.; Elnagdi, N.H. Design, synthesis, modeling studies and biological screening of novel pyrazole derivatives as potential analgesic and anti-inflammatory agents. *Bioorg. Chem.* **2019**, *89*, 103023. [CrossRef]
19. Zabiulla; Gulnaz, A.R.; Mohammed, Y.H.E.; Khanum, S.A. Design, synthesis and molecular docking of benzophenone conjugated with oxadiazole sulphur bridge pyrazole pharmacophores as anti inflammatory and analgesic agents. *Bioorg. Chem.* **2019**, *92*, 103220. [CrossRef]
20. Katoch-Rouse, R.; Pavlova, O.A.; Caulder, T.; Hoffman, A.F.; Mukhin, A.G.; Horti, A.G. Synthesis, structure–activity relationship, and evaluation of SR141716 analogues: Development of central cannabinoid receptor ligands with lower lipophilicity. *J. Med. Chem.* **2003**, *46*, 642–645. [CrossRef]
21. Tanitame, A.; Oyamada, Y.; Ofuji, K.; Fujimoto, M.; Suzuki, K.; Ueda, T.; Terauchi, H.; Kawasaki, M.; Nagai, K.; Wachi, M.; et al. Synthesis and antibacterial activity of novel and potent DNA gyrase inhibitors with azole ring. *Bioorg. Med. Chem.* **2004**, *12*, 5515–5524. [CrossRef]
22. Liu, H.; Chu, Z.-W.; Xia, D.-G.; Cao, H.-Q.; Lv, X.-H. Discovery of novel multi-substituted benzo-indole pyrazole schiff base derivatives with antibacterial activity targeting DNA gyrase. *Bioorg. Chem.* **2020**, *99*, 103807. [CrossRef]
23. Ibrahim, S.A.; Fayed, E.A.; Rizk, H.F.; Desouky, S.E.; Ragab, A. Hydrazonoyl bromide precursors as DHFR inhibitors for the synthesis of bis-thiazolyl pyrazole derivatives; antimicrobial activities, antibiofilm, and drug combination studies against MRSA. *Bioorg. Chem.* **2021**, *116*, 105339. [CrossRef]
24. Stauffer, S.R.; Coletta, C.J.; Tedesco, R.; Nishiguchi, G.; Carlson, K.; Sun, J.; Katzenellenbogen, B.S.; Katzenellenbogen, J.A. Pyrazole ligands: Structure–affinity/activity relationships and estrogen receptor- $\alpha$ -selective agonists. *J. Med. Chem.* **2000**, *43*, 4934–4947. [CrossRef]
25. Stauffer, S.R.; Huang, Y.; Coletta, C.J.; Tedesco, R.; Katzenellenbogen, J.A. Estrogen pyrazoles: Defining the pyrazole core structure and the orientation of substituents in the ligand binding pocket of the estrogen receptor. *Bioorg. Med. Chem.* **2001**, *9*, 141–150. [CrossRef]
26. Dawood, D.H.; Nossier, E.S.; Ali, M.M.; Mahmoud, A.E. Synthesis and molecular docking study of new pyrazole derivatives as potent anti-breast cancer agents targeting VEGFR-2 kinase. *Bioorg. Chem.* **2020**, *101*, 103916. [CrossRef]
27. Cheng, C.; Yun, F.; Ullah, S.; Yuan, Q. Discovery of novel cyclin-dependent kinase (CDK) and histone deacetylase (HDAC) dual inhibitors with potent in vitro and in vivo anticancer activity. *Eur. J. Med. Chem.* **2020**, *189*, 112073. [CrossRef] [PubMed]
28. Morretta, E.; Sidibè, A.; Spallarossa, A.; Petrella, A.; Meta, E.; Bruno, O.; Monti, M.C.; Brullo, C. Synthesis, functional proteomics and biological evaluation of new 5-pyrazolyl ureas as potential anti-angiogenic compounds. *Eur. J. Med. Chem.* **2021**, *226*, 113872. [CrossRef]
29. Long, J.K.; Gregory, V.; Gutteridge, S.; Taggi, A.E.; Berezna, J.F. Fungicidal Pyrazoles and their Mixtures for Protection of Crops from Phytopathological Fungi. US Patent MY157327A, 31 May 2016.
30. Taggi, A.E.; Berezna, J.F.; Long, J.K. Preparation of Pyrazoles as Fungicides. WO Patent WO2014130241, 28 August 2014.
31. Long, J.K.; Chittaboina, S.; McMahon, T.C. Preparation of Pyrazoles as Fungicides and Their Use in Fungicidal Mixtures. WO Patent WO2021183721, 16 September 2021.
32. Cantin, L.D.; Ma, X.; Akuche, C.; Liang, S.X. Preparation of Anilino-Heteroaryl-Pyrazoles Useful for the Treatment of Diabetes. WO Patent WO2005112923, 1 December 2005.
33. Rudolph, J.; Cantin, L.D.; Magnuson, S.; Bullock, W.; Bullion, A.M.; Chen, L.; Chuang, C.Y.; Liang, S.; Majumdar, D.; Ogutu, H.; et al. Preparation of Anilinopyrazoles for the Treatment of Diabetes. WO Patent WO2004050651A1, 17 June 2004.
34. Lowe, D.; Shelekhin, T.; Wang, G.; Ma, X.; Iwuagwu, C.; Ying, S.; Magnuson, S.; Rudolph, J.; Koebberling, J.; Pernerstorfer, J.; et al. Preparation of Anilinopyrazoles for the Treatment of Diabetes. WO Patent WO2007027842-A1, 8 March 2007.
35. Guisot, N. Preparation of Pyrazole Derivatives as Kinase Inhibitors. WO Patent WO2017103611A1, 22 June 2017.
36. Garnier, J.M.D.; Brzozowski, M.; Feutrell, J.T.; Lessene, G.L.; Gardner, C.; Czabotar, P.E.; Cowan, A.; Sharma, P.; Schuster-Klein, C.A.; Poitevin, C. Preparation of Amido Compounds for Treating Necroptosis and/or Inhibiting RIP1 and/or MLKL. WO Patent WO2021253098 A1, 23 December 2021.
37. Hassan, A.S.; Moustafa, G.O.; Awad, H.M.; Nossier, E.S.; Mady, M.F. Design, synthesis, anticancer evaluation, enzymatic assays, and a molecular modeling study of novel pyrazole–indole hybrids. *ACS Omega* **2021**, *6*, 12361–12374. [CrossRef] [PubMed]
38. Klueken, M.; Geist, J.; Montagne, C.; Millet, A.; Nicolas, L.; Tsuchiya, T. Active Compound Combinations. WO Patent WO2021255070 A1, 23 December 2021.
39. Venkatesha, H.M.; Saragur, R.S.; Garg, R.; Pabba, J.; Autkar, S.S. A Pesticidally Active Mixture Comprising Pyrazolopyridine Anthranilamide Compound, Oxides or Salts thereof, with Insecticides or Fungicides. WO Patent WO2022023931 A1, 3 February 2022.
40. Lim, F.P.L.; Gan, R.X.Y.; Dolzhenko, A.V. Highly selective and efficient synthesis of 3-aryl-amino-substituted 5-aminopyrazole-4-carboxylates under microwave irradiation. *Tetrahedron Lett.* **2017**, *58*, 775–778. [CrossRef]
41. Elgemeia, G.; Fathyb, N.; Zagharyc, W.; Farag, A. S-Glycosides in medicinal chemistry: Novel synthesis of cyanoethylene thioglycosides and their pyrazole derivatives. *Nucleosides Nucleotides Nucleic Acids* **2017**, *36*, 198–212. [CrossRef]
42. Lusardi, M.; Rotolo, C.; Ponassi, M.; Iervasi, E.; Rosano, C.; Spallarossa, A. One-pot synthesis and antiproliferative activity of highly functionalized pyrazole derivatives. *ChemMedChem* **2022**, *17*, e202100670. [CrossRef]
43. Hassan, A.; Mohamed, N.; Ibrahim, Y.; Mourad, A.-F.; Aboul-Fetouh, S. Charge-transfer complexes of heterocyclics of biological interest—II. Aminopyrazoles. *Spectrochim. Acta A Mol. Biomol. Spectrosc.* **1991**, *47*, 1635–1636. [CrossRef]

44. Fischer, G.; Rudorf, W.-D.; Kleinpeter, E. Study of the distribution of the  $\pi$ -electrons in push-pull alkenes by  $^1\text{H}$  and  $^{13}\text{C}$  NMR spectroscopy. *Magn. Reson. Chem.* **1991**, *29*, 212–222. [CrossRef]
45. Fischer, G.; Kleinpeter, E. Application of 2D EXSY NMR spectroscopy to the study of the dynamic behaviour of aroylcyanoketene-S,S-dimethylacetals. *Magn. Reson. Chem.* **1991**, *29*, 204–206. [CrossRef]
46. Shizheng, Z.; Chaoyue, Q.; Guoling, X.; Qianli, C. convenient synthesis of a new push-pull alkenes:  $\beta$ -alkoxyl vinyl trifluoromethyl sulfones. *Tetrahedron Lett.* **1998**, *39*, 5265–5268. [CrossRef]
47. Kleinpeter, E.; Klod, S.; Rudorf, W.-D. Electronic state of push–pull alkenes: An experimental dynamic NMR and theoretical ab initio MO study. *J. Org. Chem.* **2004**, *69*, 4317–4329. [CrossRef]
48. Pappalardo, R.R.; Marcos, E.S.; Ruiz-Lopez, M.F.; Rinaldi, D.; Rivail, J.L. Solvent effects on molecular geometries and isomerization processes: A study of push-pull ethylenes in solution. *J. Am. Chem. Soc.* **1993**, *115*, 3722–3730. [CrossRef]
49. Kleinpeter, E.; Schulenburg, A. Quantification of the push–pull effect in substituted alkenes. *Tetrahedron Lett.* **2005**, *46*, 5995–5997. [CrossRef]
50. Savych, V.I.; Mykhalchuk, V.L.; Melnychuk, P.V.; Isakov, A.O.; Savchuk, T.; Timoshenko, V.M.; Siry, S.A.; Pavlenko, S.O.; Kovalenko, D.V.; Hryshchuk, O.V.; et al. Bicyclic pyrrolidines for medicinal chemistry via [3+2]-cycloaddition. *J. Org. Chem.* **2021**, *86*, 13289–13309. [CrossRef]
51. Sofan, M.A.; El-Mekabaty, A.; Hasel, A.M.; Said, S.B. Synthesis, cytotoxicity assessment and antioxidant activity of some new thiazol-2-yl carboxamides. *J. Heterocycl. Chem.* **2021**, *58*, 1645–1655. [CrossRef]
52. Frizzo, C.P.; Hennemann, B.L.; Kuhn, B.L.; Wust, K.M.; Paz, A.V.; Martins, M.A.P.; Zanatta, N.; Bonacorso, H.G. Trends for pyrazole fragmentation determined by gas chromatography coupled with mass spectrometry. In *Gas Chromatography—Derivatization, Sample Preparation, Application*; Kusch, P., Ed.; IntechOpen: London, UK, 2018. [CrossRef]
53. Elgemeie, G.H.; Elghandour, A.H.; Elaziz, G.W.A. Novel cyanoketene N,S-acetals and pyrazole derivatives using potassium 2-cyanoethylene-1-thiolates. *Synth. Commun.* **2007**, *37*, 2827–2834. [CrossRef]

## Article

# Reaction Products of $\beta$ -Aminopropioamidoximes Nitrobenzenesulfochlorination: Linear and Rearranged to Spiropyrazolinium Salts with Antidiabetic Activity

Lyudmila Kayukova <sup>1,\*</sup> , Anna Vologzhanina <sup>2,\*</sup> , Pavel Dorovatovskii <sup>3</sup>, Gulnur Baitursynova <sup>1</sup>, Elmira Yergaliyeva <sup>1</sup>, Ayazhan Kurmangaliyeva <sup>1</sup>, Zarina Shulgau <sup>4</sup>, Sergazy Adekenov <sup>5</sup>, Zhanar Shaimerdenova <sup>5</sup> and Kydymolla Akatan <sup>6</sup> 

<sup>1</sup> JSC A. B. Bekturov Institute of Chemical Sciences, 106 Shokan Ualikhanov St., Almaty 050010, Kazakhstan; guni-27@mail.ru (G.B.); erg\_el@mail.ru (E.Y.); ayazhankb98@mail.ru (A.K.)

<sup>2</sup> A. N. Nesmeyanov Institute of Organoelement Compounds, Russian Academy of Sciences, 28 Vavilova St., B-334, 119991 Moscow, Russia

<sup>3</sup> NRC "Kurchatov Institute", 1, Akademika Kurchatova pl., 123182 Moscow, Russia; paulgemini@mail.ru

<sup>4</sup> RSE National Center for Biotechnology, Science Committee of ME&S RK, 13/5 Kurgalzhinskoe Highway, Nur-Sultan 010000, Kazakhstan; shulgau@biocenter.kz

<sup>5</sup> JSC International Research and Production Holding Phytochemistry, 4 M. Gazalieva St., Karaganda 100009, Kazakhstan; info@phyto.kz (S.A.); zh.shaimerdenova@phyto.kz (Z.S.)

<sup>6</sup> National Scientific Laboratory, S. Amanzholov East Kazakhstan State University, 18/1 Amurskaya St., Ust-Kamenogorsk 070002, Kazakhstan; ahnur.hj@mail.ru

\* Correspondence: lkayukova@mail.ru (L.K.); vologzhanina@mail.ru (A.V.); Tel.: +7-(705)-168-81-53 (L.K.)

**Citation:** Kayukova, L.; Vologzhanina, A.; Dorovatovskii, P.; Baitursynova, G.; Yergaliyeva, E.; Kurmangaliyeva, A.; Shulgau, Z.; Adekenov, S.; Shaimerdenova, Z.; Akatan, K. Reaction Products of  $\beta$ -Aminopropioamidoximes Nitrobenzenesulfochlorination: Linear and Rearranged to Spiropyrazolinium Salts with Antidiabetic Activity. *Molecules* **2022**, *27*, 2181. <https://doi.org/10.3390/molecules27072181>

Academic Editors: Vera L. M. Silva and Artur M. S. Silva

Received: 27 February 2022

Accepted: 24 March 2022

Published: 28 March 2022

**Publisher's Note:** MDPI stays neutral with regard to jurisdictional claims in published maps and institutional affiliations.



**Copyright:** © 2022 by the authors. Licensee MDPI, Basel, Switzerland. This article is an open access article distributed under the terms and conditions of the Creative Commons Attribution (CC BY) license (<https://creativecommons.org/licenses/by/4.0/>).

**Abstract:** Nitrobenzenesulfochlorination of  $\beta$ -aminopropioamidoximes leads to a set of products depending on the structure of the initial interacting substances and reaction conditions. Amidoximes, functionalized at the terminal C atom with six-membered *N*-heterocycles (piperidine, morpholine, thiomorpholine and phenylpiperazine), as a result of the spontaneous intramolecular heterocyclization of the intermediate reaction product of an  $S_N2$  substitution of a hydrogen atom in the oxime group of the amidoxime fragment by a nitrobenzenesulfonyl group, produce spiropyrazolinium *ortho*- or *para*-nitrobenzenesulfonates. An exception is *ortho*-nitrobenzenesulfochlorination of  $\beta$ -(thiomorpholin-1-yl)propioamidoxime, which is regioselective at room temperature, producing two spiropyrazolinium salts (*ortho*-nitrobenzenesulfonate and chloride), and regiospecific at the boiling point of the solvent, when only chloride is formed. The *para*-Nitrobenzenesulfochlorination of  $\beta$ -(benzimidazol-1-yl)propioamidoxime, due to the reduced nucleophilicity of the aromatic  $\beta$ -amine nitrogen atom, is regiospecific at both temperatures, and produces the *O*-*para*-nitrobenzenesulfochlorination product. The antidiabetic screening of the new nitrobenzenesulfochlorination amidoximes found promising samples with in vitro  $\alpha$ -glucosidase activity higher than the reference drug acarbose. <sup>1</sup>H-NMR spectroscopy and X-ray analysis revealed the slow inversion of six-membered heterocycles, and experimentally confirmed the presence of an unfavorable stereoisomer with an axial N–N bond in the pyrazolinium heterocycle.

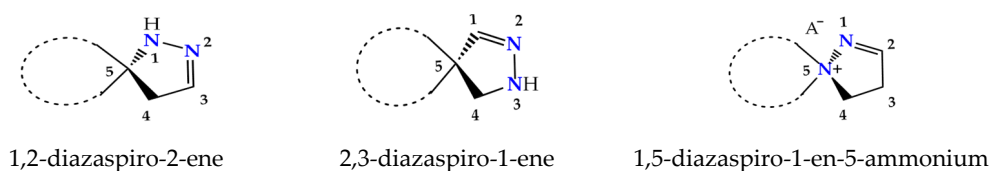
**Keywords:**  $\beta$ -aminopropioamidoximes; nitrobenzenesulfochlorination; spiropyrazolinium salts; X-ray diffraction

## 1. Introduction

Heterocycles with potential bioactive properties are of great interest, first of all, for medical chemists working in the field of heterocyclic compounds synthesis. Among the new drugs approved by the FDA in 2021, almost 50% are substances with nitrogen-containing heterocycles [1]. Pyrazoline derivatives, as prominent representatives of nitrogen-containing heterocycles, became the subject of a report on the world market of diphenylpyrazolines from Market Strides (global aggregator and publisher of market intelligence research

reports). The main segments of the diphenylpyrazoline market are divided into pharmaceutical and industrial, and address textiles, detergents, paper production, cosmetics, plastics, ceramics, and medicines [2].

Spiropyrazolines, also termed as spirocyclic hydrazine moiety, are rigid asymmetric heterocyclic structures with a chirality axis and with possible centers of chirality C-5 carbon atoms in the most studied 1,2-diazospiro- and 2,3-diazospiropyrazolines or the ammonium nitrogen atom N(+)-5 in 1,5-diazospiropyrazolinium systems (Figure 1). Thus, these compounds exhibit great synthetic potential due to an enantiomeric advantage, regioisomeric composition, reactivity, and tautomeric transformations. Essentially, 1,2- and 2,3-spiro-1-pyrazolines exist as spiro-2-pyrazolines ( $\Delta 2$  isomers) [3], although, in solutions, they exhibit an equilibrium of the imine and enamine forms [4]. As we know, the spiro-pyrazolinium salts with a 1,5-diazospiro-1-en-5-ium fragment that we obtained via the hydrolysis of 3-( $\beta$ -heteroamino)ethyl-5-aryl-1,2,4-oxadiazoles and the arylsulfochlorination of  $\beta$ -aminopropioamidoximes exist, under standard conditions, as the  $\Delta 2$  isomer [5–8]. The thermodynamic advantage of possible tautomers of the key pyrazoline moiety was estimated; it turns out that, in the case of pyrazolines, the  $\Delta 2$  isomer is much more stable than the others [9].

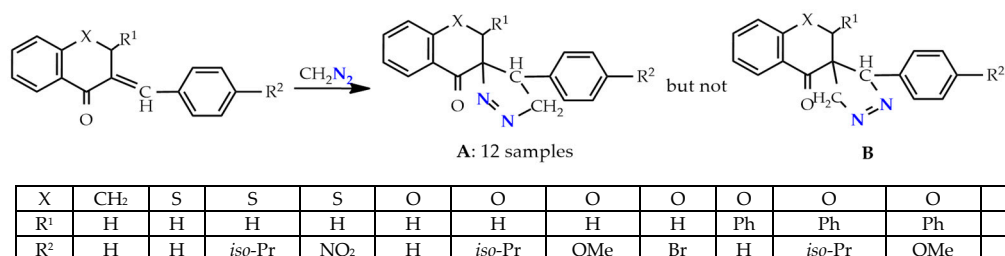


**Figure 1.** Structural isomers of spiro-pyrazolines.

Two comprehensive reviews on functionalized spiro-pyrazolines were published in 2013 and 2019 [10,11].

The most common methods for the construction of the 1,2- and 2,3-spiro-1-pyrazolines involve the formation of a new ring on an existing carbo- or heterocycle, having exocyclic C=C double bonds. The essential steps in the formation of spiro-pyrazoline systems in these cases are 1,3-cycloaddition reactions of nitrogen-containing molecules (nitrilimines [12–15] and diazoalkanes [16,17]) to double bonds, or a condensation reaction of substituted chalcones with hydrazine or its derivatives in an acidic or alkaline medium [18,19].

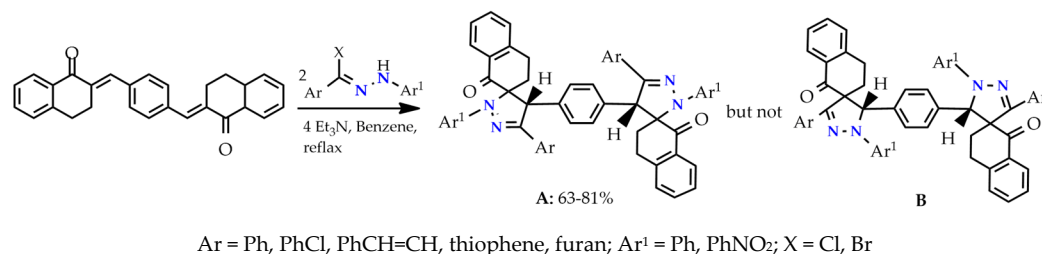
There is information about the regioselective and regiospecific syntheses of spiro-pyrazolines. The synthesis of only one stereoisomer of spiro-1-pyrazolines **A**— $\Delta 2$  1,2-diazospiropyrazolines obtained by the 1,3-dipolar cycloaddition of diazomethane to 3-arylidene-flavanones/chromanones proceeds regioselectively in one step (Scheme 1). The alternative structures **B** were rejected based on the  $^1\text{H}$  NMR and XRD, data as well as the DFT calculations [20,21].



**Scheme 1.** 1,3-Dipolar cycloaddition of diazomethane to 3-arylidene-flavanones.

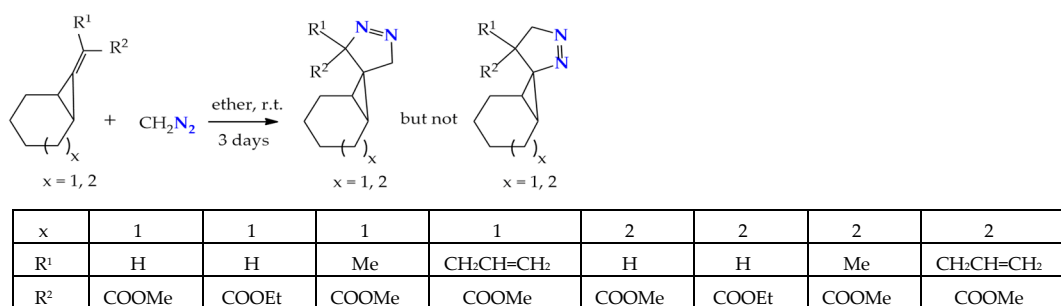
Symmetrical spiro-pyrazoline systems are formed by the 1,3-dipolar cycloaddition reaction of (*2E,2'E*)-2,2'-(1,4-phenylene bis(methanylylidene)) bis(3,4-dihydronaphthalen-1(2*H*)-one) with a hydrazinoyl halides (nitrile imines). The reaction proceeds regioselectively and only one of two possible spiro-pyrazoline regioisomers (the 1,2-diazospiropyrazoline, but

not 2,3-diazaspiropyrazoline) is formed. The best explanation for the regioselectivity of the reaction and the impossibility of the formation of the 2,3-diazaspiropyrazolines adduct is made using the molecular orbital theory in the interaction of HOMO and LUMO reagents (Scheme 2) [22].



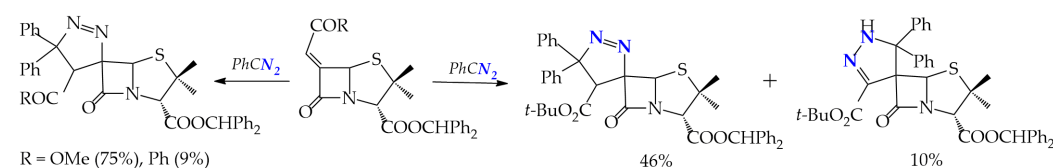
**Scheme 2.** Cycloaddition of bis-exocyclic olefins with nitrile imines.

1,3-Dipolar cycloaddition of diazomethane to a double bond activated by an electron-withdrawing group in alkylidenecyclopropanes produces 2,3-diazaspiropyrazolines in excellent amounts (95–99%). The determination of the stereochemistry of spiropyrazolines was carried out by NMR spectroscopy, including NOE experiments, which indicated that the methylene protons of the 2,3-diazaspiropyrazoline ring have NOE effects on cyclopropane protons, and this is possible when the methylene group is in the exo-position (Scheme 3) [23].



**Scheme 3.** Formation of 2,3-diazaspiro-2-ene isomers in the course of the regioselective addition of diazomethane to alkylidenecyclopropanes.

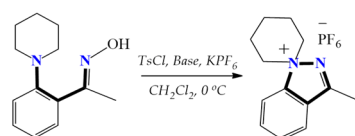
At a 1,3-dipolar addition of diphenyldiazomethane to 6-alkylidenepenicillanates, examples of regioselective and regiospecific syntheses with the formation of 1,2- and 2,3-spiropyrazoline systems are observed. Regio- and stereospecificity is observed in the interaction of diphenyldiazomethane with penicylates having Ph and COMe alkylidene substituents R to form 1,2-spiropyrazolines: (4'*S*,6*S*)-3-benzhydryl 4'-methoxycarbonyl- and (4'*S*,6*S*)-3-benzhydryl 4'-benzoyl-5',5'-diphenyl-4',5'-dihydrospiro[penicillanate-6,3'-(3*H*-pyrazole)]-3-carboxylates up to 75%. The change of the alkylidene substituent to CO<sub>2</sub>*t*-Bu leads to a stereoselective, but regioisomeric, mixture of 1,2- and 2,3-spiropyrazolines: (4'*S*,6*S*)-3-benzhydryl 4'-*tert*-butoxycarbonyl-5',5'-diphenyl-4',5'-dihydrospiro[penicillanate-6,3'-(3*H*-pyrazole)]-3-carboxylate and (6*R*)-3-benzhydryl 3'-acetyl-1',5'-dihydrospiro[penicillanate-6,4'-(4*H*-pyrazole)]-3-carboxylate in a ratio of 46 and 10% (Scheme 4) [24].



**Scheme 4.** 1,3-Dipolar addition of diphenyldiazomethane to 6-alkylidenepenicillanates (reaction conditions: DCM, 30 °C, 24 h).



Except for our own studies, no examples of 1,5-diazaspiro-1-en-5-ium spiropyrazolinium salts can be found in the literature. However, stable indazole derivatives, 1,1-disubstituted indazolium hexafluorophosphates with a nitrogen atom at the head of the bridge, were obtained utilizing the tosylation reaction. This transformation is similar to that observed in our previous studies, and includes intramolecular neighboring group participation, finally leading to strong bonding, which follows the  $S_N2$  reaction mechanism (Scheme 5) [25].



**Scheme 5.** The attainment of stable 1,1-disubstituted indazolium hexafluorophosphates.

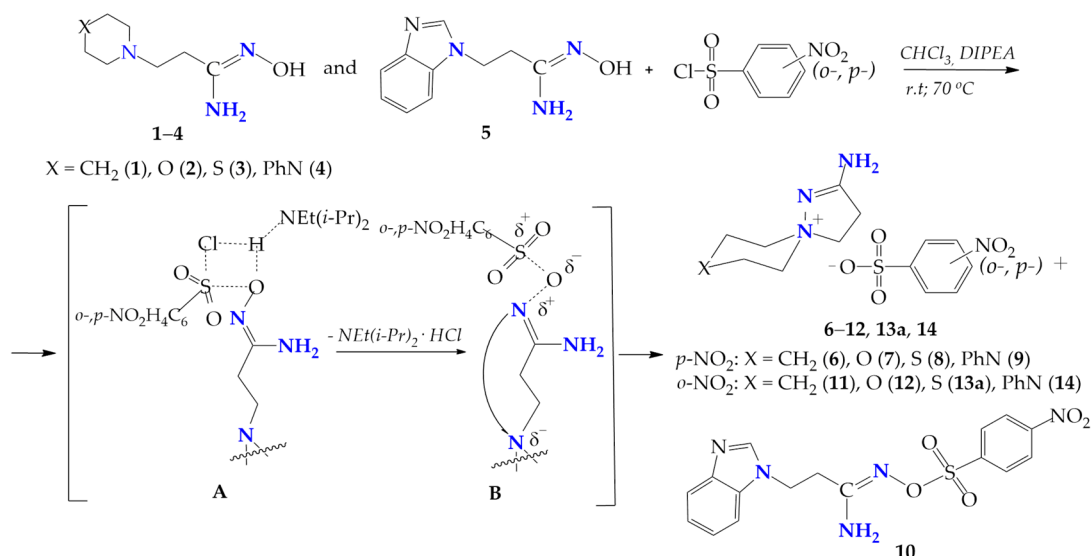
Previously, we obtained new spiropyrazolinium compounds via the hydrolysis of 3-( $\beta$ -heteroamino)ethyl-5-aryl-1,2,4-oxadiazoles [5,6], by the arylsulfochlorination (Aryl: *para*-XC<sub>6</sub>H<sub>4</sub>SO<sub>2</sub>Cl; X=CH<sub>3</sub>O, CH<sub>3</sub>, H, Br, Cl, NO<sub>2</sub>) of  $\beta$ -(morpholin-1-yl)aminopropioamidoxime [7] and by the tosylation of  $\beta$ -aminopropioamidoximes ( $\beta$ -amino group: piperidin-1-yl, morpholine-1-yl, thiomorpholin-1-yl, 4-phenylpiperazin-1-yl, benzimidazol-1-yl) at r.t. [8]. In the present study, we are interested in the regioselectivity of  $\beta$ -aminopropioamidoximes *ortho*-, *para*-nitrobenzenesulphochlorination at reaction conditions (chloroform (CHCl<sub>3</sub>), diisopropylamine (DIPEA), room temperature and 70 °C). Depending on the reactant's structure and reaction temperature, 2-amino-1,5-diazathiospiro[4.5]-dec-1-ene-5-ammonium nitrobenzenesulfonates and chloride and the product of *para*-nitrobenzenesulfochlorination, on the oxygen atom of  $\beta$ -(benzimidazol-1-yl)propioamidoxime were obtained. Among them, samples with high in vitro antidiabetic activity were found. The significance of the present work is the establishment of the ambiguity of amidoximes sulfochlorination and the possibility of obtaining a wide range of potentially biologically active products.

## 2. Results and Discussion

### 2.1. Synthesis and Spectra

The interaction of  $\beta$ -aminopropioamidoximes (1–5) with *ortho*-, *para*-nitrobenzenesulfochlorides in CHCl<sub>3</sub> was carried out at room temperature and by heating the reaction mixture to the solvent boiling point. A change in the electronic properties of the sulfochlorinating agent, the transition from tosyl chloride to *ortho*-, *para*-nitrobenzenesulfochlorides lead to an increase in the reaction time at room temperature from 15–20 h in the case of tosylation [4] to 38–120 h for *para*-benzenesulfochlorination, and up to 25–104 h for *ortho*-benzenesulfochlorination.

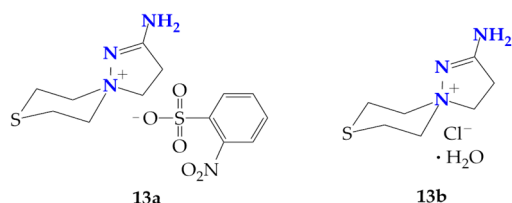
The heating of the reaction mixture at the CHCl<sub>3</sub> boiling point reduces the reaction time to 19–36 h, and to 24 h for *para*- and *ortho*-nitrobenzenesulfochlorination, respectively. The completion of  $\beta$ -aminopropioamidoximes arylsulfochlorination was confirmed by the physicochemical data (TLC, elemental analysis, m.p.), and the IR and NMR (<sup>1</sup>H and <sup>13</sup>C) spectra and X-ray data of the isolated products (6–14). On the basis of physicochemical and spectral data, it was concluded that, in the case of the nitrobenzenesulfochlorination of  $\beta$ -aminopropioamidoximes with six-membered heterocycles in the  $\beta$ -position (1–4), the main products were the nitrobenzenesulfonates of spiropyrazoline compounds 6–12, 13a, and 14; however, when the substrate was  $\beta$ -(benzimidazol-1-yl)propioamidoxime (5), only the product of *para*-nitrobenzenesulfochlorination at the oxygen atom of the amidoxime fragment 10 was isolated from the reaction mixture (Scheme 6).



**Scheme 6.** Nitrobenzenesulfochlorination of  $\beta$ -aminopropioamidoximes.

It is assumed that, in the case of the nitrobenzenesulfochlorination of  $\beta$ -aminopropioamidoximes 1–4, the *O*-nitrobenzenesulphonates of  $\beta$ -propioamidoximes formed as intermediate **B**, due to the thermodynamic advantage, rearranging into spiropyrazoline nitrobenzenesulphonates (6–12, 13a, 14). Only in the case of the benzimidazole derivative, the intermediate **B** remains stable and produces *O*-*para*-nitrobenzenesulphonate 10.

In addition, the *ortho*-nitrobenzenesulfochlorination of  $\beta$ -(thiomorpholine-1-yl)propioamidoxime (3) has the following features: at room temperature, a mixture of 2-aminospiropyrazolium *ortho*-nitrobenzenesulphonate and chloride (13a and 13b) were obtained, and carrying out the reaction at 70 °C only produces chloride 13b (Figure 2). Compound 13b was previously characterized by us [26,27].



**Figure 2.** Salts of spiropyrazolinium compounds 13a and 13b isolated at the *ortho*-nitrobenzenesulfochlorination of  $\beta$ -(thiomorpholine-1-yl)propioamidoxime.

Evidently, in this case, the *para*-nitrophenylsulfonate anion in the primarily formed 2-amino-1,5-diazaspiro[4.5]dec-1-en-5-ium *para*-nitrophenylsulfonate (13a) was exchanged for the chloride anion from DIPEA hydrochloride, releasing *para*-nitrobenzenesulfonic acid and DIPEA.

The stoichiometry of the reaction does not provide for the formation of a hydrate. We believe that the preparation of hydrate 13b can be explained by the prolonged contact of the mother liquor during the preparation of the single crystals of the *ortho*-nitrophenylsulfochlorination product of amidoxime 3 with atmospheric moisture.

When establishing the structure of nitrobenzenesulfochlorination products, a difference was noted in the values of the mobility index  $R_f$  for the products produced by the nitrobenzenesulfochlorination of amidoximes with six-membered nitrogenous heterocycles in the  $\beta$ -position (6–9, 11–14) and for the *para*-nitrobenzenesulfochlorination product of  $\beta$ -(benzimidazol-1-yl)propioamidoxime (10) ( $R_f$  0.01–0.12 and 0.75). Compounds 7 and 13b were previously described in [7] and [26,27], respectively (Table 1).

**Table 1.** Physicochemical data on the products as a result of the nitrobenzenesulfochlorination of  $\beta$ -aminopropioamidoximes (6–14).

| Compd | Yield, % |       | Time, h |       | M.p., °C | $R_f$ | Compd | Yield, % |       | Time, h |       | M.p., °C | $R_f$ |
|-------|----------|-------|---------|-------|----------|-------|-------|----------|-------|---------|-------|----------|-------|
|       | r.t.     | 70 °C | r.t.    | 70 °C |          |       |       | r.t.     | 70 °C | r.t.    | 70 °C |          |       |
| 6     | 77       | 46    | 38      | 27    | 151      | 0.12  | 11    | 77       | 75    | 35      | 29    | 153      | 0.05  |
| 7 [7] | 70       | 74    | 120     | 24    | 187–188  | 0.10  | 12    | 93       | 64    | 25      | 24    | 148      | 0.01  |
| 8     | 68       | 47    | 84      | 21    | 230      | 0.10  | 13a   | 25       | -     | 104     | 24    | 138–140  | 0.08  |
| 9     | 70       | 69    | 60      | 19    | 203      | 0.15  | 13b   | 25       | 56    | 104     | 24    | >280     | 0.08  |
| 10    | 82       | 36    | 80      | 36    | 158      | 0.75  | 14    | 79       | 81    | 34      | 24    | 185–187  | 0.08  |

In the IR spectra of compounds 6–12, 13a, and 14, there are two pairs of bands related to the characteristic stretching vibrations of a strong intensity of the NO<sub>2</sub> and SO<sub>2</sub> groups at 1515–1549 (as) cm<sup>-1</sup> and 1349–1377 (sy) cm<sup>-1</sup>, and 1207–1240 (as) cm<sup>-1</sup> and 1024–1197 (sy) cm<sup>-1</sup>, respectively, whereas, in the IR spectrum of compound 13b, there are no bands of stretching vibrations for the bonds of the NO<sub>2</sub> and SO<sub>2</sub> groups.

It is interesting that, in the <sup>1</sup>H-NMR spectra of compounds 6–9, 13a, and 13b, it was possible to fix the diastereotopic nature of the geminal protons of the methylene groups located at the ammonium nitrogen atom, which produce pairs of multiplet signals with an intensity of 2 protons at  $\delta$ : 3.35 m, 3.44 m (6); 3.41 m, 3.65 m (7); 3.60 m, 3.72 m (8); 3.49 m, 3.98 m (9); 3.10 m, 3.68 m (13a); and 3.10 m, 3.68 m (13b).

Similarly, the geminal protons of the methylene groups at the S, O, S, S, and N atoms of the  $\beta$ -heterocycles of compounds 8, 12, 13a, 13b, and 14 also appear as pairs of proton signals with an intensity of 2 protons at  $\delta$ : 2.87 m, 3.15 m (8); 3.35 m, 3.60 m (12); 2.84 m, 3.55 m (13a); 2.85 m, 3.55 m (13b); and 3.40 m, 3.71 m (14). Evidently, the effect of the slow rotation of  $\beta$ -heterocycles with the possibility of fixing the equatorial and axial protons is observed here. In addition, the diastereotopicity of these protons may be associated with the presence of an asymmetry axis inherent in the spiro compounds.

The signals of Csp<sup>3</sup> and Csp<sup>2</sup> carbon atoms in the <sup>13</sup>C-NMR spectra of compounds 6–14 are present in the characteristic regions.

We obtained a quantum-chemical confirmation of the advantageousness of the formation of spirocyclic tosylation and *para*-nitrobenzenesulfochlorination products of  $\beta$ -aminopropioamidoximes (1–4), with negative values of the Gibbs energy of the chemical reaction in the range of –119.99–163.57 kJ/mol and the disadvantage of the formation of a spirostructure for  $\beta$ -(benzimidazole-1-yl)propioamidoxime (5), with positive values of the Gibbs energy for the tosylation and *para*-nitrobenzenesulfochlorination products as 45.87 and 20.02 kJ/mol, respectively [28].

The thermodynamic advantage of the formation of 2-aminospiropyrazolylammonium sulfonates (tosylates, *para*- and *ortho*-nitrobenzenesulfonates) for a number of  $\beta$ -aminopropioamidoximes (1, 2, 4), in comparison to the formation of chloride hydrates, was identified, except for the case when the initial substrate was  $\beta$ -(thiomorpholine-1-yl)propioamidoxime 3; in this case, 2-amino-8-thia-1,5-diazaspiro[4.5]dec-1-en-5-ammonium chloride monohydrate (13b) is preferred by –8.1, –6.18, –3.08 kJ/mol, respectively [29].

It should be noted that we attempted to react  $\beta$ -(benzimidazol-1-yl)propioamidoxime (5) with *ortho*-nitrobenzenesulfonate several times, under the described conditions (CHCl<sub>3</sub>, DIPEA, r.t. and 70 °C), but, each time, a resinous reaction mixture was obtained.

## 2.2. The In Vitro Antidiabetic Screening of 2-Amino-1,5-diazaspiro[4.5]dec-1-en-5-ammonium Nitrobenzenesulphonates and Chloride Hydrate (6–9, 11–14) and 3-(1H-Benzimidazol-1-yl)-N'-[(4-nitrophenyl)sulfonyl]oxypropanimidamide (10)

The  $\alpha$ -amylase and  $\alpha$ -glucosidase inhibition tests, which hydrolyze starch in postprandial hyperglycemia, are standard tests used in the discovery and development of new antidiabetic drugs. Essentially, the regulation of  $\alpha$ -amylase and  $\alpha$ -glucosidase biological

functions (inhibition) is critical to the treatment regimen. This implies that new drug candidates with a potent inhibition of the  $\alpha$ -glucosidase and  $\alpha$ -amylase would be valuable to drug discovery and development for diabetes mellitus [30].

The in vitro antidiabetic activity of spiropyrazolilammonium *ortho*-, *para*-nitrobenzenesulfonates and chloride **6–9**, **11–14**, and the product of *O*-*para*-nitrobenzenesulfochlorination of  $\beta$ -(benzimidazol-1-yl)propioamidoxime (**10**) was assessed via the degree of inhibition of the activity of  $\alpha$ -amylase and  $\alpha$ -glucosidase by the studied substances, compared to the standard drug acarbose (Table 2). The table shows four series of experiments with different experimental values of the in vitro activity of acarbose in relation to  $\alpha$ -amylase and  $\alpha$ -glucosidase.

**Table 2.** In vitro  $\alpha$ -amylase and  $\alpha$ -glucosidase activity of nitrobenzenesulfochlorination products of  $\beta$ -aminopropioamidoximes (**6–14**).

| Compd                             | 6              | 7               | 8              | 9               | 10             | Acarbose       |
|-----------------------------------|----------------|-----------------|----------------|-----------------|----------------|----------------|
| $\alpha$ -Amylase activity, %     | 46.0 $\pm$ 2.8 | 27.7 $\pm$ 1.9  | 43.9 $\pm$ 2.1 | 42.0 $\pm$ 2.3  | 44.1 $\pm$ 2.9 | 50.3 $\pm$ 1.1 |
| $\alpha$ -Glucosidase activity, % | "0"            | 48.1 $\pm$ 22.2 | 67.1 $\pm$ 3.8 | 36.5 $\pm$ 13.2 | 61.0 $\pm$ 1.5 | 58.9 $\pm$ 1.8 |
| Compd                             | 11             | 12              | 13a            | 13b             | 14             | Acarbose       |
| $\alpha$ -Amylase activity, %     | 17.2 $\pm$ 1.2 | 9.6 $\pm$ 2.2   | 3.4 $\pm$ 1.1  | 8.4 $\pm$ 0.8   | 14.3 $\pm$ 4.1 | 34.6 $\pm$ 0.4 |
| $\alpha$ -Glucosidase activity, % | "0"            | 8.7 $\pm$ 2.2   | "0"            | "0"             | 13.0 $\pm$ 2.0 | 60.7 $\pm$ 0.7 |

All the tested compounds had an average inhibitory activity against  $\alpha$ -amylase, the values of which are less than the activity of acarbose. In regard to  $\alpha$ -glucosidase, the products of *para*-nitrobenzenesulfochlorination **8** and **10** had a pronounced inhibitory activity (61.0% and 67.1%). In the same series of experiments, the average inhibitory activity of 36.5% and 48.1% is shown by the compounds **7** and **9**. The reference drug acarbose exhibited the standard inhibitory activity of 58.9% and 50.3% in terms of  $\alpha$ -glucosidase and  $\alpha$ -amylase, respectively. In two other series of experiments, the tested *ortho*-nitro derivatives (**11–14**) did not show activity against  $\alpha$ -amylase and  $\alpha$ -glucosidase, comparable to the activity of acarbose.

The apparent difference in the antidiabetic activity of the subgroups of compounds **6–10** and **11–14** can be explained by the difference in their chemical structure. The first subgroup is derivative of *para*-nitrophenylsulfonic acid; the second subgroup is an *ortho*-nitrophenylsulfonic acid derivative. It is likely that binding to the sites of  $\alpha$ -amylase and  $\alpha$ -glucosidase enzymes responsible for increasing blood sugar is more efficient for *para*-nitrobenzenesulfonic acid derivatives (**6–10**), while *ortho*-nitrophenylsulfonic acid derivatives (**10–14**) are less efficient for the target reference antidiabetic drug acarbose.

The absence of  $\alpha$ -glucosidase activity in representatives of the subgroup of compounds **11–14** may be associated with the previously described trend of a general decrease in antidiabetic activity in the series of *ortho*-nitrophenylsulfonic acid derivatives (**10–14**), whereas the absence of  $\alpha$ -glucosidase activity for compound **6** may be a random variable.

### 2.3. X-ray Diffraction

X-ray diffraction studies of all the reaction products were carried out. They confirmed that, regardless of the synthetic conditions, the nitrobenzenesulfochlorination of  $\beta$ -aminopropioamidoximes containing piperidin-1-yl, morpholine-1-yl and 4-phenylpiperazin-1-yl as  $\beta$ -aminogroup affords spiropyrazolium nitrobenzenesulfonates **6**, **7**, **9** or **11**, **12**, **14**. As a result of the *ortho*-nitrobenzenesulfochlorination of  $\beta$ -thiomorpholin-1-ylpropioamidoxime, nitrophenylsulfonate **13a** and chloride monohydrate **13b** of the corresponding spirocation, similar to the one previously reported [29], can be obtained depending on

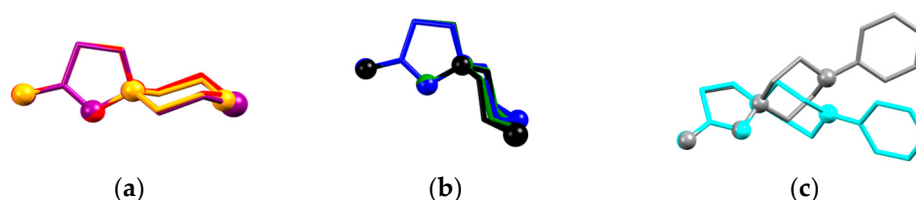
the reaction conditions. No rearrangement was detected for benzimidazol-1-yl-containing product **10** in accord with the B3LYP/6-31++G(d,p) calculations of the standard Gibbs free energies of reaction [28,29] found for N-substituted aminopyrazoles [31,32]. All salts contain one cation and one anion in the asymmetric unit (Figure S1, ESI). The quality of XRD data allowed us to locate all of the hydrogen atoms on difference Fourier maps, and undoubtedly confirmed that none of the sulfonate groups contained any hydrogen atoms.

The molecular structures of these compounds are depicted on Figure S1 (ESI), and the main geometry parameters of the cations and anions are listed in Table 3. The X-CH<sub>2</sub> bond distances increase and CH<sub>2</sub>-X-CH<sub>2</sub> angles decrease, passing from O to NPh; CH<sub>2</sub> and S. Valence angles at the positively charged N1 atom are close to ideal 109.5° values, however only N-CH<sub>2</sub> bond distances within the 6-membered ring are typical for a single N-C bond. In **10**, a similar N1-CH<sub>2</sub> bond is equal to 1.458(2) Å, due to the mesomeric effect of the benzimidazole substituent. The N-N bond in these salts varies from 1.460(2) to 1.470(2) Å, which is longer than 1.42–1.43 Å that is found for N-substituted aminopyrazoles [32,33]. Overall the conformations of the cations in **7**, **9**, **11**, **13a**, and **13b** correspond to one conformation on the six-membered ring towards the five-membered ring, while **6**, **8**, **12**, and **14** are the first examples of the inverted chair conformation (Figure 3) of this ring confirmed by means of X-ray diffraction. The difference in the two conformations manifests itself in the <sup>1</sup>H-NMR spectra (see above), and also through the N1-C1 bond length, which is generally shorter in cations with ‘novel’ conformations. In our opinion, the overall conformation of the molecule and elongation of bond distances in the pyrazole ring can be attributed to the anomeric effect [33] of the (hetero)atom in the six-membered ring. The length of the N2=C bond in all the spirocations is nearly the same as the N2=C bond distance of 1.302(2) in **10**.

**Table 3.** Selected geometrical parameters of spirocations **6–9**, **11–14** (Å and °).

|                                    | <b>6</b>              | <b>7</b> [7]          | <b>8</b>              | <b>9</b>              | <b>11</b>             | <b>12</b>             | <b>13a</b>            | <b>14</b>             |
|------------------------------------|-----------------------|-----------------------|-----------------------|-----------------------|-----------------------|-----------------------|-----------------------|-----------------------|
| N1–N2                              | 1.470(2)              | 1.466(2)              | 1.468(2)              | 1.468(4)              | 1.469(1)              | 1.473(2)              | 1.460(5)              | 1.468(1)              |
| N1–C1                              | 1.526(2)              | 1.514(3)              | 1.526(2)              | 1.530(4)              | 1.513(1)              | 1.520(2)              | 1.493(7)              | 1.518(1)              |
| C1–C2                              | 1.485(3)              | 1.495(3)              | 1.497(3)              | 1.518(4)              | 1.517(2)              | 1.513(2)              | 1.526(9)              | 1.526(2)              |
| N2=C                               | 1.298(2)              | 1.299(2)              | 1.300(2)              | 1.316(3)              | 1.311(1)              | 1.305(2)              | 1.289(6)              | 1.300(2)              |
| X–C <sub>Ar</sub>                  | 1.492(4)–<br>1.529(4) | 1.401(3)–<br>1.406(3) | 1.791(3)–<br>1.796(3) | 1.464(4)–<br>1.467(4) | 1.519(1)–<br>1.522(1) | 1.434(2)–<br>1.439(2) | 1.794(5)–<br>1.799(5) | 1.466(1)–<br>1.473(2) |
| d(C...Pz) <sup>1</sup>             | 0.302(4)              | 0.418(4)              | 0.267(3)              | 0.425(5)              | 0.457(1)              | 0.445(2)              | 0.450(7)              | 0.435(2)              |
| C <sub>Ph</sub> –NO <sub>2</sub>   | 1.472(2)              | 1.470(2)              | 1.477(2)              | 1.474(4)              | 1.472(1)              | 1.474(2)              | 1.454(6)              | 1.474(2)              |
| C <sub>Ar</sub> –X–C <sub>Ar</sub> | 112.1(2)              | 109.7(2)              | 98.2(1)               | 111.0(2)              | 109.83(9)             | 110.21(9)             | 95.5(2)               | 108.43(9)             |
| Ω <sup>2</sup>                     | 8.9(1)                | 6.6(1)                | 4.9(1)                | 6.8(1)                | 112.63(4)             | 109.74(5)             | 113.20(2)             | 125.73(5)             |

<sup>1</sup> The deviation of the C(1) atom from the mean plane formed by N–N=C–C atoms in the 5-membered pyrazole ring. <sup>2</sup> The twist angle between the mean planes of the phenyl ring and the NO<sub>2</sub> group for the anion.



**Figure 3.** Molecular conformations of the spirocation in (a) **7** (orange), **11** (red), **13a** (violet); (b) **6** (green), **12** (blue), **14** (black); and (c) **9** (grey) and **14** (cyan). The superimposed atoms are N–N=C–C atoms in the 5-membered pyrazole ring.

A prominent variation in the biological properties of these compounds can be accounted for the possibility of these cations to realize different conformations and to take part in different types of H bonds [34]. In these solids, the only donor for the H bonds is the amino group, while the sulfonate groups of the anions and heteroatoms of the cations compete to act as acceptors of H bonding. As a result, H-bonded chains are observed in

2-amino-1,5-diazathio[4.5]-dec-1-ene-5-ammonium-containing salts and tetramers in six other salts (Figure 4). The  $D^3_3(9)$  tetramers in **6**, **7**, and **11** are formed through two N–H ... N interactions and two N–H ... O ones. Similar  $D^3_3(13)$  tetramers in **12** and **14** are obtained through a similar N–H ... O cation ... anion interactions, but the cations are shifted along each other to allow for the bonding with a heteroatom of the six-membered ring. The  $R^4_4(12)$  cycles in **9** and the H-bonded chains in **8** and **13** are formed by the interactions of the amino group with sulfonate groups of two neighboring molecules. The  $G^a_d(n)$  notation of H-bonded architectures is presented in terms of [33], where **G** represents the type of pattern (**C** for chain, **S** for intramolecular hydrogen bonds, **R** for ring, and **D** for finite), **a** is the number of acceptors, **d** is the number of donors, and **n** the number of atoms in the pattern. Note that, despite the similar crystal parameters and space group of **11**–**13** (Table S1, ESI), these compounds cannot be regarded as isostructural, as they realize different packing and intermolecular (including H-bonding) interactions. Crystal packing demonstrates that, for these spirocations, heteroatoms of the six-membered cycle can take part in H bonding, and different conformations can be stabilized by means of intermolecular bonding.

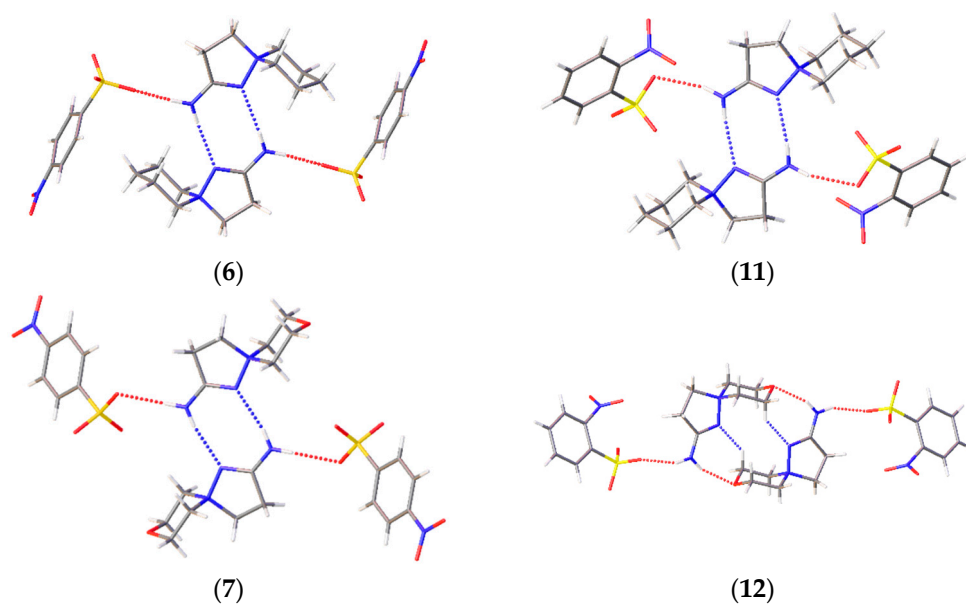
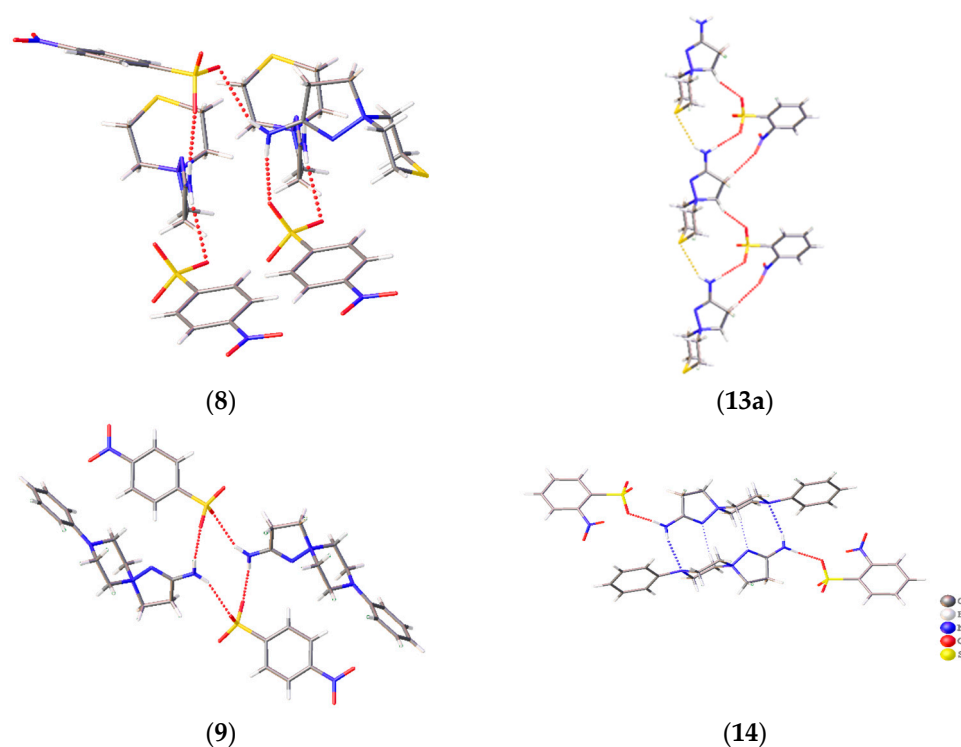


Figure 4. Cont.



**Figure 4.** H-bonding patterns in the crystal structures of the studied compounds. H bonds are depicted with dotted lines.

### 3. Materials and Methods

#### 3.1. Synthesis

The reagents were purchased from different chemical suppliers and were purified before use. FT-IR spectra were obtained on a Thermo Scientific Nicolet 5700 FTIR instrument (Thermo Fisher Scientific, Inc., Waltham, MA, USA) in KBr pellets. The  $^1\text{H}$ - and  $^{13}\text{C}$ -NMR spectra of compounds 6–10 were acquired on a Bruker Avance III 500 MHz NMR spectrometer (Bruker, BioSpin GMBH, Rheinstetten, Germany) and  $^1\text{H}$ - and  $^{13}\text{C}$ -NMR spectra of compounds 11–14 on a Jeol JNM-ECA 500 (Jeol, Tokyo 196-8558, JAPAN), (500 and 126 MHz, respectively).

The signals of the residual undeuterated solvents were used as a reference for the  $^1\text{H}$ -NMR (2.50 ppm) and  $^{13}\text{C}$ -NMR (39.5 ppm) spectra. Elemental analysis was carried out on a CE440 elemental analyzer (Exeter Analytical, Inc., Shanghai, China). The melting points were determined in glass capillaries on a PTP(M) apparatus (Khimlabpribor, Klin, Russia). The reaction progress and purity of the obtained products were controlled using Sorbfil (Sorbpolymer, Krasnodar, Russia) TLC plates coated with CTX-1A silica gel, grain size 5–17  $\mu\text{m}$ , containing UV-254 indicator. The eluent for TLC analysis was a mixture of benzene–EtOH, 1:3. The solvents for the synthesis, recrystallization, and TLC analysis (ethanol, 2-PrOH, benzene, DMF, and acetone) were purified according to the standard techniques.

#### 3.1.1. A General Procedure for the Synthesis of 2-Amino-1,5-diazaspiro[4.5]-dec-1-ene-5-ammonium *para*-Nitrobenzenesulfonates (6–9) and 3-(1*H*-Benzo[d]imidazol-1-yl)-*N'*-[(4-nitrobenzene)sulfonyl]oxypropanimidamide (10)

*The synthesis of  $\beta$ -aminopropioamidoximes 4-nitrobenzenesulfochlorinationproducts 6–10 (general method).* To a solution of 0.0029 mol of  $\beta$ -aminopropioamidoximes 1–5 in 20 mL of  $\text{CHCl}_3$ , 0.0029 mol of DIPEA was added. The reaction mixture was cooled to  $-1\text{ }^\circ\text{C}$ , and a solution of 0.0029 mol of 4-nitrobenzenesulfochloride in 2 mL of  $\text{CHCl}_3$  was added dropwise with stirring. The reaction mixture was then allowed to warm to r.t. (or heated to the boiling point (b.p.) of  $\text{CHCl}_3$ ) and stirred until the completion of the reaction. The

progress of the reaction was monitored by TLC. The formed white precipitates of the products **6–10** were filtered off and recrystallized from 2-PrOH.

**2-Amino-1,5-diazaspiro[4.5]dec-1-en-5-ammonium 4-nitrobenzenesulfonate (6).** The reaction mixture consisting of 0.5 g (0.0029 mol) of compound **1** in 20 mL of CHCl<sub>3</sub> and 0.38 g (0.0029 mol) of DIPEA was cooled to -1 °C. Then, 0.64 g (0.0029 mol) of 4-nitrobenzenesulfochloride was added dropwise. When the reaction mixture was kept at r.t. for 38 h, 0.80 g (77%) of white solid **6** was obtained (when the reaction mixture was kept at CHCl<sub>3</sub> b.p. for 27 h, 0.48 g (46%) of white solid **6** was obtained); m.p. 151 °C, *R<sub>f</sub>* 0.12. IR (KBr, cm<sup>-1</sup>): 1665 (C=N), 1607 (C=C), 1232 (SO<sub>2</sub> as) and 1190 (SO<sub>2</sub> sy), 1529 (NO<sub>2</sub> as) and 1352 (NO<sub>2</sub> sy), 3302 [N(-H)<sub>2</sub>], 2938, 2864, 2815 (C<sub>sp3</sub>-H), 3032, 3257 (C<sub>sp2</sub>-H). <sup>1</sup>H-NMR (500 MHz, DMSO-*d*<sub>6</sub>): 3.10 (t, *J* = 7.0 Hz, 2H, α-CH<sub>2</sub>), 3.81 (t, *J* = 7.0 Hz, 2H, β-CH<sub>2</sub>), 1.55 m, 1.75 m, 1.87 m, [6H, (CH<sub>2</sub>)<sub>3</sub>], 3.35 [m, 2H, N(+)(CH<sub>ax</sub>)<sub>2</sub>] and 3.44 [m, 2H, N(+)(CH<sub>eq</sub>)<sub>2</sub>], 7.23 (s, 2H, NH<sub>2</sub>), 7.83–8.21 (m, 4H, C<sub>(sp2)</sub>H). <sup>13</sup>C-NMR (126 MHz, DMSO-*d*<sub>6</sub>): 21.0, 21.9, 31.5, 60.7, 64.3 (2C), 126.0 (2C), 128.5 (2C), 138.0 (1C), 145.3 (1C), 168.5. Anal. Calcd for C<sub>14</sub>H<sub>20</sub>N<sub>4</sub>O<sub>5</sub>S (356.40): C, 47.18; H, 5.66. Found: C, 47.36; H, 5.37.

**2-Amino-8-oxa-1,5-diazaspiro[4.5]dec-1-ene-5-ammonium 4-nitrobenzenesulfonate (7).** The reaction mixture consisting of 0.5 g (0.0029 mol) of compound **2** in 20 mL of CHCl<sub>3</sub> and 0.38 g (0.0029 mol) of DIPEA was cooled to -1 °C. Then, 0.64 g (0.0029 mol) of 4-nitrobenzenesulfochloride was added dropwise. When the reaction mixture was kept at r.t. for 120 h, 0.73 g (70%) of white solid **7** was obtained (when the reaction mixture was kept at CHCl<sub>3</sub> bp for 24 h, 0.77 g (74%) of white solid **7** was obtained); m.p. 187–188 °C, *R<sub>f</sub>* 0.10. IR (KBr, cm<sup>-1</sup>): 1650 (C=N), 1600 (C=C), 1231 (SO<sub>2</sub> as) and 1194 (SO<sub>2</sub> sy), 1520 (NO<sub>2</sub> as) and 1362 (NO<sub>2</sub> sy), 3466 [N(-H)<sub>2</sub>], 2967, 2854 (C<sub>sp3</sub>-H), 3236, 3328, 3388 (C<sub>sp2</sub>-H). <sup>1</sup>H-NMR (500 MHz, DMSO-*d*<sub>6</sub>): 3.13 (t, *J* = 7.0 Hz, 2H, α-CH<sub>2</sub>), 3.92 (t, *J* = 7.0 Hz, 2H, β-CH<sub>2</sub>), 3.32 [m, 4H, O(CH<sub>2</sub>)<sub>2</sub>], 3.41 [m, 2H, N(+)(CH<sub>ax</sub>)<sub>2</sub>] and 3.65 [m, 2H, N(+)(CH<sub>eq</sub>)<sub>2</sub>], 7.28 (s, 2H, NH<sub>2</sub>), 7.80–8.19 (m, 4H, C<sub>(sp2)</sub>H). <sup>13</sup>C-NMR (126 MHz, DMSO-*d*<sub>6</sub>): 31.4, 62.1, 62.4, 63.2, 123.8 (2C), 127.4 (2C), 147.7 (1C), 154.8 (1C), 170.1. Anal. Calcd for C<sub>13</sub>H<sub>18</sub>N<sub>4</sub>O<sub>6</sub>S (358.37): C, 43.57; H, 5.06. Found: C, 43.48; H, 5.13.

**2-Amino-8-thia-1,5-diazaspiro[4.5]dec-1-en-5-ammonium 4-nitrobenzenesulfonate (8).** The reaction mixture consisting of 0.55 g (0.0029 mol) of compound **3** in 20 mL of CHCl<sub>3</sub> and 0.38 g (0.0029 mol) of DIPEA was cooled to -1 °C. Then, 0.64 g (0.0029 mol) of 4-nitrobenzenesulfochloride was added dropwise. When the reaction mixture was kept at r.t. for 84 h, 0.74 g (68%) of white solid **8** was obtained (when the reaction mixture was kept at CHCl<sub>3</sub> b.p. for 21 h, 0.51 g (47%) of white solid **8** was obtained); m.p. 230 °C, *R<sub>f</sub>* 0.10. IR (KBr, cm<sup>-1</sup>): 1642 (C=N), 1588 (C=C), 1229 (SO<sub>2</sub> as) and 1197 (SO<sub>2</sub> sy), 1519 (NO<sub>2</sub> as) and 1349 (NO<sub>2</sub> sy), 3308, 3396 [N(-H)<sub>2</sub>], 2944 (C<sub>sp3</sub>-H), 3105, 3199, 3245 (C<sub>sp2</sub>-H). <sup>1</sup>H-NMR (500 MHz, DMSO-*d*<sub>6</sub>): 3.11 (t, *J* = 7.0 Hz, 2H, α-CH<sub>2</sub>), 3.86 (t, *J* = 7.0 Hz, 2H, β-CH<sub>2</sub>), 2.87 [m, 2H, S(CH<sub>ax</sub>)<sub>2</sub>] and 3.15 [m, 2H, S(CH<sub>eq</sub>)<sub>2</sub>], 3.60 [m, 2H, N(+)(CH<sub>ax</sub>)<sub>2</sub>] and 3.72 [m, 2H, N(+)(CH<sub>eq</sub>)<sub>2</sub>], 7.37 (s, 2H, NH<sub>2</sub>), 7.83–8.20 (m, 4H, C<sub>(sp2)</sub>H). <sup>13</sup>C-NMR (126 MHz, DMSO-*d*<sub>6</sub>): 23.2, 31.4, 62.5, 64.7, 123.8 (2C), 127.3 (2C), 147.7 (1C), 154.8 (1C), 169.0. Anal. Calcd for C<sub>13</sub>H<sub>18</sub>N<sub>4</sub>O<sub>5</sub>S<sub>2</sub> (374.44): C, 41.70; H, 4.85. Found: C, 41.59; H, 4.33.

**2-Amino-8-phenyl-1,5,8-triazaspiro[4.5]dec-1-en-5-ammonium 4-nitrobenzenesulfonate (9).** The reaction mixture consisting of 0.72 g (0.0029 mol) of compound **4** in 20 mL of CHCl<sub>3</sub> and 0.38 g (0.0029 mol) of DIPEA was cooled to -1 °C. Then, 0.64 g (0.0029 mol) of 4-nitrobenzenesulfochloride was added dropwise. When the reaction mixture was kept at r.t. for 60 h, 0.88 g (70%) of white solid **9** was obtained (when the reaction mixture was kept at CHCl<sub>3</sub> b.p. for 19 h, 0.87 g (69%) of white solid **9** was obtained); m.p. 203 °C, *R<sub>f</sub>* 0.15. IR (KBr, cm<sup>-1</sup>): 1649 (C=N), 1599 (C=C), 1240 (SO<sub>2</sub> as) and 1189 (SO<sub>2</sub> sy), 1515 (NO<sub>2</sub> as) and 1350 (NO<sub>2</sub> sy), 3421 [N(-H)<sub>2</sub>], 2790, 2880, 2915 (C<sub>sp3</sub>-H), 3118, 3290 (C<sub>sp2</sub>-H). <sup>1</sup>H-NMR (500 MHz, DMSO-*d*<sub>6</sub>): 3.17 (t, *J* = 7.0 Hz, 2H, α-CH<sub>2</sub>), 3.95 (t, *J* = 7.0 Hz, 2H, β-CH<sub>2</sub>), 3.56 [m, 4H, N(CH<sub>2</sub>)<sub>2</sub>], 3.49 [m, 2H, N(+)(CH<sub>ax</sub>)<sub>2</sub>] and 3.98 [m, 2H, N(+)(CH<sub>eq</sub>)<sub>2</sub>], 7.25 (s, 2H, NH<sub>2</sub>), 7.81–8.53 (m, 9H, C<sub>(sp2)</sub>H). <sup>13</sup>C-NMR (126 MHz, DMSO-*d*<sub>6</sub>): 31.5, 44.5, 61.5, 62.9, 115.3 (2C), 120.4 (1C), 123.8 (2C), 127.4 (2C), 129.5 (2C), 147.7 (1C), 149.9 (1C), 156.7 (1C), 169.0. Anal. Calcd for C<sub>19</sub>H<sub>23</sub>N<sub>5</sub>O<sub>5</sub>S (433.48): C, 52.64; H, 5.35. Found: C, 52.35; H, 5.21.



3-(1H-benzo[d]imidazol-1-yl)-N'-[[4-nitrophenyl)sulfonyl]oxy]propanimidamide (**10**). The reaction mixture consisting of 0.59 g (0.0029 mol) of compound **5** in 20 mL of CHCl<sub>3</sub> and 0.38 g (0.0029 mol) of DIPEA was cooled to −1 °C. Then, 0.64 g (0.0029 mol) of 4-nitrobenzenesulfochloride was added dropwise. When the reaction mixture was kept at r.t. for 80 h, 0.93 g (82%) of white solid **10** was obtained (when kept at CHCl<sub>3</sub> b.p. for 36 h, 0.41 g (36%) of white solid **10** was obtained); m.p. 158 °C, *R*<sub>f</sub> 0.75. IR (KBr, cm<sup>−1</sup>): 1648 (C=N), 1617 (C=C), 1240 (SO<sub>2</sub> as) and 1187 (SO<sub>2</sub> sy), 1520 (NO<sub>2</sub> as) and 1365 (NO<sub>2</sub> sy), 3417 [N(-H)<sub>2</sub>], 2791, 2920 (C<sub>sp3</sub>-H), 3110, 3237 (C<sub>sp2</sub>-H). <sup>1</sup>H-NMR (500 MHz, DMSO-*d*<sub>6</sub>): 2.50 (t, *J* = 7.0 Hz, 2H, α-CH<sub>2</sub>), 4.33 (t, *J* = 7.0 Hz, 2H, β-CH<sub>2</sub>), 6.50 (s, 2H, NH<sub>2</sub>), 7.78–8.44 (m, 8H, C<sub>(sp2)</sub>H), 8.05 (s, 1H, C<sub>(sp2)</sub>H). <sup>13</sup>C-NMR (126 MHz, DMSO-*d*<sub>6</sub>): 31.2, 42.9, 110.8 (2C), 119.8 (2C), 121.9 (1C), 122.7 (1C), 128.5 (2C), 130.0 (2C), 133.5 (2C), 134.0 (1C), 143.7 (1C), 144.3 (1C), 144.7 (1C), 160.0. Anal. Calcd for C<sub>16</sub>H<sub>15</sub>N<sub>5</sub>O<sub>5</sub>S (389.39): C, 49.35; H, 3.88. Found: C, 49.28; H, 3.45.

### 3.1.2. A General Procedure for the Synthesis of 2-Amino-1,5-diazaspiro[4.5]-dec-1-ene-5-ammonium 2-Nitrobenzenesulfonate (**11–13a**, **14**) and 2-Amino-8-thia-1,5-diazaspiro[4.5]dec-1-en-5-ium Chloride Hydrate (**13b**)

The synthesis of β-aminopropioamidoximes 2-nitrobenzenesulfochlorination products **6–10** (general method). To a solution of 0.0029 mol of β-aminopropioamidoximes **1–5** in 20 mL of CHCl<sub>3</sub>, 0.0029 mol of DIPEA was added. The reaction mixture was cooled to −1 °C, and a solution of 0.0029 mol of 2-nitrobenzenesulfochloride in 2 mL of CHCl<sub>3</sub> was added dropwise with stirring. The reaction mixture was then allowed to warm to r.t. (or up to the b.p. of CHCl<sub>3</sub>) and stirred until the completion of the reaction. The progress of the reaction was monitored by TLC. The formed white precipitates of the products were filtered off and recrystallized from 2-PrOH.

2-Amino-1,5-diazaspiro[4.5]dec-1-en-5-ammonium 2-nitrobenzenesulfonate (**11**). The reaction mixture consisting of 0.5 g (0.0029 mol) of compound **1** in 20 mL of CHCl<sub>3</sub> and 0.38 g (0.0029 mol) of DIPEA was cooled to −1 °C. Then, 0.64 g (0.0029 mol) of 2-nitrobenzenesulfochloride was added dropwise. When the reaction mixture was kept at r.t. for 35 h, 0.80 g (77%) of white solid **11** was obtained (when the reaction mixture was kept at CHCl<sub>3</sub> b.p. for 29 h, 0.78 g (75%) of white solid **11** was obtained); m.p. 153 °C, *R*<sub>f</sub> 0.05. IR (KBr, cm<sup>−1</sup>): 1657 (C=N), 1593 (C=C), 1221, 1232 (SO<sub>2</sub> as) and 1024 (SO<sub>2</sub> sy), 1541 (NO<sub>2</sub> as) and 1377 (NO<sub>2</sub> sy), 3399 [N(-H)<sub>2</sub>], 2949 (C<sub>sp3</sub>-H), 3204, 3398 (C<sub>sp2</sub>-H). <sup>1</sup>H-NMR (500 MHz, DMSO-*d*<sub>6</sub>): 3.05 (t, *J* = 7.95 Hz, 2H, α-CH<sub>2</sub>), 3.77 (t, *J* = 7.95 Hz, 2H, β-CH<sub>2</sub>), 1.54m, 1.71m, 1.84m, [6H, (CH<sub>2</sub>)<sub>3</sub>], 3.35 [m, 4H, N(+)(CH<sub>2</sub>)<sub>2</sub>], 7.20d, 7.46–7.81 (m, 4H, C<sub>(sp2)</sub>H). <sup>13</sup>C-NMR (126 MHz, DMSO-*d*<sub>6</sub>): 21.0, 21.9(2C), 31.6, 60.7, 64.3, 122.0, 129.5, 130.5, 131.3, 140.0, 148.3, 168.6. Anal. Calcd for C<sub>14</sub>H<sub>20</sub>N<sub>4</sub>O<sub>5</sub>S (356.40): C, 47.18; H, 5.66. Found: C, 47.57; H, 5.33.

2-Amino-8-oxa-1,5-diazaspiro[4.5]dec-1-ene-5-ammonium 2-nitrobenzenesulfonate (**12**). The reaction mixture consisting of 0.5 g (0.0029 mol) of compound **2** in 20 mL of CHCl<sub>3</sub> and 0.38 g (0.0029 mol) of DIPEA was cooled to −1 °C. Then, 0.64 g (0.0029 mol) of 2-nitrobenzenesulfochloride was added dropwise. When the reaction mixture was kept at r.t. for 25 h, 0.97 g (93%) of white solid **12** was obtained (when the reaction mixture was kept at CHCl<sub>3</sub> b.p. for 24 h, 0.67 g (64%) of white solid **12** was obtained); m.p. 148 °C, *R*<sub>f</sub> 0.01. IR (KBr, cm<sup>−1</sup>): 1637 (C=N), 1593 (C=C), 1207, 1228 (SO<sub>2</sub> as) and 1022 (SO<sub>2</sub> sy), 1549 (NO<sub>2</sub> as) and 1377 (NO<sub>2</sub> sy), 3387 [N(-H)<sub>2</sub>], 2907 (C<sub>sp3</sub>-H), 3250, 3306, 3328 (C<sub>sp2</sub>-H). <sup>1</sup>H-NMR (500 MHz, DMSO-*d*<sub>6</sub>): 3.09 (t, *J* = 7.95 Hz, 2H, α-CH<sub>2</sub>), 3.88 (m, 2H, β-CH<sub>2</sub>), 3.35 [m, 2H, O(CH<sub>ax</sub>)<sub>2</sub>] and 3.60 [m, 2H, O(CH<sub>eq</sub>)<sub>2</sub>], 3.88 [m, 4H, N(+)(CH<sub>2</sub>)<sub>2</sub>], 7.20 (s, 2H, NH<sub>2</sub>), 7.45–7.81 (m, 4H, C<sub>(sp2)</sub>H). <sup>13</sup>C-NMR (126 MHz, DMSO-*d*<sub>6</sub>): 31.5, 62.2 (2C), 63.2, 122.0, 129.5, 130.6, 131.3, 140.0, 148.3, 169.2. Anal. Calcd for C<sub>13</sub>H<sub>18</sub>N<sub>4</sub>O<sub>6</sub>S (358.37): C, 43.57; H, 5.06. Found: C, 43.89; H, 5.47.

2-Amino-8-thia-1,5-diazaspiro[4.5]dec-1-en-5-ammonium 2-nitrobenzenesulfonate (**13a**) and 2-Amino-8-thia-1,5-diazaspiro[4.5]dec-1-en-5-ium chloride hydrate (**13b**). The reaction mixture consisting of 0.55 g (0.0029 mol) of compound **3** in 20 mL of CHCl<sub>3</sub> and 0.38 g (0.0029 mol) of DIPEA was cooled to −1 °C. Then, 0.64 g (0.0029 mol) of 2-nitrobenzenesulfochloride was added dropwise. When the reaction mixture was kept at r.t. for 104 h, the white precipitate

of the mixture of products **13a** and **13b** was obtained. After recrystallization, 0.16 g (25%) of **13b** was obtained. After the evaporation of the filtrate from the recrystallization to 1/2 volume. 0.27 g (25%) of 2-nitrobenzenesulfonate **13a** was formed. When the reaction mixture was kept at CHCl<sub>3</sub> b.p. for 24 h, only 0.37 g (56%) of white solid **13b** was obtained.

**13a**: m.p. 138–140 °C, *R<sub>f</sub>* 0.08. IR (KBr, cm<sup>-1</sup>): 1647 (C=N), 1604 (C=C), 1207, 1215 (SO<sub>2</sub> as) and 1024 (SO<sub>2</sub> sy), 1545 (NO<sub>2</sub> as) and 1373 (NO<sub>2</sub> sy), 3497 [N(-H)<sub>2</sub>], 2936, 2964 (C<sub>sp3</sub>-H), 3152, 3258, 3302 (C<sub>sp2</sub>-H). <sup>1</sup>H-NMR (500 MHz, DMSO-*d*<sub>6</sub>): 3.10 (t, *J* = 7.0 Hz, 2H, α-CH<sub>2</sub>), 3.83 (t, *J* = 7.95 Hz, 2H, β-CH<sub>2</sub>), 3.10 [m, 2H, S(CH<sub>ax</sub>)<sub>2</sub>] and 3.55 [m, 2H, S(CH<sub>eq</sub>)<sub>2</sub>], 3.10 [m, 2H, N(+)(CH<sub>ax</sub>)<sub>2</sub>] and 3.68 [m, 2H, N(+)(CH<sub>eq</sub>)<sub>2</sub>], 7.26 (s, 2H, NH<sub>2</sub>), 7.47–7.81 (m, 4H, C<sub>(sp2)</sub>H). <sup>13</sup>C-NMR (126 MHz, DMSO-*d*<sub>6</sub>): 23.2, 31.5, 62.6, 64.7, 122.9, 129.5, 130.6, 131.3, 139.7, 148.3, 169.1. Anal. Calcd for C<sub>13</sub>H<sub>18</sub>N<sub>4</sub>O<sub>5</sub>S<sub>2</sub> (374.44): C, 41.70; H, 4.85. Found: C, 41.67; H, 4.46.

**13b**: m.p. > 280 °C, *R<sub>f</sub>* 0.08. IR (KBr, cm<sup>-1</sup>): 1659 (C=N); 1612 [H-N; (H)<sub>2</sub>-O]; 670 [S-C]; 3135, 3230, 3380, 3384 (H-O, H-N). <sup>1</sup>H-NMR (500 MHz, DMSO-*d*<sub>6</sub>): 3.10 (t, *J* = 7.0 Hz, 2H, α-CH<sub>2</sub>), 3.85 (t, *J* = 7.95 Hz, 2H, β-CH<sub>2</sub>), 2.85 [m, 2H, S(CH<sub>ax</sub>)<sub>2</sub>] and 3.55 [m, 2H, S(CH<sub>eq</sub>)<sub>2</sub>], 3.10 [m, 2H, N(+)(CH<sub>ax</sub>)<sub>2</sub>] and 3.68 [m, 2H, N(+)(CH<sub>eq</sub>)<sub>2</sub>], 7.26 (s, 2H, NH<sub>2</sub>). <sup>13</sup>C-NMR (126 MHz, DMSO-*d*<sub>6</sub>): 23.2, 31.5, 62.6, 64.7, 169.1. Anal. Calcd for C<sub>7</sub>H<sub>16</sub>ClN<sub>3</sub>OS (225.74): C, 37.24; H, 7.14. Found: C, 37.52; H, 7.48.

*2-Amino-8-phenyl-1,5,8-triazaspiro[4.5]dec-1-en-5-ammonium 2-nitrobenzenesulfonate (14)*. The reaction mixture consisting of 0.72 g (0.0029 mol) of compound **4** in 20 mL of CHCl<sub>3</sub> and 0.38 g (0.0029 mol) of DIPEA was cooled to -1 °C. Then, 0.64 g (0.0029 mol) of 2-nitrobenzenesulfochloride was added dropwise. When the reaction mixture was kept at r.t. for 34 h, 0.99 g (79%) of white solid **14** was obtained (when reaction mixture was kept at CHCl<sub>3</sub> b.p. for 24 h 1.02 g (81%) white solid **14** was obtained); m.p. 185–187 °C, *R<sub>f</sub>* 0.08. IR (KBr, cm<sup>-1</sup>): 1647 (C=N), 1593 (C=C), 1217, 1224 (SO<sub>2</sub> as) and 1024 (SO<sub>2</sub> sy), 1535 (NO<sub>2</sub> as) and 1366 (NO<sub>2</sub> sy), 3373 [N(-H)<sub>2</sub>], 2837 (C<sub>sp3</sub>-H), 3161, 3300 (C<sub>sp2</sub>-H). <sup>1</sup>H-NMR (500 MHz, DMSO-*d*<sub>6</sub>): 3.12 (t, *J* = 7.91 Hz, 2H, α-CH<sub>2</sub>), 3.91 (t, *J* = 7.91 Hz, 2H, β-CH<sub>2</sub>), 3.40 [m, 2H, N(CH<sub>ax</sub>)<sub>2</sub>], 3.71 [m, 2H, N(CH<sub>eq</sub>)<sub>2</sub>], 3.54 [m, 4H, N(+)(CH<sub>2</sub>)<sub>2</sub>], 6.82–7.81 (m, 11H, NH<sub>2</sub>, C<sub>(sp2)</sub>H). <sup>13</sup>C-NMR (126 MHz, DMSO-*d*<sub>6</sub>): 31.6, 44.6, 61.5, 62.9, 116.4, 120.5, 122.9, 129.5, 129.7, 130.6, 131.3, 139.8, 148.3, 150.0, 169.2. Anal. Calcd for C<sub>19</sub>H<sub>23</sub>N<sub>5</sub>O<sub>5</sub>S (433.48): C, 52.64; H, 5.35. Found: C, 52.92; H, 5.63.

When reaction mixture was kept at r.t. for 34 h, 0.99 g (79%) white solid **14** was obtained [when reaction mixture was kept at CHCl<sub>3</sub> b.p. for 24 h 1.02 g (81%) white solid **14** was obtained].

### 3.2. Screening

The *in vitro* antidiabetic activity of samples **6–14** was assessed by the degree of inhibition of α-amylase and α-glucosidase activity. Pure DMSO was used as a solvent. The final concentration of the sample substances was 10 mg/mL. A total of 100 μL of α-amylase or α-glucosidase (1 U/mL) and 200 μL of the test sample solution (10 mg/mL) were added to 500 μL of phosphate buffer (0.1 M; pH 6.8). The resulting mixture was incubated for 15 min at +37 °C, and 200 μL of P-NPG solution (5 mM) was added.

Then, the resulting mixture was incubated again at +37 °C for 20 min. The reaction was stopped by the addition of 500 μL of sodium carbonate (0.1 M). Since the samples showed too much absorbance at 405 nm, they were diluted 5 times with 5 mL of water and 1 mL of sodium carbonate solution (0.1 M). A solution of α-amylase or α-glucosidase (1 U/mL) was used as a blank. As a negative control, 200 μL of pure DMSO was used in triplicate. As a reference drug, acarbose was obtained at a concentration of 10.0 mg/mL (positive control).

Simultaneously, a negative control was placed without the addition of the test compounds. All the samples were examined in triplets. The inhibitory activity was expressed as a percentage (%) of the degree of inhibition of α-glucosidase, in comparison to the negative control.

### 3.3. Single-Crystal X-ray Diffraction

The X-ray diffraction data of **8**, **9**, and **11–14** were collected on a Bruker Apex II diffractometer (Bruker AXS, Inc., Madison, WI, USA) equipped with an Oxford Cryostream cooling unit and a graphite monochromated Mo anode ( $\lambda = 0.71073 \text{ \AA}$ ). The intensities of the reflections for **10** were collected at 100 K at the “Belok” beamline of the Kurchatov Synchrotron Radiation Source (NRC “Kurchatov Institute”, Moscow, Russia), at the wavelength of  $0.745 \text{ \AA}$  using a MAR CCD 165 detector. The image integration was performed using the iMosflm software [35]. The integrated intensities were empirically corrected for the absorption using the Scala program [36]. The crystal structures were solved using SHELXT [37] program and refined with SHELXL [38] using OLEX2 software [39]. The structures were refined by the full-matrix least-squares procedure against  $F^2$ . Non-hydrogen atoms were refined anisotropically. The H(C) positions were calculated, the H(N) and H(O) atoms were located on difference Fourier maps and refined using the riding model. The details of the experiment and the crystal parameters are presented in Tables S1 and S2 (Electronic Supporting Information).

## 4. Conclusions

The set of the reaction products of  $\beta$ -aminopropioamidoximes nitrobenzenesulfochlorination depends on the structure of the initial substrates and temperature.  $\beta$ -Aminopropioamidoximes with six-membered heterocycles in the  $\beta$ -aminogroup produce good yields of 2-amino-1,5-diazaspiro[4.5]-dec-1-ene-5-ammonium nitrobenzenesulfonates at r.t. and  $\text{CHCl}_3$  b.p. An exception is the *ortho*-nitrobenzenesulfochlorination of  $\beta$ -(thiomorpholin-1-yl)propioamidoxime, when the reaction is regioselective at r.t., as two products are formed: 2-amino-1,5-diazathiospiro[4.5]-dec-1-ene-5-ammonium *ortho*-nitrobenzenesulfonate and chloride hydrate. Heating leads to a regiospecific course of the reaction with the formation of only chloride hydrate.

The *para*-Nitrobenzenesulfochlorination of  $\beta$ -(benzimidazol-1-yl)propioamidoxime produces the *O-para*-nitrobenzenesulfochlorination product. The reaction time when the reaction mixture is heated is reduced by 2–3 times. The in vitro screening of the library of nitrobenzenesulfochlorination products for antidiabetic activity reveals two samples with high  $\alpha$ -glucosidase activity exceeding the activity of the acarbose standard: products of *para*-nitrobenzenesulfochlorination of  $\beta$ -(thiomorpholin-1-yl)- and  $\beta$ -(benzimidazol-1-yl)propioamidoximes. The arsenal of the physicochemical and spectral methods made it possible to establish the structural features of the studied spiropyrazolinium organic salts. Thus, in  $\text{DMSO-}d_6$  solutions in the  $^1\text{H}$  NMR spectra, the slow inversion of six-membered nitrogen-containing  $\beta$ -heterocycles can be observed. These spiropyrazoline derivatives can be interesting objects in dynamic NMR spectroscopy, which would allow for the rotational barriers of six-membered heterocycles to be measured. It is assumed that the bulky substituted arylsulfonate anion anchors the spiroheterocycles in the most thermodynamically favorable chair-like position. According to X-ray diffraction data, the axial location of the N–N bond in the spiropyrazoline heterocycles is unambiguously determined. The NMR and XRD data demonstrate that two various conformations of spirocation are present both in solution and in solids. The cation can take part in different types of intermolecular interactions, depending on the conformation and the nature of the six-membered cycle.

**Supplementary Materials:** The following supporting information can be downloaded at: <https://www.mdpi.com/article/10.3390/molecules27072181/s1>, Figure S1: Asymmetric units of the X-rayed compounds in a representation of atoms with thermal ellipsoids ( $p = 50\%$ ); Table S1: Crystallographic data and the experimental details for compounds **6** and **8–10**; Table S2: Crystallographic data and the experimental details for compounds **11–14**; Compounds **6** and **8–14** are registered in CCDC with the numbers 2154973–2154980. Crystallographic information files are available from the Cambridge Crystallographic Data Center upon request (<http://www.ccdc.cam.ac.uk/structures>).

**Author Contributions:** Conceptualization, L.K.; methodology, G.B., E.Y. and A.K.; software, A.V., Z.S. (Zhanar Shaimerdenova); investigation, A.V., P.D., G.B., E.Y., A.K. and Z.S. (Zarina Shulgau), S.A., Z.S. (Zhanar Shaimerdenova) and K.A.; data curation, L.K.; writing—original draft preparation, L.K. and A.V.; writing—review and editing, L.K.; visualization, L.K., A.V. and E.Y.; project administration, E.Y.; funding acquisition, L.K. All authors have read and agreed to the published version of the manuscript.

**Funding:** This study was supported by the Committee of Science of the Ministry of Education and Science of the Republic of Kazakhstan (grant AP08856440). A. Vologzhanina acknowledges the support of the Ministry of Education and Science of Russia.

**Institutional Review Board Statement:** Not applicable.

**Data Availability Statement:** The data presented in this study are available in this article.

**Acknowledgments:** Single-crystal X-ray diffraction data were measured using the equipment of the Center for Molecular Studies of INEOS RAS (Moscow, Russia). SCXRD data for compound **10** were measured at the “Belok” beamline of the Kurchatov Synchrotron Radiation Source (NRC “Kurchatov Institute”, Moscow, Russia).

**Conflicts of Interest:** The authors declare no conflict of interest.

**Sample Availability:** Samples of the compounds **6–14** are available from the authors.


## References

- de la Torre, B.G.; Albericio, F. The Pharmaceutical Industry in 2021. An Analysis of FDA Drug Approvals from the Perspective of Molecules. *Molecules* **2022**, *27*, 1075. [CrossRef] [PubMed]
- Global Diphenyl Pyrazoline Market Research Report 2021—Impact of COVID-19 on the Market. Available online: <https://www.businessgrowthreports.com/TOC/19091429> (accessed on 26 March 2022).
- Lévai, A.; Simon, A.; Jenei, A.; Kálmán, G.; Jekő, J.; Tóth, G. Synthesis of spiro-1-pyrazolines by the reaction of exocyclic  $\alpha,\beta,\gamma,\delta$ -unsaturated ketones with diazomethane. *Arkivoc* **2009**, *12*, 161–172. [CrossRef]
- Dadiboyena, S.; Valente, E.J.; Hamme, A.T., II. Synthesis and Tautomerism of Spiro-Pyrazolines. *Tetrahedron Lett.* **2014**, *5514*, 2208–2211. [CrossRef] [PubMed]
- Kayukova, L.A.; Uzakova, A.B.; Vologzhanina, A.V.; Akatan, K.; Shaymardan, E.; Kabdrakhmanova, S.K. Rapid Boulton–Katritzky rearrangement of 5-aryl-3-[2-(piperidin-1-yl)ethyl]-1,2,4-oxadiazoles upon exposure to water and HCl. *Chem. Heterocycl. Compd.* **2018**, *54*, 643–649. [CrossRef]
- Kayukova, L.; Vologzhanina, A.; Praliyev, K.; Dyusembaeva, G.; Baitursynova, G.; Uzakova, A.; Bismilda, V.; Chingissova, L.; Akatan, K. Boulton–Katritzky Rearrangement of 5-Substituted Phenyl-3-[2-(morpholin-1-yl)ethyl]-1,2,4-oxadiazoles as a Synthetic Path to Spiropyrazoline Benzoates and Chloride with Antitubercular Properties. *Molecules* **2021**, *26*, 967. [CrossRef]
- Kayukova, L.A.; Praliyev, K.D.; Myrzabek, A.B.; Kainarbayeva, Z.N. Arylsulfochlorination of  $\beta$ -aminopropioamidoximes giving 2-aminospiropyrazolylammonium arylsulfonates. *Rus. Chem. Bul. (Int. Ed.)* **2020**, *69*, 496–503. [CrossRef]
- Kayukova, L.A.; Baitursynova, G.P.; Yergaliyeva, E.M.; Zhaksylyk, B.A.; Yelibayeva, N.S.; Kurmangaliyeva, A.B. Arylsulphonates of spiro-pyrazolines and O-tosilate- $\beta$ -(benzimidazol-1-yl)propioamidoxime as the products of  $\beta$ -aminopropioamidoximestosylation. *Chem. J. Kaz.* **2021**, *2*, 22–32. [CrossRef]
- Alkorta, I.; Elguero, J. The tautomerism of pyrazolines (Dihydropyrazoles). *J. Chil. Chem. Soc.* **2015**, *60*, 2966–2970. [CrossRef]
- Dadiboyena, S. Cycloadditions and condensations as essential tools in spiro-pyrazoline synthesis. *Eur. J. Med. Chem.* **2013**, *63*, 347–377. [CrossRef]
- Sadiq Zubi; Naz Sadia; Hussain Akbar Erum; Aslam Umbreen. Spiropyrazolines: A Worthy Insight into the Recent Strategies and Synthetic Applications. *Lett. Org. Chem.* **2019**, *16*, 357–391. [CrossRef]
- Liu, H.; Jia, H.; Wang, B.; Xiao, Y.; Guo, H. Synthesis of Spirobidihydropyrazole through Double 1,3-Dipolar Cycloaddition of Nitrilimines with Allenones. *Org. Lett.* **2017**, *19*, 4714–4717. [CrossRef] [PubMed]
- Monteiro, A.; Gonçalves, L.M.; Santos, M.M.M. Synthesis of novel spiro-pyrazoline oxindoles and evaluation of cytotoxicity in cancer cell lines. *Eur. J. Med. Chem.* **2014**, *79*, 266–272. [CrossRef] [PubMed]
- Rouatbi, F.; Mhiri, C.; Askri, M.; Knorr, M.; Rousselin, Y.; Kubicki, M.M. Regioselective Synthesis of Mono- and Dispiropyrazoline Derivatives via 1,3-dipolar Cycloaddition with Nitrilimines. *J. Heterocycl. Chem.* **2016**, *54*, 1152–1160. [CrossRef]
- Singh, V.; Singh, V.; Batra, S. Straightforward Strategy for the Stereoselective Synthesis of Spiro-Fused (C-5) Isoxazolino- or (C-3) Pyrazolino-(C-3) quinolin-2-ones from Baylis–Hillman Adducts by 1,3-Dipolar Cycloaddition and Reductive Cyclization. *Eur. J. Org. Chem.* **2008**, *2008*, 5446–5460. [CrossRef]
- Verma, D.; Mobin, S.; Namboothiri, I.N.N. Highly Selective Synthesis of Pyrazole and Spiropyrazoline Phosphonates via Base-Assisted Reaction of the Bestmann–Ohira Reagent with Enones. *J. Org. Chem.* **2011**, *76*, 4764–4770. [CrossRef]

17. Adamus-Grabicka, A.A.; Markowicz-Piasecka, M.; Cieślak, M.; Królewska-Golińska, K.; Hikisz, P.; Kusz, J.; Małecka, M.; Budzisz, E. Biological Evaluation of 3-Benzylidenechromanones and Their Spiropyrazolines-Based Analogues. *Molecules* **2020**, *25*, 1613. [CrossRef]
18. Dandia, A.; Joshi, R.; Sehgal, V.; Sharma, C.; Saha, M. Synthesis of novel 3-spiro indulines containing benz(g) indazole, benz(h)pyrazolo(3,4-b)quinoline and naphthisoxazol moieties. *Heterocycl. Commun.* **1996**, *2*, 281–286. [CrossRef]
19. Ibrahim, M.N.; El-Messmary, M.; Elarfi, M.G.A. Synthesis of Spiro Heterocyclic Compounds. *E-J. Chem.* **2010**, *7*, 55–58. [CrossRef]
20. Toth, G.; Szollosy, A. Synthesis and Stereochemistry of Spiropyrazolines. *J. Chem. Soc. Perkin Trans. II* **1986**, *12*, 1895–1898. [CrossRef]
21. Budzisz, E.; Paneth, P.; Geromino, I.; Muzioł, T.; Rozalski, M.; Krajewska, U.; Pipiak, P.; Ponczek, M.B.; Małecka, M.; Kupcewicz, B. The cytotoxic effect of spiroflavanone derivatives, their binding ability to human serum albumin (HSA) and a DFT study on the mechanism of their synthesis. *J. Mol. Struct.* **2017**, *1137*, 267–276. [CrossRef]
22. Farghaly, T.; Abbas, I.; Hassan, W.; Lotfy, M. Study on regioselective synthesis of bioactive bis-spiropyrazolines using molecular orbital calculations. *Eur. J. Chem.* **2014**, *5*, 577–583. [CrossRef]
23. Chowdhury, M.A.; Senboku, H.; Tokuda, M. A New Synthesis of Ring-Fused Alkylidene-cyclobutanes by Ring-Enlargement Reaction of Bicyclo[n.1.0]alkylidene Derivatives. *Tetrahedron Lett.* **2003**, *44*, 3329–3332. [CrossRef]
24. Santos, B.S.; Gomes, C.S.B.; Pinho e Melo, T.M.V.D. Synthesis of chiral spiro-pyrazoline-b-lactams and spiro-cyclopropyl b-lactams from 6-alkylidene-penicillanates. *Tetrahedron* **2014**, *70*, 3812–3821. [CrossRef]
25. Ning, Y.; Kawahata, M.; Yamaguchi, K.; Otani, Y.; Ohwada, T. Synthesis, Structure and N-N Bonding Character of 1,1-Disubstituted Indazolium Hexafluorophosphate. *Chem. Commun.* **2018**, *54*, 1881–1884. [CrossRef]
26. Kayukova, L.A.; Orazbaeva, M.A.; Gapparova, G.I.; Beketov, K.M.; Espenbetov, A.A.; Faskhutdinov, M.F.; Tashkhodjaev, B.T. Rapid acid hydrolysis of 5-aryl-3-( $\beta$ -thiomorpholinoethyl)-1,2,4-oxadiazoles. *Chem. Heterocycl. Compd.* **2010**, *46*, 879–886. [CrossRef]
27. Kayukova, L.A.; Yergaliyeva, E.M.; Vologzhanina, A.V. Redetermination of the structure of 2-amino-8-thia-1,5-di aza spiro [4.5]dec-1-en-5-ium chloride monohydrate. *Acta Cryst.* **2022**, *E78*, 164–168. [CrossRef]
28. Yergaliyeva, E.M.; Kayukova, L.A.; Bazhykova, K.B.; Gubenko, M.A.; Langer, P. Computational studies of the products of tosylation and *para*-nitrobenzenesulfonochlorination. *J. Struct. Chem.* **2021**, *62*, 1969–1975. [CrossRef]
29. Yergaliyeva, E.M.; Kayukova, L.A.; Gubenko, M.A.; Baitursynova, G.P.; Uzakova, A.B. Free energies of 2-amino-1,5-diazaspiro[4.5]dec-1-en-5-ium chlorides monohydrates and arylsulfonates formation at  $\beta$ -aminopropioamidoximes arylsulfonochlorination. *Chem. J. Kaz.* **2022**, *75*. *submitted*.
30. Akinyede, K.A.; Oyewusi, H.A.; Hughes, G.D.; Ekpo, O.E.; Oguntibeju, O.O. In Vitro Evaluation of the Anti-Diabetic Potential of Aqueous Acetone Helichrysum petiolare Extract (AAHPE) with Molecular Docking Relevance in Diabetes Mellitus. *Molecules* **2022**, *27*, 155. [CrossRef]
31. Sbit, M.; Dupont, L.; Dideberg, O.; Goblet, M.; Dejardin, J.V. Structures de l' amino-3 phényl-1 pyrazoline-2 et de l' amino-3 (m-trifluorométhylphényl)-1 pyrazoline-2. *Acta Cryst.* **1988**, *C44*, 909–912. [CrossRef]
32. Claramunt, R.M.; Cozzini, P.; Domiano, P.; Elguero, J.; Forfar, I.; Fruchier, A. Structure of 3-amino-4,5-dihydropyrazoles in acid media: X-ray structure of 3-amino-1-phenyl-4,5-dihydropyrazol-2-ium picrate and the origin of broad signals in <sup>1</sup>H NMR spectroscopy. *J. Chem. Soc. Perkin Trans. 2* **1995**, 1875–1881. [CrossRef]
33. Alabugin, I.V.; Kuhn, L.; Krivoshchapov, N.V.; Mehaffy, P.; Medvedev, M.G. Anomeric effect, hyperconjugation and electrostatics: Lessons from complexity in a classic stereoelectronic phenomenon. *Chem. Soc. Rev.* **2021**, *50*, 10212–10252. [CrossRef] [PubMed]
34. Motherwell, W.D.S.; Shields, G.P.; Allen, F.H. Automated assignment of graph-set descriptors for crystallographically symmetric molecules. *Acta Cryst.* **2000**, *B56*, 466–473. [CrossRef] [PubMed]
35. Battye, T.G.G.; Kontogiannis, L.; Johnson, O.; Powell, H.R.; Leslie, A.G.W. iMOSFLM: A new graphical interface for diffraction-image processing with MOSFLM. *Acta Cryst.* **2011**, *D67*, 271–278. [CrossRef]
36. Evans, P. Scaling and assessment of data quality. *Acta Cryst.* **2006**, *62*, 72–82. [CrossRef] [PubMed]
37. Sheldrick, G.M. SHELXT—Integrated space-group and crystal-structure determination. *Acta Cryst.* **2015**, *A71*, 3–8. [CrossRef]
38. Sheldrick, G.M. Crystal structure refinement with SHELXL. *Acta Cryst.* **2015**, *C71*, 3–8. [CrossRef]
39. Dolomanov, O.V.; Bourhis, L.J.; Gildea, R.J.; Howard, J.A.K.; Puschmann, H. OLEX2: A complete structure solution, refinement and analysis program. *J. Appl. Cryst.* **2009**, *42*, 339–341. [CrossRef]

Article

# An Orthogonal Synthetic Approach to Nonsymmetrical Bisazoly 2,4,6-Trisubstituted Pyridines

Arturo Gamonal Ruiz-Crespo, Laura Galán-Fernández, Paloma Martínez-Martín  and Juan Carlos Rodríguez-Ubis \*

Departamento de Química Orgánica, Facultad de Ciencias, Universidad Autónoma de Madrid, 28049 Madrid, Spain; arturo.gamonalrc@gmail.com (A.G.R.-C.); laura.galan@inv.uam.es (L.G.-F.); paloma.martinez1990@gmail.com (P.M.-M.)

\* Correspondence: jcrubis@uam.es

**Abstract:** A three-step synthetic route giving access to nonsymmetrical bisazoly 2,4,6-trisubstituted pyridines with different substituents on the pyrazole, indazole, and pyridine heterocycles is described. From the readily available 4-bromo-2,6-difluoropyridine, both fluorine atoms allow for easy selective stepwise substitution, and the bromine atom provides easy access to additional functionalities through both Suzuki and Sonogashira Pd(0) cross-coupling reactions. These synthons represent optimal structures as building blocks in complexation and metalloorganic structures for the tuning of their chelating and photophysical properties.

**Keywords:** pyrazolylpyridines; indazolylpyridines; nucleophilic substitution; C–C coupling

**Citation:** Gamonal Ruiz-Crespo, A.; Galán-Fernández, L.; Martínez-Martín, P.; Rodríguez-Ubis, J.C. An Orthogonal Synthetic Approach to Nonsymmetrical Bisazoly 2,4,6-Trisubstituted Pyridines. *Molecules* **2022**, *27*, 1746. <https://doi.org/10.3390/molecules27051746>

Academic Editors: Vera L. M. Silva and Artur M. S. Silva

Received: 17 February 2022

Accepted: 5 March 2022

Published: 7 March 2022

**Publisher's Note:** MDPI stays neutral with regard to jurisdictional claims in published maps and institutional affiliations.



**Copyright:** © 2022 by the authors. Licensee MDPI, Basel, Switzerland. This article is an open access article distributed under the terms and conditions of the Creative Commons Attribution (CC BY) license (<https://creativecommons.org/licenses/by/4.0/>).

## 1. Introduction

Poly-*N*-heterocyclic frameworks with extended electronic delocalization have been traditionally used as effective and stable ligands for the complexation of transition metal ions. These metal ion complexes, in particular polypyridine ligands such as 2,2':6,2''-terpyridine (**tpy**) [1–3], have been used in the design of luminescent devices or as sensitizers for light-to-electricity conversion due to their rich photophysical, photochemical [4–6], and electrochemical properties [7].

The use of 2,2':6',2''-terpyridines in a wide range of applications and in a variety of research areas has created a sizeable “pool” of different functionalized terpyridines. Therefore, a highly efficient and simple synthesis is as essential as well-defined derivatization at every ring position. While the number of publications concerning applications with terpyridine complexes has increased enormously, comparably the number of reported functionalized 2,2':6',2''-terpyridine derivatives is much lower [1,8], as many of the synthetic methods involve ring assembly reactions, which shorten and hinder access to these interesting tridentate pincer ligands.

Other terdentate pyridine-centered heteroaromatic ligands represent particularly privileged coordination frameworks. Among them, combination with side-by-sideazole rings such as pyrazole, indazole, oxazole, triazole, and tetrazole, and flanking to pyridine rings is of great interest [9,10]. The compound 2,6-bis(pyrazol-1-yl)pyridine (**bppy**) has been used as a versatile analogue to the 2,2':6',2''-terpyridine.

Based on a redox study by Jameson and colleagues on Ru(L<sub>2</sub>)<sup>2+</sup> complexes, **bppy** is a weaker π-acceptor and σ-donor. This is due to the lesser basicity of pyrazole and the higher π\* energy of the aromatic system, making **bppy** less effective in stabilizing Ru(II) because of less ligand binding strength [11,12]. However, the synthetic ease with which **bppy** may be derivatized on the 4-position of pyridine [13–15], as well as on the 3-, 4-, and 5-positions of the pyrazole rings [16,17], has led to the increasing popularity of **bppy** as a complementary platform for research into new d- and f-block metal complexes [18].

Along with **bppy**, other promising ligands in this class include 2,6-(indazol-1-yl)pyridine (**bipy**), where pyridine has a central role as a coordinating ring for this terdentate supramolecular system. In this context, the synthesis of these terdentate compounds is rather straightforward for the unsubstituted ligands [11,12,19,20] or for the symmetrically substituted pyrazole or indazole rings [16,21], but not so straightforward for ligands with different substituents on the heterocyclic rings. It is even more difficult in regards to access to non-symmetrical structures with different rings flanking the pyridine central ring or different substituents on each side [17,22,23].

These differently substituted polyheterocycles open the possibility of tuning the physico-chemical properties of their complexes. Their synthesis is very challenging with few examples described in the literature and little access to this type of nonsymmetrical bisazolyipyridine.

These **bppy** and **bipy** scaffolds are particularly attractive in comparison with terpyridine because they are easily altered by varying the substitution pattern based on the different reactivities of the azole rings compared with that of pyridine, opening the possibility of orthogonal synthesis.

In this communication, we describe a simple and straightforward method for synthetic access to versatile polysubstituted terdentate pyridine-centred heteroaromatic ligands.

By means of a combination of an azolate nucleophilic substitution reaction and palladium cross-coupling reaction (Suzuki–Miyaura- and Shonogashira-type reactions), different substitutions on the pyridine, pyrazole, and/or indazole rings are possible over the easily available 4-bromo-2,6-difluoropyridine in very mild reaction conditions.

## 2. Results and Discussion

Based on the pioneering work of Schlosser regarding the reactivity of polyfluoropyridines [24–26], the 4-bromo-2,6-difluoropyridine molecule has been described as a good alternative for accessing 2,6-dipyrazole and 2,6-diindazolepyridine derivatives [13,14,27]. The reaction conditions for the nucleophilic substitution of fluorine atoms by pyrazolate or indazolate salts are milder and much more convenient (yield, temperature, and work-up) than those of Jameson's work on the substitution of 2,6-dibromopyridine towards **bppy** [11,12]. Until recently, our work with biazolyipyridines has used a methodology based on pyrazolate substitution on 4-substituted 2,6-dibromopyridine [28,29]; however, the type of substituent at the 4-position has been limited to –OMe, –CN, and amide groups [30], and in other cases, to aromatic substituents, such as phenyl or thiophene, by more tedious synthetic access [31,32].

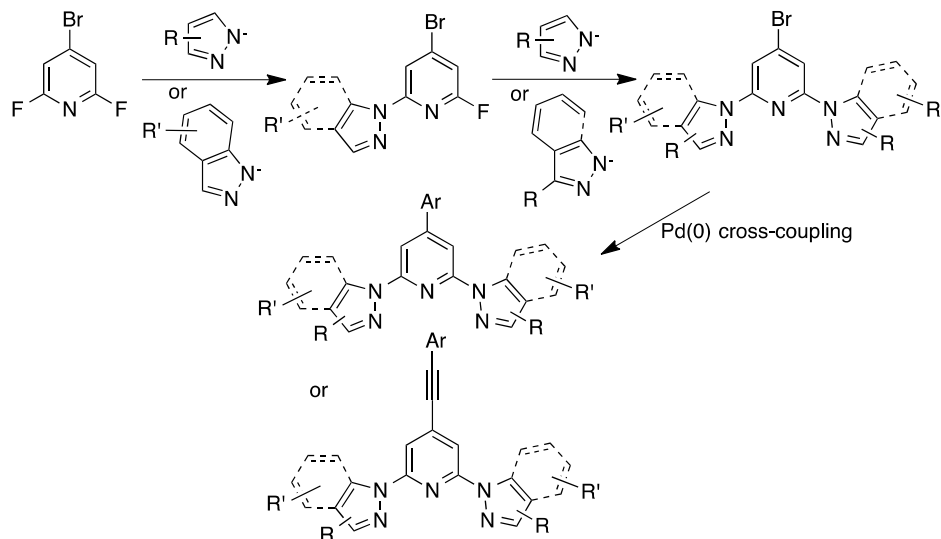
In the case of 4-bromo-2,6-difluoropyridine **1** being used as the starting material, the unreacted 4-bromine position has been exploited as an excellent functionalization board for the introduction of almost any functional group by palladium-mediated cross-coupling reactions [14].

The selective reactivity of fluorine atoms related to bromine has opened the possibility of a first orthogonal approximation to nonsymmetrical 4-substituted 2,6-bipyrazole (**bppy**), 2,6-biindazole (**bipy**), and 2-indazole-6-pyrazolepyridine (**ippy**) frameworks, which is applied in the preparation of lanthanide luminescent complexes. We are interested in these kinds of complexes for the development of a switchable lanthanide-based bioassay for DNA recognition [33].

The different substituents located on the nonsymmetrical **bppy**, **bipy**, or **ippy** units are employed with different purposes on each azole ring: as an anchoring isothiocyanate group to conjugate the DNA sequence; as an additional lanthanide coordinating group such as a carboxylic acid; and by means of the different electron-demanding groups introduced over the central pyridine ring, the opportunity to play with the photophysical properties of these ligands.

By choosing the appropriate reaction conditions, it is possible to selectively control the introduction of a substituted pyrazole or indazole ring, obtaining mono 2-pyrazole- or 2-indazole-4-bromo-6-fluoropyridine derivatives in good yields. From these compounds, it is possible to perform a second functionalization of the remaining fluorine atom by

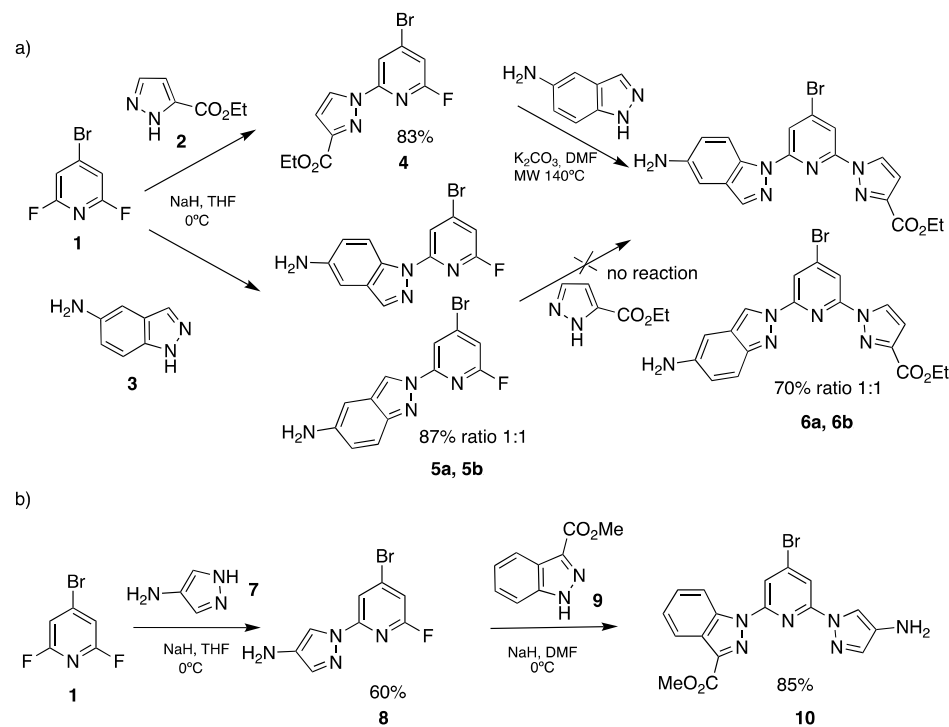
nucleophilic substitution with an adequately substituted pyrazole or indazole ring. Over the nonsymmetrical 2,6-disubstituted 4-bromopyridine, a cross-coupling reaction over the brominated position gave the terdentate ligand with very high versatile substitution (Scheme 1).



**Scheme 1.** Synthetic access to nonsymmetrical **bipy**, **bipy**, or **ippy** units.

### 2.1. Indazole Pyrazole Pyridine (**ippy**)

When accessing these ligands with indazole and pyrazole both having different substituents, we have observed that the pyrazole ring must be introduced first, as the opposite monoindazole-substituted pyridine reduces or inactivates the reactivity of the remaining fluorine atom towards the entry of pyrazole. We have studied the synthesis of these **ippy** derivatives with 5-aminoindazole, 3-methoxycarbonylindazole, 4-amino, and 3-ethoxycarbonylpyrazole, as shown in Scheme 2.

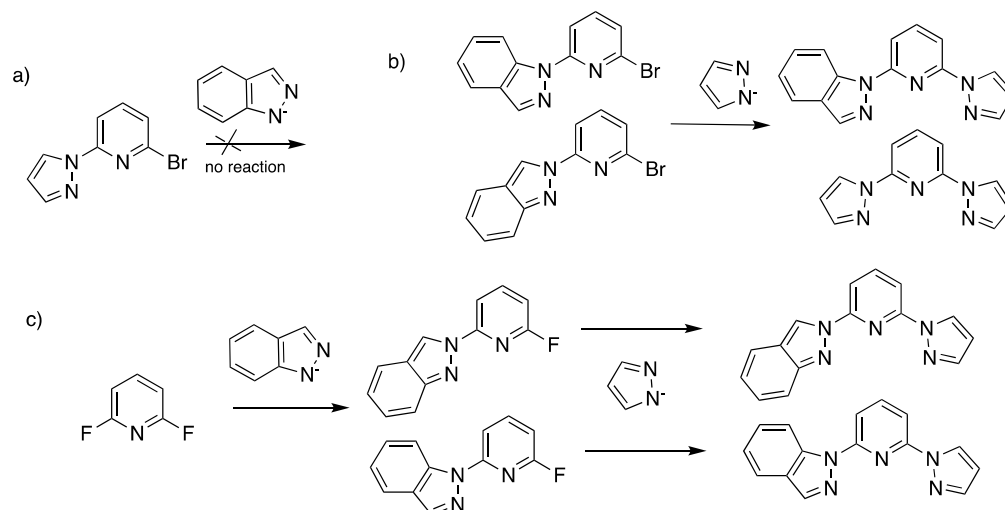


**Scheme 2.** Synthesis of **ippy** derivatives.



In both cases, Scheme 2a,b, despite the electronic demand of the substituent on the pyrazole ring (amino or ethoxycarbonyl), this heterocycle must be introduced first to obtain **4** or **8**, as any of the monosubstituted indazolepyridine prepared inactivates or reduces the reactivity of the remaining fluorine atom. In the first synthesis (Scheme 2a), the introduction of 4-ethoxycarbonylpyrazole **2** to give **4** was followed by the introduction of 5-aminoindazole **3**, giving a mixture of regioisomers (**6a** and **6b**) in a 1:1 ratio. When the first substitution with 5-amino indazole **3** was carried out in the same way as pyrazole, a 1:1 mixture of both regioisomers (**5a** and **5b**) was also obtained, but attempts to carry out the second substitution with 3-ethoxycarbonylpyrazole did not work after several attempts with different solvents and temperatures. In the case of synthesis *b*, the same order was maintained. The first ring introduced was 4-amino pyrazole **7**, giving compound **8**, followed by the introduction of 3-methoxycarbonylindazole **9**, giving **ippy 10**. When 3-methoxycarbonylindazole was first introduced, the substitution of the remaining fluorine atom with a pyrazole ring was not possible.

These results are in contrast to those reported by Halcrow and colleagues, where for the pristine pyrazole and indazole rings, the reaction to obtain **ippy** derivatives was only achieved from 2,6-dibromopyridine by the first substitution of bromine atoms with indazole and not with pyrazole (Scheme 3a,b) [22]. With 2,6-difluoropyridine (Scheme 3c) [23] as the starting material, a nonsymmetrical ligand was also obtained if the first introduced heterocycle was indazole. It seems in these cases pyrazole hampered the introduction of the indazole in contrast to our results with substituted azoles.

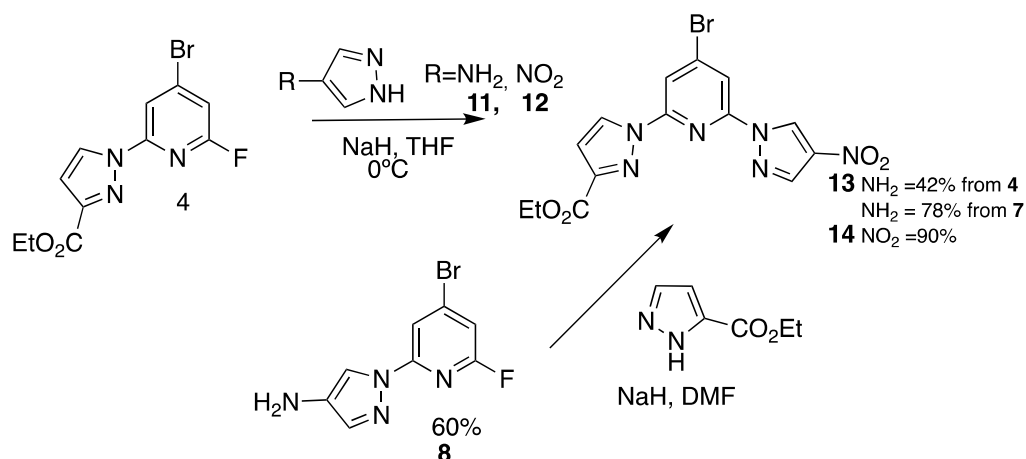


**Scheme 3.** Halcrow's results with unsubstituted pyrazole and indazole.

Electronic demand of the substituents on the azole groups could be the cause of this apparent contradiction, although the behavior described is consistent with the opposite electronic demand caused by amino and methoxycarbonyl substituents. Until the more recent communication by Halcrow describing alternative synthetic access with 2,6-difluoropyridine, the lower reactivity of the bromine atoms or the good leaving effect of the indazolate (Scheme 3b) were the tentative explanations for this behavior.

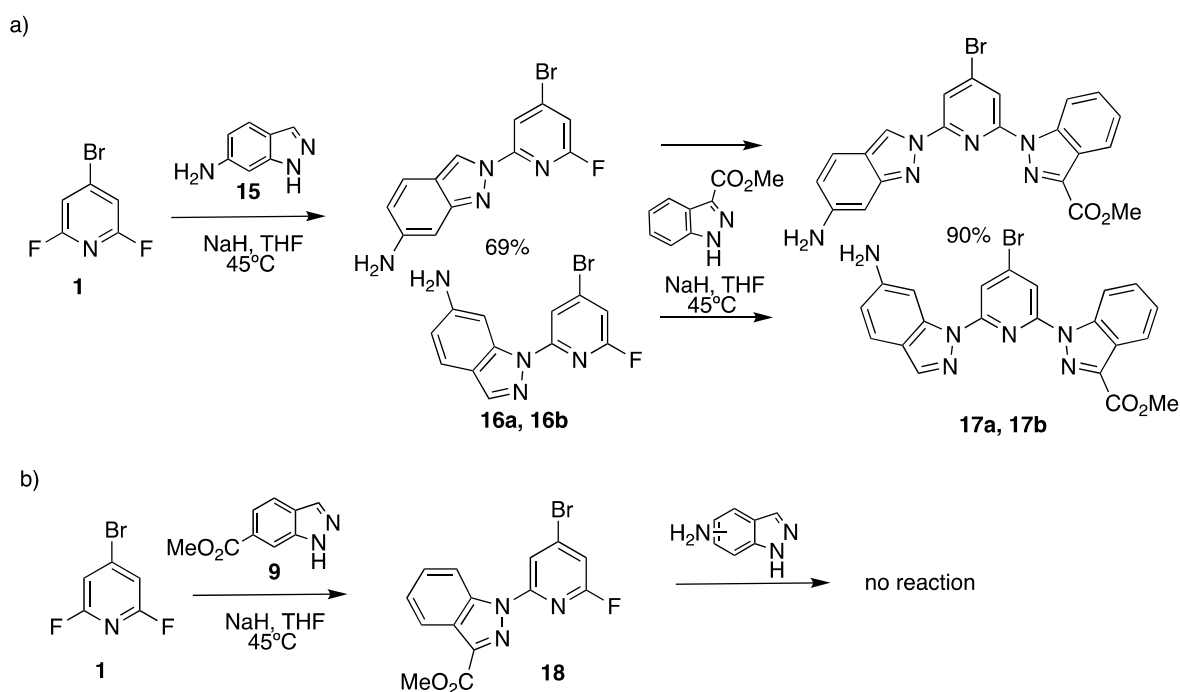
## 2.2. Bipyrazole Pyridine (**bppy**)

It is possible to obtain **bppy** derivatives from a first substitution with 3-ethoxycarbonylpyrazole, followed by a second substitution with any of the attempted 4-amino **11** and 4-nitro **12** pyrazoles. However, for the 4-aminopyrazole, the yield was only moderate (42%), whereas with 4-nitropyrazole in more gentle conditions, the **bppy** derivative was obtained in 90% yield. Due to the different electronic demands of both groups on the pyrazolate salt and the starting fluoro monosubstituted pyridine, access to this amino **bppy** was better performed in yields by the first introduction of 4-aminopyrazole, followed by a second substitution with 3-ethoxycarbonylpyrazole (Scheme 4).

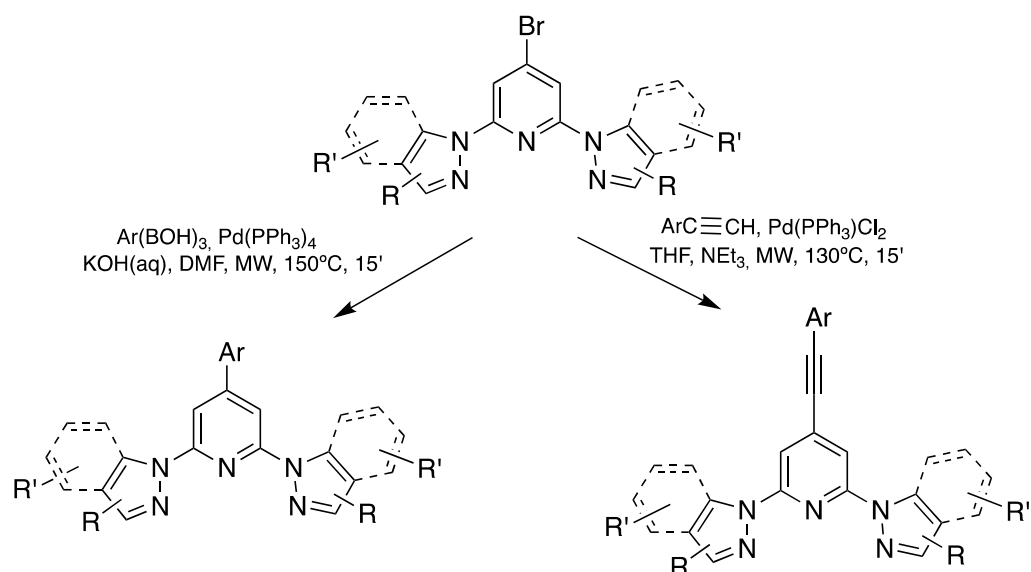
Scheme 4. Synthetic access to **bppy** derivatives.

### 2.3. Biindazole Pyridine (**bipy**)

The nonsymmetrical **bipy** compounds with 5-aminoindazole, 6-aminoindazole, and 3-methoxycarbonylindazole were obtained in the first step by the introduction of the 5- or 6-aminoindazole (represented in Scheme 5a), followed by the second step of substitution of the remaining fluorine atoms with 3-methoxycarbonylindazole. The substitution with both amino compounds (those obtained from 6-aminoindazole are the only represented in Scheme 5a, as both isomers **16a-b** or **17a-b** could be separated) drove both possible regioisomers in a 1:1 ratio. The opposite order gave no reaction when 3-methoxycarbonylindazole **9** was firstly introduced, compound **18**. The reaction of **18** with 5- or 6-aminoindazole was attempted in different solvents and at different temperatures, including microwave-mediated synthesis (Scheme 5b).

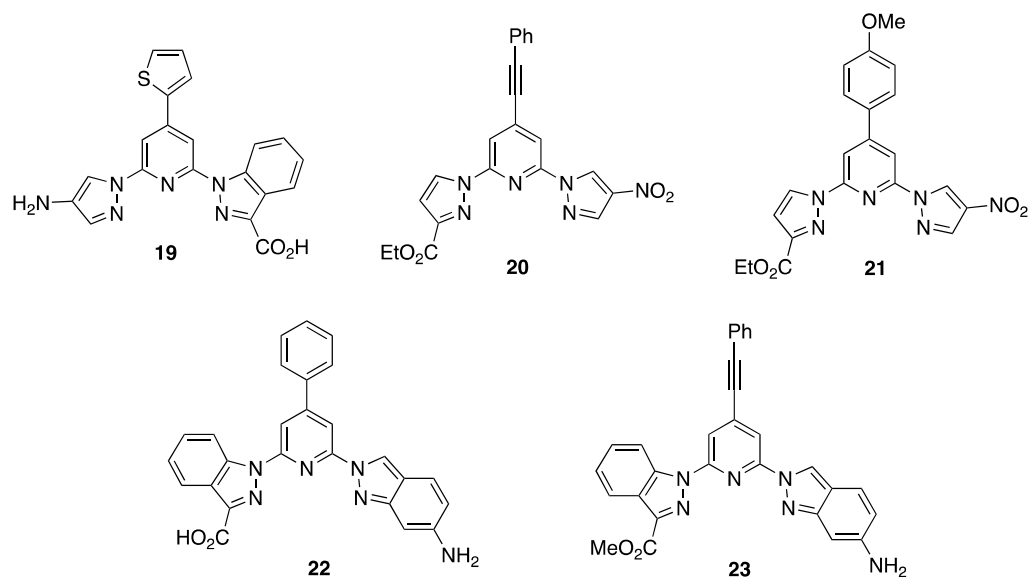
Scheme 5. Synthetic access to **bipy** derivatives.

Out of all nonsymmetrical (**ippy**, **bppy**, and **bipy**) compounds described, the bromine atom on the 4-position of pyridine was functionalized by a Suzuki and Sonogashira palladium(0) cross-coupling reaction with different arylboronic acids and arylacetylene derivatives following the general procedures described in Scheme 6.



**Scheme 6.** Synthesis of 4-substituted pyridine by Suzuki and Sonogashira reactions.

Suzuki- and Sonogashira-type reactions were carried out under microwave irradiation in only 15', with yields comparable to those under normal reflux conditions. In Suzuki reactions, it is also possible to use KOH (1 M) to obtain the hydrolyzed carboxylic acids, which is very convenient when the resultant amino acids are important to their complexing capabilities (for instance, towards lanthanide ions, as they are one of our main interests). Four examples for these coupling reactions are described for obtaining the compounds depicted in Scheme 7.



**Scheme 7.** Examples of molecules prepared from Pd-coupling reactions.

The possibility of making the bromine Pd(0) cross-coupling reaction in any of the other two synthetic steps, over the starting trihalopyridine or over the monopyrzazole or monoindazole derivatives, was proved affordable without detrimental yielding results in some of the intermediate compounds described.

### 3. Conclusions and Outlook

In summary, we have shown that by means of control of the reaction conditions it is possible to access 2,4,6-nonsymmetrically trisubstituted pyridines from readily accessible

4-bromo-2,6-difluoropyridine. The opportunities of this tri-functionalization are almost endless, and it allows for the ability to tune the electronic  $\pi$  character of these trisheterocyclic units in order to obtain the best candidates for ligands in a variety of transition and lanthanide ions complexes.

## 4. Materials and Methods

### 4.1. General Methods

All solvents (THF and DMF) were purified before use and kept dry over molecular sieves. All other reagents were of reagent grade and used as received.  $^1\text{H-NMR}$ ,  $^{13}\text{C-NMR}$ : Bruker AV-300 spectrometer (Departamento de Química Orgánica, QO). MS: VG Autospec in EI, FAB and FAB-HRMS modes (L-SIMS<sup>+</sup>), ABSciex QSTAR (ESI<sup>+</sup>, HRMS), Bruker ULTRAFLEX III (MALDI-TOF/TOF) (HRMS), spectrometers (Servicio Interdepartamental de Investigación, SidI). Elemental analyses: Perkin-Elmer CHN 2400 automatic analyzers (SidI).

### 4.2. General Synthetic Procedures

#### 4.2.1. Substitution of Fluorine Atoms by Pyrazolates or Indazolates: Method A: NaH in THF

In a round-bottom Schlenk flask under argon, the corresponding fluoropyridine (5.15 mmol) and azole (5.15 mmol) compounds were dissolved in 25 mL of dry THF. The solution was cooled to 0 °C, and NaH (60% in oil, 226 mg, 5.15 mmol) was added. The reaction mixture was left at rt for 4 h, after which 15 mL of  $\text{CH}_2\text{Cl}_2$  was added. The organic phase was washed with water (15 mL), and the aqueous phase was extracted with  $\text{CH}_2\text{Cl}_2$  ( $3 \times 10$  mL). The combined organic phases were dried over  $\text{Na}_2\text{SO}_4$  and concentrated to dryness, giving a solid that was purified by flash chromatography ( $\text{CH}_2\text{Cl}_2$ /hexane 1:1) to a white solid.

#### 4.2.2. Substitution of Fluorine Atoms by Pyrazolates or Indazolates: Method B: NaH in DMF

In a round-bottom Schlenk flask under argon, the corresponding fluoropyridine (3.5 mmol) and azole (8.3 mmol) were dissolved in 30 mL of freshly distilled DMF. The solution was cooled to 0 °C, and NaH (60% in oil, 364 mg, 9.1 mmol) was added. The reaction mixture was left at rt, then heated at 40 °C for 5 h, after which a white precipitate formed. The solid was isolated by centrifugation, and the addition of water to the liquid phase gave a second precipitate, which was also isolated by centrifugation. The combined solids were washed with warm hexane (40 mL) and water (40 mL).

#### 4.2.3. Substitution of Fluorine Atoms by Pyrazolates or Indazolates: Method C: $\text{K}_2\text{CO}_3$ in DMF and Microwave Radiation

To a microwave vial under argon contained substituted monofluorinated 4-bromopyridine (1 eq.), 3-methoxycarbonyl indazole (1.2 eq.),  $\text{K}_2\text{CO}_3$  (1.2 eq.), and dry recently distilled DMF (3 mL). The mixture was stirred at room temperature for 2 min and then heated at 140 °C for 2 h in a microwave oven (Biotage Initiator 2.5). The reaction mixture was poured on 15 mL of water and the resulting solid was isolated by centrifugation and washed 3 times with 10 mL of water. The product was purified by Flash chromatography in  $\text{CH}_2\text{Cl}_2$ :MeOH in a 95:5.

#### 4.2.4. Microwave-Assisted Suzuki-Miyaura Cross-Coupling Reaction with Boronic Acids

To a microwave vial under argon containing substituted 4-bromopyridine (0.5 mmol), the corresponding boronic acid (0.51 mmol) and  $\text{Pd}(\text{PPh}_3)_4$  (0.02 mmol) were dissolved in anhydrous THF (3.5 mL), and were stirred at room temperature for 10 min. Then, a solution of 0.5 mL KOH (1 M) was added to the mixture. The mixture was heated at 130 °C for 11 min in a microwave oven (Biotage Initiator 2.5). The solvent was removed under vacuum to yield a black residue, which was dissolved in 20 mL of  $\text{CH}_2\text{Cl}_2$  and washed with 10 mL of water. The aqueous phase was extracted with  $\text{CH}_2\text{Cl}_2$  ( $2 \times 20$  mL). The

combined organic phases were washed with brine (20 mL), dried over  $\text{Na}_2\text{SO}_4$ , filtered, and concentrated to dryness. Flash chromatography in  $\text{CH}_2\text{Cl}_2$ :hexane in a 1:1 ratio yielded the corresponding trisubstituted 2,4,6-pyridine compounds.

#### 4.2.5. Microwave-Assisted Sonogashira Cross-Coupling Reaction with Phenylacetylene

In a microwave vial under argon containing substituted 4-bromopyridine (0.46 mmol),  $\text{PdCl}_2(\text{PPh}_3)_2$  (0.061 eq.) and  $\text{CuI}$  (0.061 eq.) were dissolved in a mixture of anhydrous THF (2.5 mL) and freshly distilled  $\text{NEt}_3$  (2.2 mL), and were stirred for 5 min. Then, phenylacetylene (1.2 eq.) was added, and the mixture was heated at 120 °C for 13 min in a microwave oven (Biotage Initiator 2.5). The solvent was removed under reduced pressure to yield a dark residue, which was dissolved in 20 mL of  $\text{CH}_2\text{Cl}_2$  and washed with 15 mL of water. The aqueous phase was extracted with  $\text{CH}_2\text{Cl}_2$  ( $2 \times 20$  mL). The combined organic phases were washed with brine (20 mL), dried over  $\text{Na}_2\text{SO}_4$ , vacuum filtered, and concentrated to dryness. Flash column chromatography,  $\text{CH}_2\text{Cl}_2$ :hexane 9:1, yielded the corresponding trisubstituted 2,4,6-pyridine compounds.

### 4.3. Chemical Synthesis and Characterization

*2-(3-Ethoxycarbonyl-1-pyrazolyl)-4-bromo-6-fluoropyridine (4)*. Obtained by general method A from 4-bromo-2,6-difluoropyridine **1** (2.77 g, 14.28 mmol) and 3-ethoxycarbonylpyrazol **2** (1 g, 7.14 mmol). **4** was obtained as a white solid (1.86 g, 83%).  $^1\text{H-NMR}$  ( $\text{CDCl}_3$ )  $\delta$  (ppm) (300 MHz): 8.46 (d,  $J = 2.7$  Hz, 1H); 8.21 (dd,  $J = 1.3, 1.10$  Hz, 1H); 7.06 (dd,  $J = 2.7$  Hz, 2.59 Hz, 1H); 6.96 (d,  $J = 2.7$  Hz, 1H); 4.44 (c,  $J = 7.1$  Hz, 2H); 1.42 (t,  $J = 7.1$  Hz, 3H).  $^{13}\text{C-NMR}$  ( $\text{CDCl}_3$ )  $\delta$  (ppm) (75 MHz): 163.7, 161.7, 160.5, 147.0, 137.9, 129.0, 113.4, 111.0, 110.7, 61.8, 14.3. Anal. Calc. for  $\text{C}_{11}\text{H}_9\text{BrFN}_3\text{O}_2$ : C 42.06, H 2.89, N 13.38, found: C 42.43, H 3.16, N 13.18. MS ( $\text{FB}^+$ ):  $m/z = 314.0$  ( $[\text{M}]^+$ , 100%), 316.0 ( $[\text{M}]^+$ , 98%).

*2-(5-Aminoindazolyl)-4-bromo-6-fluoropyridine (5a, 5b)*. Obtained by general method C from 4-bromo-2,6-difluoropyridine **1** (150 mg, 0.478 mmol) and 5-aminoindazole **3** (71 mg, 0.573 mmol). A non-separable mixture of **5ab** was obtained as a white solid (13 mg, 64%). The  $^1\text{H-RMN}$  spectra were assigned from a small amount of **5a** isolated after preparative HPLC.  $^1\text{H-NMR}$  ( $\text{CDCl}_3$ )  $\delta$  (ppm) (300 MHz): **Isomer 5a**: 8.53 (d,  $J = 8.8$  Hz, 1H); 8.06 (s, 1H); 8.00 (s, 1H); 6.97 (d,  $J = 2.2$  Hz, 1H); 6.95–6.93 (m, 1H); 6.86 (m, 1H). **Isomer 5b**: 8.64 (s, 1H); 8.27 (s, 1H); 7.54 (d,  $J = 9.20$  Hz, 1H); 7.03 (m, 1H); 6.89 (d,  $J = 2.2$  Hz, 1H); 6.71 (m, 1H). Anal. Calc. for  $\text{C}_{12}\text{H}_8\text{BrFN}_4$ : C 46.93, H 2.63, N 18.24, found: C 46.73, H 2.46, N 18.18. MS ( $\text{FAB}^+$ ):  $m/z = 306.0$  ( $[\text{M}]^+$ , 100%); 308.0 ( $[\text{M}]^+$ , 97%).

*2-(5-Aminoindazolyl)-4-bromo-6-(3-ethoxycarbonyl-1-pyrazolyl)pyridine (6a, 6b)*. Obtained by general method A from 4-bromo-2-(3-ethoxycarbonyl-1-pyrazolyl)-6-fluoropyridine **4** (2.77 g, 14.28 mmol) and 5-aminoindazole **3** (1 g, 7.14 mmol). **6a, 6b** was obtained as a white solid (1.86 g, 83%).  $^1\text{H-NMR}$  ( $\text{CDCl}_3$ )  $\delta$  (ppm) (300 MHz): **Isomer 6a**: 8.55 (d,  $J = 2.5$  Hz, 1H); 8.38 (d,  $J = 8.7$  Hz, 1H); 8.13 (d,  $J = 1.2$  Hz, 1H); 8.08 (d,  $J = 1.2$  Hz, 1H); 8.01 (s, 1H); 7.04–6.95 (m, 4H); 6.87 (dd,  $J = 1.9$  Hz, 8.7 Hz, 1H); 4.47 (c,  $J = 7.1$  Hz, 4H); 1.45 (t,  $J = 7.1$  Hz, 6H). **Isomer 6b**: 8.68 (m, 1H); 8.60 (d,  $J = 2.6$  Hz, 1H); 8.31 (d,  $J = 1.2$  Hz, 1H); 8.23 (d,  $J = 1.2$  Hz, 1H); 7.55 (d,  $J = 9.2$  Hz, 1H); 7.04–6.95 (m, 4H); 6.71 (d,  $J = 1.2$  Hz, 1H); 4.47 (c,  $J = 7.1$  Hz, 4H); 1.45 (t,  $J = 7.1$  Hz, 6H). Anal. Calc. for  $\text{C}_{18}\text{H}_{15}\text{BrN}_6\text{O}_2$ : C 50.60, H 3.54, N 19.67, found: C 50.73, H 3.46, N 19.56. MS ( $\text{FAB}^+$ ):  $m/z = 427.0$  ( $[\text{M}]^+$ , 100%); 429.0 ( $[\text{M}]^+$ , 98%).

*2-(4-Amino-1H-pyrazolyl)-4-bromo-6-fluoropyridine (8)*. Obtained by general method A from 4-bromo-2,6-difluoropyridine **1** (1.05 mmol) and 4-aminopyrazole **7** (1 mmol). **8** was obtained as a white solid (60%).  $^1\text{H-RMN}$  ( $\text{CDCl}_3$ )  $\delta$  (ppm) (300 MHz): 7.98 (s, 1H); 7.97 (s, 1H); 7.47 (s, 1H); 6.93 (s, 1H).  $^{13}\text{C-NMR}$  ( $\text{CDCl}_3$ )  $\delta$  (ppm) (75 MHz): 137.13–137.01, 136.30, 131.90, 113.75, 111.67, 111.61, 108.5, 107.99. Anal. Calc. for  $\text{C}_8\text{H}_6\text{BrFN}_4$ : C 37.38, H 2.35, N 21.80, found: C 38.34, H 2.44, N 21.80. MS ( $\text{FAB}^+$ ):  $m/z = 256.0$  ( $[\text{M}]^+$ , 100%), 258.0 ( $[\text{M}]^+$ , 97%).

*2-(3-Methoxycarbonyl-1H-indazolyl)-4-bromo-6-(4-amino-1H-pyrazolyl)pyridine (10)*. Obtained by general method A from 2-(4-amino-1H-pyrazolyl)-4-bromo-6-fluoropyridine

**8** (1 mmol) and 3-methoxycarbonylindazole **9** (1.1 mmol). **10** was obtained as a white solid (84%). <sup>1</sup>H-NMR (CDCl<sub>3</sub>) δ (ppm) (300 MHz): 8.67 (d, 1H, *J* = 7.29 Hz); 8.31 (d, 1H, *J* = 8.22 Hz); 8.14 (s, 1H); 8.05 (s, 1H); 8.01 (s, 1H); 7.62 (t, 1H, *J* = 7.29 Hz); 7.48 (s, 1H); 7.45 (t, 1H, *J* = 7.34 Hz); 4.10 (s, 3H). <sup>13</sup>C-NMR (CDCl<sub>3</sub>) δ (ppm) (75 MHz): 162.54, 152.18, 150.59, 139.99, 138.54, 136.03, 134.32, 131.88, 128.78, 125.04, 124.73, 119.44, 116.90, 113.73, 112.06, 108.28, 52.48. Anal. Calc. for C<sub>17</sub>H<sub>13</sub>BrN<sub>6</sub>O<sub>2</sub>: C 49.41, H 3.17, N 20.34, found: C 49.34, H 3.24, N 20.30. MS (FAB<sup>+</sup>): *m/z* = 412.0 ([M]<sup>+</sup>, 100%), 414.0 ([M]<sup>+</sup>, 97%).

**2-(3-Ethoxycarbonyl-1H-pyrazolyl)-4-bromo-6-(4-amino-1H-pyrazolyl)pyridine (13)**. Obtained by general method A from 2-(3-ethoxycarbonyl-1H-pyrazolyl)-4-bromo-6-fluoropyridine **4** (0.46 mmol) and 4-aminopyrazole **7** (0.5 mmol). **13** was obtained as a white solid (42%). Alternatively can also be prepared from 2-(4-amino-1H-pyrazolyl)-4-bromo-6-fluoropyridine **8** and 3-ethoxycarbonylpyrazole **2** following general method A (yield 78%). <sup>1</sup>H-NMR (CDCl<sub>3</sub> 300 MHz) δ: 8.51 (1H, d, *J* = 2.27 Hz); 8.09 (1H, s); 8.00 (1H, s); 7.43 (1H, s); 6.98 (1H, s); 4.45 (2H, c, *J* = 7.18 Hz); 1.43 (3H, t, *J* = 7.18 Hz). <sup>13</sup>C-NMR (CDCl<sub>3</sub> 75 MHz) δ: 161.86, 150.58, 149.6, 146.57, 141.66, 136.55, 136.15, 128.47, 113.46, 113.03, 112.26, 110.41, 61.44, 14.32 ppm. Anal. Calc. for C<sub>14</sub>H<sub>13</sub>BrN<sub>6</sub>O<sub>2</sub>: C 44.58, H 3.47, N 22.28, found: C 44.39, H 3.52, N 22.32. MS (FAB<sup>+</sup>): *m/z* = 376.0 ([M]<sup>+</sup>, 100%), 378.0 ([M]<sup>+</sup>, 97%).

**2-(3-Ethoxycarbonyl-1H-pyrazolyl)-4-bromo-6-(4-nitro-1H-pyrazolyl)pyridine (14)**. Obtained by general method A from 2-(3-ethoxycarbonyl-1H-pyrazolyl)-4-bromo-6-fluoropyridine **4** (1 mmol) and 4-nitropyrazole **12** (1 mmol). **14** was obtained as a white solid (90%). <sup>1</sup>H-NMR (CDCl<sub>3</sub> 300 MHz) δ: 9.19 (1H, s); 8.56 (1H, d, *J* = 2.63 Hz); 8.38 (1H, d, *J* = 1.32 Hz); 8.30 (1H, s); 8.16 (1H, d, *J* = 1.32 Hz); 7.04 (1H, d, *J* = 2.63 Hz); 4.47 (2H, c, *J* = 7.24 Hz); 1.44 (3H, t, *J* = 7.23 Hz) ppm. <sup>13</sup>C-NMR (CDCl<sub>3</sub> 75 MHz) δ: 171.47, 161.39, 149.15, 146.11, 136.09, 135.69, 131.37, 128.01, 113.03, 112.57, 111.81, 109.96, 60.98, 13.87 ppm. Anal. Calc. for C<sub>14</sub>H<sub>11</sub>BrN<sub>6</sub>O<sub>4</sub>: C 41.30, H 2.72, N 20.64, found: C 41.39, H 2.42, N 20.63. FAB-HRMS *m/z* found: 406.0034, calculated for C<sub>14</sub>H<sub>11</sub>BrN<sub>6</sub>O<sub>4</sub>: 406.0025.

**2-(6-Aminoindazolyl)-4-bromo-6-fluoropyridine (16a, 16b)**. Obtained by general method A from 4-bromo-2,6-difluoropyridine **1** (1 g, 5.26 mmol) and 6-aminoindazole **15** (700.4 mg, 5.26 mmol). The resulting solid was purified by Flash chromatography (dichloromethane: MeOH, 99:1). **16a** was a white solid (450 mg, 28%) and **16b** a yellow solid (430 mg 27%).

**Isomer 16a**. <sup>1</sup>H-NMR (CDCl<sub>3</sub>) δ (ppm) (300 MHz): 8.07 (s, 1H); 8.00 (s, 1H); 7.98 (d, *J* = 1.1 Hz, 1H); 7.49 (d, *J* = 8.5 Hz, 1H); 6.87 (dd, *J* = 1.1 Hz, 2.6 Hz, 1H); 6.68 (dd, *J* = 1.9 Hz, 8.5 Hz, 1H). <sup>13</sup>C-NMR (CDCl<sub>3</sub>) δ (ppm) (300 MHz): 162.1, 154.5, 147.8, 140.6, 138.4, 136.6, 121.8, 119.5, 113.8, 113, 106.8, 98.7. Anal. Calc. for C<sub>12</sub>H<sub>8</sub>BrN<sub>4</sub>: C 46.93, H 2.63, N 18.24, found: C 46.79, H 2.81, N 18.03. MS (FAB<sup>+</sup>): *m/z* = 307.0 ([M]<sup>+</sup>, 100%); 309.0 ([M]<sup>+</sup>, 97%).

**Isomer 16b**. <sup>1</sup>H-NMR (CDCl<sub>3</sub>) δ (ppm) (300 MHz): 8.78 (s, 1H); 8.25 (s, 1H); 7.49 (d, *J* = 8.9 Hz, 1H); 7.01 (d, *J* = 1.4 Hz, 1H); 6.70 (s, 1H); 6.60 (dd, *J* = 1.4 Hz, 8.9 Hz, 1H). <sup>13</sup>C-NMR (CDCl<sub>3</sub>) δ (ppm) (300 MHz): 162.1, 150.4, 146.6, 152.5, 137.6, 121.4, 122.3, 118.4, 118, 113.5, 109.9, 95.5. Anal. Calc. for C<sub>12</sub>H<sub>8</sub>BrN<sub>4</sub>: C 46.93, H 2.63, N 18.24, found: C 47.02, H 2.81, N 18.11. MS (FAB<sup>+</sup>): *m/z* = 307.0 ([M]<sup>+</sup>, 100%); 309.0 ([M]<sup>+</sup>, 97%).

**2-(6-Aminoindazolyl)-4-bromo-6-(3-methoxycarbonyl-1H-indazolyl)pyridine (17a)**. Obtained by general method A from **16a** (1.16 mmol) and 3-methoxycarbonylindazole **9** (1.166 mmol). **9a** was obtained as a white solid (478 mg, 89%). <sup>1</sup>H-NMR (CDCl<sub>3</sub>) δ (ppm) (300 MHz): 8.69 (d, *J* = 8.5 Hz, 1H); 8.29 (d, *J* = 8.1 Hz, 1H); 8.11 (d, *J* = 1.3 Hz, 1H); 8.05 (s, 1H); 7.99 (d, *J* = 1.3 Hz, 1H); 7.97 (s, 1H); 7.58 (m, 1H); 7.55–7.53 (m, 1H); 7.46–7.41 (m, 1H); 6.70 (dd, *J* = 1.8 Hz, 8.5 Hz, 1H); 4.10 (s, 3H). <sup>13</sup>C-NMR (CDCl<sub>3</sub>) δ (ppm) (300 MHz): 163.7, 152.3, 151.2, 148.2, 144.4, 142.6, 137.2, 135.2, 128.9, 126.6, 123.1, 122.9, 122.7, 119.4, 118.6, 113.6, 112.7, 110.9, 108.7, 88.4, 53.0. Anal. Calc. for C<sub>21</sub>H<sub>15</sub>BrN<sub>6</sub>O<sub>2</sub>: C 54.44, H 3.26, N 18.14, found: C 54.10, H 3.33, N 18.31. MS (FAB<sup>+</sup>): *m/z* = 463.0 ([M]<sup>+</sup>, 100%); 465.0 ([M]<sup>+</sup>, 97%).

**2-(3-Carboxymethyl-1H-indazolyl)-4-bromo-6-fluoropyridine (18)**. Obtained by general method A from 4-bromo-2,6-difluoropyridine **1** (1 g, 5.15 mmol) and 3-carboxymethylindazole **9** (900 mg, 5.11 mmol). **18** was purified by chromatography (Hexane:dichloromethane 3:1) and isolated as a white solid (1.5 g, 84%). <sup>1</sup>H-NMR (CDCl<sub>3</sub>) δ (ppm) (300 MHz): 8.78 (d, *J* = 8.5 Hz, 1H); 8.28–8.26 (m, 2H); 7.60 (t, *J* = 7.5 Hz, 1H); 7.44 (t, *J* = 7.5 Hz, 1H); 7.04 (d,

$J = 3.0$  Hz, 1H); 4.10 (s, 3H).  $^{13}\text{C-NMR}$  ( $\text{CDCl}_3$ )  $\delta$  (ppm) (300 MHz): 163.7, 161.8, 159.7, 157.2, 142.0, 137.2, 131.4, 126.6, 122.9, 121.7, 119.4, 114.0, 108.5, 107.4, 53.0. Anal. Calc. for  $\text{C}_{21}\text{H}_{15}\text{BrN}_6\text{O}_2$ : C 54.44, H 3.26, N 18.14, found: C 54.10, H 3.33, N 18.31. MS ( $\text{ESI}^+$ ):  $m/z = 350.0$  ( $[\text{M}]^+$ , 100%), 352.0 ( $[\text{M}]^+$ , 97%).

**2-(3-Carboxy-1H-indazolyl)-4-(2-tienyl)-6-(4-amino-1H-pirazolil) piridina (19)**. Obtained by microwave-assisted Suzuki–Miyaura cross-coupling reaction with boronic acids from **10** (100.2 mg, 0.243 mmol) and tienylboronic acid (34 mg, 0.227 mmol). The product in the form of carboxylic acid **11** was isolated by centrifugation and washed with dichloromethane (60%).  $^1\text{H-NMR}$  (DMSO, 300 MHz)  $\delta$ : 8.72 (1H, d,  $J = 8.29$  Hz); 8.39 (1H, d,  $J = 7.91$  Hz); 8.32 (1H, d,  $J = 1.51$  Hz); 8.19 (1H, s); 7.90 (1H, d,  $J = 1.13$  Hz); 7.85 (1H, d,  $J = 3.77$  Hz); 7.61 (1H, d,  $J = 4.14$  Hz); 7.58 (1H, t,  $J = 7.16$  Hz); 7.52 (1H, s); 7.36 (1H, t,  $J = 7.54$  Hz); 7.21 (1H, dd,  $J_1 = 4.90$ ,  $J_2 = 3.77$  Hz) ppm.  $^{13}\text{C-NMR}$  (DMSO, 75 MHz)  $\delta$ : 153.5, 152.2, 151.6, 149.3, 139.7, 139.1, 137.6, 136.4, 130.3, 129.1, 128.9, 128.2, 127.6, 127.1, 122.9, 122.1, 117.32, 114.8, 109.2, 106.4 ppm. Anal. Calc. for  $\text{C}_{20}\text{H}_{14}\text{N}_6\text{O}_2\text{S}$ : C 59.69, H 3.51, N 20.88, found: C 59.40, H 3.61, N 20.53. MS ( $\text{ESI}^+$ ):  $m/z = 403.9$  ( $[\text{M}+\text{H}]^+$ , 100%).

**2-(3-Ethoxycarbonyl-1H-pyrazolyl)-4-phenylethynyl-6-(4-nitro-1H-pyrazolyl)pyridine (20)**. Obtained by microwave-assisted Sonogashira cross-coupling reaction with phenylacetylene from **13** (150 mg, 0.36 mmol) and phenylacetylene (0.39 mmol). The product was purified by Flash chromatography (gradient dichlorometane/hexane (20–100%)) yield 80%.  $^1\text{H-NMR}$  ( $\text{CDCl}_3$ , 300 MHz)  $\delta$ : 9.19 (1H, s); 8.57 (1H, d,  $J = 2.63$  Hz); 8.27 (1H, s); 8.23 (1H, s); 8.00 (1H, s); 7.58–7.54 (2H, m); 7.43–7.37 (3H, m); 7.01 (1H, d,  $J = 2.64$  Hz); 4.45 (2H, c,  $J = 7.02$  Hz); 1.44 (3H, t,  $J = 7.01$  Hz) ppm.  $^{13}\text{C-NMR}$  ( $\text{CDCl}_3$ , 75 MHz)  $\delta$ : 162.0, 151.3, 149.4, 136.5, 135.1, 134.9, 133.5, 132.1 (2C), 132.1, 129.5, 128.4 (2C), 128.2, 121.8, 113.7, 111.8, 110.9, 110.2, 95.3, 86.4, 61.0, 14.4 ppm. Anal. Calc. for  $\text{C}_{22}\text{H}_{16}\text{N}_6\text{O}_4$ : C 61.68, H 3.76, N 19.62, found: C 61.82, H 3.39, N 19.69. MS ( $\text{ESI}^+$ ):  $m/z = 429.1$  ( $[\text{M} + \text{H}]^+$ , 100%).

**2-(3-Ethoxycarbonyl-1H-pyrazolyl)-4-(phenyl-*p*-methoxy)-6-(4-nitro-1H-pyrazolyl)pyridine (21)**. Obtained by microwave-assisted Suzuki–Miyaura cross-coupling reaction with boronic acids from **13** (150 mg, 0.36 mmol) and *p*-methoxyphenylboronic acid (0.4 mmol). The product was isolated as a white solid 78 mg, 48% yield).  $^1\text{H-NMR}$  ( $\text{CDCl}_3$ , 300 MHz)  $\delta$ : 9.26 (1H, s); 8.63 (1H, d,  $J = 2.69$  Hz); 8.35 (1H, d,  $J = 1.25$  Hz); 8.31 (1H, s); 8.18 (1H, d,  $J = 1.32$  Hz); 7.80 (2H, d,  $J = 8.86$  Hz); 7.05 (2H, d,  $J = 8.86$  Hz); 7.04 (1H, d,  $J = 2.69$  Hz); 4.47 (2H, c,  $J = 7.10$  Hz); 3.89 (3H, s); 1.45 (3H, t,  $J = 7.10$  Hz) ppm.  $^{13}\text{C-NMR}$  ( $\text{CDCl}_3$ , 75 MHz)  $\delta$ : 161.44, 161.16, 155.32, 154.36, 149.84, 148.55, 136.98, 131.30, 128.28, 128.20, 128.08, 125.45, 114.24, 110.15, 108.92, 107.78, 61.00, 55.02, 13.87 ppm. Anal. Calc. for  $\text{C}_{21}\text{H}_{18}\text{N}_6\text{O}_5$ : C 58.06, H 4.18, N 19.35, found: C 57.23, H 3.89, N 19.29. MS ( $\text{ESI}^+$ ):  $m/z = 435.1$  ( $[\text{M} + \text{H}]^+$ , 100%).

**2-(6-Amino-1H-indazolyl)-4-phenyl-6-(3-carboxy-1H-indazolyl)pyridine (22)**. Obtained by microwave-assisted Suzuki–Miyaura cross-coupling reaction with boronic acids from **17a** (0.15 mmol) and phenylboronic acid (0.17 mmol). The product in the form of carboxylic acid **22** was isolated by centrifugation and washed with dichloromethane (89% yield).  $^1\text{H-NMR}$  ( $\text{CD}_3\text{OD}$ )  $\delta$  (ppm) (300 MHz): 9.11 (s, 1H); 8.29 (d,  $J = 8.5$  Hz, 1H); 8.05 (m, 2H); 7.93 (s, 1H); 7.73 (d,  $J = 8.5$  Hz, 1H); 7.55–7.52 (m, 2H); 7.41 (m, 1H); 7.36 (m, 1H); 7.28–7.24 (m, 3H); 7.16 (m, 2H).  $^{13}\text{C-NMR}$  ( $\text{CD}_3\text{OD}$ )  $\delta$  (ppm) (300 MHz): 165.7, 153.8, 153.5, 152.4, 140.7, 139.4, 139.0, 138.9, 138.8, 136.4, 131.7, 131.0, 130.0, 127.4, 127.2, 125.9, 125.1, 124.3, 123.8, 118.6, 115.0, 111.7, 110.6, 108.8. Anal. Calc. for  $\text{C}_{26}\text{H}_{18}\text{N}_6\text{O}_2$ : C 69.95, H 4.06, N 18.82, found: C 70.02, H 3.98, N 19.11. MS ( $\text{FAB}^+$ ):  $m/z = 446.1$  ( $[\text{M}]^+$ , 100%).

**2-(6-Amino-1H-indazolyl)-4-phenylethynyl-6-(3-methoxycarbonyl-1H-indazolyl)pyridine (23)**. Obtained by microwave-assisted Sonogashira cross-coupling reaction with phenylacetylene from **17a** (0.15 mmol) and phenylacetylene (0.17 mmol). The product was purified by Flash chromatography (gradient dichlorometane/hexane (20–100%)) yield (49 mg, 67%).  $^1\text{H-NMR}$  ( $\text{CDCl}_3$ )  $\delta$  (ppm) (300 MHz): 8.74 (d,  $J = 8.5$  Hz, 1H); 8.31 (d,  $J = 8.1$  Hz, 1H); 8.05–8.03 (m, 3H); 7.94 (s, 1H); 7.59–7.51 (m, 4H); 7.43–7.39 (m, 4H); 6.72 (dd,  $J = 1.6$  Hz, 8.5 Hz, 1H); 4.11 (s, 3H).  $^{13}\text{C-NMR}$  ( $\text{CDCl}_3$ )  $\delta$  (ppm) (300 MHz): 163.7, 151.6, 150.5, 148.2, 137.2, 135.2, 133.8, 132.0, 131.7, 128.8, 128.6, 128.1, 126.6, 124.0, 124.0, 122.9, 122.7, 119.6,

119.4, 116.2, 114.4, 113.6, 109.7, 91.9, 91.2, 89.3, 53.0. Anal. Calc. for C<sub>29</sub>H<sub>20</sub>N<sub>6</sub>O<sub>2</sub>: C 71.89, H 4.16, N 17.35, found: C 71.76, H 3.98, N 17.21. MS (FAB<sup>+</sup>): *m/z* = 484.1 ([M]<sup>+</sup>, 100%).

**Author Contributions:** Conceptualization, J.C.R.-U.; methodology, J.C.R.-U., A.G.R.-C., L.G.-F., P.M.-M.; validation, A.G.R.-C., L.G.-F. and P.M.-M.; formal analysis, A.G.R.-C., L.G.-F. and P.M.-M.; investigation, A.G.R.-C., L.G.-F. and P.M.-M.; resources, J.C.R.-U.; data curation, A.G.R.-C., L.G.-F. and P.M.-M.; writing—original draft preparation, J.C.R.-U.; writing—review and editing, J.C.R.-U.; visualization, J.C.R.-U.; supervision, J.C.R.-U.; project administration, J.C.R.-U. and L.G.-F.; funding acquisition, J.C.R.-U. All authors have read and agreed to the published version of the manuscript.

**Funding:** This research was funded by European Union Seventh Framework Programme (FP7/2007-2013) grant number 259848) And The APC was funded by ERCROS.

**Institutional Review Board Statement:** Not applicable.

**Informed Consent Statement:** Not applicable.

**Data Availability Statement:** Analytical data can be found in the archives of The Servicio Interdepartamental de Investigación of the University Autónoma de Madrid, <https://www.uam.es/uam/sidi> (accessed on 15 February 2022).

**Acknowledgments:** This research was funded through the European Union Seventh Framework Programme (FP7/2007-2013) under Grant Agreement no. 259848. Indirect funding from ERCROS S.A. (Aranjuez, Spain) through the UAM-ERCROS Chair for Pharmaceutical Chemistry is gratefully acknowledged.

**Conflicts of Interest:** The authors declare no conflict of interest.

**Sample Availability:** Samples of the final compounds **19–23** are available from the authors.

## References

- Heller, M.; Schubert, U.S. Syntheses of Functionalized 2,2':6',2''-Terpyridines. *Eur. J. Org. Chem.* **2003**, 947–961.
- Campagna, S.; Puntoriero, F.; Nastasi, F.; Bergamini, G.; Balzani, V. Photochemistry and photophysics of coordination compounds: Ruthenium. *Top. Curr. Chem.* **2007**, *280*, 117–214.
- Pal, A.K. Hanan, Design, synthesis and excited-state properties of mononuclear Ru(II) complexes of tridentate heterocyclic ligands. *G.S. Chem. Soc. Rev.* **2014**, *43*, 6184–6197. [CrossRef] [PubMed]
- Costa, R.D.; Ortí, E.; Bolink, H.J.; Monti, F.; Accorsi, G.; Armaroli, N. Luminescent ionic transition-metal complexes for light-emitting electrochemical cells. *Angew. Chem. Int. Ed.* **2012**, *51*, 8178–8211. [CrossRef]
- Dreyse, P.; Loeb, B.; Soto-Arriaza, M.; Tordera, D.; Ortí, E.; Serrano-Pérez, J.J.; Bolink, H.J. Effect of free rotation in polypyridinic ligands of Ru (II) complexes applied in light-emitting electrochemical cells. *Dalton Trans.* **2013**, *42*, 15502–15513. [CrossRef]
- Gu, J.; Yan, Y.; Helbig, B.J.; Huang, Z.; Lian, T.; Schmehl, R.H. The influence of ligand localized excited states on the photophysics of second row and third row transition metal terpyridyl complexes: Recent examples and a case study. *Coord. Chem. Rev.* **2015**, 100–109. [CrossRef]
- Schubert, U.S.; Winter, A.; Newkome, G.R. *Terpyridine-Based Materials*; Wiley-VCH: Weinheim, Germany, 2011; Chapter 4.
- Cargill-Thompson, A.M.W. The synthesis of 2, 2':6',2''-terpyridine ligands—Versatile building blocks for supramolecular chemistry. *Coord. Chem. Rev.* **1997**, *160*, 1–52. [CrossRef]
- Byrne, J.P.; Kitchen, J.A.; Gunnaugsson, T. The btp [2, 6-bis (1, 2, 3-triazol-4-yl) pyridine] binding motif: A new versatile terdentate ligand for supramolecular and coordination chemistry. *Chem. Soc. Rev.* **2014**, *43*, 5302–5325. [CrossRef]
- de Bettencourt-Dias, A.; Barber, P.S.; Bauer, S. A water-soluble pybox derivative and its highly luminescent lanthanide ion complexes. *J. Am. Chem. Soc.* **2012**, *134*, 6987–6994. [CrossRef]
- Jameson, D.L.; Kruger, K.T.; Goldsby, K.A. Redox regulation in ruthenium(II) complexes of 2,6-bis(N-pyrazolyl)pyridine ligands: Synthetically versatile analogs of 2,2':6',2''-terpyridine. *Inorg. Chem.* **1989**, 4312–4314. [CrossRef]
- Jameson, D.L.; Goldsby, K.A. 2,6-bis(N-pyrazolyl)pyridines: The convenient synthesis of a family of planar tridentate N<sub>3</sub> ligands that are terpyridine analogs. *J. Org. Chem.* **1990**, *55*, 4992–4994. [CrossRef]
- Starck, M.; Kadjane, P.; Bois, E.; Darbouret, B.; Incamps, A.; Ziessel, R.; Charbonniere, L.J. Towards libraries of luminescent lanthanide complexes and labels from generic synthons. *Chem. Eur. J.* **2011**, 9164–9179. [CrossRef] [PubMed]
- Gamonal, A.; Brunet, E.; Juanes, O.; Rodriguez-Ubis, J.C. Pd cross-coupling reactions in the access to bis-pyrazole and bis-indazole pyridine-based nona-coordinated ligands. Luminescence properties of their lanthanide complexes. *J. Photochem. Photobiol. A Chem.* **2017**, *342*, 53–58. [CrossRef]
- Halcrow, M.A. Recent advances in the synthesis and applications of 2,6-dipyrazolylpyridine derivatives and their complexes. *New J. Chem.* **2014**, *38*, 1868–1882. [CrossRef]



16. Zoppellaro, G.; Baumgarten, M. One-Step Synthesis of Symmetrically Substituted 2,6-Bis(pyrazol-1-yl)pyridine Systems. *Eur. J. Org. Chem.* **2005**, 2888–2892. [CrossRef]
17. Strohecker, D.J.; Lynch, V.M.; Holliday, B.J.; Jones, R.A. Synthesis and electronic investigation of mono- and di-substituted 4-nitro- and 4-amino-pyrazol-1-yl bis (pyrazol-1-yl) pyridine-type ligands and luminescent Eu (III) derivatives. *Dalton Trans.* **2017**, 46, 7733–7742. [CrossRef]
18. Halcrow, M.A. The synthesis and coordination chemistry of 2,6-bis(pyrazolyl)pyridines and related ligands—Versatile terpyridine analogues. *Coord. Chem. Rev.* **2005**, 249, 2880–2908. [CrossRef]
19. Brien, K.A.; Garner, C.M.; Pinney, K.G. Synthesis and characterization of 2, 6-bis-hydrazinopyridine, and its conversion to 2, 6-bis-pyrazolylpyridines. *Tetrahedron* **2006**, 62, 3663–3666. [CrossRef]
20. Basak, S.; Hui, P.; Chandrasekar, R. Regioselective, One-Pot Syntheses of Symmetrically and Unsymmetrically Halogenated 2',6'-Bispyrazolylpyridines. *Synthesis* **2009**, 23, 4042–4048.
21. Vermonden, T.; Branowska, D.; Marcelis, A.T.M.; Sudhölter, E.J.R. Synthesis of 4-functionalized terdentate pyridine-based ligands. *Tetrahedron* **2003**, 59, 5039–5045. [CrossRef]
22. Santoro, A.; Cook, L.J.K.; Kulmaczewski, R.; Barret, S.A.; Cespedes, O.; Halcrow, M.A. Iron (II) complexes of tridentate indazolylpyridine ligands: Enhanced spin-crossover hysteresis and ligand-based fluorescence. *Inorg. Chem.* **2015**, 54, 682–693. [CrossRef] [PubMed]
23. Pritchard, R.; Kilner, C.; Halcrow, M.A. Unexpected product distributions in the synthesis of 2,6-bis-(indazolyl) pyridine and 2-(pyrazol-1-yl)-6-(indazolyl) pyridine. *Tet. Lett.* **2009**, 50, 2484–2486. [CrossRef]
24. Schlosser, M.; Bobbio, C.; Rauiss, T. Regiochemically Flexible Substitutions of Di-, Tri-, and Tetrahalopyridines: The Trialkylsilyl Trick. *J. Org. Chem.* **2005**, 70, 2494–2502. [CrossRef] [PubMed]
25. Schlosser, M.; Rauiss, T.; Bobbio, C. Rerouting Nucleophilic Substitution from the 4-Position to the 2- or 6-Position of 2,4-Dihalopyridines and 2,4,6-Trihalopyridines: The Solution to a Long-Standing Problem. *Org. Lett.* **2005**, 7, 127–129. [CrossRef]
26. Schlosser, M.; Rauiss, T. The Reactivity of 2-Fluoro- and 2-Chloropyridines toward Sodium Ethoxide: Factors Governing the Rates of Nucleophilic (Het)Aromatic Substitutions. *Helv. Chim. Acta* **2005**, 88, 1240–1249. [CrossRef]
27. Kadjane, P.; Starck, M.; Camerel, F.; Hill, D.; Hildebrandt, N.; Ziesel, R.; Charbonnière, L.J. Divergent Approach to a Large Variety of Versatile Luminescent Lanthanide Complexes. *Inorg. Chem.* **2009**, 48, 4601–4603. [CrossRef]
28. Brunet, E.; Juanes, O.; Sedano, R.; Rodriguez-Ubis, J.C. Synthesis of Novel Macrocyclic Lanthanide Chelates Derived from Bis-pyrazolylpyridine. *Org. Lett.* **2002**, 4, 213–216. [CrossRef]
29. Brunet, E.; Juanes, O.; Sedano, R.; Rodriguez-Ubis, J.C. Lanthanide complexes of new polyaminocarboxylate complexes with two chromophores derived from bispyrazolylpyridine and aceto or benzophenone: Synthesis, characterization and photophysical properties. *Tetrahedron* **2005**, 61, 6757–6763. [CrossRef]
30. Brunet, E.; Juanes, O.; Sedano, R.; Rodriguez-Ubis, J.C. Lanthanide complexes of polycarboxylate-bearing dipyrazolylpyridine ligands with near-unity luminescence quantum yields: The effect of pyridine substitution. *Photochem. Photobiol. Sci.* **2002**, 1, 613–618. [CrossRef]
31. Ye, Z.; Tan, M.; Wang, G.; Yuan, J. Preparation, characterization, and time-resolved fluorometric application of silica-coated terbium (III) fluorescent nanoparticles. *Anal. Chem.* **2004**, 76, 513–518. [CrossRef]
32. Yuan, J.; Tan, M.; Wang, G. Synthesis and luminescence properties of lanthanide (III) chelates with polyacid derivatives of thienyl-substituted terpyridine analogues. *J. Lumin.* **2004**, 106, 91–101. [CrossRef]
33. Karhunen, U.; Malmi, E.; Brunet, E.; Rodriguez-Ubis, J.C.; Soukka, T. Switchable lanthanide luminescent binary probes in efficient single nucleotide mismatch discrimination. *Sens. Actuators B* **2015**, 211, 297–302. [CrossRef]

Article

# Structural Requirements of 1-(2-Pyridinyl)-5-pyrazolones for Disproportionation of Boronic Acids

Joungmo Cho <sup>1,†</sup>, Venkata Subbaiah Sadu <sup>2,†</sup>, Yohan Han <sup>1</sup>, Yunsoo Bae <sup>3</sup>, Hwajeong Lee <sup>4</sup> and Kee-In Lee <sup>1,2,\*</sup> 

<sup>1</sup> Korea Research Institute of Chemical Technology, Daejeon 34114, Korea; jmcho@kriict.re.kr (J.C.); yghan@kriict.re.kr (Y.H.)

<sup>2</sup> R&D Center, Molecules & Materials Co., Ltd., B-219 Daeduck BIZ Center, Daejeon 34013, Korea; subboo32@outlook.com

<sup>3</sup> Department of Life Science, Ewha Womans University, Seoul 03760, Korea; baey@ewha.ac.kr

<sup>4</sup> Graduate School of Pharmaceutical Sciences, Ewha Womans University, Seoul 03760, Korea; hwalee@ewha.ac.kr

\* Correspondence: kilee@kriict.re.kr

† These authors contributed equally to this work.

**Abstract:** We observed an unusual formation of four-coordinate boron(III) complexes from the reaction of 1-(2-pyridinyl)-5-pyrazolone derivatives with arylboronic acids in the basic media. The exact mechanism is not clear; however, the use of unprotected boronic acid and the presence of a bidentate ligand appeared to be the key structural requirements for the transformation. The results suggest that base-promoted disproportionation of arylboronic acid with the assistance of the [N,O]-bidentate ligation of 1-(2-pyridinyl)-5-pyrazolone should take place and facilitate the formation of pyrazole diarylborinate. Experiments to obtain a deeper understanding of its mechanism are currently underway.

**Keywords:** 1-(2-pyridinyl)-5-pyrazolone; [N,O]-bidentate ligand; arylboronic acid; base; diarylborination; four-coordinate boron(III) complex

**Citation:** Cho, J.; Sadu, V.S.; Han, Y.; Bae, Y.; Lee, H.; Lee, K.-I. Structural Requirements of 1-(2-Pyridinyl)-5-pyrazolones for Disproportionation of Boronic Acids. *Molecules* **2021**, *26*, 6814. <https://doi.org/10.3390/molecules26226814>

Academic Editors: Vera L. M. Silva and Artur M. S. Silva

Received: 20 October 2021

Accepted: 6 November 2021

Published: 11 November 2021

**Publisher's Note:** MDPI stays neutral with regard to jurisdictional claims in published maps and institutional affiliations.



**Copyright:** © 2021 by the authors. Licensee MDPI, Basel, Switzerland. This article is an open access article distributed under the terms and conditions of the Creative Commons Attribution (CC BY) license (<https://creativecommons.org/licenses/by/4.0/>).

## 1. Introduction

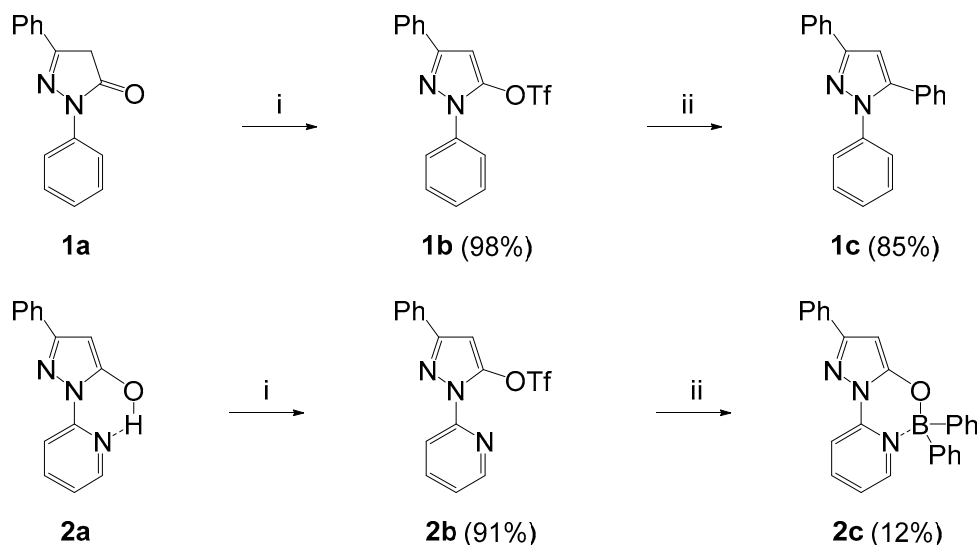
Pyrazoles are important structural units that are frequently found in many pharmaceuticals, agrochemicals, and functional materials, as they serve as core scaffolds possessing a wide range of biological activities as well as synthetic templates for organic synthesis. Indeed, a large number of arylated pyrazoles have been synthesized and proven to be effective inhibitors of COX-2, p38 MAP kinase, and CDK2/Cyclin A [1]. In particular, we were involved in the tautomeric transformations of 5-pyrazolone derivatives for the synthesis of NADPH oxidase inhibitors [2–5].

In the course of the investigation, we unexpectedly found the formation of diarylborinate complexes, particularly for the case with 1-(2-pyridinyl)-5-pyrazolone derivatives and arylboronic acids. However, the four-coordinate boron compounds have been routinely prepared from the reaction of [N,O]-bidentate ligands with triarylboranes [6] and diarylboronic acids [7]. This is a subject of great interest since four-coordinate boron(III) complexes make them very useful as luminescent materials for organic electronics and photonics, and sensing and imaging probes for biomedical purposes [8]. To the best of our knowledge, the finding is a unique instance of the formation of diarylborinates via the direct employment of arylboronic acids.

Meanwhile, this observation raised important questions, such as: “Where does it come from”? Although many questions still remain to be answered, herein we focus on reporting our early understanding of the structural requirements of 1-(2-pyridinyl)-5-pyrazolone derivatives for the disproportionation of arylboronic acids.

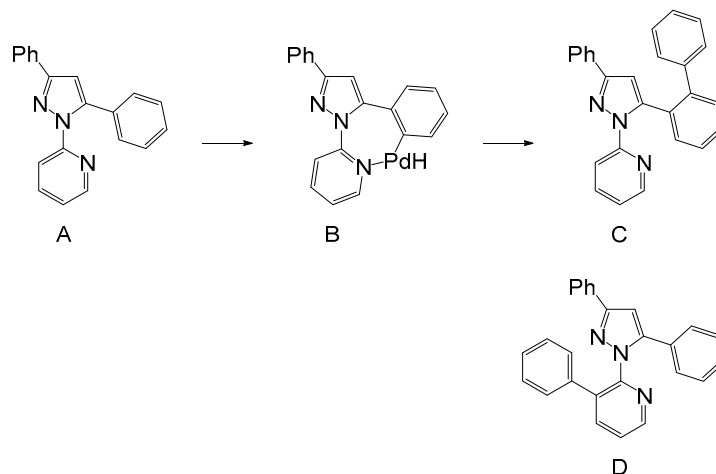
## 2. Results and Discussion

The starting pyrazolones **1a** and **2a** were prepared by the condensation of ethyl benzoylacetate with the corresponding hydrazines, respectively [9]. Pyrazole triflates **1b** and **2b** were made by treating the corresponding pyrazolones with trifluoromethanesulfonic anhydride and *N,N*-diisopropylethylamine, where chloroform is the best choice to achieve excellent chemoselectivity and high yield [10]. Suzuki–Miyaura cross-coupling of **1b** furnished the corresponding 5-phenylpyrazole **1c** in 85% yield, as shown in Scheme 1. When **2b** was used, however, an unknown product was observed in small amounts along with prolonged reaction times. The spectroscopic data apparently show the introduction of two phenyl groups into the entity, but still it was difficult to elucidate the molecular structure.



**Scheme 1.** Reagents and conditions: (i),  $\text{Tf}_2\text{O}$ , *i*- $\text{Pr}_2\text{NEt}$ ,  $\text{CHCl}_3$ , rt, 0.5 h; (ii),  $\text{PhB}(\text{OH})_2$  (3 eq),  $\text{PdCl}_2$  (dppf) (8 mol%), dppf (4 mol%),  $\text{K}_3\text{PO}_4$  (3 eq), dioxane, 100 °C, 1 h (for **1c**); 20 h (for **2c**).

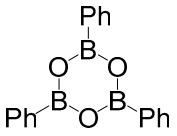
Initially, we assumed **2c** would be a biphenylated product (C) resulting from the C–H activation of a Suzuki product (A from **2b**) as the pyridine ring is known to act as a directing group via the formation of a six membered palladacycle (B), as illustrated in Scheme 2 [11]. In addition, a diarylated pyrazole (D) is conceivable, in which the pyrazole nitrogen serves as a transformable directing group, as documented in the Pd-catalyzed  $\text{sp}^2$  C–H functionalization of *N*-arylpyrazole [12]. However, the C–H activation was not the case for **2c** since this does not explain the most abundant peak observed at  $m/z = 401$ .



**Scheme 2.** Initially proposed structures for **2c**.

Next, we examined whether palladium catalysis was likely to exert influence on the disproportionation/dimerization of arylboronic acid, taking into account the detection of a palladium(II) species with a diarylborinate anion in the coupling reaction of aryl bromides with arylboronic acids catalyzed by the palladium complex [13]. Thus, in order to figure out what was really responsible for this transformation, negative control experiments were performed by the removal of each component from the reaction vessel one by one. The results are summarized in Table 1.

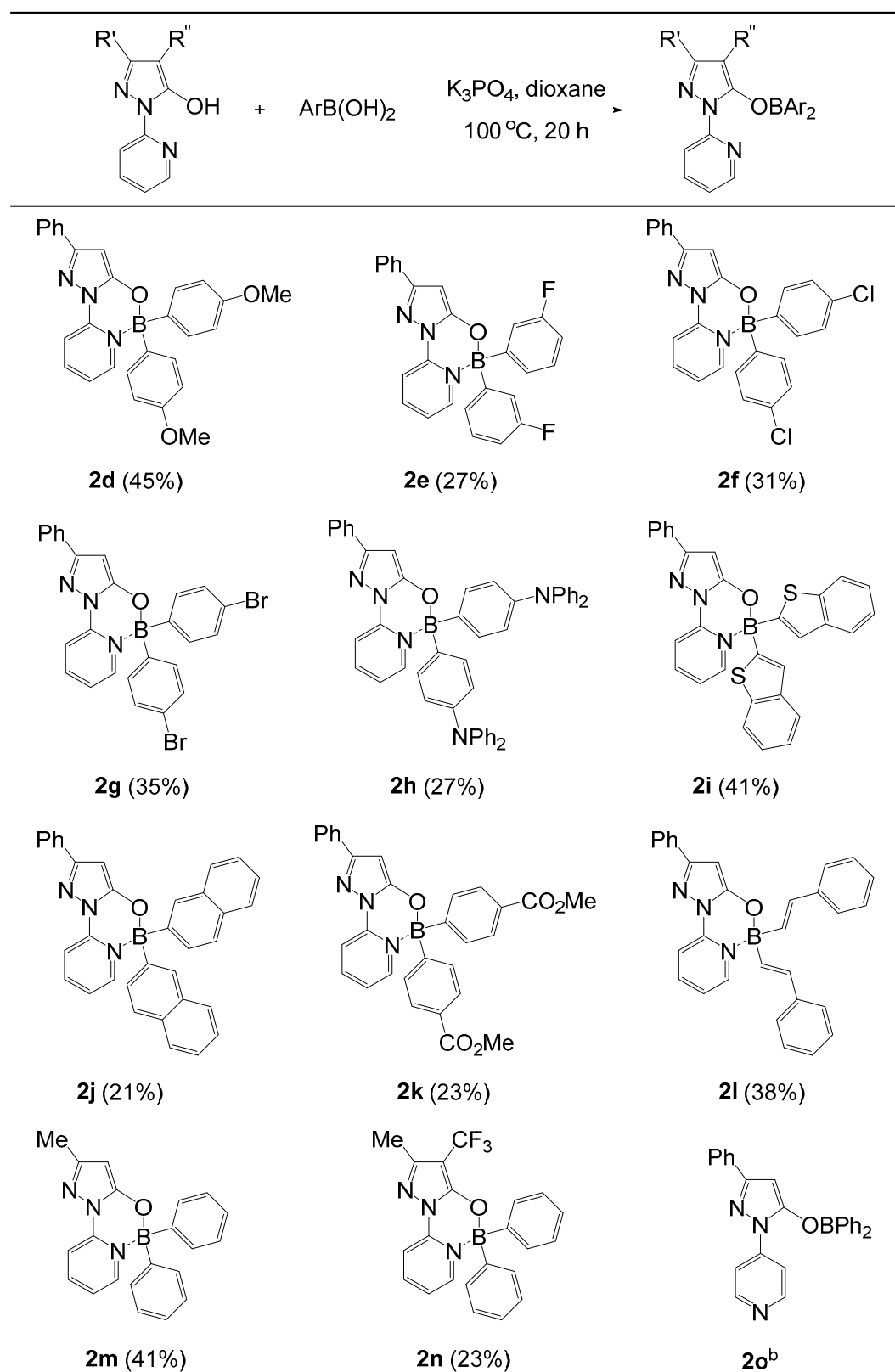
**Table 1.** Control experiments.

| Entry | Substrate <sup>a</sup> | Reaction Conditions <sup>b</sup>  | Product (Yield, %)  |
|-------|------------------------|---|---|
| 1     | <b>2b</b>              | PhB(OH) <sub>2</sub> , K <sub>3</sub> PO <sub>4</sub> , dioxane                     | <b>2c</b> (29)  |
| 2     | <b>2a</b>              | PhB(OH) <sub>2</sub> , K <sub>3</sub> PO <sub>4</sub> , dioxane                     | <b>2c</b> (37)  |
| 3     | <b>1a</b>              | PhB(OH) <sub>2</sub> , K <sub>3</sub> PO <sub>4</sub> , dioxane                     | - <sup>c</sup>  |
| 4     | <b>2a</b>              | PhB(OCMe <sub>2</sub> CMe <sub>2</sub> O), K <sub>3</sub> PO <sub>4</sub> , dioxane | - <sup>c</sup>  |
| 5     | <b>2a</b>              | PhB(OH) <sub>2</sub> , dioxane  | - <sup>c</sup>  |
| 6     | - <sup>d</sup>         | PhB(OH) <sub>2</sub> , K <sub>3</sub> PO <sub>4</sub> , dioxane                     | Ph <sub>2</sub> B(OH) +  <b>3a</b> (4%) <b>3b</b> (26%) <sup>e</sup> |
| 7     | <b>2a</b>              | <b>3a</b> , EtOH  | <b>2c</b> (81%)   |

<sup>a</sup> The structures shown in Scheme 1. <sup>b</sup> Unless otherwise indicated, the reaction conditions are as follows: substrate (1.0 mmol), boron reagent (3 eq), base (3 eq), solvent (10 mL), 100 °C, 20 h. <sup>c</sup> No reaction observed. <sup>d</sup> Without substrate. <sup>e</sup> See, Scheme 3.

When the reaction of **2b** was carried out without the palladium catalyst, this startlingly led to the same product (entry 1, Table 1). Furthermore, the use of the triflate was not a strict requirement for the transformation (entry 2). Subsequently, we ascertained that **2a** could be regenerated in the presence of a base from **2b**, presumably due to the hydrolytic instability of the triflate [14]. Another important feature was that there was no such indication from **1a** (entry 3). So far, nothing had changed when phenylboronic acid pinacol ester was used with **2a**, and the reaction was performed without the base (entries 4 and 5). To ensure a reliable formation of diarylborinate species, as the phenylboronic acid and the base were simply heated, we were able to isolate diphenylborinic acid **3a** and triphenylboroxin **3b** (entry 6). However, this could not be observed without the base. These observations demonstrate that base-induced disproportionation of boronic acids can also occur even without a chelate ligand, but will produce **3a** in lower grade. The final installation was undertaken to confirm the structure of **2c** (entry 7) by employing the reaction with diphenylborinic acid [15].

We explored the scope of the method by varying the boronic acids with different pyrazole substrates illustrated in Table 2. The reactions with 4-methoxy, 3-fluoro, 4-chloro, 4-bromo and 4-(*N,N*-diphenylamino)phenylboronic acid continually gave the products **2d–2h** in moderate yields, respectively. There were no noticeable effects with the electronic influence of boronic acid substituents. 2-Benzothienylboronic acid afforded the product **2i** at 41% yield without any issue, while 2-naphthylboronic acid afforded **2j** at 21% yield, suggesting that there was a steric effect in this transformation. Noticeably, boronic acids with sensitive functional groups such as ester (**2k**, 23%) and styrene (**2l**, 38%) were properly operated.

**Table 2.** Scope of boronic acids and pyrazole substrates <sup>a</sup>.

<sup>a</sup> Reaction conditions: pyrazole substrate (1 mmol), ArB(OH)<sub>2</sub> (3 eq), K<sub>3</sub>PO<sub>4</sub> (3 eq), dioxane (10 mL), 100 °C, 20 h; where R' = Ph, Me, R'' = H, CF<sub>3</sub>. <sup>b</sup> Not observed.

We then extended the scope of the pyrazole substrates with different substituents, such as 3-methyl and 4-trifluoromethylpyrazole, which gave **2m** (41%) and **2n** (23%), respec-

tively. Meanwhile, there was no such indication again with *N*-(4-pyridinyl)pyrazole (**2o**), indicating that *[N,O]*-bidentation is inarguably the most fundamental feature. With these results, we can deduce that *N*-(2-pyridinyl)pyrazole is stabilized by an intramolecular hydrogen bond and, thus, exists in a *syn*-periplanar orientation, which is well adjusted to accommodate an incoming boronic acid.

We primarily revealed that palladium catalysis has no role in the formation of the product. The use of unprotected boronic acid and a base is vital, and the presence of *[N,O]*-bidentate ligand seems to be the crucial structural requisite for this transformation. Previously, we reported that **1a** remains as it stands, whereas **2a** exclusively exists in the enol-form [2], and the X-ray crystal structure clearly shows that the carbonyl oxygen and pyridine nitrogen adopt an almost *syn*-periplanar arrangement that is capable of accommodating intramolecular hydrogen bonding.

Pleasingly, we were able to obtain a single crystal and determine the structure of **2c** as a six-membered pyrazole diphenylborinate complex (Figure 1). Single crystals suitable for X-ray diffraction were prepared by slow evaporation of a solution in ethyl acetate at room temperature. It is noteworthy that the crystal structure exhibited a pseudo-tetrahedral geometry around the boron center linked to two phenyl groups and with a *[N,O]*-bidentate chelating ligand. In addition, there was a broad singlet centered at 7.81 ppm in the  $^{11}\text{B}$  NMR spectrum of **2c**.

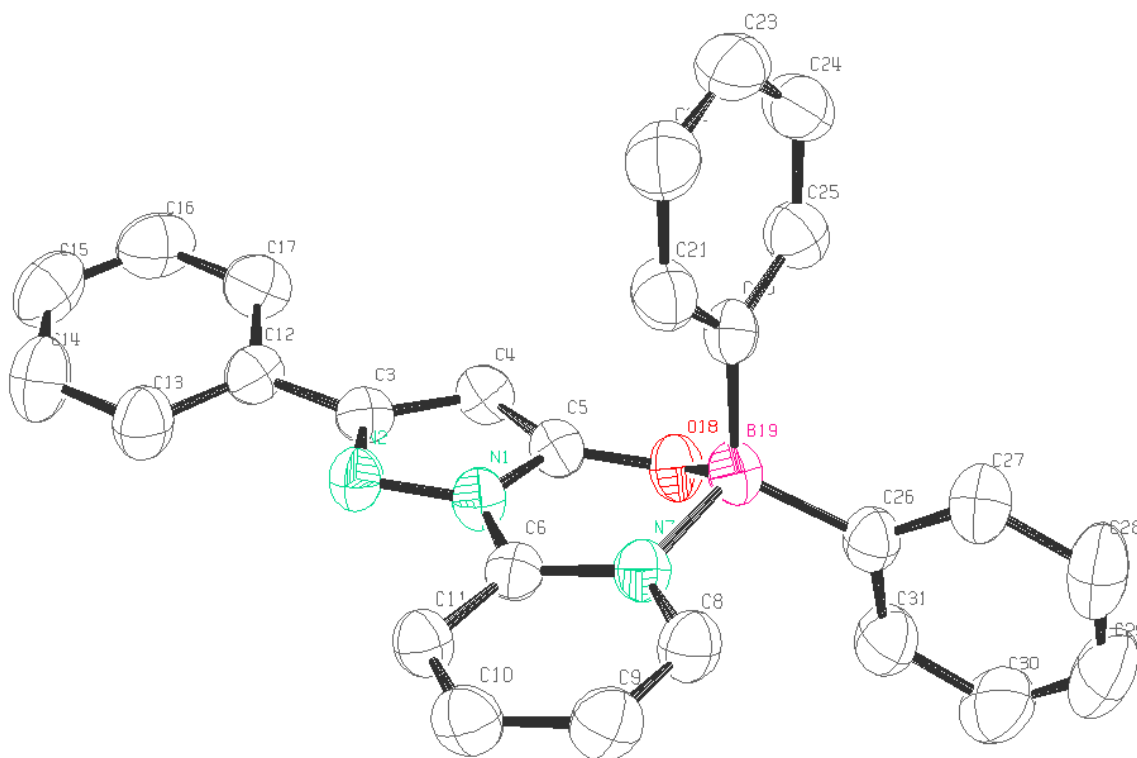


Figure 1. The crystal structure of **2c**.

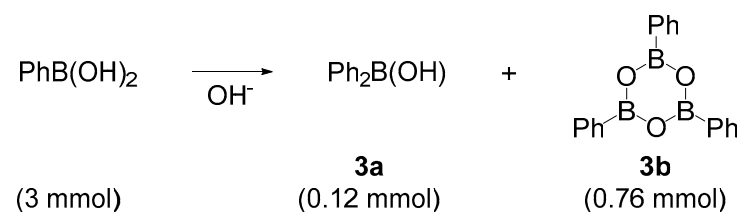
Single-crystal X-ray diffractions were measured on a Bruker APEX-II CCD diffractometer equipped with a monochromatic Mo-K $\alpha$  radiation ( $\lambda = 0.71073 \text{ \AA}$ ). The data were collected at a low temperature of 100 K by the  $\varphi$ - $\omega$  scan method. The collected data were integrated using Bruker-S SAINT software and an absorption correction was not applied. The structure was solved and refined through the least-squares method with the SHELXT and SHELXL program, respectively. All the non-hydrogen atoms were refined anisotropically and hydrogen atoms were placed in calculated positions. Table 3 presents the crystallographic data and structural refinements. Atomic coordinates and crystallo-

graphic parameters for **2c** were deposited at the Cambridge Crystallographic Data Centre (DOI: 10.5517/ccdc.csd.cc28yrgg, CCDC number: 2113966).

**Table 3.** Crystallographic data of **2c**.

| Crystal Data                     |  |   |
|----------------------------------|--|---|
| $C_{26}H_{20}BN_3O$              | $c = 11.2162 (1) \text{ \AA}$                  | $Z = 2$                                   |
| $Mr = 401.26$                    | $\alpha = 78.966 (1)^\circ$                    | Mo $K\alpha$ radiation                    |
| Triclinic, P1                    | $\beta = 81.795 (1)^\circ$                     | $\mu = 0.08 \text{ mm}^{-1}$              |
| $a = 9.7309 (1) \text{ \AA}$     | $\gamma = 79.993 (1)^\circ$                    | $T = 296 \text{ K}$                       |
| $b = 9.8830 (1) \text{ \AA}$     | $V = 1035.91 (2) \text{ \AA}^3$                | $0.44 \times 0.31 \times 0.23 \text{ mm}$ |
| Data Collection                  |  |   |
| Bruker APEXII CCD diffractometer | 5044 independent reflections                   |   |
| 19,866 measured reflections      | 3923 reflections with $I > 2\sigma(I)$         |   |
| Refinement                       |  |   |
| $R[F^2 > 2\sigma(F^2)] = 0.041$  | 280 parameters                                 |   |
| $wR(F^2) = 0.106$                | H-atom parameters constrained                  |   |
| $S = 1.03$                       | $\Delta\rho_{\max} = 0.21 \text{ e \AA}^{-3}$  |   |
| 5044 reflections                 | $\Delta\rho_{\min} = -0.19 \text{ e \AA}^{-3}$ |   |

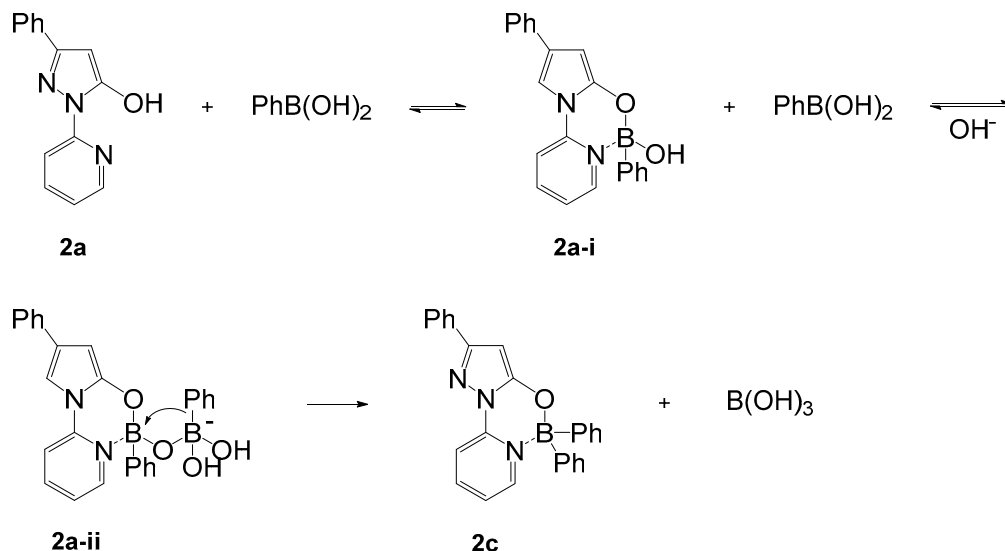
Although a number of possible explanations can be advanced for such a unique transformation, we probed that the disproportionation of arylboronic acid could be induced by the base, with or without a bidentate ligand. Firstly, when 3 mmol of phenylboronic acid and 3 mmol of potassium phosphate were simply heated without ligand, we were able to isolate 0.12 mmol of diphenylboronic acid **3a** along with triphenylboroxin **3b**, as depicted in Scheme 3. This observation demonstrates that base-induced disproportionation of boronic acids is possible even without a chelate ligand, but will produce **3a** with a lower efficiency. Meanwhile, in the presence of a bidentate ligand, the base-promoted disproportionation of arylboronic acid was accelerated, and thus, the formation of pyrazole diarylborinate occurred (entries 2 and 6, Table 1).



**Scheme 3.** Disproportionation of phenylboronic acid (entry 6, Table 1).

Based on the experimental considerations, we propose a plausible mechanism for the formation of the four-coordinate boron species facilitated by the assistance of the [N,O]-bidentate ligand, which enabled the aryl group migration between boronic acids, as illustrated in Scheme 4. We were aware that **2a** as the enol could be modulated by its complexation to phenylboronic acid (**2a-i**). Accordingly, a recent report revealed that boronic acids can disrupt the intramolecular proton transfer fluorescence through complexation with 10-hydroxybenzo[*h*]quinolone by disrupting the intramolecular hydrogen bond [16]. Considering the thermodynamics of boronic acids, entropically favorable dimeric anhydride or trimeric aggregate might be involved in this transformation [17]. Particularly, the Petasis borono–Mannich reaction [18] has been extensively studied, in which the boronic acids act as organic group donors under metal-free transition conditions, and protodeboronation [19] and boron-to-heteroatom migration [20] have also been utilized via boronate complexes derived from different types of boronic anhydride species. The base may be required to drive the initial equilibrium sufficiently toward the ‘ate’ complex (**2a-ii**)

so that boron-to-boron migration is feasible. The ‘ate’ complex is believed to be able to transfer the organic group from the anionic boron center onto a nearby electron-deficient  $sp^2$  boron through a boronic anhydride assembly.



**Scheme 4.** A plausible mechanism for the formation of **2c** induced by [N,O]-bidentate ligation.

### 3. Materials and Methods

#### 3.1. Generals

All solvents and reagents were purchased from commercial sources and used as received without further purification, unless otherwise stated. Tripotassium phosphate was crushed in mortar and dried at 70 °C in oven overnight and used. Reactions were monitored by thin layer chromatography carried out on S-2 0.25 mm E. Merck silica gel plates (60F-254, Darmstadt, Germany) using UV light as the visualizing agent and an acidic mixture of anisaldehyde or a ninhydrin solution in ethanol and heat as developing agents. E. Merck silica gel (60, particle size 0.040–0.063 mm) was used for flash column chromatography. All yields were calculated from isolated products. All NMR spectra were recorded on Bruker AV-500 instrument.  $^1\text{H}$  and  $^{13}\text{C}$  NMR spectra were referenced internally to the residual undeuterated chloroform ( $\delta_{\text{H}} = 7.26$  ppm and  $\delta_{\text{C}} = 77.0$  ppm).  $^{11}\text{B}$  NMR spectra were referenced externally to  $\text{BF}_3 \cdot \text{OEt}_2$ . The  $^{11}\text{B}$  NMR experiments were done with quartz NMR tubes (Wilmad). The NMR data were analyzed using MNova 10.0 processing software (version: MNova 14.1.0) (Mestrelab Research). The following abbreviations are used to designate multiplicities: s = singlet, d = doublet, t = triplet, q = quartet, quint = quintet, m = multiplet, br s = broad singlet. Chemical shifts are reported in ppm and coupling constants are in Hertz (Hz). High resolution mass spectra using Electronic Ionization (HRMS-EI) were recorded on Joel JMS-700 mass spectrometer. The data for X-ray structure determination were collected on Bruker SMART Apex II X-ray diffractometer equipped with graphite-monochromated  $\text{MoK}\alpha$  radiation ( $\lambda = 0.71073$  Å). The  $^1\text{H}$  and  $^{13}\text{C}$  NMR spectra for all compounds **2c–2n** prepared in this study are in Supplementary Materials.

#### 3.2. Representative Procedure for the Synthesis of Four-Coordinate Boron Complexes

A solution of **2a** (237.3 mg, 1.0 mmol),  $\text{PhB(OH)}_2$  (365.8 mg, 3.0 mmol) and  $\text{K}_3\text{PO}_4$  (636.8 mg, 3.0 mmol) in 1,4-dioxane (10 mL) was heated to reflux at 100 °C for 20 h. Subsequently, the solvent was removed by evaporation and the crude was extracted with  $\text{EtOAc}$  ( $2 \times 10$  mL). The organic layer was washed with saturated  $\text{NaHCO}_3$  and brine, and dried over anhydrous sodium sulfate. The solvent was removed under vacuum and the



residue was purified by column chromatography on silica gel (hexane/EtOAc = 7/1) to give **2c** (148.5 mg, 37% yield).

2-(5-((Diphenylboryl)oxy)-3-phenyl-1*H*-pyrazol-1-yl)pyridine (**2c**).

Yield: 37%; <sup>1</sup>H NMR (500 MHz, CDCl<sub>3</sub>): δ<sub>H</sub> 8.18–8.04 (m, 2H), 7.93 (dd, *J* = 6.2, 1.6 Hz, 1H), 7.87–7.78 (m, 2H), 7.44–7.34 (m, 3H), 7.32–7.21 (m, 11H), 5.98 (s, 1H) ppm; <sup>13</sup>C NMR (125 MHz, CDCl<sub>3</sub>): δ<sub>C</sub> 157.06, 156.6, 147.0, 143.0, 142.1, 133.0, 132.5, 129.1, 128.6, 127.6, 127.2, 126.0, 119.3, 113.4, 86.6 ppm; <sup>11</sup>B NMR (160 MHz, CDCl<sub>3</sub>): δ<sub>B</sub> 7.81 ppm; HRMS-EI *m/z* [M]<sup>+</sup> calcd for C<sub>26</sub>H<sub>20</sub>N<sub>3</sub>O, 401.1699, found 401.1692.

Atomic coordinates and crystallographic parameters for **2c** has been deposited at the Cambridge Crystallographic Data Center (DOI: 10.5517/ccdc.csd.cc28yrgg, CCDC number: 2113966). These data can be obtained free of charge from the Cambridge Crystallographic Data Center via [www.ccdc.cam.ac.uk/data\\_request/cif](http://www.ccdc.cam.ac.uk/data_request/cif) (accessed on 9 November 2021).

2-(5-((Bis(4-methoxyphenyl)boryl)oxy)-3-phenyl-1*H*-pyrazol-1-yl)pyridine (**2d**).

Yield: 45%; <sup>1</sup>H NMR (500 MHz, CDCl<sub>3</sub>): δ<sub>H</sub> 8.15 (m, 2H), 7.96 (d, *J* = 5.4 Hz, 1H), 7.85 (d, *J* = 7.05 Hz, 2H), 7.45–7.38 (m, 3H), 7.26–7.22 (m, 5H), 6.84 (d, *J* = 8.45 Hz, 4H), 5.98 (s, 1H), 3.79 (s, 6H) ppm; <sup>13</sup>C NMR (125 MHz, CDCl<sub>3</sub>): δ<sub>C</sub> 158.9, 156.9, 156.7, 147.0, 142.8, 142.0, 134.2, 132.6, 129.1, 128.6, 126.0, 119.2, 113.3, 113.2, 86.5, 55.0 ppm; HRMS (EI) *m/z* [M + H]<sup>+</sup> calcd for C<sub>28</sub>H<sub>24</sub>N<sub>3</sub>O<sub>3</sub>B, 461.1911, found 461.1911.

2-(5-((Bis(3-fluorophenyl)boryl)oxy)-3-phenyl-1*H*-pyrazol-1-yl)pyridine (**2e**).

Yield: 27%; <sup>1</sup>H NMR (500 MHz, CDCl<sub>3</sub>): δ<sub>H</sub> 8.16 (dd, *J* = 15.8, 7.7 Hz, 2H), 7.89 (dd, *J* = 16.3, 6.1 Hz, 3H), 7.44 (dt, *J* = 13.8, 6.9 Hz, 3H), 7.28 (dd, *J* = 13.6, 7.1 Hz, 3H), 7.06 (d, *J* = 7.2 Hz, 2H), 6.97 (dd, *J* = 14.9, 9.1 Hz, 4H), 6.04 (s, 1H) ppm; <sup>13</sup>C NMR (126 MHz, CDCl<sub>3</sub>): δ<sub>C</sub> 163.9, 161.98, 157.3, 156.2, 146.8, 143.5, 141.7, 132.3, 129.37 (d, *J* = 7.6 Hz), 128.68, 128.37 (d, *J* = 1.9 Hz), 126.1, 119.59, 119.2 (d, *J* = 18.2 Hz), 114.3 (d, *J* = 21.0 Hz), 114.18, 114.0, 113.7, 86.80 ppm; HRMS-EI *m/z* [M]<sup>+</sup> calcd for C<sub>26</sub>H<sub>18</sub>BF<sub>2</sub>N<sub>3</sub>O 437.1511, found 437.1509.

2-(5-((Bis(4-chlorophenyl)boryl)oxy)-3-phenyl-1*H*-pyrazol-1-yl)pyridine (**2f**).

Yield: 31%; <sup>1</sup>H NMR (500 MHz, CDCl<sub>3</sub>): δ<sub>H</sub> 8.23–8.08 (m, 2H), 7.86 (d, *J* = 6.6 Hz, 3H), 7.52–7.38 (m, 3H), 7.25 (dd, *J* = 27.6, 8.1 Hz, 9H), 6.01 (s, 1H) ppm; <sup>13</sup>C NMR (126 MHz, CDCl<sub>3</sub>): δ<sub>C</sub> 157.3, 156.3, 146.9, 143.4, 141.6, 134.3, 133.5, 132.3, 129.3, 128.7, 127.9, 126.1, 119.6, 113.7, 86.7 ppm; HRMS-EI *m/z* [M]<sup>+</sup> calcd for C<sub>26</sub>H<sub>18</sub>BCl<sub>2</sub>N<sub>3</sub>O 469.0920, found 469.0927.

2-(5-((Bis(4-bromophenyl)boryl)oxy)-3-phenyl-1*H*-pyrazol-1-yl)pyridine (**2g**).

Yield: 35%; <sup>1</sup>H NMR (500 MHz, CDCl<sub>3</sub>): δ<sub>H</sub> 8.26–8.11 (m, 2H), 7.93–7.79 (m, 3H), 7.49–7.37 (m, 7H), 7.34–7.27 (m, 4H), 7.15 (d, *J* = 8.2 Hz, 4H), 5.99 (s, 1H) ppm; <sup>13</sup>C NMR (125 MHz, CDCl<sub>3</sub>): δ<sub>C</sub> 157.3, 156.2, 143.4, 141.6, 134.6, 130.8, 129.3, 128.7, 126.1, 119.5, 113.7, 86.7, 77.3, 77.0, 76.8 ppm; HRMS-EI *m/z* [M]<sup>+</sup> calcd for C<sub>26</sub>H<sub>18</sub>BBr<sub>2</sub>N<sub>3</sub>O 566.9910, found 566.9918.

4,4'-(((3-Phenyl-1-(pyridin-2-yl)-1*H*-pyrazol-5-yl)oxy)boranediyl)bis(*N,N*-diphenylaniline) (**2h**).

Yield: 27%; <sup>1</sup>H NMR (500 MHz, CDCl<sub>3</sub>): δ<sub>H</sub> 8.11 (dd, *J* = 14.0, 7.7 Hz, 1H), 8.06–7.96 (m, 1H), 7.86 (d, *J* = 7.8 Hz, 1H), 7.54–7.32 (m, 2H), 7.21 (ddd, *J* = 19.5, 10.9, 6.7 Hz, 8H), 7.07 (d, *J* = 8.3 Hz, 4H), 7.02–6.84 (m, 5H), 5.98 (d, *J* = 1.3 Hz, 1H) ppm; <sup>13</sup>C NMR (126 MHz, CDCl<sub>3</sub>): δ<sub>C</sub> 156.7, 147.9, 146.7, 142.9, 142.1, 133.8, 129.2, 129.0, 128.6, 126.0, 124.1, 123.2, 122.3, 119.2, 113.3, 86.6 ppm; HRMS-EI *m/z* [M]<sup>+</sup> calcd for C<sub>50</sub>H<sub>38</sub>N<sub>5</sub>O, 735.3169, found 735.3177.

2-(5-((Bis(benzo[*b*]thiophen-2-yl)boryl)oxy)-3-phenyl-1*H*-pyrazol-1-yl)pyridine (**2i**).

Yield: 41%; <sup>1</sup>H NMR (300 MHz, CDCl<sub>3</sub>): δ<sub>H</sub> 8.52 (dd, *J* = 1.26, 8.67 Hz, 1H), 8.29–8.19 (m, 2H), 7.94–7.86 (m, 4H), 7.80–7.76 (m, 2H), 7.66 (dd, *J* = 0.51, 7.08 Hz, 1H), 7.49–7.37 (m, 3H), 7.35–7.24 (m, 4H), 7.71 (s, 2H), 6.42 (s, 1H) ppm; <sup>13</sup>C NMR (125 MHz, CDCl<sub>3</sub>): δ<sub>C</sub> 156.3, 155.1, 146.6, 145.7, 142.3, 142.2, 141.2, 132.2, 129.9, 129.2, 129.1, 126.3, 124.4, 124.3, 123.8, 122.7, 122.5, 113.8, 87.3 ppm; HRMS (EI) *m/z* [M + H]<sup>+</sup> calcd for C<sub>30</sub>H<sub>20</sub>N<sub>3</sub>OS<sub>2</sub>B, 513.1141, found 513.1141.

2-(5-((Di(naphthalen-2-yl)boranetyl)oxy)-3-phenyl-1*H*-pyrazol-1-yl)pyridine (**2j**).

Yield: 21%; <sup>1</sup>H NMR (500 MHz, CDCl<sub>3</sub>): δ<sub>H</sub> 8.18 (d, *J* = 8.4 Hz, 1H), 8.10 (t, *J* = 7.3 Hz, 1H), 8.02 (d, *J* = 5.1 Hz, 1H), 7.84 (dd, *J* = 12.7, 7.1 Hz, 6H), 7.77–7.67 (m, 4H), 7.61 (d, *J* = 8.1 Hz, 2H), 7.49–7.36 (m, 7H), 7.22 (t, *J* = 6.1 Hz, 1H), 6.07 (s, 1H) ppm; <sup>13</sup>C NMR

(126 MHz, CDCl<sub>3</sub>):  $\delta_C$  157.2, 156.7, 147.1, 143.2, 142.1, 133.2, 132.8, 132.5, 130.6, 129.2, 128.6, 128.1, 127.6, 127.0, 126.1, 125.5, 119.4, 113.5, 86.7 ppm; HRMS-EI  $m/z$  [M]<sup>+</sup> calcd for C<sub>34</sub>H<sub>24</sub>BN<sub>3</sub>O 501.2012, found 501.2019.

Dimethyl 4,4'-(((3-phenyl-1-(pyridin-2-yl)-1H-pyrazol-5-yl)oxy)boranediyloxy)dibenzoate (**2k**).

Yield: 23%; <sup>1</sup>H NMR (500 MHz, CDCl<sub>3</sub>):  $\delta_H$  8.17–8.04 (m, 2H), 7.93 (dd,  $J$  = 6.2, 1.6 Hz, 1H), 7.87–7.78 (m, 2H), 7.44–7.34 (m, 2H), 7.32–7.21 (m, 11H), 5.98 (s, 1H), 3.87 (s, 6H) ppm; <sup>13</sup>C NMR (125 MHz, CDCl<sub>3</sub>):  $\delta_C$  165.9, 160.0, 150.4, 145.1, 142.8, 139.3, 133.3, 130.1, 129.9, 129.2, 127.5, 121.4, 112.4, 86.8, 51.5 ppm; HRMS-EI  $m/z$  [M]<sup>+</sup> calcd for C<sub>30</sub>H<sub>24</sub>N<sub>3</sub>O<sub>5</sub>B, 517.1809, found 517.1813.

2-(5-((Di((E)-styryl)boraneyloxy)-3-phenyl-1H-pyrazol-1-yl)pyridine (**2l**).

Yield: 38%; <sup>1</sup>H NMR (300 MHz, CDCl<sub>3</sub>):  $\delta_H$  8.31 (d,  $J$  = 5.73 Hz, 1H), 8.16–8.06 (m, 2H), 7.88–7.85 (m, 2H), 7.46–7.35 (m, 6H), 7.32–7.27 (m, 6H), 7.20–7.15 (m, 2H), 6.71–6.63 (m, 4H), 5.96 (s, 1H) ppm; <sup>13</sup>C NMR (125 MHz, CDCl<sub>3</sub>):  $\delta_C$  156.9, 156.1, 146.8, 142.8, 141.3, 139.2, 139.0, 132.6, 129.1, 128.6, 128.3, 127.1, 126.3, 126.1, 119.7, 113.3, 86.35 ppm; HRMS (EI)  $m/z$  [M + H]<sup>+</sup> calcd for C<sub>30</sub>H<sub>24</sub>N<sub>3</sub>OB, 453.2012, found 453.2017.

2-(5-((Diphenylboraneyloxy)-3-methyl-1H-pyrazol-1-yl)pyridine (**2m**).

Yield: 41%; <sup>1</sup>H NMR (500 MHz, CDCl<sub>3</sub>):  $\delta_H$  8.07–8.04 (m, 2H), 7.91 (dd,  $J$  = 6.2, 1.6 Hz, 1H), 7.32–7.21 (m, 11H), 5.98 (s, 1H), 2.34 (s, 3H) ppm; <sup>13</sup>C NMR (125 MHz, CDCl<sub>3</sub>):  $\delta_C$  159.9, 150.4, 149.7, 139.3, 138.5, 133.4, 128.7, 121.4, 112.4, 91.2, 16.5 ppm; HRMS-EI  $m/z$  [M]<sup>+</sup> calcd for C<sub>21</sub>H<sub>18</sub>N<sub>3</sub>OB, 339.1543, found 339.1552.

2-(5-((Diphenylboraneyloxy)-3-methyl-4-(trifluoromethyl)-1H-pyrazol-1-yl)pyridine (**2n**).

Yield: 23%; <sup>1</sup>H NMR (500 MHz, CDCl<sub>3</sub>): <sup>1</sup>H NMR (500 MHz, CDCl<sub>3</sub>):  $\delta_H$  8.21–8.13 (m, 1H), 8.10 (d,  $J$  = 8.3 Hz, 1H), 8.02–7.95 (m, 1H), 7.41–7.34 (m, 1H), 7.32–7.21 (m, 10H), 2.12 (s, 3H). <sup>13</sup>C NMR (126 MHz, CDCl<sub>3</sub>):  $\delta_C$  153.8, 146.5, 143.5, 142.5, 132.8, 127.7, 127.4, 122.2, 120.8, 120.0, 113.6, 96.3, 5.78 ppm; HRMS-EI  $m/z$  [M]<sup>+</sup> calcd for, C<sub>22</sub>H<sub>17</sub>BF<sub>3</sub>N<sub>3</sub>O 407.1417, found 407.1411.

#### 4. Conclusions

In this study, we found a simple, mild, transition metal-free method for the preparation of four-coordinate organoboron complexes, and also discussed on the key components and the structural requirements that enable such a boron-to-boron migration. While the use of unprotected boronic acid and a base is essential, the presence of [N,O]-bidentate ligand appeared to be the key structural requirements for this transformation. Based on the control experiments, the results support that four-coordinate boron species derived from the [N,O]-bidentate ligand **2a** favor the formation of diarylboronic acid and/or disproportionation of arylboronic acid via the action of the base. The *syn*-periplanar arrangement of the [N,O]-bidentate ligand was found to be crucial. It was well organized to accommodate an incoming boronic acid, and thus, to enable to aryl group migration between boronic acids, presumably via a boronic anhydride species. Overall, the present method is particularly important in preparing four-coordinate organoboron species to ensure a completely efficient assembly of multi-component structures in a single operation. Experiments to obtain a deeper understanding of its mechanism and applications are currently underway.

**Supplementary Materials:** The following are available online. Online supplementary information contains <sup>1</sup>H and <sup>13</sup>C NMR spectra for all compounds **2c–2n** prepared in this study (**Figures S1, S2 and S4–S25**), and 11B NMR of **2c** (**Figure S3**). CCDC 2113966 contains atomic coordinates and crystallographic parameters for **2c** and these data can be obtained free of charge from the Cambridge Crystallographic Data Centre via <http://www.ccdc.cam.ac.uk/conts/retrieving.html>, accessed on 2 November 2021.

**Author Contributions:** Conceptualization, V.S.S. and K.-I.L.; synthesis and formal analysis, J.C. and V.S.S. and Y.H.; X-ray crystal study, V.S.S.; investigation, J.C., V.S.S. and K.-I.L.; biological validation, Y.B. and H.L.; writing—original draft preparation, J.C. and V.S.S.; writing—review and editing, K.-I.L. All authors have read and agreed to the published version of the manuscript.

**Funding:** This research was funded by National Research Foundation of Korea (Grant number: NRF-2017M1A2A2049100).

**Institutional Review Board Statement:** Not applicable.

**Informed Consent Statement:** Not applicable.

**Data Availability Statement:** The data presented in this study are available on request from the corresponding authors.

**Conflicts of Interest:** The authors declare no conflict of interest. The funders had no role in the design of the study; in the collection, analyses, or interpretation of data; in the writing of the manuscript, or in the decision to publish the results.

**Sample Availability:** Samples of the compounds are available from the authors.

## References

- Karrouchi, K.; Radi, S.; Ramli, Y.; Taoufik, J.; Mabkhot, Y.N.; Al-aizari, F.A.; Ansar, M. Synthesis and Pharmacological Activities of Pyrazole Derivatives: A Review. *Molecules* **2018**, *23*, 134. [CrossRef] [PubMed]
- Bin, H.-R.; Bae, Y.S.; Kim, G.; Lee, K.-I. Palladium-Catalyzed Peripheral Arylation of 5-Pyrazolones via Enolizable Bond Protection. *Synthesis* **2011**, *11*, 1783–1791.
- Joo, J.H.; Huh, J.E.; Lee, J.H.; Park, D.R.; Lee, Y.; Lee, S.G.; Choi, S.; Lee, H.J.; Song, S.W.; Jeong, Y.; et al. A novel pyrazole derivative protects from ovariectomy-induced osteoporosis through the inhibition of NADPH oxidase. *Sci. Rep.* **2016**, *6*, 22389. [CrossRef] [PubMed]
- Lee, S.G.; Lee, J.; Kim, K.M.; Lee, K.-I.; Bae, Y.S.; Lee, H.J. Pharmacokinetic Study of NADPH Oxidase Inhibitor Ewha-18278, a Pyrazole Derivative. *Pharmaceutics* **2019**, *11*, 482. [CrossRef] [PubMed]
- Sadu, V.S.; Choi, Y.M.; Kamma, K.R.; Kim, C.H.; Bae, Y.S.; Lee, K.-I. Crystal structure determination of *N*- and *O*-alkylated tautomers of 1-(2-pyridinyl)-5-hydroxypyrazole. *J. Mol. Struct.* **2020**, *1215*, 128272. [CrossRef]
- Nagata, Y.; Chujo, Y. Main-chain-type organoboron quinolate polymers: Synthesis and photoluminescence properties. *Macromolecules* **2007**, *40*, 6–8. [CrossRef]
- Marciasini, L.; Cacciuttolo, B.; Vaultier, M.; Pucheault, M. Synthesis of borinic acids and borinate adducts using diisopropylaminoborane. *Org. Lett.* **2015**, *17*, 3532–3535. [CrossRef] [PubMed]
- Frath, D.; Massue, J.; Ulrich, G.; Ziessel, R. Luminescent materials: Locking  $\pi$ -conjugated and heterocyclic ligands with boron (III). *Angew. Chem. Int. Ed.* **2014**, *53*, 2290–2310. [CrossRef] [PubMed]
- Huang, Y.-Y.; Lin, H.-C.; Cheng, K.-M.; Su, W.-N.; Sung, K.-C.; Lin, T.-P.; Huang, J.-J.; Lin, S.-K.; Wong, F.F. Efficient di-bromination of 5-pyrazolones and 5-hydroxypyrazoles by *N*-bromobenzamide. *Tetrahedron* **2009**, *65*, 9592–9597. [CrossRef]
- Dvorak, C.A.; Rudolph, D.A.; Ma, S.; Carruthers, N.I. Palladium-Catalyzed Coupling of Pyrazole Triflates with Arylboronic Acids. *J. Org. Chem.* **2005**, *70*, 4188–4190. [CrossRef] [PubMed]
- Lyons, T.W.; Sanford, M.S. Palladium-Catalyzed Ligand-Directed C–H Functionalization Reactions. *Chem. Rev.* **2010**, *110*, 1147–1169. [CrossRef] [PubMed]
- Kwak, S.H.; Gulia, N.; Daugulis, O. Synthesis of Unsymmetrical 2,6-Diarylanilines by Palladium-Catalyzed C–H Bond Functionalization Methodology. *J. Org. Chem.* **2018**, *83*, 5844–5850. [CrossRef] [PubMed]
- Crociani, B.; Antonaroli, S.; Marini, A.; Matteoli, U.; Scrivanti, A. Mechanistic study on the coupling reaction of aryl bromides with arylboronic acids catalyzed by (iminophosphine)palladium(0) complexes. Detection of a palladium(ii) intermediate with a coordinated boron anion. *Dalton Trans.* **2006**, *22*, 2698–2705. [CrossRef] [PubMed]
- Dhakal, B.; Bohé, L.; Crich, D. Trifluoromethanesulfonate Anion as Nucleophile in Organic Chemistry. *J. Org. Chem.* **2017**, *82*, 9263–9269. [CrossRef] [PubMed]
- Hagen, H.; Reinoso, S.; Albrecht, M.; Boersma, J.; Spek, A.L.; van Koten, G. *O,N*-Chelated boron aminophenolate complexes. Crystal structure of BPh<sub>2</sub>(OC<sub>6</sub>H<sub>4</sub>(CH<sub>2</sub>NMe<sub>2</sub>)-2). *J. Organomet. Chem.* **2000**, *608*, 27–33.
- Aronoff, M.R.; VanVeller, B.; Raines, R.T. Detection of Boronic acids through excited-state intramolecular proton-transfer fluorescence. *Org. Lett.* **2013**, *15*, 5382–5385. [CrossRef] [PubMed]
- Chaudhari, S.R. Screening and assignment of phenylboronic acid and its anhydride formation by NMR spectroscopy. *Chem. Phys. Lett.* **2015**, *634*, 95–97. [CrossRef]
- Candeias, N.R.; Montalbano, F.; Cal, P.M.S.D.; Gois, P.M.P. Boronic Acids and Esters in the Petasis-Borono Mannich Multicomponent Reaction. *Chem. Rev.* **2010**, *110*, 6169–6193. [CrossRef]
- Noonan, G.; Leach, A.G. A mechanistic proposal for the protodeboronation of neat boronic acids: Boronic acid mediated reaction in the solid state. *Org. Biomol. Chem.* **2015**, *13*, 2555–2560. [CrossRef]
- Voth, S.; Hollett, J.W.; McCubbin, J.A. Transition-Metal-Free Access to Primary Anilines from Boronic Acids and a Common <sup>+</sup>NH<sub>2</sub> Equivalent. *J. Org. Chem.* **2015**, *80*, 2545–2553. [CrossRef] [PubMed]

Article

# Synthesis and Antiproliferative Activity of 2,4,6,7-Tetrasubstituted-2*H*-pyrazolo[4,3-*c*]pyridines

Beatričė Razmienė <sup>1,2</sup> , Eva Řezníčková <sup>3</sup>, Vaida Dambrauskienė <sup>1</sup>, Radek Ostruszka <sup>4</sup> , Martin Kubala <sup>4</sup> , Asta Žukauskaitė <sup>5,\*</sup> , Vladimír Kryštof <sup>3,6</sup> , Algirdas Šačkus <sup>1,2</sup> and Eglė Arbačiauskienė <sup>1,\*</sup> 

- <sup>1</sup> Department of Organic Chemistry, Kaunas University of Technology, Radvilėnų pl. 19, LT-50254 Kaunas, Lithuania; beatrice.razmiene@ktu.lt (B.R.); laukaityte.vaida@gmail.com (V.D.); algirdas.sackus@ktu.lt (A.Š.)
- <sup>2</sup> Institute of Synthetic Chemistry, Kaunas University of Technology, K. Baršausko g. 59, LT-51423 Kaunas, Lithuania
- <sup>3</sup> Department of Experimental Biology, Palacký University, Šlechtitelů 27, CZ-78371 Olomouc, Czech Republic; eva.reznickova@upol.cz (E.Ř.); vladimir.krystof@upol.cz (V.K.)
- <sup>4</sup> Department of Experimental Physics, Faculty of Science, Palacký University, 17. Listopadu 12, CZ-77146 Olomouc, Czech Republic; radek.ostruszka@upol.cz (R.O.); martin.kubala@upol.cz (M.K.)
- <sup>5</sup> Department of Chemical Biology, Palacký University, Šlechtitelů 27, CZ-78371 Olomouc, Czech Republic
- <sup>6</sup> Institute of Molecular and Translational Medicine, Faculty of Medicine and Dentistry, Palacký University, Hněvotínská 5, CZ-77900 Olomouc, Czech Republic
- \* Correspondence: asta.zukauskaite@upol.cz (A.Ž.); egle.arbaciauskiene@ktu.lt (E.A.)

**Abstract:** A library of 2,4,6,7-tetrasubstituted-2*H*-pyrazolo[4,3-*c*]pyridines was prepared from easily accessible 1-phenyl-3-(2-phenylethynyl)-1*H*-pyrazole-4-carbaldehyde via an iodine-mediated electrophilic cyclization of intermediate 4-(azidomethyl)-1-phenyl-3-(phenylethynyl)-1*H*-pyrazoles to 7-iodo-2,6-diphenyl-2*H*-pyrazolo[4,3-*c*]pyridines followed by Suzuki cross-couplings with various boronic acids and alkylation reactions. The compounds were evaluated for their antiproliferative activity against K562, MV4-11, and MCF-7 cancer cell lines. The most potent compounds displayed low micromolar GI<sub>50</sub> values. 4-(2,6-Diphenyl-2*H*-pyrazolo[4,3-*c*]pyridin-7-yl)phenol proved to be the most active, induced poly(ADP-ribose) polymerase 1 (PARP-1) cleavage, activated the initiator enzyme of apoptotic cascade caspase 9, induced a fragmentation of microtubule-associated protein 1-light chain 3 (LC3), and reduced the expression levels of proliferating cell nuclear antigen (PCNA). The obtained results suggest a complex action of 4-(2,6-diphenyl-2*H*-pyrazolo[4,3-*c*]pyridin-7-yl)phenol that combines antiproliferative effects with the induction of cell death. Moreover, investigations of the fluorescence properties of the final compounds revealed 7-(4-methoxyphenyl)-2,6-diphenyl-2*H*-pyrazolo[4,3-*c*]pyridine as the most potent pH indicator that enables both fluorescence intensity-based and ratiometric pH sensing.

**Keywords:** antiproliferation; cell death; cross-coupling; cycloiodination; pyrazole; pyridine

**Citation:** Razmienė, B.; Řezníčková, E.; Dambrauskienė, V.; Ostruszka, R.; Kubala, M.; Žukauskaitė, A.; Kryštof, V.; Šačkus, A.; Arbačiauskienė, E. Synthesis and Antiproliferative Activity of 2,4,6,7-Tetrasubstituted-2*H*-pyrazolo[4,3-*c*]pyridines. *Molecules* **2021**, *26*, 6747. <https://doi.org/10.3390/molecules26216747>

Academic Editors: Vera L. M. Silva and Artur M. S. Silva

Received: 18 October 2021

Accepted: 4 November 2021

Published: 8 November 2021

**Publisher's Note:** MDPI stays neutral with regard to jurisdictional claims in published maps and institutional affiliations.

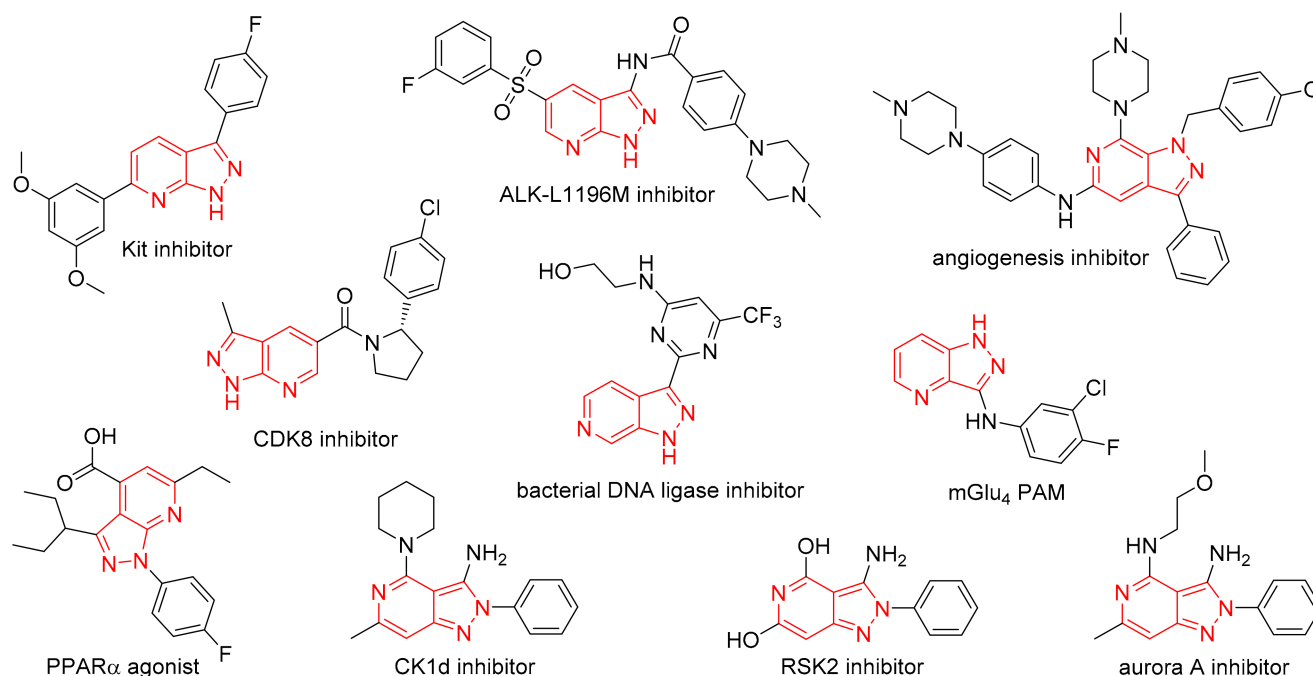


**Copyright:** © 2021 by the authors. Licensee MDPI, Basel, Switzerland. This article is an open access article distributed under the terms and conditions of the Creative Commons Attribution (CC BY) license (<https://creativecommons.org/licenses/by/4.0/>).

## 1. Introduction

Despite being rarely found in nature, presumably due to the difficulty of forming N–N bonds in living organisms, naturally occurring pyrazoles are prominent in laboratories due to their vast variety of biological activities [1]. In current medicinal chemistry, the incorporation of a pyrazole nucleus is a common practice to develop new drug-like molecules with anti-cancer, anti-diabetic, anti-viral, anti-inflammatory, anti-bacterial, anti-fungal, anti-neurodegenerative, anti-tubercular, anthelmintic, antimalarial, and photosensitizing properties [2–10], among others, thus giving rise to a great number of approved therapeutics [11]. Besides numerous biological activities, pyrazoles have also been documented to possess dyeing and fluorescence properties [12–16], and some of them can be used as colorimetric or fluorescent probes for sensing small molecules, ions, or pH [17–28], which may have applications in in vivo imaging [29–31]. Pyrazolopyridines are among the most studied condensed pyrazole systems in organic and pharmaceutical chemistry (Figure 1). For instance,

6-(3,5-dimethoxyphenyl)-3-(4-fluorophenyl)-1*H*-pyrazolo[3,4-*b*]pyridine (APcK110) is an extensively researched Kit kinase inhibitor [32–34]. More recently, various 1*H*-pyrazolo[3,4-*b*]pyridine derivatives were reported as potent ALK-L1196M [35] and CDK8 inhibitors [36], PPAR $\alpha$  agonists [37], and antimicrobial, anti-quorum-sensing, and anticancer agents [38], while 3-amino-1*H*-pyrazolo[3,4-*b*]pyridine core was identified as a novel scaffold for MELK kinase inhibitors [39]. 2-[[2-(1*H*-Pyrazolo[3,4-*c*]pyridin-3-yl)-6-(trifluoromethyl)pyrimidin-4-yl]amino]ethanol is a bacterial DNA ligase inhibitor [40], several compounds bearing 1*H*-pyrazolo[4,3-*b*]pyridin-3-amine scaffold act as positive allosteric modulators of the metabotropic glutamate receptor 4 (mGlu<sub>4</sub>) [41,42], 3-phenylpyrazolo[3,4-*c*]pyridines were reported to possess antiproliferative activity [43], and 1-(4-methoxybenzyl)-7-(4-methylpiperazin-1-yl)-*N*-[4-(4-methylpiperazin-1-yl)phenyl]-3-phenyl-1*H*-pyrazolo [3,4-*c*]pyridin-5-amine was suggested as potential angiogenesis inhibitor [44]. Among biologically active pyrazolo[4,3-*c*]pyridines, 3-amino-2-phenyl-2*H*-pyrazolo[4,3-*c*]pyridine-4,6-diol has shown inhibitory activity against p90 ribosomal S6 kinases 2 (RSK2) [45], while 3-aminopyrazolopyridinone derivatives were demonstrated to exhibit moderate inhibitory potency against CK1d, p38a, and aurora A kinases [46].



**Figure 1.** Selected examples of biologically relevant pyrazolopyridines.

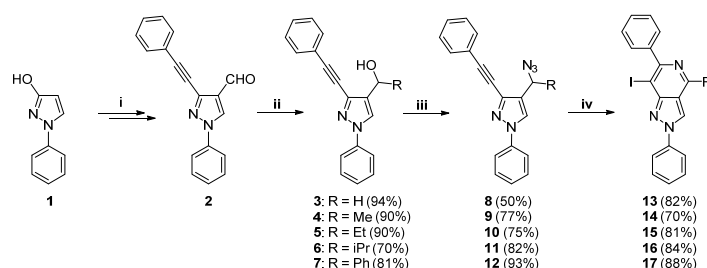
In a continuation of our work devoted to the preparation and study of the properties of various condensed and aryl coupled pyrazole derivatives [47–55], we recently reported a structure–activity relationship study on 2,4,6-trisubstituted-2*H*-pyrazolo[4,3-*c*]pyridines, several of which displayed good anticancer activity in vitro through arresting cell cycle in mitosis and the induction of apoptosis [54]. Inspired by these results, in the current work, we prepared a library of 2,4,6,7-tetrasubstituted-2*H*-pyrazolo[4,3-*c*]pyridines and examined the influence of an additional substituent at the 7-position on the biological and optical properties of the compounds.

## 2. Results and Discussion

### 2.1. Chemistry

1-Phenyl-3-(2-phenylethynyl)-1*H*-pyrazole-4-carbaldehyde **2**, which served as a starting material in this study, was prepared via a multi-step synthetic route from 1-phenyl-1*H*-pyrazol-3-ol **1** in accordance with a previously published procedure [56] (Scheme S1, Supplementary File). Then, primary alcohol **3** was obtained via the reduction of an alde-

hyde group [57] (Scheme 1). Sodium borohydride was chosen as a reducing agent, and the reaction was carried out in methanol at 0 °C under an argon atmosphere. The reaction mixture was protonated with an aqueous ammonium chloride solution to create primary alcohol **3** from the intermediate complex. For the synthesis of secondary alcohols **4–7**, carbaldehyde **2** was dissolved in THF and reacted with an appropriate alkyl or arylmagnesium halogenide at room temperature by adopting a previously reported procedure [58]. The reaction was carried out under an argon atmosphere with a dry solvent due to the sensitivity of Grignard reagents to air and moisture [59]. Although it is known that this kind of secondary alcohol might be unstable [51], all of them were successfully purified by column chromatography, and their structures were determined with spectroscopic data.



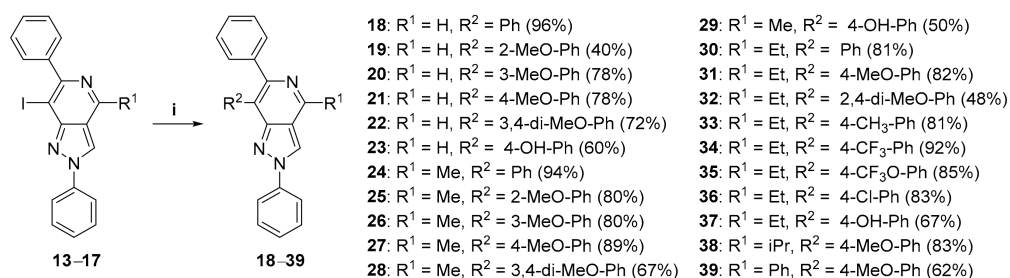
**Scheme 1.** Synthesis of 4-substituted 7-iodo-2,6-diphenyl-2H-pyrazolo[4,3-c]pyridines (**13–17**). Reagents and conditions: i: in accordance to ref. [56]; ii: NaBH<sub>4</sub> and MeOH at 0 °C for 30 min (for **3**); MeMgBr, EtMgBr, *i*PrMgCl, or PhMgBr and THF (abs.) at rt for 10 min (for **4, 5, 6** and **7**); iii: TMSN<sub>3</sub>, BF<sub>3</sub>·Et<sub>2</sub>O, and DCM at rt for 30 min; iv: K<sub>3</sub>PO<sub>4</sub> (for **13** and **17**) or NaHCO<sub>3</sub> (for **14, 15** and **16**), I<sub>2</sub>, and DCM at rt for 12 h.

The obtained alcohols **3–7** were further converted into azides **9–12**, respectively. Many methods have been developed for such a transformation, including Mitsunobu-type displacements [60,61], two-step procedures that involve a halogenated [62] or mesylated intermediate [63], the one-pot halogenation-azidation of alcohols [64], reactions with phosphitine intermediates [65], *N*-methyl-2-pyrrolidone hydrosulphate, and trimethylsilylazide (TMSN<sub>3</sub>) [51]. The latter method was chosen for the synthesis, and the reactions were performed in DCM with a catalytic amount of boron trifluoride diethyl etherate (BF<sub>3</sub>·Et<sub>2</sub>O). The reactions were carried out at room temperature under an argon atmosphere and with a dry solvent in order to protect both the boron trifluoride and TMSN<sub>3</sub> from moisture (Scheme 1). Conversion was completed in 30 minutes, and the reaction products **8–12** were furnished in 50–93% yields.

The newly synthesized azides **8–12** were further used to form the pyrazolo[4,3-c]pyridine core with iodine in the 7-position by adopting electrophilic substitution reaction conditions that were previously used to obtain 1,3,4-trisubstituted isoquinolines from 2-alkynyl benzyl azides [66]. Namely, azides **8–12** were dissolved in DCM and treated with iodine and a proper base (Scheme 1). Five equivalents of K<sub>3</sub>PO<sub>4</sub> were used for the primary azides **8** and **12**, while one equivalent of NaHCO<sub>3</sub> was used for the secondary azides **9–11**. The reactions were carried out at room temperature in the dark for 12 h, furnishing compounds **13–17** in 70–88% yields. An attempt to make use of a weaker base NaHCO<sub>3</sub> for the reaction with the primary azide **6** led to the formation of the dehalogenated side product 2,6-diphenyl-2H-pyrazolo[4,3-c]pyridine, which resulted in a troublesome purification and a lower yield of the target product.

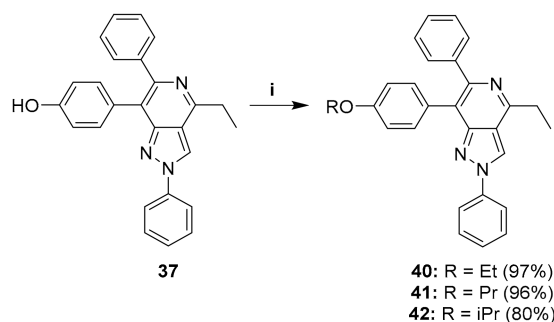
The obtained 7-iodo-2,6-diphenyl-2H-pyrazolo[4,3-c]pyridines **13–17** were further used in palladium-catalysed Suzuki–Miyaura cross-coupling reaction (Scheme 2) by adopting a previously reported procedure [67]. Namely, aromatic boronic acids were reacted with compounds **13–17** using palladium acetate as a catalyst and Cs<sub>2</sub>CO<sub>3</sub> as a base in an aqueous ethanol solution under an argon atmosphere. To ensure a short reaction time, cross-coupling reactions were carried out under microwave irradiation, thus giving rise to compounds **18–37**. Compounds **18** and **20–37** (Scheme 2) were obtained in fair to excel-

lent yields (48–96%), but the full cross-coupling conversion of **13** using 2-methoxyphenyl boronic acid could not be achieved, resulting in a lower yield of compound **19**.



**Scheme 2.** Synthesis of compounds **18–39**. Reagents and conditions: i: arylboronic acid, Pd(OAc)<sub>2</sub>, Cs<sub>2</sub>CO<sub>3</sub>, EtOH/H<sub>2</sub>O 3/1 and MW at 100 °C for 0.5–1 h.

4-ethyl-7-(4-hydroxyphenyl)-2,6-diphenyl-2H-pyrazolo[4,3-c]pyridine **37** was further subjected to hydroxyl group alkylation reactions with ethyl, propyl, and isopropyl iodides. As a result, 7-(4-alkoxyphenyl)-4-ethyl-2,6-diphenyl-2H-pyrazolo[4,3-c]pyridines **40–42** were obtained in high yields (80–97%) (Scheme 3).



**Scheme 3.** Synthesis of compounds **40–42**. Reagents and conditions: i: NaH, RI, and DMF at 70 °C for 1 h.

## 2.2. Optical Properties

The fluorescence properties of all final compounds **18–42** were first investigated in THF, with the excitation wavelength  $\lambda_{\text{ex}}$  being set to 350 nm (Table S1, Supplementary File). The emission maxima  $\lambda_{\text{em}}$  of all the compounds were located in the 437–487 nm range, which corresponds to the blue part of the visible light spectrum. A polar 4-hydroxyphenyl substituent at the 7-position bearing compounds **23**, **29**, and **37**, as well as derivatives **31–32**, **38**, **40–42** (all of which bear 4-alkoxyphenyl substituents at the 7-position and ethyl or isopropyl substituents at the 4-position), possessed the most pronounced fluorescence properties. Namely, the Stokes shifts for these compounds were in 199–205 nm range, and the quantum yield reached approximately 60–85%.

Intracellular pH plays an important role in many biological processes, and its changes from normal to abnormal levels can lead to cellular dysfunction, various diseases, and a decrease in physical performance [68]. pH-sensitive fluorescent indicators enable the precise measurement of intracellular pH, which consequently provides valuable information about ongoing physiological and pathological processes at the cellular and sub-cellular levels [69]. To assess whether the fluorescence properties of the prepared compounds are pH-dependent, they were all analysed in pH 5, 7, and 9 buffers with the excitation wavelength  $\lambda_{\text{ex}}$  set to 360 nm (Table S2, Supplementary File). The quantum yield of compounds **18**, **24**, and **30**, all of which bear phenyl substituent at the 7-position, increased at acidic pH without substantial shifts in emission maxima, which were observed to be in the 435–447 nm range. The further analysis of compound **18** in a range of pH 2–11 buffers revealed a gradual decrease in fluorescence intensity with the increase of pH (Figure S1A, Supplementary File). On the other hand, the quantum yield of 2-methoxyphenyl

or 4-methoxyphenyl substituent at the 7-position possessing compounds **19**, **21**, **25**, **27**, and **31** was higher in basic pH; moreover, in the case of 4-methoxyphenyl substituent at the 7-position bearing compounds **21**, **27**, and **31**, an acidic pH caused the red shift of the emission maxima. For instance, in the case of compound **21**, the emission spectrum was found to be composed of two partly overlapping bands (Figure S1B, Supplementary File). The short-wavelength part is pH-sensitive. It is dominant in the basic environment, and decreasing the pH from 11 to 6 caused a decrease in fluorescence intensity without a shift in emission maxima, which was maintained at 458 nm. After a further decrease of pH, it was the long-wavelength band that became more dominant, which was manifested as a gradual shift of emission maxima to 519 nm. Any other 4-alkoxyphenyl substituent at the 7-position bearing compounds only exhibited a drop of quantum yield at acidic pH without the shift of the emission maxima. A polar 4-hydroxyphenyl substituent at the 7-position bearing compounds **23**, **29**, and **37**, which possessed the highest quantum yields in THF, had the lowest quantum yields of up to 0.3% in an aqueous solution. It is well known that hydroxyphenyl groups are sensitive to photochemical reactions [70]. Typically, their  $pK_a$  drops from  $\sim 10$  in the ground state to  $\sim 3$  in the excited state, and excited-state proton transfer reactions are common in aqueous solutions. For our molecules, these reactions resulted in fluorescence quenching. Our preliminary observations suggested that most of the compounds, except for the polar derivatives **23**, **29**, and **37**, could be of potential interest as pH indicators. Considering the approximately 5-fold quantum yield increase and 40 nm blue shift of the emission spectrum maximum when moving from pH 5 to 9, the compound **21** seems to be the best pH indicator from the set of examined molecules, enabling both fluorescence-intensity-based and ratiometric pH sensing.

### 2.3. Biology

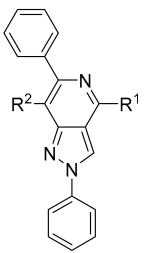
Synthesized 2*H*-pyrazolo[4,3-*c*]pyridines **18–42** were evaluated for their antiproliferative activity against three human cancer cell lines, i.e., MV4-11 (biphenotypic B myelomonocytic leukaemia cells), K562 (chronic myeloid leukaemia cells), and MCF-7 (human breast cancer cells) (Table 1). In agreement with our previous observations [54], increasing the bulkiness of the substituent at the 4-position gradually reduced or completely abolished the activity of 2*H*-pyrazolo[4,3-*c*]pyridine derivatives. Namely, while methyl-substituted compounds **24–29** possessed lower antiproliferative values than their unsubstituted counterparts **18–23**, isopropyl-, ethyl-, and phenyl-substituted compounds were mostly non-active up to the tested 10  $\mu$ M concentration. Overall, a polar 4-hydroxyphenyl substituent at the 7-position bearing the 4-unsubstituted derivative **23** proved to be the most potent.

Subsequently, the effects of the most active compound **23**, its less active 4-substituted analogues **29** and **37**, and derivative **21** were studied on K562 leukemic cells. Asynchronously growing K562 cells were treated with 10  $\mu$ M concentrations of selected compounds for 24, 48, and 72 h and analysed using immunoblotting and flow cytometry (Figure 2). Immunoblotting revealed that 48 h treatment with the most potent compound **23** was sufficient for the induction of poly(ADP-ribose) polymerase 1 (PARP-1) cleavage [71] and the activation of initiator enzyme of apoptotic cascade caspase 9 [72]. Interestingly, in addition to the clear pro-apoptotic effects, we also observed the time-dependent fragmentation of microtubule-associated protein 1-light chain 3 (LC3), which has appeared during autophagy [73]. Similar outcomes with lower efficiencies were observed in all tested compounds. In addition to cell-death-related proteins, the expression levels of proliferating cell nuclear antigen (PCNA), which plays a key role in DNA replication [74], were analysed. The results revealed that all studied compounds reduced the levels of PCNA time-dependently, with the most pronounced effect observed for compounds **23** and **29**. To independently support this observation, immunoblotting was complemented with the flow cytometric analysis of bromodeoxyuridine (BrdU) incorporation, which allowed us to recognize replicating BrdU-positive cells in the population [75] (Figure 2B). In control samples the number of proliferating cells came up to 40%, but the 10  $\mu$ M treatment with tested compounds **21**, **23**, **29**, and **37** reduced the proportion of actively proliferating

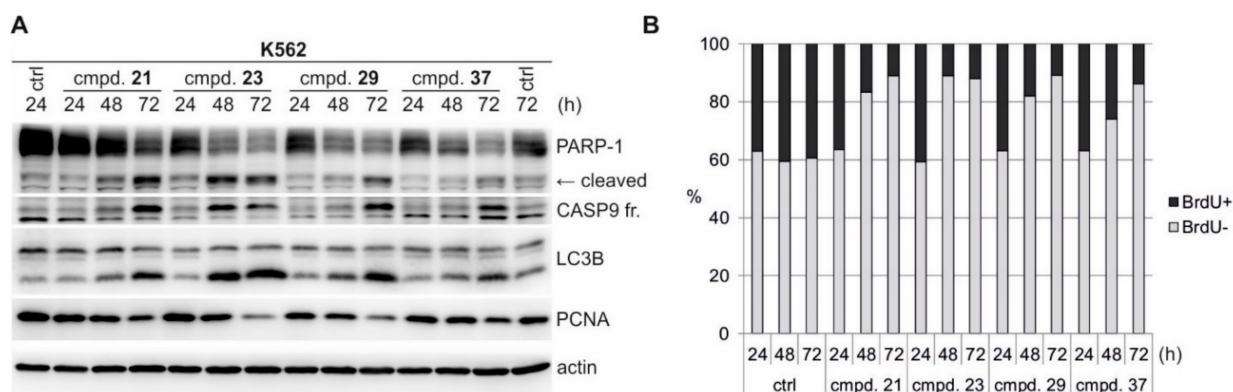


BrdU-positive cells in up to approximately 10% for the most active compounds **23** and **29**. Overall, the obtained results suggest the complex action of the compounds, combining antiproliferative effects with the induction of cell death.

**Table 1.** In vitro antiproliferative activity of 2*H*-pyrazolo[4,3-*c*]pyridine derivatives **18–42**.

| Structure   | Compound  | R <sup>1</sup> | R <sup>2</sup>         | GI <sub>50</sub> ± SD, μM * |           |            |
|---|-----------|----------------|------------------------|-----------------------------|-----------|------------|
|   |           |                |                        | MV4-11                      | K562      | MCF-7      |
|  | <b>18</b> | H              | Ph                     | 7.7 ± 2.6                   | >10       | >10        |
|   | <b>19</b> | H              | 2-MeO-Ph               | 6.5 ± 1.3                   | 7.1 ± 2.9 | 6.3 ± 2.2  |
|   | <b>20</b> | H              | 3-MeO-Ph               | 5.0 ± 1.8                   | >10       | >10        |
|   | <b>21</b> | H              | 4-MeO-Ph               | 3.5 ± 1.2                   | 4.8 ± 2.5 | 7.3 ± 0.2  |
|   | <b>22</b> | H              | 3,4-di-MeO-Ph          | 2.4 ± 1.3                   | 6.0 ± 3.8 | 4.2 ± 0.9  |
|   | <b>23</b> | H              | 4-OH-Ph                | 1.5 ± 0.7                   | 2.4 ± 1.0 | 1.6 ± 0.2  |
|   | <b>24</b> | Me             | Ph                     | >10                         | >10       | >10        |
|   | <b>25</b> | Me             | 2-MeO-Ph               | >10                         | >10       | >10        |
|   | <b>26</b> | Me             | 3-MeO-Ph               | >10                         | >10       | >10        |
|   | <b>27</b> | Me             | 4-MeO-Ph               | >10                         | >10       | 8.4 ± 2.1  |
|   | <b>28</b> | Me             | 3,4-di-MeO-Ph          | 7.6 ± 3.0                   | >10       | >10        |
|   | <b>29</b> | Me             | 4-OH-Ph                | 4.7 ± 2.7                   | 3.9 ± 0.3 | 4.1 ± 0.4  |
|   | <b>30</b> | Et             | Ph                     | >10                         | >10       | >10        |
|   | <b>31</b> | Et             | 4-MeO-Ph               | >10                         | >10       | >10        |
|   | <b>32</b> | Et             | 2,4-di-MeO-Ph          | >10                         | >10       | >10        |
|   | <b>33</b> | Et             | 4-Me-Ph                | >10                         | >10       | >10        |
|   | <b>34</b> | Et             | 4-CF <sub>3</sub> -Ph  | >10                         | >10       | >10        |
|   | <b>35</b> | Et             | 4-CF <sub>3</sub> O-Ph | >10                         | >10       | >10        |
|   | <b>36</b> | Et             | 4-Cl-Ph                | >10                         | >10       | >10        |
|   | <b>37</b> | Et             | 4-OH-Ph                | 8.0 ± 3.1                   | >10       | 3.9 ± 0.4  |
|   | <b>38</b> | iPr            | 4-MeO-Ph               | 5.7 ± 1.4                   | >10       | >10        |
|   | <b>39</b> | Ph             | 4-MeO-Ph               | >10                         | >10       | 7.9 ± 3.8  |
|   | <b>40</b> | Et             | 4-EtO-Ph               | >10                         | >10       | >10        |
|   | <b>41</b> | Et             | 4-PrO-Ph               | >10                         | >10       | >10        |
| <b>42</b>   | Et        | 4-iPrO-Ph      | >10                    | >10                         | >10       |            |
| <b>Flavopiridol</b>   |           |                |                        | 0.2 ± 0.03                  | 0.8 ± 0.1 | 0.2 ± 0.03 |

\* Data are means of at least three independent measurements.



**Figure 2.** Effect of compounds **21**, **23**, **29**, and **37** (10 μM) on K562 cell line after 24, 48, and 72 h treatment. **(A)** Immunoblotting of selected markers of cell death and proliferation. The actin level was detected to verify equal protein loading. **(B)** Analysis of BrdU incorporation. Results are representative of two independent experiments.

### 3. Materials and Methods

#### 3.1. General

All chemicals and solvents were purchased from commercial suppliers and used without further purification unless otherwise specified. The <sup>1</sup>H, <sup>13</sup>C, and <sup>15</sup>N NMR spectra were recorded in CDCl<sub>3</sub> or DMSO-*d*<sub>6</sub> solutions at 25 °C on either a Bruker Avance III 700 (700 MHz for <sup>1</sup>H, 176 MHz for <sup>13</sup>C, and 71 MHz for <sup>15</sup>N) spectrometer equipped with a 5 mm TCI <sup>1</sup>H-<sup>13</sup>C/<sup>15</sup>N/D z-gradient cryoprobe or a Jeol ECA-500 (500 MHz for <sup>1</sup>H and 126 MHz for <sup>13</sup>C) spectrometer equipped with a 5 mm Royal probe. The chemical

shifts, expressed in ppm, were relative to tetramethylsilane (TMS). The  $^{15}\text{N}$  NMR spectra were referenced to neat, external nitromethane (coaxial capillary). The  $^{19}\text{F}$  NMR spectra (376 MHz) were obtained on a Bruker Avance III 400 instrument using  $\text{C}_6\text{F}_6$  as an internal standard. FT-IR spectra were collected using the ATR method on a Bruker Vertex 70v spectrometer with an integrated Platinum ATR accessory or on a Bruker Tensor 27 spectrometer in KBr pellets. The melting points of crystalline compounds were determined in open capillary tubes with a Buchi M 565 apparatus (temperature gradient:  $2\text{ }^\circ\text{C}/\text{min}$ ) and are uncorrected. Mass spectra were recorded on Q-TOF MICRO spectrometer (Waters), analyses were performed in the positive ( $\text{ESI}^+$ ) mode, and molecular ions were recorded in  $[\text{M} + \text{H}]^+$  forms. High-resolution mass spectrometry (HRMS) spectra were obtained in the ESI mode on a Bruker MicrOTOF-Q III spectrometer. All reactions were performed in oven-dried flasks under an argon atmosphere with magnetic stirring. Reaction progress was monitored by TLC analysis on Macherey-Nagel<sup>TM</sup> ALUGRAM<sup>®</sup> Xtra SIL G/UV254 plates. TLC plates were visualized with UV light (wavelengths of 254 and 365 nm) or iodine vapour. Compounds were purified by flash chromatography in a glass column (stationary phase of silica gel, high-purity grade of 9385, pore size of  $60\text{ \AA}$ , particle size of 230–400 mesh, supplied by Sigma-Aldrich).  $^1\text{H}$ ,  $^{13}\text{C}$ , and  $^1\text{H}$ - $^{15}\text{N}$  HMBC NMR spectra, as well as the HRMS data of new compounds, are provided in Figures S2–S131 of the Supplementary Materials.

### 3.2. Chemistry

#### 3.2.1. Procedure for the Synthesis of [1-Phenyl-3-(phenylethynyl)-1H-pyrazol-4-yl]methanol **3**

1-Phenyl-3-(2-phenylethynyl)-1H-pyrazole-4-carbaldehyde **3** (560 mg, 2.06 mmol) was dissolved in MeOH (12 mL), and the solution was cooled to  $0\text{ }^\circ\text{C}$ . Subsequently,  $\text{NaBH}_4$  (156 mg, 4.12 mmol) was added under an argon atmosphere, and the mixture was stirred for 30 min. Upon completion (monitored by TLC), the reaction mixture was diluted with a saturated aqueous  $\text{NH}_4\text{Cl}$  solution (20 mL) and extracted with EtOAc ( $3 \times 30\text{ mL}$ ). The combined organic layers were dried over anhydrous  $\text{Na}_2\text{SO}_4$ , filtered, and evaporated under reduced pressure. The residue was purified by column chromatography (EtOAc/Hex, 1:3 *v/v*). Yield: 530 mg (94%), white crystalline solid, mp =  $114\text{--}115\text{ }^\circ\text{C}$ ,  $R_f = 0.18$  (EtOAc/Hex, 1:3 *v/v*).  $^1\text{H}$  NMR (700 MHz,  $\text{CDCl}_3$ ):  $\delta$  2.12 (1H, s, OH), 4.77 (2H, d,  $J = 7.0\text{ Hz}$ ,  $\text{CH}_2\text{OH}$ ), 7.28–7.32 (1H, m, NPh 4-H), 7.33–7.38 (3H, m, CPh 3,4,5), 7.42–7.46 (2H, m, NPh 3,5-H), 7.55–7.59 (2H, m, CPh 2,6-H), 7.66–7.72 (2H, m, NPh 2,6-H), 7.95 (1H, s, 5-H).  $^{13}\text{C}$  NMR (176 MHz,  $\text{CDCl}_3$ ):  $\delta$  55.9 ( $\text{CH}_2\text{OH}$ ), 80.3 ( $\text{C}\equiv\text{CPh}$ ), 93.7 ( $\text{C}\equiv\text{CPh}$ ), 119.4 (NPh C-2,6), 122.5 (C-4), 126.4 (C-5 and CPh C-1), 127.1 (NPh C-4), 128.5 (CPh C-3,5), 128.9 (CPh C-4), 129.6 (NPh C-3,5), 131.9 (CPh C-2,6), 135.6 (C-3), 139.7 (NPh C-1).  $^{15}\text{N}$  NMR (71 MHz,  $\text{CDCl}_3$ ):  $\delta$   $-163.5$  (N-1), N-2 not found. IR ( $\nu$ ,  $\text{cm}^{-1}$ ): 3373 (OH), 3126, 3066, 3056 ( $\text{CH}_{\text{arom}}$ ), 2920, 2864 ( $\text{CH}_{\text{aliph}}$ ), 1599, 1502, 1335, 1217 (C=C, C=N, C–N), 1063, 1014 ( $\text{CH}_2\text{-OH}$ ), 749, 686 (CH=CH of mono- and disubstituted benzenes). MS ( $\text{ES}^+$ ):  $m/z$  (%): 275 ( $[\text{M} + \text{H}]^+$ , 100). HRMS (ESI) for  $\text{C}_{18}\text{H}_{14}\text{N}_2\text{ONa}$  ( $[\text{M} + \text{Na}]^+$ ): requires 297.0998 and found 297.0988.

#### 3.2.2. General Procedure (A) for the Synthesis of Alcohols **4–7**

1-Phenyl-3-(2-phenylethynyl)-1H-pyrazole-4-carbaldehyde **2** (1 equivalent) was dissolved in dry THF under an argon atmosphere. Subsequently, an appropriate Grignard reagent (1.2 equivalents) was added, and the mixture was stirred at room temperature for 10 min. Upon completion (monitored by TLC), the reaction mixture was diluted with water (20 mL) and extracted with EtOAc ( $3 \times 20\text{ mL}$ ). The combined organic layers were dried over anhydrous  $\text{Na}_2\text{SO}_4$ , filtered, and evaporated under reduced pressure. The residue was purified by column chromatography.

1-[1-Phenyl-3-(phenylethynyl)-1*H*-pyrazol-4-yl]ethanol-1-ol 4

1-[1-Phenyl-3-(phenylethynyl)-1*H*-pyrazol-4-yl]ethanol-1-ol 4 was prepared in accordance with general procedure (A) from 1-phenyl-3-(2-phenylethynyl)-1*H*-pyrazole-4-carbaldehyde 2 (350 mg, 1.287 mmol) and MeMgCl (0.52 mL, 1.56 mmol) in THF (4 mL). The desired compound was purified by column chromatography (EtOAc/Hex, 1:4 *v/v*). Yield: 286 mg (70%), colourless liquid,  $R_f = 0.23$  (EtOAc/Hex, 1:5 *v/v*).  $^1\text{H NMR}$  (700 MHz,  $\text{CDCl}_3$ ):  $\delta$  1.64 (3H, d,  $J = 6.5$  Hz,  $\text{CH}_3$ ), 2.18 (1H, s, OH), 5.13 (1H, q,  $J = 6.5$  Hz, CH), 7.29–7.1 (1H, m, NPh 4-H), 7.34–7.38 (3H, m, CPh 3,4,5-H), 7.43–7.47 (2H, m, NPh 3,5-H), 7.55–7.59 (2H, m, CPh 2,6-H), 7.67–7.72 (2H, m, NPh 2,6-H), 7.92 (1H, s, 5-H).  $^{13}\text{C NMR}$  (176 MHz,  $\text{CDCl}_3$ ):  $\delta$  23.8 ( $\text{CH}_3$ ), 62.7 (CH) 80.6 ( $\text{C}\equiv\text{CPh}$ ), 93.8 ( $\text{C}\equiv\text{CPh}$ ), 119.1 (NPh C-2,6), 122.4 (CPh C-1), 124.4 (C-5), 126.9 (NPh C-4), 128.4 (CPh C-3,5), 128.7 (CPh C-4), 129.4 (NPh C-3,5), 131.5 (C-1), 131.7 (CPh C-2,6), 134.2 (C-2), 139.6 (NPh C-1).  $^{15}\text{N NMR}$  (71 MHz,  $\text{CDCl}_3$ ):  $\delta$  -75.4 (N-2), -164.4 (N-1). MS ( $\text{ES}^+$ ):  $m/z$  (%): 275 ( $[\text{M} + \text{H}]^+$ , 96).

1-[1-Phenyl-3-(phenylethynyl)-1*H*-pyrazol-4-yl]propan-1-ol 5

1-[1-Phenyl-3-(phenylethynyl)-1*H*-pyrazol-4-yl]propan-1-ol 5 was prepared in accordance with general procedure (A) from 1-phenyl-3-(2-phenylethynyl)-1*H*-pyrazole-4-carbaldehyde 2 (100 mg, 0.37 mmol) and EtMgBr (0.15 mL, 0.44 mmol) in THF (2 mL). The desired compound was purified by column chromatography (EtOAc/Hex, 1:3 *v/v*). Yield: 100 mg (90%), yellowish crystalline solid, mp = 87–88 °C,  $R_f = 0.28$  (EtOAc/Hex, 1:3 *v/v*).  $^1\text{H NMR}$  (700 MHz,  $\text{CDCl}_3$ ):  $\delta$  1.03 (3H, t,  $J = 7.7$  Hz,  $\text{CH}_3$ ), 1.93–1.99 (2H, m,  $\text{CH}_2$ ), 2.22 (1H, br s, OH), 4.87 (1H, t,  $J = 6.5$  Hz, CH), 7.29–7.32 (1H, m, NPh 4-H), 7.34–7.38 (3H, m, CPh 3,4,5-H), 7.43–7.46 (2H, m, NPh 3,5-H), 7.55–7.59 (2H, m, CPh 2,6-H), 7.68–7.72 (2H, m, NPh 2,6-H), 7.91 (1H, s, 5-H).  $^{13}\text{C NMR}$  (176 MHz,  $\text{CDCl}_3$ ):  $\delta$  10.0 ( $\text{CH}_3$ ), 30.8 ( $\text{CH}_2$ ), 68.1 (CHOH), 80.7 ( $\text{C}\equiv\text{CPh}$ ), 93.6 ( $\text{C}\equiv\text{CPh}$ ), 119.1 (NPh C-2,6), 122.5 (CPh C-4), 124.8 (C-5), 126.9 (NPh C-4), 128.4 (CPh C-3,5), 128.7 (CPh C-4), 129.4 (NPh C-3,5), 130.2 (C-4), 131.6 (CPh C-2,6), 134.5 (C-3), 139.6 (NPh C-1).  $^{15}\text{N NMR}$  (71 MHz,  $\text{CDCl}_3$ ):  $\delta$  -75.8 (N-2), -164.1 (N-1). IR (KBr,  $\nu$ ,  $\text{cm}^{-1}$ ): 3441 (OH), 3056 ( $\text{CH}_{\text{arom}}$ ), 2960, 2874 ( $\text{CH}_{\text{aliph}}$ ), 1596, 1502, 1335, 1212 (C=C, C=N, C-N), 1063, 109 ( $\text{CH}_2\text{-OH}$ ), 755, 691 (CH=CH of mono- and disubstituted benzenes). MS ( $\text{ES}^+$ ):  $m/z$  (%): 303 ( $[\text{M} + \text{H}]^+$ , 98). HRMS (ESI) for  $\text{C}_{20}\text{H}_{18}\text{N}_2\text{ONa}$  ( $[\text{M} + \text{Na}]^+$ ): requires 325.1311 and found 325.1311.

2-Methyl-1-[1-phenyl-3-(phenylethynyl)-1*H*-pyrazol-4-yl]propan-1-ol 6

2-Methyl-1-[1-phenyl-3-(phenylethynyl)-1*H*-pyrazol-4-yl]propan-1-ol 6 was prepared in accordance with general procedure (A) from 1-phenyl-3-(2-phenylethynyl)-1*H*-pyrazole-4-carbaldehyde 2 (350 mg, 1.287 mmol) and iPrMgCl (0.97 mL, 1.93 mmol) in THF (6 mL). The desired compound was purified by column chromatography (EtOAc/Hex, 1:4 *v/v*). Yield: 286 mg (70%), yellow crystalline solid, mp = 78–79 °C,  $R_f = 0.23$  (EtOAc/Hex, 1:5 *v/v*).  $^1\text{H NMR}$  (700 MHz,  $\text{CDCl}_3$ ):  $\delta$  0.98 (3H, d,  $J = 6.8$  Hz,  $\text{CH}_3$ ), 1.05 (3H, d,  $J = 6.8$  Hz,  $\text{CH}_3$ ), 2.12 (1H, s, OH), 2.15–2.12 (1H, m,  $\text{CH}(\text{CH}_3)_2$ ), 4.70 (1H, d,  $J = 6.3$  Hz,  $\text{CH-OH}$ ), 7.26–7.32 (1H, m, NPh 4-H), 7.34–7.39 (3H, m, CPh 3,4,5-H), 7.43–7.47 (2H, m, NPh 3,4-H), 7.55–7.59 (2H, m, CPh 2,6-H), 7.67–7.76 (2H, m, NPh 2,6-H), 7.91 (1H, s, 5-H).  $^{13}\text{C NMR}$  (176 MHz,  $\text{CDCl}_3$ ):  $\delta$  18.1 ( $\text{CH}_3$ ), 18.8 ( $\text{CH}_3$ ), 34.9 ( $\text{CH}(\text{CH}_3)_2$ ), 72.2 (CH-OH), 81.1 ( $\text{C}\equiv\text{CPh}$ ), 93.7 ( $\text{C}\equiv\text{CPh}$ ), 119.2 (NPh C-2,6), 122.7 (CPh C-1), 125.3 (C-5), 127.0 (NPh C-4), 128.5 (CPh C-3,5), 128.8 (CPh C-4), 129.4 (C-4), 129.6 (NPh C-3,5), 131.8 (CPh C-2,6), 134.9 (C-3), 139.7 (NPh C-1).  $^{15}\text{N NMR}$  (71 MHz,  $\text{CDCl}_3$ ):  $\delta$  -163.8 (N-1), N-2 not found. IR ( $\nu$ ,  $\text{cm}^{-1}$ ): 3383 (OH), 3054 ( $\text{CH}_{\text{arom}}$ ), 2959, 2872 ( $\text{CH}_{\text{aliph}}$ ), 1596, 1501, 1458, 1376, 1331, 1219 (C=C, C=N, C-N), 1056, 1033 (CH-OH), 963, 752, 688 (CH=CH of monosubstituted benzenes). MS ( $\text{ES}^+$ ):  $m/z$  (%): 317 ( $[\text{M} + \text{H}]^+$ , 99). HRMS (ESI) for  $\text{C}_{21}\text{H}_{20}\text{N}_2\text{ONa}$  ( $[\text{M} + \text{Na}]^+$ ): requires 339.1468 and found 339.1467.

Phenyl[1-phenyl-3-(phenylethynyl)-1*H*-pyrazol-4-yl]methanol 7

Phenyl[1-phenyl-3-(phenylethynyl)-1*H*-pyrazol-4-yl]methanol 7 was prepared in accordance with general procedure (A) from 1-phenyl-3-(2-phenylethynyl)-1*H*-pyrazole-4-

carbaldehyde **2** (100 mg, 0.37 mmol) and PhMgBr (0.15 mL, 0.44 mmol) in DCM (2 mL). The desired compound was purified by column chromatography (EtOAc/Hex, 1:7 *v/v*). Yield: 105 mg (81%), colourless liquid,  $R_f = 0.35$  (EtOAc/Hex, 1:3 *v/v*).  $^1\text{H NMR}$  (700 MHz,  $\text{CDCl}_3$ ):  $\delta$  2.54 (1H, br s, OH), 6.06 (1H, s, CH), 7.27–7.31 (1H, m, NPh 4-H), 7.31–7.33 (1H, m, C4Ph 4-H), 7.33–7.36 (3H, m, C3-Ph 3,4,5-H), 7.37–7.40 (2H, m, C4Ph 3,5-H), 7.41–7.45 (2H, m, NPh 3,5-H), 7.48–7.51 (2H, m, C3-Ph 2,6-H), 7.52–7.54 (2H, m, C4Ph 2,6-H), 7.65–7.70 (2H, m, NPh 2,6-H), 7.80 (1H, s, 5-H).  $^{13}\text{C NMR}$  (176 MHz,  $\text{CDCl}_3$ ):  $\delta$  68.8 (CH), 80.5 (C $\equiv$ CPh), 94.0 (C $\equiv$ CPh), 119.2 (NPh C-2,6), 122.4 (C3-Ph C-1), 125.5 (C-5), 126.4 (C4Ph C-2,6), 126.9 (NPh C-4), 127.9 (C4Ph C-1), 128.3 (C3-Ph C-3,5), 128.5 (C4Ph C-3,5), 128.7 (C3-Ph C-4), 129.4 (NPh C-3,5), 130.2 (C-4), 131.7 (C3-Ph C-2,6), 134.8 (C-3), 139.5 (NPh C-1), 142.6 (C4Ph C-1).  $^{15}\text{N NMR}$  (71 MHz,  $\text{CDCl}_3$ ):  $\delta$  -163.9 (N-1). MS (ES $^+$ ):  $m/z$  (%): 351 ([M + H] $^+$ , 95). HRMS (ESI) for  $\text{C}_{24}\text{H}_{18}\text{N}_2\text{O}$ Na ([M + Na] $^+$ ): requires 373.1311 and found 373.1311.

### 3.2.3. General Procedure (B) for the Synthesis of Azide–Alkynes **8–12**

To a solution of appropriate pyrazole alcohol **3–7** (1 equivalent) in dry DCM,  $\text{TMSN}_3$  (1.5 equivalents) and  $\text{BF}_3 \cdot \text{Et}_2\text{O}$  (0.2 equivalents) were added dropwise. The reaction mixture was stirred for 10–60 min under an argon atmosphere at room temperature. Upon completion (monitored by TLC), the reaction mixture was diluted with an aqueous  $\text{NaHCO}_3$  solution (10 mL) and extracted with DCM (3  $\times$  25 mL). The combined organic layers were dried over anhydrous  $\text{Na}_2\text{SO}_4$ , filtered, and evaporated under reduced pressure. The residue was purified by column chromatography.

#### 4-(Azidomethyl)-1-phenyl-3-(phenylethynyl)-1H-pyrazole **8**

4-(Azidomethyl)-1-phenyl-3-(phenylethynyl)-1H-pyrazole **8** was prepared in accordance with general procedure (B) from [1-phenyl-3-(2-phenylethynyl)-1H-pyrazol-4-yl]methanol **3** (100 mg, 0.36 mmol),  $\text{TMSN}_3$  (0.07 mL, 0.55 mmol), and  $\text{BF}_3 \cdot \text{Et}_2\text{O}$  (0.01 mL, 0.07 mmol) in DCM (1.5 mL). The desired compound was obtained after purification by column chromatography (EtOAc/Hex, 1:8 *v/v*). Yield: 54 mg (50%), light yellow liquid,  $R_f = 0.71$  (EtOAc/Hex, 1:3 *v/v*).  $^1\text{H NMR}$  (700 MHz,  $\text{CDCl}_3$ ):  $\delta$  4.44 (2H, s,  $\text{CH}_2\text{N}_3$ ), 7.31–7.35 (1H, m, NPh 4-H), 7.35–7.40 (3H, m, CPh 3,4,5-H), 7.45–7.49 (2H, m, NPh 3,5-H), 7.58–7.63 (2H, m, CPh 2,6-H), 7.69–7.74 (2H, m, NPh 2,6-H), 7.96 (1H, s, 5-H).  $^{13}\text{C NMR}$  (176 MHz,  $\text{CDCl}_3$ ):  $\delta$  44.8 ( $\text{CH}_2\text{N}_3$ ), 79.9 (C $\equiv$ CPh), 94.1 (C $\equiv$ CPh), 119.5 (NPh C-2,6), 120.9 (C-4), 122.4 (CPh C-1), 126.7 (C-5), 127.4 (NPh C-4), 128.5 (CPh C-3,5), 129.0 (CPh C-4), 129.7 (NPh C-3,5), 132.0 (CPh C-2,6), 136.5 (C-3), 139.6 (NPh C-1).  $^{15}\text{N NMR}$  (71 MHz,  $\text{CDCl}_3$ ):  $\delta$  -162.2 (N-1), -306.6 and -132.9 ( $\text{N}_3$ , one not found), N-2 not found. IR ( $\nu$ ,  $\text{cm}^{-1}$ ): 3050 ( $\text{CH}_{\text{arom}}$ ), 2921 ( $\text{CH}_{\text{aliph}}$ ), 2087 ( $\text{N}_3$ ), 1595, 1501, 1331, 1250 (C=C, C=N, C-N), 753, 688 (CH=CH of monosubstituted benzenes). MS (ES $^+$ ):  $m/z$  (%): 300 ([M + H] $^+$ , 99). HRMS (ESI) for  $\text{C}_{18}\text{H}_{14}\text{N}_5$  ([M + H] $^+$ ): requires 300.1242 and found 300.1244; for  $\text{C}_{18}\text{H}_{13}\text{N}_5\text{Na}$  ([M + Na] $^+$ ): requires 322.1065 and found 322.1063.

#### 4-(1-Azidoethyl)-1-phenyl-3-(phenylethynyl)-1H-pyrazole **9**

4-(1-Azidoethyl)-1-phenyl-3-(phenylethynyl)-1H-pyrazole **9** was prepared in accordance with general procedure (B) from 1-[1-phenyl-3-(phenylethynyl)-1H-pyrazol-4-yl]ethan-1-ol **4** (205 mg, 0.71 mmol),  $\text{TMSN}_3$  (0.14 mL, 1.07 mmol), and  $\text{BF}_3 \cdot \text{Et}_2\text{O}$  (0.02 mL, 0.14 mmol) in DCM (2 mL). The desired compound was obtained after purification by column chromatography (EtOAc/Hex, 1:4 *v/v*). Yield: 160 mg (72%), colourless oil,  $R_f = 0.72$  (EtOAc/Hex, 1:3 *v/v*).  $^1\text{H NMR}$  (700 MHz,  $\text{CDCl}_3$ ):  $\delta$  1.70 (3H, d,  $J = 7.0$  Hz,  $\text{CH}_3$ ), 4.87 (1H, q,  $J = 7.0$  Hz,  $\text{CHN}_3$ ), 7.34–7.36 (1H, m, NPh 4-H), 7.39–7.40 (3H, m, CPh 3,4,5-H), 7.48–7.51 (2H, m, NPh 3,5-H), 7.62–7.63 (2H, m, CPh 2,6-H), 7.74–7.75 (2H, m, NPh 2,6-H), 7.94 (1H, s, 5-H).  $^{13}\text{C NMR}$  (176 MHz,  $\text{CDCl}_3$ ):  $\delta$  20.7 ( $\text{CH}_3$ ), 52.7 ( $\text{CHN}_3$ ), 80.2 (C $\equiv$ CPh), 94.0 (C $\equiv$ CPh), 119.3 (NPh C-2,6), 122.4 (CPh C-1), 124.9 (C-5), 126.7 (C-4), 127.2 (NPh C-4), 128.4 (CPh C-3,5), 128.9 (CPh C-4), 129.5 (NPh C-3,5), 131.8 (CPh C-2,6), 135.1 (C-3), 139.5 (NPh C-1).  $^{15}\text{N NMR}$  (71 MHz,  $\text{CDCl}_3$ ):  $\delta$  -294.3 ( $\text{N}_3$ ), -163.3 (N-1), -133.9 ( $\text{N}_3$ ), -73.6 (N-2). IR (KBr,

$\nu$ ,  $\text{cm}^{-1}$ ): 3146 ( $\text{C}\equiv\text{CH}$ ), 3055 ( $\text{CH}_{\text{arom}}$ ), 2985, 2936 ( $\text{CH}_{\text{aliph}}$ ), 2102 ( $\text{N}_3$ ), 1597, 1549, 1502, 1216 ( $\text{C}=\text{C}$ ,  $\text{C}=\text{N}$ ), 820, 756, 688 ( $\text{CH}=\text{CH}$  of monosubstituted benzenes). MS ( $\text{ES}^+$ ):  $m/z$  (%): 314 ( $[\text{M} + \text{H}]^+$ , 100). HRMS (ESI) for  $\text{C}_{19}\text{H}_{16}\text{N}_5$  ( $[\text{M} + \text{H}]^+$ ): requires 314.1400 and found 314.1395.

#### 4-(1-Azidopropyl)-1-phenyl-3-(phenylethynyl)-1H-pyrazole 10

4-(1-Azidopropyl)-1-phenyl-3-(phenylethynyl)-1H-pyrazole **10** was prepared in accordance with general procedure (B) from 1-[1-phenyl-3-(phenylethynyl)-1H-pyrazol-4-yl]propan-1-ol **5** (100 mg, 0.33 mmol),  $\text{TMSN}_3$  (0.07 mL, 0.5 mmol), and  $\text{BF}_3\cdot\text{Et}_2\text{O}$  (0.01 mL, 0.07 mmol) in DCM (1 mL). The desired compound was obtained after purification by column chromatography (EtOAc:Hex, 1:12  $v/v$ ). Yield: 81 mg (75%), yellowish crystalline solid,  $\text{mp} = 74\text{--}75^\circ\text{C}$ ,  $R_f = 0.73$  (EtOAc/Hex, 1:3  $v/v$ ).  $^1\text{H}$  NMR (700 MHz,  $\text{CDCl}_3$ ):  $\delta$  1.06 (3H, t,  $J = 7.3\text{ Hz}$ ,  $\text{CH}_3$ ), 1.99 (2H, p,  $J = 7.2\text{ Hz}$ ,  $\text{CH}_2$ ), 4.63 (1H, t,  $J = 7.0\text{ Hz}$ ,  $\text{CH}-\text{N}_3$ ), 7.31–7.35 (1H, m, NPh 4-H), 7.36–7.40 (3H, m, CPh 3,4,5-H), 7.44–7.50 (2H, m, NPh 3,5-H), 7.57–7.63 (2H, m, CPh 2,6-H), 7.69–7.77 (2H, m, NPh 2,6-H), 7.91 (1H, s, 5-H).  $^{13}\text{C}$  NMR (176 MHz,  $\text{CDCl}_3$ ):  $\delta$  10.7 ( $\text{CH}_3$ ), 28.4 ( $\text{CH}_2$ ), 58.9 (CH), 80.2 ( $\text{C}\equiv\text{CPh}$ ), 93.8 ( $\text{C}\equiv\text{CPh}$ ), 119.2 (NPh C-2,6), 122.3 (CPh C-1), 125.1 (C-5), 125.4 (C-4), 127.1 (NPh C-4), 128.4 (CPh C-3,5), 128.8 (CPh C-4), 129.5 (NPh C-3,5), 131.7 (CPh C-2,6), 135.4 (C-3), 139.4 (NPh C-1).  $^{15}\text{N}$  NMR (71 MHz,  $\text{CDCl}_3$ ):  $\delta$   $-163.4$  (N-1),  $-134.5$  ( $\text{CH}-\text{N}=\text{N}=\text{N}$ ),  $-116.4$  ( $\text{CH}-\text{N}=\text{N}=\text{N}$ ),  $-74.4$  (N-2). IR (KBr,  $\nu$ ,  $\text{cm}^{-1}$ ): 3147 ( $\text{CH}_{\text{arom}}$ ), 2967, 2934, 2870 ( $\text{CH}_{\text{aliph}}$ ), 2092 ( $\text{N}_3$ ), 1598, 1502, 1328, 1215 ( $\text{C}=\text{C}$ ,  $\text{C}=\text{N}$ ,  $\text{C}-\text{N}$ ), 959, 757, 689 ( $\text{CH}=\text{CH}$  of monosubstituted benzenes). MS ( $\text{ES}^+$ ):  $m/z$  (%): 328 ( $[\text{M} + \text{H}]^+$ , 99). HRMS (ESI) for  $\text{C}_{20}\text{H}_{17}\text{N}_5\text{Na}$  ( $[\text{M} + \text{Na}]^+$ ): requires 350.1376 and found 350.1376.

#### 4-(Azido-2-methylpropyl)-1-phenyl-3-(phenylethynyl)-1H-pyrazole 11

4-(Azido-2-methylpropyl)-1-phenyl-3-(phenylethynyl)-1H-pyrazole **11** was prepared in accordance with general procedure (B) from 2-methyl-1-[1-phenyl-3-(phenylethynyl)-1H-pyrazol-4-yl]propan-1-ol **6** (200 mg, 0.63 mmol),  $\text{TMSN}_3$  (0.1 mL, 0.76 mmol), and  $\text{BF}_3\cdot\text{Et}_2\text{O}$  (0.02 mL, 0.13 mmol) in DCM (2 mL). The desired compound was obtained after purification by column chromatography (EtOAc/Hex, 1:10  $v/v$ ). Yield: 177 mg (82%), colourless oil,  $R_f = 0.68$  (EtOAc/Hex, 1:4  $v/v$ ).  $^1\text{H}$  NMR (700 MHz,  $\text{CDCl}_3$ ):  $\delta$  1.00 (3H, d,  $J = 6.8\text{ Hz}$ ,  $\text{CH}_3$ ), 1.06 (3H, d,  $J = 6.7\text{ Hz}$ ,  $\text{CH}_3$ ), 2.18–2.25 (1H, m,  $\text{CHCH}_3_2$ ), 4.52 (1H, d,  $J = 7.0\text{ Hz}$ ,  $\text{CH}-\text{N}_3$ ), 7.31–7.35 (1H, m, NPh 4-H), 7.37–7.40 (3H, m, CPh 3,4,5-H), 7.45–7.50 (2H, m, NPh 3,5-H), 7.56–7.62 (2H, m, CPh 2,6-H), 7.71–7.79 (2H, m, NPh 2,6-H), 7.91 (1H, s, 5-H).  $^{13}\text{C}$  NMR (176 MHz,  $\text{CDCl}_3$ ):  $\delta$  19.0 ( $\text{CH}_3$ ), 19.4 ( $\text{CH}_3$ ), 33.7 ( $\text{CH}-\text{CH}_3_2$ ), 64.2 ( $\text{CH}-\text{N}_3$ ), 80.5 ( $\text{C}\equiv\text{CPh}$ ), 93.9 ( $\text{C}\equiv\text{CPh}$ ), 119.4 (NPh C-2,6), 122.5 (CPh C-1), 124.5 (C-4), 125.6 (C-5), 127.3 (NPh C-4), 128.5 (CPh C-3,5), 129.0 (CPh C-4), 129.6 (NPh C-3,5), 131.9 (CPh C-2,6), 135.9 (C-3), 139.6 (NPh C-1).  $^{15}\text{N}$  NMR (71 MHz,  $\text{CDCl}_3$ ):  $\delta$   $-299.2$  ( $\text{N}_3$ ),  $-163.1$  (N-1),  $-134.1$  ( $\text{N}_3$ ). IR ( $\nu$ ,  $\text{cm}^{-1}$ ): 3060 ( $\text{CH}_{\text{arom}}$ ), 2963, 2873 ( $\text{CH}_{\text{aliph}}$ ), 2093 ( $\text{N}_3$ ), 1598, 1502, 1329, 1244 ( $\text{C}=\text{C}$ ,  $\text{C}=\text{N}$ ,  $\text{C}-\text{N}$ ), 753, 687 ( $\text{CH}=\text{CH}$  of monosubstituted benzenes). MS ( $\text{ES}^+$ ):  $m/z$  (%): ( $[\text{M} + \text{H}]^+$ , 99). HRMS (ESI) for  $\text{C}_{21}\text{H}_{20}\text{N}_5\text{Na}$  ( $[\text{M} + \text{Na}]^+$ ): requires 364.1533 and found 364.1533.

#### 4-[Azido(phenyl)methyl]-1-phenyl-3-(phenylethynyl)-1H-pyrazole 12

4-[Azido(phenyl)methyl]-1-phenyl-3-(phenylethynyl)-1H-pyrazole **12** was prepared in accordance with general procedure (B) from phenyl[1-phenyl-3-(phenylethynyl)-1H-pyrazol-4-yl]methanol **7** (105 mg, 0.3 mmol),  $\text{TMSN}_3$  (0.16 mL, 0.45 mmol), and  $\text{BF}_3\cdot\text{Et}_2\text{O}$  (0.01 mL, 0.06 mmol) in DCM (2 mL). The desired compound was obtained after purification by column chromatography (EtOAc/Hex, 1:7  $v/v$ ). Yield: 105 mg (93%), white crystalline solid,  $\text{mp} = 86\text{--}87^\circ\text{C}$ ,  $R_f = 0.73$  (EtOAc/Hex, 1:3  $v/v$ ).  $^1\text{H}$  NMR (700 MHz,  $\text{CDCl}_3$ ):  $\delta$  5.90 (1H, s, CH), 7.30–7.33 (1H, m, NPh 4-H), 7.33–7.39 (4H, m, C4Ph 4-H and C3-Ph 3,4,5-H), 7.40–7.44 (2H, m, C4Ph 3,5-H), 7.44–7.48 (4H, m, C4Ph 2,6-H, NPh 3,5-H), 7.48–7.52 (2H, m, C3-Ph 2,6-H), 7.68–7.72 (2H, m, NPh 2,6-H), 7.82 (1H, s, 5-H).  $^{13}\text{C}$  NMR (176 MHz,  $\text{CDCl}_3$ ):  $\delta$  60.6 (CH), 80.0 ( $\text{C}\equiv\text{CPh}$ ), 94.3 ( $\text{C}\equiv\text{CPh}$ ), 119.2 (NPh C-2,6), 122.3 (C3-Ph C-1), 125.97

(C-5), 126.0 (C-4), 127.1 (NPh C-4), 127.2 (C4Ph C-2,6), 128.3 (C3-Ph C-3,5), 128.4 (C4Ph C-4), 128.78 (C3-Ph C-4), 128.79 (C4Ph C-3,5), 129.4 (NPh C-3,5), 131.7 (C3-Ph C-2,6), 135.4 (C-3), 138.5 (C4Ph C-1), 139.4 (NPh C-1).  $^{15}\text{N}$  NMR (71 MHz,  $\text{CDCl}_3$ ):  $\delta$  -163.4 (N-1), -134.7 (N<sub>3</sub>). IR (KBr,  $\nu$ ,  $\text{cm}^{-1}$ ): 3058 ( $\text{CH}_{\text{arom}}$ ), 2097 (N<sub>3</sub>), 1597, 1502, 1303, 1227 (C=C, C=N, C-N), 958, 751, 686 (CH=CH of monosubstituted benzenes). MS (ES<sup>+</sup>):  $m/z$  (%): 376 ([M + H]<sup>+</sup>, 99). HRMS (ESI) for  $\text{C}_{24}\text{H}_{17}\text{N}_5\text{Na}$  ([M + Na]<sup>+</sup>): requires 398.1376 and found 398.1376.

### 3.2.4. General Procedure (C) for the Synthesis of 7-Iodo-2*H*-pyrazolo[4,3-*c*]pyridines 13–17

To a solution of appropriate azide-alkyne **8–12** (1 equivalent) in DCM, the appropriate base  $\text{K}_3\text{PO}_4$  (5 equivalents) or  $\text{NaHCO}_3$  (1 equivalent) and  $\text{I}_2$  (5 equivalents) were added. The reaction mixture was stirred at room temperature for 12 h. Upon completion (monitored by TLC), the reaction mixture was diluted with an aqueous  $\text{Na}_2\text{S}_2\text{O}_4$  solution (20 mL) and extracted with EtOAc (3 × 25 mL). The combined organic layers were dried over anhydrous  $\text{Na}_2\text{SO}_4$ , filtered, and evaporated under reduced pressure. The residue was purified by column chromatography.

#### 7-Iodo-2,6-diphenyl-2*H*-pyrazolo[4,3-*c*]pyridine 13

7-Iodo-2,6-diphenyl-2*H*-pyrazolo[4,3-*c*]pyridine **13** was prepared in accordance with general procedure (C) from 4-(azidomethyl)-1-phenyl-3-(2-phenylethynyl)-1*H*-pyrazole **8** (276 mg, 0.92 mmol),  $\text{K}_3\text{PO}_4$  (978 mg, 4.6 mmol), and  $\text{I}_2$  (1.472 g, 4.6 mmol) in DCM (9.8 mL). The desired compound was obtained after purification by column chromatography (EtOAc/Hex, 1:2 *v/v*). Yield: 299 mg (82%), light yellow crystalline solid, mp = 110–111 °C,  $R_f$  = 0.13 (EtOAc/Hex, 1:3 *v/v*).  $^1\text{H}$  NMR (700 MHz,  $\text{CDCl}_3$ ):  $\delta$  7.42–7.45 (1H, m, CPh 4-H), 7.46–7.52 (3H, m, CPh 3,5-H and NPh 4-H), 7.55–7.59 (2H, m, NPh 3,5-H), 7.68–7.74 (2H, m, CPh 2,6-H), 7.93–7.99 (2H, m, NPh 2,6-H), 8.77 (1H, s, 3-H), 9.13 (1H, s, 4-H).  $^{13}\text{C}$  NMR (176 MHz,  $\text{CDCl}_3$ ):  $\delta$  82.1 (C-7), 118.5 (C-3a), 121.8 (NPh, C-2,6), 123.3 (C-3), 128.1 (CPh, C-3,5), 128.4 (CPh, C-4), 129.3 (NPh, C-4), 129.9 (NPh, C-3,5), 130.1 (CPh, C-2,6), 139.9 (NPh, C-1), 142.2 (CPh, C-1), 146.1 (C-4), 153.5 (C-7a), 155.7 (C-6).  $^{15}\text{N}$  NMR (71 MHz,  $\text{CDCl}_3$ ):  $\delta$  -146.1 (N-2), -90.6 (N-1), -78.4 (N-5). IR ( $\nu$ ,  $\text{cm}^{-1}$ ): 3044, 3035 ( $\text{CH}_{\text{arom}}$ ), 1604, 1590, 1505, 1465, 1202 (C=C, C=N, C-N), 741, 700, 679 (CH=CH of monosubstituted benzenes). MS (ES<sup>+</sup>):  $m/z$  (%): 398 ([M + H]<sup>+</sup>, 100). HRMS (ESI) for  $\text{C}_{18}\text{H}_{13}\text{N}_3\text{I}$  ([M + H]<sup>+</sup>): requires 398.0149 and found 398.0149.

#### 7-Iodo-4-methyl-2,6-diphenyl-2*H*-pyrazolo[4,3-*c*]pyridine 14

7-Iodo-4-methyl-2,6-diphenyl-2*H*-pyrazolo[4,3-*c*]pyridine **14** was prepared in accordance with general procedure (C) from 4-(1-azidoethyl)-1-phenyl-3-(phenylethynyl)-1*H*-pyrazole **9** (255 mg, 0.79 mmol),  $\text{NaHCO}_3$  (69 mg, 0.82 mmol), and  $\text{I}_2$  (1034 mg, 4.07 mmol) in DCM (8.1 mL). The desired compound was obtained after purification by column chromatography (EtOAc/Hex, 1:2 *v/v*). Yield: 238 mg (72%), light yellow crystalline solid, mp = 186–189 °C,  $R_f$  = 0.43 (EtOAc/Hex, 1:2 *v/v*).  $^1\text{H}$  NMR (700 MHz,  $\text{CDCl}_3$ ):  $\delta$  2.83 (s, 3H,  $\text{CH}_3$ ), 7.40–7.43 (m, 1H, CPh 4-H), 7.46–7.49 (m, 3H, CPh 3,5-H; NPh 4-H), 7.55–7.57 (m, 2H, NPh 3,5-H), 7.67–7.69 (m, 2H, CPh 2,6-H), 7.95–7.96 (m, 2H, NPh 2,6-H), 8.72 (s, 1H, 3-H).  $^{13}\text{C}$  NMR (176 MHz,  $\text{CDCl}_3$ ):  $\delta$  22.5 ( $\text{CH}_3$ ), 79.0 (C-7), 119.0 (C-3a), 121.6 (NPh C-2,6), 123.0 (C-3), 128.0 (CPh C-3,5), 128.3 (CPh C-4), 129.0 (NPh C-4), 129.8 (NPh C-3,5), 130.0 (CPh C-2,6), 140.0 (NPh C-1), 142.5 (CPh C-1), 153.5 (C-7a), 155.3 (C-4), 155.6 (C-6).  $^{15}\text{N}$  NMR (71 MHz,  $\text{CDCl}_3$ ):  $\delta$  -147.5 (N-2), -88.5 (N-1), -80.5 (N-5). IR (KBr,  $\nu$ ,  $\text{cm}^{-1}$ ): 3131, 3107 ( $\text{CH}_{\text{arom}}$ ), 2956 ( $\text{CH}_{\text{aliph}}$ ), 1586, 1504, 1370, 1205 (C=C, C=N, C-N), 798, 768, 750, 696 (CH=CH of monosubstituted benzenes). MS (ES<sup>+</sup>):  $m/z$  (%): 412 ([M + H]<sup>+</sup>, 100). HRMS (ESI)  $\text{C}_{19}\text{H}_{15}\text{IN}_3$  ([M + H]<sup>+</sup>): requires 412.0305 and found 412.0304.

#### 4-Ethyl-7-iodo-2,6-diphenyl-2*H*-pyrazolo[4,3-*c*]pyridine 15

4-Ethyl-7-iodo-2,6-diphenyl-2*H*-pyrazolo[4,3-*c*]pyridine **15** was prepared in accordance with general procedure (C) from 4-(1-azidopropyl)-1-phenyl-3-(phenylethynyl)-1*H*-pyrazole **10** (329 mg, 1.01 mmol),  $\text{NaHCO}_3$  (85 mg, 1.01 mmol), and  $\text{I}_2$  (1278 mg, 5.03

mmol) in DCM (10 mL) the desired compound was obtained after purification by column chromatography (EtOAc/Hex, 1:6 *v/v*). Yield: 348 mg (81%), orange crystalline solid, mp = 145–146 °C,  $R_f$  = 0.39 (EtOAc/Hex, 1:3 *v/v*).  $^1\text{H}$  NMR (700 MHz,  $\text{CDCl}_3$ ):  $\delta$  1.46 (3H, t,  $J$  = 7.6 Hz,  $\text{CH}_3$ ), 3.14 (2H, q,  $J$  = 7.6 Hz,  $\text{CH}_2$ ), 7.40–7.43 (1H, m, CPh 4-H), 7.45–7.50 (3H, m, CPh 3,5-H; NPh 4-H), 7.54–7.58 (2H, m, NPh 3,5-H), 7.69–7.75 (2H, m, CPh 2,6-H), 7.93–7.98 (2H, m, NPh 2,6-H), 8.74 (1H, s, 3-H).  $^{13}\text{C}$  NMR (176 MHz,  $\text{CDCl}_3$ ):  $\delta$  13.5 ( $\text{CH}_3$ ), 29.7 ( $\text{CH}_2$ ), 78.8 (C-7), 117.8 (C-3a), 121.5 (NPh C-2,6), 122.6 (C-3), 127.8 (CPh C-3,5), 128.1 (CPh C-4), 128.9 (NPh C-4), 129.7 (NPh C-3,5), 130.0 (CPh, C-2,6), 139.8 (NPh C-1), 142.4 (CPh C-1), 153.8 (C-7a), 155.2 (C-6), 160.2 (C-4).  $^{15}\text{N}$  NMR (71 MHz,  $\text{CDCl}_3$ ):  $\delta$  –148.2 (N-2), –89.9 (N-1), –82.2 (N-5). IR (KBr,  $\nu$ ,  $\text{cm}^{-1}$ ): 3059 ( $\text{CH}_{\text{arom}}$ ), 2969, 2929 ( $\text{CH}_{\text{aliph}}$ ), 1584, 1504, 1464, 1374, 1273, 1201 (C=C, C=N, C–N), 905, 768, 698 (CH=CH of monosubstituted benzenes). MS ( $\text{ES}^+$ ):  $m/z$  (%): 425 ( $[\text{M} + \text{H}]^+$ , 99). HRMS (ESI)  $\text{C}_{20}\text{H}_{17}\text{IN}_3$  ( $[\text{M} + \text{H}]^+$ ): requires 426.0462 and found 426.0462.

#### 7-Iodo-4-isopropyl-2,6-diphenyl-2H-pyrazolo[4,3-c]pyridine 16

7-Iodo-4-isopropyl-2,6-diphenyl-2H-pyrazolo[4,3-c]pyridine **16** was prepared in accordance with general procedure (C) from 4-(azido-2-methylpropyl)-1-phenyl-3-(phenylethynyl)-1H-pyrazole **11** (177 mg, 0.52 mmol),  $\text{NaHCO}_3$  (44 mg, 0.52 mmol), and  $\text{I}_2$  (659 mg, 2.6 mmol) in DCM (5.2 mL). The desired compound was obtained after purification by column chromatography (EtOAc/Hex, 1:6 *v/v*). Yield: 191 mg (84%), white crystalline solid, mp = 134–135 °C,  $R_f$  = 0.50 (EtOAc/Hex, 1:5 *v/v*).  $^1\text{H}$  NMR (700 MHz,  $\text{CDCl}_3$ ):  $\delta$  1.49 (6H, d,  $J$  = 7.0 Hz,  $\text{CH}-(\text{CH}_3)_2$ ), 3.47 (1H, hept,  $J$  = 7.0 Hz,  $\text{CH}-(\text{CH}_3)_2$ ), 7.39–7.44 (1H, m, CPh 4-H), 7.45–7.51 (3H, m, CPh 3,5-H and NPh 4-H), 7.54–7.59 (2H, m, NPh 3,5-H), 7.74–7.82 (2H, m, CPh 2,6-H), 7.93–7.99 (2H, m, NPh 2,6-H), 8.76 (1H, s, 3-H).  $^{13}\text{C}$  NMR (176 MHz,  $\text{CDCl}_3$ ):  $\delta$  22.1 ( $\text{CH}-(\text{CH}_3)_2$ ), 35.6 ( $\text{CH}-(\text{CH}_3)_2$ ), 78.8 (C-7), 117.0 (C-3a), 121.7 (NPh C-2,6), 122.5 (C-3), 127.8 (CPh C-3,5), 128.2 (CPh C-4), 129.0 (NPh C-4), 129.8 (NPh C-3,5), 130.4 (CPh C-2,6), 140.1 (NPh C-1), 142.5 (CPh C-1), 154.3 (C-7a), 154.9 (C-6), 163.8 (C-4).  $^{15}\text{N}$  NMR (71 MHz,  $\text{CDCl}_3$ ):  $\delta$  –158.9 (N-2), –90.3 (N-1), –82.7 (N-5). IR ( $\nu$ ,  $\text{cm}^{-1}$ ): 3114, 3083, 3062 ( $\text{CH}_{\text{arom}}$ ), 2970, 2928, 2868 ( $\text{CH}_{\text{aliph}}$ ), 1584, 1507, 1468, 1391, 1212 (C=C, C=N, C–N), 1106, 1023, 915, 763, 697 (CH=CH of monosubstituted benzenes). MS ( $\text{ES}^+$ ):  $m/z$  (%): 440 ( $[\text{M} + \text{H}]^+$ , 97.7). HRMS (ESI) for  $\text{C}_{21}\text{H}_{19}\text{N}_3\text{I}$  ( $[\text{M} + \text{H}]^+$ ): requires 440.0618 and found 440.0618.

#### 7-Iodo-2,4,6-triphenyl-2H-pyrazolo[4,3-c]pyridine 17

7-Iodo-2,4,6-triphenyl-2H-pyrazolo[4,3-c]pyridine **17** was prepared in accordance with general procedure (C) from 4-[azido(phenyl)methyl]-1-phenyl-3-(phenylethynyl)-1H-pyrazole **12** (62 mg, 0.165 mmol),  $\text{K}_3\text{PO}_4$  (210 mg, 0.83 mmol), and  $\text{I}_2$  (175 mg, 0.83 mmol) in DCM (1.7 mL). The desired compound was obtained after purification by column chromatography (EtOAc/Hex, 1:8 *v/v*). Yield: 69 mg (88%), white crystalline solid, mp = 93–94 °C,  $R_f$  = 0.59 (EtOAc/Hex, 1:3 *v/v*).  $^1\text{H}$  NMR (700 MHz,  $\text{CDCl}_3$ ):  $\delta$  7.43–7.49 (2H, m, C6Ph 4-H and NPh 4-H), 7.49–7.58 (7H, m, C6Ph, NPh and C4Ph 3,5-H; C4Ph 4-H), 7.80–7.87 (2H, m, C6Ph 2,6-H), 7.94–8.00 (2H, m, NPh 2,6-H), 8.04–8.12 (2H, m, C4Ph 2,6-H), 8.90 (1H, s, 3-H).  $^{13}\text{C}$  NMR (176 MHz,  $\text{CDCl}_3$ ):  $\delta$  80.3 (C-7), 116.7 (C-3a), 121.5 (NPh C-2,6), 123.7 (C-3), 127.8 (C6Ph C-3,5), 128.2 (C6Ph C-4), 128.4 (C4Ph C-2,6), 128.9 (C4Ph C-3,5), 129.0 (NPh C-4), 129.7 (NPh C-3,5), 129.9 (C4Ph C-4), 130.2 (C6Ph C-2,6), 138.4 (C4Ph C-1), 139.7 (NPh C-1), 142.3 (C6Ph C-1), 154.5 (C-7a), 154.7 (C-4), 155.4 (C-6).  $^{15}\text{N}$  NMR (71 MHz,  $\text{CDCl}_3$ ):  $\delta$  –146.4 (N-2), –90.3 (N-1), N-5 not found. IR (KBr,  $\nu$ ,  $\text{cm}^{-1}$ ): 3058 ( $\text{CH}_{\text{arom}}$ ), 2922 ( $\text{CH}_{\text{aliph}}$ ), 1570, 1505, 1464, 1371, 1212 (C=C, C=N, C–N), 969, 750, 698 (CH=CH of monosubstituted benzenes). MS ( $\text{ES}^+$ ):  $m/z$  (%): 474 ( $[\text{M} + \text{H}]^+$ , 99). HRMS (ESI)  $\text{C}_{24}\text{H}_{17}\text{IN}_3$  ( $[\text{M} + \text{H}]^+$ ): requires 474.0462 and found 474.0462.

#### 3.2.5. General Procedure (D) for the Synthesis of 7-Substituted Pyrazolo[4,3-c]pyridine derivatives 18–39 by Suzuki–Miyaura Cross-Coupling with Boronic acids

To a solution of appropriate 7-iodo-2H-pyrazolo[4,3-c]pyridine **13–17** (1 equivalent) in a mixture of EtOH and water (3:1, *v/v*), boronic acid (1.2 equivalents),  $\text{Cs}_2\text{CO}_3$  (2 equiv-

alents), and Pd(OAc)<sub>2</sub> (0.07 equivalents) were added under argon atmosphere. The mixture was stirred at 100 °C under microwave irradiation (100 W and 300 Pa) for 0.5–1 h. Upon completion (monitored by TLC), the reaction mixture was cooled to room temperature and filtered through a pad of Celite, and the filter cake was washed with EtOAc (20 mL). The filtrate was diluted with water (20 mL) and extracted with EtOAc (3 × 25 mL). The combined organic layers were washed with brine (10 mL), dried over anhydrous Na<sub>2</sub>SO<sub>4</sub>, filtered, and evaporated under reduced pressure. The residue was purified by column chromatography.

#### 2,6,7-Triphenyl-2H-pyrazolo[4,3-c]pyridine 18

2,6,7-Triphenyl-2H-pyrazolo[4,3-c]pyridine **18** was prepared in accordance with general procedure (D) from 7-iodo-2,6-diphenyl-2H-pyrazolo[4,3-c]pyridine **13** (60 mg, 0.15 mmol), phenylboronic acid (22 mg, 0.18 mmol), Cs<sub>2</sub>CO<sub>3</sub> (98 mg, 0.3 mmol), Pd(OAc)<sub>2</sub> (2.4 mg, 0.01 mmol), EtOH (0.9 mL), and water (0.3 mL). The reaction was finished after 30 min. The desired compound was obtained after purification by column chromatography (EtOAc/Hex, 1:4 to 1:2 *v/v*). Yield: 50 mg (96%), brown crystalline solid, mp = 151–152 °C, R<sub>f</sub> = 0.08 (EtOAc/Hex, 1:3 *v/v*). <sup>1</sup>H NMR (700 MHz, CDCl<sub>3</sub>): δ 7.21–7.26 (3H, m, C6Ph 3,4,5-H), 7.28–7.31 (1H, m, C7Ph 4-H), 7.31–7.35 (2H, m, C7Ph 3,5-H), 7.42–7.46 (3H, m, C6Ph 2,6-H and NPh 4-H), 7.49–7.55 (4H, m, NPh 3,5-H and C7Ph 2,6-H), 7.89–7.94 (2H, m NPh 2,6-H), 8.66 (1H, s, 3-H), 9.32 (1H, s, 4-H). <sup>13</sup>C NMR (176 MHz, CDCl<sub>3</sub>): δ 120 (C-3a), 121.4 (NPh C-2,6), 121.8 (C-3), 123.1 (C-6), 127.2 (C6Ph C-4), 127.3 (C7Ph C-4), 127.8 (C6Ph C-2,6), 128.0 (C7Ph C-3,5), 128.7 (NPh C-4), 129.6 (NPh C-3,5), 130.5 (C7Ph C-2,6), 131.1 (C7Ph C-2,6), 135.6 (C7Ph C-1), 140.0 (NPh C-1), 140.6 (C6Ph C-1), 145.7 (C-4), 149.3 (C-4), 151.2 (C-7a). <sup>15</sup>N NMR (71 MHz, CDCl<sub>3</sub>): δ −144.9 (N-2), −96.8 (N-1), −80.5 (N-5). IR (ν, cm<sup>−1</sup>): 3502, 3081 (CH<sub>arom</sub>), 1663, 1610, 1592, 1504, 1203, 1180, 1127 (C=C, C=N, C–N), 761, 697, 688 (CH=CH of monosubstituted benzenes). MS (ES<sup>+</sup>): *m/z* (%): 348 ([M + H]<sup>+</sup>, 98). HRMS (ESI) for C<sub>24</sub>H<sub>18</sub>N<sub>3</sub> ([M + H]<sup>+</sup>): requires 348.1495 and found 348.1495.

#### 7-(2-Methoxyphenyl)-2,6-diphenyl-2H-pyrazolo[4,3-c]pyridine 19

7-(2-Methoxyphenyl)-2,6-diphenyl-2H-pyrazolo[4,3-c]pyridine **19** was prepared in accordance with general procedure (D) from 7-iodo-2,6-diphenyl-2H-pyrazolo[4,3-c]pyridine **13** (60 mg, 0.15 mmol), (2-methoxyphenyl)boronic acid (27 mg, 0.18 mmol), Cs<sub>2</sub>CO<sub>3</sub> (98 mg, 0.3 mmol), Pd(OAc)<sub>2</sub> (2.4 mg, 0.01 mmol), EtOH (0.9 mL), and water (0.3 mL). The reaction was stopped after 1 h. The desired compound was obtained after purification by column chromatography (EtOAc/Hex, 1:3 *v/v*). Yield: 23 mg (40%), light yellow crystalline solid, mp = 169–170 °C, R<sub>f</sub> = 0.08 (EtOAc/Hex, 1:3 *v/v*). <sup>1</sup>H NMR (700 MHz, CDCl<sub>3</sub>): δ 3.42 (3H, s, OCH<sub>3</sub>), 6.82–6.87 (1H, m, C7Ph), 7.00–7.03 (1H, m, C7Ph), 7.17–7.21 (1H, m, C7Ph), 7.21–7.24 (2H, m, Ph), 7.30–7.35 (1H, m, Ph), 7.39–7.42 (1H, m, Ph), 7.43–7.46 (2H, m, Ph), 7.47–7.51 (3H, m, Ph), 7.81–7.92 (2H, m, NPh, 2,6-H), 8.61 (s, 1H, 3-H), 9.34 (s, 1H, 4-H). <sup>13</sup>C NMR (176 MHz, CDCl<sub>3</sub>): δ 55.3, 111.6, 119.7, 120.1, 120.7, 121.6, 121.8, 125.1, 127.1, 127.6, 128.7, 129.3, 129.6, 129.7, 132.5, 140.3, 141.5, 145.9, 150.4, 151.6, 157.0. IR (ν, cm<sup>−1</sup>): 3062, 3019 (CH<sub>arom</sub>), 2922, 2852 (CH<sub>aliph</sub>), 1600, 1590, 1501, 1478, 1435, 1242, 1233, 1203 (C=C, C=N, C–N), 1112, 1043, 1021 (C–O–C), 763, 750, 697, 686 (CH=CH of mono- and disubstituted benzenes). MS (ES<sup>+</sup>): *m/z* (%): 378 ([M + H]<sup>+</sup>, 99). HRMS (ESI) for C<sub>25</sub>H<sub>20</sub>N<sub>3</sub>O ([M + H]<sup>+</sup>): requires 378.1601 and found 378.1601.

#### 7-(3-Methoxyphenyl)-2,6-diphenyl-2H-pyrazolo[4,3-c]pyridine 20

7-(3-Methoxyphenyl)-2,6-diphenyl-2H-pyrazolo[4,3-c]pyridine **20** was prepared in accordance with general procedure (D) from 7-iodo-2,6-diphenyl-2H-pyrazolo[4,3-c]pyridine **13** (60 mg, 0.15 mmol), (3-methoxyphenyl)boronic acid (27 mg, 0.18 mmol), Cs<sub>2</sub>CO<sub>3</sub> (98 mg, 0.3 mmol), Pd(OAc)<sub>2</sub> (2.4 mg, 0.01 mmol), EtOH (0.9 mL), and water (0.3 mL). The reaction was finished after 1 h. The desired compound was obtained after purification by column chromatography (EtOAc/Hex, 1:3 *v/v*). Yield: 44 mg (78%), white crystalline solid, mp = 71–72 °C, R<sub>f</sub> = 0.08 (EtOAc/Hex, 1:3 *v/v*). <sup>1</sup>H NMR (700 MHz, CDCl<sub>3</sub>): δ 3.66 (3H, s,



OCH<sub>3</sub>), 6.81–6.87 (1H, m, C7Ph 4-H), 7.02–7.08 (1H, m, C7Ph 2-H), 7.10–7.14 (1H, m, C7Ph 6-H), 7.21–7.29 (4H, m, C7Ph 5-H, C6Ph 3,4,5-C), 7.40–7.44 (1H, m, NPh 4-H), 7.44–7.48 (2H, m, C6Ph 2,6-H), 7.49–7.54 (2H, m, NPh 3,5-H), 7.86–7.94 (2H, m, NPh 2,6-H), 8.64 (1H, s, 3-H), 9.30 (1H, s, 4-H). <sup>13</sup>C NMR (176 MHz, CDCl<sub>3</sub>): δ 55.3 (OCH<sub>3</sub>), 113.7 (C7Ph C-4), 116.6 (C7Ph C-2), 120.2 (C-3a), 121.5 (NPh C-2,6), 121.9 (C-3), 123.0 (C-7), 123.9 (C7Ph C-6), 127.3 (C6Ph C-4), 128.0 (C6Ph C-3,5), 128.8 (NPh C-4), 129.1 (C7Ph C-5), 129.8 (NPh C-3,5), 130.6 (C6Ph C-2,6), 137.0 (C7Ph C-1), 140.2 (NPh C-1), 140.9 (C6Ph C-1), 145.9 (C-4), 149.6 (C-6), 151.2 (C-7a), 159.3 (C7Ph C-3). <sup>15</sup>N NMR (71 MHz, CDCl<sub>3</sub>): δ –145.2 (N-2), –96.9 (N-1), –79.4 (N-5). IR (ν, cm<sup>-1</sup>): 3394, 3058, 3011 (CH<sub>arom</sub>), 2920, 2849 (CH<sub>aliph</sub>), 1592, 1575, 1507, 1464, 1367, 1317, 1286, 1212 (C=C, C=N, C-N), 1150, 1051 (C-O-C), 764, 756, 699, 689 (CH=CH of mono- and disubstituted benzenes). MS (ES<sup>+</sup>): *m/z* (%): 378 ([M + H]<sup>+</sup>, 99). HRMS (ESI) for C<sub>25</sub>H<sub>20</sub>N<sub>3</sub>O ([M + H]<sup>+</sup>): requires 378.1601 and found 378.1601.

#### 7-(4-Methoxyphenyl)-2,6-diphenyl-2H-pyrazolo[4,3-c]pyridine 21

7-(4-Methoxyphenyl)-2,6-diphenyl-2H-pyrazolo[4,3-c]pyridine **21** was prepared in accordance with general procedure (D) from 7-iodo-2,6-diphenyl-2H-pyrazolo[4,3-c]pyridine **13** (60 mg, 0.15 mmol), (4-methoxyphenyl)boronic acid (27 mg, 0.18 mmol), Cs<sub>2</sub>CO<sub>3</sub> (98 mg, 0.3 mmol), Pd(OAc)<sub>2</sub> (2.4 mg, 0.01 mmol), EtOH (0.9 mL), and water (0.3 mL). The reaction was finished after 1 h. The desired compound was obtained after purification by column chromatography (EtOAc/Hex, 1:3 *v/v*). Yield: 44 mg (78%), white crystalline solid, mp = 192–193 °C, R<sub>f</sub> = 0.08 (EtOAc/Hex, 1:3 *v/v*). <sup>1</sup>H NMR (700 MHz, CDCl<sub>3</sub>): δ 3.82 (3H, s, OCH<sub>3</sub>), 6.82–6.93 (2H, m, C7Ph 3,5-H), 7.21–7.25 (1H, m, C6Ph 4-H), 7.25–7.30 (2H, m, C6Ph 3,5-H), 7.41–7.49 (5H, m, NPh 4-H, C6Ph 2,6-H, C7Ph 2,6-H), 7.50–7.56 (2H, m, NPh 3,5-H), 7.84–7.97 (2H, m, NPh 2,6-H), 8.63 (1H, s, 3-H), 9.28 (1H, s, 4-H). <sup>13</sup>C NMR (176 MHz, CDCl<sub>3</sub>): δ 55.2 (OCH<sub>3</sub>), 113.5 (C7Ph C-3,5), 120.1 (C-3a), 121.4 (NPh C-2,6), 121.7 (C-3), 122.6 (C-7), 127.0 (C6Ph C-4), 127.8 (C7Ph C-1), 127.9 (C6Ph C-3,5), 128.7 (NPh C-4), 129.6 (NPh C-3,5), 130.5 (C6Ph C-2,6), 132.4 (C7Ph C-2,6), 140.1 (NPh C-1), 140.9 (C6Ph C-1), 145.3 (C-4), 149.2 (C-6), 151.4 (C-7a), 158.9 (C7Ph C-4). <sup>15</sup>N NMR (71 MHz, CDCl<sub>3</sub>): δ –145.4 (N-2), –97.0 (N-1), –79.1 (N-5). IR (ν, cm<sup>-1</sup>): 3135, 3062, 3020 (CH<sub>arom</sub>), 2927, 2837 (CH<sub>aliph</sub>), 1589, 1503, 1438, 1290, 1252 (C=C, C=N, C-N), 1178, 1031 (C-O-C), 763, 758, 689 (CH=CH of mono- and disubstituted benzenes). MS (ES<sup>+</sup>): *m/z* (%): 378 ([M + H]<sup>+</sup>, 100). HRMS (ESI) for C<sub>25</sub>H<sub>20</sub>N<sub>3</sub>O ([M + H]<sup>+</sup>): requires 378.1603 and found 378.1601.

#### 7-(3,4-Dimethoxyphenyl)-2,6-diphenyl-2H-pyrazolo[4,3-c]pyridine 22

7-(3,4-Dimethoxyphenyl)-2,6-diphenyl-2H-pyrazolo[4,3-c]pyridine **22** was prepared in accordance with general procedure (D) from 7-iodo-2,6-diphenyl-2H-pyrazolo[4,3-c]pyridine **13** (60 mg, 0.15 mmol), (3,4-dimethoxyphenyl)boronic acid (33 mg, 0.18 mmol), Cs<sub>2</sub>CO<sub>3</sub> (98 mg, 0.3 mmol), Pd(OAc)<sub>2</sub> (2.4 mg, 0.01 mmol), EtOH (0.9 mL), and water (0.3 mL). The reaction was finished after 1 h. The desired compound was obtained after purification by column chromatography (EtOAc/Hex, 1:3 *v/v*). Yield: 44 mg (72%), white crystalline solid, mp = 163–164 °C, R<sub>f</sub> = 0.08 (EtOAc/Hex, 1:3 *v/v*). <sup>1</sup>H NMR (700 MHz, CDCl<sub>3</sub>): δ 3.61 (3H, s, 3-OCH<sub>3</sub>), 3.90 (3H, s, 4-OCH<sub>3</sub>), 6.85–6.90 (1H, m, C7Ph 5-H), 6.91–6.95 (1H, m, C7Ph 2-H), 7.21–7.30 (4H, m, C6Ph 3,4,5-H, C7Ph 6-H), 7.42–7.45 (1H, m, NPh 4H), 7.45–7.49 (2H, m, NPh 2,6-H), 7.50–7.56 (2H, m, NPh 3,5-H), 7.87–7.98 (2H, m, NPh 2,6-H), 8.65 (1H, s, 3-H), 9.28 (1H, s, 4-H). <sup>13</sup>C NMR (176 MHz, CDCl<sub>3</sub>): δ 55.7 (3-OCH<sub>3</sub>), 55.9 (4-OCH<sub>3</sub>), 110.9 (C7Ph C-5), 114.9 (C7Ph C-2), 120.3 (C-3a), 121.5 (NPh C-2,6), 121.9 (C-3), 122.8 (C-7), 124.0 (C7Ph C-6), 127.2 (C6Ph C-4), 128.0 (C7Ph C-1), 128.1 (C6Ph C-3,5), 128.8 (NPh C-4), 129.8 (NPh C-3,5), 130.5 (C6Ph C-2,6), 140.2 (NPh C-1), 141.2 (C6Ph C-1), 145.4 (C-4), 148.4 (C7Ph C-3,4), 149.4 (C-6), 151.4 (C-7a). <sup>15</sup>N NMR (71 MHz, CDCl<sub>3</sub>): δ –145.4 (N-2), –97.1 (N-1), –79.2 (N-5). IR (ν, cm<sup>-1</sup>): 3042, 3019 (CH<sub>arom</sub>), 2967, 2919, 2850 (CH<sub>aliph</sub>), 1592, 1507, 1468, 1253, 1225 (C=C, C=N, C-N), 1141, 1014 (C-O-C), 753, 699, 688 (CH=CH of mono- and disubstituted benzenes). MS (ES<sup>+</sup>): *m/z* (%): 408 ([M + H]<sup>+</sup>, 100). HRMS (ESI) for C<sub>26</sub>H<sub>22</sub>N<sub>3</sub>O<sub>2</sub> ([M + H]<sup>+</sup>): requires 408.1707 and found 408.1707.

4-(2,6-Diphenyl-2H-pyrazolo[4,3-c]pyridin-7-yl)phenol **23**

4-(2,6-Diphenyl-2H-pyrazolo[4,3-c]pyridin-7-yl)phenol **23** was prepared in accordance with general procedure (D) from 7-iodo-2,6-diphenyl-2H-pyrazolo[4,3-c]pyridine **13** (80 mg, 0.2 mmol), (4-hydroxyphenyl)boronic acid (33 mg, 0.24 mmol), Cs<sub>2</sub>CO<sub>3</sub> (131 mg, 0.4 mmol), Pd(OAc)<sub>2</sub> (3 mg, 0.014 mmol), EtOH (1.2 mL), and water (0.4 mL). The reaction was finished after 30 min. The desired compound was obtained after purification by column chromatography (EtOAc/Hex, 1:2 to 2:1 *v/v*). Yield: 44 mg (60%), yellowish crystalline solid, mp = 307–308 °C, R<sub>f</sub> = 0.18 (EtOAc/Hex, 1:2 *v/v*). <sup>1</sup>H NMR (700 MHz, DMSO-*d*<sub>6</sub>): δ 6.70–6.75 (2H, m, C7Ph 3,5-H), 7.20–7.28 (5H, m, C7Ph 2,6-H; C6Ph 3,4,5-H), 7.37–7.40 (2H, m, C6Ph 2,6-H), 7.49–7.52 (1H, m, NPh 4-H), 7.59–7.63 (2H, m, NPh 3,5-H), 8.04–8.09 (2H, m, NPh 2,6-H), 9.29 (1H, s, 4-H), 9.46 (1H, s, 3-H), 9.50 (1H, s, OH). <sup>13</sup>C NMR (176 MHz, DMSO-*d*<sub>6</sub>): δ 115.0 (C7Ph C-3,5), 119.7 (C-3a), 121.0 (NPh C-2,6), 122.3 (C-7), 124.2 (C-3), 125.8 (C7Ph C-1), 127.0 (C6Ph C-4), 127.6 (C6Ph C-3,5), 128.7 (NPh C-4), 129.8 (NPh C-3,5), 130.3 (C6Ph C-2,6), 132.0 (C7Ph C-2,6), 139.5 (NPh C-1), 140.6 (C6Ph C-1), 145.5 (C-4), 147.8 (C-6), 150.5 (C-7a), 156.7 (C7Ph C-4). <sup>15</sup>N NMR (71 MHz, DMSO-*d*<sub>6</sub>): δ –144.8 (N-2), N-1 and N-5 not found. IR (KBr, ν, cm<sup>−1</sup>): 3449 (OH), 2924 (CH<sub>arom</sub>), 1607, 1592, 1505, 1440, 1273, 1172 (C=C, C=N, C–N), 767, 695 (CH=CH of mono- and disubstituted benzenes). MS (ES<sup>+</sup>): *m/z* (%): 364 ([M + H]<sup>+</sup>, 96). HRMS (ESI) for C<sub>24</sub>H<sub>18</sub>N<sub>3</sub>O ([M + H]<sup>+</sup>): requires 364.1444 and found 364.1446.

4-Methyl-2,6,7-triphenyl-2H-pyrazolo[4,3-c]pyridine **24**

4-Methyl-2,6,7-triphenyl-2H-pyrazolo[4,3-c]pyridine **24** was prepared in accordance with general procedure (D) from 7-iodo-4-methyl-2,6-diphenyl-2H-pyrazolo[4,3-c]pyridine **14** (50 mg, 0.12 mmol), phenylboronic acid (18 mg, 0.145 mmol), Cs<sub>2</sub>CO<sub>3</sub> (79 mg, 0.24 mmol), Pd(OAc)<sub>2</sub> (1.9 mg, 0.008 mmol), EtOH (0.9 mL), and water (0.3 mL). The reaction was finished after 30 min. The desired compound was obtained after purification by column chromatography (EtOAc/Hex, 1:4 to 1:2 *v/v*). Yield: 116 mg (94%), mp = 202–205 °C, R<sub>f</sub> = 0.17 (EtOAc/Hex, 1:3 *v/v*). <sup>1</sup>H NMR (700 MHz, CDCl<sub>3</sub>): δ 2.93 (3H, s, CH<sub>3</sub>), 7.19–7.24 (3H, m, C7Ph), 7.25–7.29 (1H, m, C6Ph 4-H), 7.29–7.33 (2H, m, C6Ph 3,5-H), 7.41–7.48 (5H, m, C6Ph 2,6-H, NPh 4-H and C7Ph), 7.49–7.54 (2H, m, NPh 3,5-H), 7.89–7.91 (2H, m, NPh 2,6-H), 8.61 (1H, s, 3-H). <sup>13</sup>C NMR (176 MHz, CDCl<sub>3</sub>): δ 22.8 (CH<sub>3</sub>), 120.0 (C-3a), 121.1 (C-7), 121.3 (NPh C-2,6), 121.9 (C-3), 127.1 (C7Ph C-4), 127.2 (C6Ph C-4), 127.6 (C7Ph C-1), 127.8 (C7Ph), 127.9 (C6Ph C-3,5), 128.6 (NPh C-4), 129.6 (NPh C-3,5), 130.6 (C7Ph), 131.2 (C6Ph C-2,6), 135.7 (C6Ph C-1), 140.0 (NPh C-1), 148.8 (C-6), 151.5 (C-7a), 154.5 (C-4). <sup>15</sup>N NMR (71 MHz, CDCl<sub>3</sub>): δ –145.9 (N-2), –95.0 (N-1), –88.2 (N-5). IR (KBr, ν, cm<sup>−1</sup>): 3137, 3061 (CH<sub>arom</sub>), 2916 (CH<sub>aliph</sub>), 1588, 1545, 1505, 1476, 1371 (C=C, C=N, C–N), 762, 700, 661 (CH=CH monosubstituted benzenes). MS (ES<sup>+</sup>): *m/z* (%): 362 ([M + H]<sup>+</sup>, 100). HRMS (ESI) C<sub>25</sub>H<sub>20</sub>N<sub>3</sub> ([M + H]<sup>+</sup>): requires 362.1652 and found 362.1650.

7-(2-Methoxyphenyl)-4-methyl-2,6-diphenyl-2H-pyrazolo[4,3-c]pyridine **25**

7-(2-Methoxyphenyl)-4-methyl-2,6-diphenyl-2H-pyrazolo[4,3-c]pyridine **25** was prepared in accordance with general procedure (D) from 7-iodo-4-methyl-2,6-diphenyl-2H-pyrazolo[4,3-c]pyridine **14** (50 mg, 0.12 mmol), (2-methoxyphenyl)boronic acid (22 mg, 0.145 mmol), Cs<sub>2</sub>CO<sub>3</sub> (79 mg, 0.24 mmol), Pd(OAc)<sub>2</sub> (1.9 mg, 0.008 mmol), EtOH (0.9 mL), and water (0.3 mL). The reaction was finished after 1 h. The desired compound was obtained after purification by column chromatography (EtOAc/Hex, 1:3 *v/v*). Yield: 38 mg (80%), light yellow crystalline solid, mp = 159–160 °C, R<sub>f</sub> = 0.13 (EtOAc/Hex, 1:3 *v/v*). <sup>1</sup>H NMR (500 MHz, CDCl<sub>3</sub>): δ 2.95 (3H, s, CH<sub>3</sub>), 3.42 (3H, s, OCH<sub>3</sub>), 6.81–6.85 (1H, m, C7Ph 3-H), 6.97–7.01 (1H, m, C6Ph 4-H), 7.17–7.23 (3H, m, NPh 3,5-H and C6Ph 4-H), 7.28–7.32 (1H, m, C7Ph 4-H), 7.39–7.45 (4H, m, NPh 4-H, C6Ph 2,6-H and C7Ph 5-H), 7.47–7.51 (2H, m, C6Ph 3,5-H), 7.85–7.89 (2H, m, NPh, 2,6-H), 8.62 (1H, s, 3-H). <sup>13</sup>C NMR (126 MHz, CDCl<sub>3</sub>): δ 22.9 (CH<sub>3</sub>), 55.4 (OCH<sub>3</sub>), 111.5 (C7Ph C-3), 117.8 (C-7), 120.1 (C-3a), 120.6 (C7Ph C-5), 121.6 (NPh C-2,6), 122.2 (C-3), 125.0 (C7Ph C-1), 127.2 (C6Ph C-4), 127.6 (NPh C-3,5), 128.7 (NPh C-4), 129.2 (C7Ph C-4), 129.7 (C6Ph C-2,3,5,6), 132.6 (C7Ph C-5), 140.3 (NPh

C-1), 140.8 (C6Ph C-1), 149.8 (C-6), 151.8 (C-7a), 154.8 (C-4), 157.1 (C7Ph C-2). IR ( $\nu$ ,  $\text{cm}^{-1}$ ): 3143, 3069, 3019 ( $\text{CH}_{\text{arom}}$ ), 2955, 2922, 2853 ( $\text{CH}_{\text{aliph}}$ ), 1599, 1586, 1578, 1552, 1504, 1495, 1479, 1434, 1372, 1240, 1217 (C=C, C=N, C-N), 1046, 1022 (C-O-C), 750, 698, 685 (CH=CH of mono- and disubstituted benzenes). MS ( $\text{ES}^+$ ):  $m/z$  (%): 392 ( $[\text{M} + \text{H}]^+$ , 100). HRMS (ESI) for  $\text{C}_{26}\text{H}_{22}\text{N}_3\text{O}$  ( $[\text{M} + \text{H}]^+$ ): requires 392.1758 and found 392.1757.

#### 7-(3-Methoxyphenyl)-4-methyl-2,6-diphenyl-2H-pyrazolo[4,3-c]pyridine 26

7-(3-Methoxyphenyl)-4-methyl-2,6-diphenyl-2H-pyrazolo[4,3-c]pyridine **26** was prepared in accordance with general procedure (D) from 7-iodo-4-methyl-2,6-diphenyl-2H-pyrazolo[4,3-c]pyridine **14** (50 mg, 0.12 mmol), (3-methoxyphenyl)boronic acid (22 mg, 0.145 mmol),  $\text{Cs}_2\text{CO}_3$  (79 mg, 0.24 mmol),  $\text{Pd}(\text{OAc})_2$  (1.9 mg, 0.008 mmol), EtOH (0.9 mL), and water (0.3 mL). The reaction was finished after 30 min. The desired compound was obtained after purification by column chromatography (EtOAc/Hex, 1:3  $v/v$ ). Yield: 38 mg (80%), light yellow crystalline solid, mp = 190–191 °C,  $R_f$  = 0.18 (EtOAc/Hex, 1:3  $v/v$ ).  $^1\text{H}$  NMR (500 MHz,  $\text{CDCl}_3$ ):  $\delta$  2.97 (3H, s,  $\text{CH}_3$ ), 3.65 (3H, s,  $\text{OCH}_3$ ), 6.79–6.85 (1H, m, C7Ph 4-H), 6.96–7.03 (1H, m, C7Ph 2-H), 7.06–7.12 (1H, m, C7Ph 6-H), 7.17–7.32 (4H, m, C7Ph 5-H, C6Ph 3,4,5-H), 7.41–7.47 (1H, m, NPh 4-H), 7.50–7.55 (4H, m, NPh 3,5-H, C6Ph, 2,6-H), 7.86–7.95 (2H, m, NPh 2,6-H), 8.67 (1H, s, 3-H).  $^{13}\text{C}$  NMR (126 MHz,  $\text{CDCl}_3$ ):  $\delta$  23.1 ( $\text{CH}_3$ ), 55.2 ( $\text{OCH}_3$ ), 113.4 (C7Ph C-4), 116.6 (C7Ph C-2), 120.1 (C-3a), 120.8 (C-7), 121.3 (NPh C-2,6), 121.9 (C-3), 123.9 (C7Ph C-6), 127.2 (C6Ph C-4), 127.9 (C6Ph C-3,5), 128.6 (NPh, C-4), 129.0 (C7Ph C-5), 129.7 (NPh C-3,5), 130.6 (C6Ph C-2,6), 137.2 (C7Ph C-1), 140.1 (NPh C-1), 140.8 (C6Ph C-1), 149.3 (C-6), 151.4 (C-7a), 154.6 (C-4), 159.2 (C7Ph C-3). IR ( $\nu$ ,  $\text{cm}^{-1}$ ): 3067, 3002 ( $\text{CH}_{\text{arom}}$ ), 2954, 2923, 2852 ( $\text{CH}_{\text{aliph}}$ ), 1599, 1589, 1575, 1547, 1488, 1443, 1284, 1211 (C=C, C=N, C-N), 1160, 1049 (C-O-C), 753, 700, 686 (CH=CH of mono- and disubstituted benzenes). MS ( $\text{ES}^+$ ):  $m/z$  (%): 392 ( $[\text{M} + \text{H}]^+$ , 100). HRMS (ESI) for  $\text{C}_{26}\text{H}_{22}\text{N}_3\text{O}$  ( $[\text{M} + \text{H}]^+$ ): requires 392.1757 and found 392.1757.

#### 7-(4-Methoxyphenyl)-4-methyl-2,6-diphenyl-2H-pyrazolo[4,3-c]pyridine 27

7-(4-Methoxyphenyl)-4-methyl-2,6-diphenyl-2H-pyrazolo[4,3-c]pyridine **27** was prepared in accordance with general procedure (D) from 7-iodo-4-methyl-2,6-diphenyl-2H-pyrazolo[4,3-c]pyridine **14** (50 mg, 0.12 mmol), (4-methoxyphenyl)boronic acid (22 mg, 0.145 mmol),  $\text{Cs}_2\text{CO}_3$  (79 mg, 0.24 mmol),  $\text{Pd}(\text{OAc})_2$  (1.9 mg, 0.008 mmol), EtOH (0.9 mL), and water (0.3 mL). The reaction was finished after 30 min. The desired compound was obtained after purification by column chromatography (EtOAc/Hex, 1:3  $v/v$ ). Yield: 118 mg (89%), mp = 157–161 °C,  $R_f$  = 0.15 (EtOAc/Hex, 1:3  $v/v$ ).  $^1\text{H}$  NMR (700 MHz,  $\text{CDCl}_3$ ):  $\delta$  2.92 (3H, s,  $\text{CH}_3$ ), 3.84 (3H, s,  $\text{OCH}_3$ ), 6.88–6.89 (2H, m, C7Ph 3,5-H), 7.23–7.25 (1H, m, C6Ph 4-H), 7.27–7.30 (2H, m, C6Ph 3,5-H), 7.42–7.45 (3H, m, NPh 4-H and C7Ph 2,6-H), 7.49–7.50 (2H, m, C6Ph 2,6-H), 7.52–7.54 (2H, m, NPh 3,5-H), 7.92–7.93 (2H, m, NPh 2,6-H), 8.61 (1H, s, 3-H).  $^{13}\text{C}$  NMR (176 MHz,  $\text{CDCl}_3$ ):  $\delta$  23.2 ( $\text{CH}_3$ ), 55.3 ( $\text{OCH}_3$ ), 113.6 (C7Ph C-3,5), 120.2 (C-3a), 120.5 (C-7), 121.4 (NPh C-2,6), 121.7 (C-3), 127.0 (C6Ph C-4), 127.9 (C6Ph C-3,5), 128.3 (NPh C-4), 128.5 (C7Ph C-1), 129.7 (NPh C-3,5), 130.7 (C6Ph C-2,6), 132.5 (C7Ph C-2,6), 140.3 (NPh C-1), 141.3 (C6Ph C-1), 149.2 (C-6), 151.8 (C-7a), 154.0 (C-4), 158.7 (C7Ph C-4).  $^{15}\text{N}$  NMR (71 MHz,  $\text{CDCl}_3$ ):  $\delta$  -146.8 (N-2), -95.7 (N-1), -81.6 (N-5). IR (KBr,  $\nu$ ,  $\text{cm}^{-1}$ ): 3056, 3012 ( $\text{CH}_{\text{arom}}$ ), 2951, 2834, 2903, 2831 ( $\text{CH}_{\text{aliph}}$ ), 1607, 1598, 1588, 1507, 1247 (C=C, C=N, C-N), 1075, 1038 (C-O), 755, 728, 701, 685 (CH=CH of mono- and disubstituted benzenes). MS ( $\text{ES}^+$ ):  $m/z$  (%): 392 ( $[\text{M} + \text{H}]^+$ , 100). HRMS (ESI)  $\text{C}_{26}\text{H}_{22}\text{N}_3\text{O}$  ( $[\text{M} + \text{H}]^+$ ): requires 392.1757 and found 392.1759.

#### 7-(3,4-Dimethoxyphenyl)-4-methyl-2,6-diphenyl-2H-pyrazolo[4,3-c]pyridine 28

7-(3,4-Dimethoxyphenyl)-4-methyl-2,6-diphenyl-2H-pyrazolo[4,3-c]pyridine **28** was prepared in accordance with general procedure (D) from 7-iodo-4-methyl-2,6-diphenyl-2H-pyrazolo[4,3-c]pyridine **14** (50 mg, 0.12 mmol), (3,4-dimethoxyphenyl)boronic acid (26 mg, 0.145 mmol),  $\text{Cs}_2\text{CO}_3$  (79 mg, 0.24 mmol),  $\text{Pd}(\text{OAc})_2$  (1.9 mg, 0.008 mmol), EtOH (0.9 mL), and water (0.3 mL). The reaction was finished after 1 h. The desired compound

was obtained after purification by column chromatography (EtOAc/Hex, 1:3 *v/v*). Yield: 41 mg (67%), light yellow crystalline solid, mp = 180–181 °C,  $R_f$  = 0.12 (EtOAc/Hex, 1:3 *v/v*).  $^1\text{H}$  NMR (700 MHz,  $\text{CDCl}_3$ ):  $\delta$  2.91 (3H, s,  $\text{CH}_3$ ), 3.60 (3H, s, 3-O $\text{CH}_3$ ), 3.89 (3H, s, 4-O $\text{CH}_3$ ), 6.85–6.90 (2H, m, C7Ph 2,5-H), 7.20–7.24 (2H, m, C7Ph 6-H, C6Ph 4-H), 7.24–7.28 (2H, m, C6Ph 3,5-H), 7.41–7.44 (1H, m, NPh 4-H), 7.44–7.47 (2H, m, C6Ph 2,6-H), 7.50–7.54 (2H, m, NPh 3,5-H), 7.90–7.95 (2H, m, NPh 2,6-H), 8.62 (1H, s, 3-H).  $^{13}\text{C}$  NMR (176 MHz,  $\text{CDCl}_3$ ):  $\delta$  23.2 ( $\text{CH}_3$ ), 55.7 (3-O $\text{CH}_3$ ), 55.9 (4-O $\text{CH}_3$ ), 110.8 (C7Ph C-5), 114.9 (C7Ph C-2), 120.3 (C-3a), 120.6 (C-7), 121.4 (NPh C-2,6), 121.8 (C-3), 123.9 (C7Ph C-6), 127.1 (C6Ph C-4), 128.1 (C6Ph C-3,5), 128.3 (C7Ph C-1), 128.6 (NPh C-4), 129.7 (NPh C-3,5), 130.6 (C6Ph C-2,6), 140.3 (NPh C-1), 141.3 (CPh C-1), 148.2 (C7Ph C-4), 148.3 (C7Ph C-3), 149.3 (C-6), 151.6 (C-7a), 154.2 (C-4).  $^{15}\text{N}$  NMR (71 MHz,  $\text{CDCl}_3$ ):  $\delta$  -147.2 (N-2), -96.4 (N-1), -82.9 (N-5). IR ( $\nu$ ,  $\text{cm}^{-1}$ ): 3121, 3049, 2999 ( $\text{CH}_{\text{arom}}$ ), 2987, 2949, 2937, 2832 ( $\text{CH}_{\text{aliph}}$ ), 1589, 1519, 1508, 1481, 1465, 1256, 1231 (C=C, C=N, C-N), 1164, 1138, 1023 (C-O-C), 759, 728, 701, 686, 667 (CH=CH of mono- and trisubstituted benzenes). MS ( $\text{ES}^+$ ):  $m/z$  (%): 422 ( $[\text{M} + \text{H}]^+$ , 98). HRMS (ESI) for  $\text{C}_{27}\text{H}_{24}\text{N}_3\text{O}_2$  ( $[\text{M} + \text{H}]^+$ ): requires 422.1863 and found 422.1863.

#### 4-(4-Methyl-2,6-diphenyl-2H-pyrazolo[4,3-c]pyridin-7-yl)phenol **29**

4-(4-Methyl-2,6-diphenyl-2H-pyrazolo[4,3-c]pyridin-7-yl)phenol **29** was prepared in accordance with general procedure (D) from -iodo-4-methyl 2,6-diphenyl-2H-pyrazolo[4,3-c]pyridine **14** (80 mg, 0.2 mmol), (4-hydroxyphenyl)boronic acid (32 mg, 0.23 mmol),  $\text{Cs}_2\text{CO}_3$  (127 mg, 0.39 mmol),  $\text{Pd}(\text{OAc})_2$  (3 mg, 0.014 mmol), EtOH (1.2 mL), and water (0.4 mL). The reaction was finished after 30 min. The desired compound was obtained after purification by column chromatography (EtOAc/Hex, 1:4 to 1:2 *v/v*). Yield: 37 mg (50%), yellowish crystalline solid, mp = 269–270 °C,  $R_f$  = 0.20 (EtOAc/Hex, 1:2 *v/v*).  $^1\text{H}$  NMR (700 MHz,  $\text{DMSO}-d_6$ ):  $\delta$  2.80 (3H, s,  $\text{CH}_3$ ), 6.68–6.73 (2H, m, C7Ph 3,5-H), 7.16–7.19 (2H, m, C7Ph 2,6-H), 7.20–7.22 (1H, m, C6Ph 4-H), 7.22–7.26 (2H, m, C6Ph 3,5-H), 7.34–7.38 (2H, m, C6Ph 2,6-H), 7.46–7.49 (1H, m, NPh 4-H), 7.57–7.63 (2H, m, NPh 3,5-H), 8.04–8.08 (2H, m, NPh 2,6-H), 9.44 (1H, s, OH), 9.51 (1H, s, 3-H).  $^{13}\text{C}$  NMR (176 MHz,  $\text{DMSO}-d_6$ ):  $\delta$  22.6 ( $\text{CH}_3$ ), 114.9 (C7Ph C-3,5), 119.7 (C-3a), 120.0 (C-7), 120.6 (NPh C-2,6), 123.9 (C-3), 126.3 (C7Ph C-1), 126.7 (C6Ph C-4), 127.4 (C6Ph C-3,5), 128.4 (NPh C-4), 129.7 (NPh C-3,5), 130.3 (C6Ph C-2,6), 132.0 (C7Ph C-2,6), 139.6 (NPh C-1), 141.1 (C6Ph C-1), 148.0 (C-6), 150.9 (C-7a), 153.9 (C-4), 156.4 (C7Ph C-4).  $^{15}\text{N}$  NMR (71 MHz,  $\text{DMSO}-d_6$ ):  $\delta$  -147.2 (N-2), -80.5 (N-5), N-1 not found. IR (KBr,  $\nu$ ,  $\text{cm}^{-1}$ ): 3455 (OH), 3149 ( $\text{CH}_{\text{arom}}$ ), 2920 ( $\text{CH}_{\text{aliph}}$ ), 1609, 1591, 1509, 1397, 1264 (C=C, C=N, C-N), 828, 757, 698 (CH=CH of mono- and disubstituted benzenes). MS ( $\text{ES}^+$ ):  $m/z$  (%): 378 ( $[\text{M} + \text{H}]^+$ , 97). HRMS (ESI) for  $\text{C}_{25}\text{H}_{20}\text{N}_3\text{O}$  ( $[\text{M} + \text{H}]^+$ ): requires 378.1601 and found 378.1602.

#### 4-Ethyl-2,6,7-triphenyl-2H-pyrazolo[4,3-c]pyridine **30**

4-Ethyl-2,6,7-triphenyl-2H-pyrazolo[4,3-c]pyridine **30** was prepared in accordance with general procedure (D) from 7-iodo-4-methyl 2,6-diphenyl-2H-pyrazolo[4,3-c]pyridine **15** (80 mg, 0.19 mmol), phenylboronic acid (31 mg, 0.23 mmol),  $\text{Cs}_2\text{CO}_3$  (123 mg, 0.38 mmol),  $\text{Pd}(\text{OAc})_2$  (3 mg, 0.013 mmol), EtOH (1.2 mL), and water (0.4 mL). The reaction was finished after 30 min. The desired compound was obtained after purification by column chromatography (EtOAc/Hex, 1:5 *v/v*). Yield: 58 mg (81%), yellowish crystalline solid, mp = 179–180 °C,  $R_f$  = 0.39 (EtOAc/Hex, 1:3 *v/v*).  $^1\text{H}$  NMR (700 MHz,  $\text{CDCl}_3$ ):  $\delta$  1.54 (3H, t,  $J$  = 7.6 Hz,  $\text{CH}_3$ ), 3.23 (2H, q,  $J$  = 7.6 Hz,  $\text{CH}_2$ ), 7.19–7.23 (1H, m, C6Ph 4-H), 7.23–7.26 (2H, m, C6Ph 3,5-H), 7.26–7.29 (1H, m, C7Ph 4-H), 7.29–7.34 (2H, m, C7Ph 3,5-H), 7.40–7.44 (1H, m, NPh 4-H), 7.46–7.50 (4H, m, CPh 2,6-H), 7.50–7.53 (2H, m, NPh 3,5-H), 7.87–7.95 (2H, m, NPh 2,6-H), 8.62 (1H, s, 3-H).  $^{13}\text{C}$  NMR (176 MHz,  $\text{CDCl}_3$ ):  $\delta$  13.3 ( $\text{CH}_3$ ), 30.4 ( $\text{CH}_2$ ), 119.0 (C-3a), 120.7 (C-7), 121.2 (C-4), 121.3 (NPh C-2,6), 127.0 (C6Ph and C7Ph C-4), 127.7 (C6Ph C-3,5), 127.9 (C7Ph C-3,5), 128.4 (NPh C-4), 129.5 (NPh C-3,5), 130.7 (C6Ph C-2,6), 131.2 (C7Ph C-2,6), 136.2 (C7Ph C-1), 140.2 (NPh C-1), 141.0 (C6Ph C-1), 149.1 (C-6), 151.9 (C-7a), 159.3 (C-4).  $^{15}\text{N}$  NMR (71 MHz,  $\text{CDCl}_3$ ):  $\delta$  -147.3 (N-2), N-1 not found, -83.4 (N-5). IR (KBr,  $\nu$ ,  $\text{cm}^{-1}$ ): 3059 ( $\text{CH}_{\text{arom}}$ ), 2970, 2930 ( $\text{CH}_{\text{aliph}}$ ), 1587, 1547, 1476, 1371, 1213

(C=C, C=N, C–N), 753, 697, 686 (CH=CH monosubstituted benzenes). MS (ES<sup>+</sup>): *m/z* (%): 375 ([M + H]<sup>+</sup>, 99). HRMS (ESI) for C<sub>26</sub>H<sub>22</sub>N<sub>3</sub> ([M + H]<sup>+</sup>): requires 376.1808 and found 376.1808.

#### 4-Ethyl-7-(4-methoxyphenyl)-2,6-diphenyl-2H-pyrazolo[4,3-c]pyridine 31

4-Ethyl-7-(4-methoxyphenyl)-2,6-diphenyl-2H-pyrazolo[4,3-c]pyridine 31 was prepared in accordance with general procedure (D) from 7-iodo-4-methyl 2,6-diphenyl-2H-pyrazolo[4,3-c]pyridine 15 (80 mg, 0.19 mmol), (4-methoxyphenyl)boronic acid (34 mg, 0.23 mmol), Cs<sub>2</sub>CO<sub>3</sub> (123 mg, 0.38 mmol), Pd(OAc)<sub>2</sub> (3 mg, 0.013 mmol), EtOH (1.2 mL), and water (0.4 mL). The reaction was finished after 30 min. The desired compound was obtained after purification by column chromatography (EtOAc/Hex, 1:5 *v/v*). Yield: 63 mg (82%), yellowish crystalline solid, mp = 161–162 °C, *R<sub>f</sub>* = 0.34 (EtOAc/Hex, 1:3 *v/v*). <sup>1</sup>H NMR (700 MHz, CDCl<sub>3</sub>): δ 1.53 (3H, t, *J* = 7.6 Hz, CH<sub>3</sub>), 3.21 (2H, q, *J* = 7.6 Hz, CH<sub>2</sub>), 3.82 (3H, s, OCH<sub>3</sub>), 6.83–6.90 (2H, m, C7Ph 3,5-H), 7.19–7.23 (1H, m, C6Ph 4-H), 7.24–7.27 (2H, m, C6Ph 3,5-H), 7.40–7.44 (3H, m, C7Ph 2,6-H and NPh 4-H), 7.47–7.50 (2H, m, C6Ph 2,6-H), 7.50–7.53 (2H, m, NPh 3,5-H), 7.86–7.97 (2H, m, NPh 2,6-H), 8.61 (1H, s, 3-H). <sup>13</sup>C NMR (176 MHz, CDCl<sub>3</sub>): δ 13.3 (CH<sub>3</sub>), 30.4 (CH<sub>2</sub>), 55.1 (OCH<sub>3</sub>), 113.5 (C7Ph C-3,5), 119.0 (C-3a), 120.3 (C-7), 121.2 (C-4), 121.3 (NPh C-2,6), 126.9 (C6Ph C-4), 127.7 (C6Ph C-3,5), 128.3 (C7Ph C-1), 128.4 (NPh C-4), 129.5 (NPh C-3,5), 130.6 (C6Ph C-2,6), 132.3 (C7Ph C-2,6), 140.2 (NPh C-1), 141.2 (C6Ph C-1), 148.9 (C-6), 152.1 (C-7a), 158.6 (C7Ph C-4), 158.9 (C-4). <sup>15</sup>N NMR (71 MHz, CDCl<sub>3</sub>): δ –147.6 (N-2), N-1 not found, –83.2 (N-5). IR (KBr, *v*, cm<sup>–1</sup>): 3058, 3016 (CH<sub>arom</sub>), 2986, 2934, 2889 (CH<sub>aliph</sub>), 1607, 1507, 1462, 1376, 1290, 1248, 1176 (C=C, C=N, C–N), 1045 (C–O), 830, 753, 699, 686 (CH=CH of mono- and disubstituted benzenes). MS (ES<sup>+</sup>): *m/z* (%): 405 ([M + H]<sup>+</sup>, 99). HRMS (ESI) for C<sub>27</sub>H<sub>24</sub>N<sub>3</sub>O ([M + H]<sup>+</sup>): requires 406.1914 and found 406.1914.

#### 7-(2,4-Dimethoxyphenyl)-4-ethyl-2,6-diphenyl-2H-pyrazolo[4,3-c]pyridine 32

7-(2,4-Dimethoxyphenyl)-4-ethyl-2,6-diphenyl-2H-pyrazolo[4,3-c]pyridine 32 was prepared in accordance with general procedure (D) from 7-iodo-4-methyl 2,6-diphenyl-2H-pyrazolo[4,3-c]pyridine 15 (80 mg, 0.19 mmol), (2,4-dimethoxyphenyl)boronic acid (41 mg, 0.23 mmol), Cs<sub>2</sub>CO<sub>3</sub> (123 mg, 0.38 mmol), Pd(OAc)<sub>2</sub> (3 mg, 0.013 mmol), EtOH (1.2 mL), and water (0.4 mL). The reaction was finished after 30 min. The desired compound was obtained after purification by column chromatography (EtOAc/Hex, 1:5 *v/v*). Yield: 40 mg (48%), yellow crystalline solid, mp = 202–203 °C, *R<sub>f</sub>* = 0.24 (EtOAc/Hex, 1:3 *v/v*). <sup>1</sup>H NMR (700 MHz, CDCl<sub>3</sub>): δ 1.53 (3H, t, *J* = 7.6 Hz, CH<sub>3</sub>), 3.21 (2H, q, *J* = 7.6 Hz, CH<sub>2</sub>), 3.37 (3H, s, 2-OCH<sub>3</sub>), 3.83 (3H, s, 4-OCH<sub>3</sub>), 6.38–6.44 (1H, m, C7Ph 3-H), 6.53–6.59 (1H, m, C7Ph 5-H), 7.15–7.19 (1H, m, C6Ph 4-H), 7.19–7.25 (2H, m, C6Ph 3,5-H), 7.35–7.41 (2H, m, NPh 4-H and C7Ph 6-H), 7.45–7.51 (4H, m, C6Ph 2,6-H and NPh 3,5-H), 7.84–7.90 (2H, m, NPh 2,6-H), 8.58 (1H, s, 3-H). <sup>13</sup>C NMR (176 MHz, CDCl<sub>3</sub>): δ 13.3 (CH<sub>3</sub>), 30.4 (CH<sub>2</sub>), 55.1 (2-OCH<sub>3</sub>), 55.3 (4-OCH<sub>3</sub>), 99.1 (C7Ph C-3), 104.6 (C7Ph C-5), 116.8 (C-7), 117.9 (C7Ph C-1), 119.0 (C-3a), 121.2 (C-3), 121.4 (NPh C-2,6), 126.7 (C6Ph C-4), 127.4 (C6Ph C-3,5), 128.3 (NPh C-4), 129.5 (NPh C-3,5 and C6Ph C-2,6), 132.8 (C7Ph C-6), 140.3 (NPh C-1), 141.9 (C6Ph C-1), 149.9 (C-6), 152.4 (C-7a), 157.9 (C7Ph C-2), 159.0 (C-4), 160.5 (C7Ph C-4). <sup>15</sup>N NMR (71 MHz, CDCl<sub>3</sub>): δ –147.9 (N-2), –96.4 (N-1), –84.6 (N-5). IR (KBr, *v*, cm<sup>–1</sup>): 3134, 3058 (CH<sub>arom</sub>), 2966, 2930, 2836 (CH<sub>aliph</sub>), 1606, 1588, 1547, 1505, 1462, 1305, 1204 (C=C, C=N, C–N), 1027 (C–O), 829, 764, 705, 691 (CH=CH of mono- and trisubstituted benzenes). MS (ES<sup>+</sup>): *m/z* (%): 435 ([M + H]<sup>+</sup>, 100). HRMS (ESI) for C<sub>28</sub>H<sub>26</sub>N<sub>3</sub>O<sub>2</sub> ([M + H]<sup>+</sup>): requires 436.2020 and found 436.2020.

#### 4-Ethyl-2,6-diphenyl-7-(*p*-tolyl)-2H-pyrazolo[4,3-c]pyridine 33

4-Ethyl-2,6-diphenyl-7-(*p*-tolyl)-2H-pyrazolo[4,3-c]pyridine 33 was prepared in accordance with general procedure (D) from 7-iodo-4-methyl 2,6-diphenyl-2H-pyrazolo[4,3-c]pyridine 15 (80 mg, 0.19 mmol), (4-methylphenyl)boronic acid (31 mg, 0.23 mmol), Cs<sub>2</sub>CO<sub>3</sub> (123 mg, 0.38 mmol), Pd(OAc)<sub>2</sub> (3 mg, 0.013 mmol), EtOH (1.2 mL), and water

(0.4 mL). The reaction was finished after 30 min. The desired compound was obtained after purification by column chromatography (EtOAc/Hex, 1:8 *v/v*). Yield: 60 mg (81%), yellowish crystalline solid, mp = 179–180 °C,  $R_f$  = 0.41 (EtOAc/Hex, 1:3 *v/v*).  $^1\text{H}$  NMR (700 MHz,  $\text{CDCl}_3$ ):  $\delta$  1.52 (3H, t,  $J$  = 7.6 Hz,  $\text{CH}_2\text{CH}_3$ ), 2.34 (3H, s, Ph- $\text{CH}_3$ ), 3.19 (2H, q,  $J$  = 7.6 Hz,  $\text{CH}_2\text{CH}_3$ ), 7.09–7.14 (2H, m, C7Ph 3,5-H), 7.19–7.22 (1H, m, C6Ph 4-H), 7.23–7.25 (2H, m, C6Ph 3,5-H), 7.34–7.38 (2H, m, C6Ph 2,6-H), 7.38–7.41 (1H, m, NPh 4-H), 7.46–7.51 (4H, m, NPh 3,5-H and C7Ph 2,6-H), 7.86–7.91 (2H, m, NPh 2,6-H), 8.59 (1H, s, 3-H).  $^{13}\text{C}$  NMR (176 MHz,  $\text{CDCl}_3$ ):  $\delta$  13.3 ( $\text{CH}_2\text{CH}_3$ ), 21.3 (Ph- $\text{CH}_3$ ), 30.4 ( $\text{CH}_2\text{CH}_3$ ), 119.0 (C-3a), 120.7 (C-7), 121.2 (C-4), 121.3 (NPh C-2,6), 126.9 (C6Ph C-4), 127.7 (C6Ph C-3,5), 128.3 (NPh C-4), 128.7 (C7Ph C-3), 129.5 (NPh C-3,5), 130.6 (C7Ph C-2,6), 131.0 (C6Ph C-2,6), 133.0 (C7Ph C-1), 136.5 (C7Ph C-4), 140.2 (NPh C-1), 141.2 (C6Ph C-1), 148.9 (C-6), 152.0 (C-7a), 159.0 (C-4).  $^{15}\text{N}$  NMR (71 MHz,  $\text{CDCl}_3$ ):  $\delta$  -147.5 (N-2), -96.1 (N-1), -83.3 (N-5). IR (KBr,  $\nu$ ,  $\text{cm}^{-1}$ ): 3028 ( $\text{CH}_{\text{arom}}$ ), 2990, 2939 ( $\text{CH}_{\text{aliph}}$ ), 1587, 1505, 1463, 1377, 1211, 1045 (C=C, C=N, C-N), 822, 753, 699, 686 (CH=CH of mono- and disubstituted benzenes). MS ( $\text{ES}^+$ ):  $m/z$  (%): 389 ( $[\text{M} + \text{H}]^+$ , 98). HRMS (ESI) for  $\text{C}_{27}\text{H}_{24}\text{N}_3$  ( $[\text{M} + \text{H}]^+$ ): requires 390.1965 and found 390.1965.

#### 4-Ethyl-2,6-diphenyl-7-[4-(trifluoromethyl)phenyl]-2H-pyrazolo[4,3-c]pyridine 34

4-Ethyl-2,6-diphenyl-7-[4-(trifluoromethyl)phenyl]-2H-pyrazolo[4,3-c]pyridine **34** was prepared in accordance with general procedure (D) from 7-iodo-4-methyl 2,6-diphenyl-2H-pyrazolo[4,3-c]pyridine **15** (80 mg, 0.19 mmol), 4-(trifluoromethyl)phenylboronic acid (43 mg, 0.23 mmol),  $\text{Cs}_2\text{CO}_3$  (123 mg, 0.38 mmol),  $\text{Pd}(\text{OAc})_2$  (3 mg, 0.013 mmol), EtOH (1.2 mL), and water (0.4 mL). The reaction was finished after 30 min. The desired compound was obtained after purification by column chromatography (EtOAc/Hex, 1:8 *v/v*). Yield: 77 mg (92%), yellowish crystalline solid, mp = 203–204 °C,  $R_f$  = 0.39 (EtOAc/Hex, 1:3 *v/v*).  $^1\text{H}$  NMR (700 MHz,  $\text{CDCl}_3$ ):  $\delta$  1.54 (3H, t,  $J$  = 7.6 Hz,  $\text{CH}_3$ ), 3.19 (2H, q,  $J$  = 7.6 Hz,  $\text{CH}_2$ ), 7.22–7.28 (3H, m, C6Ph 3,4,5-H), 7.41–7.46 (3H, m, C6Ph 2,6-H, NPh 4-H), 7.50–7.54 (2H, m, NPh 3,5-H), 7.55–7.58 (2H, m, C7Ph 3,5-H), 7.59–7.63 (2H, m, C7Ph 2,6-H), 7.88–7.92 (2H, m, NPh 2,6-H), 8.64 (1H, s, 3-H).  $^{13}\text{C}$  NMR (176 MHz,  $\text{CDCl}_3$ ):  $\delta$  13.3 ( $\text{CH}_3$ ), 30.4 ( $\text{CH}_2$ ), 119.0 (C-3a), 119.2 (C-7), 121.3 (NPh C-2,6), 121.5 (C-4), 124.3 ( $\text{CF}_3$ ,  $J$  = 201.6 Hz), 124.8 (C7Ph C-3,5,  $J$  = 2.52 Hz), 127.4 (C6Ph C-4), 127.9 (C6Ph C-3,5), 128.6 (NPh C-4), 128.8 (C7Ph C-4,  $J$  = 25.2 Hz), 129.6 (NPh C-3,5), 130.7 (C6Ph C-2,6), 131.5 (C7Ph C-2,6), 140.0 (NPh C-1), 140.1 (C7Ph C-1), 140.4 (C6Ph C-1), 149.6 (C-6), 151.5 (C-7a), 160.1 (C-4).  $^{15}\text{N}$  NMR (71 MHz,  $\text{CDCl}_3$ ):  $\delta$  -146.9 (N-2), -97.4 (N-1), -83.5 (N-5).  $^{19}\text{F}$  NMR (376 MHz,  $\text{CDCl}_3$ ):  $\delta$  -65.59 (3F, s,  $\text{CF}_3$ ). IR (KBr,  $\nu$ ,  $\text{cm}^{-1}$ ): 3053 ( $\text{CH}_{\text{arom}}$ ), 2971 ( $\text{CH}_{\text{aliph}}$ ), 1585, 1484, 1327, 1130 (C=C, C=N, C-N, C-F), 759, 696 (CH=CH of mono- and disubstituted benzenes). MS ( $\text{ES}^+$ ):  $m/z$  (%): 443 ( $[\text{M} + \text{H}]^+$ , 99). HRMS (ESI) for  $\text{C}_{27}\text{H}_{21}\text{F}_3\text{N}_3$  ( $[\text{M} + \text{H}]^+$ ): requires 444.1682 and found 444.1682.

#### 4-Ethyl-2,6-diphenyl-7-[4-(trifluoromethoxy)phenyl]-2H-pyrazolo[4,3-c]pyridine 35

4-Ethyl-2,6-diphenyl-7-[4-(trifluoromethoxy)phenyl]-2H-pyrazolo[4,3-c]pyridine **35** was prepared in accordance with general procedure (D) from 7-iodo-4-methyl 2,6-diphenyl-2H-pyrazolo[4,3-c]pyridine **15** (80 mg, 0.19 mmol), 4-(trifluoromethoxy)phenylboronic acid (47 mg, 0.23 mmol),  $\text{Cs}_2\text{CO}_3$  (123 mg, 0.38 mmol),  $\text{Pd}(\text{OAc})_2$  (3 mg, 0.013 mmol), EtOH (1.2 mL), and water (0.4 mL). The reaction was finished after 30 min. The desired compound was obtained after purification by column chromatography (EtOAc/Hex, 1:8 *v/v*). Yield: 74 mg (85%), white crystalline solid, mp = 153–154 °C,  $R_f$  = 0.41 (EtOAc/Hex, 1:3 *v/v*).  $^1\text{H}$  NMR (700 MHz,  $\text{CDCl}_3$ ):  $\delta$  1.54 (3H, t,  $J$  = 7.6 Hz,  $\text{CH}_3$ ), 3.22 (2H, q,  $J$  = 7.6 Hz,  $\text{CH}_2$ ), 7.12–7.19 (2H, m, C7Ph 3,5-H), 7.22–7.28 (3H, m, C6Ph 3,4,5-H), 7.40–7.48 (3H, m, C6Ph 2,6-H, NPh 4-H), 7.49–7.56 (4H, m, NPh 3,5-H and C7Ph C-2,6), 7.87–7.94 (2H, m, NPh 2,6-H), 8.63 (1H, s, 3-H).  $^{13}\text{C}$  NMR (176 MHz,  $\text{CDCl}_3$ ):  $\delta$  13.3 ( $\text{CH}_3$ ), 30.4 ( $\text{CH}_2$ ), 119.0 (C-3a), 119.2 (C-7), 120.3 (C7Ph C-3,5), 120.5 ( $\text{CF}_3$ ,  $J$  = 176.4 Hz), 121.3 (NPh C-2,6), 121.5 (C-4), 127.2 (C6Ph C-4), 127.8 (C6Ph C-3,5), 128.6 (NPh C-4), 129.6 (NPh C-3,5), 130.6 (C6Ph C-2,6), 132.6 (C7Ph C-2,6), 134.8 (C7Ph C-4), 140.1 (NPh C-1), 140.6 (C6Ph C-1), 148.2 (C7Ph

C-1), 149.4 (C-6), 151.6 (C-7a), 159.8 (C-4).  $^{15}\text{N}$  NMR (71 MHz,  $\text{CDCl}_3$ ):  $\delta$  -147.1 (N-2), -97.4 (N-1), -83.5 (N-5).  $^{19}\text{F}$  NMR (376 MHz,  $\text{CDCl}_3$ ):  $\delta$  -60.82 (3F, s,  $\text{CF}_3$ ). IR (KBr,  $\nu$ ,  $\text{cm}^{-1}$ ): 3049 ( $\text{CH}_{\text{arom}}$ ), 2969, 2934 ( $\text{CH}_{\text{aliph}}$ ), 1586, 1507, 1367, 1259, 1225, 1168 (C=C, C=N, C-N, C-F), 757, 699, 687 (CH=CH of mono- and disubstituted benzenes). MS ( $\text{ES}^+$ ):  $m/z$  (%): 459 ( $[\text{M} + \text{H}]^+$ , 99). HRMS (ESI) for  $\text{C}_{27}\text{H}_{21}\text{F}_3\text{N}_3\text{O}$  ( $[\text{M} + \text{H}]^+$ ): requires 460.163 and found 460.1631.

#### 7-(4-Chlorophenyl)-4-ethyl-2,6-diphenyl-2H-pyrazolo[4,3-c]pyridine 36

7-(4-Chlorophenyl)-4-ethyl-2,6-diphenyl-2H-pyrazolo[4,3-c]pyridine 36 was prepared in accordance with general procedure (D) from 7-iodo-4-methyl 2,6-diphenyl-2H-pyrazolo[4,3-c]pyridine 15 (80 mg, 0.19 mmol), 4-chlorophenylboronic acid (36 mg, 0.23 mmol),  $\text{Cs}_2\text{CO}_3$  (123 mg, 0.38 mmol),  $\text{Pd}(\text{OAc})_2$  (3 mg, 0.013 mmol), EtOH (1.2 mL), and water (0.4 mL). The reaction was finished after 30 min. The desired compound was obtained after purification by column chromatography (EtOAc/Hex, 1:8 *v/v*). Yield: 65 mg (83%), yellow crystalline solid, mp = 226–227 °C,  $R_f$  = 0.49 (EtOAc/Hex, 1:3 *v/v*).  $^1\text{H}$  NMR (700 MHz,  $\text{CDCl}_3$ ):  $\delta$  1.52 (3H, t,  $J$  = 7.6 Hz,  $\text{CH}_3$ ), 3.21 (2H, q,  $J$  = 7.6 Hz,  $\text{CH}_2$ ), 7.22–7.30 (5H, m, C6Ph 3,4,5-H; C7Ph 3,5-H), 7.40–7.44 (3H, m, C7Ph 2,6-H; NPh 4-H), 7.44–7.47 (2H, m, C6Ph 2,6-H), 7.50–7.53 (2H, m, NPh 3,5-H), 7.86–7.93 (2H, m, NPh 2,6-H), 8.61 (1H, s, 3-H).  $^{13}\text{C}$  NMR (176 MHz,  $\text{CDCl}_3$ ):  $\delta$  13.3 ( $\text{CH}_3$ ), 30.4 ( $\text{CH}_2$ ), 119.0 (C-3a), 119.4 (C-7), 121.3 (NPh C-2,6), 121.4 (C-3), 127.2 (C6Ph C-4), 127.9 (C6Ph C-3,5), 128.2 (C7Ph C-3,5), 128.5 (NPh C-4), 129.6 (NPh C-3,5), 130.6 (C6Ph C-2,6), 132.5 (C7Ph C-2,6), 132.8 (C7Ph C-4), 134.6 (C7Ph C-1), 140.1 (NPh C-1), 140.6 (C6Ph C-1), 149.3 (C-6), 151.6 (C-7a), 159.7 (C-4).  $^{15}\text{N}$  NMR (71 MHz,  $\text{CDCl}_3$ ):  $\delta$  -147.3 (N-2), -97.0 (N-1), -83.3 (N-5). IR (KBr,  $\nu$ ,  $\text{cm}^{-1}$ ): 3057 ( $\text{CH}_{\text{arom}}$ ), 2991, 2939 ( $\text{CH}_{\text{aliph}}$ ), 1691, 1587, 1501, 1463, 1213, 1092 (C=C, C=N, C-N), 825, 756, 698, 688 (CH=CH of mono- and disubstituted benzenes). MS ( $\text{ES}^+$ ):  $m/z$  (%): 409 ( $[\text{M} + \text{H}]^+$ , 96). HRMS (ESI) for  $\text{C}_{26}\text{H}_{21}\text{ClN}_3$  ( $[\text{M} + \text{H}]^+$ ): requires 410.1419 and found 410.1419.

#### 4-(4-Ethyl-2,6-diphenyl-2H-pyrazolo[4,3-c]pyridin-7-yl)phenol 37

4-(4-Ethyl-2,6-diphenyl-2H-pyrazolo[4,3-c]pyridin-7-yl)phenol 37 was prepared in accordance with general procedure (D) from 7-iodo-4-methyl 2,6-diphenyl-2H-pyrazolo[4,3-c]pyridine 15 (80 mg, 0.19 mmol), (4-hydroxyphenyl)boronic acid (31 mg, 0.23 mmol),  $\text{Cs}_2\text{CO}_3$  (123 mg, 0.38 mmol),  $\text{Pd}(\text{OAc})_2$  (3 mg, 0.013 mmol), EtOH (1.2 mL), and water (0.4 mL). The reaction was finished after 30 min. The desired compound was obtained after purification by column chromatography (EtOAc/Hex, 1:8 *v/v*). Yield: 50 mg (67%), yellow-brown crystalline solid, mp = 199–200 °C,  $R_f$  = 0.17 (EtOAc/Hex, 1:3 *v/v*).  $^1\text{H}$  NMR (700 MHz,  $\text{CDCl}_3$ ):  $\delta$  1.50 (3H, t,  $J$  = 7.6 Hz,  $\text{CH}_3$ ), 2.05 (1H, s, OH), 3.21 (2H, q,  $J$  = 7.6 Hz,  $\text{CH}_2$ ), 6.58–6.64 (2H, m, C7Ph 3,5-H), 7.15–7.18 (1H, m, C6Ph C-4), 7.19–7.24 (4H, m, C6Ph 3,5-H and C7Ph 2,6-H), 7.40–7.45 (3H, m, C6Ph 2,6-H and NPh 4-H), 7.49–7.53 (2H, m, NPh 3,5-H), 7.85–7.90 (2H, m, NPh 2,6-H), 8.60 (1H, s, 3-H).  $^{13}\text{C}$  NMR (176 MHz,  $\text{CDCl}_3$ ):  $\delta$  13.6 ( $\text{CH}_3$ ), 30.1 ( $\text{CH}_2$ ), 115.3 (C7Ph C-3,5), 118.9 (C-3a), 120.7 (C-7), 121.6 (NPh C-2,6), 122.0 (C-3), 126.9 (C6Ph C-4), 127.3 (C7Ph C-1), 127.7 (C6Ph C-3,5), 128.6 (NPh C-4), 129.6 (NPh C-3,5), 130.6 (C6Ph C-2,6), 132.1 (C7Ph C-2,6), 140.0 (NPh C-1), 140.8 (C7Ph C-1), 148.9 (C-6), 152.1 (C-7a), 155.3 (C7Ph C-4), 159.0 (C-4).  $^{15}\text{N}$  NMR (71 MHz,  $\text{CDCl}_3$ ):  $\delta$  -147.5 (N-2), -98.5 (N-1), -85.0 (N-5). IR (KBr,  $\nu$ ,  $\text{cm}^{-1}$ ): 3147 (OH), 3064 ( $\text{CH}_{\text{arom}}$ ), 2963, 2932, 2873 ( $\text{CH}_{\text{aliph}}$ ), 1613, 1586, 1507, 1481, 1267, 1209 (C=C, C=N, C-N), 1040 (C-O), 816, 760, 695 (CH=CH of mono- and disubstituted benzenes). MS ( $\text{ES}^+$ ):  $m/z$  (%): 391 ( $[\text{M} + \text{H}]^+$ , 98). HRMS (ESI) for  $\text{C}_{26}\text{H}_{22}\text{N}_3\text{O}$  ( $[\text{M} + \text{H}]^+$ ): requires 392.1757 and found 392.1757.

#### 4-Isopropyl-7-(4-methoxyphenyl)-4-methyl-2,6-diphenyl-2H-pyrazolo[4,3-c]pyridine 38

4-Isopropyl-7-(4-methoxyphenyl)-4-methyl-2,6-diphenyl-2H-pyrazolo[4,3-c]pyridine 38 was prepared in accordance with general procedure (D) from 7-iodo-4-isopropyl-2,6-diphenyl-2H-pyrazolo[4,3-c]pyridine 16 (100 mg, 0.23 mmol), 4-methoxyphenylboronic acid (42 mg, 0.27 mmol),  $\text{Cs}_2\text{CO}_3$  (148 mg, 0.46 mmol),  $\text{Pd}(\text{OAc})_2$  (4 mg, 0.015 mmol), EtOH (1.5 mL), and water (0.5 mL). The reaction was finished after 1 h. The desired compound

was obtained after purification by column chromatography (EtOAc/Hex, 1:8 *v/v*). Yield: 80 mg (83%), white crystalline solid, mp = 159–160 °C,  $R_f$  = 0.54 (EtOAc/Hex, 1:3 *v/v*).  $^1\text{H}$  NMR (700 MHz,  $\text{CDCl}_3$ ):  $\delta$  1.55 (6H, d,  $J$  = 7.0 Hz,  $\text{CH}-(\text{CH}_3)_2$ ), 3.53 (1H, p,  $J$  = 7.0 Hz,  $\text{CH}-(\text{CH}_3)_2$ ), 3.83 (3H, s,  $\text{OCH}_3$ ), 6.86–6.91 (2H, m, C7Ph 3,5-H), 7.20–7.24 (1H, m, C6Ph 4-H), 7.24–7.28 (2H, m, C6Ph 3,5-H), 7.39–7.45 (3H, m, C7Ph 2,6-H and NPh 4-H), 7.50–7.55 (4H, m, C6Ph 2,6-H and NPh 3,5-H), 7.89–7.94 (2H, m, NPh 2,6-H), 8.63 (1H, s, 3-H).  $^{13}\text{C}$  NMR (176 MHz,  $\text{CDCl}_3$ ):  $\delta$  22.0 ( $\text{CH}-(\text{CH}_3)_2$ ), 36.2 ( $\text{CH}-(\text{CH}_3)_2$ ), 55.3 ( $\text{OCH}_3$ ), 113.7 (C7Ph C-3,5), 118.1 (C-3a), 120.3 (C-7), 121.2 (C-3), 121.5 (NPh C-2,6), 127.0 (C6Ph C-4), 127.8 (C6Ph C-3,5), 128.5 (NPh C-4), 128.6 (C7Ph C-1), 129.7 (NPh C-3,5), 131.0 (C6Ph C-2,6), 132.4 (C7Ph C-2,6), 140.4 (NPh C-1), 141.4 (C6Ph C-1), 148.5 (C-6), 152.6 (C-7a), 158.7 (C7Ph C-4), 162.5 (C-4).  $^{15}\text{N}$  NMR (71 MHz,  $\text{CDCl}_3$ ):  $\delta$  -147.9 (N-2), -96.8 (N-1), -83.9 (N-5). IR ( $\nu$ ,  $\text{cm}^{-1}$ ): 3136, 3041 ( $\text{CH}_{\text{arom}}$ ), 2961, 2926, 2869 ( $\text{CH}_{\text{aliph}}$ ), 1587, 1547, 1506, 1482, 1464, 1379, 1288, 1242 (C=C, C=N, C-N), 1212, 1177, 1031 (C-O-C), 763, 758, 689 (CH=CH of mono- and disubstituted benzenes). MS ( $\text{ES}^+$ ):  $m/z$  (%): 421 ( $[\text{M} + 2\text{H}]^+$ , 97.4). HRMS (ESI) for  $\text{C}_{28}\text{H}_{26}\text{N}_3\text{O}$  ( $[\text{M} + \text{H}]^+$ ): requires 420.2070 and found 420.2070.

#### 7-(4-Methoxyphenyl)-2,4,6-triphenyl-2H-pyrazolo[4,3-c]pyridine 39

7-(4-Methoxyphenyl)-2,4,6-triphenyl-2H-pyrazolo[4,3-c]pyridine 39 was prepared in accordance with general procedure (D) from 7-iodo-2,4,6-triphenyl-2H-pyrazolo[4,3-c]pyridine 17 (64 mg, 0.135 mmol), (4-methoxyphenyl)boronic acid (25 mg, 0.16 mmol),  $\text{Cs}_2\text{CO}_3$  (88 mg, 0.27 mmol),  $\text{Pd}(\text{OAc})_2$  (2 mg, 0.009 mmol), EtOH (0.9 mL), and water (0.3 mL). The reaction was finished after 45 min. The desired compound was obtained after purification by column chromatography (EtOAc/Hex, 1:10 *v/v*). Yield: 38 mg (62%), yellow crystalline solid, mp = 246–247 °C,  $R_f$  = 0.54 (EtOAc/Hex, 1:3 *v/v*).  $^1\text{H}$  NMR (700 MHz,  $\text{CDCl}_3$ ):  $\delta$  3.84 (3H, s,  $\text{CH}_3$ ), 6.88–6.92 (2H, m, C7Ph C-3,5), 7.23–7.26 (1H, m, C6Ph 4-H), 7.26–7.31 (2H, m, 3,5-H), 7.41–7.44 (1H, m, NPh 4-H), 7.48–7.54 (5H, m, C4Ph 4-H; C7Ph 2,6-H; NPh 3,5-H), 7.55–7.62 (4H, m, C6Ph 2,6-H; C4Ph 3,5-H), 7.91–7.96 (2H, m, NPh 2,6-H), 8.14–8.20 (2H, m, C4Ph 2,6-H), 8.80 (1H, s, 3-H).  $^{13}\text{C}$  NMR (176 MHz,  $\text{CDCl}_3$ ):  $\delta$  55.2 ( $\text{CH}_3$ ), 113.5 (C7Ph C-3,5), 118.1 (C-3a), 121.2 (C-7), 121.4 (NPh C-2,6), 122.3 (C-4), 127.0 (C6Ph C-4), 127.7 (C6Ph C-3,5), 128.1 (C7Ph C-1), 128.3 (C4Ph C-2,6), 128.6 (NPh C-4), 128.8 (C4Ph C-3,5), 129.4 (C4Ph C-4), 129.6 (NPh C-3,5), 130.6 (C6Ph C-2,6), 132.4 (C7Ph C-2,6), 139.7 (C4Ph C-1), 140.1 (NPh C-1), 141.1 (C6Ph C-1), 149.2 (C-6), 152.8 (C-7a), 153.4 (C-4), 158.8 (C7Ph C-4).  $^{15}\text{N}$  NMR (71 MHz,  $\text{CDCl}_3$ ):  $\delta$  -145.6 (N-2), -96.6 (N-1), N-5 not found. IR (KBr,  $\nu$ ,  $\text{cm}^{-1}$ ): 3056 ( $\text{CH}_{\text{arom}}$ ), 2924, 2833 ( $\text{CH}_{\text{aliph}}$ ), 1609, 1504, 1463, 1353, 1249, 1175 (C=C, C=N, C-N), 1038 (C-O), 838, 754, 695, 687 (CH=CH of mono- and disubstituted benzenes). MS ( $\text{ES}^+$ ):  $m/z$  (%): 454 ( $[\text{M} + \text{H}]^+$ , 96). HRMS (ESI) for  $\text{C}_{31}\text{H}_{24}\text{N}_3\text{O}$  ( $[\text{M} + \text{H}]^+$ ): requires 454.1914 and found 454.1914.

#### 3.2.6. General Procedure (E) of 4-(4-Ethyl-2,6-diphenyl-2H-pyrazolo[4,3-c]pyridin-7-yl)phenol 37 Alkylation

4-(4-Ethyl-2,6-diphenyl-2H-pyrazolo[4,3-c]pyridin-7-yl)phenol 37 (1 equivalent) was dissolved in DMF. Then, NaH (60% in mineral oil) (1.1 equivalents) was added at room temperature. Then, an appropriate amount of alkyl iodide (1.1 equivalents) was added at 70 °C and the mixture was stirred for 1 h. Upon completion (monitored by TLC), the reaction mixture was cooled to room temperature, diluted with water (20 mL), and extracted with EtOAc (3  $\times$  25 mL). The combined organic layers were washed with brine (10 mL), dried over anhydrous  $\text{Na}_2\text{SO}_4$ , filtered, and evaporated under reduced pressure. The residue was purified by column chromatography.

#### 7-(4-Ethoxyphenyl)-4-ethyl-2,6-diphenyl-2H-pyrazolo[4,3-c]pyridine 40

7-(4-Ethoxyphenyl)-4-ethyl-2,6-diphenyl-2H-pyrazolo[4,3-c]pyridine 40 was prepared in accordance with general procedure (E) from 4-ethyl-2,6-diphenyl-2H-pyrazolo[4,3-c]pyridin-7-yl)phenol 37 (60 mg, 0.15 mmol), NaH (60%) (7 mg, 0.17 mmol), ethyl iodide (0.014 mL, 0.17 mmol), and DMF (2 mL). The desired compound was obtained after



purification by column chromatography (EtOAc/Hex, 1:4 *v/v*). Yield: 62 mg (97%), yellow crystalline solid, mp = 140–141 °C,  $R_f$  = 0.38 (EtOAc/Hex, 1:3 *v/v*).  $^1\text{H}$  NMR (700 MHz,  $\text{CDCl}_3$ ):  $\delta$  1.42 (3H, t,  $J$  = 7.0 Hz,  $\text{OCH}_2\text{CH}_3$ ), 1.52 (3H, t,  $J$  = 7.6 Hz,  $\text{CH}_2\text{CH}_3$ ), 3.20 (2H, q,  $J$  = 7.6 Hz,  $\text{CH}_2\text{CH}_3$ ), 4.04 (2H, q,  $\text{OCH}_2\text{CH}_3$ ), 6.82–6.88 (2H, m, C7Ph 3,5-H), 7.19–7.23 (1H, m, C6Ph 4-H), 7.23–7.27 (2H, m, C6Ph 3,5-H), 7.37–7.43 (3H, m, NPh 4-H and C6Ph 2,6-H), 7.47–7.52 (4H, m, NPh 3,5-H and C7Ph 2,6-H), 7.88–7.93 (2H, m, NPh 2,6-H), 8.60 (1H, s, 3-H).  $^{13}\text{C}$  NMR (176 MHz,  $\text{CDCl}_3$ ):  $\delta$  13.4 ( $\text{CH}_2\text{CH}_3$ ), 14.9 ( $\text{OCH}_2\text{CH}_3$ ), 30.3 ( $\text{CH}_2\text{CH}_3$ ), 63.2 ( $\text{OCH}_2\text{CH}_3$ ), 114.0 (C7Ph C-3,5), 119.0 (C-3a), 120.4 (C-7), 121.2 (C-3), 121.3 (NPh C-2,6), 126.8 (C6Ph C-4), 127.7 (C6Ph C-3,5), 128.1 (C7Ph C-1), 128.4 (NPh C-4), 129.5 (NPh C-3,5), 130.6 (C6Ph C-2,6), 132.3 (C7Ph C-2,6), 140.1 (NPh C-1), 141.2 (C6Ph C-1), 148.8 (C-6), 152.0 (C-7a), 158.0 (C7Ph C-4), 158.8 (C-4).  $^{15}\text{N}$  NMR (71 MHz,  $\text{CDCl}_3$ ):  $\delta$  -147.6 (N-2), -96.5 (N-1), -83.8 (N-5). IR (KBr,  $\nu$ ,  $\text{cm}^{-1}$ ): 3059 ( $\text{CH}_{\text{arom}}$ ), 2983, 2930 ( $\text{CH}_{\text{aliph}}$ ), 1587, 1506, 1479, 1375, 1244, 1179 (C=C, C=N, C-N), 1047 (C-O), 826, 754, 670, 686 ( $\text{CH}=\text{CH}$  of mono- and disubstituted benzenes). MS ( $\text{ES}^+$ ):  $m/z$  (%): 419 ( $[\text{M} + \text{H}]^+$ , 97). HRMS (ESI) for  $\text{C}_{28}\text{H}_{26}\text{N}_3\text{O}$  ( $[\text{M} + \text{H}]^+$ ): requires 420.2070 and found 420.2070.

#### 4-Ethyl-2,6-diphenyl-7-(4-propoxyphenyl)-2H-pyrazolo[4,3-c]pyridine 41

4-Ethyl-2,6-diphenyl-7-(4-propoxyphenyl)-2H-pyrazolo[4,3-c]pyridine 41 was prepared in accordance with general procedure (E) from (4-ethyl-2,6-diphenyl-2H-pyrazolo[4,3-c]pyridin-7-yl)phenol 37 (60 mg, 0.15 mmol), NaH (60%) (7 mg, 0.17 mmol), 1-iodo propane (0.016 mL, 0.17 mmol), and DMF (2 mL). The desired compound was obtained after purification by column chromatography (EtOAc/Hex, 1:6 *v/v*). Yield: 64 mg (96%), yellow crystalline solid, mp = 117–118 °C,  $R_f$  = 0.41 (EtOAc/Hex, 1:3 *v/v*).  $^1\text{H}$  NMR (700 MHz,  $\text{CDCl}_3$ ):  $\delta$  1.04 (3H, t,  $J$  = 7.4 Hz,  $\text{OCH}_2\text{CH}_2\text{CH}_3$ ), 1.52 (3H, t,  $J$  = 7.6 Hz,  $\text{CH}_2\text{CH}_3$ ), 1.81 (2H, hept,  $J$  = 7.1 Hz,  $\text{OCH}_2\text{CH}_2\text{CH}_3$ ), 3.20 (2H, q,  $J$  = 7.6 Hz,  $\text{CH}_2\text{CH}_3$ ), 3.92 (2H, t,  $J$  = 6.6 Hz,  $\text{OCH}_2\text{CH}_2\text{CH}_3$ ), 6.83–6.87 (2H, m, C7Ph 3,5-H), 7.19–7.22 (1H, m, C6Ph 4-H), 7.23–7.27 (2H, m, C6Ph 3,5-H), 7.37–7.42 (3H, m, C7Ph 2,6-H and NPh 4-H), 7.47–7.51 (4H, m, NPh 3,5-H and C6Ph 2,6-H), 7.88–7.92 (2H, m, NPh 2,6-H), 8.59 (1H, s, 3-H).  $^{13}\text{C}$  NMR (176 MHz,  $\text{CDCl}_3$ ):  $\delta$  10.5 ( $\text{OCH}_2\text{CH}_2\text{CH}_3$ ), 13.4 ( $\text{CH}_2\text{CH}_3$ ), 22.6 ( $\text{OCH}_2\text{CH}_2\text{CH}_3$ ), 30.3 ( $\text{CH}_2\text{CH}_3$ ), 69.3 ( $\text{OCH}_2\text{CH}_2\text{CH}_3$ ), 114.0 (C7Ph C-3,5), 119.0 (C-3a), 120.4 (C-7), 121.2 (C-3), 121.3 (NPh C-2,6), 126.8 (C6Ph C-4), 127.7 (C6Ph C-3,5), 128.0 (C7Ph C-1), 128.3 (NPh C-4), 129.5 (NPh C-3,5), 130.6 (C6Ph C-2,6), 132.3 (C7Ph C-2,6), 140.1 (NPh C-1), 141.2 (C6Ph C-1), 148.8 (C-6), 152.0 (C-7a), 158.2 (C7Ph C-4), 158.8 (C-4).  $^{15}\text{N}$  NMR (71 MHz,  $\text{CDCl}_3$ ):  $\delta$  -147.5 (N-2), -96.2 (N-1), -83.5 (N-5). IR (KBr,  $\nu$ ,  $\text{cm}^{-1}$ ): 3045 ( $\text{CH}_{\text{arom}}$ ), 2970, 2931, 2872 ( $\text{CH}_{\text{aliph}}$ ), 1609, 1588, 1508, 1250, 1242, 1176 (C=C, C=N, C-N), 1041 (C-O), 758, 697, 687 ( $\text{CH}=\text{CH}$  of mono- and disubstituted benzenes). MS ( $\text{ES}^+$ ):  $m/z$  (%): 433 ( $[\text{M} + \text{H}]^+$ , 95). HRMS (ESI) for  $\text{C}_{29}\text{H}_{28}\text{N}_3\text{O}$  ( $[\text{M} + \text{H}]^+$ ): requires 434.2227 and found 434.2227.

#### 4-Ethyl-7-(4-isopropoxyphenyl)-2,6-diphenyl-2H-pyrazolo[4,3-c]pyridine 42

4-Ethyl-7-(4-isopropoxyphenyl)-2,6-diphenyl-2H-pyrazolo[4,3-c]pyridine 42 was prepared in accordance with general procedure (E) from (4-ethyl-2,6-diphenyl-2H-pyrazolo[4,3-c]pyridin-7-yl)phenol 37 (60 mg, 0.15 mmol), NaH (60%) (7 mg, 0.17 mmol), 2-iodo propane (0.016 mL, 0.17 mmol), and DMF (2 mL). The desired compound was obtained after purification by column chromatography (EtOAc/Hex, 1:6 *v/v*). Yield: 52 mg (80%), yellow crystalline solid, mp = 139–140 °C,  $R_f$  = 0.41 (EtOAc/Hex, 1:3 *v/v*).  $^1\text{H}$  NMR (700 MHz,  $\text{CDCl}_3$ ):  $\delta$  1.35 (6H, d,  $J$  = 6.1 Hz,  $\text{CH}(\text{CH}_3)_2$ ), 1.53 (3H, t,  $J$  = 7.6 Hz,  $\text{CH}_2\text{CH}_3$ ), 3.21 (2H, q,  $J$  = 7.6 Hz,  $\text{CH}_2\text{CH}_3$ ), 4.56 (1H, hept,  $J$  = 6.1 Hz, CH), 6.82–6.86 (2H, m, C7Ph 3,5-H), 7.20–7.23 (1H, m, C6Ph 4-H), 7.24–7.27 (2H, m, C6Ph 3,5-H), 7.38–7.43 (3H, m, NPh 4-H and C6Ph 2,6-H), 7.48–7.53 (4H, m, C6Ph 2,6-H and NPh 3,5-H), 7.89–7.94 (2H, m, NPh 2,6-H), 8.61 (1H, s, 3-H).  $^{13}\text{C}$  NMR (176 MHz,  $\text{CDCl}_3$ ):  $\delta$  13.4 ( $\text{CH}_2\text{CH}_3$ ), 22.1 ( $\text{CH}(\text{CH}_3)_2$ ), 30.3 ( $\text{CH}_2\text{CH}_3$ ), 69.7 ( $\text{OCH}_2$ ), 115.3 (C7Ph C-3,5), 119.0 (C-3a), 120.4 (C-7), 121.25 (C-3), 121.29 (NPh C-2,6), 126.8 (C6Ph C-4), 127.7 (C6Ph C-3,5), 127.9 (C7Ph C-1), 128.4 (NPh C-4), 129.5 (NPh C-3,5), 130.6 (C6Ph C-2,6), 132.3 (C7Ph C-2,6), 140.2 (NPh C-1), 141.2 (C6Ph C-1), 148.8 (C-6), 152.0 (C-7a), 156.9 (C7Ph C-4), 158.8 (C-4).  $^{15}\text{N}$  NMR (71 MHz,  $\text{CDCl}_3$ ):  $\delta$

−147.5 (N-2), −96.2 (N-1), −83.6 (N-5). IR (KBr,  $\nu$ ,  $\text{cm}^{-1}$ ): 3124, 3063 ( $\text{CH}_{\text{arom}}$ ), 2971, 2933 ( $\text{CH}_{\text{aliph}}$ ), 1608, 1588, 1507, 1280, 1238, 1182 (C=C, C=N, C–N), 1036 (C–O), 765, 702, 694 ( $\text{CH}=\text{CH}$  of mono- and disubstituted benzenes). MS ( $\text{ES}^+$ ):  $m/z$  (%): 433 ( $[\text{M} + \text{H}]^+$ , 97). HRMS (ESI) for  $\text{C}_{29}\text{H}_{28}\text{N}_3\text{O}$  ( $[\text{M} + \text{H}]^+$ ): requires 434.2227 and found 434.2227.

### 3.3. Optical Properties

The UV–vis spectra of  $10^{-4}$  mol solutions of the compounds in THF were recorded on a Shimadzu 2600 UV/vis spectrometer. The fluorescence spectra were recorded on an FL920 fluorescence spectrometer from Edinburgh Instruments. The PL quantum yields ( $\Phi_f$ ) were measured from dilute THF solutions by an absolute method using the Edinburgh Instruments integrating sphere excited with a Xe lamp. The optical densities of the sample solutions were ensured to be below 0.1 to avoid reabsorption effects. All optical measurements were performed at room temperature under ambient conditions.

A Britton–Robinson buffer (a solution consisting of 0.04 M  $\text{H}_3\text{PO}_4$ , 0.04 M  $\text{CH}_3\text{COOH}$ , and 0.04 M  $\text{H}_3\text{BO}_3$ ) was used to evaluate the pH dependence of the spectral characteristics of the compounds. The final pH values of the solutions were adjusted by 0.2 M NaOH.

- Stock solutions (4 mM) of the compounds were prepared in DMSO and further diluted in a Britton–Robinson buffer to a final concentration of 2  $\mu\text{M}$  for spectroscopic analyses. Absorption spectra at pH 5, 7, and 9 for all compounds and in the 2–11 pH range with 0.5 step for selected compounds were measured using a Specord 250 Plus spectrophotometer in appropriate Britton–Robinson buffers. The spectra were measured in the 240–450 nm interval with a step of 1 nm, a 1 nm bandpass, and an integration time of 0.5 s. The samples were placed into a quartz cuvette with an optical path of 1 cm. The baseline was measured for the cuvette containing the solvent only.
- The steady-state excitation and emission spectra of 2  $\mu\text{M}$  solutions of all the compounds at pH 5, 7, and 9 and in the 2–11 pH range with a 0.5 step for selected compounds were recorded on a Fluorolog-3 fluorimeter in the quartz cuvette with the 1 cm optical path (both in excitation and emission). Bandpasses in both the excitation and emission monochromator were set to 2 nm, and the spectra were scanned with the 1 nm step and an integration time 0.2 s per data point at 22 °C. Emission spectra were recorded in a 370–700 nm range with excitation at 360 nm.
- The quantum yield was estimated via integration of the fluorescence intensity over a range of 370–700 nm, and a 2.5  $\mu\text{M}$  quinine sulphate solution in 0.05 M  $\text{H}_2\text{SO}_4$  was used as a standard ( $\Phi_f = 60\%$ ) [76].

### 3.4. Biology

#### 3.4.1. Cell Cultures

Human cell lines were obtained from European Collection of Authenticated Cell Cultures (K562, MCF-7) or Cell Lines Service (MV4-11), and they were cultivated according to the provider's instructions. Briefly, the MCF-7 and K562 cell lines were maintained in a DMEM medium (Sigma-Aldrich, St. Louis, MO, USA), and the MV4-11 cell line was maintained in an RPMI-1640 medium. All media were supplemented with 10% foetal bovine serum (Biowest, Nuaille, France), penicillin (100 U/mL; Sigma-Aldrich, St. Louis, MO, USA), and streptomycin (100 mg/mL; Sigma-Aldrich, St. Louis, MO, USA), and cells were cultivated at 37 °C in 5%  $\text{CO}_2$ .

#### 3.4.2. Antiproliferative Activity Assay

Cells were treated in triplicate with six different doses of each compound for 72 h. After treatment, an MTT solution (Sigma-Aldrich, St. Louis, MO, USA) was added for 4 h, the formazan was subsequently dissolved by adding a 10% SDS solution (Sigma-Aldrich, St. Louis, USA), and absorbance was measured at 570 nm using a Tecan M200Pro microplate reader (Biotek, Winooski, VT, USA). The  $\text{GI}_{50}$  value, the drug concentration lethal to 50% of the cells, was calculated from the dose–response curves. Flavopiridol (MedChemExpress, Monmouth Junction, NJ, USA) was used as a reference drug.

### 3.4.3. Immunoblotting

After the treatment of the K562 cells, lysates in a RIPA buffer were prepared and proteins were separated on SDS-polyacrylamide gels and electroblotted onto nitrocellulose membranes. After blocking, overnight incubation with specific primary antibodies, and incubation with peroxidase-conjugated secondary antibodies, the peroxidase activity was detected with SuperSignal West Pico reagents (Thermo Scientific, Waltham, MA, USA) using a CCD camera LAS-4000 (Fujifilm, Tokyo, Japan). All primary antibodies were diluted in TBS containing 4% BSA and 0.1% Tween 20. The specific antibodies were purchased from Cell Signalling (Danvers, MA, USA; anti-PARP-1, clone 46D11; anti-cleaved caspase 9, clone E5Z7N; HRP-linked secondary antibodies), Sigma-Aldrich (St. Louis, MO, USA; anti-LC3B), and Santa Cruz Biotechnology (Dallas, TX, USA; anti- $\beta$ -Actin, clone C4), or they were kindly gifted by dr. B. Vojtěšek (Masaryk Memorial Cancer Institute, Brno, Czech Republic; anti-PCNA, clone PC-10).

### 3.4.4. Flow Cytometry

Asynchronously growing K562 cells were treated with a 10  $\mu$ M concentration of test compounds for 24, 48, and 72 h, and 30 min before the end of incubation, the cells were labelled with 10  $\mu$ M BrdU (Sigma-Aldrich, St. Louis, MO, USA) for 30 min. Subsequently, the cells were washed in PBS, fixed with ice-cold 70% ethanol, and denatured in 2 M HCl. After neutralization, the cells were stained with an anti-BrdU FITC-labelled antibody (eBioscience, San Diego, CA, USA) and propidium iodide (Sigma-Aldrich, St. Louis, MO, USA). Samples were then analysed by flow cytometry using a 488 nm laser (BD FACS Verse with software BD FACSuite™, version 1.0.6.; BD, Franklin Lakes, NJ, USA).

## 4. Conclusions

An efficient synthesis of 2,4,6,7-tetrasubstituted-2*H*-pyrazolo[4,3-*c*]pyridine derivatives was developed starting from easily accessible 1-phenyl-3-(2-phenylethynyl)-1*H*-pyrazole-4-carbaldehyde. The obtained compounds were evaluated for their antiproliferative activity against three cancer cell lines. Out of them, 4-(2,6-diphenyl-2*H*-pyrazolo[4,3-*c*]pyridin-7-yl)phenol **23** proved to be the most active, and further experiments revealed that it blocks proliferation and induces cell death in K562 cells. Moreover, the majority of the compounds were revealed to be pH-sensitive, and 7-(4-methoxyphenyl)-2,6-diphenyl-2*H*-pyrazolo[4,3-*c*]pyridine was found out to enable both fluorescence-intensity-based and ratiometric pH sensing.

**Supplementary Materials:** The following are available online. Scheme S1: Synthesis of 1-phenyl-3-(phenylethynyl)-1*H*-pyrazole-4-carbaldehyde (**2**) by previously published procedures. Table S1: Fundamental absorption and fluorescence characteristics of compounds **18–42** in THF ( $\lambda_{\text{ex}} = 350$  nm). Table S2: Fundamental absorption and fluorescence characteristics of compounds **18–42** in a Britton–Robinson buffer at pH 5, 7, and 9 ( $\lambda_{\text{ex}} = 360$  nm). Figure S1: Fluorescence spectra ( $\lambda_{\text{ex}} = 360$  nm) and titration profiles for compounds **18** and **21** in a Britton–Robinson buffer at pH 2–11. Figures S2–S147:  $^1\text{H}$ ,  $^{13}\text{C}$ , NMR and HRMS (ESI-TOF) spectra of compounds **3–42**,  $^{19}\text{F}$  spectra of compounds **34** and **35**, and  $^1\text{H}$ – $^{15}\text{N}$  HMBC spectra of compounds **13**, **15**, **16**, **18**, **20–24**, and **26–42**.

**Author Contributions:** Conceptualization, A.Š. and V.K.; methodology, E.A.; formal analysis, B.R., E.Ř. and M.K.; investigation, B.R., E.Ř., V.D., R.O. and M.K.; resources, A.Š., E.A. and V.K.; data curation, E.A. and V.K.; writing—original draft preparation, B.R., E.Ř., M.K. and A.Ž.; writing—review and editing, A.Ž.; visualization, E.Ř., R.O. and A.Ž.; supervision, A.Ž., V.K. and E.A.; funding acquisition, V.K. and E.A. All authors have read and agreed to the published version of the manuscript.

**Funding:** This research was funded by the European Regional Development Fund (Project ENOCH, No. CZ.02.1.01/0.0/0.0/16\_019/0000868) and by the Research Council of Lithuania (No. S-MIP-20-60).

**Institutional Review Board Statement:** Not applicable.

**Informed Consent Statement:** Not applicable.

**Data Availability Statement:** The data that support the findings of this study are available upon request.

**Acknowledgments:** The authors are grateful to A. Bieliauskas (Kaunas University of Technology) for preliminary fluorescence measurements.

**Conflicts of Interest:** The authors declare no conflict of interest. The funders had no role in the design of the study; in the collection, analyses, or interpretation of data; in the writing of the manuscript, or in the decision to publish the results.

**Sample Availability:** Not available.

## References

- Kumar, V.; Kaur, K.; Gupta, G.K.; Sharma, A.K. Pyrazole containing natural products: Synthetic preview and biological significance. *Eur. J. Med. Chem.* **2013**, *69*, 735–753. [CrossRef]
- Ansari, A.; Ali, A.; Asif, M. Shamsuzzaman Review: Biologically active pyrazole derivatives. *New J. Chem.* **2017**, *41*, 16–41. [CrossRef]
- Kucukguzel, S.G.; Senkardes, S. Recent advances in bioactive pyrazoles. *Eur. J. Med. Chem.* **2015**, *97*, 786–815. [CrossRef]
- Varvuolytė, G.; Malina, L.; Bieliauskas, A.; Hošíková, B.; Simerská, H.; Kolářová, H.; Kleizienė, N.; Kryštof, V.; Šačkus, A.; Žukauskaitė, A. Synthesis and photodynamic properties of pyrazole-indole hybrids in the human skin melanoma cell line G361. *Dyes Pigment.* **2020**, *183*, 108666. [CrossRef]
- Jayaraj, R.L.; Elangovan, N.; Dhanalakshmi, C.; Manivasagam, T.; Essa, M.M. CNB-001, a novel pyrazole derivative mitigates motor impairments associated with neurodegeneration via suppression of neuroinflammatory and apoptotic response in experimental Parkinson's disease mice. *Chem. Biol. Interact.* **2014**, *220*, 149–157. [CrossRef] [PubMed]
- Milišiūnaitė, V.; Kadlecová, A.; Žukauskaitė, A.; Doležal, K.; Strnad, M.; Voller, J.; Arbačiauskienė, E.; Holzer, W.; Šačkus, A. Synthesis and anthelmintic activity of benzopyrano[2,3-c]pyrazol-4(2H)-one derivatives. *Mol. Divers.* **2020**, *24*, 1025–1042. [CrossRef] [PubMed]
- Horrocks, P.; Pickard, M.R.; Parekh, H.H.; Patel, S.P.; Pathak, R.B. Synthesis and biological evaluation of 3-(4-chlorophenyl)-4-substituted pyrazole derivatives. *Org. Biomol. Chem.* **2013**, *11*, 4891–4898. [CrossRef] [PubMed]
- Masih, A.; Agnihotri, A.K.; Srivastava, J.K.; Pandey, N.; Bhat, H.R.; Singh, U.P. Discovery of novel pyrazole derivatives as a potent anti-inflammatory agent in RAW264.7 cells via inhibition of NF-κB for possible benefit against SARS-CoV-2. *J. Biochem. Mol. Toxicol.* **2020**, *35*, e22656. [CrossRef]
- Gogoi, P.; Shakya, A.; Ghosh, S.K.; Gogoi, N.; Gahtori, P.; Singh, N.; Bhattacharyya, D.R.; Singh, U.P.; Bhat, H.R. In silico study, synthesis, and evaluation of the antimalarial activity of hybrid dimethoxy pyrazole 1,3,5-triazine derivatives. *J. Biochem. Mol. Toxicol.* **2020**, *35*, e22682. [CrossRef]
- Karrouchi, K.; Radi, S.; Ramli, Y.; Taoufik, J.; Mabkhot, Y.N.; Al-Aizari, F.A.; Ansar, M. Synthesis and Pharmacological Activities of Pyrazole Derivatives: A Review. *Molecules* **2018**, *23*, 134. [CrossRef]
- Khan, M.F.; Alam, M.M.; Verma, G.; Akhtar, W.; Akhter, M.; Shaquiquzzaman, M. The therapeutic voyage of pyrazole and its analogs: A review. *Eur. J. Med. Chem.* **2016**, *120*, 170–201. [CrossRef] [PubMed]
- Rizk, H.F.; El-Badawi, M.A.; Ibrahim, S.A.; El-Borai, M.A. Synthesis of some novel heterocyclic dyes derived from pyrazole derivatives. *Arab. J. Chem.* **2011**, *4*, 37–44. [CrossRef]
- Karabacak, Ç.; Tilki, T.; Tuncer, B.Ö.; Cengiz, M. Antimicrobial pyrazole dyes: Synthesis, characterization, and absorption characteristics. *Res. Chem. Intermed.* **2015**, *41*, 1985–1999. [CrossRef]
- Göttinger, A.C.; Theßeling, F.A.; Hoppe, C.; Müller, T.J.J. One-Pot Coupling-Coupling-Cyclocondensation Synthesis of Fluorescent Pyrazoles. *J. Org. Chem.* **2016**, *81*, 10328–10338. [CrossRef]
- Milišiūnaitė, V.; Arbačiauskienė, E.; Bieliauskas, A.; Vilkauskaitė, G.; Šačkus, A.; Holzer, W. Synthesis of pyrazolo[4',3':3,4]pyrido[1,2-a]benzimidazoles and related new ring systems by tandem cyclisation of vic-alkynylpyrazole-4-carbaldehydes with (het)aryl-1,2-diamines and investigation of their optical properties. *Tetrahedron* **2015**, *71*, 3385–3395. [CrossRef]
- Tigreros, A.; Portilla, J. Recent progress in chemosensors based on pyrazole derivatives. *RSC Adv.* **2020**, *10*, 19693–19712. [CrossRef]
- Nayak, N.; Prasad, K.S.; Pillai, R.R.; Armaković, S.; Armaković, S.J. Remarkable colorimetric sensing behavior of pyrazole-based chemosensor towards Cu(II) ion detection: Synthesis, characterization and theoretical investigations. *RSC Adv.* **2018**, *8*, 18023–18029. [CrossRef]
- Mandal, A.K.; Suresh, M.; Suresh, E.; Mishra, S.K.; Mishra, S.; Das, A. A chemosensor for heavy-transition metal ions in mixed aqueous-organic media. *Sens. Actuators B Chem.* **2010**, *145*, 32–38. [CrossRef]
- Swami, S.; Agarwala, A.; Behera, D.; Shrivastava, R. Diaminomaleonitrile based chromo-fluorescent receptor molecule for selective sensing of Mn(II) and Zn(II) ions. *Sens. Actuators B Chem.* **2018**, *260*, 1012–1017. [CrossRef]
- Moura, N.M.M.; Núñez, C.; Santos, S.M.; Faustino, M.A.F.; Cavaleiro, J.A.S.; Neves, M.G.P.M.S.; Capelo, J.L.; Lodeiro, C. Synthesis, Spectroscopy Studies, and Theoretical Calculations of New Fluorescent Probes Based on Pyrazole Containing Porphyrins for Zn(II), Cd(II), and Hg(II) Optical Detection. *Inorg. Chem.* **2014**, *53*, 6149–6158. [CrossRef] [PubMed]

21. Garzón, L.-M.; Portilla, J. Synthesis of Novel D- $\pi$ -A Dyes for Colorimetric Cyanide Sensing Based on Hemicyanine-Functionalized N-(2-Pyridyl)pyrazoles. *Eur. J. Org. Chem.* **2019**, 2019, 7079–7088. [CrossRef]
22. Orrego-Hernández, J.; Portilla, J. Synthesis of Dicyanovinyl-Substituted 1-(2-Pyridyl)pyrazoles: Design of a Fluorescent Chemosensor for Selective Recognition of Cyanide. *J. Org. Chem.* **2017**, *82*, 13376–13385. [CrossRef]
23. Lee, H.; Berezin, M.Y.; Tang, R.; Zhegalova, N.; Achilefu, S. Pyrazole-substituted near-infrared cyanine dyes exhibit pH-dependent fluorescence lifetime properties. *Photochem. Photobiol.* **2013**, *89*, 326–331. [CrossRef]
24. Wang, F.; Duan, H.; Xing, D.; Yang, G. Novel Turn-on Fluorescence Probes for Al<sup>3+</sup> Based on Conjugated Pyrazole Schiff Base. *J. Fluoresc.* **2017**, *27*, 1721–1727. [CrossRef] [PubMed]
25. Naskar, B.; Das, K.; Mondal, R.R.; Maiti, D.K.; Requena, A.; Cerón-Carrasco, J.P.; Prodhon, C.; Chaudhuri, K.; Goswami, S. A new fluorescence turn-on chemosensor for nanomolar detection of Al<sup>3+</sup> constructed from a pyridine–pyrazole system. *New J. Chem.* **2018**, *42*, 2933–2941. [CrossRef]
26. Islam, A.S.M.; Bhowmick, R.; Mohammad, H.; Katarkar, A.; Chaudhuri, K.; Ali, M. A novel 8-hydroxyquinoline-pyrazole based highly sensitive and selective Al(III) sensor in a purely aqueous medium with intracellular application: Experimental and computational studies. *New J. Chem.* **2016**, *40*, 4710–4719. [CrossRef]
27. Ciupa, A.; Mahon, M.F.; De Bank, P.A.; Caggiano, L. Simple pyrazoline and pyrazole “turn on” fluorescent sensors selective for Cd<sup>2+</sup> and Zn<sup>2+</sup> in MeCN. *Org. Biomol. Chem.* **2012**, *10*, 8753. [CrossRef]
28. Liu, J.; Yee, K.K.; Lo, K.K.W.; Zhang, K.Y.; To, W.P.; Che, C.M.; Xu, Z. Selective Ag(I) binding, H<sub>2</sub>S sensing, and white-light emission from an easy-to-make porous conjugated polymer. *J. Am. Chem. Soc.* **2014**, *136*, 2818–2824. [CrossRef]
29. Dhara, A.; Guchhait, N.; Mukherjee, I.; Mukherjee, A.; Chandra Bhattacharya, S. A novel pyrazole based single molecular probe for multi-analyte (Zn<sup>2+</sup> and Mg<sup>2+</sup>) detection in human gastric adenocarcinoma cells. *RSC Adv.* **2016**, *6*, 105930–105939. [CrossRef]
30. Paitandi, R.P.; Sharma, V.; Singh, V.D.; Dwivedi, B.K.; Mobin, S.M.; Pandey, D.S. Pyrazole appended quinoline-BODIPY based arene ruthenium complexes: Their anticancer activity and potential applications in cellular imaging. *Dalton Trans.* **2018**, *47*, 17500–17514. [CrossRef]
31. Paitandi, R.P.; Mukhopadhyay, S.; Singh, R.S.; Sharma, V.; Mobin, S.M.; Pandey, D.S. Anticancer Activity of Iridium(III) Complexes Based on a Pyrazole-Appended Quinoline-Based BODIPY. *Inorg. Chem.* **2017**, *56*, 12232–12247. [CrossRef]
32. Faderl, S.; Pal, A.; Bornmann, W.; Albitar, M.; Maxwell, D.; Van, Q.; Peng, Z.; Harris, D.; Liu, Z.; Hazan-Halevy, I.; et al. Kit inhibitor APCK110 induces apoptosis and inhibits proliferation of acute myeloid leukemia cells. *Cancer Res.* **2009**, *69*, 3910–3917. [CrossRef]
33. Faderl, S.; Bueso-Ramos, C.; Liu, Z.; Pal, A.; Bornmann, W.; Ciurea, D.V.; Harris, D.; Hazan-Halevy, I.; Kantarjian, H.M.; Estrov, Z. Kit inhibitor APCK110 extends survival in an AML xenograft mouse model. *Investig. New Drugs* **2011**, *29*, 1094–1097. [CrossRef]
34. Faderl, S.; Bornmann, W.; Maxwell, D.; Pal, A.; Peng, Z.-H.; Shavrin, A.; Harris, D.; Van, Q.; Zhiming, L.; Verstovsek, S.; et al. APCK110, a Novel and Potent Inhibitor of c-Kit, Blocks Phosphorylation of AKT and STAT3, Induces Apoptosis, and Inhibits Proliferation of Acute Myeloid Leukemia (AML) Cells. *Blood* **2006**, *108*, 153. [CrossRef]
35. Nam, Y.; Hwang, D.; Kim, N.; Seo, H.-S.; Selim, K.B.; Sim, T. Identification of 1H-pyrazolo[3,4-b]pyridine derivatives as potent ALK-L1196M inhibitors. *J. Enzym. Inhib. Med. Chem.* **2019**, *34*, 1426–1438. [CrossRef] [PubMed]
36. Czodrowski, P.; Mallinger, A.; Wienke, D.; Esdar, C.; Pöschke, O.; Busch, M.; Rohdich, F.; Eccles, S.A.; Ortiz-Ruiz, M.J.; Schneider, R.; et al. Structure-Based Optimization of Potent, Selective, and Orally Bioavailable CDK8 Inhibitors Discovered by High-Throughput Screening. *J. Med. Chem.* **2016**, *59*, 9337–9349. [CrossRef]
37. Yoshida, T.; Oki, H.; Doi, M.; Fukuda, S.; Yuzuriha, T.; Tabata, R.; Ishimoto, K.; Kawahara, K.; Ohkubo, T.; Miyachi, H.; et al. Structural Basis for PPAR $\alpha$  Activation by 1H-pyrazolo-[3,4-b]pyridine Derivatives. *Sci. Rep.* **2020**, *10*, 7623. [CrossRef]
38. El-Gohary, N.S.; Gabr, M.T.; Shaaban, M.I. Synthesis, molecular modeling and biological evaluation of new pyrazolo[3,4-b]pyridine analogs as potential antimicrobial, antiquorum-sensing and anticancer agents. *Bioorg. Chem.* **2019**, *89*, 102976. [CrossRef]
39. Park, C.M.; Jadhav, V.B.; Song, J.-H.; Lee, S.; Won, H.Y.; Choi, S.U.; Son, Y.H. 3-Amino-1H-pyrazolopyridine Derivatives as a Maternal Embryonic Leucine Zipper Kinase Inhibitor. *Bull. Korean Chem. Soc.* **2017**, *38*, 595–602. [CrossRef]
40. Howard, S.; Amin, N.; Benowitz, A.B.; Chiarparin, E.; Cui, H.; Deng, X.; Heightman, T.D.; Holmes, D.J.; Hopkins, A.; Huang, J.; et al. Fragment-based discovery of 6-azaindazoles as inhibitors of bacterial DNA ligase. *ACS Med. Chem. Lett.* **2013**, *4*, 1208–1212. [CrossRef] [PubMed]
41. Engers, D.W.; Bollinger, S.R.; Engers, J.L.; Panarese, J.D.; Breiner, M.M.; Gregro, A.; Blobaum, A.L.; Bronson, J.J.; Wu, Y.J.; Macor, J.E.; et al. Discovery and characterization of N-(1,3-dialkyl-1H-indazol-6-yl)-1H-pyrazolo[4,3-b]pyridin-3-amine scaffold as mGlu<sub>4</sub> positive allosteric modulators that mitigate CYP1A2 induction liability. *Bioorg. Med. Chem. Lett.* **2018**, *28*, 2641–2646. [CrossRef]
42. Engers, D.W.; Blobaum, A.L.; Gogliotti, R.D.; Cheung, Y.Y.; Salovich, J.M.; Garcia-Barrantes, P.M.; Daniels, J.S.; Morrison, R.; Jones, C.K.; Soars, M.G.; et al. Discovery, Synthesis, and Preclinical Characterization of N-(3-Chloro-4-fluorophenyl)-1H-pyrazolo[4,3-b]pyridin-3-amine (VU0418506), a Novel Positive Allosteric Modulator of the Metabotropic Glutamate Receptor 4 (mGlu<sub>4</sub>). *ACS Chem. Neurosci.* **2016**, *7*, 1192–1200. [CrossRef] [PubMed]
43. Giannouli, V.; Lougiakis, N.; Kostakis, I.K.; Pouli, N.; Marakos, P.; Skaltsounis, A.-L.; Horne, D.A.; Nam, S.; Gioti, K.; Tenta, R. Design and Synthesis of New Substituted Pyrazolopyridines with Potent Antiproliferative Activity. *Med. Chem.* **2020**, *16*, 176–191. [CrossRef] [PubMed]

44. Michailidou, M.; Giannouli, V.; Kotsikoris, V.; Papadodima, O.; Kontogianni, G.; Kostakis, I.K.; Lougiakis, N.; Chatziioannou, A.; Kolisis, F.N.; Marakos, P.; et al. Novel pyrazolopyridine derivatives as potential angiogenesis inhibitors: Synthesis, biological evaluation and transcriptome-based mechanistic analysis. *Eur. J. Med. Chem.* **2016**, *121*, 143–157. [CrossRef] [PubMed]
45. Li, S.L.; Zhou, Y.; Lu, W.Q.; Zhong, Y.; Song, W.L.; Liu, K.D.; Huang, J.; Zhao, Z.J.; Xu, Y.F.; Liu, X.F.; et al. Identification of Inhibitors against p90 ribosomal S6 kinase 2 (RSK2) through structure-based virtual screening with the inhibitor-constrained refined homology model. *J. Chem. Inf. Model.* **2011**, *51*, 2939–2947. [CrossRef]
46. Smyth, L.A.; Matthews, T.P.; Collins, I. Design and evaluation of 3-aminopyrazolopyridinone kinase inhibitors inspired by the natural product indirubin. *Bioorg. Med. Chem.* **2011**, *19*, 3569–3578. [CrossRef] [PubMed]
47. Vilkauskaitė, G.; Schaaf, P.; Šačkus, A.; Krystof, V.; Holzer, W. Synthesis of pyridyl substituted pyrazolo[4,3-*c*]pyridines as potential inhibitors of protein kinases. *Arkivoc* **2014**, *2014*, 135–149. [CrossRef]
48. Holzer, W.; Vilkauskaitė, G.; Arbačiauskienė, E.; Šačkus, A. Dipyrzolo[1,5-*a*:4',3'-*c*]pyridines—A new heterocyclic system accessed via multicomponent reaction. *Beilstein J. Org. Chem.* **2012**, *8*, 2223–2229. [CrossRef]
49. Palka, B.; Di Capua, A.; Anzini, M.; Vilkauskaitė, G.; Šačkus, A.; Holzer, W. Synthesis of trifluoromethyl-substituted pyrazolo[4,3-*c*]pyridines—Sequential versus multicomponent reaction approach. *Beilstein J. Org. Chem.* **2014**, *10*, 1759–1764. [CrossRef]
50. Vilkauskaitė, G.; Šačkus, A.; Holzer, W. Sonogashira-type reactions with 5-chloro-1-phenyl-1*H*-pyrazole-4-carbaldehydes: A straightforward approach to pyrazolo[4,3-*c*]pyridines. *Eur. J. Org. Chem.* **2011**, *2011*, 5123–5133. [CrossRef]
51. Arbačiauskienė, E.; Laukaitytė, V.; Holzer, W.; Šačkus, A. Metal-Free Intramolecular Alkyne-Azide Cycloaddition To Construct the Pyrazolo[4,3-*f*][1,2,3]triazolo[5,1-*c*][1,4]oxazepine Ring System. *Eur. J. Org. Chem.* **2015**, *2015*, 5663–5670. [CrossRef]
52. Arbačiauskienė, E.; Vilkauskaitė, G.; Šačkus, A.; Holzer, W. Ethyl 3-and 5-triflyloxy-1*H*-pyrazole-4-carboxylates in the synthesis of condensed pyrazoles by Pd-catalysed cross-coupling reactions. *Eur. J. Org. Chem.* **2011**, *2011*, 1880–1890. [CrossRef]
53. Bieliauskas, A.; Krikštolaitytė, S.; Holzer, W.; Šačkus, A. Ring-closing metathesis as a key step to construct 2,6-dihydropyrano[2,3-*c*]pyrazole ring system. *Arkivoc* **2018**, *2018*, 296–307. [CrossRef]
54. Milišiūnaitė, V.; Arbačiauskienė, E.; Řezníčková, E.; Jorda, R.; Malínková, V.; Žukauskaitė, A.; Holzer, W.; Šačkus, A.; Kryštof, V. Synthesis and anti-mitotic activity of 2,4- or 2,6-disubstituted- and 2,4,6-trisubstituted-2*H*-pyrazolo[4,3-*c*]pyridines. *Eur. J. Med. Chem.* **2018**, *150*, 908–919. [CrossRef] [PubMed]
55. Milišiūnaitė, V.; Plytninkienė, E.; Bakšienė, R.; Bieliauskas, A.; Krikštolaitytė, S.; Račkauskienė, G.; Arbačiauskienė, E.; Šačkus, A. Convenient Synthesis of Pyrazolo[4',3':5,6]pyrano[4,3-*c*][1,2]oxazoles via Intramolecular Nitrile Oxide Cycloaddition. *Molecules* **2021**, *26*, 5604. [CrossRef]
56. Arbačiauskienė, E.; Martynaitis, V.; Krikštolaitytė, S.; Holzer, W.; Šačkus, A. Synthesis of 3-substituted 1-phenyl-1*H*-pyrazole-4-carbaldehydes and the corresponding ethanones by Pd-catalysed cross-coupling reactions. *Arkivoc* **2011**, *2011*, 1–21. [CrossRef]
57. Pompeu, T.E.T.; Alves, F.R.S.; Figueiredo, C.D.M.; Antonio, C.B.; Herzfeldt, V.; Moura, B.C.; Rates, S.M.K.; Barreiro, E.J.; Fraga, C.A.M.; Noël, F. Synthesis and pharmacological evaluation of new *N*-phenylpiperazine derivatives designed as homologues of the antipsychotic lead compound LASSBio-579. *Eur. J. Med. Chem.* **2013**, *66*, 122–134. [CrossRef]
58. Riva, E.; Gagliardi, S.; Martinelli, M.; Passarella, D.; Vigo, D.; Rencurosi, A. Reaction of Grignard reagents with carbonyl compounds under continuous flow conditions. *Tetrahedron* **2010**, *66*, 3242–3247. [CrossRef]
59. Goebel, M.T.; Marvel, C.S. The Oxidation of Grignard Reagents. *J. Am. Chem. Soc.* **1933**, *55*, 1693–1696. [CrossRef]
60. Besset, C.; Chambert, S.; Fenet, B.; Queneau, Y. Direct azidation of unprotected carbohydrates under Mitsunobu conditions using hydrazoic acid. *Tetrahedron Lett.* **2009**, *50*, 7043–7047. [CrossRef]
61. Mitsunobu, O. The Use of Diethyl Azodicarboxylate and Triphenylphosphine in Synthesis and Transformation of Natural Products. *Synthesis* **1981**, *1981*, 1–28. [CrossRef]
62. Bräse, S.; Banert, K. *Organic Azides: Syntheses and Applications*; John Wiley: New York, NY, USA, 2010; ISBN 9780470519981.
63. Semina, E.; Žukauskaitė, A.; Šačkus, A.; De Kimpe, N.; Mangelinckx, S. Selective Elaboration of Aminodiols towards Small Ring  $\alpha$ - and  $\beta$ -Amino Acid Derivatives that Incorporate an Aziridine, Azetidone, or Epoxide Scaffold. *Eur. J. Org. Chem.* **2016**, *2016*, 1720–1731. [CrossRef]
64. Peterson, T.; Streamland, T.; Awad, A. A Tractable and Efficient One-Pot Synthesis of 5'-Azido-5'-deoxyribonucleosides. *Molecules* **2014**, *19*, 2434–2444. [CrossRef]
65. Kuroda, K.; Hayashi, Y.; Mukaiyama, T. Conversion of tertiary alcohols to *tert*-alkyl azides by way of quinone-mediated oxidation–reduction condensation using alkyl diphenylphosphinites. *Tetrahedron* **2007**, *63*, 6358–6364. [CrossRef]
66. Fischer, D.; Tomeba, H.; Pahadi, N.K.; Patil, N.T.; Huo, Z.; Yamamoto, Y. Iodine-Mediated Electrophilic Cyclization of 2-Alkynyl-1-methylene Azide Aromatics Leading to Highly Substituted Isoquinolines and Its Application to the Synthesis of Norchelerythrine. *J. Am. Chem. Soc.* **2008**, *130*, 15720–15725. [CrossRef]
67. Žukauskaitė, Ž.; Buinauskaitė, V.; Solovjova, J.; Malinauskaitė, L.; Kveselytė, A.; Bieliauskas, A.; Ragaitė, G.; Šačkus, A. Microwave-assisted synthesis of new fluorescent indoline-based building blocks by ligand free Suzuki-Miyaura cross-coupling reaction in aqueous media. *Tetrahedron* **2016**, *72*, 2955–2963. [CrossRef]
68. Aoi, W.; Marunaka, Y. Importance of pH Homeostasis in Metabolic Health and Diseases: Crucial Role of Membrane Proton Transport. *Biomed Res. Int.* **2014**, *2014*, 598986. [CrossRef]
69. Han, J.; Burgess, K. Fluorescent indicators for intracellular pH. *Chem. Rev.* **2010**, *110*, 2709–2728. [CrossRef]
70. Tchaikovskaya, O.N.; Sokolova, I.V.; Kuznetsova, R.T.; Swetlitchnyi, V.A.; Kopylova, T.N.; Mayer, G.V. Fluorescence investigations of phenol phototransformation in aqueous solutions. *J. Fluoresc.* **2000**, *10*, 403–408. [CrossRef]

71. Diamantopoulos, P.T.; Sofotasiou, M.; Papadopoulou, V.; Polonyfi, K.; Iliakis, T.; Viniou, N.A. PARP1-driven apoptosis in chronic lymphocytic leukemia. *Biomed Res. Int.* **2014**, *2014*, 106713. [CrossRef]
72. Brady, S.C.; Allan, L.A.; Clarke, P.R. Regulation of Caspase 9 through Phosphorylation by Protein Kinase C Zeta in Response to Hyperosmotic Stress. *Mol. Cell. Biol.* **2005**, *25*, 10543–10555. [CrossRef]
73. Hansen, T.E.; Johansen, T. Following autophagy step by step. *BMC Biol.* **2011**, *9*, 39. [CrossRef]
74. Stoimenov, I.; Helleday, T. PCNA on the crossroad of cancer. *Biochem. Soc. Trans.* **2009**, *37*, 605–613. [CrossRef]
75. Wilson, G.D.; McNally, N.J.; Dische, S.; Saunders, M.I.; Des Rochers, C.; Lewis, A.A.; Bennett, M.H. Measurement of cell kinetics in human tumours in vivo using bromodeoxyuridine incorporation and flow cytometry. *Br. J. Cancer* **1988**, *58*, 423–431. [CrossRef]
76. Suzuki, K.; Kobayashi, A.; Kaneko, S.; Takehira, K.; Yoshihara, T.; Ishida, H.; Shiina, Y.; Oishi, S.; Tobita, S. Reevaluation of absolute luminescence quantum yields of standard solutions using a spectrometer with an integrating sphere and a back-thinned CCD detector. *Phys. Chem. Chem. Phys.* **2009**, *11*, 9850–9860. [CrossRef]

## Article

# Convenient Synthesis of Pyrazolo[4',3':5,6]pyrano[4,3-c][1,2]oxazoles via Intramolecular Nitrile Oxide Cycloaddition

Vaida Milišiūnaitė<sup>1</sup>, Elena Plytninkienė<sup>1,2</sup>, Roberta Bakšienė<sup>2</sup>, Aurimas Bieliauskas<sup>1</sup> , Sonata Krikštolaitytė<sup>2</sup>, Greta Račkauskienė<sup>1</sup>, Eglė Arbačiauskienė<sup>2,\*</sup>  and Algirdas Šačkus<sup>1,\*</sup>

<sup>1</sup> Institute of Synthetic Chemistry, Kaunas University of Technology, K. Baršausko g. 59, LT-51423 Kaunas, Lithuania; vaida.milisiunaite@ktu.lt (V.M.); elena.plytninkiene@ktu.lt (E.P.); aurimas.bieliauskas@ktu.lt (A.B.); greta.ragaite@ktu.lt (G.R.)

<sup>2</sup> Department of Organic Chemistry, Kaunas University of Technology, Radvilėnų pl. 19, LT-50254 Kaunas, Lithuania; roberta.ramanauskaite@gmail.com (R.B.); sonata.krikstolaityte@ktu.lt (S.K.)

\* Correspondence: egle.arbaciauskiene@ktu.lt (E.A.); algirdas.sackus@ktu.lt (A.Š.); Tel.: +370-37-451-401 (A.Š.)

**Abstract:** A simple and efficient synthetic route to the novel 3a,4-dihydro-3*H*,7*H*- and 4*H*,7*H*-pyrazolo[4',3':5,6]pyrano[4,3-c][1,2]oxazole ring systems from 3-(prop-2-en-1-yloxy)- or 3-(prop-2-yn-1-yloxy)-1*H*-pyrazole-4-carbaldehyde oximes has been developed by employing the intramolecular nitrile oxide cycloaddition (INOC) reaction as the key step. The configuration of intermediate aldoximes was unambiguously determined using NOESY experimental data and comparison of the magnitudes of <sup>1</sup>J<sub>CH</sub> coupling constants of the iminyl moiety, which were greater by approximately 13 Hz for the predominant *syn* isomer. The structures of the obtained heterocyclic products were confirmed by detailed <sup>1</sup>H, <sup>13</sup>C and <sup>15</sup>N NMR spectroscopic experiments and HRMS measurements.

**Keywords:** pyrazole; isoxazoline/isoxazole; fused ring systems; intramolecular nitrile oxide cycloaddition; 4-pyrazolaldoximes <sup>1</sup>J<sub>CH</sub>; isoxazole <sup>15</sup>N NMR; isoxazoline <sup>15</sup>N NMR

**Citation:** Milišiūnaitė, V.; Plytninkienė, E.; Bakšienė, R.; Bieliauskas, A.; Krikštolaitytė, S.; Račkauskienė, G.; Arbačiauskienė, E.; Šačkus, A. Convenient Synthesis of Pyrazolo[4',3':5,6]pyrano[4,3-c][1,2]oxazoles via Intramolecular Nitrile Oxide Cycloaddition. *Molecules* **2021**, *26*, 5604. <https://doi.org/10.3390/molecules26185604>

Academic Editors: Vera L. M. Silva and Artur M. S. Silva

Received: 27 August 2021

Accepted: 14 September 2021

Published: 15 September 2021

**Publisher's Note:** MDPI stays neutral with regard to jurisdictional claims in published maps and institutional affiliations.



**Copyright:** © 2021 by the authors. Licensee MDPI, Basel, Switzerland. This article is an open access article distributed under the terms and conditions of the Creative Commons Attribution (CC BY) license (<https://creativecommons.org/licenses/by/4.0/>).

## 1. Introduction

The 1,3-dipolar cycloaddition reaction of nitrile oxides as 1,3-dipoles and alkenes/alkynes as dipolarophiles has become an efficient tool in organic synthesis to obtain various substituted isoxazolines/isoxazoles [1–3]. The reaction was developed by Rolf Huisgen and described by Albert Padwa in their investigations on 1,3-dipolar cycloadditions [4,5]. Nitrile oxides, which are typically generated in situ, undergo subsequent 1,3-dipolar cycloaddition to form appropriate isoxazoles or isoxazolines. Numerous methods of nitrile oxide generation have been reported, mainly including the dehydration of nitroalkanes [6–8] and oxidation of aldoximes [9–11]. Alternatively, Svejstrup described the synthesis of isoxazolines and isoxazoles from hydroxyimino acids via the visible-light-mediated generation of nitrile oxides by two sequential oxidative single electron transfer processes [12]. More recently, Chen et al. reported the synthesis of fully substituted isoxazoles from nitrile oxides, which were generated in situ from copper carbene and *tert*-butyl nitrite [13].

Notably, the intramolecular nitrile oxide cycloaddition (INOC) reaction can provide a route for the preparation of isoxazoles or isoxazolines annulated to various carbo- or heterocycles. For example, the intramolecular 1,3-dipolar cycloaddition of 2-phenoxybenzoxazole *N*-oxides to neighboring benzene rings, accompanied by dearomatization, formed the corresponding isoxazolines in high yields [14]. Recently, a method for the stereoselective synthesis of novel isoxazoline/isoxazole-fused indolizidine-, pyrrolizidine- and quinolizidine-based iminosugars has been developed, employing *N*-alkenyl/alkynyl iminosugar C-nitromethyl glycosides as nitrile oxide precursors in 1,3-dipolar cycloaddition reactions [15]. The phthalate-tethered INOC strategy has also been described as a novel method for the synthesis of 12–15-membered chiral macrocycles having a bridged isoxazoline moiety in a highly regio- and diastereoselective manner [16]. Furthermore, diversity-oriented access



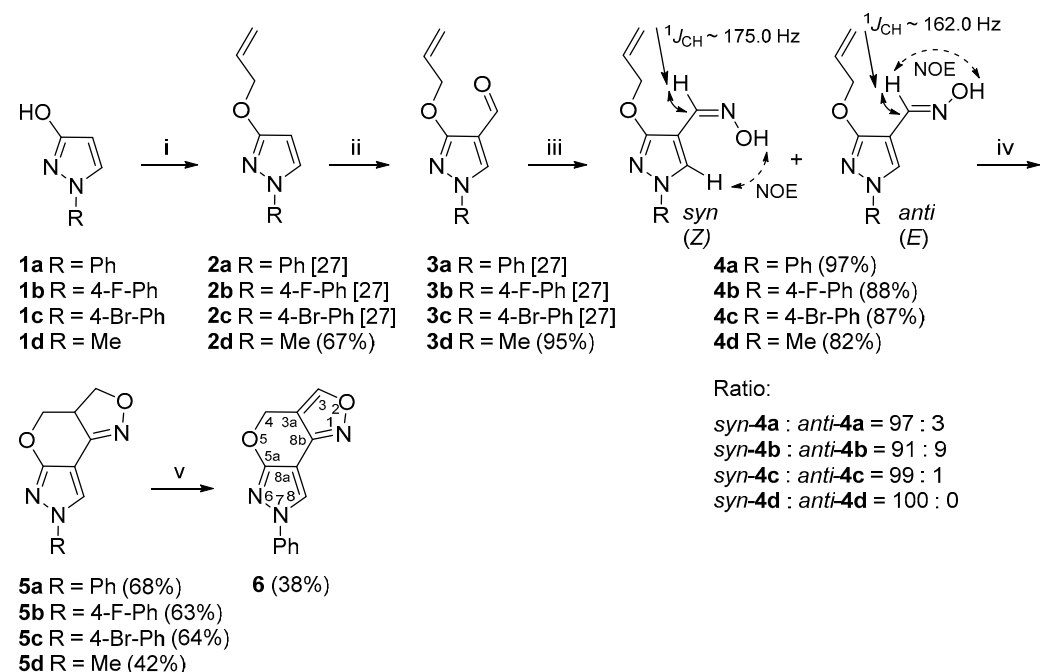
to isoxazolino and isoxazolo benzazepines as possible bromodomain and extra-terminal motif protein (BET) inhibitors has been reported via a post-Ugi heteroannulation involving the intramolecular 1,3-dipolar cycloaddition reaction of nitrile oxides with alkenes and alkynes [17]. In addition, an intramolecular 1,3-dipolar nitrile oxide cycloaddition strategy has been applied as an efficient synthesis protocol for the regio- and diastereoselective construction of highly functionalized tricyclic tetrahydroisoxazoloquinolines [18].

Fused isoxazoles or isoxazolines obtained by the INOC reaction may also serve as synthetically important intermediates for many biologically active compounds. Such compounds, including the HBV inhibitor entecavir [19,20], the antibiotic branimycin [21], the antiviral (+)-Brefeldin A [22], tricyclic isoxazoles combining serotonin (5-HT) reuptake inhibition with  $\alpha_2$ -adrenoceptor blocking activity [23] and the alkaloids meliacarpinin B [24] and Palhinine A [25], have been synthesized by employing INOC as a key step.

We previously investigated the metal-free intramolecular alkyne-azide cycloaddition reaction for the formation of the pyrazolo[4,3-*f*][1,2,3]triazolo[5,1-*c*][1,4]oxazepine ring system [26] as well as the synthesis of 2,6-dihydropyrano[2,3-*c*]pyrazole derivatives by employing the ring-closing metathesis (RCM) reaction [27]. In continuation of our interest in the synthesis and investigation of novel pyrazole-containing polyheterocyclic systems [28–33], we report herein the synthesis and structural elucidation of new 3a,4-dihydro-3*H*,7*H*- and 4*H*,7*H*-pyrazolo[4',3':5,6]pyrano[4,3-*c*][1,2]oxazole derivatives from appropriate 3-(prop-2-en-1-yloxy)- or 3-(prop-2-yn-1-yloxy)-1*H*-pyrazole-4-carbaldehyde oximes via the intramolecular nitrile oxide cycloaddition reaction.

## 2. Results

The synthetic strategy that we designed to construct the pyrazolo[4',3':5,6]pyrano[4,3-*c*][1,2]oxazole ring system employs difunctional substrates (**4a–d**) that contain an aldoxime unit next to the allyloxy group attached to the pyrazole core and can serve as intermediates for nitrile oxide generation and subsequent cycloaddition (Scheme 1).



**Scheme 1.** Synthetic route for the 3a,4-dihydro-3*H*,7*H*-pyrazolo[4',3':5,6]pyrano[4,3-*c*][1,2]oxazole ring system. Reagents and conditions: (i) NaH, DMF, 0 °C, 15 min, allylbromide, 60 °C, 1 h; (ii) DMF, POCl<sub>3</sub>, −10 °C, 15 min, 70 °C, 1 h; (iii) NH<sub>2</sub>OH·HCl, NaOAc, EtOH, reflux, 15 min; (iv) aq. NaOCl, DCM, rt, 1 h; (v) MnO<sub>2</sub>, toluene, reflux, 4 h.

As starting materials for the synthesis of compounds **4a–d**, we used 1-phenyl-, 1-(4-fluorophenyl)-, 1-(4-bromophenyl)- and 1-methylpyrazol-3-ols (**1a–d**), which are readily accessible from the oxidation of appropriate pyrazolidin-3-ones [34]. The *O*-allylation of **1a–d** with allylbromide in the presence of NaH gave *O*-allylated pyrazoles **2a–d** [27]. To introduce a formyl group to the 4-position of the pyrazole ring, we employed a previously reported Vilsmeier–Haack reaction procedure [27,35]. Heating compounds **2a–d** with Vilsmeier–Haack complex at 70 °C resulted in the formation of the desired pyrazole-4-carbaldehydes **3a–d** (Scheme 1).

In order to prepare the 3a,4-dihydro-3*H*,7*H*-pyrazolo[4',3':5,6]pyrano[4,3-*c*][1,2]oxazole derivatives **5a–d** by the INOC reaction, aldoximes **4a–d** were synthesized by the treatment of **3a–d** with hydroxylamine hydrochloride in the presence of sodium acetate [36]. As a result, the *syn*- and *anti*-3-allyloxy-4-pyrazolaldoximes were obtained in total yields of 82–97%. The <sup>1</sup>H NMR spectra of aldoximes **4a–c** showed the presence of two isomers in different ratios with a predominance of the *syn* isomer, while the compound **4d** was obtained as a pure *syn* isomer.

Over the years, the isomerism of aldoximes has been thoroughly studied and many different NMR-based approaches have been developed, mainly due to the large differences in chemical shifts, coupling constants and distinct through-space connectivities in NOESY measurements of aldoxime *syn-anti* isomers [37]. The configurational assignment of aldoximes **4a–c** was relatively easy due to the presence of both isomers, as it is well established that the resonance of the iminyl-H proton in the *syn* isomer is greatly shifted upfield by approximately  $\delta$  0.5–0.7 ppm in the <sup>1</sup>H NMR spectra compared to the *anti* isomer [38]. Moreover, the 1D selective NOESY experimental data of aldoximes **4a–c** showed that, upon irradiation of the hydroxyl proton N-OH of the predominant *syn* isomer, a strong positive NOE on the pyrazole 5-H proton was observed, while the minor isomer showed a positive NOE on the iminyl-H, therefore confirming the *anti* configuration. Finally, a heteronuclear 2D *J*-resolved NMR experiment was used in order to determine <sup>1</sup>*J*<sub>CH</sub> coupling constants throughout the series of aldoximes. It is well established from previous studies that there is a large and constant difference between the magnitudes of <sup>1</sup>*J*<sub>CH</sub> coupling constants of the iminyl moiety in *syn-anti* isomers [39], which is larger by at least 10–15 Hz for the *syn* isomer. The measurements of compounds **4a–c** showed that the relevant <sup>1</sup>*J*<sub>CH</sub> coupling constants of the iminyl moiety were around 175.0 Hz for the predominant *syn* isomer, while the minor *anti* isomer provided significantly lower coupling constant values by around 13.0 Hz. The configuration of aldoxime **4d** as a pure *syn* isomer was easily deduced from NOESY measurements and the <sup>1</sup>*J*<sub>CH</sub> coupling constant of the iminyl moiety, which was 174.5 Hz. The analysis of <sup>15</sup>N NMR spectroscopic data showed highly consistent chemical shift values within each isomer, in a range from  $\delta$  –18.2 to –25.7 ppm in the case of the *syn* isomer and in a range from  $\delta$  –15.6 to –16.5 ppm for the *anti* isomer. A comparison of the relevant NMR data of aldoximes is presented in Table S1.

Several methods for the oxidation of aldoximes to nitrile oxides are known in the literature, including the application of oxidants such as chloramine T [40,41], *N*-halosuccinimides (NXS) [42–44], hypohalites [45–47], hypervalent iodine reagents [48–50] and oxone [51–54]. The reaction conditions for 3a,4-dihydro-3*H*,7*H*-pyrazolo[4',3':5,6]pyrano[4,3-*c*][1,2]oxazole ring formation were optimized by using **4a** as a model compound (Table 1). When treating aldoxime **4a** with chloramine T in EtOH at 50 °C for 30 min, the polycyclic product **5a** was obtained in poor (20%) yield (Table 1, Entry 1). The intramolecular cyclization reaction of **4a** in the presence of the aq. NaOCl in DCM gave the desired product **5a** in 1 h in sufficient (68%) yield (Table 1, Entry 2). The experiment with TEA as an additive did not improve the yield of the product and **5a** was obtained in 52% yield (Table 1, Entry 3). A similar result showing that no additional base is required to facilitate the cycloaddition was also observed by Roy and De in their investigation on the rate enhancement of nitrile oxide cyclization and, hence, rapid synthesis of isoxazolines and isoxazoles [55].

The optimized conditions (aq. NaOCl in DCM at rt) for **5a** synthesis were also applied to the synthesis of 7-(4-fluorophenyl)-, 7-(4-bromophenyl)- and 7-methyl-3a,4-

dihydro-3*H*,7*H*-pyrazolo[4',3':5,6]pyrano[4,3-*c*][1,2]oxazoles **5b–d** to evaluate the scope of the methodology. The products were obtained in yields of 63%, 64% and 42%, respectively. In addition, we investigated whether the obtained 3*a*,4-dihydro-3*H*,7*H*-pyrazolo[4',3':5,6]pyrano[4,3-*c*][1,2]oxazole system can be further oxidized. Several oxidation reaction conditions were tested, e.g., **5a** was stirred in DMSO at 110 °C in an open atmosphere [56] or treated with a catalytic amount of Pd/C in acetic acid [57]; the best result was obtained using activated MnO<sub>2</sub> as an oxidant in toluene in a Dean–Stark apparatus for 4 h at reflux temperature [58]. Furthermore, 4*H*,7*H*-Pyrazolo[4',3':5,6]pyrano[4,3-*c*][1,2]oxazole derivative **6** was formed in 38% yield.

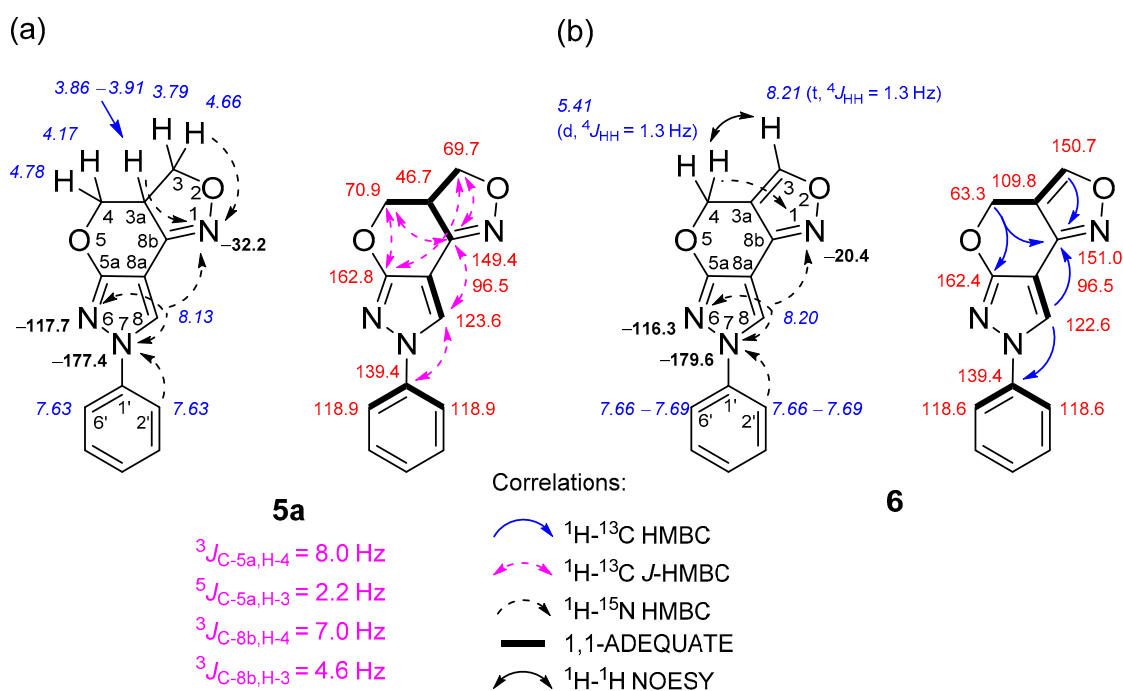
**Table 1.** Optimization of the INOC reaction conditions for **5a** synthesis.

| Entry | Conditions                        | Yield *, % |
|-------|-----------------------------------|------------|
| 1     | Chloramine T, EtOH, 50 °C, 30 min | 20         |
| 2     | 10% NaOCl, DCM, rt, 1 h           | 68         |
| 3     | 10% NaOCl, TEA, DCM, rt, 3 h      | 52         |

\* After purification by column chromatography.

A similar brief study on 5-chloropyrazole-4-carbaldehydes as synthons for intramolecular 1,3-dipolar cycloaddition was also reported by L'abbé et al. [59]. The authors noticed that 5-allyloxypyrazole-4-carbaldehyde derived from 5-chloropyrazole-4-carbaldehyde and further used as a precursor for intramolecular 1,3-dipolar cycloaddition reactions underwent a slow Claisen rearrangement to 4-allyl-5-hydroxypyrazole, even at room temperature. In contrast, we found 3-allyloxypyrazole-4-carbaldehydes to be stable. They can be stored in the laboratory at room temperature.

The formation of 3*a*,4-dihydro-3*H*,7*H*- and 4*H*,7*H*-pyrazolo[4',3':5,6]pyrano[4,3-*c*][1,2]oxazole ring systems was easily deduced after an in-depth analysis of NMR spectral data, which were obtained through a combination of standard and advanced NMR spectroscopy techniques, such as <sup>1</sup>H-<sup>13</sup>C HMBC, <sup>1</sup>H-<sup>13</sup>C *J*-HMBC, <sup>1</sup>H-<sup>15</sup>N HMBC, <sup>1</sup>H-<sup>13</sup>C HSQC, <sup>1</sup>H-<sup>13</sup>C H2BC, <sup>1</sup>H-<sup>1</sup>H COSY, <sup>1</sup>H-<sup>1</sup>H NOESY and 1,1-ADEQUATE experiments (Figure 1).



**Figure 1.** Relevant <sup>1</sup>H-<sup>13</sup>C HMBC, <sup>1</sup>H-<sup>13</sup>C *J*-HMBC, <sup>1</sup>H-<sup>15</sup>N HMBC, <sup>1</sup>H-<sup>1</sup>H NOESY and 1,1-ADEQUATE correlations and <sup>1</sup>H NMR (italics), <sup>13</sup>C NMR and <sup>15</sup>N NMR (bold) chemical shifts of compounds **5a** (a) and **6** (b).

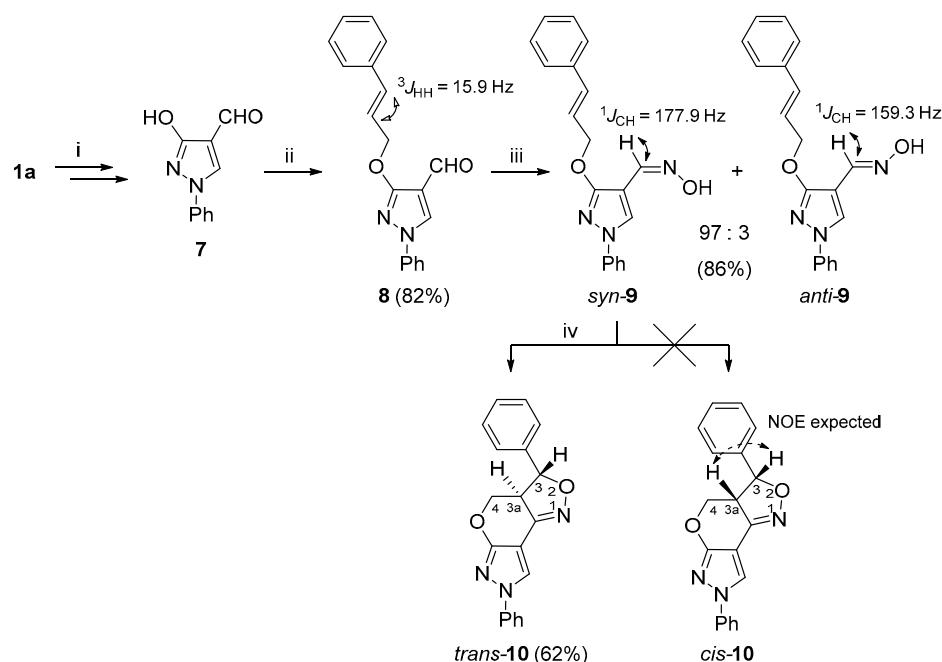
In the case of compound **5a**, the multiplicity-edited  $^1\text{H}$ - $^{13}\text{C}$  HSQC spectrum allowed us to identify the pairs of geminally coupled methylene protons, since both protons displayed cross-peaks with the same carbon. For instance, it showed two pairs of negative signals at  $\delta_{\text{H}}$  4.66, 3.79 and 4.78, 4.17 ppm, which have one-bond connectivities with the methylene carbons C-3 ( $\delta$  69.7 ppm) and C-4 ( $\delta$  70.9 ppm), respectively. The chemical shifts of these methylene groups are expected to be similar and downfield compared to a neighboring methine group at site 3a, because both are bound to the oxygen atoms O-2 and O-5. This adjacent protonated carbon C-3a ( $\delta$  46.7 ppm) relative to the aforementioned methylene sites was easily assigned from an appropriate correlation in the  $^1\text{H}$ - $^{13}\text{C}$  H2BC spectrum.

In the  $^1\text{H}$ - $^{15}\text{N}$  HMBC spectrum of **5a**, strong long-range correlations between the methylene 3-H proton at  $\delta$  4.66 ppm and the 3a-H proton at  $\delta$  3.86–3.91 ppm with the oxazole N-1 nitrogen at  $\delta$  –32.2 ppm were observed. The lack of long-range correlations with another pair of methylene protons ( $\delta$  4.78, 4.17 ppm), and the aforementioned N-1 nitrogen, strongly hinted at assigning this methylene group to site 4. In order to unambiguously discriminate between these methylene groups, the  $^1\text{H}$ - $^{13}\text{C}$  heteronuclear couplings were measured using a  $^1\text{H}$ - $^{13}\text{C}$  *J*-HMBC experiment, thus providing complimentary evidence for correct structural assignment. The *J*-HMBC spectrum showed a strong correlation between the methylene proton  $\delta$  4.78 ppm and the quaternary carbon C-5a with an 8.0-hertz coupling constant, while the proton  $\delta$  4.66 ppm correlated very weakly, with a *J* value of only 2.2 Hz, which was attributed to a  $^5J_{\text{C-5a, H-3}}$ . Finally, the pyrazole 8-H proton ( $\delta$  8.13 ppm) not only exhibited long-range HMBC correlations with neighboring N-7 “pyrrole-like” ( $\delta$  –177.4 ppm) and N-6 “pyridine-like” ( $\delta$  –117.7 ppm) nitrogen atoms, but also with the C-5a, C-8a and C-8b quaternary carbons, which were unambiguously assigned with the subsequent 1,1-ADEQUATE experiment, thus allowing all the heterocyclic moieties to be connected together. The structure of compounds **5b–d** was determined by analogous NMR spectroscopy experiments, as described above. The skeleton of the pyrazolo[4',3':5,6]pyrano[4,3-c][1,2]oxazole ring system contains three nitrogen atoms. The chemical shifts of the N-1, N-6 and N-7 atoms of compounds **5a–c** were in a range from  $\delta$  –30.9 to –32.2,  $\delta$  –116.9 to –117.7 and  $\delta$  –177.4 to –179.5 ppm, respectively, while in the case of compound **5d**, which lacked a phenyl moiety at site 7, the chemical shifts of N-1, N-6 and N-7 atoms were  $\delta$  –35.8,  $\delta$  –112.3 and  $\delta$  –194.4 ppm, respectively.

In the case of compound **6**, a comparison of the  $^1\text{H}$  NMR spectra between **5a** and **6** clearly indicated the disappearance of methine 3a-H ( $\delta$  3.86–3.91 ppm) and methylene 3-H protons ( $\delta$  4.66 and 3.79 ppm) and the formation of a new downfield methine 3-H proton signal at  $\delta$  8.21 ppm. The aforementioned methine proton that appeared as a triplet was mutually coupled with methylene 4-H protons (doublet,  $\delta$  5.41 ppm), as indicated by their *meta*-coupling ( $^4J_{\text{HH}} = 1.3$  Hz). Moreover, a comparison between the  $^1\text{H}$ - $^1\text{H}$  COSY and  $^1\text{H}$ - $^1\text{H}$  NOESY spectra showed a complete absence of COSY cross-peaks between 3-H and 4-H and only strong NOEs, which confirmed their proximity in space. This finding strongly hinted at a neighboring quaternary carbon at site 3a, which was unambiguously assigned from 1,1-ADEQUATE spectral data, where the protonated carbons C-3 ( $\delta$  150.7 ppm) and C-4 ( $\delta$  63.3 ppm) showed a sole correlation with C-3a at  $\delta$  109.8 ppm. As expected, the  $^{15}\text{N}$  chemical shifts of N-6 ( $\delta$  –116.3) and N-7 ( $\delta$  –179.6) atoms were highly comparable to those of compounds **5a–c**; only the N-1 atoms were slightly different and resonated at  $\delta$  –20.4 ppm, which is in good agreement with the data reported in the literature [60].

To expand the structural diversity of the obtained 3a,4-dihydro-3*H*,7*H*-pyrazolo[4',3':5,6]pyrano[4,3-c][1,2]oxazole system, we prepared additional *vic*-cinnamyloxy-oxime **9** as a substrate for the INOC reaction (Scheme 2). As the cinnamyloxy group turned out to be sensitive towards Vilsmeier–Haack reaction conditions, the *O*-alkylation formylation sequence of compound **1a** successfully applied to the synthesis of 3-allyloxy-pyrazole-4-carbaldehydes **3a–d** was reorganized. In short, first, the hydroxy group of pyrazol-3-ol (**1a**) was transformed to a benzyloxy group; then, the obtained 3-benzyloxy-pyrazole was formylated under the Vilsmeier–Haack reaction conditions, and the protecting OBn group was cleaved by TFA to give 3-hydroxy-1*H*-pyrazole-4-carbaldehyde **7** [35]. The

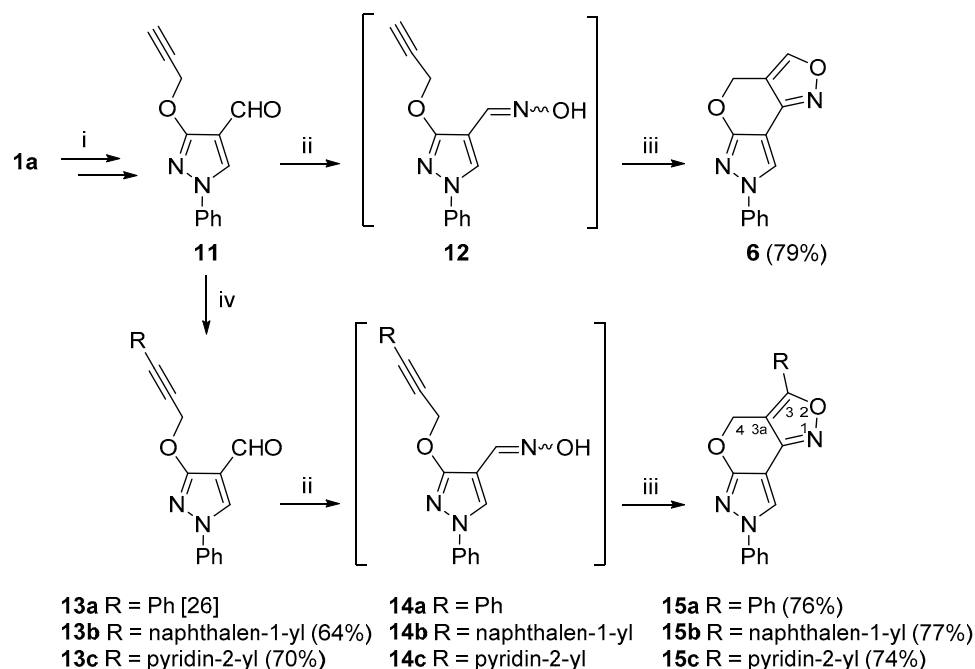
latter compound was subjected to an alkylation reaction with cinnamyl chloride and the appropriate 3-cinnamyloxy-1*H*-pyrazole-4-carbaldehyde (**8**) was obtained in very good (82%) yield. A subsequent reaction of **8** with hydroxylamine gave the aldoxime **9**, which was successfully used for the INOC reaction, and 3-phenyl-3*a*,4-dihydro-3*H*,7*H*-pyrazolo[4',3':5,6]pyrano[4,3-*c*][1,2]oxazole *trans*-**10** was obtained with a fair (62%) yield.



**Scheme 2.** Synthetic route for the 3*a*,4-dihydro-3*H*,7*H*-pyrazolo[4',3':5,6]pyrano[4,3-*c*][1,2]oxazole **10**. Reagents and conditions: (i) in accordance to ref. [35]; (ii) NaH, DMF, 0 °C, 15 min, cinnamyl chloride, 60 °C, 15 min; (iii) NH<sub>2</sub>OH·HCl, NaOAc, EtOH, reflux, 15 min; (iv) NaOCl, DCM, rt, 1 h.

While the structural elucidation of compound *trans*-**10** was straightforward and followed the same logical approach as in the case of compounds **5a–d** and **6**, determination of the relative configuration at C-3 and C-3*a* proved to be a more challenging task and was achieved by combined analysis of NOESY, *J*-coupling and molecular modeling data. For instance, the initial geometry optimizations were performed using MM2 and MMFF94 force fields [61], followed by DFT methods using B3LYP/def2-TZVP, as implemented in ORCA 5.0.0 [62], which provided the dihedral angle values between H-C(3)-C(3*a*)-H for structures *trans*-**10** (154.34°) and *cis*-**10** (19.28°). Then, the theoretical <sup>1</sup>H-<sup>1</sup>H coupling constants were calculated with the same software package following a standard procedure using a B3LYP/PCSEG-2 basis set. The dihedral angle values were used in the calculation of <sup>3</sup>*J*<sub>H3,H3*a*</sub> by the Haasnoot–de Leeuw–Altona (HLA) equation [63]. The <sup>3</sup>*J*<sub>H3,H3*a*</sub> values estimated by the HLA method were 10.0 Hz for *trans*-**10** and 8.2 Hz for *cis*-**10**, while ORCA 5.0.0 calculations were 13.4 and 10.8 Hz, respectively. The experimental value 13.1 Hz, which was obtained from the <sup>1</sup>H NMR spectrum, hinted in favor of the *trans*-**10** structure. A highly similar class of heterocycles, naphthopyranoisoxazolines, were synthesized by Liaskopoulos et al. [64], where the target compounds possessed a *trans* configuration, as confirmed by X-ray and NMR analyses, and their <sup>3</sup>*J*<sub>H3,H3*a*</sub> values were in the range of 12.2–12.5 Hz. Finally, unambiguous confirmation of *trans*-**10** assignment was obtained from the <sup>1</sup>H-<sup>1</sup>H NOESY spectrum, as it was evident from the geometrically optimized structures (Figures S80 and S81) that, in the case of *cis*-**10**, there should be a strong NOE between protons 3-H and 3*a*-H, while the NOE between 3*a*-H and the neighboring 3-phenyl group aromatic protons is not possible. However, in our case, the <sup>1</sup>H-<sup>1</sup>H NOESY spectrum showed completely opposite measurements. Moreover, a distinct NOE between protons 3-H/4-H<sub>a</sub> and 3*a*-H/4-H<sub>b</sub> is only possible if the relative configuration is *trans*-**10**.

We also investigated the INOC reaction of *vic*-alkyne–oxime substrates **12** and **14a–c** (Scheme 3). To obtain the intermediate compound **12**, firstly, 3-hydroxypyrazole **1a** was *O*-propargylated and formylated to give carbaldehyde **11** [26]. Compound **11** was then successfully converted to *4H,7H*-pyrazolo[4',3':5,6]pyrano[4,3-*c*][1,2]oxazole **6** via the INOC reaction of intermediate oxime **12**, and the targeted new polyheterocyclic compound **6** was obtained in good (79%) yield. In addition, alkyne **11** was further subjected to the Sonogashira cross-coupling reaction with various (het)arylhalides, i.e., iodobenzene, 1-iodonaphthalene and 2-bromopyridine, under the standard Sonogashira cross-coupling reaction conditions (Pd(PPh<sub>3</sub>)<sub>2</sub>Cl<sub>2</sub>, CuI, DMF, 60 °C, argon atmosphere) to give alkynes **13a–c** in good yields [26]. Compounds **13a–c** were further treated with hydroxylamine hydrochloride to provide aldoximes **14a–c**, which were used in the INOC reaction without further purification. Aldoxime **14a** was subjected to a detailed NMR analysis, and, to our delight, it was obtained as a pure *syn* isomer, which was easily elucidated from a <sup>1</sup>J<sub>CH</sub> coupling constant of the iminyl moiety, which was 179.2 Hz. Moreover, *4H,7H*-pyrazolo[4',3':5,6]pyrano[4,3-*c*][1,2]oxazoles **15a–c** were obtained in good yields.



**Scheme 3.** Synthetic route for the *4H,7H*-pyrazolo[4',3':5,6]pyrano[4,3-*c*][1,2]oxazole ring system. Reagents and conditions: (i) in accordance to ref. [26]; (ii) NH<sub>2</sub>OH·HCl, NaOAc, EtOH, reflux, 15 min; (iii) NaOCl, DCM, rt, 1 h; (iv) RX, Pd(PPh<sub>3</sub>)<sub>2</sub>Cl<sub>2</sub>, TEA, DMF, 60 °C, 15 min.

As expected, the chemical shifts of the 3-aryl-substituted compounds **15a–c** were highly similar to those of compound **6**. A distinct difference in the <sup>1</sup>H NMR spectra of the aforementioned compounds was that they contained only a singlet for the methylene 4-H protons in the area of δ 5.32–6.03 ppm, which indicated the lack of coupling partners. The data from the <sup>1</sup>H-<sup>13</sup>C HMBC spectra revealed a distinct long-range correlation between the aforementioned methylene protons and a quaternary carbon at site 3. Moreover, the protons from a neighboring 3-aryl moiety shared an HMBC cross-peak with carbon C-3 as well, thus allowing different structural fragments to be joined together. The chemical shifts of the N-1, N-6 and N-7 atoms of 3-aryl-substituted compounds were in ranges of δ –23.9 to –25.0, δ –116.4 to –117.4 and δ –179.6 to –180.1 ppm, respectively, while, in the case of compound **15c** with a pyridin-2-yl moiety, the pyridine nitrogen resonated at δ –72.8 ppm.

### 3. Materials and Methods

#### 3.1. General Information

All starting materials were purchased from commercial suppliers and were used as received. Flash column chromatography was performed on Silica Gel 60 Å (230–400 µm, Merck). Thin-layer chromatography was carried out on Silica Gel plates (Merck Kieselgel 60 F<sub>254</sub>) and visualized by UV light (254 nm). Melting points were determined on a Büchi M-565 melting point apparatus and were uncorrected. The IR spectra were recorded on a Bruker Vertex 70v FT-IR spectrometer using neat samples and are reported in frequency of absorption (cm<sup>-1</sup>). Mass spectra were obtained on a Shimadzu LCMS-2020 (ESI<sup>+</sup>) spectrometer. High-resolution mass spectra were measured on a Bruker MicrOTOF-Q III (ESI<sup>+</sup>) apparatus. The <sup>1</sup>H, <sup>13</sup>C and <sup>15</sup>N NMR spectra were recorded in CDCl<sub>3</sub>, DMSO-*d*<sub>6</sub> or TFA-*d* solutions at 25 °C on a Bruker Avance III 700 (700 MHz for <sup>1</sup>H, 176 MHz for <sup>13</sup>C, 71 MHz for <sup>15</sup>N) spectrometer equipped with a 5 mm TCI <sup>1</sup>H-<sup>13</sup>C/<sup>15</sup>N/D z-gradient cryoprobe. The chemical shifts (δ), expressed in ppm, were relative to tetramethylsilane (TMS). The <sup>15</sup>N NMR spectra were referenced to neat, external nitromethane (coaxial capillary). Full and unambiguous assignment of the <sup>1</sup>H, <sup>13</sup>C and <sup>15</sup>N NMR resonances was achieved using a combination of standard NMR spectroscopic techniques [65] such as DEPT, COSY, TOCSY, NOESY, gs-HSQC, gs-HMBC, H2BC, LR-HSQMBC and 1,1-ADEQUATE experiments [66]. Structures for molecular modeling were built using Chem3D Pro 17.0, and were optimized by MM2 and MMFF94 force fields, followed by DFT methods using B3LYP/def2-TZVP for dihedral angle measurements, and B3LYP/PCSSSEG-2 for the calculation of theoretical <sup>1</sup>H-<sup>1</sup>H coupling constants, using a standard procedure as implemented in the ORCA 5.0.0 software package. The dihedral angle values were used in the calculation of vicinal <sup>1</sup>H-<sup>1</sup>H coupling constants using the Mestre-J 1.1 software [67] and HLA (general, beta effect) equation. <sup>1</sup>H-, <sup>13</sup>C-, and <sup>1</sup>H-<sup>15</sup>N HMBC NMR spectra, and HRMS data of new compounds, are provided in Supplementary Materials as Figures S5–S79.

#### 3.2. Synthesis of 1-Methyl-3-[(prop-2-en-1-yl)oxy]-1H-pyrazole (2d)

A solution of 3-hydroxypyrazole **1d** (450 mg, 2.5 mmol) in dry DMF (5 mL) was cooled to 0 °C under an inert atmosphere, and NaH (60% dispersion in mineral oil, 60 mg, 2.5 mmol) was added portion-wise. After stirring the reaction mixture for 15 min, allyl bromide (370 mg, 3 mmol) was added dropwise. The mixture was stirred at 60 °C for 1 h, then poured into water and extracted with ethyl acetate (3 × 10 mL). The organic layers were combined, washed with brine, dried over Na<sub>2</sub>SO<sub>4</sub>, filtrated, and the solvent was evaporated. The residue was purified by flash column chromatography (SiO<sub>2</sub>, eluent: ethyl acetate/*n*-hexane, 1:7, *v/v*) to provide the desired compound **2d** as a brown liquid, yield 330 mg, 96%. IR (ν<sub>max</sub>, cm<sup>-1</sup>): 2931 (CH<sub>aliph</sub>), 1728, 1694, 1538, 1494, 1410, 1346, 1224 (–C=C, C=C, C–N, C–O–C). <sup>1</sup>H NMR (700 MHz, CDCl<sub>3</sub>): δ 3.73 (s, 3H, CH<sub>3</sub>), 4.65 (dt, *J* = 5.5, 1.5 Hz, 2H, OCH<sub>2</sub>CHCH<sub>2</sub>), 5.24 (dq, *J* = 10.6, 1.6 Hz, 1H, OCH<sub>2</sub>CHCH<sub>2</sub>), 5.40 (dq, *J* = 17.2, 1.6 Hz, 1H, OCH<sub>2</sub>CHCH<sub>2</sub>), 5.62 (d, *J* = 2.3 Hz, 1H, 4-H), 6.06 (ddt, *J* = 17.2, 10.8, 5.5 Hz, 1H, OCH<sub>2</sub>CHCH<sub>2</sub>), 7.12 (d, *J* = 2.3 Hz, 1H, 5-H). <sup>13</sup>C NMR (176 MHz, CDCl<sub>3</sub>): δ 38.9 (CH<sub>3</sub>), 69.7 (OCH<sub>2</sub>CHCH<sub>2</sub>), 90.2 (C-4), 117.4 (OCH<sub>2</sub>CHCH<sub>2</sub>), 131.2 (C-5), 133.4 (OCH<sub>2</sub>CHCH<sub>2</sub>), 163.0 (C-3). MS *m/z* (%): 139 ([M + H]<sup>+</sup>, 100). HRMS (ESI<sup>+</sup>) for C<sub>7</sub>H<sub>10</sub>N<sub>2</sub>NaO ([M + Na]<sup>+</sup>) requires 161.0685, found 161.0685.

#### 3.3. Synthesis of 1-Methyl-3-[(prop-2-en-1-yl)oxy]-1H-pyrazole-4-carbaldehyde (3d)

Phosphorus oxychloride (0.2 mL, 2.5 mmol) was added dropwise to DMF (0.23 mL, 2.5 mmol) at –10 °C temperature. Then, pyrazole **2d** (0.62 mmol) was added to the Vilsmeier–Haack complex, and the reaction mixture was heated at 70 °C temperature for 1 h. After neutralization with 10% NaHCO<sub>3</sub> solution, it was extracted with ethyl acetate (3 × 10 mL). The organic layers were combined, washed with brine, dried over Na<sub>2</sub>SO<sub>4</sub>, filtrated, and the solvent was evaporated. The residue was purified by flash column chromatography (SiO<sub>2</sub>, eluent: ethyl acetate/*n*-hexane, 1:6, *v/v*) to provide the desired compound **3c** as a brown solid, yield 400 mg, 95%, mp 59–60 °C. IR (KBr, ν<sub>max</sub>, cm<sup>-1</sup>): 3122,

3088 (CH<sub>arom</sub>), 2943, 2823 (CH<sub>aliph</sub>), 1673 (C=O), 1568, 1507, 1492, 1429, 1404, 1343, 1202, 1179, 1009 (C=N, C=C, C-N, C-O-C). <sup>1</sup>H NMR (700 MHz, CDCl<sub>3</sub>): δ 3.78 (s, 3H, CH<sub>3</sub>), 4.79 (dt, *J* = 5.6, 1.5 Hz, 2H, OCH<sub>2</sub>), 5.29 (dq, *J* = 10.5, 1.4 Hz, 1H, OCH<sub>2</sub>CHCH<sub>2</sub>), 5.43 (dq, *J* = 17.2, 1.6 Hz, 1H, OCH<sub>2</sub>CHCH<sub>2</sub>), 6.09 (ddt, *J* = 17.2, 10.5, 5.6 Hz, 1H, OCH<sub>2</sub>CHCH<sub>2</sub>), 7.69 (s, 1H, 5-H), 9.75 (s, 1H, CHO). <sup>13</sup>C NMR (176 MHz, CDCl<sub>3</sub>): δ 39.7 (CH<sub>3</sub>), 69.9 (OCH<sub>2</sub>CHCH<sub>2</sub>), 109.5 (C-4), 118.3 (OCH<sub>2</sub>CHCH<sub>2</sub>), 132.6 (C-5), 133.4 (OCH<sub>2</sub>CHCH<sub>2</sub>), 163.1 (C-3), 183.0 (CHO). MS *m/z* (%): 167 ([M + H]<sup>+</sup>, 100). HRMS (ESI<sup>+</sup>) for C<sub>8</sub>H<sub>10</sub>N<sub>2</sub>NaO<sub>2</sub> ([M + Na]<sup>+</sup>) requires 189.0634, found 189.0634

### 3.4. General Procedure for the Oxime Formation Reaction from 1H-Pyrazole-4-carbaldehydes **3a-d**

To a solution of appropriate 3-[(prop-2-en-1-yl)oxy]-1H-pyrazole-4-carbaldehyde **3a-d** (3 mmol) in EtOH (10 mL), sodium acetate (369 mg, 4.5 mmol) and hydroxylamine hydrochloride (250 mg, 3.6 mmol) were added, and the reaction mixture was refluxed for 15 min. After completion of the reaction as monitored by TLC, EtOH was evaporated, and the mixture was diluted with water (10 mL) and extracted with ethyl acetate (3 × 10 mL). The organic layers were combined, washed with brine, dried over Na<sub>2</sub>SO<sub>4</sub>, filtrated, and the solvent was evaporated. The residue was purified by flash column chromatography (SiO<sub>2</sub>, eluent: ethyl acetate/*n*-hexane, 1:6, *v/v*) to provide the desired compounds **4a-c**, as mixtures of *syn-anti* isomers or pure *syn* isomer **4d**. Due to small extent of minor isomer and heavy overlap with signals of the predominant *syn-(Z)* isomer, NMR spectroscopy data of the major isomer only are presented, while the relevant NMR spectroscopy data of the minor isomer are presented in a supplementary file, Table S1.

#### 3.4.1. N-[(Z/E)-{1-Phenyl-3-[(prop-2-en-1-yl)oxy]-1H-pyrazol-4-yl}methylidene] Hydroxylamine (**4a**)

**4a** was obtained as a mixture of *syn-* and *anti-* isomers in ratio *syn-4a:anti-4a* 97:3. Yellow solid, yield 707 mg, 97%, mp 103–104 °C. IR (ν<sub>max</sub>, cm<sup>-1</sup>): 3272 (OH), 3164, 3126, 3067, 3028 (CH<sub>arom</sub>), 2967, 2935 (CH<sub>aliph</sub>), 1641 (C=N), 1557, 1466, 1344, 1220 (C=C, C-N, C-O-C), 647, 754 (CH=CH of benzene). <sup>1</sup>H NMR (700 MHz, DMSO-*d*<sub>6</sub>): δ 4.86 (dt, *J* = 5.4, 1.4 Hz, 2H, OCH<sub>2</sub>), 5.31 (dq, *J* = 10.5, 1.4 Hz, 1H, OCH<sub>2</sub>CHCH<sub>2</sub>), 5.48 (dq, *J* = 17.2, 1.6 Hz, 1H, OCH<sub>2</sub>CHCH<sub>2</sub>), 6.14 (ddt, *J* = 17.2, 10.7, 5.4 Hz, 1H, OCH<sub>2</sub>CHCH<sub>2</sub>), 7.26–7.31 (m, 2H, Ph 4-H, CHNOH), 7.44–7.51 (m, 2H, Ph 3,5-H), 7.77–7.84 (m, 2H, Ph 2,6-H), 8.85 (s, 1H, Pz 5-H), 11.63 (s, 1H, OH). <sup>13</sup>C NMR (176 MHz, DMSO-*d*<sub>6</sub>): 69.3 (OCH<sub>2</sub>), 100.5 (Pz C-4), 117.8 (Ph C-2,6), 118.0 (OCH<sub>2</sub>CHCH<sub>2</sub>), 125.9 (Ph C-4), 129.5 (Ph C-3,5), 131.0 (Pz C-5), 133.1 (OCH<sub>2</sub>CHCH<sub>2</sub>), 134.9 (CH=N-OH), 139.1 (Ph C-1), 161.3 (Pz C-3). <sup>15</sup>N NMR (71 MHz, DMSO-*d*<sub>6</sub>): δ -184.1 (N-1), -123.0 (N-2), -19.2 (CH=N-OH). MS *m/z* (%): 244 ([M + H]<sup>+</sup>, 100). HRMS (ESI<sup>+</sup>) for C<sub>13</sub>H<sub>14</sub>N<sub>3</sub>O<sub>2</sub> ([M + H]<sup>+</sup>) requires 244.1081, found 244.1081.

#### 3.4.2. N-[(Z/E)-{4-Fluorophenyl-3-[(prop-2-en-1-yl)oxy]-1H-pyrazol-4-yl}methylidene] Hydroxylamine (**4b**)

**4b** was obtained as a mixture of *syn-* and *anti-* isomers in ratio *syn-4b:anti-4b* 91:9. Yellow solid, yield 689 mg, 88%, mp 134–136 °C. IR (ν<sub>max</sub>, cm<sup>-1</sup>): 3229 (OH), 3175, 3160, 3097 (CH<sub>arom</sub>), 2924 (CH<sub>aliph</sub>), 1669, 1564, 1502, 1390, 1224, 1209 (C=N, C=C, C-N, C-O-C, C-F), 941 (CH=CH of benzene). <sup>1</sup>H NMR (700 MHz, DMSO-*d*<sub>6</sub>): δ 4.86 (dt, *J* = 5.4, 1.4 Hz, 2H, OCH<sub>2</sub>), 5.31 (dq, *J* = 10.5, 1.3 Hz, 1H, OCH<sub>2</sub>CHCH<sub>2</sub>), 5.46 (dq, *J* = 17.3, 1.6 Hz, 1H, OCH<sub>2</sub>CHCH<sub>2</sub>), 6.14 (ddt, *J* = 17.3, 10.7, 5.4 Hz, 1H, OCH<sub>2</sub>CHCH<sub>2</sub>), 7.28 (s, 1H, CHNOH), 7.30–7.34 (m, 2H, Ph 3,5-H), 7.83–7.86 (m, 2H, Ph 2,6-H), 8.84 (s, 1H, Pz 5-H), 11.64 (s, 1H, OH). <sup>13</sup>C NMR (176 MHz, DMSO-*d*<sub>6</sub>): δ 69.3 (OCH<sub>2</sub>), 100.5 (Pz C-4), 116.17 (d, <sup>2</sup>*J*<sub>C,F</sub> = 22.9 Hz, Ph C-3,5), 118.0 (OCH<sub>2</sub>CHCH<sub>2</sub>), 119.89 (d, <sup>3</sup>*J*<sub>C,F</sub> = 8.3 Hz, Ph C-2,6), 131.2 (Pz C-5), 133.1 (OCH<sub>2</sub>CHCH<sub>2</sub>), 134.9 (CH=N-OH), 135.73 (d, <sup>4</sup>*J*<sub>C,F</sub> = 2.5 Hz, Ph C-1), 160.03 (d, <sup>1</sup>*J*<sub>C,F</sub> = 242.8 Hz, Ph C-4), 161.3 (Pz C-3). <sup>15</sup>N NMR (71 MHz, DMSO-*d*<sub>6</sub>): δ -185.8 (N-1), -122.6 (N-2), -19.2 (CH=N-OH). MS *m/z* (%): 262 ([M + H]<sup>+</sup>, 100). HRMS (ESI<sup>+</sup>) for C<sub>13</sub>H<sub>13</sub>FN<sub>3</sub>O<sub>2</sub> ([M + H]<sup>+</sup>) requires 262.0986, found 262.0986.



### 3.4.3. N-[(Z/E)-[4-Bromophenyl]-3-[(prop-2-en-1-yl)oxy]-1H-pyrazol-4-yl]methylidene] Hydroxylamine (**4c**)

**4c** was obtained as a mixture of *syn*- and *anti*- isomers in ratio *syn-4c:anti-4c* 99:1. Yellowish solid, yield 840 mg, 87%, mp 125.5–127 °C. IR (KBr,  $\nu_{\max}$ ,  $\text{cm}^{-1}$ ): 3173 (OH), 3076, 3033, 3021 ( $\text{CH}_{\text{arom}}$ ), 2848 ( $\text{CH}_{\text{aliph}}$ ), 1656, 1589, 1508, 1508, 1452, 1424, 1404, 1395, 1348, 1220, 1187, 1008 (C=N, C=C, C-N, C-O-C), 995, 955, 934, 890, 819, 803, 716 (C-Br, CH=CH of benzene).  $^1\text{H}$  NMR (700 MHz,  $\text{DMSO}-d_6$ ):  $\delta$  4.85 (dt,  $J = 5.5, 1.5$  Hz, 2H,  $\text{OCH}_2$ ), 5.30 (dq,  $J = 10.5, 1.5$  Hz, 1H,  $\text{OCH}_2\text{CHCH}_2$ ), 5.48 (dq,  $J = 17.3, 1.6$  Hz, 1H,  $\text{OCH}_2\text{CHCH}_2$ ), 6.13 (ddt,  $J = 17.1, 10.7, 5.4$  Hz, 1H,  $\text{OCH}_2\text{CHCH}_2$ ), 7.27 (s, 1H,  $\text{CHNOH}$ ), 7.62–7.67 (m, 2H, Ph 2,6-H), 7.76–7.80 (m, 2H, Ph 3,5-H), 8.88 (s, 1H, Pz 5-H), 11.67 (s, 1H, OH).  $^{13}\text{C}$  NMR (176 MHz,  $\text{DMSO}-d_6$ ):  $\delta$  69.4 ( $\text{OCH}_2$ ), 100.9 (Pz C-4), 118.05 (Ph C-4), 118.09 ( $\text{OCH}_2\text{CHCH}_2$ ), 119.7 (Ph C-2,6), 131.2 (Pz C-5), 132.3 (Ph C-3,5), 133.1 ( $\text{OCH}_2\text{CHCH}_2$ ), 134.7 (CH=N-OH), 138.4 (Ph C-4), 161.4 (Pz C-3).  $^{15}\text{N}$  NMR (71 MHz,  $\text{DMSO}-d_6$ ):  $\delta$  -186.1 (N-1), -123.6 (N-2), -18.2 (CH=N-OH). MS  $m/z$  (%): 322 ( $[\text{M} + \text{H}]^+$ , 100); 324 ( $[\text{M} + \text{H} + 2]^+$ , 100). HRMS ( $\text{ESI}^+$ ) for  $\text{C}_{13}\text{H}_{12}\text{BrN}_3\text{NaO}_2$  ( $[\text{M} + \text{Na}]^+$ ) requires 344.0005, found 344.0008.

### 3.4.4. N-[(E)-[1-Methyl-3-[(prop-2-en-1-yl)oxy]-1H-pyrazol-4-yl]methylidene] Hydroxylamine (**4d**)

Yellow solid, yield 448 mg, 82%, mp 88–89 °C. IR ( $\nu_{\max}$ ,  $\text{cm}^{-1}$ ): 3145 (OH), 3089 ( $\text{CH}_{\text{arom}}$ ), 2992, 2849, 2821 ( $\text{CH}_{\text{aliph}}$ ), 1648, 1559, 1490, 1417, 1342, 1177 (C=N, C=C, C-N, C-O-C).  $^1\text{H}$  NMR (700 MHz,  $\text{DMSO}-d_6$ ):  $\delta$  3.71 (s, 3H,  $\text{CH}_3$ ), 4.68 (dt,  $J = 5.3, 1.4$  Hz, 2H,  $\text{OCH}_2$ ), 5.25 (dq,  $J = 10.5, 1.5$  Hz, 1H,  $\text{OCH}_2\text{CHCH}_2$ ), 5.39 (dq,  $J = 17.3, 1.7$  Hz, 1H,  $\text{OCH}_2\text{CHCH}_2$ ), 6.05 (ddt,  $J = 17.2, 10.6, 5.3$  Hz, 1H,  $\text{OCH}_2\text{CHCH}_2$ ), 7.13 (s, 1H,  $\text{CHNOH}$ ), 8.19 (s, 1H, Pz 5-H), 11.19 (s, 1H, OH).  $^{13}\text{C}$  NMR (176 MHz,  $\text{DMSO}-d_6$ ):  $\delta$  38.6 ( $\text{CH}_3$ ), 69.0 ( $\text{OCH}_2$ ), 97.3 (Pz C-4), 117.5 ( $\text{OCH}_2\text{CHCH}_2$ ), 133.5 ( $\text{OCH}_2\text{CHCH}_2$ ), 135.2 (Pz C-5), 135.6 (CH=N-OH), 160.1 (Pz C-3).  $^{15}\text{N}$  NMR (71 MHz,  $\text{DMSO}-d_6$ ):  $\delta$  -199.0 (N-1), -114.8 (N-2), -25.7 (CH=N-OH). MS  $m/z$  (%): 182 ( $[\text{M} + \text{H}]^+$ , 100). HRMS ( $\text{ESI}^+$ ) for  $\text{C}_8\text{H}_{12}\text{N}_3\text{O}_2$  ( $[\text{M} + \text{H}]^+$ ) requires 182.0924, found 182.0924.  $\text{C}_8\text{H}_{11}\text{N}_3\text{NaO}_2$  ( $[\text{M} + \text{Na}]^+$ ) requires 204.0743, found 204.0743.

## 3.5. General Procedure for the Cycloaddition Reaction of Pyrazole Oximes **4a–d**

Into the solution of appropriate pyrazole (0.4 mmol) **4a–d** in DCM (5 mL), sodium hypochlorite (10% aq. solution, 0.5 mL, 0.8 mmol) was added, and the reaction mixture was stirred for 1 h at room temperature. After completion of the reaction as monitored by TLC, it was diluted with water (10 mL) and extracted with DCM ( $3 \times 10$  mL). The organic layers were combined, washed with brine, dried over  $\text{Na}_2\text{SO}_4$ , filtrated, and the solvent was evaporated. The residue was purified by flash column chromatography ( $\text{SiO}_2$ , eluent: ethyl acetate/*n*-hexane, 1:4, *v/v*) to provide the desired compounds **5a–d**.

### 3.5.1. 7-Phenyl-3a,4-dihydro-3H,7H-pyrazolo[4',3':5,6]pyrano[4,3-c][1,2]oxazole (**5a**)

White solid, yield 66 mg, 68%, mp 179–180 °C. IR ( $\nu_{\max}$ ,  $\text{cm}^{-1}$ ): 3129 ( $\text{CH}_{\text{arom}}$ ), 2953, 2922, 2852 ( $\text{CH}_{\text{aliph}}$ ), 1576, 1503, 1485, 1411, 1360, 1262, 1209, 1051 1177 (C=N, C=C, C-N, C-O-C, N-O), 813, 685 (CH=CH of benzene).  $^1\text{H}$  NMR (700 MHz,  $\text{CDCl}_3$ ):  $\delta$  3.79 (dd,  $J = 13.8, 8.0$  Hz, 1H, 3-H), 3.86–3.91 (m, 1H, 3a-H), 4.17 (dd,  $J = 12.1, 10.6$  Hz, 1H, 4-H), 4.66 (dd,  $J = 9.4, 8.1$  Hz, 1H, 3-H), 4.78 (dd,  $J = 10.5, 5.5$  Hz, 1H, 4-H), 7.29 (t,  $J = 7.4$  Hz, 1H, Ph 4-H), 7.43 (t,  $J = 8.0$  Hz, 2H, Ph 3,5-H), 7.63 (d,  $J = 7.7$  Hz, 2H, Ph 2,6-H), 8.13 (s, 1H, 8-H).  $^{13}\text{C}$  NMR (176 MHz,  $\text{CDCl}_3$ ):  $\delta$  46.7 (C-3a), 69.7 (C-3), 70.9 (C-4), 96.5 (C-8a), 118.9 (Ph C-2,6), 123.6 (C-8), 127.1 (Ph C-4), 129.6 (Ph C-3,5), 139.4 (Ph C-1), 149.4 (C-8b), 162.8 (C-5a).  $^{15}\text{N}$  NMR (71 MHz,  $\text{CDCl}_3$ ):  $\delta$  -177.4 (N-7), -117.7 (N-6), -32.2 (N-1). MS  $m/z$  (%): 242 ( $[\text{M} + \text{H}]^+$ , 100). HRMS ( $\text{ESI}^+$ ) for  $\text{C}_{13}\text{H}_{11}\text{N}_3\text{NaO}_2$  ( $[\text{M} + \text{Na}]^+$ ) requires 264.0743, found 264.0744.

3.5.2. 7-(4-Fluorophenyl)-3a,4-dihydro-3H,7H-pyrazolo[4',3':5,6]pyrano[4,3-c][1,2]oxazole (**5b**)

White solid, yield 65 mg, 63%, mp 214–215 °C. IR ( $\nu_{\max}$ ,  $\text{cm}^{-1}$ ): 3102 ( $\text{CH}_{\text{arom}}$ ), 1644, 1582, 1513, 1489, 1363, 1218 (C=N, C=C, C-N, C-O-C, N-O, C-F), 832, 600 (CH=CH of benzene).  $^1\text{H}$  NMR (700 MHz,  $\text{CDCl}_3$ ):  $\delta$  3.81 (dd,  $J = 13.8, 8.0$  Hz, 1H, 3-H), 3.87–3.93 (m, 1H, 3a-H), 4.18 (dd,  $J = 12.0, 10.7$  Hz, 1H, 4-H), 4.68 (dd,  $J = 10.5, 5.5$  Hz, 1H, 3-H), 4.80 (dd,  $J = 10.5, 5.5$  Hz, 1H, 4-H), 7.13–7.16 (m, 2H, Ph 3,5-H), 7.60–7.62 (m, 2H, Ph 2,6-H), 8.07 (s, 1H, 8-H).  $^{13}\text{C}$  NMR (176 MHz,  $\text{CDCl}_3$ ):  $\delta$  46.7 (C-3a), 69.7 (C-3), 71.0 (C-4), 96.6 (C-8a), 116.6 (d,  $^2J_{\text{C,F}} = 23.3$  Hz, Ph C-3,5), 120.8 (d,  $^3J_{\text{C,F}} = 8.0$  Hz, Ph C-2,6), 123.7 (C-8), 135.8 (d,  $^4J_{\text{C,F}} = 2.4$  Hz, Ph C-1), 149.9 (C-8b), 161.5 (d,  $^1J_{\text{C,F}} = 247.1$  Hz, Ph C-4), 162.9 (C-5a).  $^{15}\text{N}$  NMR (71 MHz,  $\text{CDCl}_3$ ):  $\delta$  -179.2 (N-7), -116.9 (N-6), -31.9 (N-1). MS  $m/z$  (%): 260 ( $[\text{M} + \text{H}]^+$ , 100). HRMS (ESI $^+$ ) for  $\text{C}_{13}\text{H}_{10}\text{FN}_3\text{NaO}_2$  ( $[\text{M} + \text{Na}]^+$ ) requires 282.0649, found 282.0648.

3.5.3. 7-(4-Bromophenyl)-3a,4-dihydro-3H,7H-pyrazolo[4',3':5,6]pyrano[4,3-c][1,2]oxazole (**5c**)

White solid, yield 82 mg, 64%, mp 255–255.5 °C. IR (KBr,  $\nu_{\max}$ ,  $\text{cm}^{-1}$ ): 3129 ( $\text{CH}_{\text{arom}}$ ), 1648, 1590, 1575, 1487, 1452, 1419, 1364, 1263, 1207, 1073, 1051, 1007 (C=N, C=C, C-N, C-O-C), 982, 942, 832, 713, 498 (C-Br, CH=CH of benzene).  $^1\text{H}$  NMR (700 MHz,  $\text{CDCl}_3$ ):  $\delta$  3.81 (dd,  $J = 13.8, 8.0$  Hz, 1H, 3-H), 3.87–3.93 (m, 1H, 3a-H), 4.18 (dd,  $J = 12.1, 10.6$  Hz, 1H, 4-H), 4.68 (dd,  $J = 9.4, 8.1$  Hz, 1H, 3-H), 4.80 (dd,  $J = 10.6, 5.5$  Hz, 1H, 4-H), 7.52–7.54 (m, 2H, Ph 2,6-H), 7.57–7.58 (m, 2H, Ph 3,5-H), 8.12 (s, 1H, 8-H).  $^{13}\text{C}$  NMR (176 MHz,  $\text{CDCl}_3$ ):  $\delta$  46.7 (C-3a), 69.8 (C-3), 71.0 (C-4), 97.0 (C-8a), 120.3 (Ph C-2,6), 120.4 (C-8), 123.5 (C-8), 132.8 (Ph C-3,5), 138.4 (Ph C-1), 149.2 (C-8b), 162.9 (C-5a).  $^{15}\text{N}$  NMR (71 MHz,  $\text{CDCl}_3$ ):  $\delta$  -179.5 (N-7), -117.6 (N-6), -30.9 (N-1). MS  $m/z$  (%): 320 ( $[\text{M}]^+$ , 100); 322 ( $[\text{M} + 2]^+$ , 100). HRMS (ESI $^+$ ) for  $\text{C}_{13}\text{H}_{10}\text{BrN}_3\text{NaO}_2$  ( $[\text{M} + \text{Na}]^+$ ) requires 341.9849, found 341.9848.

3.5.4. 7-Methyl-3a,4-dihydro-3H,7H-pyrazolo[4',3':5,6]pyrano[4,3-c][1,2]oxazole (**5d**)

White solid, yield 30 mg, 42%, mp 159–160 °C. IR ( $\nu_{\max}$ ,  $\text{cm}^{-1}$ ): 3144, 3110 ( $\text{CH}_{\text{arom}}$ ), 2996, 2946, 2867 ( $\text{CH}_{\text{aliph}}$ ), 1645, 1570, 1490, 1457, 1363, 1246, 1169, 1079, 1016 (C=N, C=C, C-N, C-O-C, N-O).  $^1\text{H}$  NMR (700 MHz,  $\text{CDCl}_3$ ):  $\delta$  3.67 (dd,  $J = 13.8, 8.1$  Hz, 1H, 3-H), 3.75 (s, 3H,  $\text{CH}_3$ ), 3.76–3.80 (m, 1H, 3a-H), 4.03 (dd,  $J = 12.1, 10.6$  Hz, 1H, 4-H), 4.55 (dd,  $J = 9.4, 8.1$  Hz, 1H, 3-H), 4.65 (dd,  $J = 10.5, 5.4$  Hz, 1H, 4-H), 7.49 (s, 1H, 8-H).  $^{13}\text{C}$  NMR (176 MHz,  $\text{CDCl}_3$ ):  $\delta$  39.7 ( $\text{CH}_3$ ), 47.0 (C-3a), 69.5 (C-3), 70.8 (C-4), 93.8 (C-8a), 127.4 (C-8), 149.8 (C-8b), 162.0 (C-5a).  $^{15}\text{N}$  NMR (71 MHz,  $\text{CDCl}_3$ ):  $\delta$  -194.4 (N-7), -112.3 (N-6), -35.8 (N-1). MS  $m/z$  (%): 180 ( $[\text{M} + \text{H}]^+$ , 100). HRMS (ESI $^+$ ) for  $\text{C}_8\text{H}_9\text{N}_3\text{NaO}_2$  ( $[\text{M} + \text{Na}]^+$ ) requires 202.0587, found 202.0586.

3.6. Oxidation of 7-Phenyl-3,3a,4,7-tetrahydropyrazolo[4',3':5,6]pyrano[4,3-c]oxazole (**5a**) with  $\text{MnO}_2$  to 7-Phenyl-4,7-dihydropyrazolo[4',3':5,6]pyrano[4,3-c]oxazole (**6**)

To a flask adapted with a Dean–Stark collector, 7-phenyl-3,3a,4,7-tetrahydropyrazolo[4',3':5,6]pyrano[4,3-c]oxazole (116 mg, 0.48 mmol), toluene (5 mL) and  $\text{MnO}_2$  (754 mg, 6 mmol) were added. The mixture was heated under reflux for 4 h, cooled to room temperature, filtered over celite, and concentrated under reduced pressure. The residue was purified by flash column chromatography ( $\text{SiO}_2$ , eluent: dichloromethane/methanol, 100:1,  $v/v$ ) to provide the desired compound as a colorless crystal, yield 43 mg, 38%, mp 205–208 °C. IR (KBr,  $\nu_{\max}$ ,  $\text{cm}^{-1}$ ): 3100 ( $\text{CH}_{\text{arom}}$ ), 1642, 1594, 1521, 1468, 1396, 1252, 1040 (C=N, C=C, C-N, C-O-C, N-O), 944, 801, 769, 684 (CH=CH of benzene).  $^1\text{H}$  NMR (700 MHz,  $\text{CDCl}_3$ ):  $\delta$  5.41 (d,  $J = 1.3$  Hz, 2H,  $\text{CH}_2$ ), 7.29–7.32 (m, 1H, Ph 4-H), 7.44–7.48 (m, 2H, Ph 3,5-H), 7.66–7.69 (m, 2H, Ph 2,6-H), 8.20 (s, 1H, 8-H), 8.21 (t,  $J = 1.3$  Hz, 1H, 3-H).  $^{13}\text{C}$  NMR (176 MHz,  $\text{CDCl}_3$ ):  $\delta$  63.3 ( $\text{CH}_2$ ), 96.5 (C-8a), 109.8 (C-3a), 118.6 (Ph C-2,6), 122.6 (C-8), 126.8 (Ph C-4), 129.6 (Ph C-3,5), 139.4 (Ph C-1), 150.7 (C-3), 151.0 (C-8b), 162.4 (C-5a).  $^{15}\text{N}$  NMR (71 MHz,  $\text{CDCl}_3$ ):  $\delta$  -179.6 (N-7), -116.3 (N-6), -20.4 (N-1). MS  $m/z$  (%): 240 ( $[\text{M} + \text{H}]^+$ , 100). HRMS (ESI $^+$ ) for  $\text{C}_{13}\text{H}_9\text{N}_3\text{NaO}_2$  ( $[\text{M} + \text{Na}]^+$ ) requires 262.0587, found 262.0589.

### 3.7. Synthesis of 1-Phenyl-3-[(2Z)-3-phenylprop-2-en-1-yl]oxy-1H-pyrazole-4-carbaldehyde (8)

A solution of 3-hydroxy-1-phenyl-1H-pyrazole-4-carbaldehyde **7** (188 mg, 1 mmol) in dry DMF (2 mL) was cooled to 0 °C under an inert atmosphere, and NaH (60% dispersion in mineral oil, 40 mg, 1 mmol) was added portion-wise. After stirring the reaction mixture for 15 min, cinnamyl chloride (185 mg, 1.2 mmol) was added dropwise. The mixture was stirred at 70 °C for 15 min, then poured into water and extracted with ethyl acetate (3 × 10 mL). The organic layers were combined, washed with brine, dried over Na<sub>2</sub>SO<sub>4</sub>, filtrated, and the solvent was evaporated. The residue was purified by flash column chromatography (SiO<sub>2</sub>, eluent: ethyl acetate/*n*-hexane, 1:4, *v/v*) to provide the desired compound as a brown solid, yield 250 mg, 82%, mp 118–119 °C. IR ( $\nu_{\max}$ , cm<sup>-1</sup>): 3096 (CH<sub>arom</sub>), 2821 (CH<sub>aliph</sub>), 1666 (C=O), 1555, 1499, 1357 (C=C, C–N, C–O–C), 964, 753, 686 (CH=CH of benzenes). <sup>1</sup>H NMR (700 MHz, CDCl<sub>3</sub>):  $\delta$  5.00 (d, *J* = 6.3 Hz, 2H, OCH<sub>2</sub>CH=CH), 6.44 (dt, *J* = 15.9, 6.3 Hz, 1H, OCH<sub>2</sub>CH=CH), 6.72 (d, *J* = 15.9 Hz, 1H, OCH<sub>2</sub>CH=CH), 7.19 (t, *J* = 7.3 Hz, 1H, CPh 4-H), 7.23–7.27 (m, 3H, CPh 3,5-H and NPh 4-H), 7.36 (d, *J* = 7.6 Hz, 2H, CPh 2,6-H), 7.39 (t, *J* = 7.9 Hz, 2H, NPh 3,5-H), 7.58 (d, *J* = 8.0 Hz, 2H, NPh 2,6-H), 8.18 (s, 1H, 5-H), 9.82 (s, 1H, CHO). <sup>13</sup>C NMR (176 MHz, CDCl<sub>3</sub>):  $\delta$  70.1 (OCH<sub>2</sub>CH=CH), 111.6 (C-4), 118.9 (NPh C-2,6), 123.6 (OCH<sub>2</sub>CH=CH), 126.8 (CPh C-2,6), 127.4 (NPh C-4), 128.2 (CPh C-4), 128.7 (CPh C-3,5), 129.58 (C-5), 129.64 (NPh C-3,5), 134.6 (OCH<sub>2</sub>CH=CH), 136.4 (CPh C-1), 139.1 (NPh C-1), 163.5 (C-3), 183.5 (CHO). MS *m/z* (%): 305 ([M + H]<sup>+</sup>, 100). HRMS (ESI<sup>+</sup>) for C<sub>19</sub>H<sub>16</sub>N<sub>2</sub>NaO<sub>2</sub> ([M + Na]<sup>+</sup>) requires 327.1104, found 327.1104.

### 3.8. Synthesis of N-[(Z/E)-{1-Phenyl-3-[(2Z)-3-phenylprop-2-en-1-yl]oxy}-1H-pyrazol-4-yl]methylidene]hydroxylamine (9)

This compound was synthesized in analogy to **4a–d**, except that pyrazole **8** was used as the adduct. Yellow solid, yield 823 mg, 86%, mp 129–130 °C. IR ( $\nu_{\max}$ , cm<sup>-1</sup>): 3161 (OH), 3022 (CH<sub>arom</sub>), 2922 (CH<sub>aliph</sub>), 1638, 1560, 1493, 1215 (C=N, C=C, C–N, C–O–C), 965, 745, 683 (CH=CH of benzene). <sup>1</sup>H NMR (700 MHz, DMSO-*d*<sub>6</sub>):  $\delta$  5.03 (d, *J* = 5.4 Hz, 2H, OCH<sub>2</sub>), 6.60 (dt, *J* = 16.0, 6.1 Hz, 1H, OCH<sub>2</sub>CH=CH), 6.86 (d, *J* = 16.0 Hz, 1H, OCH<sub>2</sub>CH=CH), 7.26–7.30 (m, 2H, NPh 4-H, CPh 4-H), 7.32 (s, 1H, CHNOH), 7.36 (t, *J* = 7.6 Hz, 2H, CPh 3,5-H), 7.49 (t, *J* = 8.0 Hz, 2H, NPh 3,5-H), 7.52 (d, *J* = 7.4 Hz, 2H, CPh 2,6-H), 7.83 (d, *J* = 7.8 Hz, 2H, NPh 2,6-H), 8.86 (s, 1H, Pz 5-H), 11.63 (s, 1H, OH). <sup>13</sup>C NMR (176 MHz, DMSO-*d*<sub>6</sub>):  $\delta$  69.3 (OCH<sub>2</sub>), 100.6 (Pz C-4), 117.8 (NPh C-2,6), 124.2 (OCH<sub>2</sub>CH=CH), 125.9 (NPh C-4), 126.6 (CPh C-2,6), 128.0 (CPh C-4), 128.7 (CPh C-3,5), 129.5 (NPh C-3,5), 131.0 (Pz C-5), 133.2 (OCH<sub>2</sub>CH=CH), 135.0 (CH=N–OH), 136.1 (CPh C-1), 139.1 (NPh C-1), 161.3 (Pz C-3). <sup>15</sup>N NMR (71 MHz, DMSO-*d*<sub>6</sub>):  $\delta$  –184.0 (N-1), –122.7 (N-2), –19.2 (CH=N–OH). MS *m/z* (%): 320 ([M + H]<sup>+</sup>, 100). HRMS (ESI<sup>+</sup>) for C<sub>19</sub>H<sub>17</sub>N<sub>3</sub>NaO<sub>2</sub> ([M + Na]<sup>+</sup>) requires 342.1213, found 342.1213.

### 3.9. Synthesis of 3,7-Diphenyl-3a,4-dihydro-3H,7H-pyrazolo[4',3':5,6]pyrano[4,3-c][1,2]oxazole (trans-10)

This compound was synthesized in analogy to **5a–d**, except that pyrazole **9** was used as the adduct. White solid, yield 79 mg, 62%, mp 195–196 °C. IR ( $\nu_{\max}$ , cm<sup>-1</sup>): 2921 (CH<sub>aliph</sub>), 1646, 1578, 1490, 1368 (C=N, C=C, C–N, C–O–C), 978, 832, 686 (CH=CH of benzene). <sup>1</sup>H NMR (700 MHz, CDCl<sub>3</sub>):  $\delta$  3.87 (ddd, *J* = 13.1, 12.2, 5.6 Hz, 1H, 3a-H), 4.34 (dd, *J* = 12.2, 10.6 Hz, 1H, 4-H), 4.74 (dd, *J* = 10.5, 5.6 Hz, 1H, 4-H), 5.16 (d, *J* = 13.1 Hz, 1H, 3-H), 7.31 (t, *J* = 7.4 Hz, 1H, NPh 4-H), 7.39–7.41 (m, 1H, CPh 4-H), 7.42–7.44 (m, 2H, CPh 3,5-H), 7.44–7.48 (m, 4H, CPh 2,6-H and NPh 3,5-H), 7.65–7.67 (m, 2H, NPh 2,6-H), 8.13 (s, 1H, 8-H). <sup>13</sup>C NMR (176 MHz, CDCl<sub>3</sub>):  $\delta$  53.4 (C-3a), 70.7 (C-4), 85.0 (C-3), 96.7 (C-8a), 118.9 (NPh C-2,6), 123.6 (C-8), 126.9 (CPh C-2,6), 127.2 (NPh C-4), 129.1 (CPh C-3,5), 129.2 (CPh C-4), 129.7 (NPh C-3,5), 136.7 (CPh C-1), 139.4 (NPh C-1), 150.3 (C-8b), 162.9 (C-5a). <sup>15</sup>N NMR (71 MHz, CDCl<sub>3</sub>):  $\delta$  –177.1 (N-7), –117.4 (N-6), –31.0 (N-1). MS *m/z* (%): 318 ([M + H]<sup>+</sup>, 100). HRMS (ESI<sup>+</sup>) for C<sub>19</sub>H<sub>15</sub>N<sub>3</sub>NaO<sub>2</sub> ([M + Na]<sup>+</sup>) requires 340.1056, found 340.1057.

### 3.10. Synthesis of 4,7-Dihydropyrazolo[4',3':5,6]pyrano[4,3-c]oxazole (6)

To a mixture of 1-phenyl-3-(prop-2-yn-1-yloxy)-1H-pyrazole-4-carbaldehyde **11** [26] (226 mg, 1 mmol) in EtOH (2 mL), sodium acetate (123 mg, 1.5 mmol) and hydroxylamine hydrochloride (104 mg, 1.5 mmol) were added portion-wise. The reaction mixture was refluxed for 15 min. After completion of the reaction as monitored by TLC, EtOH was evaporated, and the mixture was diluted with water (10 mL) and extracted with ethyl acetate (3 × 10 mL). The organic layers were combined, washed with brine, dried over Na<sub>2</sub>SO<sub>4</sub>, filtrated, and the solvent was evaporated. Obtained oxime **12** was used in the next step without further purification. To a mixture of 1-phenyl-3-(prop-2-yn-1-yloxy)-1H-pyrazole-4-carbaldehyde oxime (**12**) (approximately 1 mmol) in DCM (2 mL), 5.25% aq. NaOCl solution (2.35 mL, 2 mmol) was added dropwise. After stirring at room temperature for 1 h, the reaction mixture was then poured into water and extracted with ethyl acetate (3 × 10 mL). The organic layers were combined, washed with brine, dried over Na<sub>2</sub>SO<sub>4</sub>, filtrated, and the solvent was evaporated. The residue was purified by flash column chromatography (SiO<sub>2</sub>, eluent: ethyl acetate/*n*-hexane, 1:4, *v/v*) to provide the desired compound **6**. Yield 189 mg, 79%. The NMR, IR, MS, HRMS and mp data of compound **6** are given in Section 3.6.

### 3.11. General Sonogashira Reaction Procedure for the Synthesis of **13b,c**

To a mixture of 1-phenyl-3-(prop-2-yn-1-yloxy)-1H-pyrazole-4-carbaldehyde **11** [26] (226 mg, 1 mmol) in absolute DMF (2 mL), triethylamine (0.21 mL, 1.5 mmol), appropriate (het)aryl halide (1.1 mmol), CuI (190 mg, 0.1 mmol) and Pd(PPh<sub>3</sub>)Cl<sub>2</sub> (35 mg, 0.05 mmol) were added. The reaction mixture was stirred under an Ar atmosphere at 60 °C for 15 min. After cooling to room temperature, the reaction mixture was quenched by the addition of water (10 mL) and extracted with EtOAc (3 × 20 mL). The combined organic layers were dried over anhydrous sodium sulfate, filtered and concentrated under reduced pressure. The residue was purified by flash column chromatography (SiO<sub>2</sub>, eluent: ethyl acetate/*n*-hexane, 1:4, *v/v*) to provide the desired compounds **13b,c**.

#### 3.11.1. 3-[[3-(Naphthalen-1-yl)prop-2-yn-1-yl]oxy]-1-phenyl-1H-pyrazole-4-carbaldehyde (**13b**)

Compound **13b** was obtained from **11** according to the general Sonogashira reaction procedure using 1-iodonaphthalene (279 mg, 1.1 mmol). Colorless solid, yield 225 mg, 64%, mp 142–145 °C. IR (KBr,  $\nu_{\max}$ , cm<sup>-1</sup>): 3127, 3096 (CH<sub>arom</sub>), 2917, 2826 (CH<sub>alif</sub>), 2250 (C≡C), 1671 (CHO), 1598, 1508, 1496, 1343, 1231 (C=C, C–N, C–O–C), 986, 770, 687 (CH=CH of benzenes). <sup>1</sup>H NMR (700 MHz, CDCl<sub>3</sub>):  $\delta$  5.42 (s, 2H, CH<sub>2</sub>), 7.34–7.36 (m, 1H, Ar-H), 7.38–7.43 (m, 2H, Ar-H), 7.47–7.49 (m, 3H, NPh 3,5-H, Ar-H), 7.71–7.72 (m, 3H, NPh 2,6-H, Ar-H), 7.82–7.84 (m, 2H, Ar-H), 8.30 (s, 1H, 5-H), 8.34–8.35 (m, 1H, Ar-H), 9.93 (s, 1H, CHO). <sup>13</sup>C BMR (176 MHz, CDCl<sub>3</sub>):  $\delta$  58.1 (CH<sub>2</sub>), 85.5 (C≡CNph), 88.3 (C≡CNph), 111.8 (C-4), 118.9 (NPh C-2,6), 119.9, 125.2, 126.2, 126.6, 127.0, 127.5 (NPh C-4), 128.4, 129.4, 129.8 (NPh C-3,5), 129.8 (C-5), 131.0, 133.2, 133.6, 139.1 (NPh C-1), 162.7 (C-3), 183.3 (CHO). <sup>15</sup>N NMR (71 MHz, CDCl<sub>3</sub>):  $\delta$  -178.6 (N-1), -116.1 (N-2). MS *m/z* (%): 353 ([M + H]<sup>+</sup>, 100). HRMS (ESI<sup>+</sup>) for C<sub>23</sub>H<sub>16</sub>N<sub>2</sub>NaO<sub>2</sub> ([M + Na]<sup>+</sup>) requires 375.1104, found 375.1103.

#### 3.11.2. 1-Phenyl-3-[[3-(pyridin-2-yl)prop-2-yn-1-yl]oxy]-1H-pyrazole-4-carbaldehyde (**13c**)

Compound **13c** was obtained from **11** according to the general Sonogashira reaction procedure using 2-bromopyridine (174 mg, 1.1 mmol). Colorless solid, yield 212 mg, 70%, mp 110–113 °C. IR (KBr,  $\nu_{\max}$ , cm<sup>-1</sup>): 3100 (CH<sub>arom</sub>), 2917, 2850 (CH<sub>aliph</sub>), 2300 (C≡C), 1674 (CHO), 1561, 1501, 1466, 1357, 1209, 1020 (C=C, C–N), 757, 688 (CH=CH of benzene). <sup>1</sup>H NMR (700 MHz, CDCl<sub>3</sub>):  $\delta$  5.28 (s, 2H, CH<sub>2</sub>), 7.23–7.25 (m, 1H, Py 3-H), 7.30–7.32 (m, 1H, Ph 4-H), 7.44–7.47 (m, 3H, Ph 3,5-H, Py 5-H), 7.63–7.65 (m, 3H, Ph 2,6-H, Py 4-H), 8.27 (s, 1H, 5-H), 8.58 (s, 1H, Py 6-H), 9.88 (s, 1H, CHO). <sup>13</sup>C NMR (176 MHz, CDCl<sub>3</sub>):  $\delta$  57.5 (CH<sub>2</sub>), 83.4 (C≡CPy), 86.4 (C≡CPy), 111.5 (C-4), 118.9 (Ph C-2,6), 123.5 (Py C-5), 127.5 (Ph C-4, Py C-3), 129.7 (Ph C-3,5), 129.8 (C-5), 136.3 (Py C-4), 138.9 (Ph C-1), 142.5 (Py C-2), 150.1 (Py C-6), 162.6 (C-3), 183.3 (CHO). <sup>15</sup>N NMR (71 MHz, CDCl<sub>3</sub>):  $\delta$  -179.3 (N-1), -118.5

(N-2), pyridinyl N was not found. MS  $m/z$  (%): 304 ( $[M + H]^+$ , 100). HRMS (ESI<sup>+</sup>) for C<sub>18</sub>H<sub>13</sub>N<sub>3</sub>NaO<sub>2</sub> ( $[M + Na]^+$ ) requires 326.0900, found 326.0901.

### 3.12. General Procedure for the Synthesis of 1-Phenyl-3-(prop-2-yn-1-yloxy)-1H-pyrazole-4-carbaldehyde oximes **14a–c**

To a mixture of appropriate 1-phenyl-3-(prop-2-yn-1-yloxy)-1H-pyrazole-4-carbaldehyde **13a–c** (1 mmol) in EtOH (2 mL), sodium acetate (123 mg, 1.5 mmol) and hydroxylamine hydrochloride (104 mg, 1.5 mmol) were added portion-wise. The reaction mixture was refluxed for 15 min. After completion of the reaction as monitored by TLC, EtOH was evaporated, and the mixture was diluted with water (10 mL) and extracted with ethyl acetate (3 × 10 mL). The organic layers were combined, washed with brine, dried over Na<sub>2</sub>SO<sub>4</sub>, filtrated, and the solvent was evaporated. Obtained oximes **14a–c** were used in the next step without further purification.

Data for Selected Oxime. N-[(Z)-{1-Phenyl-3-[(3-phenylprop-2-yn-1-yl)oxy]-1H-pyrazol-4-yl)methylidene]hydroxylamine (**14a**)

White solid, yield 245 mg, 77%, mp 172–174.5 °C. IR (KBr,  $\nu_{\max}$ , cm<sup>-1</sup>): 3166 (OH), 3130, 3065, 3021 (CH<sub>arom</sub>), 2999, 2813 (CH<sub>aliph</sub>), 2237 (C≡C), 1642, 1600, 1565, 1504, 1489, 1401, 1352, 1218, 1174, 1056, 1009 (C=N, C=C, C–N, C–O–C), 996, 966, 931, 903, 874, 711, 682 (CH=CH of benzenes). <sup>1</sup>H NMR (700 MHz, DMSO-*d*<sub>6</sub>):  $\delta$  5.29 (s, 2H, CH<sub>2</sub>), 7.27 (s, 1H, CHN<sub>2</sub>OH), 7.28–7.30 (m, 1H, NPh 4-H), 7.38–7.42 (m, 3H, CPh 3-5-H), 7.47–7.50 (m, 4H, NPh 3,5-H, CPh 2,6-H), 7.82–7.83 (m, 2H, NPh 2,6-H), 8.87 (Pz 5-H), 11.65 (OH). <sup>13</sup>C NMR (176 MHz, DMSO-*d*<sub>6</sub>):  $\delta$  57.3 (CH<sub>2</sub>), 84.7 (C≡CPh), 86.3 (C≡CPh), 100.6 (Pz C-4), 118.0 (NPh C-2,6), 121.5 (CPh C-1), 126.1 (NPh C-4), 128.8 (CPh C-3,5), 129.2 (CPh C-4), 129.6 (NPh C-3,5), 131.3 (Pz C-5), 131.6 (CPh C-2,6), 134.7 (CH=N–OH), 139.1 (NPh C-1), 160.6 (Pz C-3). <sup>15</sup>N NMR (71 MHz, DMSO-*d*<sub>6</sub>):  $\delta$  –184.4 (N-1), –122.6 (N-2), –18.4 (CH=N–OH). MS  $m/z$  (%): 318 ( $[M + H]^+$ , 100). HRMS (ESI<sup>+</sup>) for C<sub>19</sub>H<sub>16</sub>N<sub>3</sub>O<sub>2</sub> ( $[M + H]^+$ ) requires 318.1237, found 318.1238.

### 3.13. General Procedure for the Synthesis of 4H,7H-Pyrazolo[4',3':5,6]pyrano[4,3-c]oxazoles **15a–c**

To a mixture of appropriate 1-phenyl-3-(prop-2-yn-1-yloxy)-1H-pyrazole-4-carbaldehyde oxime **14a–c** (approximately 1 mmol) in DCM (2 mL), 5.25% aq. NaOCl solution (2.35 mL, 2 mmol) was added dropwise. After stirring at room temperature for 1 h, the reaction mixture was quenched by the addition of water (20 mL) and extracted with DCM (3 × 20 mL). The combined organic layers were dried over anhydrous sodium sulfate, filtered and concentrated under reduced pressure. The residue was purified by flash column chromatography (SiO<sub>2</sub>, eluent: ethyl acetate/*n*-hexane, 1:4, *v/v*) to provide the desired compounds **15a–c**.

#### 3.13.1. 3,7-Diphenyl-4H,7H-pyrazolo[4',3':5,6]pyrano[4,3-c]oxazole (**15a**)

White solid, yield 239 mg, 76%, mp 209–212 °C. IR (KBr,  $\nu_{\max}$ , cm<sup>-1</sup>): 3050 (CH<sub>arom</sub>), 1640, 1602, 1526, 1453, 1405, 1375, 1340, 1048 (C=N, C=C, C–N, C–O–C), 956, 750, 725, 682 (CH=CH of benzenes). <sup>1</sup>H NMR (700 MHz, TFA-*d*):  $\delta$  6.03 (s, 2H, CH<sub>2</sub>), 7.57–7.65 (m, 10H, Ph-H), 8.63 (s, 1H, 8-H). <sup>13</sup>C NMR (700 MHz, TFA-*d*):  $\delta$  69.7 (CH<sub>2</sub>), 95.6 (C-3a), 102.6 (C-8a), 122.1 (NPh C-2,6), 124.7 (C-8), 126.3, 129.2, 130.4, 130.8, 131.4, 131.9, 134.3, 148.1, 158.4 (C-3), 166.9 (C-5a). MS  $m/z$  (%): 316 ( $[M + H]^+$ , 100). HRMS (ESI<sup>+</sup>) for C<sub>19</sub>H<sub>13</sub>N<sub>3</sub>NaO<sub>2</sub> ( $[M + Na]^+$ ) requires 338.0900, found 338.0902.

#### 3.13.2. 3-(Naphthalen-1-yl)-7-phenyl-4H,7H-pyrazolo[4',3':5,6]pyrano[4,3-c]oxazole (**15b**)

White solid, yield 281 mg, 77%, mp 202–205 °C. IR (KBr,  $\nu_{\max}$ , cm<sup>-1</sup>): 3057 (CH<sub>arom</sub>), 1646, 1598, 1530, 1472, 1395, 1256, 1047 (C=N, C=C, C–N, C–O–C), 947, 802, 772, 684 (CH=CH of benzenes). <sup>1</sup>H NMR (700 MHz, CDCl<sub>3</sub>):  $\delta$  5.32 (s, 2H, CH<sub>2</sub>), 7.23–7.25 (m, 1H, Ph 4-H), 7.40–7.42 (m, 2H, Ph 3,5-H), 7.50–7.56 (m, 4H, Nph 2,3,6,7-H), 7.63–7.64 (m, 2H,

Ph 2,6-H), 7.88–7.89 (m, 1H, Nph 5-H), 7.94–7.96 (m, 1H, Nph 4-H), 8.00–8.01 (m, 1H, Nph 8-H), 8.20 (s, 1H, 8-H).  $^{13}\text{C}$  NMR (176 MHz,  $\text{CDCl}_3$ ):  $\delta$  64.4 ( $\text{CH}_2$ ), 97.1 (C-8a), 107.7 (C-3a), 118.6 (Ph C-2,6), 122.6 (C-8), 124.3 (Nph C-1), 124.9 (Nph C-8), 125.1 (Nph C-3), 126.7 (Ph C-4), 126.8 (Nph C-6), 127.6 (Nph C-7), 127.9 (Nph C-2), 128.7 (Nph C-5), 129.6 (Ph C-3,5), 130.6 (Nph C-8a), 131.2 (Nph C-4), 133.8 (Nph C-4a), 139.5 (Ph C-1), 152.2 (C-8b), 162.5 (C-5a), 162.6 (C-3).  $^{15}\text{N}$  NMR (71 MHz,  $\text{CDCl}_3$ ):  $\delta$  -179.6 (N-7), -116.4 (N-6), -23.9 (N-1). MS  $m/z$  (%): 366 ( $[\text{M} + \text{H}]^+$ , 100). HRMS (ESI $^+$ ) for  $\text{C}_{23}\text{H}_{15}\text{N}_3\text{NaO}_2$  ( $[\text{M} + \text{Na}]^+$ ) requires 388.1056, found 388.1054.

### 3.13.3. 7-Phenyl-3-(pyridin-2-yl)-4H,7H-pyrazolo[4',3':5,6]pyrano[4,3-c]oxazole (15c)

White solid, yield 234 mg, 74%, mp 241–244 °C. IR (KBr,  $\nu_{\text{max}}$ ,  $\text{cm}^{-1}$ ): 3100 ( $\text{CH}_{\text{arom}}$ ), 1638, 1600, 1529, 1466, 1410, 1380, 1344, 1052 (C=N, C=C, C-N, C-O-C), 958, 753, 729, 685 ( $\text{CH}=\text{CH}$  of benzene).  $^1\text{H}$  NMR (700 MHz,  $\text{CDCl}_3$ ):  $\delta$  5.84 (s, 2H,  $\text{CH}_2$ ), 7.29–7.31 (m, 1H, Ph 4-H), 7.32–7.35 (m, 1H, Py 5-H), 7.45–7.48 (m, 2H, Ph 3,5-H), 7.69–7.70 (m, 2H, Ph 2,6-H), 7.85 (t,  $J = 7.7$  Hz, 1H, Py 4-H), 7.95 (d,  $J = 7.8$  Hz, 1H, Py 3-H), 8.22 (s, 1H, 8-H), 8.70 (d,  $J = 4.5$  Hz, 1H, Py 6-H).  $^{13}\text{C}$  NMR (176 MHz,  $\text{CDCl}_3$ ):  $\delta$  65.6 ( $\text{CH}_2$ ), 96.5 (C-8a), 108.8 (C-3a), 118.7 (Ph C-2,6), 121.3 (Py C-3), 122.6 (C-8), 124.2 (Py C-5), 126.8 (Ph C-4), 129.8 (Ph C-3,5), 137.1 (Py C-4), 139.7 (Ph C-1), 147.2 (Py C-2), 150.2 (Py C-6), 152.7 (C-8b), 160.6 (C-3), 162.7 (C-5a).  $^{15}\text{N}$  NMR (71 MHz,  $\text{CDCl}_3$ ):  $\delta$  -180.1 (N-7), -117.4 (N-6), -72.8 (pyridine N), -25.0 (N-1). MS  $m/z$  (%): 317 ( $[\text{M} + \text{H}]^+$ , 100). HRMS (ESI $^+$ ) for  $\text{C}_{18}\text{H}_{12}\text{N}_4\text{NaO}_2$  ( $[\text{M} + \text{Na}]^+$ ) requires 339.0852, found 339.0855.

## 4. Conclusions

In conclusion, we have developed a convenient method for the preparation of 3a,4-dihydro-3*H*,7*H*- and 4*H*,7*H*-pyrazolo[4',3':5,6]pyrano[4,3-c][1,2]oxazoles from easily obtainable 3-(prop-2-en-1-yloxy)- or 3-(prop-2-yn-1-yloxy)-1*H*-pyrazole-4-carbaldehydes by INOC reaction of intermediate oximes. The key stage—nitrile oxide preparation from the corresponding aldoximes—was carried out by oxidation with sodium hypochlorite. The method was applied for the synthesis of pyrazolo[4',3':5,6]pyrano[4,3-c][1,2]oxazoles with various substituents in the third or seventh position. In addition, extensive NMR spectroscopic studies have been undertaken using standard and advanced methods to unambiguously determine the configuration of intermediate aldoximes, showing the predominance of the *syn*-isomer, as well as the structure of new polycyclic systems.

**Supplementary Materials:** The following are available online. Table S1: Relevant NMR data of aldoximes **4a–d**, **9** and **14**, Figures S2 and S3: 1D Selective gradient NOESY spectra (**4b**), Figure S4: Heteronuclear 2D  $J$ -resolved NMR spectrum (**4b**), Figures S5–S79:  $^1\text{H}$ ,  $^{13}\text{C}$  NMR and HRMS (ESI-TOF) spectra of compounds **2d**, **3d**, **4a–d**, **5a–d**, **6**, **8–10**, **13b,c**, **14a**, **15a–c** and  $^1\text{H}$ - $^{15}\text{N}$  HMBC spectra of compounds **4a–d**, **5a–d**, **6**, **9**, **10**, **14a**, **15b,c**. Figures S80 and S81: B3LYP/def2-TZVP optimized structures of *trans*-**10** and *cis*-**10**.

**Author Contributions:** Conceptualization, A.Š.; methodology, E.A.; validation, V.M., R.B. and E.P.; formal analysis, A.B. and G.R.; investigation, E.P., V.M. and R.B.; data curation, V.M.; writing—original draft preparation, A.Š., A.B., E.A. and V.M.; writing—review and editing, S.K.; visualization A.B., A.Š. and E.A.; resources, E.A. and A.Š.; supervision, A.Š. and E.A. All authors have read and agreed to the published version of the manuscript.

**Funding:** This research was funded by the Research Council of Lithuania (No. S-MIP-20-60).

**Institutional Review Board Statement:** Not applicable.

**Informed Consent Statement:** Not applicable.

**Data Availability Statement:** The data presented in this study are available on request from the corresponding authors.

**Conflicts of Interest:** The authors declare no conflict of interest.

**Sample Availability:** Samples of the compounds are not available from the authors.

## References

1. Browder, C.C. Recent Advances in Intramolecular Nitrile Oxide Cycloadditions in the Synthesis of 2-Isoxazolines. *Curr. Org. Synth.* **2011**, *8*, 628–644. [CrossRef]
2. Plumet, J. 1,3-Dipolar Cycloaddition Reactions of Nitrile Oxides under “Non-Conventional” Conditions: Green Solvents, Irradiation, and Continuous Flow. *ChemPlusChem* **2020**, *85*, 2252–2271. [CrossRef]
3. Roscales, S.; Plumet, J. Mini-Review: Organic Catalysts in the 1,3-Dipolar Cycloaddition Reactions of Nitrile Oxides. *Heterocycles* **2019**, *99*, 725–744. [CrossRef]
4. Huisgen, R. Cycloadditions—Definition, Classification, and Characterization. *Angew. Chem. Int. Ed. Engl.* **1968**, *7*, 321–328. [CrossRef]
5. Padwa, A. Intramolecular 1,3-Dipolar Cycloaddition Reactions. *Angew. Chem. Int. Ed. Engl.* **1976**, *15*, 123–136. [CrossRef]
6. Maugein, N.; Wagner, A.; Mioskowski, C. New conditions for the generation of nitrile oxides from primary nitroalkanes. *Tetrahedron Lett.* **1997**, *38*, 1547–1550. [CrossRef]
7. Chen, W.C.; Kavala, V.; Shih, Y.H.; Wang, Y.H.; Kuo, C.W.; Yang, T.H.; Huang, C.Y.; Chiu, H.H.; Yao, C.F. Synthesis of Bicyclic Isoxazoles and Isoxazolines via Intramolecular Nitrile Oxide Cycloaddition. *Molecules* **2015**, *20*, 10910–10927. [CrossRef] [PubMed]
8. Reja, R.M.; Sunny, S.; Gopi, H.N. Chemoselective Nitrile Oxide–Alkyne 1,3-Dipolar Cycloaddition Reactions from Nitroalkane-Tethered Peptides. *Org. Lett.* **2017**, *19*, 3572–3575. [CrossRef] [PubMed]
9. Singhal, A.; Parumala, S.K.R.; Sharma, A.; Peddinti, R.K. Hypervalent iodine mediated synthesis of di- and tri-substituted isoxazoles via [3+2] cycloaddition of nitrile oxides. *Tetrahedron Lett.* **2016**, *57*, 719–722. [CrossRef]
10. Zhang, D.; Huang, Y.; Zhang, E.; Yi, R.; Chen, C.; Yu, L.; Xu, Q. Pd/Mn Bimetallic Relay Catalysis for Aerobic Aldoxime Dehydration to Nitriles. *Adv. Synth. Catal.* **2018**, *360*, 784–790. [CrossRef]
11. Wade, P.A. Additions to and Substitutions at CC  $\pi$ -Bonds. In *Comprehensive Organic Synthesis*, 2nd ed.; Trost, B.M., Fleming, I., Eds.; Elsevier Ltd.: Amsterdam, The Netherlands, 1991; Volume 3, pp. 154–196.
12. Svejstrup, T.D.; Zawodny, W.; Douglas, J.J.; Bidgeli, D.; Sheikh, N.S.; Leonori, D. Visible-light-mediated generation of nitrile oxides for the photoredox synthesis of isoxazolines and isoxazoles. *Chem. Commun.* **2016**, *52*, 12302–12305. [CrossRef]
13. Chen, R.; Ogunlana, A.A.; Fang, S.; Long, W.; Sun, H.; Bao, X.; Wan, X. In situ generation of nitrile oxides from copper carbene and *tert*-butyl nitrite: Synthesis of fully substituted isoxazoles. *Org. Biomol. Chem.* **2018**, *16*, 4683–4687. [CrossRef] [PubMed]
14. Yonekawa, M.; Koyama, Y.; Kuwata, S.; Takata, T. Intramolecular 1,3-Dipolar Cycloaddition of Nitrile *N*-Oxide Accompanied by Dearomatization. *Org. Lett.* **2012**, *14*, 1164–1167. [CrossRef]
15. Prasad, S.S.; Baskaran, S. Iminosugar C-Nitromethyl Glycoside: Stereoselective Synthesis of Isoxazoline and Isoxazole-Fused Bicyclic Iminosugars. *J. Org. Chem.* **2018**, *83*, 1558–1564. [CrossRef] [PubMed]
16. Majumdar, S.; Hossain, J.; Natarajan, R.; Banerjee, A.K.; Maiti, D.K. Phthalate tethered strategy: Carbohydrate nitrile oxide cycloaddition to 12–15 member chiral macrocycles with alkenyl chain length controlled orientation of bridged isoxazolines. *RSC Adv.* **2015**, *5*, 106289–106293. [CrossRef]
17. Balalaie, S.; Shamakli, M.; Nikbakht, A.; Alavijeh, N.S.; Rominger, F.; Rostamizadeh, S.; Bijanzadeh, H.R. Direct access to isoxazolino and isoxazolo benzazepines from 2-((hydroxyimino)methyl)benzoic acid via a post-Ugi heteroannulation. *Org. Biomol. Chem.* **2017**, *15*, 5737–5742. [CrossRef] [PubMed]
18. Bakthadoss, M.; Vinayagam, V. A novel protocol for the facile construction of tetrahydroquinoline fused tricyclic frameworks via an intramolecular 1,3-dipolar nitrile oxide cycloaddition reaction. *Org. Biomol. Chem.* **2015**, *13*, 10007–10014. [CrossRef]
19. Gioti, E.G.; Koftis, T.V.; Neokosmidis, E.; Vastardi, E.; Kotoulas, S.S.; Trakossas, S.; Tsatsas, T.; Anagnostaki, E.E.; Panagiotidis, T.D.; Zacharis, C.; et al. A new scalable synthesis of entecavir. *Tetrahedron* **2018**, *74*, 519–527. [CrossRef]
20. Zhou, B.; Li, Y. Synthesis of Entecavir (BMS-200475). *Tetrahedron Lett.* **2012**, *53*, 502–504. [CrossRef]
21. Mulzer, J.; Castagnolo, D.; Felzmann, W.; Marchart, S.; Pilger, C.; Enev, V.S. Toward the Synthesis of the Antibiotic Branimycin: Novel Approaches to Highly Substituted *cis*-Decalin Systems. *Chem. Eur. J.* **2006**, *12*, 5992–6001. [CrossRef]
22. Kim, D.; Lee, J.; Shim, P.J.; Lim, J.I.; Doi, T.; Kim, S. Role of Conformational Effects on the Regioselectivity of Macrocyclic INOC Reactions: Two New Asymmetric Total Syntheses of (+)-Brefeldin A. *J. Org. Chem.* **2002**, *67*, 772–781. [CrossRef] [PubMed]
23. Andrés, J.I.; Alcázar, J.; Alonso, J.M.; Alvarez, R.M.; Bakker, M.H.; Biesmans, I.; Cid, J.M.; De Lucas, A.I.; Fernández, J.; Font, L.M.; et al. Discovery of a New Series of Centrally Active Tricyclic Isoxazoles Combining Serotonin (5-HT) Reuptake Inhibition with  $\alpha_2$ -Adrenoceptor Blocking Activity. *J. Med. Chem.* **2005**, *48*, 2054–2071. [CrossRef] [PubMed]
24. Dong, C.; Qiao, T.; Xie, Y.; Zhang, X.; Ao, J.; Liang, G. Rapid construction of the ABD tricyclic skeleton in meliacarpinin B from carvone enabled by an INOC strategy. *Org. Chem. Front.* **2020**, *7*, 1890–1894. [CrossRef]
25. Gaugele, D.; Maier, M.E. Synthesis of the Core Structure of Palhinine A. *Eur. J. Org. Chem.* **2021**, *2021*, 2549–2556. [CrossRef]
26. Arbačiauskienė, E.; Laukaitytė, V.; Holzer, W.; Šačkus, A. Metal-Free Intramolecular Alkyne-Azide Cycloaddition To Construct the Pyrazolo[4,3-*f*][1,2,3]triazolo[5,1-*c*][1,4]oxazepine Ring System. *Eur. J. Org. Chem.* **2015**, *2015*, 5663–5670. [CrossRef]
27. Bieliauskas, A.; Krikštolaitytė, S.; Holzer, W.; Šačkus, A. Ring-closing metathesis as a key step to construct the 2,6-dihydropyrano[2,3-*c*]pyrazole ring system. *Arkivoc* **2018**, *2018*, 296–307. [CrossRef]
28. Varvuolytė, G.; Malina, L.; Bieliauskas, A.; Hošíková, B.; Simerská, H.; Kolářová, H.; Kleizienė, N.; Kryštof, V.; Šačkus, A.; Žukauskaitė, A. Synthesis and photodynamic properties of pyrazole-indole hybrids in the human skin melanoma cell line G361. *Dyes Pigment.* **2020**, *183*, 108666. [CrossRef]

29. Milišiūnaitė, V.; Kadlecová, A.; Žukauskaitė, A.; Doležal, K.; Strnad, M.; Voller, J.; Arbačiauskienė, E.; Holzer, W.; Šačkus, A. Synthesis and anthelmintic activity of benzopyrano [2,3-*c*] pyrazol-4 (2*H*)-one derivatives. *Mol. Divers.* **2020**, *24*, 1025–1042. [CrossRef] [PubMed]
30. Milišiūnaitė, V.; Paulavičiūtė, R.; Arbačiauskienė, E.; Martynaitis, V.; Holzer, W.; Šačkus, A. Synthesis of 2*H*-furo [2,3-*c*] pyrazole ring systems through silver(I) ion-mediated ring-closure reaction. *Beilstein J. Org. Chem.* **2019**, *15*, 679–684. [CrossRef]
31. Milišiūnaitė, V.; Arbačiauskienė, E.; Řezníčková, E.; Jorda, R.; Malínková, V.; Žukauskaitė, A.; Holzer, W.; Šačkus, A.; Kryštof, V. Synthesis and anti-mitotic activity of 2, 4- or 2, 6-disubstituted- and 2, 4, 6-trisubstituted-2*H*-pyrazolo [4,3-*c*] pyridines. *Eur. J. Med. Chem.* **2018**, *150*, 908–919. [CrossRef]
32. Arbačiauskienė, E.; Krikštolaitytė, S.; Mitrulevičienė, A.; Bieliauskas, A.; Martynaitis, V.; Bechmann, M.; Roller, A.; Šačkus, A.; Holzer, W. On the Tautomerism of *N*-Substituted Pyrazolones: 1,2-Dihydro-3*H*-pyrazol-3-ones versus 1*H*-Pyrazol-3-ols. *Molecules* **2018**, *23*, 129. [CrossRef] [PubMed]
33. Milišiūnaitė, V.; Arbačiauskienė, E.; Bieliauskas, A.; Vilkauskaitė, G.; Šačkus, A.; Holzer, W. Synthesis of pyrazolo [4',3':3,4] pyrido [1,2-*a*] benzimidazoles and related new ring systems by tandem cyclisation of vic-alkynylpyrazole-4-carbaldehydes with (het)aryl-1,2-diamines and investigation of their optical properties. *Tetrahedron* **2015**, *71*, 3385–3395. [CrossRef]
34. O'Brien, D.F.; Gates, J.W., Jr. Some Reactions of 3-Hydroxy-1-phenylpyrazole. *J. Org. Chem.* **1966**, *31*, 1538–1542. [CrossRef]
35. Arbačiauskienė, E.; Martynaitis, V.; Krikštolaitytė, S.; Holzer, W.; Šačkus, A. Synthesis of 3-substituted 1-phenyl-1*H*-pyrazole-4-carbaldehydes and the corresponding ethanones by Pd-catalysed cross-coupling reactions. *Arkivoc* **2011**, *11*, 1–21. [CrossRef]
36. Sankar, B.; Harikrishnan, M.; Raja, R.; Sadhasivam, V.; Malini, N.; Murugesan, S.; Siva, A. Design of a simple and efficient synthesis for bioactive novel pyrazolyl–isoxazoline hybrids. *New J. Chem.* **2019**, *43*, 10458–10467. [CrossRef]
37. Heinisch, G.; Holzer, W. Convenient and rapid determination of the configuration of aldoximes and ketoximes by means of NOE difference spectroscopy. *Tetrahedron Lett.* **1990**, *31*, 3109–3112. [CrossRef]
38. Rykowski, A.; Guzik, E.; Makosza, M.; Holzer, W. Configurational assignments of oximes derived from 5-formyl and 5-acyl-1,2,4-triazines. *J. Heterocycl. Chem.* **1993**, *30*, 413–418. [CrossRef]
39. Fraser, R.R.; Capoor, R.; Bovenkamp, J.W.; Lacroix, B.; Pagotto, J. The use of shift reagents and <sup>13</sup>C nuclear magnetic resonance for assignment of stereochemistry to oximes. *Can. J. Chem.* **1984**, *61*, 2616–2620. [CrossRef]
40. Hansen, T.V.; Wu, P.; Fokin, V.V. One-Pot Copper(I)-Catalyzed Synthesis of 3,5-Disubstituted Isoxazoles. *J. Org. Chem.* **2005**, *70*, 7761–7764. [CrossRef] [PubMed]
41. Padmavathi, V.; Reddy, K.V.; Padmaja, A.; Venugopalan, P. Unusual Reaction of Chloramine-T with Araldoximes. *J. Org. Chem.* **2003**, *68*, 1567–1570. [CrossRef] [PubMed]
42. Ledovskaya, M.S.; Rodygin, K.S.; Ananikov, V.P. Calcium-mediated one-pot preparation of isoxazoles with deuterium incorporation. *Org. Chem. Front.* **2018**, *5*, 226–231. [CrossRef]
43. Boruah, M.; Konwar, D. KF/Al<sub>2</sub>O<sub>3</sub>: Solid-Supported Reagent Used in 1,3-Dipolar Cycloaddition Reaction of Nitrile Oxide. *Synth. Comm.* **2012**, *42*, 3261–3268. [CrossRef]
44. Isaacman, M.J.; Cui, W.; Theogarajan, L.S. Rapid metal-free macromolecular coupling via In Situ nitrile oxide-activated alkene cycloaddition. *J. Polym. Sci. Part A Polym. Chem.* **2014**, *52*, 3134–3141. [CrossRef] [PubMed]
45. Minakata, S.; Okumura, S.; Nagamachi, T.; Takeda, Y. Generation of Nitrile Oxides from Oximes Using *t*-BuOI and Their Cycloaddition. *Org. Lett.* **2011**, *13*, 2966–2969. [CrossRef] [PubMed]
46. Chiacchio, U.; Corsaro, A.; Rescifina, A.; Bkaithan, M.; Grassi, G.; Piperno, A.; Privitera, T.; Romeo, G. Stereoselective synthesis of homochiral annulated sultams via intramolecular cycloaddition reactions. *Tetrahedron* **2001**, *57*, 3425–3433. [CrossRef]
47. Ravula, S.; Bobbala, R.R.; Kolli, B. Synthesis of novel isoxazole functionalized pyrazolo[3,4-*b*]pyridine derivatives; their anticancer activity. *J. Heterocyclic Chem.* **2020**, *57*, 2535–2538. [CrossRef]
48. Mendelsohn, B.A.; Lee, S.; Kim, S.; Teyssier, F.; Aulakh, V.S.; Ciufolini, M.A. Oxidation of Oximes to Nitrile Oxides with Hypervalent Iodine Reagents. *Org. Lett.* **2009**, *11*, 1539–1542. [CrossRef]
49. Yoshimura, A.; Jarvi, M.E.; Shea, M.T.; Makitalo, C.L.; Rohde, G.T.; Yusubov, M.S.; Saito, A.; Zhdankin, V.V. Hypervalent Iodine(III) Reagent Mediated Regioselective Cycloaddition of Aldoximes with Enaminones. *Eur. J. Org. Chem.* **2019**, *39*, 6682–6689. [CrossRef]
50. Jawalekar, A.M.; Reubsaet, E.; Rutjes, F.P.J.T.; van Delft, F.L. Synthesis of isoxazoles by hypervalent iodine-induced cycloaddition of nitrile oxides to alkynes. *Chem. Commun.* **2011**, *47*, 3198–3200. [CrossRef]
51. Zhao, G.; Liang, L.; Wen, C.H.E.; Tong, R. In Situ Generation of Nitrile Oxides from NaCl–Oxone Oxidation of Various Aldoximes and Their 1,3-Dipolar Cycloaddition. *Org. Lett.* **2019**, *21*, 315–319. [CrossRef]
52. Han, L.; Zhang, B.; Zhu, M.; Yan, J. An environmentally benign synthesis of isoxazolines and isoxazoles mediated by potassium chloride in water. *Tetrahedron Lett.* **2014**, *55*, 2308–2311. [CrossRef]
53. Yoshimura, A.; Zhu, C.; Middleton, K.R.; Todora, A.D.; Kastern, B.J.; Maskaev, A.V.; Zhdankin, V.V. Hypoiodite mediated synthesis of isoxazolines from aldoximes and alkenes using catalytic KI and Oxone as the terminal oxidant. *Chem. Commun.* **2013**, *49*, 4800–4802. [CrossRef]
54. Xiang, C.; Li, T.; Yan, J. Hypervalent Iodine–Catalyzed Cycloaddition of Nitrile Oxides to Alkenes. *Synth. Comm.* **2014**, *44*, 682–688. [CrossRef]
55. Roy, B.; De, R.N. Enhanced rate of intramolecular nitrile oxide cycloaddition and rapid synthesis of isoxazoles and isoxazolines. *Monatsh. Chem.* **2010**, *141*, 763–771. [CrossRef]



56. Jenkins, R.N.; Hinnant, G.M.; Bean, A.C.; Stephens, C.E. Aerobic aromatization of 1,3,5-triarylpyrazolines in open air and without catalyst. *Arkivoc* **2015**, *7*, 347–353. [CrossRef]
57. Nakamichi, N.; Kawashita, Y.; Hayashi, M. Oxidative Aromatization of 1,3,5-Trisubstituted Pyrazolines and Hantzsch 1,4-Dihydropyridines by Pd/C in Acetic Acid. *Org. Lett.* **2002**, *4*, 3955–3957. [CrossRef]
58. Vilela, G.D.; da Rosa, R.R.; Schneider, P.H.; Bechtold, I.H.; Eccher, J.; Merlo, A.A. Expedient preparation of isoxazoles from  $\Delta^2$ -isoxazolines as advanced intermediates for functional materials. *Tetrahedron Lett.* **2011**, *52*, 6569–6572. [CrossRef]
59. L'abbé, G.; Emmers, S.; Dehaen, W.; Dyllal, L.K. 5-Chloropyrazole-4-carbaldehydes as synthons for intramolecular 1,3-dipolar cycloadditions. *J. Chem. Soc. Perkin Trans. 1* **1994**, 2553–2558. [CrossRef]
60. Christl, M.; Warren, J.P.; Hawkins, B.L.; Roberts, J.D. Carbon-13 and nitrogen-15 nuclear magnetic resonance spectroscopy of nitrile oxides and related reaction products. Unexpected carbon-13 and nitrogen-15 nuclear magnetic resonance parameters of 2,4,6-trimethylbenzoxonitrile oxide. *J. Am. Chem. Soc.* **1973**, *95*, 4392–4397. [CrossRef]
61. Lewis-Atwell, T.; Townsend, P.A.; Grayson, M.N. Comparisons of different force fields in conformational analysis and searching of organic molecules: A review. *Tetrahedron* **2021**, *79*, 131865. [CrossRef]
62. Neese, F. Software update: The ORCA program system, version 4.0. *WIREs Comput. Mol. Sci.* **2018**, *8*, e1327. [CrossRef]
63. Haasnoot, C.A.G.; de Leeuw, F.A.A.M.; Altona, C. The relationship between proton-proton NMR coupling constants and substituent electronegativities—I: An empirical generalization of the Karplus equation. *Tetrahedron* **1980**, *36*, 2783–2792. [CrossRef]
64. Liaskopoulos, T.; Skoulika, S.; Tsoungas, P.G.; Varvounis, G. Novel Synthesis of Naphthopyranoisoxazoles and Versatile Access to Naphthopyranoisoxazolines. *Synthesis* **2008**, 711–718. [CrossRef]
65. Berger, S.; Braun, S. *200 and More NMR Experiments: A Practical Course*, 3rd ed.; Wiley-VCH: Weinheim, Germany, 2004; 838p.
66. Buevich, A.V.; Williamson, R.T.; Martin, G.E. NMR Structure Elucidation of Small Organic Molecules and Natural Products: Choosing ADEQUATE vs HMBC. *J. Nat. Prod.* **2014**, *77*, 1942–1947. [CrossRef] [PubMed]
67. Navarro-Vázquez, A.; Cobas, J.C.; Sardina, F.J.; Casanueva, J.; Díez, E. A Graphical Tool for the Prediction of Vicinal Proton–Proton 3JHH Coupling Constants. *J. Chem. Inf. Comput. Sci.* **2004**, *44*, 1680–1685. [CrossRef] [PubMed]

## Article

# Synthesis, Characterization, and Biological Evaluation of Some Novel Pyrazolo[5,1-*b*]thiazole Derivatives as Potential Antimicrobial and Anticancer Agents

Abdulrhman Alsayari <sup>1</sup>, Abdullatif Bin Muhsinah <sup>1</sup>, Yahya I. Asiri <sup>2</sup>, Faiz A. Al-aizari <sup>3,4</sup>, Nabila A. Kheder <sup>5</sup>, Zainab M. Almarhoon <sup>3</sup>, Hazem A. Ghabbour <sup>6</sup> and Yahia N. Mabkhot <sup>7,\*</sup>

<sup>1</sup> Department of Pharmacognosy, College of Pharmacy, King Khalid University, Abha 61441, Saudi Arabia; alsayari@kku.edu.sa (A.A.); ajmohsnah@kku.edu.sa (A.B.M.)

<sup>2</sup> Department of Pharmacology, College of Pharmacy, King Khalid University, Abha 61441, Saudi Arabia; yialmuawad@kku.edu.sa

<sup>3</sup> Department of Chemistry, College of Science, King Saud University, P.O. Box 2455, Riyadh 11451, Saudi Arabia; faizalaizari@yahoo.com (F.A.A.-a.); zalmarhoon@ksu.edu.sa (Z.M.A.)

<sup>4</sup> Department of Chemistry, Faculty of Science, Al-Baydha University, Albaydah 38018, Yemen

<sup>5</sup> Department of Chemistry, Faculty of Science, Cairo University, Giza 12613, Egypt; nabila.abdelshafy@gmail.com

<sup>6</sup> Department of Medicinal Chemistry, Faculty of Pharmacy, University of Mansoura, Mansoura 35516, Egypt; ghabbourh@yahoo.com

<sup>7</sup> Department of Pharmaceutical Chemistry, College of Pharmacy, King Khalid University, Abha 61441, Saudi Arabia

\* Correspondence: ygaber@kku.edu.sa; Tel.: +966-1724-19734

**Citation:** Alsayari, A.; Muhsinah, A.B.; Asiri, Y.I.; Al-aizari, F.A.; Kheder, N.A.; Almarhoon, Z.M.; Ghabbour, H.A.; Mabkhot, Y.N. Synthesis, Characterization, and Biological Evaluation of Some Novel Pyrazolo[5,1-*b*]thiazole Derivatives as Potential Antimicrobial and Anticancer Agents. *Molecules* **2021**, *26*, 5383. <https://doi.org/10.3390/molecules26175383>

Academic Editors: Vera L. M. Silva and Artur M. S. Silva

Received: 29 July 2021

Accepted: 31 August 2021

Published: 4 September 2021

**Publisher's Note:** MDPI stays neutral with regard to jurisdictional claims in published maps and institutional affiliations.



**Copyright:** © 2021 by the authors. Licensee MDPI, Basel, Switzerland. This article is an open access article distributed under the terms and conditions of the Creative Commons Attribution (CC BY) license (<https://creativecommons.org/licenses/by/4.0/>).

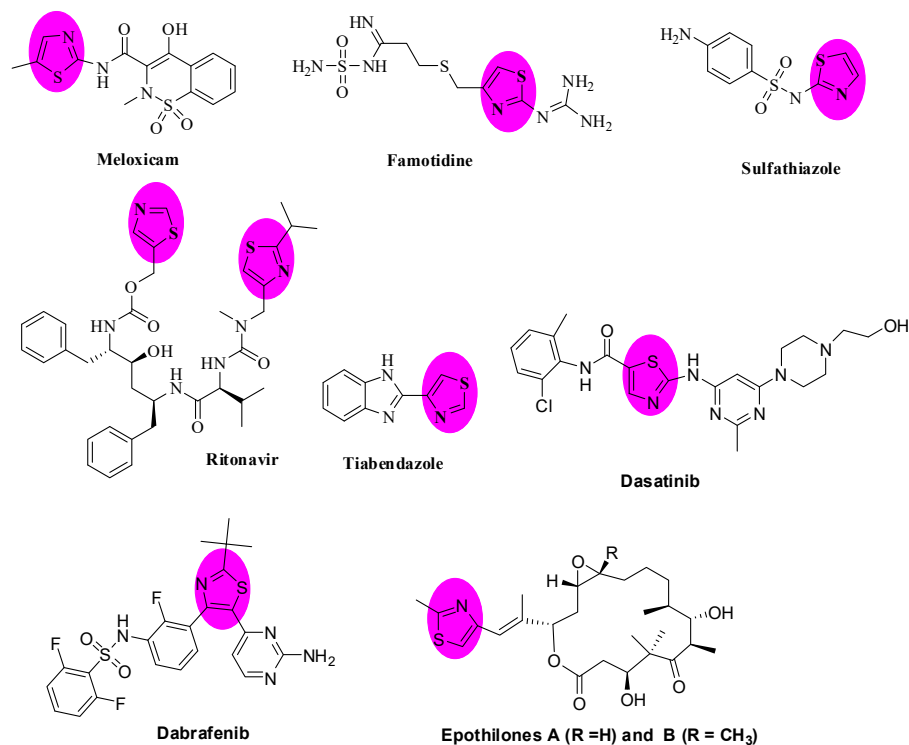
**Abstract:** The pharmacological activities of thiazole and pyrazole moieties as antimicrobial and anticancer agents have been thoroughly described in many literature reviews. In this study, a convenient synthesis of novel pyrazolo[5,1-*b*]thiazole-based heterocycles was carried out. The synthesized compounds were characterized by IR, <sup>1</sup>H and <sup>13</sup>C NMR spectroscopy and mass spectrometry. Some selected examples were screened and evaluated for their antimicrobial and anticancer activities and showed promising results. These products could serve as leading compounds in the future design of new drug molecules.

**Keywords:** pyrazolo[5,1-*b*]thiazole; X-ray crystallography; antibacterial activity; antifungal activity; anticancer activity

## 1. Introduction

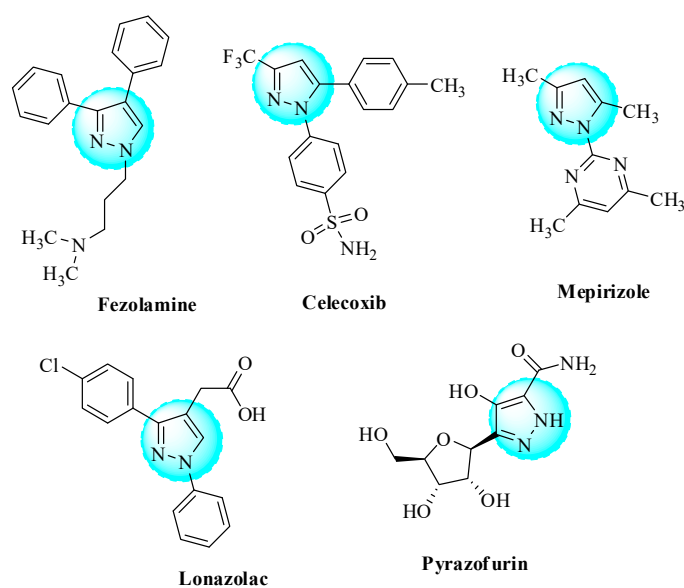
Antibiotics saved millions of lives during the twentieth century by eliminating the deadly threat of infection. In recent years, the overuse of antimicrobial agents has played a significant role in creating more resistant strains of bacteria [1], thus causing an increase in morbidity and mortality [2]. Therefore, safer, cheaper, and more effective antimicrobial agents with a new mode of action are needed [3]. Although cancer is considered the second leading cause of death, taking the lives of 9.6 million people every year [4,5], many cancers are curable if detected early and treated promptly [6]. Chemotherapy is a treatment that uses medications to destroy cancer cells. It typically works by preventing cancer cells from developing, dividing, or proliferating. However, chemotherapy has several disadvantages, one of which is a lack of selectivity leading to extreme side effects and minimal efficacy. Another is the emergence of drug resistance [7]. Therefore, there is an urgent need to design and synthesize potent and highly selective anticancer molecules that offer little-to-zero toxicity to normal cells [8]. Thiazole derivatives demonstrate many pharmacological activities [9–17]. The thiazole ring can be traced in several well-established drugs such as the non-steroidal anti-inflammatory drug meloxicam, the anti-ulcer drug famotidine, the antibacterial sulfathiazole, the antiviral ritonavir, the antiparasitic thiabendazole, and

many anticancer medicines including dasatinib, dabrafenib, and epothilones. Figure 1 shows some of the most effective drugs containing a thiazole ring [18].



**Figure 1.** Commercial drugs containing a thiazole ring.

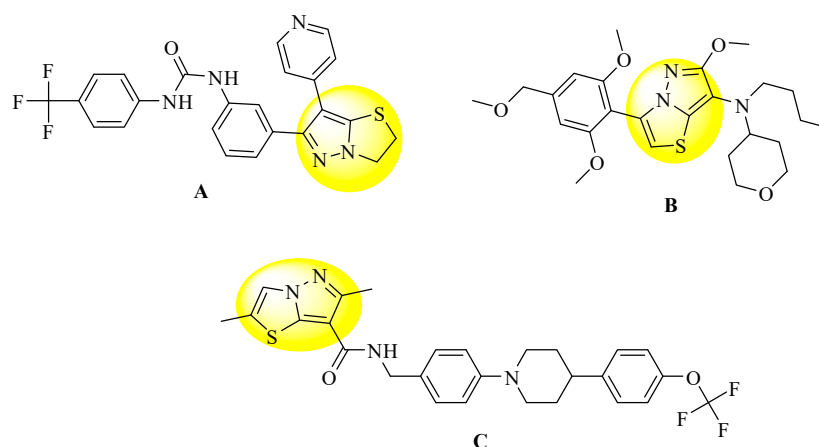
Pyrazole derivatives have been reported as antimicrobial [19], analgesic [20], anti-inflammatory [21], and anticancer agents [22]. Additionally, many pharmaceutical drugs contain the pyrazole moiety, such as the antidepressant fezolamine and the anti-inflammatories celecoxib, mepirizole, and lonazolac. Moreover, the pyrazole derivative pyrazofurin has been reported to have antiviral [23,24] and anticancer activities [24,25]. Figure 2 depicts some of the most potent drugs containing a pyrazole ring.



**Figure 2.** Commercial drug molecules containing pyrazole rings.

Many literature reviews suggest that the pharmacophore hybrids may have enhanced efficacy, fewer drug–drug interactions, and less potential to induce drug resistance [26]. In light of the significance of pyrazoles and thiazoles, numerous studies have been conducted on the synthesis and biological evaluations of new hybrid pharmacophores containing pyrazole and thiazole moieties [27–30].

Figure 3 presents three examples of pharmacologically active pyrazolo[5,1-*b*]thiazole derivatives: pyrazolo[5,1-*b*]thiazole derivative (A) (a protein kinase inhibitor for treating cancer and other diseases) [31], pyrazolothiazole (B) (a potent corticotropin-releasing factor 1 (CRF1) receptor antagonists) [32], and pyrazolo[5,1-*b*]thiazole derivative (C) (possessing a strong suppressant function against the H37Ra strain) [33] (Figure 3).



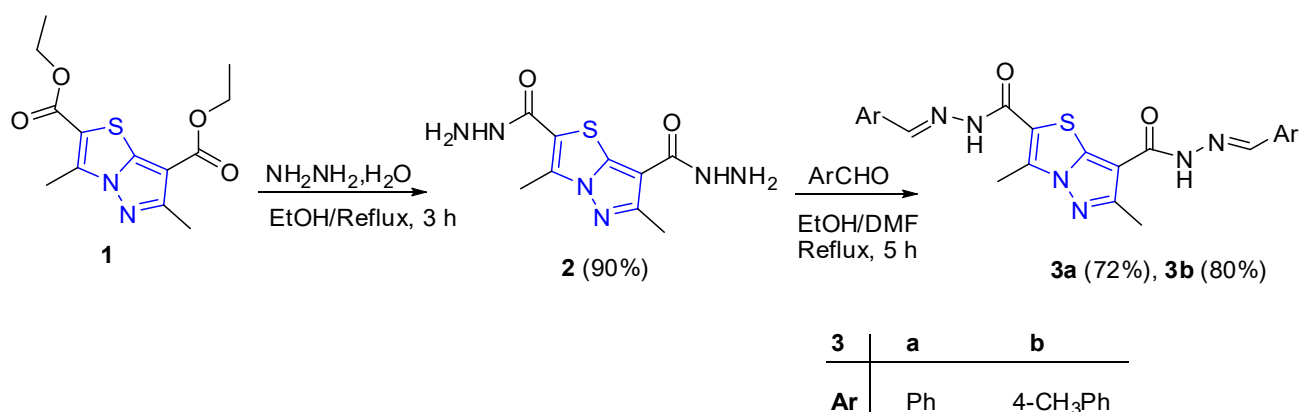
**Figure 3.** Pharmacologically active pyrazolo[5,1-*b*]thiazole derivatives.

Hydrazides are an important class of biologically active compounds [34–38]. Hydrazides and their condensation products have been reported to possess a wide range of pharmacological and biological activities, including antibacterial [34], tuberculostatic [35], HIV inhibitory [36], pesticidal [37], and antifungal [38] activities. Some of them are used as monoamine oxidase (MAO) inhibitors and serotonin antagonists in psychopharmacology [39]. Furthermore, isonicotinoyl hydrazide (isoniazid) is an excellent antituberculosis drug [40–42]. A variety of methods have been used to form hydrazides [43]. The hydrazinolysis of carboxylic acid esters in alcohol solutions is a convenient method for preparing carbohydrazides [44]. In light of this, and as part of our ongoing research on pharmacologically potent molecules [45–50], new hydrazide–hydrazones attached to pyrazolothiazole were synthesized and evaluated for their antimicrobial and anticancer activities.

## 2. Results

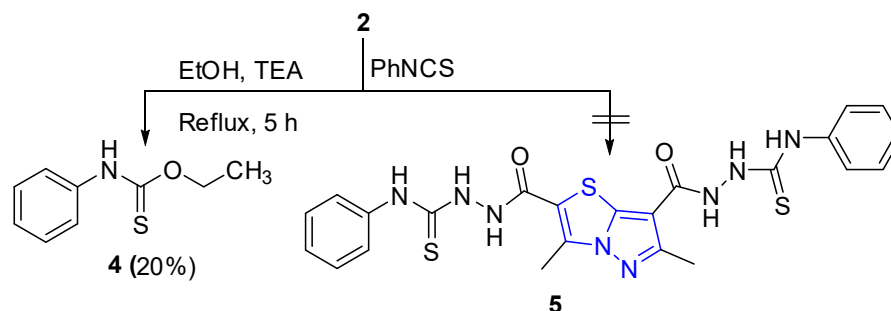
### 2.1. Chemistry

Hydrazide (2) was synthesized by treating diethyl 3,6-dimethylpyrazolo[5,1-*b*]thiazole-2,7-dicarboxylate (1) [51] with hydrazine hydrate (Scheme 1). The molecular structure was confirmed using IR, MS, and NMR analyses. Its IR spectrum showed the absence of C=O in the ester group, and the presence of absorption bands due to C=O in the amide and NHH<sub>2</sub> functions (see Experimental section). Another perfect confirmation of the structure formation obtained from NMR (<sup>1</sup>H and <sup>13</sup>C) revealed the absence of any signals due to ethoxy protons and carbons. Additionally, the mass spectrum demonstrated the molecular ion peak at the expected *m/z* value of 268 (41%). Compound 2 was reacted with the appropriate aromatic aldehyde to afford the corresponding hydrazones 3a,b (Scheme 1). Their <sup>1</sup>H NMR spectra revealed the absence of amino signals, which also confirms the presence of a signal at (6.78–6.81 ppm) for N=CH (imine group) in the hydrazone compounds.

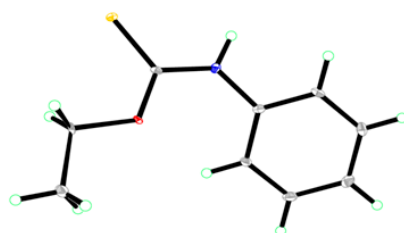


**Scheme 1.** Synthesis of pyrazolothiazoles **2** and **3a,b**.

Hydrazide **2** was reacted with phenyl isothiocyanate in ethanol and in the presence of a catalytic amount of triethylamine to afford *O*-ethyl *N*-phenylcarbamothioate (**4**) [52], rather than the expected product **5** (Scheme 2). The structure was confirmed using spectral and X-ray analysis (Figure 4). CCDC 2075096 contains the supplementary crystallographic data for this paper. These data can be obtained free of charge from the Cambridge Crystallographic Data Centre via [www.ccdc.cam.ac.uk/data\\_request/cif](http://www.ccdc.cam.ac.uk/data_request/cif). Additional information relating to compound **4** is provided in Table 1.



**Scheme 2.** Unexpected synthesis of *O*-Ethyl *N*-phenylcarbamothioate (**4**).

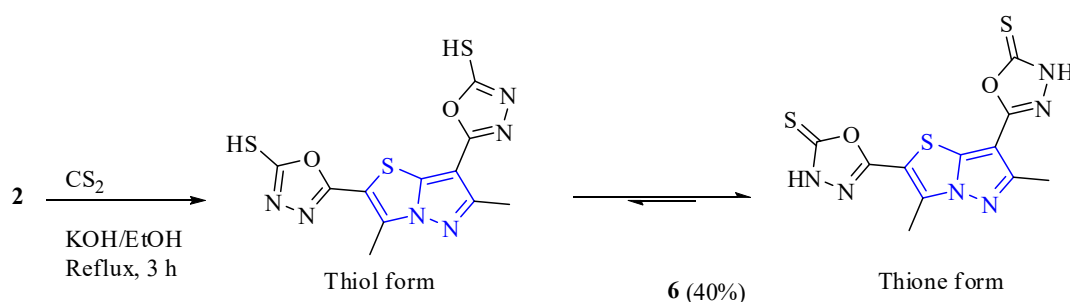


**Figure 4.** ORTEP diagram of compound **4**. Displacement ellipsoids are plotted at the 40% probability level for non-H atoms.

The ring closure reaction of acid hydrazide **2** with carbon disulfide in ethanolic KOH afforded the target compound **6** (Scheme 3). It was observed that 1,3,4-oxadiazole-2-thione derivatives exist in the thione form in solution, rather than in the thiol form [53,54]. Additionally, the thione tautomer is more stable than the thiol in the solution [54,55]. The equilibrium is even more favored towards the thione as it is better solvated than the thiol form [54]. In the <sup>1</sup>H NMR spectrum of compound **6** (Scheme 3), a signal at  $\delta$  12.9 of the NH proton was recorded.

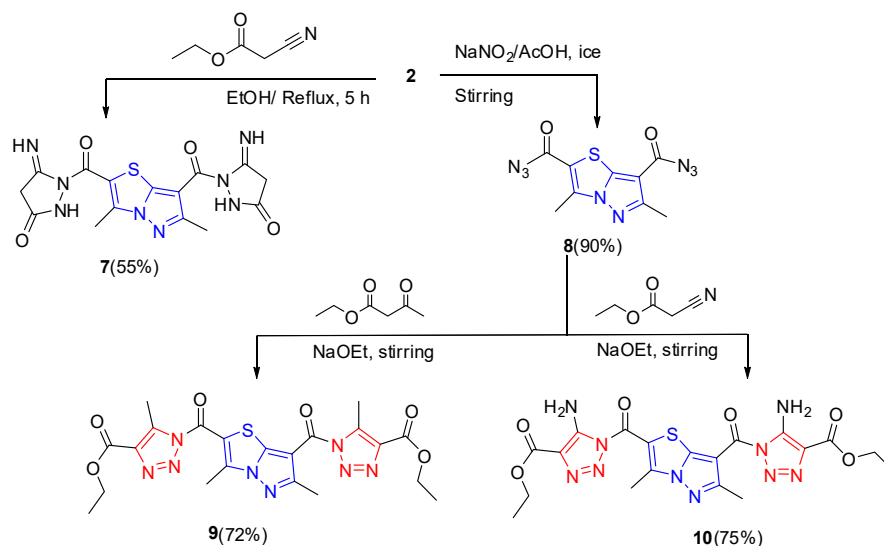
**Table 1.** Experimental details of compound 4.

| Crystal Data   |   |
|--|---|
| Chemical formula   | C <sub>9</sub> H <sub>11</sub> NOS  |
| Mr   | 181.25  |
| Crystal system, space group  | Triclinic, P-1  |
| Temperature (K)  | 293   |
| a, b, c (Å)  | 9.6587 (4), 11.7585 (5), 12.1212 (5)                                      |
| β (°)  | 88.807 (2), 84.858 (2), 84.314 (2)  |
| V (Å <sup>3</sup> )  | 1364.24 (10)  |
| Z  | 6   |
| Radiation type   | Cu Kα   |
| μ (mm <sup>-1</sup> )  | 2.76  |
| Crystal size (mm)  | 0.47 × 0.27 × 0.15  |
| Data collection  |   |
| Diffractometer   | Bruker APEX-II CCD  |
| Absorption correction  | Multi-scan<br>SADABS Bruker 2018  |
| Tmin, Tmax   | 0.932, 0.959  |
| No. of measured, independent and observed<br>[I > 2σ(I)] reflections | 12,396, 4728, 4213  |
| Rint   | 0.055   |
| Refinement   |   |
| R[F <sub>2</sub> > 2σ(F <sub>2</sub> )], wR(F <sub>2</sub> ), S      | 0.045, 0.118, 1.06  |
| No. of reflections   | 4728  |
| No. of parameters  | 341   |
| H-atom treatment   | H atoms treated by a mixture of independent<br>and constrained refinement |
| Δρmax, Δρmin (e Å <sup>-3</sup> )                                    | 0.36, -0.56   |

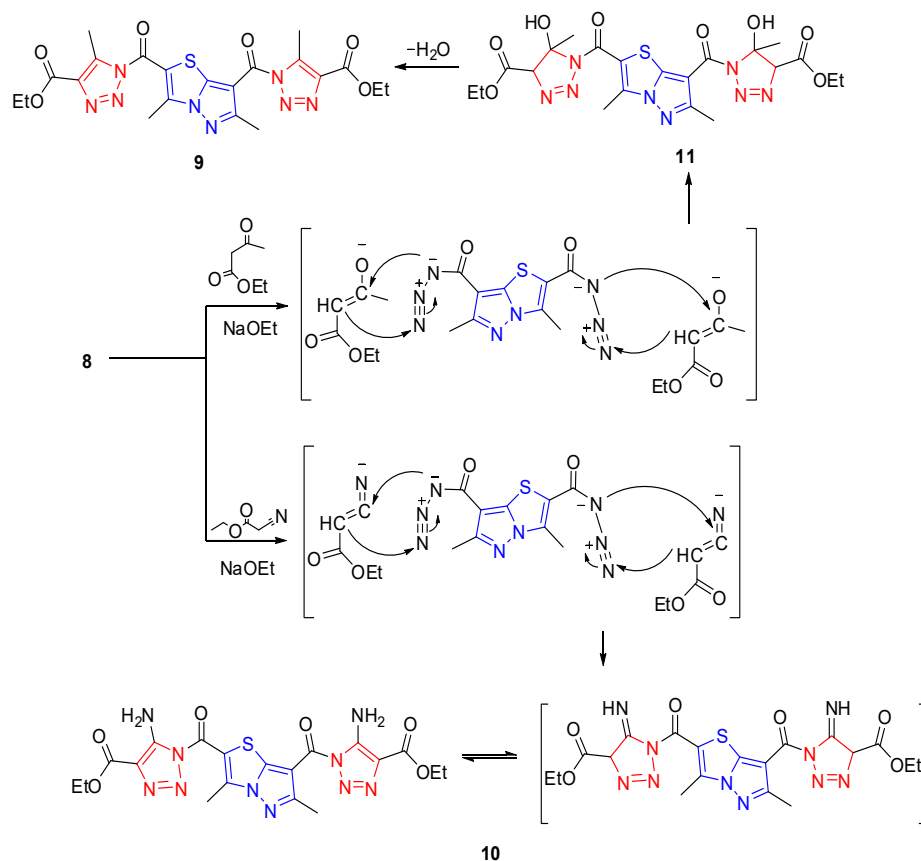
**Scheme 3.** Synthesis of 5-(2-(5-mercapto-1,3,4-oxadiazol-2-yl)-3,6-dimethylpyrazolo[5,1-*b*]thiazol-7-yl)-1,3,4-oxadiazole-2(3*H*)-thione (6).

The reaction of hydrazide 2 with ethyl cyanoacetate in absolute ethanol resulted in compound 7 as the sole product (Scheme 4). Its IR spectrum showed the absence of any absorption band due to the cyano group and the presence of the stretching bands at 3164, 1726, and 1651 cm<sup>-1</sup>, corresponding to NH and two C=O groups, respectively. Its mass spectrum demonstrated the molecular ion peak at an *m/z* value of 402. On the other hand, hydrazide 2 was converted to acyl azide 8 in the presence of sodium nitrite and acetic acid (Scheme 4). The reaction between compound 8 and ethyl acetoacetate or ethyl cyanoacetate

afforded the target compounds **9** and **10**, respectively (Scheme 4). The structures of compounds **8–10** were confirmed through analytical data and spectral analysis (See Experiment section). The suggested mechanism for the selective synthesis of compounds **9** and **10** via the reaction of hydrazide **8**, ethyl acetoacetate, or ethyl cyanoacetate in the presence of sodium ethoxide is outlined in Scheme 5 [56]. The reaction was assumed to proceed through a concerted [3+2]-cycloaddition reaction. The non-isolable intermediate **11** was further transformed into stable 1,2,3-triazole derivative **9** through rapid elimination of two water molecules induced by sodium ethoxide.



**Scheme 4.** Synthesis of bis(1,2,3-triazole) derivatives **7–10**.



**Scheme 5.** A suggested reaction mechanism for the synthesis of triazoles **9** and **10**.

## 2.2. Biological Activity Evaluation

### 2.2.1. Anticancer Screening of the Synthesized Compounds

The in vitro anti-tumor activity of the synthesized compounds was assessed against two human cancer cell lines: human hepatocellular carcinoma cell line (HepG-2) and colon carcinoma cell line (HCT-116), using the MTT assay [57]. Their activity was compared to the reference drug Doxorubicin. In addition, calculations of the tested compounds' concentrations needed to inhibit 50% of the cancerous cell population ( $IC_{50}$ ) were implemented. These are presented in Tables 2 and 3.

**Table 2.** Viability values and  $IC_{50}$  of some selected samples against hepatocellular carcinoma cell line (HepG-2).

| $IC_{50}$<br>( $\mu\text{g/mL}$ ) | Viability %                               |       |       |       |       |       |       |       | Sample    |
|-----------------------------------|---|-------|-------|-------|-------|-------|-------|-------|-----------|
|                                   | Sample Concentration ( $\mu\text{g/mL}$ ) |       |       |       |       |       |       |       |           |
|                                   | 500                                       | 250   | 125   | 62.5  | 31.25 | 15.6  | 7.8   | 3.9   |           |
| 0.36                              | 2.08                                      | 3.36  | 4.86  | 6.51  | 11.04 | 19.38 | 24.82 | 28.86 | DOX       |
| 93.2                              | 20.88                                     | 31.76 | 42.63 | 57.12 | 72.36 | 86.04 | 92.37 | 97.48 | <b>3a</b> |
| 30.5                              | 8.71                                      | 16.38 | 24.92 | 37.65 | 49.43 | 62.04 | 78.19 | 89.28 | <b>3b</b> |
| 6.9                               | 4.37                                      | 9.46  | 16.76 | 23.66 | 34.15 | 40.72 | 46.58 | 61.43 | <b>6</b>  |
| 114                               | 24.53                                     | 39.15 | 47.32 | 61.98 | 78.43 | 89.04 | 95.17 | 98.76 | <b>7</b>  |
| 12.6                              | 5.14                                      | 11.89 | 20.97 | 31.76 | 38.69 | 45.38 | 57.43 | 72.96 | <b>8</b>  |

DOX (Doxorubicin).

**Table 3.** Viability values and  $IC_{50}$  of evaluated compounds against colon carcinoma cell line (HCT-116).

| $IC_{50}$<br>( $\mu\text{g/mL}$ ) | Viability %                               |       |       |       |       |       |       |       | Sample    |
|-----------------------------------|---|-------|-------|-------|-------|-------|-------|-------|-----------|
|                                   | Sample Concentration ( $\mu\text{g/mL}$ ) |       |       |       |       |       |       |       |           |
|                                   | 500                                       | 250   | 125   | 62.5  | 31.25 | 15.6  | 7.8   | 3.9   |           |
| 0.49                              | 2.08                                      | 3.36  | 4.86  | 6.51  | 11.04 | 19.38 | 24.82 | 28.86 | DOX       |
| 86.9                              | 16.08                                     | 25.43 | 36.81 | 58.19 | 74.26 | 88.43 | 96.51 | 99.48 | <b>3b</b> |
| 13.6                              | 6.91                                      | 10.85 | 17.44 | 25.28 | 36.59 | 43.87 | 67.34 | 84.73 | <b>6</b>  |
| 28.9                              | 9.76                                      | 17.34 | 26.69 | 35.42 | 46.94 | 63.79 | 76.45 | 84.76 | <b>8</b>  |

DOX (Doxorubicin).

Of all the tested compounds, 1,3,4-oxadiazole derivative **6** exhibited the highest activity against the two tested cell lines; HepG-2 and HCT-116, with an  $IC_{50}$  = 6.9 and 13.6  $\mu\text{g/mL}$ , respectively. Having azide moiety, pyrazolothiazole derivative **8** revealed high activity against HepG-2 and HCT-116, with an  $IC_{50}$  = 12.6 and 28.9  $\mu\text{g/mL}$ , respectively.

These results support previously published results indicating that compound structures containing an 1,3,4-oxadiazole ring [58] or azide moiety [59] have potent antitumor activities.

### 2.2.2. The In Vitro Antimicrobial Assessments

Assessments of the antimicrobial activities of the synthesized compounds were performed using the inhibition zone technique [60] against six species: two fungal species (*Aspergillus fumigatus* (RCMB 002008 (4) and *Candida albicans* (RCMB 05036)), two Gram-positive bacteria (*Staphylococcus aureus* (RCMB010010 and *Bacillus subtilis* (RCMB 010067)), and two Gram-negative bacteria (*Salmonella SP.* (RCMB 010043) and *Escherichia coli* (RCMB 010052)). The standard drugs used for comparison were Amphotericin B, Gentamicin, and Ampicillin. The inhibition zone diameter (IZD) was used as the criterion for the antimicrobial activity and all results are summarized in Table 4.



**Table 4.** The in vitro antimicrobial assessment of the synthesized compounds tested at 5 mg/mL using the inhibition zone assay (inhibition zone diameter in millimeters (mm)).

| Sample          | Microorganisms |    |                        |    |                        |    |
|-----------------|----------------|----|------------------------|----|------------------------|----|
|                 | Fungi          |    | Gram-Positive Bacteria |    | Gram-Negative Bacteria |    |
|                 | AF             | CA | SA                     | BS | SSP                    | EC |
| <b>3a</b>       | 11             | 15 | 13                     | 12 | 13                     | 14 |
| <b>3b</b>       | 13             | 15 | 10                     | NA | 12                     | 14 |
| <b>4</b>        | 17             | 16 | 15                     | 14 | 15                     | 17 |
| <b>6</b>        | 18             | 15 | 14                     | 15 | 14                     | 15 |
| <b>7</b>        | NA             | 10 | 12                     | 9  | 12                     | 12 |
| <b>8</b>        | 12             | NA | 14                     | 12 | 13                     | 14 |
| <b>10</b>       | 14             | 12 | 12                     | 12 | 12                     | 14 |
| Amphotericin B. | 23             | 25 |                        |    |                        |    |
| Ampicillin      | -              | -  | 23                     | 32 |                        |    |
| Gentamycin      | -              | -  | -                      | -  | 17                     | 19 |

NA: no activity. Results of the antimicrobial evaluation are expressed as the mean of inhibition zone diameter (mm) for different compounds tested in triplicate: *Aspergillus fumigatus* (RCMB 002008 (4) (AF), *Candida albicans* (RCMB 05036) (CA), *Staphylococcus aureus* (RCMB010010) (SA), *Bacillus subtilis* (RCMB 010067) (BS), *Salmonella SP.* (RCMB 010043) (SSP), *Escherichia coli* (RCMB 010052) (EC).

The results of Table 4 illustrate the following points:

- All the tested compounds except compound **7** showed excellent activity against *Aspergillus fumigatus*. Compounds **4** and **6** were especially effective.
- All tested compounds except compound **8** showed high antifungal activity against *Candida albicans*.
- Compounds **3b**, **7**, and **8** were found to be more active against *Staphylococcus aureus* than against *Bacillus subtilis*.
- The best antibacterial activity was observed for compounds **4** and **6**: their inhibitory effect appears to be equipotent to Gentamycin against *Salmonella SP* and *Escherichia coli*.

Many thiocarbamate derivatives such as tolinaftate, tolcliate, and piritetrate are commonly used as fungicidal agents, and this explains the highest antifungal activity of compound **4** [61–65].

### 3. Materials and Methods

#### 3.1. Chemistry

##### 3.1.1. Materials and Equipment

See Supplementary Materials.

##### 3.1.2. Synthesis of 3,6-Dimethylpyrazolo[5,1-*b*]thiazole-2,7-dicarbohydrazide (**2**)

A mixture of diethyl 3,6-dimethylpyrazolo[5,1-*b*]thiazole-2,7-dicarboxylate (**1**) [51] (1.48g, 5 mmol), and hydrazine hydrate (80%, 15 mmol) in ethanol (15 mL) were refluxed for 3 h. Excess ethanol was evaporated under reduced pressure and the solid product was filtered, dried, and recrystallized from ethanol/DMF to afford target compound **2** at 90% yield; mp: 210–211 °C; IR (KBr)  $\nu_{\max}$  3338–3201(NH<sub>2</sub>+NH), 1717 (C=O) cm<sup>-1</sup>; <sup>1</sup>H NMR (CDCl<sub>3</sub>):  $\delta$  2.04 (s, 3 H, CH<sub>3</sub>), 2.16 (s, 3 H, CH<sub>3</sub>), 3.31 (s, 4H, NH<sub>2</sub>), 11.58 (s, 2 H, 2NH); <sup>13</sup>C NMR (CDCl<sub>3</sub>):  $\delta$  13.52 (CH<sub>3</sub>), 15.68 (CH<sub>3</sub>), 128.55, 129.71, 137.77, 137.86, 147.46, 186.80 (C=O); MS *m/z* (%) 268 (M<sup>+</sup>, 41%), 251 (100%). Anal. Calcd. for C<sub>9</sub>H<sub>12</sub>N<sub>6</sub>O<sub>2</sub>S (268.30): C, 40.29; H, 4.51; N, 31.32. Found: C, 40.33; H, 4.62; N, 31.25.

### 3.1.3. Synthesis of Hydrazones 3a,b

A mixture of hydrazide **2** (0.536g, 2 mmol) and appropriate aldehydes (4.2 mmol) in absolute ethanol/DMF (20mL) were refluxed for 5 h. The resulting precipitate was filtered off, washed, dried, and recrystallized by DMF/ethanol to afford the corresponding hydrazones **3a,b**.

**3a**: Yield (72%), mp. > 300 °C; IR (KBr)  $\nu_{\max}$  3274 (NH), 1714 (C=O), 1609 (C=N)  $\text{cm}^{-1}$ ;  $^1\text{H-NMR}$  ( $\text{CDCl}_3$ ):  $\delta$  1.92 (s, 3H,  $\text{CH}_3$ ), 2.20 (s, 3H,  $\text{CH}_3$ ), 6.78 (s, 2H, 2CH), 7.23–7.85 (m, 10H, ArH), 10.78 (s, 1H, NH), 11.75 (s, 1H, NH);  $^{13}\text{C-NMR}$ :  $\delta$  11.02 ( $\text{CH}_3$ ), 14.0 ( $\text{CH}_3$ ), 111.12, 128.5, 129.8, 130.3, 133.1, 135.7, 136.0, 146.2, 151.4, 163.0, 167.2 (C=O). Anal. Calcd. for  $\text{C}_{23}\text{H}_{20}\text{N}_6\text{O}_2\text{S}$  (444.51): C, 62.15; H, 4.54; N, 18.91. Found: C, 62.22; H, 4.42; N, 18.77.

**3b**: Yield (80%), mp. 260 °C; IR (KBr)  $\nu_{\max}$  3515 (NH), 1686 (C=O), 1595 (C=N)  $\text{cm}^{-1}$ ;  $^1\text{H-NMR}$  ( $\text{CDCl}_3$ ):  $\delta$ , 1.90 (s, 3H,  $\text{CH}_3$ ), 2.20 (s, 3H,  $\text{CH}_3$ ), 2.45 (s, 6H, 2 $\text{CH}_3$ ), 6.81 (s, 2H, 2CH), 7.28–7.84 (m, 8H, ArH), 11.25 (s, 2H, 2NH);  $^{13}\text{C-NMR}$ :  $\delta$  11.50 ( $\text{CH}_3$ ), 14.31 ( $\text{CH}_3$ ), 18.95 (2 $\text{CH}_3$ ), 111.30, 128.1, 129.7, 131.20, 133.1, 136.12, 136.7, 148, 151.0, 156.0, 163.0, 165.61 (C=O). Anal. Calcd. for  $\text{C}_{25}\text{H}_{24}\text{N}_6\text{O}_2\text{S}$  (472.56): C, 63.54; H, 5.12; N, 17.78. Found: C, 63.34; H, 5.22; N, 17.87.

### 3.1.4. Synthesis of O-Ethyl N-phenylcarbamothioate (4)

A mixture of hydrazide (**2**) (0.268g, 1 mmol) and phenyl isothiocyanate (0.27 g, 0.24 mL, 2 mmol) in EtOH (10 mL), in the presence of a few drops of triethylamine as a catalyst, was heated under reflux for 5 h and then allowed to cool to room temperature. The precipitated solid was filtered off, dried, and recrystallized from methanol to afford compound **4** [52] at 20% yield; mp: 55–56 °C; IR (KBr)  $\nu_{\max}$  3212 (NH), 3039, 2982 (CH)  $\text{cm}^{-1}$ ;  $^1\text{H NMR}$  ( $\text{CDCl}_3$ ):  $\delta$  1.23 (t, 3 H,  $\text{CH}_3$ ), 4.65 (q, 2 H,  $\text{CH}_2$ ), 7.20–7.46 (m, 5H, ArH), 9.12 (s, 1 H, NH);  $^{13}\text{C NMR}$  ( $\text{CDCl}_3$ ):  $\delta$ 14.90, 68.50, 121.10, 121.10, 128.40, 129.57, 129.57, 137.85 (Ar-C), 188.50 (C=S). Anal. Calcd. for  $\text{C}_9\text{H}_{11}\text{NOS}$  (181.25): C, 59.64; H, 6.12; N, 7.73. Found: C, 59.75; H, 6.07; N, 7.88.

### 3.1.5. Synthesis of Bis(1,3,4-oxadiazole) 6

Hydrazide **2** (3.75 g, 14 mmol) was dissolved in absolute ethanol (50 mL).  $\text{CS}_2$  (2.7g, 2.1 mL, 35 mmol) was then added to the solution, followed by the addition of a KOH solution (1.6 g, 28 mmol) in water (20 mL). The reaction mixture was thoroughly stirred and refluxed for 3 h until the evolution of  $\text{H}_2\text{S}$  ceased. After completion of the reaction, excess ethanol was removed under reduced pressure. The mixture was poured into a mixture of  $\text{H}_2\text{O}$ /ice and acidified with concentrated HCl. The precipitated solid was filtered off and recrystallized from ethanol/DMF, resulting in thione **6**. Yield (40%); mp. 250 °C; IR (KBr)  $\nu_{\max}$  3313 (NH), and 1116 (C=S)  $\text{cm}^{-1}$ ;  $^1\text{H NMR}$  ( $\text{CDCl}_3$ ):  $\delta$  1.31 (s, 3H,  $\text{CH}_3$ ), 2.48 (s, 3H,  $\text{CH}_3$ ), 12.90 (s, 2H, NH);  $^{13}\text{C-NMR}$   $\delta$  11.50 ( $\text{CH}_3$ ), 14.01( $\text{CH}_3$ ), 104.02, 107.30, 135.11, 142.90, 156.74, 162.21, 177.77 (C=S). Anal. Calcd. for  $\text{C}_{11}\text{H}_8\text{N}_6\text{O}_2\text{S}_3$  (352.42): C, 37.49; H, 2.29; N, 23.85; Found: C, 37.38; H, 2.18; N, 23.99.

### 3.1.6. Synthesis of Bis(pyrazole) Derivative 7

A mixture of hydrazide **2** (1.34 g, 5 mmol) and ethyl cyanoacetate (2.26 mL, 20 mmol) in ethanol (10 mL) was heated under reflux for 5 h. The precipitated solid product was filtered and recrystallized from ethanol, resulting in **7** at 55% yield; mp. 250–251 °C; IR (KBr)  $\nu_{\max}$  3164 (NH), 2982 (CH aliphatic), 1726, 1651 (2C=O), 1560 (C=N)  $\text{cm}^{-1}$ ; MS  $m/z$  (%) 402 ( $\text{M}^+$ , 4%), 400 (52%), 399 (35%), 45 (100%). Anal. Calcd. for  $\text{C}_{15}\text{H}_{14}\text{N}_8\text{O}_4\text{S}$  (402.39): Calc.: C, 44.77; H, 3.51; N, 27.85. Found: C, 44.65; H, 3.42; N, 27.93.

### 3.1.7. Synthesis 3,6-Dimethylpyrazolo[5,1-b]thiazole-2,7-dicarbonyl Azide (8)

To a suspension of hydrazide **2** (2.68 g, 10 mmol) in 30 mL of  $\text{H}_2\text{O}$ , 3.5 g (50 mmol) of sodium nitrite was added. The mixture was then cooled in ice and treated portion-wise with 3 mL (50 mmol) of acetic acid. After stirring at room temperature for 3 h, the resulting precipitate **8** was filtered, washed with  $\text{H}_2\text{O}$ , and dried: yield 90%; mp 120–121 °C; IR (KBr)

$\nu_{\max}$  2982 (CH), 2167 (N=N), 1724 (C=O), 1686 (C=O)  $\text{cm}^{-1}$ ; MS  $m/z$  (%) 290 ( $\text{M}^+$ , 14%), 40 (100%). Anal. Calcd for  $\text{C}_9\text{H}_6\text{N}_8\text{O}_2\text{S}$  (290.26): C, 37.24; H, 2.08; N, 38.60. Found: C, 37.35; H, 2.16; N, 38.49.

### 3.1.8. Synthesis of Bis(1,2,3-triazole) Derivatives 9,10

Compound 8 (0.290 g, 1 mmol) was added to a stirred solution of sodium metal (0.10 g) in ethanol (20 mL), and the mixture was left to stir at room temperature for 20 min. Either ethyl acetoacetate or ethyl cyanoacetate (2 mmol) was added while stirring. The reaction mixture was then left to stir for a further 24 h. The formed solid product was filtered off, washed with water, dried, and recrystallized from EtOH to afford the corresponding bis(1,2,3-triazole) derivatives 9 and 10, respectively.

**9.** Yield (72%), mp. 300 °C; IR (KBr)  $\nu_{\max}$  1694 (2C=O), 1594 (C=N)  $\text{cm}^{-1}$ ;  $^1\text{H-NMR}$  ( $\text{CDCl}_3$ ):  $\delta$  1.31 (s, 6H, 2 $\text{CH}_3$ ), 2.26 (s, 6H, 2 $\text{CH}_3$ ), 2.38 (s, 6H, 2 $\text{CH}_3$ ), 4.32 (q, 4H, 2 $\text{CH}_2$ );  $^{13}\text{C-NMR}$ :  $\delta$  13.40, 14.3, 15.10, 18.10, 60.75, 111.10, 130.0, 134.0, 137.20, 138.0, 145.00, 151.15, 164.93, 169.34 (C=O). Anal. Calcd. for  $\text{C}_{21}\text{H}_{22}\text{N}_8\text{O}_6\text{S}$  (514.51): C, 49.02; H, 4.31; N, 21.78. Found: C, 49.13; H, 4.37; N, 21.88.

**10.** Yield (75%), mp. 210–211 °C; IR (KBr)  $\nu_{\max}$  1697 (2C=O), 1597 (C=N)  $\text{cm}^{-1}$ ;  $^1\text{H-NMR}$  ( $\text{CDCl}_3$ ):  $\delta$  1.19 (s, 6H, 2 $\text{CH}_3$ ), 2.46 (s, 3H,  $\text{CH}_3$ ), 3.30 (s, 3H,  $\text{CH}_3$ ), 4.28 (q, 4H, 2 $\text{CH}_2$ ), 7.71 (s, 4H,  $\text{NH}_2$ );  $^{13}\text{C-NMR}$ :  $\delta$  12.40, 15.10, 19.44, 60.23, 61.75, 111.30, 131.20, 133.89, 137.20, 138.20, 146.00, 151.02, 165.93, 169.20 (C=O). Anal. Calcd. for  $\text{C}_{19}\text{H}_{20}\text{N}_{10}\text{O}_6\text{S}$  (516.49): C, 44.18; H, 3.90; N, 27.12. Found: C, 44.22; H, 3.84; N, 27.23.

## 3.2. Biological Tests

### 3.2.1. Evaluation of Antitumor Activity

The MTT assay was used to investigate the *in vitro* antitumor activity of the synthesized compounds against two human cancer cell lines: human hepatocellular carcinoma cell line (HepG-2) and colon carcinoma cell line (HCT-116) [57].

### 3.2.2. Antimicrobial Evaluation

The inhibition zone technique [60] was used to evaluate the antimicrobial activity of the synthesized compounds against six pathogens. Amphotericin B, Gentamicin, and Ampicillin were the standard medications utilized for comparison. The antimicrobial activity was measured using the inhibition zone diameter (IZD).

## 4. Conclusions

New pyrazolo[5,1-*b*]thiazole derivatives, synthesized using simple synthetic methods, can be used as leading compounds in the development of future, novel drug molecules.

**Supplementary Materials:** The following are available online, Online supplementary information includes detailed methods of the antitumor and antimicrobial evaluations, Figures S1–S4: IR, Mass,  $^1\text{H-NMR}$ , and  $^{13}\text{C-NMR}$  spectra of compound 1, Figures S5–S7: IR,  $^{13}\text{C-NMR}$  and Mass spectra of compound 2, Figures S8–S10: IR,  $^1\text{H-NMR}$ , and  $^{13}\text{C-NMR}$  spectra of compound 4, Figures S11,S12: IR, and Mass spectra of compound 7, Figures S13,S14: IR, and Mass spectra of compound 8.

**Author Contributions:** Data curation, A.A., A.B.M., Y.I.A., F.A.A.-a., H.A.G. and Y.N.M.; Formal analysis, A.A., H.A.G. and Y.N.M.; Funding acquisition, Y.N.M.; Investigation, Y.N.M.; Methodology, Y.N.M.; Project administration, Y.N.M.; Supervision, Y.I.A. and Z.M.A.; Writing—original draft, Y.N.M.; Writing—review & editing, N.A.K. All authors have read and agreed to the published version of the manuscript.

**Funding:** This work was financially supported by the Deanship of Scientific Research, King Khalid University (Grant No. R.G.P2/26/ 42).

**Institutional Review Board Statement:** Not applicable.

**Informed Consent Statement:** Not applicable.

**Data Availability Statement:** The data presented in this study are available on request from the corresponding author.

**Acknowledgments:** The financial support by the Deanship of Scientific Research (Grant No. R.G.P2/26/42), King Khalid University, Saudi Arabia is gratefully acknowledged.

**Conflicts of Interest:** The authors declare that they have no known competing financial interests or personal relationships that could have appeared to influence the work reported in this paper.

**Sample Availability:** Samples of the compounds are available from the authors.

## References

- Ventola, C.L. The antibiotic resistance crisis: Part 1: Causes and threats. *Pharm. Ther.* **2015**, *40*, 277–283.
- Chandrakantha, B.; Shetty, P.; Nambiyar, V.; Isloor, N.; Isloor, A.M. Synthesis, characterization and biological activity of some new 1,3,4-oxadiazole bearing 2-fluoro-4-methoxy phenyl moiety. *Eur. J. Med. Chem.* **2010**, *45*, 1206–1210. [CrossRef]
- Vijesh, A.M.; Isloor, A.M.; Shetty, P.; Sundershan, S.; Fun, H.K. New pyrazole derivatives containing 1,2,4-triazoles and benzoxazoles as potent antimicrobial and analgesic agents. *Eur. J. Med. Chem.* **2013**, *62*, 410–415. [CrossRef]
- Farooqi, S.I.; Arshad, N.; Channar, P.A.; Perveen, F.; Saeed, A.; Larik, F.A.; Javeed, A. Synthesis, theoretical, spectroscopic and electrochemical DNA binding investigations of 1,3,4-thiadiazole derivatives of ibuprofen and ciprofloxacin: Cancer cell line studies. *J. Photochem. Photobiol.* **2018**, *189*, 104–118. [CrossRef] [PubMed]
- Nagai, H.; Kim, Y. Cancer prevention from the perspective of global cancer burden patterns. *J. Thorac. Dis.* **2017**, *9*, 448–451. [CrossRef]
- Molina, J.R.; Yang, P.; Cassivi, S.D.; Schild, S.E.; Adjei, A.A. Non-small cell lung cancer: Epidemiology, risk factors, treatment, and survivorship. *Mayo Clin. Proc.* **2008**, *83*, 584–594. [CrossRef]
- Bhatt, P.; Kumar, M.; Jha, A. Design, Synthesis and Anticancer Evaluation of Oxa/Thiadiazolyhydrazones of Barbituric and Thiobarbituric Acid: A Collective In Vitro and In Silico Approach. *Chem. Select.* **2018**, *3*, 7060–7065. [CrossRef]
- Rashid, M.; Husain, A.; Mishra, R.; Karim, S.; Khan, S.; Ahmad, M.; Khan, S.A. Design and synthesis of benzimidazoles containing substituted oxadiazole, thiadiazole and triazolo-thiadiazines as a source of new anticancer agents. *Arab. J. Chem.* **2015**, *12*, 3202–3224. [CrossRef]
- Carter, J.S.; Kramer, S.; Talley, J.J.; Penning, T.; Collins, P.; Graneto, M.J.; Seibert, K.; Koboldt, C.; Masferrer, J.; Zweifel, B. Synthesis and activity of sulfonamide-substituted 4,5-diaryl thiazoles as selective cyclooxygenase-2 inhibitors. *Bioorg. Med. Chem. Lett.* **1999**, *9*, 1171–1174. [CrossRef]
- Hargrave, K.D.; Hess, F.K.; Oliver, J.T. N-(4-substituted-thiazolyl)oxamic acid derivatives, a new series of potent, orally active antiallergy agents. *J. Med. Chem.* **1983**, *26*, 1158–1163. [CrossRef] [PubMed]
- Bondock, S.; Khalifa, W.; Fadda, A.A. Synthesis and antimicrobial evaluation of some new thiazole, thiazolidinone and thiazoline derivatives starting from 1-chloro-3,4-dihydronaphthalene-2-carboxaldehyde. *Eur. J. Med. Chem.* **2007**, *42*, 948–954. [CrossRef] [PubMed]
- Patt, W.C.; Hamilton, H.W.; Taylor, M.D.; Ryan, M.J.; Taylor, D.G., Jr.; Connolly, C.J.C.; Doherty, A.M.; Klutchko, S.R.; Sircar, I.; Steinbaugh, B.A.; et al. Structure-activity relationships of a Series of 2-Amino-4-thiazole Containing Renin Inhibitors. *J. Med. Chem.* **1992**, *35*, 2562–2572. [CrossRef]
- Sharma, P.K.; Sawhney, S.N.; Gupta, A.; Singh, G.B.; Bani, S. Synthesis and antiinflammatory activity of some 3-(2-thiazolyl)-1,2-benzisothiazoles. *Indian J. Chem.* **1998**, *37B*, 376–381.
- Jaen, J.C.; Wise, L.D.; Caprathe, B.W.; Teclé, H.; Bergmeier, S.; Humblet, C.C.; Heffner, T.G.; Meltzner, L.T.; Pugsley, T.A. 4-(1,2,5,6-Tetrahydro-1-alkyl-3-pyridinyl)-2-thiazolamines: A novel class of compounds with central dopamine agonist properties. *J. Med. Chem.* **1990**, *33*, 311–317. [CrossRef]
- Ergenc, N.; Capan, G.; Gunay, N.S.; Ozkirimli, S.; Gungor, M.; Ozbey, S.; Kendi, E. Synthesis and hypnotic activity of new 4-thiazolidinone and 2-thioxo-4,5-imidazolidinedione derivatives. *Arch. Pharm. Pharm. Med. Chem.* **1999**, *332*, 343–347. [CrossRef]
- Tsuji, K.; Ishikawa, H. Synthesis and anti-pseudomonal activity of new 2-isocephems with a dihydroxypyridone moiety at C-7. *Bioorg. Med. Chem. Lett.* **1994**, *4*, 1601–1606. [CrossRef]
- Bell, F.W.; Cantrell, A.S.; Hogberg, M.; Jaskunas, S.R.; Johansson, N.G.; Jordon, C.L.; Kinnick, M.D.; Lind, P.; Morin, J.M., Jr.; Noreen, R.; et al. Phenethylthiazolethiourea (PETT) Compounds, a New Class of HIV-1 Reverse Transcriptase Inhibitors. 1. Synthesis and Basic Structure-Activity Relationship Studies of PETT Analogs. *J. Med. Chem.* **1995**, *38*, 4929–4936. [CrossRef] [PubMed]
- Sharma, P.C.; Bansal, K.K.; Sharma, A.; Sharma, D.; Deep, A. Thiazole-containing compounds as therapeutic targets for cancer therapy. *Eur. J. Med. Chem.* **2020**, *188*, 112016. [CrossRef] [PubMed]
- Isloor, A.M.; Kalluraya, B.; Shetty, P. Regioselective reaction: Synthesis, characterization and pharmacological studies of some new Mannich bases derived from 1,2,4-triazoles. *Eur. J. Med. Chem.* **2009**, *44*, 3784–3787. [CrossRef]
- Isloor, A.M.; Kalluraya, B.; Rao, M. Sydnone derivatives: Part IV; synthesis of 3-aryl-4-(substituted pyrazolidene hydrazine-4-thiazolyl) sydnones as possible analgesic and anticonvulsant agents. *J. Saudi Chem. Soc.* **2000**, *4*, 265–270.

21. Kalluraya, B.; Isloor, A.M.; Shenoy, S. Synthesis and biological activity of 6-substituted-3-[4-(3-substituted pyrazolidene) hydrazino-4-thiazolyl] coumarins. *Indian J. Heterocycl. Chem.* **2001**, *11*, 159–162.
22. Sunil, D.; Isloor, A.M.; Shetty, P. Synthesis, characterization and anticancer activity of 1,2,4-Triazolo [3,4-b]-1,3,4-thiadiazoles on Hep G2 cell lines. *Der. Pharma Chem.* **2009**, *1*, 19–26.
23. Canonico, P.G.; Jahrling, P.B.; Pannier, W.L. Antiviral efficacy of pyrazofurin against selected RNA viruses. *Antivir. Res.* **1982**, *2*, 331–337. [CrossRef]
24. Westhead, J.E.; Price, H.D. Quantitative assay of pyrazofurin a new antiviral, antitumor antibiotic. *Antimicrob. Agents Chemother.* **1974**, *5*, 90–91. [CrossRef]
25. Ardiansah, B.A.Y.U. Recent reports on pyrazole-based bioactive compounds as candidate for anticancer agents. *Asian J. Pharm. Clin. Res.* **2017**, *12*, 45. [CrossRef]
26. Pulici, M.; Marchionni, C.; Piutti, C.; Gasparri, F. Bicyclic pyrazoles as protein kinase inhibitors. WO 2010070060 (2010). *Chem. Abstr.* **2010**, *153*, 87782.
27. Desai, N.; Trivedi, A.; Pandit, U.; Dodiya, A.; Rao, V.K.; Desai, P. Hybrid Bioactive Heterocycles as Potential Antimicrobial Agents: A Review. *Mini Rev. Med. Chem.* **2016**, *16*, 1500–1526. [CrossRef]
28. Mahajan, N.S.; Pattana, S.R.; Jadhav, R.L.; Pimpodhar, N.V.; Manikrao, A.M. Synthesis of some thiazole compounds of biological interest containing mercapta group. *Int. J. Chem. Sci.* **2008**, *6*, 800–806.
29. Rizk, H.; El-Borai, M.A.; Ragab, A.; Ibrahim, S.A. Design, synthesis, biological evaluation and molecular docking study based on novel fused pyrazolothiazole scaffold. *J. Iran. Chem. Soc.* **2020**, *17*, 2493–2505. [CrossRef]
30. Chandanshive, J.Z.; Bonini, B.F.; Tiznado, W.; Escobar, C.A.; Caballero, J.; Femoni, C.; Fochi, M.; Franchini, M.C. 1,3-Dipolar Cycloaddition of Nitrile Imines with Cyclic  $\alpha$ - $\beta$ -Unsaturated Ketones: A Regiochemical Route to Ring-Fused Pyrazoles. *Eur. J. Org. Chem.* **2011**, *25*, 4806–4813. [CrossRef]
31. Abdel-Wahab, B.F.; Mohamed, H.A. Pyrazolothiazoles: Synthesis and Applications. *Phosphorus Sulfur Silicon Relat. Elem.* **2013**, *188*, 1680–1693. [CrossRef]
32. Takahashi, Y.; Hashizume, M.; Shin, K.; Terauchi, T.; Takeda, K.; Hibi, S.; Murata-Tai, K.; Fujisawa, M.; Shikata, K.; Taguchi, R.; et al. Design, synthesis, and structure-activity relationships of novel pyrazolo[5,1-b]thiazole derivatives as potent and orally active corticotropin-releasing factor 1 receptor antagonists. *J. Med. Chem.* **2012**, *55*, 8450–8463. [CrossRef]
33. Lu, X.; Tang, J.; Liu, Z.; Li, M.; Zhang, T.; Zhang, X.; Ding, K. Discovery of new chemical entities as potential leads against Mycobacterium tuberculosis. *Bioorg. Med. Chem. Lett.* **2016**, *26*, 5916–5919. [CrossRef]
34. Rollas, S.; Gulerman, N.; Erdeniz, H. Synthesis and antimicrobial activity of some new hydrazones of 4-fluorobenzoic acid hydrazide and 3-acetyl-2,5-disubstituted-1,3,4-oxadiazolines. *Farmaco* **2002**, *57*, 171–174. [CrossRef]
35. Pavan, F.R.; Maia, P.I.D.S.; Leite, S.R.; Deflon, V.M.; Batista, A.A.; Sato, D.N.; Leite, C.Q. Thiosemicarbazones, semicarbazones, dithiocarbazates and hydrazide/hydrazones: Anti-Mycobacterium tuberculosis activity and cytotoxicity. *Eur. J. Med. Chem.* **2010**, *45*, 1898–1905. [CrossRef]
36. Marastoni, M.; Baldisserotto, A.; Trapella, C.; McDonald, J.; Bortolotti, F.; Tomatis, R. HIV protease inhibitors: Synthesis and activity of N-aryl-N'-hydroxyalkyl hydrazide pseudopeptides. *Eur. J. Med. Chem.* **2005**, *5*, 445–451. [CrossRef] [PubMed]
37. Tabanca, N.; Ali, A.; Bernier, U.R.; Khan, I.A.; Kocyigit-Kaymakcioglu, B.; Oruç-Emre, E.E.; Unsalan, S.; Rollas, S. Biting deterrence and insecticidal activity of hydrazide-hydrazones and their corresponding 3-acetyl-2,5-disubstituted 2,3-dihydro-1,3,4-oxadiazoles against Aedes aegypti. *Pest. Manag. Sci.* **2013**, *69*, 703–708. [CrossRef]
38. Turan-Zitouni, G.; Altintop, M.D.; Özdemir, A.; Demirci, F.; Mohsen, U.A.; Kaplancıklı, Z.A. Synthesis and antifungal activity of new hydrazide derivatives. *J. Enzyme Inhib. Med. Chem.* **2013**, *28*, 1211–1216. [CrossRef]
39. Vardanyan, R.S.; Hruby, V.J. Antidepressants. In *Synthesis of Essential Drugs*; Elsevier: Amsterdam, The Netherlands, 2006; pp. 103–116.
40. Patole, J.; Sandbhor, U.; Padhye, S.; Deobagkar, D.N.; Ansonc, C.E.; Powell, A. Structural chemistry and in vitro antitubercular activity of acetylpyridine benzoyl hydrazone and its copper complex against Mycobacterium smegmatis. *Bioorg. Med. Chem. Lett.* **2004**, *13*, 51–55. [CrossRef]
41. Maccari, R.; Ottana, R.; Vigorita, M.G. In vitro advanced antimycobacterial screening of isoniazid-related hydrazones, hydrazides and cyanoboranes: Part 14. *Bioorg. Med. Chem. Lett.* **2005**, *15*, 2509–2513. [CrossRef]
42. Bottari, B.; Maccari, R.; Monforte, F.; Ottana, R.; Vigorita, M.G.; Bruno, G.; Nicolo, F.; Rotondo, A.; Rotondo, E. Nickel(II) 2,6-diacetylpyridine bis(isonicotinoylhydrazonate) and bis(benzoylhydrazonate) complexes: Structure and antimycobacterial evaluation. Part XI. *Bioorg. Med. Chem.* **2001**, *9*, 2203–2211. [CrossRef]
43. Al-Ajely, M.S.; Yaseen, A.N. Synthesis and Characterization of Some New Hydrazides and Their Derivatives. *Ibn AL-Haitham J. For. Pure Appl. Sci.* **2017**, *28*, 103–112.
44. Elshaarawy, R.F.; Janiak, C. 2-Thiophenecarbohydrazides: A novel efficient method for the synthesis of 2-thiophenecarbohydrazide. *Z. Nat. B* **2011**, *66*, 1202–1208.
45. Khodair, A.I.; Ahmed, A.; Emam, D.R.; Kheder, N.A.; Elmalki, F.; Hadda, T.B. Synthesis, Antiviral, DFT and Molecular Docking Studies of Some Novel 1,2,4-Triazine Nucleosides as Potential Bioactive Compounds. *Carbohydr. Res.* **2021**, *500*, 108246. [CrossRef] [PubMed]

46. Gomha, S.M.; Edrees, M.M.; Muhammad, Z.A.; Kheder, N.A.; Abu-Melha, S.; Saad, A.M. Synthesis, Characterization, and Antimicrobial Evaluation of Some New 1,4-Dihydropyridines-1,2,4-Triazole Hybrid Compounds. *Polycycl. Aromat. Compd.* **2020**. [CrossRef]
47. Hadda, T.B.; Deniz, F.S.S.; Orhan, I.E.; Zgou, H.; Rauf, A.; Mabkhot, Y.N.; Bennani, B.; Emam, D.R.; Kheder, N.A.; Asayari, A.; et al. Spiro Heterocyclic Compounds as Potential Anti-Alzheimer agents (Part 2): Their Metal Chelation Capacity, POM Analyses and DFT Studies. *Med. Chem.* **2021**, *17*. [CrossRef]
48. Mabkhot, Y.; Algarni, H.; Alsayari, A.; bin Muhsinah, A.; Kheder, N.A.; Almarhoon, Z.; Al-Aizari, F. Synthesis, X-ray Analysis, Biological Evaluation and Molecular Docking Study of New Thiazoline Derivatives. *Molecules* **2019**, *24*, 1654. [CrossRef]
49. Mabkhot, Y.; Alharbi, M.; Al-Showiman, S.; Soliman, S.; Kheder, N.A.; Frey, W.; Asayari, A.; Bin Muhsinah, A.; Algarni, H. A novel synthesis, X-ray analysis and computational studies of (Z)-ethyl 2-((Z)-5-((dimethylamino)methylene)-4-oxo-3-phenylthiazolidin-2-ylidene)acetate as a potential anticancer agent. *BMC Chem.* **2019**, *13*, 35. [CrossRef]
50. Abu-Melha, S.; Edrees, M.M.; Salem, H.H.; Kheder, N.A.; Gomha, S.M.; Abdelaziz, M.R. Synthesis and biological evaluation of some novel thiazole-based heterocycles as potential anticancer and antimicrobial agents. *Molecules* **2019**, *24*, 539. [CrossRef] [PubMed]
51. Al-aizari, F.A. Synthesis of Some Thioxothiazole Derivatives and Evaluation of their Biological Activity. Ph.D. Thesis, King Saud University, Riyadh, Saudi Arabia, 2017.
52. Sahoo, S.K.; Chakraborty, S.; Patel, B.K. A one-pot conversion of di-substituted thiourea to O-organyl arylthiocarbamate using FeCl<sub>3</sub>. *J. Sulphur Chem.* **2012**, *33*, 143–153. [CrossRef]
53. Horning, D.E.; Muchowski, J.M. Five-membered Heterocyclic Thiones. Part I. 1,3,4-Oxadiazole-2-thione. *Can. J. Chem.* **1972**, *50*, 3079–3082. [CrossRef]
54. Tomi, I.H.; Al-Qaisi, A.H.; Al-Qaisi, Z.H. Synthesis, characterization and effect of bis-1,3,4-oxadiazole rings containing glycine moiety on the activity of some transferase enzymes. *J. King Saud Univ. Sci.* **2011**, *23*, 23–33. [CrossRef]
55. Thurston, D.E.; Pysz, I. *Chemistry and Pharmacology of Anticancer Drugs*, 2nd ed.; CRC Press: Boca Raton, FL, USA, 2021. [CrossRef]
56. Ramachary, D.B.; Gujral, J.; Peraka, S.; Reddy, G.S. Triazabicyclodecene as an Organocatalyst for the Regiospecific Synthesis of 1,4,5-Trisubstituted N-Vinyl-1,2,3-triazoles. *Eur. J. Org. Chem.* **2017**, *3*, 459–464. [CrossRef]
57. Mosmann, T. Rapid colorimetric assay for cellular growth and survival: Application to proliferation and cytotoxicity assays. *J. Immunol. Methods* **1983**, *65*, 55–63. [CrossRef]
58. Glomb, T.; Szymankiewicz, K.; Świątek, P. Anti-cancer activity of derivatives of 1,3,4-oxadiazole. *Molecules* **2018**, *23*, 3361. [CrossRef]
59. Fu, D.J.; Fu, L.; Liu, Y.C.; Wang, J.W.; Wang, Y.Q.; Han, B.K.; Li, X.R.; Zhang, C.; Li, F.; Song, J.; et al. Structure-activity relationship studies of β-lactam-azide analogues as orally active antitumor agents targeting the tubulin colchicine site. *Sci. Rep.* **2017**, *7*, 12788. [CrossRef]
60. Ghorab, M.M.; Alsaied, M.S.; El-Gaby, M.S.; Safwat, N.A.; Elaasser, M.M.; Soliman, A.M. Biological evaluation of some new N-(2,6-dimethoxypyrimidinyl)thioureido benzenesulfonamide derivatives as potential antimicrobial and anticancer agents. *Eur. J. Med. Chem.* **2016**, *124*, 299–310. [CrossRef] [PubMed]
61. Petranyi, G.; Ryer, N.S.; Stutz, A. Allylamine derivatives: New class of synthetic antifungal agents inhibiting fungal squalene epoxidase. *Science* **1984**, *224*, 1239–1241. [CrossRef]
62. Ryder, N.S.; Dupont, M.C. Inhibition of squalene epoxidase by allylamine antimycotic compounds. A comparative study of the fungal and mammalian enzymes. *Biochem. J.* **1985**, *230*, 765–770.
63. Ryder, N.S.; Frank, I.; Dupont, M.C. Ergosterol biosynthesis inhibition by the thiocarbamate antifungal agents tolinaftate and tolciclate. *Antimicrob. Agents Chemother.* **1986**, *29*, 858–860. [CrossRef] [PubMed]
64. Morita, T.; Iwata, K.; Nozawa, Y. Inhibitory effect of a new mycotic agent, piritetrate on ergosterol biosynthesis in pathogenic fungi. *Med. Vet. Mycol.* **1989**, *27*, 17–25. [CrossRef] [PubMed]
65. Iwatani, W.; Arika, T.; Yamaguchi, H. Two mechanisms of butenafine action in *Candida albicans*. *Antimicrob. Agents Chemother.* **1993**, *37*, 785–788. [CrossRef] [PubMed]

Review

# Recent Developments in Reactions and Catalysis of Protic Pyrazole Complexes

Wei-Syuan Lin<sup>1</sup> and Shigeki Kuwata<sup>2,\*</sup> 

<sup>1</sup> Department of Chemical Science and Engineering, School of Materials and Chemical Technology, Tokyo Institute of Technology, 2-12-1 E4-1 O-okayama, Meguro-ku, Tokyo 152-8552, Japan; lin.w.ae@m.titech.ac.jp

<sup>2</sup> Department of Applied Chemistry, College of Life Sciences, Ritsumeikan University, 1-1-1 Noji-higashi, Kusatsu 525-8577, Shiga, Japan

\* Correspondence: skuwata@fc.ritsumei.ac.jp

**Abstract:** Protic pyrazoles (*N*-unsubstituted pyrazoles) have been versatile ligands in various fields, such as materials chemistry and homogeneous catalysis, owing to their proton-responsive nature. This review provides an overview of the reactivities of protic pyrazole complexes. The coordination chemistry of pincer-type 2,6-bis(1*H*-pyrazol-3-yl)pyridines is first surveyed as a class of compounds for which significant advances have made in the last decade. The stoichiometric reactivities of protic pyrazole complexes with inorganic nitrogenous compounds are then described, which possibly relates to the inorganic nitrogen cycle in nature. The last part of this article is devoted to outlining the catalytic application of protic pyrazole complexes, emphasizing the mechanistic aspect. The role of the NH group in the protic pyrazole ligand and resulting metal–ligand cooperation in these transformations are discussed.

**Keywords:** pyrazole; pyrazolato; pincer ligand; metal–ligand cooperation; homogeneous catalysis; bifunctional catalysis; transfer hydrogenation; hydrazine

**Citation:** Lin, W.-S.; Kuwata, S. Recent Developments in Reactions and Catalysis of Protic Pyrazole Complexes. *Molecules* **2023**, *28*, 3529. <https://doi.org/10.3390/molecules28083529>

Academic Editors: Vera L. M. Silva and Artur M. S. Silva

Received: 16 March 2023

Revised: 12 April 2023

Accepted: 13 April 2023

Published: 17 April 2023



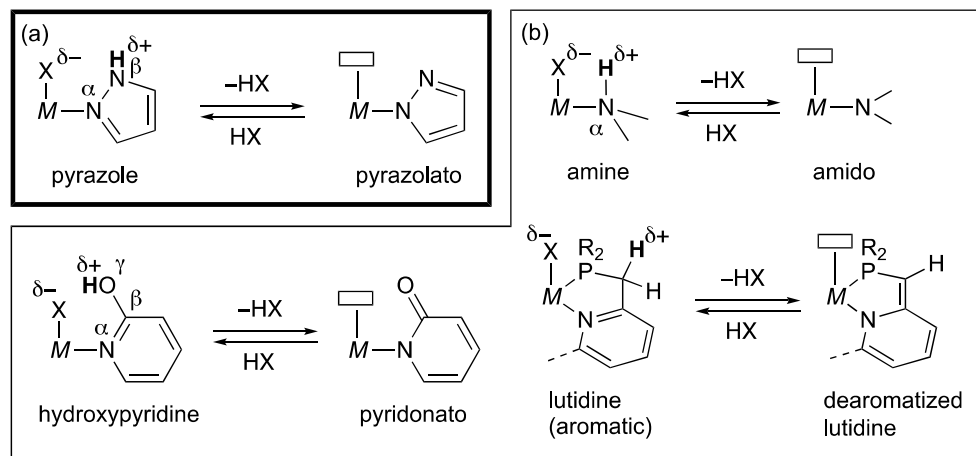
**Copyright:** © 2023 by the authors. Licensee MDPI, Basel, Switzerland. This article is an open access article distributed under the terms and conditions of the Creative Commons Attribution (CC BY) license (<https://creativecommons.org/licenses/by/4.0/>).

## 1. Introduction

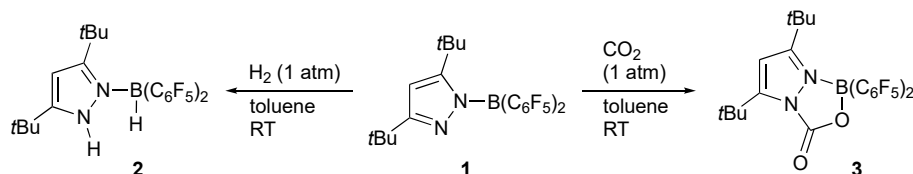
Pyrazole is an aromatic five-membered N-heterocycle containing a potentially Brønsted acidic NH group adjacent to a Schiff-base nitrogen atom. This amphiprotic character gives rise to the rich coordination chemistry of pyrazoles. Unlike aprotic N-heterocycles, such as pyridine, pyrazole can be deprotonated easily, and the resulting pyrazolate anion bridges two metal centers to form di- or polynuclear complexes in some cases. The NH group also provides a clue to integration of pyrazole units, making multidentate ligands, such as poly(pyrazolyl)borates [1]. The flexible ligand design based on the easy construction of the pyrazole ring [2–4] and N-functionalization has led to the structural diversity of the pyrazole complexes [5–8] and their applications in various fields, including materials chemistry [9], homogeneous catalysis [10,11], bioinorganic modeling [12], supramolecular chemistry [13–15], and medicinal chemistry [16].

Coordination of a pyrazole to a Lewis acidic metal center renders the pyrazole NH proton more acidic [2]. The increased Brønsted acidity causes intra- and intermolecular hydrogen bonding as well as facile deprotonation that switches the coordination mode from a lone-pair donating L-type to a covalent X-type. These events should make an electronic impact on the complex. It is to be emphasized that the deprotonation in the position  $\beta$  to the metal may be coupled with ligand dissociation on the metal center. As illustrated in Scheme 1a, elimination of HX or outer sphere transfer of nucleophilic group X along with a proton from such a “ $\beta$ -protic” pyrazole complex would yield a coordinatively unsaturated pyrazolato complex. Bond cleavage of pronucleophile HX on this complex regenerates the pyrazole complex. The interconversion associated with change in the coordination mode of the pyrazole rather than the formal oxidation state of the metal would mediate various

bond activation and transfer of HX. Such metal–ligand cooperative transformations have also been known for related proton-responsive ligands [17–26], exemplified in Scheme 1b. Nevertheless, difference in ligand acidity and relative positions to the metal center in the protic pyrazole complexes brings about their unique reactivities. Tamm and co-workers demonstrated that the pyrazolylborane **1** reacts with dihydrogen gas at room temperature to afford the zwitterionic pyrazolium borate **2** (Scheme 2) [27]. Heterocumulenes, such as carbon dioxide, also react with **1** to give the corresponding adduct **3**, for example [28]. These reactions showcase the pyrazole-based bifunctional reactivities operating even in the field of transition-metal-free, frustrated Lewis pair chemistry.



**Scheme 1.** (a) Elimination and addition of pronucleophiles HX in pyrazole complexes. (b) Representative examples of related metal–ligand cooperative interconversion.



**Scheme 2.** Bifunctional reactions of a pyrazolylborane as a frustrated Lewis pair.

In this review, we outline the reactivities of the β-protic pyrazole complexes of transition metals. The proton-responsive nature and catalytic application of this class of complexes were surveyed about a decade ago [10,11]. This article updates these earlier reviews by focusing on their stoichiometric and catalytic reactivities. Special attention will be paid to the mechanistic aspects in the discussion on the catalysis. Protic pyrazoles are also known as modules in spin-crossover materials [29–33] and phosphorescent complexes [34], which are not covered in this review. The readers can also refer to papers [33,35,36] to learn the design and synthesis of specific classes of protic pyrazole ligands.

## 2. Reactions of Protic Pyrazole Complexes

### 2.1. Pincer-Type Complexes Bearing Protic Pyrazole Arms

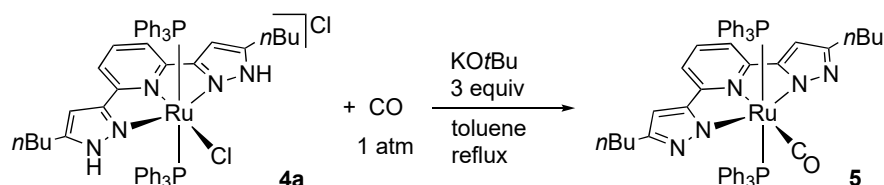
Chelation has been a rational strategy to ensure the coordination of pyrazoles for metal–ligand cooperative reactivities [35,37]. During the last decade, significant advances have been made particularly in the coordination chemistry of 2,6-bis(1*H*-pyrazol-3-yl)pyridines (R<sup>2</sup>LH<sub>2</sub>; R represents the substituent at the 5-position of the pyrazole ring), which place the two protic pyrazole groups at trans positions rigorously, owing to the rigid pincer-type framework [38]. This class of compounds have long been used as a ligand in iron(II) complexes showing thermal and photochemical spin-state transitions [29–33]. The protic pyrazole groups therein greatly affect the spin-crossover properties of the complexes through hydrogen bonding interaction with surrounding counteranion and solvent. In this



section, we describe the transition metal  $R^LH_2$  complexes and related pincer-type pyrazole complexes, focusing on their stoichiometric reactivities, which originate mostly from the protic pyrazole units.

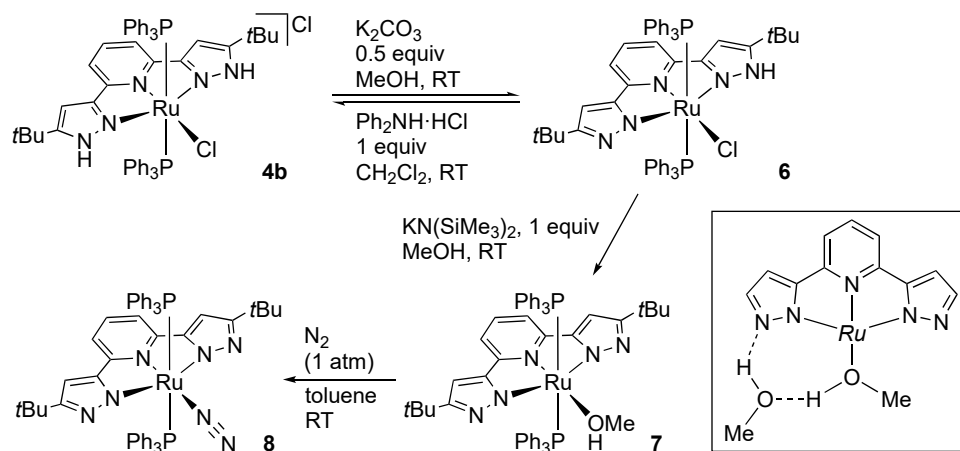
### 2.1.1. Bis(1*H*-pyrazol-3-yl)pyridine Complexes Ruthenium and Osmium

In 2010, Thiel and co-workers reported that deprotonation of the  $nBuLH_2$ -ligated ruthenium(II) complex **4a** under carbon monoxide leads to the formation of the bis(pyrazolato) carbonyl complex **5** (Scheme 3) [39]. The result shows the diprotic nature of the pincer-type complex **4a**. The  $nBuL$  complex **5** is also obtained by the dehydrogenative coordination of  $nBuLH_2$  to  $[RuH_2(CO)(PPh_3)_3]$ .



**Scheme 3.** Dehydrochlorination of a protic pincer-type ruthenium complex in the presence of carbon monoxide.

Soon after that, our group demonstrated that the deprotonation can be done stepwise and reversible at least in the first step [40]. Thus, the ruthenium(II) complex **4b** having a *tert*-butyl substituted pincer ligand,  $tBuLH_2$ , undergoes reversible deprotonation by equimolar amount of a base to afford the pyrazole–pyrazolato complex **6** (Scheme 4). The partial deprotonation of the pincer ligand is established by the  $^1H$  NMR spectrum of **6**, showing the  $D_2O$ -exchangeable NH resonance at  $\delta$  10.17 with only 1H intensity as well as inequivalence of the two pyrazole arms. The single crystal X-ray analysis allows the detailed structural comparison between the pyrazole and deprotonated pyrazolato rings. The deprotonated pyrazole group lacks neighboring hydrogen bond acceptors and features a smaller  $N_\alpha N_\beta C$  angle ( $106.8(4)^\circ$ ) due to the increased *s* character of the lone pair electrons on the deprotonated nitrogen atom [10,41]. Complete deprotonation of the pyrazole arms is achieved by an additional base in methanol, giving the bis(pyrazolato) methanol complex **7**. In the crystal of **7**, a hydrogen bonding network involving a co-crystallized methanol is observed (inset). The methanol ligand in **7** is replaced by molecular nitrogen and oxygen to yield the dinitrogen complex **8** and a side-on peroxo complex, respectively.

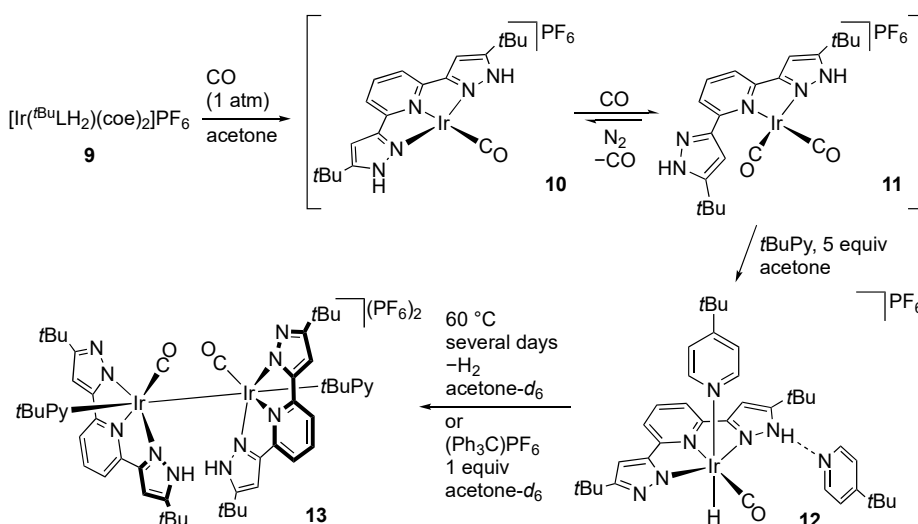


**Scheme 4.** Stepwise dehydrochlorination of the protic pincer-type ruthenium complex **4b**.

Some osmium complexes having  $^R\text{LH}_2$  or its deprotonated form are known [42,43]. Substitution reactions of  $[\text{OsCl}_2(\text{H}_2\text{O})(^t\text{BuLH}_2)]$  by bio-relevant molecules are reported [43].

### Rhodium and Iridium

Goldberg and co-workers reported the reactivities of the iridium(I) complex  $[\text{Ir}(^t\text{BuLH}_2)(\text{coe})_2]\text{PF}_6$  (**9**; coe = cyclooctene) bearing labile coe ligands (Scheme 5) [44]. The coe ligands are easily displaced by carbon monoxide, giving the bis(carbonyl) complex **11** featuring  $\kappa^2$ -coordination of the  $^t\text{BuLH}_2$  ligand. When **11** is dissolved in acetone- $d_6$  under  $\text{N}_2$ , a monocarbonyl species **10** having equivalent pyrazole arms is observed, suggesting an equilibrium between **10** and **11**. Addition of 4-*tert*-butylpyridine (*t*BuPy) to **11** results in an oxidative addition of one of the two pyrazole NH groups to afford the hydrido-iridium(III) pyrazolato complex **12**. Co-crystallization of an additional pyridine, which is engaged in hydrogen bonding with the pyrazole arm of the  $^t\text{BuLH}$  ligand, has been confirmed by X-ray analysis. Deprotonation of **12** affords the bis(pyrazolato) complex  $[\text{IrH}(\text{CO})(^t\text{BuPy})(^t\text{BuL})]$ . Triphenylphosphine also reacts with the carbonyl complex **11** with oxidative addition of the pyrazole arm; however, the isolated product is  $[\text{IrH}(\text{CO})(\text{PPh}_3)_2(^t\text{BuLH})]\text{PF}_6$ , having a  $\kappa^2$ -bound  $^t\text{BuLH}$  ligand. Interestingly, thermolysis of **12** leads to dinuclear reductive elimination of  $\text{H}_2$  to give the diiridium(II) complex **13**. Complex **13** is also formed by treatment of **12** with  $(\text{Ph}_3\text{C})\text{PF}_6$ . Deprotonation of the dicationic complex **13** yields the bis(pyrazolato) complex  $[\{\text{Ir}(\text{CO})(^t\text{BuPy})(^t\text{BuL})\}_2]$ . Isolation of the iridium complexes ranging from Ir(I) to Ir(III) indicates the electronic flexibility of the  $^R\text{LH}_n$  ( $n = 0-2$ ) ligands.



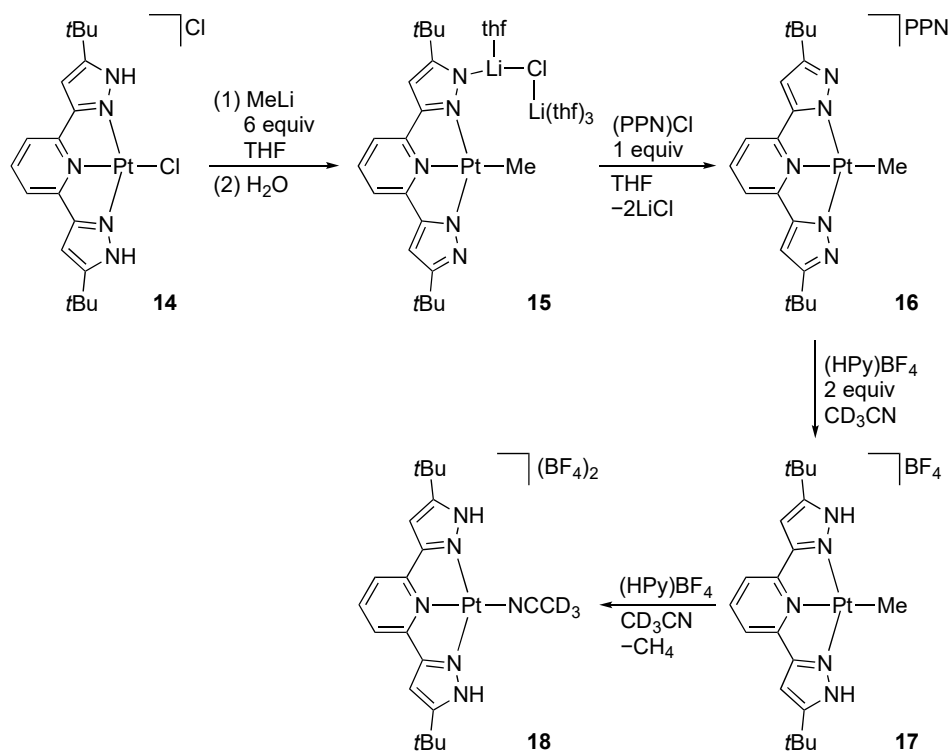
**Scheme 5.** Synthesis and reactions of  $^t\text{BuLH}_2$  iridium complexes. coe = cyclooctene; *t*BuPy = 4-*tert*-butylpyridine.

On the other hand, Bogojeski and Bugarčić [45] and we [46] reported the synthesis and crystal structures of the trichlorido rhodium(III) and iridium(III) complexes  $[\text{MCl}_3(^t\text{BuLH}_2)]$  ( $\text{M} = \text{Rh}, \text{Ir}$ ), respectively. The kinetics of the substitution reactions of the rhodium complex with small biomolecules, such as amino acids, is studied [45].

### Platinum

Goldberg and co-workers [47] demonstrated that reaction of the chlorido complex **14** with methyllithium results in methylation of the platinum center, along with deprotonation of the  $^t\text{BuLH}_2$  ligand to afford the methyl complex **15** with a dangling lithium cation on one of the two pyrazolato arms (Scheme 6). In the solution of THF- $d_8$ , the pincer ligand in **15** is symmetric, and the lithium cation is removed by the treatment with bis(triphenylphosphine)iminium (PPN) chloride to give the anionic complex **16**. The methyl bis(pyrazolato) complex **16** undergoes three-step protonation with a pyridinium tetrafluoroborate. While the first protonation product is insoluble and remains uncharacterized,

following protonation yields the cationic methyl complex **17** and acetonitrile complex **18** sequentially. Thus, the first site of protonation is the pyrazolato ligand rather than the Pt–Me bond. Methane release from  $[\text{PtMe}(\text{tBuLH}_2)]\text{Cl}$ , a chloride salt of **17**, is not observed in  $\text{C}_6\text{D}_6$  until  $180\text{ }^\circ\text{C}$ , indicating that the high energy barrier for the intramolecular proton transfer to the methyl ligand.

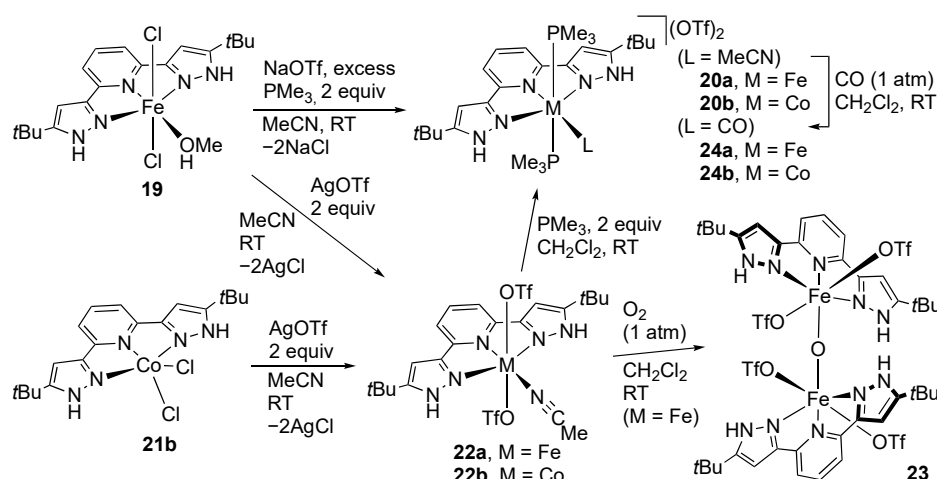


**Scheme 6.** Reactions of the bis(pyrazolato) pincer-type platinum complex **14**. PPN =  $(\text{PPh}_3)_2\text{N}^+$ ; Hpy = 2,6-dimethoxypyridinium cation.

In this connection, uncharged bis(pyrazolato) phosphine complexes  $[\text{Pt}(\text{PPh}_3)(\text{R}^{\text{L}})]$  are also synthesized [48]. The complexes display green phosphorescence in solution and in the solid state; however, the reactivities are unknown.

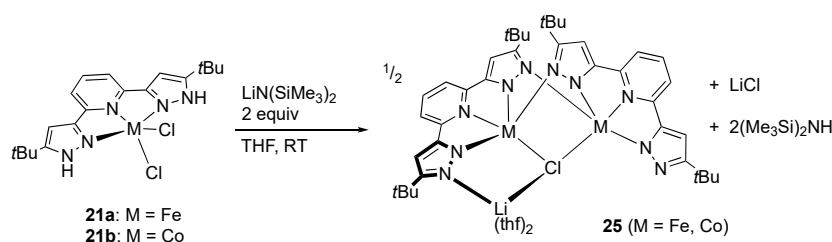
#### First-Row Transition Metals

The 3d transition metal complexes of  $\text{R}^{\text{L}}\text{LH}_2$  have been known much earlier [49]. Most of the studies were, however, limited to their structural determination, except for the spin-crossover properties of the iron(II) complexes with the Fe:ligand ratio of 1:2 until recently. In 2013, we synthesized a 1:1 complex **19** of iron(II) and  $\text{tBuLH}_2$  and uncovered the reactivity [50]. The paramagnetic dichlorido complex **19** is converted to the diamagnetic phosphine complex **20a** with the aid of sodium triflate. Complex **20a** catalyzes disproportionation of hydrazine (vide infra). We later obtained the cobalt and manganese analogues  $[\text{MCl}_2(\text{tBuLH}_2)]$  ( $\text{M} = \text{Co}$  (**21b**), Mn) and explored the ligand substitution reactions of **19** and **21b**, as summarized in Scheme 7 [49]. The iron and cobalt complexes, **19** and **21b**, are converted into the high-spin, triflate complexes **22**, upon treatment with silver triflate in acetonitrile. The iron complex **22a** reacts with dioxygen to give the oxido-bridged diiron(III) complex **23** [49,51]. The two pincer ligands in **23** are almost perpendicular, and the protic pyrazole arms make a hydrogen bond with the triflate ligand on the opposite iron center. The low-spin phosphine and carbonyl complexes, **20** and **24**, can further be derivatized by sequential ligand replacement of the triflate complexes of **22**. The ammine complex  $[\text{Fe}(\text{NH}_3)(\text{PMe}_3)_2(\text{tBuLH}_2)](\text{OTf})_2$  is obtained similarly [50].



**Scheme 7.** Ligand substitution of iron and cobalt complexes of  $t\text{BuLH}_2$ .

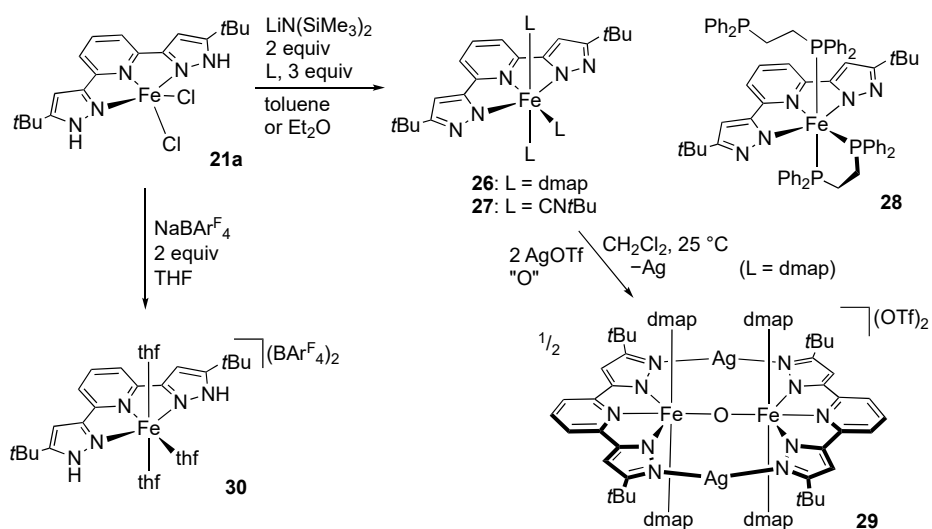
Following that, Caulton and co-workers reported dehydrochlorination of the iron(II) and cobalt(II) complexes **21** with two equiv of a lithium silylamide in THF (Scheme 8) [52,53]. Full dehydrochlorination is, however, not achieved, and the products are the monochlorido-bridged, anionic complexes **25**. For cobalt, the reactions in diethyl ether or toluene yield single crystals of unexpected polynuclear complexes, apparently caused by partial dissociation of the  $t\text{BuLH}_2$ . Complexes **25** can be regarded as lithium chloride adducts of dimers of the expected two-fold dehydrochlorination products  $\text{M}^{t\text{BuL}}$  with coordinative unsaturation.



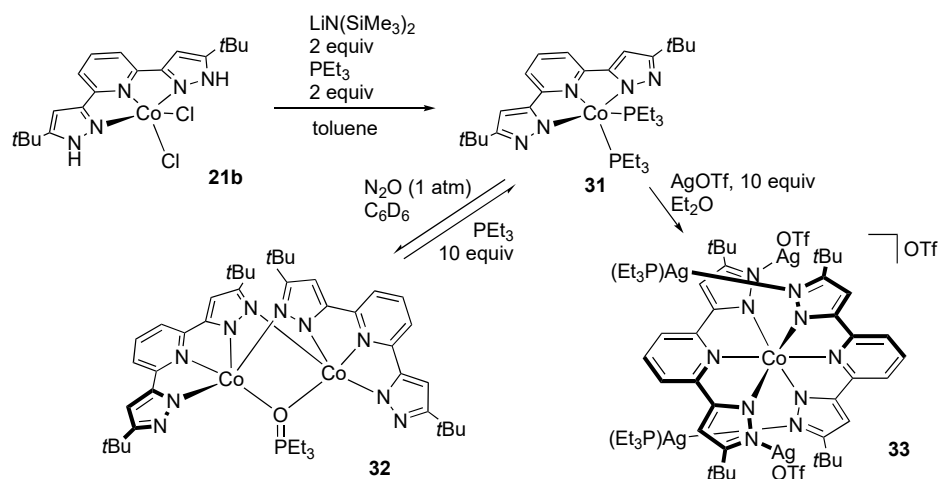
**Scheme 8.** Dehydrochlorination of the iron and cobalt complexes of  $t\text{BuLH}_2$ , **21**.

In contrast, treatment of the iron complex **21a** in the presence of two-electron donor ligands results in complete dissociation of the chloride ligands to give the bis(pyrazolato) complexes, such as **26–28** (Scheme 9) [52]. The 4-dimethylaminopyridine (DMAP) complex **26** is paramagnetic, while the isocyanide complex **27** as well as the diphosphine complex **28** obtained similarly is diamagnetic. The DMAP complex **26** is further converted to the oxido-bridged Fe(III)<sub>2</sub> complex **29** upon treatment with silver triflate, although the oxidant remains unclear [54]. In **29**, the Lewis-basic pyrazolate arms are bridged by the silver cation. On the other hand, chloride abstraction of **21a** with two equiv of  $\text{NaBAr}^{\text{F}}_4$  ( $\text{Ar}^{\text{F}} = \text{C}_6\text{H}_3(\text{CF}_3)_{2-3,5}$ ) in THF leads to the formation of the dicationic THF complex **30** [52], which, however, is found to decompose into  $[\text{Fe}(t\text{BuLH}_2)_2]^{2+}$  with ligand redistribution during recrystallization from dichloromethane.

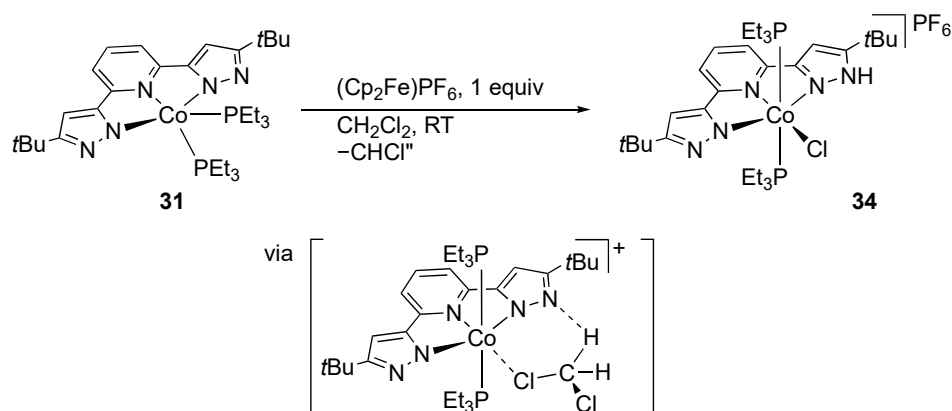
As in the case of the iron analogue **21a**, dehydrochlorination of the cobalt(II) complex **21b** in the presence of triethylphosphine affords the bis(phosphine) complex **31** (Scheme 10) [55]. Subsequent treatment with nitrous oxide results in oxidation of the phosphine ligand to yield the (phosphine oxide)-bridged dinuclear complex **32**. This complex catalyzes oxidation of  $\text{PEt}_3$  and  $\text{PPh}_3$  with nitrous oxide or  $\text{O}_2$ , owing to the interconversion between **31** and **32**. Meanwhile, the ligand basicity of **31** was suggested by the formation of the cobalt(III) complex **33** with each pyrazolato arm binding to a silver center [54]. Even cooperation of Lewis acid–Brønsted base centers is proposed for the oxidation of **31** in dichloromethane to give the cobalt(III) chlorido complex **34** (Scheme 11) [56].



**Scheme 9.** Dehydrochlorination of the  $^t\text{BuLH}_2$  iron complex **21a** in the presence of donor ligands. dmap = 4-dimethylaminopyridine.

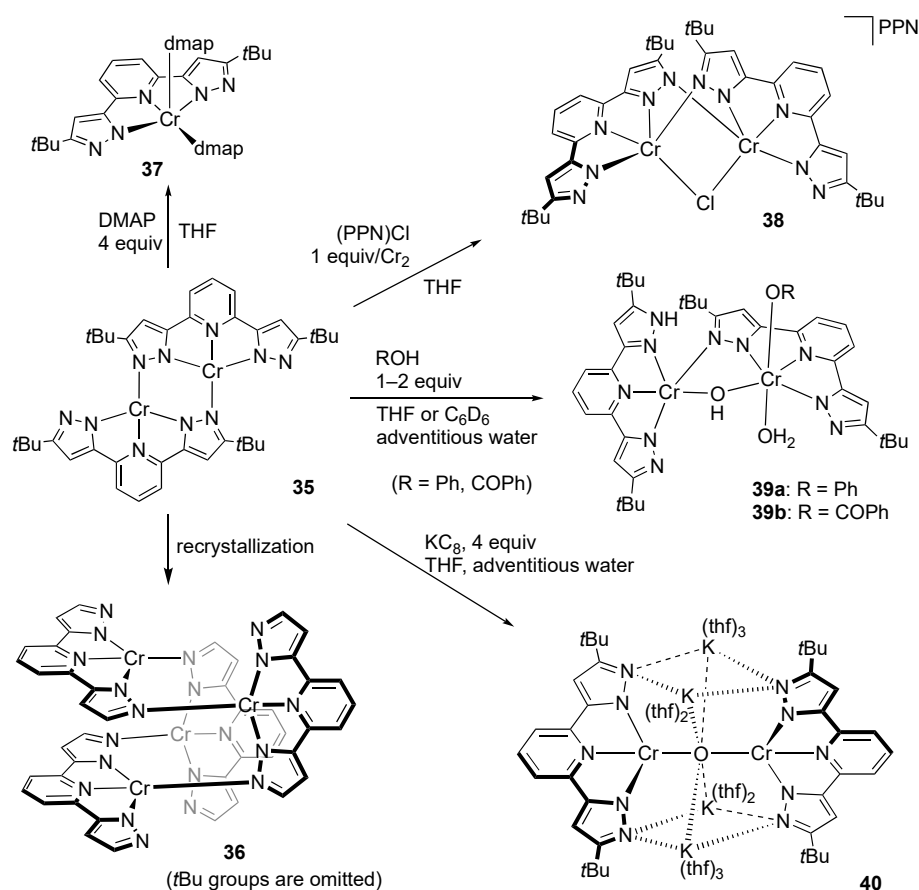


**Scheme 10.** Dehydrochlorination and subsequent reactions of the  $^t\text{BuLH}_2$  cobalt complex **21b**.



**Scheme 11.** Oxidation of a  $^t\text{BuLH}_2$  cobalt complex in dichloromethane.

Synthesis of the elusive, coligand-free bis(pyrazolato) complexes  $M^R L$  has been achieved for chromium(II) by redox-neutral, salt metathesis reaction of  $K_2^{tBu}L$  [54] with  $CrCl_2$  or treatment of a chromium(II) silylamide and  $^{tBu}LH_2$  [57]. The primary product was claimed to be the bis(pyrazolato)-type dimer **35**, which subsequently converts into the tetramer **36** during recrystallization (Scheme 12). Owing to the coordinative unsaturation, **35** reacts with four equiv of DMAP to give the mononuclear bis(dmap) complex **37** with a square-pyramidal geometry. In contrast, addition of chloride anion to **35** affords the anionic monochlorido complex **38**, maintaining the pyrazolato-bridged dichromium(II) core.



**Scheme 12.** Reactions of the pyrazolato-bridged dichromium complex **35**. PPN =  $(Ph_3P)_2N^+$ ; DMAP = 4-dimethylaminopyridine.

Cooperative reactivities of the Lewis acidic metal center and Brønsted basic pyrazolato nitrogen atoms in **35** are also reported. Treatment of **35** with phenol does not result in simple redox-neutral acid–base reaction to give a phenoxido–pyrazole complex; instead, the Cr(II)Cr(III) mixed-valent phenoxido complex **39a** is obtained (Scheme 12) [57]. The oxidation has been explained by evolution of dihydrogen gas, which, however, is not detected in the reaction mixture. Benzoic acid similarly reacts with **35** to yield the corresponding benzoate complex **39b**. On the other hand, treatment of **35** with an equimolar amount of 2-naphthol (NapOH) results in partial dissociation of the pincer ligand to afford the trinuclear Cr(II)Cr(III)<sub>2</sub> complex  $[(^{tBu}LH_2)Cr(ONap)(\mu_2-ONap)_2]_2Cr(Cl)_2$ , wherein the two chloride counteranions are accommodated between the pyrazole rings through hydrogen bonding [57].

Chemical reduction of **35** with four equiv of  $KC_8$  suggests that the pincer-type bis(1*H*-pyrazol-3-yl)pyridine ligand is redox non-innocent. The reaction eventually yields the oxido-bridged dichromium complex  $[K_4(thf)_{10}][Cr_2^{tBu}L_2(\mu_2-O)]$  (**40**), possibly after reactions with adventitious water and dihydrogen evolution as postulated in the previous reactions (Scheme 12) [58]. The X-ray analysis of **40** revealed that the C–C bond distances

around the 4-position of the pyridine ring (1.420(10)–1.439(10) Å) are much longer than the distances of the C2–C3 and C5–C6 bonds (1.352(9)–1.367(8) Å), indicating reduction in the pincer ligand  ${}^t\text{BuL}$  with an unpaired electron at the 4-position of the pyridine ring. The DFT calculation also supports the description of the oxidation state of **40** as  $\text{Cr(II)}({}^t\text{BuL}^{\bullet-})$  rather than  $\text{Cr(I)}({}^t\text{BuL})$ .

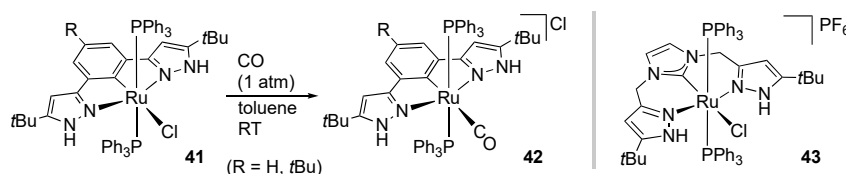
In addition, reduction of **35** with two equiv of  $\text{KC}_8$  as well as oxidation of **35** with ferrocenium cation is examined [58]. Recrystallization of the reaction products again results in uptake of adventitious water to produce oxido-bridged tri- and tetranuclear complexes, respectively, with ambiguous reaction stoichiometry. The reduced species is trapped with carbon dioxide to afford a carbonato-bridged, dianionic–dinuclear complex [59]. On the other hand, the oxidation of **35** with a quinone gives rise to the formation of a bis(semiquinone)  $\text{Cr(III)}_2$  complex [58].

### 2.1.2. Modified 1*H*-Pyrazol-3-yl Pincer Complexes

Partial replacement of the components in the protic pincer ligand  ${}^R\text{LH}_2$ , the central pyridine and flanking pyrazoles, should tune the properties of their metal complexes as in other pincer-type complexes. This section provides an overview of the reactivities of protic pyrazole complexes obtained by ligand modification of  ${}^R\text{LH}_2$ .

#### Modification at Pincer Center

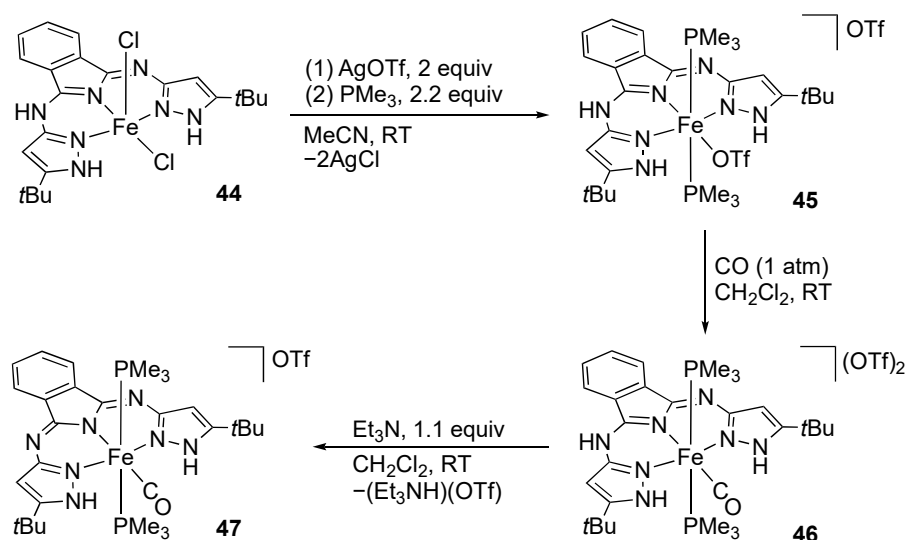
Introduction of a strong  $\sigma$ -donor as the central ligating atom in the protic pincer framework should affect the reactivities of the trans ligand in particular. We reported ligand substitution of the NCN pincer-type ruthenium complexes **41**, which are obtained by cyclometalation of the corresponding 1,3-bis(1*H*-pyrazol-3-yl)benzenes (Scheme 13) [46]. Owing to the trans effect of the central aryl group in the pincer ligand, the substitution takes place even at room temperature to give **42**, in contrast to the reaction of the NNN pincer-type analogue **4b** at 100 °C with the aid of a Lewis acid [60]. An iridium complex, bearing this NCN pincer ligand, is also synthesized in a similar manner [46].



**Scheme 13.** Ligand substitution of an NCN pincer-type protic pyrazole ruthenium complex.

We also installed an N-heterocyclic carbene (NHC) unit in the center of the pincer framework furnished with two protic pyrazoles [61]. The increase in the electron density of the resulting ruthenium complexes, such as **43**, is indicated by the CV measurements. Meanwhile, the CO stretching frequency of the carbonyl derivative is *higher* than that of the pyridine-centered counterpart  $[\text{Ru}(\text{CO})(\text{PPh}_3)_2({}^t\text{BuL})]$  (1989 vs. 1964  $\text{cm}^{-1}$ ). The DFT calculations suggest that the twist of the pincer ligand due to the increase in the chelate size in the NHC-centered pincer may lead to delocalization of the metal d-orbital to the pyrazole  $\pi$ -orbitals, which reduces  $\pi$ -back donation to the carbonyl ligand.

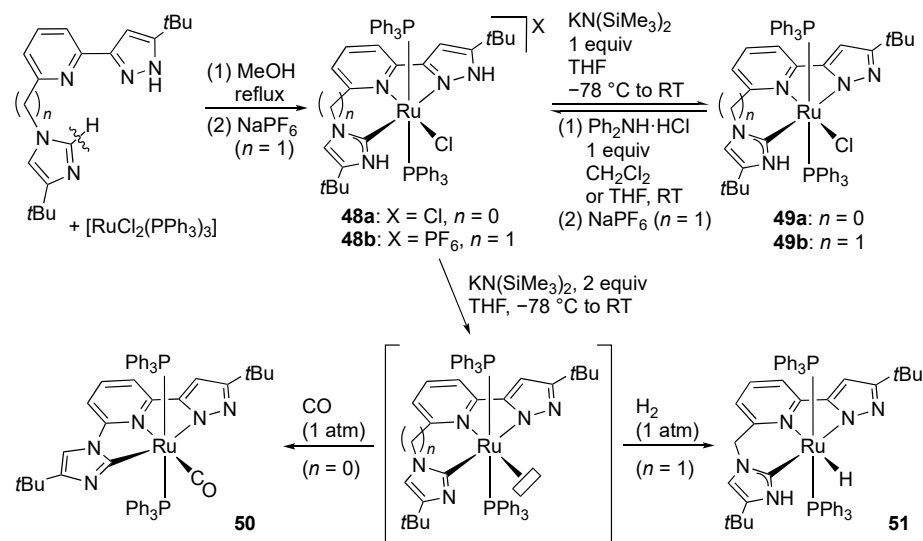
In addition to the C-centered pincer ligands, a novel triprotic NNN pincer ligand bearing a donating central nitrogen atom has been developed recently. The reaction of iron(II) chloride with 1,3-bis(1*H*-pyrazol-3-ylimino)isoindoline results in tautomerization of the ligand to give the 3-amino-1-imino-1*H*-isoindole complex **44** (Scheme 14). This dichloridoiron(II) complex exhibits reactivities similar to those of the  ${}^t\text{BuLH}_2$  complex **19** shown in Scheme 7 [62]. The CO stretching frequency of the carbonyl complex **46** (1963  $\text{cm}^{-1}$ ) is much lower than that of the  ${}^t\text{BuLH}_2$  analogue **24a** (2005  $\text{cm}^{-1}$ ) [49], indicating the donating nature of the central isoindole unit. Importantly, **46** undergoes deprotonation of the chelate backbone rather than the pyrazole groups to afford the isoindolin-2-yl complex **47** bearing a monoanionic bis(pyrazole) pincer ligand.



**Scheme 14.** Reactions of isoindoline-based pincer-type protic pyrazole iron complexes.

### Unsymmetrical Pincer-Type Complexes

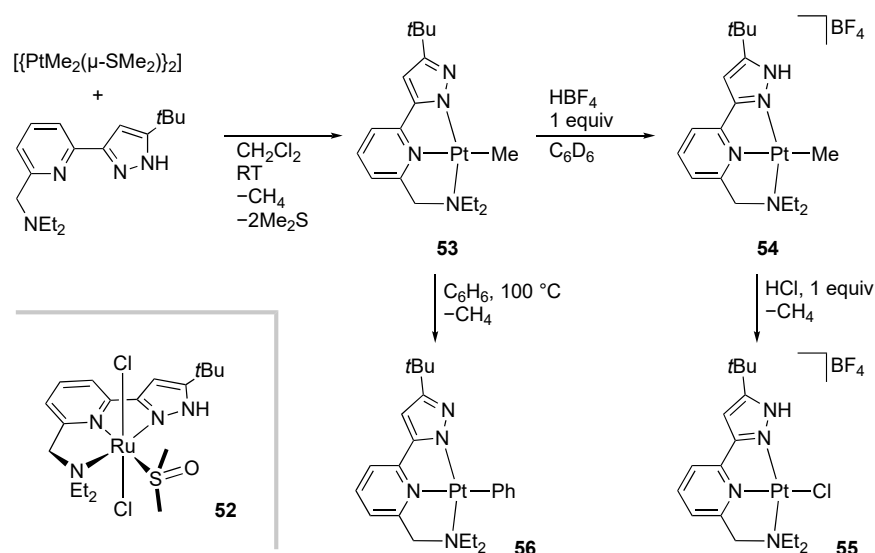
Replacement of one of the two pyrazole arms in pincer-type  $^R\text{LH}_2$  ligands by other donor groups has also been investigated. Such desymmetrization modifies the numbers and acidity of the protic sites as well as the electronic and steric properties of the metal center. We revealed that tautomerization of imidazole assisted by chelation with a pyrazolylpyridine unit results in the formation of the protic pincer-type ruthenium(II) complexes **48**, having protic pyrazole and N-heterocyclic carbene (pNHC [63]) arms (Scheme 15) [60,64]. These complexes undergo reversible deprotonation to afford the corresponding pyrazolato complexes **49**, showing that protic pyrazole is more acidic than pNHC. Exhaustive deprotonation of **48a** under carbon monoxide gives the pyrazolato–imidazolyl carbonyl complex **50** [60]. Similar treatment of **48b** under dihydrogen results in heterolytic cleavage of H<sub>2</sub> to yield the hydrido complex **51**, in which the proton derived from H<sub>2</sub> goes to the more Brønsted basic imidazolyl arm [64].



**Scheme 15.** Synthesis and reactions of CNN pincer-type pyrazole ruthenium complexes bearing a pNHC arm.

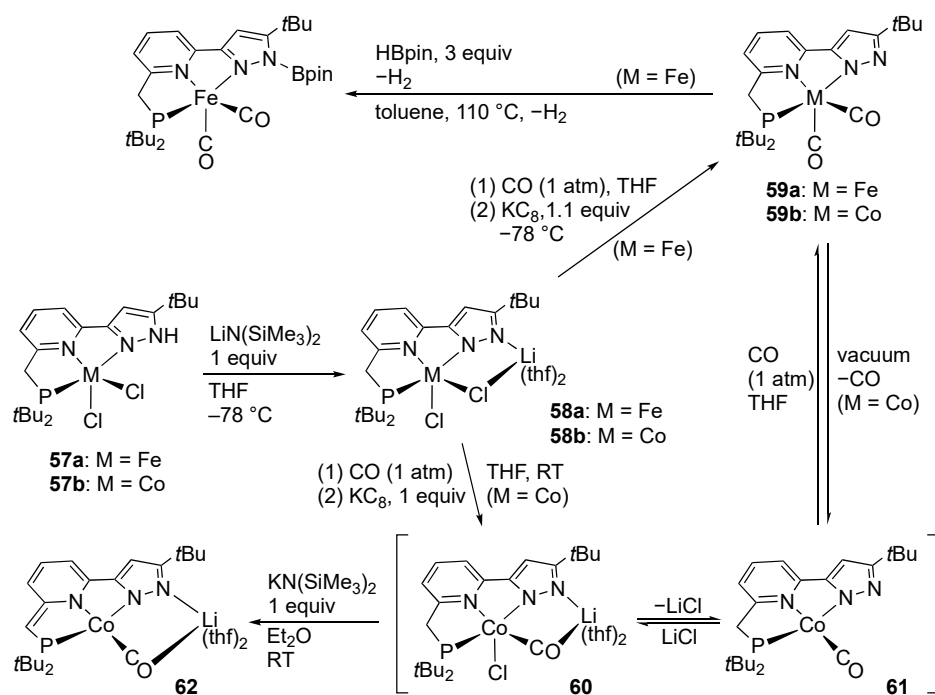


A tertiary amino group can also be incorporated into the protic pincer framework to afford unsymmetrical pincer-type complexes with a hemilabile arm. After our isolation of the ruthenium(II) and iron(II) complexes, such as **52** [65], Goldberg and co-workers reported the reactivities of the platinum(II) complexes bearing this unsymmetrical protic pincer ligand (Scheme 16) [47]. The methyl–pyrazolato complex **53**, obtained from a dimethylplatinum(II) complex and the free ligand, undergoes protonation at the pyrazolato arm rather than the methyl ligand, as observed in the symmetrical bis(pyrazolato) complex **16** (vide supra). The reaction of **54** with hydrogen chloride leads to methane evolution to afford the chlorido complex **55**. In contrast, intramolecular proton migration from the NH group to the methyl ligand appears more difficult. The methyl complex **54**, with a deuterium-labeled NH group, releases only unlabeled CH<sub>4</sub> after being subjected to the temperature higher than 100 °C. The absence of CDH<sub>3</sub> generation indicates that the methane is derived from an external proton source rather than the NH group. Interestingly, heating of the methyl–pyrazolato complex **53** in benzene results in the formation of the phenyl complex **56**. The reaction in C<sub>6</sub>D<sub>6</sub> revealed concurrent site-specific deuteration of the methylene hydrogens in the ethyl groups of the pincer ligand, which implies the hemilabile nature of the dialkylaminomethyl arm.



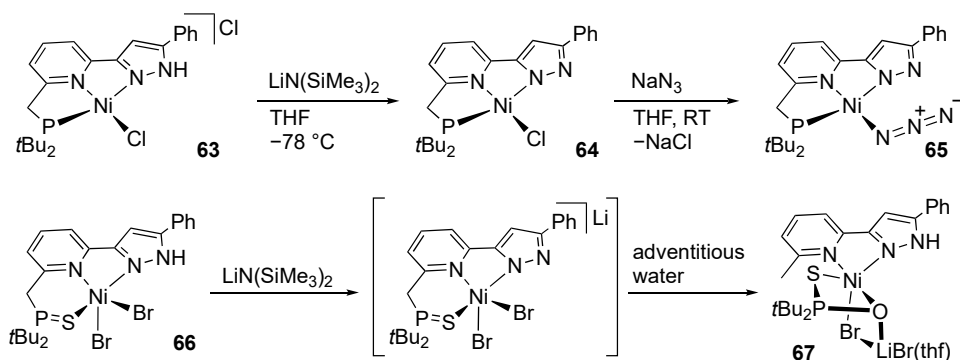
**Scheme 16.** Synthesis and reactions of NNN pincer-type pyrazole platinum complexes bearing an aminomethyl arm.

Caulton and co-workers reported the iron [66] and cobalt [67] complexes bearing a PNN pincer-type protic pyrazole ligand (Scheme 17). The dichlorido iron(II) and cobalt(II) complexes **57** with a distorted square-pyramidal geometry are deprotonated with lithium silylamide to afford the *N*-lithiated complexes **58**. Subsequent treatment with KC<sub>8</sub> under carbon monoxide yields the iron(I) and cobalt(I) complexes **59–61**. Further reduction of the iron complex **59a** with KC<sub>8</sub> results in the formation of a monoanionic dicarbonyl iron(0) complex. The iron complex **59a** also undergoes *N*-borylation of the pyrazolato arm with concurrent hydrogen evolution [66]. On the other hand, treatment of the mixture of the cobalt complexes **60** and **61** with an additional base leads to the second deprotonation at the methylene group of the pincer ligand to afford **62** with a dearomatized pyridine moiety [67], as in the related lutidine-based pincer-type complexes [17]. The result substantiates the diprotic nature of the PNN pincer-type ligand bearing a protic pyrazole arm.



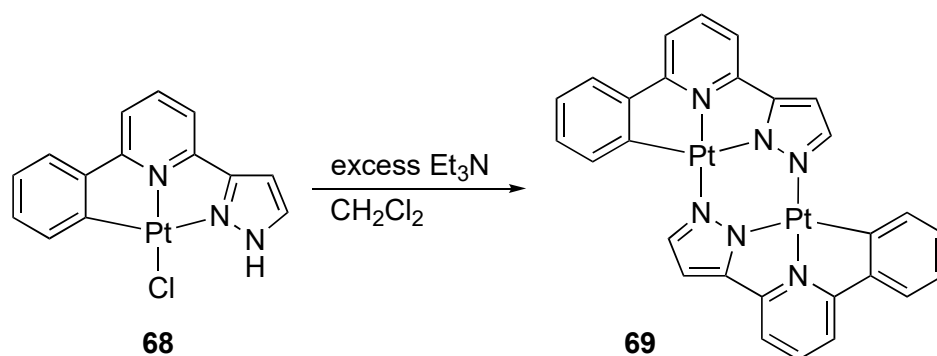
**Scheme 17.** Reactions of iron and cobalt complexes bearing a protic PNN pincer-type ligand.

The square-planar nickel(II) complex **63**, bearing a PNN pincer-type pyrazole ligand is also reported (Scheme 18) [68]. As expected, deprotonation of **63** affords the corresponding pyrazolato complex **64**, which is subsequently converted to the azido complex **65**. Meanwhile, deprotonation of the SNN pincer-type complex **66** results in P–C bond cleavage of the pincer ligand to give the pyrazole complex **67** with a trigonal bipyramidal geometry. The methyl hydrogen atom as well as pyrazole proton is believed to be derived from adventitious water. The reaction in rigorously dried THF leads to redistribution of the nickel–pincer unit in **66** to give a bis(pincer ligand)-type nickel complex.



**Scheme 18.** Deprotonation and subsequent reactions of PNN and SNN pincer-type nickel complexes.

Previously, Lam and co-workers reported a CNN pincer-type pyrazole complex **68**, wherein one of the two protic pyrazolyl groups in the  $\text{H}^2\text{LH}_2$  ligand is replaced by a phenyl group (Scheme 19) [69]. This complex undergoes dehydrochlorination to afford the pyrazolato-bridged dinuclear complex **69**, as observed in bidentate 2-(1*H*-pyrazol-3-yl)pyridine complexes [70,71].

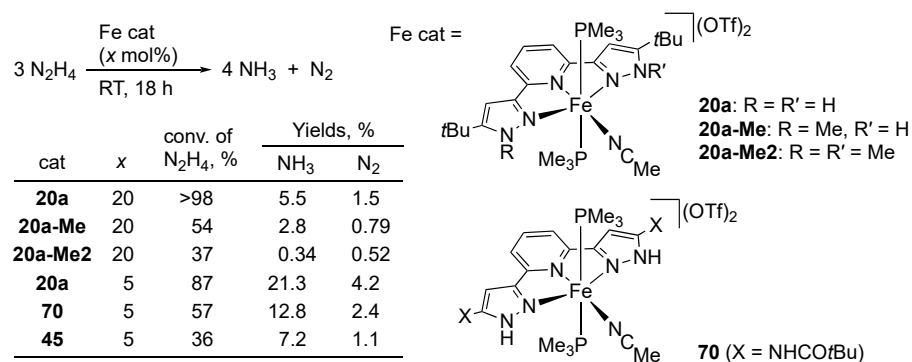


**Scheme 19.** Dehydrochlorination and dimerization of a protic pincer complex of platinum.

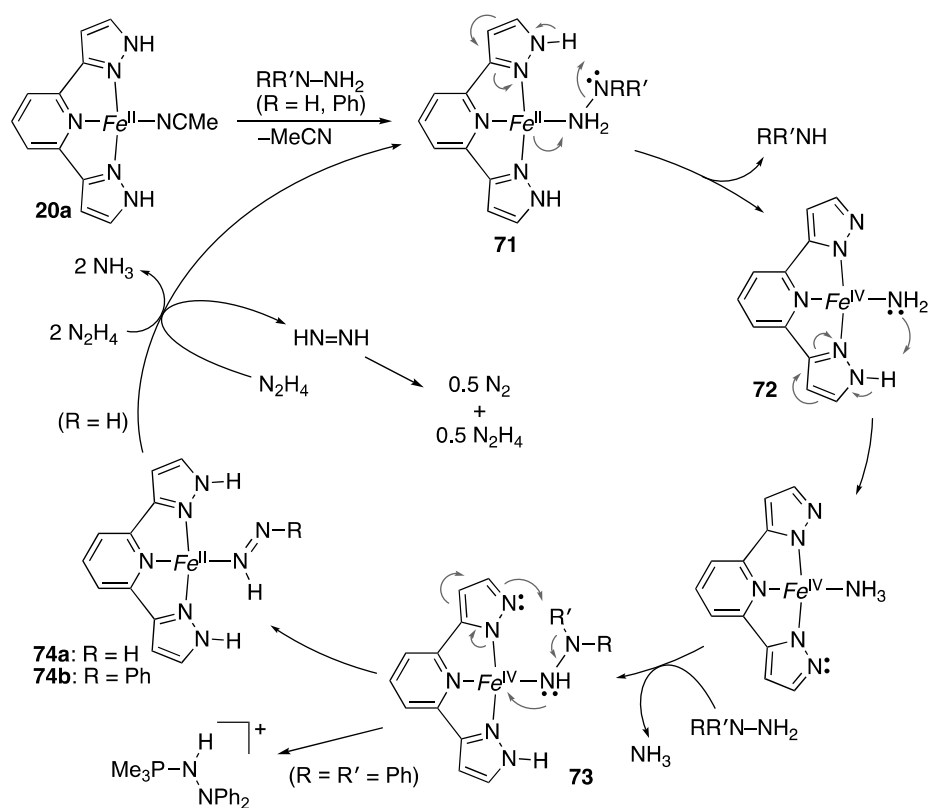
### 2.2. Redox Reactions of Hydrazines and Azobenzene

Given the expanded  $\pi$ -conjugated structure, the pincer-type  $R^LH_2$  ligands may be expected to function as an electron reservoir in addition to a proton source. The electron transfer coupled with proton transfer in the second coordination sphere appears crucial in various enzymatic transformations, including biological nitrogen fixation. In this context, reactions of protic pyrazole complexes with partially reduced dinitrogen species, such as hydrazine, have been investigated.

We revealed that the iron(II)  $t^{\text{Bu}}LH_2$  complex **20a** catalyzes N–N bond cleavage of hydrazine as shown in Scheme 20 [50]. The pivotal role of the pyrazole NH groups is suggested by the reactions of the N-methylated derivatives, **20a-Me** and **20a-Me2**, which are sluggish and much more complicated. The catalytic activities of the amide-substituted complex **70** [72] as well as the isoindoline-based pincer complex **45** [62] are also lower than that of **20a**. Control experiments and theoretical calculations [73] led to the proposed mechanism summarized in Scheme 21, featuring multiple and bidirectional proton-coupled electron transfer (PCET) between the metal–ligand bifunctional platform and the hydrazine substrate. The pyrazole NH group promotes heterolytic N–N bond cleavage of the coordinated hydrazine in **71** through a hydrogen bond with the distal nitrogen atom. The second pyrazole NH group in the pincer ligand behaves as an acid–base catalyst for substitution of the amido ligand in **72** by the second molecule of hydrazine to afford the hydrazido(1–) complex **73**. The calculations also suggest some radical character of the  $\kappa N$ -nitrogen ligands in these high-valent iron species **72** and **73**, and hence a mixed electronic structure of  $Fe^{IV}(NH_2^-)$  and  $Fe^{III}(NH_2^\bullet)$ , for example [73]. Following PCET from the hydrazido(1–) ligand to the high-valent iron–bis(pyrazolato) fragment would yield the iron(II) diazene complexes **74**. In fact, the phenyldiazeno complex **74b** is isolated in the reaction of phenylhydrazine. An X-ray analysis revealed that the phenyldiazeno ligand in **74b** benefits from stabilization by hydrogen-bonding interactions with the two pyrazole NH units and counteranion. Meanwhile, the reaction of 1,1-diphenylhydrazine results in reductive elimination of a hydrazinophosphonium salt from the hydrazido(1–) iron(IV) complex **73** bearing trimethylphosphine ligands (omitted in Scheme 21) due to the lack of the distal hydrogen atom. Finally, the diazeno complex **74a** releases free diazene, which disproportionates to dinitrogen and hydrazine. An alternative scenario that merits comments involves a direct reaction of **74a** with hydrazine to give two moles of ammonia. The proposed  $2H^+ / 2e^-$  shuttling may be applicable to other multielectron redox processes.

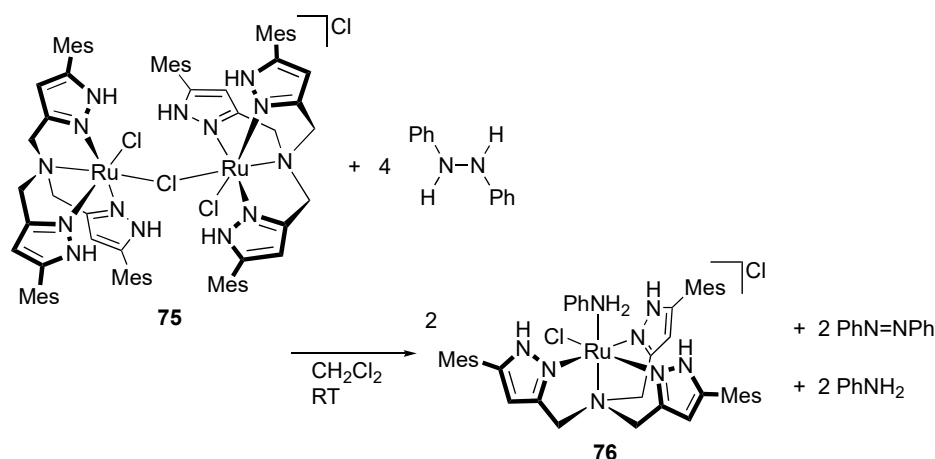


**Scheme 20.** Catalytic disproportionation of hydrazine with protic pincer-type iron complexes.



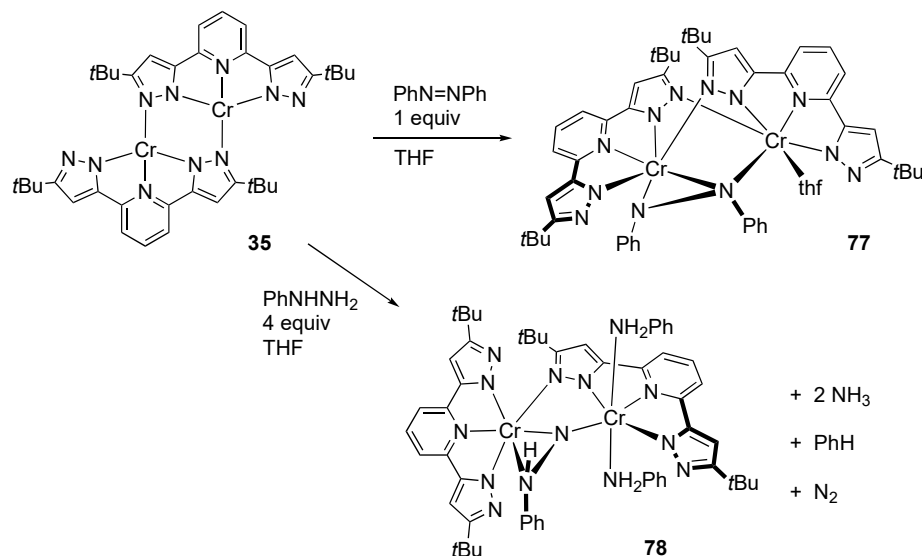
**Scheme 21.** Proposed mechanism for catalytic disproportionation of hydrazine with a protic pincer-type iron complex. Fe = Fe(PMe<sub>3</sub>)<sub>2</sub><sup>2+</sup>. The total charge of the iron complexes (+2) and *tert*-butyl groups in the pincer ligand are omitted.

Similar disproportionation of a substituted hydrazine is reported for a triprotic, tripodal tris(1*H*-pyrazol-3-ylmethyl)amine complex [74]. Treatment of the chlorido-bridged diruthenium(II) complex **75** with 1,2-diphenylhydrazine results in N–N bond cleavage to afford the aniline complex **76** (Scheme 22) [75]. Concurrent formation of azobenzene along with free aniline indicates disproportionation of two moles of 1,2-diphenylhydrazine to azobenzene and two moles of aniline in this transformation. The aniline ligand in **76** is engaged in hydrogen bonding network with the protic pyrazole units along with the chloride counteranion. The disproportionation proceeds catalytically when an excess of 1,2-diphenylhydrazine is added to **75**. An analogous complex of a tetradentate ligand having non-protic pyridylmethyl arms displays no catalytic activity, even in the presence of external protic pyrazole as a proton source, indicating that the proton-responsive unit in the second coordination sphere is responsible for the N–N bond cleavage.



**Scheme 22.** N–N bond cleavage of 1,2-diphenylhydrazine by a tripodal protic pyrazole ruthenium complex. Mes = 2,4,6-Me<sub>3</sub>C<sub>6</sub>H<sub>2</sub>.

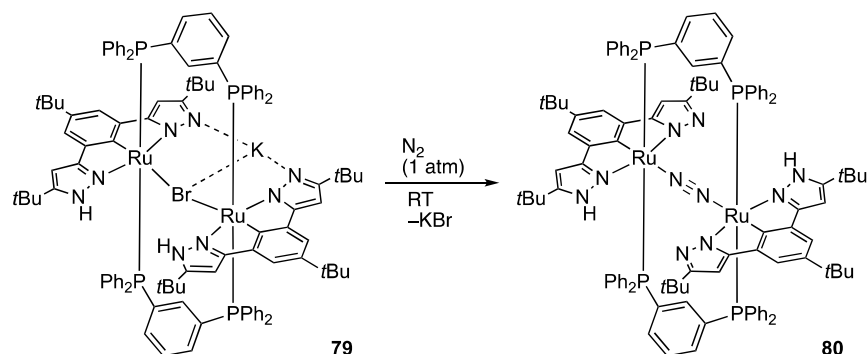
Caulton's group demonstrated that the reaction of dichromium(II) complex **35** (vide supra) [57] with azobenzene yields the paramagnetic chromium(III) complex **77** having an unsymmetrically bridged PhNNPh unit (Scheme 23) [76]. The N–N distance of 1.471(9) Å indicates that the N=N bond is reduced by the chromium(II) centers in **35** to give the hydrazido(2−) ligand. A benzo[*c*]cinnoline derivative, featuring η<sup>2</sup>:η<sup>2</sup>-coordination of the azo group and lack of the THF ligand, is also characterized. Reduction of these hydrazido(2−) complexes with KC<sub>8</sub> is further examined. Only the benzo[*c*]cinnoline derivative undergoes N–N bond cleavage upon treatment with an excess of the reductant.



**Scheme 23.** Reaction of the pyrazolato-bridged dichromium complex with azobenzene and phenylhydrazine.

Electron transfer from the dichromium(II) complex **35** to phenylhydrazine gives rise to the formation of the phenylhydrazido(2−)-bridged di(aniline)dichromium(III) complex **78** (Scheme 23) [77]. The two aniline ligands, derived from N–N bond cleavage of phenylhydrazine, bind to one of the two chromium atoms at trans positions and form intramolecular hydrogen bonding with the protic pyrazoles on the other chromium center. While the reaction stoichiometry should be rather complicated, ammonia and benzene were detected as the fission products in the reaction mixture.

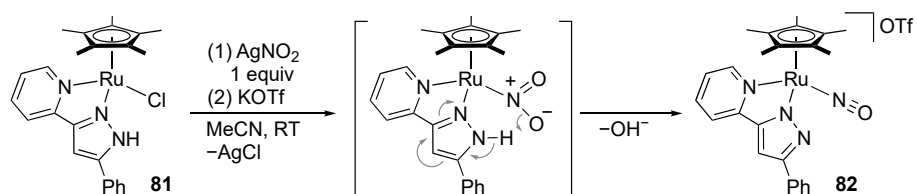
Even dinitrogen is coordinated to proton-responsive pyrazole-based complexes, as in the mononuclear  $t\text{BuL}$  complex **8** [40]. The NCN pincer-type dinuclear complex **79**, supported by two linking diphosphine ligands, reacts with dinitrogen to afford the dinitrogen-bridged diruthenium(II) complex **80** (Scheme 24) [78]. Unfortunately, no further transformation of the dinitrogen ligand in this multiproton-responsive cavity has not been reported.



**Scheme 24.** Synthesis of a dinitrogen-bridged diruthenium complex bearing protic pyrazole ligands.

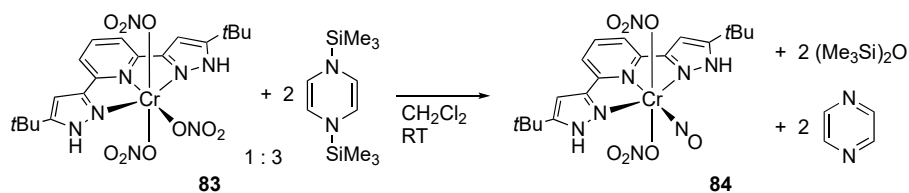
### 2.3. Nitrate Reduction

Reduction of nitrogen oxides constitutes the inorganic nitrogen cycle in nature. Better understanding of the reaction may be important to address the issue of the coastal eutrophication caused by excessive use of nitrogen fertilizer. We found that the reaction of the ruthenium(II) complex **81** with silver nitrite leads to N–O bond cleavage of the nitro anion, giving the nitrosylruthenium(II) complex **82** (Scheme 25) [41]. The dehydrative conversion is most likely assisted by proton transfer from the pyrazole ligand, and the overall reaction is redox neutral.



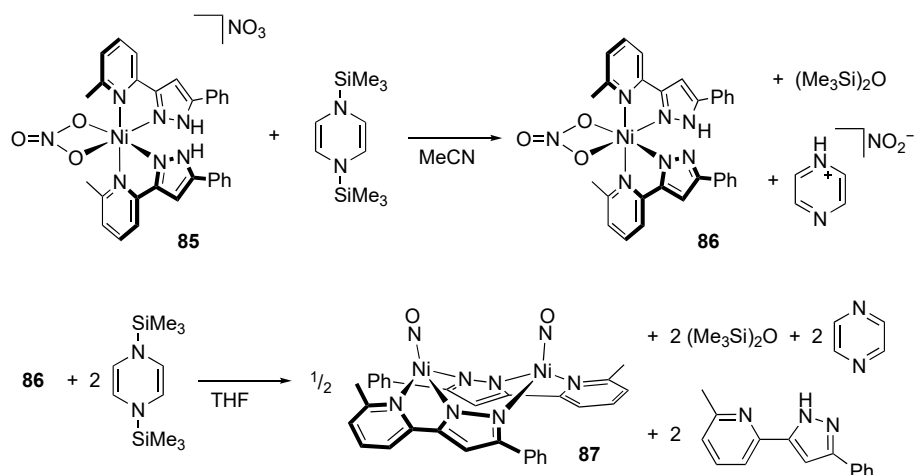
**Scheme 25.** Dehydrative conversion of a nitrite ion to a nitrosyl ligand on a protic pyrazole complex of ruthenium.

Caulton's group demonstrated that  $N,N'$ -disilyldihydropyrazines, whose usefulness in salt-free reduction was uncovered by Mashima and co-workers [79], are effective for deoxygenation of  $\text{NO}_x$  ligands on protic pyrazole complexes. Thus, the tris(nitrate) chromium(III) complex **83**, bearing a protic bis(pyrazole)-type pincer ligand [80], reacted with three equiv of an  $N,N'$ -disilyldihydropyrazine to afford the nitrosyl–nitrate chromium(I) complex **84** (Scheme 26) [81]. The reaction byproducts, hexamethyldisiloxane and pyrazine, were detected in the reaction mixture via  $^1\text{H}$  NMR spectroscopy. It is to be noted that the reaction takes place without any damage on the pyrazole NH protons.



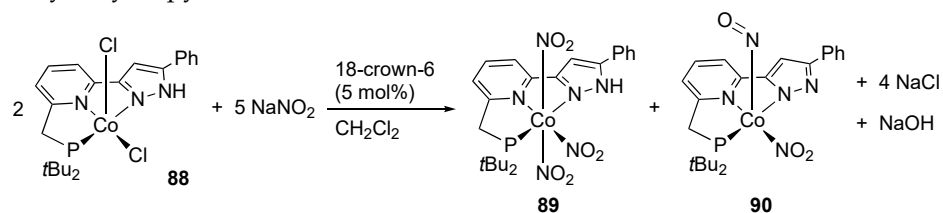
**Scheme 26.** Deoxygenation of a nitrate ligand with  $N,N'$ -disilyldihydropyrazine on a protic pyrazole complex of chromium.

Similarly, treatment of the bis(1*H*-pyrazol-3-ylpyridine)nickel(II) nitrate complex **85** with an equimolar amount of the disilyldihydropyrazine results in deoxygenation of the nitrate and formation of mono-deprotonated product **86** (Scheme 27) [71]. The NH proton remaining on a pyrazole ring in **86** is identified by the larger  $N_{\alpha}N_{\beta}C$  angle. The deoxygenated product in this transformation, nitrite ion, was not detected; however, further deoxygenation of **86** affords the diamagnetic nickel(0) complex **87**, having linear nitrosyl ligands derived from deoxygenation of the nitrate ligand. Thermodynamics of deoxygenation of the  $NO_x$  ligands with a disilyldihydropyrazine was also investigated theoretically for manganese complexes bearing a PNN pincer-type protic pyrazole ligand [82].



**Scheme 27.** Deoxygenation of a nitrate ion with *N,N'*-disilyldihydropyrazine on a protic pyrazole complex of nickel.

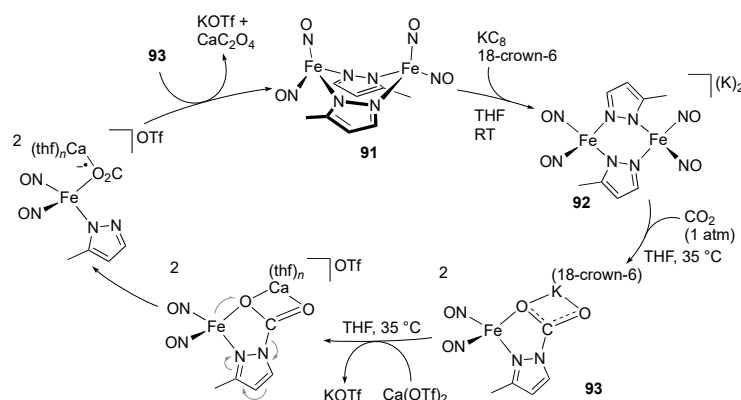
The PNN pincer-type cobalt(II) dichlorido complex **88** bearing a protic pyrazole arm reacts with sodium nitrite to afford the tris(nitrito-*N*)cobalt(III) complex **89** and bent nitrosyl cobalt(III) complex **90** [83]. Although the yields and ratio of **89** and **90** are not described, the reaction stoichiometry shown in Scheme 28 has been proposed along with proton transfer from the pyrazole moiety to the bridging nitrite in a dinuclear intermediate. The compounds **89** and **90** are independently obtained by the reaction of the pincer ligand with a cobalt(III) complex  $Na_3[Co(NO_2)_6]$  followed by deoxygenation and deprotonation with a disilyldihydropyrazine [83].



**Scheme 28.** Reaction of a protic, PNN pincer-type cobalt complex with sodium nitrite.

#### 2.4. CO<sub>2</sub> Reduction

Liaw, Lu, and co-workers demonstrated that the pyrazolato-bridged  $\{Fe(NO)_2\}_2$  complex **91** undergoes two-electron reduction to give the dianionic complex **92** (Scheme 29) [84]. Subsequent reaction with carbon dioxide results in nucleophilic attack of the pyrazolato ligand, resulting in the formation of the mononuclear CO<sub>2</sub> adduct **93**. Interestingly, addition of an equimolar amount of calcium triflate yields calcium oxalate and regenerates the dinuclear complex **91**. A calcium-assisted one-electron transfer from the iron center to the CO<sub>2</sub> unit followed by bimolecular coupling with **93** is proposed for the last step of this synthetic cycle.



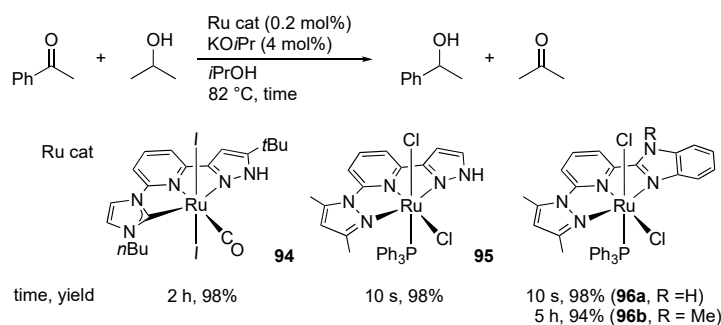
**Scheme 29.** Synthetic cycle for reduction of carbon dioxide to oxalate promoted by a pyrazolato iron complex.

### 3. Catalysis of Protic Pyrazole Complexes

In addition to the aerobic oxidation of phosphines (Section 2.1.1) and catalytic disproportionation of hydrazines (Section 2.2), the catalytic application of protic pyrazole complexes to various chemical transformations has been investigated. This section focuses on recent work along with studies in which the role of the protic pyrazole ligand is evident or discussed. A previous review on this topic is available [11].

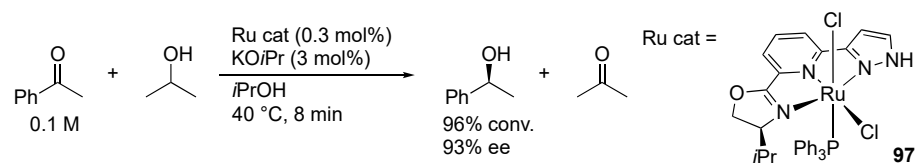
#### 3.1. Hydrogenation and Transfer Hydrogenation

In 2008, Yu's group demonstrated that the protic pincer-type ruthenium(II) complex **94** catalyzes transfer hydrogenation of acetophenones with 2-propanol in the presence of an excess of a base (Scheme 30) [85]. Introduction of a non-protic pyrazole arm instead of the NHC in **94** significantly accelerates the reaction with **95** [86,87]. It is to be noted that the imidazole complex **96a** with an NH group at a remoter position  $\gamma$  to the metal displays catalytic activity comparable with **95**, whereas the non-protic analogue **96b** is much less effective [88,89]. These results may suggest an inner-sphere mechanism involving  $\beta$ -hydrogen elimination of an alkoxide intermediate instead of a pyrazole-aided outer-sphere hydrogen transfer. The NH group in the pincer ligand may still operate to facilitate the dissociation of the halido ligand and to increase the nucleophilic character of the hydrido intermediate through deprotonation of the NH unit. Even asymmetric transfer hydrogenation of aryl ketones has been achieved with protic pincer-type complexes, such as **97**, bearing an optically active oxazolanyl group in the chelate framework (Scheme 31) [90]. We [46] and Halcrow [91] also reported that  $^R\text{LH}_2$  and related NCN pincer-type ruthenium(II) complexes **4** and **41** promote catalytic transfer hydrogenation of acetophenone with 2-propanol in the presence of alkoxide bases. The reactivities parallel with stoichiometric hydrogenation transfer in other protic pyrazole complexes [92,93].



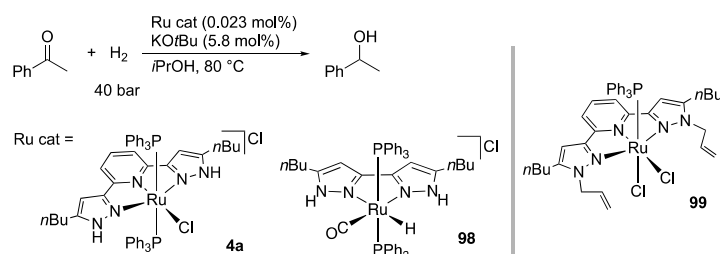
**Scheme 30.** Transfer hydrogenation of acetophenone catalyzed by pincer-type pyrazole ruthenium complexes.





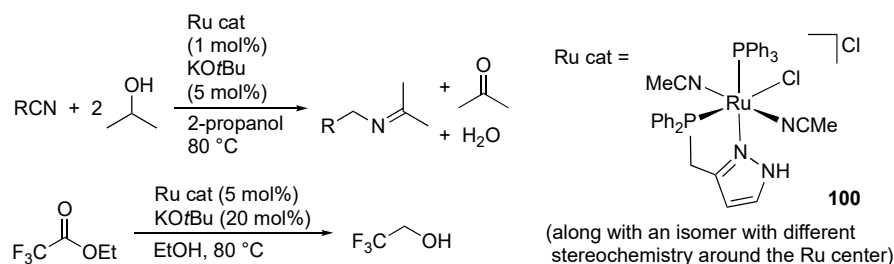
**Scheme 31.** Asymmetric transfer hydrogenation of acetophenone catalyzed by a protic, pincer-type pyrazole ruthenium complex.

Thiel and co-workers demonstrated that the diprotic ruthenium(II) complexes **4a** and **98** catalyze not only transfer hydrogenation but also hydrogenation of acetophenone (Scheme 32) [39]. Theoretical calculations suggest that outer sphere hydrogen transfer from the anticipated hydrido–pyrazole intermediate to the carbonyl substrate as well as the heterolytic cleavage of dihydrogen at the coordinatively unsaturated pyrazolato complex is facile. On the other hand, in the transfer hydrogenation reaction, the efficiency of the non-protic analogues, such as **99**, is comparable or even higher in some cases [94–97], implying that such metal–pyrazole cooperating mechanism is less probable. Catalytic hydrogenation with the  $t^{\text{Bu}}\text{LH}_2$  analogue **4b** is also reported [65].



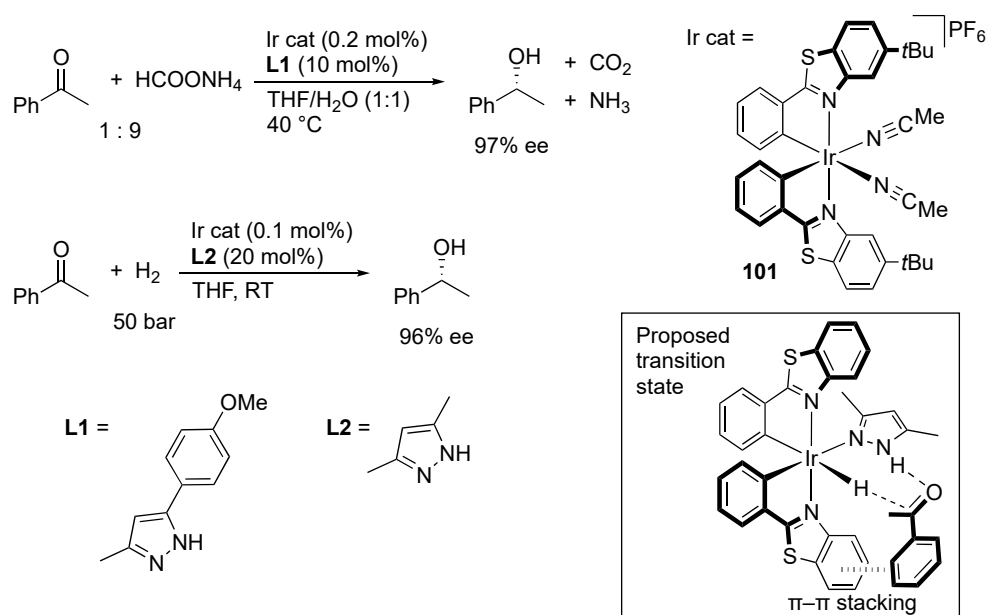
**Scheme 32.** Hydrogenation of acetophenone catalyzed by diprotic pyrazole ruthenium complexes.

Nikonov's group uncovered that the ruthenium(II) complexes, typified by **100**, bearing a P–N chelate protic pyrazole ligand, promote transfer hydrogenation of not only acetophenone [98] but also nitriles, heteroaromatics, alkynes, alkenes, and esters [99]. In the reaction of aromatic and aliphatic nitriles with 2-propanol, the initially formed amine product further reacts with acetone, a byproduct of the transfer hydrogenation in 2-propanol, to afford the ketimines as the final product (Scheme 33). No further reduction of the ketimines to secondary amines is observed. In the transfer hydrogenation of inner alkynes, semi-hydrogenation products, alkenes, are obtained with *E*-selectivity. The *E*-alkenes would be formed by the isomerization of *Z*-alkenes initially generated. Actually, *cis*-stilbene isomerizes to *trans*-stilbene under the catalytic conditions. When the substituents on alkynes are less bulky, further reduction takes place to give the corresponding alkanes. Meanwhile, the conversion of a terminal alkyne is very low. Scheme 33 also illustrates catalytic transfer hydrogenation of ethyl trifluoroacetate to 1,1,1-trifluoroethanol. In this reaction, ethanol is oxidized to ethyl acetate through Tishchenko reaction, and whole process can be viewed as ester metathesis [100].



**Scheme 33.** Transfer hydrogenation of nitriles and ethyl trifluoroacetate catalyzed by a protic pyrazole ruthenium complex.

Gong, Meggers, and co-workers revealed that the chiral-at-metal iridium(III) complex **101** catalyzes asymmetric transfer hydrogenation of ketones in the presence of protic pyrazoles (Scheme 34) [101]. Other additives, such as  $PnBu_3$ , 2,6-diaminopyridine, and imidazole, leads to much lower catalytic activity and enantioselectivity as the reaction without the protic pyrazoles. An X-ray analysis of a related chlorido-pyrazole complex suggests that the NH unit would be placed in the optimum orientation for efficient bifunctional hydrogen transfer to the ketone substrate (inset). Further, attractive  $\pi$ - $\pi$  interaction between the C-N chelate ligand and the arene ring in the substrate is proposed to realize the high enantioselectivity. This binary catalyst system is also effective for asymmetric hydrogenation of acetophenone [102]. In addition, the catalyst serves as a photoredox mediator, which allows asymmetric hydrogenation and photoredox transformation sequences without isolation of the chiral alcohol intermediate. On the other hand, half-sandwich C-N chelate pyrazole complexes of iridium(III) are known to catalyze transfer hydrogenation of acetophenone with 2-propanol [93].

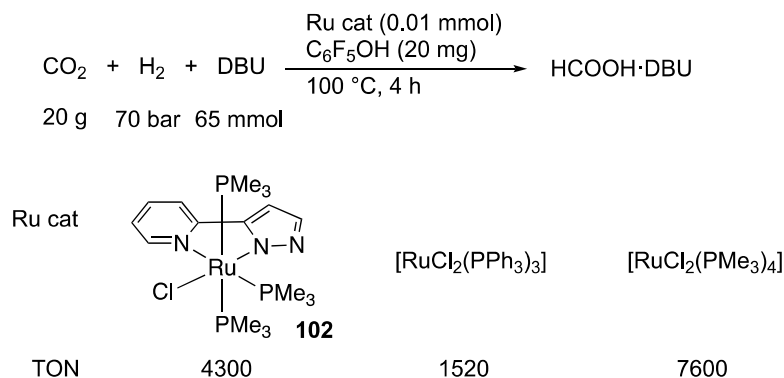


**Scheme 34.** Asymmetric transfer hydrogenation and hydrogenation of acetone mediated by a chiral iridium complex and protic pyrazoles binary catalysts. In inset, *tert*-butyl groups are omitted.

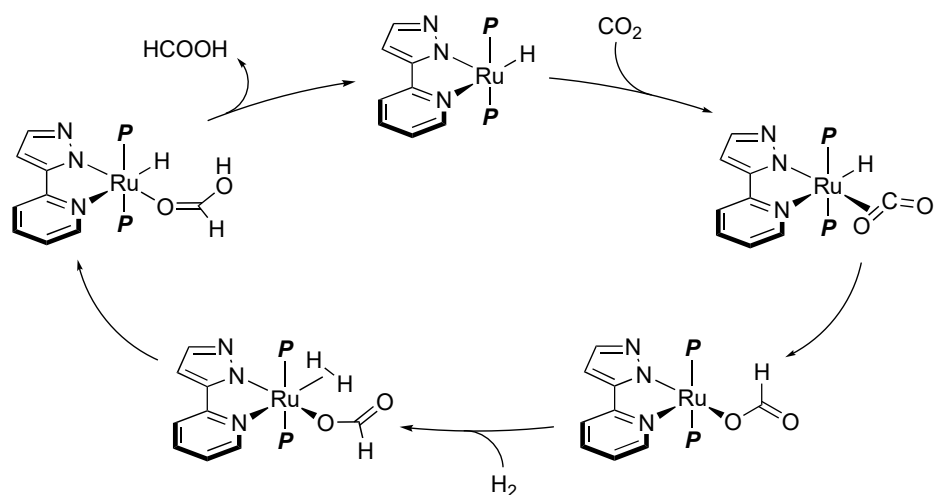
Niedner-Schatteburg, van Wüllen, and Thiel's team demonstrated that the pyrazolato-ruthenium(II) complex **102** catalyzes hydrogenation of carbon dioxide under supercritical conditions (Scheme 35), in addition to transfer hydrogenation of acetophenone with 2-propanol [103]. The  $CO_2$  hydrogenation activity of **102** is almost comparable with those of the conventional dichloridoruthenium(II) phosphine complexes. A mechanism without any proton response of the pyrazolato group is proposed on the basis of theoretical calculations (Scheme 36). A major role of the ionizable pyrazole in the chelate appears to be to make the chelate ligand anionic and more electron-donating [104]. The stronger trans influence of the pyrazolato moiety leads to generation of a vacant site, where carbon dioxide is coordinated. Subsequent insertion into the Ru-H bond gives a formate ligand, which mediates heterolytic cleavage of dihydrogen.

Himeda, Ertem, and co-workers described the half-sandwich iridium(III) complexes bearing proton-responsive ligands as efficient  $CO_2$  hydrogenation catalysts in basic aqueous solutions (Scheme 37) [105,106]. The protic pyrazole group brings about better catalytic activity than the *N*-methylpyrazole group (**103a** vs. **103b** and **104a** vs. **104b**). The performance of the pyrazole complexes **103** is, however, not so prominent when compared with that of the imidazole complexes **105**. Meanwhile, introduction of an OH group at the 6-position of the pyridine ring significantly accelerates the reaction (**104** and **106**). These

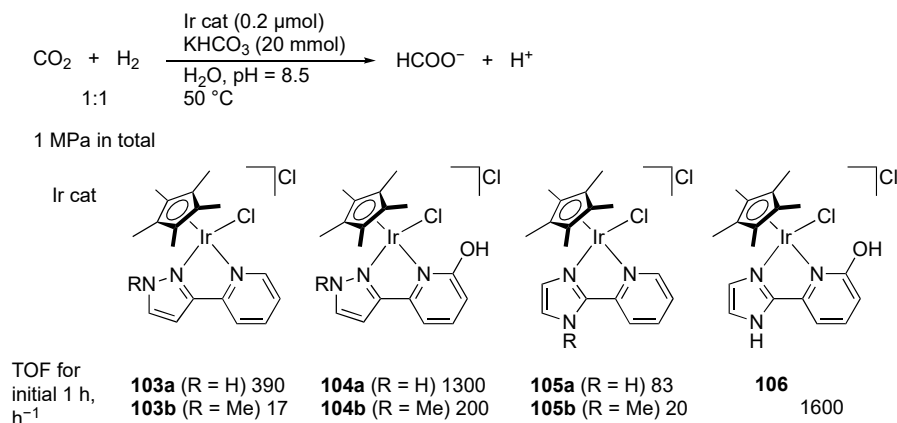
observations as well as DFT calculations led to the mechanistic proposal that the proton-responsive site on the diazole rings offers strong electron donation to the iridium center through its deprotonation. Still, the diazolato unit may also provide a proton acceptor site for the H<sub>2</sub> heterolysis even in the absence of an OH group.



**Scheme 35.** Hydrogenation of carbon dioxide catalyzed by ruthenium complexes. DBU = 1,8-diazabicyclo [5.4.0]undec-7-ene.



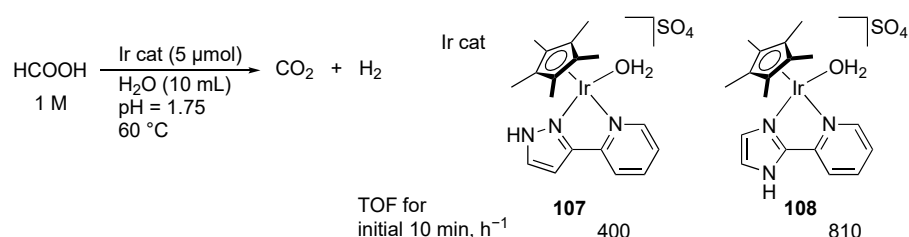
**Scheme 36.** Proposed mechanism for hydrogenation of carbon dioxide with a pyrazolato ruthenium catalyst. *P* = PMe<sub>3</sub>.



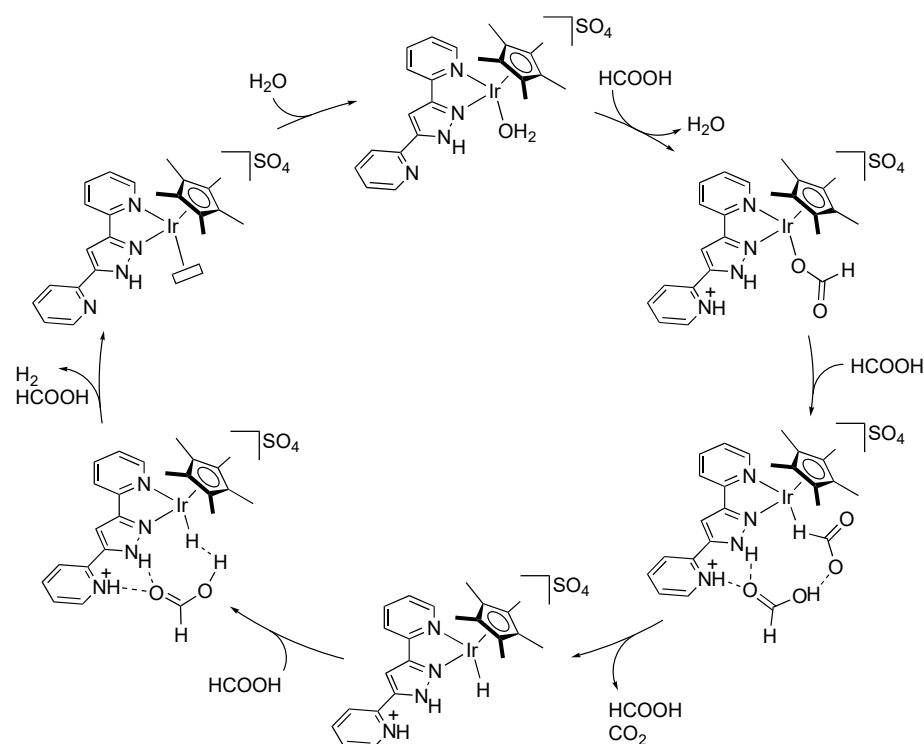
**Scheme 37.** Hydrogenation of carbon dioxide catalyzed by iridium complexes.

### 3.2. Hydrogen Evolution

Dehydrogenation of formic acid, a reverse reaction of CO<sub>2</sub> hydrogenation, is also catalyzed with protic pyrazole complexes. Wang, Himeda, and co-workers revealed that the 2-(1*H*-pyrazol-3-yl)pyridine iridium(III) complex **107** promotes hydrogen evolution from formic acid under acidic conditions (Scheme 38) [107]. The catalytic activity of **107** is less than that of the imidazole analogue **108** with a remoter  $\gamma$ -NH group, suggesting that the azole units mainly have a role in increasing the electron donation to the metal center through their deprotonation. Interestingly, introduction of a pendant pyridyl group on the pyrazole unit improves the catalytic activity [108]. The proposed mechanism involves a two-point hydrogen bonding between protic pyrazole–pyridinium unit and an external formic acid in the second coordination sphere (Scheme 39). The proton relay would facilitate the protonation to the hydrido ligand.

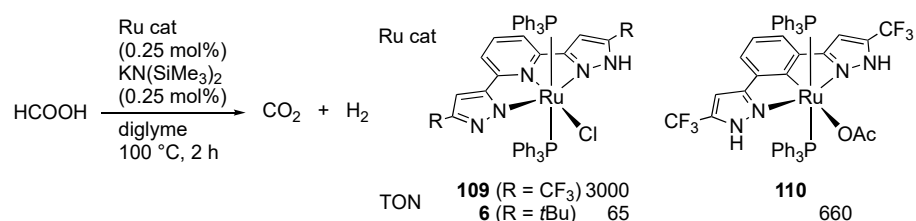


**Scheme 38.** Dehydrogenation of formic acid catalyzed by iridium complexes.



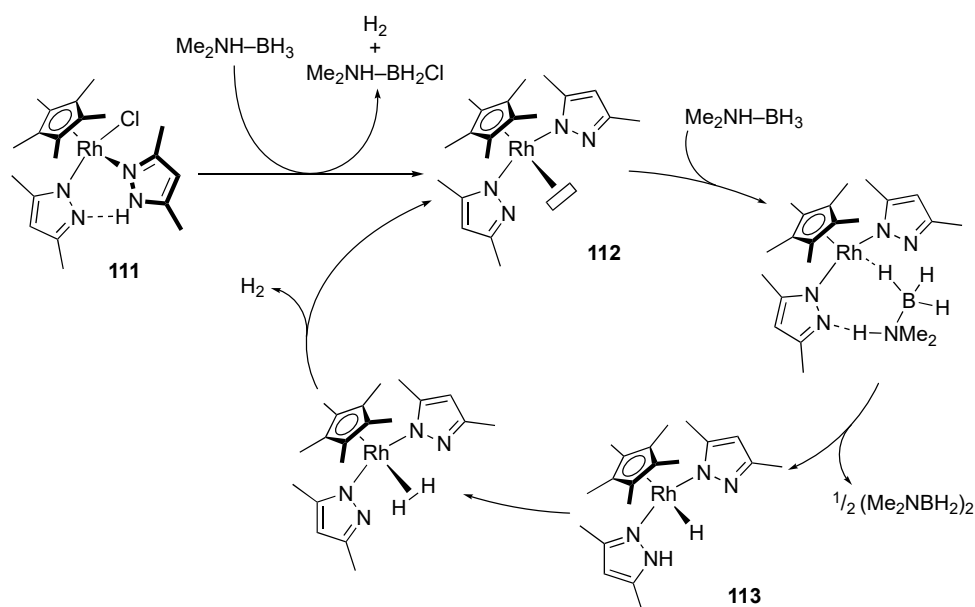
**Scheme 39.** Proposed mechanism for dehydrogenation of formic acid catalyzed by an iridium complex bearing a pyridine-appended protic pyrazolylpyridine chelate ligand.

We reported hydrogen evolution from formic acid catalyzed by the CF<sub>3</sub>LH ruthenium(II) complex **109** (Scheme 40) [109]. The catalytic activity of the less acidic <sup>t</sup>BuLH analogue **6** is poor, indicating the importance of proton transfer from the protic pyrazole arm in the catalysis. The reaction with the NCN pincer-type complex **110** is also much slower.



**Scheme 40.** Dehydrogenation of formic acid catalyzed by protic pincer-type ruthenium complexes.

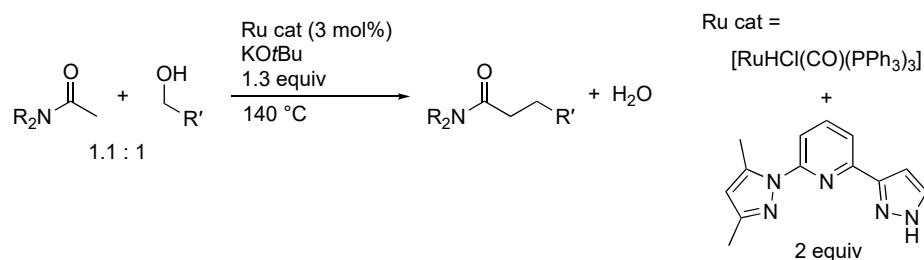
In addition to formic acid, amine–boranes have attracted much attention in terms of chemical H<sub>2</sub>-storage. Pal and Nozaki reported hydrogen evolution from dimethylamine–borane promoted by the pyrazole–pyrazolato rhodium(III) complex **111** [110]. On the basis of theoretical calculations as well as the fact that [(Cp\**RhCl*)<sub>2</sub>] and the free pyrazole are catalytically inactive in separate runs, a metal–pyrazole cooperative mechanism is proposed, as shown in Scheme 41. Dehydrochlorination of the catalyst precursor **111** generates the coordinatively unsaturated bis(pyrazole) complex **112**. The Lewis acidic rhodium center and Brønsted basic pyrazolato ligand in **112** dehydrogenates dimethylamine–borane substrate in a cooperative manner. The resulting hydrido complex **113** releases dihydrogen gas guided by an intramolecular hydrogen bond to regenerate **112**.



**Scheme 41.** Proposed mechanism for dehydrogenation of an amine–borane catalyzed by a protic pyrazole rhodium complex.

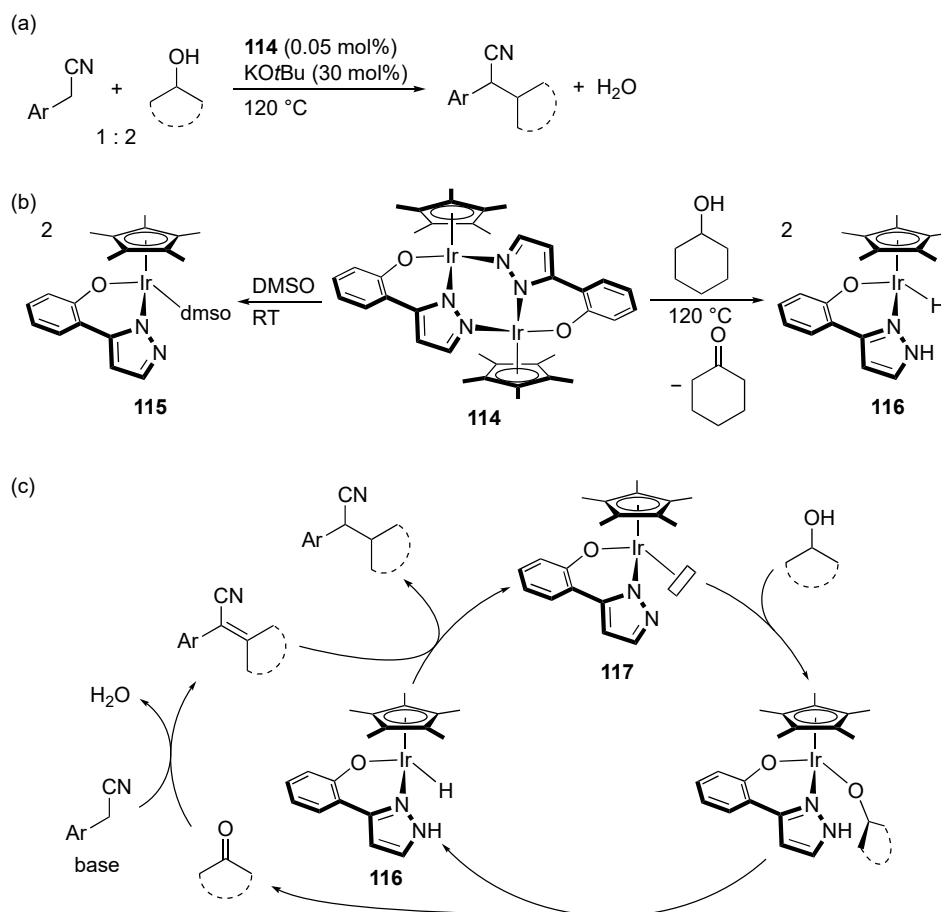
### 3.3. Borrowing Hydrogen Catalysis

Owing to their hydrogen transfer ability, protic pyrazole complexes also exhibit borrowing hydrogen catalysis, wherein the catalyst first borrows hydrogen atoms from the alcohol substrate and then returns them after the bond formation of the resulting carbonyl intermediate [111]. Ryu and co-workers applied a pincer-type ligand in the Yu's transfer hydrogenation catalyst (Section 3.1) to  $\alpha$ -alkylation of amides with primary alcohols (Scheme 42) [112]. As in typical borrowing hydrogen transformations, initial dehydrogenative oxidation of the primary alcohol followed by dehydrative condensation of the resulting aldehyde and amide is proposed. Subsequent transfer hydrogenation from the catalyst would yield the  $\alpha$ -alkylation product.



**Scheme 42.**  $\alpha$ -Alkylation of amides with primary alcohols catalyzed by a protic pyrazole ruthenium complex.

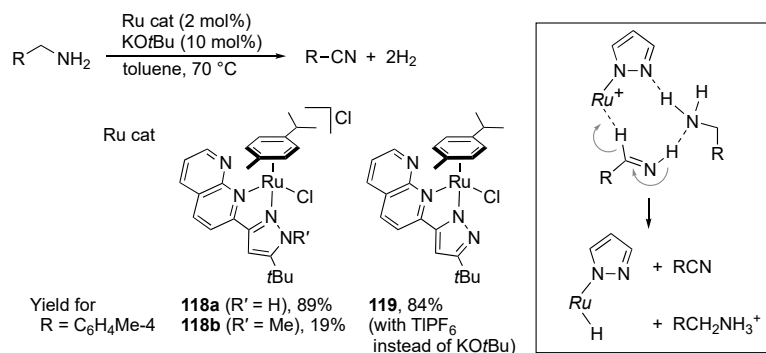
Bagh's group demonstrated that the pyrazolato-bridged diiridium(III) complex **114** promotes  $\alpha$ -alkylation of arylacetonitriles with secondary alcohols (Scheme 43) [113]. When the catalyst precursor **114** is dissolved in DMSO, the DMSO complex **115** is obtained, whereas reaction of **114** with cyclohexanol affords the hydrido-pyrazole complex **116** with liberation of cyclohexanone (Scheme 43b). Formation of these mononuclear N–O chelate complexes suggests that the catalysis involves initial split of the pyrazolato dimer complex **114** into a coordinatively unsaturated pyrazolato complex **117**, which then undergoes transfer hydrogenation from the secondary alcohol to give the hydrido-pyrazole complex **116** (Scheme 43c). Following steps in borrowing hydrogen cycle were also supported by the stoichiometric reactions.



**Scheme 43.** (a)  $\alpha$ -Alkylation of arylacetonitriles with secondary alcohols catalyzed by a pyrazolato-bridged diiridium complex. (b) Stoichiometric reactivities of the dinuclear catalyst precursor. (c) Proposed mechanism.

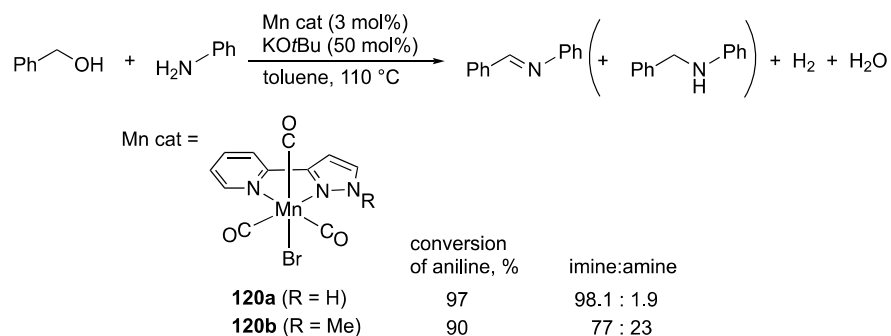
### 3.4. Dehydrogenative Oxidation

If the hydride intermediate in the borrowing hydrogen catalysis somehow releases dihydrogen gas instead of returning the hydrogen atoms to give the redox-neutral product, the net reaction would turn to be dehydrogenative oxidation. Hölscher, Bera, and co-workers described acceptorless double dehydrogenation of primary amines catalyzed by the ruthenium(II) complex **118a** bearing an N–N chelate protic pyrazole ligand (Scheme 44) [114]. Both aromatic and aliphatic nitriles are obtained in this manner. Secondary amines are also converted to the corresponding imines under the reaction conditions. The poor activity of the *N*-methylated analogue **118b** indicates the crucial role of the pyrazole NH group in the catalysis. Meanwhile, the uncharged pyrazolato complex **119** with a Lewis acid displays catalytic performance comparable with that of **118a** even in the absence of base. A coordinatively unsaturated pyrazolato complex is thus suggested to be a catalytically active species. Computational study proposed that the pyrazole unit is not involved directly in the abstraction of hydride from the amine substrate, but dehydrogenation of an imine intermediate occurs in a concerted, metal–ligand cooperative manner with the aid of an external substrate molecule in the second coordination sphere (inset). The resultant hydrido complex would undergo protonation with ammonium cation to evolve dihydrogen gas.



**Scheme 44.** Acceptorless dehydrogenation of primary amines catalyzed by protic pyrazole ruthenium complexes.

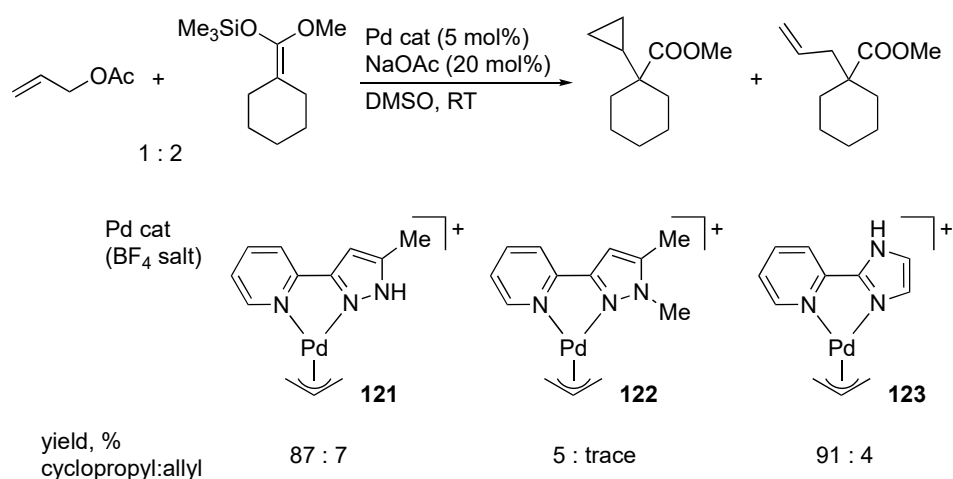
Chai and co-workers reported synthesis of imines catalyzed by the protic pyrazole manganese(I) complex **120a** (Scheme 45) [115]. The non-protic analogue **120b** exhibits lower conversion and brings about increased formation of the amine byproduct through the borrowing hydrogen pathway, although the detailed reason is not mentioned. The reaction is proposed to proceed via dehydrative condensation of aniline and benzaldehyde, which is formed by dehydrogenative oxidation of benzyl alcohol with a coordinatively unsaturated pyrazolato complex.



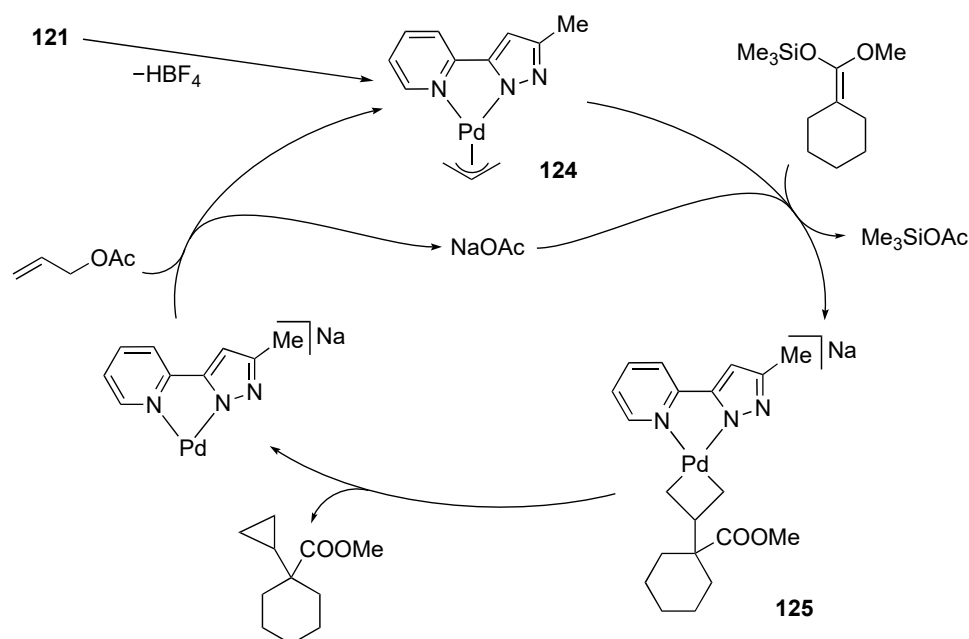
**Scheme 45.** Acceptorless dehydrogenative coupling of benzyl alcohol and aniline catalyzed by pyrazole manganese complexes.

## 3.5. Transformation of Allylic and Propargylic Compounds

Satake and co-workers demonstrated that the N–N chelate pyridylpyrazole palladium(II) complex **121** catalyzes the reaction of allylic acetates and ketene silyl acetals, as shown in Scheme 46 [116]. The significance of the NH group therein is evident by comparison with the catalytic performance of the non-protic complex **122**. On the other hand, the position of the NH group appears unimportant since the protic imidazole complex **123** bearing a  $\gamma$ -NH group displays similar catalytic activity and even better selectivity for cyclopropanation over allylation [117]. The proposed mechanism is illustrated in Scheme 47. Deprotonation of the catalyst precursor **121** gives the uncharged pyrazolato complex **124**, which undergoes nucleophilic attack of the ketene silyl acetal to afford the palladacyclobutane complex **125**. The major role of the NH group would be to make the chelate ligand a better  $\sigma$ -donor, which directs the attack of nucleophile at the central carbon rather than the terminal carbon atoms [118]. Use of chiral oxazolidinones as the chelate tether realizes asymmetric cyclopropanation of a ketene silyl acetal with moderate stereoselectivity [119].



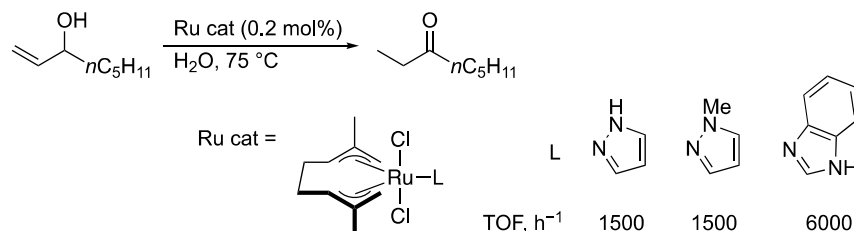
**Scheme 46.** Cyclopropanation of ketene silyl acetal with allyl acetate catalyzed by pyrazole palladium complexes.



**Scheme 47.** Proposed mechanism for catalytic cyclopropanation.

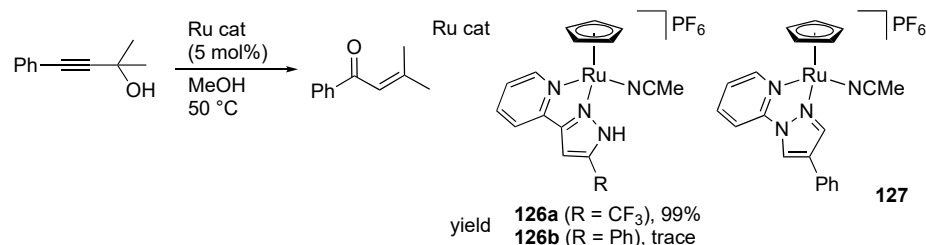


Jimeno, Lledós, and co-workers described isomerization of allylic alcohols mediated by protic azole ruthenium(IV) catalyst precursors in water (Scheme 48) [120,121]. Because the *N*-methylated pyrazole and  $\gamma$ -protic imidazole complexes exhibit similar and much higher catalytic performance, respectively, the aqua ligand rather than the protic azoles is proposed as an acid–base catalytic site to promote the metal–ligand cooperative hydrido migration from the allylic carbon to the vinyl carbon atom.

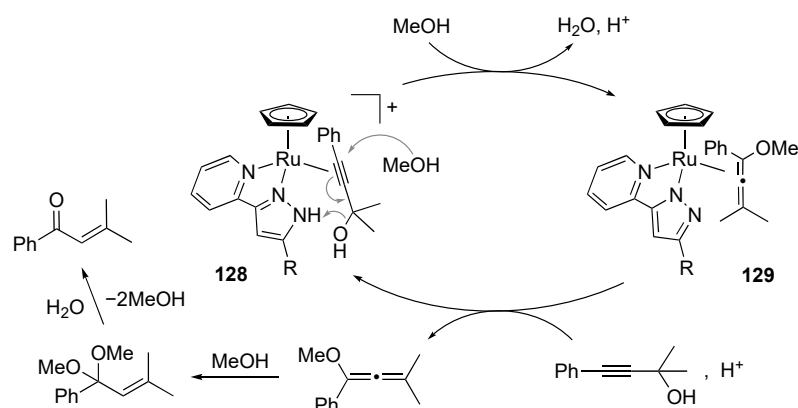


**Scheme 48.** Isomerization of an allylic alcohol to a ketone catalyzed by azole ruthenium complexes.

We uncovered that the protic pyrazole ruthenium(II) complexes **126** catalyze isomerization of 1,1-dimethyl-3-phenylprop-2-yn-1-ol to 3-methyl-1-phenylbut-2-en-1-one in methanol (Scheme 49) [122]. The reaction, known as Meyer–Schuster rearrangement [123,124], does not occur with non-protic analogue **127** as well as a substitution-inert isocyanide complex, whereas the complex **126b** with a less electron-withdrawing phenyl substituent requires a more elevated temperature (reflux, 87%). These observations indicate that both Lewis acidic metal center and Brønsted acidic NH group in **126** are necessary for this catalysis. A proposed mechanism is shown in Scheme 50. The  $\pi$ -bound propargylic alcohol in **128** undergoes an  $S_N2'$ -type propargylic substitution by the solvent methanol with the aid of the intramolecular  $NH\cdots O$  hydrogen bonding in the second coordination sphere to afford the allene complex **129**. Dissociation and solvolysis of the allene would yield an acetal, which is finally converted to the enone product via hydrolysis.

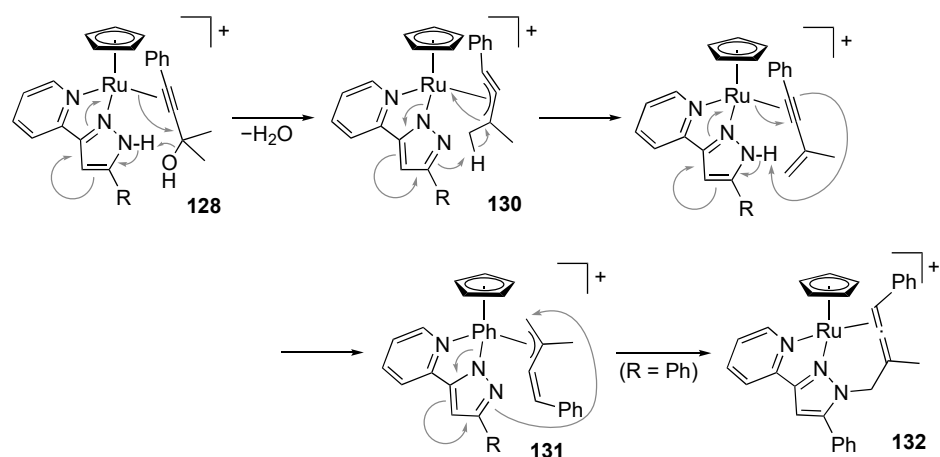


**Scheme 49.** Isomerization of a propargylic alcohol to an enone catalyzed by pyrazole ruthenium complexes.



**Scheme 50.** Proposed mechanism for isomerization of a propargylic alcohol catalyzed by protic pyrazole ruthenium complexes.

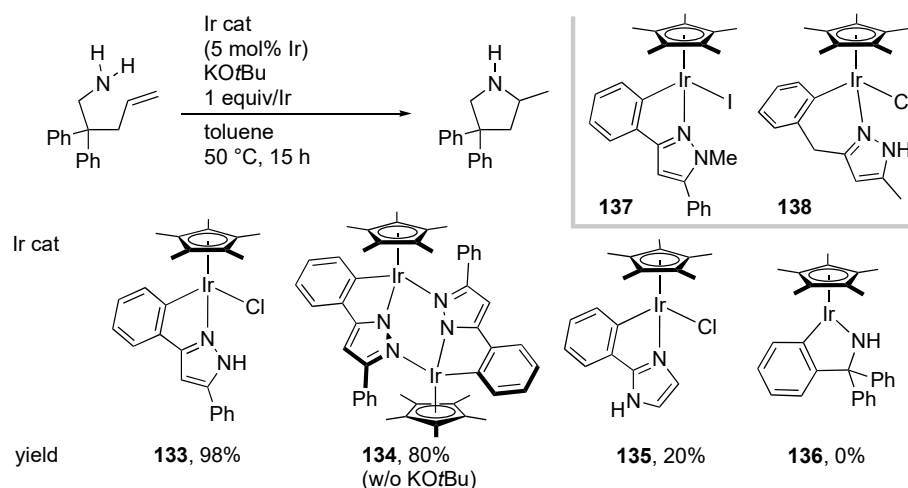
Use of less nucleophilic solvents, such as 1,2-dichloroethane and 1,4-dioxane, completely switches the reaction outcome. In the absence of the external nucleophile, a two-point interaction between the protic pyrazole complex and the substrate would lead to facile C–O bond cleavage, giving the  $\eta^3$ -propargyl complex **130** (Scheme 51). Involvement of **130** in the Meyer–Schuster rearrangement in methanol (Scheme 50) is less likely because the nucleophilic addition to  $\eta^3$ -propargyl ligands generally takes place at the central carbon atom [125] and would fail to provide the observed product. The pyrazolato unit in **130** mediates proton migration in the  $\eta^3$ -propargyl ligand to afford the  $\eta^3$ -butadienyl complex **131**, which is isolable in the case of R = CF<sub>3</sub>. When the pyrazolato ligand in **131** is more nucleophilic (R = Ph), intramolecular addition to the terminal carbon in the  $\eta^3$ -butadienyl ligand occurs to give the *N*-allenylmethylpyrazole complex **132**.



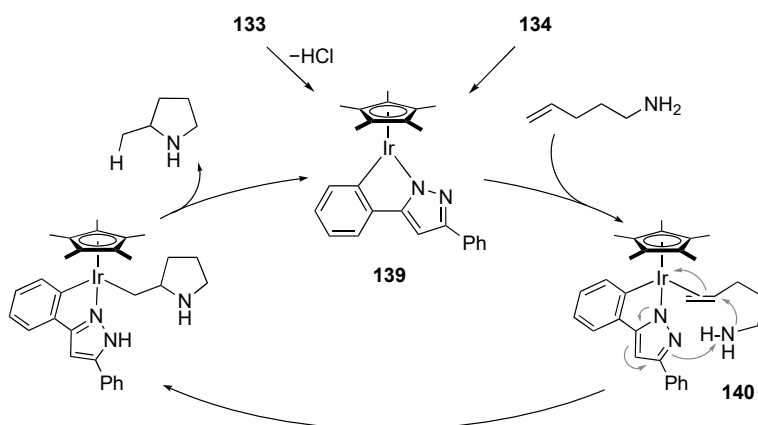
**Scheme 51.** Transformation of a propargylic alcohol on protic pyrazole ruthenium complexes in less nucleophilic solvents.

### 3.6. Hydroamination of Alkenes

The metal–ligand bifunctional nature of protic pyrazole complexes is further applied to catalytic hydroamination of alkenes, in which both amine and olefin functional groups are activated simultaneously. We disclosed that the C–N chelate protic pyrazole iridium(III) complex **133** promotes cyclization of aminoalkenes with the aid of an equimolar amount of an alkoxide base (Scheme 52). The catalyst is compatible with various functional groups such as ester, bromo, cyano, and hydroxy groups. The pyrazolato-bridged dimer **134**, obtained by dehydrochlorination of **133**, exhibits catalytic activity similar to **133** even in the absence of the base. Meanwhile, the catalytic performance of the related complexes, **135** and **136**, having a proton-responsive site at the positions  $\gamma$  and  $\alpha$  to the iridium center, respectively, is poor. Additionally, catalytically inactive are the *N*-methylated derivative **137** and the six-membered chelate analogue **138** [93]. These results indicate that an exquisitely positioned proton-responsive site with appropriate direction and acidity is crucial for the catalysis. Scheme 53 illustrates a proposed mechanism featuring the metal–ligand cooperation. The olefin part in the aminoalkene substrate binds to the coordinatively unsaturated mononuclear pyrazolato complex **139**, derived from dehydrochlorination of the chlorido complex **133** or split of the pyrazolato dimer **134**. The activated olefin is attacked by the amino group with increased nucleophilic character owing to intramolecular hydrogen bond with the pyrazolato unit. The tight-fitting assembly in transition state **140** is supported by the large negative activation entropy provided by kinetic experiments. Subsequent proton transfer from the pyrazole unit to the Ir–C bond yields the product and regenerates the unsaturated pyrazolato complex **139**.



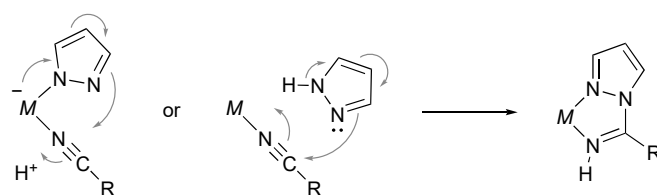
**Scheme 52.** Cyclization of an aminoalkene catalyzed by iridium complexes.



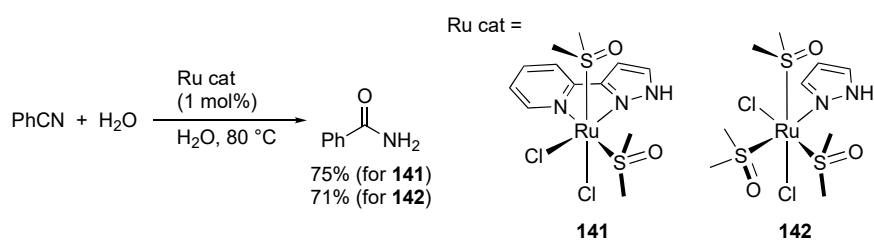
**Scheme 53.** Proposed mechanism for cyclization of aminoalkenes catalyzed by a protic pyrazole iridium complex. Substituents of aminoalkenes are omitted.

### 3.7. Hydration of Nitriles

Metal-mediated coupling of nitrile and pyrazole to give a stable chelate pyrazolylamidino ligand, illustrated in Scheme 54, has been known for a long time. Nevertheless, a certain type of protic pyrazole complex catalyzes hydration of nitriles. Rodríguez, Romero, and co-workers reported hydration of benzonitriles and acrylonitrile catalyzed by the pyrazole complexes, such as **141** and **142** (Scheme 55) [126,127]. The reaction is proposed to proceed via nucleophilic attack of water or hydroxide anion to the coordinated nitrile. Although the role of the pyrazole ligand in this catalytic reaction is not mentioned, the proton-responsive pyrazole ligand may increase the nucleophilic character of water through hydrogen bonding in the second coordination sphere.



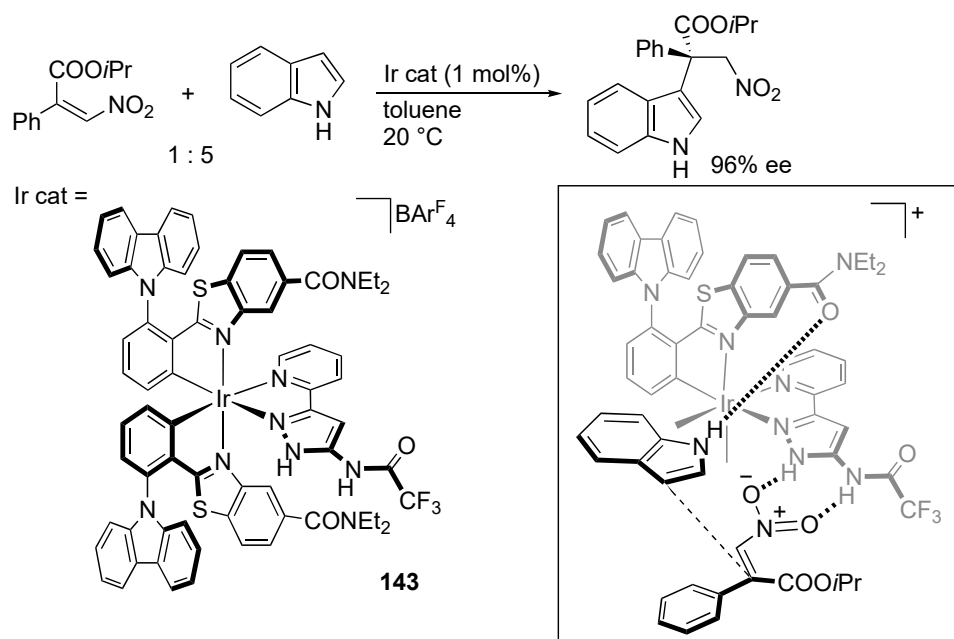
**Scheme 54.** Coupling of pyrazole and nitrile on a metal center.



**Scheme 55.** Catalytic hydration of benzonitrile with protic pyrazole ruthenium complexes.

### 3.8. Catalysis with Coordinatively Saturated Complexes

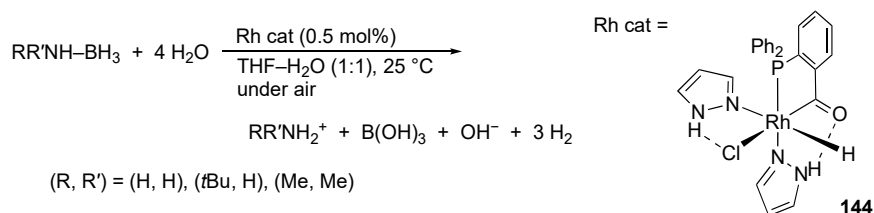
In their seminal work on chiral-at-metal complexes [128,129], Gong and Meggers described ligand-centered catalysis of protic pyrazole complexes. For example, the iridium complex **143** bearing an amido-substituted protic pyrazole ligand catalyzes asymmetric 1,4-addition of indoles to  $\beta$ -nitroacrylates (Scheme 56) [130]. As the well-known thiourea organocatalysis [131], the amidopyrazole unit serves as a hydrogen bond donor to the nitroalkene. The chiral metal center in the catalyst **143** is coordinatively saturated and inert; however, the carboxamide substituent in the C–N chelate acts as a hydrogen bond acceptor for the indole, making the complex bifunctional.



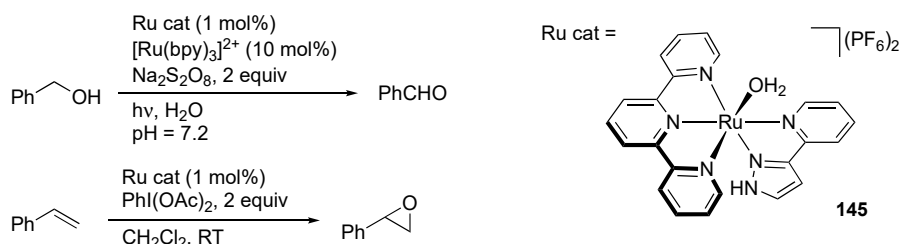
**Scheme 56.** Asymmetric 1,4-addition of indole to a  $\beta$ -nitroacrylate catalyzed by a protic pyrazole iridium complex.  $\text{Ar}^{\text{F}} = \text{C}_6\text{H}_3(\text{CF}_3)_2\text{-3,5}$ .

### 3.9. Miscellaneous

Suzuki–Miyaura coupling reactions with bis(pyrazole) palladium(II) complexes [132] as well as a binary system of  $\text{PdCl}_2$  and  $\text{PhLH}_2$  [133] are reported. Garralda and co-workers described hydrolysis of ammonia–borane and amine–boranes catalyzed by the rhodium(III) bis(pyrazole) complexes, such as **144** (Scheme 57) [134]. Rodríguez and Romero reported the ruthenium(II) complex **145** bearing a protic pyrazole ligand catalyzes photochemical oxidation of alcohols in water in the presence of a sacrificial oxidant along with  $[\text{Ru}(\text{bpy})_3]^{2+}$  as a photosensitizer (Scheme 58) [135]. Chemical oxidation of alkenes to epoxides is also promoted. Unfortunately, the mechanisms for these reactions and the role of the protic pyrazole ligand therein are not discussed.



**Scheme 57.** Hydrolysis of amine–boranes catalyzed by a protic pyrazole rhodium complex.



**Scheme 58.** Oxidation of an alcohol and alkene catalyzed by a protic pyrazole ruthenium complex.

#### 4. Conclusions

It is now apparent that the protic pyrazoles are versatile non-innocent ligands, owing to their ability to place a proton-responsive site in the second coordination sphere. The deprotonation of the  $\beta$ -NH unit turns the pyrazole ligand to a stronger  $\sigma$ -donor. In both protonated and deprotonated forms, the ligand-based hydrogen bonding and electrostatic interactions at the  $\beta$ -position allows efficient substrate recognition and activation as well as additional tuning of the electronic properties of the metal center. Importantly, these events in the outer coordination sphere are linked with the metal-centered reactions in some cases. Such metal–ligand cooperation can be compared with those of related proton-responsive ligand systems (Scheme 1); however, the stiff five-membered structure that fixes the proton with an azole acidity in the metal–pyrazole plane makes the reactivity of protic pyrazole complexes distinctive. Additionally, facile redox of the metal–pyrazole framework coupled with deprotonation is implied for  $\pi$ -delocalized, bis(pyrazole)-type  $^t\text{BuLH}_2$  complexes (Scheme 21 and compound **40** in Scheme 12). The metal–ligand cooperative catalysis thus has been explored for various types of reactions, typified by transfer hydrogenation and functionalization of unsaturated carbon–carbon bonds. The role of the NH groups therein, however, appears to depend on the catalyst systems. In some reactions, control experiments with  $\gamma$ -protic imidazole complexes indicate that the presence of the ionizable NH group is prerequisite for the catalysis but the position is unimportant. The protic pyrazole ligand in this case would remain deprotonated during the catalytic turnover and serve only to increase the electron density of the metal center. Further studies are needed to elucidate the conditions under which the metal–ligand cooperation is exerted. These efforts will lead to improvement and deeper mechanistic understanding of the catalysis of protic pyrazole complexes. The metal–ligand cooperation has also been applied to activation of small inorganic molecules. A future target in this direction will undoubtedly be multiproton-coupled multielectron reduction of inert molecules, such as carbon dioxide and dinitrogen, with polyprotic pyrazole complexes. In these studies, novel design of protic pyrazole ligands will continue to be a major subject to create more sophisticated metal–ligand cooperation platforms for both stoichiometric and catalytic transformations unique to protic pyrazole complexes. Facile construction of the pyrazole rings will be advantageous in the synthesis of the pyrazole ligands whose Brønsted acidity and deployment are controlled by the substituents on the ring and chelate framework.

**Author Contributions:** Writing—original draft preparation, W.-S.L.; writing—review and editing, S.K. All authors have read and agreed to the published version of the manuscript.

**Funding:** This research was funded by JSPS KAKENHI Grant Number JP19H02732.

**Institutional Review Board Statement:** Not applicable.

**Data Availability Statement:** Data sharing is not applicable to this article.

**Conflicts of Interest:** The authors declare no conflict of interest.

## References

1. Trofimenko, S. Recent Advances in Poly(pyrazolyl)borate (Scorpionate) Chemistry. *Chem. Rev.* **1993**, *93*, 943–980. [CrossRef]
2. Halcrow, M.A. Pyrazoles and Pyrazolides—Flexible Synthons in Self-Assembly. *Dalton Trans.* **2009**, *38*, 2059–2073. [CrossRef] [PubMed]
3. Neto, J.S.S.; Zeni, G. Alkynes and Nitrogen Compounds: Useful Substrates for the Synthesis of Pyrazoles. *Chem. Eur. J.* **2020**, *26*, 8175–8189. [CrossRef] [PubMed]
4. Sloop, J.C.; Holder, C.; Henary, M. Selective Incorporation of Fluorine in Pyrazoles. *Eur. J. Org. Chem.* **2015**, *2015*, 3405–3422. [CrossRef]
5. Bhaumik, P.K.; Ghosh, K.; Chattopadhyay, S. Synthetic Strategies, Crystal Structures and Biological Activities of Metal Complexes with the Members of Azole Family: A Review. *Polyhedron* **2021**, *200*, 115093. [CrossRef]
6. Ionel, H. Inverse Coordination. Organic Nitrogen Heterocycles as Coordination Centers. A Survey of Molecular Topologies and Systematization. Part Five-Membered and Smaller Rings. *J. Coord. Chem.* **2019**, *72*, 2127–2159. [CrossRef]
7. Sethi, S.; Jena, S.; Das, P.K.; Behera, N. Synthetic Approach and Structural Diversities of Pyridylpyrazole Derived Late Transition Metal Complexes. *J. Mol. Struct.* **2019**, *1193*, 495–521. [CrossRef]
8. Doidge, E.D.; Roebuck, J.W.; Healy, M.R.; Tasker, P.A. Phenolic Pyrazoles: Versatile Polynucleating Ligands. *Coord. Chem. Rev.* **2015**, *288*, 98–117. [CrossRef]
9. Lu, C.-W.; Wang, Y.; Chi, Y. Metal Complexes with Azolate-Functionalized Multidentate Ligands: Tactical Designs and Optoelectronic Applications. *Chem. Eur. J.* **2016**, *22*, 17892–17908. [CrossRef]
10. Kuwata, S.; Ikariya, T.  $\beta$ -Protic Pyrazole and N-Heterocyclic Carbene Complexes: Synthesis, Properties, and Metal–Ligand Cooperative Bifunctional Catalysis. *Chem. Eur. J.* **2011**, *17*, 3542–3556. [CrossRef]
11. Kuwata, S.; Ikariya, T. Metal–Ligand Bifunctional Reactivity and Catalysis of Protic N-Heterocyclic Carbene and Pyrazole Complexes Featuring  $\beta$ -NH Units. *Chem. Commun.* **2014**, *50*, 14290–14300. [CrossRef] [PubMed]
12. Kuwata, S. Design of Multiproton-Responsive Metal Complexes as Molecular Technology for Transformation of Small Molecules. In *Molecular Technology: Energy Innovation*; Yamamoto, H., Kato, T., Eds.; Wiley-VCH: Weinheim, Germany, 2018; pp. 81–103. ISBN 978-3-527-34163-4.
13. Pérez, J.; Riera, L. Pyrazole Complexes and Supramolecular Chemistry. *Eur. J. Inorg. Chem.* **2009**, *2009*, 4913–4925. [CrossRef]
14. Perez, J.; Riera, L. Organometallic Complexes as Anion Hosts. *Chem. Commun.* **2008**, *44*, 533–543. [CrossRef] [PubMed]
15. Perez, J.; Riera, L. Stable Metal–Organic Complexes as Anion Hosts. *Chem. Soc. Rev.* **2008**, *37*, 2658–2667. [CrossRef]
16. Ansari, A.; Ali, A.; Asif, M. Shamsuzzaman Review: Biologically Active Pyrazole Derivatives. *New J. Chem.* **2016**, *41*, 16–41. [CrossRef]
17. Khusnutdinova, J.R.; Milstein, D. Metal–Ligand Cooperation. *Angew. Chem. Int. Ed.* **2015**, *54*, 12236–12273. [CrossRef]
18. Kar, S.; Milstein, D. Sustainable Catalysis with Fluxional Acridine-Based PNP Pincer Complexes. *Chem. Commun.* **2022**, *58*, 3731–3746. [CrossRef]
19. Elsbey, M.R.; Baker, R.T. Strategies and Mechanisms of Metal–Ligand Cooperativity in First-Row Transition Metal Complex Catalysts. *Chem. Soc. Rev.* **2020**, *49*, 8933–8987. [CrossRef]
20. Cotman, A.E. Escaping from Flatland: Stereoconvergent Synthesis of Three-Dimensional Scaffolds via Ruthenium(II)-Catalyzed Noyori–Ikariya Transfer Hydrogenation. *Chem. Eur. J.* **2021**, *27*, 39–53. [CrossRef]
21. Akter, M.; Anbarasan, P. (Cyclopentadienone)iron Complexes: Synthesis, Mechanism and Applications in Organic Synthesis. *Chem. Asian J.* **2021**, *16*, 1703–1724. [CrossRef]
22. Gonçalves, T.P.; Dutta, I.; Huang, K.-W. Aromaticity in Catalysis: Metal Ligand Cooperation via Ligand Dearomatization and Rearomatization. *Chem. Commun.* **2021**, *57*, 3070–3082. [CrossRef] [PubMed]
23. Fujita, K. Development and Application of New Iridium Catalysts for Efficient Dehydrogenative Reactions of Organic Molecules. *Bull. Chem. Soc. Jpn.* **2019**, *92*, 344–351. [CrossRef]
24. Matsunami, A.; Kayaki, Y. Upgrading and Expanding the Scope of Homogeneous Transfer Hydrogenation. *Tetrahedron Lett.* **2018**, *59*, 504–513. [CrossRef]
25. Hale, L.V.A.; Szymczak, N.K. Hydrogen Transfer Catalysis beyond the Primary Coordination Sphere. *ACS Catal.* **2018**, *8*, 6446–6461. [CrossRef]
26. Dub, P.A.; Gordon, J.C. The Role of the Metal-Bound N–H Functionality in Noyori-Type Molecular Catalysts. *Nat. Rev. Chem.* **2018**, *2*, 396–408. [CrossRef]

27. Theuergarten, E.; Schlüns, D.; Grunenberg, J.; Daniliuc, C.G.; Jones, P.G.; Tamm, M. Intramolecular Heterolytic Dihydrogen Cleavage by a Bifunctional Frustrated Pyrazolylborane Lewis Pair. *Chem. Commun.* **2010**, *46*, 8561–8563. [CrossRef]
28. Theuergarten, E.; Schlösser, J.; Schlüns, D.; Freytag, M.; Daniliuc, C.G.; Jones, P.G.; Tamm, M. Fixation of Carbon Dioxide and Related Small Molecules by a Bifunctional Frustrated Pyrazolylborane Lewis Pair. *Dalton Trans.* **2012**, *41*, 9101–9110. [CrossRef]
29. Cook, L.J.K.; Mohammed, R.; Sherborne, G.; Roberts, T.D.; Alvarez, S.; Halcrow, M.A. Spin State Behavior of Iron(II)/Dipyrazolylpyridine Complexes. New Insights from Crystallographic and Solution Measurements. *Coord. Chem. Rev.* **2015**, *289–290*, 2–12. [CrossRef]
30. Halcrow, M.A. Recent Advances in the Synthesis and Applications of 2,6-Dipyrazolylpyridine Derivatives and Their Complexes. *New J. Chem.* **2014**, *38*, 1868–1882. [CrossRef]
31. Craig, G.A.; Roubeau, O.; Aromí, G. Spin State Switching in 2,6-Bis(pyrazol-3-yl)pyridine (3-Bpp) Based Fe(II) Complexes. *Coord. Chem. Rev.* **2014**, *269*, 13–31. [CrossRef]
32. Olguín, J.; Brooker, S. Spin Crossover Active Iron(II) Complexes of Selected Pyrazole-Pyridine/Pyrazine Ligands. *Coord. Chem. Rev.* **2011**, *255*, 203–240. [CrossRef]
33. Halcrow, M.A. The Synthesis and Coordination Chemistry of 2,6-Bis(pyrazolyl)pyridines and Related Ligands—Versatile Terpyridine Analogues. *Coord. Chem. Rev.* **2005**, *249*, 2880–2908. [CrossRef]
34. Li, T.-Y.; Wu, J.; Wu, Z.-G.; Zheng, Y.-X.; Zuo, J.-L.; Pan, Y. Rational Design of Phosphorescent Iridium(III) Complexes for Emission Color Tunability and Their Applications in OLEDs. *Coord. Chem. Rev.* **2018**, *374*, 55–92. [CrossRef]
35. Grotjahn, D.B.; Van, S.; Combs, D.; Lev, D.A.; Schneider, C.; Incarvito, C.D.; Lam, K.-C.; Rossi, G.; Rheingold, A.L.; Rideout, M.; et al. Substituent Control of Hydrogen Bonding in Palladium(II)-Pyrazole Complexes. *Inorg. Chem.* **2003**, *42*, 3347–3355. [CrossRef]
36. Grotjahn, D.B.; Van, S.; Combs, D.; Lev, D.A.; Schneider, C.; Rideout, M.; Meyer, C.; Hernandez, G.; Mejorado, L. New Flexible Synthesis of Pyrazoles with Different, Functionalized Substituents at C3 and C5. *J. Org. Chem.* **2002**, *67*, 9200–9209. [CrossRef]
37. Grotjahn, D.B. Bifunctional Catalysts and Related Complexes: Structures and Properties. *Dalton Trans.* **2008**, *37*, 6497–6508. [CrossRef]
38. Labrum, N.S.; Chen, C.-H.; Caulton, K.G. A New Face for Bis(pyrazol-3-yl)pyridine: Incompatible Geometric Preferences Dictates Unprecedented Pincer Ligand Connectivity. *Inorg. Chim. Acta* **2019**, *485*, 54–57. [CrossRef]
39. Jozak, T.; Zabel, D.; Schubert, A.; Thiel, W.R. Ruthenium Complexes Bearing N–H Acidic Pyrazole Ligands. *Eur. J. Inorg. Chem.* **2010**, *2010*, 5135–5145. [CrossRef]
40. Yoshinari, A.; Tazawa, A.; Kuwata, S.; Ikariya, T. Synthesis, Structures, and Reactivities of Pincer-Type Ruthenium Complexes Bearing Two Proton-Responsive Pyrazole Arms. *Chem. Asian J.* **2012**, *7*, 1417–1425. [CrossRef]
41. Kashiwame, Y.; Watanabe, M.; Araki, K.; Kuwata, S.; Ikariya, T. Synthesis, Structure, and Proton-Transfer Reactions of Brønsted Acidic Pyridylpyrazole Complexes of Ruthenium. *Bull. Chem. Soc. Jpn.* **2011**, *84*, 251–258. [CrossRef]
42. Liao, J.-L.; Chi, Y.; Su, Y.-D.; Huang, H.-X.; Chang, C.-H.; Liu, S.-H.; Lee, G.-H.; Chou, P.-T. Os(II) Metal Phosphors Bearing Tridentate 2,6-Di(pyrazol-3-yl)pyridine Chelate: Synthetic Design, Characterization and Application in OLED Fabrication. *J. Mater. Chem. C* **2014**, *2*, 6269–6282. [CrossRef]
43. Petrović, A.Z.; Čočić, D.C.; Bockfeld, D.; Živanović, M.; Milivojević, N.; Virijević, K.; Janković, N.; Scheurer, A.; Vraneš, M.; Bogojeski, J.V. Biological Activity of Bis(pyrazolylpyridine) and Terpyridine Os(II) Complexes in the Presence of Biocompatible Ionic Liquids. *Inorg. Chem. Front.* **2021**, *8*, 2749–2770. [CrossRef]
44. Kuo, J.L.; Goldberg, K.I. Metal/Ligand Proton Tautomerism Facilitates Dinuclear H<sub>2</sub> Reductive Elimination. *J. Am. Chem. Soc.* **2020**, *142*, 21439–21449. [CrossRef] [PubMed]
45. Milutinović, M.M.; Bogojeski, J.V.; Klisurić, O.; Scheurer, A.; Elmroth, S.K.C.; Bugarčić, Z.D. Synthesis and Structures of a Pincer-Type Rhodium(III) Complex: Reactivity toward Biomolecules. *Dalton Trans.* **2016**, *45*, 15481–15491. [CrossRef] [PubMed]
46. Toda, T.; Saitoh, K.; Yoshinari, A.; Ikariya, T.; Kuwata, S. Synthesis and Structures of NCN Pincer-Type Ruthenium and Iridium Complexes Bearing Protic Pyrazole Arms. *Organometallics* **2017**, *36*, 1188–1195. [CrossRef]
47. Zahora, B.A.; Gau, M.R.; Goldberg, K.I. Synthesis and Reactivity of Pt<sup>II</sup> Methyl Complexes Supported by Pyrazolate Pincer Ligands. *Organometallics* **2020**, *39*, 1230–1237. [CrossRef]
48. Galstyan, A.; Naziruddin, A.R.; Cebrián, C.; Iordache, A.; Daniliuc, C.G.; Cola, L.D.; Strassert, C.A. Correlating the Structural and Photophysical Features of Pincer Luminophores and Monodentate Ancillary Ligands in Pt<sup>II</sup> Phosphors. *Eur. J. Inorg. Chem.* **2015**, *2015*, 5822–5831. [CrossRef]
49. Umehara, K.; Kuwata, S.; Ikariya, T. Synthesis, Structures, and Reactivities of Iron, Cobalt, and Manganese Complexes Bearing a Pincer Ligand with Two Protic Pyrazole Arms. *Inorg. Chim. Acta* **2014**, *413*, 136–142. [CrossRef]
50. Umehara, K.; Kuwata, S.; Ikariya, T. N–N Bond Cleavage of Hydrazines with a Multiproton-Responsive Pincer-Type Iron Complex. *J. Am. Chem. Soc.* **2013**, *135*, 6754–6757. [CrossRef]
51. Nikovsky, I.A.; Polezhaev, A.V.; Melnikova, E.K.; Nelyubina, Y.V. New Iron(III) Oxo Complex with Substituted 2,6-Bis(pyrazol-3-yl)pyridine. *Russ. J. Inorg. Chem.* **2020**, *65*, 864–869. [CrossRef]
52. Cook, B.J.; Polezhaev, A.V.; Chen, C.-H.; Pink, M.; Caulton, K.G. Deprotonation, Chloride Abstraction, and Dehydrohalogenation as Synthetic Routes to Bis-Pyrazolate Pyridyl Iron(II) Complexes. *Eur. J. Inorg. Chem.* **2017**, *2017*, 3999–4012. [CrossRef]
53. Cook, B.J.; Chen, C.-H.; Pink, M.; Caulton, K.G. Dehydrohalogenation of Proton Responsive Complexes: Versatile Aggregation Viapyrazolate Pincer Ligand Arms. *Dalton Trans.* **2018**, *47*, 2052–2060. [CrossRef] [PubMed]

54. Cook, B.J.; Pink, M.; Chen, C.-H.; Caulton, K.G. Electrophile Recruitment as a Structural Element in Bis-Pyrazolate Pyridine Complex Aggregation. *Eur. J. Inorg. Chem.* **2018**, *2018*, 5160–5166. [CrossRef]
55. Cook, B.J.; Chen, C.-H.; Caulton, K.G. A Multifunctional Pincer Ligand for Cobalt-Promoted Oxidation by N<sub>2</sub>O. *Chem. Eur. J.* **2018**, *24*, 5962–5966. [CrossRef] [PubMed]
56. Cook, B.J.; Pink, M.; Pal, K.; Caulton, K.G. Electron and Oxygen Atom Transfer Chemistry of Co(II) in a Proton Responsive, Redox Active Ligand Environment. *Inorg. Chem.* **2018**, *57*, 6176–6185. [CrossRef]
57. Labrum, N.S.; Pink, M.; Chen, C.-H.; Caulton, K.G. Reactivity of an Unusual Divalent Chromium Aggregate Supported by a Multifunctional Bis(pyrazolate) Pincer Ligand. *Eur. J. Inorg. Chem.* **2019**, *2019*, 1932–1940. [CrossRef]
58. Labrum, N.S.; Curtin, G.M.; Jakubikova, E.; Caulton, K.G. The Influence of Nucleophilic and Redox Pincer Character as Well as Alkali Metals on the Capture of Oxygen Substrates: The Case of Chromium(II). *Chem. Eur. J.* **2020**, *26*, 9547–9555. [CrossRef]
59. Labrum, N.S.; Chen, C.-H.; Caulton, K.G. A Bis-Pyrazolate Pincer on Reduced Cr Deoxygenates CO<sub>2</sub>: Selective Capture of the Derived Oxide by Cr<sup>III</sup>. *Chem. Eur. J.* **2019**, *25*, 7935–7940. [CrossRef]
60. Toda, T.; Yoshinari, A.; Ikariya, T.; Kuwata, S. Protic N-Heterocyclic Carbene Versus Pyrazole: Rigorous Comparison of Proton- and Electron-Donating Abilities in a Pincer-Type Framework. *Chem. Eur. J.* **2016**, *22*, 16675–16683. [CrossRef]
61. Toda, T.; Kuwata, S. Central N-Heterocyclic Carbene Moieties in Protic Pincer-Type Bis(pyrazole) Ligands: Perturbation on Steric and Electronic Properties of Ruthenium Center. *J. Organomet. Chem.* **2020**, *917*, 121270. [CrossRef]
62. Toda, T.; Kuwata, S. Synthesis, Structures, and Reactivities of Iron Complexes Bearing an Isoindoline-Based, Polyprotic Pincer-Type Pyrazole Ligand. *Z. Anorg. Allg. Chem.* **2021**, *647*, 1471–1477. [CrossRef]
63. Kuwata, S.; Hahn, F.E. Complexes Bearing Protic N-Heterocyclic Carbene Ligands. *Chem. Rev.* **2018**, *118*, 9642–9677. [CrossRef] [PubMed]
64. Toda, T.; Kuwata, S.; Ikariya, T. Unsymmetrical Pincer-Type Ruthenium Complex Containing β-Protic Pyrazole and N-Heterocyclic Carbene Arms: Comparison of Brønsted Acidity of NH Groups in Second Coordination Sphere. *Chem. Eur. J.* **2014**, *20*, 9539–9542. [CrossRef] [PubMed]
65. Toda, T.; Kuwata, S.; Ikariya, T. Synthesis and Structures of Ruthenium and Iron Complexes Bearing an Unsymmetrical Pincer-Type Ligand with Protic Pyrazole and Tertiary Aminoalkyl Arms. *Z. Anorg. Allg. Chem.* **2015**, *641*, 2135–2139. [CrossRef]
66. Polezhaev, A.V.; Liss, C.J.; Telser, J.; Chen, C.-H.; Caulton, K.G. A PNNH Pincer Ligand Allows Access to Monovalent Iron. *Chem. Eur. J.* **2018**, *24*, 1330–1341. [CrossRef] [PubMed]
67. Polezhaev, A.V.; Chen, C.; Losovyj, Y.; Caulton, K.G. A Multifunctional Pincer Ligand Supports Unsaturated Cobalt: Five Functionalities in One Pincer. *Chem. Eur. J.* **2017**, *23*, 8039–8050. [CrossRef] [PubMed]
68. Cabelof, A.C.; Carta, V.; Chen, C.-H.; Pink, M.; Caulton, K.G. Pincers with Diverse Donors and Their Interconversion: Application to Ni(II). *Z. Anorg. Allg. Chem.* **2021**, *647*, 1524–1529. [CrossRef]
69. Koo, C.-K.; Ho, Y.-M.; Chow, C.-F.; Lam, M.H.-W.; Lau, T.-C.; Wong, W.-Y. Synthesis and Spectroscopic Studies of Cyclometalated Pt(II) Complexes Containing a Functionalized Cyclometalating Ligand, 2-Phenyl-6-(1H-pyrazol-3-yl)-pyridine. *Inorg. Chem.* **2007**, *46*, 3603–3612. [CrossRef] [PubMed]
70. Arroyo, M.; Gómez-Iglesias, P.; Anton, N.; García-Rodríguez, R.; Alegria, E.C.B.A.; Pombeiro, A.J.L.; Miguel, D.; Villafaña, F. Homo- and Heteropolymetallic 3-(2-Pyridyl)pyrazolate Manganese and Rhenium Complexes. *Dalton Trans.* **2014**, *43*, 4009–4020. [CrossRef]
71. Cabelof, A.C.; Carta, V.; Caulton, K.G. A Proton-Responsive Ligand Becomes a Dimetal Linker for Multisubstrate Assembly via Nitrate Deoxygenation. *Chem. Commun.* **2021**, *57*, 2780–2783. [CrossRef]
72. Nakahara, Y.; Toda, T.; Kuwata, S. Iron and Ruthenium Complexes Having a Pincer-Type Ligand with Two Protic Amidepyrazole Arms: Structures and Catalytic Application. *Polyhedron* **2018**, *143*, 105–110. [CrossRef]
73. Tanaka, H.; Hitaoka, S.; Umehara, K.; Yoshizawa, K.; Kuwata, S. Mechanistic Study on Catalytic Disproportionation of Hydrazine by a Protic Pincer-Type Iron Complex through Proton-Coupled Electron Transfer. *Eur. J. Inorg. Chem.* **2020**, *2020*, 1472–1482. [CrossRef]
74. Yamagishi, H.; Konuma, H.; Kuwata, S. Stereoselective Synthesis of Chlorido-Phosphine Ruthenium Complexes Bearing a Pyrazole-Based Protic Tripodal Amine Ligand. *Polyhedron* **2017**, *125*, 173–178. [CrossRef]
75. Yamagishi, H.; Nabeya, S.; Ikariya, T.; Kuwata, S. Protic Ruthenium Tris(pyrazol-3-ylmethyl)amine Complexes Featuring a Hydrogen-Bonding Network in the Second Coordination Sphere. *Inorg. Chem.* **2015**, *54*, 11584–11586. [CrossRef]
76. Labrum, N.S.; Cabelof, A.C.; Caulton, K.G. A Dimeric Chromium(II) Pincer as an Electron Shuttle for N=N Bond Scission. *Chem. Eur. J.* **2020**, *26*, 13915–13926. [CrossRef]
77. Labrum, N.S.; Caulton, K.G. [Cr(Pincer<sup>2-</sup>)<sub>2</sub>] as an Electron Shuttle for Reductively Promoted Hydrazine Disproportionation. *Dalton Trans.* **2019**, *48*, 11642–11646. [CrossRef]
78. Toda, T.; Suzuki, S.; Kuwata, S. Metallo-Supramolecular Assembly of Protic Pincer-Type Complexes: Encapsulation of Dinitrogen and Carbon Disulfide into a Multiproton-Responsive Diruthenium Cage. *Chem. Commun.* **2019**, *55*, 1028–1031. [CrossRef]
79. Saito, T.; Nishiyama, H.; Tanahashi, H.; Kawakita, K.; Tsurugi, H.; Mashima, K. 1,4-Bis(trimethylsilyl)-1,4-diaza-2,5-cyclohexadienes as Strong Salt-Free Reductants for Generating Low-Valent Early Transition Metals with Electron-Donating Ligands. *J. Am. Chem. Soc.* **2014**, *136*, 5161–5170. [CrossRef]
80. Labrum, N.S.; Seo, J.; Chen, C.-H.; Pink, M.; Beagan, D.M.; Caulton, K.G. Di- and Trivalent Chromium Bis(pyrazol-3-yl)pyridine Pincer Complexes with Good Leaving Groups. *Inorg. Chim. Acta* **2019**, *486*, 483–491. [CrossRef]



81. Seo, J.; Cabelof, A.C.; Chen, C.-H.; Caulton, K.G. Selective Deoxygenation of Nitrate to Nitrosyl Using Trivalent Chromium and the Mashima Reagent: Reductive Silylation. *Chem. Sci.* **2018**, *10*, 475–479. [CrossRef]
82. Cabelof, A.C.; Erny, A.M.; Beagan, D.M.; Caulton, K.G. A Redox Cascade of  $\text{NO}_x^-$  Complexes: Structures and Nitrogen Deoxygenation Thermodynamics. *Polyhedron* **2021**, *200*, 115119. [CrossRef]
83. Cabelof, A.C.; Carta, V.; Chen, C.-H.; Caulton, K.G. Nitrogen Oxyanion Reduction by Co(II) Augmented by a Proton Responsive Ligand: Recruiting Multiple Metals. *Dalton Trans.* **2020**, *49*, 7891–7896. [CrossRef] [PubMed]
84. Tseng, Y.-T.; Ching, W.-M.; Liaw, W.-F.; Lu, T.-T. Dinitrosyl Iron Complex [K-18-crown-6-ether][ $(\text{NO})_2\text{Fe}(\text{MePyrCO}_2)$ ]: Intermediate for Capture and Reduction of Carbon Dioxide. *Angew. Chem. Int. Ed.* **2020**, *59*, 11819–11823. [CrossRef] [PubMed]
85. Zeng, F.; Yu, Z. Ruthenium(II) Complexes Bearing a Pyridyl-Supported Pyrazolyl-N-Heterocyclic Carbene (NNC) Ligand and Their Catalytic Activity in the Transfer Hydrogenation of Ketones. *Organometallics* **2008**, *27*, 6025–6028. [CrossRef]
86. Jin, W.; Wang, L.; Yu, Z. A Highly Active Ruthenium(II) Pyrazolyl-Pyridyl-Pyrazole Complex Catalyst for Transfer Hydrogenation of Ketones. *Organometallics* **2012**, *31*, 5664–5667. [CrossRef]
87. Liu, T.; Wang, L.; Wu, K.; Wang, Q.; Yu, Z. Mono- and Multinuclear Pincer-Type Ru(II) Complex Catalysts and Their Catalytic Applications. *Inorg. Chim. Acta* **2023**, *551*, 121458. [CrossRef]
88. Zeng, F.; Yu, Z. Exceptionally Efficient Unsymmetrical Ruthenium(II) NNN Complex Catalysts Bearing a Pyridyl-Based Pyrazolyl-Imidazolyl Ligand for Transfer Hydrogenation of Ketones. *Organometallics* **2008**, *27*, 2898–2901. [CrossRef]
89. Zeng, F.; Yu, Z. Construction of Highly Active Ruthenium(II) NNN Complex Catalysts Bearing a Pyridyl-Supported Pyrazolyl-Imidazolyl Ligand for Transfer Hydrogenation of Ketones. *Organometallics* **2009**, *28*, 1855–1862. [CrossRef]
90. Ye, W.; Zhao, M.; Yu, Z. Ruthenium(II) Pyrazolyl-Pyridyl-Oxazolonyl Complex Catalysts for the Asymmetric Transfer Hydrogenation of Ketones. *Chem. Eur. J.* **2012**, *18*, 10843–10846. [CrossRef]
91. Roberts, T.D.; Halcrow, M.A. Supramolecular Assembly and Transfer Hydrogenation Catalysis with Ruthenium(II) Complexes of 2,6-Di(1H-pyrazol-3-yl)pyridine Derivatives. *Polyhedron* **2016**, *103*, 79–86. [CrossRef]
92. Kashiwame, Y.; Kuwata, S.; Ikariya, T. Metal-Pyrazole Bifunction in Half-Sandwich C–N Chelate Iridium Complexes: Pyrazole-Pyrazolato Interconversion and Application to Catalytic Intramolecular Hydroamination of Aminoalkene. *Chem. Eur. J.* **2010**, *16*, 766–770. [CrossRef] [PubMed]
93. Kashiwame, Y.; Ikariya, T.; Kuwata, S. Synthesis, Structures, and Reactivities of Six-Membered C–N Chelate Protic Pyrazole Complexes of Iridium. *Polyhedron* **2021**, *197*, 115036. [CrossRef]
94. Ghoochany, L.T.; Farsadpour, S.; Sun, Y.; Thiel, W.R. New N,N,N-Donors Resulting in Highly Active Ruthenium Catalysts for Transfer Hydrogenation at Room Temperature. *Eur. J. Inorg. Chem.* **2011**, *2011*, 3431–3437. [CrossRef]
95. Zhu, Z.; Zhang, J.; Fu, H.; Yuan, M.; Zheng, X.; Chen, H.; Li, R. Construction of Pincer-Type Symmetrical Ruthenium(II) Complexes Bearing Pyridyl-2,6-Pyrazolyl Arms: Catalytic Behavior in Transfer Hydrogenation of Ketones. *RSC Adv.* **2014**, *4*, 52734–52739. [CrossRef]
96. Dayan, O.; Dayan, S.; Kani, I.; Cetinkaya, B. Ruthenium(II) Complexes Bearing Pyridine-Based Tridentate and Bidentate Ligands: Catalytic Activity for Transfer Hydrogenation of Aryl Ketones. *Adv. Organomet. Chem.* **2012**, *26*, 663–670. [CrossRef]
97. Gunnaz, S.; Ozdemir, N.; Dayan, S.; Dayan, O.; Cetinkaya, B. Synthesis of Ruthenium(II) Complexes Containing Tridentate Triamine ('NNN') and Bidentate Diamine Ligands (NN'): As Catalysts for Transfer Hydrogenation of Ketones. *Organometallics* **2011**, *30*, 4165–4173. [CrossRef]
98. Alshakova, I.D.; Korobkov, I.; Kuzmina, L.G.; Nikonov, G.I. Ruthenium Complexes with a Pyrazole-Phosphine Ligand. *J. Organomet. Chem.* **2017**, *853*, 68–73. [CrossRef]
99. Alshakova, I.D.; Gabidullin, B.; Nikonov, G.I. Ru-Catalyzed Transfer Hydrogenation of Nitriles, Aromatics, Olefins, Alkynes and Esters. *ChemCatChem* **2018**, *10*, 4860–4869. [CrossRef]
100. Dubey, A.; Khaskin, E. Catalytic Ester Metathesis Reaction and Its Application to Transfer Hydrogenation of Esters. *ACS Catal.* **2016**, *6*, 3998–4002. [CrossRef]
101. Tian, C.; Gong, L.; Meggers, E. Chiral-at-Metal Iridium Complex for Efficient Enantioselective Transfer Hydrogenation of Ketones. *Chem. Commun.* **2016**, *52*, 4207–4210. [CrossRef]
102. Zhang, X.; Qin, J.; Huang, X.; Meggers, E. Sequential Asymmetric Hydrogenation and Photoredox Chemistry with a Single Catalyst. *Org. Chem. Front.* **2018**, *5*, 166–170. [CrossRef]
103. Muller, K.; Sun, Y.; Heimermann, A.; Menges, F.; Niedner-Schatteburg, G.; van Wüllen, C.; Thiel, W.R. Structure–Reactivity Relationships in the Hydrogenation of Carbon Dioxide with Ruthenium Complexes Bearing Pyridinylazolato Ligands. *Chem. Eur. J.* **2013**, *19*, 7825–7834. [CrossRef] [PubMed]
104. Hashiguchi, B.G.; Young, K.J.H.; Yousufuddin, M.; Goddard, W.A.; Periana, R.A. Acceleration of Nucleophilic CH Activation by Strongly Basic Solvents. *J. Am. Chem. Soc.* **2010**, *132*, 12542–12545. [CrossRef] [PubMed]
105. Suna, Y.; Himeda, Y.; Fujita, E.; Muckerman, J.T.; Ertem, M.Z. Iridium Complexes with Proton-Responsive Azole-Type Ligands as Effective Catalysts for  $\text{CO}_2$  Hydrogenation. *ChemSusChem* **2017**, *10*, 4535–4543. [CrossRef] [PubMed]
106. Onishi, N.; Xu, S.; Manaka, Y.; Suna, Y.; Wang, W.-H.; Muckerman, J.T.; Fujita, E.; Himeda, Y.  $\text{CO}_2$  Hydrogenation Catalyzed by Iridium Complexes with a Proton-Responsive Ligand. *Inorg. Chem.* **2015**, *54*, 5114–5123. [CrossRef]
107. Manaka, Y.; Wang, W.-H.; Suna, Y.; Kambayashi, H.; Muckerman, J.T.; Fujita, E.; Himeda, Y. Efficient  $\text{H}_2$  Generation from Formic Acid Using Azole Complexes in Water. *Catal. Sci. Technol.* **2014**, *4*, 34–37. [CrossRef]




108. Wang, W.-H.; Wang, H.; Yang, Y.; Lai, X.; Li, Y.; Wang, J.; Himeda, Y.; Bao, M. Synergistic Effect of Pendant N Moieties for Proton Shuttling in the Dehydrogenation of Formic Acid Catalyzed by Biomimetic Ir<sup>III</sup> Complexes. *ChemSusChem* **2020**, *13*, 5015–5022. [CrossRef]
109. Nakahara, Y.; Toda, T.; Matsunami, A.; Kayaki, Y.; Kuwata, S. Protic NNN and NCN Pincer-Type Ruthenium Complexes Featuring (Trifluoromethyl)pyrazole Arms: Synthesis and Application to Catalytic Hydrogen Evolution from Formic Acid. *Chem. Asian J.* **2018**, *13*, 73–80. [CrossRef]
110. Pal, S.; Iwasaki, T.; Nozaki, K. Metal–Ligand Cooperative  $\kappa_1$ -N-Pyrazolate Cp\*Rh<sup>III</sup>-Catalysts for Dehydrogenation of Dimethylamine-Borane at Room Temperature. *Dalton Trans.* **2021**, *50*, 7938–7943. [CrossRef]
111. Reed-Berendt, B.G.; Latham, D.E.; Dambatta, M.B.; Morrill, L.C. Borrowing Hydrogen for Organic Synthesis. *ACS Cent. Sci.* **2021**, *7*, 570–585. [CrossRef]
112. Kuwahara, T.; Fukuyama, T.; Ryu, I. Ruthenium Hydride/Nitrogen Tridentate Ligand-Catalyzed  $\alpha$ -Alkylation of Acetamides with Primary Alcohols. *RSC Adv.* **2013**, *3*, 13702–13704. [CrossRef]
113. Panda, S.; Saha, R.; Sethi, S.; Ghosh, R.; Bagh, B. Efficient  $\alpha$ -Alkylation of Arylacetonitriles with Secondary Alcohols Catalyzed by a Phosphine-Free Air-Stable Iridium(III) Complex. *J. Org. Chem.* **2020**, *85*, 15610–15621. [CrossRef] [PubMed]
114. Dutta, I.; Yadav, S.; Sarbajna, A.; De, S.; Hölscher, M.; Leitner, W.; Bera, J.K. Double Dehydrogenation of Primary Amines to Nitriles by a Ruthenium Complex Featuring Pyrazole Functionality. *J. Am. Chem. Soc.* **2018**, *140*, 8662–8666. [CrossRef] [PubMed]
115. Chai, H.; Yu, K.; Liu, B.; Tan, W.; Zhang, G. A Highly Selective Manganese-Catalyzed Synthesis of Imines under Phosphine-Free Conditions. *Organometallics* **2020**, *39*, 217–226. [CrossRef]
116. Satake, A.; Nakata, T. Novel  $\eta^3$ -Allylpalladium–Pyridinylpyrazole Complex: Synthesis, Reactivity, and Catalytic Activity for Cyclopropanation of Ketene Silyl Acetal with Allylic Acetates. *J. Am. Chem. Soc.* **1998**, *120*, 10391–10396. [CrossRef]
117. Satake, A.; Koshino, H.; Nakata, T. Cyclopropanation of Ketene Silyl Acetals with Allylic Acetates Using  $\eta^3$ -Allylpalladium–Pyridinylimidazole Catalysts. *Chem. Lett.* **1999**, *28*, 49–50. [CrossRef]
118. Aranyos, A.; Szabó, K.J.; Castaño, A.M.; Bäckvall, J.-E. Central versus Terminal Attack in Nucleophilic Addition to ( $\pi$ -Allyl)palladium Complexes. Ligand Effects and Mechanism. *Organometallics* **1997**, *16*, 1058–1064. [CrossRef]
119. Satake, A.; Kadohama, H.; Koshino, H.; Nakata, T. Asymmetric Cyclopropanation of Ketene Silyl Acetal with Allylic Acetate Catalyzed by a Palladium Complex. *Tetrahedron Lett.* **1999**, *40*, 3597–3600. [CrossRef]
120. Diez, J.; Gimeno, J.; Lledós, A.; Suárez, F.J.; Vicent, C. Imidazole Based Ruthenium(IV) Complexes as Highly Efficient Bifunctional Catalysts for the Redox Isomerization of Allylic Alcohols in Aqueous Medium: Water as Cooperating Ligand. *ACS Catal.* **2012**, *2*, 2087–2099. [CrossRef]
121. Bellarosa, L.; Diez, J.; Gimeno, J.; Lledós, A.; Suárez, F.J.; Ujaque, G.; Vicent, C. Highly Efficient Redox Isomerisation of Allylic Alcohols Catalysed by Pyrazole-Based Ruthenium(IV) Complexes in Water: Mechanisms of Bifunctional Catalysis in Water. *Chem. Eur. J.* **2012**, *18*, 7749–7765. [CrossRef]
122. Tashima, N.; Ohta, S.; Kuwata, S. Metal–Ligand Cooperative C–O Bond Cleavage of Propargylic Alcohol with Protic Pyrazole Complexes of Ruthenium. *Faraday Discuss.* **2019**, *220*, 364–375. [CrossRef] [PubMed]
123. Justaud, F.; Hachem, A.; Grée, R. Recent Developments in the Meyer-Schuster Rearrangement. *Eur. J. Org. Chem.* **2021**, *2021*, 514–542. [CrossRef]
124. Cadierno, V.; Crochet, P.; García-Garrido, S.E.; Gimeno, J. Metal-Catalyzed Transformations of Propargylic Alcohols into  $\alpha,\beta$ -Unsaturated Carbonyl Compounds: From the Meyer–Schuster and Rupe Rearrangements to Redox Isomerizations. *Dalton Trans.* **2010**, *39*, 4015–4031. [CrossRef] [PubMed]
125. Wojcicki, A. Allenyls and Propargyls: Versatile Ligands in Transition-Metal Chemistry. *Inorg. Chem. Commun.* **2002**, *5*, 82–97. [CrossRef]
126. Ferrer, Í.; Rich, J.; Fontrodona, X.; Rodríguez, M.; Romero, I. Ru(II) Complexes Containing DMSO and Pyrazolyl Ligands as Catalysts for Nitrile Hydration in Environmentally Friendly Media. *Dalton Trans.* **2013**, *42*, 13461–13469. [CrossRef] [PubMed]
127. Ferrer, Í.; Fontrodona, X.; Rodríguez, M.; Romero, I. Ru(II)-DMSO Complexes Containing Azole-Based Ligands: Synthesis, Linkage Isomerism and Catalytic Behaviour. *Dalton Trans.* **2016**, *45*, 3163–3174. [CrossRef]
128. Zhang, L.; Meggers, E. Steering Asymmetric Lewis Acid Catalysis Exclusively with Octahedral Metal-Centered Chirality. *Acc. Chem. Res.* **2017**, *50*, 320–330. [CrossRef]
129. Zhang, L.; Meggers, E. Stereogenic-Only-at-Metal Asymmetric Catalysts. *Chem. Asian J.* **2017**, *12*, 2335–2342. [CrossRef]
130. Chen, L.-A.; Tang, X.; Xi, J.; Xu, W.; Gong, L.; Meggers, E. Chiral-at-Metal Octahedral Iridium Catalyst for the Asymmetric Construction of an All-Carbon Quaternary Stereocenter. *Angew. Chem. Int. Ed.* **2013**, *52*, 14021–14025. [CrossRef]
131. Vera, S.; García-Urricelqui, A.; Mielgo, A.; Oiárbide, M. Progress in (Thio)urea- and Squaramide-Based Brønsted Base Catalysts with Multiple H-Bond Donors. *Eur. J. Org. Chem.* **2023**, *26*, e202201254. [CrossRef]
132. Agarwal, P.; Thirupathi, N.; Nethaji, M. Syntheses, Structural Aspects, Solution Behavior, and Catalytic Utility of Cyclopalladated  $N,N',N''$ -Triarylguanidines [ $\kappa^2$ (C,N)Pd(Pyrazole)<sub>2</sub>X] (X = Br, OC(O)CF<sub>3</sub>, and PF<sub>6</sub>) in Suzuki–Miyaura Coupling Reactions of Aryl Bromides. *Organometallics* **2016**, *35*, 3112–3123. [CrossRef]
133. Yang, Q.; Wang, L.; Lei, L.; Zheng, X.-L.; Fu, H.; Yuan, M.; Chen, H.; Li, R.-X. PdCl<sub>2</sub>-2,6-Bis(1,5-diphenyl-1H-pyrazol-3-yl)pyridine Catalyzed Suzuki–Miyaura Cross-Coupling. *Catal. Commun.* **2012**, *29*, 194–197. [CrossRef]

134. Nacienceno, V.S.; Azpeitia, S.; Ibarlucea, L.; Mendicute-Fierro, C.; Rodriguez-Dieguez, A.; Seco, J.M.; Sebastian, E.S.; Garralda, M.A. Stereoselective Formation and Catalytic Activity of Hydrido(acylphosphane)(chlorido)(pyrazole)rhodium(III) Complexes. Experimental and DFT Studies. *Dalton Trans.* **2015**, *44*, 13141–13155. [CrossRef] [PubMed]
135. Manrique, E.; Fontrodona, X.; Rodríguez, M.; Romero, I. A Ruthenium(II) Aqua Complex as Efficient Chemical and Photochemical Catalyst for Alkene and Alcohol Oxidation. *Eur. J. Inorg. Chem.* **2019**, *2019*, 2124–2133. [CrossRef]

**Disclaimer/Publisher's Note:** The statements, opinions and data contained in all publications are solely those of the individual author(s) and contributor(s) and not of MDPI and/or the editor(s). MDPI and/or the editor(s) disclaim responsibility for any injury to people or property resulting from any ideas, methods, instructions or products referred to in the content.

Review

# Recent Applications of the Multicomponent Synthesis for Bioactive Pyrazole Derivatives

Diana Becerra <sup>1</sup>, Rodrigo Abonia <sup>2</sup> and Juan-Carlos Castillo <sup>1,\*</sup>

<sup>1</sup> Escuela de Ciencias Química, Facultad de Ciencias, Universidad Pedagógica y Tecnológica de Colombia, Avenida Central del Norte, Tunja 150003, Colombia; diana.becerra08@uptc.edu.co

<sup>2</sup> Research Group of Heterocyclic Compounds, Department of Chemistry, Universidad del Valle, A.A. 25360, Cali 76001, Colombia; rodrigo.abonia@correounivalle.edu.co

\* Correspondence: juan.castillo06@uptc.edu.co; Tel.: +57-8-740-5626 (ext. 2425)

**Abstract:** Pyrazole and its derivatives are considered a privileged *N*-heterocycle with immense therapeutic potential. Over the last few decades, the pot, atom, and step economy (PASE) synthesis of pyrazole derivatives by multicomponent reactions (MCRs) has gained increasing popularity in pharmaceutical and medicinal chemistry. The present review summarizes the recent developments of multicomponent reactions for the synthesis of biologically active molecules containing the pyrazole moiety. Particularly, it covers the articles published from 2015 to date related to antibacterial, anticancer, antifungal, antioxidant,  $\alpha$ -glucosidase and  $\alpha$ -amylase inhibitory, anti-inflammatory, antimycobacterial, antimalarial, and miscellaneous activities of pyrazole derivatives obtained exclusively via an MCR. The reported analytical and activity data, plausible synthetic mechanisms, and molecular docking simulations are organized in concise tables, schemes, and figures to facilitate comparison and underscore the key points of this review. We hope that this review will be helpful in the quest for developing more biologically active molecules and marketed drugs containing the pyrazole moiety.

**Keywords:** multicomponent reactions (MCRs); pyrazole derivatives; biological activity; medicinal chemistry; drug discovery

**Citation:** Becerra, D.; Abonia, R.; Castillo, J.-C. Recent Applications of the Multicomponent Synthesis for Bioactive Pyrazole Derivatives. *Molecules* **2022**, *27*, 4723. <https://doi.org/10.3390/molecules27154723>

Academic Editors: Vera L. M. Silva and Artur M. S. Silva

Received: 7 July 2022

Accepted: 20 July 2022

Published: 23 July 2022

**Publisher's Note:** MDPI stays neutral with regard to jurisdictional claims in published maps and institutional affiliations.



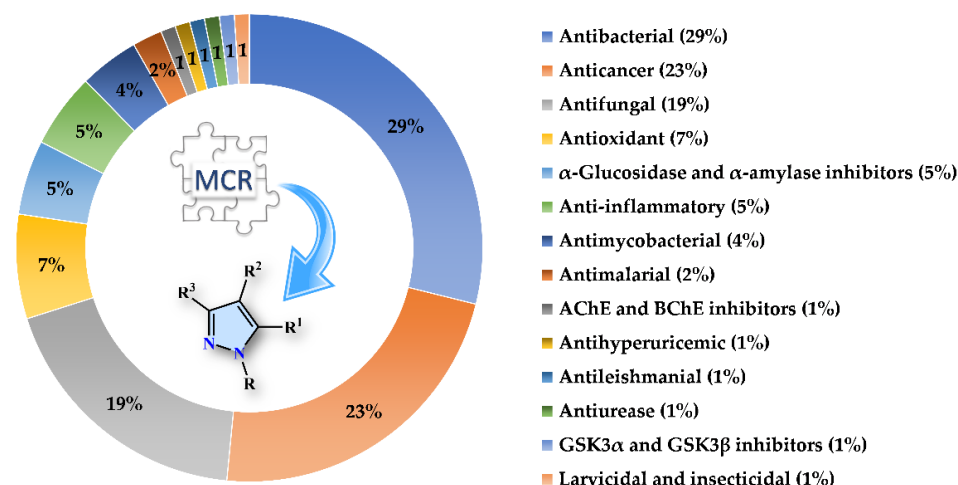
**Copyright:** © 2022 by the authors. Licensee MDPI, Basel, Switzerland. This article is an open access article distributed under the terms and conditions of the Creative Commons Attribution (CC BY) license (<https://creativecommons.org/licenses/by/4.0/>).

## 1. Introduction

Multicomponent reactions (MCRs) are one-pot reactions employing three or more components to form a product, where most of the atoms of all starting materials are substantially incorporated in the final product [1]. To date, MCRs have innumerable advantages over sequential multistep synthesis such as operational simplicity, saving time and energy (step efficiency), proceeding with high convergence (process efficiency), exhibiting a very high bond-forming index (BFI), and are highly compatible with a range of unprotected orthogonal functional groups [1,2]. Thereby, MCRs are considered a powerful alternative to synthesize complex organic molecules in a high chemo-, regio-, and stereoselective manner with a plethora of applications in agrochemistry [3], polymer chemistry [4], combinational chemistry [5], medicinal chemistry [6], and especially drug discovery programs [7]. Importantly, MCRs allow the incorporation of diverse scaffold shapes by using MCR variants such as Strecker (1850) [8], Hantzsch (1881) [9], Biginelli (1891) [10], Mannich (1912) [11], Passerini (1921) [12], Kabachnik–Fields (1952) [13], Asinger (1956) [14], Ugi (1959) [15], Gewald (1966) [16], Van Leusen (1977) [17], and Groebke–Blackburn–Bienaymé (1998) [18], among others. Although most of the MCRs were discovered in the second half of the twentieth century, their use has grown enormously over the last four decades due to the demand for organic molecules in medicinal chemistry and drug discovery programs. It is estimated that approximately 5% of the commercially available drugs can be synthesized by an MCR strategy [19]. For instance, Nifedipine (Hantzsch), Telaprevir (Passerini), and

Crixivan (Ugi) are valuable examples of marketed drugs obtained through this synthetic strategy [19].

On the other hand, pyrazole is a “biologically privileged” five-membered *N*-heteroaromatic compound containing two nitrogen atoms in adjacent positions. Nowadays, pyrazole and its derivatives have attracted considerable attention due to their broad spectrum of pharmaceutical and biological properties [20–22], proving to be significant structural components of active pharmaceutical ingredients (APIs) and diverse pyrazole-based compounds. It is exemplified by the number of FDA-approved drugs containing the pyrazole scaffold, such as Celecoxib, Lonazolac, Mepirizole, Rimonabant, Difenamizole, Betazole, Fezolamine, Tepoxalin, Pyrazofurin, and Deracoxib, among other marketed drugs [20,21]. The innumerable applications in medicinal chemistry, biomedical science, and drug discovery have stimulated the academia and pharmaceutical industry for developing new, efficient, and simple synthetic protocols to prepare structurally diverse pyrazole derivatives [23–25]. Quite impressively, 1241 publications and 148 reviews have been reported in the Scopus database from 2015 to date searching for the keywords “pyrazole derivatives” and “biological activity”. In particular, 64 of such publications have been dedicated to the use of MCRs for the synthesis of biologically active pyrazole derivatives or at least tested for any biological properties. This review tries to provide more insight into MCR-based synthetic routes of pyrazole derivatives, as well as the analysis of some plausible synthetic mechanisms, a comprehensive picture of its diverse biological activity data, and a detailed discussion of molecular docking studies showing how pyrazole-based compounds interact with therapeutically relevant targets. Hence, this review covers articles published from 2015 to date related to antibacterial, anticancer, antifungal, antioxidant,  $\alpha$ -glucosidase and  $\alpha$ -amylase inhibitory, anti-inflammatory, antimycobacterial, antimalarial, and miscellaneous activities of pyrazole derivatives obtained exclusively via an MCR (Figure 1). It is worth noting that 71% of the articles found suitable for this review corresponded mainly to pyrazole derivatives displaying antibacterial (29%), anticancer (23%), and antifungal (19%) activities, respectively. For better comprehension, the content of this review has been organized and discussed through different biological activities displayed or evaluated for the target pyrazole derivatives, as shown in Figure 1.



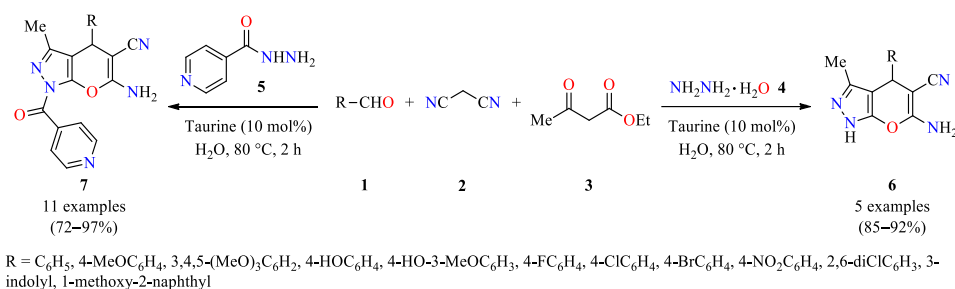
**Figure 1.** Bibliometric graphic depicting the percentage of articles associated with each biological activity screened from 2015 to date [data were collected searching in Scopus for the keywords: “pyrazole derivatives”, “biological activity”, and “multicomponent reactions”].

## 2. Multicomponent Synthesis of Biologically Active Pyrazole Derivatives

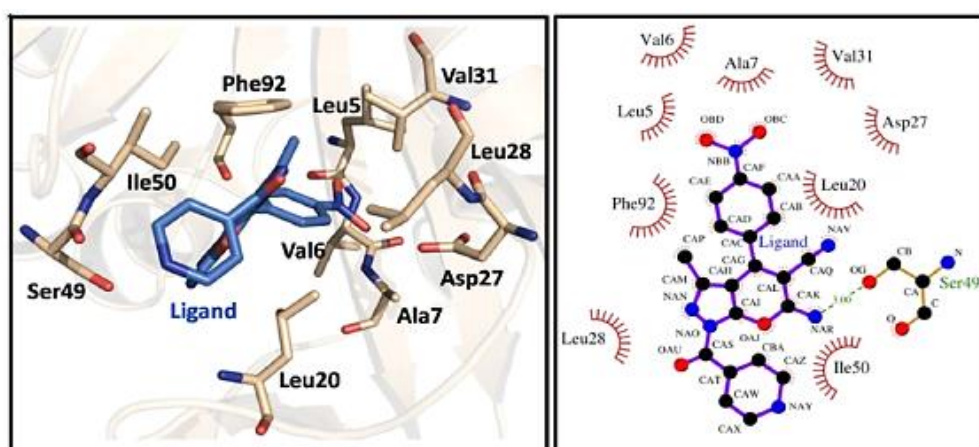
### 2.1. Antibacterial Activity

It is well known that over the past few decades antibiotic deposits have become less effective worldwide due to their overuse and the emerging antimicrobial drug resistance. Particularly, drug resistance has been developed by common bacterial pathogens against frequently prescribed drugs (amphotericin B, fluconazole, penicillin, and chloram-

phenicol, among others). Hence, it is an emerging field of study as it relates to a global health challenge, thereby numerous strategies will be required to develop new therapeutic compounds as antibacterial agents. In this regard, the broad-scale pharmaceutical applications of pyrano[2,3-*c*]pyrazole, including its appearance in numerous biologically important scaffolds, manifest its significant demand worldwide [26]. For example, the taurine-catalyzed four-component reaction of diverse (hetaryl)aldehydes **1**, malononitrile **2**, ethyl acetoacetate **3**, and hydrazine hydrate **4** in water at 80 °C for 2 h afforded 1,4-dihydropyrano[2,3-*c*]pyrazoles **6** in 85–92% yields (Scheme 1) [26]. Under the same optimized conditions, the four-component reaction was extended to isoniazid **5** leading to densely substituted products **7** in 72–97% yields. After completion of the reaction by TLC, the formed solid was filtered, washed with hot water, and recrystallized in ethanol to afford the desired product. The recyclability of the taurine catalyst was studied under optimized conditions. Accordingly, the catalyst was reused for up to three recycles without an appreciable loss of catalytic activity. This protocol is distinguished by its broad substrate scope, short reaction times, low catalyst loading, and could be applied in various organic transformations to achieve the complexity of the targeted architecture. Later, all synthesized 1,4-dihydropyrano[2,3-*c*]pyrazoles **7** were evaluated for their plausible antibacterial potential through *in silico* molecular docking analysis against the Staphylococcal drug target enzyme DHFR (PDB ID: 2w9g) and its trimethoprim-resistant variant S1DHFR (PDB ID: 2w9s). Remarkably, compound **7** (R = 4-NO<sub>2</sub>C<sub>6</sub>H<sub>4</sub>) exhibited an excellent mode of binding against DHFR and S1DHFR with a binding energy of –8.8 Kcal/mol and –8.7 Kcal/mol, respectively. As shown in Figure 2, the docked **7** (R = 4-NO<sub>2</sub>C<sub>6</sub>H<sub>4</sub>) at the wild-type DHFR active site forms one hydrogen bond between the amino group and Ser49 residue.



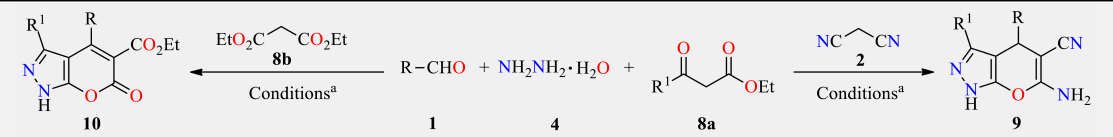
**Scheme 1.** Taurine-catalyzed four-component synthesis and *in silico*-based analysis of 1,4-dihydropyrano [2,3-*c*]pyrazoles **6** and **7**.



**Figure 2.** Molecular docking of compound **7** (R = 4-NO<sub>2</sub>C<sub>6</sub>H<sub>4</sub>) with *Staphylococcus aureus* wild-type DHFR (PDB ID: 2w9g). The left panel shows the zoomed-in view of the ligand interactions with the DHFR active site amino acid residues in the 3D space. The right panel shows the 2D representation of the array of ligand–protein interactions. Hydrogen bond formation is indicated by the green dotted line, whereas hydrophobic interactions are indicated by the spiked arcs. Image adapted from Mali et al. [26].

The time-efficient synthesis of pyrano[2,3-*c*]pyrazole derivatives **9** and **10** in 85–93% yields could be easily accomplished by the Knoevenagel condensation/Michael addition/imine–enamine tautomerism/*O*-cyclization sequence through a four-component reaction of (hetero)aromatic aldehydes **1**, hydrazine hydrate **4**,  $\beta$ -ketoesters **8** as ethyl acetoacetate **8a** or diethyl malonate **8b**, and enolizable active methylene compounds as malononitrile **2** or diethyl malonate **8b**, respectively, catalyzed by piperidine (5 mol%) with vigorous stirring in an aqueous medium for 20 min at room temperature (Table 1) [27]. The synthesized compounds were screened against Gram-positive (*Bacillus subtilis*, *Clostridium tetani*, and *Streptococcus pneumoniae*) and Gram-negative (*Salmonella typhi*, *Pseudomonas aeruginosa*, and *Vibrio cholerae*) bacterial strains using the broth microdilution method in the presence of ciprofloxacin as the standard drug. Remarkably, the compound **9k** displayed better activity against Gram-positive and Gram-negative bacterial strains with MIC values of 0.10–1.00  $\mu\text{g}/\text{mL}$  and 0.50–2.50  $\mu\text{g}/\text{mL}$ , respectively, when compared to ciprofloxacin as a standard drug (MIC = 3.12–6.25  $\mu\text{g}/\text{mL}$  and 3.12  $\mu\text{g}/\text{mL}$ , respectively), (Table 1). Later, the compound **9k** was evaluated for the binding mode determination and the antimicrobial in silico study against penicillin-binding protein PBPb (PDB ID: 3UDI). Molecular docking results showed that the compound **9k** has a tremendous binding affinity towards PBPb with binding of energy of  $-7.3$  Kcal/mol. The compound **9k** was capable of forming four hydrogen bonds and five hydrophobic interactions with the key amino acid residues in the PBPb binding pocket.

**Table 1.** Four-component synthesis and antimicrobial evaluation of pyrano[2,3-*c*]pyrazole derivatives **9** and **10**.



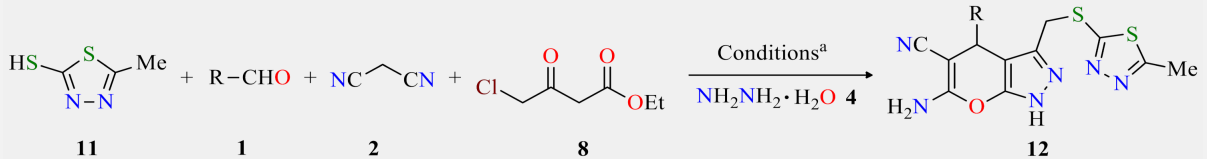
| Compound                   | R                                  | R <sup>1</sup> | Yield <b>9</b><br>(%) | Yield <b>10</b><br>(%) | MIC ( $\mu\text{g}/\text{mL}$ ) |       |       |       |       |       |
|----------------------------|------------------------------------|----------------|-----------------------|------------------------|---------------------------------|-------|-------|-------|-------|-------|
|                            |                                    |                |                       |                        | BS                              | CT    | SP    | ST    | PA    | VC    |
| <b>9a</b>                  | 2-OHC <sub>6</sub> H <sub>4</sub>  | Me             | 92                    | –                      | 3.57                            | 3.57  | 5.00  | 1.87  | 1.25  | 3.125 |
| <b>9b</b>                  | 4-MeC <sub>6</sub> H <sub>4</sub>  | Me             | 91                    | –                      | 1.25                            | 0.10  | 3.125 | 3.57  | 7.50  | 1.87  |
| <b>9c</b>                  | 4-MeOC <sub>6</sub> H <sub>4</sub> | Me             | 91                    | –                      | 3.125                           | 7.50  | 2.50  | 6.25  | 1.25  | 1.00  |
| <b>9d</b>                  | C <sub>6</sub> H <sub>5</sub>      | Me             | 93                    | –                      | 3.57                            | 1.00  | 1.25  | 5.00  | 1.87  | 6.25  |
| <b>9e</b>                  | 2-Furanyl                          | Me             | 90                    | –                      | 2.50                            | 1.87  | 5.00  | 6.25  | 3.57  | 1.25  |
| <b>9f</b>                  | 2-OHC <sub>6</sub> H <sub>4</sub>  | EtO            | 91                    | –                      | 3.125                           | 1.87  | 2.50  | 5.00  | 3.125 | 6.25  |
| <b>9g</b>                  | 4-MeC <sub>6</sub> H <sub>4</sub>  | EtO            | 89                    | –                      | 1.00                            | 1.25  | 3.75  | 3.125 | 5.00  | 0.93  |
| <b>9h</b>                  | 4-MeOC <sub>6</sub> H <sub>4</sub> | EtO            | 90                    | –                      | 0.75                            | 1.00  | 1.25  | 3.75  | 2.50  | 5.00  |
| <b>9i</b>                  | C <sub>6</sub> H <sub>5</sub>      | EtO            | 91                    | –                      | 1.00                            | 2.50  | 3.75  | 2.50  | 3.125 | 6.25  |
| <b>9j</b>                  | 9-Anthracenyl                      | EtO            | 86                    | –                      | 1.25                            | 0.93  | 1.87  | 3.75  | 3.125 | 7.50  |
| <b>9k</b>                  | 2-Furanyl                          | EtO            | 91                    | –                      | 0.10                            | 1.00  | 0.10  | 0.50  | 0.75  | 2.50  |
| <b>10a</b>                 | 2-OHC <sub>6</sub> H <sub>4</sub>  | Me             | –                     | 89                     | 1.87                            | 0.93  | 1.25  | 3.125 | 1.87  | 5.00  |
| <b>10b</b>                 | 4-MeC <sub>6</sub> H <sub>4</sub>  | Me             | –                     | 85                     | 1.87                            | 1.00  | 2.50  | 5.00  | 3.57  | 6.25  |
| <b>10c</b>                 | 4-MeOC <sub>6</sub> H <sub>4</sub> | Me             | –                     | 86                     | 1.87                            | 3.125 | 6.25  | 1.87  | 6.25  | 7.50  |
| <b>10d</b>                 | C <sub>6</sub> H <sub>5</sub>      | Me             | –                     | 88                     | 3.125                           | 1.00  | 2.50  | 3.75  | 1.25  | 5.00  |
| <b>10e</b>                 | 2-Furanyl                          | Me             | –                     | 86                     | 0.75                            | 0.10  | 1.25  | 1.87  | 2.50  | 3.125 |
| Ciprofloxacin <sup>b</sup> | –                                  | –              | –                     | –                      | 6.25                            | 6.25  | 3.125 | 3.125 | 3.125 | 3.125 |

<sup>a</sup> Reaction conditions: (hetero)aromatic aldehyde **1** (1 mmol), hydrazine hydrate **4** (1 mmol), ethyl acetoacetate **8a** or diethyl malonate **8b** (1 mmol), malononitrile **2** or diethyl malonate **8b** (1 mmol), and piperidine (5 mol%) at room temperature for 20 min. <sup>b</sup> Positive control for the study. BS (*Bacillus subtilis*), CT (*Clostridium tetani*), SP (*Streptococcus pneumoniae*), ST (*Salmonella typhi*), PA (*Pseudomonas aeruginosa*), VC (*Vibrio cholerae*).

In 2019, Reddy et al. developed the solvent-free synthesis of highly substituted pyrano[2,3-*c*]pyrazoles **12** in 81–91% yields through a five-component reaction of 5-methyl-1,3,4-thiadiazole-2-thiol **11**, diverse aldehydes **1**, malononitrile **2**, ethyl 4-chloro-3-oxobutanoate **8** (R = CH<sub>2</sub>Cl), and hydrazine hydrate **4** catalyzed by montmorillonite K10 at 65–70 °C for 5 h (Table 2) [28].

The synthesized compounds were screened against Gram-positive (*Staphylococcus aureus* and *Bacillus subtilis*) and Gram-negative (*Proteus vulgaris* and *Escherichia coli*) bacterial strains using ciprofloxacin as a standard drug. It was found that at a 50 µg/well concentration, the pyrano[2,3-*c*]pyrazoles **12** showed a diameter of growth of the inhibition zone ranging from 0 to 21 mm and 0 to 31 mm against Gram-positive and Gram-negative bacterial strains, respectively, in comparison to ciprofloxacin (21 to 23 mm and 31 to 32 mm, respectively) [28]. Interestingly, the compounds **12d** and **12f** showed better antibacterial efficacy at a 50 µg/well concentration against *Staphylococcus aureus*, *Bacillus subtilis*, *Proteus vulgaris*, and *Escherichia coli* with a zone of inhibition in the range of 15–27 mm and 16–31 mm, respectively, when compared to ciprofloxacin (21–32 mm). In addition, the minimum inhibitory concentration (MIC) and minimum bactericidal concentration (MBC) results of most active compounds **12d** and **12f** were determined against *Staphylococcus aureus*, *Bacillus subtilis*, *Proteus vulgaris*, and *Escherichia coli*. Particularly, compound **12d** showed better MIC and MBC values in the range of 12.5–50 µg/mL and 25–100 µg/mL, in comparison to ciprofloxacin (MIC = 6.25–12.5 µg/mL). It is noteworthy that compound **12d** and ciprofloxacin displayed the same MIC value (6.25 µg/mL) against *Bacillus subtilis*.

**Table 2.** Solvent-free five-component synthesis of pyrano[2,3-*c*]pyrazoles **12** as antimicrobial agents.

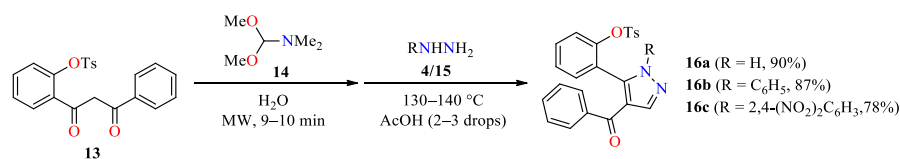


| Compound                   | R   | Yield <b>12</b> (%) | Zone of Inhibition (mm) |             |            |             |            |             |            |             |
|----------------------------|---|---------------------|-------------------------|-------------|------------|-------------|------------|-------------|------------|-------------|
|                            |   |                     | SA                      |             | BS         |             | PV         |             | EC         |             |
|                            |   |                     | 50 µg/Well              | 100 µg/Well | 50 µg/Well | 100 µg/Well | 50 µg/Well | 100 µg/Well | 50 µg/Well | 100 µg/Well |
| <b>12a</b>                 | C <sub>6</sub> H <sub>5</sub>                   | 85                  | 11                      | 13          | 13         | 15          | 16         | 20          | 20         | 24          |
| <b>12b</b>                 | 2-MeOC <sub>6</sub> H <sub>4</sub>              | 81                  | 3                       | 6           | 5          | 6           | 6          | 9           | 10         | 12          |
| <b>12c</b>                 | 3-OHC <sub>6</sub> H <sub>4</sub>               | 86                  | 6                       | 9           | 8          | 9           | 10         | 13          | 12         | 16          |
| <b>12d</b>                 | 4-ClC <sub>6</sub> H <sub>4</sub>               | 91                  | 15                      | 16          | 18         | 21          | 22         | 26          | 27         | 31          |
| <b>12e</b>                 | 2-OHC <sub>6</sub> H <sub>4</sub>               | 82                  | 8                       | 10          | 9          | 11          | 11         | 15          | 14         | 18          |
| <b>12f</b>                 | 4-NO <sub>2</sub> C <sub>6</sub> H <sub>4</sub> | 90                  | 16                      | 19          | 21         | 24          | 25         | 28          | 31         | 34          |
| <b>12g</b>                 | 4-FC <sub>6</sub> H <sub>4</sub>                | 87                  | 16                      | 18          | 19         | 22          | 23         | 27          | 29         | 33          |
| <b>12h</b>                 | 4-OHC <sub>6</sub> H <sub>4</sub>               | 89                  | 9                       | 10          | 10         | 12          | 13         | 18          | 17         | 21          |
| <b>12i</b>                 | 4-MeOC <sub>6</sub> H <sub>4</sub>              | 84                  | 5                       | 7           | 6          | 7           | 8          | 11          | 11         | 13          |
| <b>12j</b>                 | 2-MeC <sub>6</sub> H <sub>4</sub>               | 82                  | 0                       | 0           | 0          | 0           | 0          | 0           | 0          | 0           |
| <b>12k</b>                 | 4-MeC <sub>6</sub> H <sub>4</sub>               | 86                  | 0                       | 0           | 0          | 0           | 0          | 0           | 0          | 0           |
| <b>12l</b>                 | 2-ClC <sub>6</sub> H <sub>4</sub>               | 83                  | 14                      | 16          | 17         | 19          | 20         | 24          | 25         | 29          |
| <b>12m</b>                 | 3-FC <sub>6</sub> H <sub>4</sub>                | 88                  | 13                      | 15          | 14         | 16          | 17         | 23          | 22         | 26          |
| <b>12n</b>                 | 4-BrC <sub>6</sub> H <sub>4</sub>               | 85                  | 10                      | 12          | 11         | 13          | 14         | 19          | 19         | 23          |
| Ciprofloxacin <sup>b</sup> | –   | –                   | 21                      | 24          | 23         | 26          | 31         | 33          | 32         | 36          |

<sup>a</sup> Reaction conditions: 2-thioly-5-methyl-1,3,4-thiadiazole **11** (1.1 mmol), aldehyde **1** (1 mmol), malononitrile **2** (1 mmol), ethyl 4-chloro-3-oxobutanoate **8** (1 mmol), hydrazine hydrate **4** (1 mmol), and montmorillonite K10, 65–70 °C, 5 h. <sup>b</sup> Positive control for the study. SA (*Staphylococcus aureus*), BS (*Bacillus subtilis*), PV (*Proteus vulgaris*), EC (*Escherichia coli*).

In 2019, Kendre's group published the microwave-assisted synthesis of pyrazoles **16a–c** in 78–90% yields by the three-component reaction of 1-phenyl-3-(2-(tosyloxy)phenyl)propane-1,3-dione **13**, *N,N*-dimethylformamide dimethyl acetal **14**, and different amines such as hydrazine **4** (R = H) and derivatives **15b,c** catalyzed by acetic acid (2–5 drops) in water, maintaining the temperature in the range of 115–140 °C for 9–10 min (Scheme 2) [29]. The pyrazole derivatives **16** were screened against Gram-positive (*Bacillus subtilis* and *Staphylococcus aureus*) and Gram-negative (*Escherichia coli* and *Pseudomonas aeruginosa*) bacterial strains using ampicillin as the standard drug. It was found that pyrazoles **16a–c** showed an inhibition zone in the range of 10–22, in comparison to ampicillin (21–24 mm). Interestingly, compound **16c** showed better antibacterial efficacy against *Escherichia coli*, *Bacillus Subtilis*, and *Pseudomonas aeruginosa* with a zone of inhibition of 17, 20, and 22 mm, respectively, when compared to ampicillin (21, 24, and 22 mm, respectively).





**Scheme 2.** Three-component synthesis of pyrazoles **16a–c** with antimicrobial activity.

Foroughifar's group reported in 2018 the ultrasound-assisted synthesis of pyrano[2,3-*c*]pyrazoles **18** in 84–94% yields via a four-component reaction of aromatic aldehydes **1**, malononitrile **2**, ethyl 3-oxo-3-phenylpropanoate **17**, and hydrazine hydrate **4** catalyzed by graphene oxide (10 mol%) with vigorous stirring in an aqueous medium for 2–6 min at room temperature (Table 3) [30]. The recyclability of the heterogeneous catalyst was studied under optimized conditions. Accordingly, the carbocatalyst was reused in up to five cycles without an appreciable loss of catalytic activity. Later, the synthesized compounds were screened against Gram-negative (*Escherichia coli* and *Pseudomonas aeruginosa*) and Gram-positive (*Staphylococcus saprophyticus* and *Staphylococcus aureus*) bacterial strains using the broth microdilution method in the presence of cefazolin as a standard drug. The synthesized compounds showed remarkable antibacterial activity against Gram-negative and Gram-positive bacterial strains with MIC values in the range of 20–45 µg/mL, in comparison to cefazolin (MIC > 35 µg/mL). Interestingly, the compounds **18a** and **18h** displayed the highest activity against Gram-negative bacterial strains with MIC values ranging from 20 to 25 µg/mL, while the compounds **18a**, **18f**, and **18g** displayed the highest activity against Gram-positive bacterial strains with MIC values ranging from 20 to 25 µg/mL, in comparison to cefazolin (MIC > 35 µg/mL).

**Table 3.** Ultrasound-assisted four-component synthesis of pyrano[2,3-*c*]pyrazoles **18** as antimicrobial agents.

| Compound               | R                 | Yield <b>18</b> (%) | MIC (µg/mL) |     |     |     |
|------------------------|-------------------|---------------------|-------------|-----|-----|-----|
|                        |                   |                     | EC          | PA  | SS  | SA  |
| <b>18a</b>             | H                 | 94                  | 20          | 30  | 25  | 20  |
| <b>18b</b>             | 4-Me              | 85                  | 25          | 35  | 45  | 25  |
| <b>18c</b>             | 3-NO <sub>2</sub> | 89                  | 30          | 45  | 45  | 40  |
| <b>18d</b>             | 3-OH              | 84                  | 30          | 30  | 30  | 30  |
| <b>18e</b>             | 2-Me              | 87                  | 25          | 40  | 35  | 35  |
| <b>18f</b>             | 2-NO <sub>2</sub> | 92                  | 35          | 45  | 35  | 20  |
| <b>18g</b>             | 4-MeO             | 85                  | 35          | 30  | 25  | 35  |
| <b>18h</b>             | 4-Br              | 93                  | 40          | 25  | 45  | 45  |
| <b>18i</b>             | 4- <i>i</i> Pr    | 86                  | 45          | 40  | 35  | 40  |
| <b>18j</b>             | 2-Cl              | 90                  | 35          | 30  | 45  | 35  |
| Cefazolin <sup>b</sup> | –                 | –                   | >35         | >35 | >35 | >35 |

<sup>a</sup> Reaction conditions: Aldehyde **1** (1 mmol), malononitrile **2** (1 mmol), ethyl 3-oxo-3-phenylpropanoate **17** (1 mmol), hydrazine hydrate **4** (1.5 mmol), and graphene oxide (10 mol%) in H<sub>2</sub>O (5 mL) at r.t for 2–6 min under ultrasound irradiation. <sup>b</sup> Positive control for the study. EC (*Escherichia coli*), PA (*Pseudomonas aeruginosa*), SS (*Staphylococcus saprophyticus*), SA (*Staphylococcus aureus*).

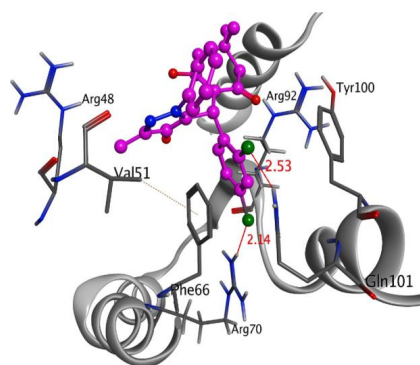
In 2018, Bakar et al. reported the synthesis of pyrazole-dimedone derivatives **21** in 40–78% yields via a four-component reaction of 3-methyl-1-phenyl-1*H*-pyrazol-4(5*H*)-one **19**, diverse aldehydes **1**, and dimedone **20** mediated by Et<sub>2</sub>NH in water at an ambient temperature for 1–12 h (Table 4) [31]. The synthesized pyrazolic salts **21** were evaluated against

three Gram-positive bacterial strains including *Staphylococcus aureus*, *Enterococcus faecalis*, and *Bacillus subtilis* using ciprofloxacin as the standard drug. The pyrazolic salts **21a–o** showed a diameter of growth of the inhibition zone in the range of 10–24 mm and MIC values in the range of 8–64 µg/L against all Gram-positive bacterial strains, in comparison to ciprofloxacin (24–27 mm and ≤0.25 µg/L, respectively). Overall, the pyrazolic salts **21e** and **21l** were the most active compounds against *Staphylococcus aureus* with a MIC value of 16 µg/L. Moreover, compound **21b** was the most active against *Enterococcus faecalis* with a MIC value of 16 µg/L. Ultimately, compound **21k** displayed better antibacterial efficacy against *Bacillus subtilis* with a zone of inhibition of 20 mm and a MIC value of 8 µg/L, when compared to ciprofloxacin (25 mm and ≤0.25 µg/L, respectively). Later, a docking simulation was performed to predict the mode of inhibition against the thymidylate kinase (TMK) (PDB ID: 4QGG) from *Staphylococcus aureus*. Although compound **21a** was moderately active against the *Staphylococcus aureus* bacterial strain, it showed more interactions with the TMK protein from *Staphylococcus aureus*. The docking molecular of **21a** displayed the highest negative score of −6.86 kcal/mol, which is comparable to ciprofloxacin (−6.90 kcal/mol). As shown in Figure 3, the chlorine atoms at the 2 and 4 positions were engaged in the formation of two halogen bonds with the amino groups of Arg70 and Gln101, respectively. Moreover, the dichloro-substituted benzene ring along with the pyrazole ring displayed various π–π and π–cation interactions with the crucial residues Phe66 and Arg92. Apart from this, the carbon atom located at the R position and methyl of the pyrazole ring formed hydrophobic interactions with Arg48 and Phe66. Unfortunately, the authors did not show the docking molecular for compounds **21e** and **21l**, which were the most active against *Staphylococcus aureus* with a MIC value of 16 µg/L (Table 4).

**Table 4.** Four-component synthesis and antibacterial evaluation of pyrazole-dimedone derivatives **21**.

| Compound                   | R   | Yield <b>21</b> (%) | SA       |            | EF       |            | BS       |            |
|----------------------------|---|---------------------|----------|------------|----------|------------|----------|------------|
|                            |   |                     | CPM (mm) | MIC (µg/L) | CPM (mm) | MIC (µg/L) | CPM (mm) | MIC (µg/L) |
| <b>21a</b>                 | 2,4-diClC <sub>6</sub> H <sub>3</sub>           | 78                  | 13       | 32         | 14       | 32         | 12       | 32         |
| <b>21b</b>                 | C <sub>6</sub> H <sub>5</sub>                   | 62                  | 15       | 32         | 13       | 16         | 15       | 16         |
| <b>21c</b>                 | 4-ClC <sub>6</sub> H <sub>4</sub>               | 50                  | 13       | 32         | 24       | 32         | 16       | 32         |
| <b>21d</b>                 | 4-MeC <sub>6</sub> H <sub>4</sub>               | 62                  | 16       | 32         | 16       | 32         | 18       | 32         |
| <b>21e</b>                 | 3-MeC <sub>6</sub> H <sub>4</sub>               | 66                  | 19       | 16         | 15       | 32         | 14       | 64         |
| <b>21f</b>                 | 4-BrC <sub>6</sub> H <sub>4</sub>               | 71                  | 14       | 32         | 13       | 64         | 15       | 32         |
| <b>21g</b>                 | 3-BrC <sub>6</sub> H <sub>4</sub>               | 70                  | 14       | 32         | 15       | 32         | 16       | 32         |
| <b>21h</b>                 | 4-NO <sub>2</sub> C <sub>6</sub> H <sub>4</sub> | 52                  | 12       | 64         | 14       | 32         | 16       | 32         |
| <b>21i</b>                 | 3-NO <sub>2</sub> C <sub>6</sub> H <sub>4</sub> | 63                  | 14       | 32         | 12       | 64         | 17       | 32         |
| <b>21j</b>                 | 4-MeOC <sub>6</sub> H <sub>4</sub>              | 64                  | 10       | 64         | 13       | 32         | 10       | 32         |
| <b>21k</b>                 | 4-FC <sub>6</sub> H <sub>4</sub>                | 57                  | 13       | 32         | 13       | 32         | 20       | 8          |
| <b>21l</b>                 | 4-CF <sub>3</sub> C <sub>6</sub> H <sub>4</sub> | 76                  | 16       | 16         | 16       | 32         | 16       | 32         |
| <b>21m</b>                 | 2,6-diClC <sub>6</sub> H <sub>3</sub>           | 40                  | 15       | 32         | 13       | 32         | 12       | 32         |
| <b>21n</b>                 | 2-Naphthyl                                      | 76                  | 14       | 32         | 13       | 32         | 15       | 32         |
| <b>21o</b>                 | 2-Thienyl                                       | 75                  | 13       | 32         | 20       | 32         | 15       | 16         |
| Ciprofloxacin <sup>a</sup> | –   | –                   | 27       | ≤0.25      | 24       | ≤0.25      | 25       | ≤0.25      |

<sup>a</sup> Positive control for the study. SA (*Staphylococcus aureus*), EF (*Enterococcus faecalis*), BS (*Bacillus subtilis*).



**Figure 3.** Docking molecular of the compound **21a** (magenta) with crucial residues of thymidylate kinase target protein (PDB ID: 4QGG) from *Staphylococcus aureus*. Image adapted from Barakat et al. [31].

On the other hand, an efficient one-pot multicomponent reaction of 3-(2-bromoacetyl) coumarins **22**, thiosemicarbazide **23**, and substituted acetophenones **24** in *N,N*-dimethylformamide, followed by Vilsmeier–Haack formylation reaction conditions, afforded the coumarin-containing thiazolyl-3-aryl-pyrazole-4-carbaldehydes **25** with high yields and short reaction times [32]. During this approach, thiazole and pyrazole rings are formed along with a functional group (-CHO) on the pyrazole ring in a regioselective manner. Subsequently, products **25** were screened against Gram-negative (*Escherichia coli*, *Klebsiella pneumoniae*, and *Proteus vulgaris*) and Gram-positive (*Methicillin-resistant Staphylococcus aureus*, *Bacillus Subtilis*, and *Bacillus cereus*) bacterial strains by using the agar well diffusion method in the presence of gentamycin sulfate and ampicillin as standard drugs [32]. As shown in Table 5, the synthesized compounds **25** showed low to moderate antibacterial activity with MIC values ranging from 72.8 to 150 µg/mL, in comparison to gentamycin sulfate (MIC = 2–45 µg/mL) and ampicillin (MIC = 4–10 µg/mL) as standard drugs. In particular, the compound **25n** showed moderate MIC values of 86.5, 79.1, and 72.8 µg/mL against *Escherichia coli*, *Klebsiella pneumoniae*, and *Bacillus cereus*, respectively. Similarly, the compound **25m** also exhibited a moderate MIC value of 98.2 µg/mL against *Bacillus subtilis*.

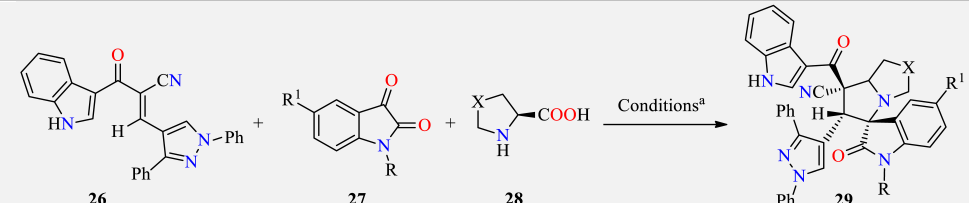
**Table 5.** One-pot three-component synthesis and antibacterial activity of coumarin substituted thiazolyl-3-aryl-pyrazole-4-carbaldehydes **25**.

|                         |     |                |                | MIC (µg/mL)  |       |                |                |       |       |       |
|-------------------------|-----|----------------|----------------|--------------|-------|----------------|----------------|-------|-------|-------|
| Compound                | R   | R <sup>1</sup> | R <sup>2</sup> | Yield 25 (%) | EC    | KP             | PV             | MRSA  | BS    | BC    |
| <b>25a</b>              | H   | H              | H              | 84           | 135   | 150            | 133            | 150   | 132   | 145   |
| <b>25b</b>              | H   | Cl             | H              | 80           | 134.6 | 129            | 130            | 150   | 129.5 | 138.6 |
| <b>25c</b>              | Cl  | Cl             | H              | 75           | 119.6 | 118            | 131.5          | 115   | 123   | 117   |
| <b>25d</b>              | H   | Br             | H              | 80           | 118.1 | 116.8          | 124            | 116   | 125   | 129   |
| <b>25e</b>              | Br  | Br             | H              | 85           | 115.6 | 119            | 120            | 116.8 | 118   | 119   |
| <b>25f</b>              | H   | Benzo          | H              | 78           | 132.8 | 150            | 150            | 135   | 122.8 | 138.9 |
| <b>25g</b>              | H   | Cl             | Cl             | 77           | 126.3 | 117.4          | 130.7          | 134   | 112.2 | 110.8 |
| <b>25h</b>              | Cl  | Cl             | Cl             | 73           | 110.9 | 105            | 113            | 112.5 | 110.7 | 112   |
| <b>25i</b>              | H   | Br             | Cl             | 83           | 117.5 | 115            | 127.5          | 122.9 | 119.7 | 115   |
| <b>25j</b>              | MeO | H              | Cl             | 82           | 125.3 | 129            | 132.3          | 139   | 132.6 | 126   |
| <b>25k</b>              | H   | H              | Me             | 77           | 132.5 | 150            | 150            | 150   | 150   | 135   |
| <b>25l</b>              | H   | Br             | Me             | 82           | 134.6 | 124            | 121.8          | 138.1 | 125   | 126   |
| <b>25m</b>              | Cl  | Cl             | Me             | 81           | 101.3 | 100.9          | 105            | 115.6 | 98.2  | 100.1 |
| <b>25n</b>              | Br  | Br             | Me             | 85           | 86.5  | 79.1           | 100.7          | 105.9 | 92.4  | 72.8  |
| <b>25o</b>              | MeO | H              | Me             | 82           | 132.7 | 150            | 142            | 150   | 150   | 136   |
| Gentamycin <sup>b</sup> | –   | –              | –              | –            | 2     | 4              | 4              | 22    | 45    | 10    |
| Ampicillin <sup>b</sup> | –   | –              | –              | –            | 10    | – <sup>c</sup> | – <sup>c</sup> | 4     | 5     | 4     |

<sup>a</sup> Reaction conditions: 3-(2-bromoacetyl)coumarin derivative **22** (1 mmol), thiosemicarbazide **23** (1 mmol), substituted acetophenone **24** (1 mmol), DMF (5 mL), POCl<sub>3</sub> (5 mmol), 0–60 °C, 5–6 h. <sup>b</sup> Positive control for the study. <sup>c</sup> Not determined. EC (*Escherichia coli*), KP (*Klebsiella pneumoniae*), PV (*Proteus vulgaris*), MRSA (*Methicillin-resistant Staphylococcus aureus*), BS (*Bacillus subtilis*), and BC (*Bacillus cereus*).

Interestingly, a series of highly functionalized spiro pyrrolidine-oxindoles **29** in 80–93% yields have been synthesized through a 1,3-dipolar cycloaddition reaction between dipolarophile (*E*)-3-(1,3-diphenyl-1*H*-pyrazol-4-yl)-2-(1*H*-indole-3-carbonyl)acrylonitrile **26** and an azomethine ylide formed in situ from isatin derivatives **27** and amino acids such as *L*-proline **28a** and *L*-thioprolines **28b** in refluxing methanol for 2 h (Table 6) [33]. The reaction mixture was allowed to cool at room temperature, filtered, and the resulting crude was recrystallized in ethanol to afford spiro pyrrolidine-oxindoles **29** in a diastereoselective manner. The spiro pyrrolidine-oxindoles **29** were screened against Gram-negative (*Salmonella typhimurium*, *Klebsiella pneumoniae*, *Proteus vulgaris*, *Shigella flexneri*, and *Enterobacter aerogenes*) and Gram-positive (*Micrococcus luteus*, *Staphylococcus epidermidis*, *Staphylococcus aureus*, and *Methicillin-resistant Staphylococcus aureus*) bacterial strains using the disc diffusion method in the presence of streptomycin as a standard drug [33]. The synthesized compounds showed low to moderate antibacterial activity against Gram-negative and Gram-positive bacterial strains with MIC values in the range of 31.2–500 µg/mL, in comparison to streptomycin (MIC = 6.25–30 µg/mL). Interestingly, compound **29a** displayed the highest activity against Gram-negative bacterial strains with MIC values in the range of 31.2–125 µg/mL, except for *Salmonella typhimurium* (MIC = 250 µg/mL). However, compounds **29c** and **29e** showed the highest activity against *Salmonella typhimurium* with a MIC value of 125 µg/mL. Furthermore, compound **29a** showed better activity against Gram-positive bacterial strains with a MIC value of 31.2 µg/mL, except for *Staphylococcus epidermidis* (MIC = 62.5 µg/mL).

**Table 6.** Three-component synthesis and antibacterial activity of spiro pyrrolidine-oxindoles **29**.

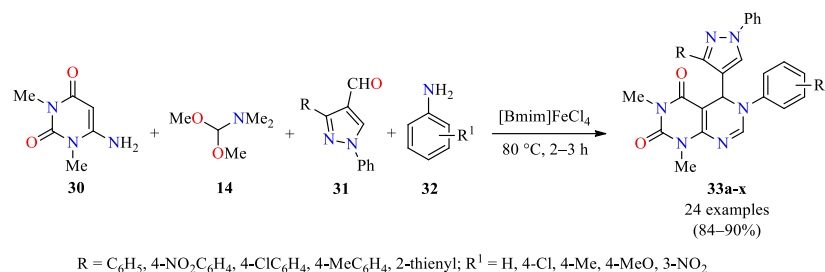


| Compound                  | R               | R <sup>1</sup>  | X               | Yield <b>29</b> (%) | MIC (µg/mL)    |      |                |                |                |      |      |      |      |
|---------------------------|-----------------|-----------------|-----------------|---------------------|----------------|------|----------------|----------------|----------------|------|------|------|------|
|                           |                 |                 |                 |                     | ST             | KP   | PV             | SF             | ML             | EA   | SE   | SA   | MRSA |
| <b>29a</b>                | H               | H               | CH <sub>2</sub> | 92                  | 250            | 31.2 | 125            | 31.2           | 31.2           | 62.5 | 62.5 | 31.2 | 31.2 |
| <b>29b</b>                | Allyl           | H               | CH <sub>2</sub> | 86                  | 500            | 500  | 250            | 250            | 250            | 250  | 125  | 125  | 250  |
| <b>29c</b>                | <i>n</i> -Butyl | H               | CH <sub>2</sub> | 90                  | 125            | 250  | 250            | – <sup>c</sup> | 500            | 500  | 62.5 | 125  | 500  |
| <b>29d</b>                | Me              | H               | CH <sub>2</sub> | 93                  | 500            | 500  | 250            | 250            | 500            | 250  | 250  | 250  | 125  |
| <b>29e</b>                | Propargyl       | H               | CH <sub>2</sub> | 87                  | 125            | 250  | 250            | 500            | 500            | 250  | 125  | 500  | 250  |
| <b>29f</b>                | H               | NO <sub>2</sub> | CH <sub>2</sub> | 80                  | 250            | 250  | 125            | 500            | 500            | 250  | 250  | 125  | 500  |
| <b>29g</b>                | H               | H               | S               | 91                  | 500            | 500  | 500            | 500            | 500            | 500  | 500  | 500  | 500  |
| <b>29h</b>                | Allyl           | H               | S               | 88                  | 250            | 500  | 500            | 500            | 500            | 250  | 125  | 250  | 500  |
| <b>29i</b>                | Benzyl          | H               | S               | 86                  | 250            | 250  | 500            | 500            | 250            | 250  | 125  | 62.5 | 500  |
| <b>29j</b>                | <i>n</i> -Butyl | H               | S               | 93                  | 250            | 500  | 500            | 500            | 250            | 500  | 250  | 250  | 500  |
| <b>29k</b>                | Me              | H               | S               | 89                  | – <sup>c</sup> | 500  | 500            | 500            | – <sup>c</sup> | 250  | 500  | 125  | 500  |
| Streptomycin <sup>b</sup> | –               | –               | –               | –                   | 30             | 6.25 | – <sup>c</sup> | 6.25           | 6.25           | 25   | 6.25 | 6.25 | 6.25 |

<sup>a</sup> Reaction conditions: (*E*)-3-(1,3-diphenyl-1*H*-pyrazol-4-yl)-2-(1*H*-indole-3-carbonyl)acrylonitrile **26** (1 mmol), isatin derivative **27** (1 mmol), and amino acid **28** (1.1 mmol), MeOH (5 mL), reflux, 3 h. <sup>b</sup> Positive control for the study. <sup>c</sup> Not determined. ST (*Salmonella typhimurium*), KP (*Klebsiella pneumoniae*), PV (*Proteus vulgaris*), SF (*Shigella flexneri*), ML (*Micrococcus luteus*), EA (*Enterobacter aerogenes*), SE (*Staphylococcus epidermidis*), SA (*Staphylococcus aureus*), MRSA (*Methicillin-resistant Staphylococcus aureus*).

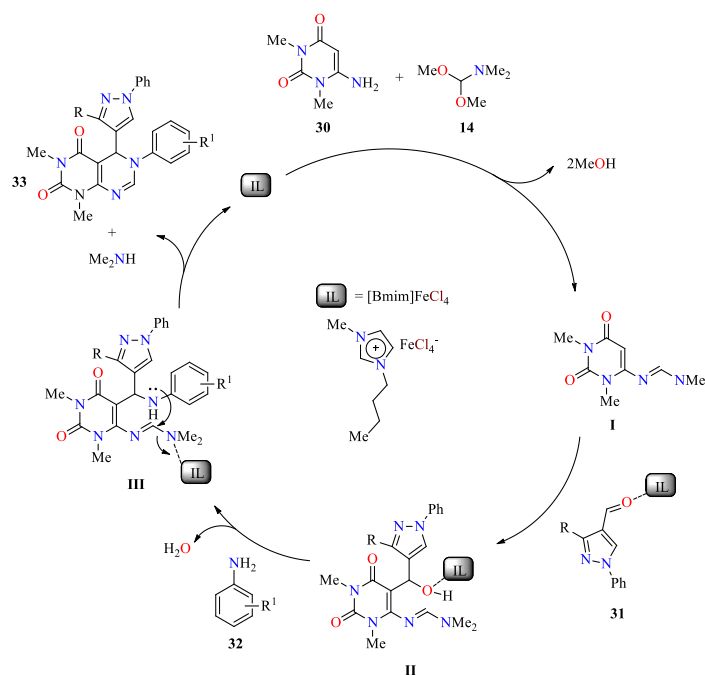
In 2017, Suresh et al. described an efficient synthesis of pyrazole-based pyrimido[4,5-*d*]pyrimidines **33** in 84–90% yields through a four-component reaction from 6-amino-1,3-dimethyluracil **30**, *N,N*-dimethylformamide dimethyl acetal **14**, 1-phenyl-3-(4-substituted-phenyl)-4-formyl-1*H*-pyrazoles **31**, and primary aromatic amines **32** using the ionic liquid [Bmim]FeCl<sub>4</sub> as both catalyst and solvent at 80 °C for 2–3 h (Scheme 3) [34]. Although the reaction was optimized with various solvents such as water, ethanol, acetic acid, DMF, nitrobenzene, and toluene under reflux or heating conditions, the yields were disappointing. However, the use of ionic liquids was conducted to improve the yields. An interesting trend was observed with the types of substituents on 1-phenyl-3-(4-phenyl)-4-formyl-1*H*-substituted pyrazoles **31** and primary aromatic amines **32**. Overall, the presence of

electron-withdrawing substituents (85–90%) generated higher yields than electron-donating substituents (78–84%). Finally, the ionic liquid catalyst was reused in up to four cycles without an appreciable loss in catalytic activity.



**Scheme 3.** Four-component synthesis of pyrazole-based pyrimido[4,5-*d*]pyrimidines **33** mediated by [Bmim]FeCl<sub>4</sub>.

The plausible mechanism for the synthesis of pyrazole-based pyrimido[4,5-*d*]pyrimidines **33** is illustrated in Scheme 4. Initially, the [Bmim]FeCl<sub>4</sub>-catalyzed condensation reaction between 6-amino-1,3-dimethyluracil **30** and *N,N*-dimethylformamide dimethyl acetal **14** generated the amidine intermediate **I**, which reacted with 1-phenyl-3-(4-substituted-phenyl)-4-formyl-1*H*-pyrazole **31** to furnish intermediate **II**. Then, the [Bmim]FeCl<sub>4</sub>-catalyzed nucleophilic substitution of the hydroxyl group of the intermediate **II** by the amine group of the aromatic amine **32** gave the intermediate **III**, which participated in the intramolecular nucleophilic addition/elimination of the Me<sub>2</sub>NH sequence to form the pyrimido[4,5-*d*]pyrimidine system **33**.



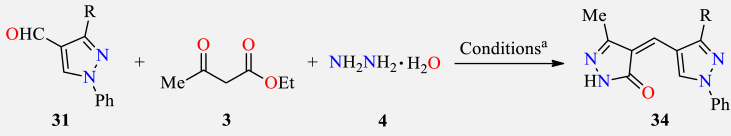
**Scheme 4.** Proposed mechanism for the synthesis of pyrazole-based pyrimido[4,5-*d*]pyrimidines **33** mediated by [Bmim]FeCl<sub>4</sub> (IL).

The synthesized compounds **33** were screened for their antibacterial activity against Gram-positive (*Bacillus subtilis*, *Staphylococcus aureus*, *Staphylococcus aureus* MLS-16, and *Micrococcus luteus*) and Gram-negative (*Klebsiella planticola*, *Escherichia coli*, and *Pseudomonas aeruginosa*) bacterial strains using ciprofloxacin as a positive control. Overall, the compounds **33c** (R = 4-NO<sub>2</sub>C<sub>6</sub>H<sub>4</sub>, R<sup>1</sup> = 4-Me), **33l** (R = 4-MeC<sub>6</sub>H<sub>4</sub>, R<sup>1</sup> = 4-Cl), and **33m** (R = 4-MeC<sub>6</sub>H<sub>4</sub>, R<sup>1</sup> = 4-Me) were the most active against *Bacillus subtilis*, *Staphylococcus aureus*, *Staphylococcus*

*aureus* MLS16, and *Micrococcus luteus* with MIC values in the range of 3.9–15.6 µg/mL, in comparison to ciprofloxacin (MIC = 0.9 µg/mL). Notably, the compound **33l** showed better activity against *Bacillus subtilis* and *Staphylococcus aureus* with an MBC value of 7.8 µg/mL, when compared to ciprofloxacin (MBC = 0.9 and 1.9 µg/mL, respectively).

Very recently, a series of 4-[(3-aryl-1-phenyl-1*H*-pyrazol-4-yl)methylidene]-2,4-dihydro-3*H*-pyrazol-3-ones **34** were synthesized through a one-pot three-component reaction of 3-aryl-1-phenyl-1*H*-pyrazole-4-carbaldehydes **31**, ethyl acetoacetate **3**, and hydrazine hydrate **4** in the presence of sodium acetate as a base under refluxing ethanol for 1 h (Table 7) [35]. After completion of the reaction (TLC), the mixture was cooled to room temperature, and the precipitate was filtered, washed with water, dried, and purified by column chromatography to afford compounds **34** in 82–92% yields. All synthesized compounds **34** were screened against Gram-positive (*Staphylococcus aureus* and *Bacillus subtilis*) and Gram-negative (*Pseudomonas aeruginosa* and *Escherichia coli*) bacterial strains using norfloxacin as a positive control. These compounds showed acceptable antibacterial activity against Gram-positive and Gram-negative bacterial strains with a zone of inhibition in the range of 7.9–17.2 mm, when compared to norfloxacin (19.2–25.6 mm). Interestingly, compound **34b** exerted the better antibacterial potency against *Staphylococcus aureus* with a zone of inhibition of 17.2 mm, while the compound **34a** displayed the highest activity against *Bacillus subtilis*, *Pseudomonas aeruginosa*, and *Escherichia coli* with a zone of inhibition of 12.0, 13.5, and 14.3 mm, respectively.

**Table 7.** One-pot three-component synthesis and antibacterial activity of 4-[(3-aryl-1-phenyl-1*H*-pyrazol-4-yl)methylidene]-2,4-dihydro-3*H*-pyrazol-3-ones **34**.

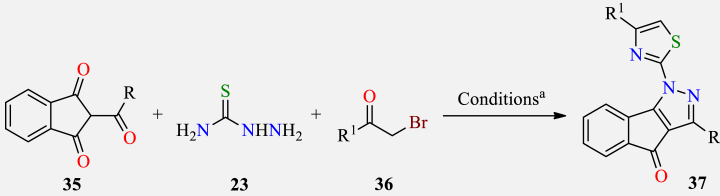
|  |   |                     |                         |      |      |      |
|--|---|---------------------|-------------------------|------|------|------|
| Compound   | R   | Yield <b>34</b> (%) | Zone of Inhibition (mm) |      |      |      |
|  |   |                     | SA                      | BS   | PA   | EC   |
| <b>34a</b>   | C <sub>6</sub> H <sub>5</sub>                       | 84                  | 15.8                    | 12.0 | 13.5 | 14.3 |
| <b>34b</b>   | 4-FC <sub>6</sub> H <sub>4</sub>                    | 85                  | 17.2                    | 11.6 | 12.0 | 11.5 |
| <b>34c</b>   | 4-ClC <sub>6</sub> H <sub>4</sub>                   | 88                  | 14.0                    | 8.9  | 10.9 | 10.8 |
| <b>34d</b>   | 4-BrC <sub>6</sub> H <sub>4</sub>                   | 88                  | 14.1                    | 8.0  | 11.2 | 10.5 |
| <b>34e</b>   | 4-MeC <sub>6</sub> H <sub>4</sub>                   | 90                  | 9.0                     | 8.4  | 9.6  | 10.2 |
| <b>34f</b>   | 4-MeOC <sub>6</sub> H <sub>4</sub>                  | 92                  | 10.0                    | 7.9  | 8.8  | 9.2  |
| <b>34g</b>   | 3-MeOC <sub>6</sub> H <sub>4</sub>                  | 85                  | 12.2                    | 9.4  | 12.0 | 8.0  |
| <b>34h</b>   | 4-OHC <sub>6</sub> H <sub>4</sub>                   | 82                  | 9.6                     | 11.0 | 9.7  | 9.7  |
| <b>34i</b>   | 4-NO <sub>2</sub> C <sub>6</sub> H <sub>4</sub>     | 82                  | 14.8                    | 8.8  | 10.3 | 11.8 |
| <b>34j</b>   | 2,4-(Cl) <sub>2</sub> C <sub>6</sub> H <sub>3</sub> | 86                  | 15.6                    | 10.8 | 12.1 | 12.0 |
| Norfloxacin <sup>b</sup>   | –   | –                   | 25.6                    | 19.2 | 24.2 | 24.0 |

<sup>a</sup> Reaction conditions: 3-aryl-1-phenyl-1*H*-pyrazole-4-carbaldehyde **31** (1 mmol), ethyl acetoacetate **3** (1 mmol), hydrazine hydrate **4** (1 mmol), and sodium acetate (2 mmol), EtOH (5 mL), reflux, 1 h. <sup>b</sup> Positive control for the study. SA (*Staphylococcus aureus*), BS (*Bacillus subtilis*), PA (*Pseudomonas aeruginosa*), EC (*Escherichia coli*).

A series of thiazole-tethered indenopyrazoles **37** were efficiently synthesized through a one-pot three-component reaction (Table 8) [36]. Initially, a mixture of 2-acyl-(1*H*)-indene-1,3-(2*H*)-diones **35** and thiosemicarbazide **23** in dry methanol was refluxed for 10–15 min. Thereafter, sodium acetate,  $\alpha$ -bromoketones **36**, and methanol/glacial acetic acid (2:1, *v/v*) were slowly added. The resulting reaction mixture was refluxed for 5–8 h. On completion of the reaction, the formed solid was filtered and purified by column chromatography to afford the corresponding indenopyrazoles **37** in 53–80% yields (Table 8). All synthesized compounds **37** were screened for their antimicrobial activity against Gram-positive (*Staphylococcus aureus* and *Bacillus subtilis*) and Gram-negative (*Pseudomonas aeruginosa* and *Escherichia coli*) bacterial strains showing MIC values in the range of 0.0270–0.0652 µmol/mL and 0.0270–0.0629 µmol/mL, respectively, when compared to

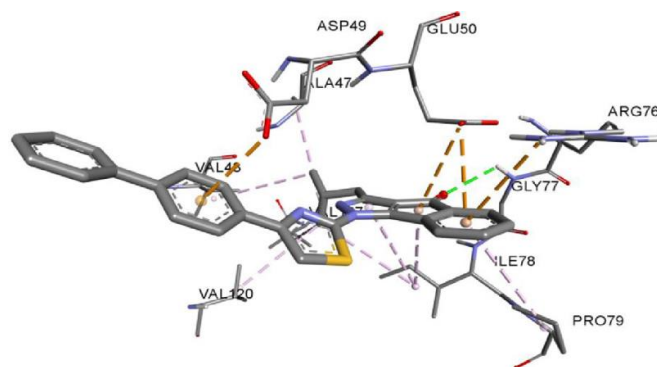
ciprofloxacin (MIC = 0.0094  $\mu\text{mol/mL}$ ) as a positive control. Interestingly, the indenopyrazole **37d** displayed the highest potency against all the tested microbial strains with MIC values ranging from 0.0270 to 0.0541  $\mu\text{mol/mL}$ , in comparison to the standard drug ciprofloxacin (MIC = 0.0094  $\mu\text{mol/mL}$ ). To determine the binding conformation, molecular docking of indenopyrazole **37d** was performed in the binding site of DNA gyrase of *Escherichia coli* (PDB ID: 1KZN). As shown in Figure 4, the carbonyl group of indene moiety forms one hydrogen bond with Gly77. The pyrazole ring interacts with Ile78 via  $\pi$ -alkyl interactions, while the phenyl group present on the thiazole ring interacts with Asp49 via  $\pi$ -anion interactions. Finally, the  $\pi$ -electrons of the indene moiety interact with Glu50 and Arg76 via  $\pi$ -anion and  $\pi$ -cation interactions, respectively.

**Table 8.** One-pot three-component synthesis of 3-alkyl-1-(4-(aryl/heteroaryl)thiazol-2-yl)indeno[1,2-c]pyrazol-4(1H)-ones **37** as antibacterial agents.



| Compound                   | R           | R <sup>1</sup> | Yield <b>37</b> (%) | MIC ( $\mu\text{mol/mL}$ ) |        |        |        |
|----------------------------|-------------|----------------|---------------------|----------------------------|--------|--------|--------|
|                            |             |                |                     | SA                         | BS     | PA     | EC     |
| <b>37a</b>                 | Me          | Biphenyl       | 74                  | 0.0297                     | 0.0595 | 0.0297 | 0.0297 |
| <b>37b</b>                 | Et          | Biphenyl       | 78                  | 0.0288                     | 0.0576 | 0.0288 | 0.0288 |
| <b>37c</b>                 | <i>i</i> Pr | Biphenyl       | 72                  | 0.0559                     | 0.0559 | 0.0559 | 0.0559 |
| <b>37d</b>                 | <i>i</i> Bu | Biphenyl       | 80                  | 0.0270                     | 0.0541 | 0.0270 | 0.0270 |
| <b>37e</b>                 | Me          | 2-Naphthyl     | 72                  | 0.0317                     | 0.0635 | 0.0317 | 0.0317 |
| <b>37f</b>                 | Et          | 2-Naphthyl     | 75                  | 0.0613                     | 0.0613 | 0.0306 | 0.0613 |
| <b>37g</b>                 | <i>i</i> Pr | 2-Naphthyl     | 79                  | 0.0593                     | 0.0593 | 0.0593 | 0.0593 |
| <b>37h</b>                 | <i>i</i> Bu | 2-Naphthyl     | 76                  | 0.0287                     | 0.0574 | 0.0287 | 0.0287 |
| <b>37i</b>                 | Me          | 2-Benzofuranyl | 63                  | 0.0326                     | 0.0652 | 0.0326 | 0.0326 |
| <b>37j</b>                 | Et          | 2-Benzofuranyl | 60                  | 0.0629                     | 0.0629 | 0.0629 | 0.0629 |
| <b>37k</b>                 | <i>i</i> Pr | 2-Benzofuranyl | 58                  | 0.0607                     | 0.0607 | 0.0607 | 0.0607 |
| <b>37l</b>                 | <i>i</i> Bu | 2-Benzofuranyl | 53                  | 0.0293                     | 0.0587 | 0.0293 | 0.0293 |
| Ciprofloxacin <sup>b</sup> | –           | –              | –                   | 0.0094                     | 0.0094 | 0.0094 | 0.0094 |

<sup>a</sup> Reaction conditions: 2-acyl-(1H)-indene-1,3-(2H)dione **35** (1 mmol), thiosemicarbazide **23** (1 mmol), MeOH (30 mL), reflux, 10–15 min, then  $\alpha$ -bromoketone **36** (5 mmol), sodium acetate (5 mmol), MeOH/AcOH (2:1, *v/v*) (20 mL), reflux, 5–8 h. <sup>b</sup> Positive control for the study. SA (*Staphylococcus aureus*), BS (*Bacillus subtilis*), PA (*Pseudomonas aeruginosa*), EC (*Escherichia coli*).

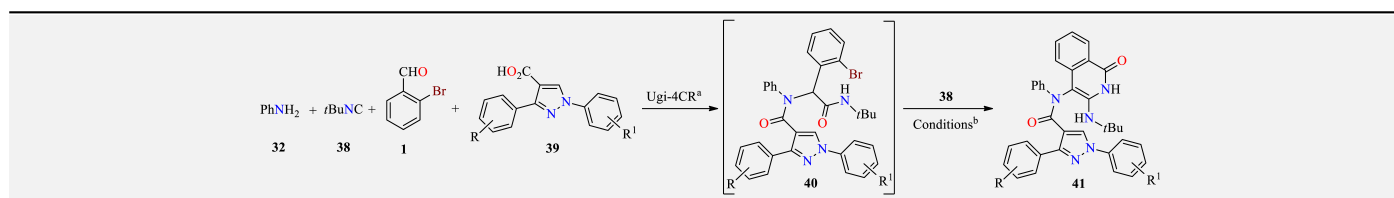


**Figure 4.** Docking molecular of indenopyrazole **37d** with crucial residues of DNA gyrase of *Escherichia coli* (PDB ID: 1KZN). Image adapted from Mor et al. [36].

The Ugi multicomponent reaction (MCR) is one of the most predominant isocyanide-based MCRs, attracting a wide diversity of fascinated chemists owing to its four-component

transformation and remarkable functional tolerance [37,38]. Viewing the significance of the *N*-containing heterocycles (particularly pyrazole and isoquinolone derivatives) in countless areas, mainly in medicinal chemistry, a Ugi-mediated research work focused on the synthesis of the hybrid molecules of these two structural pharmacophores was undertaken [39]. Thus, the microwave-assisted ligand-free palladium-catalyzed post-Ugi reaction for the synthesis of isoquinolone and pyrazole-mixed pharmacophore derivatives **41** was achieved from pyrazole-substituted amides **40** (synthesized using the Ugi reaction). In this approach, intermediate amides **40** were obtained in 77–96% yield from an Ugi four-component type reaction of anilines **32**, *t*-butyl isocyanide **38**, benzaldehydes **1**, and a variety of pyrazole carboxylic acids **39** in MeOH at 40 °C for approximately 18 h, as shown in Table 9. Subsequently, after optimization of the reaction conditions, the isocyanide **38** insertion and successive intramolecular cyclization process of the intermediates **40** was achieved in the presence of PdCl<sub>2</sub> and Cs<sub>2</sub>CO<sub>3</sub> as a base in DMF as the solvent at 150 °C under microwave irradiation, affording the target pyrazole derivatives **41**. It was found that irrespective of the substituents on the pyrazole scaffold in **40**, all the representative reactions could produce moderate to good yields of **41**. Moreover, among the various isocyanides **38** being tested with **40** for this transformation, only *t*-butyl isocyanide **38** was found to be constructed efficiently in the hybrid structures **41** and hence it was the only isocyanide employed in this investigation. Then, the synthesized target compounds **41** were subjected to in vitro antibacterial activity against five clinical bacterial strains (i.e., *Staphylococcus aureus*, *Escherichia coli*, *Enterococcus faecalis*, *Streptococcus pyogenes*, and *Vibrio cholera*), according to Clinical and Laboratory Standard Institute (CLSI) protocols [40]. The activities of **41** in terms of their MICs ranged from 250 μM to 20.85 μM, as shown in Table 9. The results obtained were further described with the help of DFT and molecular orbital calculations, showing that pyrazole derivatives **41e** and **41g** revealed good antibacterial activity compared to the standard drug kanamycin.

**Table 9.** Schematic route for the multicomponent synthesis of pyrazole-based Ugi products **41** and their in vitro antibacterial activities (MIC) against five bacterial strains.



| Compound               | R    | R <sup>1</sup>    | Yield of <b>41</b> (%) | Antibacterial Activity of the Synthesized Compounds <b>41</b> (in μM) |       |      |      |       |
|------------------------|------|-------------------|------------------------|---|-------|------|------|-------|
|                        |      |                   |                        | SA  | EC    | EF   | EP   | VC    |
| <b>41a</b>             | H    | H                 | 91                     | >250  | >250  | >250 | >250 | >250  |
| <b>41b</b>             | 4-Br | H                 | 51                     | >250  | >250  | >250 | >250 | >250  |
| <b>41c</b>             | 4-Me | H                 | 76                     | >250  | >250  | >250 | >250 | >250  |
| <b>41d</b>             | H    | 4-F               | 88                     | >250  | >250  | >250 | >250 | >250  |
| <b>41e</b>             | H    | 4-NO <sub>2</sub> | 79                     | 20.85   | 31.5  | >250 | 200  | 41.25 |
| <b>41f</b>             | H    | 4-Cl              | 87                     | 90.5  | 100   | 200  | >250 | 125   |
| <b>41g</b>             | H    | 3,5-diCl          | 81                     | 37.25   | 37.25 | >250 | >250 | 90.5  |
| Kanamycin <sup>c</sup> | –    | –                 | –                      | 31.3  | 3.9   | 62.5 | 62.5 | 62.5  |

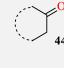
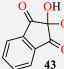
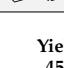
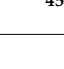






<sup>a</sup> Reaction conditions: **32** (1 mmol), **38** (1 mmol), **1** (1 mmol), **39** (1.2 mmol) in MeOH (3 mL), 35–40 °C, 15–18 h, 77–96%. <sup>b</sup> Reaction conditions: **40a** (1 mmol), *t*-butyl isocyanide **38** (1.2 mmol), catalyst Pd(OAc)<sub>2</sub> (10 mol%), base Cs<sub>2</sub>CO<sub>3</sub> (2 mmol), solvent DMF (2.5 mL), MWI (150 °C), 15 min under inert (N<sub>2</sub>) conditions. SA (*Staphylococcus aureus*), EC (*Escherichia coli*), EF (*Enterococcus faecalis*), EP (*Streptococcus pyogenes*), VC (*Vibrio cholera*). <sup>c</sup> Positive control for the study, commonly used antibacterial drug.

On the basis that 4*H*-pyrans and 4*H*-pyran-annulated heterocyclic frameworks represent an excellent structural motif that is often found in naturally occurring compounds with a broad spectrum of remarkable biological activities, [41,42] a library of spiropyrans



**45** were synthesized via a one-pot four-component reaction of various-type cyclic CH-acids **44**, malononitrile **2**, cyanoacetohydrazide **42**, and ninhydrin **43** in EtOH at reflux under catalyst-free conditions, as shown in Table 10 [43]. The obtained products **45** were subsequently tested in vitro for antibacterial effects on the Gram-negative strain *Escherichia coli* and the Gram-positive strain *Staphylococcus aureus* by using the disk diffusion method and using tetracycline and DMSO as positive and negative controls, respectively. Results showed an inhibition zone of 4–15 mm for compounds **45** against *Staphylococcus aureus* (except **45d**, **45h**, and **45j**), while *Escherichia coli* was resistant against all compounds **45** tested (Table 10). Moreover, it was found that compounds **45a**, **45b**, **45f**, **45g**, and **45i** displayed the best MICs against *Staphylococcus aureus*.

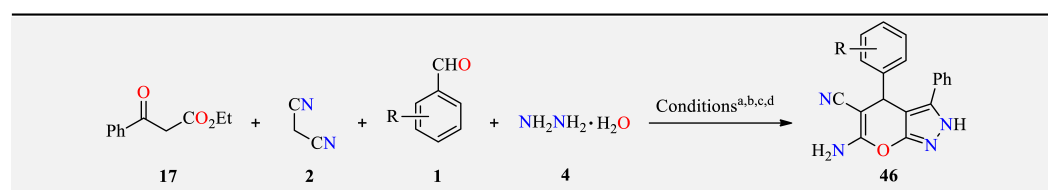
**Table 10.** Multicomponent synthesis and antimicrobial activity of spiroindenopyridazine-4*H*-pyrane derivatives **45**.

| Compound                  | Reagent 44  | Yield of 45 (%) | Antibacterial Activity of the Synthesized Compounds 45 (in $\mu\text{M}$ ) |                         |                         |
|---------------------------|---|-----------------|--|-------------------------|-------------------------|
|                           |   |                 | MIC'S (mM) SA  | Inhibition Zone (mm) SA | Inhibition Zone (mm) EC |
| 45a                       |    | 95              | 5  | 7                       | — <sup>a</sup>          |
| 45b                       |    | 97              | 5  | 5                       | —                       |
| 45c                       |    | 93              | 50   | 7                       | —                       |
| 45d                       |    | 98              | —  | —                       | —                       |
| 45e                       |   | 97              | 10   | 9                       | —                       |
| 45f                       |  | 93              | 5  | 5                       | —                       |
| 45g                       |  | 98              | 5  | 15                      | —                       |
| 45h                       |  | 96              | —  | —                       | —                       |
| 45i                       |  | 90              | 5  | 4                       | —                       |
| 45j                       |  | 92              | —  | —                       | —                       |
| Tetracycline <sup>b</sup> | —   | —               | —  | 30                      | 23                      |
| DMSO                      | —   | —               | —  | 0                       | 0                       |

<sup>a</sup> inactive at concentration 50 mM. <sup>b</sup> Positive control for the study. SA (*Staphylococcus aureus*), EC (*Escherichia coli*).

As mentioned before, pyran-annulated heterocyclic compounds have interested synthetic organic chemists and biochemists because of their biological [44] and pharmacological activities [45]. Additionally, many chemical reactions have used ionic liquids such as green alternative media for volatile organic solvents because of their low vapor pressures, chemical and thermal stability, nonflammability, high ionic conductivity, and wide electrochemical potential window [46]. Based on the above findings, a simple and highly efficient synthesis of a series of pyrano[2,3-*c*]pyrazole-5-carbonitrile derivatives **46** by a one-pot, four-component reaction with ethyl benzoylacetate **17**, malononitrile **2**, aryl aldehydes **1**, and hydrazine hydrate **4** was achieved [47]. Reactions were performed under several catalytic conditions such as choline chloride:thiourea (DES) and choline chloride:urea as ionic liquid catalysts under reflux and ultrasonic irradiation conditions in short reaction times with high yields (Table 11). It was also observed that the best results according to the reaction conditions in the presence of catalyst choline were with chloride:thiourea, because of the acidic strength of thiourea compared with urea. Overall, the method provided several advantages such as a shorter reaction time with high yields, mild reaction conditions, and environmental friendliness. Furthermore, all compounds **46** were subsequently evaluated for their *in vitro* antibacterial activity against two Gram-positive bacteria (*Staphylococcus saprophyticus* and *Staphylococcus aureus*) and two Gram-negative bacteria (*Escherichia coli* and *Pseudomonas aeruginosa*), compared with cefazolin regarding the minimum inhibitory concentration (MIC). Interestingly, several of the obtained compounds **46** were more active than cefazolin (MIC values < 35), as shown in Table 11.

**Table 11.** Multicomponent synthesis and their *in vitro* antibacterial activity of pyranopyrazole derivatives **46** using ChCl•2 thiourea and ChCl•2 thiourea as catalysts, under both ultrasonic irradiation and reflux conditions.



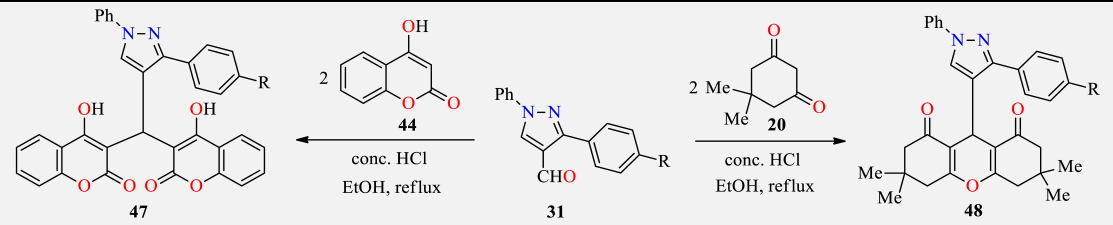
| Compound               | R                    | Yield of <b>46</b> (%)  | Antibacterial Activity of the Synthesized Compounds <b>46</b> (MIC in $\mu\text{g}\cdot\text{mL}^{-1}$ ) |     |     |     |
|------------------------|----------------------|---|--|-----|-----|-----|
|                        |                      |   | EC   | PA  | SS  | SA  |
| <b>46a</b>             | H                    | (98) <sup>a</sup> , (95) <sup>c</sup>   | 25   | 20  | 30  | 35  |
| <b>46b</b>             | 4-Me                 | (94) <sup>a</sup> , (80) <sup>b</sup> , (90) <sup>c</sup> , (76) <sup>d</sup> | 30   | 40  | 35  | 30  |
| <b>46c</b>             | 3-NO <sub>2</sub>    | (93) <sup>a</sup> , (83) <sup>b</sup> , (92) <sup>c</sup> , (80) <sup>d</sup> | 30   | 40  | 25  | 40  |
| <b>46d</b>             | 3-OH                 | (94) <sup>a</sup> , (89) <sup>b</sup>   | 35   | 20  | 35  | 35  |
| <b>46e</b>             | 2-Me                 | (97) <sup>a</sup>   | 35   | 20  | 30  | 40  |
| <b>46f</b>             | 4-OH                 | (97) <sup>a</sup> , (88) <sup>b</sup>   | 25   | 40  | 30  | 25  |
| <b>46g</b>             | 2-NO <sub>2</sub>    | (93) <sup>a</sup>   | 30   | 20  | 35  | 30  |
| <b>46h</b>             | 2-OH                 | (88) <sup>a</sup> , (69) <sup>b</sup>   | 40   | 20  | 40  | 35  |
| <b>46i</b>             | 4-OMe                | (98) <sup>a</sup> , (73) <sup>b</sup>   | 40   | 45  | 30  | 30  |
| <b>46j</b>             | 4-Cl                 | (91) <sup>a</sup> , (80) <sup>b</sup> , (90) <sup>c</sup> , (82) <sup>d</sup> | 30   | 35  | 35  | 35  |
| <b>46k</b>             | 4-Br                 | (89) <sup>a</sup>   | 35   | 30  | 30  | 30  |
| <b>46l</b>             | 4-N(Me) <sub>2</sub> | (96) <sup>a</sup> , (75) <sup>b</sup>   | 30   | 25  | 25  | 35  |
| <b>46m</b>             | 4- <i>i</i> Pr       | (89) <sup>a</sup> , (80) <sup>b</sup>   | 30   | 45  | 35  | 35  |
| <b>46n</b>             | 4-NO <sub>2</sub>    | (91) <sup>a</sup> , (89) <sup>b</sup>   | 30   | 45  | 15  | 35  |
| <b>46o</b>             | 2-Cl                 | (89) <sup>a</sup>   | 25   | 30  | 35  | 15  |
| <b>46p</b>             | 3-Br                 | (96) <sup>a</sup>   | 15   | 20  | 35  | 25  |
| Cefazolin <sup>e</sup> | —                    | —   | >35  | >35 | >35 | >35 |

<sup>a</sup> Reaction conditions: <sup>a</sup> (EtOH, reflux at 80 °C, catalyst ChCl•2 thiourea 10 mol%), <sup>b</sup> (EtOH, reflux at 80 °C, catalyst ChCl•2 urea 10 mol%), <sup>c</sup> (sonication at rt, catalyst ChCl•2 thiourea 10 mol%), <sup>d</sup> (sonication at rt, catalyst ChCl•2 urea 10 mol%). EC (*Escherichia coli*), PA (*Pseudomonas aeruginosa*), SS (*Staphylococcus saprophyticus*), SA (*Staphylococcus aureus*). <sup>e</sup> Cefazolin is taken as a standard drug for this study.

Due to functionalized coumarins playing a prominent role in medicinal chemistry and being intensively used as scaffolds for drug development [48,49], an efficient synthesis of a series of pyrazolylbiscoumarin **47** and pyrazolylxanthenedione **48** hybrid derivatives

was established [50]. The synthesis of the title compounds **47** was achieved using a simple acid-catalyzed pseudo three-component condensation reaction of the corresponding 1*H*-pyrazole-4-carbaldehydes **31** and two equivalents of type 4-hydroxycoumarin **44** in refluxing ethanol in the presence of concentrated HCl, as shown in Table 12. Similarly, treatment of 1*H*-pyrazole-4-carbaldehydes **31** and two equivalents of dimedone **20** under the same reaction conditions afforded the pyrazolyloxanthenedione derivatives **48**, as shown in Table 12. All the synthesized compounds **47** and **48** were screened for their antibacterial activity against the Gram-positive bacteria *Staphylococcus aureus* and the Gram-negative bacteria *Klebsiella pneumoniae*, using the commercial antibiotic streptomycin as the standard drug. The tested compounds exhibited a variable degree of antibacterial activity, showing the inhibition zone size ranging from 6 to 21 mm as shown in Table 12. Particularly, compounds **47a** and **48a** displayed higher biological activity; however, none of the synthesized compounds **47/48** were superior to the standard drug streptomycin.

**Table 12.** Pseudo three-component synthesis and antibacterial evaluation of pyrazolylbiscoumarins **47** and pyrazolyloxanthenediones **48**.



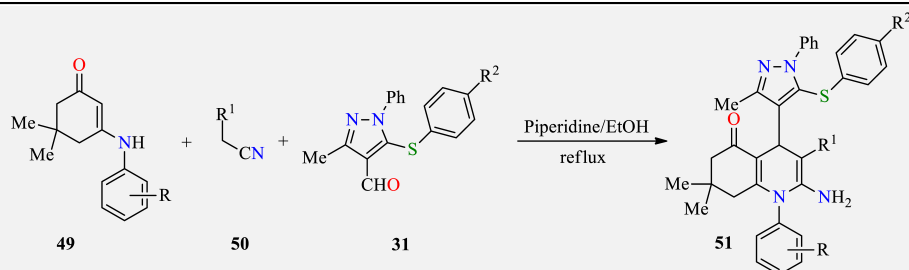
| Compound                  | R               | Yield of 47/48 (%) | Activity (Zone of Inhibition in mm) at Various Concentrations in ppm |     |     |     |    |     |     |     |
|---------------------------|-----------------|--------------------|--|-----|-----|-----|----|-----|-----|-----|
|                           |                 |                    | SA   |     |     |     | KP |     |     |     |
|                           |                 |                    | 50   | 100 | 150 | 250 | 50 | 100 | 150 | 250 |
| <b>47a</b>                | H               | 80                 | 11   | 13  | 15  | 19  | 13 | 14  | 16  | 17  |
| <b>47b</b>                | Me              | 82                 | 7  | 9   | 11  | 12  | 9  | 11  | 12  | 14  |
| <b>47c</b>                | OMe             | 84                 | –  | 8   | 10  | 14  | 6  | 9   | 12  | 15  |
| <b>47d</b>                | Br              | 86                 | 6  | 8   | 11  | 13  | 8  | 11  | 13  | 16  |
| <b>47e</b>                | NO <sub>2</sub> | 82                 | 10   | 13  | 14  | 17  | 11 | 12  | 14  | 16  |
| <b>48a</b>                | H               | 83                 | 13   | 17  | 18  | 19  | 16 | 18  | 20  | 22  |
| <b>48b</b>                | Me              | 82                 | 8  | 11  | 13  | 14  | 9  | 11  | 14  | 17  |
| <b>48c</b>                | OMe             | 86                 | –  | 7   | 9   | 12  | –  | 8   | 9   | 11  |
| <b>48d</b>                | Br              | 80                 | 6  | 8   | 10  | 11  | 7  | 9   | 10  | 12  |
| <b>48e</b>                | NO <sub>2</sub> | 84                 | –  | 7   | 9   | 13  | –  | 8   | 12  | 14  |
| Streptomycin <sup>a</sup> | –               | –                  |  | 21  |     |     |    | 25  |     |     |

SA (*Staphylococcus aureus*), KP (*Klebsiella pneumoniae*). <sup>a</sup> Positive control for the study.

Due to fluorine playing a crucial role in improving pharmacodynamic and pharmacokinetic properties of drugs molecules [51], and considering the fact that fluoro-substituted pyrazoles are a class of heterocycles occupying a remarkable position in medicinal chemistry because of their variety of pharmacological activities [52,53], a multicomponent cyclocondensation reaction was implemented for the synthesis of a series of fluorinated 5-(phenylthio)pyrazole-based polyhydroquinoline derivatives **51** [54]. This approach proceeded by incorporating various fluorinated enaminones **49**, different active methylene compounds **50**, and phenylthio-1-phenyl-1*H*-pyrazole-4-carbaldehydes **31** in a one-pot process in the presence of piperidine as a basic catalyst under refluxing EtOH, affording the targeted compounds **51** in good to excellent yield (71–84%), as shown in Table 13. All the synthesized compounds **51** were evaluated in vitro for their antibacterial activity using the broth microdilution method according to National Committee for Clinical Laboratory Standards [55]. Three Gram-positive (*Bacillus subtilis*, *Clostridium tetani*, and *Streptococcus pneumoniae*) and three Gram-negative (*Salmonella typhi*, *Escherichia coli*, and *Vibrio cholerae*) bacteria were chosen for antibacterial screening using ampicillin, ciprofloxacin, norfloxacin,

and chloramphenicol as the standard antibacterial agents. The results indicated that compound **51** showed moderate to very good antibacterial activity in comparison with the activity displayed by the standard drugs, as shown in Table 13.

**Table 13.** Three-component synthesis of pyrazolo-quinolines **51** and their in vitro antibacterial activity (MIC) against six bacterial strains.



| Compound                     | R                 | R <sup>1</sup>     | R <sup>2</sup> | Yield of <b>51</b> (%) | Antibacterial Activity of Compounds <b>51</b> (MIC in µg/mL) |      |      |      |     |      |
|------------------------------|-------------------|--------------------|----------------|------------------------|--|------|------|------|-----|------|
|                              |                   |                    |                |                        | SP   | BS   | CT   | EC   | ST  | VC   |
| <b>51a</b>                   | 4-F               | CN                 | Cl             | 81                     | 500  | 500  | 250  | 100  | 250 | 250  |
| <b>51b</b>                   | 4-F               | CO <sub>2</sub> Et | Cl             | 79                     | 100  | 500  | 62.5 | 200  | 500 | 200  |
| <b>51c</b>                   | 4-F               | CONH <sub>2</sub>  | Cl             | 73                     | 200  | 200  | 500  | 250  | 200 | 200  |
| <b>51d</b>                   | 4-F               | CN                 | Me             | 84                     | 62.5   | 250  | 125  | 200  | 200 | 1000 |
| <b>51e</b>                   | 4-F               | CO <sub>2</sub> Et | Me             | 76                     | 500  | 250  | 1000 | 250  | 250 | 1000 |
| <b>51f</b>                   | 4-CF <sub>3</sub> | CN                 | Me             | 72                     | 500  | 500  | 500  | 250  | 100 | 62.5 |
| <b>51g</b>                   | 4-CF <sub>3</sub> | CO <sub>2</sub> Et | Me             | 80                     | 100  | 100  | 500  | 500  | 200 | 500  |
| <b>51h</b>                   | 2,4-F             | CN                 | Me             | 79                     | 100  | 62.5 | 100  | 100  | 500 | 500  |
| <b>51i</b>                   | 2,4-F             | CO <sub>2</sub> Et | Me             | 73                     | 200  | 500  | 250  | 500  | 100 | 100  |
| <b>51j</b>                   | 2,4-F             | CN                 | Cl             | 75                     | 500  | 500  | 200  | 100  | 200 | 200  |
| <b>51k</b>                   | 2,4-F             | CO <sub>2</sub> Et | Cl             | 78                     | 100  | 1000 | 250  | 200  | 200 | 100  |
| <b>51l</b>                   | 2,4-F             | CONH <sub>2</sub>  | Cl             | 81                     | 500  | 500  | 200  | 500  | 500 | 500  |
| <b>51m</b>                   | 4-F               | CN                 | F              | 83                     | 200  | 100  | 200  | 62.5 | 100 | 500  |
| <b>51n</b>                   | 4-F               | CO <sub>2</sub> Et | F              | 71                     | 500  | 100  | 500  | 100  | 200 | 500  |
| <b>51o</b>                   | CF <sub>3</sub>   | CN                 | F              | 72                     | 200  | 200  | 62.5 | 62.5 | 100 | 100  |
| <b>51p</b>                   | CF <sub>3</sub>   | CO <sub>2</sub> Et | F              | 77                     | 500  | 1000 | 200  | 500  | 500 | 100  |
| Ampicillin <sup>a</sup>      | –                 | –                  | –              | –                      | 100  | 250  | 250  | 100  | 100 | 100  |
| Norfloxacin <sup>a</sup>     | –                 | –                  | –              | –                      | 10   | 100  | 50   | 10   | 10  | 10   |
| Chloramphenicol <sup>a</sup> | –                 | –                  | –              | –                      | 50   | 50   | 50   | 50   | 50  | 50   |
| Ciprofloxacin <sup>a</sup>   | –                 | –                  | –              | –                      | 25   | 50   | 100  | 25   | 25  | 25   |

SP (*Streptococcus pneumoniae*), BS (*Bacillus subtilis*), CT (*Clostridium tetani*), EC (*Escherichia coli*), ST (*Salmonella typhi*), VC (*Vibrio cholerae*). <sup>a</sup> Positive control for the study.

It is known that pyrazoles, imidazoles, dihydropyrimidinones (DHPMs), and 1,4-dihydropyridines (DHPs) are considered to be important chemical synthons of various physiological significance and pharmaceutical utility [56,57]. Based on these precedents, Viveka, et al. considered constructing hybrid molecular architectures by combining pyrazole with biologically active DHPMs, DHPs, and imidazole pharmacophores through a multicomponent reaction sequence [58]. In this sense, a series of pyrazole-containing pyrimidine **52**, 1,4-dihydropyridine **53**, and imidazole **54** derivatives were synthesized in acceptable to good yields using substituted type 4-formylpyrazole **31** as a key intermediate by following the Biginelli reaction, the classical Hantzsch condensation, and the Debus reaction, respectively, as described in Table 14. The synthesized products were screened for their in vitro antibacterial properties by the disc diffusion method against *Staphylococcus aureus*, *Escherichia coli*, *Pseudomonas aeruginosa*, and *Klebsiella pneumoniae* using streptomycin as the standard drug. The activities and the minimum inhibitory concentration (MIC) of the pyrazole derivatives **52**, **53**, and **54** are presented in Table 14. In general, the results showed that the various compounds **52**, **53**, and **54** displayed variable inhibitory effects on the growth of the bacteria depending on the nature of the substituents with the pyrazole;

particularly, compounds **52c** and **52f** displayed the highest activity. Additionally, from these studies, it is concluded that pyrimidinone-incorporated halo-substituted 1,3-diarylpyrazole was shown to be a better molecule from a biological activity point of view, and these molecules could be designed as potential drugs after further structural modifications.

**Table 14.** Multicomponent synthesis of pyrimidine-, dihydropyridine-, and imidazole-based pyrazoles **52**, **53**, and **54** and their in vitro antibacterial activity.

| Compound                  | R  | R <sup>1</sup> | Yield of <b>52</b> , <b>53</b> , <b>54</b> (%) | Antibacterial Activity of the Synthesized Compounds <b>52</b> , <b>53</b> , <b>54</b> (MIC in $\mu\text{g}\cdot\text{mL}^{-1}$ ) <sup>c</sup> |            |           |           |
|---------------------------|----|----------------|--|---|------------|-----------|-----------|
|                           |    |                |  | SA  | EC         | PA        | KP        |
| <b>52a</b>                | Cl | OEt            | 90   | 25 (13)   | 25 (14)    | NP        | 50 (9)    |
| <b>52b</b>                | Cl | Ome            | 88   | 12.5 (15)   | 12.5 (15)  | 25 (10)   | 25 (11)   |
| <b>52c</b>                | Cl | Me             | 77   | 6.25 (18)   | 6.25 (18)  | 6.25 (19) | 12.5 (12) |
| <b>52d</b>                | F  | Oet            | 89   | 12.5 (12)   | 12.5 (14)0 | NP        | 12.5 (11) |
| <b>52e</b>                | F  | Ome            | 80   | 25 (12)   | 12.5 (13)  | 50 (10)   | 25 (11)   |
| <b>52f</b>                | F  | Me             | 72   | 12.5 (16)   | 6.25 (16)  | 6.25 (17) | 6.25 (19) |
| <b>53a</b>                | Cl | Oet            | 74   | 12.5 (14)   | 12.5 (14)  | 25 (11)   | 25 (12)   |
| <b>53b</b>                | Cl | Ome            | 79   | 50 (9)  | 25 (11)    | NP        | 100 (4)   |
| <b>53c</b>                | Cl | Me             | 64   | 50 (10)   | 50 (11)    | 50 (9)    | NP        |
| <b>53d</b>                | F  | Oet            | 72   | 25 (11)   | 25 (10)    | NP        | 12.5 (12) |
| <b>53e</b>                | F  | Ome            | 65   | 12.5 (13)   | 12.5 (15)  | 25 (10)   | 12.5 (15) |
| <b>53f</b>                | F  | Me             | 62   | 50 (7)  | 50 (8)     | 100 (8)   | NP        |
| <b>54a</b>                | Cl | –              | 86   | NP  | 25 (12)    | 12.5 (10) | NP        |
| <b>54b</b>                | F  | –              | 78   | 50 (10)   | 25 (11)    | 25 (9)    | 100 (5)   |
| Streptomycin <sup>d</sup> | –  | –              | –  | 6.25 (20)   | 6.25 (17)  | 6.25 (19) | 6.25 (18) |

<sup>a</sup> Biginelli reaction conditions: A mixture of compound **31** (2 mol), type keto-derivative **3** (2.2 mol), urea (3 mol), and HCl (0.5 mL) in ethanol was heated to reflux for 6 h. <sup>b</sup> Hantzsch reaction conditions: A mixture of compound **31** (1.0 mol), type keto-derivative **3** (2 mol), and ammonium acetate (1.1 mol) in ethanol (20 mL) was refluxed for 8 h. <sup>c</sup> Values in brackets correspond to zone of inhibition in mm. SA (*Staphylococcus aureus*), EC (*Escherichia coli*), PA (*Pseudomonas aeruginosa*), KP (*Klebsiella pneumonia*). <sup>d</sup> Positive control for the study.

Research on the design of synthetic protocols with an efficient atom economy and catalyst-free under ultrasound irradiation conditions has received specific attention [59]. In this sense, an efficient multicomponent method for the synthesis of biologically active 1,3,4-thiadiazole-1*H*-pyrazol-4-yl thiazolidin-4-one hybrids **57** was reported [60], from the reaction of 5-(substituted phenyl)-1,3,4-thiadiazol-2-amines **55**, type pyrazole-4-carbaldehyde **31**, and 2-mercaptoacetic acid **56** in ethanol under ultrasound irradiation. It was found that reactions gave the desired products **57** in 91–97% yield, in short times (55–65 min) at 50 °C as shown in Table 15. All the obtained pyrazol-4-yl-thiazolidin-4-ones **57** were screened for their antibacterial activity. Among the screened hybrids **57**, derivatives with 4-nitro and 3-nitro groups substituted on the phenyl ring showed fourfold (MBC = 156.3  $\mu\text{g}/\text{cm}^3$ ) and twofold (MBC = 312.5  $\mu\text{g}/\text{cm}^3$ ), respectively, stronger potency against the *Pseudomonas aeruginosa* strain as compared to the standard ciprofloxacin. Moreover, SAR studies revealed the importance of the functional groups on the phenyl ring of the 1,3,4-thiadiazol-2-amine moiety for varying bacterial activity. Thus, the electron-withdrawing (NO<sub>2</sub>) group at *para*-

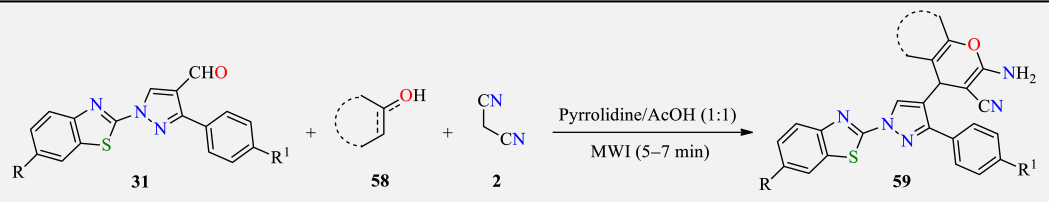
and *meta*-positions played a significant role in enhancing the antibacterial activity, as shown in Table 15.

**Table 15.** Three-component synthesis of thiadiazole-1*H*-pyrazol-4-yl-thiazolidin-4-ones **57** and their in vitro antibacterial activity (MBC) against six bacterial strains.

| Compound                   | R                 | Yield of <b>57</b> (%) <sup>a</sup> | Antibacterial Activity of Compounds <b>57</b> (MBC in µg/mL) |           |           |           |           |           |
|----------------------------|-------------------|-------------------------------------|--|-----------|-----------|-----------|-----------|-----------|
|                            |                   |                                     | <i>MRSA</i>  | <i>SA</i> | <i>EC</i> | <i>PA</i> | <i>ST</i> | <i>KP</i> |
| <b>57a</b>                 | H                 | 96 (74)                             | 1250   | 625       | 2500      | 2500      | 625       | 625       |
| <b>57b</b>                 | 4-F               | 94 (62)                             | 625  | 625       | 625       | 312.5     | 625       | 625       |
| <b>57c</b>                 | 4-Br              | 95 (56)                             | 625  | 312.5     | 312.5     | 312.5     | 625       | 625       |
| <b>57d</b>                 | 3-F               | 91 (55)                             | 1250   | 78.5      | 312.5     | 2500      | 312.5     | 625       |
| <b>57e</b>                 | 3-Cl              | 94 (58)                             | 1250   | 625       | 312.5     | 1250      | 9.8       | 625       |
| <b>57f</b>                 | 3-Br              | 93 (60)                             | 156.3  | 625       | 156.3     | 312.5     | 625       | 625       |
| <b>57g</b>                 | 4-NO <sub>2</sub> | 97 (64)                             | 625  | 39.1      | 4.9       | 156.3     | 312.5     | 500       |
| <b>57h</b>                 | 3-NO <sub>2</sub> | 92 (56)                             | 312.5  | 156.3     | 39.1      | 625       | 625       | 156.3     |
| <b>57i</b>                 | 4-Me              | 96 (57)                             | 2500   | 2500      | 1250      | 1250      | 2500      | 1250      |
| <b>57j</b>                 | 4-OMe             | 95 (61)                             | 1250   | 625       | 1250      | 1250      | 1250      | 1250      |
| <b>57k</b>                 | 3,4,5-OMe         | 91 (62)                             | 1250   | 625       | 1250      | 2500      | 625       | 625       |
| <b>57l</b>                 | 3,4-OMe           | 93 (60)                             | 2500   | 625       | 625       | 2500      | 625       | 1250      |
| Ciprofloxacin <sup>b</sup> | –                 | –                                   | 625  | 39.1      | 1.22      | 625       | 1.22      | 4.9       |

<sup>a</sup> Yields in brackets were obtained under conventional heating at 50 °C. *MRSA* (Methicillin-resistant *Staphylococcus aureus*), *SA* (*Staphylococcus aureus*), *EC* (*Escherichia coli*), *PA* (*Pseudomonas aeruginosa*), *ST* (*Salmonella typhimurium*), *KP* (*Klebsiella pneumoniae*). <sup>b</sup> Positive control for the study.

Among all the various organocatalysts, the pyrrolidine-acetic acid catalyst is one of the most versatile for many important organic reactions and asymmetric transformations [61]. Based on this, an efficient method for the synthesis of fused pyran-pyrazole derivatives **59** was developed through a one-pot, three-component, solvent-free reaction of type 1*H*-pyrazole-4-carbaldehyde **31**, various active methylenes **58**, and malononitrile **2** under microwave irradiation in the presence of pyrrolidine-acetic acid (10 mol%) as a bifunctional catalyst, affording products **59** in good yields, as shown in Table 16 [62]. Some highlights of this protocol were associated with the solvent-free reaction conditions, shorter reaction time, greater selectivity, and straightforward workup procedure. The synthesized compounds **59** were investigated against a representative panel of six pathogenic strains using the broth microdilution MIC method for their in vitro antimicrobial activity. The investigation of the antimicrobial activity data revealed that some compounds **59** showed good to excellent antibacterial activity against the representative species when compared with the standard drugs such as ampicillin, ciprofloxacin, and norfloxacin. Particularly, compounds **59c**, **59e**, **59h**, **59m**, **59n**, **59o**, **59q**, **59r**, and **59t** were found to be the most efficient antimicrobials in the series, as shown in Table 16.

**Table 16.** Microwave-assisted three-component synthesis of pyrano-pyrazole derivatives **59** and their in vitro antibacterial activity evaluation against a panel of six pathogenic strains.


| Compound                     | Reagent 58 | R  | R <sup>1</sup> | Yield of 59 (%) | Antibacterial Activity of Compounds 59 (MIC in µg/mL) |     |      |      |     |     |
|------------------------------|------------|----|----------------|-----------------|---|-----|------|------|-----|-----|
|                              |            |    |                |                 | BS  | CT  | SA   | EC   | ST  | VC  |
| 59a                          |            | H  | F              | 71              | 250   | 250 | 500  | 200  | 200 | 250 |
| 59b                          |            | H  | Me             | 83              | 250   | 100 | 250  | 500  | 500 | 250 |
| 59c                          |            | Me | F              | 78              | 250   | 100 | 125  | 200  | 250 | 200 |
| 59d                          |            | Me | Me             | 79              | 500   | 500 | 500  | 200  | 250 | 500 |
| 59e                          |            | H  | F              | 78              | 100   | 250 | 500  | 250  | 500 | 250 |
| 59f                          |            | H  | Me             | 72              | 200   | 500 | 100  | 250  | 250 | 200 |
| 59g                          |            | Me | F              | 75              | 250   | 250 | 250  | 200  | 250 | 250 |
| 59h                          |            | Me | Me             | 70              | 250   | 250 | 250  | 125  | 100 | 125 |
| 59i                          |            | H  | F              | 73              | 250   | 100 | 500  | 100  | 200 | 100 |
| 59j                          |            | H  | Me             | 83              | 200   | 250 | 500  | 125  | 100 | 250 |
| 59k                          |            | Me | F              | 81              | 100   | 100 | 62.5 | 200  | 125 | 125 |
| 59l                          |            | Me | Me             | 84              | 500   | 200 | 200  | 100  | 200 | 100 |
| 59m                          |            | H  | F              | 75              | 200   | 100 | 500  | 200  | 250 | 200 |
| 59n                          |            | H  | Me             | 86              | 500   | 500 | 200  | 200  | 200 | 500 |
| 59o                          |            | Me | F              | 70              | 125   | 500 | 500  | 125  | 100 | 100 |
| 59p                          |            | Me | Me             | 82              | 100   | 100 | 500  | 200  | 250 | 100 |
| 59q                          |            | H  | F              | 68              | 250   | 500 | 250  | 100  | 125 | 250 |
| 59r                          |            | H  | Me             | 73              | 500   | 250 | 250  | 250  | 250 | 500 |
| 59s                          |            | Me | F              | 75              | 250   | 250 | 250  | 62.5 | 100 | 250 |
| 59t                          |            | Me | Me             | 76              | 250   | 250 | 500  | 250  | 500 | 250 |
| Ampicillin <sup>a</sup>      | —          | —  | —              | —               | 100   | 250 | 100  | 100  | 100 | 250 |
| Norfloxacin <sup>a</sup>     | —          | —  | —              | —               | 10  | 50  | 10   | 10   | 10  | 100 |
| Chloramphenicol <sup>a</sup> | —          | —  | —              | —               | 50  | 50  | 50   | 50   | 50  | 50  |
| Ciprofloxacin <sup>a</sup>   | —          | —  | —              | —               | 50  | 100 | 25   | 25   | 25  | 50  |

BS (*Bacillus subtilis*), CT (*Clostridium tetani*), SA (*Staphylococcus aureus*), EC (*Escherichia coli*), ST (*Salmonella typhi*), VC (*Vibrio cholerae*). <sup>a</sup> Positive control for the study.

Due to the fact pyrazole and pyrimidine-2,4,6-trione heterocycles are interesting pharmacophores for pharmaceutical targets in synthetic and natural products [63], as well as being used as a precursor for the construction of condensed heterocyclic systems [64], a series of pyrazole-thiopyrimidine-trione derivatives **61** was synthesized via a one-pot multi-component reaction in aqueous media with the purpose of identifying new drugs as antibacterial agents [65]. Thus, a cascade Aldol–Michael additions of *N,N*-diethyl thiobarbituric acid **60**, 3-methyl-1-phenyl-1*H*-pyrazol-5(4*H*)-one **19**, and aldehydes **1** mediated by aqueous Et<sub>2</sub>NH as a catalyst afforded the pyrazole-thiobarbituric acid derivatives **61** in (63–88%) yield with a broad substrate scope under mild reaction conditions, as shown in Table 17.

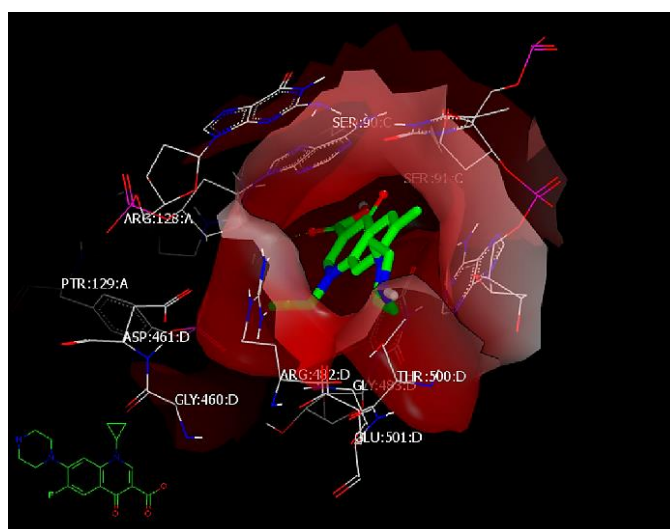
The new compounds **61** were evaluated for their antibacterial activity against three Gram-positive bacterial strains. Compound **61c** exhibited the best activity against *Staphylococcus aureus* and *Staphylococcus faecalis* with MIC = 16 µg/L. However, compounds **61l** and **61o** were the most active against *Bacillus subtilis* with MIC = 16 µg/L. Molecular docking studies for the final compounds **61** and the standard drug ciprofloxacin were performed using the OpenEye program, with different target proteins to explore their mode of action. Molecular modeling gave the comparative consensus scores of synthesized compounds **61** with two targets: DNA topoisomerase II (PDB ID 5BTC) [66] and gyrase B (PDB ID 4URM) proteins [67]. Thus, the docking with DNA Topoisomerase II (5BTC) for the standard drug

ciprofloxacin had a consensus score of 1 through the hydrophobic–hydrophobic interaction and formed HB with ARG:128:A through the oxygen of its carbonyl (Figure 5).

**Table 17.** Three-component synthesis of pyrazole-thiobarbituric derivatives **61** and their in vitro antibacterial activity against three Gram-positive bacterial strains.

| Antibacterial Activity of Compounds <b>61</b> (MBC in $\mu\text{g/L}$ ) <sup>a</sup> |   |                                     |          |                         |          |                         |          |                         |
|--|---|-------------------------------------|----------|-------------------------|----------|-------------------------|----------|-------------------------|
| Compound   | Ar  | Yield of <b>61</b> (%) <sup>a</sup> | SA       |                         | EF       |                         | BS       |                         |
|  |   |                                     | CPM (mm) | MIC ( $\mu\text{g/L}$ ) | CPM (mm) | MIC ( $\mu\text{g/L}$ ) | CPM (mm) | MIC ( $\mu\text{g/L}$ ) |
| <b>61b</b>   | Ph  | 83                                  | 13       | 32                      | 15       | 32                      | 12       | 32                      |
| <b>61c</b>   | 4-ClC <sub>6</sub> H <sub>4</sub>                 | 84                                  | 12       | 32                      | 12       | 32                      | 10       | 32                      |
| <b>61d</b>   | 4-MeC <sub>6</sub> H <sub>4</sub>                 | 73                                  | 14       | 16                      | 12       | 16                      | 11       | 32                      |
| <b>61e</b>   | 3-MeC <sub>6</sub> H <sub>4</sub>                 | 73                                  | Nil      | 128                     | 9        | 128                     | 11       | 64                      |
| <b>61f</b>   | 4-BrC <sub>6</sub> H <sub>4</sub>                 | 78                                  | Nil      | 128                     | 10       | 64                      | 11       | 64                      |
| <b>61g</b>   | 4-BrC <sub>6</sub> H <sub>4</sub>                 | 88                                  | Nil      | 128                     | 10       | 64                      | 11       | 64                      |
| <b>61h</b>   | 3-BrC <sub>6</sub> H <sub>4</sub>                 | 88                                  | Nil      | 128                     | 10       | 64                      | 11       | 64                      |
| <b>61i</b>   | 4-NO <sub>2</sub> C <sub>6</sub> H <sub>4</sub>   | 73                                  | 13       | 32                      | 12       | 64                      | 11       | 64                      |
| <b>61j</b>   | 4-NO <sub>2</sub> C <sub>6</sub> H <sub>4</sub>   | 73                                  | 13       | 32                      | 16       | 32                      | 11       | 64                      |
| <b>61k</b>   | 3-NO <sub>2</sub> C <sub>6</sub> H <sub>4</sub>   | 72                                  | 14       | 32                      | 16       | 32                      | 13       | 32                      |
| <b>61l</b>   | 4-MeOC <sub>6</sub> H <sub>4</sub>                | 69                                  | 14       | 32                      | 18       | 16                      | 13       | 32                      |
| <b>61m</b>   | 4-CF <sub>3</sub> C <sub>6</sub> H <sub>4</sub>   | 63                                  | 13       | 64                      | 10       | 32                      | 11       | 32                      |
| <b>61n</b>   | 2,4-Cl <sub>2</sub> C <sub>6</sub> H <sub>3</sub> | 68                                  | 13       | 32                      | 20       | 32                      | 15       | 16                      |
| <b>61o</b>   | 2,6-Cl <sub>2</sub> C <sub>6</sub> H <sub>3</sub> | 65                                  | 13       | 32                      | 24       | 32                      | 16       | 32                      |
| <b>61p</b>   | 2-Naphthyl  | 67                                  | 14       | 32                      | 11       | 32                      | 11       | 32                      |
| <b>61q</b>   | Thiophen-2-yl                                     | 78                                  | 14       | 32                      | Nil      | 32                      | 11       | 16                      |
| Ciprofloxacin <sup>b</sup>   | –   | –                                   | 27       | $\leq 0.25$             | 24       | $\leq 0.25$             | 25       | $\leq 0.25$             |

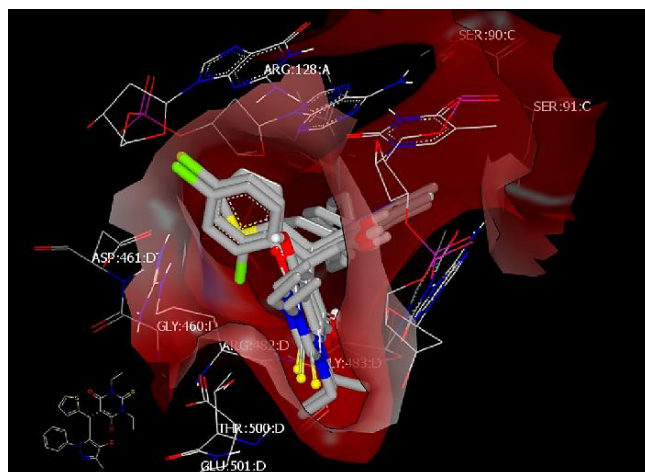
<sup>a</sup> SA (*Staphylococcus aureus*), EF (*Staphylococcus faecalis*), BS (*Bacillus subtilis*), ST (*Salmonella typhimurium*), KP (*Klebsiella pneumonia*). <sup>b</sup> Standard drug.



**Figure 5.** Visual representation of ciprofloxacin docked with 5BTC, showing hydrophobic–hydrophobic interaction and hydrogen bonding with ARG 128:A, as shown by Vida. Image adapted from Elshaier et al. [65].

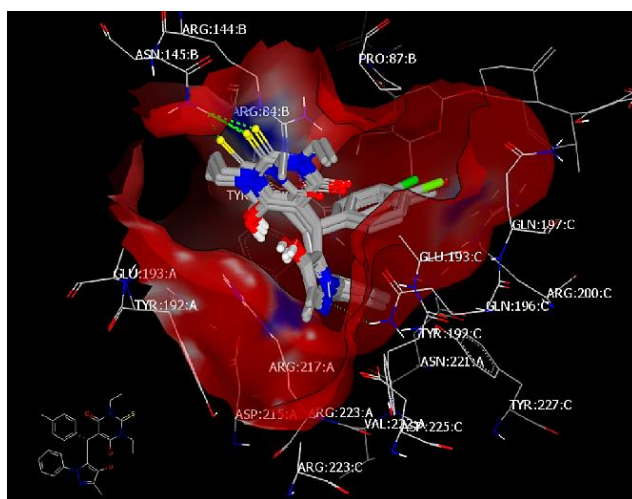


Meanwhile, the docking mode with DNA Topoisomerase II (5BTC) for the most active compounds showed a hydrophobic–hydrophobic interaction with the receptor. Compound **61c** with a consensus score of 29, compound **61o** with a consensus score of 10, and compound **61i** with a consensus score of 54 exhibited hydrophobic–hydrophobic interactions and overlay each other (Figure 6).



**Figure 6.** Visual representation of compounds **61c**, **61o**, and **61i** docked with 5BTC, showing no hydrogen bond interaction, as shown by Vida. Image adapted from Elshaier et al. [65].

Regarding the molecular docking with Gyrase B (PDB ID 4URM), compound **61c** (consensus score: 24) showed an HB interaction with ASN 145:A through the sulfur atom of the thiobarbiturate ring and overlay with **61a**, **61d**, and **61f** with the same HB. However, **61a** showed extra HB with GLN 196:A through the N of pyrazole (Figure 7).

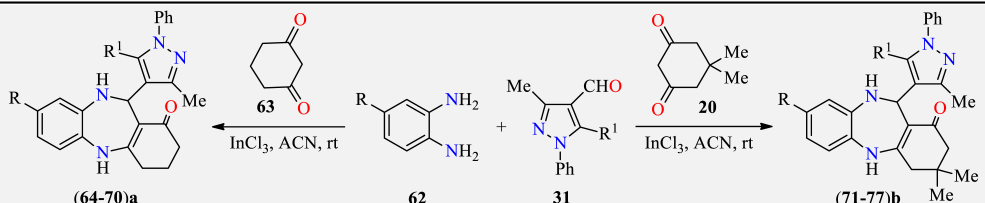


**Figure 7.** Visual representation of compound **61d** docked with 4URM and overlay with **61c**, **61a**, and **61f**. The compounds showed hydrogen bonding between the sulfur of the pyrimidine ring and ASN 145:A, as shown by Vida. Image adapted from Elshaier et al. [65].

Diazepine and pyrazole, which represent seven- and five-membered nitrogen-containing rings, respectively, are structures of great importance in the development of newer molecular assemblies, finding a wide range of applications in diverse fields [68,69]. In this regard, pyrazole-appended benzodiazepines were envisaged as interesting molecular templates, anticipated to have new bioprofiles [70]. Thus, several pyrazolyl-dibenzo[*b,e*][1,4]diazepinone scaffolds (**64–70a**)/(**71–77b**) were synthesized in acceptable to good yields by assembling, via a three-component approach, 5-substituted 3-methyl-1-phenyl-pyrazole-4-carbaldehydes

**31** of varied natures with different cyclic diketones **20/63** and aromatic diamines **62** in the presence of indium chloride in acetonitrile at room temperature, as shown in Table 18. It is assumed that the aprotic nature of acetonitrile might have favored this reaction, as it gave poor results in protic solvents such as ethanol and water.

**Table 18.** Three-component synthesis of pyrazolo-diazepinones (**64–70**)a/(**71–77**)b and their in vitro antibacterial activity (MIC) against six bacterial strains.



| Compound                     | R    | R <sup>1</sup>                    | Yield of<br>( <b>64–70</b> )a/( <b>71–77</b> )b<br>(%) | Antibacterial Activity of Compounds ( <b>64–70</b> )a/( <b>71–77</b> )b (MIC in µg/mL) |      |      |                        |     |      |
|------------------------------|------|-----------------------------------|--|--|------|------|------------------------|-----|------|
|                              |      |                                   |  | Gram-Positive Bacteria   |      |      | Gram-Negative Bacteria |     |      |
|                              |      |                                   |  | SP   | VC   | EC   | EC                     | EC  | EC   |
| <b>64a</b>                   | H    | PhO                               | 87   | 250  | 500  | 250  | 500                    | 500 | 500  |
| <b>64'a</b>                  | COPh | PhO                               | 76   | 100  | 250  | 500  | 500                    | 250 | 500  |
| <b>65a</b>                   | H    | MeC <sub>6</sub> H <sub>4</sub> O | 67   | 250  | 250  | 500  | 250                    | 500 | 250  |
| <b>65'a</b>                  | COPh | MeC <sub>6</sub> H <sub>4</sub> O | 78   | 200  | 250  | 250  | 500                    | 250 | 200  |
| <b>66a</b>                   | H    | ClC <sub>6</sub> H <sub>4</sub> O | 79   | 250  | 250  | 500  | 200                    | 500 | 500  |
| <b>66'a</b>                  | COPh | ClC <sub>6</sub> H <sub>4</sub> O | 89   | 125  | 125  | 500  | 250                    | 250 | 250  |
| <b>67a</b>                   | H    | PhS                               | 87   | 200  | 200  | 500  | 500                    | 500 | 500  |
| <b>67'a</b>                  | COPh | PhS                               | 74   | 250  | 250  | 250  | 250                    | 500 | 500  |
| <b>68a</b>                   | H    | ClC <sub>6</sub> H <sub>4</sub> S | 87   | 125  | 250  | 250  | 500                    | 250 | 250  |
| <b>68'a</b>                  | COPh | ClC <sub>6</sub> H <sub>4</sub> S | 73   | 200  | 200  | 200  | 250                    | 250 | 200  |
| <b>69a</b>                   | H    | Allyl-S                           | 86   | 125  | 250  | 500  | 250                    | 500 | 500  |
| <b>69'a</b>                  | COPh | Allyl-S                           | 64   | 250  | 250  | 500  | 100                    | 500 | 500  |
| <b>70a</b>                   | H    | Bn-S                              | 64   | 200  | 250  | 500  | 200                    | 500 | 500  |
| <b>70'a</b>                  | COPh | Bn-S                              | 69   | 500  | 200  | 500  | 250                    | 500 | 500  |
| <b>71b</b>                   | H    | PhO                               | 79   | 200  | 200  | 500  | 200                    | 250 | 250  |
| <b>71'b</b>                  | COPh | PhO                               | 69   | 62.5   | 125  | 500  | 250                    | 250 | 500  |
| <b>72b</b>                   | H    | MeC <sub>6</sub> H <sub>4</sub> O | 77   | 200  | 200  | 250  | 50                     | 250 | 200  |
| <b>72'b</b>                  | COPh | MeC <sub>6</sub> H <sub>4</sub> O | 72   | 125  | 125  | 200  | 200                    | 100 | 125  |
| <b>73b</b>                   | H    | ClC <sub>6</sub> H <sub>4</sub> O | 87   | 125  | 200  | 125  | 125                    | 125 | 200  |
| <b>73'b</b>                  | COPh | ClC <sub>6</sub> H <sub>4</sub> O | 75   | 62.5   | 62.5 | 100  | 62.5                   | 100 | 62.5 |
| <b>74b</b>                   | H    | PhS                               | 89   | 200  | 250  | 500  | 250                    | 250 | 200  |
| <b>74'b</b>                  | COPh | PhS                               | 86   | 200  | 200  | 250  | 200                    | 200 | 200  |
| <b>75b</b>                   | H    | ClC <sub>6</sub> H <sub>4</sub> S | 79   | 125  | 200  | 250  | 200                    | 250 | 200  |
| <b>75'b</b>                  | COPh | ClC <sub>6</sub> H <sub>4</sub> S | 68   | 62.5   | 125  | 62.5 | 125                    | 50  | 100  |
| <b>76b</b>                   | H    | Allyl-S                           | 58   | 250  | 250  | 500  | 250                    | 250 | 500  |
| <b>76'b</b>                  | COPh | Allyl-S                           | 76   | 200  | 200  | 500  | 250                    | 200 | 250  |
| <b>77b</b>                   | H    | Bn-S                              | 70   | 250  | 250  | 500  | 500                    | 250 | 500  |
| <b>77'b</b>                  | COPh | Bn-S                              | 72   | 250  | 500  | 500  | 500                    | 500 | 500  |
| Gentamycin <sup>a</sup>      | –    | –                                 | –  | 0.5  | 5    | 1    | 5                      | 5   | 0.05 |
| Ampicillin <sup>a</sup>      | –    | –                                 | –  | 100  | 250  | 250  | 100                    | 100 | 100  |
| Chloramphenicol <sup>a</sup> | –    | –                                 | –  | 50   | 50   | 50   | 50                     | 50  | 50   |
| Ciprofloxacin <sup>a</sup>   | –    | –                                 | –  | 50   | 100  | 50   | 25                     | 25  | 25   |
| Norfloxacin <sup>a</sup>     | –    | –                                 | –  | 10   | 50   | 100  | 10                     | 10  | 10   |

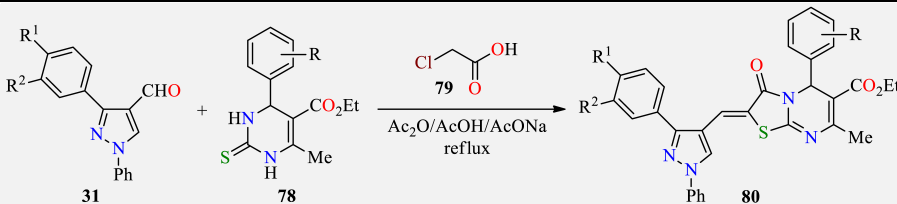
SP (*Streptococcus pneumoniae*), CT (*Clostridium tetani*), BS (*Bacillus subtilis*), ST (*Salmonella typhi*), VC (*Vibrio cholera*), EC (*Escherichia coli*). <sup>a</sup> Standard drugs.

Structures of the obtained compounds (**64–70**)a/(**71–77**)b were confirmed by spectroscopic techniques, and based on single-crystal X-ray diffraction data of the representative compound **75b**. All obtained heterocycles (**64–70**)a/(**71–77**)b were screened, in vitro, for their antibacterial activity against three Gram-positive (*Streptococcus pneumoniae*, *Clostridium tetani*, and *Bacillus subtilis*) and three Gram-negative (*Salmonella typhi*, *Vibrio cholera*, and *Escherichia coli*) bacterial strains. Results showed that compounds **73b**, **73'b**, and **75'b** bearing a chlorophenyl-tethered pyrazolyl moiety displayed excellent to moderate inhibitory power against all six bacterial species, compared with the standard drugs gentamycin, ampicillin, chloramphenicol, ciprofloxacin, and norfloxacin, as shown in Table 18.

Due to the rapidly increasing incidence of antimicrobial resistance representing a serious problem worldwide, the development of new and different antimicrobial drugs has been a very important objective for many research programs directed toward the design of new antimicrobial agents [71]. For this purpose, a series of pyrazole-integrated

thiazolo[2,3-*b*]dihydropyrimidinone derivatives **80** were synthesized via the MCR approach in a single framework as potential antimicrobial agents [72]. In this protocol, the highly activated intermediates **31** and **78** were reacted with monochloroacetic acid **79** and anhydrous sodium acetate in an acetic acid-acetic anhydride medium, resulting in the formation of the target compounds **80** in acceptable to good yields, as shown in Table 19. The synthesized compounds **80** were evaluated for their in vitro antibacterial activity against a Gram-positive organism (*Staphylococcus aureus*), Gram-negative organisms (*Klebsiella pneumoniae*, *Pseudomonas aeruginosa*, and *Escherichia coli*), and compared with that of the standard drug streptomycin. The zone of inhibition was determined by the agar well diffusion method. Remarkably, as observed in the antibacterial activity described in Table 19, compounds **80a**, **80b**, and **80d** showed good activity for all the tested species that contained electron-withdrawing 3,4-dichloro phenyl groups on the pyrazole ring, indicating that such a substitution is a favorable site for high activity in future developments.

**Table 19.** Three-component synthesis of thiazolo[2,3-*b*]dihydropyrimidinones **80** and their in vitro antibacterial activity against four bacterial strains.



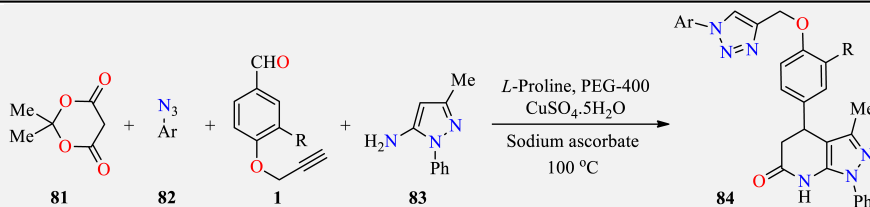
| Compound                  | R                      | R <sup>1</sup> | R <sup>2</sup> | Yield of <b>80</b> (%) | Antibacterial Activity of Compounds <b>80</b><br>(Zone of Inhibition in mm) |      |      |      |
|---------------------------|------------------------|----------------|----------------|------------------------|---|------|------|------|
|                           |                        |                |                |                        | EC  | SA   | PA   | KP   |
| <b>80a</b>                | 3-F, 4-Me              | Cl             | Cl             | 91                     | 17.9  | 15.9 | 15.9 | 15.4 |
| <b>80b</b>                | 2,5-(OMe) <sub>2</sub> | Cl             | Cl             | 89                     | 17.5  | 15.2 | 14.4 | 16.2 |
| <b>80c</b>                | H                      | Cl             | Cl             | 67                     | 11.2  | 11.9 | 10.6 | 12.9 |
| <b>80d</b>                | 4-OMe                  | Cl             | Cl             | 88                     | 16.3  | 13.7 | 15.2 | 14.4 |
| <b>80e</b>                | 3-F, 4-Me              | F              | F              | 72                     | 12.2  | 12.4 | 11.1 | 10.4 |
| <b>80f</b>                | 2,5-(OMe) <sub>2</sub> | F              | F              | 74                     | 9.9   | 9.5  | 11.7 | 10.3 |
| <b>80g</b>                | H                      | F              | F              | 81                     | 7.1   | 5.3  | 10.6 | 8.1  |
| <b>80h</b>                | 4-OMe                  | F              | F              | 73                     | 9.3   | 9.1  | 7.2  | 9.4  |
| <b>80i</b>                | 3-F, 4-Me              | Cl             | H              | 59                     | 9.5   | 11.2 | 12.2 | 10.6 |
| <b>80j</b>                | 2,5-(OMe) <sub>2</sub> | Cl             | H              | 72                     | 11.6  | 8.2  | 11.6 | 12.4 |
| <b>80k</b>                | H                      | Cl             | H              | 70                     | 7.7   | 5.2  | 10.4 | 5.1  |
| <b>80l</b>                | 4-OMe                  | Cl             | H              | 49                     | 10.9  | 11.5 | 10.1 | 7.0  |
| <b>80m</b>                | 3-F, 4-Me              | F              | H              | 66                     | 8.1   | 9.9  | 5.4  | 9.6  |
| <b>80n</b>                | 2,5-(OMe) <sub>2</sub> | F              | H              | 75                     | 10.1  | 11.4 | 11.6 | 12.8 |
| <b>80o</b>                | H                      | F              | H              | 86                     | 7.2   | 9.6  | 11.4 | 9.1  |
| <b>80p</b>                | 4-OMe                  | F              | H              | 76                     | 7.4   | 10.0 | 11.2 | 11.1 |
| Streptomycin <sup>a</sup> | –                      | –              | –              | –                      | 18.5  | 16.2 | 19.2 | 16.6 |

EC (*Escherichia coli*), SA (*Staphylococcus aureus*), PA (*Pseudomonas aeruginosa*), KP (*Klebsiella pneumoniae*). <sup>a</sup> Standard drug for the study.

Considering that molecular hybridization using a multicomponent approach is an effective strategy for the synthesis of new bioactive compounds and is being used in modern medicinal chemistry [73,74], a series of heterocyclic compounds containing pyrazolo[3,4-*b*]pyridin-6(7*H*)-one linked 1,2,3-triazoles **84** were synthesized to develop new pharmacophores with promising biological activities [75]. In this approach, the novel molecular hybrids **84** containing pyrazole, pyridinone, and 1,2,3-triazole were obtained from a one-pot four-component reaction of Meldrum's acid **81**, substituted aryl azides **82**, 4-(prop-2-yn-1-yloxy)aryl aldehydes **1**, and 3-methyl-1-phenyl-1*H*-pyrazol-5-amine **83** using *L*-proline as a basic organocatalyst, aq. solution of CuSO<sub>4</sub>·5H<sub>2</sub>O and aq. solution of sodium ascorbate as catalysts at 100 °C through click chemistry in PEG-400 as a highly efficient and green media.

Thus, a diverse library of 4-(4-((1-(aryl)-1*H*-1,2,3-triazol-4-yl)aryl)-3-methyl-1-phenyl-4,5-dihydro-1*H*-pyrazolo[3,4-*b*]pyridin-6(7*H*)-ones **84** was obtained in high yields, as shown in Table 20.

**Table 20.** Four-component synthesis of 1*H*-1,2,3-triazole-tethered pyrazolo[3,4-*b*]pyridin-6(7*H*)-ones **84** and their in vitro antibacterial activity against four bacterial strains.



| Compound                   | Ar                                    | R   | Yield of <b>84</b> (%) | Antibacterial Activity of Compounds <b>84</b><br>(Diameter of Growth of Inhibition Zone (mm)) |      |      |      |
|----------------------------|---------------------------------------|-----|------------------------|---|------|------|------|
|                            |                                       |     |                        | SA  | BS   | SE   | BC   |
| <b>84a</b>                 | 4-MeOC <sub>6</sub> H <sub>4</sub>    | H   | 82                     | 16.0  | 17.3 | 19.6 | 18.6 |
| <b>84b</b>                 | 3-Cl,4-FC <sub>6</sub> H <sub>3</sub> | H   | 90                     | 15.3  | 16.3 | 17.3 | 14.3 |
| <b>84c</b>                 | 4-FC <sub>6</sub> H <sub>4</sub>      | H   | 86                     | 15.3  | 15.6 | 16.3 | 16.3 |
| <b>84d</b>                 | 4-BrC <sub>6</sub> H <sub>4</sub>     | H   | 84                     | 14.3  | 16.3 | 15.3 | 17.0 |
| <b>84e</b>                 | 4-MeC <sub>6</sub> H <sub>4</sub>     | H   | 80                     | 18.6  | 20.3 | 19.3 | 21.6 |
| <b>84f</b>                 | 3-ClC <sub>6</sub> H <sub>4</sub>     | H   | 84                     | 16.0  | 17.3 | 20.6 | 19.3 |
| <b>84g</b>                 | 3-Cl,4-FC <sub>6</sub> H <sub>3</sub> | MeO | 92                     | 17.3  | 19.3 | 20.6 | 18.6 |
| <b>84h</b>                 | 4-FC <sub>6</sub> H <sub>4</sub>      | MeO | 84                     | 15.3  | 15.6 | 17.3 | 16.6 |
| <b>84i</b>                 | 4-BrC <sub>6</sub> H <sub>4</sub>     | MeO | 86                     | 14.6  | 16.3 | 15.3 | 16.3 |
| <b>84j</b>                 | 4-MeOC <sub>6</sub> H <sub>4</sub>    | MeO | 80                     | 19.3  | 21.6 | 20.3 | 21.3 |
| <b>84k</b>                 | 4-MeC <sub>6</sub> H <sub>4</sub>     | MeO | 82                     | 21.6  | 22.3 | 22.6 | 23.6 |
| <b>84l</b>                 | 3-ClC <sub>6</sub> H <sub>4</sub>     | MeO | 84                     | 18.6  | 20.3 | 18.6 | 19.3 |
| Ciprofloxacin <sup>a</sup> | –                                     | –   | –                      | 26.6  | 24.0 | 19.6 | 23.0 |

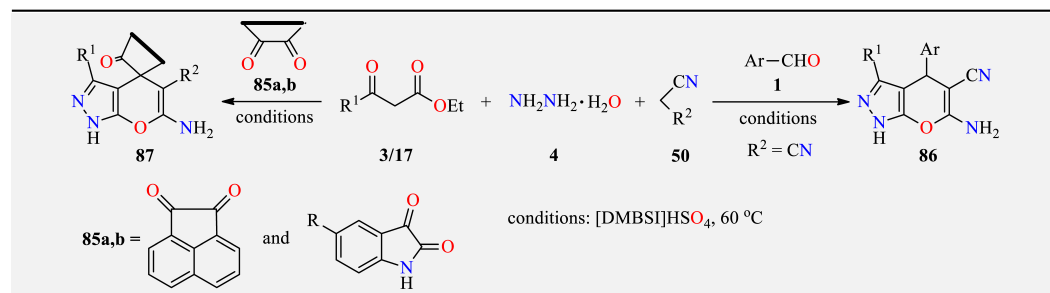
SA (*Staphylococcus aureus*), BS (*Bacillus subtilis*), SE (*Staphylococcus epidermidis*), BC (*Bacillus cereus*). <sup>a</sup> Standard drug for the study.

The structure of the synthesized compounds **84** was confirmed by the single-crystal X-ray diffraction analysis for compound **84e**. The in vitro antibacterial activity of all obtained compounds **84** was evaluated against six antibacterial strains. Four Gram-positive bacteria (*Staphylococcus aureus*, *Staphylococcus epidermidis*, *Bacillus subtilis*, and *Bacillus cereus*) and two Gram-negative bacteria (*Escherichia coli* and *Pseudomonas aeruginosa*) were used in this study. The antibacterial activity of all compounds **84** was evaluated by the agar well diffusion method using ciprofloxacin as a standard. The results of the antibacterial activity evaluation revealed that all compounds possessed good activity against Gram-positive bacterial strains and no activity against Gram-negative bacterial strains, that is, *Escherichia coli* and *Pseudomonas aeruginosa*, as shown in Table 20. Particularly, results showed that compound **84k** displayed the best antibacterial activity with a diameter of growth of the inhibition zone of 21.6 mm against *Staphylococcus aureus*, 22.6 mm against *Staphylococcus epidermidis*, 22.3 mm against *Bacillus subtilis*, and 23.6 mm against *Bacillus cereus* bacteria. The structure–activity relationship study of these compounds revealed that compounds **84e**, **84k**, having a methyl group on phenyl group attached to the triazole ring in the molecule, showed better activity compared to other compounds.

It is well known that ionic liquids have become excellent alternatives to organic solvents and catalysts for a large array of organic reactions, due to their favorable properties [76]. To expand their previous application of the SO<sub>3</sub>H-functional Brønsted-acidic halogen-free ionic liquid 1,2-dimethyl-*N*-butanesulfonic acid imidazolium hydrogen sulfate ([DMBSI]HSO<sub>4</sub>) in the synthesis of heterocyclic compounds [77], Mamaghani, et al. reported a rapid, straightforward, and highly efficient one-pot synthesis of pyrano[2,3-*c*]pyrazole derivatives **86** and spiro-conjugated pyrano[2,3-*c*]pyrazoles **87** in the presence of [DMBSI]HSO<sub>4</sub> as a catalyst via a one-pot four-component reaction under solvent-free

conditions [78]. In this approach, the reaction of  $\beta$ -ketoesters **3/17**, hydrazine hydrate **4**, malononitrile **50** ( $R^2 = \text{CN}$ ), and aromatic aldehydes **1** in the presence of  $[\text{DMBSI}]\text{HSO}_4$  in solvent-free conditions at  $60^\circ\text{C}$  afforded pyrano-pyrazole derivatives **86** in good to excellent yields (Table 21). Additionally, the reaction of equimolar amounts of  $\beta$ -ketoesters **3/17**, hydrazine hydrate **4**, alkyl cyanides **50**, and 1,2-diketones **85a,b** under the aforementioned optimized solvent-free conditions afforded the spiro-conjugated pyrano-pyrazoles **87** in high yields (85–96%), as shown in Table 22.

**Table 21.** Four-component synthesis of pyrano[2,3-*c*]pyrazoles **86** and their in vitro antibacterial activity against three bacterial strains.



| Compound                  | Ar   | $R^1$ | Yield of <b>86</b> (%) | Antibacterial Activity of Compounds <b>86</b> (Diameter of Growth of Inhibition Zone (mm)) |    |    |
|---------------------------|--|-------|------------------------|--|----|----|
|                           |  |       |                        | ML   | BS | PA |
| <b>86a</b>                | 4-ClC <sub>6</sub> H <sub>4</sub>                    | Me    | 95                     | –  | 11 | –  |
| <b>86b</b>                | 4-MeC <sub>6</sub> H <sub>4</sub>                    | Me    | 90                     | –  | –  | –  |
| <b>86c</b>                | 4-MeOC <sub>6</sub> H <sub>4</sub>                   | Me    | 88                     | –  | –  | –  |
| <b>86d</b>                | 3-ClC <sub>6</sub> H <sub>4</sub>                    | Me    | 95                     | –  | –  | –  |
| <b>86e</b>                | Pyridine-3-yl  | Me    | 95                     | –  | –  | –  |
| <b>86f</b>                | 3-MeOC <sub>6</sub> H <sub>4</sub>                   | Me    | 90                     | –  | –  | –  |
| <b>86g</b>                | Naphtalen-1-yl                                       | Me    | 85                     | –  | –  | –  |
| <b>86h</b>                | Thiophen-2-yl  | Me    | 95                     | –  | –  | –  |
| <b>86i</b>                | 9H-Fluoren-2-yl                                      | Me    | 86                     | 10   | 8  | –  |
| <b>86j</b>                | 2,4-Cl <sub>2</sub> C <sub>6</sub> H <sub>3</sub>    | Me    | 96                     | –  | –  | –  |
| <b>86k</b>                | 3,4-(MeO) <sub>2</sub> C <sub>6</sub> H <sub>3</sub> | Me    | 87                     | 14   | –  | –  |
| <b>86l</b>                | Naphtalen-2-yl                                       | Me    | 86                     | 16   | 11 | –  |
| <b>86m</b>                | 4-ClC <sub>6</sub> H <sub>4</sub>                    | Ph    | 90                     | –  | –  | –  |
| <b>86n</b>                | 3-NO <sub>2</sub> C <sub>6</sub> H <sub>4</sub>      | Ph    | 95                     | 8  | 8  | –  |
| <b>86o</b>                | 3-BrC <sub>6</sub> H <sub>4</sub>                    | Ph    | 94                     | –  | –  | –  |
| Erythromycin <sup>a</sup> | –  | –     | –                      | 10   | 12 | 10 |
| Tetracycline <sup>a</sup> | –  | –     | –                      | 16   | 14 | 18 |

ML (*Micrococcus Luteus*), BS (*Bacillus subtilis*), PA (*Pseudomonas aeruginosa*). <sup>a</sup> Standard drug for the study.

**Table 22.** Four-component synthesis of spiro-conjugated pyrano[2,3-*c*]pyrazoles **87** and their in vitro antibacterial activity against three bacterial strains.

| Compound                  | $R^2$              | $R^1$ | R  | Yield of <b>87</b> (%) | Antibacterial Activity of Compounds <b>87</b> (Diameter of Growth of Inhibition Zone (mm)) |    |    |
|---------------------------|--------------------|-------|----|------------------------|--|----|----|
|                           |                    |       |    |                        | ML   | BS | PA |
| <b>87a</b>                | CN                 | Me    | –  | 96                     | –  | –  | –  |
| <b>87b</b>                | CO <sub>2</sub> Et | Me    | –  | 93                     | 8  | 8  | –  |
| <b>87c</b>                | CN                 | Pr    | –  | 96                     | 8  | 5  | –  |
| <b>87d</b>                | CN                 | Me    | H  | 96                     | –  | –  | 10 |
| <b>87e</b>                | CN                 | Pr    | H  | 95                     | 8  | –  | –  |
| <b>87f</b>                | CN                 | Ph    | H  | 88                     | –  | –  | –  |
| <b>87g</b>                | CN                 | Me    | Cl | 85                     | 14   | –  | –  |
| Erythromycin <sup>a</sup> | –                  | –     | –  | –                      | 10   | 12 | 10 |
| Tetracycline <sup>a</sup> | –                  | –     | –  | –                      | 16   | 14 | 18 |

ML (*Micrococcus Luteus*), BS (*Bacillus subtilis*), PA (*Pseudomonas aeruginosa*). <sup>a</sup> Standard drug for the study.

The antibacterial activity of some of the synthesized compounds **86a–o** and **87a–g** was examined against both Gram-negative (*Pseudomonas aeruginosa* and *Escherichia coli*)

and Gram-positive (*Micrococcus luteus* and *Bacillus subtilis*) bacteria, using tetracycline and erythromycin as standard drugs. The results revealed that most of the compounds (**86a–o** and **87a–g**) exhibited moderate activity toward *Micrococcus luteus* as revealed by the diameters of their inhibition zones. In addition, the results also showed that most of these compounds were not active against *Escherichia coli* and *Pseudomonas aeruginosa*, as shown in Tables 21 and 22.

It is well known that eco-friendly reaction paths, environmentally friendly catalysts, solvents, and prepared novel biologically active heterocycles have been becoming imperative key points for several unending investigation programs [79,80]. In this way, the development of a method for the synthesis of thioether-linked pyranopyrazoles **88** was performed via a reusable green catalyst, green solvent, and multicomponent domino approach [81]. Thus, the five-component reaction between the commercially available type 5-phenyl-1,3,4-oxadiazole-2-thiol **11**, aromatic aldehydes **1**, type phenyl hydrazine **15**, ethyl 4-chloro-3-oxobutanoate **8**, and malononitrile **2** in an ethanol–water solvent mixture at 70 °C using the Montmorillonite K-10 clay catalyst afforded products **88** in the range of 81–89% yield, as shown in Table 23. In this way, the K-10 catalyst behaved as a key point to promote this scientific path. Because of its acid catalytic nature to rapidly initiate the reactions, reusability, simple work-up process, time minimization, inexpensive nature, natural solvent compatibility, suppression of the side products leading to its cost reduction and eco-friendliness, the use of the K-10 catalyst highly improved this protocol compared to its catalyst-free analog procedure. Subsequently, the obtained compounds **88** were tested for their antibacterial properties against Gram-positive *Bacillus subtilis* and *Staphylococcus aureus* and Gram-negative *Escherichia coli* and *Pseudomonas aeruginosa* human pathogens under the disc diffusion method, using tetracycline as a drug base, as shown in Table 23. The outcomes organized in Table 23 indicate that compound **88e** revealed outstanding antibacterial inhibition compared to all other active compounds against the four bacteria. In addition, it showed noticeable activity towards *Escherichia coli* and *Pseudomonas aeruginosa* pathogens and inhibition zone values more than the reference drug tetracycline. Moreover, compound **88n** also exhibited very good inhibition zone values, indicating that these two active compounds may be used to support further investigation as a way to ascertain new antibacterial agents.

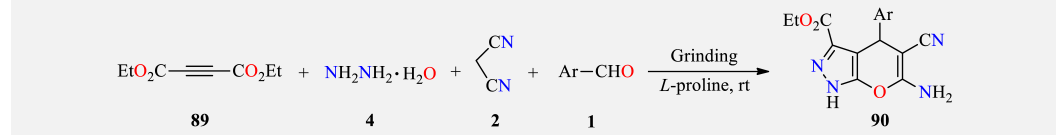
**Table 23.** Five-component synthesis of dihydropyrano[2,3-*c*]pyrazoles **88** and their in vitro antibacterial activity against four bacterial strains.

| Compound                  | Ar  | Yield of <b>88</b> (%) | Antibacterial Activity of Compounds <b>88</b> (Zone of Inhibition (in mm) at conc. 100 mg/mL after 24 h) |      |                        |      |
|---------------------------|---|------------------------|--|------|------------------------|------|
|                           |   |                        | Gram-Positive Bacteria   |      | Gram-Negative Bacteria |      |
|                           |   |                        | BS   | SA   | EC                     | PA   |
| <b>88a</b>                | 4-MeOC <sub>6</sub> H <sub>4</sub>              | 81                     | –  | –    | –                      | –    |
| <b>88b</b>                | 4-MeC <sub>6</sub> H <sub>4</sub>               | 85                     | 3.8  | 3.0  | 2.9                    | 2.6  |
| <b>88c</b>                | 4-HOC <sub>6</sub> H <sub>4</sub>               | 84                     | 9.1  | 8.8  | 8.7                    | 8.0  |
| <b>88d</b>                | Ph  | 82                     | 4.9  | 4.6  | 4.5                    | 4.3  |
| <b>88e</b>                | 4-FC <sub>6</sub> H <sub>4</sub>                | 80                     | 18.8   | 17.1 | 17.5                   | 15.2 |
| <b>88f</b>                | 3-FC <sub>6</sub> H <sub>4</sub>                | 83                     | 13.6   | 12.2 | 10.9                   | 9.6  |
| <b>88g</b>                | 3-HOC <sub>6</sub> H <sub>4</sub>               | 84                     | 5.6  | 5.1  | 5.6                    | 5.6  |
| <b>88h</b>                | 2-HOC <sub>6</sub> H <sub>4</sub>               | 86                     | 7.5  | 7.4  | 6.3                    | 7.0  |
| <b>88i</b>                | 2-MeC <sub>6</sub> H <sub>4</sub>               | 83                     | –  | 2.8  | –                      | –    |
| <b>88j</b>                | 2-MeOC <sub>6</sub> H <sub>4</sub>              | 89                     | –  | –    | –                      | –    |
| <b>88k</b>                | 2-ClC <sub>6</sub> H <sub>4</sub>               | 88                     | 11.4   | 10.4 | 10.2                   | 9.1  |
| <b>88l</b>                | 4-ClC <sub>6</sub> H <sub>4</sub>               | 82                     | 15.6   | 13.1 | 12.7                   | 11.0 |
| <b>88m</b>                | 4-BrC <sub>6</sub> H <sub>4</sub>               | 84                     | 9.8  | 9.3  | 8.9                    | 8.2  |
| <b>88n</b>                | 4-NO <sub>2</sub> C <sub>6</sub> H <sub>4</sub> | 83                     | 16.2   | 15.2 | 15.3                   | 13.7 |
| Tetracycline <sup>a</sup> | –   | –                      | 19.4   | 18.1 | 16.8                   | 14.2 |

BS (*Bacillus subtilis*), SA (*Staphylococcus aureus*), EC (*Escherichia coli*), PA (*Pseudomonas aeruginosa*). <sup>a</sup> Standard drug for this study.

Similarly to that previously described [78], Ambethkar, et al. reported an efficient grinding protocol for the synthesis of dihydropyrano[2,3-*c*]pyrazole derivatives **90**, in excellent yields, from a four-component reaction between acetylene ester **89**, hydrazine hydrate **4**, aryl aldehydes **1**, and malononitrile **2** in the presence of *L*-proline under solvent-free conditions, as shown in Table 24 [82]. The reaction tolerated various electron-withdrawing and electron-donating substituents in the *ortho*, *meta*, and *para* positions on the ring of the corresponding aromatic aldehydes **1**, as well as heteroaromatic aldehydes. The structures of the synthesized compounds **90** were deduced by spectroscopic techniques and confirmed by X-ray crystallography for compound **90h**. Compounds **90** were further evaluated for their in vitro antibacterial activities against four bacterial strains (*Staphylococcus albus*, *Streptococcus pyogenes*, *Klebsiella pneumoniae*, and *Pseudomonas aeruginosa*), using amikacin as the standard drug. This study was carried out by the agar well diffusion method using DMSO as a negative control. The antimicrobial data revealed that the compounds **90a**, **90g**, **90h**, **90i**, **90j**, **90k**, and **90l** showed activity against the four bacterial strains evaluated, as shown in Table 24.

**Table 24.** Four-component synthesis of dihydropyrano[2,3-*c*]pyrazole **90** and their in vitro antibacterial activity against four bacterial strains.

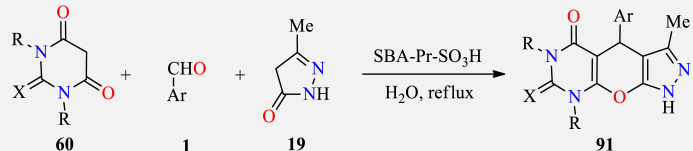
|  |   |                        |  |      |      |      |
|--|---|------------------------|--|------|------|------|
| Compound   | Ar  | Yield of <b>90</b> (%) | Antibacterial Activity of Compounds <b>90</b> (Inhibition Zone (mm)) |      |      |      |
|  |   |                        | SAI  | SP   | KP   | PA   |
| <b>90a</b>   | Ph  | 79                     | 17   | 7    | 9    | 12   |
| <b>90b</b>   | 4-MeC <sub>6</sub> H <sub>4</sub>               | 80                     | 12   | R    | R    | 10   |
| <b>90c</b>   | 2-ClC <sub>6</sub> H <sub>4</sub>               | 69                     | 12   | R    | R    | 10   |
| <b>90d</b>   | 4-ClC <sub>6</sub> H <sub>4</sub>               | 88                     | R  | R    | R    | R    |
| <b>90e</b>   | 4-FC <sub>6</sub> H <sub>4</sub>                | 93                     | R  | 4    | 10   | R    |
| <b>90f</b>   | 2-furyl   | 65                     | R  | R    | 13   | 3    |
| <b>90g</b>   | 2-thienyl                                       | 69                     | 7  | 9    | 5    | 4    |
| <b>90h</b>   | 4-EtC <sub>6</sub> H <sub>4</sub>               | 82                     | 15   | 15   | 7    | 7    |
| <b>90i</b>   | 4-HOC <sub>6</sub> H <sub>4</sub>               | 88                     | 22   | 13   | 15   | 12   |
| <b>90j</b>   | 2-MeOC <sub>6</sub> H <sub>4</sub>              | 72                     | 15   | 11   | 17   | 7    |
| <b>90k</b>   | 4-HO, 3-MeOC <sub>6</sub> H <sub>3</sub>        | 78                     | 10   | 8    | 12   | 9    |
| <b>90l</b>   | 4-MeOC <sub>6</sub> H <sub>4</sub>              | 81                     | 8  | 10   | 9    | 7    |
| <b>90m</b>   | 4-NO <sub>2</sub> C <sub>6</sub> H <sub>4</sub> | 92                     | 11   | 9    | 13   | 8    |
| Control <sup>a</sup>   | –   | –                      | R  | R    | R    | R    |
| Amikacin <sup>b</sup>  | –   | –                      | 26.6   | 24.0 | 19.6 | 23.0 |

SAI (*Staphylococcus albus*), SP (*Streptococcus pyogenes*), KP (*Klebsiella pneumoniae*), PA (*Pseudomonas aeruginosa*). <sup>a</sup> DMSO. <sup>b</sup> Standard drug for the study. Not active (R, inhibition zone < 2 mm); weak activity (2–8 mm); moderate activity (9–15 mm); strong activity (> 15 mm).

Propyl sulfonic acid-functionalized SBA-15 as a heterogeneous Brønsted acid, with its hexagonal structure, high surface area, and large pore size, exhibits efficient catalytic activity in a variety of organic reactions [83]. In this regard, the design and optimization of a convenient three-component approach for the synthesis of a series of tricyclic fused pyrazolopyranopyrimidine derivatives **91** using SBA-Pr-SO<sub>3</sub>H as a nanocatalyst was performed [84]. The morphology of the SBA-Pr-SO<sub>3</sub>H catalyst was verified by SEM and TEM images. The results confirmed that the hexagonally ordered mesoporous structure of SBA-15 silica was well retained after the chemical grafting reaction. In this approach, the one-pot three-component reaction of barbituric acids **60**, aromatic aldehydes **1**, and type 3-methyl-5-pyrazolone **19** under reflux conditions in water and the presence of a catalytic amount of SBA-Pr-SO<sub>3</sub>H afforded the target products **91** in 89–96%, as shown in Table 25. The mild reaction conditions, reusability, both electron-rich and electron-deficient aldehy-

des tolerance, high product yields, short reaction times, and simple work-up procedures were some advantages of this method.

**Table 25.** SBA-Pr-SO<sub>3</sub>H-Catalyzed three-component synthesis of pyrazolopyranopyrimidines **91** and their in vitro antibacterial activity against four bacterial strains.



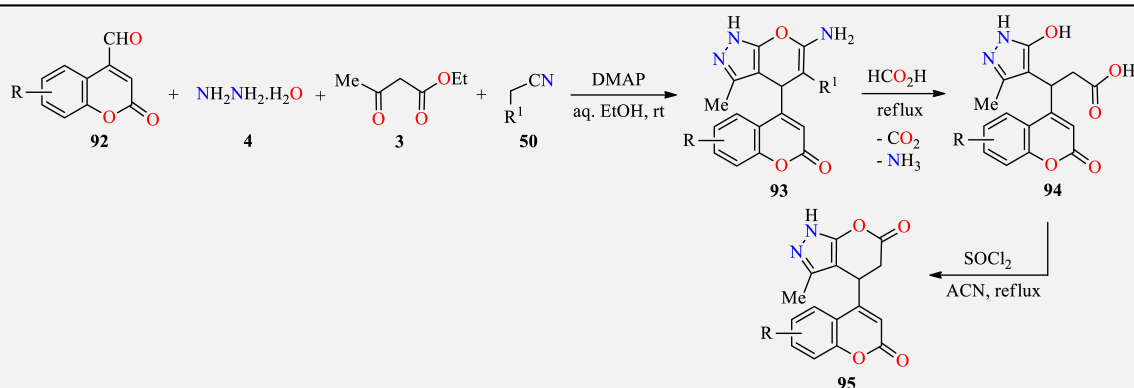
| Compound                     | Ar  | R  | X | Yield of <b>91</b> (%) | Antibacterial Activity of Compounds <b>91</b><br>(Inhibition Zone (mm)) |    |    |    |
|------------------------------|---|----|---|------------------------|---|----|----|----|
|                              |   |    |   |                        | BS  | EA | EC | PA |
| <b>91a</b>                   | 4-ClC <sub>6</sub> H <sub>4</sub>               | H  | O | 92                     | 20  | 24 | 12 | 0  |
| <b>91b</b>                   | 4-MeC <sub>6</sub> H <sub>4</sub>               | H  | O | 93                     | 18  | 22 | 12 | 0  |
| <b>91c</b>                   | Ph  | H  | O | 94                     | 15  | 21 | 13 | 0  |
| <b>91d</b>                   | 2-MeOC <sub>6</sub> H <sub>4</sub>              | H  | O | 95                     | 14  | 19 | 12 | 0  |
| <b>91e</b>                   | 3-NO <sub>2</sub> C <sub>6</sub> H <sub>4</sub> | H  | O | 89                     | 16  | 24 | 0  | 0  |
| <b>91f</b>                   | 4-ClC <sub>6</sub> H <sub>4</sub>               | Me | O | 90                     | 21  | 24 | 12 | 0  |
| <b>91g</b>                   | 4-MeC <sub>6</sub> H <sub>4</sub>               | Me | O | 91                     | 19  | 23 | 14 | 0  |
| <b>91h</b>                   | Ph  | Me | O | 96                     | 21  | 25 | 26 | 0  |
| <b>91i</b>                   | 4-MeC <sub>6</sub> H <sub>4</sub>               | H  | S | 91                     | 16  | 20 | 12 | 0  |
| Chloramphenicol <sup>a</sup> | –   | –  | – | –                      | 26  | 22 | 24 | 8  |
| Gentamicin <sup>a</sup>      | –   | –  | – | –                      | 28  | 20 | 20 | 18 |

BS (*Bacillus subtilis*), SA (*Staphylococcus aureus*), EC (*Escherichia coli*), PA (*Pseudomonas aeruginosa*). <sup>a</sup> Standard drugs for the study.

The compounds **91** were screened in vitro using the disc diffusion method (IZ). The microorganisms used were *Pseudomonas aeruginosa* and *Escherichia coli* as Gram-negative bacteria, and *Staphylococcus aureus* and *Bacillus subtilis* as Gram-positive bacteria. The activities of each compound were compared with chloramphenicol and gentamicin as references. The inhibition zones of compounds **91** around the discs are shown in Table 25. All compounds **91** exhibited significant antibacterial activities against *Staphylococcus aureus* when compared with the reference drugs. All compounds **91** were able to inhibit the growth of *Bacillus subtilis* and *Escherichia coli*. No compound showed antibiotic activity against *Pseudomonas aeruginosa*.

Coumarin analogs are a group of privileged bioactive oxygen heterocycles, found substantially in nature with a wide range of structural modifications [85,86]. Knowing the synthetic and biological value of coumarin, but also pyrazole and pyran scaffolds, an investigation directed toward hybridization of these three pharmacophoric motifs in a single molecule was performed. In this sense, the synthesis, characterization, and biological studies of a series of coumarin-based pyrano[2,3-*c*]pyrazoles **93**, pyrazolylpropanoic acids **94**, and dihydropyrano[2,3-*c*]pyrazol-6(1*H*)-ones **95** using conventional methods was established [87]. Products **93** were obtained through a base-catalyzed one-pot four-component approach when a mixture of hydrazine hydrate **4**, ethyl acetoacetate **3**, formylcoumarin **92**, and type nitrile **50** in the presence of DMAP as a base was vigorously stirred at room temperature under an open atmosphere. The corresponding pyrano[2,3-*c*]pyrazole-5-carbonitriles **93** were obtained in a range of 86–94%. Subsequently, the treatment of compounds **93** with formic acid under reflux afforded the pyrazolylpropanoic acids **94** as pure white products in 77–89%. Finally, the intramolecular cyclization of propanoic acids **94** with thionyl chloride in ACN at reflux generated the tail-tail pyranone (pyranone-4-pyranone or C<sub>4</sub>-C<sub>4</sub> pyranone) derivatives **95** in 81–85%, as shown in Table 26. The structures of the synthesized compounds were deduced by spectroscopic techniques and particularly confirmed by X-ray crystallography for compound **93b**.



**Table 26.** Four-component synthesis of coumarin-substituted pyrazoles **93**, **94**, and **95** and their in vitro antibacterial activity (MIC) against four bacterial strains.

| Compound                   | R         | R <sup>1</sup>     | Yield of <b>93</b> , <b>94</b> and <b>95</b> (%) | Antibacterial Activity of Compounds <b>93</b> , <b>94</b> and <b>95</b><br>(Minimum Inhibitory Concentration in µg/mL (MIC)) |       |       |       |
|----------------------------|-----------|--------------------|--|--|-------|-------|-------|
|                            |           |                    |  | SA   | SF    | EC    | PA    |
| <b>93a</b>                 | 6-Me      | CN                 | 94   | 6.25   | 12.5  | 12.5  | 12.5  |
| <b>93b</b>                 | 6-OMe     | CN                 | 91   | 3.125  | 12.5  | 6.25  | 1.56  |
| <b>93c</b>                 | 6-Cl      | CN                 | 89   | 3.125  | 6.25  | 3.125 | 12.5  |
| <b>93d</b>                 | 7-Me      | CN                 | 92   | 6.25   | 12.5  | 0.78  | 3.125 |
| <b>93e</b>                 | 7,8-Benzo | CN                 | 90   | 6.25   | 12.5  | 25.0  | 25.0  |
| <b>93f</b>                 | 6-Me      | CO <sub>2</sub> Et | 92   | 3.125  | 6.25  | 12.5  | 6.25  |
| <b>93g</b>                 | 6-OMe     | CO <sub>2</sub> Et | 89   | 1.56   | 3.125 | 6.25  | 6.25  |
| <b>93h</b>                 | 6-Cl      | CO <sub>2</sub> Et | 86   | 3.125  | 12.5  | 6.25  | 50.0  |
| <b>93i</b>                 | 7-Me      | CO <sub>2</sub> Et | 91   | 3.125  | 25.0  | 3.125 | 12.5  |
| <b>93j</b>                 | 7,8-Benzo | CO <sub>2</sub> Et | 88   | 3.125  | 12.5  | 6.25  | 6.25  |
| <b>94a</b>                 | 6-Me      | –                  | 89   | 3.125  | 12.5  | 12.5  | 25.0  |
| <b>94b</b>                 | 6-OMe     | –                  | 80   | 0.78   | 1.56  | 3.125 | 6.25  |
| <b>94c</b>                 | 6-Cl      | –                  | 77   | 1.56   | 6.25  | 25.0  | 50.0  |
| <b>94d</b>                 | 7-Me      | –                  | 82   | 3.125  | 6.25  | 6.25  | 12.5  |
| <b>94e</b>                 | 7,8-Benzo | –                  | 89   | 6.25   | 12.5  | 6.25  | 12.5  |
| <b>95a</b>                 | 6-Me      | –                  | 85   | 6.25   | 12.5  | 3.125 | 12.5  |
| <b>95b</b>                 | 6-OMe     | –                  | 82   | 3.125  | 6.25  | 6.25  | 6.25  |
| <b>95c</b>                 | 6-Cl      | –                  | 81   | 6.25   | 12.5  | 6.25  | 12.5  |
| <b>95d</b>                 | 7-Me      | –                  | 84   | 6.25   | 6.25  | 12.5  | 6.25  |
| <b>95e</b>                 | 7,8-Benzo | –                  | 83   | 12.5   | 12.5  | 12.5  | 6.25  |
| Ciprofloxacin <sup>a</sup> | –         | –                  | –  | 6.25   | 6.25  | 3.125 | 6.25  |

SA (*Staphylococcus aureus*), SF (*Staphylococcus faecalis*), EC (*Escherichia coli*), PA (*Pseudomonas aeruginosa*). <sup>a</sup> Standard drug for the study.

The synthesized compounds **93**, **94**, and **95** were also screened for their antibacterial activity using ciprofloxacin as a standard drug. The susceptibility of the test organisms to synthetic compounds was assessed using a broth dilution assay as the minimum inhibitory concentration (MIC) and four microorganisms for the study: Two Gram-positive (*Staphylococcus aureus* and *Staphylococcus faecalis*) and two Gram-negative (*Escherichia coli* and *Pseudomonas aeruginosa*) strains. The study revealed that almost all tested compounds showed excellent antibacterial activity against Gram-positive (*Staphylococcus aureus* and *Staphylococcus faecalis*) bacterial strains. However, in the case of Gram-negative (*Escherichia coli* and *Pseudomonas aeruginosa*) bacterial strains, only some of the synthesized compounds showed selective antibacterial activity, as shown in Table 26. Among all these synthesized scaffolds, compounds **93g** and **94b** were highly active and more potent than the remaining derivatives in both biological, as well as molecular docking simulation, studies performed with *Staphylococcus aureus* dihydropteroate synthetase (DHPS).

## 2.2. Anticancer Activity

Analysis of the database of U.S. FDA-approved drugs reveals that approximately 60% of unique small-molecule drugs contain an aza-heterocycle [88]. Particularly, aza-heterocycles play an important role in the development of clinically viable anticancer drugs [89,90]. As a result, innumerable synthetic approaches for preparing diversely functionalized aza-heterocycles with anticancer properties have been successfully described during the last decade [91–95]. In this way, the coumarin-containing thiazolyl-3-aryl-pyrazole-4-carbaldehydes **25a–o**, obtained via the three-component synthetic approach discussed previously in Section 2.1. Antibacterial activity (Table 5) [32], were also evaluated for their *in vitro* cytotoxic activity against three human cancer cell lines (DU-145, MCF-7, and HeLa) at three different concentrations (2.5, 5.0, and 100  $\mu\text{M}$ ) by adopting the MTT assay method in the presence of Doxorubicin as a standard reference drug. As shown in Table 27, the synthesized compounds showed moderate to good anticancer activity with  $\text{IC}_{50}$  values ranging from 5.75  $\mu\text{M}$  to 100  $\mu\text{M}$ . In most cases, the compounds exhibited greater cytotoxic activity on the HeLa cell line. In particular, the compounds **25m** and **25n** showed excellent cytotoxic activity against the HeLa cell line with  $\text{IC}_{50}$  values of 5.75  $\mu\text{M}$  and 6.25  $\mu\text{M}$ , respectively, when compared to Doxorubicin (3.92  $\mu\text{M}$ ). Afterward, molecular docking studies were performed to validate *in vitro* results and elucidate the importance of different types of interactions to inhibit the function of the probable target human microsomal cytochrome P450 2A6 (1z11.pdb) enzyme. Overall, the compounds **25m** and **25n** showed the lowest binding energy with  $-11.72$  kcal/mol and  $-11.95$  kcal/mol, respectively. Among the most key interacting residues, Ile366 and Cys439 actively participate in the formation of hydrogen bonding with the compounds **25m** and **25n**.

**Table 27.** Cytotoxic activity of coumarin-substituted thiazolyl-3-aryl-pyrazole-4-carbaldehydes **25**.

| Compound                 | R   | R <sup>1</sup> | R <sup>2</sup> | IC <sub>50</sub> ( $\mu\text{M}$ ) |                |                |
|--------------------------|-----|----------------|----------------|------------------------------------|----------------|----------------|
|                          |     |                |                | DU-145                             | MCF-7          | HeLa           |
| <b>25a</b>               | H   | H              | H              | – <sup>a</sup>                     | – <sup>a</sup> | – <sup>a</sup> |
| <b>25b</b>               | H   | Cl             | H              | – <sup>a</sup>                     | – <sup>a</sup> | 12.82          |
| <b>25c</b>               | Cl  | Cl             | H              | 41.05                              | 76.33          | 13.75          |
| <b>25d</b>               | H   | Br             | H              | 35.01                              | 18.16          | 11.02          |
| <b>25e</b>               | Br  | Br             | H              | 27.97                              | 22.23          | 13.69          |
| <b>25f</b>               | H   | Benzo          | H              | 11.91                              | 39.46          | 13.11          |
| <b>25g</b>               | H   | Cl             | Cl             | 14.86                              | 18.67          | 9.51           |
| <b>25h</b>               | Cl  | Cl             | Cl             | 30.90                              | 21.74          | 10.29          |
| <b>25i</b>               | H   | Br             | Cl             | 22.32                              | 85.03          | 9.46           |
| <b>25j</b>               | MeO | H              | Cl             | 38.18                              | 71.68          | 41.89          |
| <b>25k</b>               | H   | H              | Me             | 50.23                              | 69.45          | 37.36          |
| <b>25l</b>               | H   | Br             | Me             | 20.86                              | 35.17          | 14.13          |
| <b>25m</b>               | Cl  | Cl             | Me             | 14.71                              | 14.56          | 5.75           |
| <b>25n</b>               | Br  | Br             | Me             | 10.81                              | 24.52          | 6.25           |
| <b>25o</b>               | MeO | H              | Me             | 31.42                              | 42.57          | 28.19          |
| Doxorubicin <sup>b</sup> | –   | –              | –              | 2.49                               | 3.18           | 3.92           |

<sup>a</sup> Not determined. <sup>b</sup> Standard drug for the study.

In addition, Sharma et al. developed a time-efficient and simple synthesis of pyrazolopyrazole derivatives **96** in 77–94% yields through a four-component reaction of (hetero)aromatic aldehydes **1**, malononitrile **2**, hydrazine hydrate **4**, ethyl acetoacetate **3**, and triethylamine in EtOH at an ambient temperature for 1–2 h (Table 28) [96]. Alternatively,

the same reaction was conducted under microwave irradiation at 60 °C for 3–5 min to afford the expected products in 70–87% yields. Later, the pyranopyrazole derivatives **96** were evaluated for their *in vitro* anticancer activity against the Hep3B Hepatocellular carcinoma cell line. As shown in Table 28, the synthesized compounds showed anticancer activity with IC<sub>50</sub> values ranging from 10 µg/mL to 128 µg/mL. Overall, the presence of certain heteroatom substituents at the 3-position of the pharmacophore may be crucial to enhancing the anticancer activity.

**Table 28.** Four-component synthesis and anticancer activity of pyranopyrazole derivatives **96**.

| Compound   | R   | Yield <b>96</b> (%) |          | IC <sub>50</sub> (µg/mL) |
|------------|---|---------------------|----------|--------------------------|
|            |   | Method A            | Method B | Hep3B                    |
| <b>96a</b> | 3-HOC <sub>6</sub> H <sub>4</sub>               | 88                  | 82       | 32                       |
| <b>96b</b> | 4-BrC <sub>6</sub> H <sub>4</sub>               | 82                  | 80       | 16                       |
| <b>96c</b> | 3-BrC <sub>6</sub> H <sub>4</sub>               | 80                  | 77       | 10                       |
| <b>96d</b> | 3-NO <sub>2</sub> C <sub>6</sub> H <sub>4</sub> | 86                  | 81       | 32                       |
| <b>96e</b> | 3-Thiophenyl                                    | 88                  | 80       | 24                       |
| <b>96f</b> | 2-Pyrrolyl                                      | 85                  | 80       | 128                      |
| <b>96g</b> | 3-Indolyl                                       | 81                  | 79       | 64                       |
| <b>96h</b> | 4-ClC <sub>6</sub> H <sub>4</sub>               | 77                  | 70       | 96                       |
| <b>96i</b> | 2-IC <sub>6</sub> H <sub>4</sub>                | 80                  | 75       | 96                       |
| <b>96j</b> | C <sub>6</sub> H <sub>5</sub>                   | 86                  | 81       | 128                      |
| <b>96k</b> | <i>n</i> -Butyl                                 | 82                  | 83       | 20                       |
| <b>96l</b> | 4-MeC <sub>6</sub> H <sub>4</sub>               | 88                  | 87       | 20                       |
| <b>96m</b> | 4-Pyridinyl                                     | 94                  | 85       | 48                       |
| <b>96n</b> | 2-FC <sub>6</sub> H <sub>4</sub>                | 90                  | 87       | 32                       |

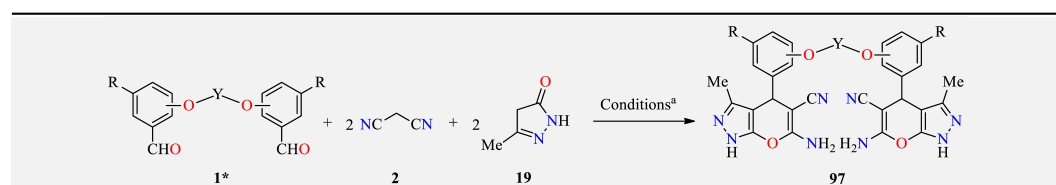
Method A: Aldehyde **1** (2.2 mmol), malononitrile **2** (2.2 mmol), hydrazine hydrate **4** (2.0 mmol), ethyl acetoacetate **3** (2.0 mmol), Et<sub>3</sub>N (3.0 mmol), EtOH (4 mL), 1–2 h, r.t. Method B: Aldehyde **1** (2.2 mmol), malononitrile **2** (2.2 mmol), hydrazine hydrate **4** (2.0 mmol), ethyl acetoacetate **3** (2.0 mmol), Et<sub>3</sub>N (3.0 mmol), EtOH (4 mL), 3–5 min, 60 °C, MWI.

The 1*H*-1,2,3-triazole tethered pyrazolo[3,4-*b*]pyridin-6(7*H*)-ones **84a–l**, obtained via the multicomponent synthetic approach discussed previously in Section 2.1. Antibacterial activity, was also subjected to apoptosis studies on ovarian follicles of goats (*Capra hircus*) (Table 20) [75]. In summary, all compounds **84a–l** caused cellular degeneration and induced apoptosis within the granulosa cells at a 10 µM dose concentration and 6 h exposure duration with the percentage of apoptosis ranging from 22.15% to 41.35% in comparison with the control (9.21%) (Table 20). In particular, the compounds **84b** (R = H, Ar = 3-Cl-4-FC<sub>6</sub>H<sub>3</sub>), **84e** (R = H, Ar = 4-MeC<sub>6</sub>H<sub>4</sub>), and **84l** (R = MeO, Ar = 3-ClC<sub>6</sub>H<sub>4</sub>) displayed the maximum incidence of apoptotic attributes within granulosa cells (37.50%, 36.08%, and 41.35%, respectively). To assess the DNA fragmentation within granulosa cells, an important hallmark of apoptosis, a TUNEL assay was performed using the DAB stain. Overall, the maximum incidence of DNA fragmentation was observed after treatment with compounds **84b**, **84e**, and **84l**.

In 2017, Salama and collaborators designed the synthesis of *bis*-1,4-dihydropyrano[2,3-*c*]pyrazole-5-carbonitrile derivatives **97** in high yields by a pseudo-five-component reaction of *bis*-aldehydes **1\***, malononitrile **2**, and pyrazolone **19** catalyzed by piperidine in refluxing ethanol for 3 h (Table 29) [97]. All synthesized compounds **97a–f** were evaluated for their *in vitro* anticancer activity against *Lung* A549, *Breast* MCF-7, and *Liver* HepG2 cell lines with IC<sub>50</sub> values ranging from 0.014 mM to 3.34 mM. Overall, the compound **97e** gave the highest cytotoxic values against the three selected lines of A549, MCF-7, and HEPG2 with IC<sub>50</sub> values of 0.37, 0.31, and 0.014 mM, respectively. Later, a molecular docking simulation was performed to investigate the interactions of the compound **97e** with vascular endothelial

growth factor receptor 2 (VEGFR2) (PDB code: 3wze). It forms two hydrogen bonds with Arg1066 through an amino group and His816 through a cyano group. Furthermore, the compound **97e** forms three  $\pi$ -cation interactions between Arg1027 and the pyrazole ring, as well as His816 and Arg1027 with the 4-aryl group. Additionally, the compound **97e** showed a higher potent binding mode than the standard inhibitor Sorafenib.

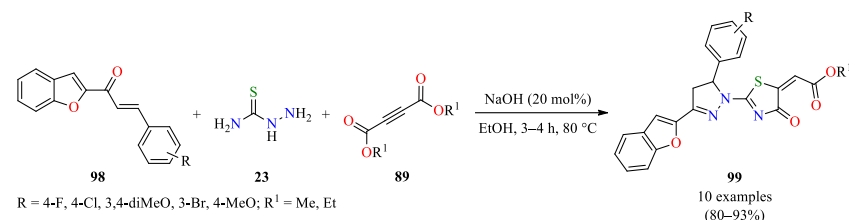
**Table 29.** Pseudo five-component synthesis and anticancer activity of *bis*-1,4-dihydropyrano[2,3-*c*]pyrazole-5-carbonitrile derivatives **97**.



| Compound   | R  | Y                               | Yield <b>97</b> (%) | IC <sub>50</sub> (mM) |       |       |
|------------|----|---------------------------------|---------------------|-----------------------|-------|-------|
|            |    |                                 |                     | A549                  | MCF-7 | HEPG2 |
| <b>97a</b> | H  | (CH <sub>2</sub> ) <sub>2</sub> | 87                  | 0.46                  | 2.30  | 3.34  |
| <b>97b</b> | Br | (CH <sub>2</sub> ) <sub>2</sub> | 85                  | 0.98                  | 1.99  | 0.99  |
| <b>97c</b> | H  | (CH <sub>2</sub> ) <sub>3</sub> | 82                  | 0.78                  | 0.29  | 0.42  |
| <b>97d</b> | Br | (CH <sub>2</sub> ) <sub>3</sub> | 79                  | 0.71                  | 1.56  | 0.46  |
| <b>97e</b> | H  | (CH <sub>2</sub> ) <sub>4</sub> | 85                  | 0.37                  | 0.31  | 0.014 |
| <b>97f</b> | Br | (CH <sub>2</sub> ) <sub>4</sub> | 83                  | 0.64                  | 0.79  | 0.33  |

<sup>a</sup> Reaction conditions: *bis*-aldehyde **1\*** (1 mmol), malononitrile **2** (2.2 mmol), 3-methyl-1*H*-pyrazol-5(4*H*)-one **19** (2.2 mmol), piperidine (0.2 mL), EtOH (5 mL), reflux, 3 h.

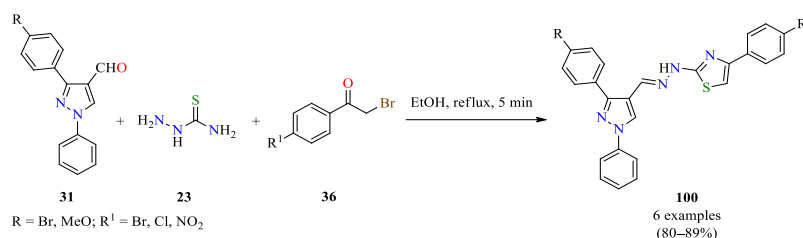
Some groups are interested in the use of  $\alpha,\beta$ -unsaturated ketones to access functionalized pyrazoline derivatives. For instance, Yakaiah and colleagues described the synthesis of pyrazolo-oxothiazolidine derivatives **99** with 80–93% yields through a three-component reaction of benzofuran-based chalcones **98**, thiosemicarbazide **23**, and dialkyl acetylenedicarboxylates **89** catalyzed by NaOH (20 mol%) in ethanol at 80 °C (Scheme 5) [98]. The synthesized compounds were evaluated for their antiproliferative activity against the A549 Lung cancer cell line with IC<sub>50</sub> values ranging from 0.81  $\mu\text{g}/\text{mL}$  to > 5  $\mu\text{g}/\text{mL}$ . Especially, the compound **99f** (R = 4-F, R<sup>1</sup> = Me, IC<sub>50</sub> = 0.81  $\mu\text{g}/\text{mL}$ ) showed higher activity than the standard drug sorafenib (IC<sub>50</sub> = 3.78  $\mu\text{g}/\text{mL}$ ). Molecular docking studies indicated that compound **99f** had the greatest affinity for the catalytic site of the receptor VEGFR2 (PDB ID code: 4AGD and 4ASD). The binding mode of compound **99f** with the active site of VEGFR2 (PDB ID code: 4AGD) showed one hydrogen bond between the oxothiazolidine-containing carbonyl group and CYS919. In the case of VEGFR2 (PDB ID code: 4ASD), the oxygen atom of the benzofuran ring and carbonyl group formed two hydrogen bonds with residues ASP1046 and ARG1027, respectively.



**Scheme 5.** Three-component synthesis of pyrazolo-oxothiazolidine derivatives **99** as antiproliferative agents.

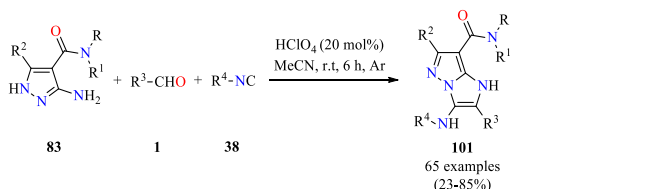
The multicomponent synthesis of highly functionalized *N*-heterocycles as apoptosis inducers has been successfully implemented. For instance, a mixture of 3-aryl-1-phenyl-1*H*-pyrazole-4-carbaldehydes **31**, thiosemicarbazide **23**, and  $\alpha$ -bromoacetophenones **36** in refluxing ethanol for 5 min afforded a series of (*E*)-2-(2-((3-aryl-1-phenyl-1*H*-pyrazol-4-yl)methylene)hydrazinyl)-4-arylthiazoles **100** (Scheme 6) [99]. The solids were filtered

and recrystallized from ethanol to afford pyrazole derivatives with high yields and short reaction times. The percentage of apoptosis was investigated in granulosa cells of ovarian antral follicles after treatment with compounds at a 10  $\mu$ M concentration for a 6 h exposure duration. The compounds **100b** (R = Br, R<sup>1</sup> = Cl) and **100e** (R = MeO, R<sup>1</sup> = Cl) showed the maximum potency to induce apoptosis with percentages of apoptosis of 23.45% and 25.61%, respectively, in comparison with the control (5.14%). Moreover, the microphotograph of granulosa cells with a TUNEL assay revealed that all compounds induced DNA fragmentation. As expected, the compounds **100b** and **100e** induced the maximum DNA damage, indicating apoptotic cells with fragmented DNA.



**Scheme 6.** Three-component synthesis of (*E*)-2-((3-aryl-1-phenyl-1*H*-pyrazol-4-yl)methylene)hydrazinyl-4-arylthiazoles **100** as apoptosis inducers.

Remarkably, the Groebke–Blackburn–Bienaymé reaction has been used to efficiently prepare diverse azole-fused imidazoles of biological interest. For instance, a series of imidazo[1,2-*b*]pyrazoles **101** were prepared in moderate to high yields through a GBB-type three-component reaction of 3-amino-1*H*-pyrazole-4-carboxamides **83**, aldehydes **1**, and isocyanides **38** catalyzed by HClO<sub>4</sub> (20 mol%) in acetonitrile at an ambient temperature for 6 h (Scheme 7) [100]. Since an oxidative minor side reaction yielding dehydrogenated 3-imino derivatives of the target products was observed, an argon atmosphere was employed. The antitumor activity of all imidazo[1,2-*b*]pyrazole-7-carboxamides **101** was evaluated against two human (*Acute promyelocytic leukemia* HL-60 and *Breast adenocarcinoma* MCF-7) and one murine (Mammary carcinoma 4T1) cancer cell lines using doxorubicin as a positive control. Among 27 primary carboxamides, the compound **101a** (R = R<sup>1</sup> = R<sup>2</sup> = H, R<sup>3</sup> = *t*-Bu, R<sup>4</sup> = 2,4,4-trimethylpentan-2-yl) showed the most significant cytotoxic activity against HL-60, MCF-7, and 4T1 cell lines with IC<sub>50</sub> values of 1.24, 1.49, and 1.88  $\mu$ M, respectively. From 38 secondary and tertiary carboxamides, the compound **101b** (R = H, R<sup>1</sup> = 4-FC<sub>6</sub>H<sub>4</sub>, R<sup>2</sup> = H, R<sup>3</sup> = *t*-Bu, R<sup>4</sup> = 2,4,4-trimethylpentan-2-yl) displayed the highest potency against HL-60, MCF-7, and 4T1 cell lines with IC<sub>50</sub> values ranging from 0.183  $\mu$ M to 7.43  $\mu$ M. Finally, the annexin V PI assay revealed that the most potent derivatives **101a** and **101b** induced apoptosis in HL-60 cells.

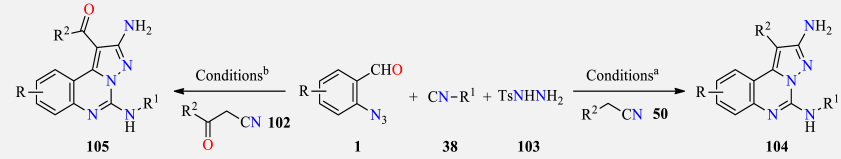


R = H, 2-MeC<sub>6</sub>H<sub>4</sub>, 3,5-(Me)<sub>2</sub>C<sub>6</sub>H<sub>3</sub>, 4-*i*PrC<sub>6</sub>H<sub>4</sub>, 4-MeOC<sub>6</sub>H<sub>4</sub>, 2,4-(MeO)<sub>2</sub>C<sub>6</sub>H<sub>3</sub>, 2-MeC<sub>6</sub>H<sub>4</sub>, 2-CF<sub>3</sub>C<sub>6</sub>H<sub>4</sub>, 3-CF<sub>3</sub>C<sub>6</sub>H<sub>4</sub>, 4-CF<sub>3</sub>C<sub>6</sub>H<sub>4</sub>, 2-FC<sub>6</sub>H<sub>4</sub>, 3-FC<sub>6</sub>H<sub>4</sub>, 4-FC<sub>6</sub>H<sub>4</sub>, 4-ClC<sub>6</sub>H<sub>4</sub>, 4-BrC<sub>6</sub>H<sub>4</sub>, 4-NO<sub>2</sub>C<sub>6</sub>H<sub>4</sub>, 4-CNC<sub>6</sub>H<sub>4</sub>, 4-EtO<sub>2</sub>CC<sub>6</sub>H<sub>4</sub>, 4-MeSC<sub>6</sub>H<sub>4</sub>, 4-Me<sub>2</sub>NC<sub>6</sub>H<sub>4</sub>, 2,4-(F)<sub>2</sub>C<sub>6</sub>H<sub>3</sub>, 3,4-(F)<sub>2</sub>C<sub>6</sub>H<sub>3</sub>, 4-FC<sub>6</sub>H<sub>4</sub>CH<sub>2</sub>, 2-fluoro-5-pyridinyl  
R<sup>1</sup> = H, Me, Bu, *t*-Bu, cyclopropyl, cyclopentyl, cyclohexyl, benzyl, C<sub>6</sub>H<sub>5</sub>, 2-pyridinyl, 3-pyridinyl, 4-pyridinyl, 2-thiazolyl, 3-isoxazolyl  
R<sup>2</sup> = H, Me  
R<sup>3</sup> = C<sub>6</sub>H<sub>5</sub>, 4-MeOC<sub>6</sub>H<sub>4</sub>, 4-AcO-3-MeOC<sub>6</sub>H<sub>3</sub>, 2,4,6-(MeO)<sub>3</sub>C<sub>6</sub>H<sub>2</sub>, 4-FC<sub>6</sub>H<sub>4</sub>, 4-CF<sub>3</sub>C<sub>6</sub>H<sub>4</sub>, 3,4-(F)<sub>2</sub>C<sub>6</sub>H<sub>3</sub>, 3-pyridinyl, cyclohexyl, heptyl, *t*-Bu, Et, cyclopropyl, *i*-Pr, 2-methylpent-4-en-2-yl  
R<sup>4</sup> = *t*-Bu, CH<sub>2</sub>CO<sub>2</sub>Me, 4-MeOC<sub>6</sub>H<sub>4</sub>, cyclohexyl, 2,4,4-trimethylpentan-2-yl

**Scheme 7.** Three-component synthesis and anticancer activity of imidazo[1,2-*b*]pyrazole-7-carboxamide derivatives **101**.

In 2019, Ansari and colleagues developed a Pd-catalyzed one-pot four-component protocol for the synthesis of highly functionalized pyrazolo[1,5-*c*]quinazolines **104**/**105** (Table 30) [101]. Initially, a mixture of type 2-azidobenzaldehyde **1**, isocyanide **38**, and tosyl hydrazide **103** in the presence of palladium acetate (7.5 mol%) as a catalyst in toluene was stirred at an ambient temperature for 15 min to generate azomethine imine in situ, then the acetonitrile derivative **50** and DABCO were added, and the reaction was stirred at 100 °C for 2 h to afford pyrazolo[1,5-*c*]quinazolines **104**. For aroylacetonitrile **102**, a similar methodology was developed for the synthesis of target compounds **105** with the addition of iodine (10 mol%) as a catalyst. The presence of electron-withdrawing groups on the  $\alpha$ -position of acetonitrile such as CN, COOR<sup>2</sup>, and COR<sup>2</sup> was essential for their participation in the reaction. For instance, compound **104d** was not formed due to the absence of such groups. The reaction proceeds with good functional group tolerance, excellent regioselectivity, a high atom economy, and low catalyst loading under simple reaction conditions. Target compounds **104** and **105** were screened for their antiproliferative potential against MDA-MB-231, A549, and H1299 cell lines using erlotinib and gefitinib as standard drugs. Notably, compound **105b** showed the most significant cytotoxic activity against MDA-MB-231, A549, and H1299 cell lines with IC<sub>50</sub> values of 1.93, 1.06, and 1.32  $\mu$ M, respectively, when compared to erlotinib and gefitinib. Next, the inhibition of **105b** in comparison to erlotinib toward the ATP-dependent phosphorylation of EGFR was investigated at concentrations of 100, 250, and 500 nM. The results suggested that compound **105b** possesses the most potent EGFR inhibition with an IC<sub>50</sub> value of 157.63 nM, in comparison to erlotinib (IC<sub>50</sub> = 201.34 nM). Additionally, compound **105b** elevated ROS levels and altered the mitochondrial potential, resulting in apoptosis via the G1 phase.

**Table 30.** Pd-Catalyzed one-pot four-component reaction of pyrazolo[1,5-*c*]quinazolines **104** and **105** as potential EGFR inhibitors.

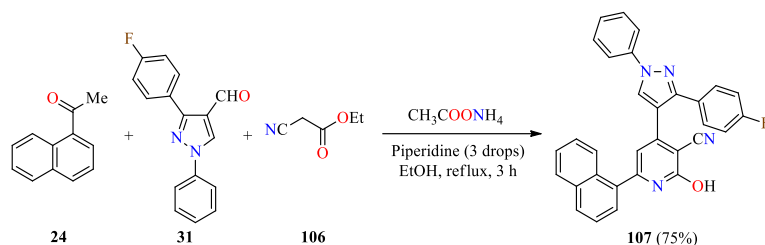


| Compound               | R    | R <sup>1</sup>                                    | R <sup>2</sup>                     | Yield 104/105 (%) | IC <sub>50</sub> ( $\mu$ M) |       |       |
|------------------------|------|---|------------------------------------|-------------------|-----------------------------|-------|-------|
|                        |      |   |                                    |                   | MDA-MB-231                  | A549  | H1299 |
| <b>104a</b>            | H    | <i>t</i> Bu                                       | CN                                 | 93                | 6.86                        | 3.98  | 4.97  |
| <b>104b</b>            | H    | CMe <sub>2</sub> CH <sub>2</sub> CMe <sub>3</sub> | CN                                 | 86                | 1.96                        | 2.87  | 2.02  |
| <b>104c</b>            | 4-Br | <i>t</i> Bu                                       | CN                                 | 75                | 5.89                        | 4.98  | 6.35  |
| <b>104d</b>            | 4-Br | <i>t</i> Bu                                       | Ph                                 | 0                 | –                           | –     | –     |
| <b>104e</b>            | 4-Cl | <i>t</i> Bu                                       | CN                                 | 82                | 7.98                        | 5.93  | 4.86  |
| <b>104f</b>            | 4-Cl | CMe <sub>2</sub> CH <sub>2</sub> CMe <sub>3</sub> | CN                                 | 78                | 5.65                        | 4.56  | 4.93  |
| <b>104g</b>            | 5-Cl | CMe <sub>2</sub> CH <sub>2</sub> CMe <sub>3</sub> | CN                                 | 89                | 8.54                        | 10.44 | 9.34  |
| <b>104h</b>            | 5-Cl | CMe <sub>2</sub> CH <sub>2</sub> CMe <sub>3</sub> | CO <sub>2</sub> Me                 | 76                | 7.83                        | 5.27  | 5.01  |
| <b>104i</b>            | H    | <i>t</i> Bu                                       | CO <sub>2</sub> Me                 | 84                | 7.90                        | 8.33  | 6.65  |
| <b>104j</b>            | H    | CMe <sub>2</sub> CH <sub>2</sub> CMe <sub>3</sub> | CO <sub>2</sub> Me                 | 73                | 4.69                        | 2.78  | 4.94  |
| <b>104k</b>            | H    | <i>t</i> Bu                                       | CO <sub>2</sub> Et                 | 77                | 8.83                        | 4.89  | 6.99  |
| <b>104l</b>            | H    | CMe <sub>2</sub> CH <sub>2</sub> CMe <sub>3</sub> | CO <sub>2</sub> Et                 | 79                | 7.82                        | 5.89  | 4.75  |
| <b>104m</b>            | H    | <i>t</i> Bu                                       | CO <sub>2</sub> <i>i</i> Pr        | 77                | 4.76                        | 3.29  | 3.47  |
| <b>104n</b>            | H    | CMe <sub>2</sub> CH <sub>2</sub> CMe <sub>3</sub> | CO <sub>2</sub> <i>i</i> Pr        | 80                | 9.36                        | 6.35  | 5.96  |
| <b>105a</b>            | H    | CMe <sub>2</sub> CH <sub>2</sub> CMe <sub>3</sub> | C <sub>6</sub> H <sub>5</sub>      | 87                | 5.28                        | 6.84  | 7.22  |
| <b>105b</b>            | H    | CMe <sub>2</sub> CH <sub>2</sub> CMe <sub>3</sub> | 4-FC <sub>6</sub> H <sub>4</sub>   | 71                | 1.93                        | 1.06  | 1.32  |
| <b>105c</b>            | H    | CMe <sub>2</sub> CH <sub>2</sub> CMe <sub>3</sub> | 2-ClC <sub>6</sub> H <sub>4</sub>  | 65                | 5.97                        | 6.45  | 7.84  |
| <b>105d</b>            | H    | CMe <sub>2</sub> CH <sub>2</sub> CMe <sub>3</sub> | 4-MeOC <sub>6</sub> H <sub>4</sub> | 75                | 2.45                        | 1.74  | 2.04  |
| <b>105e</b>            | 5-Cl | CMe <sub>2</sub> CH <sub>2</sub> CMe <sub>3</sub> | C <sub>6</sub> H <sub>5</sub>      | 70                | 3.49                        | 2.69  | 3.22  |
| Erlotinib <sup>c</sup> | –    | –   | –                                  | –                 | 4.56                        | 2.98  | 3.33  |
| Gefitinib <sup>c</sup> | –    | –   | –                                  | –                 | 6.85                        | 2.65  | 3.02  |

<sup>a</sup> Reaction conditions: 2-azidobenzaldehyde **1** (1 equiv), isocyanide **38** (1.2 equiv), TsNHNH<sub>2</sub> **103** (1 equiv), Pd(OAc)<sub>2</sub> (7.5 mol%), 4 Å MS (200 mg), PhMe (1.0 mL), 100 °C, 10 min, then active methylene compound **50** (2 equiv), DABCO (3 equiv), 100 °C, 3 h. <sup>b</sup> Reaction conditions: 2-azidobenzaldehyde **1** (1 equiv), isocyanide **38** (1.2 equiv), TsNHNH<sub>2</sub> **103** (1.1 equiv), Pd(OAc)<sub>2</sub> (7.5 mol%), 4 Å MS (200 mg), PhMe (1.0 mL), 100 °C, 10 min, then aroylacetonitrile **102** (2 equiv), DABCO (3 equiv), I<sub>2</sub> (10 mol%), 100 °C, 3 h. <sup>c</sup> Standard drug for the study.

Furthermore, the molecular docking studies of the most potent EGFR inhibitor **105b** within the active site of the EGFR protein (PDB ID: 1M17) showed that the compound perfectly fits into the ATP domain of EGFR and has a much better docking score ( $-9.10$  kcal/mol) than erlotinib ( $-7.20$  kcal/mol); thus, revealing that smaller and polar substitutions on the pyrazole ring are essential for binding with EGFR.

Recently, the piperidine-catalyzed four-component reaction of 1-(naphthalen-1-yl)ethanone **24**, 3-(4-fluorophenyl)-1-phenyl-1*H*-pyrazole-4-carbaldehyde **31**, ethyl 2-cyanoacetate **106**, and ammonium acetate in refluxing ethanol for 3 h was reported for the regioselective synthesis of 4-(3-(4-fluorophenyl)-1-phenyl-1*H*-pyrazol-4-yl)-2-hydroxy-6-(naphthalen-1-yl)nicotinonitrile **107** in 75% yields (Scheme 8) [102]. Although the scope of the reaction was not further studied, compound **107** was employed in the construction of an important library of diversely functionalized *N*-heterocycles containing pyridine and pyrazole moieties without using a multicomponent approach. Next, the anticancer activity of compound **107** was screened against HepG2 and HeLa cell lines using a standard MTT assay in the presence of doxorubicin as a standard drug. Thus, compound **107** showed a low cytotoxic effect with  $IC_{50}$  values of  $20.00$   $\mu$ M and  $35.58$   $\mu$ M for HepG2 and HeLa cell lines, respectively, when compared to doxorubicin ( $IC_{50} = 4.50$   $\mu$ M and  $5.57$   $\mu$ M, respectively).



**Scheme 8.** Four-component synthesis of 4-(3-(4-fluorophenyl)-1-phenyl-1*H*-pyrazol-4-yl)-2-hydroxy-6-(naphthalen-1-yl)nicotinonitrile **107** with anticancer activity.

Importantly, a green and efficient synthesis of 4,5-dihydropyrano[2,3-*c*]pyrazol-6(2*H*)-one derivatives **108** is described by the four-component reaction of aromatic aldehydes **1**, Meldrum's acid **81**, methyl acetoacetate **3**, and hydrazine hydrate **4** catalyzed by potassium carbonate (10 mol%) in water–ethanol (5.0 mL, 1:1) at reflux for 2–4 h (Table 31) [103]. This protocol provides several advantages such as environmental friendliness, short reaction times, good yields (59–85%), and a simple workup procedure. The cytotoxic activity of synthesized compounds **108a–l** was evaluated by MTT assay on A2780, MCF-7, and PC-3 cell lines using doxorubicin as a standard drug. The compounds **108g** in the A2780 cell line ( $IC_{50} = 104$   $\mu$ M), **108g** and **108i** in the MCF-7 cell line ( $IC_{50} = 87$  and  $23$   $\mu$ M, respectively), and **108g–i** in the PC-3 cell line ( $IC_{50} = 60$ ,  $50$ , and  $31$   $\mu$ M, respectively) showed the best results close to the control drug doxorubicin (Table 31). Therefore, the compounds **108g** and **108h** were adopted for the identification of mechanisms of action on A2780 and MCF-7 cell lines. In summary, the compound **108h** increased caspase-3 and caspase-9 activation in the A2780 cell line, while the compound **108g** significantly increased caspase-9 activation in the MCF-7 cell line.

**Table 31.** Four-component synthesis and in vitro anticancer activity of 4,5-dihydropyrano[2,3-*c*]pyrazol-6(2*H*)-one derivatives **108**.

| Compound                 | R                        | Yield <b>108</b> (%) | IC <sub>50</sub> (μM) |       |      |
|--------------------------|--------------------------|----------------------|-----------------------|-------|------|
|                          |                          |                      | A2780                 | MCF-7 | PC-3 |
| <b>108a</b>              | 3-MeO                    | 66                   | 150                   | 165   | 90   |
| <b>108b</b>              | 4-MeO                    | 65                   | 150                   | NA    | 165  |
| <b>108c</b>              | 2,3-(MeO) <sub>2</sub>   | 60                   | 150                   | 120   | 100  |
| <b>108d</b>              | 2-OH-4-MeO               | 80                   | NA <sup>b</sup>       | NA    | NA   |
| <b>108e</b>              | 2,4-(OH) <sub>2</sub>    | 85                   | 150                   | NA    | 75   |
| <b>108f</b>              | 2,4-(MeO) <sub>2</sub>   | 68                   | NA                    | 101   | NA   |
| <b>108g</b>              | 2,5-(MeO) <sub>2</sub>   | 74                   | 104                   | 87    | 60   |
| <b>108h</b>              | 3,4-(MeO) <sub>2</sub>   | 75                   | 150                   | NA    | 50   |
| <b>108i</b>              | 3,5-(MeO) <sub>2</sub>   | 70                   | NA                    | 23    | 31   |
| <b>108j</b>              | 2,3,4-(OH) <sub>3</sub>  | 80                   | NA                    | NA    | NA   |
| <b>108k</b>              | 2,3,4-(MeO) <sub>3</sub> | 60                   | NA                    | NA    | NA   |
| <b>108l</b>              | 3,4,5-(MeO) <sub>3</sub> | 59                   | NA                    | NA    | NA   |
| Doxorubicin <sup>a</sup> | –                        | –                    | 3.70                  | 4.76  | 5.25 |

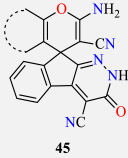
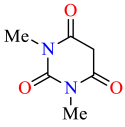
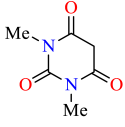
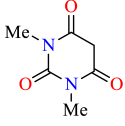
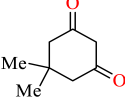
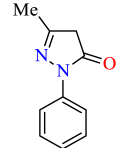
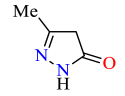
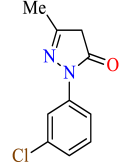
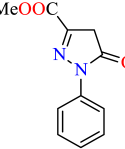
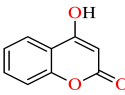
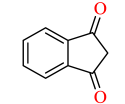
<sup>a</sup> Standard drug for the study. <sup>b</sup> NA = not active.

Additional to the antibacterial activity previously discussed in Table 10 (Section 2.1. Antibacterial activity) for the spiroindenopyridazine-4*H*-pyrans **45** obtained via a four-component synthesis [43], their cytotoxic activity on non-small cell *lung* cancer (A549), *Breast* cancer (MCF-7), Human malignant *melanoma* (A375), *Prostate* cancer (PC-3 and LNCaP), and normal cells HDF (human dermal fibroblast) were also investigated using the MTT colorimetric assay in the presence of etoposide as a positive control. As shown in Table 32, the compounds have no inhibition effect on two cancer cell lines (MCF-7 and PC-3) and Normal cells HDF. Moreover, the compound **45a** displayed the highest cytotoxicity against A549, A375, and LNCaP cell lines with IC<sub>50</sub> values of 40, 70.7, and 32.1 μM, respectively, when compared to etoposide (IC<sub>50</sub> = 60, 25.3, and 90 μM, respectively). Interestingly, inverted fluorescent microscopy images showed that compound **45a** induced cell death in A549 cells. Treatment with **45a** leads to both the up-regulated expression of Bax and the down-regulated expression of Bcl-2 in A549 cells, confirming mitochondria-mediated apoptosis.

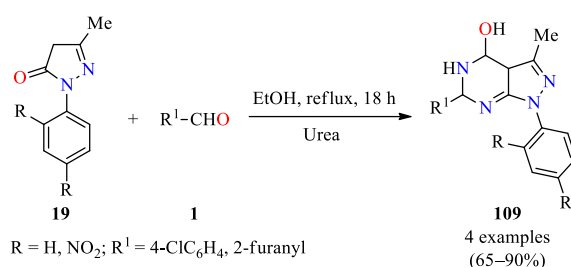
In 2020, Alharthy reported the synthesis of pyrazolo[3,4-*d*]pyrimidin-4-ol derivatives **109** via a three-component reaction of 1-aryl-3-methyl-1*H*-pyrazol-5-ones **19**, urea, and (hetero)aromatic aldehydes **1** in refluxing EtOH for 18 h (Scheme 9) [104]. The reaction mixture was filtered, dried, and recrystallized from ethanol to afford compounds in 65–90% yields. The cytotoxic activity of all synthesized compounds was evaluated against MCF-7 (*Breast* cancer) and A549 (*Lung* cancer) cell lines using doxorubicin as a standard drug. Overall, the compound **109a** (R = H, R<sup>1</sup> = 4-ClC<sub>6</sub>H<sub>4</sub>) displayed better inhibitory activity against MCF-7 and A549 cell lines with IC<sub>50</sub> values of 74 μM and 11.5 μM, respectively, when compared to doxorubicin (IC<sub>50</sub> = 35.2 μM and 9.80 μM, respectively).



**Table 32.** Evaluation of spiroindenopyridazine-4*H*-pyrans **45** against the cancer cell lines A549, PC-3, MCF-7, A375, LNCaP, and Normal cell HDF <sup>a</sup>.

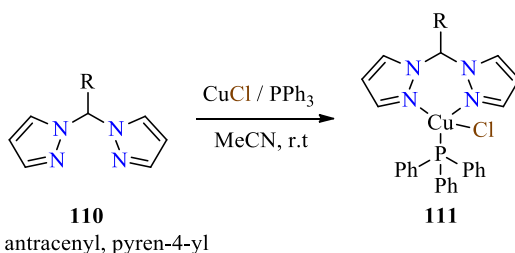
| Compound               | Cyclic CH-Acid <b>44</b><br>in Table 10   | IC <sub>50</sub> (μM) |      |       |      |       |      |
|------------------------|---|-----------------------|------|-------|------|-------|------|
|                        |   | A549                  | PC-3 | MCF-7 | A375 | LNCaP | HDF  |
|                        |    |                       |      |       |      |       |      |
| 45a                    |    | 40                    | >100 | >100  | 70.7 | 32.1  | >100 |
| 45b                    |    | >100                  | >100 | >100  | >100 | >100  | >100 |
| 45c                    |    | >100                  | >100 | >100  | >100 | >100  | >100 |
| 45d                    |  | >100                  | >100 | >100  | >100 | >100  | >100 |
| 45e                    |  | >100                  | >100 | >100  | >100 | >100  | >100 |
| 45f                    |  | >100                  | >100 | >100  | >100 | >100  | >100 |
| 45g                    |  | >100                  | >100 | >100  | >100 | >100  | >100 |
| 45h                    |  | >100                  | >100 | >100  | >100 | >100  | >100 |
| 45i                    |  | >100                  | >100 | >100  | >100 | >100  | >100 |
| 45j                    |  | >100                  | >100 | >100  | >100 | >100  | >100 |
| Etoposide <sup>b</sup> | –   | 60                    | 40   | 30    | 25.3 | 90    | >100 |

<sup>a</sup> Reaction conditions: Cyanoaceto-hydrazide **42** (1 mmol), ninhydrin **43** (1 mmol), malononitrile **2** (1 mmol), cyclic CH-acid **44** (1 mmol), EtOH (10 mL), reflux, 6–12 h. <sup>b</sup> Standard drug for the study.



**Scheme 9.** Three-component synthesis of pyrazolo[3,4-*d*]pyrimidin-4-ol derivatives **109** with anti-cancer activity.

Considerable interest in pyrazole-containing copper(I) complexes have been stimulated by promising pharmacological applications, fluorescence sensing, and catalytic properties [105,106]. For instance, the copper(I) complexes **111** with pyrazole-linked triphenylphosphine moieties have been described as photostable and cost-effective fluorescent probes for simultaneously tracking mitochondria and nucleolus via live cell imaging techniques, in a single run and within a timeframe of just 30 min [107]. Both metallo-complexes **111** were synthesized via a three-component reaction of *bis*-pyrazole derivatives **110**, copper(I) chloride, and triphenylphosphine in HPLC-grade acetonitrile at room temperature (Scheme 10). These metallo-complexes were found to be the least cytotoxic to HeLa cells, and even at a 20  $\mu\text{M}$  treatment concentration, approximately 90% of cell viability was observed in both cases. Moreover, both complexes were found to be photostable when torched with 10% of a 100 mW laser for up to 10 min.

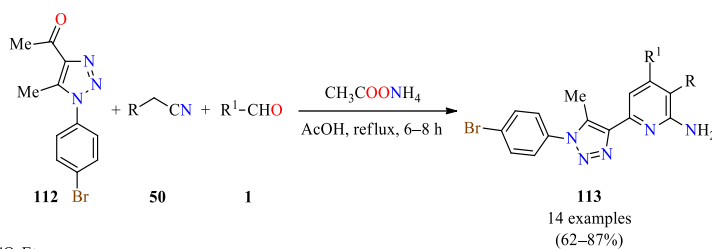


**Scheme 10.** Three-component synthesis of copper(I) complexes **111** with pyrazole-linked triphenylphosphine moieties as mitochondria- and nucleolus-labelling probes.

The pyrazolyl-dibenzo[*b,e*][1,4]diazepinones (**64–70a**) and (**71–77b**) were obtained via a multicomponent synthetic approach and previously discussed in Section 2.1. Antibacterial activity (Table 18) [70]. These compounds were also screened for their antiproliferative potential against six human cancer cell lines using a sulforhodamine B (SRB) assay in the presence of cisplatin, etoposide, and camptothecin as standard drugs. In particular, the compounds **73b** ( $\text{R} = \text{H}, \text{R}^1 = 4\text{-ClC}_6\text{H}_4\text{O}$ ) and **75b** ( $\text{R} = \text{H}, \text{R}^1 = 4\text{-ClC}_6\text{H}_4\text{S}$ ) showed better antiproliferative activity against A549 (*Lung* cancer), HBL-100 (*Breast* cancer), HeLa (*Cervix* cancer), SW1573 (*Lung* cancer), T-47D (*Breast* cancer), and WiDr (*Colon* cancer) cell lines with  $\text{GI}_{50}$  values ranging from 2.6–5.1  $\mu\text{M}$  and 1.8–7.5  $\mu\text{M}$ , respectively, when compared to *cis*-platin ( $\text{GI}_{50} = 1.9\text{--}26 \mu\text{M}$ ), etoposide ( $\text{GI}_{50} = 1.4\text{--}23 \mu\text{M}$ ), and camptothecin ( $\text{GI}_{50} = 0.23\text{--}2.0 \mu\text{M}$ ). Docking studies were performed for compounds **73b** and **75b** along with etoposide in the active site of human topoisomerase II alpha (PDB ID: 5GWK) [70]. The oxygen atom of the carbonyl group of guanine, a part of DNA, forms a hydrogen bond with the NH group of the diazepine ring of the compound **73b**. However, compound **75b** did not form any hydrogen bond with the DNA. Etoposide showed a docking score of  $-3.59$ , which is better than compounds **73b** ( $-1.37$ ) and **75b** ( $-0.95$ ). In addition, etoposide displayed lower binding energy ( $-70.81 \text{ kcal/mol}$ ) than compounds **73b** and **75b** ( $-31.78 \text{ kcal/mol}$  and  $-25.97 \text{ kcal/mol}$ , respectively).

In 2021, Rashdan et al., described the synthesis of 1,2,3-triazolyl-pyridine hybrids **113** through a four-component reaction of 1,2,3-triazole derivatives **112**, active methylene com-

pounds **50**, (hetero)aromatic aldehydes **1**, and ammonium acetate in refluxing acetic acid for 6–8 h (Scheme 11) [108]. After the completion of the reaction, the mixture was cooled and the precipitated products were filtered, washed with water, dried, and recrystallized from ethanol to give 1,2,3-triazolyl-pyridine hybrids **113** in 62–87% yields. The cytotoxic activities of all synthesized compounds were screened against HepG2 Hepatocellular carcinoma and BALB/3T3 (Murine fibroblast) cell lines using an MTT assay and the standard drug doxorubicin. Overall, the compounds **113d** (R = CN, R<sup>1</sup> = 3-(1-(4-bromophenyl)-5-methyl-1H-1,2,3-triazol-4-yl)-1-phenyl-1H-pyrazole-4-yl) and **113e** (R = CN, R<sup>1</sup> = 3-(1-(3-nitrophenyl)-5-methyl-1H-1,2,3-triazol-4-yl)-1-phenyl-1H-pyrazole-4-yl) showed an excellent anticancer activity against HepG2 cell line with IC<sub>50</sub> values of 0.64 µg/mL and 1.08 µg/mL, respectively, in comparison to the reference drug (IC<sub>50</sub> = 3.56 µg/mL). Meanwhile, they did not show toxicity on the Normal cell lines (BALAB/3T3).

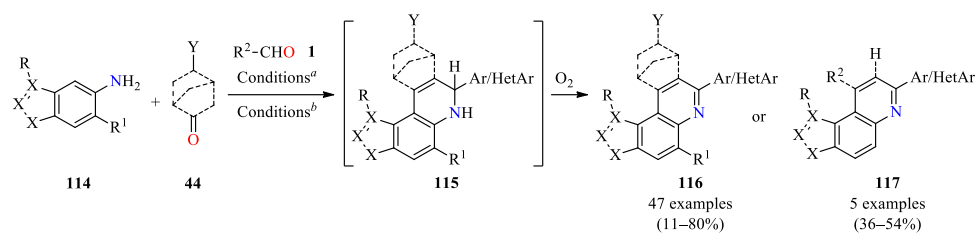


R = CN, CO<sub>2</sub>Et

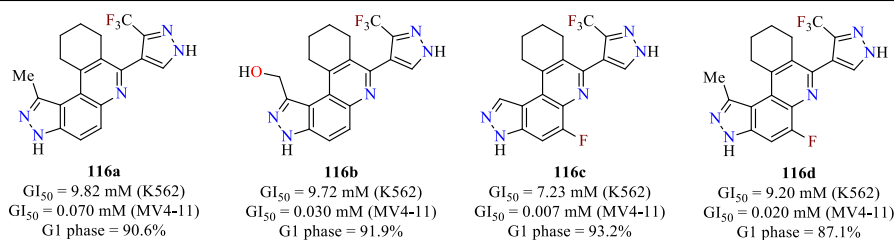
R<sup>1</sup> = C<sub>6</sub>H<sub>5</sub>, 4-MeOC<sub>6</sub>H<sub>4</sub>, 4-OH-3-MeOC<sub>6</sub>H<sub>3</sub>, 2-thiophenyl, 2-furanyl, 3-(1-(4-bromophenyl)-5-methyl-1H-1,2,3-triazol-4-yl)-1-phenyl-1H-pyrazole-4-yl, 3-(1-(3-nitrophenyl)-5-methyl-1H-1,2,3-triazol-4-yl)-1-phenyl-1H-pyrazole-4-yl

**Scheme 11.** Four-component synthesis and anticancer evaluation of 1,2,3-triazolyl-pyridine hybrids **113**.

Very recently, novel 3H-pyrazolo[4,3-f]quinolines **116/117** were rapidly assembled through a one-pot Doebner/Povarov-type MCR utilizing arylamines **114** and (hetero)aromatic aldehydes **1** to form Schiff bases, which subsequently reacted with the enol form of cyclic or acyclic ketones **44** in the presence of catalytic acid to give an intermediate **115** that is readily oxidized by air to form a quinoline core (Scheme 12) [109]. Authors explored how various modifications on compounds **116/117** affected the proliferation of K562 (*Chronic myelogenous leukemia*, CML) and MV4-11 (*Acute myeloid leukemia*, AML) cell lines in the presence of quizartinib (GI<sub>50</sub> = > 20 µM and 0.002 µM, respectively) and dinaciclib (GI<sub>50</sub> = 0.013 µM and 0.007 µM, respectively) as positive controls. Overall, the compounds **116/117** exhibited antiproliferative activity against K562 and MV4-11 cell lines with GI<sub>50</sub> values ranging from 3.28 to > 100 µM and 0.007 to > 100 µM, respectively. The most potent inhibitors **116a**, **116b**, **116c**, and **116d** caused the accumulation of >80% of treated MV4-11 cells in the G1 phase. These compounds blocked the proliferation of K562 and MV4-11 cell lines with GI<sub>50</sub> values ranging from 7.23 to 9.82 µM and 7 to 70 nM, respectively (Scheme 12). Finally, molecular docking was performed between compound **116a** and active (activation loop-out, DFG-in, homology model) and inactive kinase conformation (DFG-out, PDB: 4XUF). The compound **116a** adopted a binding mode corresponding to type I FLT3 kinase inhibitors. The 3H-pyrazole ring formed a hydrogen bond with Cys694 in the hinge region, while the 3-trifluoromethyl moiety formed C–F⋯H–N and C–F⋯C=O interactions with Arg834 and Asp698, respectively.

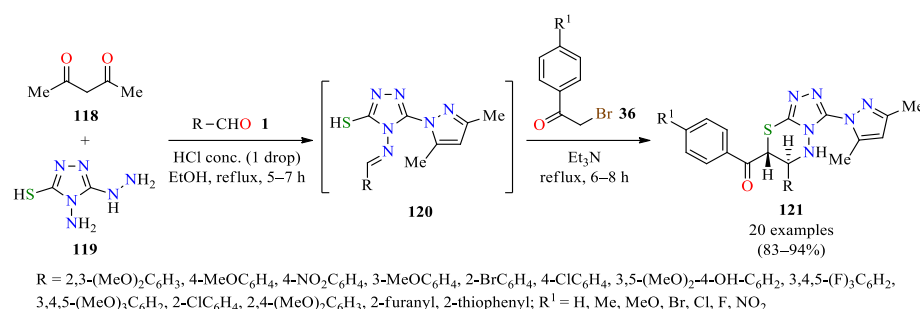


R = H, F, Cl, Br, I, Me, CN, CH<sub>2</sub>OH, CO<sub>2</sub>Me, 4-(methylpiperazin-1-yl)prop-1-yn-1-yl); R<sup>1</sup> = F, Br, CF<sub>3</sub>, piperidine  
 X = C, N, NH, NMe, S; Y = *N*-methylpiperazine, morpholine, CN, CO<sub>2</sub>Me, CO<sub>2</sub>H, CF<sub>3</sub>, NHAc, OH  
 R<sup>2</sup> = Et, cyclopropyl, 3-Cl-4-FC<sub>6</sub>H<sub>3</sub>, 3,5-diFC<sub>6</sub>H<sub>3</sub>, 4-pyridinyl



**Scheme 12.** Three-component synthesis and anticancer evaluation of 3*H*-pyrazolo[4,3-*f*]quinoline derivatives **116** and **117**. Reaction conditions: (a) (i) EtOH, reflux, 2 h, and (ii) cyclic ketone **44**, catalyst HCl, reflux, 12 h; (b) (i) THF, reflux, 2 h, and (ii) acyclic ketone or acetophenone **44** and I<sub>2</sub> (10 mol%), reflux, 12 h.

Recently, pyrazole and dihydrothiadiazine skeletons were obtained by a one-pot four-component reaction [110]. Initially, a mixture of acetylacetone **118**, 4-amino-5-hydrazinyl-4*H*-1,2,4-triazole-3-thiol **119**, and diverse aldehydes **1** catalyzed by one drop of concentrated HCl in refluxing ethanol for 5–7 h afforded pyrazole-based intermediates **120** (Scheme 13). Then, substituted phenacyl bromides **36** and an excess of triethylamine (one drop of HCl was neutralized by one mole of Et<sub>3</sub>N) were added, and the resulting mixture was continued under reflux for 6–8 h. Finally, the reaction mixture was cooled to room temperature, and the formed solid was filtered and recrystallized from ethanol to afford pyrazole-based dihydrothiadiazine derivatives **121** in 83–94% yields. From the mechanistic perspective, the hydrazino functional group of compound **119** underwent cyclocondensation with acetylacetone **118** to form a pyrazole ring. Then, an appropriate amount of different aldehydes **1** and substituted phenacyl bromides **36** reacted with amine (–NH<sub>2</sub>) and thiol (–SH) groups mediated by HCl and Et<sub>3</sub>N, respectively, leading to dihydrothiadiazine derivatives **121** (Scheme 13). The synthesized compounds **121a–t** were screened for their antitumoral activity against LN-229 (*Glioblastoma*), Capan-1 (*Pancreatic adenocarcinoma*), HCT-116 (*Colorectal carcinoma*), NCI-H460 (*Lung carcinoma*), DND-41 (*Acute lymphoblastic leukemia*), HL-60 (*Acute myeloid leukemia*), K-562 (*Chronic myeloid leukemia*), and Z-138 (*Non-Hodgkin lymphoma*) cell lines using docetaxel (a microtubule depolymerization inhibitor) and staurosporine (a pan-kinase inhibitor) as positive controls. Overall, the compounds **121j** (R = 3,4,5-(F)<sub>3</sub>C<sub>6</sub>H<sub>2</sub>, R<sup>1</sup> = Me) and **121q** (R = 2-Furanyl, R<sup>1</sup> = MeO) displayed better activity against eight cancer cell lines with IC<sub>50</sub> values in the range of 1.9–56.0 μM and 0.4–2.5 μM, respectively, in comparison to docetaxel (IC<sub>50</sub> = 0.0009–0.0087 μM) and staurosporine (IC<sub>50</sub> = 0.0004–0.0229 μM) as standard drugs. In addition, immune fluorescence analysis of tubulin in HEp-2 cells was performed with compounds **121j** and **121q** and compared to DMSO (vehicle control) and vincristine (positive control). Remarkably, these compounds inhibit the polymerization of tubulin in a dose-dependent manner.



**Scheme 13.** One-pot four-component synthesis and anticancer evaluation of 3-(1*H*-pyrazol-1-yl)-6,7-dihydro-5*H*-[1,2,4]triazolo[3,4-*b*][1,3,4]thiadiazine derivatives **121**.

Importantly, pyrazole-based 1,4-naphthoquinones **123** were rapidly assembled through a four-component reaction of ethylacetoacetate **3**, 2-hydroxy-1,4-naphthoquinone **122**, hydrazine derivatives **4/15**, and diverse aromatic aldehydes **1** catalyzed by V<sub>2</sub>O<sub>5</sub> (5 mol%) in refluxing ethanol for 1 h (Table 33) [111]. This protocol was distinguished by its short reaction times, high yields, the use of a green solvent, and broad substrate scope. Moreover, some compounds were screened for their anticancer activity against the HeLa (*Cervical cancer*) cell line using the MTT colorimetric assay and doxorubicin as a positive control. These compounds showed good to excellent anticancer activity with IC<sub>50</sub> values in the range of 2.9–25.12 μM, in comparison to doxorubicin (IC<sub>50</sub> = 5.1 μM). Notably, the compounds **123i**, **123f**, and **123b** resulted in being more active than doxorubicin with IC<sub>50</sub> values of 2.9, 4.36, and 4.81 μM, respectively.

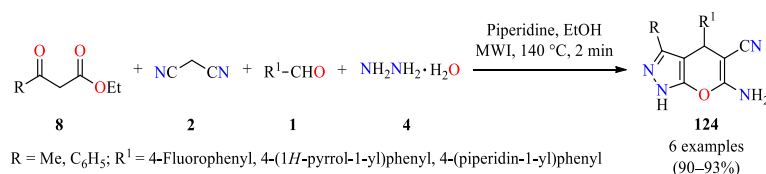
**Table 33.** Four-component synthesis and anticancer evaluation of pyrazole-based 1,4-naphthoquinones **123**.

| Compound                 | R                                  | R <sup>1</sup>                           | Yield <b>123</b> (%) | IC <sub>50</sub> (μM) |
|--------------------------|------------------------------------|--|----------------------|-----------------------|
|                          |                                    |  |                      | HeLa                  |
| <b>123a</b>              | C <sub>6</sub> H <sub>5</sub>      | 4-MeOC <sub>6</sub> H <sub>4</sub>       | 95                   | – <sup>c</sup>        |
| <b>123b</b>              | C <sub>6</sub> H <sub>5</sub>      | 3-OHC <sub>6</sub> H <sub>4</sub>        | 96                   | 4.81                  |
| <b>123c</b>              | C <sub>6</sub> H <sub>5</sub>      | C <sub>6</sub> H <sub>5</sub>            | 93                   | 22.08                 |
| <b>123d</b>              | C <sub>6</sub> H <sub>5</sub>      | 3-Me-4-ClC <sub>6</sub> H <sub>3</sub>   | 92                   | 25.12                 |
| <b>123e</b>              | C <sub>6</sub> H <sub>5</sub>      | 2-OHC <sub>6</sub> H <sub>4</sub>        | 91                   | – <sup>c</sup>        |
| <b>123f</b>              | C <sub>6</sub> H <sub>5</sub>      | 3-MeO-4-BzOC <sub>6</sub> H <sub>3</sub> | 93                   | 4.36                  |
| <b>123g</b>              | C <sub>6</sub> H <sub>5</sub>      | 2-OH-3-MeOC <sub>6</sub> H <sub>3</sub>  | 89                   | – <sup>c</sup>        |
| <b>123h</b>              | C <sub>6</sub> H <sub>5</sub>      | 2-BrC <sub>6</sub> H <sub>4</sub>        | 86                   | 9.18                  |
| <b>123i</b>              | H                                  | 2-OH-4-MeOC <sub>6</sub> H <sub>3</sub>  | 88                   | 2.9                   |
| <b>123j</b>              | 2-EtC <sub>6</sub> H <sub>4</sub>  | 2-OH-3-MeOC <sub>6</sub> H <sub>3</sub>  | 94                   | – <sup>c</sup>        |
| <b>123k</b>              | 4-MeOC <sub>6</sub> H <sub>4</sub> | 2-OH-3-MeOC <sub>6</sub> H <sub>3</sub>  | 92                   | – <sup>c</sup>        |
| <b>123l</b>              | 2-BrC <sub>6</sub> H <sub>4</sub>  | 2-OH-3-MeOC <sub>6</sub> H <sub>3</sub>  | 98                   | – <sup>c</sup>        |
| Doxorubicin <sup>b</sup> | –                                  | –  | –                    | 5.1                   |

<sup>a</sup> Reaction conditions: Ethyl acetoacetate **3** (1 mmol), 2-hydroxy-1,4-naphthoquinone **122** (1 mmol), hydrazine derivative **4/15** (1 mmol), aldehyde **1** (1 mmol), V<sub>2</sub>O<sub>5</sub> (5 mol%), EtOH (5 mL), 80 °C, 1 h. <sup>b</sup> Standard drug for the study. <sup>c</sup> Not determined.

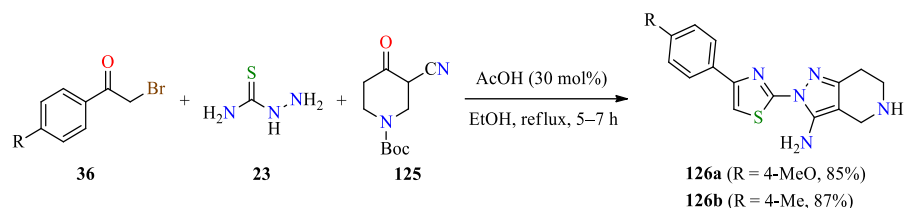
Very recently, 1,4-dihydropyrano[2,3-*c*]pyrazole derivatives **124** were obtained in excellent yields through a piperidine-catalyzed four-component reaction of β-ketoesters **8**, malononitrile **2**, aryl/heteroaryl aldehydes **1**, and hydrazine hydrate **4** in ethanol under microwave heating at 140 °C for 2 min (Scheme 14) [112]. After completion of the reaction, the product was filtered, washed with methanol, and recrystallized from ethanol. The

pyrazole derivatives **124a–f** were evaluated for their antitumor activity against four human cancer cell lines: PC-3 (*Prostate cancer*), SKOV-3 (*Ovarian cancer*), HeLa (*Cervical cancer*), and A549 (*Non-small cell lung cancer*), and two normal cell lines: Human fetal lung (HFL-1) and Human diploid fibroblasts (WI-38) using the MTT colorimetric assay in the presence of vinblastine and doxorubicin as standard drugs. These compounds displayed good cytotoxicity against PC-3, SKOV-3, HeLa, and A549 with IC<sub>50</sub> values in the range of 2.0–5.5, 2.0–4.2, 1.1–3.9, and 1.1–20.9 μM, respectively, when compared to vinblastine and doxorubicin (IC<sub>50</sub> = 2.7–3.1 and 1.4–2.2 μM, respectively). Overall, the compound **124c** (R = Me, R<sup>1</sup> = 4-(1*H*-pyrrol-1-yl)phenyl) displayed the highest cytotoxicity against PC-3 and HeLa cell lines with IC<sub>50</sub> values of 2.0 and 1.1 μM, respectively. In addition, the compounds **124a** (R = Me, R<sup>1</sup> = 4-fluorophenyl) and **124e** (R = Me, R<sup>1</sup> = 4-(piperidin-1-yl)phenyl) showed better cytotoxicity against SKOV-3 and A549 cell lines with IC<sub>50</sub> values of 2.0 and 1.1 μM, respectively. Molecular docking studies were performed for all synthesized compounds against His-tag human thymidylate synthase (HT-hTS) in a complex with 2'-deoxyuridine 5'-monophosphate (dUMP) (PDB: 6QXH) [112]. The compounds **124a** (R = Me, R<sup>1</sup> = 4-fluorophenyl), **124b** (R = C<sub>6</sub>H<sub>5</sub>, R<sup>1</sup> = 4-fluorophenyl), and **124f** (R = C<sub>6</sub>H<sub>5</sub>, R<sup>1</sup> = 4-(piperidin-1-yl)phenyl) stabilized in a TS binding pocket similar to dUMP through an arrangement of the pyranopyrazole cluster in perpendicular mode with Tyr270 via a hydrogen bond interaction, while the compounds **124c** (R = Me, R<sup>1</sup> = 4-(1*H*-pyrrol-1-yl)phenyl) and **124d** (R = C<sub>6</sub>H<sub>5</sub>, R<sup>1</sup> = 4-(1*H*-pyrrol-1-yl)phenyl) occupied the binding pocket by interaction with Asn238.



**Scheme 14.** Microwave-assisted four-component synthesis of 1,4-dihydropyrano[2,3-*c*]pyrazoles **124** as anticancer agents.

Interestingly, thiazolyl-based pyrazoles **126** were obtained in good yields through a three-component reaction of substituted phenacyl bromides **36**, thiosemicarbazide **23**, and 1-boc-3-cyano-4-piperidone **125** catalyzed by acetic acid (30 mol%) in refluxing ethanol for 5–7 h (Scheme 15) [113]. After the completion of the reaction, the mixture was cooled to room temperature, and the precipitate was filtered, washed, and recrystallized from ethanol. The anticancer activity of synthesized compounds was screened against three human cancer cell lines: HeLa (*Cervical cancer*), A549 (*Lung cancer*), and MDA-MB-231 (*Breast cancer*) using the MTT colorimetric assay in the presence of combretastatin A-4 as a positive control. The compounds **126a** (R = 4-MeO) and **126b** (R = 4-Me) showed good cytotoxicity against HeLa, A549, and MDA-MB-231 cell lines with IC<sub>50</sub> values in the range of 3.60–4.17 μM and 4.61–5.29 μM, respectively. Besides, thiazolyl-based pyrazoles and combretastatin A-4 were docked into the colchicine binding site of β-tubulin (PDB: 4YJ2), finding that compounds **126a** (−8.79 kcal/mol) and **126b** (−8.77 kcal/mol) have better docking scores than combretastatin A-4 (−8.45 kcal/mol). The compound **126a** interacted via two hydrogen bonds with Gln136 and Glh200.



**Scheme 15.** Three-component synthesis and anticancer evaluation of thiazolyl-based pyrazoles **126**.

A series of 6-amino-1,4-dihydropyrano[2,3-*c*]pyrazole-5-carbonitriles **127** were synthesized in high yields via a one-pot multicomponent approach [114]. Initially, a mixture of  $\beta$ -keto esters **8**, aryl hydrazines **15**, and zinc triflate (10 mol%) was irradiated under microwave at 80 °C for 10 min. Then, aromatic aldehydes **1** and malononitrile **2** were added to the above reaction mixture. The resulting mixture was further irradiated under microwave at 120 °C for 15 min to afford pyrazole derivatives **127a–f** under solvent-free conditions. The anticancer activity of compounds was investigated against four human cancer cell lines: 786-0 (*Renal cancer*), A431 (*Epidermal carcinoma*), MCF-7 (*Breast cancer*), and U-251 (*Human glioblastoma*) employing doxorubicin as a positive control. As shown in Table 34, the compound **127h** with –NO<sub>2</sub> and –OMe groups displayed significant activity with an IC<sub>50</sub> value of 9.9  $\mu$ g/mL against the 786-0 cell line. Furthermore, the compounds **127b** (IC<sub>50</sub> = 22.78  $\mu$ g/mL), **127i** (IC<sub>50</sub> = 21.98  $\mu$ g/mL), and **127j** (IC<sub>50</sub> = 19.98  $\mu$ g/mL) with –OH or –Br groups on phenyl ring showed moderate activity against the A431 cell line, when compared to doxorubicin (IC<sub>50</sub> = 1.6  $\mu$ g/mL). Moreover, the compounds **127h** and **127j** showed better activity against MCF-7 and U-251 cell lines with IC<sub>50</sub> values of 31.87 and 25.78  $\mu$ g/mL, respectively, in comparison to doxorubicin (IC<sub>50</sub> = 2.1 and 1.9  $\mu$ g/mL, respectively).

**Table 34.** Zn(OTf)<sub>2</sub>-catalyzed one-pot four-component synthesis of 6-amino-1,4-dihydropyrano[2,3-*c*]pyrazole-5-carbonitriles **127** as anticancer agents.

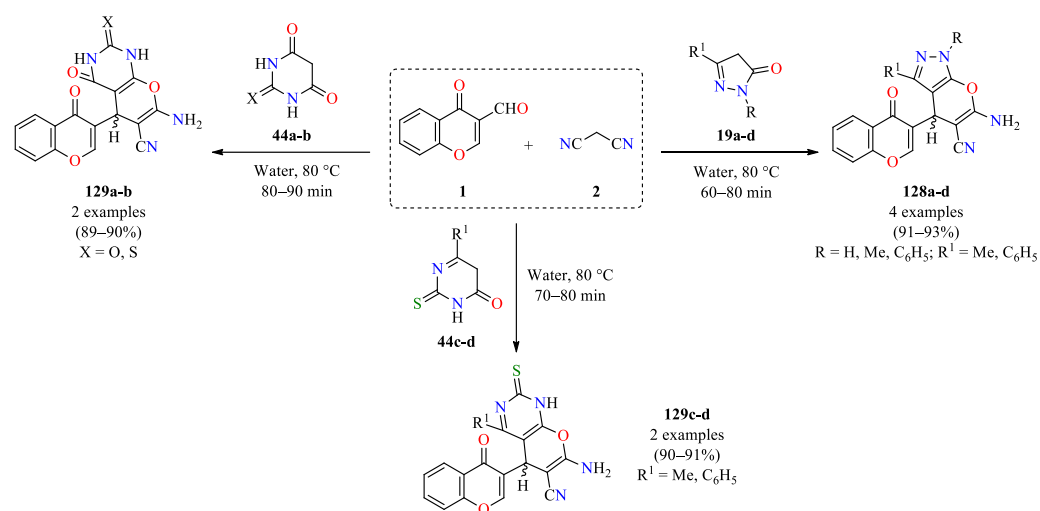
| Compound                 | R               | R <sup>1</sup>                                  | R <sup>2</sup>                                  | Yield <b>127</b> (%) | IC <sub>50</sub> ( $\mu$ g/mL) |       |       |       |
|--------------------------|-----------------|---|---|----------------------|--------------------------------|-------|-------|-------|
|                          |                 |   |   |                      | 786-0                          | A431  | MCF-7 | U-251 |
| <b>127a</b>              | CF <sub>3</sub> | C <sub>6</sub> H <sub>5</sub>                   | C <sub>6</sub> H <sub>5</sub>                   | 93                   | 19.81                          | 55.87 | 89.76 | 30.89 |
| <b>127b</b>              | CF <sub>3</sub> | C <sub>6</sub> H <sub>5</sub>                   | 4-BrC <sub>6</sub> H <sub>4</sub>               | 98                   | 21.98                          | 22.78 | 47.88 | 33.98 |
| <b>127c</b>              | CF <sub>3</sub> | 4-ClC <sub>6</sub> H <sub>4</sub>               | C <sub>6</sub> H <sub>5</sub>                   | 95                   | 66.41                          | 55.98 | 54.87 | 55.78 |
| <b>127d</b>              | CF <sub>3</sub> | 4-ClC <sub>6</sub> H <sub>4</sub>               | 4-MeOC <sub>6</sub> H <sub>4</sub>              | 92                   | 31.86                          | 41.34 | 44.65 | 97.98 |
| <b>127e</b>              | CH <sub>3</sub> | 3-NO <sub>2</sub> C <sub>6</sub> H <sub>4</sub> | C <sub>6</sub> H <sub>5</sub>                   | 92                   | 55.78                          | >100  | 66.54 | 55.98 |
| <b>127f</b>              | CH <sub>3</sub> | 3-NO <sub>2</sub> C <sub>6</sub> H <sub>4</sub> | 3-Br-4-MeO-C <sub>6</sub> H <sub>3</sub>        | 99                   | 78.98                          | >100  | 55.78 | 97.98 |
| <b>127g</b>              | CH <sub>3</sub> | 3-NO <sub>2</sub> C <sub>6</sub> H <sub>4</sub> | 4-NO <sub>2</sub> C <sub>6</sub> H <sub>4</sub> | 97                   | 17.43                          | >100  | >100  | >100  |
| <b>127h</b>              | CH <sub>3</sub> | 3-NO <sub>2</sub> C <sub>6</sub> H <sub>4</sub> | 4-MeOC <sub>6</sub> H <sub>4</sub>              | 98                   | 9.9                            | 66.54 | 31.87 | 73.67 |
| <b>127i</b>              | CH <sub>3</sub> | 3-NO <sub>2</sub> C <sub>6</sub> H <sub>4</sub> | 2-OHC <sub>6</sub> H <sub>4</sub>               | 94                   | 21.98                          | 21.98 | 47.89 | 33.98 |
| <b>127j</b>              | CH <sub>3</sub> | 3-NO <sub>2</sub> C <sub>6</sub> H <sub>4</sub> | 5-Br-2-OH-C <sub>6</sub> H <sub>3</sub>         | 96                   | 45.89                          | 19.98 | 39.87 | 25.78 |
| Doxorubicin <sup>b</sup> | –               | –   | –   | –                    | 0.99                           | 1.6   | 2.1   | 1.9   |

<sup>a</sup> Reaction conditions:  $\beta$ -keto esters **8** (1 mmol), aryl hydrazines **15** (1.1 mmol), and zinc triflate (10 mol%), MWI, 80 °C, 10 min, then aromatic aldehydes **1** (1 mmol) and malononitrile **2** (1.1 mmol), MWI, 120 °C, 15 min. <sup>b</sup> Standard drug for the study.

Ali and colleagues described a one-pot three-component reaction of 4-oxo-4*H*-chromene-3-carbaldehyde **1**, malononitrile **2**, and cyclic active methylene compounds such as pyrazolones **19a–d** and diverse pyrimidinones **44a–d** in water at 80 °C for 60–90 min to afford a series of new 4-(4-oxo-4*H*-chromen-3-yl)pyrano[2,3-*c*]pyrazoles **128a–d** and 5-(4-oxo-4*H*-chromen-3-yl)pyrano[2,3-*d*]pyrimidines **129a–d** in 91–93% and 89–91% yields, respectively (Scheme 16) [115].

The antiproliferative activity of synthesized compounds **128a–d** and **129a–d** was evaluated against three human cancer cell lines: PC-3 (*Prostate cancer*), SKOV3 (*Ovarian cancer*), and HeLa (*Cervical cancer*) using the sulforhodamine B (SRB) assay in the presence of doxorubicin as a standard drug [115]. The IC<sub>50</sub> values obtained after 72 h of incubation are reported in Table 35. The compounds **128** showed antiproliferative activity against PC-3, SKOV3, and HeLa cell lines with IC<sub>50</sub> values in the range of 9.7–190.3, 16.5–234.3, and 8.4–91.3  $\mu$ g/mL, respectively, in comparison to doxorubicin (IC<sub>50</sub> = 2.1, 2.3, and 1.9  $\mu$ g/mL,

respectively). In addition, compounds **129** showed antiproliferative activity against PC-3, SKOV3, and HeLa cell lines with IC<sub>50</sub> values in the range of 8.9–73.4, 4.7–35.5, and 11.3–32.8 µg/mL, respectively. Particularly, compound **129a** displayed the best cytotoxic effect against PC-3, SKOV3, and HeLa cell lines with IC<sub>50</sub> values of 8.9, 4.7, and 11.3 µg/mL, respectively (Table 35). Furthermore, compound **128c** showed a promising cytotoxic effect in Cervical cancer (HeLa) with an IC<sub>50</sub> value of 8.4 µg/mL, and a moderate cytotoxicity against Prostate cancer (PC-3) and Ovarian cancer (SKOV3) with IC<sub>50</sub> values of 13.2 and 16.5 µg/mL, respectively. In general, the 5-(4-oxo-4H-chromen-3-yl)pyrano[2,3-d]pyrimidines **129** resulted in being more active than 4-(4-oxo-4H-chromen-3-yl)pyrano[2,3-c]pyrazoles **128**. It should be noted that the 3-methyl-1-phenylpyrazole fragment in **128c** improved the cytotoxicity in comparison to other pyrazole derivatives. Likewise, the barbituric acid fused to the pyran core in **129a** showed higher activity than thiobarbituric acid moiety in **129b**, while the 6-phenylthiouracil moiety in **129d** displayed a better antiproliferative effect than the 6-methylthiouracil moiety in **129c**.



**Scheme 16.** Three-component synthesis and anticancer activity of new 4-(4-oxo-4H-chromen-3-yl)pyrano[2,3-c]pyrazoles **128a–d** and 5-(4-oxo-4H-chromen-3-yl)pyrano[2,3-d]pyrimidines **129a–d**.

**Table 35.** Anticancer activity of compounds **128** and **129** against PC-3, SKOV3, and HeLa cell lines.

| Compound                 | R                             | R <sup>1</sup>                | X | Yield 128/129 (%) | IC <sub>50</sub> (µg/mL) |       |      |
|--------------------------|-------------------------------|-------------------------------|---|-------------------|--------------------------|-------|------|
|                          |                               |                               |   |                   | PC-3                     | SKOV3 | HeLa |
| <b>128a</b>              | H                             | Me                            | – | 92                | 9.7                      | 35.6  | 25.9 |
| <b>128b</b>              | H                             | C <sub>6</sub> H <sub>5</sub> | – | 93                | 34.2                     | 55.4  | 32.5 |
| <b>128c</b>              | Me                            | C <sub>6</sub> H <sub>5</sub> | – | 91                | 13.2                     | 16.5  | 8.4  |
| <b>128d</b>              | C <sub>6</sub> H <sub>5</sub> | C <sub>6</sub> H <sub>5</sub> | – | 93                | 190.3                    | 234.3 | 91.3 |
| <b>129a</b>              | –                             | –                             | O | 89                | 8.9                      | 4.7   | 11.3 |
| <b>129b</b>              | –                             | –                             | S | 90                | 73.4                     | 9.3   | 14.3 |
| <b>129c</b>              | –                             | Me                            | – | 91                | 42.1                     | 35.5  | 32.8 |
| <b>129d</b>              | –                             | C <sub>6</sub> H <sub>5</sub> | – | 90                | 18.9                     | 5.4   | 15.9 |
| Doxorubicin <sup>a</sup> | –                             | –                             | – | –                 | 2.1                      | 2.3   | 1.9  |

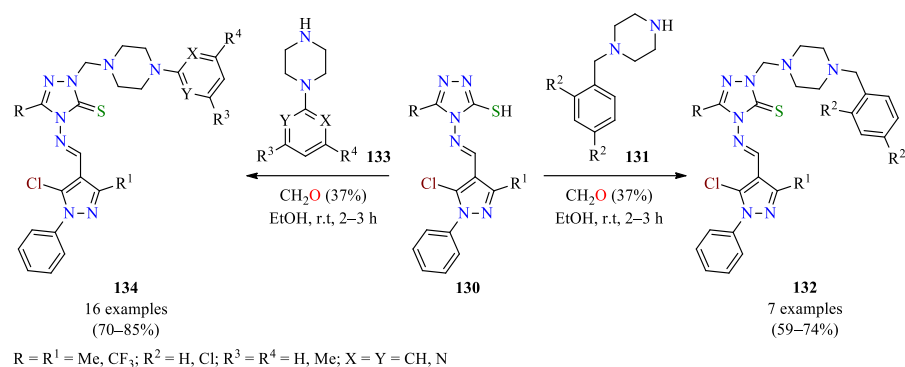
<sup>a</sup> Standard drug for the study.



### 2.3. Antifungal Activity

Currently, the incidence and severity of fungal diseases have increased in patients with increased vulnerability such as neonates, burns patients, cancer patients receiving chemotherapy, patients with acquired immunodeficiency syndrome, and organ transplant patients [116]. Moreover, the use of standard antifungal therapies has been limited due to problems of toxicity, low efficacy rates, and resistance to antifungal drugs [117]. These reasons have given rise to the design and production of new chemical libraries of aza-heterocycles with distinct action or multitargeted combination therapy [116–119]. In this way, several pyrazole-containing pyrimidines **52**, 1,4-dihydropyridines **53**, and imidazoles **54** were prepared via multicomponent synthetic approaches and discussed in Section 2.1. Antibacterial activity (Table 14) [58]. Moreover, all of these compounds were screened for their antifungal activity against *Aspergillus niger* and *Aspergillus flavus* using itraconazole as a positive control. In most cases, the pyrimidines **52** showed appreciable antifungal activity against *Aspergillus niger* and *Aspergillus flavus* with MIC values of 6.25–25 µg/mL and 12.5–25 µg/mL, respectively. In particular, the compound **52f** (R = F, R<sup>1</sup> = MeO) showed excellent antifungal activity against *Aspergillus niger* and *Aspergillus flavus* with MIC values of 6.25 µg/mL and 12.5 µg/mL, respectively, in comparison to itraconazole (MIC = 6.25 µg/mL for both strains). Moreover, the 1,4-dihydropyridines **53** showed some degree of inhibition for both fungal strains with MIC values ranging from 12.5 to >100 µg/mL. However, imidazoles **54** showed that imidazole and pyrazole rings did not contribute to antifungal efficacy.

The Mannich reaction has provided elegant and efficient solutions for the carbon–carbon and carbon–nitrogen bond formation via an iminium intermediate [120,121]. According to thione–thiol tautomerism, Wang et al. reported that the thione form undergoes a Mannich reaction via the N–H at the  $\alpha$ -position of the thiocarbonyl group [121]. As a result, the Mannich reaction of 1,2,4-triazole-3-thiol forms **130**, formaldehyde solution (37 wt. % in H<sub>2</sub>O), and 4-(substituted benzyl)piperazines **131** in ethanol at room temperature for 2–3 h afforded 1,2,4-triazole-5(4H)-thiones **132** in acceptable yields (Scheme 17). The reaction was successfully extended to 4-(substituted pyrimidyl/phenyl/pyridyl)piperazines **133** under the same reaction conditions to give 1,2,4-triazole-5(4H)-thiones **134** in good yields. The crude reaction was placed in a refrigerator overnight, and the resulting precipitate was filtered and recrystallized from ethanol to give products. Later, the 1,2,4-triazole-5(4H)-thiones **132** and **134** were screened for their in vitro fungicidal activity against six plant fungal pathogens, including *Alternaria solani* Sorauer, *Gibberella sanbinetti*, *Fusarium omysporum*, *Cercospora arachidicola*, *Physalospora piricola*, and *Rhizoctonia cerealis* using triadimefon, carbendazim, and chlorothalonil as positive controls. It was found that at a 50 µg/mL concentration, most of the compounds **132** and **134** exhibited significant fungicidal activities against *Alternaria solani* Sorauer, *Physalospora piricola*, and *Rhizoctonia cerealis* with the inhibition of 26.7–47.6%, 12.5–75.0%, and 35.7–98.0%, respectively, when compared to triadimefon (31.3%, 71.4%, and 98.0%, respectively). Several compounds displayed favorable activities against other plant fungal pathogens, such as compound **134g** (R = CF<sub>3</sub>, R<sup>1</sup> = Me, R<sup>3</sup> = Me, R<sup>4</sup> = H, X = Y = N) with 62.5% inhibition against *Gibberella sanbinetti*, and compounds **132g** (R = R<sup>1</sup> = CF<sub>3</sub>, R<sup>2</sup> = Cl) and **134p** (R = R<sup>1</sup> = CF<sub>3</sub>, R<sup>3</sup> = R<sup>4</sup> = Me, X = Y = N) with 75.0% inhibition against *Cercospora arachidicola*, which were more effective than triadimefon (52.9% and 66.7%, respectively).



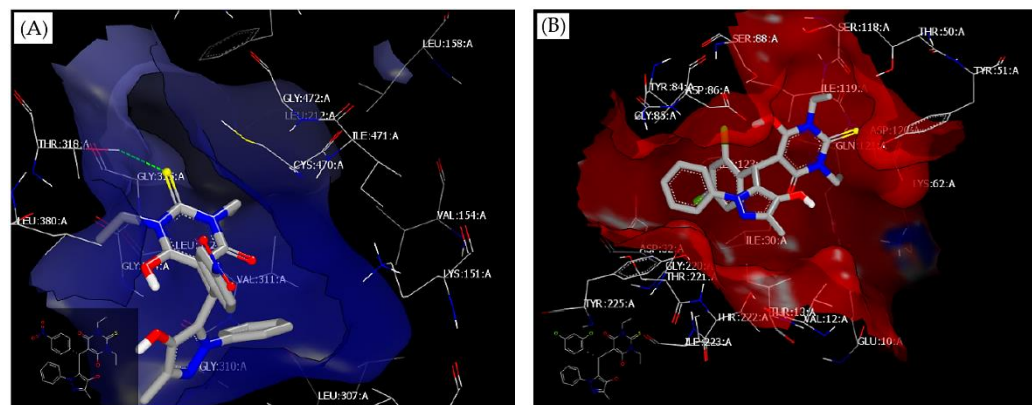
**Scheme 17.** Three-component synthesis and antifungal activity of highly functionalized 1,2,4-triazole-5(4H)-thiones **132** and **134**.

On the other hand, a series of 1*H*-1,2,3-triazole tethered pyrazolo[3,4-*b*]pyridin-6(7*H*)-ones **84a–l** was obtained via the multicomponent synthetic approach discussed in Section 2.1. Antibacterial activity (Table 20) [75]. The antifungal activity of these compounds was evaluated against *Candida albicans* and *Saccharomyces cerevisiae*. The diameter of growth of the inhibition zone (mm) and MIC value ( $\mu\text{g}/\text{mL}$ ) of all compounds was determined using amphotericin-B as a standard drug. Overall, the pyrazolo[3,4-*b*]pyridin-6(7*H*)-ones **84a–l** showed a diameter of growth of the inhibition zone in the range of 12.3–16.3 mm and 14.3–16.6 mm for *Candida albicans* and *Saccharomyces cerevisiae*, respectively, when compared to amphotericin-B (17.6 mm and 18.3 mm, respectively). Moreover, the compounds **84a–l** showed MIC values in the range of 64–256  $\mu\text{g}/\text{mL}$  for both *Candida albicans* and *Saccharomyces cerevisiae*, when compared to amphotericin-B (100  $\mu\text{g}/\text{mL}$  for both cases). Interestingly, the compound **84k** ( $R = \text{MeO}$ ,  $\text{Ar} = 4\text{-MeC}_6\text{H}_4$ ) showed the highest activity against *Candida albicans* with a diameter of growth of the inhibition zone of 16.3 mm and a MIC value of 64  $\mu\text{g}/\text{mL}$ . Furthermore, compound **84k** displayed the highest activity against *Saccharomyces cerevisiae* with a diameter of growth of the inhibition zone of 16.6 mm and a MIC value of 64  $\mu\text{g}/\text{mL}$ .

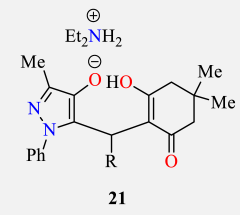
In the same way, the series of pyrazole-thiobarbituric acid derivatives **61**, obtained via a four-component synthetic approach and discussed in Section 2.1. Antibacterial activity (Table 17) [65], was also evaluated for their antifungal activity against *Candida albicans* by the diffusion method and serial dilution method using fluconazole as a standard drug (Table 36). Overall, compounds **61** showed MIC values in the range of 4–64  $\mu\text{g}/\text{L}$  against *Candida albicans*. In particular, the compounds **61h** and **61i** exerted significant activity against *Candida albicans* with a MIC value of 4  $\mu\text{g}/\text{L}$ , in comparison to fluconazole (MIC = 0.5  $\mu\text{g}/\text{L}$ ). Later, docking molecular was performed for all compounds and fluconazole against Lanosterol 14  $\alpha$ -demethylase (CYP51A1) (PDB ID code: 4WMZ). The fluconazole (consensus score of 57) forms two hydrogen bonds with Thr318 via the nitrogen atom of the triazole moiety and Leu312 via the oxygen atom of the hydroxyl group. The compound **61h** (consensus score of 55) forms one hydrogen bond between Thr318 and the sulfur atom of the thiocarbonyl group (Figure 8A), while the compound **61i** (consensus score of 48) interacts with Thr318 via hydrophobic–hydrophobic interactions (Figure 8B).

**Table 36.** Antifungal evaluation of pyrazole-thiobarbituric acid derivatives **61**.

| Compound                 | Ar  | <i>Candida albicans</i> |            |
|--------------------------|---|-------------------------|------------|
|                          |   | CPM (mm)                | MIC (μg/L) |
| <b>61a</b>               | 4-FC <sub>6</sub> H <sub>4</sub>                | 18                      | 8          |
| <b>61b</b>               | C <sub>6</sub> H <sub>5</sub>                   | 16                      | 16         |
| <b>61c</b>               | 4-ClC <sub>6</sub> H <sub>4</sub>               | 16                      | 16         |
| <b>61d</b>               | 4-MeC <sub>6</sub> H <sub>4</sub>               | 11                      | 64         |
| <b>61e</b>               | 3-MeC <sub>6</sub> H <sub>4</sub>               | 12                      | 64         |
| <b>61f</b>               | 4-BrC <sub>6</sub> H <sub>4</sub>               | 15                      | 32         |
| <b>61g</b>               | 3-BrC <sub>6</sub> H <sub>4</sub>               | 14                      | 32         |
| <b>61h</b>               | 4-NO <sub>2</sub> C <sub>6</sub> H <sub>4</sub> | 20                      | 4          |
| <b>61i</b>               | 3-NO <sub>2</sub> C <sub>6</sub> H <sub>4</sub> | 14                      | 32         |
| <b>61j</b>               | 4-MeOC <sub>6</sub> H <sub>4</sub>              | 17                      | 16         |
| <b>61k</b>               | 4-CF <sub>3</sub> C <sub>6</sub> H <sub>4</sub> | 16                      | 16         |
| <b>61l</b>               | 2,4-diClC <sub>6</sub> H <sub>3</sub>           | 21                      | 4          |
| <b>61m</b>               | 2,6-diClC <sub>6</sub> H <sub>3</sub>           | 15                      | 16         |
| <b>61n</b>               | 2-Naphthyl                                      | 16                      | 16         |
| <b>61o</b>               | 2-Thiophenyl                                    | 17                      | 8          |
| Fluconazole <sup>a</sup> | –   | 28                      | 0.5        |

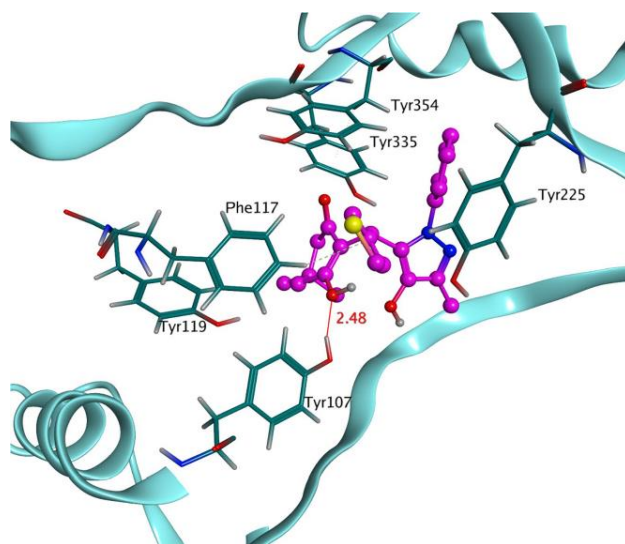
<sup>a</sup> Standard drug for the study.**Figure 8.** Ligand–receptor interaction profiles by molecular docking. (A) Interactions between 4WMZ and **61h**, and (B) interactions between 4WMZ and **61l**. Image adapted from Elshaier et al. [65].

The pyrazole-dimedone derivatives **21a–o**, obtained via a three-component synthetic approach and discussed in Section 2.1. Antibacterial activity (Table 4) [31], were also evaluated for their antifungal activity against *Candida albicans* with MIC values in the range of 4–32 μg/L and a diameter of growth of the inhibition zone in the range of 13–21 mm, when compared to fluconazole as a standard drug (0.5 μg/L and 28 mm, respectively) (Table 37). Remarkably, the pyrazole-dimedone **21o** bearing thiophene was the most active against *Candida albicans* with a MIC value of 4 μg/L. The docking molecular of the compound **21o** against *N*-myristoyl transferase (NMT) (PDB ID code: 1IYL) from *Candida albicans* displayed a docking score of  $-8.7$  kcal/mol and molecular interactions with the NMT enzyme. As shown in Figure 9, the hydroxyl group of the dimedone ring formed one hydrogen bond with Tyr107 at a distance of 2.48 Å. Apart from this, multiple hydrophobic and  $\pi$ - $\pi$  electrostatic interactions were observed with crucial residues such as Tyr107, Phe117, Tyr119, Tyr225, and Tyr335.

**Table 37.** Antifungal evaluation of pyrazole-dimedone derivatives **21**.


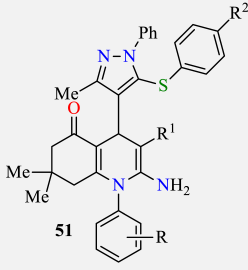
| Compound                 | R   | <i>Candida albicans</i> |            |
|--------------------------|---|-------------------------|------------|
|                          |   | CPM (mm)                | MIC (µg/L) |
| <b>21a</b>               | 2,4-diClC <sub>6</sub> H <sub>3</sub>           | 14                      | 32         |
| <b>21b</b>               | C <sub>6</sub> H <sub>5</sub>                   | 15                      | 32         |
| <b>21c</b>               | 4-ClC <sub>6</sub> H <sub>4</sub>               | 15                      | 16         |
| <b>21d</b>               | 4-MeC <sub>6</sub> H <sub>4</sub>               | 16                      | 16         |
| <b>21e</b>               | 3-MeC <sub>6</sub> H <sub>4</sub>               | 14                      | 32         |
| <b>21f</b>               | 4-BrC <sub>6</sub> H <sub>4</sub>               | 14                      | 32         |
| <b>21g</b>               | 3-BrC <sub>6</sub> H <sub>4</sub>               | 14                      | 32         |
| <b>21h</b>               | 4-NO <sub>2</sub> C <sub>6</sub> H <sub>4</sub> | 17                      | 16         |
| <b>21i</b>               | 3-NO <sub>2</sub> C <sub>6</sub> H <sub>4</sub> | 14                      | 32         |
| <b>21j</b>               | 4-MeOC <sub>6</sub> H <sub>4</sub>              | 13                      | 32         |
| <b>21k</b>               | 4-FC <sub>6</sub> H <sub>4</sub>                | 15                      | 16         |
| <b>21l</b>               | 4-CF <sub>3</sub> C <sub>6</sub> H <sub>4</sub> | 14                      | 32         |
| <b>21m</b>               | 2,6-diClC <sub>6</sub> H <sub>3</sub>           | 16                      | 16         |
| <b>21n</b>               | 2-Naphthyl                                      | 14                      | 32         |
| <b>21o</b>               | 2-Thiophenyl                                    | 21                      | 4          |
| Fluconazole <sup>a</sup> | –   | 28                      | 0.5        |

<sup>a</sup> Standard drug for the study.



**Figure 9.** Docking molecular of the compound **21o** with *N*-myristoyl transferase (PDB ID code: 1IYL) from *Candida albicans*. Image adapted from Barakat et al. [31].

Similarly, the polyhydroquinoline derivatives **51a–p**, obtained via a three-component process and discussed in Section 2.1. Antibacterial activity (Table 13) [54], were also screened for their antifungal activity against *Candida albicans* and *Aspergillus fumigatus* using griseofulvin as a positive control (Table 38). The compounds **51j**, **51k**, and **51n** were found to be more active than griseofulvin (MIC = 500 µg/mL) against *Candida albicans*. Moreover, the compounds **51i** and **51l** showed the same antifungal activity as griseofulvin (MIC = 100 µg/mL) against *Aspergillus fumigatus*.

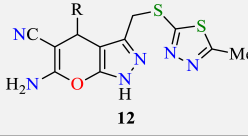
**Table 38.** Antifungal activity of polyhydroquinoline derivatives 51.


| Compound                  | R                 | R <sup>1</sup>    | R <sup>2</sup> | <i>C. albicans</i> | <i>A. fumigatus</i> |
|---------------------------|-------------------|-------------------|----------------|--------------------|---------------------|
|                           |                   |                   |                | MIC (µg/mL)        | MIC (µg/mL)         |
| 51a                       | 4-F               | CN                | 4-Cl           | >1000              | >1000               |
| 51b                       | 4-F               | COOEt             | 4-Cl           | 1000               | >1000               |
| 51c                       | 4-F               | CONH <sub>2</sub> | 4-Cl           | 1000               | 500                 |
| 51d                       | 4-F               | CN                | 4-Me           | 500                | 500                 |
| 51e                       | 4-F               | COOEt             | 4-Me           | 500                | >1000               |
| 51f                       | 4-CF <sub>3</sub> | CN                | 4-Me           | 1000               | >1000               |
| 51g                       | 4-CF <sub>3</sub> | COOEt             | 4-Me           | 1000               | 1000                |
| 51h                       | 2,4-diF           | CN                | 4-Me           | 500                | >1000               |
| 51i                       | 2,4-diF           | COOEt             | 4-Me           | 500                | 100                 |
| 51j                       | 2,4-diF           | CN                | 4-Cl           | 250                | 1000                |
| 51k                       | 2,4-diF           | COOEt             | 4-Cl           | 250                | 1000                |
| 51l                       | 2,4-diF           | CONH <sub>2</sub> | 4-Cl           | 1000               | 100                 |
| 51m                       | 4-F               | CN                | 4-F            | 1000               | 1000                |
| 51n                       | 4-F               | COOEt             | 4-F            | 250                | 1000                |
| 51o                       | 4-CF <sub>3</sub> | CN                | 4-F            | 500                | 500                 |
| 51p                       | 4-CF <sub>3</sub> | COOEt             | 4-F            | 500                | 250                 |
| Griseofulvin <sup>a</sup> | –                 | –                 | –              | 500                | 100                 |

<sup>a</sup> Standard drug for the study.

The pyrano[2,3-*c*]pyrazole derivatives **12**, obtained via a four-component process and discussed in Section 2.1. Antibacterial activity (Table 2) [28], were also screened for their antifungal activity against *Aspergillus flavus* and *Aspergillus niger* using ketoconazole as a standard drug (Table 39). It was found that at a 50 µg/well concentration, the compounds showed a diameter of growth of the inhibition zone in the range of 2–23 mm and 8–30 mm against *Aspergillus flavus* and *Aspergillus niger*, respectively, in comparison to ketoconazole (28 mm and 33 mm, respectively). In particular, compound **12f** showed better antifungal efficacy against *Aspergillus flavus* and *Aspergillus niger* with a diameter of growth of the inhibition zone of 23 mm and 30 mm, respectively, at a 50 µg/well concentration.

The pyrazolyl-dibenzo[*b,e*][1,4]diazepinones (**64–70**)**a** and (**71–77**)**b**, obtained via a multicomponent process and discussed in Section 2.1. Antibacterial (Table 18) [70], were also evaluated for their antifungal activity. The MIC values for such compounds against *Aspergillus fumigates* and *Candida albicans* were determined using griseofulvin as a standard drug. The compounds showed MIC values ranging from 250 to > 500 µg/mL and 250 to 1000 µg/mL against *Aspergillus fumigates* and *Candida albicans*, respectively, when compared to griseofulvin (MIC = 100 µg/mL and 500 µg/mL, respectively). Although compounds are very poor in their antifungal potency against *Aspergillus fumigates*, the resistance in many cases against *Candida albicans* is not disappointing. For instance, the compounds **65a** (R = H, R<sup>1</sup> = 4-MeC<sub>6</sub>H<sub>4</sub>O), **75b** (R = H, R<sup>1</sup> = 4-ClC<sub>6</sub>H<sub>4</sub>S), **66a** (R = H, R<sup>1</sup> = 4-ClC<sub>6</sub>H<sub>4</sub>O), **66'a** (R = COC<sub>6</sub>H<sub>5</sub>, R<sup>1</sup> = 4-ClC<sub>6</sub>H<sub>4</sub>O), and **74b** (R = H, R<sup>1</sup> = C<sub>6</sub>H<sub>5</sub>S) displayed better activity against *Candida albicans* with MIC values of 250 µg/mL, in comparison to griseofulvin (MIC = 500 µg/mL).

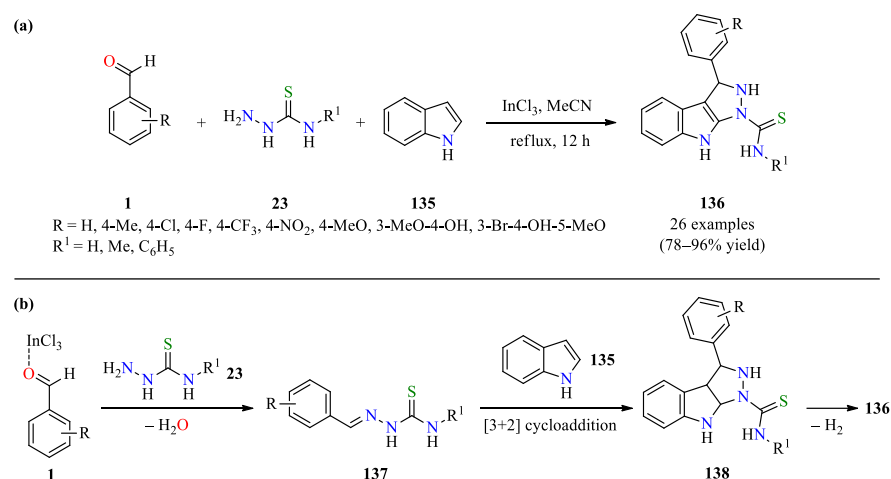
**Table 39.** Antifungal activity of pyrano[2,3-c]pyrazole derivatives **12**.


| Compound                  | R   | Zone of Inhibition (mm)   |             |                          |             |
|---------------------------|---|---------------------------|-------------|--------------------------|-------------|
|                           |   | <i>Aspergillus flavus</i> |             | <i>Aspergillus niger</i> |             |
|                           |   | 50 µg/Well                | 100 µg/Well | 50 µg/Well               | 100 µg/Well |
| <b>12a</b>                | C <sub>6</sub> H <sub>5</sub>                   | 15                        | 20          | 22                       | 25          |
| <b>12b</b>                | 2-MeOC <sub>6</sub> H <sub>4</sub>              | 5                         | 9           | 10                       | 12          |
| <b>12c</b>                | 3-OHC <sub>6</sub> H <sub>4</sub>               | 10                        | 14          | 16                       | 19          |
| <b>12d</b>                | 4-ClC <sub>6</sub> H <sub>4</sub>               | 20                        | 24          | 27                       | 29          |
| <b>12e</b>                | 2-OHC <sub>6</sub> H <sub>4</sub>               | 11                        | 15          | 18                       | 20          |
| <b>12f</b>                | 4-NO <sub>2</sub> C <sub>6</sub> H <sub>4</sub> | 23                        | 27          | 30                       | 33          |
| <b>12g</b>                | 4-FC <sub>6</sub> H <sub>4</sub>                | 22                        | 26          | 28                       | 31          |
| <b>12h</b>                | 4-OHC <sub>6</sub> H <sub>4</sub>               | 13                        | 17          | 19                       | 22          |
| <b>12i</b>                | 4-MeOC <sub>6</sub> H <sub>4</sub>              | 9                         | 11          | 13                       | 15          |
| <b>12j</b>                | 2-MeC <sub>6</sub> H <sub>4</sub>               | 2                         | 6           | 8                        | 11          |
| <b>12k</b>                | 4-MeC <sub>6</sub> H <sub>4</sub>               | 7                         | 10          | 11                       | 13          |
| <b>12l</b>                | 2-ClC <sub>6</sub> H <sub>4</sub>               | 19                        | 23          | 25                       | 28          |
| <b>12m</b>                | 3-FC <sub>6</sub> H <sub>4</sub>                | 18                        | 21          | 23                       | 26          |
| <b>12n</b>                | 4-BrC <sub>6</sub> H <sub>4</sub>               | 13                        | 18          | 21                       | 23          |
| Ketoconazole <sup>a</sup> | –   | 28                        | 31          | 33                       | 35          |

<sup>a</sup> Standard drug for the study.

Recently, Makhanya et al. reported the InCl<sub>3</sub>-catalyzed synthesis of fused indolo-pyrazoles (FIPs) **136** up to 96% yield. In this approach, FIPs **136** were successfully obtained through a three-component reaction between aromatic aldehydes **1**, thiosemicarbazide derivatives **23**, and indole **135** in the presence of a catalytic amount of InCl<sub>3</sub> in acetonitrile under reflux conditions (Scheme 18a) [122]. This approach shows a broad substrate scope and excellent functional group tolerance with diverse electron-rich and electron-deficient aromatic substrates. A plausible mechanism proposed by the authors is shown in Scheme 18b. The mechanism is triggered by the InCl<sub>3</sub>-catalyzed condensation reaction between aromatic aldehyde **1** and thiosemicarbazide derivative **23** to afford intermediate **137**. Thereafter, the [3+2] annulation reaction between indole **135** and Schiff base **137** and subsequent aromatization of the intermediate **138** enables the construction of a fused indolo-pyrazole scaffold. The antifungal activity was evaluated based on the diameter of the zone of inhibition (mm) against *Candida albicans*, *Candida utilis*, *Saccharomyces cerevisiae*, *Aspergillus flavus*, and *Aspergillus niger* using Amphotericin B as a standard drug. Overall, the compounds **136a–z** showed a diameter of growth of the inhibition zone ranging from 0 to 23 mm, in comparison to amphotericin-B (22 to 32 mm). Particularly, compound **136t** (R = 4-Cl, R<sup>1</sup> = Me) showed moderate potency against *Candida albicans* and *Candida utilis* with an inhibition diameter of 15 and 14 mm, respectively, while the compound **136x** (R = 4-MeO, R<sup>1</sup> = Me) showed good activity against *Saccharomyces cerevisiae* with an inhibition diameter of 20 mm, when compared to amphotericin-B (32, 30, and 29 mm, respectively).

Some spiropyrrolidine-oxindoles **29**, obtained from a three-component process and discussed in Section 2.1. Antibacterial (Table 6) [33], were also screened for their antifungal activity against *Candida albicans* and *Malassezia pachydermatis* using ketoconazole as a positive control (Table 40). Overall, the compounds showed a diameter of growth of the inhibition zone in the range of 9–12 mm and 8–10 mm for *Candida albicans* and *Malassezia pachydermatis*, respectively, when compared to ketoconazole (28 mm and 26 mm, respectively). Moreover, the compounds showed MIC values in the range of 125–500 µg/mL for *Candida albicans* and *Malassezia pachydermatis*, when compared to ketoconazole (MIC = 25 µg/mL). Remarkably, compound **29j** showed better activity against *Candida albicans* and *Malassezia pachydermatis* with a MIC value of 125 µg/mL. Unfortunately, the diameter of the growth of the inhibition zone for compound **29j** was not reported.



**Scheme 18.** (a) Three-component synthesis of fused indolo-pyrazoles **136** for evaluation of their antifungal activity, (b) plausible mechanism for the synthesis of compounds **136**.

**Table 40.** Antifungal activity of spiropyrrolidine-oxindoles **29**.

| Compound                  | R               | R <sup>1</sup>  | X               | <i>C. albicans</i> |                | <i>M. pachydermatis</i> |                |
|---------------------------|-----------------|-----------------|-----------------|--------------------|----------------|-------------------------|----------------|
|                           |                 |                 |                 | CPM (mm)           | MIC (µg/mL)    | CPM (mm)                | MIC (µg/mL)    |
| <b>29a</b>                | H               | H               | CH <sub>2</sub> | 10                 | 125            | 8                       | 500            |
| <b>29b</b>                | Allyl           | H               | CH <sub>2</sub> | – <sup>b</sup>     | 250            | – <sup>b</sup>          | 500            |
| <b>29c</b>                | <i>n</i> -Butyl | H               | CH <sub>2</sub> | – <sup>b</sup>     | 500            | – <sup>b</sup>          | – <sup>b</sup> |
| <b>29d</b>                | Me              | H               | CH <sub>2</sub> | – <sup>b</sup>     | – <sup>b</sup> | – <sup>b</sup>          | – <sup>b</sup> |
| <b>29e</b>                | Propargyl       | H               | CH <sub>2</sub> | 10                 | – <sup>b</sup> | 9                       | – <sup>b</sup> |
| <b>29f</b>                | H               | NO <sub>2</sub> | CH <sub>2</sub> | 11                 | 250            | – <sup>b</sup>          | 500            |
| <b>29g</b>                | H               | H               | S               | 9                  | 125            | 8                       | 250            |
| <b>29h</b>                | Allyl           | H               | S               | 12                 | 250            | 10                      | – <sup>b</sup> |
| <b>29i</b>                | Benzyl          | H               | S               | – <sup>b</sup>     | 500            | – <sup>b</sup>          | 500            |
| <b>29j</b>                | <i>n</i> -Butyl | H               | S               | – <sup>b</sup>     | 125            | – <sup>b</sup>          | 125            |
| <b>29k</b>                | Me              | H               | S               | – <sup>b</sup>     | – <sup>b</sup> | – <sup>b</sup>          | – <sup>b</sup> |
| Ketoconazole <sup>a</sup> | –               | –               | –               | 28                 | 25             | 26                      | 25             |

<sup>a</sup> Standard drug for the study. <sup>b</sup> Not determined.

All the pyrazole derivatives **9** and **10**, synthesized from four-component processes, each one, and discussed in Section 2.1. Antibacterial (Table 1) [27], were also screened against *Candida krusei*, *Aspergillus fumigatus*, and *Aspergillus niger* using the Broth microdilution method in the presence of griseofulvin and nystatin as standard drugs (Table 41). Overall, the compounds showed a good antifungal activity with MIC values in the range of 3.75–12.5 µg/mL against three strains of fungi, in comparison to griseofulvin (MIC = 1.25–3.12 µg/mL) and nystatin (MIC = 1.00–1.25 µg/mL). Notably, compounds **9c** and **10e** displayed better antifungal activity against *Candida krusei* with a MIC value of 3.75 µg/mL. In addition, the compounds **9e** and **10c** showed a MIC value of 3.75 µg/mL against *Aspergillus fumigatus* and *Aspergillus niger*, respectively, which were almost equally active compared to griseofulvin (MIC = 1.25 µg/mL) and nystatin (MIC = 1.00 µg/mL) as standard drugs.

**Table 41.** Antifungal evaluation of pyrazole derivatives **9** and **10**.

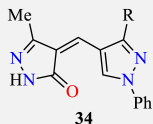
| Compound                  | R                                  | R <sup>1</sup> | MIC (µg/mL)           |                              |                          |
|---------------------------|------------------------------------|----------------|-----------------------|------------------------------|--------------------------|
|                           |                                    |                | <i>Candida krusei</i> | <i>Aspergillus fumigatus</i> | <i>Aspergillus niger</i> |
| <b>9a</b>                 | 2-OHC <sub>6</sub> H <sub>4</sub>  | Me             | 5.00                  | 6.25                         | 7.50                     |
| <b>9b</b>                 | 4-MeC <sub>6</sub> H <sub>4</sub>  | Me             | 7.50                  | 10.0                         | 12.5                     |
| <b>9c</b>                 | 4-MeOC <sub>6</sub> H <sub>4</sub> | Me             | 3.75                  | 5.00                         | 7.50                     |
| <b>9d</b>                 | C <sub>6</sub> H <sub>5</sub>      | Me             | 5.00                  | 6.25                         | 7.50                     |
| <b>9e</b>                 | 2-Furanyl                          | Me             | 10.0                  | 3.75                         | 7.50                     |
| <b>9f</b>                 | 2-OHC <sub>6</sub> H <sub>4</sub>  | EtO            | 12.5                  | 8.75                         | 6.25                     |
| <b>9g</b>                 | 4-MeC <sub>6</sub> H <sub>4</sub>  | EtO            | 8.75                  | 10.0                         | 7.50                     |
| <b>9h</b>                 | 4-MeOC <sub>6</sub> H <sub>4</sub> | EtO            | 8.75                  | 7.50                         | 6.25                     |
| <b>9i</b>                 | C <sub>6</sub> H <sub>5</sub>      | EtO            | 12.5                  | 10.0                         | 8.75                     |
| <b>9j</b>                 | 9-Anthracenyl                      | EtO            | 12.5                  | 5.00                         | 7.50                     |
| <b>9k</b>                 | 2-Furanyl                          | EtO            | 8.75                  | 7.50                         | 10.0                     |
| <b>10a</b>                | 2-OHC <sub>6</sub> H <sub>4</sub>  | Me             | 8.75                  | 7.50                         | 6.25                     |
| <b>10b</b>                | 4-MeC <sub>6</sub> H <sub>4</sub>  | Me             | 8.75                  | 12.5                         | 6.25                     |
| <b>10c</b>                | 4-MeOC <sub>6</sub> H <sub>4</sub> | Me             | 6.25                  | 10.0                         | 3.75                     |
| <b>10d</b>                | C <sub>6</sub> H <sub>5</sub>      | Me             | 7.50                  | 5.00                         | 8.75                     |
| <b>10e</b>                | 2-Furanyl                          | Me             | 3.75                  | 8.75                         | 12.5                     |
| Griseofulvin <sup>a</sup> | –                                  | –              | 3.12                  | 1.25                         | 1.25                     |
| Nystatin <sup>a</sup>     | –                                  | –              | 1.25                  | 1.00                         | 1.00                     |

<sup>a</sup> Positive control for the study.

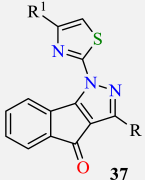
The synthesis of 4-[(3-aryl-1-phenyl-1*H*-pyrazol-4-yl)methylidene]-2,4-dihydro-3*H*-pyrazol-3-ones **34a–j** was reported by Sivaganesh et al. [35] and previously discussed in Section 2.1. Antibacterial (Table 7). The obtained compounds were also screened against *Aspergillus niger* and *Sclerotium rolfisii* fungal strains at a 500 µg/mL concentration by the disc diffusion method using ketoconazole as a standard drug (Table 42). These compounds showed acceptable activity against *Aspergillus niger* and *Sclerotium rolfisii* with a zone of inhibition in the range of 6.8–9.8 mm and 8.5–13.2 mm, respectively, when compared to ketoconazole (18.3 mm and 22.1 mm, respectively). Interestingly, compounds **34a** and **34j** showed the best antifungal potency against *Aspergillus niger* and *Sclerotium rolfisii* with a zone of inhibition of 9.8 mm and 13.2 mm, respectively. In addition, the compounds **34h**, **34c**, and **34a** displayed moderate activity against *Sclerotium rolfisii* with a zone of inhibition of 11.3, 12.0, and 12.8 mm, respectively.

In the same way, a series of 3-alkyl-1-(4-(aryl/heteroaryl)thiazol-2-yl)indeno[1,2-*c*]pyrazol-4(1*H*)-ones **37a–l** was reported by Mor et al. [36], and previously discussed in Section 2.1. Antibacterial (Table 8). These compounds were also screened for their antifungal activity against *Candida albicans* and *Aspergillus niger* showing MIC values in the range of 0.0067–0.0635 µmol/mL and 0.0270–0.1258 µmol/mL, respectively, when compared to fluconazole (MIC = 0.0408 µmol/mL) as a positive control (Table 43). Interestingly, the indenopyrazole **37d** displayed the highest potency against *Candida albicans* and *Aspergillus niger* with MIC values of 0.0067 and 0.0270 µmol/mL, respectively, in comparison to the standard drug fluconazole (MIC = 0.0408 µmol/mL).



**Table 42.** Antifungal activity of 4-[(3-aryl-1-phenyl-1H-pyrazol-4-yl)methylidene]-2,4-dihydro-3H-pyrazol-3-ones 34.


| Compound                  | R   | Zone of Inhibition (mm)  |                           |
|---------------------------|---|--------------------------|---------------------------|
|                           |   | <i>Aspergillus niger</i> | <i>Sclerotium rolfsii</i> |
| 34a                       | C <sub>6</sub> H <sub>5</sub>                       | 9.8                      | 12.8                      |
| 34b                       | 4-FC <sub>6</sub> H <sub>4</sub>                    | 8.2                      | 10.2                      |
| 34c                       | 4-ClC <sub>6</sub> H <sub>4</sub>                   | 6.9                      | 12.0                      |
| 34d                       | 4-BrC <sub>6</sub> H <sub>4</sub>                   | 7.7                      | 9.8                       |
| 34e                       | 4-MeC <sub>6</sub> H <sub>4</sub>                   | 8.0                      | 10.2                      |
| 34f                       | 4-MeOC <sub>6</sub> H <sub>4</sub>                  | 7.8                      | 8.5                       |
| 34g                       | 3-MeOC <sub>6</sub> H <sub>4</sub>                  | 6.8                      | 9.0                       |
| 34h                       | 4-OHC <sub>6</sub> H <sub>4</sub>                   | 6.9                      | 11.3                      |
| 34i                       | 4-NO <sub>2</sub> C <sub>6</sub> H <sub>4</sub>     | 7.9                      | 10.8                      |
| 34j                       | 2,4-(Cl) <sub>2</sub> C <sub>6</sub> H <sub>3</sub> | 8.9                      | 13.2                      |
| Ketoconazole <sup>a</sup> | –   | 18.3                     | 22.1                      |

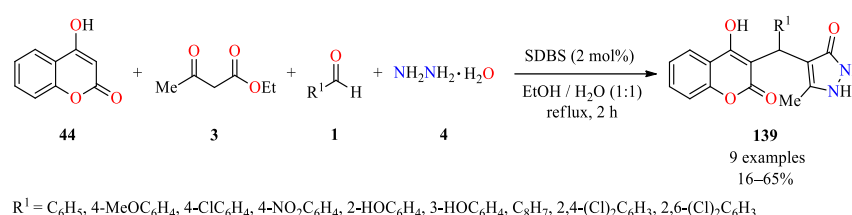
<sup>a</sup> Standard drug for the study.**Table 43.** Antifungal activity of 3-alkyl-1-(4-(aryl/heteroaryl)thiazol-2-yl)indeno[1,2-c]pyrazol-4(1H)-ones 37.


| Compound                 | R           | R <sup>1</sup> | MIC (μmol/mL)           |                          |
|--------------------------|-------------|----------------|-------------------------|--------------------------|
|                          |             |                | <i>Candida albicans</i> | <i>Aspergillus niger</i> |
| 37a                      | Me          | Biphenyl       | 0.0297                  | 0.0595                   |
| 37b                      | Et          | Biphenyl       | 0.0144                  | 0.1153                   |
| 37c                      | <i>i</i> Pr | Biphenyl       | 0.0139                  | 0.1118                   |
| 37d                      | <i>i</i> Bu | Biphenyl       | 0.0067                  | 0.0270                   |
| 37e                      | Me          | 2-Naphthyl     | 0.0635                  | 0.0635                   |
| 37f                      | Et          | 2-Naphthyl     | 0.0153                  | 0.1227                   |
| 37g                      | <i>i</i> Pr | 2-Naphthyl     | 0.0148                  | 0.0593                   |
| 37h                      | <i>i</i> Bu | 2-Naphthyl     | 0.0071                  | 0.0574                   |
| 37i                      | Me          | 2-Benzofuranyl | 0.0163                  | 0.0652                   |
| 37j                      | Et          | 2-Benzofuranyl | 0.0157                  | 0.1258                   |
| 37k                      | <i>i</i> Pr | 2-Benzofuranyl | 0.0151                  | 0.0607                   |
| 37l                      | <i>i</i> Bu | 2-Benzofuranyl | 0.0146                  | 0.0293                   |
| Fluconazole <sup>a</sup> | –           | –              | 0.0408                  | 0.0408                   |

<sup>a</sup> Standard drug for the study.

Alternatively, a one-pot multicomponent protocol has been described for the synthesis of various benzylpyrazolyl-coumarins **139** in 16–65% yields through a reaction of 4-hydroxycoumarin **44**, ethyl acetoacetate **3**, diverse aldehydes **1**, and hydrazine hydrate **4** catalyzed by sodium dodecyl benzene sulfonate (SDBS, 2 mol%) in an ethanol–water mixture at reflux for 2 h (Scheme 19) [123]. This new approach is distinguished by its short reaction time, recovery of the catalyst, and reuse without loss of activity. The synthesized compounds **139a–i** were screened against *Candida albicans* by the disk diffusion technique using ketoconazole as a standard drug. The compounds **139a–i** showed moderate antifungal activity with a diameter of the inhibition zone in the range of 7–11 mm at a 5 mg/mL

concentration, in comparison to ketoconazole (22  $\mu\text{g}/\text{mL}$ ). Moreover, the compounds **139a–i** showed MIC values ranging from  $\geq 125$  to  $\geq 500$   $\mu\text{g}/\text{mL}$  against *Candida albicans*, when compared to ketoconazole (6.25  $\mu\text{g}/\text{mL}$ ). Interestingly, the compound **139e** ( $R^1 = 2\text{-OHC}_6\text{H}_4$ ) showed the highest antifungal activity with a MIC value of  $\geq 125$   $\mu\text{g}/\text{mL}$ . Docking molecular was performed for compound **139e** and ketoconazole against *N*-myristoyl transferase (NMT) (PDB ID code: 1IYL) from *Candida albicans*. The compound **139e** showed better binding energy ( $-14.16$  kcal/mol) than the standard drug ketoconazole ( $-12.91$  kcal/mol). According to the docking calculations results, the phenyl ring of chromen-2-one and the 2-hydroxyphenyl moiety of compound **139e** formed  $\pi$ - $\pi$  interactions with Phe176 and Phe117. The hydroxyl group of chromen-2-one ring formed a hydrogen bond with Leu451. In addition, the oxygen atom and phenyl ring of the chromen-2-one moiety formed a hydrogen bond and  $\pi$ -anion interaction with Tyr107 and Leu451, respectively. Apart from this, multiple hydrophobic interactions were observed with crucial residues such as Val108 and Leu415.



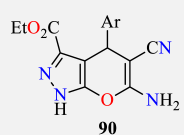
**Scheme 19.** One-pot four-component synthesis and antifungal activity of benzylpyrazolyl-coumarin derivatives **139**.

#### 2.4. Antioxidant Activity

Antioxidants are radical scavengers that help in delaying or preventing oxidation by trapping free radicals such as the superoxide radical ( $\text{O}_2^{\bullet-}$ ), hydroxyl radical ( $\text{OH}^{\bullet}$ ), and lipid peroxide radicals [124,125]. In consequence, they are essential to relieve the oxidative stress and production of reactive oxygen species (ROS), and subsequently decrease diverse degenerative diseases of aging [125,126]. Due to their protective roles in food and pharmaceutical products, the discovery of heterocyclic compounds with antioxidant properties continues to be of great interest to the scientific community. For instance, a series of dihydropyrano[2,3-*c*]pyrazole derivatives **90** was reported by Ambethkar et al. [82], and previously discussed in Section 2.1. Antibacterial (Table 24). These compounds were also screened for their antioxidant activity against 2,2-diphenyl-1-picrylhydrazyl (DPPH) radical scavenger at concentrations ranging from 25 to 100  $\mu\text{g}/\text{mL}$  using ascorbic acid as a reference (Table 44). Notably, the compounds **90i** and **90k** at a 100  $\mu\text{g}/\text{mL}$  concentration displayed significant scavenging capacity with 60.65% and 57.82% inhibition, respectively, when compared to the ascorbic acid (98.85%). These results revealed that the presence of a hydroxyl group at the *para* position could extend the  $\pi$ -conjugation for stabilizing the formed free radical.

A series of pyrazole-containing pyrimidines **52**, 1,4-dihydropyridines **53**, and imidazoles **54**, obtained via a multicomponent approach and previously discussed in Section 2.1. Antibacterial activity (Table 14) [58], were also screened for their antioxidant activity. In summary, the pyrimidine derivatives **52c** ( $R = \text{Cl}, R^1 = \text{Me}$ ) and **52f** ( $R = \text{F}, R^1 = \text{Me}$ ) displayed better DPPH radical scavenging activity with 89.41% and 83.34%, respectively, as compared to glutathione (89.09%). By comparing the antioxidant results, a gradual decrease in the activity of the acetyl ( $-\text{CO}-\text{Me}$ ) substituent was observed, followed by methoxy ( $-\text{CO}-\text{OMe}$ ) and ethoxy ( $-\text{CO}-\text{OEt}$ ) ester substituents. These results showed that modulation of the basic structure through ring substituents and/or additional functionalization decreases the antioxidant activity.

**Table 44.** Antioxidant activity of dihydropyrano[2,3-*c*]pyrazole derivatives **90**.

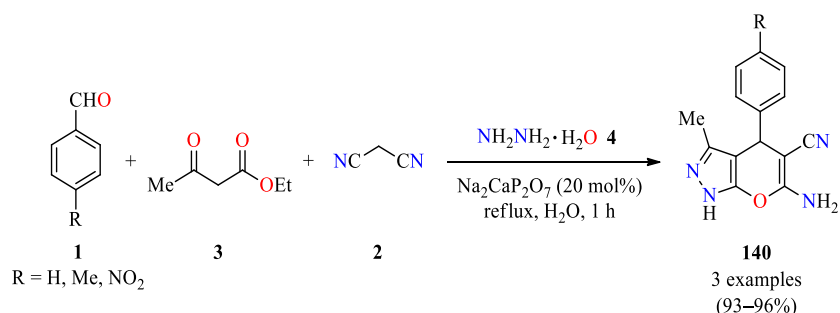
|  |   |                          |                          |                          |                           |
|--|---|--------------------------|--------------------------|--------------------------|---------------------------|
| Compound   | Ar  | % Inhibition at 25 µg/mL | % Inhibition at 50 µg/mL | % Inhibition at 75 µg/mL | % Inhibition at 100 µg/mL |
| <b>90a</b>   | C <sub>6</sub> H <sub>5</sub>                   | 16.16                    | 25.54                    | 37.23                    | 48.45                     |
| <b>90b</b>   | 4-MeC <sub>6</sub> H <sub>4</sub>               | 13.12                    | 23.64                    | 34.86                    | 43.84                     |
| <b>90c</b>   | 2-ClC <sub>6</sub> H <sub>4</sub>               | 15.52                    | 25.13                    | 38.52                    | 47.69                     |
| <b>90d</b>   | 4-ClC <sub>6</sub> H <sub>4</sub>               | 15.86                    | 25.23                    | 36.14                    | 45.70                     |
| <b>90e</b>   | 4-FC <sub>6</sub> H <sub>4</sub>                | 16.26                    | 25.17                    | 35.23                    | 46.81                     |
| <b>90f</b>   | 2-Furanyl                                       | 14.54                    | 21.22                    | 25.31                    | 32.21                     |
| <b>90g</b>   | 2-Thiophenyl                                    | 18.14                    | 26.46                    | 39.76                    | 42.11                     |
| <b>90h</b>   | 4-EtC <sub>6</sub> H <sub>4</sub>               | 14.14                    | 24.22                    | 30.52                    | 39.50                     |
| <b>90i</b>   | 4-HOC <sub>6</sub> H <sub>4</sub>               | 22.75                    | 30.46                    | 48.11                    | 60.65                     |
| <b>90j</b>   | 2-MeOC <sub>6</sub> H <sub>4</sub>              | 17.24                    | 26.61                    | 38.54                    | 49.41                     |
| <b>90k</b>   | 3-MeO-4-OHC <sub>6</sub> H <sub>3</sub>         | 21.62                    | 27.42                    | 45.12                    | 57.82                     |
| <b>90l</b>   | 4-MeOC <sub>6</sub> H <sub>4</sub>              | 17.64                    | 24.25                    | 34.36                    | 44.11                     |
| <b>90m</b>   | 4-NO <sub>2</sub> C <sub>6</sub> H <sub>4</sub> | 17.25                    | 28.41                    | 36.19                    | 45.64                     |
| Ascorbic acid <sup>a</sup>   | –   | 29.34                    | 55.84                    | 90.07                    | 98.85                     |

<sup>a</sup> Reference compound.

Additional to the antibacterial activity previously discussed in Table 2 (Section 2.1. Antibacterial activity) for the pyranopyrazole derivatives **12** obtained via a five-component synthesis [28], their DPPH and H<sub>2</sub>O<sub>2</sub> radical scavenging activity were also investigated using ascorbic acid as a standard drug. In a DPPH assay, the compounds **12a** (R = 4-MeOC<sub>6</sub>H<sub>4</sub>) and **12j** (R = 2-MeOC<sub>6</sub>H<sub>4</sub>) showed higher IC<sub>50</sub> values of 34.35 µg/mL and 35.93 µg/mL, respectively, when compared to the standard drug (39.51 µg/mL). In the H<sub>2</sub>O<sub>2</sub> radical scavenging assay, compound **12a** (38.71 µg/mL) displayed similar activity to standard ascorbic acid (39.47 µg/mL), whereas compound **12j** (44.05 µg/mL) exhibited moderate activity. Importantly, the results of DPPH and H<sub>2</sub>O<sub>2</sub> radical scavenging activity studies showed a linear correlation.

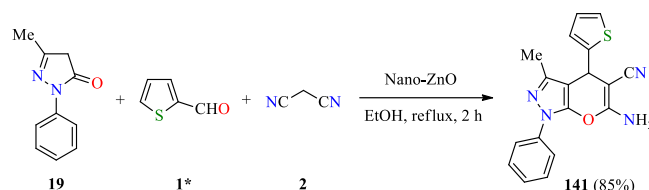
The pyrazolyl-dibenzo[*b,e*][1,4]diazepinones (**64–70a**) and (**71–77b**) were obtained via a multicomponent synthetic approach and previously discussed in Section 2.1. Antibacterial activity (Table 18) [70]. In addition, ferric reducing antioxidant power (FRAP) values were determined using Benzie and Strain's modified FRAP method. Overall, the compounds **65a** (R = R<sup>1</sup> = H, R<sup>2</sup> = 4-MeC<sub>6</sub>H<sub>4</sub>O), **77b** (R = H, R<sup>1</sup> = Me, R<sup>2</sup> = PhCH<sub>2</sub>S), and **75b** (R = H, R<sup>1</sup> = Me, R<sup>2</sup> = 4-ClC<sub>6</sub>H<sub>4</sub>S) registered better FRAP values with 459, 464, and 468 (mm/100 g), respectively, indicating that they are good in resistance to the reduction of the ferric tripyridyl triazine (Fe(III)-TPTZ) complex into a blue color ferrous tripyridyl triazine (Fe(II)-TPTZ) complex.

Recently, the Na<sub>2</sub>CaP<sub>2</sub>O<sub>7</sub>-catalyzed synthesis of pyrano[2,3-*c*]pyrazoles derivatives **140** has been successfully implemented through a four-component reaction of aromatic aldehydes **1**, ethyl acetoacetate **3**, malononitrile **2**, and hydrazine hydrate **4** in refluxing water for 1 h (Scheme 20) [127]. In the DPPH assay, the compounds **140a** (R = H) and **140b** (R = Me) showed significant scavenging effects, while the compound **140c** (R = NO<sub>2</sub>) displayed a very low effect. In addition, the pyrano[2,3-*c*]pyrazole derivatives **140** had cytoprotective properties against the harmful effects of stressors, such as H<sub>2</sub>O<sub>2</sub> and SNP (sodium nitroprusside) by quenching free radicals, while improving the activities of antioxidant enzymes.



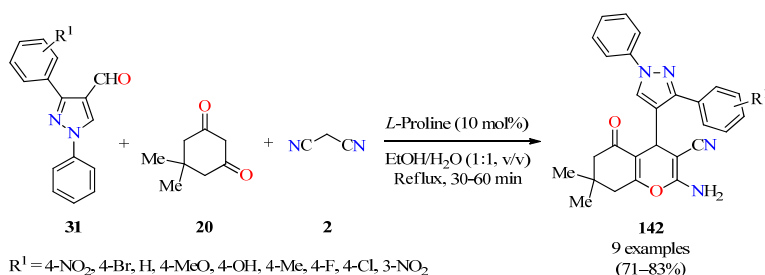
**Scheme 20.**  $\text{Na}_2\text{CaP}_2\text{O}_7$ -Catalyzed four-component synthesis of pyrano[2,3-*c*]pyrazole derivatives **140** and evaluation of their antioxidant activity.

Very recently, the nano-ZnO-catalyzed reaction of 5-methyl-2-phenyl-2,4-dihydro-3*H*-pyrazol-3-one **19**, thiophene-2-carbaldehyde **1\***, and malononitrile **2** in refluxing ethanol for 2 h has been reported for the synthesis of the pyrano 2,3-*c*]pyrazole-5-carbonitrile **141** in 85% yield (Scheme 21) [128]. Although the scope of the reaction was not further studied, compound **141** was used in the construction of an important library of highly functionalized pyrano[2,3-*c*]pyrazole derivatives without using a multicomponent approach. The synthesized compound **141** was screened for its antioxidant activity. As a result, it exhibited a total antioxidant activity of 22.26 U/mL, which is similar to standard ascorbic acid (29.40 U/mL).



**Scheme 21.** Three-component synthesis of the pyrano[2,3-*c*]pyrazole-5-carbonitrile **141** and evaluation of its antioxidant activity.

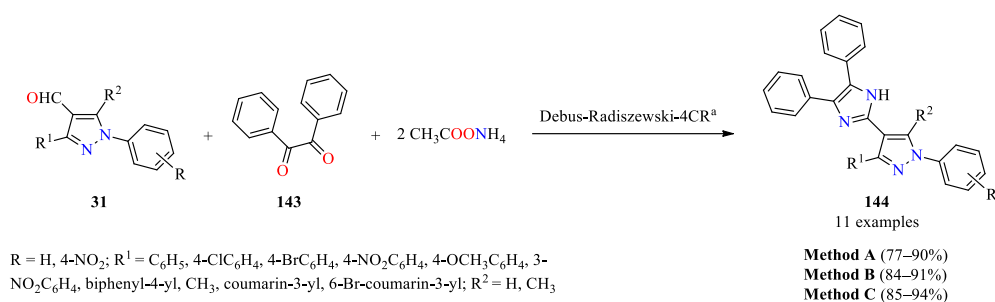
The eco-friendly three-component reaction of 3-aryl-1-phenyl-1*H*-pyrazole-4-carbaldehydes **31**, dimedone **20**, and malononitrile **2** catalyzed by *L*-proline (10 mol%) in refluxing aqueous ethanol for 30–60 min has been reported for the synthesis of tetrahydrobenzo[*b*]pyran derivatives **142** (Scheme 22) [129]. The solids were filtered and washed with a mixture of ethanol/water (1:1, *v/v*) to afford pyrazole derivatives **142** in 71–83% yields. All the synthesized compounds **142a–i** were screened for their antioxidant activity against the 2,2-diphenyl-1-picrylhydrazyl (DPPH) radical scavenger at the concentration of 1.0 mM using ascorbic acid as a positive control. Notably, the compounds **142a** ( $\text{R}^1 = 4\text{-NO}_2$ ) and **142b** ( $\text{R}^1 = 4\text{-Br}$ ) at a 1.0 mM concentration showed better scavenging capacity with 61.87% and 60.62% inhibition, respectively, when compared to the ascorbic acid (72.00%).



**Scheme 22.** Three-component synthesis of tetrahydrobenzo[*b*]pyran derivatives **142** with antioxidant activity.

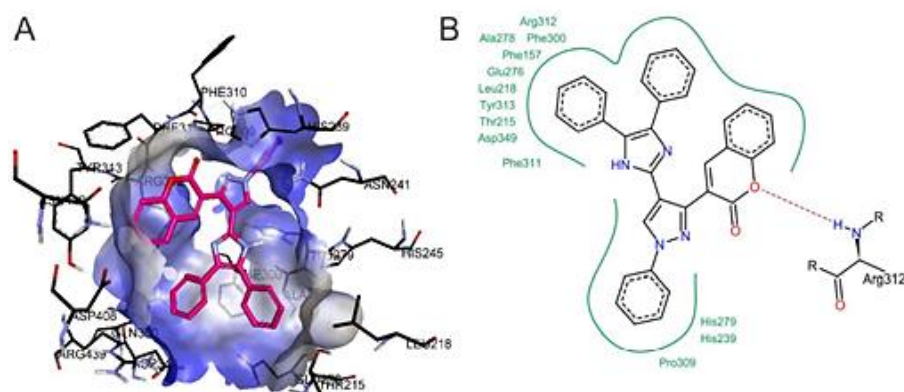
### 2.5. $\alpha$ -Glucosidase and $\alpha$ -Amylase Inhibitory Activity

Type 2 diabetes is the most common form of diabetes, which is a challenging metabolic disease characterized by insulin resistance, leading to hyperglycemia or abnormal blood glucose levels and damage to various physiological processes in the body [130]. The significant increase in the number of people affected by this disease and its worldwide spread makes blood glucose control very complex in patients affected by type 2 diabetes [131,132]. Other problems are the side effects of antidiabetic drugs currently used for its treatment [133,134]. One aspect to be taken into account in the development of new antidiabetic drugs is the relationship between diabetes mellitus and the inhibition of hydrolase enzymes such as  $\alpha$ -glucosidases and  $\alpha$ -amylases, showing that the incorporation ofazole-type heterocycles such as pyrazole, imidazole, and triazole, among others, is required in the design of new antihyperglycemic agents with higher activity than acarbose [135]. For instance, Chaudhry et al. described a multicomponent Debus–Radiszewski reaction to efficiently prepare imidazolylpyrazoles **144** in 77–90% yields from pyrazole-4-carbaldehydes **31** obtained by the Vilsmeier–Haack formylation reaction [24,136], benzil **143**, and ammonium acetate in refluxing acetic acid for 2 h (Scheme 23). The same reaction was conducted under microwave heating using a domestic oven to afford products **144** in 84–91% yields after short reaction times (2–3 min) [137]. Finally, the use of glutamic acid (15 mol%) as a catalyst at reflux for 15–20 min furnished products **144** in 85–94% yields.



**Scheme 23.** Pseudo four-component synthesis of imidazolylpyrazoles **144** as  $\alpha$ -glucosidase inhibitors.

In vitro  $\alpha$ -glucosidase inhibition assays of imidazolylpyrazoles **144a–k** showed an inhibitory effect compared to control acarbose ( $\text{IC}_{50} = 38.25 \mu\text{M}$ ), with the most potent inhibitors being those that contain substituents such as the coumarinyl ring, which exhibited percentages of inhibition at 98.56% (0.5 mM) with an  $\text{IC}_{50}$  value of 2.78  $\mu\text{M}$  in compound **144j** ( $\text{R}^1 = \text{coumarin-3-yl}$ ,  $\text{R} = \text{R}^2 = \text{H}$ ) and 97.69% (0.5 mM) with an  $\text{IC}_{50}$  value of 2.95  $\mu\text{M}$  in compound **144k** ( $\text{R}^1 = 6\text{-Br-coumarin-3-yl}$ ,  $\text{R} = \text{R}^2 = \text{H}$ ) [137]. According to molecular docking studies, the activity of the compound **144j** can be explained through a hydrogen bond interaction between the oxygen atom of the coumarin ring and Arg312 at the active site of the oligo-1,6-glucosidase (PDB ID: 3A4A) from *Saccharomyces cerevisiae* (Figure 10). The imidazolylpyrazoles containing electron-withdrawing groups such as  $\text{R}^1 = 4\text{-ClC}_6\text{H}_4$  (**144b**),  $4\text{-BrC}_6\text{H}_4$  (**144c**), and  $4\text{-NO}_2\text{C}_6\text{H}_4$  (**144h**), where  $\text{R}$  and  $\text{R}^2 = \text{H}$ , have markedly improved activity via the binding of the substrate with the target positions. Therefore, the comparative study has helped to find some key structural elements that could give rise to promising anti-diabetic compounds.



**Figure 10.** (A) Overall structure of the oligo-1,6-glucosidase (PDB ID: 3A4A) from *Saccharomyces cerevisiae* with compound **144j**, and (B) 2D interactions for compound **144j**. Image adapted from Chaudhry et al. [137].

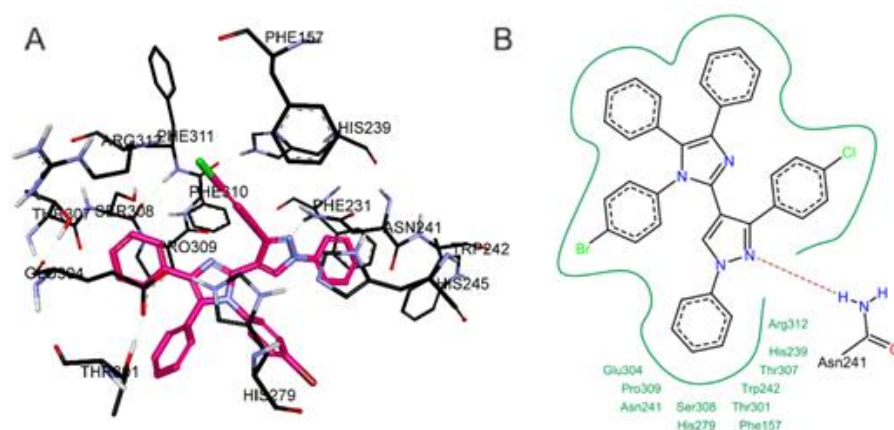
The same authors carried out structural modifications to generate imidazole–pyrazole hybrids as potent  $\alpha$ -glucosidase inhibitors [138]. Thus, the multicomponent Debus–Radziszewski reaction of pyrazole-4-carbaldehydes **31**, benzyl **143**, substituted anilines **32**, and ammonium acetate under microwave irradiation afforded a series of imidazole–pyrazole hybrids **145** in 69–88% yields. This multicomponent approach shows high compatibility with pyrazole-4-carbaldehydes **31** containing electron-donating and electron-withdrawing groups. The imidazolypyrazoles **145** were screened against  $\alpha$ -glucosidase using acarbose as a standard drug (Table 45). In particular, the compounds containing electron-withdrawing substituents such as **145f** and **145m** showed a better inhibitory effect with  $IC_{50}$  values of 25.19  $\mu$ M and 33.62  $\mu$ M, respectively, when compared to acarbose ( $IC_{50}$  = 38.25  $\mu$ M).

**Table 45.** Multicomponent Debus–Radziszewski synthesis of imidazolypyrazoles **145** as  $\alpha$ -glucosidase inhibitors.

| Compound              | R                 | R <sup>1</sup>        | Yield of <b>145</b> (%) | $\alpha$ -Glucosidase Inhibition |                      |
|-----------------------|-------------------|-----------------------|-------------------------|----------------------------------|----------------------|
|                       |                   |                       |                         | Percentage Inhibition (%)        | $IC_{50}$ ( $\mu$ M) |
| <b>145a</b>           | 4-MeO             | 4-MeO                 | 75                      | 99.56                            | 178.82               |
| <b>145b</b>           | 4-MeO             | 4-Br                  | 70                      | 91.12                            | 162.93               |
| <b>145c</b>           | 4-MeO             | 3,5-(Me) <sub>2</sub> | 81                      | 96.13                            | 182.17               |
| <b>145d</b>           | 4-Cl              | 4-MeO                 | 78                      | 98.65                            | 168.92               |
| <b>145e</b>           | 4-Cl              | 4-Cl                  | 69                      | 93.19                            | 85.71                |
| <b>145f</b>           | 4-Cl              | 4-Br                  | 73                      | 96.21                            | 25.19                |
| <b>145g</b>           | 4-Cl              | 3,5-(Me) <sub>2</sub> | 84                      | 89.54                            | 132.81               |
| <b>145h</b>           | 4-Br              | 4-MeO                 | 82                      | 89.76                            | 104.75               |
| <b>145i</b>           | 4-Br              | 4-Cl                  | 71                      | 87.25                            | 84.61                |
| <b>145j</b>           | 4-Br              | 3,5-(Me) <sub>2</sub> | 81                      | 75.23                            | 412.42               |
| <b>145k</b>           | 3-NO <sub>2</sub> | 4-Cl                  | 77                      | 96.76                            | 42.23                |
| <b>145l</b>           | 3-NO <sub>2</sub> | 4-MeO                 | 84                      | 95.79                            | 43.14                |
| <b>145m</b>           | 3-NO <sub>2</sub> | 4-Br                  | 81                      | 97.52                            | 33.62                |
| <b>145n</b>           | 3-NO <sub>2</sub> | 3,5-(Me) <sub>2</sub> | 88                      | 91.25                            | 58.73                |
| Acarbose <sup>b</sup> | –                 | –                     | –                       | 92.23                            | 38.25                |

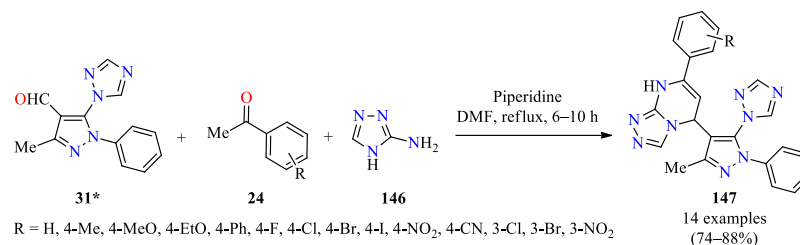
<sup>a</sup> Reaction conditions: Pyrazole-4-carbaldehydes **31**, benzyl **143**, substituted anilines **32**, and ammonium acetate, AcOH, MWI. <sup>b</sup> Reference compound.

Later, a homology model was constructed using oligo-1,6-glucosidase (PDB ID: 3A4A) from *Saccharomyces cerevisiae* as the protein template because it exhibits one of the best results and also shares 72% identity and 85% similarity of the  $\alpha$ -glucosidase sequence. Figure 11 shows 3D and 2D interactions of the most likely coupled conformation of the compound **145f** with the homology model. It was found that imidazolopyrazole **145f** presented a significant fit to the binding cavity, with the hydrogen bond interaction between the unsubstituted nitrogen atom of the pyrazole ring and Asn241 being important [138].

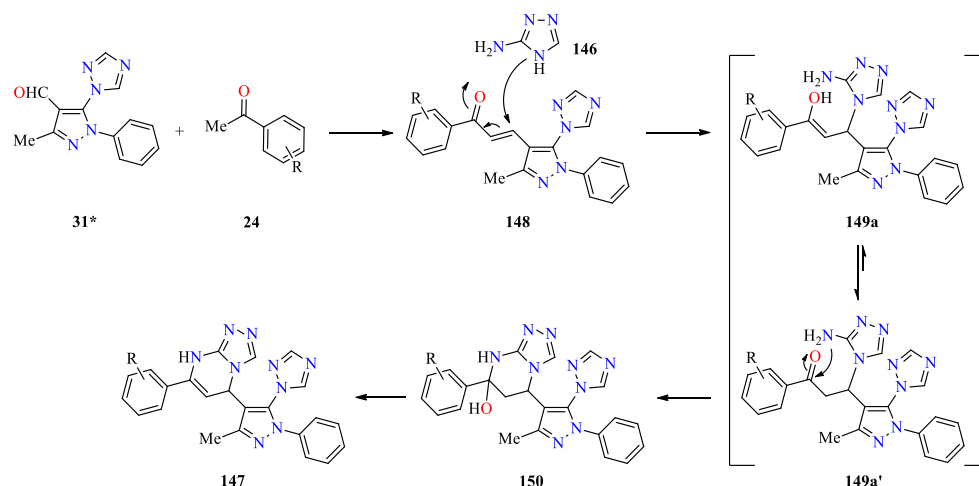


**Figure 11.** (A) The overall structure of the oligo-1,6-glucosidase (PDB ID: 3A4A) from *Saccharomyces cerevisiae* with compound **145f**, and (B) 2D interactions for compound **145f**. Image adapted from Chaudhry et al. [138].

Remarkably, Pogaku et al. described an interesting one-pot multicomponent approach to synthesize new pyrazole-triazolopyrimidine hybrids **147** as potent  $\alpha$ -glucosidase inhibitors (Scheme 24) [139]. The synthesis of compounds involved an optimization process varying the base, solvent, and reaction time. Thus, the one-pot three-component reaction of pyrazole-4-carbaldehydes **31\***, substituted acetophenones **24**, 4*H*-1,2,4-triazol-3-amine **146**, and a slight excess of piperidine in refluxing DMF for 6–10 h afforded pyrazole-triazolopyrimidine hybrids **147** in 74–88% yields. The plausible mechanism for the synthesis of pyrazole derivatives **147** is illustrated in Scheme 25. Initially, Claisen–Schmidt condensation of pyrazole-4-carbaldehydes **31\*** with substituted acetophenones **24** afforded chalcones **148**, which subsequently reacted with 4*H*-1,2,4-triazol-3-amine **146** to generate enol/keto intermediates **149a/149a'**. Finally, keto forms suffered an intramolecular cyclization/dehydration sequence to give pyrazole-triazolopyrimidine hybrids **147**.



**Scheme 24.** Three-component synthesis of pyrazole-triazolopyrimidine hybrids **147** as  $\alpha$ -glucosidase inhibitors.



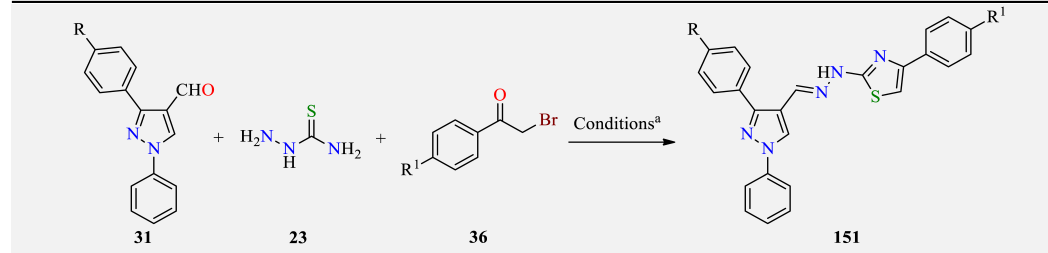
**Scheme 25.** The plausible mechanism for the synthesis of pyrazole-triazolopyrimidine hybrids **147**.

The synthesized compounds **147** were tested against  $\alpha$ -glucosidase using acarbose as a standard drug [139]. It was observed that compounds substituted with electron-withdrawing groups on the phenyl ring showed higher inhibitory activity against  $\alpha$ -glucosidase than compounds with electron-donating groups. Among them, the compounds **147h** (R = 4-Cl), **147f** (R = 4-F), and **147i** (R = 4-NO<sub>2</sub>) exhibited the highest inhibitory activity with IC<sub>50</sub> values of 12.45, 14.47, and 17.27  $\mu$ M, when compared to acarbose (IC<sub>50</sub> = 12.68  $\mu$ M). Moreover, in silico docking studies of the ligand **147h** with the active site of the  $\alpha$ -glucosidase (PDB ID: 3WY1) were performed using the GOLD 5.6 tool. From the two chains of  $\alpha$ -glucosidase, the A chain with the polyacrylic acid as the crystalline co-ligand was selected. The compound **147h** forms hydrophobic, van der Waals, and hydrogen bond interactions with various amino acids of the active site of  $\alpha$ -glucosidase. The formation of a hydrogen bond between the nitrogen atom of the triazole and the oxygen atom of the Asp202 was observed, as well as a hydrogen bond between Asp62 and the nitrogen atom of the pyrazole moiety. In addition, the residue Asp333 forms two hydrogen bonds with nitrogen atoms of triazole and pyrimidine rings.

In 2019, Duhan et al. described the three-component synthesis of thiazole-clubbed pyrazole hybrids **151** from 1-aryl-3-phenyl-1H-pyrazole-4-carbaldehydes **31**, thiosemicarbazide **23**, and substituted  $\alpha$ -bromoacetophenones **36** in refluxing EtOH for 5 min (Table 46) [140]. The formed solids were filtered, dried, and recrystallized from ethanol to afford thiazole–pyrazole hybrids **151** in 71–89% yields after short reaction times. All synthesized pyrazole derivatives **151** were screened for their  $\alpha$ -amylase activity at three different concentrations (12.5, 25, and 50  $\mu$ g/mL) using acarbose as a standard drug. At a 50  $\mu$ g/mL concentration, the synthesized compounds **151a–r** exhibited a percentage of inhibition in the range from 70.04% to 89.15%, when compared to acarbose (77.96%). In particular, the compounds **151g** and **151h** displayed a significant percentage of inhibition with values of 89.15% and 88.42%, respectively, in comparison to acarbose (77.96%).

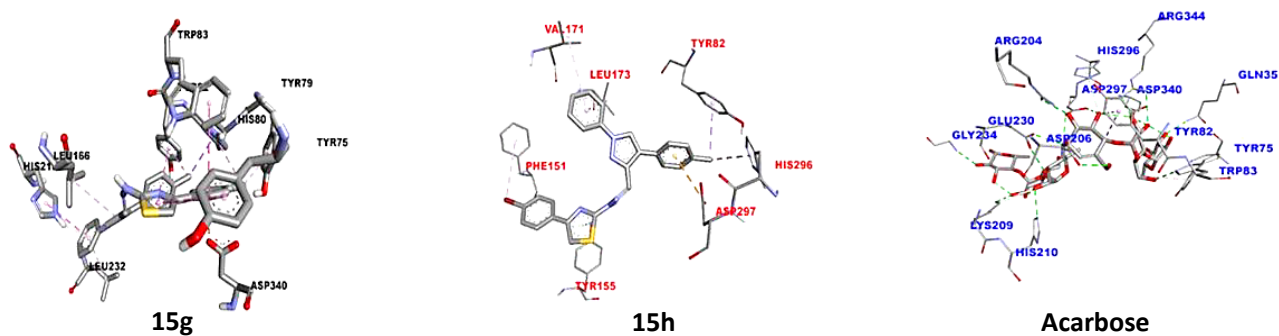
Additionally, molecular docking studies of the most potent compounds **151g** and **151h** were performed with the active site residues of *Aspergillus oryzae*  $\alpha$ -amylase (PDB ID: 7TAA) to establish the binding conformation and interactions associated with the activity [140]. As shown in Figure 12, compound **151g** showed four hydrophobic, one hydrogen bond, and one electrostatic interaction, while compound **151h** displayed one electrostatic, one hydrogen bond, and eleven hydrophobic interactions. As a result, the binding interactions found for compounds **151g** and **151h** with  $\alpha$ -amylase were similar to those responsible for  $\alpha$ -amylase inhibition by acarbose.



**Table 46.** Three-component synthesis and  $\alpha$ -amylase activity of thiazole–pyrazole hybrids **151**.


| Compound              | R   | R <sup>1</sup>  | Yield <b>151</b> (%) | % Inhibition at 12.5 $\mu$ g/mL | % Inhibition at 25 $\mu$ g/mL | % Inhibition at 50 $\mu$ g/mL |
|-----------------------|-----|-----------------|----------------------|---------------------------------|-------------------------------|-------------------------------|
| <b>151a</b>           | Br  | Br              | 85                   | 56.80                           | 61.21                         | 82.72                         |
| <b>151b</b>           | Br  | Cl              | 80                   | 61.03                           | 68.38                         | 80.33                         |
| <b>151c</b>           | Br  | NO <sub>2</sub> | 88                   | 68.57                           | 71.51                         | 82.90                         |
| <b>151d</b>           | MeO | Br              | 82                   | 58.82                           | 67.46                         | 79.04                         |
| <b>151e</b>           | MeO | Cl              | 80                   | 69.49                           | 75.55                         | 82.17                         |
| <b>151f</b>           | MeO | NO <sub>2</sub> | 89                   | 55.15                           | 64.71                         | 77.94                         |
| <b>151g</b>           | Me  | Br              | 85                   | 65.81                           | 72.06                         | 89.15                         |
| <b>151h</b>           | Me  | Cl              | 87                   | 62.13                           | 71.69                         | 88.42                         |
| <b>151i</b>           | Me  | NO <sub>2</sub> | 83                   | 48.35                           | 52.21                         | 79.96                         |
| <b>151j</b>           | F   | Br              | 79                   | 57.35                           | 70.59                         | 81.25                         |
| <b>151k</b>           | F   | Cl              | 86                   | 60.29                           | 64.71                         | 77.21                         |
| <b>151l</b>           | F   | NO <sub>2</sub> | 78                   | 55.33                           | 67.83                         | 86.03                         |
| <b>151m</b>           | Cl  | Br              | 71                   | 67.28                           | 76.84                         | 83.82                         |
| <b>151n</b>           | Cl  | Cl              | 83                   | 68.87                           | 71.32                         | 84.74                         |
| <b>151o</b>           | Cl  | NO <sub>2</sub> | 83                   | 56.07                           | 67.10                         | 81.99                         |
| <b>151p</b>           | H   | Br              | 81                   | 52.39                           | 61.40                         | 75.18                         |
| <b>151q</b>           | H   | Cl              | 82                   | 40.99                           | 58.82                         | 70.04                         |
| <b>151r</b>           | H   | NO <sub>2</sub> | 87                   | 52.94                           | 60.48                         | 78.13                         |
| Acarbose <sup>b</sup> | –   | –               | –                    | 67.25                           | 71.17                         | 77.96                         |

<sup>a</sup> Reaction conditions: 1-aryl-3-phenyl-1H-pyrazole-4-carbaldehydes **31** (1 mmol), thiosemicarbazide **23** (1.1 mmol), and substituted  $\alpha$ -bromoacetophenones **36** (1 mmol), EtOH (10 mL), reflux, 5 min. <sup>b</sup> Reference compound.



**Figure 12.** 3D Interactions of compounds **151g**, **151h**, and acarbose with binding sites of *Aspergillus oryzae*  $\alpha$ -amylase (PDB ID: 7TAA). Image adapted from Duhan et al. [140].

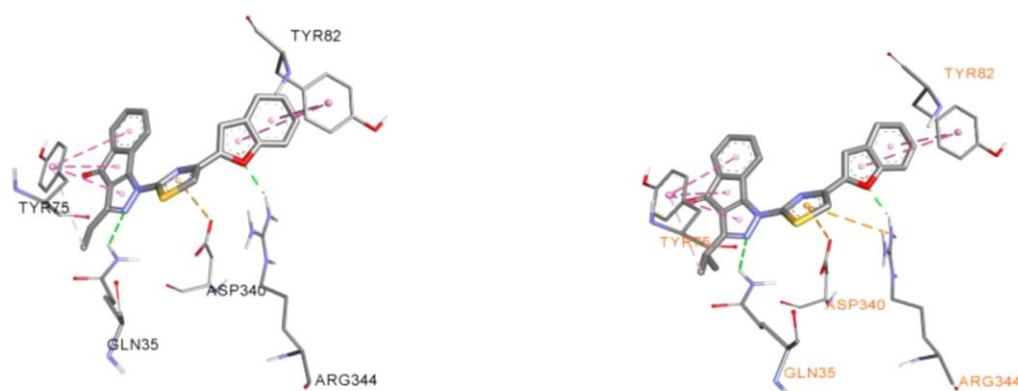
On the other hand, a series of 3-alkyl-1-(4-(aryl/heteroaryl)thiazol-2-yl)indeno[1,2-*c*]pyrazol-4(1*H*)-ones **37a–l** was obtained via the one-pot three-component approach discussed in Section 2.1. Antibacterial activity (Table 8) [36]. The pyrazole derivatives **37a–l** were also screened for their  $\alpha$ -amylase activity by using the starch-iodine method in the presence of acarbose as a standard drug (Table 47). Overall, compounds **37a–l** showed IC<sub>50</sub> values in the range of 0.46–20.51  $\mu$ M, when compared to acarbose (IC<sub>50</sub> = 0.11  $\mu$ M). Interestingly, compounds **37j** and **37k** resulted in being the best inhibitors of  $\alpha$ -amylase with IC<sub>50</sub> values of 0.79  $\mu$ M and 0.46  $\mu$ M, respectively. In addition, the compounds **37i** and **37l** displayed good inhibitory activity with IC<sub>50</sub> values of 0.94  $\mu$ M and 0.89  $\mu$ M, respectively, whereas the compounds **37a**, **37e**, **37f**, and **37h** were found to be moderately active with IC<sub>50</sub> values in the range of 3.21–6.88  $\mu$ M. To determine the binding conformation, molecular docking for indenopyrazoles **37j** and **37k** was performed in the active site of *Aspergillus*

*oryzae*  $\alpha$ -amylase (PDB ID: 7TAA). The binding affinity of compounds **37j**, **37k**, and acarbose are  $-8.7$ ,  $-9.0$ , and  $-10.1$  kcal/mol, respectively. As shown in Figure 13, the oxygen atom of the benzofuran ring forms a hydrogen bond with Arg344, while the nitrogen atom of the pyrazole ring interacts with Gln35 via a hydrogen bond. The indenopyrazole and benzofuran ring form  $\pi$ - $\pi$  stacked interactions with Tyr75 and the aromatic ring of the Tyr82, respectively. Finally, the thiazole ring forms  $\pi$ -anion interactions with Asp340 in both compounds, and  $\pi$ -cation interactions with Arg344 only in compound **37k**.

**Table 47.**  $\alpha$ -Amylase activity of 3-alkyl-1-(4-(aryl/heteroaryl)thiazol-2-yl)indeno[1,2-*c*]pyrazol-4(1*H*)-ones **37**.

| Compound              | R           | R <sup>1</sup> | IC <sub>50</sub> ( $\mu$ M) |
|-----------------------|-------------|----------------|-----------------------------|
| <b>37a</b>            | Me          | Biphenyl       | 5.29                        |
| <b>37b</b>            | Et          | Biphenyl       | 10.05                       |
| <b>37c</b>            | <i>i</i> Pr | Biphenyl       | 20.51                       |
| <b>37d</b>            | <i>i</i> Bu | Biphenyl       | 10.78                       |
| <b>37e</b>            | Me          | 2-Naphthyl     | 6.88                        |
| <b>37f</b>            | Et          | 2-Naphthyl     | 4.17                        |
| <b>37g</b>            | <i>i</i> Pr | 2-Naphthyl     | 18.31                       |
| <b>37h</b>            | <i>i</i> Bu | 2-Naphthyl     | 3.21                        |
| <b>37i</b>            | Me          | 2-Benzofuranyl | 0.94                        |
| <b>37j</b>            | Et          | 2-Benzofuranyl | 0.79                        |
| <b>37k</b>            | <i>i</i> Pr | 2-Benzofuranyl | 0.46                        |
| <b>37l</b>            | <i>i</i> Bu | 2-Benzofuranyl | 0.89                        |
| Acarbose <sup>a</sup> | –           | –              | 0.11                        |

<sup>a</sup> Reference compound.



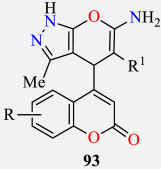
**Figure 13.** 3D Interactions of indenopyrazoles **37j** (left) and **37k** (right) with binding sites of *Aspergillus oryzae*  $\alpha$ -amylase (PDB ID: 7TAA). Image adapted from Mor et al. [36].

## 2.6. Anti-Inflammatory Activity

Inflammation is part of the complex biological response of vascular tissues to harmful stimuli, such as pathogens, damaged cells, or irritants [141,142]. Essentially, inflammation involves the production of pro-inflammatory mediators, an influx of innate immune cells, and tissue destruction [141,142]. In this sense, steroidal and non-steroidal anti-inflammatory drugs have been extensively employed to inhibit the production of pro-inflammatory prostaglandins (PGs) [143]. In recent decades, NSAIDs have become a widely used therapeutic group due to fewer adverse effects or other side effects such as

renal impairment and gastric ulcers [143]. In consequence, the development of efficient and safer anti-inflammatory drugs is still highly desired in chemical biology and drug design. In this way, the series of 4-coumarinylpyrano[2,3-*c*]pyrazole derivatives **93**, obtained via a one-pot four-component approach and discussed in Section 2.1. Antibacterial activity (Table 26) [87], was also subjected to an anti-inflammatory effect against the denaturation of hen's egg albumin method at the concentration of 31.25  $\mu\text{M}$  with aceclofenac as a standard drug (Table 48). Compounds **93** showed very high activity against the denaturation of protein with inhibition percentages ranging from 7.60% to 51.43%. Remarkably, the compounds **93g**, **93h**, and **93j** showed excellent activity with inhibition percentages of 51.43%, 39.06%, and 37.65%, respectively, which are more active compared to the standard aceclofenac drug (5.50%). Moreover, the anti-inflammatory activity was also screened using the Human Red Blood Cell (HRBC) membrane stabilization technique at the concentration of 100  $\mu\text{M}$  with the standard acetyl salicylic acid drug. Notably, the compounds **93g**, **93h**, and **93j** exhibited good activity with inhibition percentages of 54.06%, 39.86%, and 38.56%, respectively, in comparison with the standard acetyl salicylic acid drug (36.16%).

**Table 48.** Anti-inflammatory activity of 4-coumarinylpyrano[2,3-*c*]pyrazoles **93**.

| <br><b>93</b> |           |                |  |  |
|--|-----------|----------------|--|--|
| Compound   | R         | R <sup>1</sup> | % Inhibition of Egg Albumin in 31.25 $\mu\text{M}$ | % Inhibition of Erythrocyte in 100 $\mu\text{M}$ |
| <b>93a</b>   | 6-Me      | CN             | 10.33  | 28.36  |
| <b>93b</b>   | 6-MeO     | CN             | 19.13  | 32.66  |
| <b>93c</b>   | 6-Cl      | CN             | 28.04  | 36.06  |
| <b>93d</b>   | 7-Me      | CN             | 7.60   | 28.16  |
| <b>93e</b>   | 7,8-Benzo | CN             | 14.44  | 28.86  |
| <b>93f</b>   | 6-Me      | COOEt          | 24.82  | 36.06  |
| <b>93g</b>   | 6-MeO     | COOEt          | 51.43  | 54.06  |
| <b>93h</b>   | 6-Cl      | COOEt          | 39.06  | 39.86  |
| <b>93i</b>   | 7-Me      | COOEt          | 28.67  | 36.16  |
| <b>93j</b>   | 7,8-Benzo | COOEt          | 37.65  | 38.56  |
| Acceclofenac <sup>a</sup>  | –         | –              | 5.50   | –  |
| Acetyl salicylic acid <sup>a</sup>   | –         | –              | –  | 36.16  |

<sup>a</sup> Reference compound.

The thiazolo[2,3-*b*]dihydropyrimidinones **80a–p**, obtained via a three-component synthetic approach and discussed in Section 2.1. Antibacterial activity (Table 19) [72], was also screened for its anti-inflammatory activity using the carrageenan-induced paw edema method of inflammation in rats at successive intervals of 1, 2, and 4 h compared with the standard indomethacin drug. The tested compounds **80a–p** exhibited moderate anti-inflammatory activity within 2 h, while the activity increased and reached peak level at 4 h and declined after 4 h. Remarkably, the compounds **80a** (R = 3-F-4-Me, R<sup>1</sup> = R<sup>2</sup> = Cl), **80e** (R = 3-F-4-Me, R<sup>1</sup> = R<sup>2</sup> = F), and **80i** (R = 3-F-4-Me, R<sup>1</sup> = Cl, R<sup>2</sup> = H) showed potent anti-inflammatory activity at 4 h with 85.33%, 81.32%, and 80.75% inhibition of the edema, respectively, which is comparable with the standard indomethacin drug (86.76%). Later, the synthesized compounds **80a–p** were docked into the active sites of the COX-2 enzyme. The molecular docking revealed that compounds **80a**, **80e**, and **80i** were more selective towards the COX-2 active site with calculated binding energy of  $-540.47$ ,  $-315.73$ , and  $-129.88$  kcal/mol, respectively, involving a hydrogen bonding between the nitrogen atom of the pyrimidine ring and hydrogen atom of the amino group into ARG 120. These results are in good agreement with experimental results.

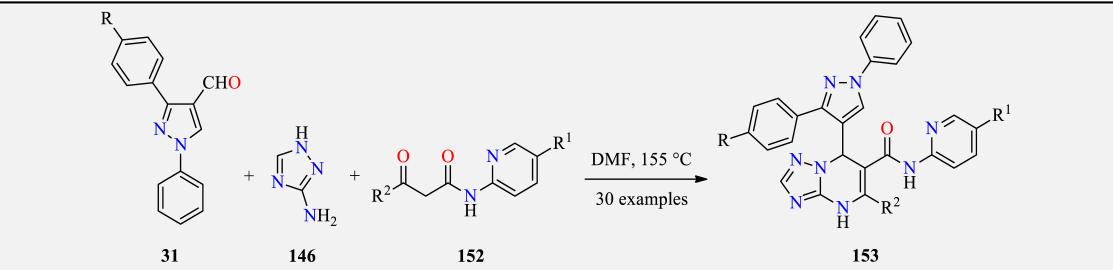
Similarly, the pyrazole derivatives **16a–c**, obtained via a three-component process and discussed in Section 2.1. Antibacterial activity (Scheme 2) [29], were also screened for their anti-inflammatory activity in rats at successive intervals of 1, 2, 4, and 6 h. The standard indomethacin drug (10 mg/kg) and tested heterocycles (50 mg/kg) were administered to the rats 30 min before the injection of 0.1 mL of 1% carrageenan suspension in normal saline. The reduction in edema volume reached a maximum level at 6 h ranging from 9.30% to 13.31%, which is compared to the standard indomethacin drug (16.27%). In particular, pyrazole derivatives **16a** (R = H) and **16c** (R = 2,4-(NO<sub>2</sub>)<sub>2</sub>C<sub>6</sub>H<sub>3</sub>) displayed the highest reduction in edema volume with 13.31% and 12.26%, respectively.

The pyrano[2,3-*c*]pyrazole-5-carbonitrile **141**, obtained via a multicomponent process and discussed in Section 2.4. Antioxidant (Scheme 21) [128], was also evaluated for its anti-inflammatory activity using celecoxib and quercetin as standard drugs. Notably, the compound **141** exhibited significant activity against COX-1 and COX-2 enzymes with values of 5.47 and 0.25 μM, respectively, in comparison to the standard celecoxib (14.60 and 0.04 μM, respectively). It also inhibited the LOX enzyme with a value of 4.43 μM, which is comparable to the standard quercetin (3.35 μM).

Tetrahydrobenzo[*b*]pyran derivatives **142**, obtained from a three-component process and discussed in Section 2.4. Antioxidant (Scheme 22) [129], were also screened for their anti-inflammatory activity using the protein denaturation method at the concentration of 1.0 mM using diclofenac as a standard drug. Importantly, the compounds **142i** (R<sup>1</sup> = 3-NO<sub>2</sub>), **142a** (R<sup>1</sup> = 4-NO<sub>2</sub>), and **142d** (R<sup>1</sup> = 4-MeO) exhibited good activity with inhibition percentages of 69.72%, 65.13%, and 63.30%, respectively, in comparison with the standard diclofenac drug (90.21%).

## 2.7. Antimycobacterial Activity

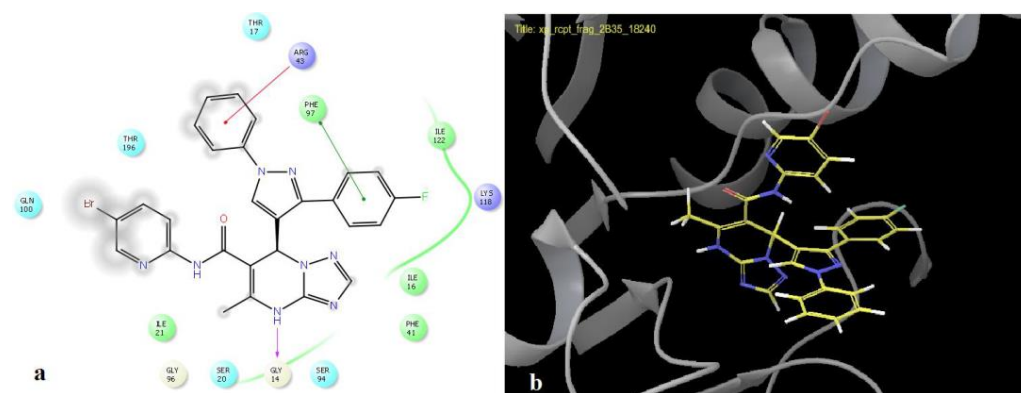
Tuberculosis (TB) is a disease caused by *Mycobacterium tuberculosis* that claims approximately 1.5 million deaths every year [144]. When *M. tuberculosis* is not treated adequately, it takes the form of MDR-TB (multidrug-resistant TB) and XDR-TB (extensive-drug resistant TB) [144]. Thus, the re-emergence of tuberculosis has stimulated the search for new drugs against drug-resistant organisms, preferably acting on new targets [145,146]. Screening of new compounds has been carried out in several mycobacteria models. The main model used remains the infective agent, *M. tuberculosis* with H37Rv and H37Ra as virulent and avirulent reference strains, respectively [145,146]. In this way, Patel's group reported the synthesis of thirteen examples of pyrazole-linked triazolo[1,5-*a*]pyrimidines **153** through a three-component reaction of pyrazole-4-carbaldehyde derivatives **31**, 1*H*-1,2,4-triazol-3-amine **146**, and β-ketoamides **152** containing a pyridine nucleus in refluxing DMF for specific time intervals as visualized by TLC (Table 49) [147]. After cooling, acetone (10 mL) was added, and the reaction mixture was stirred overnight at room temperature. Then, the solid was filtered, recrystallized from ethanol, and dried in the air. Later, the compounds **153** were evaluated for their anti-tuberculosis activity against *Mycobacterium tuberculosis* strain H37Rv using the Lowenstein–Jensen medium and broth dilution technique. The most significant results are summarized in Table 49. Particularly, the compounds **153a–e** inhibited *Mycobacterium tuberculosis* ranging from 95% to 99% at a 6.25 μg/mL concentration. Further, the secondary screening results showed that the compounds **153a** and **153b** inhibited the *mycobacterium* strain at MIC 3.13 and 1.56 μg/mL, respectively, while the compounds **153c**, **153d**, and **153e** inhibited *Mycobacterium tuberculosis* at a MIC lower than 1.0 μg/mL. In summary, the triazolo[1,5-*a*]pyrimidine derivatives **153** exhibited moderate anti-TB activity as compared to Isoniazid (MIC = 0.3 μg/mL) but good anti-TB activity as compared to Ethambutol and Rifampicin (MIC = 0.5 and 3.12 μg/mL, respectively).

**Table 49.** Three-component synthesis of pyrazole-linked triazolo[1,5-*a*]pyrimidines **153** as anti-tubercular agents.


| Compound                | R               | R <sup>1</sup> | R <sup>2</sup> | % Inhibition at 6.25 µg/mL | MIC (µg/mL) | IC <sub>50</sub> Enzyme Inhibition (µg/mL) | CC <sub>50</sub> VERO Cells (µg/mL) |
|-------------------------|-----------------|----------------|----------------|----------------------------|-------------|--|-------------------------------------|
| <b>153a</b>             | H               | Br             | Me             | 95                         | 3.13        | 0.85                                       | 25                                  |
| <b>153b</b>             | NO <sub>2</sub> | Br             | Me             | 96                         | 1.56        | 0.28                                       | 25                                  |
| <b>153c</b>             | Cl              | Br             | Me             | 98                         | 0.78        | 0.11                                       | 20                                  |
| <b>153d</b>             | F               | H              | Me             | 99                         | 0.78        | 0.16                                       | 20                                  |
| <b>153e</b>             | F               | Br             | Me             | 99                         | 0.39        | 0.11                                       | 20                                  |
| Isoniazid <sup>a</sup>  | –               | –              | –              | 99                         | 0.3         | –  | –                                   |
| Rifampicin <sup>a</sup> | –               | –              | –              | 99                         | 0.5         | –  | –                                   |
| Ethambutol <sup>a</sup> | –               | –              | –              | 99                         | 3.12        | –  | –                                   |

<sup>a</sup> Reference compounds.

It should be noted that compounds **153a–e** were found to be non-toxic against Vero cells (IC<sub>50</sub> ≥ 20 µg/mL), while compounds **153c–e** displayed good mycobacterial enoyl-reductase (InhA) inhibitory potency with IC<sub>50</sub> values of 0.11, 0.16, and 0.11 µg/mL, respectively (Table 49). In addition, molecular docking studies were performed for the most active compounds **153a–e** against the active site of the InhA enzyme (PDB: 2B35). As shown in Figure 14, the significant binding affinities with docking energies ranging from −44.89 to −56.60 kcal/mol and the RMS deviation values were observed to fall in the range of 2–3 Å, which can be considered to be an acceptable value of deviation [147]. As shown in Figure 14, the compound **153c** with binding energy of −49.48 kcal/mol and the considerably high XP glide score of −9.07 binds with the InhA active site forming a hydrogen bond between NH of the dihydropyrimidine ring and oxygen of the carboxylate group of Gly14 at a distance of 2.17 Å. Furthermore, π–π stacking was observed between the two phenyl rings linked to the pyrazole ring with the phenyl ring of Phe97 and amine group of Arg43, respectively.

**Figure 14.** (a) 2D model enumerating the interactions between ligand **153c** and InhA enzyme, (b) 3D model of compound **153c** in the binding pocket of the InhA enzyme. Image adapted from Bhattacharya et al. [147].

Similarly, the polyhydroquinoline derivatives **51a–p**, obtained via a three-component process and discussed in Section 2.1. Antibacterial activity (Table 13) [54], were also screened against the *Mycobacterium tuberculosis* H37Rv strain at a 250 µg/mL concentration using isoniazid and rifampicin as standard drugs (Table 50). Remarkably, the polyhydroquinoline derivatives **51e**, **51i**, and **51l** exhibited significant antituberculosis activity with percentages of inhibition of 94%, 95%, and 91%, respectively, which are comparable to isoniazid and rifampicin (99% and 98%, respectively).

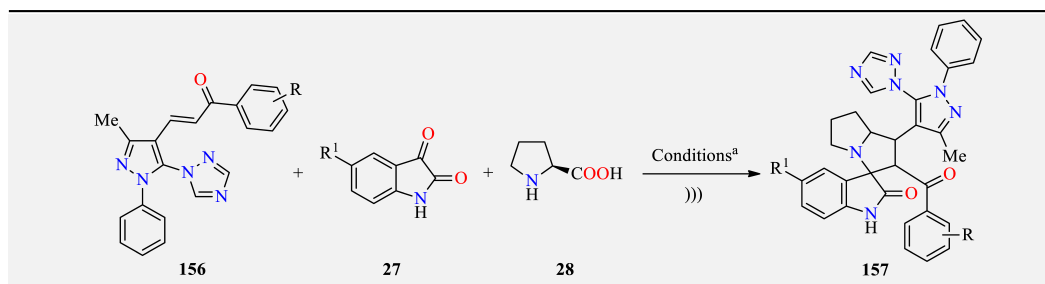
**Table 50.** Antituberculosis activity of polyhydroquinoline derivatives **51**.

**51**

| Compound                | R                 | R <sup>1</sup>    | R <sup>2</sup> | % Inhibition at 250 µg/mL |
|-------------------------|-------------------|-------------------|----------------|---------------------------|
| <b>51a</b>              | 4-F               | CN                | 4-Cl           | 65                        |
| <b>51b</b>              | 4-F               | COOEt             | 4-Cl           | 20                        |
| <b>51c</b>              | 4-F               | CONH <sub>2</sub> | 4-Cl           | 30                        |
| <b>51d</b>              | 4-F               | CN                | 4-Me           | 46                        |
| <b>51e</b>              | 4-F               | COOEt             | 4-Me           | 94                        |
| <b>51f</b>              | 4-CF <sub>3</sub> | CN                | 4-Me           | 46                        |
| <b>51g</b>              | 4-CF <sub>3</sub> | COOEt             | 4-Me           | 50                        |
| <b>51h</b>              | 2,4-diF           | CN                | 4-Me           | 73                        |
| <b>51i</b>              | 2,4-diF           | COOEt             | 4-Me           | 95                        |
| <b>51j</b>              | 2,4-diF           | CN                | 4-Cl           | 79                        |
| <b>51k</b>              | 2,4-diF           | COOEt             | 4-Cl           | 89                        |
| <b>51l</b>              | 2,4-diF           | CONH <sub>2</sub> | 4-Cl           | 91                        |
| <b>51m</b>              | 4-F               | CN                | 4-F            | 67                        |
| <b>51n</b>              | 4-F               | COOEt             | 4-F            | 80                        |
| <b>51o</b>              | 4-CF <sub>3</sub> | CN                | 4-F            | 65                        |
| <b>51p</b>              | 4-CF <sub>3</sub> | COOEt             | 4-F            | 87                        |
| Isoniazid <sup>a</sup>  | –                 | –                 | –              | 99                        |
| Rifampicin <sup>a</sup> | –                 | –                 | –              | 98                        |

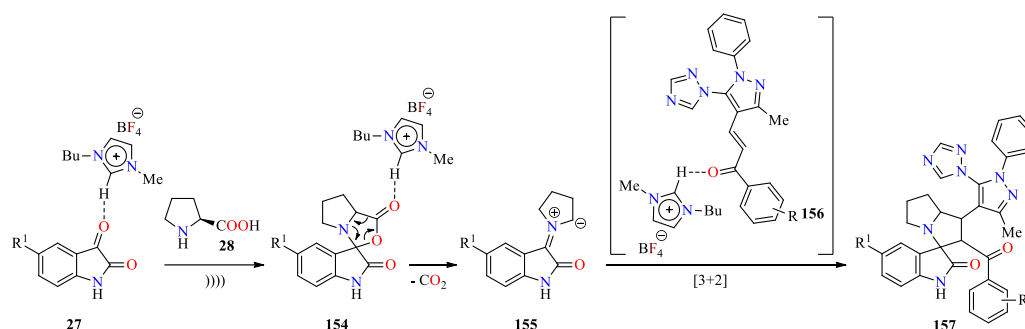
<sup>a</sup> Reference compounds.

Ultrasonic irradiation has been frequently used in the synthesis of diverse *N*-heterocyclic systems of biological interest [105]. For instance, a series of 1,2,4-triazol-1-yl-pyrazole-based spirooxindolopyrrolizidines **157** have been synthesized in 76–92% yields by an ultrasound-assisted three-component reaction of pyrazole-based chalcones **156**, substituted isatins **27**, and *L*-proline **28** using an ionic liquid ([Bmim]BF<sub>4</sub>) at 60 °C for 6–16 min (Table 51) [148]. The [Bmim]BF<sub>4</sub> is reused in up to five cycles without a significant change in yields and catalytic activity. This multicomponent approach is distinguished by its operational simplicity, high yielding, short reaction time, as well as easy separation and recyclability of the [Bmim]BF<sub>4</sub>. The plausible mechanism for the synthesis of compounds **157** is depicted in Scheme 26. It should be mentioned that the ionic liquid can act as both a solvent and catalyst through the interaction of its electron-deficient hydrogen atom with the oxygen atom of carbonyl groups. This interaction facilitates the polarization of the carbonyl group of isatin **27** to react with *L*-proline **28** for the formation of intermediate **154**, and subsequent decarboxylation leads to the highly reactive azomethine ylide **155**. Ultimately, the 1,3-dipolar cycloaddition reaction between the adjacent double bond of dipolarophile **156** and azomethine ylide **155** affords the spirooxindolopyrrolizidine system **157**.

**Table 51.** Ultrasound-assisted three-component synthesis of 1,2,4-triazol-1-yl-pyrazole-based spirooxindolopyrrolidines **157** as antitubercular agents.

| Compound                | R                 | R <sup>1</sup> | Yield <b>157</b> (%) | MIC (μg/mL) | Cytotoxicity % Inhibition at 25 μg/mL <sup>c</sup> |
|-------------------------|-------------------|----------------|----------------------|-------------|--|
| <b>157a</b>             | H                 | H              | 92                   | >25         | – <sup>d</sup>                                     |
| <b>157b</b>             | 4-Me              | H              | 83                   | >25         | – <sup>d</sup>                                     |
| <b>157c</b>             | 4-MeO             | H              | 78                   | 12.5        | – <sup>d</sup>                                     |
| <b>157d</b>             | 4-Cl              | H              | 86                   | 6.25        | 16.85  |
| <b>157e</b>             | 4-Br              | H              | 84                   | 1.56        | 27.15  |
| <b>157f</b>             | 3-NO <sub>2</sub> | H              | 92                   | >25         | – <sup>d</sup>                                     |
| <b>157g</b>             | 4-NO <sub>2</sub> | H              | 90                   | 6.25        | 29.61  |
| <b>157h</b>             | H                 | Cl             | 89                   | 0.78        | 19.76  |
| <b>157i</b>             | 4-Me              | Cl             | 80                   | 25.0        | – <sup>d</sup>                                     |
| <b>157j</b>             | 4-MeO             | Cl             | 76                   | 3.12        | 21.65  |
| <b>157k</b>             | 4-Cl              | Cl             | 82                   | 1.56        | 17.91  |
| <b>157l</b>             | 4-Br              | Cl             | 81                   | 1.56        | 26.43  |
| <b>157m</b>             | 3-NO <sub>2</sub> | Cl             | 90                   | 6.25        | 18.96  |
| <b>157n</b>             | 4-NO <sub>2</sub> | Cl             | 88                   | 1.56        | 24.94  |
| <b>157o</b>             | H                 | Br             | 85                   | 3.12        | 18.62  |
| <b>157p</b>             | 4-MeO             | Br             | 79                   | 25.0        | – <sup>d</sup>                                     |
| <b>157q</b>             | 4-Cl              | Br             | 85                   | 1.56        | 22.36  |
| <b>157r</b>             | 4-Br              | Br             | 80                   | 1.56        | 21.97  |
| <b>157s</b>             | 3-NO <sub>2</sub> | Br             | 86                   | 6.25        | 20.08  |
| <b>157t</b>             | 4-NO <sub>2</sub> | Br             | 85                   | 6.25        | 26.40  |
| Ethambutol <sup>b</sup> | –                 | –              | –                    | 1.56        | – <sup>d</sup>                                     |

<sup>a</sup> Reaction conditions: Pyrazole-based chalcones **156** (1.0 mmol), substituted isatins **27** (1.0 mmol), and L-proline **28** (1.0 mmol) in [Bmim]BF<sub>4</sub> (3.0 mL) at 60 °C for 6–16 min under ultrasound irradiation. <sup>b</sup> Reference compound. <sup>c</sup> The cytotoxicity was determined in the RAW 264.7 cell line. <sup>d</sup> Not determined.

**Scheme 26.** Plausible mechanism for the ultrasound-assisted multicomponent synthesis of spirooxindolopyrrolidines **157**.

The compounds **157a–p** were screened against the *Mycobacterium tuberculosis* H37Rv strain using ethambutol as a standard drug (Table 51) [148]. Most compounds **157** exhibited significant anti-TB activity with MIC values ranging from 0.78 to 12.5 μg/mL, except for compounds **157a**, **157b**, **157f**, **157i**, and **157p**, which presented MIC values equal to or greater than 20 μg/mL. Remarkably, the compound **157h** displayed higher anti-TB activity

(MIC = 0.78 µg/mL) than the standard drug ethambutol (MIC = 1.56 µg/mL). Additionally, the cytotoxicity of the most potent anti-TB compounds was screened against the RAW 264.7 cell line at a 25 µg/mL concentration by adopting the MTT assay. In summary, the promising antituberculosis active compounds **157e**, **157h**, **157k**, **157l**, **157n**, **157q**, and **157r** exhibited a lower percentage of inhibition ranging from 17.91% to 27.15%.

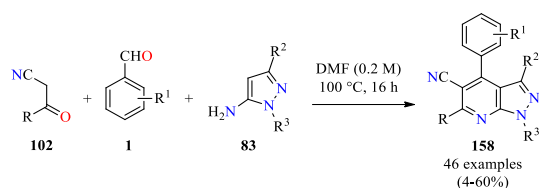
The pyrazolyl-dibenzo[*b,e*][1,4]diazepinones (**64–70a**) and (**71–77b**) were obtained via a multicomponent synthetic approach and previously discussed in Section 2.1. Antibacterial activity (Table 18) [70]. These compounds exhibited anti-TB activity ranging from 6% to 90% at a 250 µg/mL concentration using isoniazid as a standard drug. In particular, the synthesized compounds **66a** (R = H, R<sup>1</sup> = 4-ClC<sub>6</sub>H<sub>4</sub>O), **66'a** (R = COPh, R<sup>1</sup> = 4-ClC<sub>6</sub>H<sub>4</sub>O), **75b** (R = H, R<sup>2</sup> = 4-ClC<sub>6</sub>H<sub>4</sub>S), and **75'b** (R = COPh, R<sup>2</sup> = 4-ClC<sub>6</sub>H<sub>4</sub>S) displayed better anti-TB activity with percentages of inhibition of 86%, 85%, 90%, and 88%, respectively, which are comparable to the standard drug isoniazid (99%).

### 2.8. Antimalarial Activity

Malaria is a disease caused by the parasite *Plasmodium*, which is transmitted by the bite of an infected mosquito belonging to the *Anopheles* genus [149]. Among the five *Plasmodium* species, *Plasmodium falciparum* is considered responsible for approximately 90% of malaria deaths worldwide [150,151]. For that reason, developing novel antimalarials with remarkable activity against all five human-infecting *Plasmodium* species is still highly desirable [150,151]. In this way, the polyhydroquinoline derivatives **51a–p**, obtained via a three-component process and discussed in Section 2.1. Antibacterial activity (Table 13) [54], were also screened for their in vitro antimalarial activity using chloroquine and quinine as standard drugs. Overall, the compounds **51a** (R = 4-F, R<sup>1</sup> = CN, R<sup>2</sup> = 4-Cl), **51c** (R = 4-F, R<sup>1</sup> = CONH<sub>2</sub>, R<sup>2</sup> = 4-Cl), and **51d** (R = 4-F, R<sup>1</sup> = CN, R<sup>2</sup> = 4-Me) exhibited IC<sub>50</sub> values of 0.065, 0.085, and 0.076 µM, respectively, which is remarkable against *Plasmodium falciparum* as compared to chloroquine and quinine (IC<sub>50</sub> = 0.020 and 0.268 µM, respectively). Later, molecular docking was performed between ligands (**51a**, **51c**, **51d**, chloroquine, and quinine) and the receptor wild-type *Plasmodium falciparum* dihydrofolate reductase-thymidylate synthase (PDB ID: 4DPD) [54]. The molecules interacted with the active pockets of protein by forming an H-bond. The docking scores of molecules **51a**, **51c**, and **51d** were found to be −27.88, −28.78, and −27.82, respectively, which were not as good compared to the standard drugs chloroquine and quinine with values of −49.93 and −45.82, respectively. The cyano group of compounds **51a** and **51d** and the carbonyl group of the amide **51c** interacted with the active pockets of the enzyme, forming hydrogen bonds with TYR 365. In addition, the C=O of the cyclohexane ring formed a hydrogen bond with LYS 297.

The pyrazolo[3,4-*b*]pyridine core has been proven to be antimalarial for overcoming the burden of resistance in *Plasmodium falciparum* [151]. Consequently, the simple and efficient synthesis of functionalized pyrazolo[3,4-*b*]pyridines continues to be an important factor in modern drug discovery [152]. In this way, Eagon et al. developed the three-component reaction of aryl-3-oxopropanenitrile derivatives **102**, aromatic aldehydes **1**, and *N*-aryl-5-aminopyrazoles **83** in DMF at 100 °C for 16 h to afford densely substituted pyrazolo[3,4-*b*]pyridines **158** (Scheme 27) [153]. In most cases, compounds **158** were obtained in low to moderate yields because the crude product was purified via trituration with methanol or absolute ethanol, and subsequent filtration and drying. Later, all synthesized compounds **158** were tested against the chloroquine-sensitive *Plasmodium falciparum* 3D7 strain grown in the presence of O-positive erythrocytes with EC<sub>50</sub> values ranging from 0.0692 to 2.04 µM. Overall, most compounds displayed sub-micromolar potency against the intraerythrocytic stage of the parasite, with the most potent compound **158w** (R = 4-*t*ButC<sub>6</sub>H<sub>4</sub>, R<sup>1</sup> = 2-OH, R<sup>2</sup> = Me, R<sup>3</sup> = C<sub>6</sub>H<sub>5</sub>) presenting an EC<sub>50</sub> value of 0.0692 µM. Additional blood stage assays of the compound **158w** showed a moderate killing profile with no activity against the gametocyte stage of the parasite.





R = C<sub>6</sub>H<sub>5</sub>, 2-MeC<sub>6</sub>H<sub>4</sub>, 3-MeC<sub>6</sub>H<sub>4</sub>, 4-MeC<sub>6</sub>H<sub>4</sub>, 3-EtC<sub>6</sub>H<sub>4</sub>, 4-EtC<sub>6</sub>H<sub>4</sub>, 4-PrC<sub>6</sub>H<sub>4</sub>, 4-*i*-PrC<sub>6</sub>H<sub>4</sub>, 4-*t*-ButC<sub>6</sub>H<sub>4</sub>, 3-MeOC<sub>6</sub>H<sub>4</sub>, 4-MeOC<sub>6</sub>H<sub>4</sub>, 3,4-(OCH<sub>2</sub>O)C<sub>6</sub>H<sub>3</sub>, 4-FC<sub>6</sub>H<sub>4</sub>, 4-ClC<sub>6</sub>H<sub>4</sub>, 4-IC<sub>6</sub>H<sub>4</sub>, 4-CF<sub>3</sub>C<sub>6</sub>H<sub>4</sub>, 4-CNC<sub>6</sub>H<sub>4</sub>, 4-NO<sub>2</sub>C<sub>6</sub>H<sub>4</sub>, 4-MeSO<sub>2</sub>C<sub>6</sub>H<sub>4</sub>, 2-naphthyl, 1,2,3,4-tetrahydronaphthalen-2-yl  
 R<sup>1</sup> = H, 2-Me, 2-MeO, 2-EtO, 2-HO, 3-HO, 4-HO, 2-NO<sub>2</sub>, 2-CN, 2-I, 2-Br, 2-Cl, 2-F, 2-CF<sub>3</sub>, 2-CF<sub>3</sub>O, 2-MeSO<sub>2</sub>, 2-COOH, 2-COOMe, 2-ethynyl  
 R<sup>2</sup> = Me, cyclopropyl, C<sub>6</sub>H<sub>5</sub>  
 R<sup>3</sup> = C<sub>6</sub>H<sub>5</sub>, 2-MeC<sub>6</sub>H<sub>4</sub>, 3-MeC<sub>6</sub>H<sub>4</sub>, 4-MeC<sub>6</sub>H<sub>4</sub>

**Scheme 27.** Three-component synthesis of densely substituted pyrazolo [3,4-*b*]pyridines **158** as antimalarial agents.

## 2.9. Miscellaneous Activities

### 2.9.1. AChE and BChE Inhibitory Activity

Alzheimer's disease (AD) is a progressive neurological disorder and the most common cause of dementia in the elderly. It is widely known that one of the possible treatments is the inhibition of acetylcholinesterase (AChE) and butyrylcholinesterase (BChE) to maintain the levels of the neurotransmitter ACh [154,155]. Currently, three AChE inhibitors have been approved by the US Food and Drug Administration for AD therapy: Donepezil, rivastigmine, and galantamine; however, these drugs neither cure nor stop the progression of the disease [154,155]. In the search for new ChE inhibitors, Derabli et al. provided the synthesis, docking studies, and in vitro anticholinesterase activity of new tacrine-pyranopyrazole analogs via a one-pot four-component reaction [156]. By mixing (hetero)aromatic aldehydes **1**, malononitrile **2**, and 3-methyl-1*H*-pyrazol-5-one **19** in refluxing 1,2-dichloroethane (DCE) generates pyrano[2,3-*c*]pyrazole intermediates **160**. Then, AlCl<sub>3</sub>-mediated Friedländer condensation with cyclohexanone **159** in the same flask gave rise to a library of tacrine-pyranopyrazoles **161** with good to excellent yields (Table 52). The use of aromatic or heterocyclic aldehydes did not have a significant impact on the yields.

**Table 52.** One-pot four-component synthesis and in vitro anticholinesterase activity of new tacrine-pyranopyrazole analogues **161**.

| Compound                 | R  | AChE IC <sub>50</sub> (μM) | BChE IC <sub>50</sub> (μM) |
|--------------------------|--|----------------------------|----------------------------|
| <b>161a</b>              | C <sub>6</sub> H <sub>5</sub>                        | 1.23                       | 36.01                      |
| <b>161b</b>              | 4-ClC <sub>6</sub> H <sub>4</sub>                    | 1.66                       | >68.15                     |
| <b>161c</b>              | 4-Br-C <sub>6</sub> H <sub>4</sub>                   | 1.80                       | 11.64                      |
| <b>161d</b>              | 4-NO <sub>2</sub> C <sub>6</sub> H <sub>4</sub>      | 5.80                       | 2.73                       |
| <b>161e</b>              | 4-MeSC <sub>6</sub> H <sub>4</sub>                   | 0.058                      | >66.05                     |
| <b>161f</b>              | 2,4-(Me) <sub>2</sub> C <sub>6</sub> H <sub>3</sub>  | 0.29                       | 39.03                      |
| <b>161g</b>              | 2,4-(MeO) <sub>2</sub> C <sub>6</sub> H <sub>3</sub> | 0.26                       | 31.11                      |
| <b>161h</b>              | 2-Cl-5-NO <sub>2</sub> C <sub>6</sub> H <sub>3</sub> | 1.04                       | 2.50                       |
| <b>161i</b>              | 2-Cl-6-NO <sub>2</sub> C <sub>6</sub> H <sub>3</sub> | 1.77                       | 1.84                       |
| <b>161j</b>              | Biphenyl-4-yl  | 0.044                      | >61.20                     |
| <b>161k</b>              | 3-Pyridinyl  | 0.33                       | 4.26                       |
| <b>161l</b>              | 2-MeO-1-naphthyl                                     | 0.13                       | 11.35                      |
| Galantamine <sup>a</sup> | –  | 21.82                      | 40.72                      |
| Tacrine <sup>a</sup>     | –  | 0.26                       | 0.05                       |

<sup>a</sup> Reference compounds.

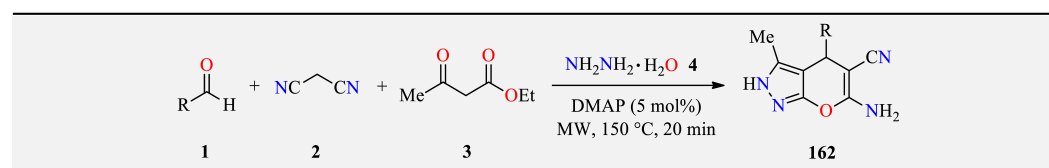
The corresponding tacrine-pyranopyrazoles were evaluated on their in vitro anticholinesterase activity [156]. The data obtained for the inhibition of AChE/BChE by target compounds **161a–l** demonstrated that the majority of compounds had higher selectivity towards AChE than BChE with IC<sub>50</sub> values ranging from 0.044 to 5.80 μM, wherein com-

pounds **161e** and **161j** were found to be most active inhibitors against AChE with  $IC_{50}$  values of 0.058 and 0.044  $\mu\text{M}$ , respectively, in comparison to Galantamine as the reference drug ( $IC_{50} = 21.82 \mu\text{M}$ ). Afterward, molecular modeling simulation of compound **161j** with the AChE receptor showed two hydrogen bonds with Ser286 and one hydrogen bond with Tyr70. The *S* configuration was rotated in the opposite way to direct the biphenyl ring in the same direction as the *R* isomer. Since it was inversely oriented, it formed three hydrogen bonds with different amino acid residues such as Arg289 (two hydrogen bonds) and Tyr334 (one hydrogen bond). The amino group and pyrazole ring seemed to act as the pharmacophores for these interactions.

### 2.9.2. Antihyperuricemic Activity

Xanthine oxidase (XO) is a complex molybdoflavoprotein that catalyzes the hydroxylation of xanthine and hypoxanthine by using molecular oxygen as an electron acceptor [157]. However, XO produces reactive oxygen species leading to oxidative damage to the tissue and a variety of clinical disorders [157]. In this sense, purine-based xanthine oxidase inhibitors such as allopurinol, pterin, and 6-formylpterin have been successfully utilized to prevent XO-mediated tissue damage. However, these inhibitors have been reported to be associated with Steven–Johnson syndrome and worsening of renal function in some patients [157,158]. In 2015, Kaur et al. developed the solvent-free four-component reaction of (hetero)aromatic aldehydes **1**, malononitrile **2**, ethyl 3-oxobutanoate **3**, and hydrazine hydrate **4** in the presence of DMAP as a catalyst under microwave heating at 150 °C for 20 min, affording pyrano[2,3-*c*]pyrazole derivatives **162** in high yields (Table 53) [158]. Later, an in vitro xanthine oxidase assay was conducted by the authors. Among a series of 19 compounds, 6 compounds were found to display a % age inhibition of >80%. It should be noted that molecules exhibiting % age inhibition of more than 80% at 50  $\mu\text{M}$  were further tested for the xanthine oxidase inhibitory activity using allopurinol as a reference inhibitor ( $IC_{50} = 8.29 \mu\text{M}$ ). Remarkably, non-purine xanthine oxidase inhibitors **162l** and **162m** displayed the most potent inhibition against the enzyme with  $IC_{50}$  values of 3.2 and 2.2  $\mu\text{M}$ , respectively.

**Table 53.** Microwave-assisted four-component synthesis of pyrano[2,3-*c*]pyrazoles **162** as non-purine xanthine oxidase inhibitors.



| Compound                 | R  | % Age Inhibition (50 $\mu\text{M}$ ) <sup>b</sup> | XO $IC_{50}$ ( $\mu\text{M}$ ) |
|--------------------------|--|---|--------------------------------|
| <b>162a</b>              | C <sub>6</sub> H <sub>5</sub>                          | 83  | 12.4                           |
| <b>162b</b>              | 4-FC <sub>6</sub> H <sub>4</sub>                       | 45  | –                              |
| <b>162c</b>              | 3-OHC <sub>6</sub> H <sub>4</sub>                      | 24  | –                              |
| <b>162d</b>              | 3-ClC <sub>6</sub> H <sub>4</sub>                      | 62  | –                              |
| <b>162e</b>              | 2-OHC <sub>6</sub> H <sub>4</sub>                      | 27  | –                              |
| <b>162f</b>              | 4-BrC <sub>6</sub> H <sub>4</sub>                      | 85  | 6.4                            |
| <b>162g</b>              | 2-MeOC <sub>6</sub> H <sub>4</sub>                     | 48  | –                              |
| <b>162h</b>              | 4-MeOC <sub>6</sub> H <sub>4</sub>                     | 38  | –                              |
| <b>162i</b>              | 4-NO <sub>2</sub> C <sub>6</sub> H <sub>4</sub>        | 82  | 8.4                            |
| <b>162j</b>              | 4-OHC <sub>6</sub> H <sub>4</sub>                      | 45  | –                              |
| <b>162k</b>              | 1-Naphthyl   | 54  | –                              |
| <b>162l</b>              | 2-Furanyl  | 84  | 3.2                            |
| <b>162m</b>              | 2-Thiophenyl   | 89  | 2.2                            |
| <b>162n</b>              | 2-Indolyl  | 44  | –                              |
| <b>162o</b>              | 3,4-(MeO) <sub>2</sub> C <sub>6</sub> H <sub>3</sub>   | 55  | –                              |
| <b>162p</b>              | 2,3,4-(MeO) <sub>3</sub> C <sub>6</sub> H <sub>2</sub> | 52  | –                              |
| <b>162q</b>              | 4-ClC <sub>6</sub> H <sub>4</sub>                      | 88  | 4.0                            |
| <b>162r</b>              | 4-Pyridinyl  | 79  | –                              |
| <b>162s</b>              | 3-Me-2-thiophenyl                                      | 74  | –                              |
| Allopurinol <sup>a</sup> | –  | –   | 8.29                           |

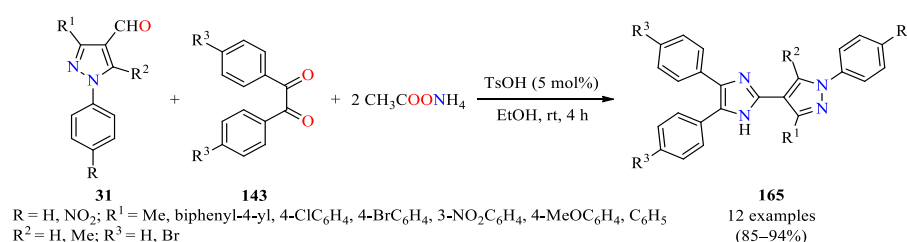
<sup>a</sup> Reference compound. <sup>b</sup> The compounds exhibiting % age inhibition of more than 80% at 50  $\mu\text{M}$  were further tested for the XO inhibitory activity.

### 2.9.3. Antileishmanial Activity

Leishmaniasis is a chronic infection caused by a protozoan parasite that belongs to the genus *Leishmania*. Among all forms of leishmaniasis, visceral leishmaniasis (VL) is the most serious form of the disease [159]. In recent years, several therapeutic options for VL have been employed such as the oral drug miltefosine, the aminoglycoside antibiotic paromomycin, and pentamidine [159,160]. Nevertheless, major concerns such as teratogenicity, nephrotoxicity, hepatotoxicity, ototoxicity, and unaffordable cost are associated with current antileishmanial chemotherapeutic agents [159,160]. Note that combining two or more potentially bioactive moieties to construct heterocyclic scaffolds is a known process in drug discovery [160]. In 2017, Anand et al. reported the three-component reaction of indole-based 5-aminopyrazoles **163**, aryl aldehydes **1**, and cyclic 1,3-diketones **44** in acetic acid at 100–110 °C for 2 h to afford pyrazolodihydropyridine derivatives **164** in 55–80% yields (Table 54) [161]. Most of the compounds were purified by crystallization in EtOH without the need for column chromatography. Later, in vitro antileishmanial activity of pyrazolodihydropyridines was evaluated at 25  $\mu\text{M}$  and 50  $\mu\text{M}$  concentrations against extracellular promastigotes and intracellular amastigotes of luciferase-expressing *Leishmania donovani*. As shown in Table 54, the compounds **164d** and **164j** displayed excellent activity with parasite killing >95% at 50  $\mu\text{M}$ . Remarkably,  $\text{IC}_{50}$  values of **164d** and **164j** were found to be 7.36  $\mu\text{M}$  and 4.05  $\mu\text{M}$  against amastigotes, respectively, which is better than the antileishmanial drug miltefosine ( $\text{IC}_{50} = 9.46 \mu\text{M}$ ).

### 2.9.4. Antiurease Activity


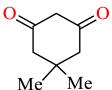
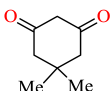
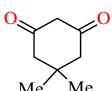
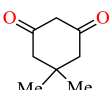
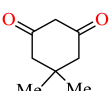
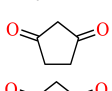
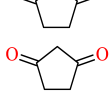
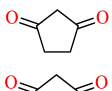
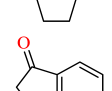
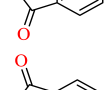
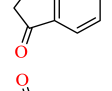
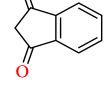
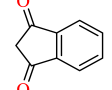
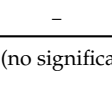
From a medicinal perspective, urease is the major virulence factor of some lethal bacterial pathogens such as *Mycobacterium tuberculosis*, *Proteus mirabilis*, and *Helicobacter pylori*, among others [162]. Generally, it causes infections of the gastrointestinal tract, gastric ulcers, kidney stones, hepatic coma, and the risk of developing gastric cancer [163]. As a contribution to this topic, Chaudhry et al. reported a pseudo-four-component reaction of pyrazole-4-carbaldehyde **31**, symmetrical 1,2-diarylethane-1,2-diones **143**, and ammonium acetate catalyzed by *p*-toluenesulfonic acid in ethanol at ambient temperature, affording a series of imidazolopyrazole derivatives **165** up to 94% yield in short reaction times (4 h) (Scheme 28) [164]. This TsOH-catalyzed approach resulted in being a simple and convergent method to prepare products via the formation of four C-N bonds in one-step.



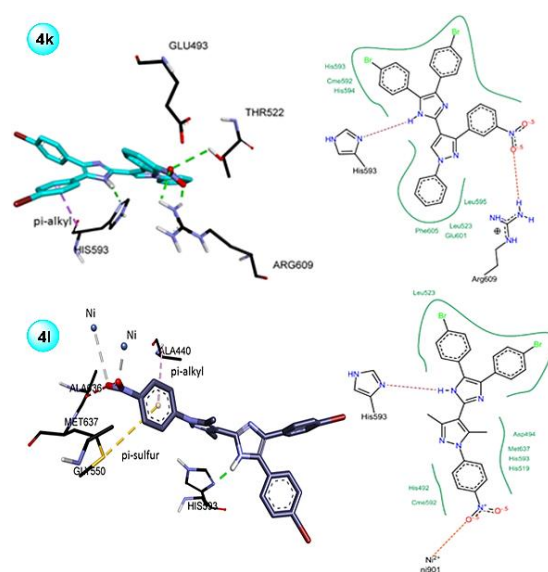
**Scheme 28.** Pseudo-four-component synthesis of imidazolopyrazoles **165** as antiurease agents.

The twelve synthesized compounds were tested for their antiurease activity with  $\text{IC}_{50}$  values ranging from 0.7 to 154.6  $\mu\text{M}$ . Seven compounds were more potent compared to the standard thiourea ( $\text{IC}_{50} = 21.26 \mu\text{M}$ ) as a positive control. Remarkably, the compounds **165k** (R = R<sup>1</sup> = H, R<sup>2</sup> = 3-NO<sub>2</sub>C<sub>6</sub>H<sub>4</sub>, and R<sup>3</sup> = Br) and **165l** (R = NO<sub>2</sub>, R<sup>1</sup> = R<sup>2</sup> = Me, and R<sup>3</sup> = Br) have excellent activity with  $\text{IC}_{50}$  values of 0.7 and 1.0  $\mu\text{M}$ , respectively. Afterward, molecular docking studies were performed to understand the interaction mode of best inhibitors **165k** and **165l** with the active site of urease. The crystal structure of Jack bean's (*Canavalia ensiformis*) urease [PDB ID: 4GY7, 1.49 Å] was selected for the study. As shown in Figure 15, the oxygen of the nitro group of inhibitor **165k** bonded with NH of ARG609 amino acid through a hydrogen bond, whereas, in the case of inhibitor **165l**, the nitro group seemed to interact with the embedded Ni<sup>2+</sup> ion.

**Table 54.** Three-component synthesis and in vitro antileishmanial activity of pyrazolodihydropyridines **164**.

| Compound                 | R   | R <sup>1</sup>  | Reagent 44  | Promastigotes GI (%) |            | Amastigotes GI (%) |                  |
|--------------------------|---|---|---|----------------------|------------|--------------------|------------------|
|                          |   |   |   | 25 $\mu$ M           | 50 $\mu$ M | 25 $\mu$ M         | 50 $\mu$ M       |
| <b>164a</b>              | 4-ClC <sub>6</sub> H <sub>4</sub>                   | 4-ClC <sub>6</sub> H <sub>4</sub>                         |    | 62.5                 | 65.4       | NSI <sup>b</sup>   | NSI <sup>b</sup> |
| <b>164b</b>              | 4-FC <sub>6</sub> H <sub>4</sub>                    | 4-ClC <sub>6</sub> H <sub>4</sub>                         |    | 54.3                 | 65.3       | NSI                | NSI              |
| <b>164c</b>              | 4-ClC <sub>6</sub> H <sub>4</sub>                   | 3,4,5-(MeO) <sub>3</sub> C <sub>6</sub> H <sub>2</sub>    |    | 79.3                 | 86.7       | 23.6               | 28.2             |
| <b>164d</b>              | 3,4-(Cl) <sub>2</sub> C <sub>6</sub> H <sub>3</sub> | 2,5-(MeO) <sub>2</sub> C <sub>6</sub> H <sub>3</sub>      |    | 85.9                 | 90.6       | 91.5               | 95.8             |
| <b>164e</b>              | 3,4-(Cl) <sub>2</sub> C <sub>6</sub> H <sub>3</sub> | 3,4-(MeO) <sub>2</sub> C <sub>6</sub> H <sub>3</sub>      |  | 52.3                 | 59.5       | NSI                | NSI              |
| <b>164f</b>              | 4-ClC <sub>6</sub> H <sub>4</sub>                   | 2-Thiophenyl  |  | 82.5                 | 86.5       | 43.8               | 51.7             |
| <b>164g</b>              | 4-ClC <sub>6</sub> H <sub>4</sub>                   | 2,5-(MeO) <sub>2</sub> C <sub>6</sub> H <sub>3</sub>      |  | 85.5                 | 93.2       | 37.3               | 42.6             |
| <b>164h</b>              | 4-ClC <sub>6</sub> H <sub>4</sub>                   | 3,4,5-(MeO) <sub>3</sub> C <sub>6</sub> H <sub>2</sub>    |  | 78.4                 | 81.2       | 45.2               | 59.6             |
| <b>164i</b>              | 4-ClC <sub>6</sub> H <sub>4</sub>                   | 4-OH-3,5-(MeO) <sub>2</sub> C <sub>6</sub> H <sub>2</sub> |  | 79.1                 | 89.6       | 25.2               | 30.7             |
| <b>164j</b>              | 3,4-(Cl) <sub>2</sub> C <sub>6</sub> H <sub>3</sub> | 3,4-(MeO) <sub>2</sub> C <sub>6</sub> H <sub>3</sub>      |  | 91.7                 | 93.3       | 96.8               | 97.3             |
| <b>164k</b>              | 4-FC <sub>6</sub> H <sub>4</sub>                    | 4-OH-3,5-(MeO) <sub>2</sub> C <sub>6</sub> H <sub>2</sub> |  | 56.5                 | 66.9       | NSI                | NSI              |
| <b>164l</b>              | 4-ClC <sub>6</sub> H <sub>4</sub>                   | 4-ClC <sub>6</sub> H <sub>4</sub>                         |  | 49.1                 | 62.4       | NSI                | NSI              |
| <b>164m</b>              | 4-FC <sub>6</sub> H <sub>4</sub>                    | 4-ClC <sub>6</sub> H <sub>4</sub>                         |  | 54.2                 | 68.3       | NSI                | NSI              |
| <b>164n</b>              | 4-ClC <sub>6</sub> H <sub>4</sub>                   | 2,3,4-(MeO) <sub>3</sub> C <sub>6</sub> H <sub>2</sub>    |  | 64.2                 | 67.4       | NSI                | NSI              |
| <b>164o</b>              | 4-ClC <sub>6</sub> H <sub>4</sub>                   | 2-Thiophenyl  |  | 65.3                 | 69.2       | NSI                | NSI              |
| Miltefosine <sup>a</sup> | –   | –   | –   | 100                  | 100        | 99.8               | 100              |

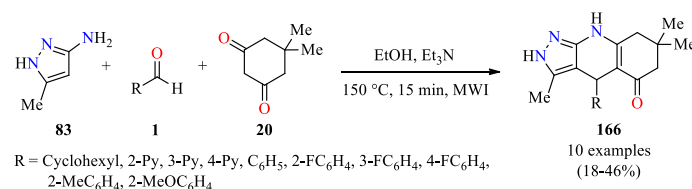
<sup>a</sup> Reference compound. <sup>b</sup> NSI (no significant inhibition).



**Figure 15.** 3D and 2D Interactions of compounds **165k** and **165l** with the amino acids of 4GY7. Image adapted from Chaudhry et al. [164].

### 2.9.5. GSK3 $\alpha$ and GSK3 $\beta$ Inhibitors

Glycogen Synthase Kinase 3 (GSK3) is a key regulator of insulin-dependent glycogen synthesis, which has been shown to function as a master regulator of multiple signaling pathways, including insulin signaling, neurotrophic factor signaling, neurotransmitter signaling, and microtubule dynamics [165,166]. In this context, Wagner et al. reported the discovery of a novel pyrazolo-tetrahydroquinolinone scaffold **166** with selective and potent GSK3 inhibition. The tricyclic compounds **166** were prepared through a three-component reaction of 5-methyl-1*H*-pyrazol-3-amine **83**, aldehydes **1**, 5,5-dimethylcyclohexane-1,3-dione **20**, and triethylamine in ethanol under microwave heating at 150 °C for 15 min (Scheme 29) [167]. The racemic compounds **166** were obtained in low to moderate yields after a simple filtration process. IC<sub>50</sub> values for GSK3 $\alpha$  and GSK3 $\beta$  inhibition were measured in a mobility shift microfluidic assay measuring the phosphorylation of a synthetic substrate. It was noted that the tested racemic compounds **166** inhibit GSK3 $\alpha$  and GSK3 $\beta$  with IC<sub>50</sub> values ranging from 0.018 to >33.33  $\mu$ M and 0.051 to >33.33  $\mu$ M, respectively. Afterward, the enantiomers of BRD4003 (R = C<sub>6</sub>H<sub>5</sub>) were separated by chiral HPLC and the absolute stereochemistry of each enantiomer was determined indirectly via a high-resolution *h*GSK3 $\beta$  co-crystal structure of the closely related analog. Remarkably, the (*S*)-enantiomer strongly inhibits GSK3 $\alpha$  and GSK3 $\beta$  (IC<sub>50</sub> 0.343  $\mu$ M and 0.468  $\mu$ M, respectively). In contrast, the (*R*)-enantiomer weakly inhibits GSK3 $\alpha$  and GSK3 $\beta$  (IC<sub>50</sub> 4.27  $\mu$ M and 7.27  $\mu$ M, respectively).



**Scheme 29.** Microwave-assisted three-component synthesis of pyrazolo-tetrahydroquinolinones **166** as GSK3 $\alpha$  and GSK3 $\beta$  inhibitors.

### 2.9.6. Larvicidal and Insecticidal Activity

Malaria remains a major public health challenge with an estimated 229 million cases recorded in 2019 [168]. The disease spreads from one person to another via the bite of a female mosquito of the genus *Anopheles* [169]. There are 465 to 474 described *Anopheles*

species with 70 of its members recognized to transmit the *Plasmodium* parasite to humans [170]. Therefore, the control of *Anopheles arabiensis* populations still represents the best line of defense. In this way, fused indolo-pyrazoles (FIPs) **136** were prepared via a multicomponent approach and discussed in Section 2.3. Antifungal activity (Scheme 18) [122] and were also screened for larvae mortality. It should be mentioned that *Anopheles arabiensis* mosquitoes were obtained from a colonized strain from Zimbabwe, which had been reared according to the WHO (1975) guidelines in an insectary simulating the temperature (27.5 °C), humidity (70 %), and lighting (12/12) of a malaria-endemic environment. Each container was monitored for larval mortality at 24 h intervals for three days [122]. The percentage mortality was calculated relative to the initial number of exposed larvae. Overall, seven FIPs produced more than 60% mortality at a dose of 4.0 µM. The highest activity was detected for **136c** (R = 4-Cl, R<sup>1</sup> = H), **136r** (R = H, R<sup>1</sup> = Me), and **136v** (R = 4-CF<sub>3</sub>, R<sup>1</sup> = Me), which was comparable to the positive control Temephos, an effective emulsifiable organophosphate larvicide used by the malarial control program. Additionally, the insecticidal activity assessment was conducted by exposing susceptible adult mosquitoes to a treated surface, by following WHO protocol (1975). Deltamethrin (15 g/ L, K-Othrine) was used as a positive control. The effect of FIPs **136** was measured by determining the knock-down rate, which was based on temporary paralysis of mosquitoes during a 60 min exposure period, and mortality 24 h post-exposure. Overall, the FIPs **136a** (R = R<sup>1</sup> = H), **136c** (R = 4-Cl, R<sup>1</sup> = H), and **136p** (R = 3-MeO-4-OH, R<sup>1</sup> = C<sub>6</sub>H<sub>5</sub>) showed a 40% knock-down of activity within the first 60 min of exposure. After 24 h, the mortality of *Anopheles arabiensis* adults exposed to FIPs **136a**, **136c**, and **136p** was nearly 80%, which was comparable to the positive control K-Othrine.

### 3. Conclusions

In the present comprehensive review, a variety of MCR-based approaches applied to the synthesis of biologically active pyrazole derivatives was described. Particularly, it covered the articles published from 2015 to date related to antibacterial, anticancer, antifungal, antioxidant,  $\alpha$ -glucosidase and  $\alpha$ -amylase inhibitory, anti-inflammatory, antimycobacterial, and antimalarial activities, among others, of pyrazole derivatives obtained exclusively through MCRs, giving significant insight into reported MCR-based synthetic routes of pyrazole derivatives, as well as various plausible synthetic mechanisms, a comprehensive view of their diverse biological activity data, and some discussions on molecular docking studies showing how the obtained pyrazole-based compounds interacted with therapeutically relevant targets for potential pharmaceutical applications.

**Author Contributions:** Conceptualization; writing—original draft preparation; writing—review and editing, D.B., R.A. and J.-C.C.; supervision, J.-C.C. All authors have read and agreed to the published version of the manuscript.

**Funding:** This research received no external funding.

**Institutional Review Board Statement:** Not applicable.

**Informed Consent Statement:** Not applicable.

**Data Availability Statement:** Data sharing is not applicable.

**Acknowledgments:** D.B. and J.-C.C. acknowledge the Dirección de Investigaciones at the Universidad Pedagógica y Tecnológica de Colombia (Project SGI 3312). R.A. thanks MINCIENCIAS and Universidad del Valle for partial financial support. The authors thank Daniela Becerra-Córdoba for designing the graphical abstract.

**Conflicts of Interest:** The authors declare no conflict of interest.

## References

1. Hulme, C. Applications of multicomponent reactions in drug discovery–lead generation to process development. In *Multicomponent Reactions*, 1st ed.; Zhu, J., Bienaymé, H., Eds.; WILEY-VCH: Weinheim, German, 2005; Volume 1, pp. 311–341.
2. Dömling, A.; Wang, W.; Wang, K. Chemistry and biology of multicomponent reactions. *Chem. Rev.* **2012**, *112*, 3083–3135. [CrossRef]
3. Ramachary, D.B.; Jain, S. Sequential one-pot combination of multi-component and multi-catalysis cascade reactions: An emerging technology in organic synthesis. *Org. Biomol. Chem.* **2011**, *9*, 1277–1300. [CrossRef] [PubMed]
4. Kakuchi, R. Multicomponent reactions in polymer synthesis. *Angew. Chem. Int. Ed.* **2014**, *53*, 46–48. [CrossRef] [PubMed]
5. Abonia, R.; Castillo, J.; Insuasty, B.; Quiroga, J.; Nogueras, M.; Cobo, J. Efficient catalyst-free four-component synthesis of novel  $\gamma$ -aminoethers mediated by a Mannich type reaction. *ACS Comb. Sci.* **2013**, *15*, 2–9. [CrossRef] [PubMed]
6. Insuasty, D.; Castillo, J.; Becerra, D.; Rojas, H.; Abonia, R. Synthesis of biologically active molecules through multicomponent reactions. *Molecules* **2020**, *25*, 505. [CrossRef]
7. Younus, H.A.; Al-Rashida, M.; Hameed, A.; Uroos, M.; Salar, U.; Rana, S.; Khan, K.M. Multicomponent reactions (MCR) in medicinal chemistry: A patent review (2010–2020). *Expert. Opin. Ther. Pat.* **2021**, *31*, 267–289. [CrossRef]
8. Strecker, A. Ueber die künstliche Bildung der Milchsäure und einen neuen, dem glycocoll homologen körper. *Ann. Chem. Pharm.* **1850**, *75*, 27–45. [CrossRef]
9. Hantzsch, A. Condensationprodukte aus aldehydammoniak und ketoniartigen verbindungen. *Chem. Ber.* **1881**, *14*, 1637–1638. [CrossRef]
10. Biginelli, P. Ueber aldehyduramide des acetessigäthers. *Chem. Ber.* **1891**, *24*, 1317. [CrossRef]
11. Mannich, C.; Krösche, W. Ueber ein kondensationsprodukt aus formaldehyd, ammoniak und antipyrin. *Arch. Pharm.* **1912**, *250*, 647–667. [CrossRef]
12. Passerini, M. Sopra gli isonitrili (I). Composto del *p*-isonitrilazobenzolo con acetone ed acido acetico. *Gazz. Chim. Ital.* **1921**, *51*, 126–129.
13. Fields, E.K. The synthesis of esters of substituted amino phosphonic acids. *J. Am. Chem. Soc.* **1952**, *74*, 1528–1531. [CrossRef]
14. Asinger, F. Über die gemeinsame einwirkung von schwefel und ammoniak auf ketone. *Angew. Chem.* **1956**, *68*, 413. [CrossRef]
15. Ugi, I.; Meyr, R.; Fetzer, U.; Steinbrückner, C. Versuche mit isonitrilen. *Angew. Chem.* **1959**, *71*, 373–388. [CrossRef]
16. Gewalt, K.; Schinke, E.; Böttcher, H. Heterocyclen aus CH-aciden nitrilen, VIII. 2-Amino-thiophene aus methylenaktiven nitrilen, carbonylverbindungen und schwefel. *Chem. Ber.* **1966**, *99*, 94–100. [CrossRef]
17. Oldenzil, O.H.; Van Leusen, D.; Van Leusen, A.M. Chemistry of sulfonylmethyl isocyanides. 13. A general one-step synthesis of nitriles from ketones using tosylmethyl isocyanide. Introduction of a one-carbon unit. *J. Org. Chem.* **1977**, *42*, 3114–3118. [CrossRef]
18. Bienaymé, H.; Bouzid, K. A new heterocyclic multicomponent reaction for the combinatorial synthesis of fused 3-aminoimidazoles. *Angew. Chem. Int. Ed.* **1998**, *37*, 2234–2237. [CrossRef]
19. Boltjes, A.; Dömling, A. The Groebke-Blackburn-Bienaymé reaction. *Eur. J. Chem.* **2019**, *2019*, 7007–7049. [CrossRef]
20. Naim, M.J.; Alam, O.; Nawaz, F.; Alam, J.; Alam, P. Current status of pyrazole and its biological activities. *J. Pharm. Bioallied Sci.* **2016**, *8*, 2–17. [CrossRef] [PubMed]
21. Karrouchi, K.; Radi, S.; Ramli, Y.; Taoufik, J.; Mabkhot, Y.N.; Al-aizari, F.A.; Ansar, M. Synthesis and pharmacological activities of pyrazole derivatives: A review. *Molecules* **2018**, *23*, 134. [CrossRef]
22. Ebenezer, O.; Shapi, M.; Tuszynski, J.A. A review of the recent development in the synthesis and biological evaluations of pyrazole derivatives. *Biomedicines* **2022**, *10*, 1124. [CrossRef]
23. Maddila, S.; Jonnalagadda, S.B.; Gangu, K.K.; Maddila, S.N. Recent advances in the synthesis of pyrazole derivatives using multicomponent reactions. *Curr. Org. Synth.* **2017**, *14*, 634–6531. [CrossRef]
24. Castillo, J.-C.; Portilla, J. Recent advances in the synthesis of new pyrazole derivatives. In *TARGETS IN HETEROCYCLIC SYSTEMS: Chemistry and Properties*; Attanasi, O.A., Merino, P., Spinelli, D., Eds.; Società Chimica Italiana: Rome, Italy, 2018; Volume 22, pp. 194–223. Available online: [https://www.soc.chim.it/sites/default/files/ths/22/chapter\\_9.pdf](https://www.soc.chim.it/sites/default/files/ths/22/chapter_9.pdf) (accessed on 6 July 2022).
25. Sadeghpour, M.; Olyaei, A. Recent advances in the synthesis of bis(pyrazolyl)methanes and their applications. *Res. Chem. Intermed.* **2021**, *47*, 4399–4441. [CrossRef]
26. Mali, G.; Shaikh, B.A.; Garg, S.; Kumar, A.; Bhattacharyya, S.; Erande, R.D.; Chate, A.V. Design, synthesis, and biological evaluation of densely substituted dihydropyrano[2,3-*c*]pyrazoles via a taurine-catalyzed green multicomponent approach. *ACS Omega* **2021**, *6*, 30734–30742. [CrossRef]
27. El-Assaly, S.A.; Ismail, A.E.H.A.; Bary, H.A.; Abouelenein, M.G. Synthesis, molecular docking studies, and antimicrobial evaluation of pyrano[2,3-*c*]pyrazole derivatives. *Curr. Chem. Lett.* **2021**, *10*, 309–328. [CrossRef]
28. Reddy, G.M.; Garcia, J.R.; Zyryanov, G.V.; Sravya, G.; Reddy, N.B. Pyranopyrazoles as efficient antimicrobial agents: Green, one-pot and multicomponent approach. *Bioorg. Chem.* **2019**, *82*, 324–331. [CrossRef] [PubMed]
29. Kendre, B.V.; Landge, M.G.; Bhusare, S.R. Synthesis and biological evaluation of some novel pyrazole, isoxazole, benzoxazepine, benzothiazepine and benzodiazepine derivatives bearing an aryl sulfonate moiety as antimicrobial and anti-inflammatory agents. *Arab. J. Chem.* **2019**, *12*, 2091–2097. [CrossRef]

30. Dehbalaei, M.G.; Foroughifar, N.; Pasdar, H. Facile green one-pot synthesis of pyrano[2,3-*c*]pyrazole and 1,8-dioxo-decahydroacridine derivatives using graphene oxide as a carbocatalyst and their biological evaluation as potent antibacterial agents. *Biointerface Res. Appl. Chem.* **2018**, *8*, 3016–3022.
31. Barakat, A.; Al-Majid, A.M.; Al-Qahtany, B.M.; Ali, M.; Teleb, M.; Al-Agamy, M.H.; Naz, S.; Ul-Haq, Z. Synthesis, antimicrobial activity, pharmacophore modeling and molecular docking studies of new pyrazole-dimedone hybrid architectures. *Chem. Cent. J.* **2018**, *12*, 29. [CrossRef]
32. Vaarla, K.; Kesharwani, R.K.; Santosh, K.; Rao, R.; Kotamraju, S.; Toopurani, M.K. Synthesis, biological activity evaluation and molecular docking studies of novel coumarin substituted thiazolyl-3-aryl-pyrazole-4-carbaldehydes. *Bioorg. Med. Chem. Lett.* **2015**, *25*, 5797–5803. [CrossRef]
33. Kathirvelan, D.; Haribabu, J.; Reddy, B.S.R.; Balachandran, C.; Duraipandiyar, V. Facile and diastereoselective synthesis of 3,2'-spiropyrrolidine-oxindoles derivatives, their molecular docking and antiproliferative activities. *Bioorg. Med. Chem. Lett.* **2015**, *25*, 389–399. [CrossRef] [PubMed]
34. Suresh, L.; Kumar, P.S.V.; Poornachandra, Y.; Kumar, C.G.; Chandramouli, G.V.P. Design, synthesis and evaluation of novel pyrazolo-pyrimido[4,5-*d*]pyrimidine derivatives as potent antibacterial and biofilm inhibitors. *Bioorg. Med. Chem. Lett.* **2017**, *27*, 1451–1457. [CrossRef] [PubMed]
35. Sivaganesh, T.; Padmaja, P.; Reddy, P.N. Efficient one-pot synthesis of pyrazole–pyrazol-3-one hybrid analogs and evaluation of their antimicrobial activity. *Russ. J. Org. Chem.* **2022**, *58*, 81–86. [CrossRef]
36. Mor, S.; Khatri, M. Synthesis, antimicrobial evaluation,  $\alpha$ -amylase inhibitory ability and molecular docking studies of 3-alkyl-1-(4-(aryl/heteroaryl)thiazol-2-yl)indeno[1,2-*c*]pyrazol-4(1*H*)-ones. *J. Mol. Struct.* **2022**, *1249*, 131526. [CrossRef]
37. Zidan, A.; El-Naggar, A.M.; Abd El-Sattar, N.E.A.; Ali, A.K.; El Kaïm, L. Raising the diversity of Ugi reactions through selective alkylations and allylations of Ugi adducts. *Front. Chem.* **2019**, *7*, 20. [CrossRef] [PubMed]
38. Rocha, R.O.; Rodrigues, M.O.; Neto, B.A.D. Review on the Ugi multicomponent reaction mechanism and the use of fluorescent derivatives as functional chromophores. *ACS Omega* **2020**, *5*, 972–979. [CrossRef]
39. Pandya, K.M.; Battula, S.; Naik, P.J. Pd-catalyzed post-Ugi intramolecular cyclization to the synthesis of isoquinolone-pyrazole hybrid pharmacophores & discover their antimicrobial and DFT studies. *Tetrahedron Lett.* **2021**, *81*, 153353. [CrossRef]
40. Anantharaman, A.; Rizvi, M.S.; Sahal, D. Synergy with rifampin and kanamycin enhances potency, kill kinetics, and selectivity of *DeNovo*-designed antimicrobial peptides. *Antimicrob. Agents Chemother.* **2010**, *54*, 1693–1699. [CrossRef]
41. Makino, M.; Fujimoto, Y. Flavanones from *Baeckea frutescens*. *Phytochemistry* **1999**, *50*, 273–277. [CrossRef]
42. Bhavanarushi, S.; Kanakaiah, V.; Yakaiah, E.; Saddanapu, V.; Addlagatta, A.; Rani, V.J. Synthesis, cytotoxic, and DNA binding studies of novel fluorinated condensed pyrano pyrazoles. *Med. Chem. Res.* **2013**, *22*, 2446–2454. [CrossRef]
43. Safari, F.; Hosseini, H.; Bayat, M.; Ranjbar, A. Synthesis and evaluation of antimicrobial activity, cytotoxic and pro-apoptotic effects of novel spiro-4*H*-pyran derivatives. *RSC Adv.* **2019**, *9*, 24843–24851. [CrossRef] [PubMed]
44. Mobinikhaledi, A.; Foroughifar, N.; Moseleh, T.; Hamta, A. Synthesis of some novel chromenopyrimidine derivatives and evaluation of their biological activities. *Iranian J. Pharm. Res.* **2014**, *13*, 873–879.
45. Parmar, N.J.; Pansuriya, B.R.; Parmar, B.D.; Barad, H.A. Solvent-free, one-pot synthesis and biological evaluation of some new dipyrazolo[3,4-*b*:4',3'-*e*]pyranylquinolones and their precursors. *Med. Chem. Res.* **2014**, *23*, 42–56. [CrossRef]
46. Plechkova, N.V.; Seddon, K.R. Applications of ionic liquids in the chemical industry. *Chem. Soc. Rev.* **2008**, *37*, 123–150. [CrossRef]
47. Dehbalaei, M.G.; Foroughifar, N.; Pasdar, H.; Khajeh-Amiri, A.; Foroughifar, N.; Alikarami, M. Choline chloride based thiourea catalyzed highly efficient, eco-friendly synthesis and anti-bacterial evaluation of some new 6-amino-4-aryl-2,4-dihydro-3-phenylpyrano[2,3-*c*]pyrazole-5-carbonitrile derivatives. *Res. Chem. Intermed.* **2017**, *43*, 3035–3051. [CrossRef]
48. Jung, J.-C.; Park, O.-S. Synthetic approaches and biological activities of 4-hydroxycoumarin derivatives. *Molecules* **2009**, *14*, 4790–4803. [CrossRef]
49. Hussain, H.; Hussain, J.; Al-Harrasi, A.; Krohn, K. The chemistry and biology of bicoumarins. *Tetrahedron* **2012**, *68*, 2553–2578. [CrossRef]
50. Neena; Nain, S.; Bhardwaj, V.; Kumar, R. Efficient synthesis and antibacterial evaluation of a series of pyrazolylbiscoumarin and pyrazolylxanthenedione derivatives. *Pharm. Chem. J.* **2015**, *49*, 254–258. [CrossRef]
51. Böhm, H.J.; Banner, D.; Bendels, S.; Kansy, M.; Kuhn, B.; Müller, K.; Obst-Sander, U.; Stahl, M. Fluorine in medicinal chemistry. *ChemBioChem* **2004**, *5*, 637–643. [CrossRef]
52. Karad, S.C.; Purohit, V.B.; Avalani, J.R.; Sapariya, N.H.; Raval, D.K. Design, synthesis, and characterization of a fluoro substituted novel pyrazole nucleus clubbed with 1, 3, 4-oxadiazole scaffolds and their biological applications. *RSC Adv.* **2016**, *6*, 41532–41541. [CrossRef]
53. Karad, S.C.; Purohit, V.B.; Raval, D.K.; Kalaria, P.N.; Avalani, J.R.; Thakor, P.; Thakkar, V.R. Green synthesis and pharmacological screening of polyhydroquinoline derivatives bearing a fluorinated 5-aryloxypyrazole nucleus. *RSC Adv.* **2015**, *5*, 16000–16009. [CrossRef]
54. Sapariya, N.H.; Vaghasiya, B.K.; Thummar, R.P.; Kamani, R.D.; Patel, K.H.; Thakor, P.; Thakkar, S.S.; Ray, A.; Raval, D.K. Synthesis, characterization, in silico molecular docking study and biological evaluation of a 5-(phenylthio)pyrazole based polyhydroquinoline core moiety. *New J. Chem.* **2017**, *41*, 10686–10694. [CrossRef]
55. NCCLS (National Committee for Clinical Laboratory Standards). *Performance Standards for Antimicrobial Susceptibility Testing: Twelfth Informational Supplement* (2002); NCCLS: Albany, NY, USA, 2002; ISBN 1-56238-454-6.



56. Malladi, S.; Isloor, A.M.; Peethambar, S.K.; Fun, H.K. Synthesis of new 3-aryl-4-(3-aryl-4, 5-dihydro-1H-pyrazol-5-yl)-1-phenyl-1H-pyrazole derivatives as potential antimicrobial agents. *Med. Chem. Res.* **2013**, *22*, 2654–2664. [CrossRef]
57. Baranda, A.B.; Alonso, R.M.; Jimenez, R.M.; Weinmann, W. Instability of calcium channel antagonists during sample preparation for LC–MS–MS analysis of serum samples. *Forensic Sci. Int.* **2006**, *156*, 23–34. [CrossRef]
58. Viveka, S.; Dinesha; Madhu, L.N.; Nagaraja, G.K. Synthesis of new pyrazole derivatives via multicomponent reaction and evaluation of their antimicrobial and antioxidant activities. *Monatsh. Chem.* **2015**, *146*, 1547–1555. [CrossRef]
59. Aboelnaga, A.; El-Sayed, T.H. Click synthesis of new 7-chloroquinoline derivatives by using ultrasound irradiation and evaluation of their biological activity. *Green. Chem. Lett. Rev.* **2018**, *11*, 254–263. [CrossRef]
60. Kerru, N.; Gummidi, L.; Bhaskaruni, S.V.H.S.; Maddila, S.N.; Jonnalagadda, S.B. Ultrasound-assisted synthesis and antibacterial activity of novel 1,3,4-thiadiazole-1H-pyrazol-4-yl-thiazolidin-4-one derivatives. *Monatsh. Chem.* **2020**, *151*, 981–990. [CrossRef]
61. Adib, M.; Ansari, S.; Fatemi, S.; Bijanzadeh, H.R.; Zhu, L.G. A multi-component synthesis of 3-aryl-1-(arylmethylideneamino)pyrrolidine-2,5-diones. *Tetrahedron* **2010**, *66*, 2723–2727. [CrossRef]
62. Patel, H.B.; Gohil, J.D.; Patel, M.P. Microwave-assisted, solvent-free, one-pot, three-component synthesis of fused pyran derivatives containing benzothiazole nucleus catalyzed by pyrrolidine-acetic acid and their biological evaluation. *Monatsh. Chem.* **2017**, *148*, 1057–1067. [CrossRef]
63. Abunada, N.M.; Hassaneen, H.H.; Kandile, N.G.; Miqdad, O.A. Synthesis and antimicrobial activity of some new pyrazole, fused pyrazolo[3,4-*d*]pyrimidine and pyrazolo[4,3-*e*][1,2,4]-triazolo[1,5-*c*]pyrimidine derivatives. *Molecules* **2008**, *13*, 1501–1517. [CrossRef]
64. Barakat, A.; Al-Majid, A.M.; Shahidu, M.I.; Warad, I.; Masand, V.H.; Yousuf, S.; Choudhary, M.I. Molecular structure investigation and biological evaluation of Michael adducts derived from dimedone. *Res. Chem. Intermed.* **2016**, *42*, 4041–4053. [CrossRef]
65. Elshaier, Y.A.M.M.; Barakat, A.; Al-Qahtany, B.M.; Al-Majid, A.M.; Al-Agamy, M.H. Synthesis of pyrazole-thiobarbituric acid derivatives: Antimicrobial activity and docking studies. *Molecules* **2016**, *21*, 1337. [CrossRef]
66. Blower, T.R.; Williamson, B.H.; Kerns, R.J.; Berger, J.M. Crystal structure and stability of gyrase-fluoroquinolone cleaved complexes from *Mycobacterium tuberculosis*. *Proc. Natl. Acad. Sci. USA* **2016**, *113*, 1706–1713. [CrossRef] [PubMed]
67. Lu, J.; Patel, S.; Sharma, N.; Soisson, S.M.; Kishii, R.; Takei, M.; Fukuda, Y.; Lumb, K.J.; Singh, S.B. Structures of kbidelomycin bound to *Staphylococcus aureus* GyrB and ParE showed a novel U-shaped binding mode. *ACS Chem. Biol.* **2014**, *19*, 2023–2031. [CrossRef] [PubMed]
68. Reddy, T.S.; Kulhari, H.; Reddy, V.G.; Rao, A.V.S.; Bansal, V.; Kamal, A.; Shukla, R. Synthesis and biological evaluation of pyrazolo–triazole hybrids as cytotoxic and apoptosis inducing agents. *Org. Biomol. Chem.* **2015**, *13*, 10136–10149. [CrossRef]
69. Thurston, D.E.; Bose, D.S. Synthesis of DNA–interactive pyrrolo[2,1-*c*][1,4]benzodiazepines. *Chem. Rev.* **1994**, *94*, 433–465. [CrossRef]
70. Brahmabhatt, G.C.; Sutariya, T.R.; Atara, H.D.; Parmar, N.J.; Gupta, V.K.; Lagunes, I.; Padrón, J.M.; Murumkar, P.R.; Yadav, M.R. New pyrazolyl-dibenzo[*b,e*][1,4]diazepinones: Room temperature one-pot synthesis and biological evaluation. *Mol. Divers.* **2020**, *24*, 355–377. [CrossRef] [PubMed]
71. Li, X.; Ma, S. Advances in the discovery of novel antimicrobials targeting the assembly of bacterial cell division protein FtsZ. *Eur. J. Med. Chem.* **2015**, *95*, 1–15. [CrossRef]
72. Viveka, S.; Dinesha; Nagaraja, G.K.; Shama, P.; Basavarajaswamy, G.; Rao, K.P.; Sreenivasa, M.Y. One pot synthesis of thiazolo[2,3-*b*]dihydropyrimidinone possessing pyrazole moiety and evaluation of their anti-inflammatory and antimicrobial activities. *Med. Chem. Res.* **2018**, *27*, 171–185. [CrossRef]
73. Gediya, L.K.; Njar, V.C. Promise and challenges in drug discovery and development of hybrid anticancer drugs. *Expert. Opin. Drug Discov.* **2009**, *4*, 1099–1111. [CrossRef]
74. Viegas-Junior, C.; Danuello, A.; da Silva Bolzani, V.; Barreiro, E.J.; Fraga, C.A.M. Molecular hybridization: A useful tool in the design of new drug prototypes. *Curr. Med. Chem.* **2007**, *14*, 1829–1852. [CrossRef]
75. Sindhu, J.; Singh, H.; Khurana, J.M.; Bhardwaj, J.K.; Saraf, P.; Sharma, C. Synthesis and biological evaluation of some functionalized 1H-1,2,3-triazole tethered pyrazolo[3,4-*b*]pyridin-6(7H)-ones as antimicrobial and apoptosis inducing agents. *Med. Chem. Res.* **2016**, *25*, 1813–1830. [CrossRef]
76. Song, C.E. Enantioselective chemo- and bio-catalysis in ionic liquids. *Chem. Commun.* **2004**, 1033–1043. [CrossRef] [PubMed]
77. Nia, R.H.; Mamaghani, M.; Shirini, F.; Tabatabaeian, K.; Heidary, M. Rapid and efficient synthesis of 1,4-dihydropyridines using a sulfonic acid functionalized ionic liquid. *Org. Prep. Proc. Int.* **2014**, *46*, 152–163. [CrossRef]
78. Mamaghani, M.; Nia, R.H.; Shirini, F.; Tabatabaeian, K.; Rassa, M. An efficient and eco-friendly synthesis and evaluation of antibacterial activity of pyrano[2,3-*c*]pyrazole derivatives. *Med. Chem. Res.* **2015**, *24*, 1916–1926. [CrossRef]
79. Reddy, G.M.; Garcia, J.R. Synthesis of pyranopyrazoles under eco-friendly approach by using acid catalysis. *J. Heterocycl. Chem.* **2017**, *54*, 89–94. [CrossRef]
80. Zaki, M.E.A.; Soliman, H.A.; Hiekal, O.A.; Rashad, A.E.Z. Pyrazolopyranopyrimidines as a class of anti-inflammatory agents. *Naturforsch.* **2006**, *61*, 1–5. [CrossRef] [PubMed]
81. Reddy, G.M.; Garcia, J.R.; Reddy, V.H.; Kumari, A.K.; Zyryanov, G.V.; Yuvaraja, G. An efficient and green approach: One pot, multi component, reusable catalyzed synthesis of pyranopyrazoles and investigation of biological assays. *J. Saudi Chem. Soc.* **2019**, *23*, 263–273. [CrossRef]

82. Ambethkar, S.; Padmini, V.; Bhuvanesh, N. A green and efficient protocol for the synthesis of dihydropyrano[2,3-*c*]pyrazole derivatives via a one-pot, four component reaction by grinding method. *J. Adv. Res.* **2015**, *6*, 975–985. [CrossRef]
83. Ziarani, G.M.; Lashgari, N.; Badiei, A. Sulfonic acid-functionalized mesoporous silica (SBA-Pr-SO<sub>3</sub>H) as solid acid catalyst in organic reactions. *J. Mol. Catal. A: Chem.* **2015**, *397*, 166–191. [CrossRef]
84. Ziarani, G.M.; Aleali, F.; Lashgari, N.; Badiei, A.; Soorki, A.A. Efficient synthesis and antimicrobial evaluation of pyrazolopyranopyrimidines in the presence of SBA-Pr-SO<sub>3</sub>H as a nanoporous acid catalyst. *Iran. J. Pharm. Res.* **2018**, *17*, 525–534.
85. Souza, L.G.; Rennó, M.N.; Figueroa-Villar, J.D. Coumarins as cholinesterase inhibitors: A review. *Chem. Biol. Interact.* **2016**, *254*, 11–23. [CrossRef] [PubMed]
86. Sahoo, C.R.; Sahoo, J.; Mahapatra, M.; Lenka, D.; Sahu, P.K.; Dehury, B.; Padhy, R.N.; Paidsetty, S.K. Coumarin derivatives as promising antibacterial agent(s). *Arab. J. Chem.* **2021**, *14*, 102922. [CrossRef]
87. Chougala, M.M.; Samundeeswari, S.; Holiyachi, M.; Shastri, L.A.; Dodamani, S.; Jalalpure, S.; Dixit, S.R.; Joshi, S.D.; Sunagar, V.A. Synthesis, characterization and molecular docking studies of substituted 4-coumarinylpyrano[2,3-*c*]pyrazole derivatives as potent antibacterial and anti-inflammatory agents. *Eur. J. Med. Chem.* **2017**, *125*, 101–116. [CrossRef] [PubMed]
88. Vitaku, E.; Smith, D.T.; Njardarson, J.T. Analysis of the structural diversity, substitution patterns, and frequency of nitrogen heterocycles among US FDA approved pharmaceuticals. *J. Med. Chem.* **2014**, *57*, 10257–10274. [CrossRef]
89. Martins, P.; Jesus, J.; Santos, S.; Raposo, L.R.; Roma-Rodrigues, C.; Baptista, P.V.; Fernandes, A.R. Heterocyclic anticancer compounds: Recent advances and the paradigm shift towards the use of nanomedicine's tool box. *Molecules* **2015**, *20*, 16852–16891. [CrossRef]
90. Lang, D.K.; Kaur, R.; Arora, R.; Saini, B.; Arora, S. Nitrogen-containing heterocycles as anticancer agents: An overview. *Anticancer Agents Med. Chem.* **2020**, *20*, 2150–2168. [CrossRef]
91. Abonia, R.; Insuasty, D.; Castillo, J.; Insuasty, B.; Quiroga, J.; Nogueras, M.; Cobo, J. Synthesis of novel quinoline-2-one based chalcones of potential anti-tumor activity. *Eur. J. Med. Chem.* **2012**, *57*, 29–40. [CrossRef]
92. Insuasty, B.; Becerra, D.; Quiroga, J.; Abonia, R.; Nogueras, M.; Cobo, J. Microwave-assisted synthesis of pyrimido[4,5-*b*][1,6]naphthyridin-4(3*H*)-ones with potential antitumor activity. *Eur. J. Med. Chem.* **2013**, *60*, 1–9. [CrossRef]
93. Castillo, J.-C.; Jiménez, E.; Portilla, J.; Insuasty, B.; Quiroga, J.; Moreno-Fuquen, R.; Kennedy, A.R.; Abonia, R. Application of a catalyst-free Domino Mannich/Friedel-Crafts alkylation reaction for the synthesis of novel tetrahydroquinolines of potential antitumor activity. *Tetrahedron* **2018**, *74*, 932–947. [CrossRef]
94. Serrano-Sterling, C.; Becerra, D.; Portilla, J.; Rojas, H.; Macías, M.; Castillo, J.-C. Synthesis, biological evaluation and X-ray crystallographic analysis of novel (*E*)-2-cyano-3-(het)arylacrylamides as potential anticancer agents. *J. Mol. Struct.* **2021**, *1244*, 130944. [CrossRef]
95. Insuasty, D.; García, S.; Abonia, R.; Insuasty, B.; Quiroga, J.; Nogueras, M.; Cobo, J.; Borosky, G.L.; Laali, K.K. Design, synthesis, and molecular docking study of novel quinoline-based bis-chalcones as potential antitumor agents. *Arch. Pharm.* **2021**, *354*, e2100094. [CrossRef]
96. Sharma, A.; Chowdhury, R.; Dash, S.; Pallavi, B.; Shukla, P. Fast microwave assisted synthesis of pyranopyrazole derivatives as new anticancer agents. *Curr. Microv. Chem.* **2016**, *3*, 78–84. [CrossRef]
97. Salama, S.K.; Mohamed, M.F.; Darweesh, A.F.; Elwahy, A.H.M.; Abdelhamid, I.A. Molecular docking simulation and anticancer assessment on human breast carcinoma cell line using novel bis(1,4-dihydropyrano[2,3-*c*]pyrazole-5-carbonitrile) and bis(1,4-dihydropyrazolo[4',3':5,6]pyrano[2,3-*b*]pyridine-6-carbonitrile) derivatives. *Bioorg. Chem.* **2017**, *71*, 19–29. [CrossRef] [PubMed]
98. Yakaiah, S.; Kumar, P.S.V.; Rani, P.B.; Prasad, K.D.; Aparna, P. Design, synthesis and biological evaluation of novel pyrazolo-oxothiazolidine derivatives as antiproliferative agents against human lung cancer cell line A549. *Bioorg. Med. Chem. Lett.* **2018**, *28*, 630–636. [CrossRef]
99. Kumar, P.; Duhan, M.; Kadyan, K.; Bhardwaj, J.K.; Saraf, P.; Mittal, M. Multicomponent synthesis of some molecular hybrid containing thiazole pyrazole as apoptosis inducer. *Drug Res.* **2018**, *68*, 72–79. [CrossRef]
100. Demjén, A.; Alföldi, R.; Angyal, A.; Gyuris, M.; Hackler, L.; Szebeni, G.J.; Wölfling, J.; Puskás, L.G.; Kanizsai, I. Synthesis, cytotoxic characterization, and SAR study of imidazo[1,2-*b*]pyrazole-7-carboxamides. *Arch. Pharm.* **2018**, *351*, e1800062. [CrossRef]
101. Ansari, A.J.; Joshi, G.; Yadav, U.P.; Maurya, A.K.; Agnihotri, V.K.; Kalra, S.; Kumar, R.; Singh, S.; Sawant, D.M. Exploration of Pd-catalysed four-component tandem reaction for one-pot assembly of pyrazolo[1,5-*c*]quinazolines as potential EGFR inhibitors. *Bioorg. Chem.* **2019**, *93*, 103314. [CrossRef]
102. El-Sayed, A.A.; Amr, A.E.G.E.; EL-Ziaty, A.K.; Elsayed, E.A. Cytotoxic effects of newly synthesized heterocyclic candidates containing nicotinonitrile and pyrazole moieties on hepatocellular and cervical carcinomas. *Molecules* **2019**, *24*, 1965. [CrossRef]
103. Hosseinzadeh, L.; Mahmoudian, N.; Ahmadi, F.; Adibi, H. Synthesis of 4-phenyl-4,5-dihydropyrano[2,3-*b*]pyrazolone derivatives with activated potassium carbonate: Evaluation of anticancer activity on cancer cell lines and apoptosis mechanism. *J. Rep. Pharm. Sci.* **2019**, *8*, 262–269. [CrossRef]
104. Alharthy, R.D. Design and synthesis of novel pyrazolo[3,4-*d*]pyrimidines: In vitro cytotoxic evaluation and free radical scavenging activity studies. *Pharm. Chem. J.* **2020**, *54*, 273–278. [CrossRef]
105. Castillo, J.-C.; Bravo, N.-F.; Tamayo, L.-V.; Mestizo, P.-D.; Hurtado, J.; Macías, M.; Portilla, J. Water-compatible synthesis of 1,2,3-triazoles under ultrasonic conditions by a Cu(I) complex-mediated click reaction. *ACS Omega* **2020**, *5*, 30148–30159. [CrossRef] [PubMed]

106. Komarnicka, U.K.; Starosta, R.; Plotek, M.; Almeida, R.F.M.; Jeżowska-Bojczuk, M.; Kyzioł, A. Copper(I) complexes with phosphine derived from sparfloxacin. Part II: A first insight into the cytotoxic action mode. *Dalton Trans.* **2016**, *45*, 5052–5063. [CrossRef]
107. Rani, M.R.; Singh, A.; Garg, N.; Kaur, N.; Singh, N. Mitochondria- and nucleolus-targeted copper(I) complexes with pyrazole-linked triphenylphosphine moieties for live cell imaging. *Analyst* **2020**, *145*, 83–90. [CrossRef]
108. Rashdan, H.R.M.; Shehadi, I.A.; Abdelmonsef, A.H. Synthesis, anticancer evaluation, computer-aided docking studies, and ADMET prediction of 1,2,3-triazolyl-pyridine hybrids as human aurora B kinase inhibitors. *ACS Omega* **2021**, *6*, 1445–1455. [CrossRef] [PubMed]
109. Dayal, N.; Řezníčková, E.; Hernandez, D.E.; Peřina, M.; Torregrosa-Allen, S.; Elzey, B.D.; Škerlová, J.; Ajani, H.; Djukic, S.; Vojáčková, V.; et al. 3H-Pyrazolo[4,3-f]quinoline-based kinase inhibitors inhibit the proliferation of acute myeloid leukemia cells *in vivo*. *J. Med. Chem.* **2021**, *64*, 10981–10996. [CrossRef] [PubMed]
110. Jilloju, P.C.; Persoons, L.; Kurapati, S.K.; Schols, D.; De Jonghe, S.; Daelemans, D.; Vedula, R.R. Discovery of (±)-3-(1H-pyrazol-1-yl)-6,7-dihydro-5H-[1,2,4]triazolo[3,4-b][1,3,4]thiadiazine derivatives with promising *in vitro* anticoronavirus and antitumoral activity. *Mol. Divers.* **2021**, 1–15. [CrossRef]
111. Vairaperumal, V.; Perumal, M.; Sengodu, P.; Shanumuganthan, S.; Paramasivam, M. V<sub>2</sub>O<sub>5</sub>-Catalyzed one-pot multicomponent of pyrazol naphthoquinone as scaffolds for potential bioactive compounds: Synthesis, structural study and cytotoxic activity. *ChemistrySelect* **2019**, *4*, 3006–3010. [CrossRef]
112. Fouda, A.M.; El-Nassag, M.A.A.; Elhenawy, A.A.; Shati, A.A.; Alfaifie, M.Y.; Elbehairi, S.E.I.; Alam, M.M.; El-Agrody, A.M. Synthesis of 1,4-dihydropyrano[2,3-c]pyrazole derivatives and exploring molecular and cytotoxic properties based on DFT and molecular docking studies. *J. Mol. Struct.* **2022**, *1249*, 131555. [CrossRef]
113. Mamidala, S.; Aravilli, R.K.; Vaarla, K.; Peddi, S.R.; Gondru, R.; Manga, V.; Vedula, R.R. A facile one-pot, three-component synthesis of a new series of thiazolyl pyrazoles: Anticancer evaluation, ADME and molecular docking studies. *Polycycl. Aromat. Compd.* **2022**; *in press*. [CrossRef]
114. Parikh, P.H.; Timaniya, J.B.; Patel, M.J.; Patel, K.P. Microwave-assisted synthesis of pyrano[2,3-c]pyrazole derivatives and their anti-microbial, anti-malarial, anti-tubercular, and anti-cancer activities. *J. Mol. Struct.* **2022**, *1249*, 131605. [CrossRef]
115. Ali, T.E.; Assiria, M.A.; Shatic, A.A.; Alfaific, M.Y.; Elbehairic, S.E.I. Facile green one-pot synthesis and antiproliferative activity of some novel functionalized 4-(4-oxo-4H-chromen-3-yl)-pyrano[2,3-c]pyrazoles and 5-(4-oxo-4H-chromen-3-yl)-pyrano[2,3-d]pyrimidines. *Russ. J. Org. Chem.* **2022**, *58*, 106–113. [CrossRef]
116. Kathiravan, M.K.; Salake, A.B.; Chothe, A.S.; Dudhe, P.B.; Watode, R.P.; Mukta, M.S.; Gadhwe, S. The biology and chemistry of antifungal agents: A review. *Bioorg. Med. Chem.* **2012**, *20*, 5678–5698. [CrossRef] [PubMed]
117. Shafiei, M.; Peyton, L.; Hashemzadeh, M.; Foroumadi, A. History of the development of antifungal azoles: A review on structures, SAR, and mechanism of action. *Bioorg. Chem.* **2020**, *104*, 104240. [CrossRef]
118. Abonia, R.; Garay, A.; Castillo, J.C.; Insuasty, B.; Quiroga, J.; Noguerras, M.; Cobo, J.; Butassi, E.; Zacchino, S. Design of two alternative routes for the synthesis of naftifine and analogues as potential antifungal agents. *Molecules* **2018**, *23*, 520. [CrossRef] [PubMed]
119. Elejalde, N.-R.; Macías, M.; Castillo, J.-C.; Sortino, M.; Svetaz, L.; Zacchino, S.; Portilla, J. Synthesis and *in vitro* antifungal evaluation of novel *N*-substituted 4-aryl-2-methylimidazoles. *ChemistrySelect* **2018**, *3*, 5220–5227. [CrossRef]
120. Abonia, R.; Castillo, J.; Insuasty, B.; Quiroga, J.; Noguerras, M.; Cobo, J. An efficient synthesis of 7-(arylmethyl)-3-*tert*-butyl-1-phenyl-6,7-dihydro-1H,4H-pyrazolo[3,4-d][1,3]oxazines. *Eur. J. Org. Chem.* **2010**, *2010*, 6454–6463. [CrossRef]
121. Wang, B.-L.; Zhang, L.-Y.; Zhan, Y.-Z.; Zhang, Y.; Zhang, X.; Wang, L.-Z.; Li, Z.-M. Synthesis and biological activities of novel 1,2,4-triazole thiones and bis(1,2,4-triazole thiones) containing phenylpyrazole and piperazine moieties. *J. Fluor. Chem.* **2016**, *184*, 36–44. [CrossRef]
122. Makhanya, T.R.; Gengan, R.M.; Kasumbwe, K. Synthesis of fused indolo-pyrazoles and their antimicrobial and insecticidal activities against *anopheles arabiensis* mosquito. *ChemistrySelect* **2020**, *5*, 2756–2762. [CrossRef]
123. Halit, S.; Benazzouz-Touami, A.; Makhloufi-Chebli, M.; Bouaziz, S.T.; Ahriz, K.I. Sodium dodecyl benzene sulfonate-catalyzed reaction for green synthesis of biologically active benzylpyrazolyl-coumarin derivatives, mechanism studies, theoretical calculations. *J. Mol. Struct.* **2022**, *1261*, 132908. [CrossRef]
124. Apak, R.; Özyürek, M.; Güçlü, K.; Çapanoğlu, E. Antioxidant activity/capacity measurement. 1. Classification, physicochemical principles, mechanisms, and electron transfer (ET)-based assays. *J. Agric. Food Chem.* **2016**, *64*, 997–1027. [CrossRef] [PubMed]
125. Chanda, K.; Rajeshwaria; Hiremathada, A.; Singh, M.; Santos, M.A.; Keria, R.S. A review on antioxidant potential of bioactive heterocycle benzofuran: Natural and synthetic derivatives. *Pharmacol. Rep.* **2017**, *69*, 281–295. [CrossRef] [PubMed]
126. Gulcin, I. Antioxidants and antioxidant methods: An updated overview. *Arch. Toxicol.* **2020**, *94*, 651–715. [CrossRef] [PubMed]
127. Addoum, B.; Khalfi, B.E.; Idiken, M.; Sakoui, S.; Derdak, R.; Filali, O.A.; Elmakssoudi, A.K.; Soukri, A. Synthesis, characterization of pyrano[2,3-c]pyrazoles derivatives and determination of their antioxidant activities. *Iran. J. Toxicol.* **2021**, *15*, 175–194. [CrossRef]
128. Amer, M.M.K.; Abdellattif, M.H.; Mouneir, S.M.; Zordok, W.A.; Shehab, W.S. Synthesis, DFT calculation, pharmacological evaluation, and catalytic application in the synthesis of diverse pyrano[2,3-c]pyrazole derivatives. *Bioorg. Chem.* **2021**, *114*, 105136. [CrossRef]

129. Kate, P.; Pandit, V.; Jawale, V.; Bachute, M. L-Proline catalyzed one-pot three-component synthesis and evaluation for biological activities of tetrahydrobenzo[*b*]pyran: Evaluation by green chemistry metrics. *J. Chem. Sci.* **2022**, *134*, 4. [CrossRef]
130. Suresh, L.; Onkara, P.; Kumar, P.S.V.; Pydisetty, Y.; Chandramouli, G.V.P. Ionic liquid-promoted multicomponent synthesis of fused tetrazolo[1,5-*a*]pyrimidines as  $\alpha$ -glucosidase inhibitors. *Bioorg. Med. Chem. Lett.* **2016**, *26*, 4007–4014. [CrossRef]
131. Naim, M.J.; Alam, M.J.; Nawaz, F.; Naidu, V.; Aaghaz, S.; Sahu, M.; Siddiqui, N.; Alam, O. Synthesis, molecular docking and anti-diabetic evaluation of 2,4-thiazolidinedione based amide derivatives. *Bioorg. Chem.* **2017**, *73*, 24–36. [CrossRef]
132. Cho, N.; Shaw, J.; Karuranga, S.; Huang, Y.; da Rocha Fernandes, J.; Ohlrogge, A.; Malanda, B. IDF Diabetes Atlas: Global estimates of diabetes prevalence for 2017 and projections for 2045. *Diabetes Res. Clin. Pract.* **2018**, *38*, 271–281. [CrossRef]
133. Özil, M.; Emirik, M.; Etlík, S.Y.; Ülker, S.; Kahveci, B. A simple and efficient synthesis of novel inhibitors of alpha-glucosidase based on benzimidazole skeleton and molecular docking studies. *Bioorg. Chem.* **2016**, *68*, 226–235. [CrossRef]
134. Nikookar, H.; Khanaposhtani, M.M.; Imanparast, S.; Faramarzi, M.A.; Ranjbar, P.R.; Mahdavi, M.; Larijani, B. Design, synthesis and in vitro  $\alpha$ -glucosidase inhibition of novel dihydropyrano[3,2-*c*]quinoline derivatives as potential anti-diabetic agents. *Bioorg. Chem.* **2018**, *77*, 280–286. [CrossRef] [PubMed]
135. Ozil, M.; Emirik, M.; Belduz, A.; Ulker, S. Molecular docking studies and synthesis of novel bisbenzimidazole derivatives as inhibitors of  $\alpha$ -glucosidase. *Bioorg. Med. Chem.* **2016**, *24*, 5103–5114. [CrossRef] [PubMed]
136. Abdel-Wahab, B.F.; Khidre, R.E.; Farahat, A.A. Pyrazole-3(4)-carbaldehyde: Synthesis, reactions and biological activity. *ARKIVOC* **2011**, (*i*), 196–245. [CrossRef]
137. Chaudhry, F.; Naureen, S.; Huma, R.; Shaukat, A.; al-Rashida, M.; Asif, N.; Ashraf, M.; Munawar, M.; Ain Khan, M. In search of new  $\alpha$ -glucosidase inhibitors: Imidazolylpyrazole derivatives. *Bioorg. Chem.* **2017**, *71*, 102–109. [CrossRef]
138. Chaudhry, F.; Naureen, S.; Ashraf, M.; al-Rashida, M.; Jahan, B.; Ali Munawar, M.; Ain Khan, M. Imidazole-pyrazole hybrids: Synthesis, characterization and in-vitro bioevaluation against  $\alpha$ -glucosidase enzyme with molecular docking studies. *Bioorg. Chem.* **2019**, *82*, 267–273. [CrossRef]
139. Pogaku, V.; Gangarapu, K.; Basavoju, S.; Tatapudic, K.K.; Katragadda, S.B. Design, synthesis, molecular modelling, ADME prediction and antihyperglycemic evaluation of new pyrazole-triazolopyrimidine hybrids as potent  $\alpha$ -glucosidase inhibitors. *Bioorg. Chem.* **2019**, *93*, 103307. [CrossRef]
140. Duhan, M.; Singh, R.; Devi, M.; Sindhu, J.; Bhatia, R.; Kumar, A.; Kumar, P. Synthesis, molecular docking and QSAR study of thiazole clubbed pyrazole hybrid as  $\alpha$ -amylase inhibitor. *J. Biomol. Struct. Dyn.* **2019**, *39*, 91–107. [CrossRef]
141. Bertolini, A.; Ottani, A.; Sandrini, M. Selective COX-2 inhibitors and dual acting anti-inflammatory drugs: Critical remarks. *Curr. Med. Chem.* **2002**, *9*, 1033–1043. [CrossRef]
142. Rao, P.P.N.; Kabir, S.N.; Mohamed, T. Nonsteroidal anti-inflammatory drugs (NSAIDs): Progress in small molecule drug development. *Pharmaceuticals* **2010**, *3*, 1530–1549. [CrossRef]
143. Sharma, S.; Kumar, D.; Singh, D.; Monga, V.; Kumar, B. Recent advancements in the development of heterocyclic anti-inflammatory agents. *Eur. J. Med. Chem.* **2020**, *200*, 112438. [CrossRef]
144. Kumar, V.; Patel, S.; Jain, R. New structural classes of antituberculosis agents. *Med. Res. Rev.* **2018**, *38*, 684–740. [CrossRef] [PubMed]
145. Campaniço, A.; Moreira, R.; Lopes, F. Drug discovery in tuberculosis. New drug targets and antimycobacterial agents. *Eur. J. Med. Chem.* **2018**, *150*, 525–545. [CrossRef] [PubMed]
146. Shetye, G.S.; Franzblau, S.G.; Cho, S. New tuberculosis drug targets, their inhibitors, and potential therapeutic impact. *Transl. Res.* **2020**, *220*, 68–97. [CrossRef] [PubMed]
147. Bhatt, J.D.; Chudasama, C.J.; Patel, K.D. Pyrazole clubbed triazolo[1,5-*a*]pyrimidine hybrids as an anti-tubercular agents: Synthesis, in vitro screening and molecular docking study. *Bioorg. Med. Chem.* **2015**, *23*, 7711–7716. [CrossRef]
148. Pogaku, V.; Krishna, V.S.; Sriram, D.; Rangan, K.; Basavoju, S. Ultrasonication-ionic liquid synergy for the synthesis of new potent anti-tuberculosis 1,2,4-triazol-1-yl-pyrazole based spirooxindolopyrrolizidines. *Bioorg. Med. Chem. Lett.* **2019**, *29*, 1682–1687. [CrossRef] [PubMed]
149. Ashton, T.D.; Devine, S.M.; Möhrle, J.J.; Laleu, B.; Burrows, J.N.; Charman, S.A.; Creek, D.J.; Sleeb, B.E. The development process for discovery and clinical advancement of modern antimalarials. *J. Med. Chem.* **2019**, *62*, 10526–10562. [CrossRef] [PubMed]
150. Insuasty, B.; Montoya, A.; Becerra, D.; Quiroga, J.; Abonia, R.; Robledo, S.; Vélez, I.D.; Upegui, Y.; Nogueras, M.; Cobo, J. Synthesis of novel analogs of 2-pyrazoline obtained from [(7-chloroquinolin-4-yl)amino]chalcones and hydrazine as potential antitumor and antimalarial agents. *Eur. J. Med. Chem.* **2013**, *67*, 252–262. [CrossRef] [PubMed]
151. Silva, T.B.; Bernardino, A.M.R.; Ferreira, M.L.G.; Rogerio, K.R.; Carvalho, L.J.M.; Beochat, N.; Pinheiro, L.C.S. Design, synthesis, and anti-*P. falciparum* activity of pyrazolopyridine-sulfonamide derivatives. *Bioorg. Med. Chem.* **2016**, *24*, 4492–4498. [CrossRef]
152. Charris-Molina, A.; Castillo, J.-C.; Macías, M.; Portilla, J. One-step synthesis of fully functionalized pyrazolo[3,4-*b*]pyridines via isobenzofuranone ring opening. *J. Org. Chem.* **2017**, *82*, 12674–12681. [CrossRef]
153. Eagon, S.; Hammill, J.T.; Sigal, M.; Ahn, K.J.; Tryhorn, J.E.; Koch, G.; Belanger, B.; Chaplan, C.A.; Loop, L.; Kashtanova, A.S.; et al. Synthesis and structure–activity relationship of dual-stage antimalarial pyrazolo[3,4-*b*]pyridines. *J. Med. Chem.* **2020**, *63*, 11902–11919. [CrossRef]
154. Bautista-Aguilera, Ó.M.; Ismaili, L.; Iriepa, I.; Diez-Iriepa, D.; Chabchoub, F.; Marco-Contelles, J.; Pérez, M. Tacrines as Therapeutic Agents for Alzheimer’s Disease. V. Recent Developments. *Chem. Rec.* **2021**, *21*, 162–174. [CrossRef]

155. Dighe, S.N.; Deora, G.S.; De la Mora, E.; Nachon, F.; Chan, S.; Parat, M.-O.; Brazzolotto, X.; Ross, B.P. Discovery and structure–activity relationships of a highly selective butyrylcholinesterase inhibitor by structure-based virtual screening. *J. Med. Chem.* **2016**, *59*, 7683–7689. [CrossRef] [PubMed]
156. Derabli, C.; Boualia, I.; Abdelwahab, A.B.; Boulcina, R.; Bensouici, C.; Kirsch, G.; Debache, A. A cascade synthesis, in vitro cholinesterases inhibitory activity and docking studies of novel Tacrine-pyranopyrazole derivatives. *Bioorganic Med. Chem. Lett.* **2018**, *28*, 2481–2484. [CrossRef]
157. Prusis, P.; Dambrova, M.; Andrianov, V.; Rozhkov, E.; Semenikhina, V.; Piskunova, I.; Ongwae, E.; Lundstedt, T.; Kalvinsh, I.; Wikberg, J.E.S. Synthesis and quantitative structure–activity relationship of hydrazones of *N*-amino-*N'*-hydroxyguanidine as electron acceptors for xanthine oxidase. *J. Med. Chem.* **2004**, *47*, 3105–3110. [CrossRef]
158. Kaur, R.; Naaz, F.; Sharma, S.; Mehndiratta, S.; Gupta, M.K.; Bedi, P.M.S.; Nepali, K. Screening of a library of 4-aryl/heteroaryl-4*H*-fused pyrans for xanthine oxidase inhibition: Synthesis, biological evaluation and docking studies. *Med. Chem. Res.* **2015**, *24*, 3334–3349. [CrossRef]
159. Sangshetti, J.N.; Khan, F.A.K.; Kulkarni, A.A.; Arote, R.; Patil, R.H. Antileishmanial drug discovery: Comprehensive review of the last 10 years. *RSC Adv.* **2015**, *5*, 32376–32415. [CrossRef]
160. Insuasty, B.; Ramírez, J.; Becerra, D.; Echeverry, C.; Quiroga, J.; Abonia, R.; Robledo, S.M.; Vélez, I.D.; Upegui, Y.; Muñoz, J.A.; et al. An efficient synthesis of new caffeine-based chalcones, pyrazolines and pyrazolo[3,4-*b*][1,4]diazepines as potential antimalarial, antitrypanosomal and antileishmanial agents. *Eur. J. Med. Chem.* **2015**, *93*, 401413. [CrossRef]
161. Anand, D.; Yadav, P.K.; Patel, O.P.S.; Parmar, N.; Maurya, R.K.; Vishwakarma, P.; Raju, K.S.R.; Taneja, I.; Wahajuddin, M.; Kar, S.; et al. Antileishmanial activity of pyrazolopyridine derivatives and their potential as an adjunct therapy with miltefosine. *J. Med. Chem.* **2017**, *60*, 1041–1059. [CrossRef]
162. Rutherford, J.C. The emerging role of urease as a general microbial virulence factor. *PLoS Pathog.* **2014**, *10*, e1004062. [CrossRef]
163. Valenzuela-Valderrama, M.; Cerda-Opazo, P.; Backert, S.; González, M.F.; Carrasco-Véliz, N.; Jorquera-Cordero, C.; Wehinger, S.; Canales, J.; Bravo, D.; Quest, A.F.G. The *Helicobacter pylori* urease virulence factor is required for the induction of hypoxia-induced factor-1 $\alpha$  in gastric cells. *Cancers* **2019**, *11*, 799. [CrossRef] [PubMed]
164. Chaudhry, F.; Naureen, S.; Aslam, M.; Al-Rashida, M.; Rahman, J.; Huma, R.; Fatima, J.; Khan, M.; Munawar, M.A.; Khan, M.A. Identification of imidazolylpyrazole ligands as potent urease inhibitors: Synthesis, antiurease activity and in silico docking studies. *ChemistrySelect* **2020**, *5*, 11817–11821. [CrossRef]
165. Vasdev, N.; Garcia, A.; Stableford, W.T.; Young, A.B.; Meyer, J.H.; Houle, S.; Wilson, A.A. Synthesis and ex vivo evaluation of carbon-11 labelled *N*-(4-methoxybenzyl)-*N'*-(5-nitro-1,3-thiazol-2-yl)urea ([<sup>11</sup>C]AR-A014418): A radiolabelled glycogen synthase kinase-3 $\beta$  specific inhibitor for PET studies. *Bioorg. Med. Chem. Lett.* **2005**, *15*, 5270–5273. [CrossRef]
166. Monte, F.L.; Kramer, T.; Gu, J.; Anumala, U.R.; Marinelli, L.; La Pietra, V.; Novellino, E.; Franco, B.; Demedts, D.; Van Leuven, F.; et al. Identification of glycogen synthase kinase-3 inhibitors with a selective sting for glycogen synthase kinase-3 $\alpha$ . *J. Med. Chem.* **2012**, *55*, 4407–4424. [CrossRef] [PubMed]
167. Wagner, F.F.; Bishop, J.A.; Gale, J.P.; Shi, X.; Walk, M.; Ketterman, J.; Patnaik, D.; Barker, D.; Walpita, D.; Campbell, A.J.; et al. Inhibitors of glycogen synthase kinase 3 with exquisite kinome-wide selectivity and their functional effects. *ACS Chem. Biol.* **2016**, *11*, 1952–1963. [CrossRef]
168. Vantaux, A.; Riehle, M.M.; Piv, E.; Farley, E.J.; Chy, S.; Kim, S.; Corbett, A.G.; Fehrman, R.L.; Pepey, A.; Eiglmeier, K.; et al. Anopheles ecology, genetics and malaria transmission in northern Cambodia. *Sci. Rep.* **2021**, *11*, 6458. [CrossRef]
169. Rich, S.M.; Xu, G. Resolving the phylogeny of malaria parasites. *Proc. Natl. Acad. Sci. USA* **2011**, *108*, 12973–12974. [CrossRef] [PubMed]
170. Sinka, M.E.; Bangs, M.J.; Mangiun, S.; Rubio-Palis, Y.; Chareoviriyaphap, T.; Coetzee, M.; Mbogo, C.M.; Hemingway, J.; Patil, A.P.; Temperley, W.H.; et al. A global map of dominant malaria vectors. *Parasite Vectors* **2012**, *5*. [CrossRef]

Review

# Revisiting the Chemistry of Vinylpyrazoles: Properties, Synthesis, and Reactivity

Vera L. M. Silva \*  and Artur M. S. Silva 

LAQV-REQUIMTE, Department of Chemistry, University of Aveiro, 3810-193 Aveiro, Portugal; artur.silva@ua.pt

\* Correspondence: verasilva@ua.pt; Tel.: +351-234-370704

**Abstract:** Vinylpyrazoles, also known as pyrazolyl olefins, are interesting motifs in organic chemistry but have been overlooked. This review describes the properties and synthetic routes of vinylpyrazoles and highlights their versatility as building blocks for the construction of more complex organic molecules. Concerning the reactivity of vinylpyrazoles, the topics surveyed herein include their use in cycloaddition reactions, free-radical polymerizations, halogenation and hydrohalogenation reactions, and more recently in transition-metal-catalyzed reactions, among other transformations. The current state of the art about vinylpyrazoles is presented with an eye to future developments regarding the chemistry of these interesting compounds. Styrylpyrazoles were not considered in this review, as they were the subject of a previous review article published in 2020.

**Keywords:** pyrazoles; vinylpyrazoles; biological activity; synthesis; reactivity

## 1. Introduction

Pyrazoles have attracted increased attention in recent years owing to their widespread applications in medicine [1–15], agriculture, [16] materials science [17–20], and catalysis [21,22]. In this review, the chemistry of a particular kind of pyrazoles, the vinylpyrazoles, is revisited. Vinylpyrazoles (vinyl-1*H*-pyrazoles), also known as pyrazolyl olefins, are characterized by the presence of a vinyl group linked at one of the pyrazoles' ring positions (N-1, C-3, C-4, C-5) (Figure 1). There are few examples of vinylpyrazoles despite their interesting properties. These compounds are interesting building blocks for the synthesis of more complex pyrazoles endowed with biological activities and for other advanced structures, such as indazoles, among others. For example, some 5-vinylpyrazoles were found to be potent DNA gyrase inhibitors with antibacterial activity against Gram-(+) bacteria [23], while others have been used as additives in the production of rubbers [24–26]. Furthermore, these compounds present interesting physicochemical properties, such as tautomerism and isomerism, owing to the presence of the vinyl group. Consequently, several spectroscopic studies on vinylpyrazoles have been reported [27–35]. For example, Skvortsova and coworkers performed several <sup>1</sup>H- and <sup>13</sup>C-NMR spectral analyses for evaluation of electronic and steric effects in 1-vinylpyrazoles [28]. They showed that the substituents on the pyrazole ring had an effect on the conformation of the vinyl group; 5-methyl-1-vinylpyrazoles had predominantly *S-cis*-N<sup>2</sup> orientation, while 1-vinylpyrazoles without substituents at C-5 were a mixture of conformers. These observations were confirmed six years later by Vashchenko and Afonin [35]. Despite their interesting structural features and chemistry, vinylpyrazoles have been overlooked, and their reactivity has not been much explored. However, the discovery of several tools in modern organic synthesis in the last decades, mainly related to metathesis, transition-metal-catalyzed and C-H activation reactions, and visible light-driven and green organometallic transformations, among others, may open novel opportunities towards the investigation of the vinylpyrazoles reactivity and versatility in organic synthesis. This review intends to show the current state of the art with an eye to future perspectives concerning the chemistry and reactivity studies of vinylpyrazoles.

**Citation:** Silva, V.L.M.; Silva, A.M.S. Revisiting the Chemistry of Vinylpyrazoles: Properties, Synthesis, and Reactivity. *Molecules* **2022**, *27*, 3493. <https://doi.org/10.3390/molecules27113493>

Academic Editor: Gianfranco Favi

Received: 11 May 2022

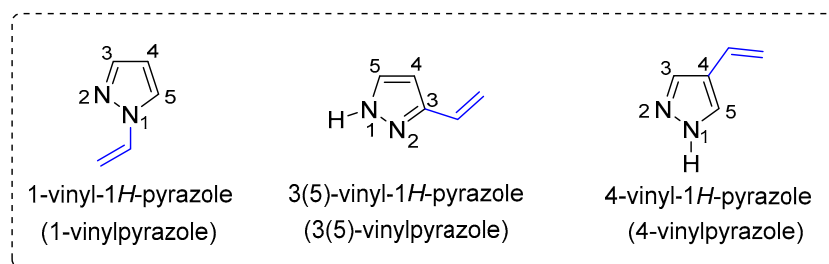
Accepted: 26 May 2022

Published: 29 May 2022

**Publisher's Note:** MDPI stays neutral with regard to jurisdictional claims in published maps and institutional affiliations.



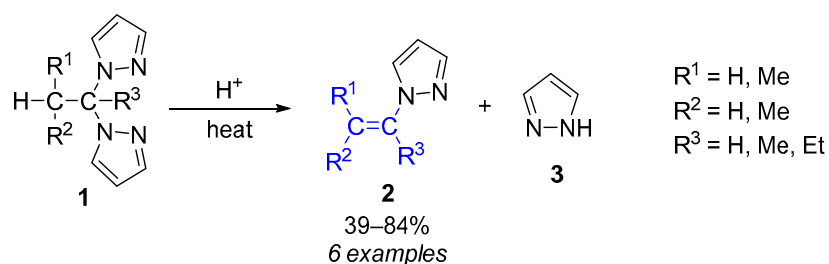
**Copyright:** © 2022 by the authors. Licensee MDPI, Basel, Switzerland. This article is an open access article distributed under the terms and conditions of the Creative Commons Attribution (CC BY) license (<https://creativecommons.org/licenses/by/4.0/>).



**Figure 1.** Structures of 1-vinylpyrazole, 3(5)-vinylpyrazoles, and 4-vinylpyrazole. For sake of simplicity, throughout the manuscript, the nomenclature 1-vinylpyrazole is adopted instead of 1-vinyl-1*H*-pyrazole.

## 2. Synthesis of Vinylpyrazoles

One of the first methods described in the literature for the synthesis of 1-vinylpyrazoles, namely 3,5-dimethyl-1-vinylpyrazole and 3-methyl-5-phenyl-1-vinylpyrazole, was the reaction of acetylene with 3,5-dimethylpyrazole and 3-methyl-5-phenylpyrazole using high pressure [36]. The compounds 1-vinylpyrazole and 3,5-dimethyl-1-vinylpyrazole were also prepared by dehydration of the corresponding alcohols, 1-( $\beta$ -hydroxyethyl)pyrazole and 3,5-dimethyl-1-( $\beta$ -hydroxyethyl)pyrazole. These alcohols were obtained by condensing 1,1,3,3-tetraethoxypropane and acetylacetone, respectively, with  $\beta$ -hydroxyethyl hydrazine [36]. Later, 1-vinylpyrazoles were prepared starting from pyrazoles with free NH and different substituents at C-4 by reaction with boiling vinyl acetate in the presence of mercuric(II) sulfate as a catalyst for 1–7 h. The catalyst was directly produced in the reaction medium from mercuric(II) acetate and sulfuric acid added dropwise [37]. The 1-vinylpyrazoles were obtained in very good yields (70–86%). Electron-acceptor groups at C-4 of the pyrazole nucleus increased the acidity of the NH group and accelerated the reaction. In 1970, Trofimenko reported the synthesis of 1-vinylpyrazoles and their analogs containing alkyl substituents on the vinyl group by acid-catalyzed cracking of geminal bis(1-pyrazolyl)alkanes **1**, obtained from the reaction of pyrazole with acetals or ketals [38]. At around 200 °C and in the presence of an acid such as *p*-toluenesulfonic acid, the bis(1-pyrazolyl)alkanes **1** containing  $\beta$ -hydrogens underwent fragmentation to 1-vinylpyrazole **2** and pyrazole **3** (Scheme 1).

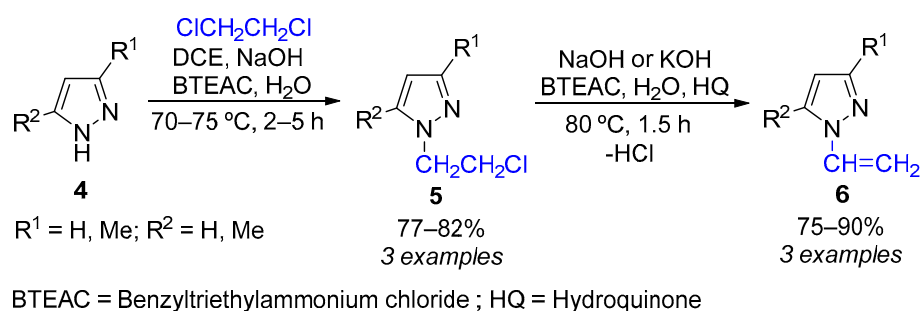


**Scheme 1.** Synthesis of 1-vinylpyrazoles **2** from geminal bis(1-pyrazolyl)alkanes **1** [38].

Other methods for the preparation of 1-vinylpyrazoles include the dehydrohalogenation of 1-(2-haloethyl)pyrazoles with potassium hydroxide in ethanol [39]. However, the treatment of 1-(2-bromoethyl)-5-hydroxy-(3-methyl- and 3-phenyl)pyrazoles under the same reaction conditions afforded the corresponding 2,3-dihydro-(6-methyl- and -6-phenyl)pyrazolo[3,2-*b*]oxazoles. On the other hand, the treatment of 5-benzoyloxy-1-(2-bromoethyl)-(3-methyl- and -3-phenyl)pyrazoles with sodium *t*-butoxide in butanol gave 5-hydroxy-(3-methyl- and -3-phenyl)-1-vinylpyrazoles.

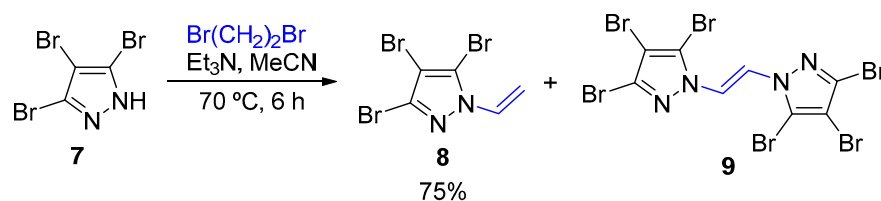
Another interesting method that allowed the formation of 1-vinylpyrazoles used water as solvent under phase transfer catalysis conditions (PTC). This method involved the *N*-alkylation of pyrazole **4** with dichloroethane (DCE) followed by dehydrochlorination of

the obtained 1-(2-chloroethyl)pyrazoles **5**, which proceeded smoothly in water under PTC conditions to the formation of 1-vinylpyrazoles **6** in 75–90% yield (Scheme 2) [40].



**Scheme 2.** Synthesis of 1-vinylpyrazoles **6** by dehydrochlorination of 1-(2-chloroethyl)pyrazoles **5** [40].

The reaction of 3,4,5-tribromopyrazole **7** with 1,2-dibromoethane and triethylamine followed by the elimination of HBr gave 3,4,5-tribromo-1-vinylpyrazole **8** in 75% overall yield (Scheme 3) [41]. The formation of 1,2-bis(3,4,5-tribromopyrazol-1-yl)ethane **9** by substitution of both bromine atoms of 1,2-dibromoethane could be suppressed by performing the reaction in acetonitrile using a large excess of triethylamine.

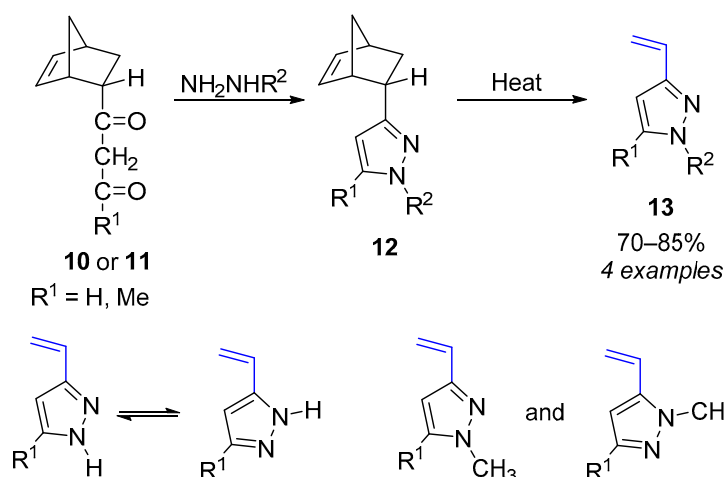


**Scheme 3.** Synthesis of 1-vinylpyrazoles **8** from 3,4,5-tribromopyrazoles **7** and 1,2-dibromoethane [41].

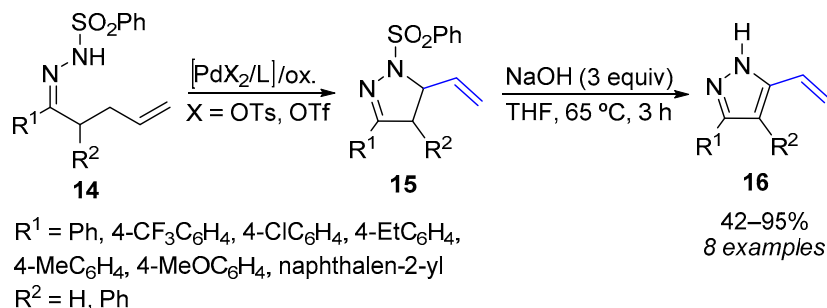
Only a few examples of the synthesis of 3- and 5-vinylpyrazoles are known, especially when one of the nitrogens bears a proton. In 1976, Sharp reported the synthesis of 3-vinylpyrazoles by thermolysis and rearrangement of 3*H*-1,2-diazepines [42]. Later, Ponticello demonstrated that the cracking of the adducts **12**, prepared by a condensation–cyclization reaction of a  $\beta$ -ketoaldehyde **10** ( $\text{R}^1 = \text{H}$ ) or a  $\beta$ -diketone **11** ( $\text{R}^1 = \text{Me}$ ) with hydrazine or its derivatives, afforded 3(5)-vinylpyrazoles **13** in good yield (Scheme 4) [43]. When  $\text{R}^1 = \text{H}$ , the two tautomers corresponding to the 3- and 5-vinylpyrazoles are indistinguishable, since very easy interconversion might be expected through ions formed by addition and loss of a proton. As expected, condensation of methyl hydrazine with  $\beta$ -ketoaldehyde or  $\beta$ -diketone each gave two isomeric pyrazoles. Substitution on nitrogen prevents tautomerism; thus, the two isomers were not identical.

Furthermore, 5-vinylpyrazoles **16** could be obtained by aromatization of 5-vinylpyrazolines **15** generated from *N*-sulfonyl,*C*-homoallyl-hydrazones **14** via Pd-catalyzed C–H oxidative C,*N*-cyclization through a 5-*exo-trig* process from a  $\pi$ -allyl complex intermediate when the Pd(II) center is associated to noncoordinating anions such as tosylates or triflates. Indeed, 5-vinylpyrazolines with electron-active substituents at the *p*-position of the phenyl ring and hindered pyrazolines could be converted to the corresponding pyrazoles in moderate-to-high yields through a base-induced eliminative aromatization process (Scheme 5) [44].



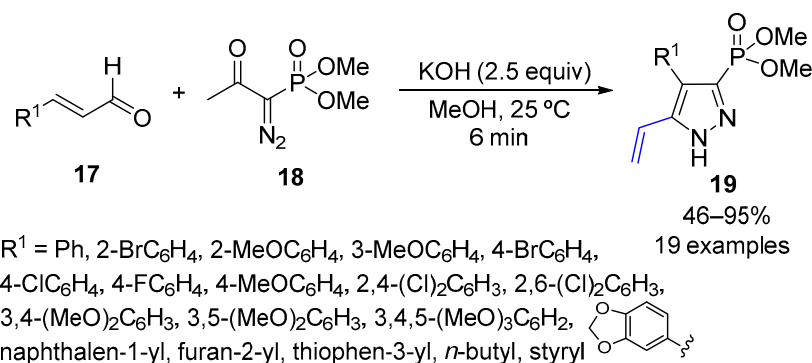


**Scheme 4.** Synthesis of 3(5)-vinylpyrazoles **13** [43].



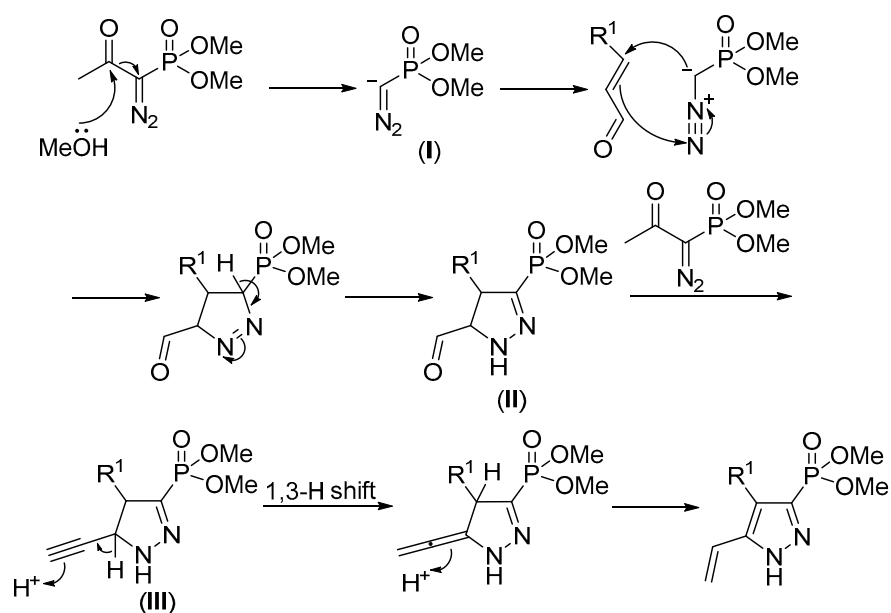
**Scheme 5.** Synthesis of 5-vinylpyrazoles **16** by base-induced eliminative aromatization of 5-vinylpyrazolines **15** [44].

Mohan and coworkers developed a rapid synthesis of 5(3)-vinylpyrazoles under mild conditions. The reaction was based on the versatility and dual reactivity of Bestmann–Ohira reagent (BOR) **18** as a homologation reagent and cycloaddition reactant in a domino reaction with a cinnamaldehyde **17** (Scheme 6) [45]. The sequence involved a formal 1,3-dipolar cycloaddition/Horner–Wadsworth–Emmons (HWE) homologation of the resulting pyrazoline carbaldehydes followed by a 1,3-H shift to give the 5(3)-vinylpyrazoles.



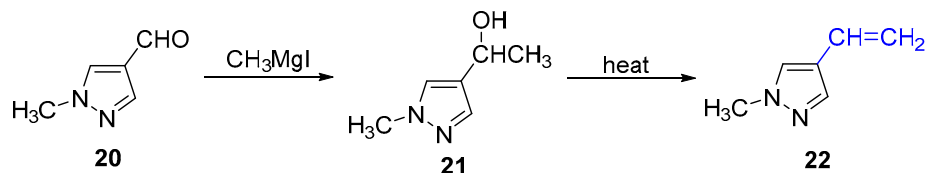
**Scheme 6.** Domino reaction for the synthesis of functionalized 5(3)-vinylpyrazoles **19** using Bestmann–Ohira reagent **18** [45].

The reaction mechanism started with the methanolysis of BOR and generation of a diazomethyl anion **I**. Then, a 1,3-dipolar cycloaddition of **I** to cinnamaldehydes gave pyrazoline carbaldehydes **II**. Reaction of pyrazolines **II** with another molecule of BOR generated pyrazoline alkyne intermediates **III**, which after a 1,3-H shift followed by aromatization produced 5(3)-vinylpyrazoles **19** (Scheme 7).



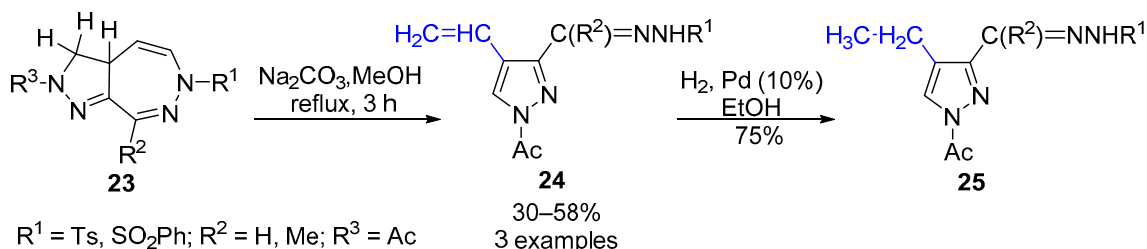
**Scheme 7.** Plausible domino reaction mechanism [45].

There have also been some reports on the synthesis of 4-vinylpyrazoles. For example, the decarboxylation of  $\beta$ -(1-phenyl-4-pyrazolyl)acrylic acid afforded 1-phenyl-4-vinylpyrazole [46,47]. Another method involved the reaction of 1-methyl-1*H*-pyrazole-4-carbaldehyde **20** with the Grignard reagent methylmagnesium iodide to produce the corresponding alcohol **21**, which upon heating afforded 1-methyl-4-vinyl-1*H*-pyrazole **22** (Scheme 8) [48].



**Scheme 8.** Synthesis of 1-methyl-4-vinylpyrazole **22** from 1-methylpyrazole-4-carbaldehyde **20** [48].

When tetrahydropyrazolo[3,4-*d*][1,2]diazepines (**23**) bearing arylsulfonyl groups at N-6 and acetyl groups at N-2 were treated with methanolic sodium carbonate (1 g per g of **23**), the corresponding 4-vinylpyrazole-3(5)-carbaldehyde tosyl and phenylsulphonylhydrazones **24** were obtained. Catalytic hydrogenation of the vinyl function gave 4-ethylpyrazoles **25** (Scheme 9) [49].



**Scheme 9.** Synthesis of 4-vinylpyrazoles **24** from tetrahydropyrazolo[3,4-*d*][1,2]diazepines **23** [49].

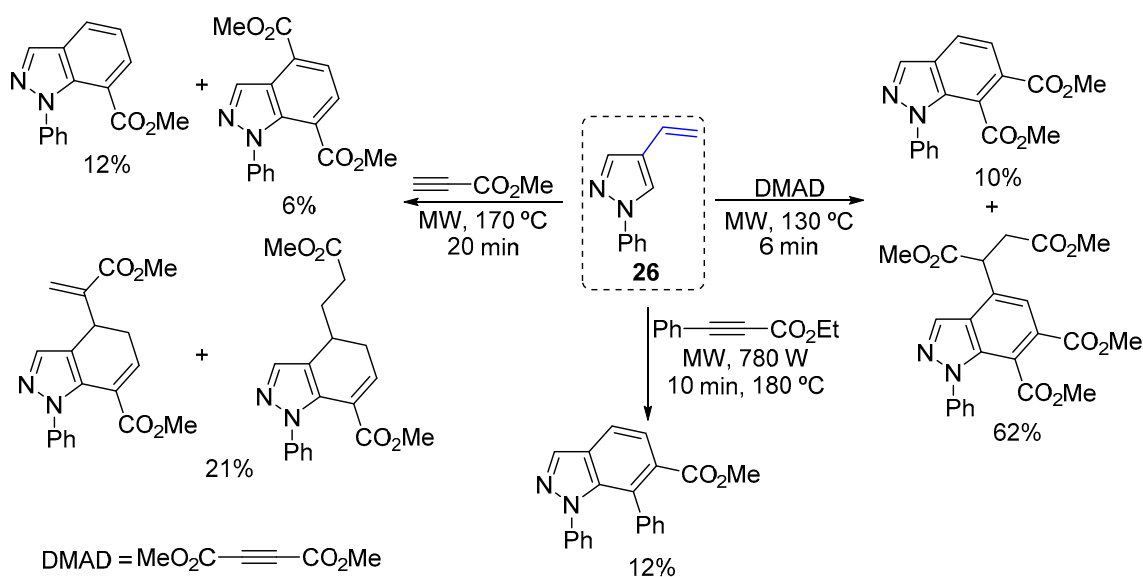
### 3. Reactivity of Vinylpyrazoles

Vinylpyrazole and substituted vinylpyrazoles do not resemble enamines in reactivity. This is in accord with the nonavailability of electrons from the N-1 to stabilize dipolar structures of transition states such as those commonly invoked to account for the reactivity

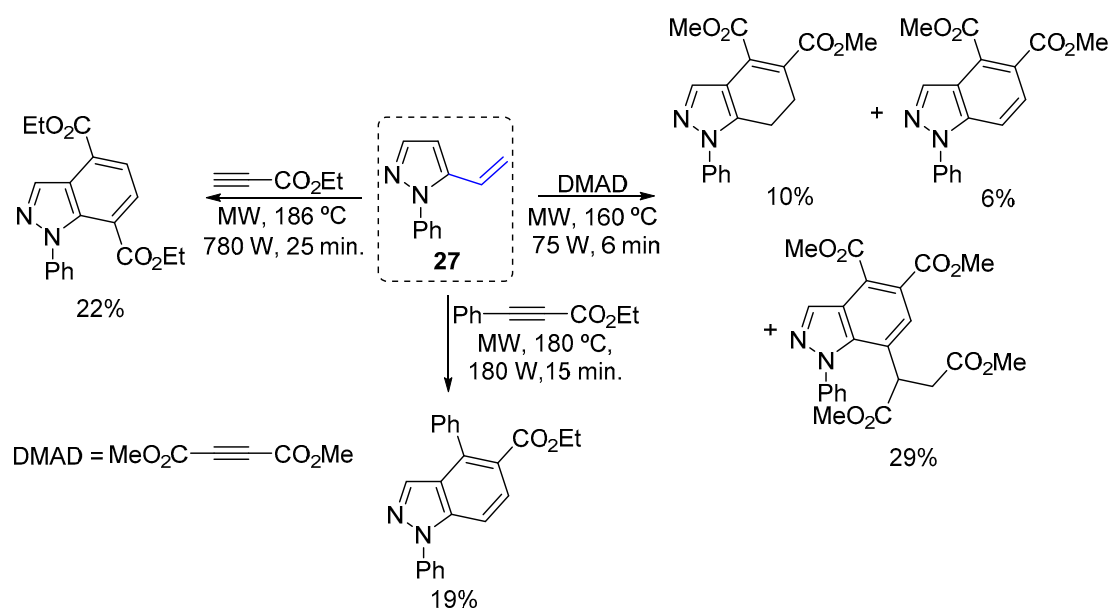
of enamines. Vinylpyrazoles coexist with pyrazole and show no tendency to add it back. The shelf life of vinylpyrazoles is good, and no polymerization in the neat liquid is observed even after 2 years [27–35]. Some reactions with vinylpyrazoles have been described in the literature. However, the reactivity of these scaffolds has been barely explored. Some examples of vinylpyrazoles' transformations are described in the following subsections.

### 3.1. Cycloaddition Reactions

Diels–Alder (DA) cycloadditions are amongst the most elegant reactions for rapidly building complex cyclic compounds. Vinylpyrazoles are very reluctant to react as dienes in DA cycloadditions because of the loss of aromaticity of the pyrazole ring on [4 + 2] cycloadduct formation being much less reactive than vinylpyrroles and vinylindoles. Harsh reaction conditions are required, such as sealed vessels and high pressures (8–10 atm) and temperatures (120–140 °C) for long reaction times (several days), to obtain very low or moderate yields [50,51]. So far, the vinylpyrazoles have been used as dienes in Diels–Alder reactions for the preparation of compounds with medicinal interest, being these ones of the most described reactions of vinylpyrazoles in literature. In 1996, Díaz-Ortiz et al. studied the effect of microwaves in solvent-free conditions in the improvement of the reactivity of vinylpyrazoles. They found that 4-vinylpyrazoles **26** reacted with dienophiles, such as methyl and ethyl propiolate, dimethyl acetylenedicarboxylate, *N*-phenylmaleimide, or tetracyanoethene, to form 1:1 adducts [52]. The cycloaddition occurred rapidly (6–30 min), and the yields, while generally fair, were superior to those of conventional methods. Moreover, with microwave activation, it was possible to use low-reactive dienophiles such as ethyl phenylpropiolate, and other intermediate products not observed in conventional methods were isolated and characterized. This type of reaction also occurred with 3- and 5-vinylpyrazoles [53]. Since DA reactions of vinylpyrazoles have been the subject of several publications, only some examples are provided for the reaction of 4- and 5-vinylpyrazoles **26** and **27** with some common dienophiles (Schemes 10 and 11) [53].



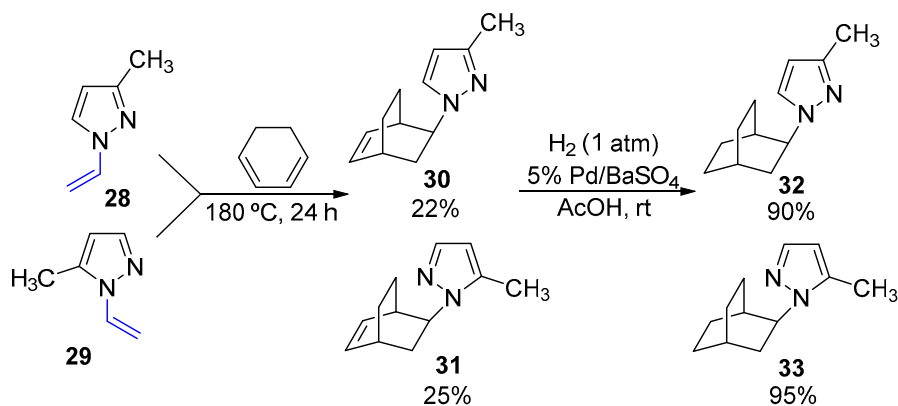
**Scheme 10.** Diels–Alder reactions of 1-phenyl-4-vinylpyrazole **26** with different dienophiles [53].



**Scheme 11.** Diels–Alder reactions of 1-phenyl-5-vinylpyrazole **27** with different dienophiles [53].

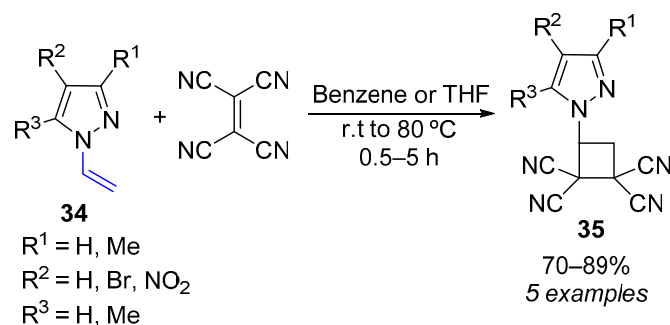
Sepúlveda-Arques et al. investigated the effects of the presence of substituents either on the pyrazole ring nitrogen or in the vinyl group on the improvement of the yields of the cycloadducts obtained from the Diels–Alder reactions. They showed that the reactivity was not limited to one kind of substituent on the nitrogen ring but was nonetheless limited and that it failed with small changes by substitution on the vinyl group [54].

Few data on the reactivity of 3- and 5-methyl-1-vinylpyrazoles **28** and **29** as dienophiles are available in the literature. Asratyan and coworkers studied the behavior of these pyrazoles as dienophiles in the reaction with cyclohexa-1,3-diene (Scheme 12) [55]. Although  $^1\text{H}$ - and  $^{13}\text{C}$ -NMR data showed that 5-methyl-1-vinylpyrazole **29** existed mainly as the *S-cis*- $\text{N}^2$  isomer, while 3-methyl-1-vinylpyrazole **28** was a roughly equimolar mixture of steric isomers [28], no characteristic differences were found in the behavior of these compounds in the cycloaddition. The reaction with the diene proceeded only at 180 °C to give the product in low yields. When reaction temperature is increased to 220 °C, fast polymerization of the diene and dienophile occurred. The authors suggested that the spatial location of the vinyl group in 1-vinylpyrazoles **28** and **29** with respect to N-2 took no part in the Diels–Alder reaction. The obtained products **30** and **31** went through a hydrogenation reaction to afford compounds **32** and **33**.



**Scheme 12.** Diels–Alder reaction of 3- and 5-methyl-1-vinylpyrazoles **28** and **29** with cyclohexa-1,3-diene [55].

In aprotic solvents, 1-vinylpyrazoles **34** reacted with tetracyanoethylene. The reaction gave mainly 1-(2,2,3,3-tetracyano-1-cyclobutyl)pyrazoles **35** as a result of a [2 + 2] cycloaddition involving the formation of a  $\pi$ - $\pi$  complex at the first stage (Scheme 13) [56]. The reaction occurred in benzene at room temperature for 1-vinylpyrazole but required heating at 80 °C for its 3-methyl and 5-methyl derivatives, while 2–5% of the product was obtained for 4-bromo-1-vinylpyrazole, and 3,5-dimethyl-4-nitropyrazole did not react to give the [2 + 2]-cycloaddition product. Using a more polar solvent such as THF or without a solvent, excess vinylpyrazoles gave high yields of the corresponding 1-(2,2,3,3-tetracyano-1-cyclobutyl)pyrazoles **35** at room temperature.



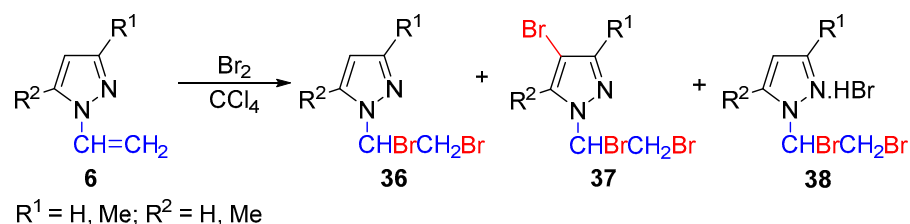
**Scheme 13.** [2 + 2] Cycloaddition of 1-vinylpyrazoles **34** with tetracyanoethylene [56].

### 3.2. Polymerization Reactions

Polymerization of vinylpyrazoles has been performed with azo initiators [38]. The rate and extent of polymerization depends on the nature of the substituents on the vinyl group. For example, neat 1-vinylpyrazole polymerizes almost explosively, while 1-(propen-2-yl)pyrazole polymerizes to a lesser extent, and the more heavily substituted the analogs are, the slower the polymerization is. In dilute benzene, 1-vinylpyrazole solution was cleanly polymerized to polymers of molecular weight 150,000–330,000. Furthermore, 1-vinylpyrazole polymerized under free-radical initiation to a high polymer. In this case, the same trend was observed; the extent of polymerization diminished with increasing substitution on the vinyl group. Nikitenko and coworkers studied the free-radical polymerization of 3-methyl-1-vinylpyrazole and 5-methyl-1-vinylpyrazole separately, as individual substances and not as a mixture of isomers [57]. In both cases, the rate of polymerization was proportional to 0.5 order with respect to the initiator azobisisobutyronitrile (AIBN) concentration. When the concentration of monomer was low ( $\leq 3M$ ), the reaction followed first-order kinetics, but for higher initial concentrations, the order was lower than the unit. The overall rate of polymerization was found to be higher for 5-methyl-1-vinylpyrazole.

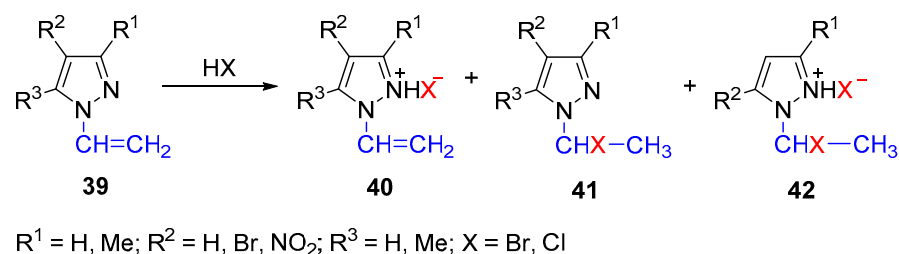
### 3.3. Halogenation and Hydrohalogenation Reactions

Compared with 1-vinylimidazoles and 1-vinyltriazoles, 1-vinylpyrazoles show a different behavior in bromination reactions [58]. With 1-vinylimidazoles, the formation of a complex with the halogen occurs, while with 1-vinyltriazoles, addition of bromine to the double bond of the vinyl group occurs. Notably, 1-vinylpyrazoles **6** do not form complexes with bromine. The bromination in carbon tetrachloride at  $-20$  °C affords a complex mixture of products that is difficult to separate. The main reaction products are 1-(1',2'-dibromo)ethylpyrazoles **36** and the product of electrophilic substitution at C-4 **37**; however, the coordination of the released hydrogen bromide with the pyrazoles present in the reaction mixture also produces hydrohalides **38** (Scheme 14). Higher percentages of **36** can be obtained by increasing the temperature, by adding the vinylpyrazole to a solution of bromine, and by using an excess of bromine, but the stability of the bromination products depends on the position and number of substituents in the pyrazole ring, especially methyl groups.



**Scheme 14.** Halogenation and hydrohalogenation of 1-vinylpyrazoles **6** [58].

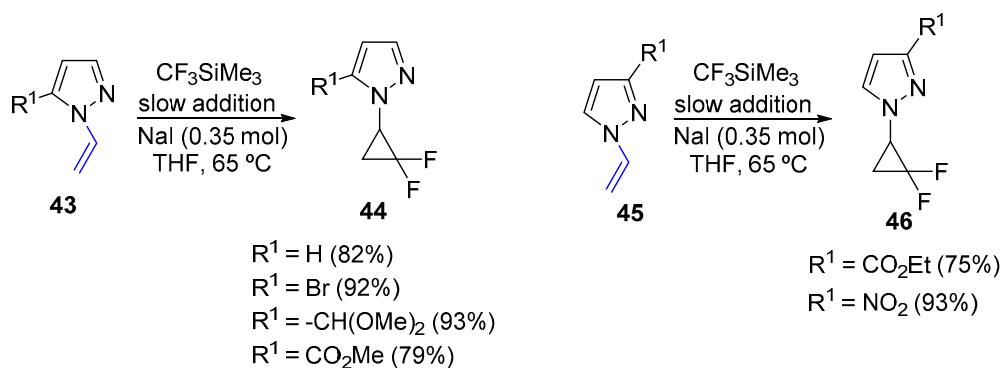
The products of the hydrohalogenation of vinylpyrazoles depend on the structure of the pyrazole itself and the nature of the hydrogen halide. Skvortsova and coworkers investigated the hydrohalogenation of a series of vinylpyrazoles **39**, (1-vinylpyrazole, 4-bromo-1-vinylpyrazole, 3-methyl-1-vinylpyrazole, 5-methyl-1-vinylpyrazole, 3,5-dimethyl-1-vinylpyrazole, and 4-nitro-3,5-dimethyl-1-vinylpyrazole) (Scheme 15) [59]. At  $-150\text{ }^\circ\text{C}$ , addition of hydrogen halides to all 1-vinylpyrazoles occurred only at the N-2 with formation of salts **40**. However, the hydrohalides of the less basic vinylpyrazoles (1-vinylpyrazole, 4-bromo-1-vinylpyrazole, and 4-nitro-3,5-dimethyl-1-vinylpyrazole) decomposed rapidly. On the other hand, at  $20\text{--}25\text{ }^\circ\text{C}$ , 1-vinylpyrazole and 4-bromo-1-vinylpyrazole added predominantly hydrogen halides at the double bond of the vinyl group, with formation of 1-(1'-haloethyl)pyrazoles **41**, which was in accordance with Markovnikov's rule. Then, the resulting compounds **41** underwent further hydrohalogenation at the N-2 to give compounds **42**. Under these conditions, the more basic alkyl-substituted 1-vinylpyrazoles produced the corresponding hydrohalides. Addition of hydrogen halides to the double bond of the vinyl group of 4-nitro-3,5-dimethyl-1-vinylpyrazole was more difficult, since the nitro group decreased the nucleophilicity not only of the N-2 but of the double bond of the vinyl group. The reaction of 4-bromo-1-vinylpyrazole with HBr formed a mixture of products, whereas the reaction with HCl proceeded most specifically [59].



**Scheme 15.** Main products formed in the hydrohalogenation of 1-vinylpyrazoles **39** [59].

### 3.4. Difluorocyclopropanation Reactions

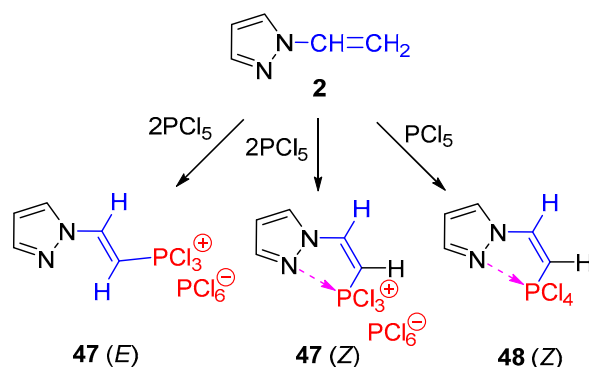
Fluorinated cyclopropanes have become extraordinary structural motifs with huge importance in organic synthesis, drug discovery, and agrochemistry. In fact, highly potent compounds bearing a *gem*-difluorocyclopropyl group were disclosed in recent patents [60–63]. In most of the compounds reported in the literature, the *gem*-difluorocyclopropyl is attached to a carbon atom, while the corresponding N-linked analogues are less common. N-vinylpyrazoles **43** and **45** undergo difluorocyclopropanation with  $\text{CF}_3\text{SiMe}_3\text{-NaI}$  system with formation of the corresponding N-difluorocyclopropyl derivatives **44** and **46** in very good yield (Scheme 16). These compounds are stable and undergo further regioselective functionalization to afford *gem*-difluorocyclopropylpyrazole amines, carboxylic acids, aldehydes, bromides, and boronic derivatives [64]. It is noteworthy that this method is not successful for the preparation of other azole derivatives, such as imidazoles, triazoles, and tetrazoles, possibly because of the presence of a nucleophilic nitrogen atom (in the case of the imidazole) or electronic effects for the other representatives.



**Scheme 16.** Difluorocyclopropanation of 1-vinylpyrazoles **43** and **45** [64].

### 3.5. Phosphorylation Reactions

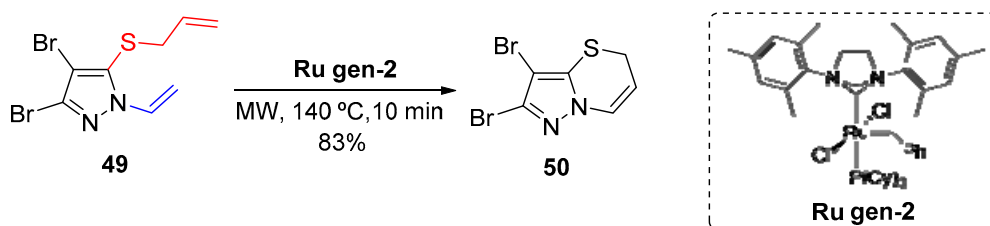
The phosphorylation of 1-vinylpyrazole **2** with phosphorus pentachloride afforded phosphorylated azoles **47** and **48** (Scheme 17) [65]. Krivdin and coworkers studied the effects of intramolecular and intermolecular coordination on  $^{31}\text{P}$  nuclear shielding both experimentally and theoretically, with a special emphasis on the calculation of  $^{31}\text{P}$  shielding constants. They noticed dramatic  $^{31}\text{P}$  nuclear shielding to approximately 150 ppm on changing the phosphorus coordination number by one (+ (90–120) ppm for tetracoordinated phosphorus, – (20–40) ppm for pentacoordinated phosphorus, and – (200–220) ppm for hexacoordinated phosphorus) and suggested that  $^{31}\text{P}$ -NMR chemical shifts could serve as an unambiguous criterion of intra- or intermolecular coordination involving phosphorus.



**Scheme 17.** Phosphorylation of 1-vinylpyrazole **2** [65].

### 3.6. Ring-Closing Metathesis Reactions

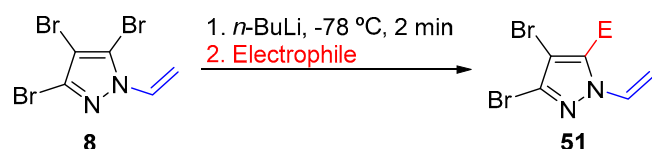
The *N*-vinylated pyrazoles are also useful intermediates for Grubbs' ring closure metathesis reaction (RCM) to generate novel heterocycles [41,66]. For example, 5*H*-pyrazolo[5,1-*b*][1,3]thiazine **50** was obtained in 83% yield, in a short reaction time, by microwave irradiation of 1-vinylpyrazole **49** with Grubbs' second-generation catalyst (**Ru gen-2**) (Scheme 18) [41,67], which in this reaction was more reactive than Grubbs' first generation [68,69] and the Hoveyda–Grubbs' catalyst [70].



**Scheme 18.** Ring closure metathesis reaction of 1-vinylpyrazole **49** with formation of 5*H*-pyrazolo[5,1-*b*][1,3]thiazine **50** [41].

### 3.7. Organometallic Reactions

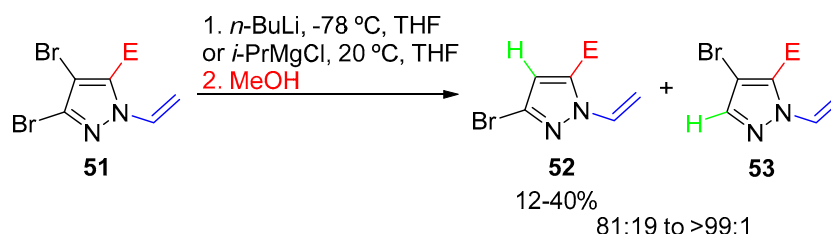
The vinyl group is a stable and versatile *N*-protection group for bromine–lithium exchange reactions in pyrazoles that can be removed easily under mild conditions. Begtrup and coworkers demonstrated that 3,4,5-tribromo-1-vinylpyrazole **8**, underwent regioselective bromine–lithium exchange at the 5-position. Subsequent addition of an electrophile gave 5-substituted 3,4-dibromo-1-vinylpyrazoles **51** (Scheme 19) [41]. A range of electrophiles can be introduced at the 5-position. Longer lithiation time (10–15 min) led to lower yields of the 5-substituted product because of the low stability of the pyrazole anion.



| Electrophile                    | E                    | Yield (%) |
|---------------------------------|----------------------|-----------|
| NH <sub>4</sub> Cl              | H                    | 80        |
| Cl <sub>6</sub> C <sub>2</sub>  | Cl                   | 82        |
| MeI                             | Me                   | 78        |
| DMF                             | CHO                  | 66        |
| Ph <sub>2</sub> CO              | CHPh <sub>2</sub> OH | 81        |
| TsCN                            | CN                   | 26        |
| TBDMSCl                         | TBDMS                | 77        |
| Me <sub>2</sub> S <sub>2</sub>  | SMe                  | 84        |
| All <sub>2</sub> S <sub>2</sub> | SAll                 | 77        |
| Ph <sub>2</sub> PCl             | PPh <sub>2</sub>     | 59        |
| Bu <sub>3</sub> SnCl            | SnBu <sub>3</sub>    | 77        |

**Scheme 19.** Bromine–lithium exchange of 3,4,5-tribromo-1-vinylpyrazole **8** and reactions with different electrophiles [41].

The 5-substituted 3,4-dibromo-1-vinylpyrazoles **51** can undergo subsequent bromine–lithium or bromine–magnesium exchange using *n*-BuLi or *i*-PrMgCl together with protons from methanol as the electrophile, affording compounds **52** and **53**. The reaction occurred preferentially at C-4, with the regioselectivity between C-3- and C-4 being influenced by the nature of the metal and the 5-substituent (Scheme 20) [41]. Begtrup and coworkers found that bromine–lithium exchange took place with higher regioselectivity than bromine–magnesium exchange.

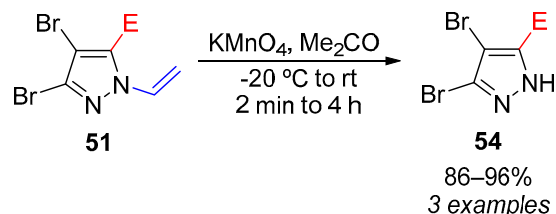


**Scheme 20.** Regioselectivity of bromine–lithium and bromine–magnesium exchange in 5-substituted 3,4-dibromo-1-vinylpyrazoles **51** [41].

The vinyl group can be removed from the 5-substituted compounds **51** by mild treatment with KMnO<sub>4</sub>, affording the corresponding NH-pyrazoles **54**. Depending on the substituents, slightly different conditions may be required (Scheme 21) [41]. For example, the vinyl group of 3,4,5-tribromo-1-vinylpyrazole (E = Br) and 3,4-dibromo-5-methyl-1-



vinylpyrazole (E = Me) could be removed smoothly in excellent yield (96% for both) by treatment with a 2% solution of  $\text{KMnO}_4$  at room temperature and at 10 °C. When oxidation sensitive groups such as SMe (E = SMe) are present, the devinylation should be performed at  $-20$  to  $-10$  °C to avoid concurrent oxidation of SMe to  $\text{SO}_2\text{Me}$ .



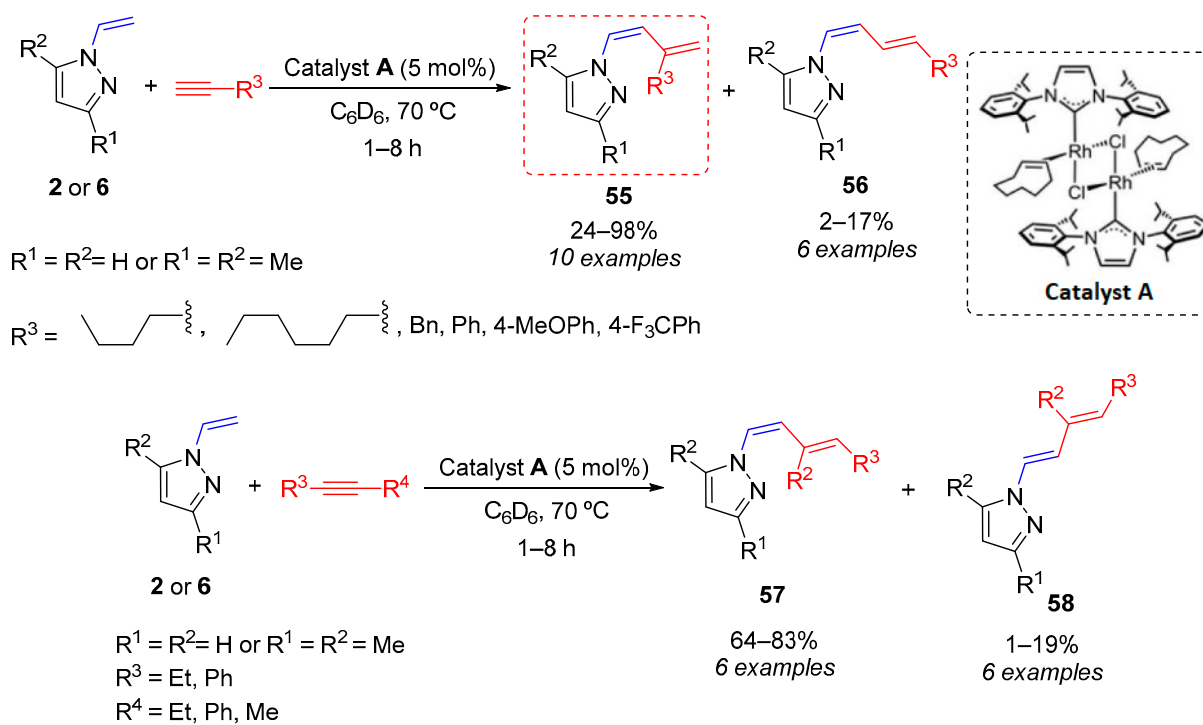
**Scheme 21.** Cleavage of the vinyl group of 5-substituted 1-vinylpyrazoles **51** [41].

### 3.8. Transition-Metal-Catalyzed Reactions

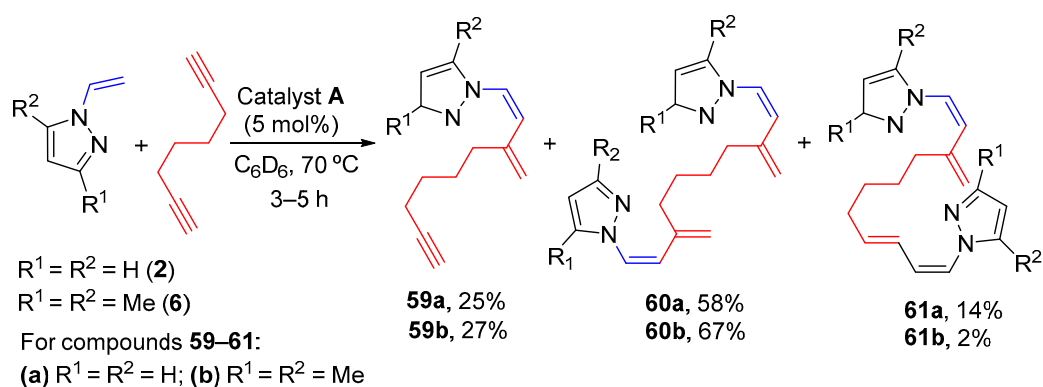
Transition-metal-catalyzed reactions have gained increasing interest in organic chemistry over the last years because of their versatility and high levels of chemo-, regio-, and stereoselectivity. Many transition-metal complexes of Pd, Au, Zn, Co, Rh, Ru, Mo, Ni, Cu, and Fe have been developed as catalysts to accelerate these organic reactions. One of the hottest topics in transition metal catalysis is the development of highly efficient catalysts for direct C-H bond functionalization reactions. Preferentially, these reactions should be performed in mild conditions (room temperature, weak base, air atmosphere) to allow easy access to nitrogen-containing compounds such as pyrazoles frequently found in pharmaceuticals, crop-protection chemicals, and products for material sciences.

#### C-H Activation Reactions

Among the transition-metal-catalyzed reactions, C-C bond formation via C-H activation has gaining increasing interest as a very powerful, selective, and atom-economical tool in organic synthesis [71]. Aromatic protons have been commonly involved in this process, but functionalization of the vinyl C-H bond is more challenging because of competitive polymerization or Michael addition reactions, and electron-rich olefins are much less reactive [72]. The 1-vinylpyrazoles **2** and **6** underwent coupling with alkynes via C-H activation to afford Markovnikov-selective butadienylpyrazole derivatives **55** and **57** under mild conditions [73]. This reaction was efficiently catalyzed by the rhodium(I)-*N*-heterocyclic carbene catalyst **A** ( $\text{A} = [\text{Rh}(\mu\text{-Cl})(\text{IPr})(\eta^2\text{-coe})]_2$ ) (Rh-NHC). The reaction occurred both with terminal or internal alkynes (Scheme 22) and with terminal diynes (Scheme 23) in mild conditions. With terminal diynes, a mixture of monohydrovinylated *Z/gem* product **59** and the doubly coupled derivatives bis-*Z/gem* **60** and *Z/gem Z/E* **61** was obtained (Scheme 23). The presence of the carbene ligand in the rhodium catalyst was found to be essential for the catalytic coupling and C-H activation of the electron-rich pyrazolyl olefin. Moreover, 1-vinylpyrazole **2** ( $\text{R}^1 = \text{R}^2 = \text{H}$ ) was more reactive than 3,5-dimethyl-1-vinylpyrazole **6** ( $\text{R}^1 = \text{R}^2 = \text{Me}$ ), but the reaction with the former presented slightly lower selectivity. It is worth mentioning that even with the diynes, the selectivity trend towards Markovnikov addition products was maintained, with disubstituted pyrazole **6** being slightly more selective than **2**. Contrarily to aromatic alkynes, aliphatic terminal alkynes were preferentially hydrovinylated without dimerization, cyclotrimerization, or polymerization of the alkyne.

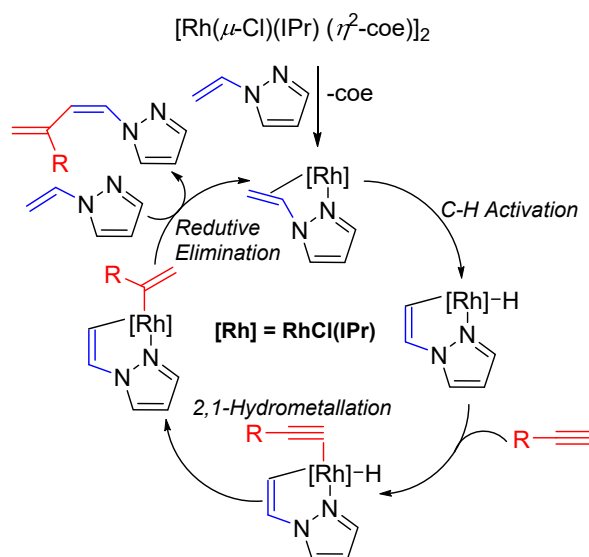


**Scheme 22.** Coupling reaction of 1-vinylpyrazoles **2** and **6** with terminal and internal alkynes mediated by Rh-NHC catalyst [73].



**Scheme 23.** Coupling reaction of 1-vinylpyrazoles **2** and **6** with terminal diynes mediated by Rh-NHC catalyst [73].

The reaction mechanism started with the C-H activation of the vinylpyrazole assisted by nitrogen coordination to the metallic center. Then, alkyne coordination, insertion, and reductive elimination took place to afford the coupling product (Scheme 24) [73].



**Scheme 24.** Plausible catalytic cycle for the coupling reaction of 1-vinylpyrazole **2** with alkynes [73].

### 3.9. Miscellaneous

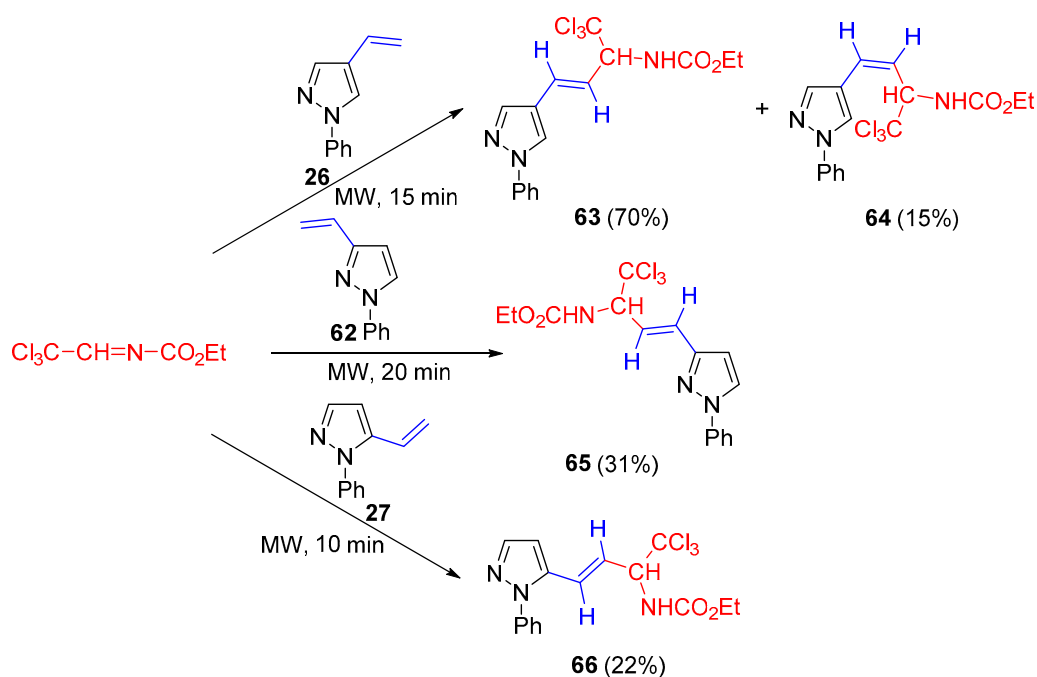
#### 3.9.1. Reaction with Ethyl *N*-Trichloroethylidenecarbamate

The reaction of vinylpyrazoles **26**, **62**, and **27** with *N*-trichloroethylidenecarbamate, which participates in cycloaddition reactions as a dienophile, as a dipolarophile, and even as a heterodiene, did not afford any cycloaddition product. Under microwave heating, the result of the reaction was found to depend on the nature of the diene and the substitution of the pyrazole ring. In fact, an electrophilic substitution reaction occurred through the exocyclic double bond, which was activated by conjugation with the pyrazole ring, to give Michael addition to the conjugated imine system (Scheme 25) [74]. Even in the 3- and 5-substituted pyrazoles **62** and **27**, the reaction occurred at the double bond and not in the activated C-4 of the pyrazole ring. A mixture of *trans*-**63** and *cis*-**64** isomers was obtained with pyrazole **26** (although the *cis* was obtained in 15% yield), while the thermodynamic *trans* isomer **65** and **66** was the only product observed in the reactions of pyrazoles **62** and **27**, respectively. Under conventional heating in an oil bath, no reaction occurred under similar conditions of temperature and time, and the starting vinylpyrazoles were not recovered because of dimerization in these conditions.

#### 3.9.2. Reaction with Alkanethiols

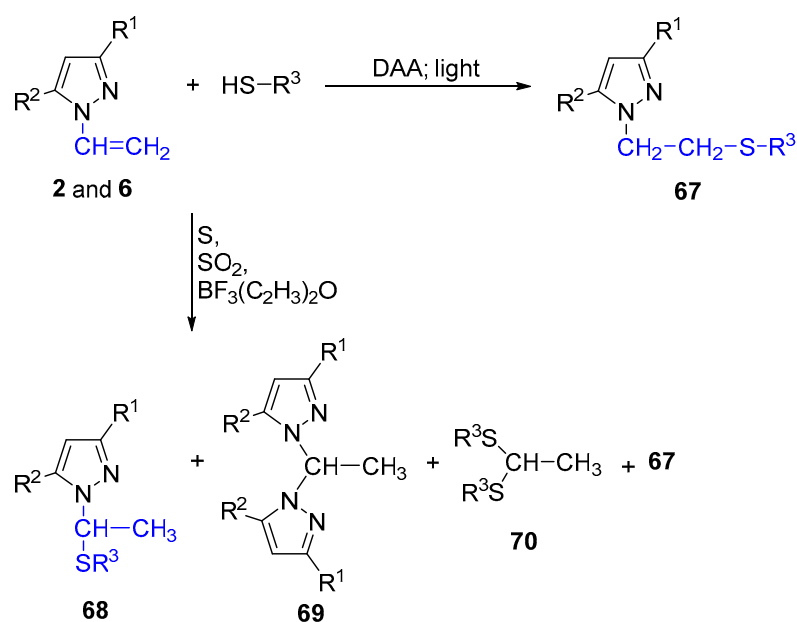
Pyrazoles containing sulfur atoms have interesting biological activities and are used as drugs [75]. This type of pyrazoles can be prepared from vinylpyrazoles and their alkyl derivatives, which are known to react with thiols via either ionic or free radical mechanisms, with the formation of  $\alpha$ - and  $\beta$ -addition products, depending on whether the addition follows the Markovnikov rule or not, respectively [76].

The method of radical thiylation yields more stable products and is easily and rapidly conducted not only with heating, catalysts, and irradiation with UV light but at 20 °C without special initiation, being a more convenient method of synthesis of pyrazoles with sulfur-containing substituents.



**Scheme 25.** Reactions of 1-phenylvinylpyrazoles **26**, **62**, and **27** with ethyl *N*-trichloroethylidene carbamate [74].

$\beta$ -Addition products, the 1-(pyrazolyl-1)-2-(alkylthio)ethanes (Scheme 26, **67.1a–e**–**67.3a–e**, **67.4b,d,e**), were formed, in 80–85% yield, in the reaction of thiols with 1-vinylpyrazoles **2** and **6**. The ease of the radical addition was a function of both the reactants and the reaction conditions, namely the temperature. Methyl substituted 1-vinylpyrazoles **6** reacted more energetically than **2**, and the reaction time was reduced to 0.5–2 h by increasing the temperature to 80 °C and using AIBN (1%) as a radical initiator. In the presence of ionic initiators ( $\text{BF}_3(\text{C}_2\text{H}_5)_2\text{O}$ ,  $\text{SO}_2$ , S) with heating, the reaction followed two competing pathways, with the formation of a mixture of  $\alpha$ - and  $\beta$ -addition products **68** and **67**, the ratio of which depended on the reaction conditions used, together with 1,1-bis(pyrazol-1-yl)ethanes **69** and 1,1-bis(*R*-thio)ethanes **70**, formed as a result of disproportionation of 1-(pyrazol-1-yl)-1-(*R*-thio)ethanes **68.1a–d**, **68.4a–d**. The authors isolated some products of  $\alpha$ -addition **68.2b–68.4b**, **68.4a,c,d**, thioacetals **70a–c**, and pyrazoles **69.1–69.4**. Thylation of vinylpyrazole **6.4** ( $\text{R}^1 = \text{R}^2 = \text{Me}$ ) with butane-1-thiol (**b**) afforded only the product of  $\beta$ -addition **67.4b**, with *p*-toluenesulfonic acid (3%, 9%, 90 °C, 8 h). In the presence of elemental sulfur, the addition of thiols to alkenes followed the Markovnikov rule, and sulfur inhibited radical processes. Total yields of thylation for vinylpyrazole **67.4b** were no greater than 53% in the presence of 3, 9, and 15 mol% of sulfur in heating at 90 °C for 14 h. Increasing the temperature to 120 °C, the yield increased to 80–83%. In similar conditions (120 °C, 14 h, 9 mol%), the yield for the formation of vinylpyrazoles **67.1–67.3** was slightly lower (70–75%), and the concentration of  $\alpha$ - and  $\beta$ -addition products was 95:5–90:10. When  $\text{BF}_3(\text{C}_2\text{H}_5)_2\text{O}$  was used (9 mol%, 120 °C, 14 h), the product of the  $\beta$ -addition was the main compound. Addition of radical process inhibitors such as benzoquinone or hydroquinone (3–6%) allowed increasing the concentration of  $\alpha$ -products **68** to 95–98%, although  $\beta$ -addition was not completely suppressed.



DAA = *N,N*-Diallylamine

For compounds **67–70**:

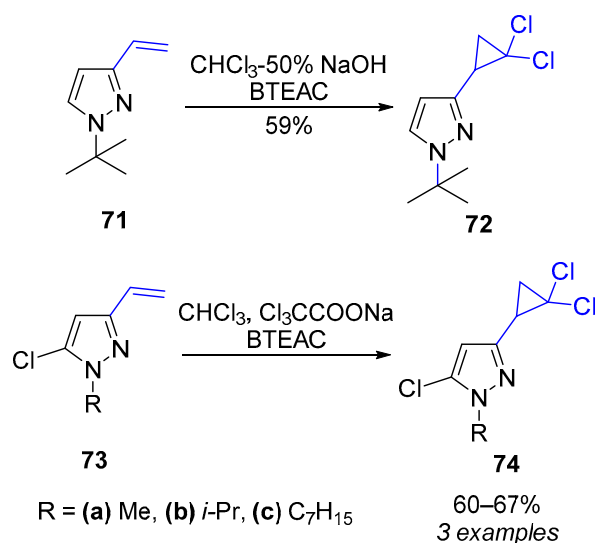
(**1**)  $\text{R}^1 = \text{R}^2 = \text{H}$ ; (**2**)  $\text{R}^1 = \text{Me}$ ,  $\text{R}^2 = \text{H}$ ; (**3**)  $\text{R}^1 = \text{H}$ ,  $\text{R}^2 = \text{Me}$ ; (**4**)  $\text{R}^1 = \text{R}^2 = \text{Me}$

$\text{R}^3 =$  (**a**)  $\text{C}_2\text{H}_5$ ; (**b**)  $\text{C}_4\text{H}_9$ ; (**c**)  $-\text{CH}_2-\underset{\text{CH}_3}{\text{CH}}-\text{CH}_3$ ; (**d**)  $-\text{H}_2\text{C}-\text{C}_6\text{H}_4$ ; (**e**)  $-\text{H}_2\text{C}-\text{C}_4\text{H}_3\text{O}$

**Scheme 26.** Reactions of 1-vinylpyrazoles **2** and **6** with alkanethiols [76].

### 3.9.3. Reaction with Dichlorocarbene

Furthermore, 3-vinylpyrazoles **71** react with dichlorocarbene, generated from chloroform or sodium trichloroacetate, to afford new cyclopropylpyrazoles **72** [77], which are interesting precursors of bisheterocycles such as 5-(pyrazol-4-yl)isoxazolines. Popov and coworkers synthesized 1-*t*-butyl-3-(2,2-dichlorocyclopropyl)-1*H*-pyrazole **72** by reaction of vinylpyrazole **71** with chloroform and sodium hydroxide under PTC. The reaction was carried out at 60 °C (10 min), and compound **72** was obtained in 59% yield (Scheme 27). The reactions of 1-alkyl-5-chloro-3-vinyl-1*H*-pyrazoles **73a–c** under analogous conditions did not afford the target dichlorocyclopropane derivatives. In fact, 1-alkyl-5-chloro-3-(2,2-dichlorocyclopropyl)-1*H*-pyrazoles **74a–c** were obtained in good yield only when dichlorocarbene was generated under neutral conditions, by thermal decomposition of sodium trichloroacetate in chloroform in the presence of benzyltriethylammonium chloride (BTEAC) as PTC (Scheme 27) [77].



**Scheme 27.** Synthesis of 3-(2,2-dichlorocyclopropyl)pyrazoles **72** and **74** [77].

#### 4. Conclusions

Few methods have been reported in the literature for the synthesis of vinylpyrazoles, especially for the preparation of 3(5)- and 4-vinylpyrazoles. In addition, most of the reported methods used harsh conditions and/or toxic reagents and suffered from a lack of generality and/or substrate scope. Thus, novel methods for the synthesis of these interesting pyrazole scaffolds are highly desirable. Furthermore, reactivity studies with vinylpyrazoles have been scarce and mainly restricted to Diels–Alder cycloadditions, polymerization reactions, and halogenation and dehydrohalogenation reactions. The application of the novel tools and concepts of modern organic chemistry to vinylpyrazoles, namely solid supported synthesis, transition-metal catalysis using the more classical and novel catalysts, and visible-light-photoinduced and greener organometallic reactions, may open great opportunities for the development of novel methods of synthesis and transformations of vinylpyrazoles. From our point of view, of high interest will be the investigation of transition-metal-catalyzed reactions of vinylpyrazoles, and especially the more challenging C–H activation reactions, visible-light-photoinduced reactions, and greener organometallic reactions that allow the introduction of different electrophiles in the pyrazole ring, towards the development of more environmentally friendly, atom-economic, and selective transformation of vinylpyrazoles into more advanced molecules with therapeutical interest.

**Author Contributions:** Conceptualization, V.L.M.S. and A.M.S.S.; writing—original draft preparation, V.L.M.S.; writing—review and editing, V.L.M.S. and A.M.S.S. All authors have read and agreed to the published version of the manuscript.

**Funding:** This work received financial support from the University of Aveiro, Fundação para a Ciência e Tecnologia, FCT/MEC, through the financial support of the LAQV-REQUIMTE (UIDB/50006/2020). V. L. M. Silva thanks funding through FCT under the Scientific Employment Stimulus—Institutional Call—reference CEECINST/00026/2018.

**Institutional Review Board Statement:** Not applicable.

**Informed Consent Statement:** Not applicable.

**Data Availability Statement:** Not applicable.

**Conflicts of Interest:** The authors declare no conflict of interest.

**Sample Availability:** Not applicable.

## References

1. Pérez-Fernández, R.; Goya, P.; Elguero, J. A review of recent progress (2002–2012) on the biological activities of pyrazoles. *Arxivoc* **2014**, *2014*, 233. [CrossRef]
2. Küçükgülzel, S.G.; Senkardes, S. Recent advances in bioactive pyrazoles. *Eur. J. Med. Chem.* **2015**, *97*, 786–815. [CrossRef]
3. Abrigach, F.; Touzani, R. Pyrazole derivatives with NCN junction and their biological activity: A review. *Med. Chem.* **2016**, *6*, 292–298. [CrossRef]
4. Faria, J.V.; Vegi, P.F.; Miguita, A.G.C.; dos Santos, M.S.; Boechat, N.; Bernardino, A.M.R. Recently reported biological activities of pyrazole compounds. *Bioorg. Med. Chem.* **2017**, *25*, 5891–5903. [CrossRef]
5. Ansari, A.; Ali, A.; Asif, M. Biologically active pyrazole derivatives. *New J. Chem.* **2017**, *41*, 16–41. [CrossRef]
6. Silva, V.L.M.; Elguero, J.; Silva, A.M.S. Current progress on antioxidants incorporating the pyrazole core. *Eur. J. Med. Chem.* **2018**, *156*, 394–429. [CrossRef]
7. Gomes, P.M.O.; Silva, A.M.S.; Silva, V.L.M. Pyrazoles as key scaffolds for the development of fluorine-18-labeled radiotracers for positron emission tomography (PET). *Molecules* **2020**, *25*, 1722. [CrossRef]
8. Secci, D.; Bolasco, A.; Chimenti, P.; Carradori, S. The state of the art of pyrazole derivatives as monoamine oxidase inhibitors and antidepressant/anticonvulsant agents. *Curr. Med. Chem.* **2011**, *18*, 5114–5144. [CrossRef]
9. Silva, V.L.M.; Silva, A.M.S.; Pinto, D.C.G.A.; Jagerovic, N.; Callado, L.F.; Cavaleiro, J.A.S.; Elguero, J. Synthesis and pharmacological evaluation of chlorinated *N*-alkyl-3 and -5-(2-hydroxyphenyl)pyrazoles as CB<sub>1</sub> cannabinoid ligands. *Monatsh. Chem.* **2007**, *138*, 797–811. [CrossRef]
10. Silva, V.L.M.; Silva, A.M.S.; Pinto, D.C.G.A.; Rodríguez, P.; Gomez, M.; Jagerovic, N.; Callado, L.F.; Cavaleiro, J.A.S.; Elguero, J.; Fernandez-Ruiz, J. Synthesis and pharmacological evaluation of new (*E*)- and (*Z*)-3-aryl-4-styryl-1*H*-pyrazoles as potential cannabinoid ligands. *Arxivoc* **2010**, *2010*, 226–247. [CrossRef]
11. Marques, J.; Silva, V.L.M.; Silva, A.M.S.; Marques, M.P.M.; Braga, S.S. Ru(II) trithiacyclononane 5-(2-hydroxyphenyl)-3-[(4-methoxystyryl)pyrazole], a complex with facile synthesis and high cytotoxicity against PC-3 and MDA-MB-231 cells. *Complex Met.* **2014**, *1*, 7–12. [CrossRef]
12. Chowdary, B.N.; Umashankara, M.; Dinesh, B.; Girish, K.; Baba, A.R. Development of 5-(aryl)-3-phenyl-1*H*-pyrazole derivatives as potent antimicrobial compounds. *Asian J. Chem.* **2019**, *31*, 45–50. [CrossRef]
13. Carreira, A.R.F.; Pereira, D.M.; Andrade, P.B.; Valentão, P.; Silva, A.M.S.; Braga, S.S.; Silva, V.L.M. Novel styrylpyrazole-glucosides and their dioxolo-bridged doppelgangers: Synthesis and cytotoxicity. *New J. Chem.* **2019**, *43*, 8299–8310. [CrossRef]
14. Rocha, S.; Lucas, M.; Silva, V.L.M.; Gomes, P.M.O.; Silva, A.M.S.; Araújo, A.N.; Aniceto, N.; Guedes, R.C.; Corvo, M.L.; Fernandes, E.; et al. Pyrazoles as novel protein tyrosine phosphatase 1B (PTP1B) inhibitors: An in vitro and in silico study. *Int. J. Biol. Macromol.* **2021**, *181*, 1171–1182. [CrossRef]
15. Rocha, S.; Aniceto, N.; Guedes, R.C.; Albuquerque, H.M.T.; Silva, V.L.M.; Silva, A.M.S.; Corvo, M.L.; Fernandes, E.; Freitas, M. An In Silico and an In Vitro Inhibition Analysis of Glycogen Phosphorylase by Flavonoids, Styrylchromones, and Pyrazoles. *Nutrients* **2022**, *14*, 306. [CrossRef]
16. Giornal, F.; Pazenok, S.; Rodefeld, L.; Lui, N.; Vors, J.-P.; Leroux, F.R. Synthesis of diversely fluorinated pyrazoles as novel active agrochemical ingredients. *J. Fluor. Chem.* **2013**, *152*, 2–11. [CrossRef]
17. Garcia, H.; Iborra, S.; Miranda, M.A.; Morera, I.M.; Primo, J. Pyrazoles and isoxazoles derived from 2-hydroxyaryl phenylethynyl ketones: Synthesis and spectrophotometric evaluation of their potential applicability as sunscreens. *Heterocycles* **1991**, *32*, 1745–1748. [CrossRef]
18. Catalan, J.; Fabero, F.; Claramunt, R.M.; Santa Maria, M.D.; Foces-Foces, M.C.; Cano, F.H.; Martinez-Ripoll, M.; Elguero, J.; Sastre, R. New ultraviolet stabilizers: 3- and 5-(2'-hydroxyphenyl)pyrazoles. *J. Am. Chem. Soc.* **1992**, *114*, 5039–5048. [CrossRef]
19. Willy, B.; Müller, T.J.J. Rapid one-pot, four-step synthesis of highly fluorescent 1,3,4,5-tetrasubstituted pyrazoles. *Org. Lett.* **2011**, *13*, 2082–2085. [CrossRef]
20. Dorlars, A.; Schellhammer, C.-W.; Schroeder, J. Heterocycles as Structural Units in New Optical Brighteners. *Angew. Chem. Int. Ed.* **1975**, *14*, 665–679. [CrossRef]
21. Trofimenko, S. Coordination chemistry of pyrazole-derived ligands. *Chem. Rev.* **1972**, *72*, 497–509. [CrossRef]
22. Busev, A.I.; Akimov, V.K.; Gusev, S.I. Pyrazolone Derivatives as Analytical Reagents. *Russ. Chem. Rev.* **1965**, *34*, 237. [CrossRef]
23. Tanitame, A.; Oyamada, Y.; Ofuji, K.; Suzuki, K.; Ito, H.; Kawasaki, M.; Wachi, M.; Yamagishi, J.-I. Potent DNA gyrase inhibitors; novel 5-vinylpyrazole analogues with Gram-positive antibacterial activity. *Bioorg. Med. Chem. Lett.* **2004**, *14*, 2863–2866. [CrossRef]
24. Farberov, M.I. An investigation of pyrazoles LVII. Synthesis of 1- and 4-Vinylpyrazoles. *Khim. Nauka Prom.* **1959**, *4*, 90.
25. Jacobi, H.R. An investigation of pyrazoles LVII. Synthesis of 1- and 4-Vinylpyrazoles. *Ktmststoffe* **1953**, *43*, 381.
26. Grandberg, I.I.; Sharova, G.I. An investigation of pyrazoles LVII. Synthesis of 1- and 4-Vinylpyrazoles. *Khimiya Geterotsiklicheskikh Soedin.* **1968**, *4*, 325–326.
27. Chipanina, N.N.; Kazakova, N.A.; Shestova, L.A.; Domnina, E.S.; Skvortsova, G.G.; Frolov, Y.L. Spectroscopic evidence of donor-acceptor interactions of 1-ethyl and 1-vinylpyrazoles. *J. Appl. Spectrosc.* **1975**, *23*, 946–949. [CrossRef]
28. Es'kova, L.A.; Voronov, V.K.; Domnina, E.S.; Skvortsova, G.G. NMR spectra and structure of 1-vinylpyrazoles. *Russ. Chem. Bull.* **1985**, *34*, 922–926. [CrossRef]

29. Es'kova, L.A.; Voronov, V.K.; Domnina, E.S.; Olivson, A.I.; Chipanina, N.N.; Petrova, E.V.; Shulunova, A.I.; Enikeeva, E.I.; Skvortsova, G.G. NMR and IR spectroscopic study of the structure of quaternary salts of 1-vinylpyrazoles. *Russ. Chem. Bull.* **1985**, *34*, 917–921. [CrossRef]
30. Danovich, D.K.; Voronov, V.K.; Es'kova, L.A. Quantum-chemical investigation of the electronic structure and geometry of 1-vinylpyrazole derivatives. *Russ. Chem. Bull.* **1988**, *37*, 278–283. [CrossRef]
31. Afonin, A.V.; Voronov, V.K.; Es'kova, L.A.; Domnina, E.S.; Petrova, E.V.; Zasyad'ko, O.V. Direct  $^{13}\text{C}$ - $^1\text{H}$  coupling constants in the vinyl group of 1-vinylpyrazoles. *Russ. Chem. Bull.* **1987**, *36*, 180–182. [CrossRef]
32. Turchaninov, V.K.; Ermikov, A.F.; Es'kova, L.A.; Shagun, V.A. Conformational structure of 1-vinylpyrazoles from photoelectron and electron spectroscopic data. *J. Struct. Chem.* **1988**, *29*, 639–641. [CrossRef]
33. Afonin, A.V.; Danovich, D.K.; Voronov, V.K.; Es'kova, L.A.; Baikalova, L.V.; Domina, E.S. Rotational isomerism in 1-vinylpyrazoles and 1-vinylimidazoles from  $^1\text{H}$  and  $^{13}\text{C}$  NMR data and quantum-chemical calculations. *Chem. Heterocycl. Compd.* **1990**, *26*, 1121–1125. [CrossRef]
34. Afonin, A.V.; Voronov, V.K.; Domnina, E.S.; Es'kova, L.A.; Baikalova, L.V.; Trzhtinskaya, B.V.; Enikeeva, E.I.; Vashchenko, A.V.  $^{15}\text{N}$  NMR spectra and specific intramolecular interactions in *N*-vinylazoles. *Chem. Heterocycl. Compd.* **1991**, *27*, 845–848. [CrossRef]
35. Afonin, A.V.; Vashchenko, A.V. Analysis of influence of the 5-methyl group on internal rotation of the vinyl group in 1-vinylpyrazoles by the AM-I method. *Russ. Chem. Bull.* **1991**, *40*, 1838–1840. [CrossRef]
36. Jones, N.O. Chem. Abstr., 6T, 1077h. British Patent 887, 365, 1962.
37. Grandberg, I.I.; Sharova, G.I. Studies on pyrazoles LX. Synthesis of *N*-Vinylpyrazoles. *Chem. Heterocycl. Compd.* **1968**, *4*, 797–798. [CrossRef]
38. Trofimenko, S. Vinylpyrazoles. *J. Org. Chem.* **1970**, *35*, 3459–3462. [CrossRef]
39. Ochi, H.; Miyasaka, T.; Arakawa, K. Studies of Heterocyclic Compounds. XVI. Synthesis of 1-Vinylpyrazoles by Dehydrohalogenation of 1-(2-Haloethyl)pyrazoles. *Yakugaku Zasshi J. Pharm. Soc. Jpn.* **1978**, *98*, 165–171. [CrossRef]
40. Attarian, O.S.; Matsuyan, S.G.; Martirosyan, S.S. Synthesis of *N*-Vinylpyrazoles. *Chem. Heterocycl. Compd.* **2005**, *41*, 452–455. [CrossRef]
41. Iddon, B.; Tønder, J.E.; Hosseini, M.; Begtrup, M. The *N*-vinyl group as a protection group of the preparation of 3(5)-substituted pyrazoles via bromine–lithium exchange. *Tetrahedron* **2007**, *63*, 56–61. [CrossRef]
42. Anderson, C.D.; Sharp, J.T.; Stefaniuk, E.; Strathdee, R.S. The thermal and photochemical reactions of 3*H*-1,2-diazepines: A new variation on the diazepine-pyrazole rearrangement. *Tetrahedron Lett.* **1976**, *17*, 305–308. [CrossRef]
43. Ponticello, I.S. Preparation of New Heterocyclic Monomers: Vinylisoxazoles, Vinylpyrazoles, and Vinylpyrazolones. *J. Polym. Sci. A Polym. Chem.* **1975**, *13*, 415–423. [CrossRef]
44. Mboyi, C.D.; Duhayon, C.; Canac, Y.; Chauvin, R. From *N*-sulfonyl,*C*-homoallyl-hydrazones to pyrazole and pyridazine (*N*2)-heterocycles: The ultimate aromatization process. *Tetrahedron* **2014**, *70*, 4957–4968. [CrossRef]
45. Ahamad, S.; Gupta, A.K.; Kant, R.; Mohanan, K. Domino reaction involving the Bestmann–Ohira reagent and  $\alpha,\beta$ -unsaturated aldehydes: Efficient synthesis of functionalized pyrazoles. *Org. Biomol. Chem.* **2015**, *13*, 1492–1499. [CrossRef] [PubMed]
46. Finar, I.L.; Saunders, K.J. An Investigation of pyrazoles LVII. Synthesis of 1- and 4-vinylpyrazoles. *J. Chem. Soc.* **1963**, *4*, 3967. [CrossRef]
47. Grandberg, I.I.; Sharova, G.I. An investigation of pyrazoles. *Chem. Heterocycl. Compd.* **1970**, *4*, 241–242. [CrossRef]
48. Timmermans, P.; Vijtewaal, A.P.; Habraken, C.I. Pyrazoles XI. The synthesis of 1,1'-dimethylbipyrazolylys. *J. Heterocycl. Chem.* **1972**, *9*, 1373. [CrossRef]
49. Frost, J.R.; Streith, J. Polyaza-azulenes. Part 1. Synthesis and Reactions of Some 2,3,3a,6-Tetrahydropyrazolo[3,4-*d*][1,2]diazepines. *J. Chem. Soc. Perkin Trans. 1* **1978**, *11*, 1297–1303. [CrossRef]
50. Simón, M.M.; Sepúlveda-Arques, J. New cycloaddition reactions of 1-phenyl-4-vinylpyrazole. *Tetrahedron* **1986**, *42*, 6683–6686. [CrossRef]
51. Simón, M.M.; Laviada, M.J.A.; Sepúlveda Arques, J. Cycloadditions with 1-phenyl-5-vinylpyrazole. *J. Chem. Soc. Perkin Trans. 1* **1990**, 2749–2750. [CrossRef]
52. Diaz-Ortiz, A.; Carrillo, J.R.; Díez-Barra, E.; de la Hoz, A.; Gómez-Escalonilla, M.J.; Moreno, A.; Langa, F. Diels–Alder Cycloaddition of Vinylpyrazoles. Synergy between Microwave Irradiation and Solvent-Free Conditions. *Tetrahedron* **1996**, *52*, 9237–9248. [CrossRef]
53. Díaz-Ortiz, A.; de la Hoz, A.; Langa, F. Microwave irradiation in solvent-free conditions: An eco-friendly methodology to prepare indazoles, pyrazolopyridines and bipyrazoles by cycloaddition reactions. *Green Chem.* **2000**, *2*, 165–172. [CrossRef]
54. Sepúlveda-Arques, J.; Medio-Simon, M.; Piqueres-Vidal, L. Cycloaddition Reactions of 1-*tert*-Butyl-4-vinylpyrazole. *Monatsh. Chem.* **1989**, *120*, 1113–1118. [CrossRef]
55. Attaryana, O.S.; Baltayan, A.O.; Asratyan, G.V. Diels–Alder Reactions of 3- and 5-Methyl-1-vinylpyrazoles with Cyclohexa-1,3-diene and Hydrogenation of the Reaction Products. *Russ. J. Gen. Chem.* **2008**, *78*, 626–628. [CrossRef]
56. Es'kova, L.A.; Petrova, E.V.; Turchaninov, V.K.; Domina, E.S.; Afonin, A.V. Reaction of 1-vinylpyrazoles with tetracyanoethylene. *Chem. Heterocycl. Compd.* **1989**, *25*, 768–771. [CrossRef]
57. Nikitenko, E.E.; Martynenko, A.L.; Ostrovsky, S.A.; Rusak, E.E.; Kryuchkov, E.E.; Topchiev, D.A. The reactivity of 3-methyl- and 5-methyl-1-vinylpyrazoles in free-radical polymerization. *Russ. Chem. Bull.* **1993**, *42*, 378–380. [CrossRef]



58. Es'kova, L.A.; Domnina, E.S.; Skvortsova, G.G.; Voronov, V.K.; Chipanina, N.N.; Kazakova, N.A. Bromination of 1-vinylpyrazoles. *Chem. Heterocycl. Compd.* **1978**, *14*, 774–776. [CrossRef]
59. Es'kova, L.A.; Voronov, V.K.; Domnina, E.S.; Skvortsova, G.G. Hydrohalogenation of 1-vinylpyrazoles. *Russ. Chem. Bull.* **1985**, *34*, 2359–2362. [CrossRef]
60. Marcin, L.R.; Higgins, M.A.; Bronson, J.J.; Zusi, F.C.; Macor, J.E.; Ding, M. Triazolopyridine ether derivatives and their use in neurological and psychiatric disorders. WO 2015/042243, 26 March 2015.
61. Giovannini, R.; Bertani, B.; Ferrara, M.; Lingard, I.; Mazzaferro, R.; Rosenbrock, H. Phenyl-3-aza-bicyclo[3.1.0]hex-3-yl-methanones and the use thereof as medicament. WO2013/17657, 7 February 2013.
62. Lim, J.; Kelley, E.H.; Methot, J.L.; Zhou, H.; Petrocchi, A.; Mansoor, U.F.; Fischer, C.; O'Boyle, B.M.; Guerin, D.J.; Bienstock, E.; et al. Novel compounds that are ERK inhibitors. WO 2013/063214, 2 May 2013.
63. Dilger, A.K.; Corte, J.R.; De Lucca, I.; Fang, T.; Yang, W.; Wang, Y.; Pabbisetty, K.B.; Ewing, W.R.; Zhu, Y.; Wexler, R.R.; et al. Macrocyclic factor xia inhibitors condensed with heterocycles. WO 2015/116882, 6 August 2015.
64. Nosik, P.S.; Poturai, A.S.; Pashko, M.O.; Melnykov, K.P.; Ryabukhin, S.V.; Volochnyuk, D.M.; Grygorenko, O.O. *N*-Difluorocyclopropyl-Substituted Pyrazoles: Synthesis and Reactivity. *Eur. J. Org. Chem.* **2019**, *2019*, 4311–4319. [CrossRef]
65. Chernyshev, K.A.; Larina, L.I.; Chirkina, E.A.; Krivdin, L.B. The effects of intramolecular and intermolecular coordination on  $^{31}\text{P}$  nuclear shielding: Phosphorylated azoles. *Magn. Reson. Chem.* **2012**, *50*, 120–127. [CrossRef]
66. Lam, P.Y.S.; Vincent, G.; Bonne, D.; Clark, C.G. Copper-promoted/catalyzed C-N and C-O bond cross-coupling with vinylboronic acid and its utilities. *Tetrahedron Lett.* **2003**, *44*, 4927–4931. [CrossRef]
67. Scholl, M.; Ding, S.; Lee, C.W.; Grubbs, R.H. Synthesis and Activity of a New Generation of Ruthenium-Based Olefin Metathesis Catalysts Coordinated with 1,3-Dimesityl-4,5-dihydroimidazol-2-ylidene Ligands. *Org. Lett.* **1999**, *1*, 953–956. [CrossRef] [PubMed]
68. Schwab, P.; France, M.B.; Ziller, J.W.; Grubbs, R.H. A Series of Well-Defined Metathesis Catalysts—Synthesis of  $[\text{RuCl}_2(=\text{CHR}')(\text{PR}_3)_2]$  and Its Reactions. *Angew. Chem. Int. Ed. Engl.* **1995**, *34*, 2039–2041. [CrossRef]
69. Schwab, P.; Grubbs, R.H.; Ziller, J.W. Synthesis and Applications of  $\text{RuCl}_2(=\text{CHR}')(\text{PR}_3)_2$ : The Influence of the Alkylidene Moiety on Metathesis Activity. *J. Am. Chem. Soc.* **1996**, *118*, 100–110. [CrossRef]
70. Garber, S.B.; Kingsbury, J.S.; Gray, B.L.; Hoveyda, A.H. Efficient and Recyclable Monomeric and Dendritic Ru-Based Metathesis Catalysts. *J. Am. Chem. Soc.* **2000**, *122*, 8168–8179. [CrossRef]
71. Seregin, I.V.; Gevorgyan, V. Direct transition metal-catalyzed functionalization of heteroaromatic compounds. *Chem. Soc. Rev.* **2007**, *36*, 1173–1193. [CrossRef] [PubMed]
72. Colby, D.A.; Bergman, R.G.; Ellman, J.A. Rhodium-Catalyzed C–C Bond Formation via Heteroatom-Directed C–H Bond Activation. *Chem. Rev.* **2010**, *110*, 624–655. [CrossRef]
73. Azipiroz, R.; Rubio-Pérez, L.; Di Giuseppe, A.; Passarelli, V.; Lahoz, F.J.; Castarlenas, R.; Pérez-Torrente, J.J.; Oro, L.A. Rhodium(I)-*N*-Heterocyclic Carbene Catalyst for Selective Coupling of *N*-Vinylpyrazoles with Alkynes via C-H Activation. *ACS Catal.* **2014**, *4*, 4244–4253. [CrossRef]
74. Carrillo, J.; Díaz-Ortiz, A.; de la Hoz, A.; Gómez-Escalonilla, M.J.; Moreno, A.; Prieto, P. The Effect of Focused Microwaves on the Reaction of Ethyl *N*-Trichloroethylidene carbamate with Pyrazole Derivatives. *Tetrahedron* **1999**, *55*, 9623–9630. [CrossRef]
75. Akhmetova, V.R.; Akhmediev, N.S.; Ibragimov, A.G. Sulfur-Containing Pyrazoles, Pyrazolines and Indazoles. In *N-Heterocycles*; Ameta, K.L., Kant, R., Penoni, A., Maspero, A., Scapinello, L., Eds.; Springer: Singapore, 2022; pp. 275–312. [CrossRef]
76. Es'kova, L.A.; Erushnikova, L.P.; Afonin, A.V.; Domnina, E.S. Interaction of 1-vinylpyrazoles with alkanethiols. *Russ. Chem. Bull.* **1992**, *41*, 1462–1465. [CrossRef]
77. Kobelevskaya, V.A.; Popov, A.V.; Nikitin, A.Y.; Levkovskaya, G.G. Directed Synthesis of 3-(2,2-Dichlorocyclopropyl)pyrazoles. *Russ. J. Org. Chem.* **2017**, *53*, 144–146. [CrossRef]

Review

# 1*H*-Pyrazolo[3,4-*b*]quinolines: Synthesis and Properties over 100 Years of Research

Andrzej Danel <sup>1,\*</sup>, Ewa Gondek <sup>1</sup>, Mateusz Kucharek <sup>2</sup>, Paweł Szlachcic <sup>2</sup> and Arkadiusz Gut <sup>3</sup> 

<sup>1</sup> Faculty of Materials Engineering and Physics, Cracow University of Technology, Podchorążych Str. 1, 30-084 Krakow, Poland; egondek@pk.edu.pl

<sup>2</sup> Faculty of Food Technology, University of Agriculture in Krakow, Balicka Str. 122, 30-149 Krakow, Poland; mateusz.kucharek@urk.edu.pl (M.K.); pawel.szlachcic@urk.edu.pl (P.S.)

<sup>3</sup> Faculty of Chemistry, Jagiellonian University, Gronostajowa Str. 2, 30-387 Krakow, Poland; arkadiusz.gut@uj.edu.pl

\* Correspondence: rrdanela@cyf-kr.edu.pl

**Abstract:** This paper summarises a little over 100 years of research on the synthesis and the photophysical and biological properties of 1*H*-pyrazolo[3,4-*b*]quinolines that was published in the years 1911–2021. The main methods of synthesis are described, which include Friedländer condensation, synthesis from anthranilic acid derivatives, multicomponent synthesis and others. The use of this class of compounds as potential fluorescent sensors and biologically active compounds is shown. This review intends to summarize the abovementioned aspects of 1*H*-pyrazolo[3,4-*b*]quinoline chemistry. Some of the results that are presented in this publication come from the laboratories of the authors of this review.

**Keywords:** biological properties; fluorescence; fluorescent sensors; Friedländer condensation; multicomponent reaction; 1*H*-pyrazolo[3,4-*b*]quinolines

**Citation:** Danel, A.; Gondek, E.; Kucharek, M.; Szlachcic, P.; Gut, A. 1*H*-Pyrazolo[3,4-*b*]quinolines: Synthesis and Properties over 100 Years of Research. *Molecules* **2022**, *27*, 2775. <https://doi.org/10.3390/molecules27092775>

Academic Editors: Vera L. M. Silva and Artur M. S. Silva

Received: 1 March 2022

Accepted: 22 April 2022

Published: 26 April 2022

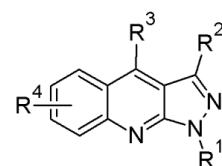
**Publisher's Note:** MDPI stays neutral with regard to jurisdictional claims in published maps and institutional affiliations.



**Copyright:** © 2022 by the authors. Licensee MDPI, Basel, Switzerland. This article is an open access article distributed under the terms and conditions of the Creative Commons Attribution (CC BY) license (<https://creativecommons.org/licenses/by/4.0/>).

## 1. Introduction

1*H*-Pyrazolo[3,4-*b*]quinolines are three-membered azaheterocyclic systems that are composed of a pyrazole-and-quinoline fragment (Figure 1). The parent structure can be modified with a number of substituents that have a great influence on the physical, photophysical and biological properties.



$R^1$  = H, alkyl, aryl, substituted aryl

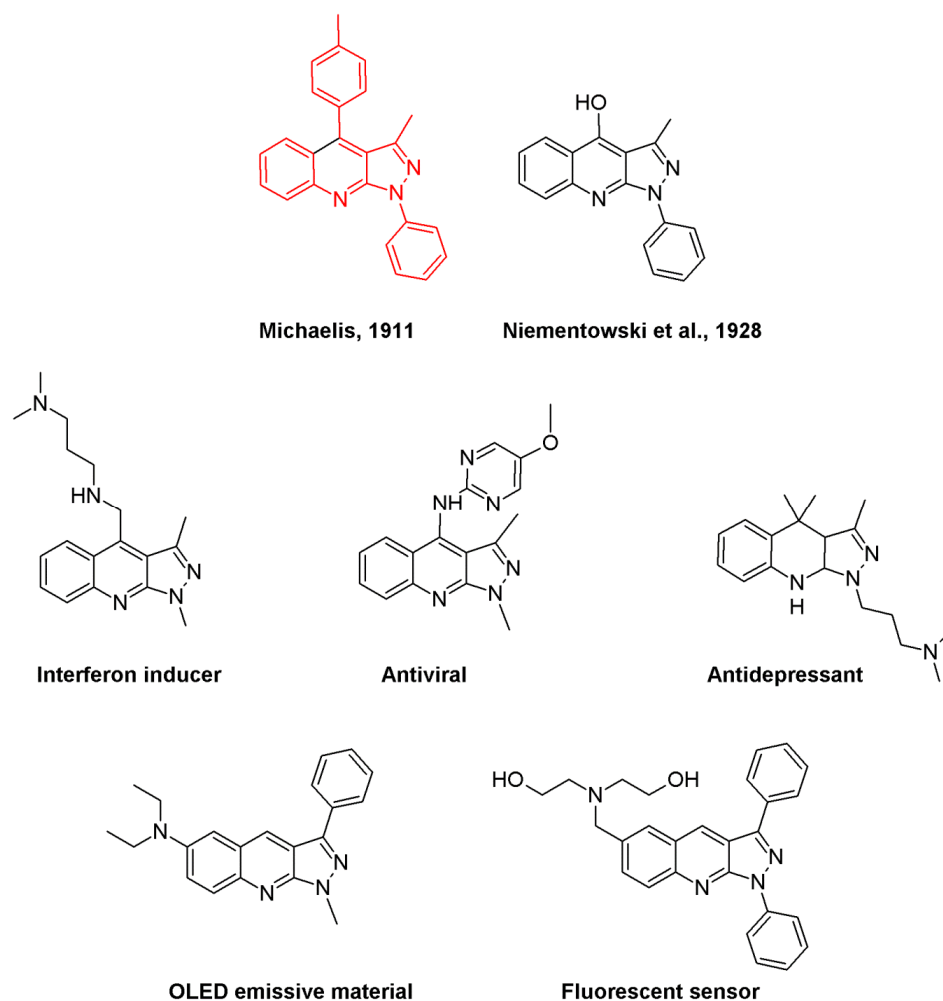
$R^2$  = H, alkyl, aryl, substituted aryl

$R^3$  = H, alkyl, aryl, substituted aryl, OH, OR, halogen,  $NH_2$ , NHR,  $NR_2$

$R^4$  = H, alkyl, halogen, OR, OH, CN,  $NO_2$ , COOR,  $NR_2$

**Figure 1.** The structure of 1*H*-pyrazolo[3,4-*b*]quinoline.

The first synthesis of this class of compounds was described in 1911 by Michaelis; however, the author incorrectly presented their structures. He concluded that the obtained compounds were a benzylidene derivative of 5-*N*-phenylamino-3-methyl-1-phenylpyrazole. This structure is marked in red in Figure 2 [1]. His results were later verified by other researchers. For this reason, the discoverer of this class of compounds should be considered as Niementowski and colleagues, who in their work presented the first structure of 1*H*-pyrazolo[3,4-*b*]quinoline in 1928 [2]. In the interwar period, there were some works by Koćwa, who also synthesised this system [3,4]. The remaining works on the synthesis of these compounds were published after 1945.

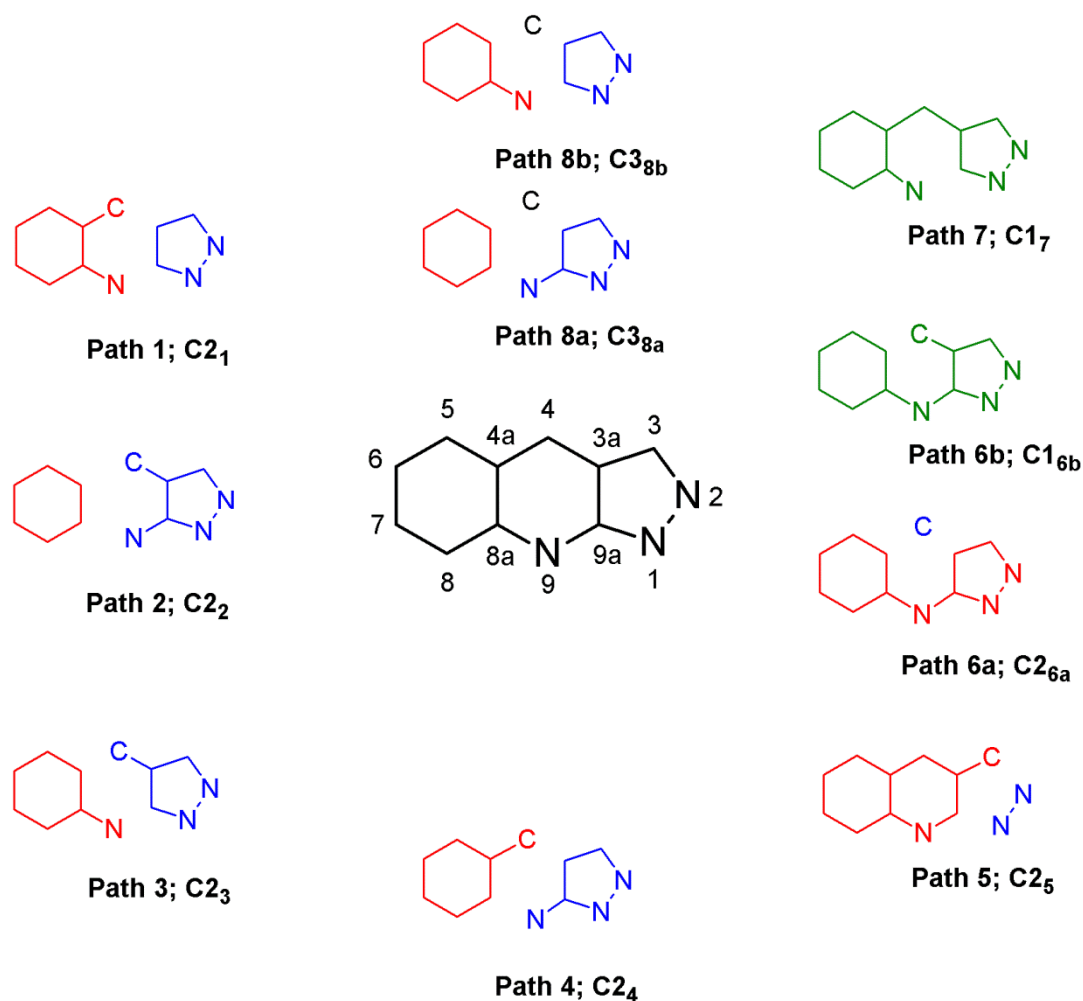


**Figure 2.** Various 1*H*-pyrazolo[3,4-*b*]quinoline structures.

Michaelis noticed that the compounds that were obtained by him were characterised by intense fluorescence, and, indeed, a significant part of pyrazolo[3,4-*b*]quinolines exhibits emission properties, both in solutions and even in a solid state. These properties have been used in the synthesis of fluorescent sensors for various cations [5]. In addition, pyrazolo[3,4-*b*]quinolines were tested as emission materials in organic electroluminescent cells (OLEDs). The summary of this research was published some time ago in our review article [6]. It is also necessary to mention the biological properties of this class of compounds, which were largely studied in the first stage of 1*H*-pyrazolo[3,4-*b*]quinoline development, and it is now observed that more and more research groups are interested in these heterocycles. This aspect will be discussed later in this review (Figure 2).

## 2. The Main Synthesis Method of 1*H*-Pyrazolo[3,4-*b*]quinoline

The following scheme for the synthesis of pyrazoloquinolines is based on the methodology for the synthesis of the quinoline system, which is described in detail in one of the Houben–Weil volumes on quinoline synthesis [7] (Figure 3). The first and oldest method of pyrazoloquinolines synthesis is a two-component reaction (C<sub>2</sub>), in which the Friedländer condensation of anthranilaldehyde, *o*-aminoacetophenones and *o*-aminobenzophenones, and the appropriate pyrazolones, are used (Figure 3; Path 1). As a result of the reaction, a bond is formed between the N9 nitrogen and the C9a carbon, and between the C3a and C4 carbon atoms. The reaction is limited by the availability of *o*-aminocarbonyl compounds. The synthesis of the Niementowski and Pfitzinger quinolines can also be used here, although to a lesser extent than in the first case.



**Figure 3.** Various methods for constructing the 1H-pyrazolo[3,4-b]quinoline carbon skeleton.

The second path is essentially the reverse of the first methodology, where the *o*-aminocarbonyl system is linked to the pyrazole moiety. In a two-component reaction (C2<sub>2</sub>), a bond is formed between the C8a carbon and the N9 nitrogen, and between the carbons C4a and C4 (Figure 3; Path 2).

The two-component reaction (C2<sub>3</sub>) in which one of the reactants is an aromatic amine and the other is a pyrazole derivative is one of the most valuable syntheses of the pyrazoloquinoline system. The entire spectrum of substituted anilines is commercially available, while the synthesis of pyrazole derivatives that contain an aldehyde or ketone group is not difficult. In this reaction, a bond is formed between C4 and C4a carbon, and between nitrogen N9 and C9a carbon (Figure 3; Path 3).

The reaction of 5-aminopyrazoles and the *o*-halogen derivatives of aromatic carboxylic acids has some importance in the synthesis of pyrazoloquinolines that are substituted at the 4-chlorine/bromine or hydroxyl position. In this two-component reaction (C2<sub>4</sub>), a bond is formed between the nitrogen atom N9 and the carbon C8a, and between the carbon carbon and the carbon C3a (Figure 3; Path 4).

After studying the literature on the synthesis of pyrazoloquinolines, it seems that Path 5 is one of the most exploited procedures for synthesising this system. It uses quinoline derivatives (aldehydes, nitriles) and the appropriate hydrazines. The resulting derivatives are later further modified, and most often in terms of the synthesis of biologically active compounds. In this two-component reaction (C2<sub>5</sub>), a bond is formed between the C9a carbon and the N1 nitrogen, and between the N2 nitrogen and the C3 carbon (Figure 3; Path 5).

Another synthetic procedure of pyrazoloquinolines is a two-component reaction (C2<sub>6a</sub>) and a one-component reaction (C1<sub>6b</sub>). Both routes are based on 5-*N*-arylpyrazole derivatives. In the first case, cyclization takes place with the use of an aromatic aldehyde, and, in the second case, an ester group is used, which is attached to the pyrazole ring in position 4. In the first situation, bonds between the C4 and C4a/C3a carbons are formed. In the second case, bonds between C4 and C4a are formed. The ring-closure is also performed by using the Vilsmeier–Haack formylation reaction (Figure 3; Path 6).

The use of a one-component system (C1<sub>7</sub>), where the reductive cyclization of the *o*-nitrobenzylidene system is used, is practically irrelevant when it comes to the synthesis of pyrazoloquinolines. A bond is formed between the nitrogen N9 and the C9a carbon in the pyrazole ring (Figure 3; Path 7).

Finally, we should mention multicomponent reactions, which are very popular in the synthesis of heterocyclic systems. This method is suitable for both the synthesis of the fully aromatic pyrazoloquinoline system, or with the hydrogenated moiety in either the middle ring or the carbocyclic system. The N9-nitrogen-contributing system may be an amine pyrazole or an aromatic amine (C3<sub>8a</sub> or C3<sub>8b</sub>). The C4-bound fragment is most often derived from an aromatic or an aliphatic aldehyde (Figure 3; Path 8).

### 2.1. The Friedländer Synthesis Based on *o*-Aminoaldehydes, *o*-Aminoacetophenones and *o*-Aminobenzophenones

The Friedländer condensation of *o*-aminocarbonyl compounds **1** (R<sup>3</sup> = H, alkyl, aryl) with carbonyl systems that contain the active  $\alpha$ -methylene group **2** is one of the most important methods of quinoline **3** synthesis [8–13] (Figure 4) (Scheme 1).

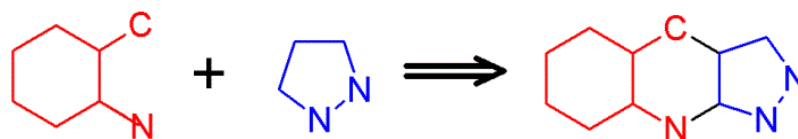
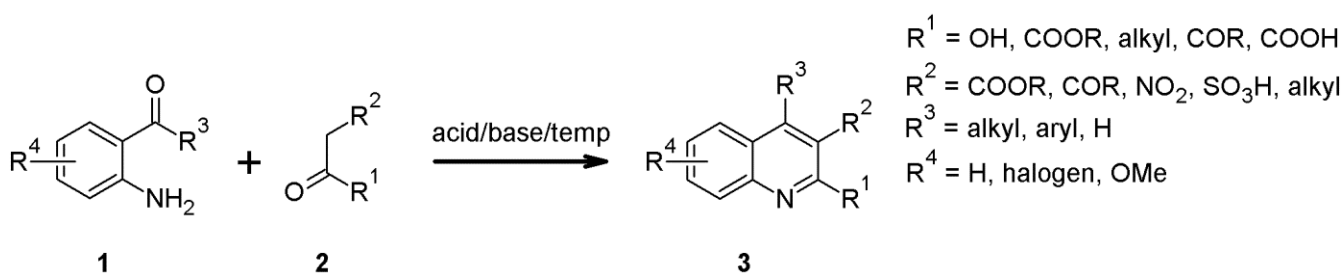
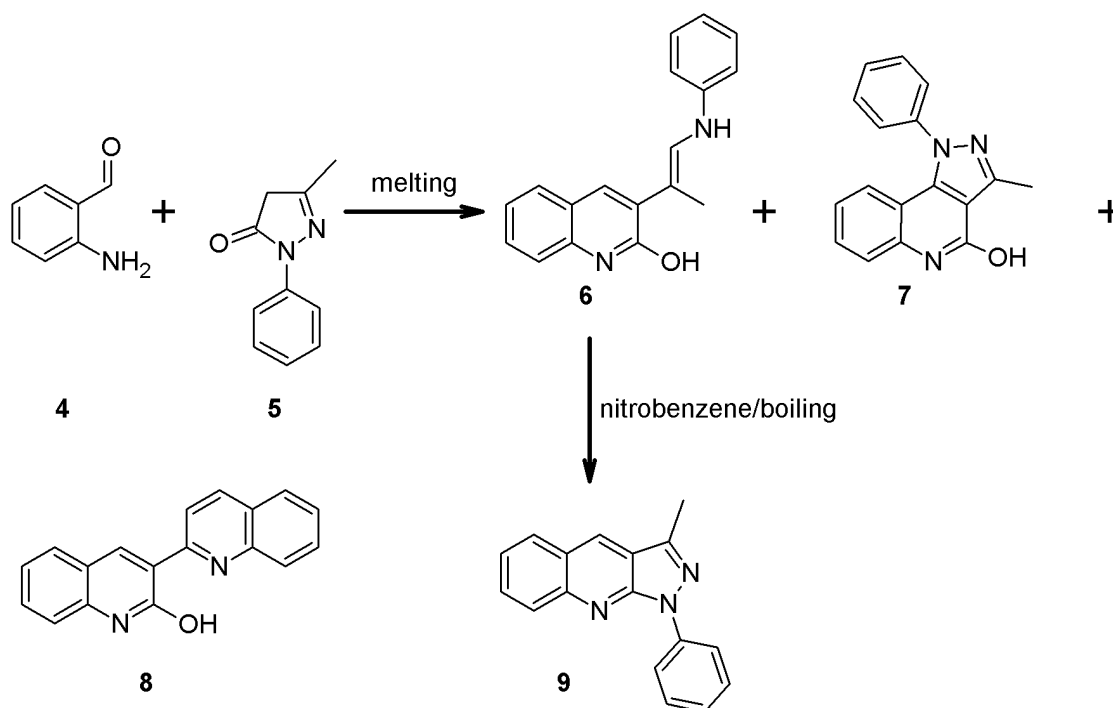


Figure 4. Path 1: C2<sub>1</sub>: C4-C3a; N9-C9a.



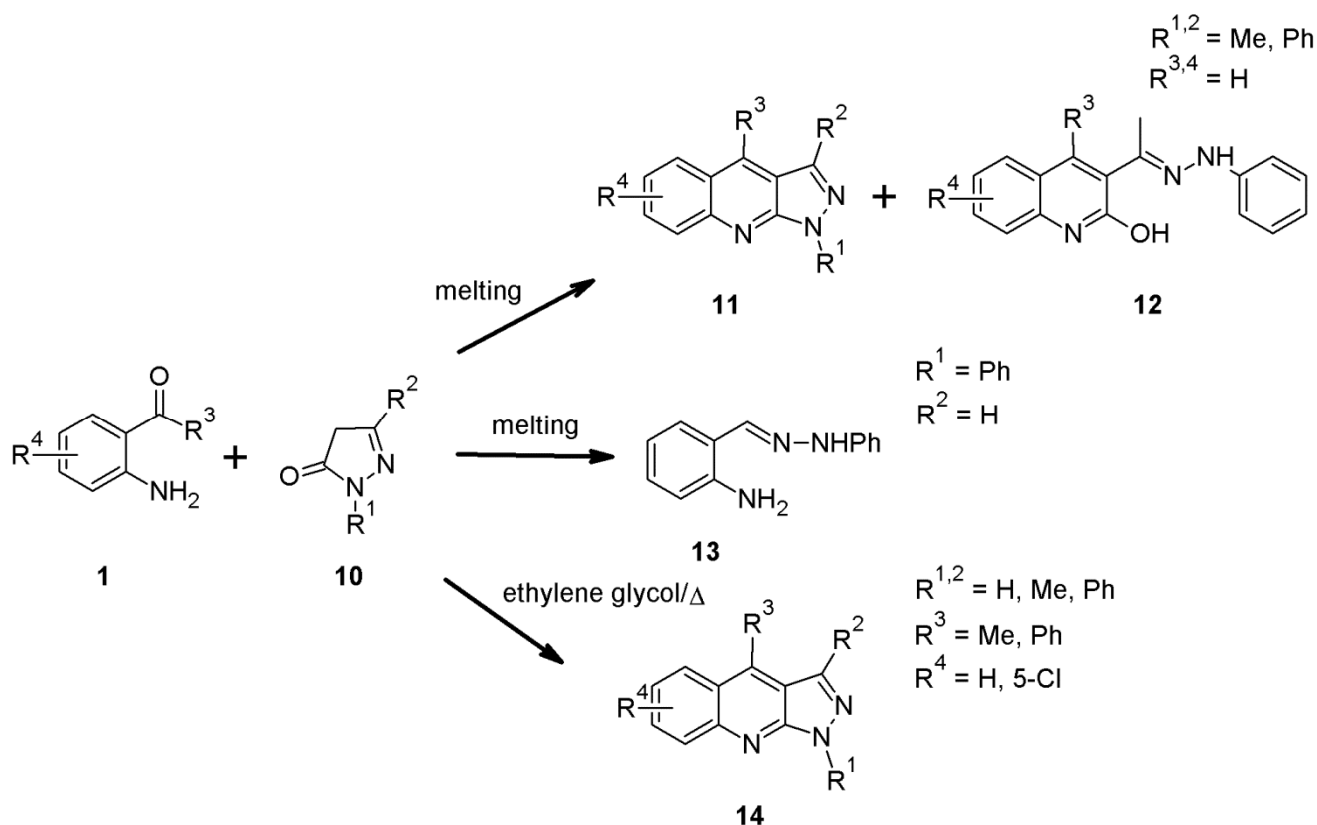
Scheme 1. The Friedländer condensation leading to quinoline derivatives.

The reaction can be catalysed by acids and bases, but it also takes place in an inert environment. We start the description of synthetic PQ methods with the oldest results that were published by Niementowski and colleagues, who used the Friedländer condensation of anthranilaldehyde **4** and 5-methyl-2-phenyl-4*H*-pyrazol-3-one **5** (Scheme 2) [2]. As a result, three products were obtained: phenylhydrazone of 3-acetylquinolone **6**; 3-methyl-1-phenyl-1*H*-pyrazolo[4,3-*c*]quinoline **7**; and 3-(2-quinolyl)-quinolin-2-ol **8**. The heating of phenylhydrazone **6** in the boiling of C<sub>6</sub>H<sub>5</sub>NO<sub>2</sub> led to the formation of 1-methyl-3-phenyl-1*H*-pyrazolo[3,4-*b*]quinoline **9**. Thus, this compound can be described as the first synthesised pyrazoloquinoline.



**Scheme 2.** The first attempt at the Friedländer synthesis of 1*H*-pyrazolo[3,4-*b*]quinolines [2].

As for further research on the use of the Friedländer condensation for the synthesis of PQs, a mention should be made of the work of Tomasik et al., which describes a complete synthesis that uses nine pyrazolones **10** substituted with the methyl, phenyl and hydrogen groups with *o*-aminobenzaldehyde **4** (Scheme 3) [14].



**Scheme 3.** Friedländer-based synthesis of 1*H*-pyrazolo[3,4-*b*]quinolines—an extension.

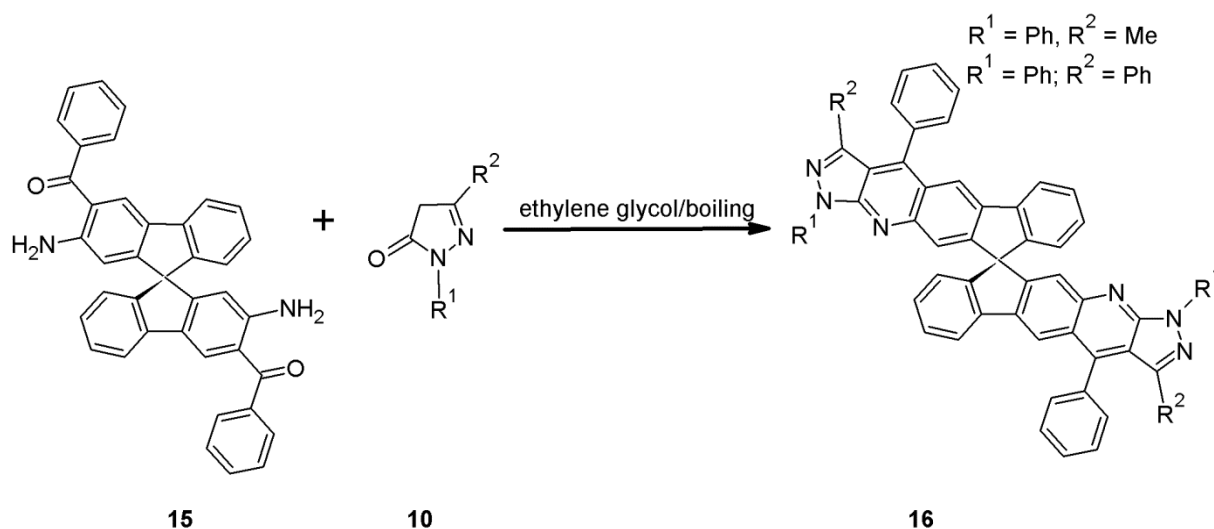
The syntheses were conducted within 150–260 °C in melt. The reaction mixtures were separated by column chromatography or crystallisation. PQs **11** were obtained in the cases of five pyrazolones (**10**:  $R^{1,2} = \text{Ph}$ ;  $R^{1,2} = \text{Me}$ ;  $R^1 = \text{Me}/R^2 = \text{Ph}$ ;  $R^1 = \text{H}/R^2 = \text{Me, Ph}$ ). In the case of 1,3-dimethylpyrazol-5-one (**10**:  $R^{1,2} = \text{Me}$ ), it was possible to isolate the intermediate product, which was the 4-benzylidene derivative, which suggests that the first step in some of these reactions is the reaction between the aldehyde group and the  $\alpha$ -methylene group of the pyrazolone. In the next step, the pyrazolone ring is opened and compound **12** is formed, which then cyclizes to form pyrazoloquinoline **11**. In other cases, 3-acylquinoline alkyl/arylhydrazones **12** or other products were obtained, such as **13** (ca. 100%) in the case when pyrazolone **10** ( $R^1 = \text{Ph}$ ,  $R^2 = \text{H}$ ) is used.

Paczkowski et al. investigated pyrazolo[3,4-*b*]quinolines as potential photoinitiators for free radical polymerisation. They prepared these compounds via Friedländer condensation that was conducted in boiling glacial acetic acid [15].

Danel, as an *o*-aminocarbonyl component **1**, applied *o*-aminoacetophenone, *o*-aminobenzophenone and 5-chloro-2-aminobenzophenone, and a complete set of pyrazolones substituted with methyl, phenyl and hydrogen **10** ( $R^{1,2} = \text{H, Me, Ph}$ ) (Scheme 3) [16]. The reaction was carried out in boiling ethylene glycol. Contrary to the two previously mentioned syntheses, in this case, all pyrazoloquinolines **14** were obtained in a single stage, although with different yields (20–85%). Sabitha et al. applied a microwave-assisted condensation of **1** ( $R^3 = \text{H, Me}$ ;  $R^4 = \text{H}$ ) and **10** ( $R^1 = \text{Ph}$ ,  $R^2 = \text{Me}$ ) that was supported on clay, which led to 1*H*-pyrazolo[3,4-*b*]quinolines [17].

As mentioned in the introduction, a significant part of pyrazoloquinolines exhibit intense fluorescence, which makes them good luminophores for the fabrication of electroluminescent devices. However, high luminescence efficiency is only one of the many conditions that must be met by candidates for luminophores. The others are a high thermal stability and a high glass-transition temperature. This can be achieved by using spiro compounds, which are just such systems [18]. The introduction of the 9,9'-spirobifluorene system increases the stiffness of the molecule and prevents packing and the intermolecular interactions in the film (after vacuum sputtering on the ITO anode), which hinders crystallisation and increases the  $T_g$  value. The tetrahedral nature of the carbon at the centre of the spiro of the system that links the two coupled systems serves as a breaking fragment for this coupling so that the optical and electronic properties of the system are preserved [19].

Tao et al. synthesised two spiro PQs **16** systems by using the Friedländer condensation of *o*-aminobenzophenones on the basis of spirobifluorene **15** (Scheme 4) [20].



**Scheme 4.** Synthesis of spirobifluorene-based 1*H*-pyrazolo[3,4-*b*]quinolines.

## 2.2. The Friedländer Synthesis Based on Pyrazole Derivatives

The previously mentioned Friedländer condensation procedures included either the appropriate aldehyde or ketone attached to a carbocyclic ring. One drawback of this synthesis is that the work of obtaining *o*-aminocarbonyl systems **1** is quite troublesome, and aldehydes are often not very stable reagents [21]. The reverse approach is also possible, where pyrazole *o*-aminoaldehyde **18** is used (Figure 5) (Schemes 5 and 6).

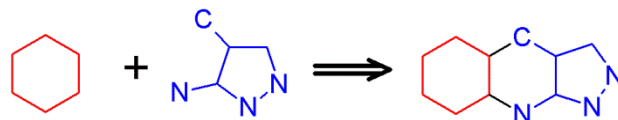
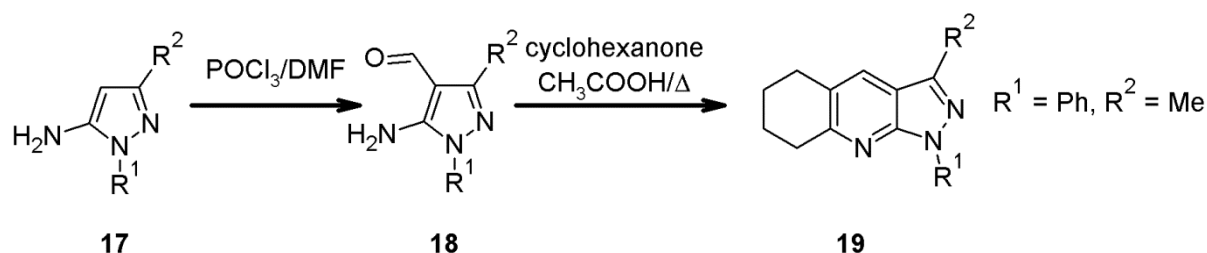
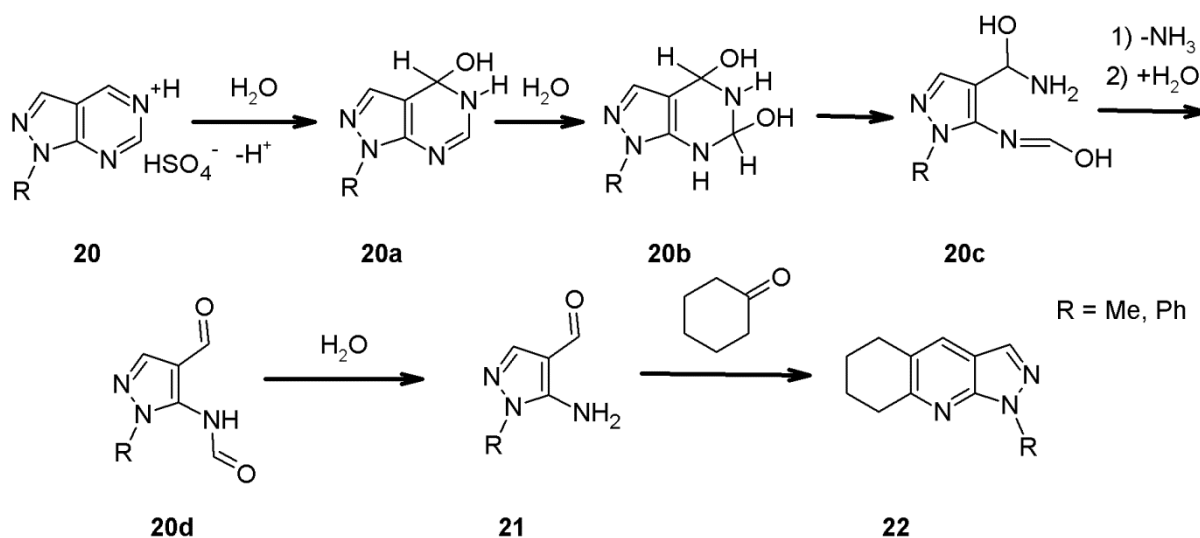


Figure 5. Path 2: C<sub>22</sub>: C<sub>4</sub>-C<sub>4a</sub>; N<sub>9</sub>-C<sub>8a</sub>.



Scheme 5. 1*H*-Pyrazolo[3,4-*b*]quinoline synthesis from 2-amino-4-pyrazolecarbaldehyde.



Scheme 6. 1*H*-Pyrazolo[3,4-*b*]quinoline synthesis from pyrazolo[3,4-*d*]pyrimidine derivatives.

Breitmaier and Häuvel prepared pyrazole aldehyde **18** by the formylation of 5-amino-3-methyl-1-phenylpyrazole **17**. This aldehyde **18** was condensed with cyclohexanone in glacial acetic acid, which yielded 5,6,7,8-tetrahydro-1*H*-pyrazolo[3,4-*b*]quinoline **19** (Scheme 5) [22].

Instead of cyclohexanone, other cyclic ketones can be applied [23]. Higashino et al. prepared pyrazoloquinoline **22** by using aldehyde **21** that was prepared from 1*H*-pyrazolo[3,4-*d*]pyrimidine salts **20** and reactive carbonyl compounds, such as cyclohexanone/cyclopentanone with ethoxide ion as a catalyst (Scheme 6) [6].

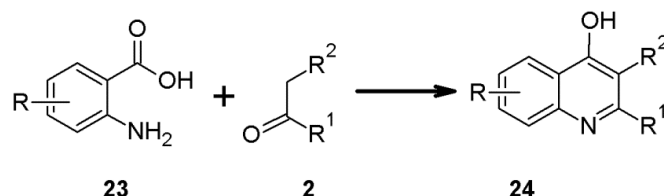
The authors propose a number of structures (**20a–d**) that can form as intermediates, but they have not isolated any of them. Aldehyde **21** can also be prepared by reducing 5-amino-1-methyl(phenyl)-1*H*-pyrazole-4-carbonitrile with Raney-nickel alloy and formic acid [24].



### 2.3. 1*H*-Pyrazolo[3,4-*b*]quinoline Syntheses Based on Anthranilic Acid and Anthranilic Acid Derivatives

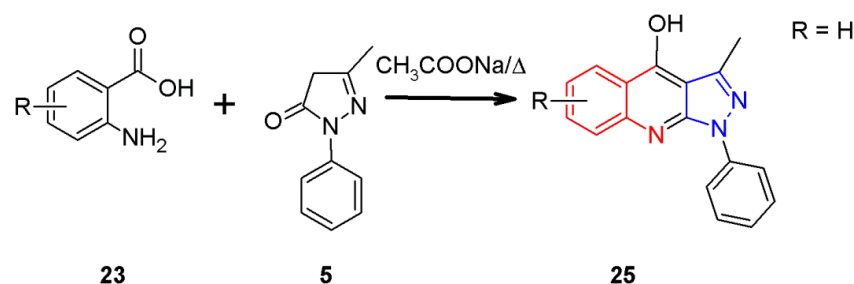
Path 1: C2<sub>1</sub>: C4-C3a; N9-C9a (Figure 4)

Another classic method of synthesising the quinoline **3** is the Niementowski reaction, in which anthranilic acid **23** and ketones **2** (or aldehydes) are used. As a result, 4-hydroxyquinolines **24** are formed (Scheme 7) [25].



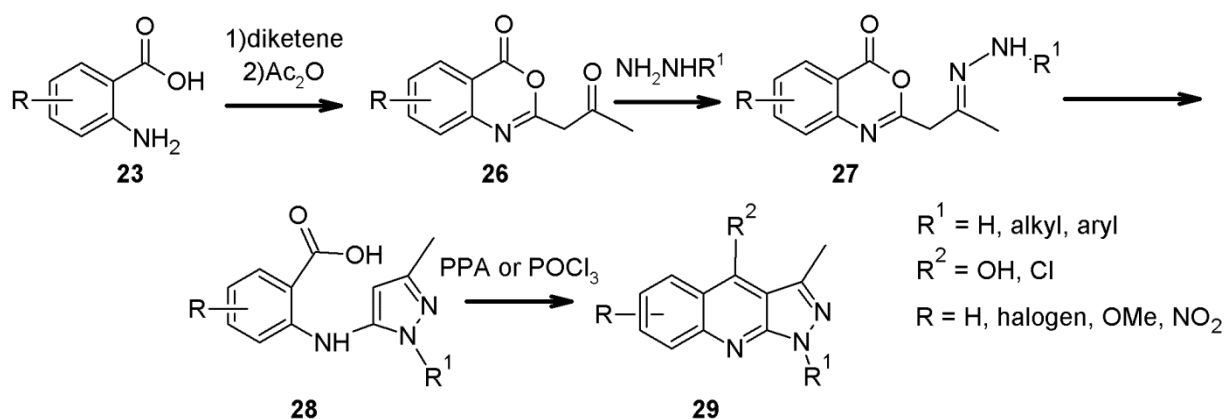
**Scheme 7.** Niementowski's quinoline synthesis.

The first attempt to synthesise pyrazoloquinoline by using Niementowski's synthesis was made by Ghosh in 1937 through the reaction of anthranilic acid **23** and pyrazolone **5** in the presence of anhydrous CH<sub>3</sub>COONa. The product of the reaction was to be 4-hydroxy-3-methyl-1-phenyl-1*H*-pyrazolo[3,4-*b*]quinoline **25** (Scheme 8) [26].



**Scheme 8.** An attempt to apply anthranilic acid for 4-hydroxy-1*H*-pyrazolo[3,4-*b*]quinoline synthesis.

The reaction was re-examined by Tomasik and co-workers, and it turned out that compound **25** does not arise under these conditions. In the reaction mixture, only traces of two 1*H*-pyrazolo[3,4-*b*]quinolines were found: 1-phenyl-3-methyl-1*H*-pyrazolo[3,4-*b*]quinoline (**14**; R<sup>1</sup> = Ph, R<sup>2</sup> = Me, R<sup>3,4</sup> = H) and 1-phenyl-3,4-methyl-1*H*-pyrazolo[3,4-*b*]quinoline (**14**; R<sup>1</sup> = Ph, R<sup>2,3</sup> = Me, R<sup>4</sup> = H); however, both of them were formed as byproducts. 4-Hydroxy derivative **25** was not formed in this reaction. To prove it, the compound was obtained by another synthetic method, and it was compared to the obtained products by using TLC (Scheme 9); it was not detected in the reaction mixture, according to the Gosh procedure [27,28].

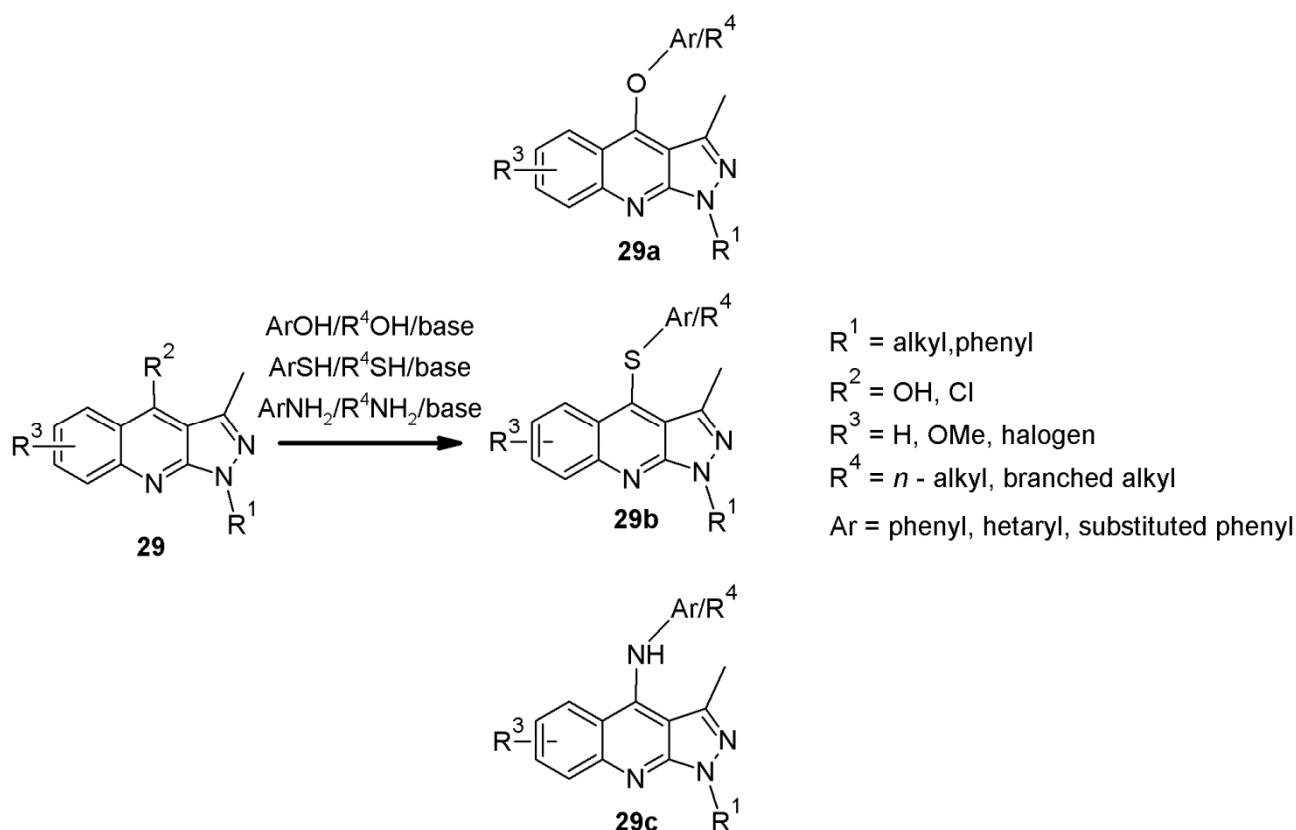


**Scheme 9.** Indirect use of anthranilic acid in synthesis of 1*H*-pyrazolo[3,4-*b*]quinolines.

After studying a large number of publications on the synthesis of the compounds that are the subject of this review, it seems that, so far, it has not been possible to obtain pyrazoloquinolines by the direct reaction of anthranilic acid and pyrazolones.

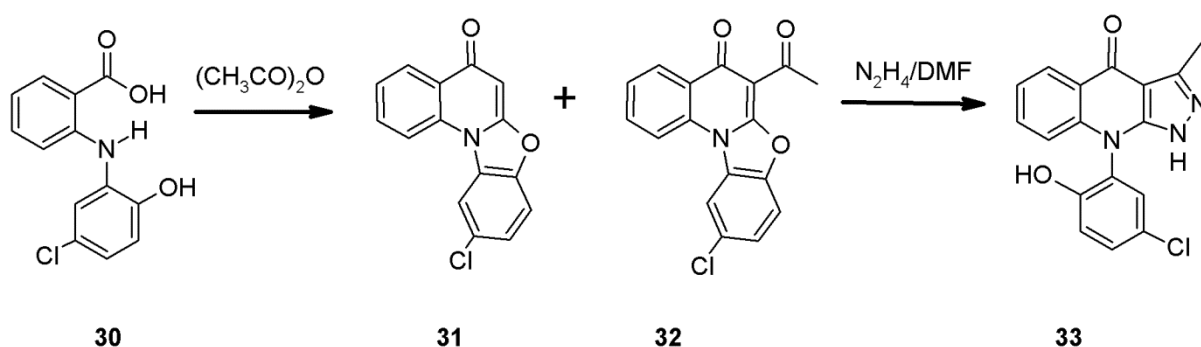
On the other hand, anthranilic acid **23** and its derivatives, in turn, are a valuable substrate for the indirect synthesis of pyrazoloquinolines **29** (Scheme 9). Anthranilic acid **23** is reacted with diketene and acetic anhydride, which yields 2-acetyl-4*H*-3,1-benzoxazin-4-one **26**, which is easily separated from a reaction mixture by filtration. In the next step, **26** is converted to the pyrazole derivative **28** by reaction with the appropriate hydrazine. There is no need to isolate the intermediate **27**. The final step in this reaction sequence is heating **28** in polyphosphoric acid (PPA) or phosphorus oxychloride (POCl<sub>3</sub>), depending on whether we want to obtain the 4-hydroxy derivative or the compound that contains the chlorine atom in the 4 position (**29**: R<sup>2</sup> = OH or R<sup>2</sup> = Cl).

This reaction cycle was used by Stein et al. and by Crenshaw et al. to prepare 4-hydroxy and 4-chloro derivatives (**29**: R<sup>2</sup> = OH or Cl), which were then used to synthesize a whole range of compounds with biological activity, which will be discussed later in this review [29,30]. The 4-chloro derivatives **29** (R<sup>2</sup> = Cl) were then reacted with phenols, thiophenols and amines, which yielded phenoxy **29a**, thiophenoxy **29b** and amine-substituted **29c** derivatives. These compounds showed antimalarial, antibacterial or interferon-inducing effects (Scheme 10).



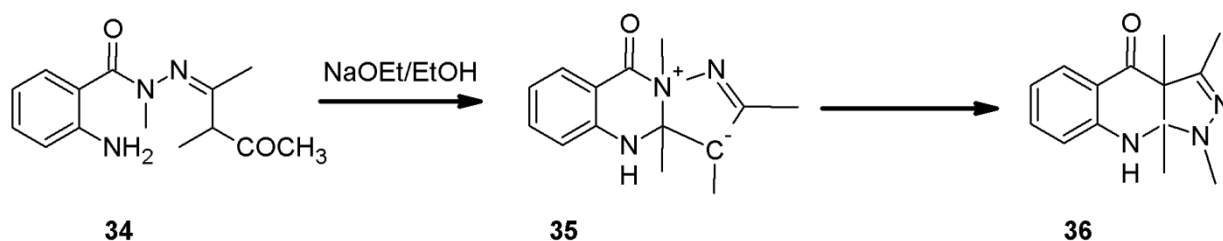
**Scheme 10.** 4-chloro/hydroxy derivatives of pyrazoloquinolines as a source for biologically active compounds.

In the previous reaction, acetic anhydride was the reagent in one of several steps where anthranilic acid played an important role. On the other hand, Kim used it to cyclise *N*-(2-hydroxyphenyl)anthranilic acid **30**, which resulted in two derivatives: **31** and a very small amount of **32** (1.7% yield). The reaction of **32** with hydrazine hydrate yielded a derivative of 1,9-dihydro-3-methyl-4*H*-pyrazolo[3,4-*b*]quinoline-4-one **33** (Scheme 11) [31].



**Scheme 11.** *N*-Arylamide of anthranilic acid as a source for pyrazolo[3,4-*b*]quinoline synthesis.

In concluding the discussion of the use of anthranilic acid derivatives, one could also mention the publication of Gal et al., which concerns the transformation of the modified hydrazides of acid **34**. Different products were formed, depending on the reaction conditions (e.g., **35**). When the reaction was run in the presence of sodium ethoxide, the product was pyrazolo[3,4-*b*]quinoline **36** (Scheme 12) [32].



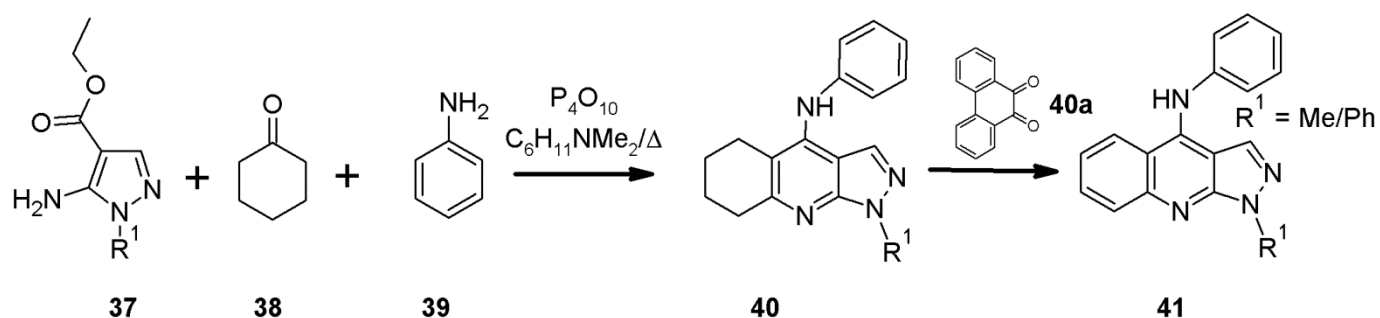
**Scheme 12.** Hydrazide of anthranilic acid as a precursor for pyrazolo[3,4-*b*]quinoline synthesis.

Contrary to the reaction that is shown in Scheme 10, the last two reactions (Schemes 11 and 12) have no preparative significance.

#### 2.4. 1*H*-Pyrazolo[3,4-*b*]quinoline Syntheses Based on 4-amino-3-carboxypyrazole Derivatives

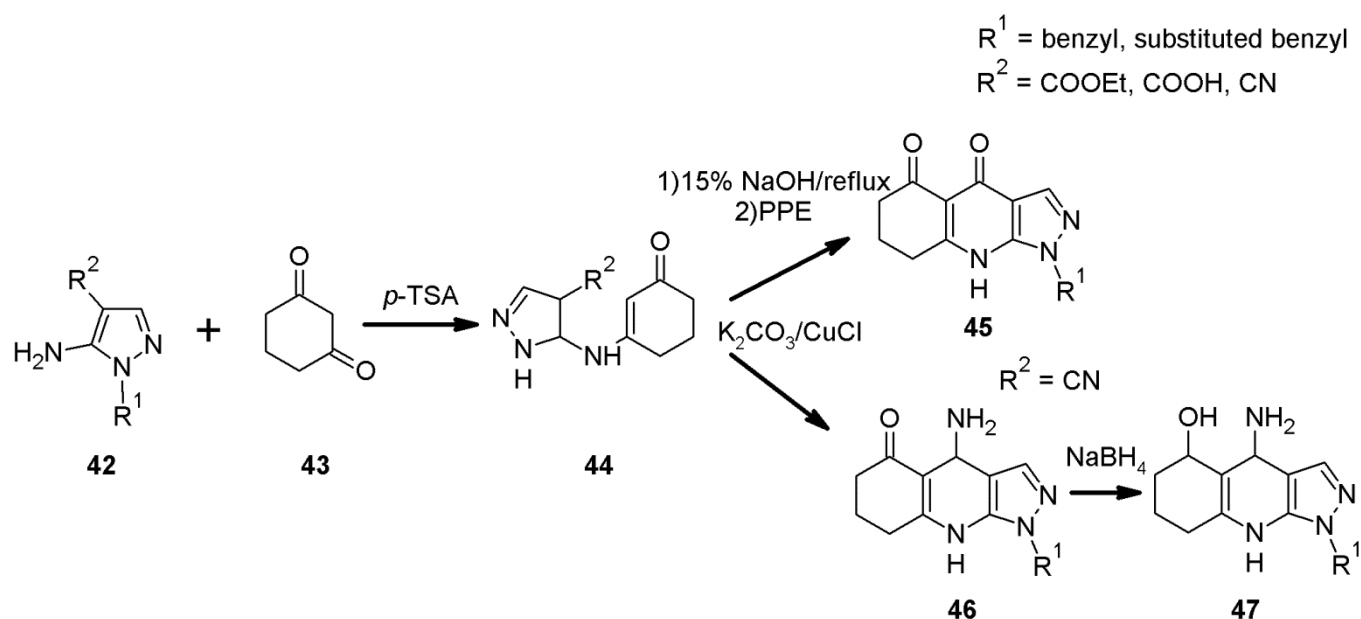
Path 2: C<sub>2,2</sub>: C4-C4a; N9-C8a (Figure 5)

As in the case of the Friedländer condensation, in this case as well, the derivatives of pyrazoles, such as 5-amino-1*H*-pyrazole-4-carboxylic acid derivatives **37**, can be used. Pedersen obtained 4-*N*-phenyl-1*H*-pyrazolo[3,4-*b*]quinoline **40** by reacting pyrazole derivative **37**, cyclohexanone **38** and aniline **39** in the presence of phosphorus pentoxide and *N,N*-dimethyl-*N*-cyclohexylamine. This reaction looks similar to a multicomponent one, but all of the atoms that make up the backbone matrix come only from **37** and **38**. The next step was to oxidise 5,6,7,8-tetrahydro-1*H*-pyrazolo[3,4-*b*]quinolin-4-amine **40** to a fully aromatic **41** with 9,10-phenantrenoquinone **40a** (Scheme 13) [33,34].



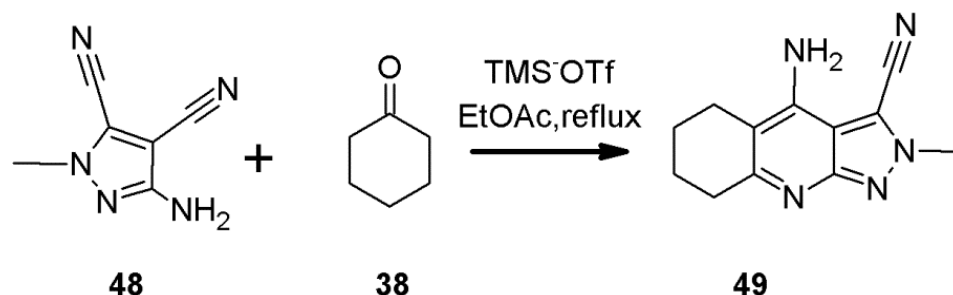
**Scheme 13.** Synthesis of pyrazolo[3,4-*b*]quinoline based on ethyl ester of 3-amino-4-carboxyethylpyrazole.

One of the research groups, which was looking for new drugs for the treatment of Alzheimer's disease, prepared a series of 5,6,7,8-tetrahydropyrazolo[3,4-*b*]quinoline derivatives, such as **45** and **46**, which were then transformed into other systems (e.g., **47**) [35]. Aminopyrazoles **42** were prepared from the appropriate benzylhydrazines and ethoxymethylenemalononitrile (**42**:  $R^2 = \text{CN}$ ) or ethyl ethoxymethylenecyanoacetate (**42**:  $R^2 = \text{COOEt}$ ). In the next turn, they were reacted with 1,3-cyclohexanedione **43** in the presence of *p*-toluenesulfonic acid (*p*-TSA). As a result, enamino ketones **44** were formed. In the case of the enemino ketone **44**, where  $R^2$  was a COOEt substituent, the compound was hydrolysed to produce a derivative with the COOH carboxyl group (**44**:  $R^2 = \text{COOH}$ ). Next, cyclisation was performed in the presence of polyphosphoric esters (PPE) afforded **45**. The use of potassium carbonate and copper(I) chloride in the case of **44** ( $R^2 = \text{CN}$ ) promotes the formation of **46**, respectively (Scheme 14).



**Scheme 14.** 3-Amino-4-pyrazolo carbocyclic acid and its ester as a source for pyrazoloquinoline synthesis.

Campbell and Firor prepared pyrazolo[3,4-*b*]quinolines **46** by cadmium-chloride- or copper-acetate-promoted cyclisations of pyrazolo enaminones **44** ( $R^2 = \text{CN}$ ,  $R^1 = \text{alkyl}$ ) [36]. Instead of toxic cadmium chloride, zinc chloride can also be used [37]. The system with the carbocyclic ring without any functional group can be prepared by starting from cyclohexanone **38** and 4-amino-1-methyl-pyrazole-2,3-dicarbonitrile **48** (Scheme 15) [38].



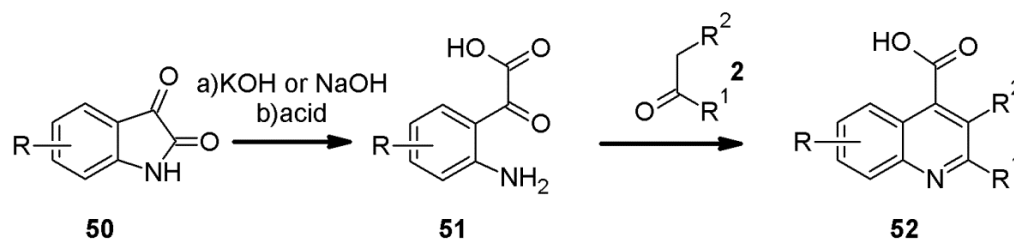
**Scheme 15.** 5-Amino-2-methyl-pyrazole-3,4-dicarbonitrile in the synthesis of pyrazolo[3,4-*b*]quinoline derivatives.

The resulting 2*H*-pyrazolo[3,4-*b*]quinoline-3-carbonitriles **49** was subjected to further transformations in order to find new pharmacologically active compounds.

### 2.5. The Pfitzinger Synthesis of 1H-pyrazolo[3,4-b]quinolines

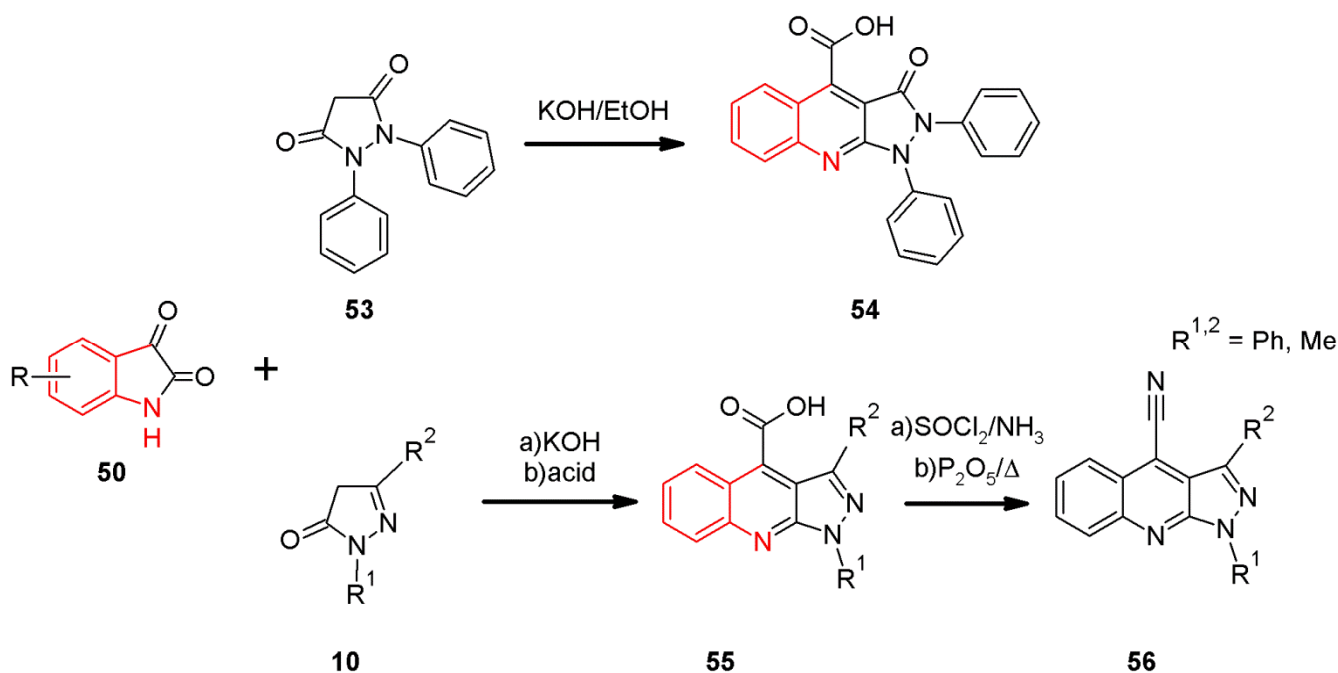
Path 1: C2<sub>1</sub>: C4-C3a; N9-C9a (Figure 4)

One of the classic named chemical reactions that leads to the quinoline system is the Pfitzinger synthesis [39,40]. It uses isatin or its derivatives **50**, which are easier to obtain than *o*-aminobenzaldehydes. The reaction is carried out in a basic environment, at which point the opening of the heterocyclic ring takes place to form a keto-acid **51**, which is then condensed with aldehydes/ketones **2**. Additionally, the final product, **52**, can be decarboxylated (Scheme 16).



**Scheme 16.** The Pfitzinger synthesis of quinoline.

The use of isatin **50** for the synthesis of pyrazolo[3,4-*b*]quinolines, where this system is built into the backbone, is very limited. One of the reactions is the synthesis that is reported by Fabrini [41]. A reaction between isatine **50** and 1,2-diphenylpyrazolidine-3,5-dione **53** afforded 1H-pyrazolo[3,4-*b*]quinolin-3-one-4-carboxylic acid **54**. In a similar fashion, Seshadri combined isatin **50** and 1,3-disubstituted pyrazolin-5-ones **10** under basic conditions and obtained 4-carboxylic acids **55**, and with nitriles **56** after subsequent reactions of **55** with SOCl<sub>2</sub> and P<sub>2</sub>O<sub>5</sub> (Scheme 17) [42].



**Scheme 17.** Synthesis of pyrazolo[3,4-*b*]quinolines from isatine.

Recently, a few studies have appeared on multicomponent pyrazoloquinolines syntheses where isatins and their derivatives are used. The end product is the *spiro*-type systems, where isatin brings C-4 carbon to the overall structure. These reactions will be discussed in the final section on the synthesis of this class of compounds.

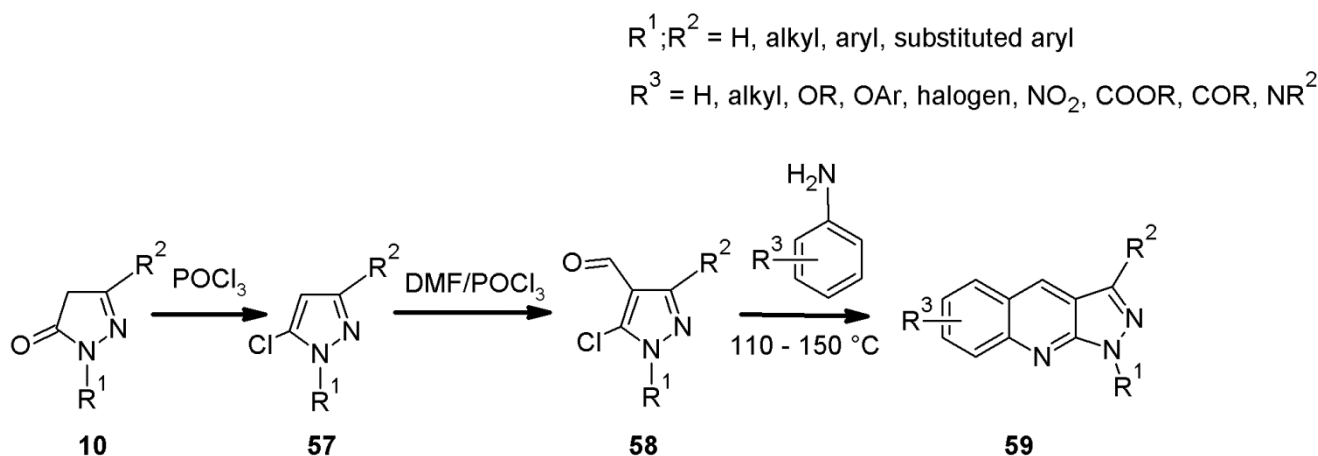
### 2.6. 1*H*-Pyrazolo[3,4-*b*]quinoline Syntheses Based on 5-chloro-4-aryl/formylpyrazoles and 4-benzylidene-1,3-disubstituted-pyrazol-5-ones

Another method of pyrazoloquinolines synthesis is the use of aromatic amines and 4 substituted pyrazole derivatives such as aldehydes, ketones or benzylidene ones (Figure 6).



**Figure 6.** Path 3: C2<sub>3</sub>: N9-C9a; C4-C4a.

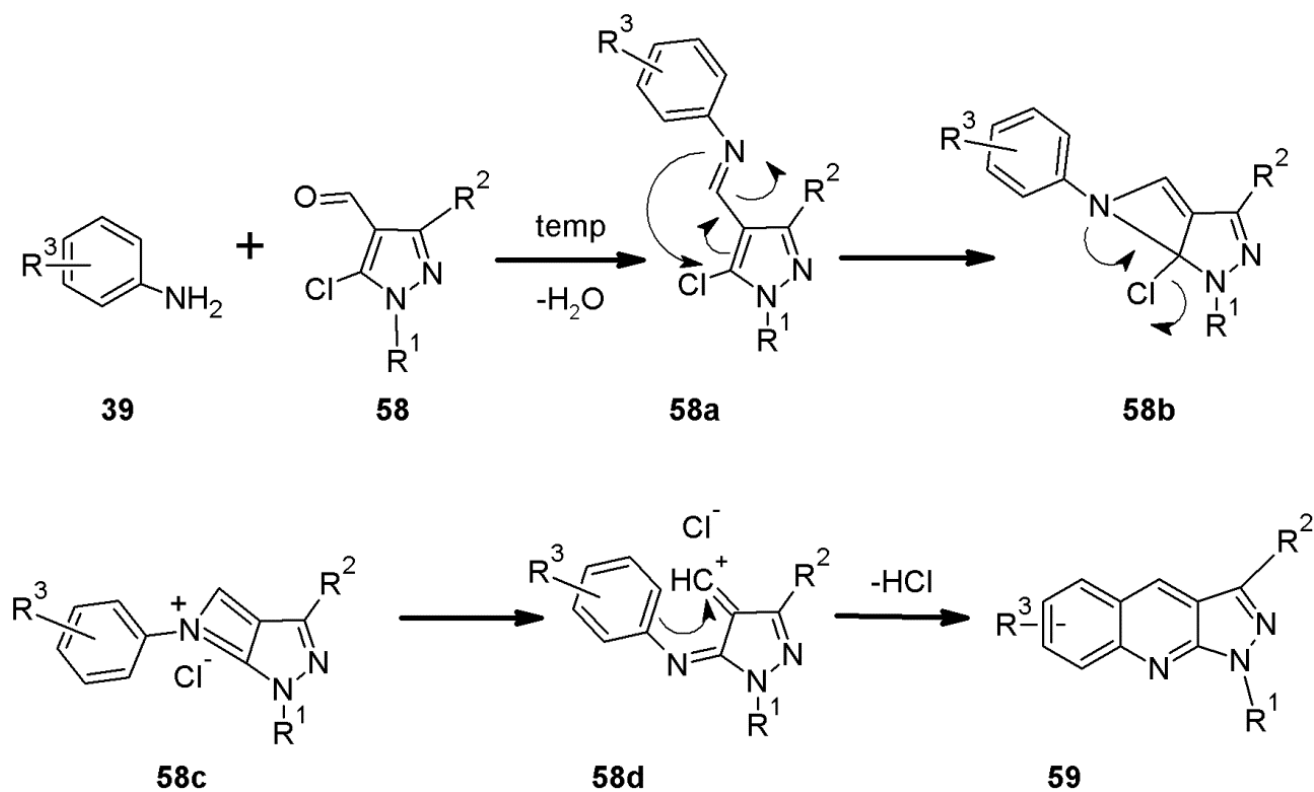
In 1963, Brack published a work on the synthesis of pyrazoloquinolines that was based on the reactions of aromatic amines **39** and 5-chloro-4-formylpyrazoles **58** [43,44]. The latter compounds were obtained by the formylation of the appropriate 5-chloropyrazoles **57** [45]. They can also be obtained in one step in the Vilsmeier–Haack reaction by treating the pyrazolones **10** with a DMF / POCl<sub>3</sub> mixture [46]. The original Brack's reaction was carried out in melt within 110–150 °C (Scheme 18).



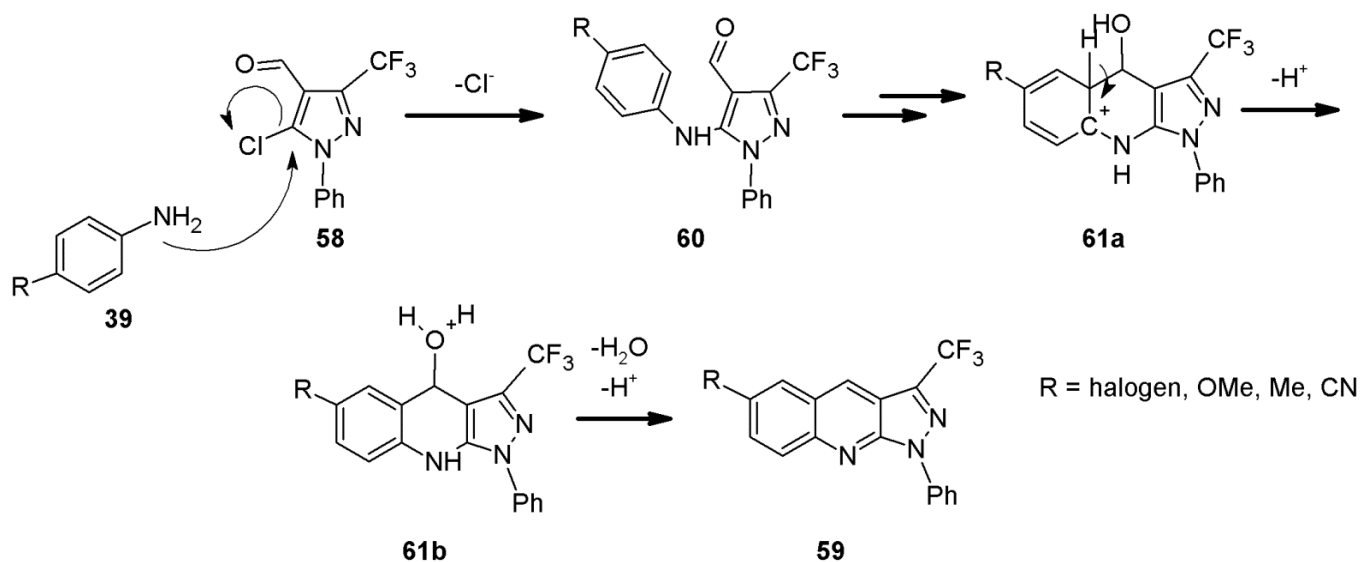
**Scheme 18.** Synthesis of 1*H*-pyrazolo[3,4-*b*]quinolines, according to Brack's protocol.

Two possible schemes for this reaction have been found in the literature. One was proposed by Brack (Scheme 19). The reaction starts from the formation of Schiff base **58a** from aniline **39** and aldehyde **58**. In the next steps, several rearrangements take place with the formation of the final pyrazoloquinoline **59**.

Another mechanism was proposed a few years ago that consists of the nucleophilic substitution of the chlorine atom in pyrazole **58** by an amino group in **39** with subsequent ring formation, and the elimination of the water molecule and hydrogen cation, which leads to the aromatisation of the system (intermediates **60-61b**) (Scheme 20) [47]. It seems, however, that the experimental data support the former; therefore, it was possible to isolate the intermediate product, which was Schiff's base **58a**, which was formed from pyrazole aldehyde **58** and substituted aniline **39**. The authors of the later paper were not able to isolate amine derivative **60**.

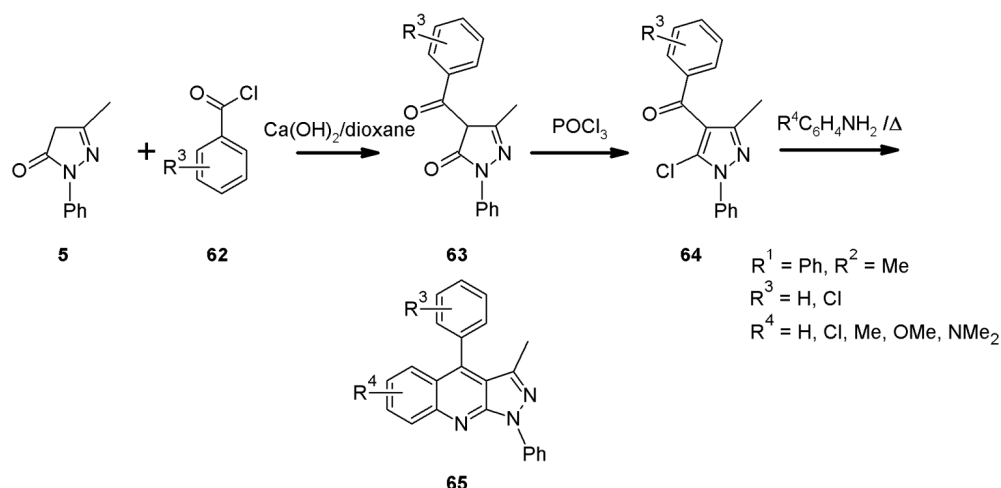


Scheme 19. The possible mechanism of Brack's synthesis.



Scheme 20. An alternative mechanism of Brack's 1H-pyrazolo[3,4-b]quinoline synthesis.

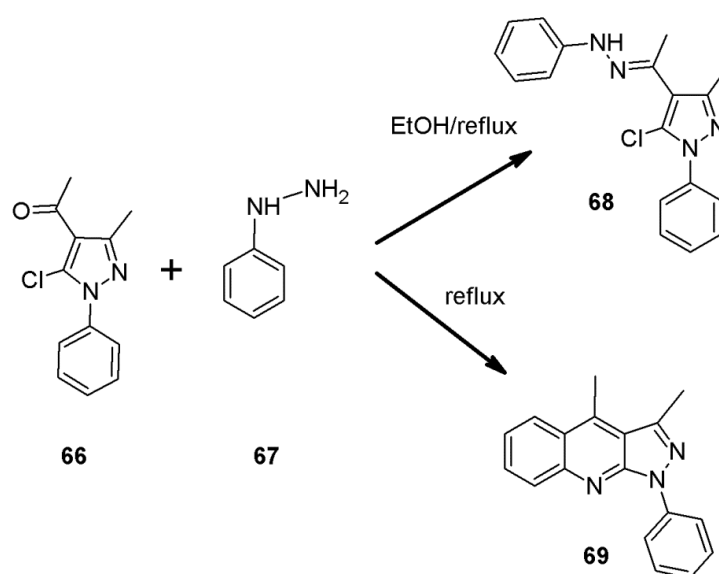
In the original work of Brack, the author limited himself mainly to three 5-chloro-4-formylpyrazole aldehydes (58;  $R^1 = \text{Me}$ ,  $R^2 = \text{Ph}$ ;  $R^1 = \text{Ph}$ ,  $R^2 = \text{Me}$ ;  $R^1 = \text{tetrahydro-1,1-dioxo-3-thienyl}$ ,  $R^2 = \text{Me}$ ) and a few aromatic amines. However, this reaction has many more possibilities, as is shown in several later works by other authors [48]. The use of 5-chloro-4-arylpurazoles **64** is an extension of the scope of two-component reactions with aromatic amines  $R^4\text{C}_6\text{H}_4\text{NH}_2$  and pyrazole systems with aldehyde function **58** [49] (Scheme 21).



**Scheme 21.** Synthesis of 1*H*-pyrazolo[3,4-*b*]quinolines based on 4-aryl-5-chloropyrazoles.

Pyrazole derivatives **64** can be synthesised either by the acylation of 5-chloropyrazoles with aromatic acid chlorides **62** and aluminum chloride, or by reacting pyrazolones **10** and acid chlorides **62**, followed by chlorination with phosphorus oxychloride [50] (Scheme 21). In contrast to the reaction with aldehydes **58**, this reaction required much more severe conditions and it lasted from 2 to 3 h at 220 °C. In one case, the authors isolated an intermediate product, which was the product of the nucleophilic amine substitution of the aromatic chlorine atom at the 5 position of the pyrazole ring. This proves a different mechanism than in the case of the original Brack reaction with pyrazole aldehyde **58** (Scheme 19), and it would, in a way, confirm the mechanism that was proposed for this reaction by Wan et al. (Scheme 20) [50].

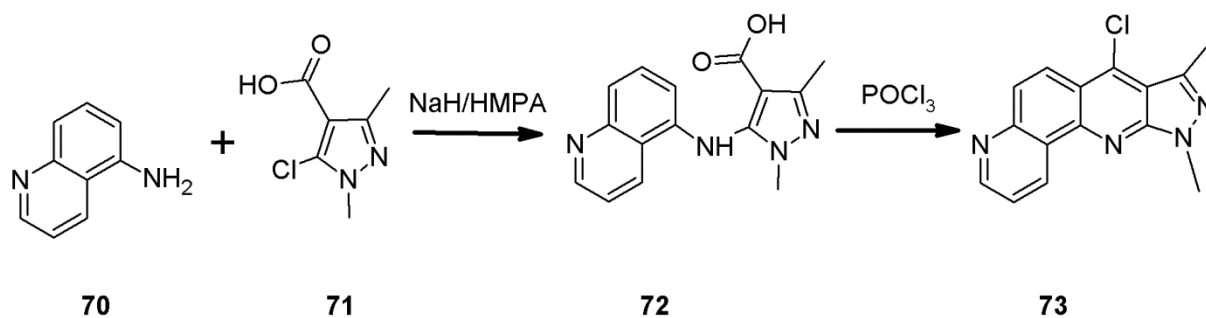
Gonzales and El Guero probably describe the only reaction where the 4 acetyl derivatives of chloropyrazole **66** and phenylhydrazine **67** were used for the synthesis of pyrazoloquinoline **69**. Depending on the reaction conditions, either the corresponding phenylhydrazone **68** or pyrazoloquinoline **69** are obtained. In the latter case, the authors suggest that phenylhydrazine decomposes under the influence of high temperatures, and the resulting aniline reacts with the chlorine atom with subsequent cyclisation to pyrazoloquinoline [51] (Scheme 22).



**Scheme 22.** Reaction of phenylhydrazine with 4-acetyl-5-chloro-3-methyl-1-phenylpyrazole.



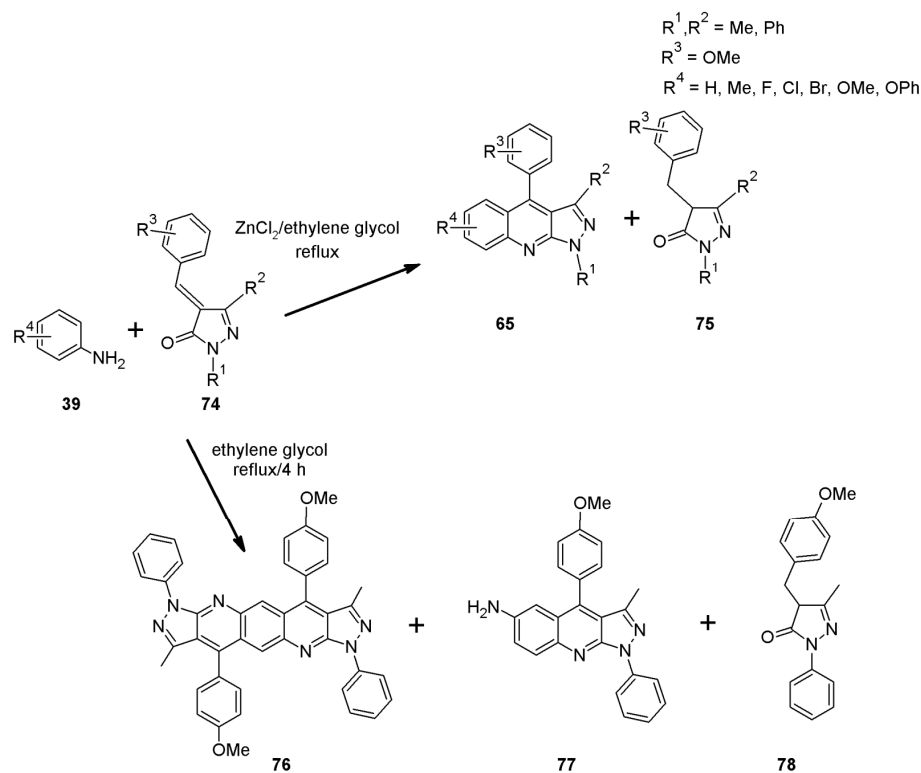
Crenshaw et al. synthesised 10*H*-pyrido[2,3-*h*]pyrazolo[3,4-*b*]quinoline **73** by starting from 5-aminoquinoline **70** and 5-chloro-1,3-dimethylpyrazolo-4-carboxylic acid **71** [52] (Scheme 23). The purpose of this reaction was to confirm the structure of product **73** that was unexpectedly formed by the ring closure of the derivative **28** ( $R^1 = \text{Me}$ ,  $R = 4\text{-NO}_2$ ), instead of the expected 4-chloro-7-nitro-1,3-dimethyl-1*H*-pyrazolo[3,4-*b*]quinoline **29** ( $R^1 = \text{Me}$ ,  $R^2 = \text{Cl}$ ,  $R = 7\text{-NO}_2$ ) (Scheme 9).



**Scheme 23.** Synthesis of 10*H*-pyrido[2,3-*h*]pyrazolo[3,4-*b*]quinoline.

Regardless of the analysis of the structure of compound **73** by using the  $^1\text{H}$  NMR spectrum, the authors synthesised it by reactions of aminoquinoline **70** and pyrazole acid **71** in the presence of sodium hydride, and they then cyclised the intermediate **72** with  $\text{POCl}_3$ .

Tomasik et al. report a new method toward 1*H*-pyrazolo[3,4-*b*]quinolines that uses anilines **39** and benzylidene derivatives **74** (Scheme 24). This reaction produces derivatives that are substituted with a phenyl group (or a substituted phenyl group) in position 4 of the parent backbone **65**. As a side product, compound **75** was isolated. It is an excellent alternative to Friedländer condensation, where 2-aminobenzophenones **1** ( $R^3 = \text{Ph}$ ) are used (Scheme 3) [1,53].



**Scheme 24.** Synthesis of pyrazolo[3,4-*b*]quinolines from 4-benzylidenepyrazol-3-ones and anilines.

While searching for the literature on the synthesis of pyrazoloquinolines, we came across a work where a whole series of syntheses of various pyrazole derivatives with potential biological effects were described [54]. Among them was the synthesis that uses the benzylidene derivative **74** ( $R^1 = \text{Ph}$ ,  $R^2 = \text{Me}$ ,  $R^3 = p\text{-OMe}$ ) and 1,4-phenylenediamine **39** ( $R^4 = p\text{-NH}_2$ ) (Scheme 24). The authors took into account the possibility of the formation of a condensed **76** system, but they did not find it in the reaction products. They only describe that they received compound **77**, which was supposed to be a pyrazoloquinoline and a side product **78**. However, they did not provide evidence of this in the form of  $^1\text{H}$  NMR and  $^{13}\text{C}$  NMR spectra for both of them. The obtained substance (**77**) was white, which is in contradiction to our research to date. We have obtained a whole range of variously substituted 1,4-diphenyl-3-methyl-1*H*-pyrazoloquinolines, which are always yellow crystalline substances, and are, in addition, also strongly fluorescing, which the authors of the publication did not mention. Thus, it seems to us that they failed to obtain **77**.

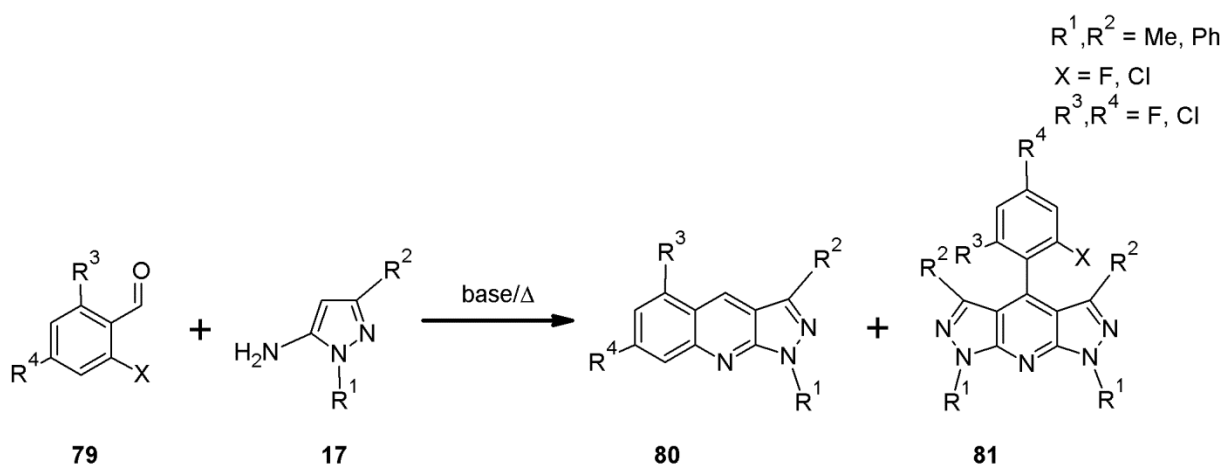
### 2.7. 1*H*-Pyrazolo[3,4-*b*]quinoline Syntheses Based on Aminopyrazoles

The procedure that was developed by Brack is an extremely effective tool for the synthesis of pyrazoloquinolines. There is also the possibility of using substituted *o*-halogenobenzoic aldehydes and aminopyrazoles (Figure 7).



**Figure 7.** Path 4; C2<sub>4</sub>: C4-C3a; N9-C8a.

Szlachcic et al. have published a very extensive work on the use of variously substituted *o*-halogeno benzaldehydes **79** for the synthesis of pyrazoloquinolines **80** [55] (Scheme 25). The authors focused on regioselective reactions, which would allow the preparation of mono- and disubstituted pyrazoloquinoline halogen derivatives, which could be used later for further reactions (e.g., nucleophilic substitution with aliphatic or aromatic amines), and which could be used, for example, as luminophores for the construction of electroluminescent cells.

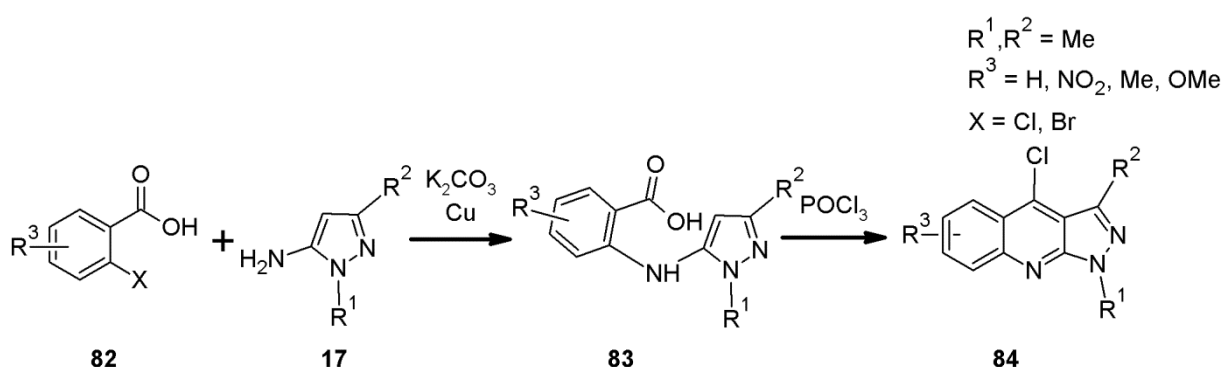


**Scheme 25.** Synthesis of pyrazolo[3,4-*b*]quinolines from 3-aminopyrazoles and halogenated aromatic aldehydes.

In the case of monosubstituted aldehydes **79** ( $R^{3,4} = \text{H}$ ,  $X = \text{F, Cl, Br, I}$ ), it has been observed that, besides pyrazoloquinoline **80**, bis-pyrazolo[3,4-*b*;3',4'-*e*]pyridine **81** is also formed; however, in the case of *o*-fluorobenzaldehyde, pyrazoloquinoline was the final product. The opposite tendency was observed for *o*-iodobenzaldehyde **79** ( $R^{3,4} = \text{H}$ ,  $X = \text{I}$ ). Pentafluorobenzaldehyde yielded only pyrazoloquinoline **80**. As part of the work, the

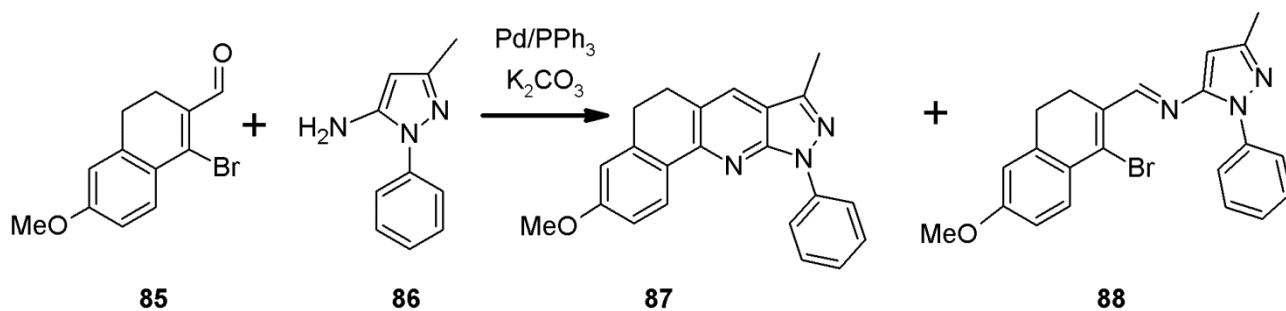
influence of the base on the course of the reaction was also investigated, and it turned out that bases such as DABCO or quinoline favored the formation of **80** but not of **81**. The influence of the substituents in the aminopyrazole **17** was also of some importance, and so the system with the phenyl group in position 3 (**17**;  $R^2 = \text{Ph}$ ) favored the formation of PQ, while the methyl group contributed to the formation of more **81**. Dehaen et al. investigated the reaction pentafluorobenzaldehyde and 5-chloro-4-formylpyrazoles **17** with 5-amino-1,2-azoles. Depending on the reaction conditions, the positions of the halogen atom in relation to the carbonyl group pyrazolo[3,4-*b*]quinolines **80**, bis-pyrazolo[3,4-*b*; 4',3'-*e*]pyridines **81** and isoxazolo[5,4-*b*]quinolines were formed [56].

Another reaction route is the use of *o*-halogen-substituted benzoic acids **82** and 1,3-disubstituted 5-aminopyrazoles **17**. As a result of the Ullmann-type reaction that is catalysed by copper, an intermediate **83** is formed. In the next step, it can be transformed into **84** by heating with  $\text{POCl}_3$  (Scheme 26). This reaction was used, inter alia, by Siminoff and other researchers for the synthesis of **84** from anthranilic acid **23** and diketene [34,57,58] (Scheme 9).



**Scheme 26.** Synthesis of pyrazolo[3,4-*b*]quinolines from 3-aminopyrazoles and ortho-chloro/bromo benzoic acid.

Boruah et al. employed a palladium catalysed reaction of  $\beta$ -bromovinyl aldehyde **85** with **86**, which yielded pyrazolo[3,4-*b*]quinoline **87** and Schiff base **88** (Scheme 27) [59].

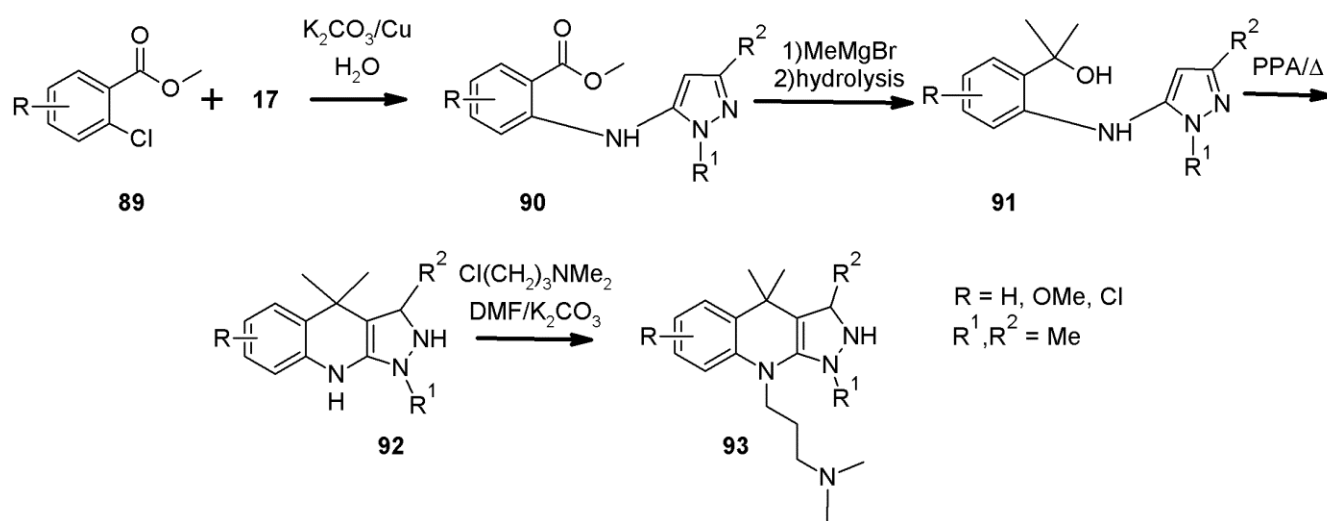


**Scheme 27.** Application of  $\beta$ -bromovinyl aldehyde in synthesis of 1*H*-pyrazolo[3,4-*b*]quinolines.

The ratio of the products that were obtained depended on the conditions under which the reaction was carried out. Thus, during heating at 120 °C for 24 h, the Schiff's base **88** dominated in the reaction mixture, while the reaction that was carried out in the microwave field, without a solvent, for 15 min, favored the formation of pyrazoloquinoline **87**. As a catalyst, 2.5 mol% palladium acetate has been proven to be the best.

At the end of the description of the use of the *o*-halogen derivatives of acids, esters and aldehydes, we want to mention the use of a benzyl alcohol derivative that has been cyclised to pyrazoloquinoline. In 1974, Horace de Wald synthesised a series of pyrazoloquinolines **93** as potential antidepressants [60]. As a starting material, he applied the methyl ester of 2-chlorobenzoic acid **89**. The Ullmann reaction with 1,3-dimethyl-5-amino pyrazole **17** afforded the formation of **90**. This compound was reacted with Grignard

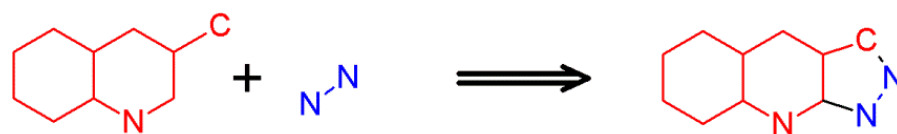
reagent  $\text{CH}_3\text{MgBr}$ , and it was hydrolysed to yield an alcohol **91**, which was cyclised to **92** with PPA at 85–110 °C (Scheme 28).



**Scheme 28.** Benzyl alcohol derivatives as a substrate for pyrazolo[3,4-*b*]quinoline synthesis.

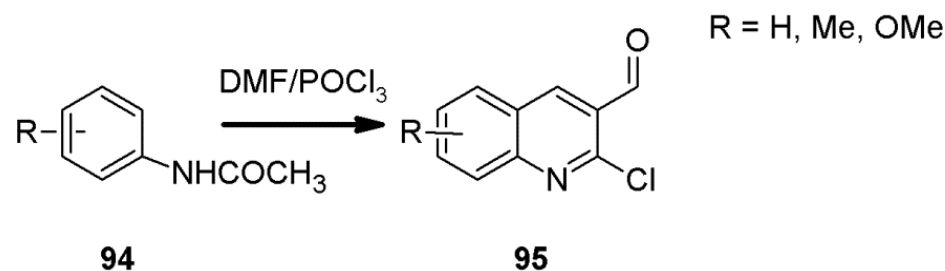
### 2.8. 1*H*-Pyrazolo[3,4-*b*]quinoline Synthes Based on Quinoline Derivatives

The most common way to obtain pyrazolo[3,4-*b*]quinolines by using the fifth path is by the reaction of the hydrazines  $\text{RNHNH}_2$  ( $\text{R} = \text{H, aryl}$ ) with quinoline derivatives (Figure 8).



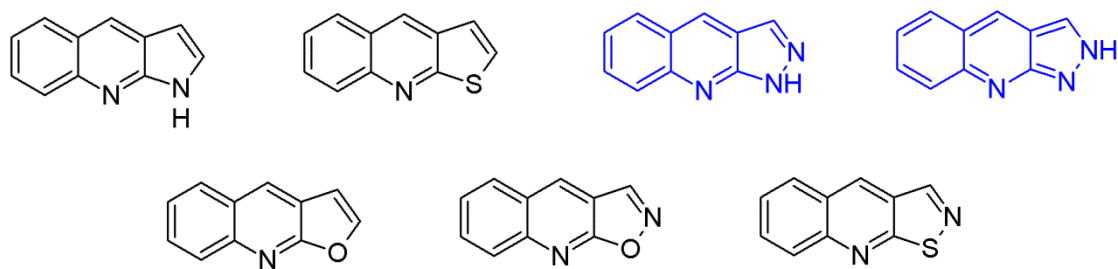
**Figure 8.** Path 5; C2<sub>5</sub>:N1-C9a; N2-C3.

Some modifications are also possible, in which 2-chloro/2-aminoquinolino-3-carbonitrile or 3-acetylquinolin-2(1*H*)-one can also be used. In 1978, Meth-Cohn et al. described the synthesis of the 5-chloro-4-formylquinoline derivatives **95** by the formulation of Vilsmeier–Haack-substituted acetanilides **94** (Scheme 29) [61–63].



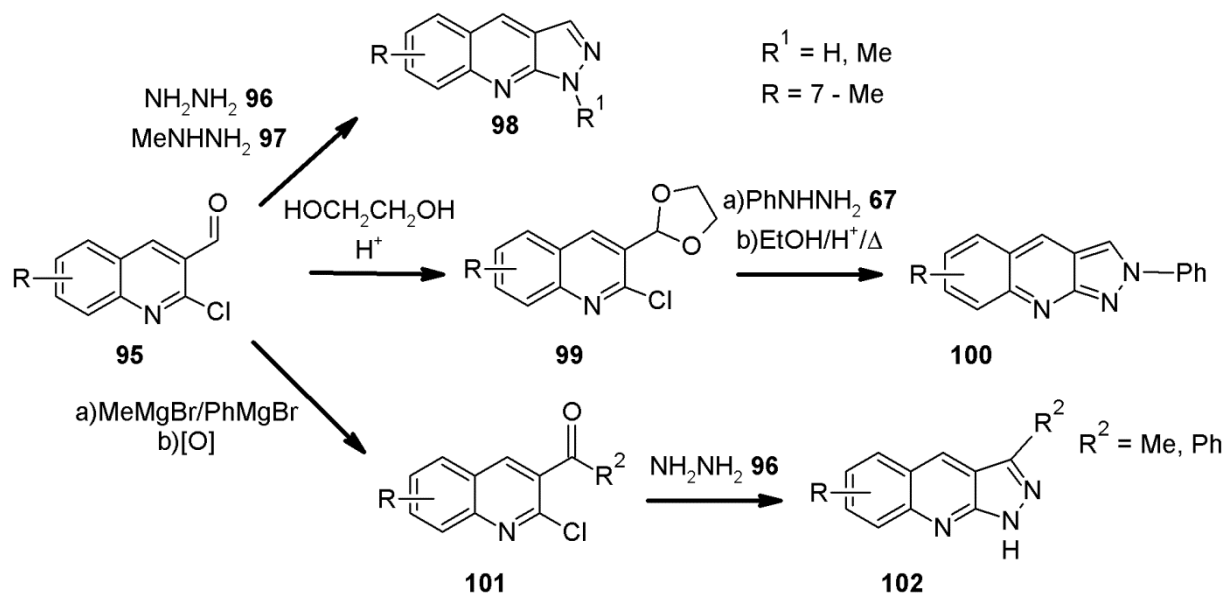
**Scheme 29.** Synthesis of 5-chloro-4-formylquinolines, according to Meth-Cohn protocol.

The resulting compound, 5-chloro-4-formylquinoline **95**, can be transformed into a wide variety of fused heterocyclic derivatives, including 1*H*- or 2*H*-pyrazolo[3,4-*b*]quinolines (Figure 9) [64].



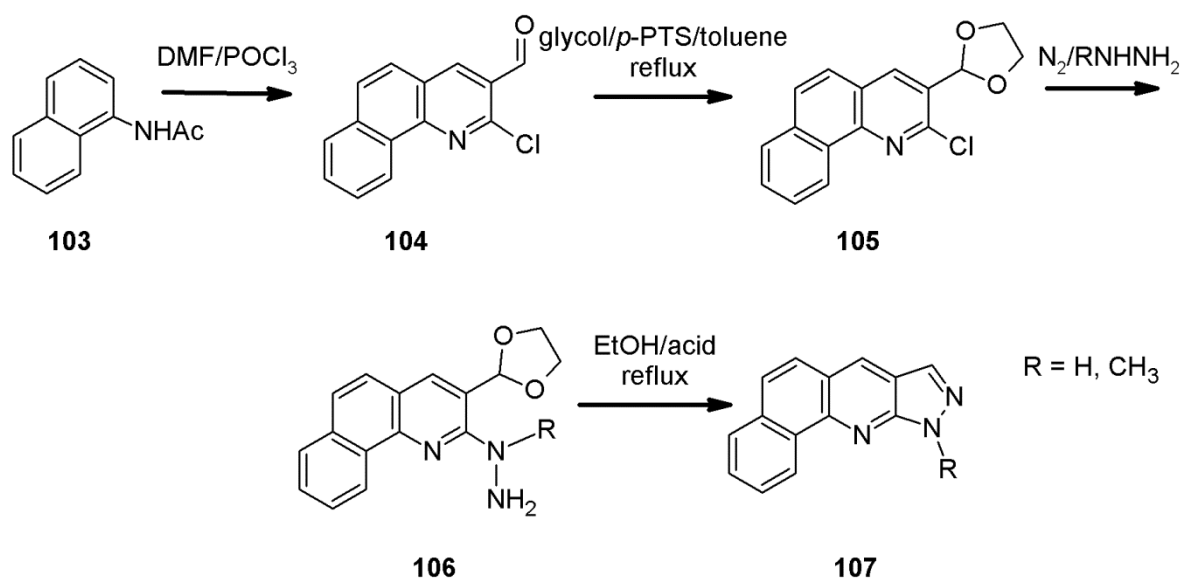
**Figure 9.** Some heterocycles prepared from 2-chloro-4-formyl quinoline [64].

Some simple procedures of transforming 2-chloro-3-formylquinolines **95** into pyrazoloquinolines are depicted in Scheme 30. Thus, Hayes et al. carried out the reaction between **95** and hydrazine **96** or methylhydrazine **97**. The immediate attack at the aldehyde group forms 1,7-dimethyl-1*H*-pyrazolo[3,4-*b*]quinoline **98**. On the other hand, when the aldehyde group is protected, such as in **99**, hydrazine substitutes the chlorine atom at position 2, and with the subsequent deacetylation with acid in alcoholic solution and the cyclisation to the pyrazole ring. The formation of 2*H*-pyrazolo[3,4-*b*]quinolines **100** is observed. The third modification consists of reacting the Grignard reagent with an aldehyde group in **95**, and the resulting alcohol is oxidised with chromium (VI) compounds to the ketone **101**. Reaction with hydrazine or arylhydrazine leads to the formation of 1*H*-pyrazolo[3,4-*b*]quinolines **102** [65].



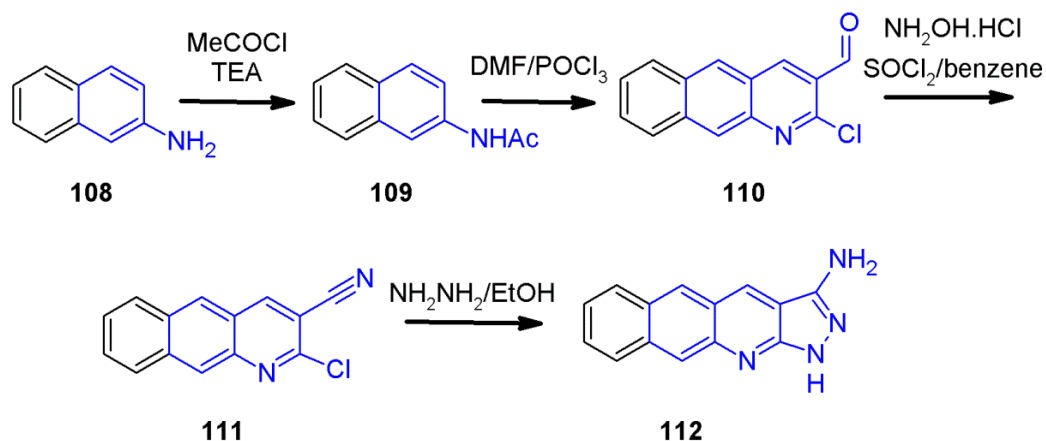
**Scheme 30.** 1*H*-Pyrazolo[3,4-*b*]quinoline syntheses from 2-chloro-3-formylquinolines [61].

Other researchers have applied the same methodologies, and sometimes with the application of MW irradiation [65–74]. Mane et al. investigated the influence of baker's yeast on the synthesis of tetrahydrobenzo[*a*]xanthene-11-ones and pyrazolo[3,4-*b*]quinolines. They reacted substituted aldehydes **95** and hydrazine **96** or phenylhydrazine **67** in water and obtained pyrazolo[3,4-*b*]quinolines **98** ( $R = H, Me, Cl, OMe, R^1 = H, Ph$ ), with the yield of 79–90% [75]. In 1999, Kerry et al. formylated *N*-acetylo-1-naphthylamine **103** to produce 2-chlorobenzo[*h*]quinoline-3-carbaldehyde **104**. In the next turn, the aldehyde group was protected by transformation into acetal **105** and was reacted with methylhydrazine **97** or hydrazine **96**, which formed compound **106**. This one was heated in boiling ethanol that was acidified with HCl, which afforded 10-methyl-10*H*-benzo[*h*]pyrazolo[3,4-*b*]quinoline **107** (Scheme 31) [76]. These derivatives were synthesised as potential topoisomerase inhibitors.



**Scheme 31.** Synthesis of benzo[*h*]pyrazolo[3,4-*b*]quinolines.

When 2-naphthylamine **108** is used instead of 1-naphthylamine, the aldehyde **110** can be obtained by carrying out the same chemical transformations (e.g., acetyl derivative **109**) as for the previously described reactions. Maheira converted **109** into an oxime by reaction with hydroxylamine hydrochloride and, with the subsequent treatment with SOCl<sub>2</sub> in boiling benzene, he obtained 2-chloro-benzo[*g*]quinoline-3-carbonitrile **111**. Further reaction with hydrazine **96** gave **112**. In the next turn, 3-aminoderivative **112** was coupled with various pyrazol-5-ones, which formed a series of azo dyes for polyester fibers (Scheme 32) [77,78].

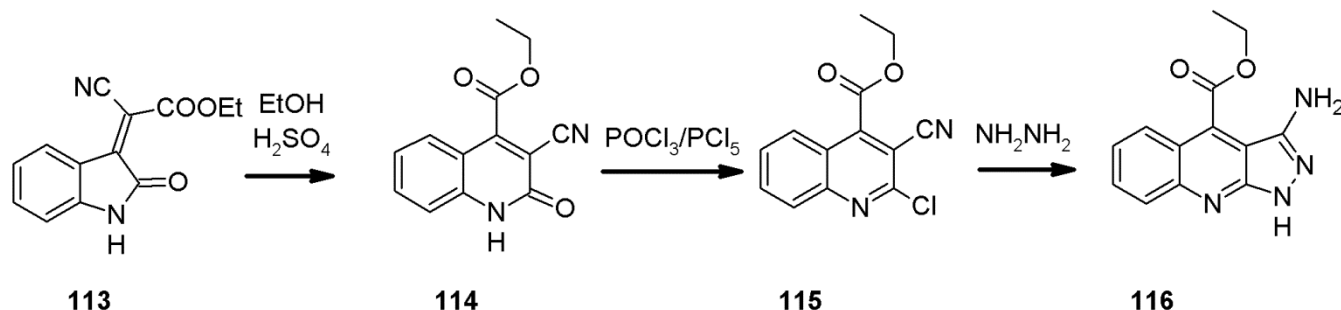


**Scheme 32.** Synthesis of 1*H*-benzo[*g*]pyrazolo[3,4-*b*]quinoline-3-ylamine.

The same synthetic protocol can be used for **95** by the transformation of it into oxime, 2-chloroquinoline-3-carbonitrile and then into 3-amino-1*H*-pyrazolo[3,4-*b*]quinoline, which is then modified in various ways to search for potential compounds of biological activity (Scheme 32—structures marked in blue) [79].

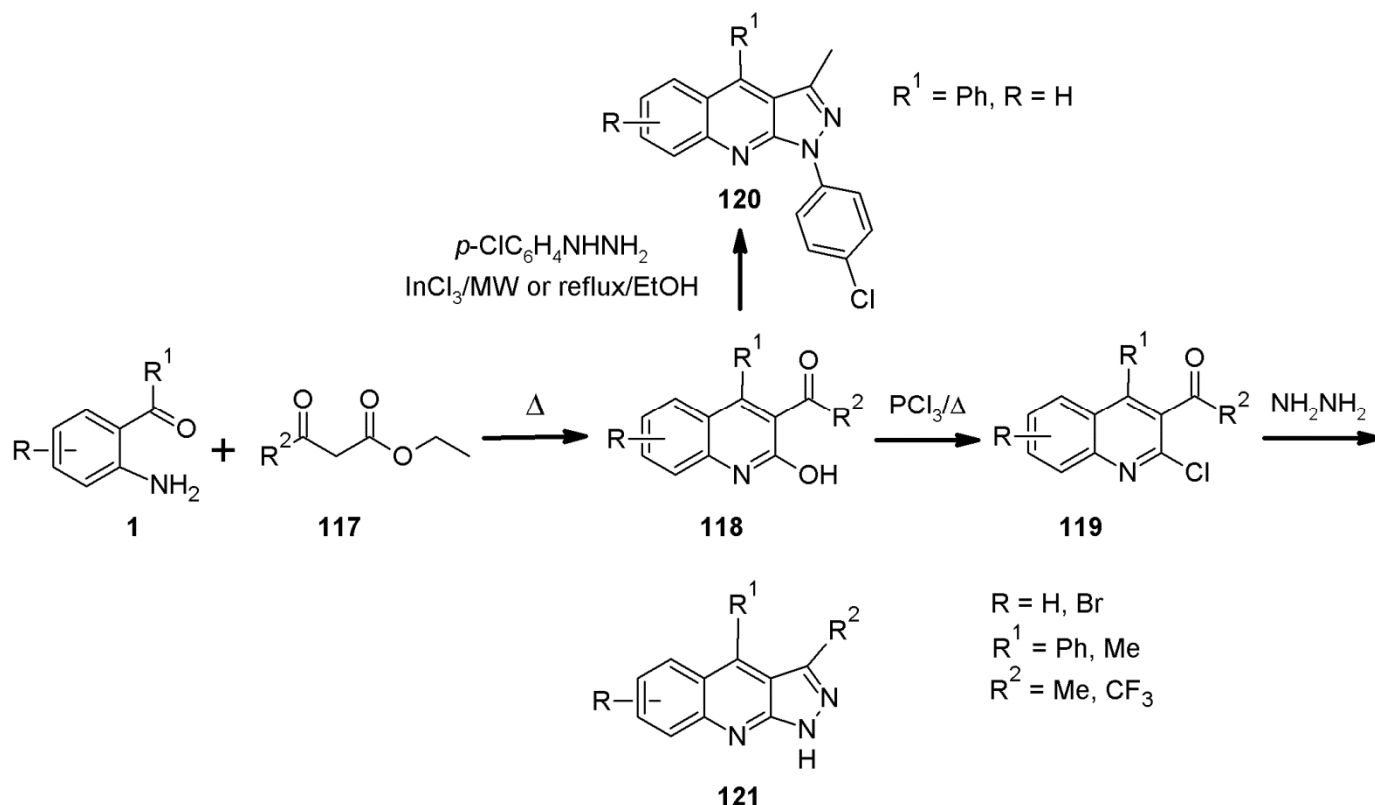
Section 2.5 discusses the few cases where isatin and pyrazolones are used in the Pfitzinger reaction for the synthesis of pyrazoloquinolines. Here, we have another one of the few cases that uses this compound, and specifically its derivative **113**, which is formed as a result of the reaction of isatin **50** with ethyl cyanoacetate. The reaction with ethanol acidified with sulphuric acid afforded ethyl 3-cyano-2-oxo-1,2-dihydroquinoline-4-carboxylate **114**. Heating with a mixture of phosphorus oxychloride and phosphorus trichloride causes the introduction of the chlorine atom in the 2 position of the quinoline system, which

results in the formation of compound **115**. The last step is the reaction with hydrazine, which gives pyrazoloquinoline **116**. This compound offers multiple possibilities for further functionalization and for obtaining a whole range of derivatives (e.g., by modifying the ester and amino groups, or by adding substituents to the nitrogen atom N1 (Scheme 33) [80]).



**Scheme 33.** Synthesis of ethyl 3-amino-1H-pyrazolo[3,4-b]quinoline-4-carboxylate.

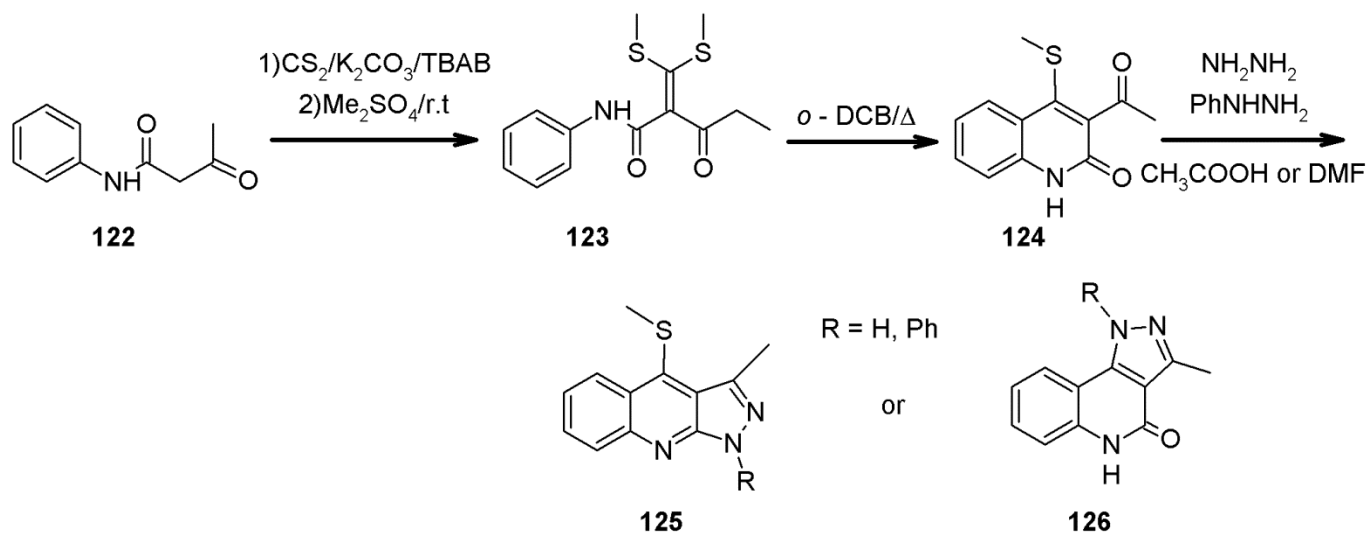
Another substrate for the synthesis of pyrazolo[3,4-b]quinolines is 2-hydroxy-3-acetylquinoline **118**, which is easily prepared from ethyl acetoacetate **117** and *o*-aminoacetophenone/benzophenone **1** (Scheme 34). Arasakumar et al. applied 3-acetyl-4-phenyl-chinolin-2-one **118** and *p*-chlorophenylhydrazine for the synthesis of substituted 1H-pyrazolo[3,4-b]quinoline **120** [81]. Researchers have studied the effects of various Lewis acids (e.g., SnCl<sub>4</sub>, AlCl<sub>3</sub>, TiCl<sub>4</sub>, etc.), as well as of the microwave field, on the reaction yield. The best results were achieved with indium chloride (InCl<sub>3</sub>).



**Scheme 34.** Syntheses of 1H-pyrazolo[3,4-b]quinolines from 2-hydroxy-3-acylquinolines.

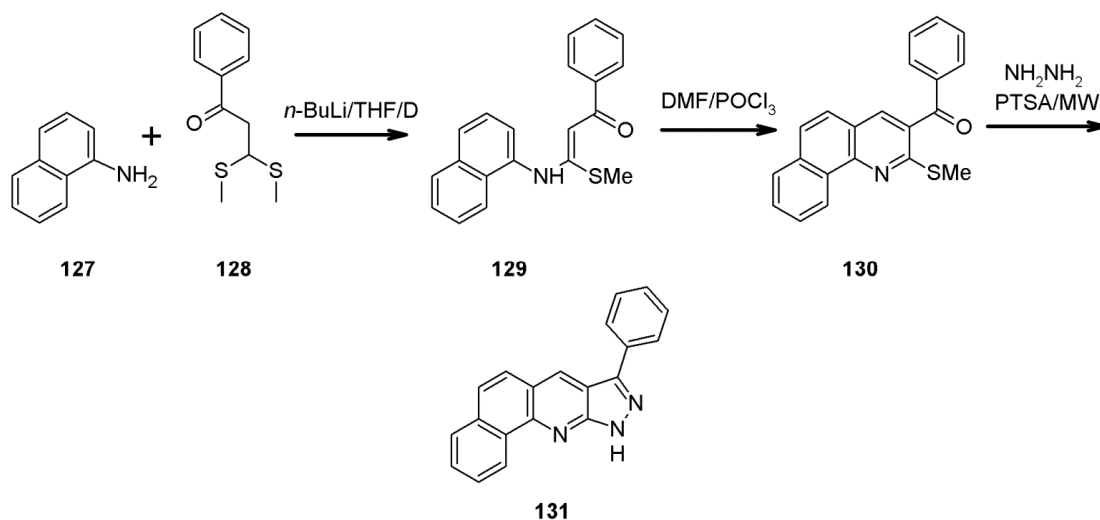
Compound **118** can be subjected to the reaction with phosphorus trichloride (PCl<sub>3</sub>) to give 2-chloro-3-acylquinolines **119**, which is reacted with hydrazine. The product is 3,4-disubstituted-1H-pyrazolo[3,4-b]quinoline **121** [82]. The free position in nitrogen N1 allows for numerous modifications of these compounds in terms of the biological

properties [83]. 3-Acetyl-4-(methylthio)quinolin-2(1*H*)-one **124** is an example of another quinolin-2-one-based system that can be used both for the synthesis of pyrazoloquinolines and for other heterocycles as well [84]. It can be easily prepared from acetoacetanilide **122** by reacting with carbon disulfide in the presence of tetrabutylammonium bromide (TBAB), with the subsequent methylation yielding ketene dithioacetal **123**. In the next step, the **123** is cyclised by boiling in *o*-dichlorobenzene. Reactions with hydrazine or phenylhydrazine in acetic acid lead to the formation of the corresponding pyrazoloquinolines **125**. On the other hand, when DMF is used as a reaction medium instead, **125** angular pyrazolo[4,3-*c*]quinolin-2-ones **126** are formed (Scheme 35) [85].



**Scheme 35.** Synthesis of 4-methylthio-1*H*-pyrazolo[3,4-*b*]quinolines.

The use of 2-naphthylamine **108** and the Meth-Cohn procedure allows for the synthesis of benzo[*h*]pyrazolo[3,4-*b*]quinoline (Scheme 32). Similarly, 1-naphthylamine **127** can be reacted with  $\alpha$ -oxoketene dithioacetal **128** and *n*-BuLi to form  $\alpha$ -oxoketene-*N,S*-naphthylaminoacetal **129**, which forms 2-methylthio-3-benzoyl-4-methylquinolines **130** upon the cyclisation by  $\text{POCl}_3$ /DMF. The reaction with hydrazine under microwave irradiation afforded the formation of **131** (Scheme 36) [86].



**Scheme 36.** Syntheses of 2-methylthio-3-benzoyl-4-methylquinolines and related 1*H*-pyrazolo[3,4-*b*]quinolines.



The same procedure can be applied to aromatic amines or diamines and, as a result, other heterocyclic systems, such as phenanthrolines, can be obtained.

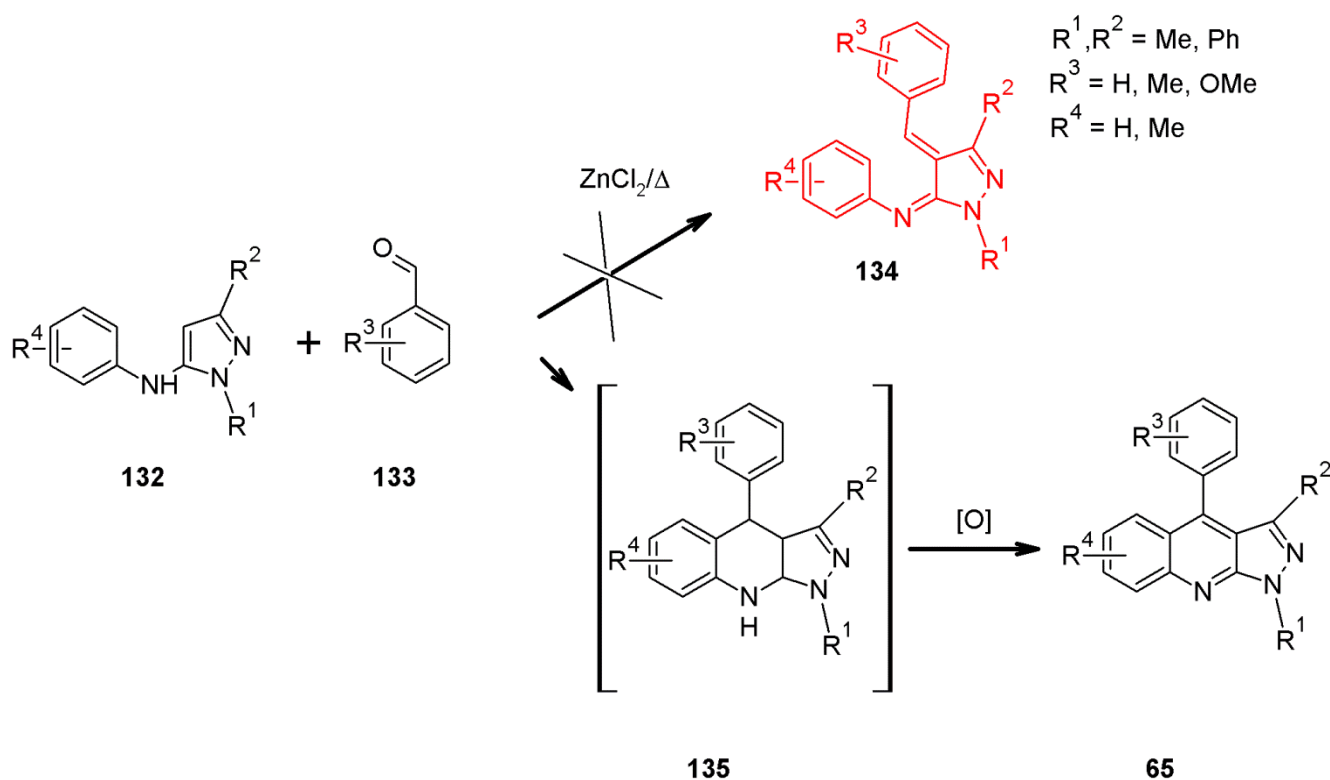
### 2.9. 1*H*-Pyrazolo[3,4-*b*]quinoline Syntheses Based on 5-arylaminoaminopyrazoles

One of the oldest methods of pyrazoloquinolines synthesis are the two-component reactions of 5-arylamino pyrazoles and aromatic aldehydes (Figure 10).



**Figure 10.** Path 6a; C2<sub>6a</sub>: C4-C4a; C4-C3a.

In 1911, Michaelis heated 5-*N*-arylamino-1,3-disubstituted pyrazoles **132** with some aromatic aldehydes **133** in the presence of anhydrous ZnCl<sub>2</sub> and obtained compounds to which he assigned a structure **134** (Scheme 37) [1]. He described them as yellow crystalline substances with a strong blue fluorescence in a toluene solution. Our group was interested in these types of compounds from the point of view of applying them to organic electroluminescent cells. The syntheses described by Michaelis were repeated, and the chemical structures of the compounds that were obtained were analysed by using <sup>1</sup>H NMR spectroscopy. It turned out that the structure of Michaelis **134** did not correspond to any of the compounds that he received, but that it did match the pyrazoloquinolines of **65** [87].

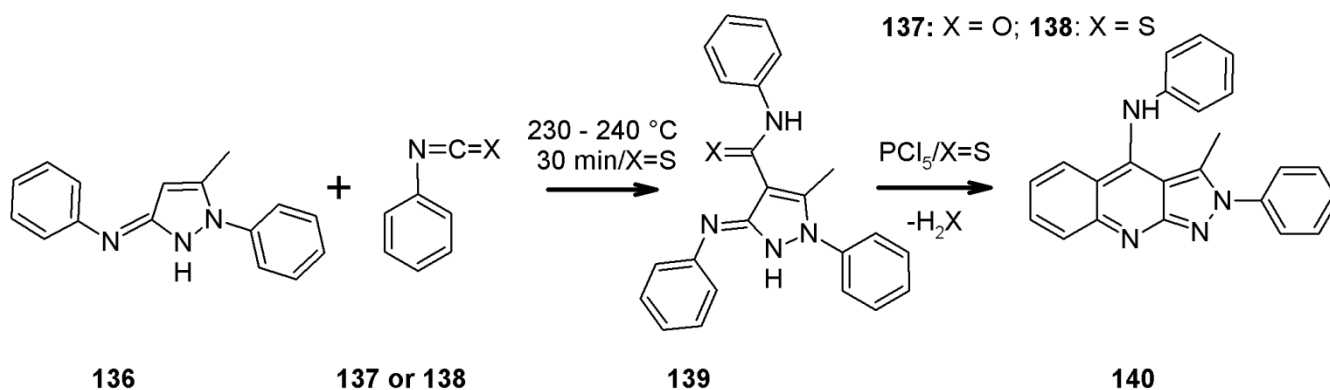


**Scheme 37.** Correction and verification of the Michaelis' 1*H*-pyrazolo[3,4-*b*]quinoline synthesis.

In several cases, it was possible to isolate intermediate **135**, which oxidises over time to form pyrazolo[3,4-*b*]quinoline **65**. The modified Michaelis method turned out to be a very good method for the synthesis of **65**, and it complements the Friedländer condensation, in which *o*-aminobenzophenones are used. However, it provides more possibilities with regard to the introduction of substituents to the phenyl ring in position 4 and the modification of the carbocyclic ring. The starting 5-*N*-arylamino-pyrazoles **132** can

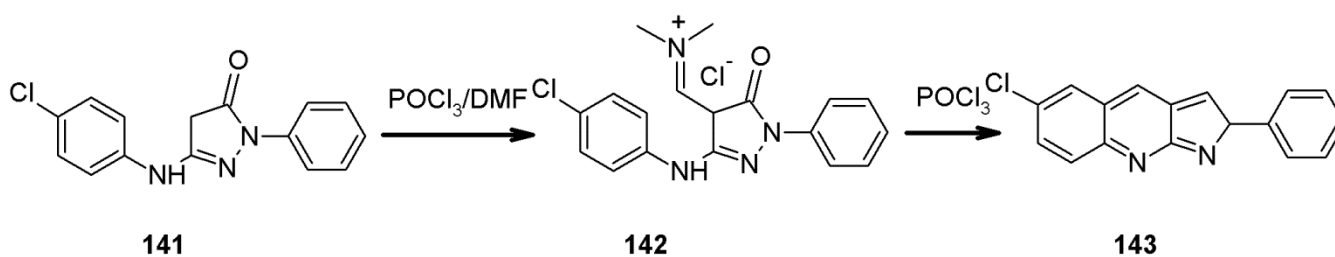
be obtained from commercial 1,3-disubstituted 5-aminopyrazoles and the corresponding aryl halides by the procedures that are described by Buchwald [88].

The next two-component procedure with *N*-arylpyrazoles is one of the oldest synthetic pyrazoloquinolines methods (Scheme 38). In 1936, Koćwa published a series of papers in which he obtained 2*H*-pyrazolo[3,4-*b*]quinolines **140** by reacting aryl isocyanates **137** or isothiocyanates **138** with *N*-arylpyrazoles **136** [3,4]. By heating *N*-[5-methyl-1-phenyl-1,2-dihydro-3*H*-pyrazol-3-ylidene]aniline **136** with phenyl isocyanate **137** at a temperature of 230–240 °C, product **140** is formed, while, in the case of phenyl isothiocyanate **138**, intermediate **139** was isolated, which then cyclised to **140** by heating with  $\text{PCl}_5$  at a temperature of 100–110 °C in 15 min (Scheme 38).



**Scheme 38.** Reactions of isocyanates and isothiocyanates with *N*-arylpyrazole with isolation of intermediate products.

In 1976, Purnaprajna and Seshadri, as a result of the Vilsmeier–Haack formylation of 1-phenyl-3-(*p*-chloroanilino)-5-pyrazolone **141**, isolated 4-dimethylaminomethylene derivative **142**. In the next stage, they cyclised it by using phosphorus oxychloride to produce 3,6-dichloro-2-phenyl-2*H*-pyrazolo[3,4-*b*]quinoline **143** (Scheme 39) [89].



**Scheme 39.** Ring closure by Vilsmeier–Haack formylation reaction.

For a long time, this was only one example of such reaction. It was not until 2021 that Kucharek and colleagues developed a one-step cyclisation reaction of 5-*N*-arylpyrazoles **132** in the presence of dimethylformamide diethyl acetal (DMF-DEA)/ $\text{POCl}_3$  at 80 °C. The yields of the obtained pyrazoloquinolines **59** ranged between 27 and 97% [90].

We include in this part one more synthesis, in which the 5-*N*-arylamino derivatives of pyrazoles with the ester group in the 4 position of the pyrazole ring are obtained (Figure 11. Path 6b).

This compound can be easily prepared in a one-pot reaction by starting from aniline **39**, carbon disulfide, chloroacetic acid and hydrazine, which yields thiosemicarbazide **144**. A subsequent reaction with ethyl 2-chloroacetoacetate **145** produced pyrazole ester **146**. The hydrolysis of **146** in EtOH/KOH and the cyclisation of the resulting acid with  $\text{POCl}_3$  yielded chloro derivative **147** (Scheme 40) [33,91–93].

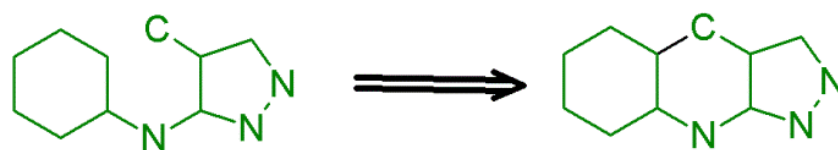
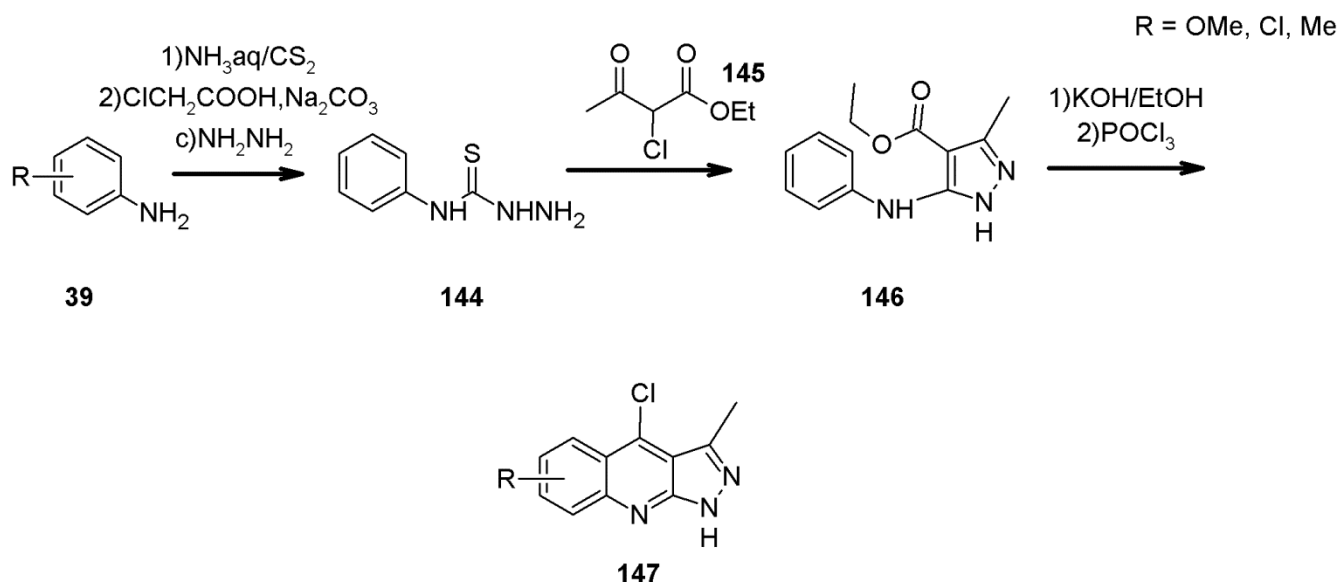


Figure 11. Path 6b: C1<sub>6b</sub>: C4-C4a.



Scheme 40. Synthesis of 5-chloro-3-methyl-1H-pyrazolo[3,4-b]quinoline derivatives.

#### 2.10. 1H-Pyrazolo[3,4-b]quinoline Syntheses Based on 4-arylidene pyrazoles

Another one-component procedure is the synthesis which uses 4-arylidene substituted pyrazole derivatives (Figure 12).

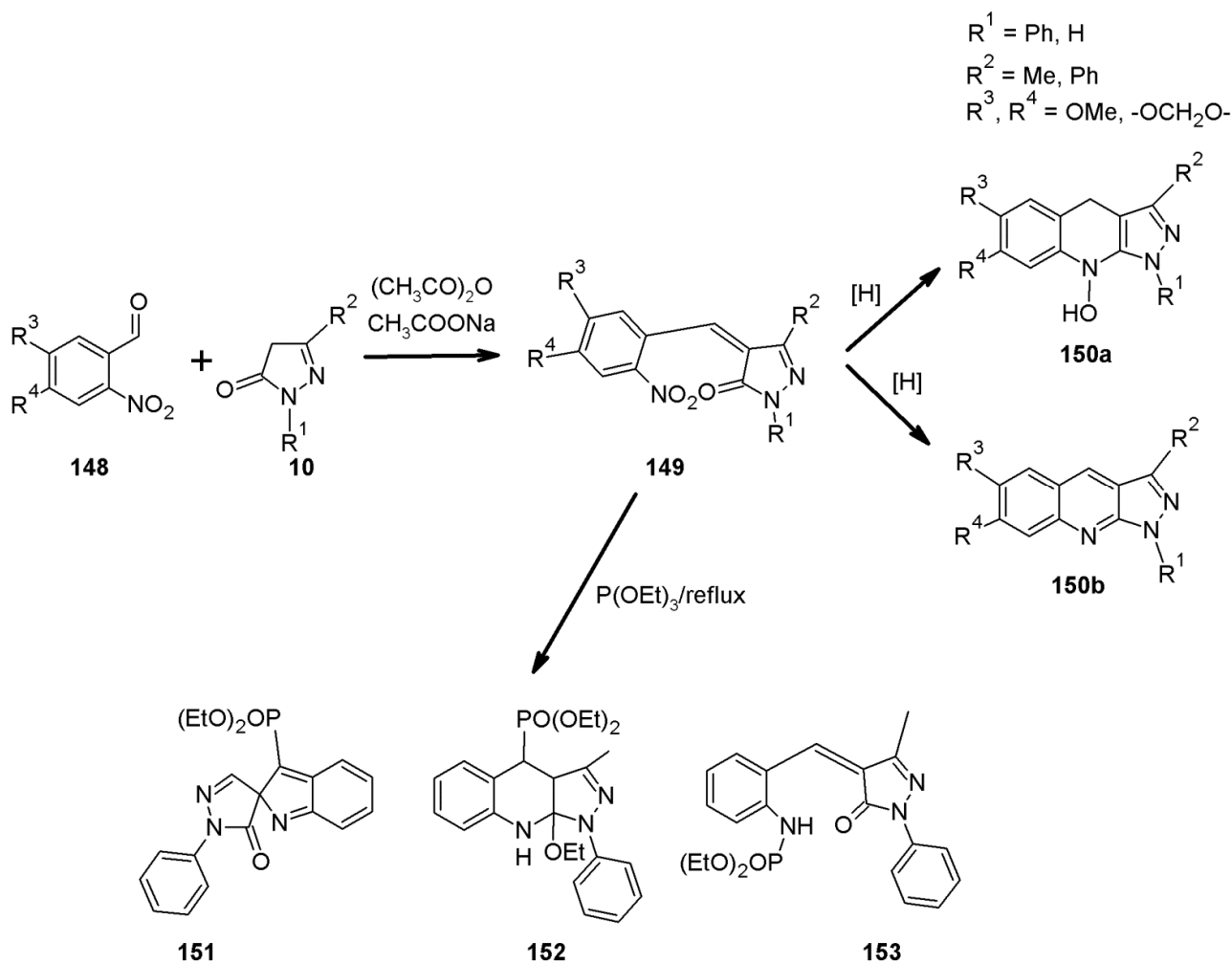


Figure 12. Path 7; C1<sub>7</sub>: N9-C3a.

Coutts and Edwards reacted *o*-nitrobenzaldehyde **148** and pyrazolone **10**, which yielded 4-(2-nitrobenzylidene)-2-pyrazolin-5-ones **149** [94]. The next step was to use several methods of reductive cyclisation, such as cyclohexene/Pd(C), NaBH<sub>4</sub> as well as zinc and acetic acid. The end product was 9-hydroxypyrazolo[3,4-*b*]quinolines **150a**. After changing the reaction conditions as a result of reductive cyclisation, they obtained pyrazolo[3,4-*b*]quinoline **150b** [95] (Scheme 41). The prereaction between *o*-nitrobenzaldehyde **148** and the corresponding pyrazolone **10** may be an alternative to avoid the synthesis of the anthranilic aldehyde **1** (R<sup>3</sup> = H, R<sup>4</sup> = H, halogen, OMe) that is needed for the Friedländer condensation (Scheme 3).

As part of the research on nitrenes, Kametani and colleagues performed reductive cyclisation reactions on 4-(4,5-methylenedioxy-2-nitrobenzylidene)-2-phenyloxazolones by using triethyl phosphite (P(OEt)<sub>3</sub>). These compounds were prepared from 4,5-dimethoxy-2-nitrobenzaldehyde (**145**; R<sup>3,4</sup> = OMe) and *N*-benzoylglycine. The reaction resulted in the formation of 2-phenyloxazolo[5,4-*b*]quinoline [96]. Nishiwaki also tried to cyclise 4-(2-nitrobenzylidene)-2-pyrazolin-5-ones **149** by using P(OEt)<sub>3</sub> as the reducing agent. However, instead of the expected pyrazoloquinolines, a whole range of other products were

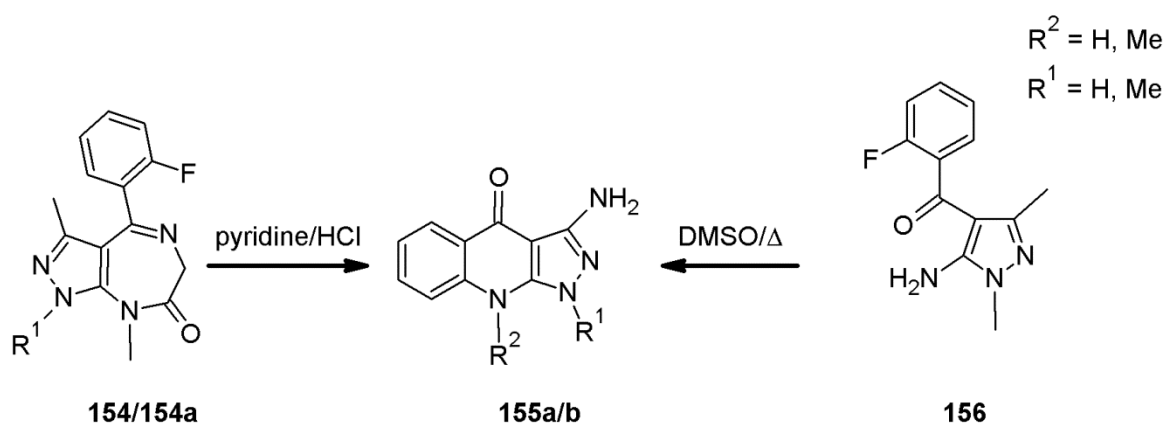
isolated from the reaction mixture, the structures (e.g., **151**, **152**, **153**) of which are shown in Scheme 41 [97]. Tomasik and Danel used reductive cyclisation with iron powder and glacial acetic acid to synthesise pyrazoloquinolines **150** from *o*-nitrobenzylidene derivatives **149**, however with moderate yields [98].



**Scheme 41.** *o*-Nitrobenzaldehyde as an equivalent for *o*-aminobenzaldehyde in the synthesis of pyrazolo[3,4-*b*]quinolines.

In concluding the discussion of the use of single-component systems, one could mention the work of DeWald on the metabolites of Zolazepam **154** ( $R^1 = \text{Me}$ ). After the administration of Zolazepam to rats, the metabolite **154a** ( $R^1 = \text{H}$ ) was found in their urine. In order to synthesise it, the Zolazepam was demethylated with boiling pyridine hydrochloride; however, the reaction was unsuccessful, and instead of **154a**, **155a** was obtained ( $R^2 = \text{Me}$ ,  $R^1 = \text{H}$ ). Compound **156** was synthesised to obtain an isomer **155b** ( $R^2 = \text{H}$ ,  $R^1 = \text{Me}$ ) (Scheme 42) [99].

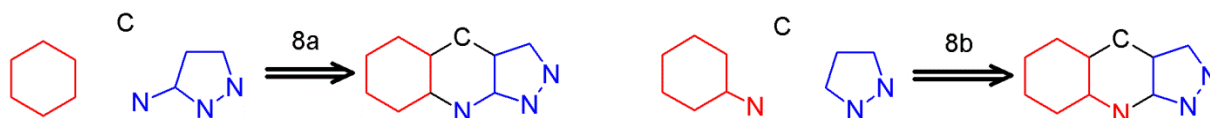
To sum up, the synthesis of pyrazoloquinolines with the use of a single-component system (e.g., **148**) is of no practical importance in the light of other, much more efficient methods.



**Scheme 42.** Investigation on Zolazepam metabolites.

### 2.11. Multicomponent 1*H*-Pyrazolo[3,4-*b*]quinoline Synthesis

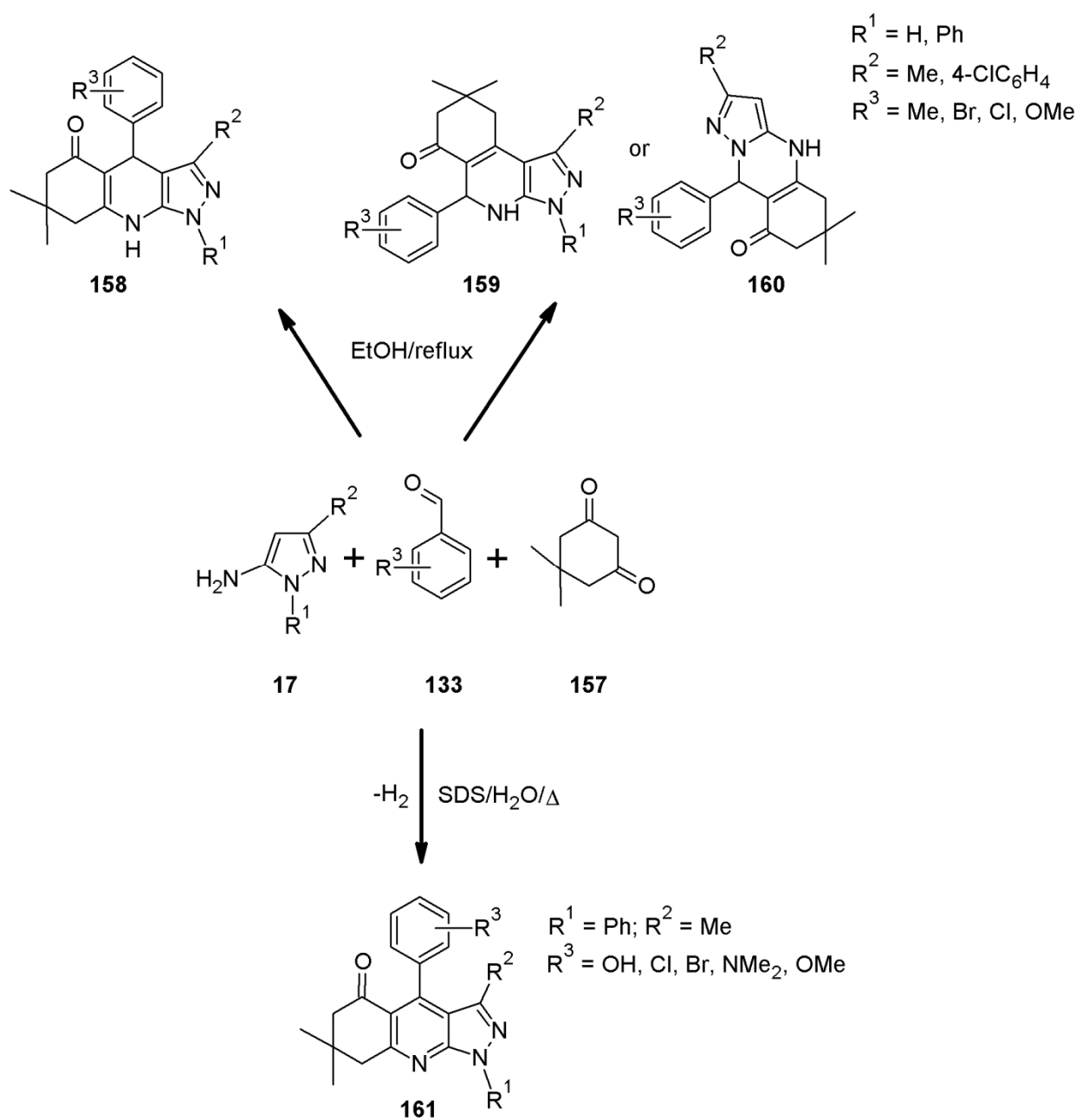
In recent years, the significant development of multicomponent reactions in organic chemistry has been observed, including the syntheses of heterocyclic compounds [100,101]. Many review publications and monographs on this issue have been published [102,103]. As far as pyrazoloquinolines are concerned, the multicomponent reactions described so far in the literature are limited to the two methodologies presented below (Figure 13).



**Figure 13.** Path 8a; C4-C4a, C4-C3a, C8a-N9. Path 8b; C4-C4a, N9-C9a, C4-C3a.

The first reaction of this type was described by Hormaza et al. in 1998. Pyrazoloquinoline derivatives **158** were obtained by heating the amino pyrazole **17**, aromatic aldehyde **138** and the corresponding cyclic 1,3-dione **157**. The authors proved that the reaction is regioselective with the formation of linear pyrazoloquinoline **158** when  $R^1 = H$  or Ph. The angular derivatives **159** or **160** (for  $R^1 = H$ ) were not formed (Scheme 43) [104].

Nogueras et al. investigated the mechanism of the abovementioned reaction. After carrying out a few experiments, they came to the conclusion that the first step is the Knoevenagel condensation between dimedone **157** and aldehyde **133**, and then, in the Michael addition, there is the attachment of aminopyrazole **17** with the subsequent cyclocondensation between the dimedone carbonyl group and the pyrazole amino group [105]. This reaction has been modified many times in terms of different reaction conditions. These modifications include conducting reactions in the microwave field, with or without a catalyst such as *L*-proline [106,107]. One of the important synthetic aspects of green chemistry is the use of ultrasound in organic synthesis. This approach was used by Maddila and colleagues for the synthesis of pyrazoloquinolines. The reactions took several minutes, and the yields of the products that were obtained were relatively high (in the order of 70–98%) [108]. Other modifications to this reaction consisted of the use of various catalysts, such as  $H_3PW_{12}O_{14}$  or nanomagnetic cellulose in ionic liquids [109,110]. In all mentioned cases, when dimedone **157** was used, the central heterocyclic ring was hydrogenated. In some cases, a fully aromatic ring was produced (Scheme 43). Thus, Shi and Wang used sodium 1-dodecanesulfonate SDS as a catalyst in the aqueous reaction medium for the same components (**17**, **133** and **157**) [111]. The end product was a system with a fully aromatic pyridine fragment **161**. The authors mentioned in the paper that the mechanism of this reaction is not fully understood, and especially how the hydrogen molecule is lost from the structure. The same reaction that was carried out in polyethylene glycol PEG-400 yielded the same product with an aromatic pyridine fragment [112].

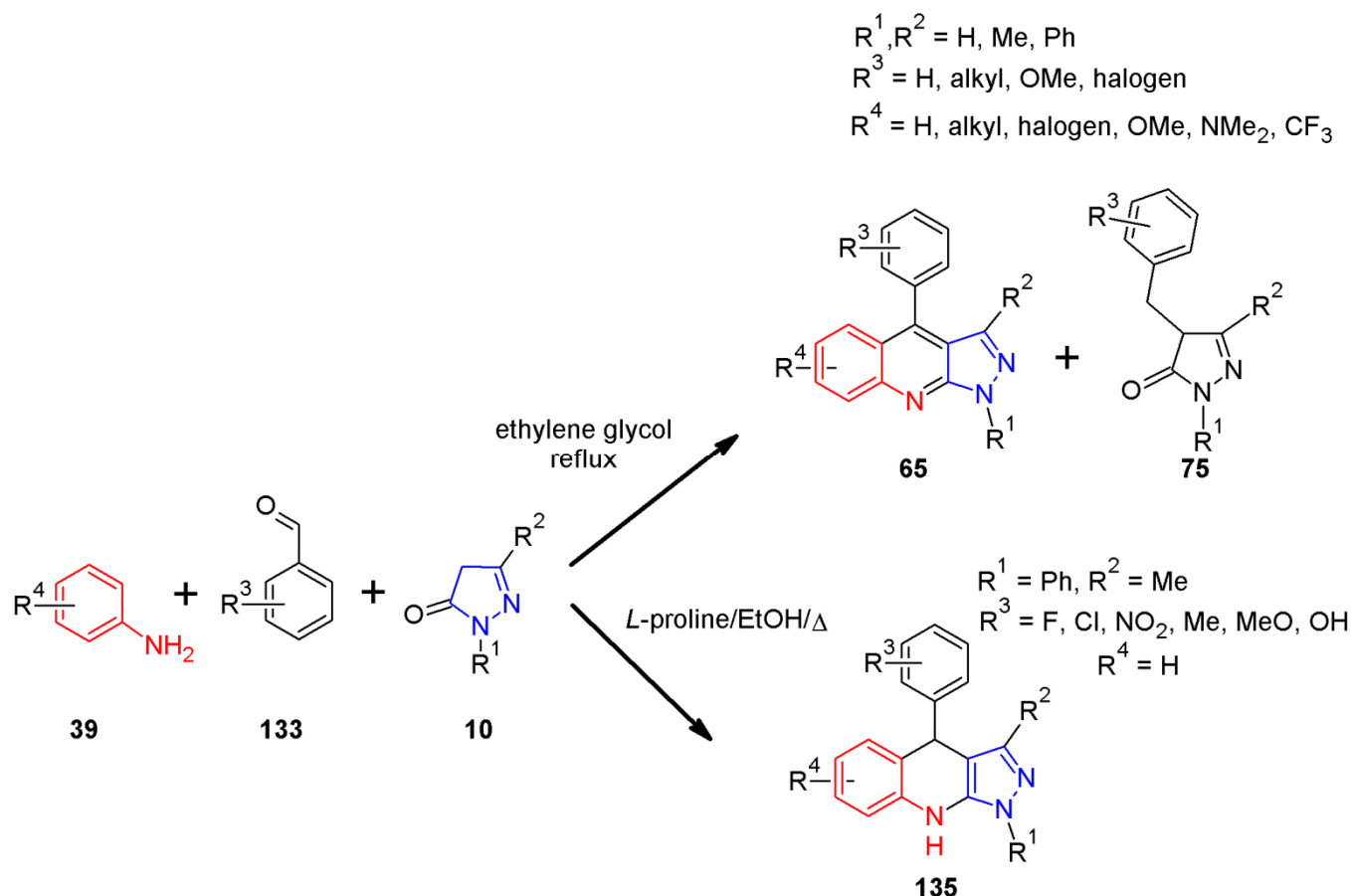


**Scheme 43.** The first three-component synthesis of 4-aryl-4,7,8,9-tetrahydro-6H-pyrazolo[3,4-b]quinolin-5-ones.

Contrary to the previously described multicomponent reactions (Path 8a; C4-C4a, C4-C3a, C8a-N9), Tomasik et al. synthesised fully aromatic pyrazolo[3,4-*b*]quinolines **65** (Path 8b; C4-C4a, N9-C9a, C4-C3a) (Scheme 44) [113].

The final compounds **65** are obtained by heating a mixture of aromatic amine **39**, aromatic aldehyde **133** and pyrazolone **10** in ethylene glycol for two hours. After cooling and digestion with methanol/ethanol, the pyrazoloquinolines precipitate as a crystalline solid. The yields of the reactions are in the range of 20–33%, although some authors have claimed that they obtained pyrazoloquinolines **65** in the order of 50–60% by this method [114]. Aromatic amines **39** can contain both electron-donating groups and electron-withdrawing groups in the *o*, *m*, or *para* positions. Aromatic aldehydes **133** can include various benzaldehyde derivatives, as well as naphthalene-1/2-carbaldehyde, but it is unable to obtain derivatives of 9-formylanthracene. Despite moderate yields, it seems to be

the best method of obtaining 4 substituted aryl pyrazoloquinolines, which successfully replaces the Friedländer synthesis by using substituted *o*-aminobenzophenones. Hedge and Shetty describe a multicomponent synthesis of 1,4-diphenyl-3-methyl-4,9-dihydro-1*H*-pyrazolo[3,4-*b*]quinolines **135** that used *L*-proline as the catalyst (Scheme 44) [115]. The components were the same as in Tomasik et al.'s procedure, but the final product was not aromatised in the final step (Path 8b; C4-C4a, N9-C9a, C4-C3a).



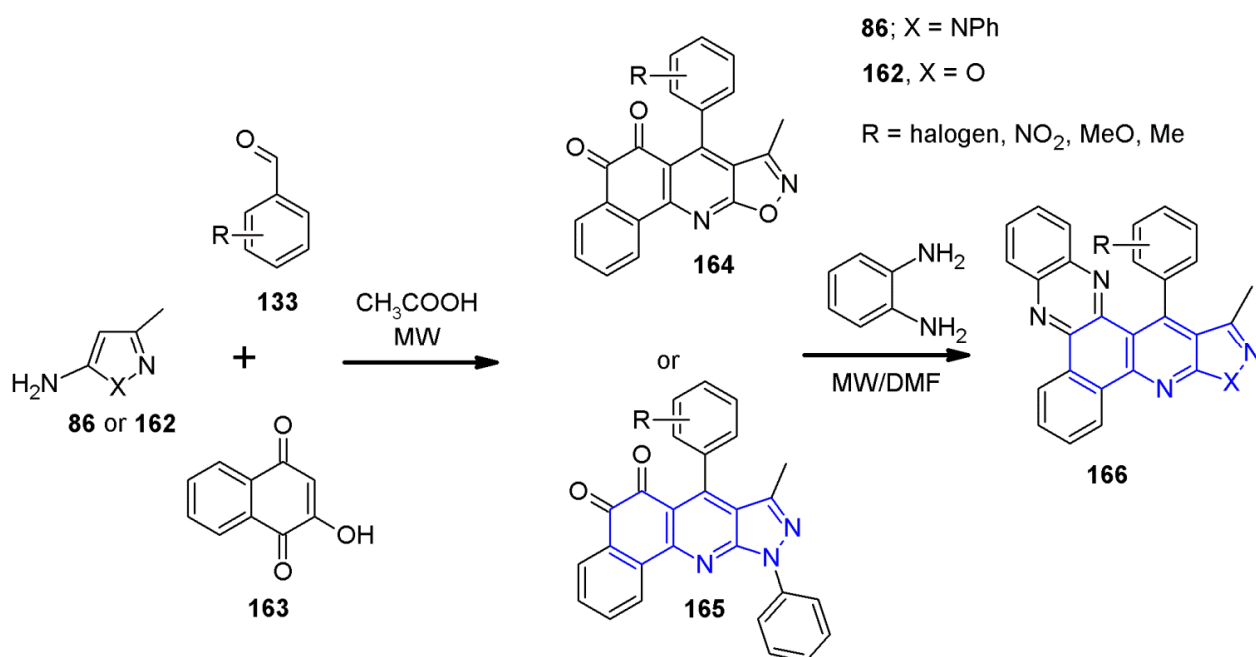
**Scheme 44.** The first multicomponent synthesis of aromatic 1*H*-pyrazolo[3,4-*b*]quinolines.

Another group of multicomponent reactions are those that use 2-hydroxynaphthalene-1,4-dione **163**. Li et al. synthesised two series of compounds: benzo[*h*]isoxazolo[5,4-*b*]quinolines **164** from 5-amino-3-methyloxazole **162**, and benzo[*h*]pyrazolo[3,4-*b*]quinolines **165** by applying 5-amino-3-methyl-1-phenylpyrazole **86** (Scheme 45) [116].

In the next stage, the authors subjected the obtained systems (**164** and **165**) to reactions with 1,2-diaminobenzene in order to obtain the quinoxaline derivatives **166**. All the steps that are described were carried out under microwave irradiation.

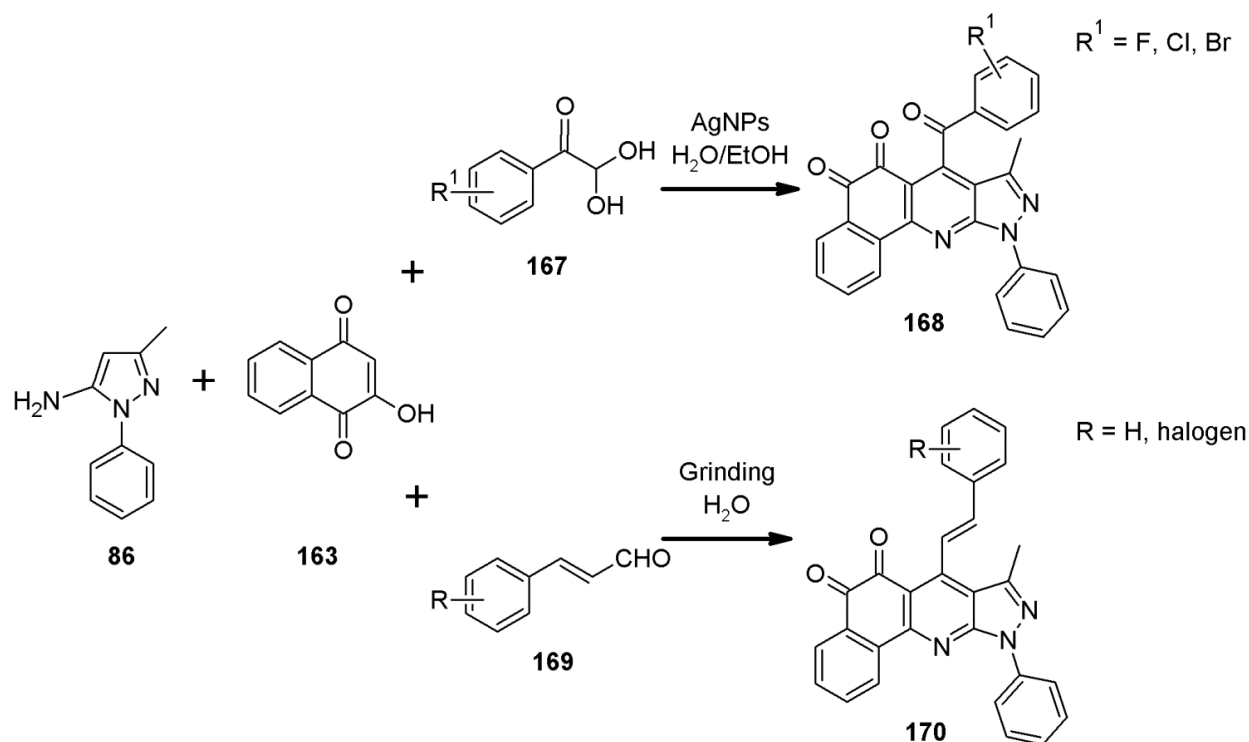
The reaction that was performed by Rajesh et al. is described as a “*sequential four-component reaction*”, which makes it a kind of record holder among the multicomponent reactions that are used for the synthesis of pyrazoloquinolines **165**. They reacted 3-aminocrotononitrile and phenylhydrazine with an addition of *L*-proline for 10 min in boiling water, and they then added an equimolar mixture of aldehyde **138** and dione **163**. The whole mixture was then heated for 1–1.5 h [117].

Quiroga et al. synthesised a series of benzo[*h*]pyrazolo[3,4-*b*]quinolines **165** via a three-component reaction under microwave irradiation [118]. When they used **86** ( $X = \text{NH}$ ), the middle heterocyclic ring was unsaturated. The formation of the linear benzo[*g*]pyrazolo[3,4-*b*]quinoline system was not observed. The resulting compounds were screened against some *Mycobacterium* strains.



**Scheme 45.** Syntheses of benzo[*h*]pyrazolo[3,4-*b*]quinolin-5,6-diones and derivatives.

Khalafy et al. conducted research on the influence of silver nanoparticles (AgNPs) on the course of the reaction. The aryl glyoxal hydrates **167** were used as the C-4 carbon incorporation reagent in the three-component reaction. The end product is 7-benzoyl-benzo[*h*]pyrazolo[3,4-*b*]quinolin-5,6-diones **168**. It should be emphasised that the reactions were carried out in a water–alcohol environment at a temperature of 60 °C, and in most cases, they were completed within 60 min [119] (Scheme 46).



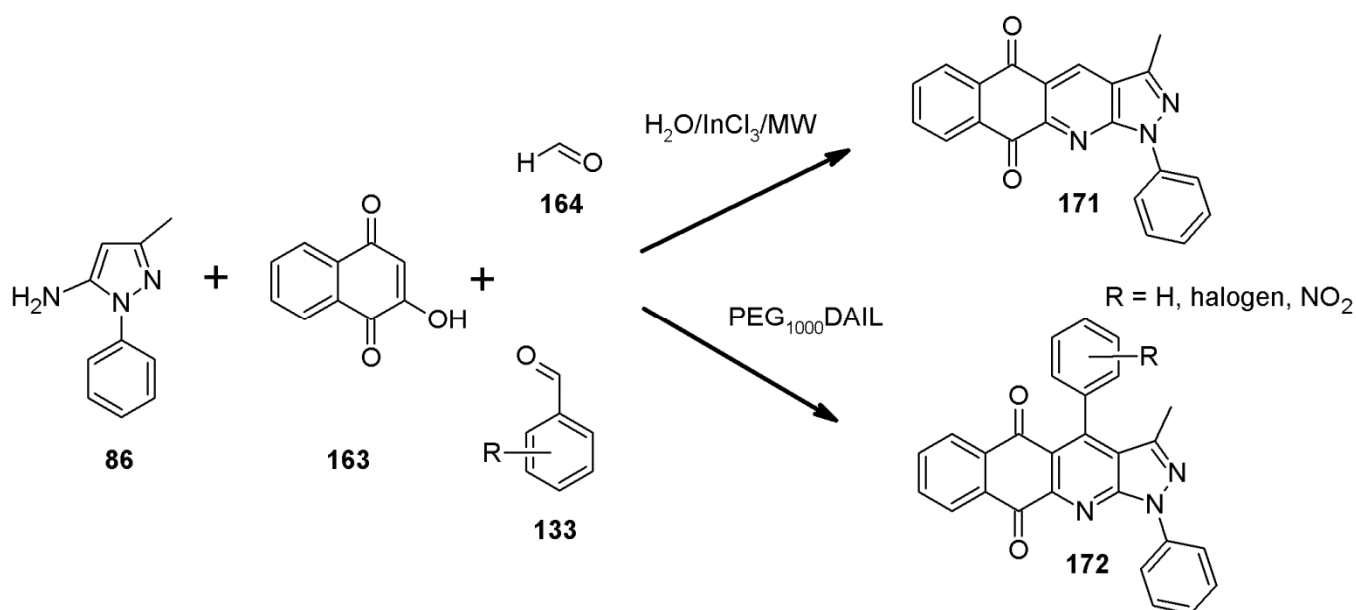
**Scheme 46.** Syntheses of benzo[*h*]pyrazolo[3,4-*b*]quinolin-5,6-diones.



Another multicomponent reaction for the synthesis of pyrazoloquinoline derivatives **170** differs from the others by the procedure in which ingredients such as aminopyrazole **86**, 2-hydroxy-1,4-naphthalenedione **163** and cinnamaldehyde **169** are ground in a mortar with a little addition of water. The authors call it, “liquid assisted grinding or LAG.” After grinding is completed, the product is simply recrystallised from an appropriate solvent (Scheme 46) [120].

The multicomponent reactions with the use of **163** that have been described so far led to the preparation of angular benzo[*g*]pyrazolo[3,4-*b*]quinolin-5,6-diones (e.g., **165**, **168** or **169**). It is also possible to obtain a linear system of the mentioned heterocyclic system.

Gutierrez, in the three-component reaction of aminopyrazole **86**, 2-hydroxy-1,4-naphthalenedione **163** and formaldehyde **164**, and indium chloride ( $\text{InCl}_3$ ) as a catalyst, obtained 3-methyl-1-phenyl-naphthalen [2,3-*e*]pyrazolo[3,4-*b*]pyridine-5,10-dione **171** (Scheme 47) [121]. The reactions were carried out by using either conventional heating (40–60 h) or by heating in a microwave field (10–20 min).



**Scheme 47.** Three-component reactions catalysed by  $\text{InCl}_3$  in synthesis of linear pyrazolo[3,4-*b*]quinoline skeleton.

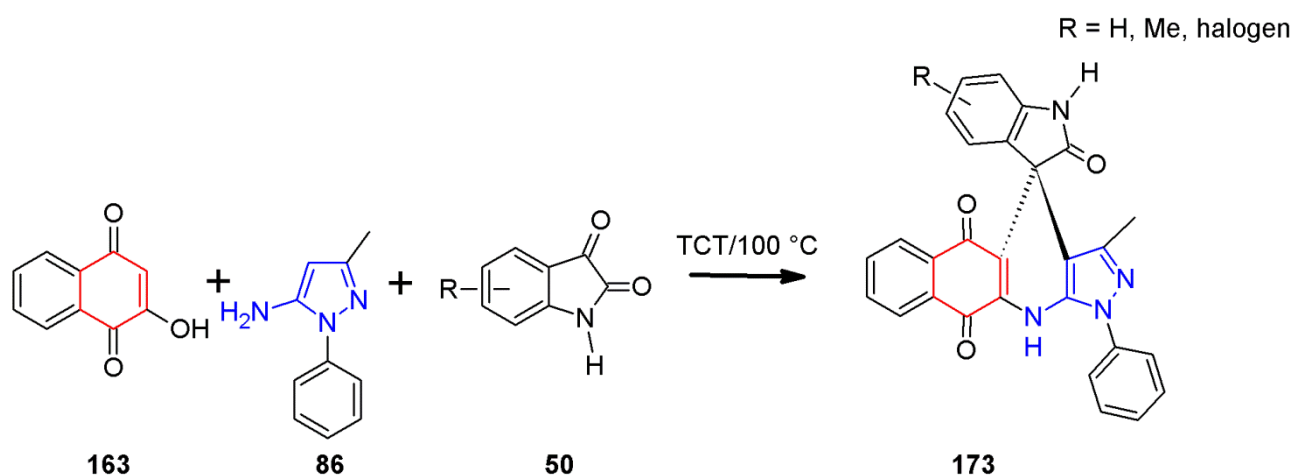
Indium chloride ( $\text{InCl}_3$ ), as a catalyst, was also used in the three-component reaction to synthesise not only pyrazoloquinolines, but also pyrimidine derivatives. Instead of formaldehyde, the authors used a number of aromatic aldehydes. In the case of 1,3-cyclohexanedione, a product with a hydrogenated pyridine ring was obtained, and, in the case of 1,3-pentanedione and naphthalene-2-hydroxy-1,4-dione, which are products with aromatic pyridine fragments, were obtained [122]. Wu et al., as a catalyst, used a 10–15 mol% amount of  $(\text{NH}_4)_2\text{HPO}_4$  for 2-hydroxynaphthalene-1,4-dione **163**, aromatic aldehyde **133** and 5-amino-3-methyl-1-phenylpyrazole **86** three-component reactions [123]. The isolated yields of the benzo[*h*]pyrazolo[3,4-*b*]quinolines ranged from 80–95%.

Due to the concern for the protection of the natural environment, we have observed an increasing tendency to change the approach to organic synthesis. This is manifested, inter alia, by the use of water as the reaction medium, or by the use of ionic liquids. One such example is PEG<sub>1000</sub>-based dicationic acid ionic liquid, which has been used by Ren et al. in the synthesis of linear benzo[*h*]pyrazolo[3,4-*b*]quinolines **172** in three-component reactions from **163**, **133** and **86** [124]. The authors presented a possible mechanism of this reaction that consists of the addition of an aldehyde **133** to **163**, followed by a Michael’s

addition of aminopyrazole **86**, the cyclisation of the resulting adduct with the subsequent oxidation with air and the final formation of **172** (Scheme 47).

*L*-proline is a frequently used catalyst in multicomponent reactions. Karamthulla et al. used it in the synthesis of linear 2*H*-benzo[*g*]pyrazolo[3,4-*b*]quinolone-5,10(4*H*,11*H*)-dione derivatives [125]. The reaction that was performed differed slightly in terms of the choice of components, and, namely, by the fact that 3-amino-5-methylpyrazole was used instead of the 1-phenyl-3-methyl-5-aminopyrazole **86**. Contrary to the reactions that are shown in Scheme 47, no aromatisation of the pyridine ring was observed.

In multicomponent reactions where pyrazoloquinolines are synthesised, isatin is sometimes used. We mentioned it in the context of the Pfitzinger reaction that was described earlier. In this case, isatin made a significant contribution to the construction of the pyrazoloquinolines skeleton (Scheme 17). In the three-component reactions that are depicted in Scheme 48, it contributes only carbon 4 in the skeleton (Path 8a; C4-C4a, C4-C3a, C8a-N9). Wu et al. obtained spiro[benzo[*h*]pyrazolo[3,4-*b*]quinoline-4,3'-indoline] **173** by reacting dione **163**, aminopyrazole **86** and isatin, or its derivative **50**, in the presence of wet cyanuric chloride (TCT) [126].

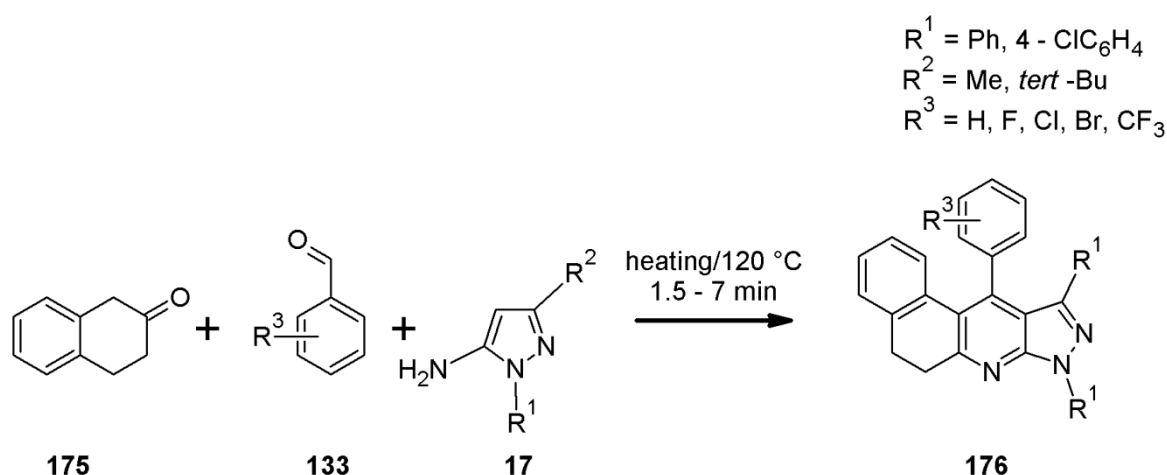


**Scheme 48.** Synthesis of spiro[benzo[*h*]pyrazolo[3,4-*b*]quinoline-4,3'-indoline.

Dabiri conducted the abovementioned reaction in the presence of *L*-proline (10 mol%) in boiling water for 6–7.5 h. The researchers additionally conducted additional studies by replacing isatin with acenaphylen-1,2-dione. The yields of the corresponding spiro derivatives were in the range of 50–70% [127]. Spiro compounds based on pyrazoloquinolines (i.e., spiro[indoline-3,4'-pyrazolo[3,4-*b*]quinoline]-2,5'(6'*H*) dione) can also be obtained without any catalysts, as was proven by Rong and his colleagues by heating isatin **50**, dimedone **157** (or 1,3-cyclohexanedione **43**) and 3-amino-1*H*-pyrazole in water or dilute acetic acid [128]. This reaction meets 100% of the requirements of the so-called “green chemistry”.

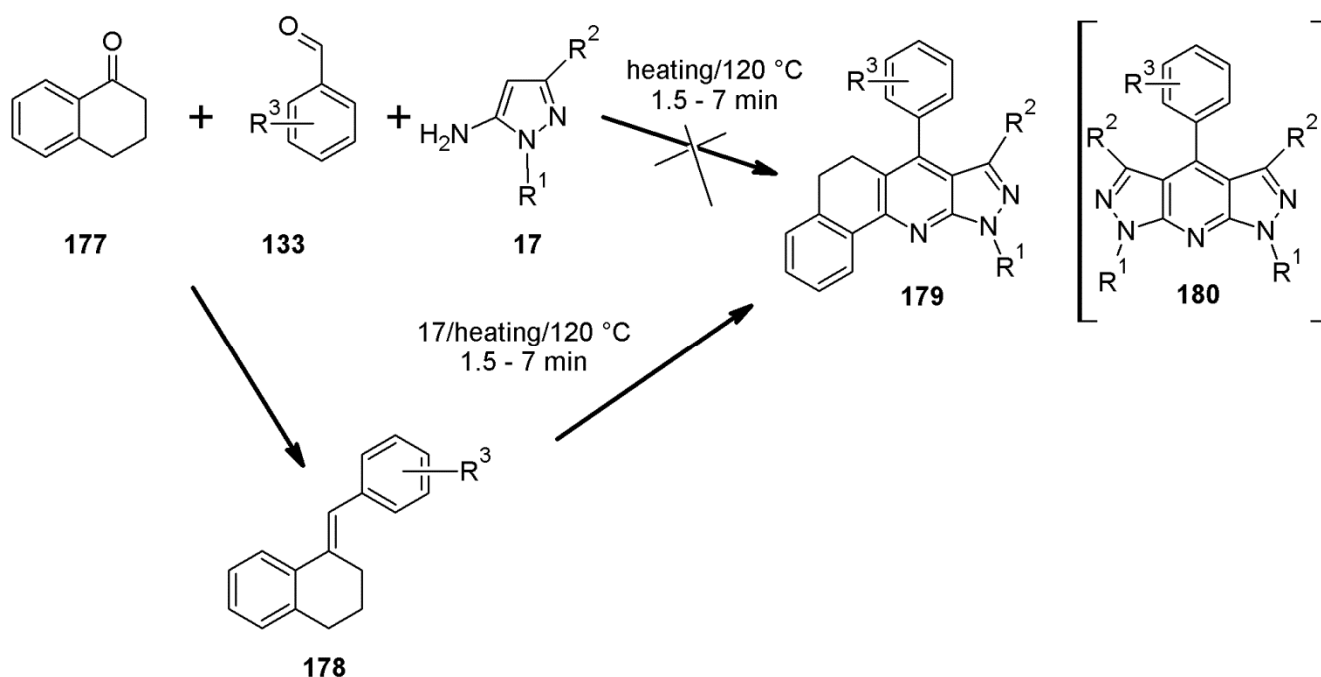
The catalysts that have been discussed so far in multicomponent reactions were of a homogeneous nature. Baradani and colleagues used  $\text{Fe}_3\text{O}_4@\text{Cu}(\text{OH})_x$  as a catalyst in the three-component reaction of dimedone **173**, aminopyrazole **86** and 5,6-dihydro-4*H*-pyrrolo[3,2,1-*ij*]quinoline-1,2-dione, instead of isatin [129]. The reactions were carried out in the environment of water/ethanol with the addition of a nanocatalyst, and they lasted from 8 to 9 h. After the reaction was completed, the catalyst was removed with a strong magnet. The final product was separated and purified with chromatographic techniques.

In the literature, you can find descriptions of three-component reactions that use  $\beta$ -tetralone **175** or  $\alpha$ -tetralone **177** for the synthesis of angular benzo[*f*]-**197** or benzo[*g*]pyrazoloquinolines **200**. The reactions were carried out by melting the reagents [130]. The first of the abovementioned reactions ran smoothly and produced the expected benzo[*f*] derivative **176** (Scheme 49).



**Scheme 49.**  $\beta$ -Tetralone as a substrate for benzo[*f*]pyrazolo[3,4-*b*]quinoline synthesis.

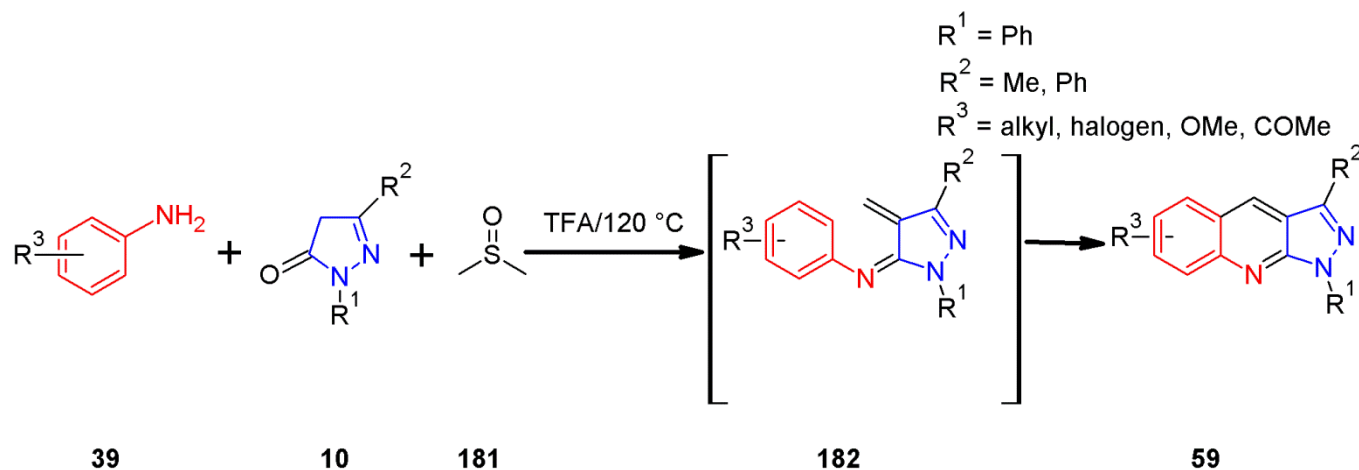
Quiroga and co-workers tried to repeat the earlier procedure to obtain the benzo[*h*]isomer **179**, and unfortunately, in this case, they were not successful. The main product turned out to be *bis*-pyrazolo[3,4-*b*;3',4'-*e*]pyridine **180**. Therefore, they changed the procedure and first synthesised a 2-arylidene derivative of  $\alpha$ -tetralone **178**, which was then reacted with aminopyrazole **17** by melting. This time, a derivative **179** was obtained (Scheme 50).



**Scheme 50.**  $\alpha$ -Tetralone as a substrate for benzo[*h*]pyrazolo[3,4-*b*]quinoline synthesis.

Sathiyarayanan et al. prepared benzo[*f*]pyrazolo[3,4-*b*]quinolines **176** by heating  $\beta$ -tetralone **175**, aminopyrazole **17** and aromatic aldehyde **133** in ethanol/ $\text{CH}_3\text{COOH}$  and tin chloride ( $\text{SnCl}_2$ ) (10 mol%) [131]. The reaction also proceeded with cyclohexanone and cyclopentanone, but it failed with  $\alpha$ -tetralone and 2-hydroxynaphthalene-1,4-dione **163**. The resulting compounds exhibited intense emission properties in solution, and in the solid state as well. Moreover, when the  $R^3$  was  $\text{NMe}_2$ , the compound exhibited aggregation-induced emission AIE. To conclude our review of the most important pyrazoloquinoline reactions in the last 100 years, we were very pleased with the work that was published by Tiwari et al. in 2021 [132]. It is a very universal method that allows one to obtain a whole range of pyrazoloquinolines **59** from commercial ingredients, such as aromatic amines

39, pyrazolones 10 and dimethylsulfoxide 181. The reaction proceeds in the presence of trifluoroacetic anhydride TFA. The authors proposed the mechanism of this reaction, where one of the intermediate steps is the azadiene system 182, which is annulated and then aromatised to produce the final pyrazolo[3,4-*b*]quinoline 59 (Scheme 51).



**Scheme 51.** Three-component reaction with DMSO as source of C-4 atom in pyrazolo[3,4-*b*]quinoline skeleton.

Perhaps this reaction will be an alternative to the procedure that was developed by Brack in 1965 (Scheme 19), which allows the obtention of all of the possible combinations of the substituents for 10 ( $R^1, R^2 = \text{H, Me, Ph}$ ) in the pyrazole ring. Tiwari et al. employed only two pyrazolone derivatives 10 ( $R^1 = \text{Ph}, R^2 = \text{Me}$  and  $R^{1,2} = \text{Ph}$ ). Finally, it may be mentioned that the authors expected a completely different result; thus, this is an example of serendipity in organic chemistry.

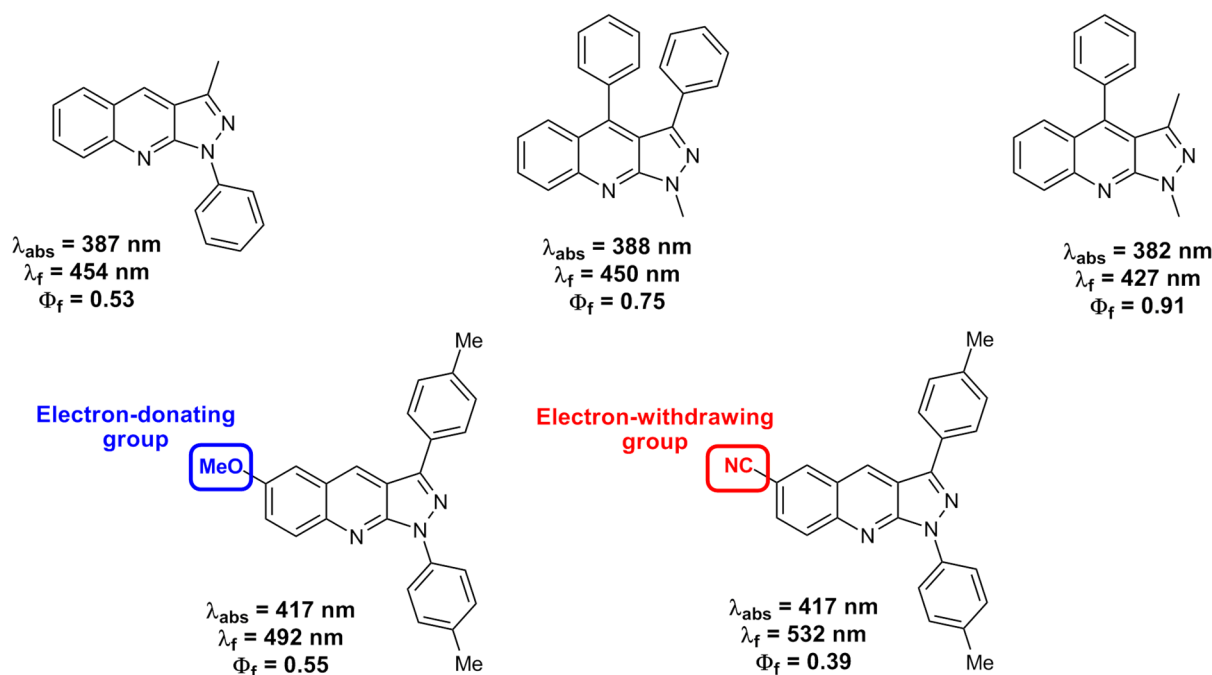
### 3. Photophysical Physical Properties of 1*H*-Pyrazolo[3,4-*b*]quinolines and Their Application

In view of the ever-growing demand for many high-tech and biomedical applications, the group of 1*H*-pyrazolo[3,4-*b*]quinolines has gained considerable interest from the scientific community, which is mainly due to their intrinsic optical and photophysical characteristics. Over the past decades, many researchers have made some efforts to understand the relationship between the structure and the optical properties of these compounds. However, even though the establishment of the structure obtained by Niementowski was made in 1928 [2], it was only in the late 1990s and mid 2000s that a number of reports related to the spectroscopic characteristics and the computational analysis of 1*H*-pyrazolo[3,4-*b*]quinoline derivatives (see Figure 1 in the Introduction) were published [133–138].

#### 3.1. Structure–Property Relationship

Structurally, pyrazoloquinolines are the products of the ring fusion of the heteroaromatic pyrazole and quinoline moieties, which gives rise to a rigid D- $\pi$ -A system (Figure 14). Separately, these building blocks play a crucial role in the design of many functional materials. For instance, quinoline scaffolds are frequently used as electron-accepting components in light-harvesting systems [139,140], or as optical limiters [141]. Furthermore, quinoline-based molecules exhibit highly efficient electron-transporting properties that are combined with thermal and redox robustness and high photoluminescence quantum yields. These features are of paramount importance in the construction of many high-tech devices, such as organic optoelectronics (OLEDs) [142,143], photodiode detectors [144] and photovoltaic cells (OPVs) [145]. On the other hand, the pyrazole unit often acts as an electron donor in chromophore systems, which is due to the presence of two electron-rich adjacent nitrogen atoms [146,147]. Especially in conjunction with various electron acceptors (e.g., electron-





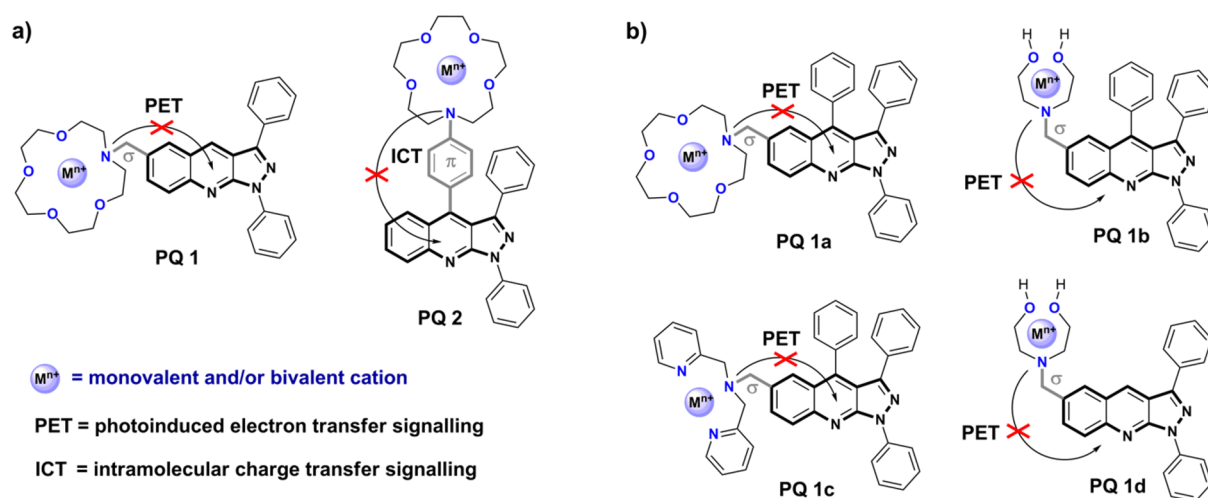
**Figure 15.** Structures and photophysical properties of differently substituted 1*H*-pyrazolo[3,4-*b*]quinolines. The data presented were measured in chloroform [158].

A tremendous variety of synthetic approaches has led to an extension of the portfolio of pyrazoloquinolines with tunable luminescence features. Exemplarily, an introduction of additional electron-donating and electron-withdrawing groups within the chromophore results in the formation of spatially extended dipolar (or quadrupolar) systems. A considerable charge separation within the electronically excited states of these molecules results in a redshift of the emission bands, which noticeably proceeds with an increase in the solvent polarity [138,159,163]. However, the fluorescence intensity of such organic dyes decreases at the same time, which is due to an enhancement of the rate of nonradiative decay via intramolecular rotations within excited ICT states [164,165]. Another significant process that leads to the rapid deactivation of excited states is referred to as “photoinduced electron transfer (PET)” [166–169]. In this case, an electron donor (e.g., dialkylamine group) and the luminophore are commonly separated by a short alkyl spacer, which electronically disconnects the  $\pi$ -conjugation between the receptor and the electron donor units. The excitation of such a system is followed by the PET process, which leads to an immediate nonradiative decay to the ground state. However, most of the pyrazoloquinolines that are substituted with dialkyl and diaryl amines are deliberately designed for the in-active interruption of the aforementioned fluorescence-quenching mechanisms, which makes them promising “turn-on” sensors.

### 3.2. Application of Pyrazoloquinolines in Fluorescence Sensing

Since the electroluminescence properties of 1*H*-pyrazolo[3,4-*b*]quinolines have been frequently reported for many years [20,47,170–174], in this review, we focus on their use as efficient fluorescence probes. The operation of many fluorescent indicators is based on a noticeable enhancement of the fluorescence emission upon the addition of metal cations to the fluorescing medium. Exemplarily, in 2002, Rurack et al. reported the synthesis of two aza-crown-modified 1,3-diphenyl-pyrazoloquinolines that exhibited high fluorometric sensitivity to  $\text{Na}^+$  and  $\text{Ca}^{2+}$  cations (see Figure 16a) [5]. The main concept of this study relied upon the structural connection between the nitrogen lone pair of the analyte receptor and the chromophore system, either by a  $\sigma$ -spacer (compound **PQ 1**) or by a perpendicular  $\pi$ -conjugated arrangement (compound **PQ 2**). Derivative **PQ 1** proved to be weakly emissive in polar solvents ( $\Phi_{\text{f}} = 0.02$  in acetonitrile, compared to  $\Phi_{\text{f}} = 0.54$  in hexane), which

was mainly due to the PET-fluorescence-quenching mechanism. On the contrary, pyrazoloquinoline **PQ 2** showed an intense dual emission from LE and ICT fluorescent species ( $\Phi_f = 0.18$  in acetonitrile, compared to  $\Phi_f = 0.37$  in hexane). Furthermore, both derivatives showed highly desirable effects in the presence of analyte species (i.e., metal ions) on the basis of two different sensing mechanisms. The authors demonstrated that dye **PQ 1** readily bound monovalent  $\text{Na}^+$  and bivalent  $\text{Ca}^{2+}$  cations, with a concomitant increase in the fluorescence intensity. These observations were in unambiguous agreement with a proposed PET-signalling mechanism. More interestingly, pyrazoloquinoline **PQ 2** performed as a dual emissive sensor with a high fluorescence output for both states of the detection system: bound and unbound. In this case, the presence of bivalent  $\text{Ca}^{2+}$  cations alternated the nature of the excited state of the fluorophore from the low-lying ICT state to the blue-shifted LE state, with a significant enhancement in the emission (from  $\Phi_f = 0.18$  to  $\Phi_f = 0.35$  in acetonitrile) at the same time. In contrast, the addition of  $\text{Na}^+$  ions to **PQ 2** did not change its spectral characteristics markedly.

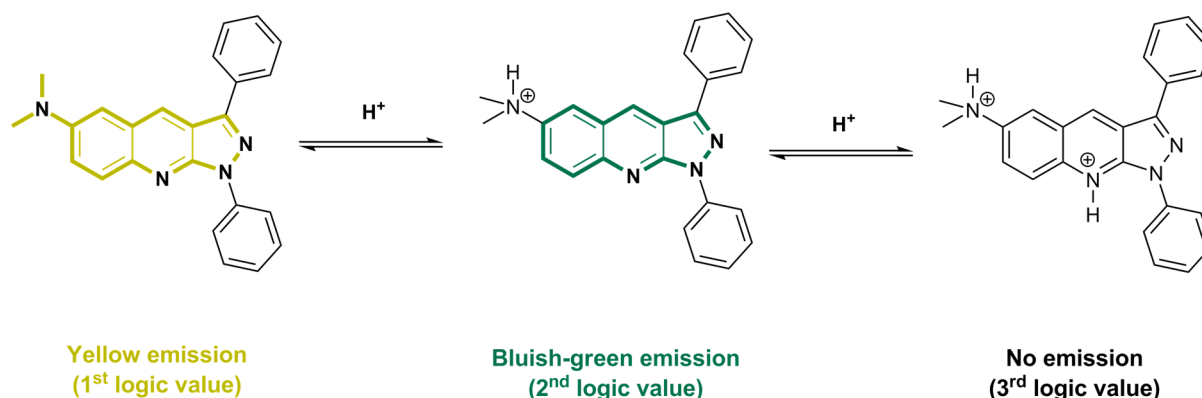


**Figure 16.** Structures of pyrazoloquinoline-based cation-sensitive fluorescence probes: (a) aza-crown-modified derivatives, reported by Rurack in 2002 [5]; (b) PET-signalling derivatives, investigated by Mac et al. between 2010 and 2013 [175–177].

Since the aforementioned studies on pyrazoloquinoline-based sensors were reported, almost a decade passed until this stem was followed. Then, between 2010 and 2013, Mac and co-workers published a series of articles on ion-sensitive pyrazoloquinolines, which varied by the molecular architecture of the receptor unit (see Figure 16b) [175–177]. All of the sensors presented (**PQ 1a–d**) were designed for PET signalling, and they maintained the connection between the receptor unit and the pyrazoloquinoline chromophore via the non-conjugated methylene spacer. In addition, the authors extended their studies to a wide range of metal cations, including monovalent  $\text{Li}^+$ ,  $\text{Na}^+$  and  $\text{Ag}^+$ , and bivalent  $\text{Ca}^{2+}$ ,  $\text{Ba}^{2+}$ ,  $\text{Mg}^{2+}$ ,  $\text{Zn}^{2+}$ ,  $\text{Cd}^{2+}$  and  $\text{Pb}^{2+}$  cations. The results obtained were consistent, which showed that these “turn-on” fluorescent cation indicators were more sensitive to the presence of bivalent cations than to monovalent species. Interestingly, for compound **PQ 1c**, an increased sensitivity and selectivity to  $\text{Zn}^{2+}$  and  $\text{Mg}^{2+}$  arose from a predominant complexation of these cations with two molecules of the sensing system. Furthermore, noticeable bathochromic shifts of the fluorescence bands were observed for  $\text{M}_2\text{Zn}^{2+}$  and  $\text{M}_2\text{Mg}^{2+}$  complexes. These findings were explained by the formation of excimer species  $[\text{M}^{2+}(\text{MM})]^*$ , which was confirmed by quantum chemical calculations [177]. In 2013, the same research group demonstrated a detailed study on the pyrazoloquinoline derivative **PQ 1d**, which was a direct precursor for the synthesis of the aza-crown fluorescence probe **PQ 1**, previously reported by Rurack [5]. It was found that this compound can act as a highly efficient sensor for many bivalent cations and that, more importantly, its selectivity

can be easily enhanced by the addition of small amounts of water to the fluorescing medium.

Three years later, Uchacz et al. investigated a series of donor-acceptor 1*H*-pyrazolo[3,4-*b*]quinolines that were substituted with different amine donors (i.e., *N,N*-dimethylamine, *N,N*-diphenylamine, *N,N*-phenyl-1-naphthylamine and carbazole groups), with the aim of implementing them as pH-sensitive molecular logic switches [178]. The authors showed that, in the presence of trifluoroacetic acid (the input signal), the fluorescence of the investigated pyrazoloquinolines was almost completely quenched, which was due to the formation of a nonemissive protonated adduct. Interestingly, pyrazoloquinoline substituted with the *N,N*-dimethylamine group presented a more advanced ternary logic behavior (see Figure 17). The nonprotonated state of this compound showed considerable fluorescence (yellow emission, first logic value), which, upon the first protonation of the nitrogen of the dimethylamino moiety, shifted hypsochromically and slightly decreased (bluish-green emission, second logic value). The second protonation, which involved the nitrogen of the quinoline core, quenched the fluorescence quantitatively (no emission, third logic value). Basically, reading the fluorescence response as an output that is dependent on the presence of proton input signals yielded functional luminescent molecules with the potential for multilevel logic switching, which ranged from binary to ternary responses.



**Figure 17.** Schematic representation of 1*H*-pyrazolo[3,4-*b*]quinoline-based pH-sensitive ternary logic gate reported by Uchacz et al. in 2016 [178].

With regard to all of these results, it can be concluded that the scope of pyrazoloquinoline-based fluorescence probes is still amenable to further investigation. For instance, the up-to-date studies were mainly focused on the PET-signalling mechanism, with only minute mention of the intramolecular rotation-dependent quenching of the excited ICT states. Currently, a plethora of photophysical studies are devoted to many different ICT state-related phenomena, such as TICT, PICT, PPT, TADF, umpolung-ICT and so forth [179–183], which can be used as output signals for analyte compounds. Furthermore, the presented studies focus mostly on inorganic ion-sensing, which leaves future prospects for the many biomedical applications of pyrazoloquinoline fluorophores, such as fluorescence bioimaging, photosensitized diagnoses or therapies.

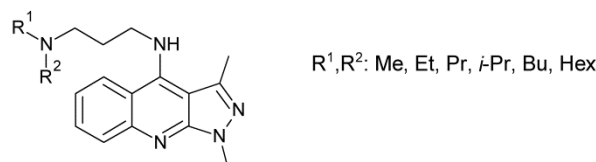
#### 4. Biological Properties of 1*H*-Pyrazolo[3,4-*b*]quinolines

Nitrogen-heterocycles are the most common heterocyclic compounds that occur in living organisms [184], and they are also very often tested as compounds that show biological activity [185,186]. Thus, it is not unusual that pyrazoloquinoline derivatives have attracted the attention of researchers who deal with the biological activity of organic compounds. It is advisable to divide pyrazoloquinoline derivatives into groups according to the kind of biological activity that they possess.



#### 4.1. Hypolipemic and Hypocholesteremic Activity

The method of synthesis that was developed by Stein et al. and Crenshaw et al. [29,30] produced, inter alia, 4-chloro-1,3-dimethyl-1*H*-pyrazolo[3,4-*b*]quinolines, which, after functionalization with different amine derivatives (Figure 18), were tested for their hypolipemic and hypocholesteremic activity in rats [187].

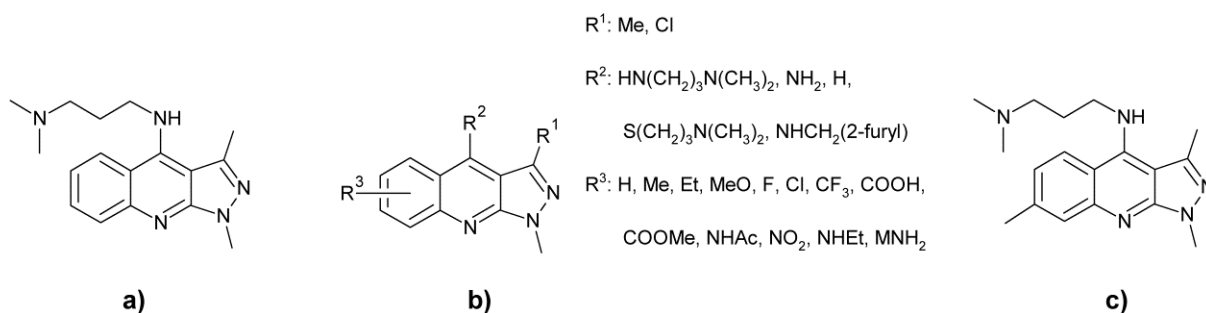


**Figure 18.** 4-[(3-( $R^1, R^2$ -Amino)propylamino)-1,3-dimethyl-1*H*-pyrazolo[3,4-*b*]quinolines.

The compounds were suspended in a carboxymethyl cellulose solution at a dose of 100–400 mg/kg, compared to a carboxymethyl cellulose solution only, and were administered to rats daily for 4 days. After the administration, the rats were tested for their cholesterol and phospholipid concentrations in serum, and the results show that, with the maximum dose of 400 mg/kg, the concentration was reduced significantly: by –51% for cholesterol and by –47% for phospholipids.

#### 4.2. Interferon-Production-Inducing Activity

Interferons are an important group of signalling proteins that are released by cells in response to some viruses [188], and interferon-inducing drugs are one of the weapons in the fight against viruses [189]. 4-[(3-(Dimethylamino)propylamino)-1,3-dimethyl-1*H*-pyrazolo[3,4-*b*]quinoline (Figure 19), which was obtained by Stein et al. [29], was tested as a low-molecular-weight interferon inducer by Siminoff et al. [190].



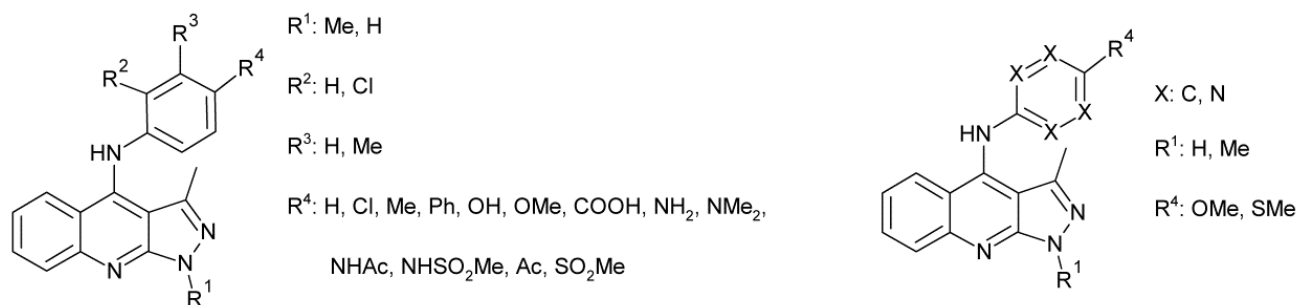
**Figure 19.** (a) 4-[(3-(dimethylamino)propylamino)-1,3-dimethyl-1*H*-pyrazolo[3,4-*b*]quinoline; (b) 4- $R^2$ -1-methyl-3- $R^1$ -(5,6,7 or 8)- $R^3$ -1*H*-pyrazolo[3,4-*b*]quinoline; and (c) 4-[(3-(dimethylamino)propylamino)-1,3,7-trimethyl-1*H*-pyrazolo[3,4-*b*]quinoline.

The compound was administered to female mice by the oral or parenteral route, and the administration was repeated. In concentrations of 200 mg/kg or higher, the response of the interferon production was very high, and it protected the mouse L cells against infection by the vesicular stomatitis virus or the mouse picornavirus. The animals also became hyperresponsive to repeated stimulation. The following research in the Siminoff group also showed that other derivatives of 1,3-dimethyl-1*H*-pyrazolo[3,4-*b*]quinoline, which contained the substituent at the 4 position, which is attached by the NH moiety, and with a side chain of at least three carbons and terminating with the second amino function (Figure 19b), also have significant interferon-inducing activity [30]. In the subsequent research, Siminoff analyzed which cells in mice are the major target for interferon induction by 4-[(3-(dimethylamino)propylamino)-1,3-dimethyl-1*H*-pyrazolo[3,4-*b*]quinoline (Figure 19a) [191]. The analysis of the results shows that the type of adherent leukocytes that are resident in the spleen is a major target of interferon induction. The other derivatives (Figure 19b) were also tested by Siminoff and Crenshaw in the cultures of spleen

adherent leukocytes [192]. The results show that some of the derivatives also showed high interferon-inducing activity. One of the derivatives, 4-[(3-(dimethylamino)propylamino)-1,3,7-trimethyl-1*H*-pyrazolo[3,4-*b*]quinoline hydrochloride (Figure 19c), was also tested by Kern et al. [193], and again, the compound induced high levels of circulating interferon, which effected, with significantly reduced mortality, the mice that were infected with the Rochester mouse virus, *Herpesvirus hominis*, Semliki forest virus and the vesicular stomatitis virus. The authors also observed the strong hyporeactivity of the interferon after multiple doses of 4-[(3-(dimethylamino)propylamino)-1,3,7-trimethyl-1*H*-pyrazolo[3,4-*b*]quinoline hydrochloride.

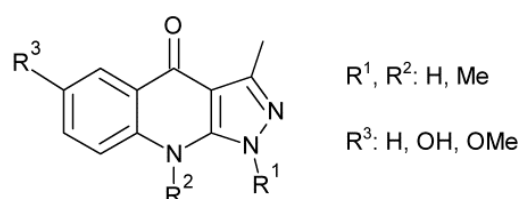
#### 4.3. Antiviral Activity

Many virus infections in humans are self-cured by the immune system of the organism, and, for many others, vaccinations provide immunity to infection. However, there are some diseases that must be cured by the use of antiviral drugs (e.g., HIV, herpes viruses, hepatitis). A huge family of 1*H*-pyrazolo[3,4-*b*]quinoline derivatives (Figure 20), which were obtained by the method of Stein et al. [29] and then functionalised, were synthesised and tested for antiviral activity by the group from the Research Institute for Pharmacy and Biochemistry in Prague in the 1980s [194–201].



**Figure 20.** 4-(substituted-phenylamino)-1-*R*<sup>1</sup>-3-methyl-1*H*-pyrazolo[3,4-*b*]quinolines and 4-(4-substituted-pyrimidin-2-ylamino)-1-*R*<sup>1</sup>-3-methyl-1*H*-pyrazolo[3,4-*b*]quinolines.

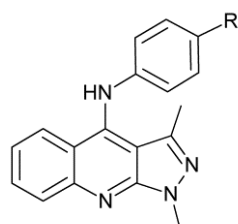
Anilino derivatives were tested against the A2-Hongkong virus and against the encephalomyocarditis (EMC) virus in vivo in mice. Some of them showed high activity against one or the other virus, and some of them were effective against both. In the case of 4-[(4-methylphenyl)amino]- and 4-[(5-methoxy-2-pyrimidin-2-yl)amino]- derivatives, which were administered orally, the survival time was extended after infection with the A2-Hongkong virus by 50 and 67 days, respectively. In the case of 4-[(4-hydroxyphenyl)amino]-, 4-[(4-octadecaoxyphenyl)amino]- and 4-[(3,4-methylenedioxyphenyl)amino]- derivatives that were administered subcutaneously, the time of survival against the EMC virus was increased by 70, 83 and 95 days, respectively [194,198]. The keto derivatives (Figure 21) were tested against the same viruses as aniline-derivatives: against the A2-Hongkong virus and against the encephalomyocarditis (EMC) virus in vivo in mice, and after oral or subcutaneous administration.



**Figure 21.** 4,9-dihydro-3-methyl-4-oxo-1*H*(2*H*)-pyrazolo[3,4-*b*]quinolines.

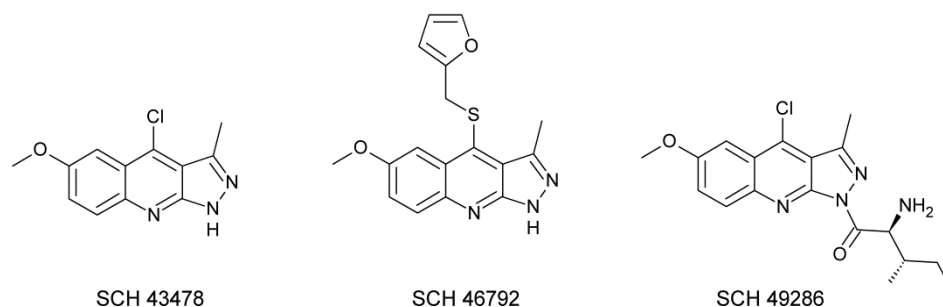
The most potent against the A2-Hongkong virus was 4,9-dihydro-3,9-dimethyl-4-oxo-1*H*(2*H*)-pyrazolo[3,4-*b*]quinoline, which extended the survival by 55%. In the case

of the EMC virus, the compounds were much more effective, and for 4,9-dihydro-3-methyl-4-oxo-1*H*(2*H*)-pyrazolo[3,4-*b*]quinoline and 4,9-dihydro-6-methoxy-3-methyl-4-oxo-1*H*(2*H*)-pyrazolo[3,4-*b*]quinoline, the survival was extended by 96% or by 80–100%, respectively [195,200,201]. Some of the compounds were also tested in vitro against different microbes (e.g., *Streptococcus faecalis*, *Escherichia coli* or *Candida albicans*); however, none of the studied derivatives had significant inhibitory effects [195]. The authors from the Research Institute for Pharmacy and Biochemistry in Prague were so satisfied with the results that they obtained for some of the tested pyrazoloquinoline derivatives that they patented them in Czechoslovakia [202–208]. One of the compounds that was obtained by Rádl et al. [194], 4-[(4-methoxyphenyl)amino]-1,3-dimethyl-1*H*-pyrazolo[3,4-*b*]quinoline (Figure 22, R = OMe), was included in the modeling procedure for the binding site identification and the docking study of human  $\beta$ -arrestin by Chintha et al. [209].



**Figure 22.** 4-[(4-R-phenyl)amino]-1,3-dimethyl-1*H*-pyrazolo[3,4-*b*]quinoline.

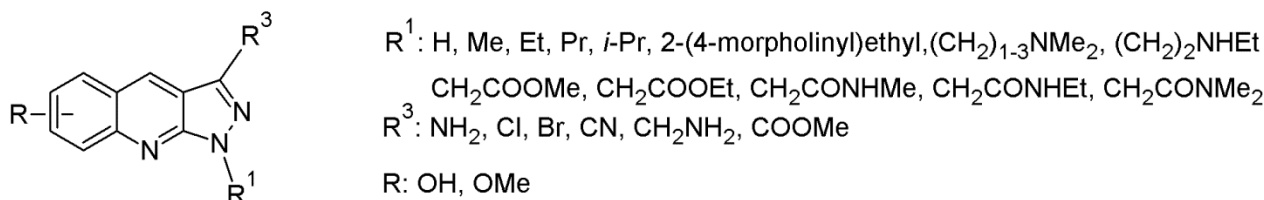
Unfortunately, the results for that compound were not amazing. Another derivative, 4-[(4-ethoxyphenyl)amino]-1,3-dimethyl-1*H*-pyrazolo[3,4-*b*]quinoline (Figure 22, R = OEt), was used by Vyas et al. [210] as one of the known potential apoptosis inducers that are used to generate pharmacophore models with their apoptosis-inducing activity, for the same reason that Kemnitzer et al. used 4-[(4-propionylphenyl)amino]-1,3-dimethyl-1*H*-pyrazolo[3,4-*b*]quinoline (Figure 22, R = COC<sub>2</sub>H<sub>5</sub>) as the reference in apoptosis-inducer studies [211]. Different pyrazoloquinoline derivatives have attracted attention as antiviral compounds against the herpes simplex virus. Albin et al. tested the activity of three earlier synthesized [200,212] derivatives (Figure 23) against herpes simplex virus type 2 (HSV-2) [213].



**Figure 23.** 4-chloro-3-methyl-6-methoxy-1*H*-pyrazolo[3,4-*b*]quinoline (SCH 43478); 4-[(furan-2-yl)methylsulfanyl]-3-methyl-6-methoxy-1*H*-pyrazolo[3,4-*b*]quinoline (SCH 46792); and (2*S*,3*S*)-2-amino-1-(4-chloro-6-methoxy-3-methyl-1*H*-pyrazolo[3,4-*b*]quinolin-1-yl)-3-methylpentan-1-one (SCH 49286).

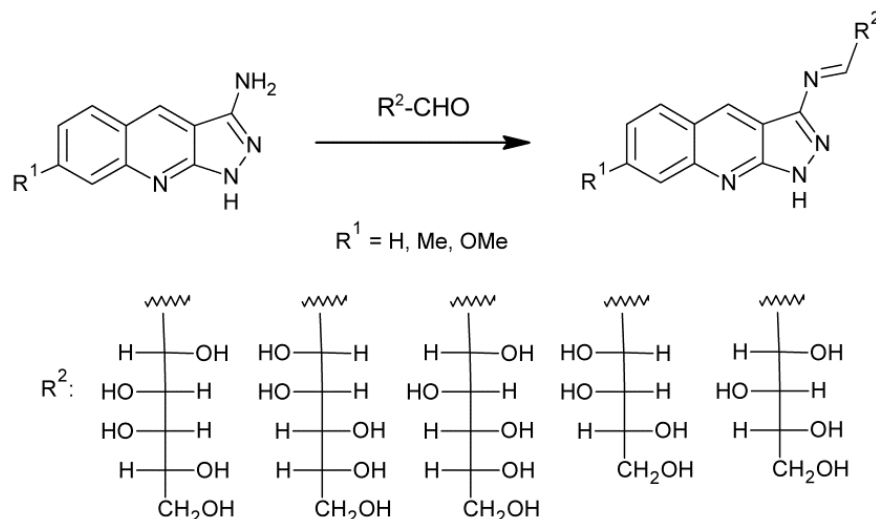
In vitro tests were performed with African green monkey kidney (Vero) cells, human diploid lung (WI-38) cells, human epithelial (HeLa) cells and human foreskin fibroblast (FS-85) cells. The monolayers of the cells were infected with HSV-2 in the presence or absence of the compounds SCH 43478, 46792 and 49286. The results were compared with those that were obtained with Acyclovir (ACV), which is the most popular drug that is used against herpes simplex. The inhibition of the HSV-2 plaque formation in Vero cells was achieved with concentrations lower than those for ACV; however, for the other cell

lines, ACV is more effective. The cytotoxicity of all of the studied compounds against the tested cell lines was comparable to the effect of ACV. It is important to say that the compounds of interest were effective only when added shortly after infection; if added after 3 h or later, they were ineffective, which is a much worse result than that obtained for the ACV. Another broad group of 3-amino-1*H*-pyrazolo[3,4-*b*]quinolines (Figure 24) were studied by Bell and Ackerman [214].



**Figure 24.** 1*H*-Pyrazolo[3,4-*b*]quinoline derivatives examined by Bell and Ackerman in [214].

The authors tested the synthesised compounds against HSV-2 in vitro on mouse embryo fibroblast monolayers. Some of the studied compounds exhibited high activity (comparable or higher than that of Acyclovir), but they were never tested again. A different group of researchers synthesised 3-amino-1*H*-pyrazolo[3,4-*b*]quinoline that was derivatised with monosaccharides at the amino group (Figure 25), and they tested those against herpes simplex virus type 1 (HSV-1) [215].



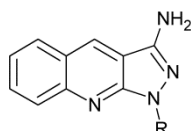
**Figure 25.** 1*H*-Pyrazolo[3,4-*b*]quinoline derivatives examined by Bekhit et al. [215].

African green monkey kidney (Vero) cells were infected with HSV-1. From the tested group, most of the compounds did not show significant cytotoxicity at the concentrations that are safe for living cells. Only two derivatives were borderline cytotoxic: 7-methyl- and 7-methoxy-3-amino-1*H*-pyrazolo[3,4-*b*]quinoline that was derivatised with pentoses. The authors from the same research group also tested another group of derivatives, and they found that simple 7-methoxy-3-amino-1*H*-pyrazolo[3,4-*b*]quinoline has an in vitro anti-HSV-1 activity that is comparable to Acyclovir [216]. The authors also show that the compound of interest has low toxicity (tested in vivo in male mice), even when administered through the parenteral route (nontoxic up to 80 mg/kg). The compounds that were obtained by Bekhit et al. [215] (Figure 25) were tested by Arif et al. for their potential cytotoxic activity [217,218]. At a 100  $\mu\text{M}$  concentration, some of the compounds showed high cytotoxicity against human breast carcinoma cell lines (MCF-7 and MDA-MB-231); however, at the same time, they were comparably cytotoxic to normal human breast epithelial cell lines (MCF-10A and MCF-12A). The 7-Methoxy-3-amino-1*H*-pyrazolo[3,4-*b*]quinoline antiviral activity against HIV Type 1 was tested together with other different heterocyclic

compounds [219]. Unfortunately, the compound did not show significant activity against that type of virus.

#### 4.4. Antibacterial Activity

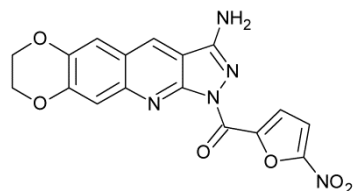
Because of the rising bacterial resistance to antibiotics [220], there is a constant need to invent new drugs. Pyrazoloquinoline derivatives have been also tested in this field. A group of pyrazoloquinoline derivatives was tested by El-Sayed and Aboul-Enein [221]. The authors started with 3-amino-1*H*-pyrazolo[3,4-*b*]quinoline and they substituted it at the amino group (Figure 26).



R: H, C<sub>6</sub>H<sub>5</sub>, 4-BrC<sub>6</sub>H<sub>4</sub>, 4-ClC<sub>6</sub>H<sub>4</sub>, 4-FC<sub>6</sub>H<sub>4</sub>, 4-NO<sub>2</sub>C<sub>6</sub>H<sub>4</sub>

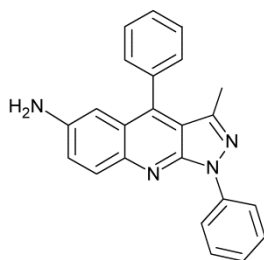
**Figure 26.** 1-Substituted-3-amino-1*H*-pyrazolo[3,4-*b*]quinolines.

The compounds were then tested against *E. coli*, *S. aureus*, *C. albicans* and *A. niger*, and they were compared with ampicillin and ketoconazole. The preliminary results indicated that none of the tested compounds had activity higher than ampicillin against *E. coli*. 1-(4-fluorophenyl)- and 1-(4-nitrophenyl)-3-amino-1*H*-pyrazolo[3,4-*b*]quinoline achieved results that were comparable to ampicillin against *S. aureus*. Both compounds also have high activity against *C. albicans* and *A. niger*, with the second of them even higher than ketoconazole. In the case of *A. niger*, 1-(4-chlorophenyl)-3-amino-1*H*-pyrazolo[3,4-*b*]quinoline also showed high activity. Another family of differently substituted 3-amino-1*H*-pyrazolo[3,4-*b*]quinolines was synthesised by Lapa et al. [222]. Among the group, one compound, (Figure 27) exhibited in vitro activity against *S. aureus*, *S. epidermidis* and *S. pneumonia* that was comparable to Kanamycin (MIC = 4.0–8.0 µg/mL).



**Figure 27.** 3-amino-1-(5-nitro-2-furoyl)-6,7-ethylenedioxy-1*H*-pyrazolo[3,4-*b*]quinoline.

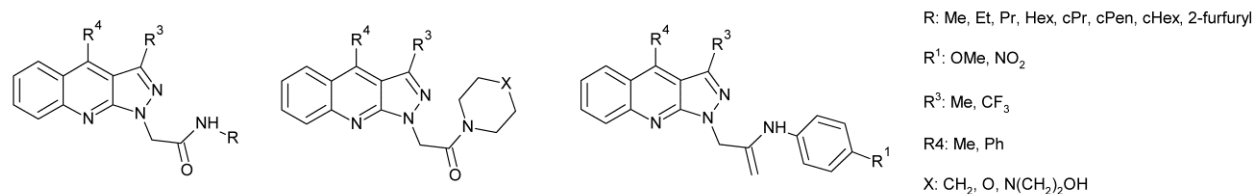
Against *Mycobacterium smegmatis*, the compound was even more active than Kanamycin. A different amino derivative was tested by Hamama et al. [54]. The authors used the Path 3 synthetic methodology (Figure 3), reacted arylidene compound 74 with 1,4-phenylenediamine and obtained 6-amino-3-methyl-1,4-diphenyl-1*H*-pyrazolo-[3,4-*b*]quinoline (Figure 28).



**Figure 28.** 6-amino-3-methyl-1,4-diphenyl-1*H*-pyrazolo[3,4-*b*]quinoline.

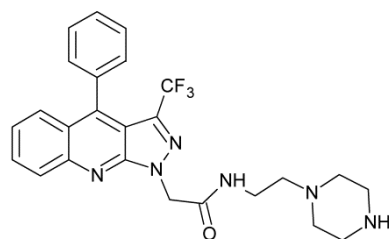
The in vitro activity of the compound against *Bacillus subtilis* and *Escherichia coli* was a little lower than that found for Ampicillin. Pyrazoloquinolines of a totally different struc-

ture were studied by Quiroga et al. [118] (Scheme 45). The authors obtained a series of benzo[*h*]pyrazolo[3,4-*b*]quinolin-5,6-diones (**165**), between which 3-methyl-1,4-diphenyl-, 3-methyl-4-(4-methylphenyl)-1-phenyl- and 3-methyl-4-(4-fluorophenyl)-1-phenyl- seemed to be the most promising and presented the strongest in vitro activity against some *Mycobacterium* spp. For two active compounds, the authors also presented the XRD measurement results. The results indicate that the research should be continued. Another group of pyrazoloquinoline derivatives that were differently substituted at N-1 (Figure 29) were synthesised and tested by Jitender et al. [83].



**Figure 29.** 1*H*-Pyrazolo[3,4-*b*]quinoline, synthesised and tested by Jitender et al. [83].

A group of 32 compounds was tested for antibacterial activity against different Gram-positive (*S. aureus*, *B. subtilis*, *M. luteus*) and Gram-negative (*E. coli*, *K. planticola*, *P. aeruginosa*) bacteria. From the group, only four compounds had some activity, and the most potent was 2-(4-phenyl-3-(trifluoromethyl)-1*H*-pyrazolo[3,4-*b*]quinolin-1-yl)-*N*-(2-(piperazin-1-yl)ethyl) acetamide (Figure 30), which, with an MIC at 3.9–7.8 µg/mL, was a little worse than the value that was found for Ciprofloxacin (the reference in the study).



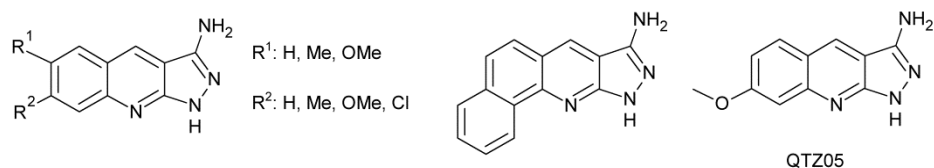
**Figure 30.** 2-(4-phenyl-3-(trifluoromethyl)-1*H*-pyrazolo[3,4-*b*]quinolin-1-yl)-*N*-(2-(piperazin-1-yl)ethyl) acetamide.

Better results were obtained in the activity against *Candida albicans* spp.; for all the tested species, 2-(4-phenyl-3-(trifluoromethyl)-1*H*-pyrazolo[3,4-*b*]quinolin-1-yl)-*N*-(2-(piperazin-1-yl)ethyl) acetamide was as active as the Miconazole biofilm inhibition assay of the studied compound, which was comparable to the results for Ciprofloxacin against Gram-positive and Gram-negative bacteria, and to the results for Miconazole against *C. albicans*. All of the 32 compounds were also tested for their cytotoxicity against the HeLa, HepG2, A549 and COLO 205 cancer cells lines, but the IC<sub>50</sub> (µM) values had to be at least one level of magnitude higher than those found for 5-fluorouracil (as a reference) in order to attract more attention as an anticancer drug.

#### 4.5. Anticancer Activity

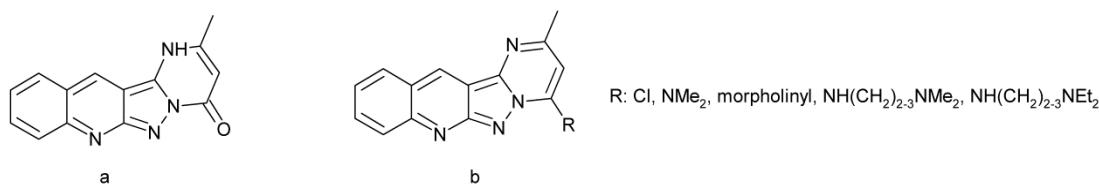
Cancer is a leading cause of death (after cardiovascular diseases), and, in 2020, there were nearly 10 million deaths that were attributed to it (WHO). At the moment, world medicine has many anticancer drugs, but most of them are also cytotoxic to normal cells, and especially to those that are rapidly dividing. Thus, there is still a need for new highly selective anticancer drugs [223,224]. 7-Methoxy-3-amino-1*H*-pyrazolo[3,4-*b*]quinoline, which appeared to be as active as Acyclovir against HSV-1 [216], was also tested as an inhibitor of the growth of cancer cells. Karthikeyan et al. tested the cytotoxicity of a group of 3-amino-1*H*-pyrazolo[3,4-*b*]quinolines (Figure 31) against ten cancer cell lines, including

breast, colon, prostate, brain and ovarian, in comparison to a noncancerous cell line, the human embryonic kidney [225].



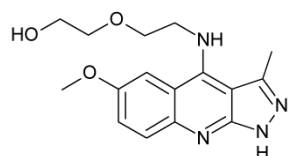
**Figure 31.** 3-amino-1*H*-pyrazolo[3,4-*b*]quinoline derivatives tested by Karthikeyan et al. [225].

The cytotoxicity was determined by MTT assay by using different concentrations for every compound, in the range of 0.1–100  $\mu$ M. The most potent in the series turned out to be 7-methoxy-3-amino-1*H*-pyrazolo[3,4-*b*]quinoline (QTZ05), which was effective against all of the tested colon cancer cell lines (HCT-116, HCT-15, HT-29 and LOVO) and the brain cancer cell line (LN-229) at a concentration of 10.2  $\mu$ M or lower. As can be seen (Figures 2 and 4 in [225]), the compound of interest decreased the density and the colony size. Additionally, as the authors point out, the HCT116 cells that survived were unable to replicate. The results indicate that 7-methoxy-3-amino-1*H*-pyrazolo[3,4-*b*]quinoline produces an increase in the number of cells in the sub G1 phase of the cell cycle. The authors also checked the ability of the studied compound to induce apoptosis. The same authors (Karthikeyan et al.) also studied a different group of 1*H*-pyrazolo[3,4-*b*]quinoline derivatives (Figure 32) in the search for an anticancer drug [79,226].



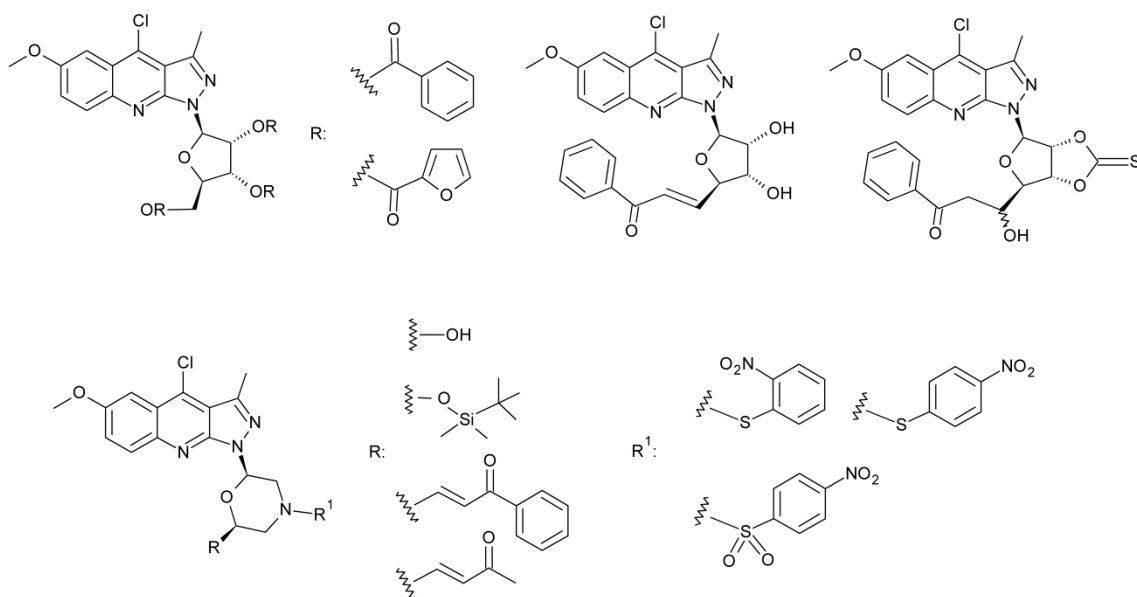
**Figure 32.** The structures of: (a) 2-methylpyrimido[1'',2'':1,5]pyrazolo[3,4-*b*]quinoline-4(1*H*)-one; and (b) 4-*R*-2-methylpyrimido[1'',2'':1,5]pyrazolo[3,4-*b*]quinolines.

2-Methylpyrimido[1'',2'':1,5]pyrazolo[3,4-*b*]quinoline-4(1*H*)-one (Figure 32a) appeared to be the most active against colon cancer cells (HCT-116 and S1) and prostate cancer cells (PC3 and DU-145) at concentrations of 0.6–1.2  $\mu$ M. At the same time, it was 10–15 times less cytotoxic to normal cells (canine kidney MDCK, mouse fibroblasts NIH/3T3 and human embryonic kidney HEK293/pcDNA.3.1.). 2-Methylpyrimido-[1'',2'':1,5]pyrazolo[3,4-*b*]quinoline-4(1*H*)-one was also found to be the most active in reversing the ABCG-2-mediated resistance to mitoxantrone, doxorubicin and cisplatin, which are common anticancer drugs. Mutations in Ras proteins are able to lead to unregulated cell division and are found in a significant number of human cancers [227]. For this reason, the identification of drugs that inhibit, either directly or indirectly, the transforming activity of the Ras protein is important in the search for an effective treatment of cancer [228]. 6-Methoxy-4-[2-[(2-hydroxyethoxy)ethyl]amino]-3-methyl-1*H*-pyrazolo[3,4-*b*]quinoline (SCH 51344, Figure 33) was one of the compounds that was tested as a possible *ras*-transformation inhibitor.



**Figure 33.** The structure 6-methoxy-4-[2-[(2-hydroxyethoxy)ethyl]amino]-3-methyl-1*H*-pyrazolo[3,4-*b*]quinoline (SCH 51344).

Kumar et al. carefully studied the mechanism of inhibition [229–232]. Pyrazoloquinoline SCH 51344, specifically, inhibits the RAS-mediated cell morphology pathway (H-, K- and N-RAS V12-induced membrane ruffling). The treatment of RAS-transformed cells with SCH 51344 restored organised actin filament bundles. Moreover, the anchorage-independent growth of K-RAS, which transformed NIH 3T3 cells and human colon and pancreatic tumor-derived cells (DLD-1, Panc-1, SW-480), was inhibited by SCH 51344. The authors also show that SCH 51344 is not cytotoxic to normal cells. Their studies show that the compound selectively suppressed oncogene-transformed growth without the gross effect on the normal signalling pathway. Gelman et al. also found that SCH 51344 suppresses *src-*, *ras-* and *raf-* induced oncogenic transformation by more than 90% at a 40  $\mu$ M concentration of the pyrazoloquinoline [233]. The oncogenic growth potentials of rat-6/*ras* and *raf* are more sensitive to SCH 51344 than rat-6/*src* cells because they are more dependent on pathways that are blocked by the compound. (S)-Crizotinib was tested as an anticancer drug by Huber et al., and the obtained results were compared to (R) enantiomer and SCH 51344 [234,235]. The authors, by using the proteomic approach, identified the target of SCH 51344 as the human mutT homologue MTH1 (NUDT1). The analysis of that pyrazoloquinoline was only one step to the main goal, which was the study concerning (S)-crizotinib. SCH 51344 was also one of the compounds that was tested by Ursu and Waldman as a small molecule target that binds to MTH1, with a comparison to (R)- and (S)-crizotinib [236]. The authors tested a few molecules of different structures by linker-based target identification techniques. The authors attached SCH 51344 to sepharose and proved that MTH1 is a primary target of the compound. The result was also confirmed in vitro by isothermal titration calorimetry and an MTH1 catalytic assay. SCH 51344 (6-methoxy-4-[2-[(2-hydroxyethoxy)ethyl]amino]-3-methyl-1H-pyrazolo[3,4-b]quinoline) is now commercially available as an MTH1 inhibitor [237]. It is in use as one of the reference compounds in research that concerns anticancer drugs [238–243]. Different pyrazoloquinoline derivatives, functionalized with ribose or morpholine moieties (Figure 34), have been also tested as antitumor agents [244–246].

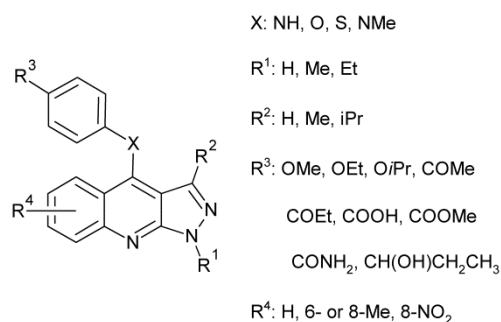


**Figure 34.** Selected (most effective) 1-substituted-4-chloro-3-methyl-6-methoxy-1H-pyrazolo[3,4-b]quinoline derivatives.

The mechanism of inhibition is probably the binding to an allosteric region of the *Ras* p21 protein, which leads to conformational change and prevents the binding of  $^3$ H-GDP to the protein. The best results have been obtained for 1-[4-chloro-3-methyl-6-methoxy-1H-pyrazolo[3,4-b]quinoliny]l-1-ribofuranoside-tribenzoate-, tris(2-furoate)-,



4-(*E*-2-benzoylphenyl),4-[(1-hydroxy-2-benzoyl)ethyl]-2,3-thiocarbonate: a >70% inhibition at 10, 10.5, 10 and 1.5  $\mu\text{M}$  concentrations, respectively. For the morpholine series, eight derivatives showed >70% inhibition at a <10 $\mu\text{M}$  concentration. One of the ways of anticancer drug action is by inducing the apoptosis of tumor cells [247]. 4-Phenylamino pyrazolo[3,4-*b*]quinolines, which have been tested for their antiviral activity [194,198], have also brought attention to themselves as potential apoptosis inducers. Zhang et al. tested a group of *N*-phenyl-1*H*-pyrazolo-[3,4-*b*]quinolin-4-amines (Figure 35) as potent apoptosis inducers [57].



**Figure 35.** Pyrazolo[3,4-*b*]quinolines tested by Zhang et al. [57].

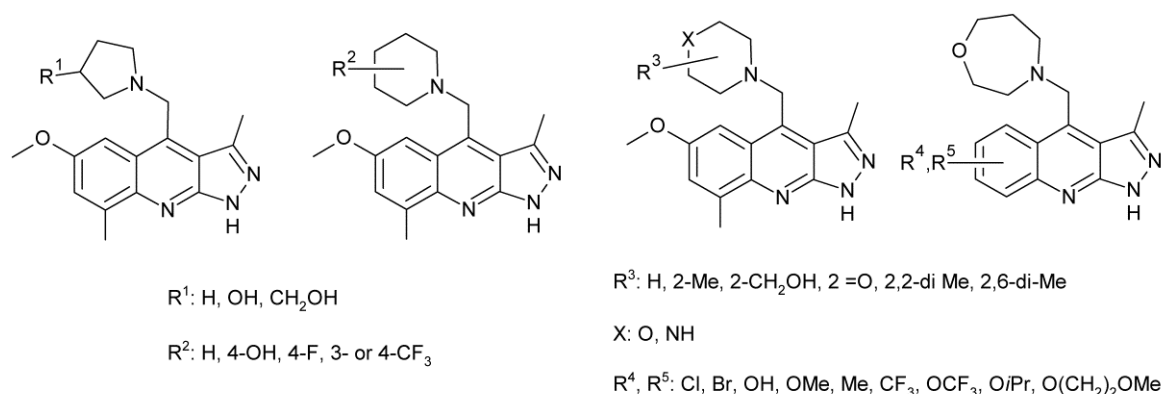
The authors tested the activity of the synthesised derivatives against the human breast cancer (T47D), colon cancer (HCT116) and liver cancer (SNU 398) cell lines in vitro. The most active against the chosen cancer cells appeared to be 1,3-dimethyl-*N*-(4-propionylphenyl)-1*H*-pyrazolo[3,4-*b*]quinolin-4-amine (Figure 35, X = NH, R<sup>1</sup>, R<sup>2</sup> = Me, R<sup>3</sup> = COEt, R<sup>4</sup> = H), which was about 6 ÷ 13-fold more potent than the reference, *N*-(4-acetylphenyl)-2,3-dihydro-1*H*-cyclopenta[*b*]quinolin-9-amine. The authors also tested the cell proliferation activity of the same compound and they again obtained very promising results; however, the research has not been continued.

#### 4.6. Antiparasitic Activity

Al-Qahtani et al. tested the effect of the series of pyrazoloquinoline derivatives that were obtained earlier by Bekhit et al. [215] (Figure 25) on the growth of *Leishmania donovani* protozoan parasites [248]. The *L. donovani* (strain DD8) were cultures in Schneider's medium with four different concentrations of drugs (50–400  $\mu\text{M}$ ), and they were compared to Amphotericin B-treated cells and to an untreated control. The results indicate that some of the derivatives exhibited an activity that was comparable to the classic drug Amphotericin B; however, the effect was observed after 12 h compared to 6 h for Amph. B. The research has been never repeated.

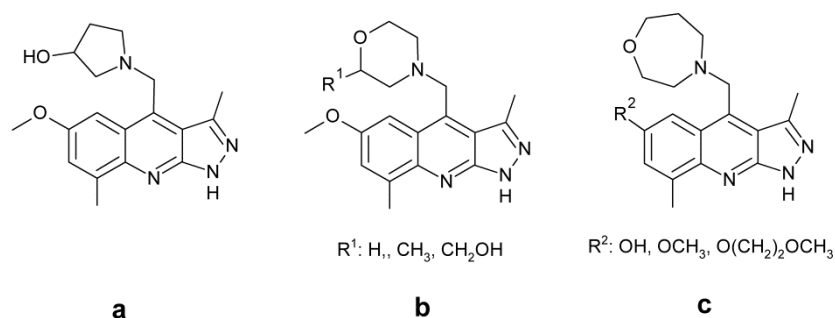
#### 4.7. Treatment of Schizophrenia

As schizophrenia is affecting circa 1% of the world's population [249], and because the already existing drugs enable only a small portion of patients to lead independent lives, there is still the need for improved treatment of schizophrenia. Antipsychotic drugs, which are used in the treatment of schizophrenia, are mostly dopamine 2 (D2) receptor antagonists [250]. PDE10, which is a dual cAMP/cGMP phosphodiesterase, and which belongs to a family of degradative enzymes that hydrolyse the second messengers that terminate signal transduction, is expressed at high levels in the striatal medium spiny neurons. The inhibition of PDE10, and the following blocking of the degradation of cGMP and cAMP, should mimic the effect of a D2 receptor antagonist and a D1 receptor agonist, which is an ideal profile for an antipsychotic drug. A wide family of different pyrazoloquinoline derivatives was tested in the search for potent PDE10 inhibitors for the treatment of schizophrenia. In the first group, which was analyzed by Yang et al. and Ho et al. [91,92], 3-methyl-1*H*-pyrazolo[3,4-*b*]quinolines could be found, which were substituted at position 4 with different saturated heterocyclic rings (Figure 36).



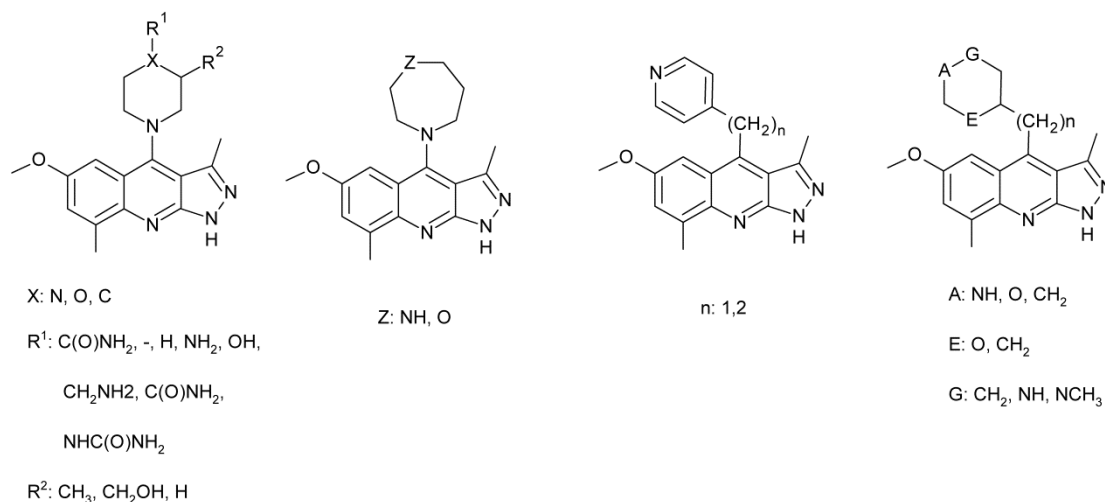
**Figure 36.** 1*H*-Pyrazolo[3,4-*b*]quinolines synthesized and tested by Yang et al. and Ho et al. [91,92].

The synthesised compounds were tested for their affinity to the cloned human recombinant, PDE10A1, by measuring their ability to compete with [ $^3H$ ]cAMP. The strongest binding affinities were obtained for one pyrrolidine derivative (Figure 37a), three morpholine-derivatized compounds (Figure 37b) and three 1,4-oxazepane-derivatives (Figure 37c) with  $K_i$  0.6–5 nM.



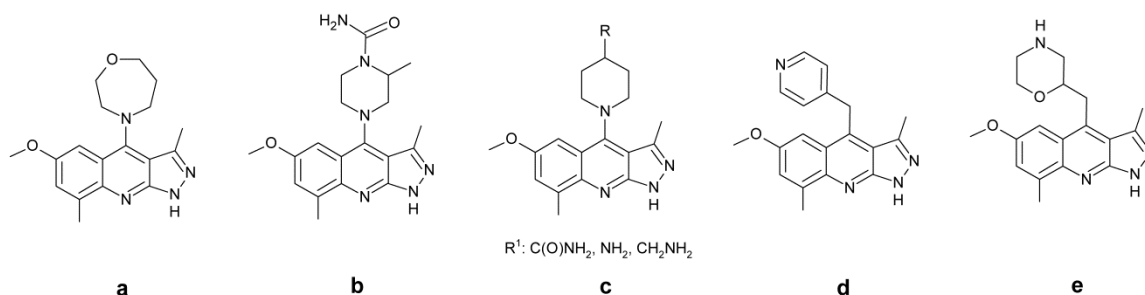
**Figure 37.** (a) *N*-[6-Methoxy-3,8-dimethyl-1*H*-pyrazolo[3,4-*b*]quinolinyl]methyl-3-hydroxypyrrolidine; (b) *N*-[6-methoxy-3,8-dimethyl-1*H*-pyrazolo[3,4-*b*]quinolinyl]methyl-2- $R^1$ -morpholines; (c) *N*-[6- $R^2$ -8-methyl-1*H*-pyrazolo[3,4-*b*]quinolinyl]methyl-1,4-oxazepanes.

One of the following, *N*-[6-methoxy-3,8-dimethyl-1*H*-pyrazolo[3,4-*b*]quinolinyl]-methylmorpholine, was used for co-crystallisation with PDE10A, and the obtained crystals were studied with XRD. The second group was obtained by Ho et al. [92] and it is presented in Figure 38.



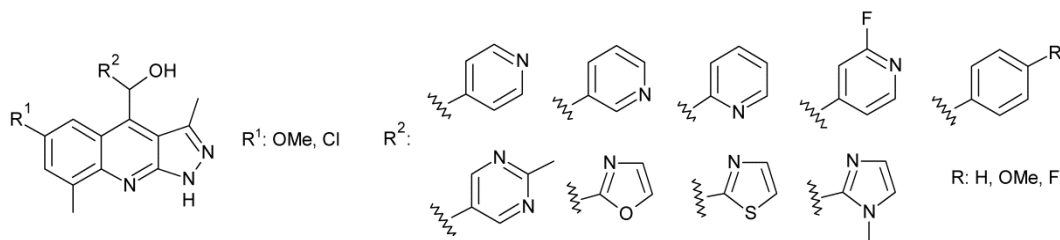
**Figure 38.** 1*H*-Pyrazolo[3,4-*b*]quinolines synthesized and tested by Ho et al. [92].

The strongest binding affinities were obtained for one 1,4-oxazepane-derivative derivative (Figure 39a), one piperazine-derivative (Figure 39b), three piperidine-derivatized compounds (Figure 39c), one pyridine-derivative (Figure 39d) and one morpholine-derivatised compound (Figure 39e) with  $K_i$  0.6–5 nM.



**Figure 39.** (a) 4-[6-Methoxy-3,8-dimethyl-1H-pyrazolo[3,4-b]quinolinyl]-1,4-oxazepane; (b) 1-[6-methoxy-3,8-dimethyl-1H-pyrazolo[3,4-b]quinolinyl]-4-carboxamid-3-methylpiperazine; (c) 1-[6-methoxy-3,8-dimethyl-1H-pyrazolo[3,4-b]quinolinyl]-4-R-piperidines; (d) 4-[6-methoxy-3,8-dimethyl-1H-pyrazolo[3,4-b]quinolinyl]methylpyridine; and (e) 2-[6-methoxy-3,8-dimethyl-1H-pyrazolo[3,4-b]quinolinyl]methylmorpholine.

One of the tested piperazine derivatives had been co-crystallised with PDE10A. Both author groups (Yang et al. and Ho et al.) state that they had been planning to perform *in vivo* evaluations; however, we could not find any further results concerning the pyrazoloquinolines described above. In the different families of pyrazoloquinoline derivatives, the moiety in position 4 was secondary alcohol with an aromatic moiety (Figure 40) or some other substituents (they are not presented here because of worse results).

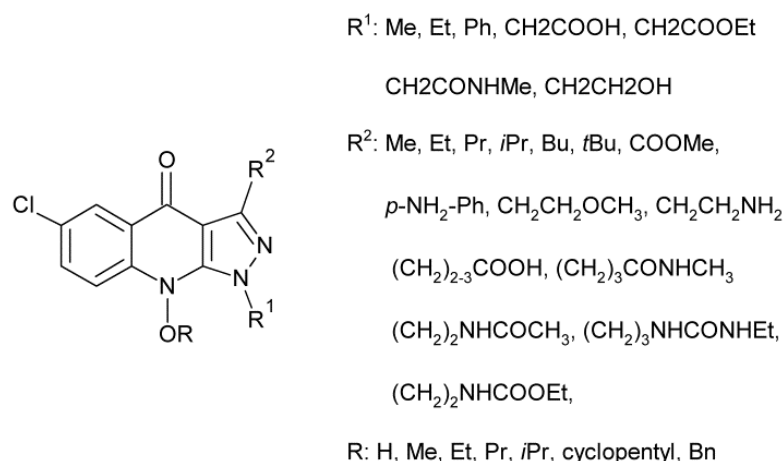


**Figure 40.** 1H-Pyrazolo[3,4-b]quinolines synthesised and tested by McElroy et al. [93].

The most potent *in vitro* binding to PDE10A appeared to be 4-[(4-pyridyl)hydroxymethyl]- and 4-[[4-(3-fluoropyridyl)] hydroxymethyl]-6-methoxy-3,8-dimethyl-1H-pyrazolo[3,4-b]quinoline, with a  $K_i$  equal to 0.06–0.07 nM. The first of them was explored extensively by Wu et al. by 3D-QSAR, molecular docking and molecular dynamics simulations [251], together with other derivatives that were obtained by McElroy et al. [93]. Three of the derivatives: 4-[(4-pyridyl)hydroxymethyl]-6-methoxy-3,8-dimethyl-1H-pyrazolo[3,4-b]quinoline, 1-[6-methoxy-3,8-dimethyl-1H-pyrazolo[3,4-b]quinolinyl]methyl-4-fluoropiperidine and 1-[6-methoxy-3,8-dimethyl-1H-pyrazolo[3,4-b]quinolinyl]-4-methoxypiperidine, which were studied earlier [91–93], have been used as the reference compounds in the search for new PDE10A inhibitors on the basis of the quinazoline derivatives [252].

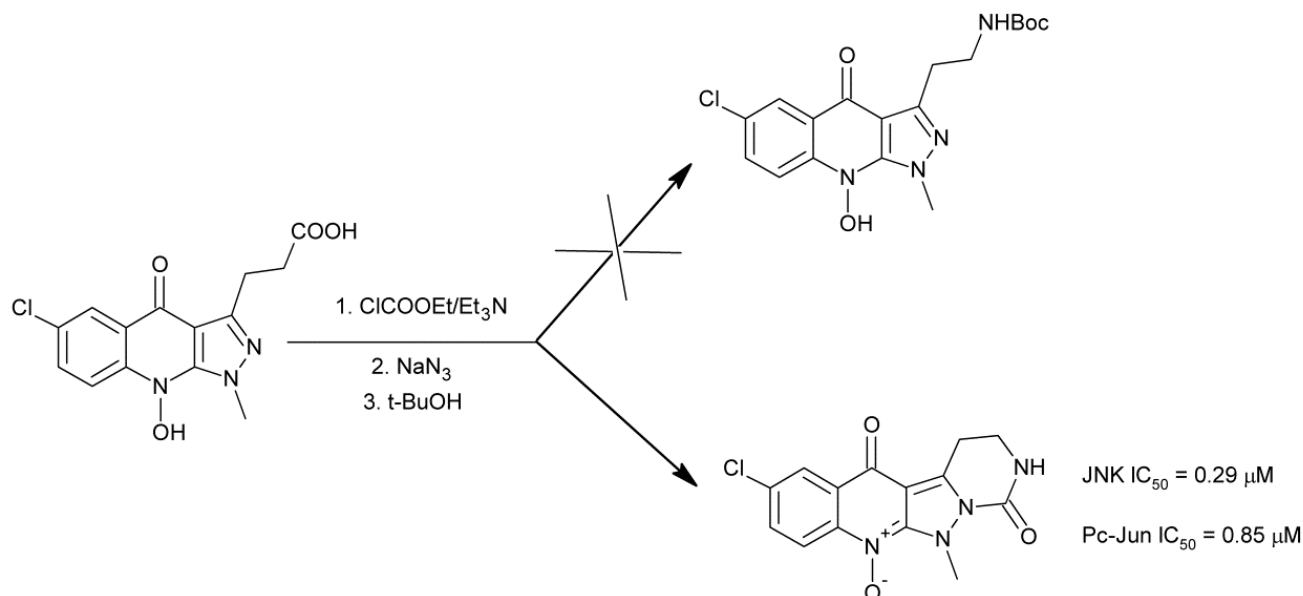
#### 4.8. Treatment of Diabetes

Type 2 diabetes is now one of the most prevalent metabolic diseases worldwide [253]. Patients with type 2 diabetes are insulin resistant, and so there is still a need to find drugs that can help to increase insulin sensitivity. C-Jun N-terminal kinase-1 (JNK1) is one of the mitogen-activated protein kinases that probably plays a key role in linking insulin resistance and obesity [254]. Liu et al. synthesised a group of 1,9-dihydro-9-hydroxy pyrazolo[3,4-b]quinolin-4-ones derivatives (Figure 41) and tested them as JNK inhibitors [255].



**Figure 41.** The structure of 1,9-dihydro-9-hydroxypyrazolo[3,4-*b*]quinolin-4-ones derivatives.

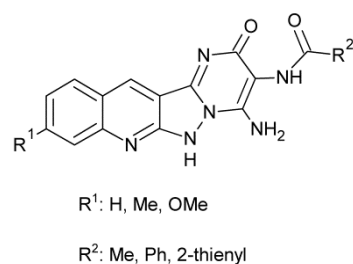
All of the obtained compounds were tested in a JNK1 enzymatic inhibition assay and in a cell-based assay by measuring the inhibition of the TNF $\alpha$  (tumor necrosis factor)-stimulated phosphorylation of c-Jun in HepG2 (human liver cancer) cells. The most potent (JNK1 IC<sub>50</sub> < 1  $\mu$ M) appeared to be derivatives with R = H, R<sup>2</sup> = Me and R<sup>1</sup> = Et, and Bu, (CH<sub>2</sub>)<sub>3</sub>CONHMe, (CH<sub>2</sub>)<sub>2</sub>NHCOMe, (CH<sub>2</sub>)<sub>3</sub>NHCONHEt or (CH<sub>2</sub>)<sub>2</sub>NHCOOEt. The authors were also able to grow the co-crystals of one of the derivatives (R = H, R<sup>1</sup>, R<sup>2</sup> = Me, JNK1 IC<sub>50</sub> = 1.22  $\mu$ M), bound into the ATP site of JNK1, and they analysed the interactions between the protein and the inhibitor. The most potent against JNK1 and also Pc-Jun proved to be the compound that was serendipitously found by the authors who tried to convert carboxylic acid to amine (Figure 42).



**Figure 42.** The most potent unexpected product of acid derivatisation.

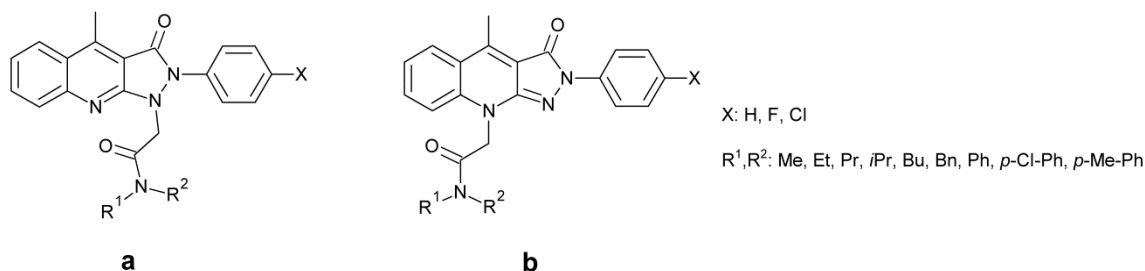
#### 4.9. Benzodiazepine Receptor Inhibitor

The group of pyrazoloquinolines that were substituted by fusing the pyrazole ring with a purine moiety were synthesised by the functionalisation of 3-amino-1*H*-pyrazolo-[3,4-*b*]quinoline derivatives by El-Sayed et al. (Figure 43) [256].



**Figure 43.** 1*H*-Pyrazolo[3,4-*b*]quinolines, synthesised and tested by El-Sayed et al. [256].

The authors tested the benzodiazepine receptor (BZR) binding affinity of nine different derivatives, and they observed the best results for 2-thienyl substituent at the 2 position: an 83% inhibition of specific [<sup>3</sup>H]Ro15-1788 (Flumazenil) binding at a 10 μM concentration was achieved for 2-(2-thienyl)quinolino[2',3'-5,4](3-pyrazolino)[3,2-*b*]purin-4-one (R<sub>1</sub> = H, R<sub>2</sub> = 2-thienyl). It is important to say that the K<sub>i</sub> value for the tested compound is three levels of magnitude higher than that found for Flumazenil. The authors have not continued their research. A different group of pyrazoloquinoline derivatives (Figure 44) were tested by Cappelli et al. as translocator protein (TSPO) ligands [257].



**Figure 44.** Pyrazoloquinoline derivatives obtained by Cappelli et al. [257].

TSPO is an alternative binding site of diazepam [258]; however, what is more important is that a dramatic increase in the TSPO density occurs in glial cells in response to brain inflammation or injury. Many neuropathological conditions (e.g., Alzheimer's disease, Parkinson's disease) also increase the TSPO density [259]. The authors decided to synthesise the pyrazoloquinolines that are shown in Figure 44 because they are structurally similar to alpidem, which is a known drug that is used for the treatment of anxiety [260]. The authors performed *in vitro* binding experiments to rat cerebral cortex membranes together with *in vivo* light/dark box tests in mice (for the most promising derivatives). Both experiments showed that the highest TSPO binding affinities were achieved *in vitro* by *N*-R<sub>2</sub>-2-[2-(4-*X*-phenyl)-4-methyl-3-oxo-2*H*-pyrazolo[3,4-*b*]quinolin-9(3*H*)-yl]-*N*-R<sub>1</sub>-acetamides (Figure 44b). The IC<sub>50</sub> values for all of these derivatives were lower than 1 nM. Moreover, the antianxiety activity of one of the derivatives (*N*-butyl-2-[2-phenyl-4-methyl-3-oxo-2*H*-pyrazolo[3,4-*b*]quinolin-9(3*H*)-yl]-*N*-methylacetamide) was high, at 10 mg/kg dose, which was comparable to the value that was found for emapunil with the same dose, and for diazepam with a 1 mg/kg dose. The biological activity studies were combined with a detailed structural analysis, including XRD and computational calculations. The obtained results indicate that these group of pyrazoloquinoline derivatives could be a group of new TSPO modulators, and that they are worth further research.

#### 4.10. Singlet-Oxygen-Generating Activity for SPA

A scintillation proximity assay (SPA) is a biochemical screening radio-isotopic method that is used for the sensitive and rapid measurement of a broad range of biological processes [261]. Pai et al. used 4-[(4-aminophenyl)sulfanyl]-6-methoxy-3-methyl-1*H*-pyrazolo[3,4-*b*]quinoline (SCH 46891), which was obtained earlier by Afonso et al. [212], as one of the tested potent inhibitors of the phosphopeptide binding to the growth factor

receptor-bound protein 2 (*Grb2*) SH2 domain [262]. The studies reveal that the inhibition of the *Grb2* SPA by SCH 46891 was light-dependent. The compound was inactive when the assay plates were kept dark. The same light-dependent inhibition property was found for the tyrosine-protein kinase (*Syk*) SH2 domain via SPA. The authors concluded that the light-dependent inhibition mechanism is based on the singlet-oxygen-generating property of SCH 46891 upon irradiation (positive reaction with singlet oxygen trap 2-methylfuran, and the suppression of the inhibition activity by singlet oxygen quenchers).

#### 4.11. Pregnancy Interceptive

In 1991, Mehrotra et al. [263] tested 3-amino-6,7-dimethoxy-1*H*-pyrazolo[3,4-*b*]quinoline as a potential pregnancy interceptor in vivo in hamsters and guinea pigs. When the compound was used in the early postimplantation schedule, it interrupted the pregnancy partially; however, it was ineffective in the preimplantation schedule. The same compound was tested in vitro on growing trophoblasts, and it appeared to prevent growth and to cause the degeneration of the cells. The results led the authors to the conclusion that the compound intercepts pregnancy probably through a direct effect on the embryo attachment site. The research was never continued or repeated with that, nor with any other pyrazoloquinoline derivative.

## 5. Conclusions

In summary, the main aim of this review was to introduce readers to the methods and procedures that are used for the 1*H*-pyrazolo[3,4-*b*]quinoline skeleton synthesis, and to familiarize them with some of the photophysical and biological properties. The work is based on publications that appeared in the years 1911–2021. During this period, approx. 350 publications and patents were published, and, to the best of our knowledge, this is the first study of this type. We wanted to collect, in this review, all of the most important synthetic methods to create a kind of guide for researchers who are involved in the synthesis of nitrogen-condensed heterocycles, and who may decide to direct their interests there.

By studying the development of the synthetic methods of 1*H*-pyrazolo[3,4-*b*]quinolines over the last one hundred years, a significant revolution in the approach to preparative methods can be noticed, and especially in the last ten years. In the initial period, syntheses based on classical reactions (e.g., the Friedländer condensation or modifications of the Niementowski reaction) were used. Nowadays, an increasing number of publications can be found that describe three-/four-component reactions, and reactions that are carried out in an aqueous environment with the use of a microwave field, or with ultrasounds and ionic liquids, which are catalysed with palladium compounds and nanoparticles, or that are even mediated with baker's yeast. All of these procedures are part of the so-called "green chemistry".

These methods lead to the synthesis of the basic skeleton, as well as functionalized systems, which offer further possibilities for structural modifications with hydroxyl, halogen or amino moieties. The latter aspect is especially important for chemists in the pharmaceutical industry.

The first synthesised 1*H*-pyrazolo[3,4-*b*]quinolines attracted the attention of researchers with their emissive properties, and they were applied as optical brighteners in the 1960s. Later studies show that, in some cases, the quantum yield of the fluorescence was equal to one, and that, in addition, these compounds turned out to be very resistant to temperature or oxidation. For this reason, they were used as emission materials for the fabrication of organic light-emitting diodes (OLEDs) that work on the basis of the phenomenon of fluorescence. In recent years, however, very efficient emissive materials that are based on the phenomenon of phosphorescence or thermally activated delayed fluorescence TADF have appeared, and so it should not be expected that pyrazoloquinolines will be used in the future to fabricate OLEDs. However, by taking into account their very good emissive properties and their stability, it can be expected that they will be used as fluorescent sensors for various analytes, as dyes for synthetic fibers, as dyes for fluorescence microscopy or as materials for the security features of banknotes based on fluorescence.

The third aspect of the use of pyrazoloquinolines are their biological properties, which have been studied since the 1970s, and which were started by Siminoff and Crenshaw, who investigated the antimalarial properties of these compounds. Currently, the spectrum of biological properties is much broader and includes a variety of tests, among which the research on antibacterial, antiviral and anticancer properties is at the forefront. This resulted in, among other things, the commercialization of some preparations, such as, for example, 6-methoxy-4-[2-[(2-hydroxyethoxy)ethyl]amino]-3-methyl-1*H*-pyrazolo[3,4-*b*]quinoline, which is now commercially available as an MTH1 inhibitor. Therefore, further studies towards the investigation of novel pharmacologically active 1*H*-pyrazolo[3,4-*b*]quinolines are highly desirable.

**Author Contributions:** Conceptualisation, A.D.; writing—the synthetic part, A.D. and M.K.; schematic drawing for the synthetic part, E.G.; writing—the photophysical part, A.G.; writing—the pharmacological part, P.S. All authors have read and agreed to the published version of the manuscript.

**Funding:** This research received no external funding.

**Acknowledgments:** I would like to thank Piotr Tomasiak for many years of cooperation and for introducing me to the fascinating world of heterocyclic chemistry (A.D.). The authors (A.D.; E.G.; M.K.; P.S.) would like to thank the Krakow University of Technology and the University of Agriculture in Krakow for the financial support.

**Conflicts of Interest:** The authors declare no conflicts of interest.

## References

1. Michaelis, A. Über 5-Aminopyrazole und über Iminopyrine. I. Über substituierte 5-Iminopyrazolone und über 5-Aminopyrazole. *Justus Liebigs Ann. Chem.* **1911**, *385*, 1–43. [CrossRef]
2. Musierowicz, A.; Niementowski, S.; Tomasiak, Z. Kondensacja fenylo-1-metylo-3-okso-5-[dwuchydropirazolu] i [chloro-2]-fenylo-1-metylo-3-okso-[dwuhydro-4,5-pyrazolu] z o-aminobenzaldehydem. *Roczn. Chemii* **1928**, *8*, 325–344.
3. Koćwa, A. Reactions in the pyrazolone series. II. Reactions of arylimine derivatives of 1-phenyl-5-methyl-3-pyrazolone with carbanilide or phenyl isocyanate,  $\alpha$ -naphthyl isocyanate, and thiocarbanilide or phenyl isothiocyanate. *Bull. Intern. Acad. Polon. Sci.* **1936**, 382–389.
4. Koćwa, A. Reactions in the pyrazolone series. III. Reactions of arylimine derivatives of 1-phenyl-3-methyl-5-pyrazolone with carbanilide or phenyl isocyanate,  $\alpha$ -naphthyl isocyanate, or with thiocarbanilide or phenyl isothiocyanate. *Bull. Intern. Acad. Polon. Sci.* **1936**, 390–402.
5. Rettig, W.; Rurack, K.; Danel, A.; Rotkiewicz, K.; Grabka, D.; Spieles, M. 1,3-Diphenyl-1*H*-pyrazolo[3,4-*b*]quinoline: A versatile fluorophore for the design of brightly emissive molecular sensors. *Org. Lett.* **2002**, *4*, 4647–4650. [CrossRef]
6. Danel, A.; Gondek, E.; Kityk, I. 1*H*-pyrazolo[3,4-*b*]quinoline and 1*H*-pyrazolo[3,4-*b*]quinoxaline derivatives as promising materials for optoelectronic applications. *Opt. Mater.* **2009**, *32*, 267–273. [CrossRef]
7. Reimann, E. Chinoline. In *Houben-Weyl Methods of Organic Chemistry*, 4th ed.; Hetarenes II-Part 1; Büchel, K.H., Falbe, J., Hageman, H., Hanack, M., Klamann, D., Krecher, R., Kropf, H., Regitz, M., Schaumann, E., Eds.; Georg Thieme Verlag Stuttgart: New York, NY, USA, 1991; Volume E7a, pp. 290–493.
8. Friedländer, P. Ueber o-Amidobenzaldehyd. *Chem. Ber.* **1882**, *15*, 2572–2575. [CrossRef]
9. Marco-Contelles, J.; Perez-Mayoral, E.; Samadi, A.; Carreiras, M.C.; Soriano, E. Recent advances in Friedlander reaction. *Chem. Rev.* **2009**, *109*, 2652–2671. [CrossRef]
10. Cheng, C.-C.; Yan, S.-J. The Friedlander synthesis of quinolines. *Org. React.* **1982**, *28*, 37–201. [CrossRef]
11. Fallah-Mehrjarch, M. Friedlander synthesis of poly-substituted quinolones: A mini review. *Mini-Rev. Org. Chem.* **2017**, *14*, 187–196. [CrossRef]
12. Ramann, G.A.; Cowen, B.J. Recent advances in metal-free quinoline synthesis. *Molecules* **2016**, *21*, 986. [CrossRef] [PubMed]
13. Nainwal, L.M.; Tasneem, S.; Akhtar, W.; Verma, G.; Faraz Khan, M.; Parvez, S.; Shaquiquzzaman, M.; Akhter, M.; Amumtaz Alam, M. Green recipes to quinoline: A review. *Eur. J. Med. Chem.* **2019**, *164*, 121–170. [CrossRef] [PubMed]
14. Abramovitch, R.; Tomasiak, P.; Tomasiak, D. Friedländer Condensation of 1*H*-Pyrazolin-5-ones with o-Aminobenzaldehydes. Synthesis of 1*H*-Pyrazolo[3,4-*b*]quinolines. *J. Heterocycl. Chem.* **1983**, *20*, 1539–1543. [CrossRef]
15. Kucybała, Z.; Przyjazna, B.; Linden, L.-A.; Paczkowski, J. Developmnet of new dyeing photoinitiators for free radical polymerization based on 1*H*-pyrazolo[3,4-*b*]quinoline skeleton. IV. *Polym. Bull.* **2000**, *45*, 327–334. [CrossRef]
16. Danel, A. Synthesis of Pyrazolo[3,4-*b*]quinolines as Luminophores for Electroluminescent Devices. Ph.D. Thesis, Jagiellonian University, Krakow, Poland, 1996.
17. Sabitha, G.; Babu, R.S.; Reddy, S.B.V.; Yadav, J.S. Microwave Assisted Friedländer Condensation Catalyzed by Clay. *Synth. Commun.* **1999**, *29*, 4403–4408. [CrossRef]

18. Qu, Y.-K.; Zheng, Q.; Fan, J.; Liao, L.-S.; Jiang, Z.-Q. Spiro compounds for organic-light emitting diodes. *Acc. Mater. Res.* **2021**, *2*, 1261–1271. [CrossRef]
19. Salbeck, J.; Pudzich, R.; Fuhrmann, T. Spiro compounds for organic electroluminescence and related applications. *Adv. Polym. Sci.* **2006**, *107*, 1011–1065. [CrossRef]
20. Chen, C.-H.; Wu, F.-I.; Shu, C.-F.; Chien, C.-H.; Tao, Y.-T. Spirobifluorene-based pyrazoloquinolines: Efficient blue electroluminescent materials. *J. Mater. Chem.* **2004**, *14*, 1585–1589. [CrossRef]
21. Caluve, P. Heteroannulations with *o*-aminoaldehydes. *Tetrahedron* **1980**, *36*, 2359–2407. [CrossRef]
22. Häufel, J.; Breitmaier, E. Synthesis of Pyrazolo Heteroaromatic Compounds by Means of 5-Amino-3-methyl-1-phenylpyrazole-4-carbaldehyde. *Angew. Chem. Int. Ed.* **1974**, *13*, 604. [CrossRef]
23. Jachak, N.M.; Avhale, A.B.; Medhane, V.J.; Toche, R.B. A convenient route for the synthesis of pyrazolo[3,4-d]pyrimidine, pyrazolo[3,4-b][1,6]naphthiridine and pyrazolo[3,4-b]quinoline derivatives. *J. Heterocycl. Chem.* **2006**, *43*, 1169–1175. [CrossRef]
24. Higashino, T.; Iwai, Y.; Hayashi, E. Studies on Pyrazolo[3,4-d]pyrimidine Derivatives. IV. On 1-methyl- and 1-phenyl-1H-pyrazolo[3,4-d]pyrimidine 5-oxide. *Chem. Pharm. Bull.* **1976**, *24*, 3120–3134. [CrossRef]
25. Niementowski, S. Synthesen der Chinolinderivate. *Chem. Ber.* **1894**, *27*, 1394–1403. [CrossRef]
26. Ghosh, T.N. Quinoline derivatives. *J. Indian Chem. Soc.* **1937**, *14*, 123–126.
27. Menzel, K.H.; Putter, R.; Wolfrum, G. Synthesen und reaktionen neuer ortho-kondensierter pyrazoloverbindungen. *Angew. Chem.* **1962**, *21*, 839–847. [CrossRef]
28. Danel, A.; Tomasik, P.; Kappe, T.; Gheath, A.H. Attempted Niementowski condensation of anthranilic acid and its ester with 3-methyl-1-phenylpyrazolin-5-one. *Polish J. Chem.* **1996**, *70*, 302–309.
29. Stein, R.G.; Biel, J.H.; Singh, T. Antimalarials. 4-Substituted 1H-pyrazolo[3,4-b]quinolones. *J. Med. Chem.* **1970**, *13*, 153–155. [CrossRef]
30. Crenshaw, R.R.; Luke, G.M.; Siminoff, P. Interferon inducing activities of derivatives of 1,3-dimethyl-4-(3-dimethylaminopropylamino)-1H-pyrazolo[3,4-b]quinoline and related compounds. *J. Med. Chem.* **1976**, *19*, 262–275. [CrossRef]
31. Kim, D.H. Further studies on the reaction of *N*-(2-hydroxyphenyl)anthranilic acid with acetic anhydride. *J. Heterocycl. Chem.* **1981**, *18*, 1389–1392. [CrossRef]
32. Gal, M.; Feher, Ö.; Tihanyi, E.; Horvath, G.; Jerkovitch, G.; Argay, G.; Kálman, A. The ring closure and rearrangement of 1-(2-amino)-benzoyl-1-methylhydrazones of  $\beta$ -dicarbonyl compounds: On the formation and crystal structure of 3a,9a-dihydro-1,3,3a,9a-tetramethyl-4H-pyrazolo[3,4-b]quinolin-4-one. *Tetrahedron Lett.* **1980**, *21*, 1567–1570. [CrossRef]
33. Nielsen, S.; Pedersen, E.B. Synthesis of 4-arylamino-5,6,7,8-tetrahydro-1H-pyrazolo[3,4-b]quinolones and the corresponding *N*-Mannich bases. *Liebigs Ann. Chem.* **1986**, *1986*, 1728–1735. [CrossRef]
34. Nielsen, S.; Pedersen, E.B. Synthesis of 4-arylamino-5,6,7,8-tetrahydro-1H-pyrazolo[3,4-b]quinolones and 5,6,7,8-tetrahydrogenated analogs. *Chem. Scr.* **1986**, *26*, 331–336.
35. Gatta, F.; Pomponi, M.; Maurizio, M. Synthesis of 7,8-dihydro-6H-pyrazolo[3,4-b]quinolin-5-ones and related derivatives. *J. Heterocycl. Chem.* **1991**, *28*, 1301–1307. [CrossRef]
36. Campbell, J.B.; Firor, J.W. Synthesis of tricyclic aminopyridines by a cadmium promoted cyclization. *J. Org. Chem.* **1995**, *60*, 5243–5249. [CrossRef]
37. Deeb, A.; El-Mobayed, M.; Essawy, A.N.; El-Hamid, A.A.; Mohamid, A.; El-Hamid, A. Heterocyclic synthesis from 3-amino-4-cyanompyrazole. *Collect. Czech. Chem. Commun.* **1990**, *55*, 728–733. [CrossRef]
38. Silva, D.; Chioua, M.; Samadi, A.; Carreiras, C.M.; Jimeno, M.-L.; Mendes, E.; De los Rios, C.; Romero, A.; Villarroya, M.; Lopez, M.G.; et al. Synthesis and pharmacological assessment of diversity substituted pyrazolo[3,4-b]quinoline, and benzo[b]pyrazolo[4,3-g][1,8]naphthyridine. *Eur. J. Med. Chem.* **2011**, *46*, 4676–4681. [CrossRef]
39. Pfitzinger, W. Chinolinderivate aus isatinsäure. *J. Prakt. Chem.* **1886**, *33*, 100. [CrossRef]
40. Shvekgheimer, M.G.-A. The Pfitzinger reaction. *Chem. Heterocycl. Compd.* **2004**, *40*, 257–294. [CrossRef]
41. Musante, C.; Fabbrini, L. Contribution to the knowledge of malonyldiphenylhydrazine and its derivatives. *Gazz. Chim. Ital.* **1954**, *84*, 595–605.
42. Holla, D.C.; Seshadri, S. A new synthesis of pyrazolo[3,4-b]quinoline derivatives. *Bull. Chem. Soc. Jpn.* **1984**, *57*, 2984–2986. [CrossRef]
43. Brack, A. Über kondensierte Pyrazolopyridine. *Liebigs Ann. Chem.* **1965**, *681*, 105–110. [CrossRef]
44. Brack, A. 1H-Pyrazolo[3,4-b]quinolines. DE1186867, 11 May 1962.
45. Butler, D.E.; De Wald, H.A. New general methods for the substitution of 5-chloropyrazoles. The synthesis of 1,3-dialkyl-5-chloropyrazol-4-yl aryl ketones and new 1,3-dialkyl-2-pyrazolin-5-ones. *J. Org. Chem.* **1971**, *36*, 2542–2547. [CrossRef]
46. Obakachi, V.A.; Kushwaha, N.D.; Kushwaha, B.; Mahlalela, M.C.; Shinde, S.R.; Kehinde, I.; Karpoomath, R. Design and synthesis of pyrazolone-based compounds as potent blockers of SARS-CoV-2 viral entry into the host cells. *J. Mol. Struct.* **2021**, *1241*, 130665. [CrossRef] [PubMed]
47. Wan, W.; Wang, H.; Lin, H.; Wang, J.; Jiang, Y.; Jiang, H.; Zhu, S.; Wang, Z.; Hao, J. Synthesis, electrochemical, photochemical, and electroluminescent properties of organic dyes containing pyrazolo[3,4-b]quinoline chromophore. *Dyes Pigments* **2015**, *121*, 138–146. [CrossRef]
48. Porai-Koshits, B.A.; Kvitko, I.Y.; Shutkova, E.A. Synthesis and transformations of chloropyrazolealdehydes. *Pharm. Chem. J.* **1970**, *4*, 138–143. [CrossRef]



49. Hennig, L.; Müller, T.; Grosche, M. Syntheses von Pyrazolo[3,4-*b*]chinolinen aus 4-Aroyl-5-chloropyrazolen. *J. Prakt. Chem.* **1990**, *332*, 693–698. [CrossRef]
50. El-Shehry, M.; El-Telbani, E.M.; Swellem, R. Synthesis of polyfunctional substituted pyrazoles. *J. Chem. Res.* **2009**, *10*, 625–629. [CrossRef]
51. Gonzales, E.; Elguero, J. Action des hydrazines sur les acetyl-4-chloro-5(ou 3)methyl-3 (ou 5) pyrazoles: Formation d'une pyrazolo[3,4-*b*]quinoline, d'hydrazones et de cetazines. *J. Heterocycl. Chem.* **1986**, *23*, 999–1001. [CrossRef]
52. Crenshaw, R.R.; Luke, G.M.; Whitehead, D.F. Unexpected formation of a 10*H*-pyrido[2,3-*h*]pyrazolo[3,4-*b*]quinoline derivative, A new ring system. *J. Heterocycl. Chem.* **1976**, *13*, 155–156. [CrossRef]
53. Chaczatryan, K.; Chaczatryan, G.; Danel, A.; Tomasik, P. The synthesis of 4-aryl-1*H*-pyrazolo[3,4-*b*]quinolines by cyclization of 4-arylidene-pyrazolin-5-ones with anilines. *ARKIVOC* **2001**, *VI*, 63–69. [CrossRef]
54. Hamama, S.W.; El-Gohary, H.G.; Soliman, M.; Zoorob, H.H. A versatile synthesis, PM-3-Semiempirical, antibacterial, and antitumor evaluation of some bioactive pyrazoles. *J. Heterocycl. Chem.* **2012**, *49*, 543–554. [CrossRef]
55. Szlachcic, P.; Kucharek, M.; Jarosz, B.; Danel, A.; Stadnicka, K. Facile and regioselective synthesis of substituted 1*H*-pyrazolo[3,4-*b*]quinolones from 2-fluorobenzaldehydes and 1*H*-pyrazol-5-amines. *J. Heterocycl. Chem.* **2016**, *54*, 1729–1745. [CrossRef]
56. Abramov, M.A.; Ceulemans, E.; Jackers, C.; Van der Auweraer, M.; Dehaen, W. Reactions of 5-amino-1,2-azoles with aromatic and heterocyclic *o*-chloroaldehydes: [1+1] versus [2+1] cyclocondensation. *Tetrahedron* **2001**, *57*, 9123–9129. [CrossRef]
57. Zhang, H.-Z.; Classen, G.; Crogran-Grundy, C.; Tseng, B.; Drewe, J.; Cai, S.X. Discovery and structure—Activity relationship of *N*-phenyl-1*H*-pyrazolo[3,4-*b*]quinolin amines as a new series of potent apoptosis inducers. *Bioorg. Med. Lett.* **2008**, *16*, 222–231. [CrossRef]
58. Pamukcu, R.; Piazza, A. Method for Inhibiting Neoplastic Cells by Exposure to Substituted *N*-cycloalkylmethyl-1-*H*-pyrazolo[3,4-*b*]quinoline-4-amines. U.S. Patent 5,942,520, 24 August 1999.
59. Shekarro, K.; Kaishap, P.P.; Saddanapu, A.A.; Gogoi, S.; Boruah, R.C. Microwave—Assisted palladium mediated efficient synthesis of pyrazolo[3,4-*b*]pyridines, pyrazolo[3,4-*b*]quinolines, pyrazolo[1,5-*a*]pyrimidines and pyrazolo[1,5-*a*]quinazolines. *RSC Adv.* **2014**, *4*, 24001. [CrossRef]
60. De Wald, H. 9-Substituted-4,9-dihydro-1,3,4,4-tetraalkyl-1*H*-pyrazolo[3,4-*b*]quinolines. U.S. Patent 3,790,576, 5 February 1974.
61. Meth-Cohn, O.; Narine, B.; Tarnowski, B. A versatile new synthesis of quinolones and related fused pyridines, Part 5. The synthesis of 2-chloroquinolone-3- carbaldehydes. *J. Chem. Soc. Perkin Trans. 1* **1981**, 1520–1530. [CrossRef]
62. Hayes, R.; Meth-Cohn, O. A versatile new synthesis of quinolones and related fused pyridines. Part 10. Routes to quinolines with fused azacycles. *Tetrahedron Lett.* **1982**, *23*, 1613–1615. [CrossRef]
63. Marson, C.M. Reactions of carbonyl compounds with (monohalo) methyleniminium salts (Vilsmeier reagents). *Tetrahedron* **1992**, *48*, 3659–3726. [CrossRef]
64. Meth-Cohn, O. The synthesis of pyridines, quinolones and other related systems by the Vilsmeier and the reversed Vilsmeier method. *Heterocycles* **1993**, *35*, 539–557. [CrossRef]
65. Bhat, B.N.; Bhaduri, A.P. Syntheses of substituted pyrazolo[3,4-*b*]quinolines, 3,4-dihydro-4-oxopyrimido[4',5':4,5]thieno[2,3-*b*]quinoline and pyrido[1',2':1,2]pyrimido[4,5-*b*]quinoline. *J. Heterocycl. Chem.* **1986**, *23*, 925–928. [CrossRef]
66. Rajendran, S.P.; Manomani, M.; Vijayalakshmi, S. Synthesis of pyrazolo[3,4-*b*]quinolines and their 1-phenyl derivatives. *Org. Prep. Procedures Int.* **2009**, *26*, 383–385. [CrossRef]
67. Kidwai, M.; Negi, N. Synthesis of some novel substituted quinolones as potent analgesic agents. *Monatsh. Chem.* **1997**, *128*, 85–89. [CrossRef]
68. Mogilaiah, K.; Sudhakar, G.R.; Reddy, N.V. Microwave assisted synthesis of pyrazolo[3,4-*b*]quinoline containing 1,8-naphthyridine moiety. *Indian J. Chem.* **2003**, *42B*, 1753–1755.
69. Selvi, S.T.; Nadaraj, V.; Mohan, S.; Sasi, R.; Hema, M. Solvent free synthesis and evaluation of antimicrobial activity of pyrimido[4,5-*b*] and pyrazolo[3,4-*b*]quinolines. *Bioorg. Med. Lett.* **2006**, *14*, 3896–3903. [CrossRef]
70. Mali, J.R.; Pratap, U.R.; Jawale, D.V.; Mane, R.A. Water mediated one-pot synthetic route for pyrazolo[3,4-*b*]quinolines. *Tetrahedron Lett.* **2010**, *51*, 3980–3982. [CrossRef]
71. Paul, S.; Gupta, M.; Gupta, R.; Loupy, A. Microwave assisted solvent free synthesis of pyrazolo[3,4-*b*]quinolones and pyrazolo[3,4-*c*]pyrazoles using *p*-TsOH. *Tetrahedron Lett.* **2001**, *42*, 3827–3829. [CrossRef]
72. El-Bordany, E.A.; Aziz, A.A.; Abou-Elmagd, W.S.I.; Hashem, A.I. Synthesis and spectroscopic characterization of some novel pyrazoloquinoline, pyrazolotetrazine and thiazolidinone derivatives. *J. Heterocycl. Chem.* **2018**, *55*, 291–296. [CrossRef]
73. Munir, R.; Javid, N.; Zia-ur-Rehman, M.; Zaheer, M.; Huma, R.; Roohi, A.; Athar, M.M. Synthesis of novel *N*-acylhydrazones and their C-N/*N*-N bond conformational characterization by NMR spectroscopy. *Molecules* **2021**, *26*, 4908. [CrossRef]
74. Teixeira, F.C.; Lucas, C.; Curto, M.J.M.; Andre, V.; Duarte, T.M.; Teixeira, A.P.S. Synthesis of novel pyrazolo[3,4-*b*]quinoline—Bisphosphonic acids and unexpected intramolecular cyclization and phosphorylation reaction. *Org. Biomol. Chem.* **2021**, *19*, 2533–2545. [CrossRef]
75. Chavan, A.S.; Kharat, A.S.; Bhosle, M.; Dhumal, S.T.; Mane, R.A. Water mediated and Baker yeast accelerated novel synthetic protocols for tetrahydrobenzo[*a*]xanthene -11-ones and pyrazolo[3,4-*b*]quinolones. *Synth. Commun.* **2021**, *51*, 1963–1973. [CrossRef]
76. Kerry, M.; Boyd, G.W.; Mackay, S.P.; Meth-Cohn, O.; Platt, L. The synthesis of benzo[*h*]quinolones as topoisomerase inhibitors. *J. Chem. Soc. Perkin Trans. 1* **1999**, 2315–2321. [CrossRef]

77. Parekh, N.M.; Sahoo, S.K.; Maheiria, K.C. Quantum chemical studies and dyeing performance of some novel benzoquinoline based heterocyclic monoazo dyes on polyester fiber. *Dye. Pigment.* **2012**, *95*, 142–148. [CrossRef]
78. Parekh, N.M.; Maheira, K.C. Synthesis of heterocyclic monoazo dyes derived from 1H-benzo[g]pyrazolo[3,4-b]quinoline-3-ylamine: Their antimicrobial activity and their dyeing performance on various fibers. *Res. Chem. Intermed.* **2012**, *38*, 885–901. [CrossRef]
79. Karthikeyan, C.; Lee, C.; Moore, J.; Mittal, R.; Suswam, E.A.; Abbot, K.L.; Pondugula, S.R.; Manne, U.; Narayanan, N.K.; Trivedi, P.; et al. IND-2, a pyrimido[1'',2'':1,5]pyrazolo[3,4-b]quinoline derivative circumvents multi-drug resistance and causes apoptosis in colon cancer cells. *Bioorg. Med. Chem.* **2015**, *23*, 602–611. [CrossRef] [PubMed]
80. Yoshida, K.; Otomasu, H. Synthesis of 1H-pyrazolo[3,4-b]pyridine and related compounds. *Yakugaku Zasshi* **1976**, *96*, 33–36. [CrossRef]
81. Arasakumar, T.; Mathusalini, S.; Lakshmi, K.; Mohan, S.P.; Ata, A.; Lin, C.-H. An object oriented synthetic approach toward angular and linear fused pyrazoloquinolines of biological importance with InCl<sub>3</sub> catalyst. *Synth. Commun.* **2016**, *46*, 232–241. [CrossRef]
82. Vostrova, L.N.; Gerenga, S.A.; Kiridenk, A.M.; Grenaderowa, M.V.; Kharchenko, S.L.; Abramovitch, A.E.; Dimitrieva, T.N. 2-Heterylquinoline derivatives. *Ukr. Chim. Zh.* **1992**, *58*, 578–781.
83. Jintender Dev, G.; Poornachandra, Y.; Reddy, K.R.; Kumar, R.N.; Ravikumar, N.; Swaroop, K.; Ranjithreddy, P.; Kumar, G.S.; Nanubolu, J.B.; Ganesh, K.; et al. Synthesis of novel pyrazolo[3,4-b]quinolinyl acetamide analogs, their evaluation for antimicrobial and anticancer activities, validation by molecular modelling and COMFA analysis. *Eur. J. Med. Chem.* **2017**, *130*, 223–239. [CrossRef]
84. Hassan, M.M.; Othman, E.; Abass, M. Substituted quinolinones. 18. 3-Acetyl-4-methylthiopyridin-2(1H)-one as useful synthon intermediate for synthesis of some new quinolinones. *Res. Chem. Intermed.* **2013**, *39*, 1209–1225. [CrossRef]
85. Abass, M.; Hassanin, H.M.; Allimony, H.; Hassan, H. Substituted quinolinones. 27. Regioselective synthesis of pyrazolo-, oxazolo-, and triazepinoquinoline derivatives. *Chem. Heterocycl. Compd.* **2015**, *51*, 1023–1029. [CrossRef]
86. Mahat, P.K.; Venkatesh, C.; Kumar, U.K.S.; Ila, H.; Junjappa, H. Reaction of  $\alpha$ -oxoketene-N,S-arylaminoacetals with Vilsmeier Reagents: An efficient route to highly functionalized quinolones and their benzo/hetero-fused analogues. *J. Org. Chem.* **2003**, *68*, 3966–3975. [CrossRef] [PubMed]
87. Danel, A.; Chaczatrian, K.; Tomasik, P. Microwave-assisted, facile route to 1H-pyrazolo[3,4-b]quinolines. *ARKIVOC* **2000**, *1*, 51–57. [CrossRef]
88. Kucharek, M.; Danel, A. Palladium catalysed amino group arylation of 1,3-disubstituted-1H-pyrazolo-5-amine based on Buchwald-Hartwig reaction. *Chem. Heterocycl. Compd.* **2021**, *57*, 633–639. [CrossRef]
89. Purnaprajna, V.; Seshadri, S. Studies in the Vilsmeier—Haack reaction: Part XII. Synthesis of the 2-phenylpyrazolo[3,4-b]quinoline system. *Indian J. Chem. Sect B* **1976**, *14B*, 971–972. [CrossRef]
90. Kucharek, M.; Danel, A.; Gut, A. Synthesis of 1,3,6-trisubstituted -1H-pyrazolo[3,4-b]quinolines based on intramolecular condensation of 5-N-aryl-1H-pyrazole-5-amine derivatives. *Chem. Heterocycl. Compd.* **2021**, submitted.
91. Yang, S.-W.; Smotryski, J.; McElroy, W.T.; Tan, Z.; Ho, G.; Tulshian, D.; Greeniee, W.J.; Guzzi, M.; Zhang, X.; Mullins, D.; et al. Discovery of orally active pyrazoloquinolines as potent PDE10 inhibitors for the management of schizophrenia. *Bioorg. Med. Lett.* **2012**, *22*, 235–239. [CrossRef]
92. Ho, G.D.; Yang, S.-W.; Smotryski, J.; Bercovici, A.; Nechuta, T.; Smith, E.M.; McElroy, W.; Tan, Z.; Tulshian, D.; McKittrick, B.; et al. The discovery of potent, selective, and orally active pyrazoloquinolines as potent PDE10A inhibitors for the treatment of Schizophrenia. *Bioorg. Med. Lett.* **2012**, *22*, 1019–1022. [CrossRef]
93. McElroy, W.T.; Tan, Z.; Basu, K.; Yang, S.-W.; Smotryski, J.; Ho, G.D.; Tulshian, D.; Greenlee, W.J.; Mullins, D.; Guzzi, M.; et al. Pyrazoloquinolines as PDE10A inhibitors: Discover of a tool compound. *Bioorg. Med. Lett.* **2012**, *22*, 1335–1339. [CrossRef]
94. Coutts, R.T.; Edwards, J.B. The preparation of 9-hydroxypyrazolo[3,4-b]quinolines. *Can. J. Chem.* **1966**, *44*, 2009–20014. [CrossRef]
95. Coutts, R.T.; El-Hawari, A.-M. Derivatives of 2-pyrazolin-5-one.V. Preparation and properties of 1',2'-dihydrospiro[[2]pyrazoline-4,3'(4'H)-quinoline]-5-one derivatives and related compounds. *Can. J. Chem.* **1977**, *55*, 2856–2866. [CrossRef]
96. Kametani, T.; Yamanaka, T.; Ogasawara, K. Nitrenes. Part IV. Synthesis of oxazolo[5,4-b]quinoline through a nitrene intermediate. *J. Chem. Soc. C* **1969**, 385–387. [CrossRef]
97. Nishiwaki, T.; Fukuhara, G.; Takahashi, T. Studies on heterocyclic chemistry. Part XVI. Reaction of 4-o-nitrobenzylidene - $\Delta^2$ -pyrazoli-5-ones with trialkyl phosphites: Synthesis of phosphorus-substituted pyrazolo[3,4-b]quinoline derivatives. *J. Chem. Soc. Perkin Trans. I* **1973**, *15*, 1606–1609. [CrossRef]
98. Danel, A.; Tomasik, P. Condensation of 2-nitrobenzaldehyde with pyrazolin-5-ones. Structure of 4-(2-nitrobenzylidene)pyrazolin-5-ones and their reductive cyclization. *Polish J. Chem.* **1995**, *69*, 1013–1017. [CrossRef]
99. DeWald, H. The synthesis of 4-(o-fluorophenyl)-6,8-dihydro-3,8-dimethyl-pyrazolo[3,4-e][1,4]diazepin-7(H)one, A metabolite of Zolazepam. *J. Heterocycl. Chem.* **1974**, *11*, 1061–1062. [CrossRef]
100. Shi, F.; Zhang, S.; Wu, S.-S.; Gao, Y.; Tu, S.-J. A diversity oriented synthesis of pyrazolo[4,3-f]quinoline derivatives with potential biactivities via microwave—Assisted multicomponent reactions. *Mol. Divers.* **2011**, *15*, 497–505. [CrossRef]
101. De Andrade, A.; Dos Santos, G.C.; Da Silva-Filho, L.C. Synthesis of quinoline derivatives by multicomponent reaction using niobium pentachloride as Lewis Acid. *J. Heterocycl. Chem.* **2015**, *52*, 273–277. [CrossRef]

102. Jiang, B.; Rajale, T.; Wever, W.; Tu, S.-J.; Li, G. Multicomponent reactions for the synthesis of heterocycles. *Chem. Asian. J.* **2010**, *5*, 2318–2335. [CrossRef]
103. Chebanov, V.A.; Gura, K.A.; Desenko, S.M. Aminoazoles as key reagents in multicomponent heterocyclizations. In *Synthesis of Heterocycles via Multicomponent Reactions I: Topics in Heterocyclic Chemistry*; Springer: Berlin/Heidelberg, Germany, 2010; Volume 23, pp. 41–84. [CrossRef]
104. Quiroga, J.; Insuasty, B.; Hormanza, A.; Saitz, C.; Jullian, C. Syntheses of 4-Aryl-4,7,8,9-tetrahydro-6H-pyrazolo[3,4-*b*]quinolin-5-ones. *J. Heterocycl. Chem.* **1998**, *35*, 575–578. [CrossRef]
105. Quiroga, J.; Mejia, D.; Insuasty, B.; Abonia, R.; Nogueras, M.; Sanchez, A.; Cobo, J.; Low, N.J. Regioselective synthesis of 4,7,8,9-tetrahydro-2H-pyrazolo[3,4-*b*]quinolin-5(6H)-ones. Mechanism and structural analysis. *Tetrahedron* **2001**, *57*, 6947–6953. [CrossRef]
106. Bhattacharjee, D.; Kshiar, B.; Myrboh, B. L-Proline as an efficient enantioinduction organocatalyst in the solvent-free synthesis of pyrazolo[3,4-*b*]quinoline derivatives via one-pot multicomponent reaction. *RSC Adv.* **2016**, *6*, 95944. [CrossRef]
107. Khumalo, M.R.; Maddila, S.N.; Maddila, S.; Jonnalagadda, S.B. A multicomponent, facile and catalyst-free microwave-assisted protocol for the synthesis of pyrazolo[3,4-*b*]quinolines under green conditions. *RSC Adv.* **2019**, *9*, 30768. [CrossRef]
108. Devi, L.; Nagraraju, K.; Maddila, S.; Jonnalagadda, S.B. A green, efficient protocol for the catalyst free synthesis of tetrahydro-1H-pyrazolo[3,4-*b*]quinolin-5(4H)-ones supported by ultrasonic irradiation. *Chem. Data Collect.* **2020**, *30*, 100566. [CrossRef]
109. Zahedifar, M.; Shojaei, R.; Sheibani, H. Convenient regioselective reaction in presence of H<sub>3</sub>PW<sub>12</sub>O<sub>40</sub>: Synthesis and characterization of pyrazolo[3,4-*b*]quinoline-3,5-diones. *Res. Chem. Intermed.* **2018**, *44*, 873–882. [CrossRef]
110. Zahedifar, M.; Pouramiri, B.; Razavi, R. Triethanolamine lactate-supported nanomagnetic cellulose: A green and efficient catalyst for the synthesis of pyrazolo[3,4-*b*]quinolines and theoretical study. *Res. Chem. Intermed.* **2020**, *46*, 2749–2765. [CrossRef]
111. Wang, H.-Y.; Shi, D.-Q. Three-component one-pot synthesis of pyrazolo[3,4-*b*]quinolin-5(6H)-one derivatives in aqueous media. *J. Heterocycl. Chem.* **2012**, *49*, 212–216. [CrossRef]
112. Kamakar, K.; Murthy, N.S.; Ramesh, K.; Satish, G.; Nanubolu, J.B.; Nageswar, Y.V.D. Polyethylene glycol (PEG-400): An efficient and recyclable reaction medium for the synthesis of pyrazolo[3,4-*b*]quinoline. *Tetrahedron Lett.* **2012**, *53*, 2897–2903. [CrossRef]
113. Tomasik, P.; Chaczatryan, K.; Chaczatryan, G.; Danel, A. Facile synthesis of 4-aryl-1H-pyrazolo[3,4-*b*]quinolines. *Polish J. Chem.* **2003**, *77*, 1141–1147.
114. Hu, Y.; Liu, Y.-F.; Zhang, J.; Zhang, Y.-Z.; Bi, F.-L. Synthesis of 1,3,4-triphenyl-1H-pyrazolo[3,4-*b*]quinoline derivatives under microwave irradiation. *Ziran Kexueban* **2012**, *42*, 241–244.
115. Hedge, H.; Shetty, N.S. Facile one-pot multicomponent synthesis of 1H-pyrazolo[3,4-*b*]quinolones using L-proline as a catalyst. *Chem. Heterocycl. Compd.* **2017**, *53*, 883–886. [CrossRef]
116. Jaing, B.; Zhang, G.; Ma, N.; Shi, F.; Tu, S.-J.; Kaur, P.; Li, G. A new rapid multicomponent domino reaction for the formation of functionalized benzo[*h*]pyrazolo[3,4-*b*]quinolines. *Org. Biomol. Chem.* **2011**, *9*, 3834–3838. [CrossRef]
117. Rajesh, S.M.; Bala, B.D.; Perumal, S.; Menedez, J.C. L-Proline—Catalysed sequential four component “on water” protocol for the synthesis of structurally complex heterocyclic ortho-quinones. *Green Chem.* **2011**, *13*, 3248–3254. [CrossRef]
118. Quiroga, J.; Diaz, Y.; Bueno, J.; Insuasty, B.; Abonia, R.; Ortiz, A.; Nogueras, M.; Cobo, J. Microwave induced three-component synthesis and antimicrobial activity of benzopyrazolo[3,4-*b*]quinolindiones. *Eur. J. Med. Chem.* **2014**, *74*, 216–224. [CrossRef] [PubMed]
119. Khalafy, J.; Arlan, F.M.; Marjani, A.P.; Sarchami, V. One-pot, three-component synthesis of polyfunctionalized benzo[*h*]pyrazolo[3,4-*b*][1,6]naphthyridine and benzo[*g*]pyrazolo[3,4-*b*]quinoline derivatives in the presence of silver nanoparticles (AgNPs). *J. Heterocycl. Chem.* **2020**, *57*, 3961–3969. [CrossRef]
120. Yadaw, R.; Parvin, T. Multicomponent synthesis of styryl linked benzo[*h*]pyrazolo[3,4-*b*]quinoline-5,6(10H)-diones by liquid assisted grinding. *New. J. Chem.* **2021**, *45*, 10388–10395. [CrossRef]
121. Polo, E.; Ferrer-Perutz, K.; Trilleras, J.; Quiroga, J.; Gutierrez, M. Microwave—Assisted one pot synthesis in water carbonylpyrazolo[3,4-*b*]pyridine derivatives catalysed by InCl<sub>3</sub> and sonochemical assisted condensation with aldehydes to obtain new chalcone derivatives containing the pyrazolopyridinic moiety. *RSC Adv.* **2017**, *7*, 50044–50055. [CrossRef]
122. Khurana, J.M.; Chaudhary, A.; Nand, B.; Lumb, A. Aqua mediated indium(II) chloride catalysed synthesis of fused pyrimidines and pyrazoles. *Tetrahedron Lett.* **2012**, *53*, 3018–3022. [CrossRef]
123. Wu, L.-Q.; Dong, R.-Y.; Yang, C.-G.; Yan, F.-L. Synthesis of 4-aryl-3-methyl-1-phenyl-1H-benzo[*h*]pyrazolo[3,4-*b*]quinoline-5,10-diones using diammonium hydrogen phosphate as an efficient and versatile catalyst in water. *J. Chin. Chem. Soc.* **2010**, *57*, 19–23. [CrossRef]
124. Re, Y.-M.; Jin, S.; Yan, H.-J.; Zhang, Z. PEG<sub>1000</sub>-Based dicationic acidic ionic liquid catalysed one-pot synthesis of 4-aryl-3-methyl-1-phenyl-1H-benzo[*h*]pyrazolo[3,4-*b*]quinoline-5,10-diones via multicomponent reactions. *Catalysis* **2015**, *5*, 1649–1656. [CrossRef]
125. Karamthulla, S.; Pal, S.; Parvin, T.; Choudhury, L.H. L-Proline catalysed multicomponent reactions: Facile access to 2H-benzo[*g*]pyrazolo[3,4-*b*]quinoline-5,10(4H,11H)-dione derivatives. *RSC Adv.* **2014**, *4*, 15319–15324. [CrossRef]
126. Yin, A.; Yang, L.; Wu, L. Synthesis of spiro[pyrazolo[3,4-*b*]pyridine-4,3'-indoline] and spiro[benzo[*h*]pyrazolo[3,4-*b*]quinoline-4,3'-indoline] derivatives using wet cyanuric chloride under solvent free condition. *J. Chem. Sci.* **2013**, *125*, 601–606. [CrossRef]
127. Dabiri, M.; Tisseh, Z.N.; Nobahar, M.; Bazgir, A. Organic reaction in water: A highly efficient and environmentally friendly synthesis of spiro compounds catalysed by L-proline. *Helv. Chim. Acta* **2011**, *94*, 824–830. [CrossRef]

128. Zhu, G.; Gao, L.; Yu, Q.; Qin, Y.; Xi, J.; Rong, L. An efficient synthesis of 1',7',8',9'-tetrahydrospiro[indoline-3,4'-pyrazolo[3,4-b]quinoline]2,5'(6'H)-dione derivatives in aqueous medium. *J. Heterocycl. Chem.* **2018**, *55*, 871–878. [CrossRef]
129. Baradarani, M.M.; Saatluo, B.; Ghabeli, S.; Shokri, Z.; Shahbazi, M.; Joule, J.A. Synthesis of hexahydrospiro[pyrazolo[3,4-b]quinoline-4,1'-pyrrolo[3,2,1-ij]quinoline-2',5'(1H,4'H)-diones] from 5,6 dihydro-4H-pyrrolo[3,2,1-ij]quinoline-1,2-dione using Fe<sub>3</sub>O<sub>4</sub>@Cu(OH)<sub>x</sub> as Nanoacatalyst. *J. Heterocycl. Chem.* **2019**, *56*, 1999–2007. [CrossRef]
130. Quiroga, J.; Portilla, J.; Serrano, H.; Abonia, R.; Insuasty, B.; Nogueras, M.; Cobo, J. Regioselective synthesis of fused benzopyrazolo[3,4-b]quinolines under solvent-free conditions. *Tetrahedron Lett.* **2007**, *48*, 1987–1990. [CrossRef]
131. Manickam, S.; Balijapalli, U.; Sathiyarayan, K.I. SnCl<sub>2</sub>-catalyzed synthesis of dihydro-5H-benzof[pyrazolo[3,4-b]quinoline and dihydroindeno[2,1-b]pyrazolo[4,3-e]pyridine with high fluorescence and their photophysical properties. *New. J. Chem.* **2018**, *42*, 860–871. [CrossRef]
132. Yadav, P.; Awasthi, A.; Gokulnath, S.; Tiwari, D.K. DMSO as a methine source in TFA-mediated one pot tandem regioselective synthesis of 3 substituted -1-aryl-1H-pyrazolo[3,4-b]quinolines from anilines and pyrazolones. *J. Org. Chem.* **2021**, *86*, 2658–2666. [CrossRef]
133. Pietrzycki, W.; Danel, A.; Tomasik, P. Quantum chemical ci-1 analysis of uv absorption spectra of 1h-pyrazolo[3,4-b]quinoline system. *Bull. Soc. Chim. Belges* **1994**, *103*, 725–741. [CrossRef]
134. Gondek, E.; Kościel, E.; Sanetra, J.; Danel, A.; Wisła, A.; Kityk, A.V. Optical absorption of 1H-pyrazolo[3,4-b]quinoline and its derivatives. *Spectrochim. Acta Part A Mol. Biomol. Spectrosc.* **2004**, *60*, 3101–3106. [CrossRef]
135. Gondek, E.; Kityk, I.V.; Sanetra, J.; Szlachcic, P.; Armatys, P.; Wisła, A.; Danel, A. New-synthesized pyrazoloquinoline as promising luminescent materials. *Optics Laser Technol.* **2006**, *38*, 487–492. [CrossRef]
136. Kościel, E.; Gondek, E.; Kityk, A.V. Optical absorption of 1-phenyl-3-methyl-1H-pyrazolo[3,4-b]quinoline derivatives: Molecular dynamics modeling. *Opt. Commun.* **2007**, *280*, 95–102. [CrossRef]
137. Kościel, E.; Gondek, E.; Pokładko, M.; Jarosz, B.; Vlokh, R.O.; Kityk, A.V. Photoluminescence of 1,3-dimethyl pyrazoloquinoline derivatives. *Mater. Chem. Phys.* **2009**, *114*, 860–867. [CrossRef]
138. Kościel, E.; Gondek, E.; Jarosz, B.; Danel, A.; Nizioł, J.; Kityk, A.V. Photoluminescence of 1-phenyl-3-methyl pyrazoloquinoline derivatives. *Spectrochim. Acta Part A Mol. Biomol. Spectrosc.* **2009**, *72*, 582–590. [CrossRef] [PubMed]
139. Yu, J.; He, K.; Li, Y.; Tan, H.; Zhu, M.; Wang, Y.; Liu, Y.; Zhu, W.; Wu, H. A novel near-infrared-emitting cyclometalated platinum (II) complex with donor–acceptor–acceptor chromophores. *Dyes Pigment.* **2014**, *107*, 146–152. [CrossRef]
140. Slodek, A.; Matussek, M.; Filapek, M.; Szafraniec-Gorol, G.; Szłapa, A.; Grudzka-Flak, I.; Szczurek, M.; Malecki, J.G.; Maron, A.; Schab-Balcerzak, E.; et al. Small Donor-Acceptor Molecules Based on a Quinoline-Fluorene System with Promising Photovoltaic Properties. *Eur. J. Org. Chem.* **2016**, *2016*, 2500–2508. [CrossRef]
141. Yan, Z.; Guang, S.; Xu, H.; Liu, X.-Y. Quinoline-based azo derivative assembly: Optical limiting property and enhancement mechanism. *Dyes Pigment.* **2013**, *99*, 720–726. [CrossRef]
142. dos Santos, G.C.; Servilha, R.O.; de Oliveira, E.F.; Lavarda, F.C.; Ximenes, V.F.; da Silva-Filho, L.C. Theoretical-Experimental Photophysical Investigations of the Solvent Effect on the Properties of Green- and Blue-Light-Emitting Quinoline Derivatives. *J. Fluoresc.* **2017**, *27*, 1709–1720. [CrossRef]
143. Goel, A.; Kumar, V.; Singh, S.P.; Sharma, A.; Prakash, S.; Singh, C.; Anand, R.S. Non-aggregating solvatochromic bipolar benzof[quinolines and benzo[a]acridines for organic electronics. *J. Mater. Chem.* **2012**, *22*, 14880. [CrossRef]
144. EL-Shabaan, M.M.; Gaml, E.A. Fluorescent quinoline carboxylate derivative: Study on the optical properties and photo diode application. *Phys. B Condens. Matter* **2022**, *626*, 413578. [CrossRef]
145. Onozawa-Komatsuzaki, N.; Funaki, T.; Kasuga, K.; Nakazawa, Y.; Sayama, K.; Sugihara, H. Synthesis and Electrochemical Properties of 2,6-Bis(quinoline-2-yl)pyridyl Ruthenium Complexes as Near-Infrared Sensitizers for Dye-Sensitized Solar Cells. *Jpn. J. Appl. Phys.* **2012**, *51*, 10NE11. [CrossRef]
146. Lanke, S.K.; Sekar, N. Pyrazole based NLOphores: Synthesis, photophysical, DFT, TDDFT studies. *Dye. Pigment.* **2016**, *127*, 116–127. [CrossRef]
147. Barberá, J.; Clays, K.; Giménez, R.; Houbrechts, S.; Persoons, A.; Serrano, J.L. Versatile optical materials: Fluorescence, non-linear optical and mesogenic properties of selected 2-pyrazoline derivatives. *J. Mater. Chem.* **1998**, *8*, 1725–1730. [CrossRef]
148. Willy, B.; Müller, T.J.J. Rapid One-Pot, Four-Step Synthesis of Highly Fluorescent 1,3,4,5-Tetrasubstituted Pyrazoles. *Org. Lett.* **2011**, *13*, 2082–2085. [CrossRef] [PubMed]
149. Götzinger, A.C.; Theßeling, F.A.; Hoppe, C.; Müller, T.J.J. One-Pot Coupling–Coupling–Cyclocondensation Synthesis of Fluorescent Pyrazoles. *J. Org. Chem.* **2016**, *81*, 10328–10338. [CrossRef]
150. Castillo, J.-C.; Tigreros, A.; Portilla, J. 3-Formylpyrazolo[1,5-a]pyrimidines as Key Intermediates for the Preparation of Functional Fluorophores. *J. Org. Chem.* **2018**, *83*, 10887–10897. [CrossRef] [PubMed]
151. Taydakov, I.V.; Akkuzina, A.A.; Avetisov, R.I.; Khomyakov, A.V.; Saifutayrov, R.R.; Avetissov, I.C. Effective electroluminescent materials for OLED applications based on lanthanide 1,3-diketones bearing pyrazole moiety. *J. Lumin.* **2016**, *177*, 31–39. [CrossRef]
152. Lewińska, G.; Khachatryan, K.; Danel, K.S.; Danel, Z.; Sanetra, J.; Marszałek, K.W. Investigations of the Optical and Thermal Properties of the Pyrazoloquinoline Derivatives and Their Application for OLED Design. *Polymers* **2020**, *12*, 2707. [CrossRef] [PubMed]

153. García, M.; Romero, I.; Portilla, J. Synthesis of Fluorescent 1,7-Dipyridyl-bis-pyrazolo[3,4-b:4',3'-e]pyridines: Design of Reversible Chemosensors for Nanomolar Detection of Cu 2+. *ACS Omega* **2019**, *4*, 6757–6768. [CrossRef]
154. Orrego-Hernández, J.; Lizarazo, C.; Cobo, J.; Portilla, J. Pyrazolo-fused 4-azafluorenones as key reagents for the synthesis of fluorescent dicyanovinylidene-substituted derivatives. *RSC Adv.* **2019**, *9*, 27318–27323. [CrossRef]
155. Kanwal, I.; Rasool, N.; Zaidi, S.H.M.; Zakaria, Z.A.; Bilal, M.; Hashmi, M.A.; Mubarak, A.; Ahmad, G.; Shah, S.A.A. Synthesis of Functionalized Thiophene Based Pyrazole Amides via Various Catalytic Approaches: Structural Features through Computational Applications and Nonlinear Optical Properties. *Molecules* **2022**, *27*, 360. [CrossRef]
156. Bhalekar, S.; Bhagwat, A.; Sekar, N. 3 Fluorescent styryl chromophores with rigid (pyrazole) donor and rigid (benzothiophene-dioxide) acceptor—Complete density functional theory (DFT), TDDFT and nonlinear optical study. In *Computational Chemistry*; De Gruyter: Berlin, Germany, 2021; pp. 33–60.
157. Makowska-Janusik, M.; Gondek, E.; Kityk, I.V.; Wisła, J.; Sanetra, J.; Danel, A. Second-order optical effects in several pyrazoloquinoline derivatives. *Chem. Phys.* **2004**, *306*, 265–271. [CrossRef]
158. Nizioł, J.; Danel, A.; Boiteux, G.; Davenas, J.; Jarosz, B.; Wisła, A.; Seytre, G. Optical properties of new pyrazolo[3,4-b] quinoline and its composites. *Synth. Met.* **2002**, *127*, 175–180. [CrossRef]
159. Gašiorski, P.; Danel, K.S.; Matusiewicz, M.; Uchacz, T.; Vlokh, R.; Kityk, A.V. Synthesis and Spectroscopic Study of Several Novel Annulated Azulene and Azafluoranthene Based Derivatives. *J. Fluoresc.* **2011**, *21*, 443–451. [CrossRef] [PubMed]
160. Misra, R.; Bhattacharyya, S.P. *Intramolecular Charge Transfer: Theory and Applications*; Wiley-VCH Verlag GmbH & Co. KGaA: Weinheim, Germany, 2018; ISBN 978-3-527-34156-6.
161. Grabowski, Z.R.; Rotkiewicz, K.; Rettig, W. Structural Changes Accompanying Intramolecular Electron Transfer: Focus on Twisted Intramolecular Charge-Transfer States and Structures. *Chem. Rev.* **2003**, *103*, 3899–4032. [CrossRef] [PubMed]
162. Gondek, E.; Danel, A.; Nizioł, J.; Armatys, P.; Kityk, I.V.; Szlachcic, P.; Karelus, M.; Uchacz, T.; Chwast, J.; Lakshminarayana, G. Some spirobiindane based 1H-pyrazolo[3,4-b] quinoline chromophore as novel chromophore for light-emitting diodes. *J. Lumin.* **2010**, *130*, 2093–2099. [CrossRef]
163. Kolbus, A.; Grabka, D.; Danel, A.; Szary, K. Spectral properties of 1H-pyrazolo[3,4-b]quinoline substituted with *N,N*-diethylamine moiety. *Opt. Mater.* **2016**, *57*, 102–106. [CrossRef]
164. Rettig, W. Photoinduced charge separation via twisted intramolecular charge transfer states. In *Electron Transfer I. Topics in Current Chemistry*; Springer-Verlag GmbH: Berlin, Heidelberg, Germany, 1994; pp. 253–299.
165. Grabowski, Z.R.; Rotkiewicz, K.; Siemiarczuk, A. Dual fluorescence of donor-acceptor molecules and the Twisted Intramolecular Charge Transfer (ICT) states. *J. Lumin.* **1979**, *18–19*, 420–424. [CrossRef]
166. Michl, J. Electronic structure of aromatic  $\pi$ -electron systems as reflected in their MCD spectra. *Pure Appl. Chem.* **1980**, *52*, 1549–1563. [CrossRef]
167. Miura, T.; Urano, Y.; Tanaka, K.; Nagano, T.; Ohkubo, K.; Fukuzumi, S. Rational Design Principle for Modulating Fluorescence Properties of Fluorescein-Based Probes by Photoinduced Electron Transfer. *J. Am. Chem. Soc.* **2003**, *125*, 8666–8671. [CrossRef]
168. Fox, M.A. Photoinduced Electron Transfer. *Photochem. Photobiol.* **1990**, *52*, 617–627. [CrossRef]
169. Rurack, K.; Resch-Genger, U. Rigidization, preorientation and electronic decoupling—the ‘magic triangle’ for the design of highly efficient fluorescent sensors and switches. *Chem. Soc. Rev.* **2002**, *31*, 116–127. [CrossRef]
170. Mu, L.; He, Z.; Kong, X.; Liang, C.; Wang, Y.; Danel, A.; Kulig, E.; Milburn, G.H.W. Towards Color Stable Blue Primary for Displays: Suppress Field-Dependent Color Change in a Multilayered Electroluminescent Device. *J. Disp. Technol.* **2011**, *7*, 96–104. [CrossRef]
171. Gašiorski, P.; Gondek, E.; Danel, K.S.; Pokladko-Kowar, M.; Armatys, P.; Kityk, A.V. Green electroluminescence from azafluoranthene derivatives in polymer based electroluminescent devices. *Opt. Mater.* **2013**, *35*, 681–684. [CrossRef]
172. Jaglarz, J.; Kępińska, M.; Sanetra, J. Thermo-optical properties of 1H[3,4-b] quinoline films used in electroluminescent devices. *Opt. Mater.* **2014**, *36*, 1275–1280. [CrossRef]
173. Tao, Y.T.; Balasubramaniam, E.; Danel, A.; Wisła, A.; Tomasik, P. Pyrazoloquinoline derivatives as efficient blue electroluminescent materials. *J. Mater. Chem.* **2001**, *11*, 768–772. [CrossRef]
174. Danel, K.S.; Gondek, E.; Pokladko, M.; Kityk, I.V. 4-(*p-N,N*-Diarylphenyl)substituted 1H-pyrazolo[3,4-b]quinolines as novel luminophors for organic light emitting diode—synthesis, electroluminescent devices. *J. Mater. Sci. Mater. Electron.* **2009**, *20*, 171–176. [CrossRef]
175. Mac, M.; Uchacz, T.; Danel, A.; Musiolik, H. Applications of Fluorescent Sensor Based on 1H-pyrazolo[3,4-b]quinoline in Analytical Chemistry. *J. Fluoresc.* **2013**, *23*, 1207–1215. [CrossRef]
176. Mac, M.; Uchacz, T.; Wróbel, T.; Danel, A.; Kulig, E. New Fluorescent Sensors Based on 1H-pyrazolo[3,4-b]quinoline Skeleton. *J. Fluoresc.* **2010**, *20*, 525–532. [CrossRef]
177. Mac, M.; Uchacz, T.; Danel, A.; Danel, K.; Kolek, P.; Kulig, E. A New Fluorescent Sensor Based on 1H-pyrazolo[3,4-b]quinoline Skeleton. Part 2. *J. Fluoresc.* **2011**, *21*, 375–383. [CrossRef]
178. Uchacz, T.; Szlachcic, P.; Wojtasik, K.; Mac, M.; Stadnicka, K. Amino derivatives of 1,3-diphenyl-1H-pyrazolo[3,4-b]quinoline—Photophysics and implementation of molecular logic switches. *Dyes Pigment.* **2016**, *124*, 277–292. [CrossRef]
179. Paisley, N.R.; Tonge, C.M.; Hudson, Z.M. Stimuli-Responsive Thermally Activated Delayed Fluorescence in Polymer Nanoparticles and Thin Films: Applications in Chemical Sensing and Imaging. *Front. Chem.* **2020**, *8*, 229. [CrossRef]

180. Gerasimova, M.A.; Tomilin, F.N.; Malyar, E.Y.; Varganov, S.A.; Fedorov, D.G.; Ovchinnikov, S.G.; Slyusareva, E.A. Fluorescence and photoinduced proton transfer in the protolytic forms of fluorescein: Experimental and computational study. *Dyes Pigment.* **2020**, *173*, 107851. [CrossRef]
181. Meng, X.; You, L.; Li, S.; Sun, Q.; Luo, X.; He, H.; Wang, J.; Zhao, F. An ICT-based fluorescence enhancement probe for detection of Sn<sup>2+</sup> in cancer cells. *RSC Adv.* **2020**, *10*, 37735–37742. [CrossRef]
182. Sasaki, S.; Drummen, G.P.C.; Konishi, G. Recent advances in twisted intramolecular charge transfer (TICT) fluorescence and related phenomena in materials chemistry. *J. Mater. Chem. C* **2016**, *4*, 2731–2743. [CrossRef]
183. Yan, C.; Guo, Z.; Chi, W.; Fu, W.; Abedi, S.A.A.; Liu, X.; Tian, H.; Zhu, W.-H. Fluorescence upconverting enables light-up sensing of N-acetyltransferases and nerve agents. *Nat. Commun.* **2021**, *12*, 3869. [CrossRef] [PubMed]
184. Jacobi, P.A. *Introductory Heterocyclic Chemistry*; John Wiley & Sons: Hoboken, NJ, USA, 2018; ISBN 978-1-119-41759-0.
185. Kerru, N.; Gummidi, L.; Maddila, S.; Gangu, K.K.; Jonnalagadda, S.B. A Review on Recent Advances in Nitrogen-Containing Molecules and Their Biological Applications. *Molecules* **2020**, *25*, 1909. [CrossRef] [PubMed]
186. Heravi, M.M.; Zadsirjan, V. Prescribed drugs containing nitrogen heterocycles: An overview. *RSC Adv.* **2020**, *10*, 44247–44311. [CrossRef]
187. Graeve, R.E.; Pociask, J.R.; Stein, R.G. Dialkylamino Alkylamino Pyrazolo(3,4b) quinolines. U.S. Patent 3600393A, 17 August 1971.
188. De Andrea, M.; Ravera, R.; Gioia, D.; Gariglio, M.; Landolfo, S. The interferon system: An overview. *Eur. J. Paediatr. Neurol.* **2002**, *6* (Suppl. A), A41–A46. [CrossRef] [PubMed]
189. Bagheri, A.; Moezzi, S.M.I.; Mosaddeghi, P.; Parashkouhi, S.N.; Hoseini, S.M.F.; Badakhshan, F.; Negahdaripour, M. Interferon-inducer antivirals: Potential candidates to combat COVID-19. *Int. Immunopharmacol.* **2021**, *91*, art.107245. [CrossRef]
190. Siminoff, P.; Bernard, A.M.; Hursky, V.S.; Price, K.E. BL-20803, a New, Low-Molecular-Weight Interferon Inducer. *Antimicrob. Agents Chemother.* **1973**, *3*, 742–743. [CrossRef]
191. Siminoff, P. Target Cells for Interferon Induction by BL-20803. *J. Infect. Dis.* **1976**, *133*, A37–A42. [CrossRef]
192. Siminoff, P.; Crenshaw, R.R. Simulation of Interferon Production in Mice and in Mouse Spleen Leukocytes by Analogues of BL-20803. *Antimicrob. Agents Chemother.* **1977**, *11*, 571–573. [CrossRef] [PubMed]
193. Kern, E.R.; Hamilton, J.R.; Overall, J.C.; Glasgow, L.A. Antiviral Activity of BL-3849A, a Low-Molecular-Weight Oral Interferon Inducer. *Antimicrob. Agents Chemother.* **1976**, *10*, 691–696. [CrossRef] [PubMed]
194. Rádl, S.; Zikán, V.; Šmejkal, F. Příprava některých 4-anilino-1,3-dimethyl-1H-pyrazolo(3,4-b)chinolinů s protivirovým účinkem. *Ceskoslov. Farm.* **1984**, *33*, 429–432.
195. Rádl, S.; Zikán, V.; Šmejkal, F. Syntheses of 1, 2, and 9-methyl derivatives of 4,9-dihydro-3-methyl-4-oxo-1H(2H)-pyrazolo[3,4-b]quinoline and their antiviral activity. *Coll. Czechoslov. Chem. Commun.* **1985**, *50*, 1057–1063. [CrossRef]
196. Rádl, S.; Zikán, V.; Šmejkal, F. Příprava některých 4-fenoxy- a 4-fenylotioderivátů 1H-pyrazolo/3,4-b/chinolinu s protivirovým účinkem. *Ceskoslov. Farm.* **1985**, *34*, 119–122.
197. Rádl, S.; Roubínek, F.; Šmejkal, F.; Zikán, V. Příprava některých 1-substituovaných 4-dialkylaminoalkylamino-3-methyl-1H-pyrazolo/3,4-b/chinolinů s protivirovým účinkem. *Ceskoslov. Farm.* **1985**, *34*, 190–193.
198. Rádl, S.; Zikán, V.; Šmejkal, F. Příprava 4-(hydroxyanilino)-a4-(alkoxyanilino)derivátů 1,3-dimethyl-1H-pyrazolo/3,4-b/chinolinu s potenciálním protivirovým účinkem. *Ceskoslov. Farm.* **1985**, *34*, 383–385.
199. Rádl, S.; Roubínek, F.; Zikán, V.; Šmejkal, F. Příprava některých 1-substituovaných 4-alkylamin-3-methyl-1H-pyrazolo(3,4-b)chinolinů s potenciálním protivirovým účinkem. *Ceskoslov. Farm.* **1986**, *34*, 105–109.
200. Rádl, S.; Zikán, V. Syntheses of 1, 2, and 9-methyl derivatives of 4,9-dihydro-6-methoxy-3-methyl-4-oxo-1H(2H)-pyrazolo[3,4-b]quinoline and 4,9-dihydro-6-hydroxy-3-methyl-4-oxo-1H(2H)-pyrazolo[3,4-b]quinoline and their antiviral activity. *Coll. Czechoslov. Chem. Commun.* **1987**, *52*, 788–792. [CrossRef]
201. Rádl, S.; Zikán, V. Synthesis and biological activity of some basic-substituted 4,9-dihydro-3-methyl-4-oxo-1H(2H)-pyrazolo[3,4-b]quinolines. *Coll. Czechoslov. Chem. Commun.* **1988**, *53*, 1812–1819. [CrossRef]
202. Zikán, V.; Rádl, S.; Šmejkal, F.; Zelená, D. Substituované 4-anilino-1,3-dimethyl-1H-pyrazolo/3,4-b/chinoliny a Způsoby Jejich Přípravy. CS Patent 233445B1, 14 March 1985.
203. Zikán, V.; Rádl, S.; Šmejkal, F.; Zelená, D. Substituované 4,9-dihydro-3-methyl-4-oxo-1H-pyrazolo(3,4-b)chinoliny a Spůsob Jejich Výroby. CS Patent 235167B1, 15 May 1985.
204. Zikán, V.; Rádl, S. Substituované 4-fenoxy-3-methyl-1H-pyrazolo(3,4-b)chinoliny a Způsoby Jejich Přípravy. CS Patent 235176B1, 15 May 1985.
205. Zikán, V.; Rádl, S.; Šmejkal, F.; Zelená, D. 4-Karboxyalkylamino-1,3-dimethyl-1H-pyrazolo(3,4-b)chinoliny a Způsob Jejich Přípravy. CS Patent 235177B1, 15 May 1985.
206. Zikán, V.; Rádl, S. 4-Chlor-6-methoxy-3-methyl-1H-pyrazolo(3,4-b)chinolin a Jeho N1-methylderivát. CS Patent 252340B1, 13 August 1987.
207. Zikán, V.; Rádl, S. O,N-substituované 4,9-dihydro-6-hydroxy-1,3-dimethyl-4-oxo-1H-pyrazolo(3,4-b)chinoliny. CS Patent 252341B1, 13 August 1987.
208. Zikán, V.; Rádl, S.; Šmejkal, F. 4,9-dihydro-6-methoxy-3-methyl-4-oxo-1H-pyrazolo(3,4-b)chinolin. CS Patent 252621B1, 17 September 1987.
209. Chinthia, C.; Gupta, N.; Ghate, M.; Vyas, V.K. Homology modeling, binding site identification, and docking study of human  $\beta$ -arrestin: An adaptor protein involved in apoptosis. *Med. Chem. Res.* **2014**, *23*, 1189–1201. [CrossRef]





210. Vyas, V.K.; Qureshi, G.; Dayani, H.; Jha, A.; Ghate, M. Pharmacophore-based identification and in vitro validation of apoptosis inducers as anticancer agents. *SAR QSAR Environmental Res.* **2020**, *31*, 869–881. [CrossRef] [PubMed]
211. Kemnitzer, W.; Kuemmerle, J.; Zhang, H.-Z.; Kasibhatla, S.; Tseng, B.; Drewe, J.; Cai, S.X. Discovery of 3-aryl-5-aryl-1,2,4-oxadiazoles as a new series of apoptosis inducers. 2. Identification of more aqueous soluble analogs as potential anticancer agents. *Bioorg. Med. Chem. Lett.* **2009**, *19*, 4410–5515. [CrossRef] [PubMed]
212. Afonso, A.; Kelly, J.M.; Chackalamannil, S. 4-Substituted Pyrazoloquinoline Derivatives. U.S. Patent 5506236A, 9 April 1996.
213. Albin, R.; Chase, R.; Risano, C.; Lieberman, M.; Ferrari, E.; Skelton, A.; Buontempo, P.; Cox, S.; DeMartino, J.; Wright-Minogue, J.; et al. SCH 43478 and analogs: In vitro activity and in vivo efficacy of novel agents for herpesvirus type 2. *Antiviral Res.* **1997**, *35*, 139–146. [CrossRef]
214. Bell, M.R.; Ackerman, J.H. Pyrazolo[3,4-b]quinolines and Their Use as Antiviral Agents. U.S. Patent 4920128A, 24 April 1990.
215. Bekhit, A.A.; El-Sayed, O.A.; Aboul-Enein, H.Y.; Siddiqui, Y.M.; Al-Ahdal, M.N. Synthesis of Aldehyde-sugar Derivatives of Pyrazoloquinoline as Inhibitors of Herpes Simplex Virus Type 1 Replication. *J. Enzym. Inhib. Med. Chem.* **2004**, *19*, 33–38. [CrossRef]
216. Bekhit, A.A.; El-Sayed, O.A.; Aboul-Enein, H.Y.; Siddiqui, Y.M.; Al-Ahdal, M.N. Evaluation of Some Pyrazoloquinolines as Inhibitors of Herpes Simplex Virus Type 1 Replication. *Arch. Pharm.* **2005**, *338*, 74–77. [CrossRef]
217. Arif, J.M.; Kunhi, M.; Subramanian, M.P.; Bekhit, A.A.; El-Sayed, O.A.; Al-Hussein, K.; Aboul-Enein, H.Y.; Al-Khodairy, F.M. Evaluation of Cytotoxic Potential of Newly Synthesized Antiviral Aminopyrazoloquinoline Derivatives. *Int. J. Biomedical Sci.* **2007**, *3*, 194–198.
218. Arif, J.M.; Kunhi, M.; Subramanian, M.P.; Bekhit, A.A.; El-Sayed, O.A.; Al-Hussein, K.; Aboul-Enein, H.Y.; Al-Khodairy, F.M. Cytotoxic and genotoxic potentials of newly synthesized antiviral aminopyrazoloquinoline derivatives. *Med. Chem. Res.* **2008**, *17*, 297–304. [CrossRef]
219. Shuck-Lee, D.; Chen, F.F.; Willard, R.; Raman, S.; Ptak, R.; Hammarskjöld, M.-L.; Rekosh, D. Heterocyclic Compounds That Inhibit Rev-RRE Function and Human Immunodeficiency Virus Type 1 Replication. *Antimicrob. Agents Chemother.* **2008**, *52*, 3169–3179. [CrossRef]
220. Magiorakos, A.-P.; Srinivasan, A.; Carey, R.B.; Carmeli, Y.; Falagas, M.E.; Giske, C.G.; Harbarth, S.; Hindler, J.F.; Kahlmeter, G.; Olsson-Liljequist, B.; et al. Multidrug-resistant, extensively drug-resistant and pandrug-resistant bacteria: An international expert proposal for interim standard definitions for acquired resistance. *Clin. Microbiol. Infect.* **2012**, *18*, 268–281. [CrossRef]
221. El-Sayed, O.A.; Aboul-Enein, H.Y. Synthesis and Antimicrobial Activity of Novel Pyrazolo[3,4-b]quinoline Derivatives. *Arch. Pharm.* **2001**, *334*, 117–120. [CrossRef]
222. Lapa, G.B.; Bekker, O.B.; Mirchink, E.P.; Danilenko, V.N.; Preobrazhenskaya, M.N. Regioselective acylation of congeners of 3-amino-1H-pyrazolo[3,4-b]quinolines, their activity on bacterial serine/threonine protein kinases and in vitro antibacterial (including antimycobacterial) activity. *J. Enzym. Inhib. Med. Chem.* **2012**, *28*, 1088–1093. [CrossRef] [PubMed]
223. Nurgali, K.; Jagoe, R.T.; Abalo, R. Editorial: Adverse Effects of Cancer Chemotherapy: Anything New to Improve Tolerance and Reduce Sequelae? *Front. Pharmacol.* **2018**, *9*, 245. [CrossRef] [PubMed]
224. Garattini, S.; Bertele, V. Efficacy, safety, and cost of new anticancer drugs. *BMJ* **2002**, *325*, 269–271. [CrossRef]
225. Karthikeyan, C.; Amawi, H.; Viana, A.G.; Sanglard, L.; Hussein, N.; Saddler, M.; Ashby, C.R., Jr.; Moorthy, N.S.H.N.; Trivedi, P.; Tiwari, A.K. 1H-Pyrazolo[3,4-b]quinoline-3-amine derivatives inhibit growth of colon cancer cells via apoptosis and sub G1 cell cycle arrest. *Bioorg. Med. Chem. Lett.* **2018**, *28*, 2244–2249. [CrossRef]
226. Karthikeyan, C.; Malla, R.; Ashby, C.R., Jr.; Amawi, H.; Abbott, K.L.; Moore, J.; Chen, J.; Balch, C.; Lee, C.; Flannery, P.C.; et al. Pyrimido[1'',2'':1,5]pyrazolo[3,4-b]quinolines: Novel compounds that reverse ABCG2-mediated resistance in cancer cells. *Cancer Lett.* **2016**, *376*, 118–126. [CrossRef]
227. Goodsell, D.S. The Molecular Perspective: The *ras* Oncogene. *The Oncologist* **1999**, *4*, 263–264. [CrossRef]
228. Downward, J. Targeting RAS signaling pathways in cancer therapy. *Nat. Rev. Cancer* **2003**, *3*, 11–22. [CrossRef]
229. Kumar, C.C.; Prorock-Rogers, C.; Kelly, J.; Dong, Z.; Lin, J.-J.; Armstrong, L.; Kung, H.-F.; Weber, M.J.; Afonso, A. SCH 51344 Inhibits *ras* Transformation by a Novel Mechanism. *Cancer Res.* **1995**, *55*, 5106–5117.
230. Walsh, A.B.; Dhanasekaran, M.; Bar-Sagi, D.; Kumar, C.C. SCH 51344-induced reversal of RAS-transformation is accompanied by the specific inhibition of the RAS and RAC-dependent cell morphology pathway. *Oncogene* **1997**, *15*, 2553–2560. [CrossRef]
231. Kumar, C.C.; Ohashi, K.; Nagata, K.; Walsh, A.; Bar-Sagi, D.; Mizuno, K. SCH 51344, An Inhibitor of RAS/RAC-Mediated Cell Morphology Pathway. *Ann. N. Y. Acad. Sci.* **1999**, *886*, 122–131. [CrossRef] [PubMed]
232. Kumar, C.C. Inhibition of RAS-transformation by SCH51344. *Gan Kagaku Ryoho (Jpn. J. Cancer Chemother.)* **1997**, *24*, 1503–1511.
233. Gelman, I.H.; Xi, Q.; Kumar, C.C. Reexpression of the Major PKC Substrate, SSeCKS, Correlates with the Tumor-Suppressive Effects of SCH51344 on Rat-6/*src* and Rat-6/*ras* Fibroblasts but Not on Rat-6/*raf* Fibroblasts. *Ann. N. Y. Acad. Sci.* **1999**, *886*, 221–224. [CrossRef] [PubMed]
234. Huber, K.V.M.; Salah, E.; Radic, B.; Gridling, M.; Elkins, J.M.; Stukalov, A.; Jemth, A.-S.; Göktürk, C.; Sanjiv, K.; Strömberg, K.; et al. Stereospecific targeting of MTH1 by (S)-crizotinib as an anticancer strategy. *Nature* **2014**, *508*, 222–227. [CrossRef]
235. Huber, K.; Superti-Furga, G. Aminoheteroaryl Compounds as MTH1 Inhibitors. WO Patent 2014/033136A1, 6 March 2014.
236. Ursu, A.; Waldmann, H. Hide and seek: Identification and confirmation of small molecule protein targets. *Bioorg. Med. Chem. Lett.* **2015**, *25*, 3079–3086. [CrossRef]
237. SCH 51344, Cat. No. 5280. Available online: [https://www.tocris.com/products/sch-51344\\_5280](https://www.tocris.com/products/sch-51344_5280) (accessed on 1 March 2022).

238. Nieborowska-Sikorska, M.; Maifrede, S.; Dasgupta, Y.; Sullivan, K.; Flis, S.; Le, B.V.; Solecka, M.; Belyaeva, E.A.; Kubovcakova, L.; Nawrocki, M.; et al. Ruxolitinib-induced defects in DNA repair cause sensitivity to PARP inhibitors in myeloproliferative neoplasms. *Blood* **2017**, *130*, 2848–2859. [CrossRef]
239. Kawamura, T.; Kawatani, M.; Muroi, M.; Kondoh, Y.; Futamura, Y.; Aono, H.; Tanaka, M.; Honda, K.; Osada, H. Proteomic profiling of small-molecule inhibitors reveals dispensability of MTH1 for cancer cell survival. *Sci. Rep.* **2016**, *6*, art.26521. [CrossRef]
240. Papeo, G. MutT Homolog 1 (MTH1): The Silencing of a Target. *J. Med. Chem.* **2016**, *59*, 2343–2345. [CrossRef]
241. Zhou, N.; Xu, Y.; Liu, X.; Wang, Y.; Peng, J.; Luo, X.; Zheng, M.; Chen, K.; Jiang, H. Combinatorial Pharmacophore-Based 3D-QSAR Analysis and Virtual Screening of FGFR1 Inhibitors. *Int. J. Mol. Sci.* **2015**, *16*, 13407–13425. [CrossRef]
242. Huber, K.; Superti-Furga, G. Aminoheteroaryl Compounds as MTH1 Inhibitors. U.S. Patent 2016/0015702A1, 21 January 2016.
243. Bökel, C.; Weidemann, T. Methods and Compositions for Reducing Interleukin-4 or Interleukin-13 Signaling. U.S. Patent 2013/0084275A1, 4 April 2013.
244. Wolin, R.; Wang, D.; Kelly, J.; Afonso, A.; James, L.; Kirschmeier, P.; McPhail, A.T. Synthesis and evaluation of pyrazolo[3,4-b]quinoline ribofuranosides and their derivatives as inhibitors of oncogenic Ras. *Bioorg. Med. Chem. Lett.* **1996**, *6*, 195–200. [CrossRef]
245. Wolin, R.L.; Afonso, A.; Kelly, J.M.; Njoroge, F.G. Pyrazoloquinolines. U.S. Patent 5,595,998A, 21 January 1997.
246. Wolin, R.L.; Afonso, A. Pyrazoloquinolines. U.S. Patent 5597821A, 28 January 1997.
247. Kaufmann, S.H.; Earnshaw, W.C. Induction of Apoptosis by Cancer Chemotherapy. *Exp. Cell Res.* **2000**, *256*, 42–49. [CrossRef] [PubMed]
248. Al-Qahtani, A.; Siddiqui, Y.M.; Bekhit, A.A.; El-Sayed, O.A.; Aboul-Enein, H.Y.; Al-Ahdal, M.N. Effect of Pyrazoloquinoline Derivatives on the Growth of Leishmania donovani Promastigotes. *Arch. Pharm.* **2005**, *338*, 484–487. [CrossRef] [PubMed]
249. Javitt, D.C. Balancing therapeutic safety and efficacy to improve clinical and economic outcomes in schizophrenia: A clinical review. *Am. J. Manag. Care* **2014**, *20* (Suppl. 8), 160–165.
250. Lally, J.; MacCabe, J.H. Antipsychotic medication in schizophrenia: A review. *Br. Med. Bull.* **2015**, *114*, 169–179. [CrossRef] [PubMed]
251. Wu, Q.; Gao, Q.; Guo, H.; Li, D.; Wang, J.; Gao, W.; Han, C.; Li, Y.; Yang, L. Inhibition mechanism exploration of quinoline derivatives as PDE10A inhibitors by in silico analysis. *Mol. BioSyst.* **2013**, *9*, 386–397. [CrossRef] [PubMed]
252. Kjellgren, E.R.; Glue, O.E.S.; Reinholdt, P.; Meyer, J.E.; Kongsted, J.; Poongavanam, V. A comparative study of binding affinities for 6,7-dimethoxy-4-pyrrolidylquinoxalines as phosphodiesterase 10A inhibitors using the linear interaction energy method. *J. Mol. Graph. Model.* **2015**, *61*, 44–52. [CrossRef] [PubMed]
253. Khan, M.A.B.; Hashim, M.J.; King, J.K.; Govender, R.D.; Mustafa, H.; Al Kaabi, J. Epidemiology of Type 2 Diabetes—Global Burden of Disease and Forecasted Trends. *J. Epidemiol. Glob. Health* **2020**, *10*, 107–111. [CrossRef] [PubMed]
254. Yung, J.H.M.; Giacca, A. Role of c-Jun N-terminal Kinase (JNK) in Obesity and Type 2 Diabetes. *Cells* **2020**, *9*, 706. [CrossRef]
255. Liu, M.; Xin, Z.; Clampitt, J.E.; Wang, S.; Gum, R.J.; Haasch, D.L.; Trevillyan, J.M.; Abad-Zapatero, C.; Fry, E.H.; Sham, H.L.; et al. Synthesis and SAR of 1,9-dihydro-9-hydroxypyrazolo[3,4-b]quinoline-4-ones as novel, selective c-Jun N-terminal kinase inhibitors. *Bioorg. Med. Chem. Lett.* **2006**, *16*, 2590–2594. [CrossRef]
256. El-Sayed, O.A.; Habib, N.S.; Aboul-Enein, H.Y.; Costa, B.; Lucacchini, A.; Martini, C. Synthesis and Benzodiazepine Receptor Binding Activity of 2,9-Disubstituted Quinolone[2',3'-5,4](3-pyrazolino)[3,2-b]purin-4-ones. *Arch. Pharm.* **2002**, *335*, 207–212. [CrossRef]
257. Cappelli, A.; Bini, G.; Valenti, S.; Giuliani, G.; Paolino, M.; Anzini, M.; Vomero, S.; Giorgi, G.; Giordani, A.; Stasi, L.P.; et al. Synthesis and Structure—Activity Relationship Studies in Translocator Protein Ligands Based on a Pyrazolo[3,4-b]quinoline Scaffold. *J. Med. Chem.* **2011**, *54*, 7165–7175. [CrossRef] [PubMed]
258. Papadopoulos, V.; Baraldi, M.; Guilarte, T.R.; Knudsen, T.B.; Lacapère, J.J.; Lindemann, P.; Norenberg, M.D.; Nutt, D.; Weizman, A.; Zhang, M.R.; et al. Translocator protein (18 kDa): New nomenclature for the peripheral-type benzodiazepine receptor based on its structure and molecular function. *Trends Pharmacol. Sci.* **2006**, *27*, 402–409. [CrossRef]
259. Dimitrova-Shumkovska, J.; Krstanoski, L.; Veenman, L. Diagnostic and Therapeutic Potential of TSPO Studies Regarding Neurodegenerative Diseases, Psychiatric Disorders, Alcohol Use Disorders, Traumatic Brain Injury, and Stroke: An Update. *Cells* **2020**, *9*, 870. [CrossRef]
260. Sanger, D.J.; Zivkovic, B. Discriminative stimulus effects of alpidem, a new imidazopyridine anxiolytic. *Psychopharmacology* **1994**, *113*, 395–403. [CrossRef] [PubMed]
261. Glickman, J.F.; Schmid, A.; Ferrand, S. Scintillation Proximity Assays in High-Throughput Screening. *Assay Drug Dev. Technol.* **2008**, *6*, 433–455. [CrossRef] [PubMed]
262. Pai, J.J.-K.; Kirkup, M.P.; Frank, E.A.; Pachter, J.A.; Bryant, R.W. Compounds Capable of Generating Singlet Oxygen Represent a Source of Artifactual Data in Scintillation Proximity Assays Measuring Phosphopeptide Binding to SH2 Domains. *Anal. Biochem.* **1999**, *270*, 33–40. [CrossRef] [PubMed]
263. Mehrotra, P.K.; Shukla, R.; Dwivedi, A.; Srivastava, R.P.; Bhat, N.; Seth, M.; Bhaduri, A.P.; Kamboj, V.P. Pregnancy interceptive efficacy and biological profile of 3-amino-6,7-dimethyl-1H-pyrazolo[3,4-b]quinoline (compound 85/83) in rodents. *Contraception* **1991**, *43*, 507–519. [CrossRef]



Review

# 1*H*-Pyrazolo[3,4-*b*]pyridines: Synthesis and Biomedical Applications

Ana Donaire-Arias , Ana Maria Montagut, Raimon Puig de la Bellacasa , Roger Estrada-Tejedor, Jordi Teixidó   
and José I. Borrell \* 

Grup de Química Farmacèutica, IQS School of Engineering, Universitat Ramon Llull, Via Augusta 390, E-08017 Barcelona, Spain; anaariasd@iqs.url.edu (A.D.-A.); ana.montagut@iqs.url.edu (A.M.M.); raimon.puig@iqs.url.edu (R.P.d.l.B.); roger.estrada@iqs.url.edu (R.E.-T.); jordi.teixido@iqs.url.edu (J.T.)

\* Correspondence: j.i.borrell@iqs.url.edu; Tel.: +34-660-921-791

**Abstract:** Pyrazolo[3,4-*b*]pyridines are a group of heterocyclic compounds presenting two possible tautomeric forms: the 1*H*- and 2*H*-isomers. More than 300,000 1*H*-pyrazolo[3,4-*b*]pyridines have been described which are included in more than 5500 references (2400 patents) up to date. This review will cover the analysis of the diversity of the substituents present at positions N1, C3, C4, C5, and C6, the synthetic methods used for their synthesis, starting from both a preformed pyrazole or pyridine, and the biomedical applications of such compounds.

**Keywords:** 1*H*-pyrazolo[3,4-*b*]pyridines; substitution pattern; synthesis; biological activity

**Citation:** Donaire-Arias, A.; Montagut, A.M.; Puig de la Bellacasa, R.; Estrada-Tejedor, R.; Teixidó, J.; Borrell, J.I. 1*H*-Pyrazolo[3,4-*b*]pyridines: Synthesis and Biomedical Applications. *Molecules* **2022**, *27*, 2237. <https://doi.org/10.3390/molecules27072237>

Academic Editors: Vera L. M. Silva and Artur M. S. Silva

Received: 25 February 2022

Accepted: 23 March 2022

Published: 30 March 2022

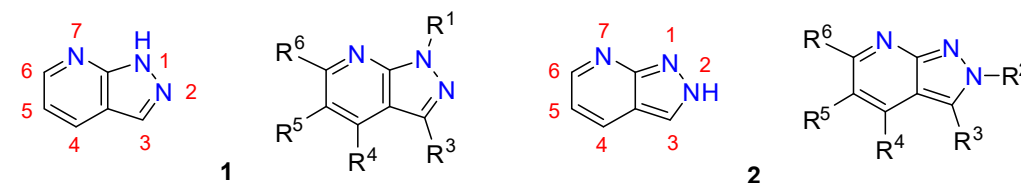
**Publisher's Note:** MDPI stays neutral with regard to jurisdictional claims in published maps and institutional affiliations.



**Copyright:** © 2022 by the authors. Licensee MDPI, Basel, Switzerland. This article is an open access article distributed under the terms and conditions of the Creative Commons Attribution (CC BY) license (<https://creativecommons.org/licenses/by/4.0/>).

## 1. Introduction

Pyrazolo[3,4-*b*]pyridines are one of the bicyclic heterocyclic compounds which are members of the family of pyrazolopyridines formed by five congeners (the [3,4-*b*], [3,4-*c*], [4,3-*c*], [4,3-*b*], and [1,5-*a*]), which are the possible fusions of a pyrazole and a pyridine ring [1]. They can present two isomeric structures: 1*H*-pyrazolo[3,4-*b*]pyridines (1) and 2*H*-pyrazolo[3,4-*b*]pyridines (2) (Figure 1). The first monosubstituted 1*H*-pyrazolo[3,4-*b*]pyridine ( $R^3 = \text{Ph}$ ) was synthesized by Ortoleva in 1908 upon treatment of diphenylhydrazone and pyridine with iodine [2]. Only three years later, Bulow synthesized three *N*-phenyl-3-methyl substituted derivatives 1 ( $R^1 = \text{Ph}$ ,  $R^3 = \text{Me}$ ), starting from 1-phenyl-3-methyl-5-amino-pyrazole which was treated with 1,3-diketones in glacial AcOH, following a widely used strategy [3].



**Figure 1.** Structure of 1*H*- and 2*H*-pyrazolo[3,4-*b*]pyridines (1 and 2) and diversity centers present on them.

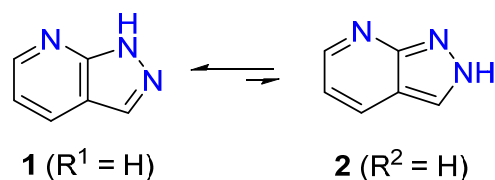
Since then, structures 1 and 2 have attracted the interest of medicinal chemists due to the close similitude with the purine bases adenine and guanine, an interest that is clearly illustrated by the more than 300,000 structures 1 (5000 references, including nearly 2400 patents) and around 83,000 structures 2 (nearly 2700 references, including 1500 patents) included in SciFinder [4] and 180 reviews, including some on the synthesis of such structures [5–8]. These compounds present up to five diversity centers that allow a wide range of possible combinations of substituents capable of addressing different biological activities.

Our group, like others, was attracted by the versatility of such compounds and used them as scaffolds for the synthesis of tyrosine kinase inhibitors (TKI). The analysis of the

different reviews accessible in the literature showed that, to the best of our knowledge, there is no review covering both the synthetic methods used for their synthesis and the biological activities achieved with these structures.

Consequently, we decided to carry out a review of the literature covering the structural, synthetic, and biological aspects of pyrazolo[3,4-*b*]pyridines, but previously, we analyzed the information available, taking some preliminary decisions:

- (a) The review will cover only those compounds that present a fully unsaturated pyridine ring, not taking into account other degrees of unsaturation. Nevertheless, the presence of hydroxy groups at C4 or C6 will be covered, and consequently, the corresponding pyridone tautomers will be included due to the greater stability of the 4-oxo or 6-oxo derivatives.
- (b) In the case of pyrazolo[3,4-*b*]pyridines not substituted at the nitrogen atoms of the pyrazole ring, two tautomeric forms are possible: the 1*H*- (**1**,  $R^1 = H$ ) and the 2*H*-pyrazolo[3,4-*b*]pyridine (**2**,  $R^2 = H$ ) (Figure 2). Although such tautomerism could complicate the diversity analysis of such compounds, the AM1 calculations of Alkorta and Elguero clearly showed the greater stability of the 1*H*-tautomer by a difference of 37.03 kJ/mol (almost 9 kcal/mol) [9].



**Figure 2.** Tautomeric 1*H*-pyrazolo[3,4-*b*]pyridine (**1**) and 2*H*-pyrazolo[3,4-*b*]pyridine (**2**).

Although the number of pyrazolopyridines **2** seems to be around 83,000, most of them are compounds with  $R^2 = H$ . When the search is repeated with the elimination of tautomerism, only about 4900 2*H*-pyrazolo[3,4-*b*]pyridines **2** ( $R^2 = H$ ) remain, included in only 130 references. In many cases, the 2-NH tautomer is only favored when the pyridine ring is not fully dehydrogenated, thus being a tetrahydropyridone [10,11]. Such behavior is in agreement with our experimental results and DFT calculations for C4–C5 fused pyrazole-3-amines, which pointed out that the only way to majorly observe the 2*H*-tautomer is to have the pyrazole ring fused to a non-aromatic ring [12]. Thus, the N1 substituted isomers **1** present aromatic circulation in both rings, thanks to the double bond that can be drawn in the fusion of both rings while N2 substituted structures **2** only allow a peripheric circulation due to the positions of the double bonds in the pyrazole ring. Therefore, the different aromatic circulation has a high impact on the relative stability of the isomers.

Convergently, the total number of the 2-substituted derivatives **2** is drastically reduced to around 19,000, which includes  $R^2 = Me$  (18.28%, 110 references) [13],  $R^2 = Ph$  (8.58%, 213 references) [14], and  $R^2 = \text{heterocycle}$  (56.86%, 35 references) [15]. In most cases, the regioselectivity is achieved by starting from an adequately substituted pyrazole.

Moreover, a search carried out at DrugBank (<https://www.drugbank.ca/>, accessed on 8 March 2022), a database containing information on drugs and drug targets, has revealed that there are 14 1*H*-pyrazolo[3,4-*b*]pyridines **1** in different phases of research: 7 are classified as Experimental (having shown biological activity), 5 are classified as Investigational (included in some of the approval phases), and 2 have already been approved. On the contrary, there is not a single 2*H*-pyrazolo[3,4-*b*]pyridine **2** in any of these stages.

- (c) To the best of our knowledge, there are only five specific reviews on pyrazolopyridines prior to this review. Three of them are devoted to the synthesis of such compounds [6–8], the most recent being from 2012 [6]. The other two cover biological aspects, either from a general perspective (a review from 1985, [16]) or a very specific point of view (kinase inhibitors, 2013 [17]). Furthermore, 5591 references cover the 300,000 1*H*-pyrazolo[3,4-*b*]pyridines included in SciFinder, but 3005 of them (almost 54%) are from 2012 or later (1413 being patents).

Consequently, taking into account the preceding considerations, the rather low number of 2*H*-pyrazolo[3,4-*b*]pyridines **2**, and the low impact of such isomers in drugs under development, we decided to focus the present review only on the structural, synthetic, and biological aspects of 1*H*-pyrazolo[3,4-*b*]pyridines **1**, paying special attention to the period from 2012 to 2022.

## 2. Structural Features of 1*H*-Pyrazolo[3,4-*b*]pyridines: Substitution Patterns

The first aspect addressed in this review is the analysis of the diversity already covered at the different substitution positions present in the Markush formula of **1** by the molecules included in SciFinder. Such information is not directly accessible from SciFinder or other computerized databases due to the huge number of structures **1** included (more than 300,000), so analysis with specialized software is not possible. Consequently, we have explored the substitution patterns at N1, C3, C4, C5, and C6 one by one in order to obtain a picture of the diversity covered.

### 2.1. Substitution Pattern at N1

The analysis of the diversity at N1 included in Table 1 shows that almost one-third of the more than 300,000 compounds **1** have a methyl group at N1 followed by those presenting other alkyl groups (around 23%) or a phenyl group (15%). The number of unsubstituted pyrazoles is around 20%. Such distribution agrees with the synthetic methods used for the synthesis of compounds **1** from a pyrazole ring that requires to be substituted to avoid the formation of two regioisomers (see Section 3).

**Table 1.** Substitution pattern at N1 of 1*H*-pyrazolo[3,4-*b*]pyridines **1**<sup>1</sup>.

| R <sup>1</sup> | Structures <b>1</b> (%) | Number of References | Selected References |
|----------------|-------------------------|----------------------|---------------------|
| H              | 19.70                   | 2520                 | [18,19]             |
| Me             | 31.78                   | 986                  | [20,21]             |
| Alkyl          | 23.27                   | 823                  | [22,23]             |
| Cycloalkyl     | 0.70                    | 47                   | [24,25]             |
| Ph             | 15.17                   | 1077                 | [26,27]             |
| Heterocycle    | 2.33                    | 284                  | [27,28]             |
| Other          | 7.05                    | -                    | -                   |

<sup>1</sup> The selected references included in Tables 1–5 have been selected using two criteria: (1) if possible, to select recent representative examples from the literature, and (2) when available, to select a paper published in a journal rather than a patent.

### 2.2. Substitution Pattern at C3

The diversity analysis included in Table 2 clearly shows that more than three-quarters of the diversity is covered by the substituents hydrogen and methyl. Other substituents, such as phenyl, cycloalkyl, and heterocyclic rings, on one side, or an amino group and a hydroxy group as the carbonyl tautomer on the other side, only have minor contributions. Such a ratio is directly connected with the more employed synthetic methodologies used for the construction of these heterocycles although the importance of amino and carbonyl groups in the biological activities of pyrazolopyridines cannot be dismissed.

**Table 2.** Substitution pattern at C3 of 1*H*-pyrazolo[3,4-*b*]pyridines **1**.

| R <sup>3</sup>  | Structures <b>1</b> (%) | Number of References | Selected References |
|-----------------|-------------------------|----------------------|---------------------|
| H               | 30.83                   | 2049                 | [19,28]             |
| Me              | 46.77                   | 1395                 | [29,30]             |
| Cycloalkyl      | 4.01                    | 98                   | [31,32]             |
| Ph              | 2.12                    | 540                  | [27,33]             |
| Heterocycle     | 4.88                    | 1138                 | [32,33]             |
| NH <sub>2</sub> | 4.69                    | 727                  | [18,34]             |
| OH              | 2.17                    | 239                  | [35,36]             |
| Other           | 4.52                    | -                    | -                   |

### 2.3. Substitution Pattern at C4, C5, and C6

The chemical diversity present at C4, C5, and C6 (Tables 3–5) is usually interconnected because it depends on the building block used for the construction of the pyridine ring that usually is an  $\alpha,\beta$ -unsaturated ketone, or a 1,3-dicarbonyl compound. The percentages of the R<sup>4</sup> substituents are in agreement with such a synthetic approach, that being mainly a hydrogen atom, methyl, phenyl, or heterocyclic ring. The hydroxy group as the keto tautomer shows the use of ester groups during the formation of the pyridine ring that finally ends as a pyridone. A different origin has the amido group present at C4 that usually comes from the manipulation of a cyano or ester group present at such a position and not from the direct formation of the pyridine ring.

**Table 3.** Substitution pattern at C4 of 1*H*-pyrazolo[3,4-*b*]pyridines 1.

| R <sup>4</sup> | Structures 1 (%) | Number of References | Selected References |
|----------------|------------------|----------------------|---------------------|
| H              | 37.33            | 3003                 | [37,38]             |
| Me             | 6.59             | 389                  | [18,27]             |
| Ph             | 2.29             | 660                  | [10,39]             |
| Heterocycle    | 2.42             | 355                  | [27,40]             |
| OH             | 0.89             | 312                  | [41,42]             |
| N-substituent  | 4.54             | 980                  | [43,44]             |
| CONHR          | 38.30            | 148                  | [29,45]             |
| Other          | 7.63             | -                    | -                   |

In the case of C5, the most usual substituent is a hydrogen atom because, in most of the cases, the starting  $\alpha,\beta$ -unsaturated ketone, or a 1,3-dicarbonyl compound has no substituent at  $\alpha$ -position of the corresponding compound. Only in a small percentage of cases is there a substituent at such a position. Once more, the presence of amide groups at C5 is remarkably high, a group that usually comes from the manipulation of a cyano group conveniently introduced at such a position.

**Table 4.** Substitution pattern at C5 of 1*H*-pyrazolo[3,4-*b*]pyridines 1.

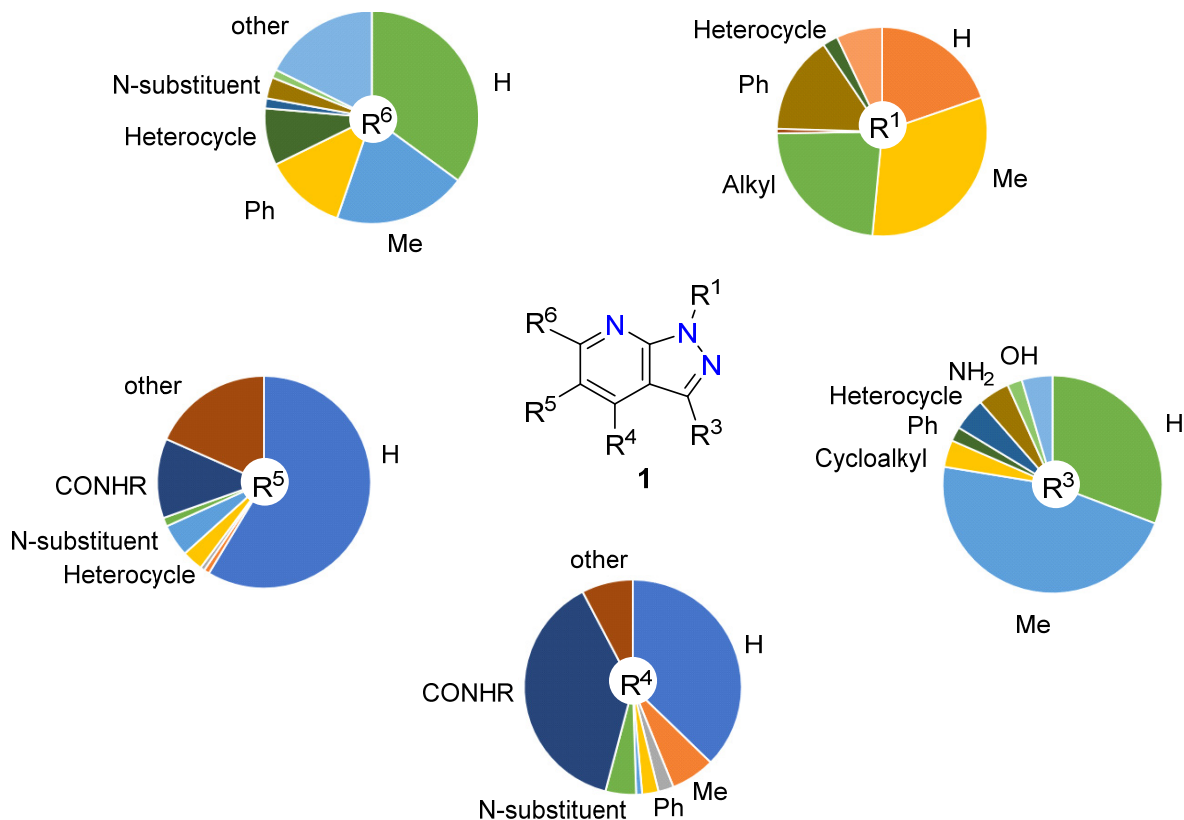
| R <sup>5</sup> | Structures 1 (%) | Number of References | Selected References |
|----------------|------------------|----------------------|---------------------|
| H              | 58.61            | 2753                 | [26,34]             |
| Me             | 0.84             | 87                   | [46,47]             |
| Ph             | 0.66             | 211                  | [19,48]             |
| Heterocycle    | 3.18             | 349                  | [49,50]             |
| N-substituent  | 4.90             | 231                  | [51,52]             |
| Halogen        | 1.34             | 583                  | [18,19]             |
| CONHR          | 12.13            | 430                  | [53,54]             |
| Other          | 18.34            | -                    | -                   |

Finally, as for the diversity at C6, the distribution of substituents agrees with the main use of  $\alpha,\beta$ -unsaturated ketones where the end substituent of the system is a hydrogen atom, a methyl, phenyl, or heterocyclic ring.

**Table 5.** Substitution pattern at C6 of 1*H*-pyrazolo[3,4-*b*]pyridines 1.

| R <sup>6</sup> | Structures 1 (%) | Number of References | Selected References |
|----------------|------------------|----------------------|---------------------|
| H              | 35.10            | 3270                 | [19,55]             |
| Me             | 20.15            | 679                  | [18,27]             |
| Ph             | 12.44            | 509                  | [33,56]             |
| Heterocycle    | 8.65             | 300                  | [57,58]             |
| OH             | 1.52             | 334                  | [59,60]             |
| N-substituent  | 3.22             | 565                  | [61,62]             |
| Carbonyl group | 1.27             | 92                   | [63,64]             |
| Other          | 17.64            | -                    | -                   |

Once the diversity of the substituents at the various positions of the 1*H*-pyrazolo[3,4-*b*]pyridines has been analyzed, a more visual comparison of the diversities covered at positions N1, C3, C4, C5, and C6 of structures 1 included in SciFinder is possible, as shown in Figure 3.



**Figure 3.** Diversity analysis of the substituents present at positions N1, C3, C4, C5, and C6 of 1*H*-pyrazolo[3,4-*b*]pyridines 1.

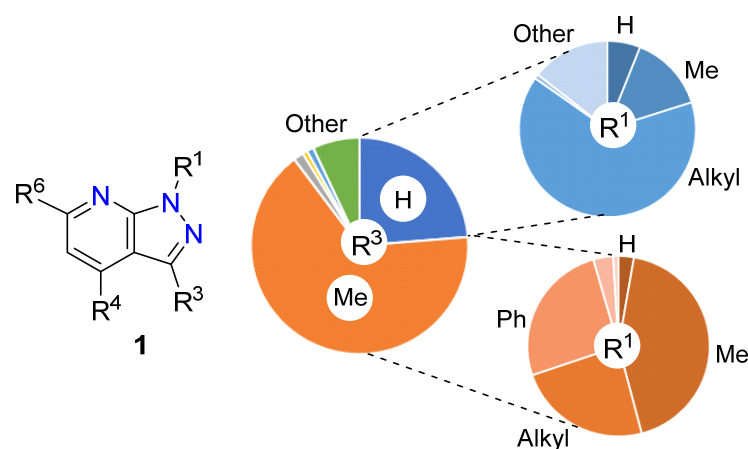
Although the one-by-one analysis of the substituents present at the different positions of the pyrazolopyridine system gives a good picture of the diversity already covered, it would certainly be more interesting to have an idea of the more common di- and trisubstitution patterns. Therefore, a search of the most common combinations of substituents at C3, C4, and C5 was carried out with the following results: 46.83% of the compounds described correspond to a 4,6-disubstituted pattern, 22.04% to 5-monosubstituted compounds, 7.76% to 3,4,5-trisubstituted structures, and 3.37% to unsubstituted pyrazolopyridines.

To see the correlation between such preferred substitution patterns at the pyridine ring and the corresponding substituents at N1 and C3, we have prepared Figures 4 and 5, which correspond to the most abundant 4,6-disubstituted and 5-monosubstituted patterns.

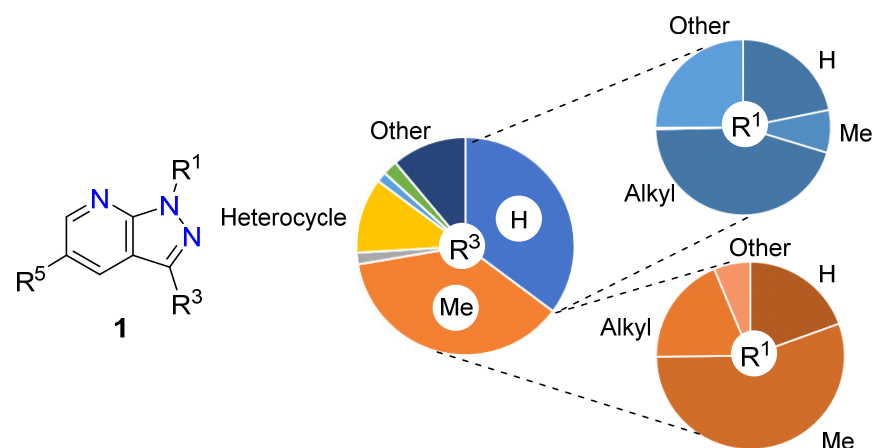
In the case of the 4,6-disubstituted 1*H*-pyrazolo[3,4-*b*]pyridines, the most common substituent at position C3 is a methyl group (66.06%) followed by a hydrogen atom (23.69%). Correspondingly, for R<sup>3</sup> = H, the most abundant R<sup>1</sup> is a methyl group (14.07%) and an alkyl group (64.66%), while for R<sup>3</sup> = Me the most abundant R<sup>1</sup> is a methyl group (43.20%), an alkyl group (23.89%), or a phenyl group (25.74%). These results correlate with the use of a 1-substituted 3-methyl-1*H*-pyrazole or a 1-substituted 1*H*-pyrazole as starting material to afford the 3-methyl (R<sup>3</sup> = Me) and 3-unsubstituted (R<sup>3</sup> = H) 4,6-disubstituted 1*H*-pyrazolo[3,4-*b*]pyridines 1, respectively.

On the other hand, the situation with the substituents being more abundant at position C3 of the 5-monosubstituted 1*H*-pyrazolo[3,4-*b*]pyridines is more equilibrated, as the hydrogen atom (35.20%) and methyl group (37.20%) are virtually tied. Moreover, the presence of R<sup>1</sup> = H reaches higher values than in the case of the 4,6-disubstituted pyrazolopyridines:

21.82% when  $R^3 = H$  and 19.47% when  $R^3 = Me$ . Once more, the preferred substituents at  $R^1$  are the methyl group (55.37%) when  $R^3 = Me$  and the alkyl group (44.96%) when  $R^3 = H$ .



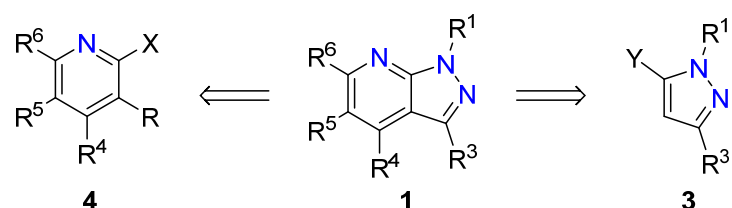
**Figure 4.** Diversity analysis of the 4,6-disubstituted 1*H*-pyrazolo[3,4-*b*]pyridines **1**.



**Figure 5.** Diversity analysis of the 5-monosubstituted 1*H*-pyrazolo[3,4-*b*]pyridines **1**.

### 3. Synthetic Approaches to 1*H*-Pyrazolo[3,4-*b*]pyridines

1*H*-Pyrazolo[3,4-*b*]pyridines **1** are bicyclic heterocyclic systems, and therefore, there are many different strategies to achieve such a structure. This review, however, will focus on two major strategies: the formation of a pyridine ring into an existing pyrazole ring **3** and the formation of the pyrazole ring into a preexisting pyridine ring **4** (Scheme 1).



**Scheme 1.** Retrosynthetic analysis of 1*H*-pyrazolo[3,4-*b*]pyridines **1**.

Therefore, it is possible to make a first classification of the synthetic methods depending on which of the two strategies shown in Scheme 1 is being used.

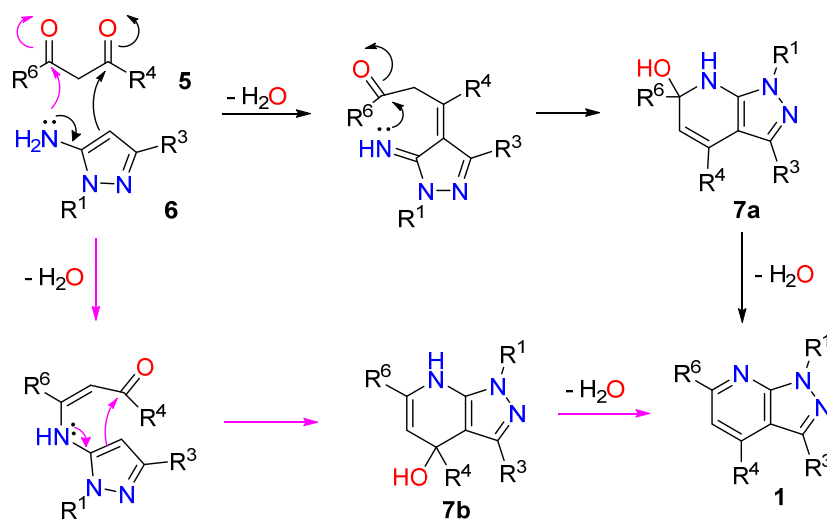
#### 3.1. Pyridine Formation onto a Preexisting Pyrazole Ring

Those reactions are characterized by using different pyrazole derivatives to synthesize the pyridine ring. Most of the reactions that can be found in the literature use

3-aminopyrazole as the starting material, which generally acts as a 1,3-NCC-dinucleophile, reacting therefore with a 1,3-CCC-biselectrophile. The different reactions will be classified according to the nature of the 1,3-CCC-biselectrophile used.

### 3.1.1. 1,3-Dicarbonyl Compounds and Derivatives as 1,3-CCC-Biselectrophiles

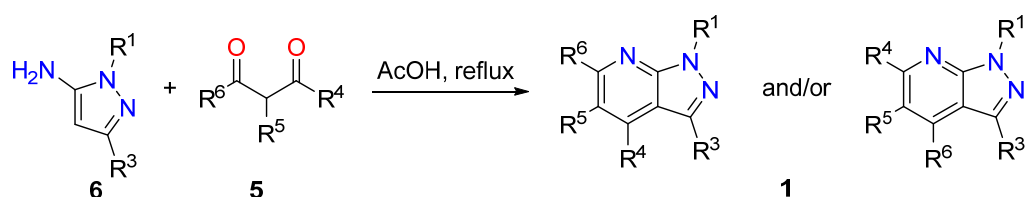
Dicarbonyl compounds **5** have two electrophilic positions (the carbonyl groups) and a nucleophilic one (the  $\alpha$  position in between the two carbonylic groups). Since the compound reacts as a 1,3-CCC-biselectrophile, the two carbonyl groups are the ones involved in the reaction. There is a strong debate on the mechanism for this type of reaction and two different proposals arise from literature as commented below (Scheme 2).



**Scheme 2.** Different mechanistic proposals for the formation of 1*H*-pyrazolo[3,4-*b*]pyridines **1** from 5-aminopyrazole **6** as the 1,3-NCC-dinucleophile and a dicarbonyl compound **5** as the 1,3-CCC-biselectrophile.

5-Aminopyrazole **6** has two different reactive points that can act as a nucleophile: the amino group ( $-\text{NH}_2$ ) and the  $\text{sp}^2$  carbon at its  $\beta$  position. The reaction starts with the nucleophilic attack of one of those nucleophiles onto one of the two carbonyl groups followed by dehydration. Unfortunately, there is no consensus regarding which of the two nucleophiles reacts in the first place. The first attack is followed by the second nucleophile reacting with the unreacted carbonyl group, leading to the formation of a 6-member ring **7a** or **7b** (depending on the initial attack) which, after dehydration, forms the pyrazolo[3,4-*b*]pyridine system **1**. This mechanism is the one taking place for the majority of dicarbonyl compounds and derivatives, adapting it to the nature of each reactant.

The vast majority of the reactions reported in literature follow the same conditions (Scheme 3). AcOH is commonly used as a solvent, and the reaction is carried out at reflux temperature or microwave (MW) irradiation, with reaction times that may vary depending on the substituents present [65,66]. It is also possible to carry out this reaction using water as a solvent at 90 °C for 16 h [67] or using MeOH and HCl at room temperature for 16 h [68].

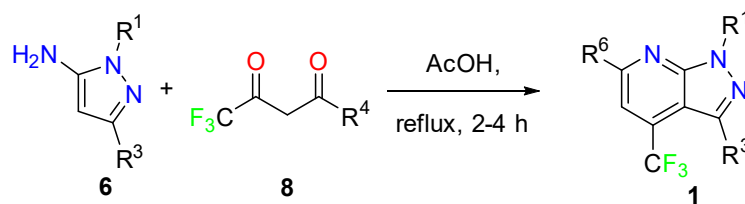


**Scheme 3.** Reaction conditions for the synthesis of 1*H*-pyrazolo[3,4-*b*]pyridines **1** using 1,3-dicarbonyl compounds **5** and 5-aminopyrazole **6** as starting materials.

As it can be seen from the reaction mechanism, if the 1,3-dicarbonyl compound is nonsymmetrical, two regioisomers can be formed [66]. The proportions among the products will depend on the relative electrophilicity of the two carbonyl groups. If the two are very similar, the proportions are going to be near 50%, but if they are very different, it is possible to carry out the reaction having regioselectivity higher than 80%.

As mentioned, there is no consensus on the order of the attack of the two nucleophiles, and it is even possible to find authors performing very similar reactions but claiming opposite results, obtaining yields higher than 60% in both cases. On the one hand, Ghaedi et al. performed the reaction using ethyl 2,4-dioxo-4-phenylbutanoate derivatives as starting materials, achieving final molecules with yields ranging from 60 to 90%. The resulting 1*H*-pyrazolo[3,4-*b*]pyridines present a COOEt group at the R<sup>6</sup> position [63]. On the other hand, Ibrahim et al. used ethyl acetoacetate derivatives as starting materials, compounds that present one carbonyl group with higher electrophilicity than the other, as it so happens, with 2,4-dioxo-4-phenylbutanoate derivatives. The reaction was carried out using the same conditions above, but the results ended up being the opposite. The molecules described by Ibrahim, with yields ranging from 62 to 76%, seem to have the hydroxy group at the R<sup>4</sup> position, and not at the R<sup>6</sup> as described by Ghaedi [42]. This example shows how difficult it can be to determine not only the mechanism, but also the structure of the molecules obtained. Since there are no big differences between the NMR spectra of the two regioisomers, it might be difficult to determine which one is present unless both are available.

To clarify the mechanism and avoid the presence of both regioisomers, Emelina et al. used 1,1,1-trifluoropentane-2,4-dione (8) and its derivatives to differentiate the two carbonyl groups present in the initial reactant (Scheme 4) [66].

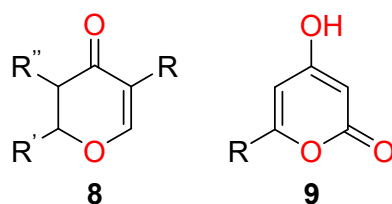


**Scheme 4.** Synthesis of 1*H*-pyrazolo[3,4-*b*]pyridines **1** using 5-aminopyrazole **6** and 1,1,1-trifluoropentane-2,4-dione (**8**) and its derivatives as starting materials.

They concluded that, since the carbonyl group having the CF<sub>3</sub> group is more electrophilic, it should be the one reacting in the first place. The results show that, once the pyridine ring gets formed, the CF<sub>3</sub> stays at the R<sup>4</sup> position, meaning that the amino group from the 5-aminopyrazole **6** reacts in second place. To assign the position of the CF<sub>3</sub> group, they used <sup>1</sup>H-NMR and <sup>13</sup>C-NMR to look after the long-range coupling constants between the fluorine atoms from the CF<sub>3</sub> group and the H and C atoms from the R<sup>3</sup> group [66].

This type of reaction can be performed with a wide range of 1,3-CCC-biselectrophiles, such as the ones included in Table 6.

All of the 1,3-CCC-biselectrophiles listed in Table 6 are open-chain compounds; however, some six-membered cyclic 1,3-CCC-biselectrophiles that get opened during the reaction have also been used to construct the 1*H*-pyrazolo[3,4-*b*]pyridine skeleton (Figure 6).



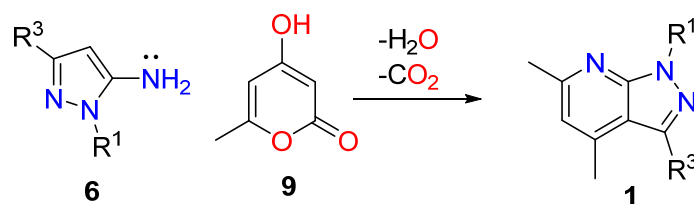
**Figure 6.** The general structure of the six-membered cyclic 1,3-CCC-biselectrophiles used to construct 1*H*-pyrazolo[3,4-*b*]pyridines.



**Table 6.** Different examples of 1,3-CCC-biselectrophiles used to synthesize 1*H*-pyrazolo[3,4-*b*]pyridines.

| 1,3-CCC-Biselectrophiles | Reference |
|--------------------------|-----------|
|                          | [67]      |
|                          | [42]      |
|                          | [42]      |
|                          | [63,65]   |
|                          | [66]      |
|                          | [68]      |

In the case of 2,3-dihydro-4*H*-pyran-4-ones **8**, the reaction works in a very similar way as the other 1,3-dicarbonyl compounds, but with 4-hydroxy-2*H*-pyran-2-ones **9**, the reaction involves a decarboxylation, as depicted in Scheme 5.

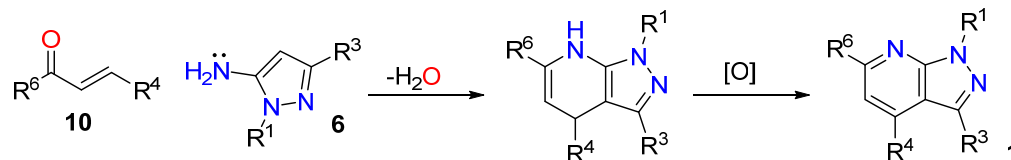
**Scheme 5.** Synthesis of 1*H*-pyrazolo[3,4-*b*]pyridines from 4-hydroxy-2*H*-pyran-2-ones **9**.

The conditions for those reactions vary depending on the author, Jouha et al., that used molecule **9** as the initial reactant, carrying out the reaction under microwave irradiation at 180 °C for 3 h using BuOH the solvent and TsOH as the catalyst. The final product presented methyl groups at positions R<sup>3</sup>, R<sup>4</sup>, and R<sup>6</sup>; therefore, no regioselectivity issues were present, and the final product was obtained with a 98% yield [69]. Ianoshenko et al. published three different papers about this matter, proposing two different reaction conditions. On one hand, they tested the same conditions used for the 1,3-dicarbonyl reactants, using AcOH at reflux temperature for 1 h, obtaining yields up to 98%. On the other hand, they used DMF, TMSCl at 100 °C for 1 h, obtaining yields up to 93% [70–72].

In none of the cases were regioselectivity problems reported; this could be due to either a mistake in analyzing the results or the higher selectivity of this subtype of reactions over the traditional 1,3-dicarbonyl condensations described above.

### 3.1.2. Michael Acceptors Used as 1,3-CCC-Biselectrophiles

$\alpha,\beta$ -Unsaturated ketones **10** have also been used as 1,3-CCC-biselectrophiles in the formation of 1*H*-pyrazolo[3,4-*b*]pyridines **1** by reacting them with 5-aminopyrazole **6**. Michael acceptors react similarly to 1,3-dicarbonyl compounds (Scheme 6).



**Scheme 6.** Synthesis of 1*H*-pyrazolo[3,4-*b*]pyridines using  $\alpha,\beta$ -unsaturated ketones **10** and 5-aminopyrazole **6** as initial reactants.

The  $sp^2$  carbon in  $\beta$  to the amino group is the one believed to be the most nucleophilic and, therefore, is the one that seems to attack in the first place, performing a Michael addition. Unfortunately, there is no complete agreement on that matter. Accordingly, the amino group ( $NH_2$ ) would react in the second place, attacking the carbonyl group of the Michael acceptor, and leaving a hydroxyl group. After the elimination of water and spontaneous oxidation, the pyrazolo[3,4-*b*]pyridine would be formed. This last spontaneous oxidation step takes place in more than one of the mechanisms proposed in the literature. It is not clear how the oxidation proceeds, but some hypotheses have been made. Among them, the most plausible is oxidation due to the atmospheric oxygen. Alternatively, some authors propose a disproportionation of the molecule, but in this case, a 50:50 mixture of the oxidized and reduced products would be obtained, a result not clearly described in any of the manuscripts.

Such a reaction is carried out under both acidic and basic conditions. Stepaniuk et al. compared different reaction conditions, selecting either acetic acid at reflux for 12 h or  $HCl/1,4$ -dioxane in EtOH at 100 °C for 18 h, with yields ranging from 44 to 99% [73]. Han et al. performed the reaction using 1.0 M NaOH in glycol as a solvent at 120 °C for 5–12 min, affording in all cases yields above 90% [74]. Many authors have used Lewis acids as catalysts,  $CuCl_2$ ,  $ZrCl_4$ , or  $ZnCl_2$  [75–77], instead of Brønsted–Lowry acids. Shi et al. performed this reaction without a catalyst by using the ionic liquid [bmim]Br as a solvent, keeping the yields between 80 and 96% [78].

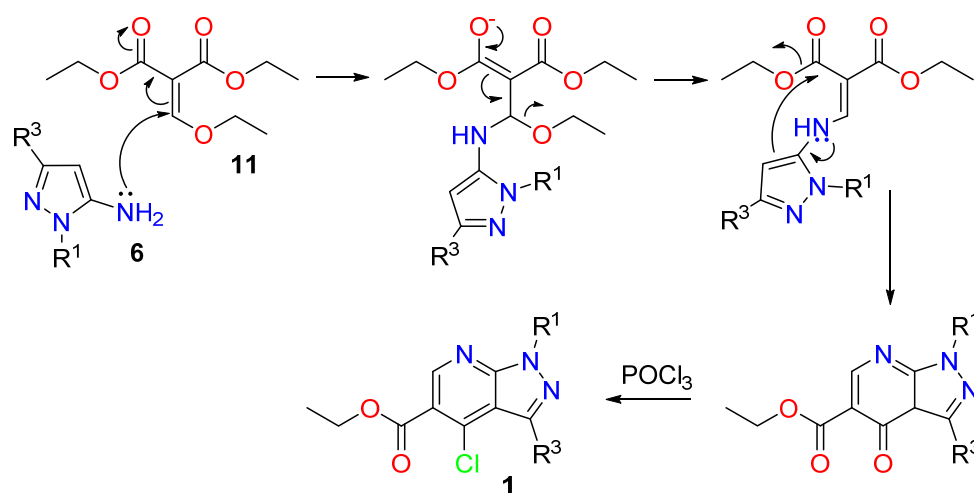
Since this reaction is the result of the attack of two nucleophilic centers on two electrophilic centers, it is also possible to achieve two different regioisomers. Stepaniuk et al. performed an analysis of the effect of the reaction conditions on the final regioisomer ratios. They concluded that the regioselectivity of the reaction was very sensitive to small changes, not only on the conditions, but also on the structure of the initial reactants [73].

### 3.1.3. Diethyl 2-(Ethoxymethylene)malonate as 1,3-CCC-Biselectrophile (Gould–Jacobs Reaction)

The Gould–Jacobs reaction is often used for the synthesis of quinolines or 4-hydroxyquinoline derivatives using aniline and diethyl 2-(ethoxymethylene)malonate **11** as starting materials. 1*H*-Pyrazolo[3,4-*b*]pyridines can be obtained by using 3-aminopyrazole **6** (or its derivatives) instead of aniline. The product obtained, in the majority of the cases, is a 4-chloro substituted 1*H*-pyrazolo[3,4-*b*]pyridine **1** [79–83].

The mechanism proposed in the literature for the formation of 1*H*-pyrazolo[3,4-*b*]pyridines **1** by the Gould–Jacobs reaction is depicted in Scheme 7.

In this case, the amino group of the 3-aminopyrazole **6** would react in the first place, attacking the enol ether group present in **11**, causing the elimination of ethanol. The subsequent nucleophilic attack on one of the two ester groups present eliminates ethanol as well. Finally, the carbonyl group present in the 6-membered ring reacts with  $POCl_3$ , forming the corresponding 4-chloro-1*H*-pyrazolo[3,4-*b*]pyridines **1**. Since the 1,3-CCC-biselectrophile is symmetrical, there are no regioselectivity problems.



**Scheme 7.** Gould-Jacobs reaction mechanism for the synthesis of 4-chloro 1H-pyrazolo[3,4-b]pyridines **1** from diethyl 2-(ethoxymethylene)malonate **11**.

The reaction conditions used for such protocols are often very similar. The reaction can be performed by using ethanol as solvent at reflux temperature, followed by the treatment with POCl<sub>3</sub> [79,82]. Since diethyl 2-(ethoxymethylene)malonate **11** is liquid at room temperature, it is possible to perform the reaction without any solvent, using 100–110 °C for times between 1.5 and 12 h [80,81,83,84]. Rimland et al. performed the reaction without any solvent at 160 °C for 5 h using SOCl<sub>2</sub> instead of POCl<sub>3</sub> in the last step [83].

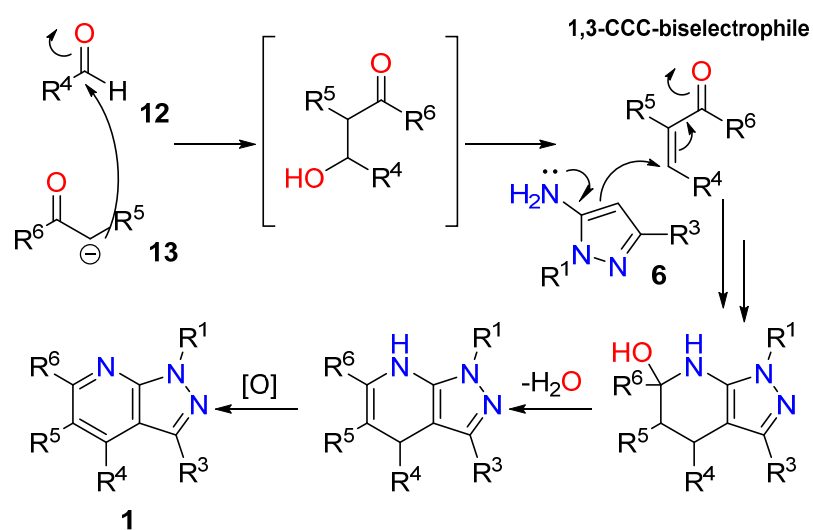
As the electrophile used for the reaction is always the same, the variations in the structure of the final product come from the substituents present in the pyrazole reagent (R<sup>1</sup> and R<sup>3</sup>). In all cases, the final product is 4-chloro substituted 1H-pyrazolo[3,4-b]pyridine **1**, except for Pan et al., which obtained the 4-hydroxy substituted compound because the POCl<sub>3</sub> was not included [84].

The Gould–Jacobs reaction is a simple way to achieve 4-chloro-1H-pyrazolo[3,4-b]pyridines, but it is not very versatile due to the limitations in the nature of the substituents accessible. Nevertheless, it is an interesting strategy for further derivatization of the 1H-pyrazolo[3,4-b]pyridines formed.

### 3.1.4. In Situ Formation of the 1,3-CCC-Biselectrophiles or the 1,3-NCC-Dinucleophiles

One way to overcome regioselectivity problems is to generate in situ the 1,3-CCC-biselectrophile by using an aldehyde **12**, a carbonyl compound **13** bearing at least an α-hydrogen atom, and a conveniently substituted pyrazole **6**. Many authors have described the use of such a three-component reaction in very high yields without reporting regioselectivity issues, agreeing, in all cases, on how the mechanism is taking place (Scheme 8) and which isomer is being formed [40,64,85–90].

The reaction starts with the formation of the 1,3-CCC-biselectrophile by a carbonyl condensation between the α-carbon of the carbonyl compound **13** (usually a ketone) and the aldehyde **12**, followed by the elimination of water. Once the electrophile is formed, the mechanism is similar to the one described in Scheme 6, including a Michael addition of the 5-aminopyrazole **6** to the in-situ-formed α,β-unsaturated compound, followed by a closing of the pyridine ring with the subsequent elimination of water and final oxidation to yield the 1H-pyrazolo[3,4-b]pyridine scaffold **1**. Ezzrati et al. performed this reaction in both the presence and absence of air. When the reaction was carried out in the absence of air at 50 °C during 40–60 min, the final molecule contained a dihydropyridine instead of a pyridine ring. They were able to convert such a compound to the desired pyrazolopyridine by dissolving the intermediate in ethanol at reflux for 10–30 min in the presence of air [85]. Such a result leads to the conclusion that air may be necessary to carry out the oxidation reaction.



**Scheme 8.** Mechanism of the three-component reaction for the formation of 1*H*-pyrazolo[3,4-*b*]pyridines **1**.

This protocol is frequently carried out with a catalyst. Shi et al. used *L*-proline to help the carbonyl condensation by forming an imine between the amino group of the *L*-proline and the aldehyde. The reaction is carried out using EtOH as solvent at 80 °C for 30–60 min [89]. Acids or bases are commonly used as catalysts as well—to assist with deprotonation in case of a base, or to increase electrophilicity if an acid is used. El-borai et al. used acetic acid (or a mixture of acetic acid and triethylamine) to catalyze the reaction, using high temperatures (150 to 160 °C). The reaction takes 15 to 20 min to complete, with yields ranging from 65 to 88% when only acetic acid is present, and from 86 to 98% when a combination of both catalysts is used. It is important to mention that the initial reactants were not the same and thus the different yields could be due to other elements besides the present catalysts [64].

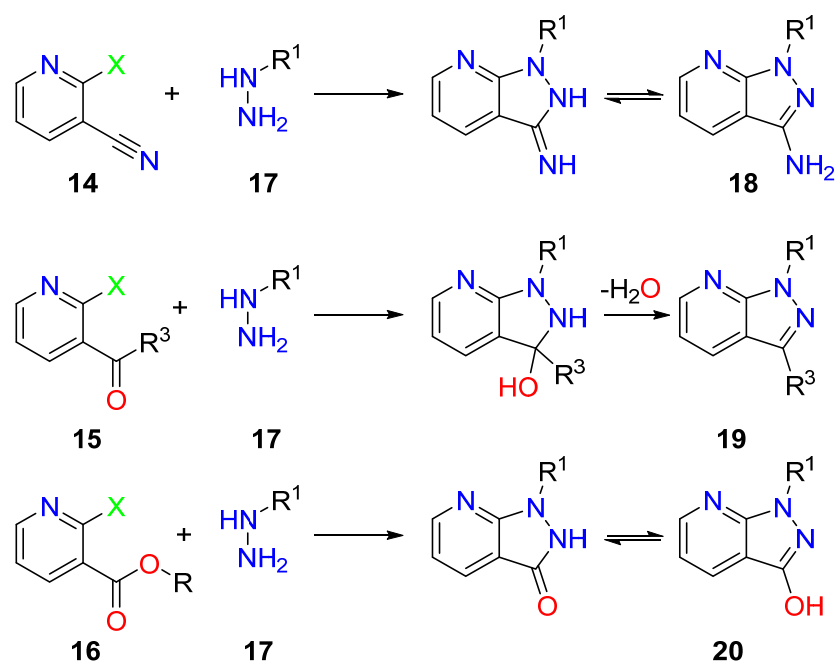
To make the reaction greener, some authors have used ionic liquids as both solvents and catalysts [40,87,90]. Jadhav et al. used [Et<sub>3</sub>NH][HSO<sub>4</sub>] as the ionic liquid, demonstrating that it can be recycled up to five times without losing its capability of performing the reaction. This is a very interesting approach in terms of waste reduction, lower temperatures (60 °C), higher yields (90–96%), and safer reaction conditions [40]. The reaction has also been carried out without a catalyst by Ezzrati and Rahmati et al., using ethanol and water as solvents, respectively, or even without any solvent or catalyst by Quiroga et al. under microwave irradiation at 200 °C during 9 min [85,86,88].

There are some examples of the 1,3-NCC-dinucleophile being generated in situ. Hamama et al. and Marzouk et al. used 3-pyrazolones that reacted with ammonia to generate the 3-aminopyrazole ring [91,92].

### 3.2. Pyrazole Formation onto a Preexisting Pyridine Ring

As previously commented, pyrazolo[3,4-*b*]pyridines can be also synthesized starting from a pyridine derivative and closing the pyrazole ring. Those reactions are usually carried out using hydrazine **17** (or substituted hydrazine) and a pyridine ring **14–16** containing a good leaving group at position C2 and an electrophilic group at position C3 (Scheme 9).

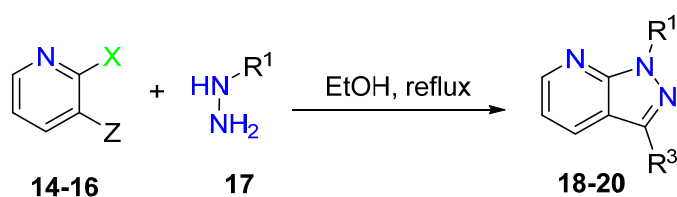
The leaving group most widely used in these reactions is a chlorine atom, while the electrophilic group is chosen among carbonyl groups (aldehyde, ketone, or ester groups) or a cyano group. Depending on the electrophilic group, the final compounds **18–20** present as the R<sup>3</sup> substituent a hydrogen atom, an alkyl or aryl group, a carbonyl group, or an amino group, respectively. The other diversity centers included in the final pyrazolo[3,4-*b*]pyridine must be present in the initial pyridine (R<sup>4</sup>, R<sup>5</sup>, and R<sup>6</sup>) and the hydrazine (R<sup>1</sup>).



**Scheme 9.** Formation of 1*H*-pyrazolo[3,4-*b*]pyridines **18–20** starting from a preexisting pyridine ring (**14–16**) and hydrazine (or substituted hydrazine) **17**.

The mechanism is very similar for the three different options. In all the cases, the reaction starts with the nucleophilic attack of the hydrazine **17** to both electrophilic positions of the corresponding pyridine ring **14–16**: the chloro substituted carbon and the electrophilic group at position C3. After this step, the corresponding intermediate evolves to the final 1*H*-pyrazolo[3,4-*b*]pyridines **18–20**, either by tautomerization (in the case of a C3 nitrile or ester group) or by elimination of water (in the case of aldehydes or ketones). It is important to mention that it is not clear in which tautomeric form is present the carbonyl group at position C3 since some authors draw the keto form and others draw the enol form.

Since the reactions are very similar regardless of the groups present at C3 of the pyridine ring, the reaction conditions are also very similar. As an example, Scheme 10 shows the conditions mostly used for the reaction:



**Scheme 10.** Typical reaction conditions used for the synthesis of 1*H*-pyrazolo[3,4-*b*]pyridines starting from a preformed pyridine ring.

Most authors use hydrazine hydrate as the initial reactant, using ethanol as solvent at reflux temperature; the reaction time needed ranges from 2 h to more than 15 h [93–96]. Arafa and Hussein performed the reaction at 50 °C using a sonicator, allowing them to obtain the product in 15 min [97]. Since hydrazine hydrate is liquid at room temperature, some authors perform the reaction without a solvent, with the reaction times going from 3 to 10 h [98–101].

There is too much variation among the reaction conditions used to compare the two methods and properly discuss a decrease in the reaction time by eliminating the solvent. Mali et al. performed the reaction without solvent at reflux temperature and under microwave irradiation, thus reducing the reaction time from 7–10 h to 1.5–2 h [101]. Orlikova et al. also performed the reaction without solvent but at 150 °C, and using ethanol

as a solvent at reflux temperature; in both cases, the reaction times were very similar: 2 h without solvent and 2–3 h using ethanol.

Other solvents can be used to perform the reaction, like DMF, either at reflux temperature or around 100 °C [102,103]; BuOH at reflux temperature [104]; or ethylene glycol at 165 °C [105,106]. It is also possible to find authors who have used acids or bases to favor the reaction. Thus Al-kaabi and Elgemeie used Et<sub>3</sub>N, and the reaction was complete after 3 h [107], and Teixeira et al. and Selvi et al. used TsOH at reflux (3 h) and microwave-assisted heating (4–13 min, 320 W), respectively [38,108].

As can be seen, there is not a standardized method for carrying out this type of reaction.

Table 7 includes the different pyridine reactants that have been used.

**Table 7.** Pyridine reactants used for the synthesis of 1*H*-pyrazolo[3,4-*b*]pyridines.

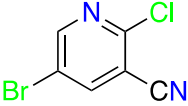
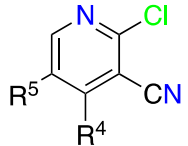
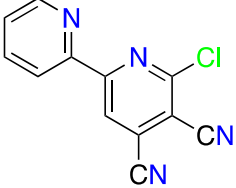
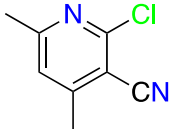
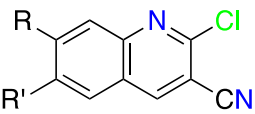
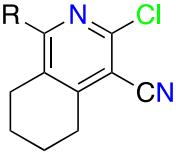
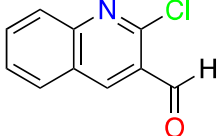
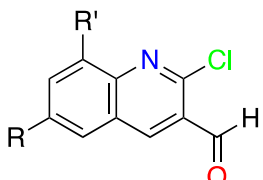
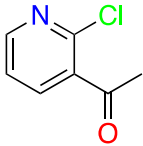
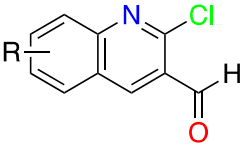
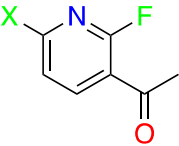
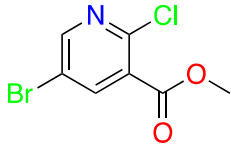
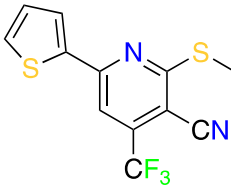
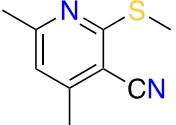
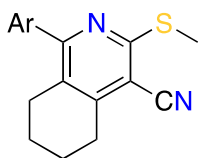
| Initial Pyridine  | Reference |
|---|-----------|
|    | [93,94]   |
|    | [46]      |
|  | [97]      |
|  | [104]     |
|  | [103]     |
|  | [100]     |
|  | [38]      |
|  | [101]     |

Table 7. Cont.

| Initial Pyridine  | Reference |
|---|-----------|
|    | [105]     |
|    | [108]     |
|    | [106]     |
|    | [95,96]   |
|  | [98,99]   |
|  | [102]     |
|  | [107]     |

### 3.3. Other Reactions

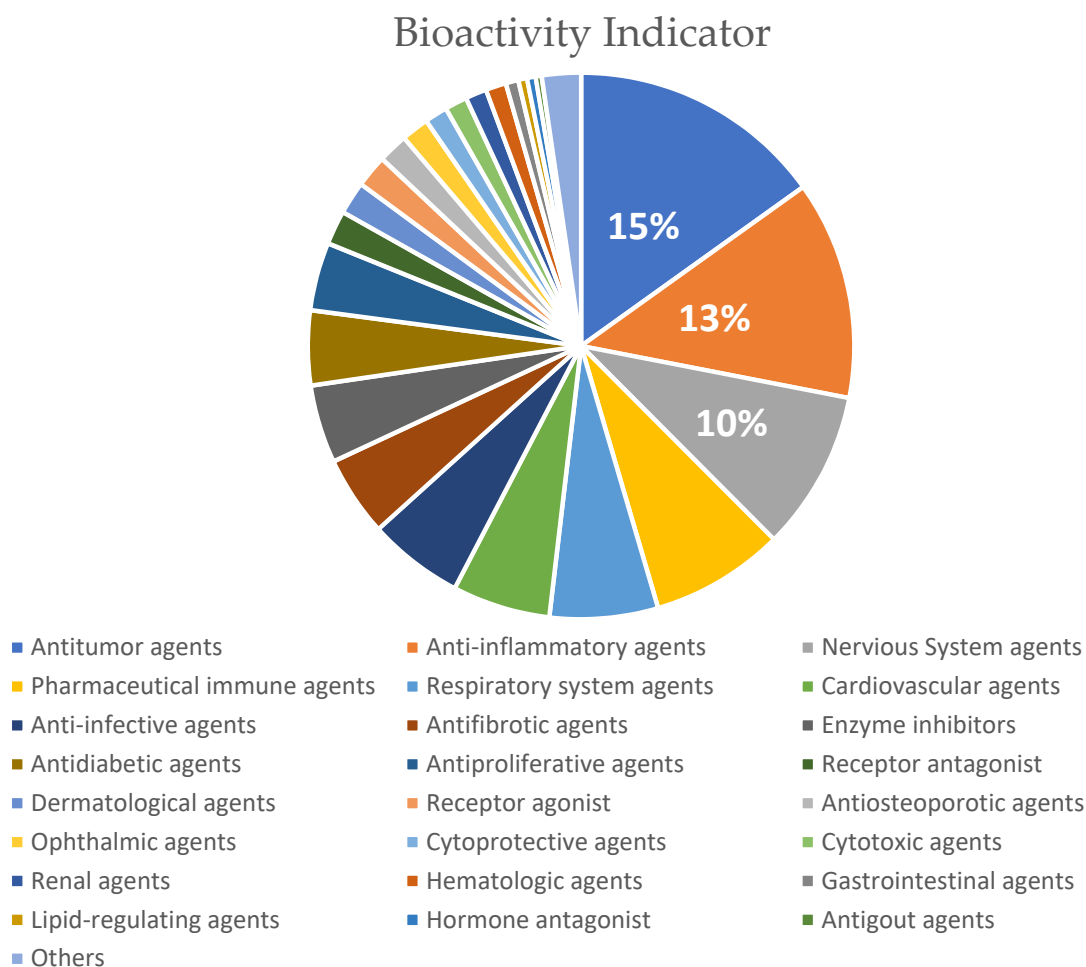
The above classification has been made to systematize the reactions used to synthesize 1*H*-pyrazolo[3,4-*b*]pyridines **1**. Even though most of the references that can be found in the literature can be classified in that way, there is a pool of reactions that do not fit into any of the categories mentioned [91,109–116].

## 4. Biomedical Applications of 1*H*-Pyrazolo[3,4-*b*]pyridines

1*H*-Pyrazolo[3,4-*b*]pyridines **1** have been extensively used as a scaffold for the synthesis of small molecules looking for therapeutic properties to treat different diseases. From all the molecules containing a pyrazolo[3,4-*b*]pyridine core (more than 300,000 reported molecules), 156,660 molecules have been synthesized for therapeutic purposes.

According to the literature, the most relevant, important part of the overall biomedical applications' bioactivity indicators for 1*H*-pyrazolo[3,4-*b*]pyridines are antitumor agents (22,675 molecules), anti-inflammatory agents (19,416 molecules), and nervous system agents

(14,203 molecules). More concretely, they account for 38% of the biomedical applications (Figure 7).



**Figure 7.** Bioactivity indicators of the potential therapeutic uses of 1*H*-pyrazolo[3,4-*b*]pyridines.

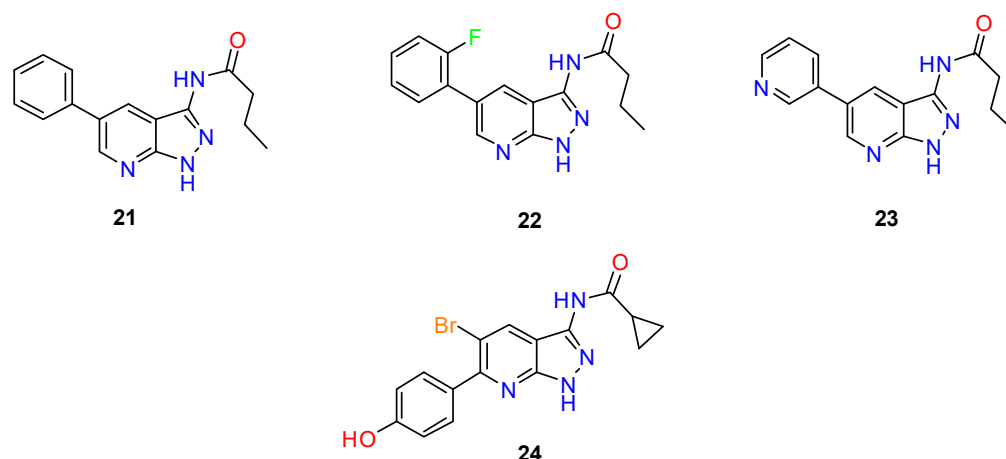
In the following part of this review, we focus on these three main biomedical applications because they represent more than a third of the overall bioactivity indicators, as well as the different pattern substitutions of the pyrazolo[3,4-*b*]pyridine scaffold selected for each disease, giving more importance to the major ones.

#### 4.1. Antitumor Agents

The use of 1*H*-pyrazolo[3,4-*b*]pyridines **1** as a scaffold for antitumor agents corresponds to 15% of the biomedical applications. In most of them, the selected substituents are at R<sup>3</sup> and R<sup>5</sup> (8112 molecules, 36% of this group of compounds), followed by disubstitution at R<sup>3</sup> and R<sup>4</sup> (1375 molecules), monosubstitution at R<sup>3</sup> (1208 molecules), and other substitution patterns, which include around 1000 molecules each. An analysis of the type of substituents present in the most abundant group has shown that 5897 structures (almost 26% of the structures reported with anticancer activity) present a combination of substituents in which R<sup>1</sup> = R<sup>4</sup> = R<sup>6</sup> = H, and R<sup>3</sup> and R<sup>5</sup> are heterocyclic rings.

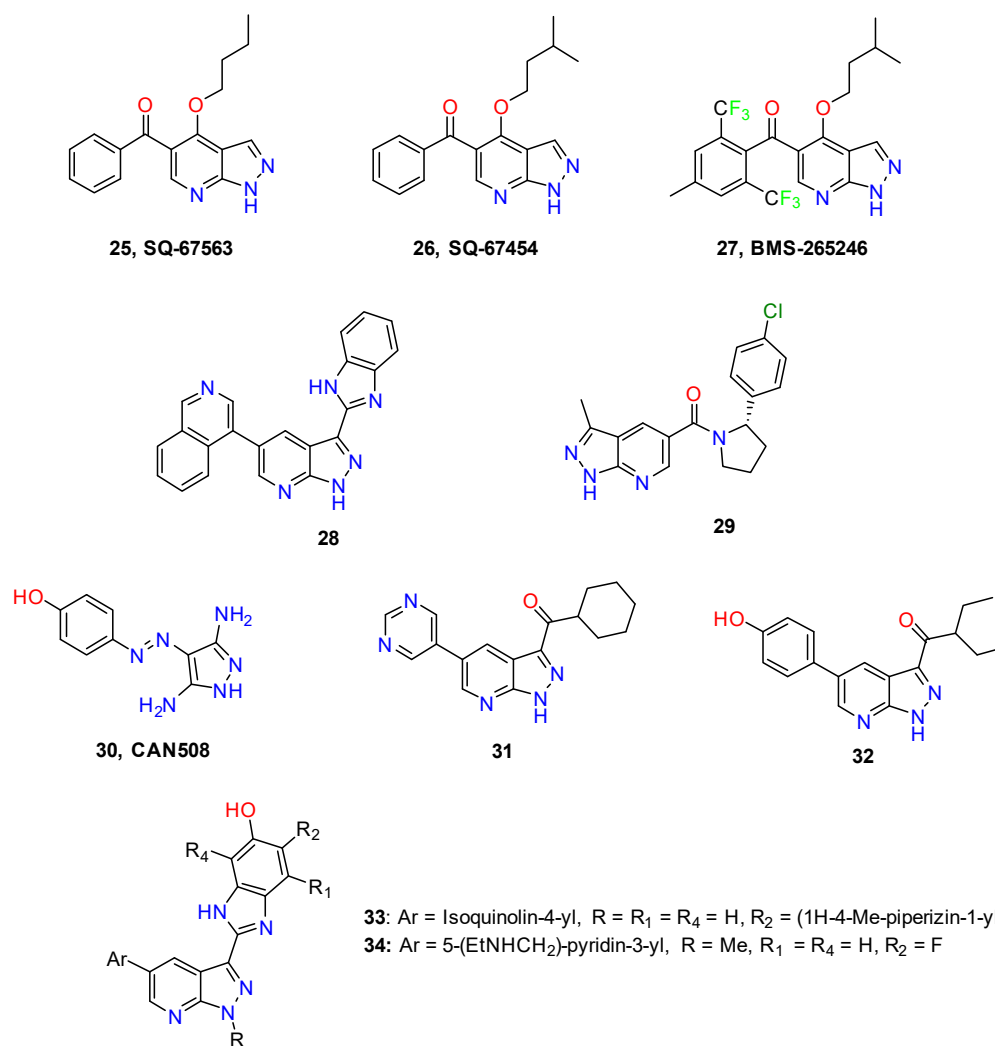
1*H*-Pyrazolo[3,4-*b*]pyridines derivatives **21**, **22**, and **23** (Figure 8) have been described as potent inhibitors of hGSK-3 $\alpha$  (IC<sub>50</sub> = 56  $\pm$  6 nM, 18  $\pm$  2 nM, and 11  $\pm$  2 nM, respectively) [94]. Further optimization of these promising small molecules was performed, resulting in molecule **24** with an IC<sub>50</sub> of 0.8  $\pm$  0.4 nM [117].





**Figure 8.** 1*H*-Pyrazolo[3,4-*b*]pyridines as inhibitors of hGSK-3 $\alpha$ .

Cyclin-dependent kinases (CDKs) are encouraging drug targets for various human diseases, in particular for cancer. SAR studies of compounds **25** and **26** (Figure 9) led to the discovery of an excellent CDK1/CDK2 selective inhibitor **27**, BMS-265246 (CDK1/cycB  $IC_{50}$  = 6 nM and CDK2/cycE  $IC_{50}$  = 9 nM) [118].



**Figure 9.** 1*H*-Pyrazolo[3,4-*b*]pyridines as inhibitors of CDKs.

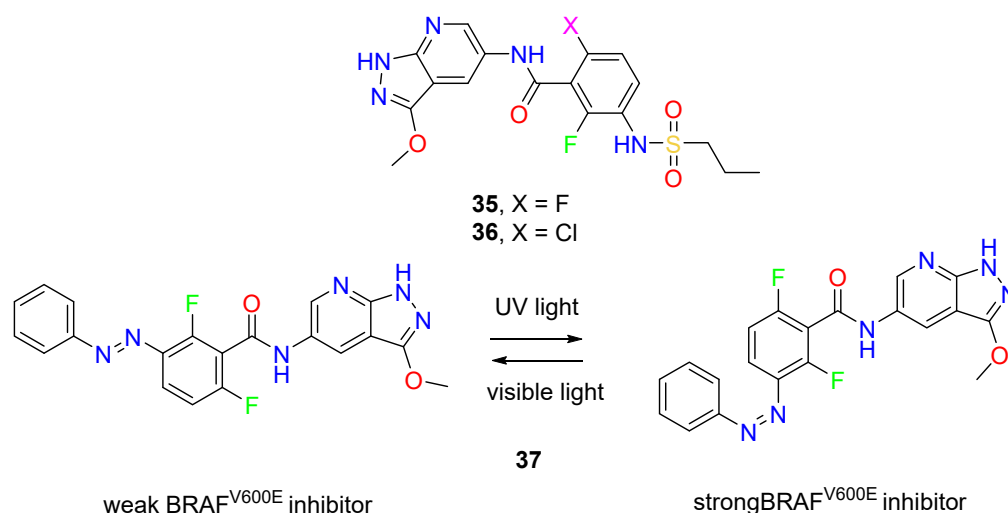
Compound **28** inhibits CDK1 activity with an  $IC_{50}$  of 23 nM. This inhibitory activity has been observed by a reduced amount of  $^{33}P$ -cATP incorporated into the immobilized substrate in a FlashPlate assay format. **28** has also shown inhibition growth of HeLa cervical adenocarcinoma, A375 malignant melanoma, and HCT-116 colon carcinoma cells, with  $IC_{50}$  values of 1.7, 0.87, and 0.55  $\mu$ M, respectively. Moreover, this compound also exhibits inhibition of VEGFR-2 kinase, a receptor tyrosine kinase implicated in angiogenesis, another important mechanism for tumor progression with an  $IC_{50}$  value of 1.46  $\mu$ M [119].

In the growth of colorectal cancer, multiple lines of evidence propose that the mediator-complex-associated, cyclin-dependent kinase (CDK8) may act as an oncogene. Compound **29** (MSC2530818) is a structure-based, designed small molecule that exhibits outstanding kinase selectivity, biochemical and cellular potency, microsomal stability, and is orally bioavailable. This compound shows an in-vivo, oral, pharmacokinetic profile in mice, rats, and dogs. It also evidences reduction of the tumor-growth rates of established human SW620 colorectal carcinoma xenografts using two different oral dosing schedules. Considering its huge activity, compound **29** went into preclinical, in-vivo, animal efficacy and safety studies [53].

Molecule **30** (CAN508) has been used for a scaffold-hopping strategy, and the scaffold alteration using the 1*H*-pyrazolo[3,4-*b*]pyridine core appears to cause a positive alteration in the selectivity profile of the inhibitors. Compound **31** exhibits an excellent inhibitor activity against CDK2 and CDK9 ( $IC_{50}$  values of 0.36  $\mu$ M and 1.8  $\mu$ M, respectively). Furthermore, compound **32** evidences extraordinary selectivity towards CDK2 (265-fold over CDK9) [120].

1*H*-Pyrazolo[3,4-*b*]pyridine analogs **33** and **34** also manifest a selective and potent cyclin-dependent kinase and cellular antiproliferative inhibition. These compounds have shown an excellent in-vitro inhibition of the cellular proliferation in HeLa, HCT116, and A375 human tumor cell lines [121].

About 7% of all cancers present the V600E mutation of B-Raf kinase, which results in the constitutive activation of the MAPK signaling pathway. Molecules **35** and **36** (Figure 10) have been structure-based designed for inhibiting B-Raf<sup>V600E</sup>. These compounds have shown to be potent, selective, and orally bioavailable debutants that inhibited tumor growth in a mouse xenograft model driven by B-Raf<sup>V600E</sup> [67].

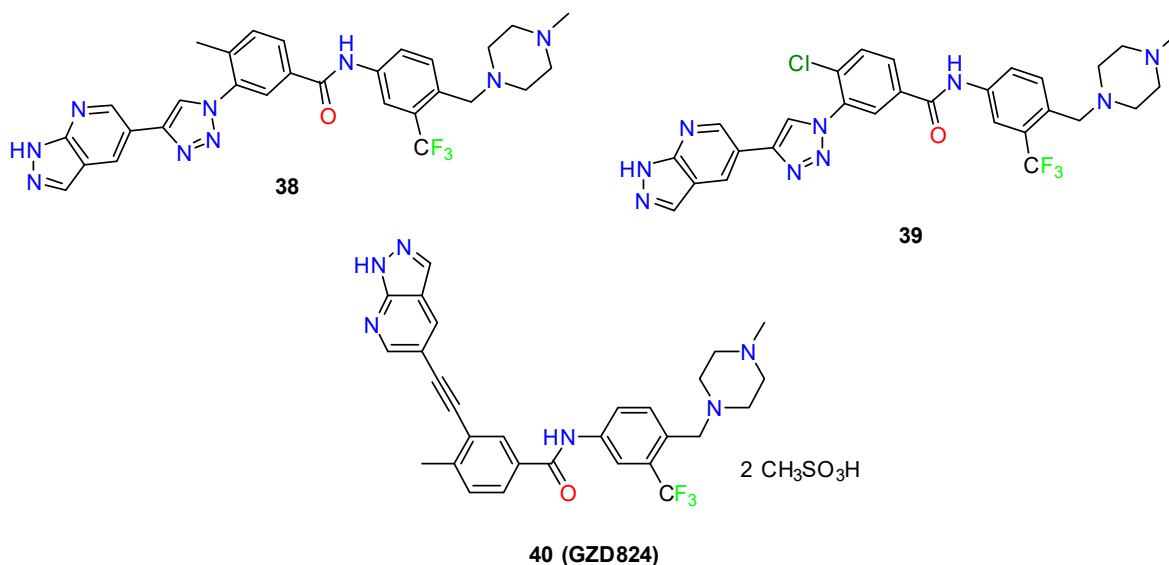


**Figure 10.** 1*H*-Pyrazolo[3,4-*b*]pyridines as BRAF<sup>V600E</sup> inhibitors.

Moreover, one of the most difficult types of cancer to treat is metastatic melanoma; the inhibition of BRAF<sup>V600E</sup> mutant kinase is its main current therapy. Nevertheless, the inhibition of BRAF by small molecules in cancer patients provokes an increase of wild-type BRAF activity in healthy tissue, causing side effects and the formation of new tumors. Hoorens et al. have developed the BRAF<sup>V600E</sup> kinase inhibitor **37** (Figure 10), the activity

of which can be switched on and off in a reversible way with light. Consequently, the drug can be selectively activated at the desired site of action, avoiding side effects. This small molecule contains in its structure an azobenzene photoswitch that, once activated with light, increases the inhibitory activity by 10-fold compared with the non-activated form [122].

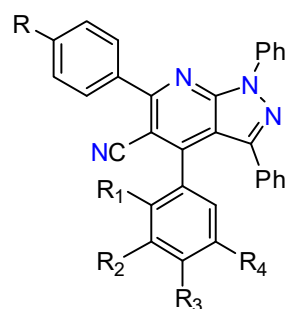
Lead compounds **38** and **39** (Figure 11) have been described for their strong inhibition activity towards a broad spectrum of Bcr-Abl mutants, such as the gatekeeper T315I and p-loop mutations, which are associated with disease progression in chronic myelogenous leukemia (CML). They resolutely inhibited the kinase activities of Bcr-Abl<sup>WT</sup> and Bcr-Abl<sup>T315I</sup> with IC<sub>50</sub> values of 0.60, 0.36, and 1.12, 0.98 nM, respectively [123].



**Figure 11.** Inhibitors for the treatment of chronic myelogenous leukemia (CML).

GZD824 **40** is another small molecule described for the treatment of CML that includes a 1H-pyrazolo[3,4-b]pyridine moiety. Such a compound is an orally bioavailable inhibitor against a broad spectrum of Bcr-Abl mutants, including T315I. This promising compound has a K<sub>d</sub> value of 0.32 and 0.71 nM for Bcr-Abl<sup>WT</sup> and Bcr-Abl<sup>T315I</sup>, respectively. It also effectively suppresses the proliferation of Bcr-Abl-positive K562 and Ku812 human CML cells with IC<sub>50</sub> values of 0.2 and 0.13 nM, respectively. Its bioavailability is 48.7%, and it presents a half-life of 10.6 h. Moreover, it stimulates tumor regression in mouse xenograft tumor models and greatly improves the survival of mice, altogether making GZD824 a potential lead aspirant for the development of Bcr-Abl inhibitors [95].

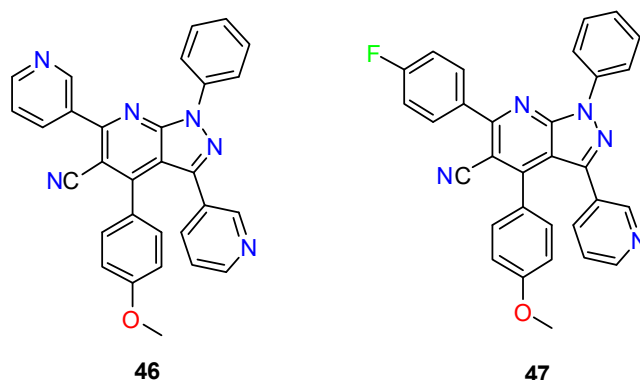
A series of 1H-pyrazolo[3,4-b]pyridine derivatives (**41**, **42**, **43**, **44**, and **45**, among others), have been designed as potential anticancer agents (Figure 12). They have been screened for their antitumor activity in vitro, with compound **41** having been tested with a full-panel, five-dose assay to assess its GI<sub>50</sub>, TGI, and IC<sub>50</sub> values. Compound **41** exhibits broad-spectrum antiproliferative activities over the whole National Institute cancer (NCI) panel, with excellent growth inhibition. Its full-panel GI<sub>50</sub> (the mean activity value for the entire panel, MG-MID) value equals 2.16 mM and subpanel GI<sub>50</sub> (MG-MID) range is 1.92–2.86 mM. Moreover, 1H-pyrazolo[3,4-b]pyridines **41**, **42**, **43**, **44**, and **45** have been tested for their antiproliferative activity against a panel of leukemia cell lines (K562, MV4-11, CEM, RS4;11, ML-2, and KOPN-8), where they showed excellent antileukemic activity. These results make compounds **42**, **43**, **44**, and **45** encouraging lead molecules to stimulate optimization to frame more robust and efficient anticancer candidates [124].



|    | R                | R <sub>1</sub> | R <sub>2</sub>         | R <sub>3</sub> | R <sub>4</sub> |
|----|------------------|----------------|------------------------|----------------|----------------|
| 41 | H                | H              | H                      | OH             | H              |
| 42 | 4-Me             | H              | H                      | OH             | H              |
| 43 | 4-Me             | H              | -O-CH <sub>2</sub> -O- |                | H              |
| 44 | OCH <sub>3</sub> | H              | H                      | OH             | H              |
| 45 | F                | H              | H                      | OH             | H              |

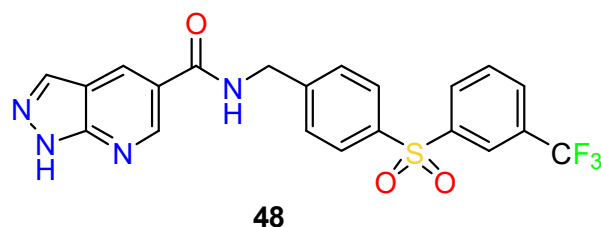
**Figure 12.** Other 1*H*-pyrazolo[3,4-*b*]pyridines proposed as anticancer agents.

Compounds **46** and **47** (Figure 13) demonstrated antitumor activity against a liver cell line with an IC<sub>50</sub> of 3.73 μM and 3.43 μM, respectively [64].



**Figure 13.** Pyrazolo[3,4-*b*]pyridines against liver cancer cell lines.

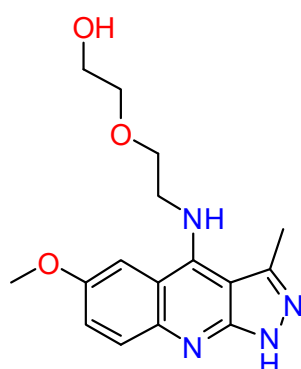
The human nicotinamide phosphoribosyltransferase (NAMPT) is involved in the first step of the conversion of nicotinamide (NAM) to the biologically important enzyme co-factor nicotinamide adenine dinucleotide (NAD). Compound **48** (Figure 14) was identified after structure-based design studies and exhibits nanomolar antiproliferation activities against human tumor lines in in vitro cell culture experiments. This compound has an IC<sub>50</sub> = 6.1 nM and an IC<sub>50</sub> = 4.3 nM for NAMPT BC and A2780 cells, respectively [125].



**Figure 14.** 1*H*-Pyrazolo[3,4-*b*]pyridine inhibitor of NAMPT BC and A2780 cells.

The rat sarcoma virus (RAS) is a guanosine-nucleotide-binding protein. Specifically, it is a single subunit, small GTPase. Activated RAS GTPase signaling is a crucial motor of oncogenic alteration and malignant disease. The use of cellular models of RAS-dependent cancers has driven the identification of molecule **49** (SCH51344) (Figure 15) as a human

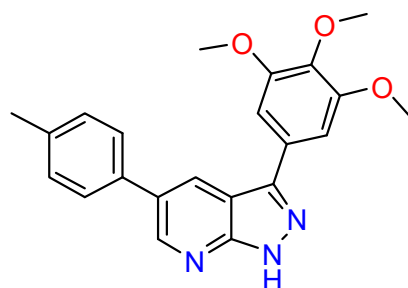
mutT homolog MTH1 (also known as NUDT1) inhibitor, a nucleotide pool sanitizing enzyme [126].



**49, SCH 51344**

**Figure 15.** 1*H*-Pyrazolo[3,4-*b*]pyridine active in cellular models of RAS-dependent cancers.

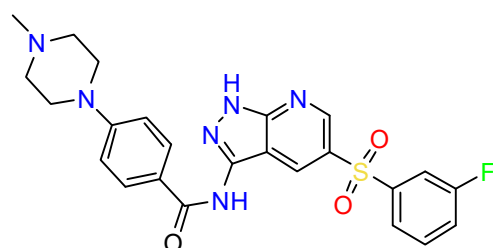
Compound **50** (Figure 16) has been designed as a tubulin polymerization inhibitor targeting the colchicine site. It has been tested by MTT assays for its antiproliferative activity against three human cancer cell lines (SGC-7901, A549, and HeLa). **50** exhibits noticeable in vitro potential activity because SGC-7901 has an  $IC_{50} = 13$  nM, and it could significantly inhibit tubulin polymerization and strongly disrupt the cytoskeleton [127].



**50**

**Figure 16.** 1*H*-Pyrazolo[3,4-*b*]pyridine active as a tubulin polymerization inhibitor.

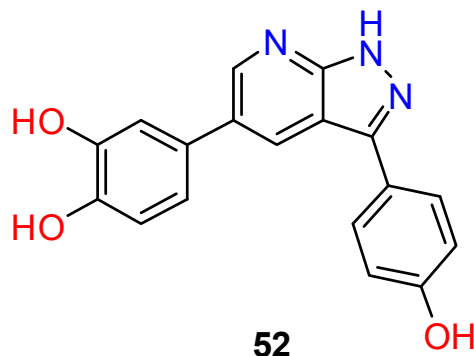
An encouraging molecular target for non-small cells lung carcinoma (NSCLC) is the anaplastic lymphoma kinase (ALK). Compound **51** (Figure 17) has been described for its excellent inhibitory activity against ALK-L1196M ( $IC_{50} < 0.5$  nM) and ALK-wt. Moreover, **51** shows a remarkable inhibition of ROS1 ( $IC_{50} < 0.5$  nM) and displays excellent selectivity over c-Met. **51** resolutely suppresses proliferation of ALK-L1196M-Ba/F3 and H2228 cells boarding EML4-ALK via apoptosis and the ALK signaling blockade [128].



**51**

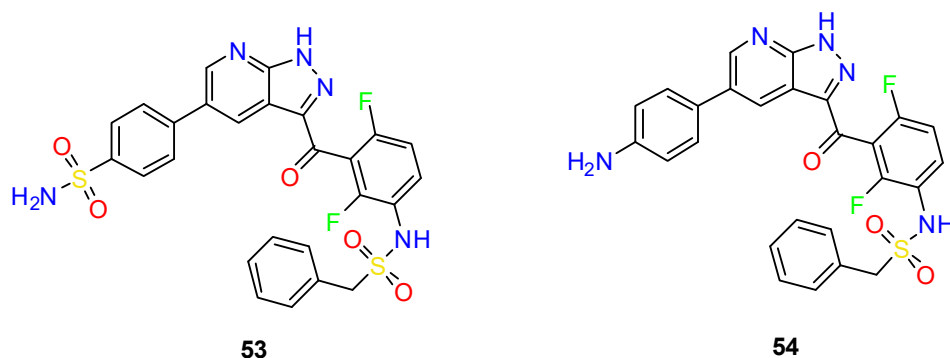
**Figure 17.** 1*H*-Pyrazolo[3,4-*b*]pyridine active against non-small cell lung carcinoma (NSCLC).

Compound 52 (Figure 18) has been found to have an excellent DYRK1B inhibitory enzymic activity with an  $IC_{50} = 3$  nM, cell proliferation inhibitory activity ( $IC_{50} = 1.6$   $\mu$ M) against HCT116 colon cancer cells, and inhibitory activity in a patient-derived colon cancer organoids model and a 3D spheroids assay model of SW480 and SW620 [18,19].



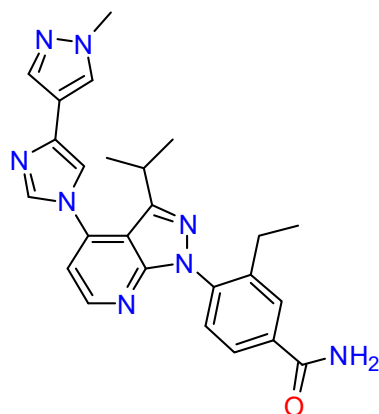
**Figure 18.** 1*H*-Pyrazolo[3,4-*b*]pyridine active against HCT116 colon cancer cells.

Mitogen-activated protein kinase 4 (MKK4) has recently been identified as the main regulator in hepatocyte regeneration. A scaffold-hopping approach has been performed to obtain compounds 53 and 54 (Figure 19), which show high affinity to MKK4 in the low nanomolar range and a selectivity profile from a multiparameter-optimization due to the essential antitargets (MKK7 and JNK1) and off-targets (BRAF, MAP4K5, and ZAK) in the MKK4 pathway [28].



**Figure 19.** 1*H*-Pyrazolo[3,4-*b*]pyridine active against mitogen-activated protein kinase 4 (MKK4).

Pimitespib (55, TAS-116, Figure 20) shows an inhibitory effect on the phosphorylation of KIT-Asp818Tyr, which is a c-kit gene that contains a germline Asp820Tyr mutation at exon 17. This mutation causes multiple gastrointestinal stromal tumors (GISTs). This small molecule can decrease the cecal tumor volume in model mice; thus, it seems to inhibit *in vivo* tumor progression. These studies suggest that Pimitespib can be a potential drug to control multiple GISTs in patients with germline KIT-Asp820Tyr [129].



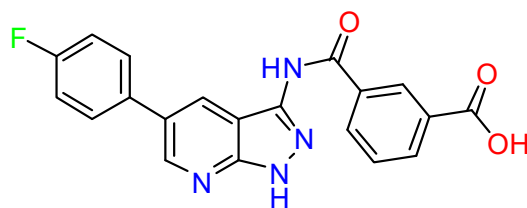
**55, Pimitepsib (TAS-116)**

**Figure 20.** Pimitepsib (TAS-116) active against gastrointestinal stromal tumors (GISTs).

#### 4.2. Anti-Inflammatory Agents

The use of 1*H*-pyrazolo[3,4-*b*]pyridines as scaffolds for anti-inflammatory agents corresponds to 13% of the overall biomedical applications of such structures. The main combination of substituents used for such biological activity is the disubstitution at  $R^3$  and  $R^5$  (7045 molecules, 36% of this group). A total of 1761 pyrazolo[3,4-*b*]pyridines (9% of this group) include a trisubstitution at positions  $R^1$ ,  $R^4$ , and  $R^5$ . Other substitution patterns used less often are the combinations  $R^3$ - $R^4$ - $R^6$ ,  $R^3$ - $R^4$ , and  $R^1$ - $R^3$ - $R^4$ - $R^6$ , with 981, 961, and 908 molecules, respectively. In this case, the combination of substituents in which  $R^1 = R^4 = R^6 = H$  and  $R^3$  and  $R^5$  are heterocyclic rings covers 30% of the total number of structures claimed as having an anti-inflammatory activity (5856 compounds).

The repression of spleen tyrosine kinase (Syk) is an encouraging approach for the treatment of several allergic and autoimmune disorders, such as rheumatoid arthritis, asthma, and allergic rhinitis. Compound **56** (Figure 21) presents great Syk inhibitory activity ( $IC_{50} = 1.2 \mu M$ ), representing a good lead compound for further optimization [130].

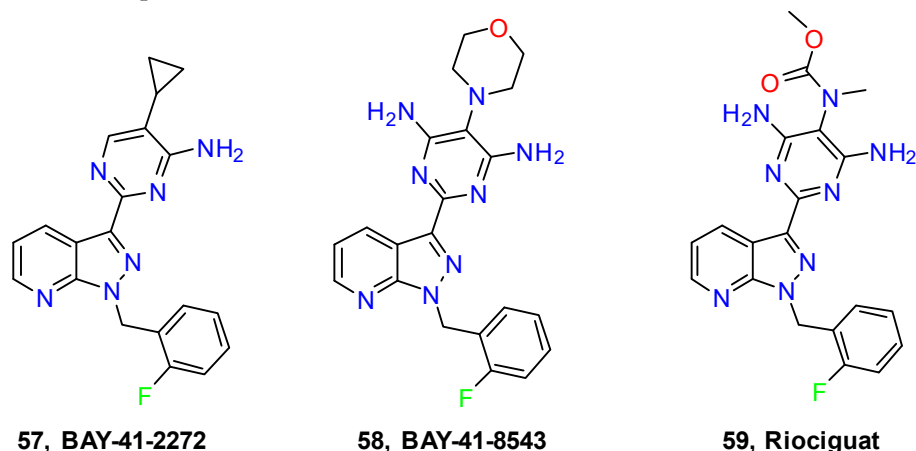


**56**

**Figure 21.** 1*H*-Pyrazolo[3,4-*b*]pyridine for the treatment of several allergic and autoimmune disorders.

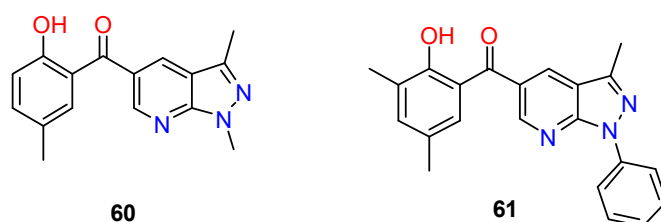
Although pulmonary hypertension (PH) is a cardiovascular disease, its known inflammatory basis led us to include it in this section [131]. Soluble guanylate cyclase (sGC) is an essential signal-transduction enzyme activated by nitric oxide (NO). The pathogenesis of cardiovascular and other diseases can be a consequence of impairments of the NO–sGC signaling pathway. The stimulation of sGC is a promising treatment for pulmonary hypertension (PH), a disease related to a poor prognosis. Pyrazolopyridines **57** (BAY 41-2272) and **58** (BAY 41-8543) (Figure 22) exhibited favorable effects in experimental models of PH, despite their being related to unfavorable drug metabolism and pharmacokinetic (DMPK) properties. Riociguat (**59**) (Figure 22) is a designed compound found by SAR exploration that improves the DMPK profile and shows excellent effects on pulmonary hemodynamics and exercise capacity in patients with PH. Riociguat was investigated in phase III clinical trials for the oral treatment of PH [132] and approved in the USA, Europe, and other regions

for patients with pulmonary arterial hypertension and marketed by Bayer under the trade name Adempas.



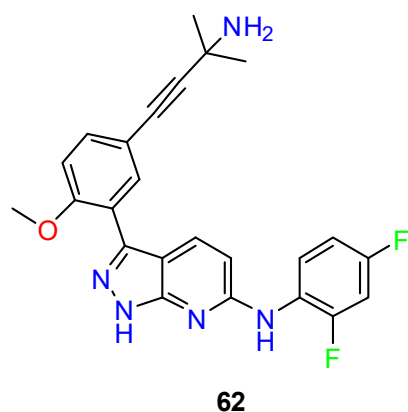
**Figure 22.** 1H-Pyrazolo[3,4-b]pyridines for the treatment of pulmonary arterial hypertension.

Molecules **60** and **61** (Figure 23) exhibit promising anti-inflammatory activity against TNF- $\alpha$  and IL-6. In concrete, against IL-6 with 60–65% inhibition at 10  $\mu$ M. Moreover, they show potent IL-6 inhibitory activity, with an IC<sub>50</sub> of 0.2 and 0.3  $\mu$ M, respectively [133].



**Figure 23.** 1H-Pyrazolo[3,4-b]pyridines with anti-inflammatory activity against TNF- $\alpha$  and IL-6.

The inhibition of p38 $\alpha$  is one of the major targets in developing anti-inflammatory drugs due to its prominent role in regulating inflammatory cytokines, such as TNF $\alpha$  and IL-1. Molecule **62** (Figure 24) has potent p38 $\alpha$  inhibitor activity and excellent in vivo activity upon oral administration in animal models of rheumatoid arthritis [134].

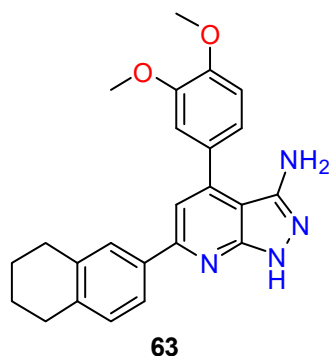


**Figure 24.** 1H-Pyrazolo[3,4-b]pyridine with potent p38 $\alpha$  inhibitor activity.

The study of the activity of molecule **63** (Figure 25) on macrophage growth, phagocytosis of FITC-zymosan, radical scavenging affinity against OH $\cdot$ , ROO $\cdot$ , and O<sub>2</sub><sup>-</sup>, and macrophage binding affinity to fluorescein isothiocyanate-conjugated bacterial lipopolysaccharide (FITC-LPS), together with its affection for the inflammatory mediators (nitric oxide

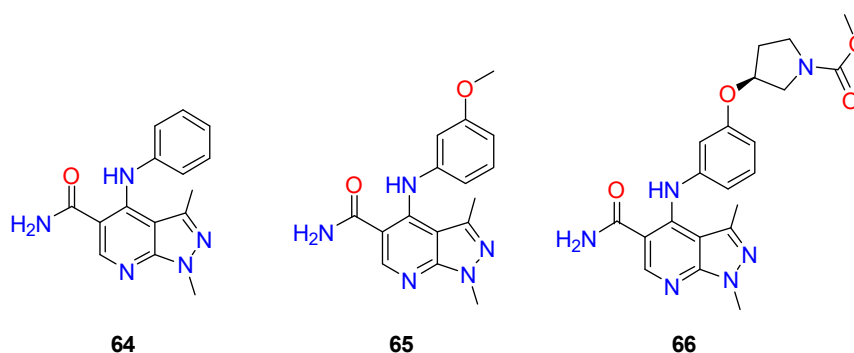


(NO), tumor necrosis factor- $\alpha$  (TNF- $\alpha$ ), prostaglandin E-2 (PGE-2), cyclooxygenase-2 (COX-2), and 5-lipoxygenase (5-LO)) in LPS-stimulated macrophages, have converted it into a promising multipotent anti-inflammatory agent [135].



**Figure 25.** 1*H*-Pyrazolo[3,4-*b*]pyridine with multipotent anti-inflammatory activity.

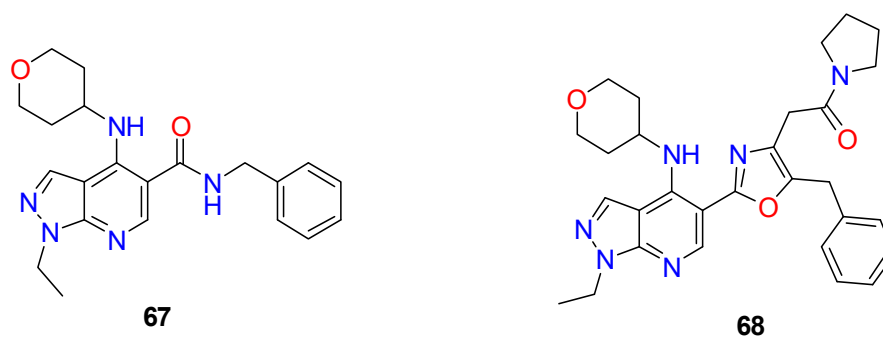
4-Anilinopyrazolopyridine derivative **64** (Figure 26) led to the optimization of phosphodiesterase 4 (PDE4) inhibitors. Compounds **65** and **66** present improved therapeutic capacity with fewer side effects, being orally active compounds. Compound **66** shows much higher bioavailability than compounds **64** and **65** [136].



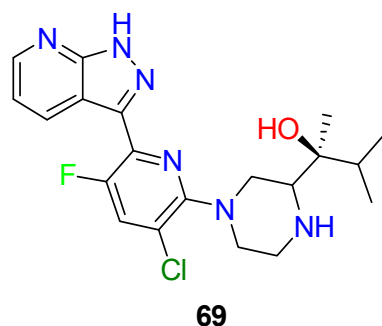
**Figure 26.** 1*H*-Pyrazolo[3,4-*b*]pyridines active against phosphodiesterase 4 (PDE4).

Compound **67** (Figure 27) was discovered after the optimization of a high-throughput screening hit. This molecule exhibits potent and selective inhibition activity against phosphodiesterase 4 (PDE4) with a  $pIC_{50}$  of 8.5, thus being a promising target for the treatment of chronic obstructive pulmonary disease (COPD). Moreover, molecule **67** also inhibits LPS-induced TNF- $\alpha$  production from isolated human peripheral blood mononuclear cells and has a promising rat pharmacokinetic profile for oral dosing [137]. Compound **68** (Figure 27) was found to have excellent potent inhibitory activity against PDE4. This compound was discovered after SAR studies of the 5-position. Thus, optimization using X-ray crystallography and computational modeling led to **68** with sub-nM inhibition of LPS-induced TNF- $\alpha$  production from isolated human peripheral blood mononuclear cells [138].

T cell activation and survival strongly depend on protein kinase C  $\theta$  (PKC $\theta$ ). Recent studies show that T cell responses associated with autoimmune diseases are PKC $\theta$ -dependent. Selective and potent inhibition of PKC $\theta$  is likely to block autoimmune T cell responses without compromising antiviral immunity. Molecule **69** (Figure 28) was discovered by using structure-based rational design and has shown to be a potent and selective PKC $\theta$  inhibitor [139].



**Figure 27.** 1*H*-Pyrazolo[3,4-*b*]pyridines active against phosphodiesterase 4 (PDE4).

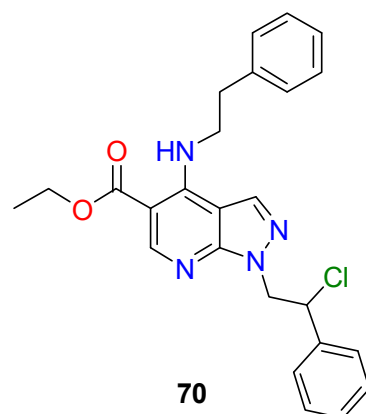


**Figure 28.** 1*H*-Pyrazolo[3,4-*b*]pyridine active against protein kinase C  $\theta$  (PKC $\theta$ ).

#### 4.3. Nervous System Agents

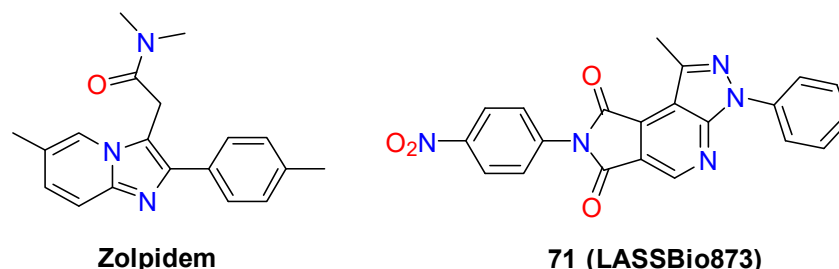
The use of pyrazolo[3,4-*b*]pyridines as a scaffold for the treatment of nervous system diseases corresponds to 10% of the overall biomedical applications. A total of 2799 molecules (20% of this category) presents a disubstitution  $R^3$  and  $R^5$ , while 2044 compounds (14% of this group) include a trisubstitution at  $R^1$ - $R^4$ - $R^5$ . Lower amounts of molecules (1337, 964, and 881 molecules) present substituents at  $R_1$ - $R_4$ - $R_5$ - $R_6$ ,  $R_3$ - $R_4$ - $R_6$ , and  $R_1$ - $R_3$ - $R_4$ - $R_6$ , respectively. In this category the situation concerning the nature of substituents present at the different positions is not so clear, but 1509 structures (10% of the total) present  $R^1$  = alkyl (or alky-substituted),  $R^3$  = H,  $R^5$  = carbonyl group, and  $R^6$  not equal to a hydrogen atom.

Adenosine is a neurotransmitter distributed through a wide variety of tissues in mammals.  $A_1$ -adenosine receptor ( $A_1$ AR) is an adenosine receptor that modulates adenosine effects together with  $A_{2A}$ ,  $A_{2B}$ , and  $A_3$ . Affinity data at  $A_1$ AR,  $A_{2A}$ AR, and  $A_{3A}$ AR in bovine membranes reveal that **70** (Figure 29) binds selectively and with a high-affinity  $A_1$ AR over  $A_{2A}$ AR and  $A_3$ AR [140].



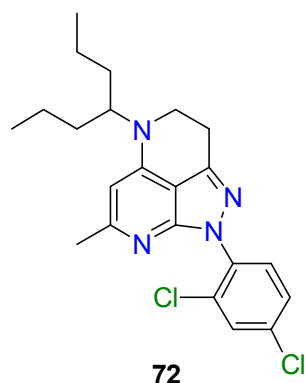
**Figure 29.** Pyrazolo[3,4-*b*]pyridine binding selectively with  $A_1$ -adenosine receptor ( $A_1$ AR).

Compound **71** (LASSBio873, Figure 30) was structurally designed by using the analgesic and sedative drug Zolpidem as a lead compound, which is used to treat anxiety disorders linked to the neuronal inhibition induced by  $\gamma$ -aminobutyric acid (GABA), the main inhibitory neurotransmitter in the mammalian central nervous system (CNS). Molecule **76** presents not only a potent ability to induce sedation but also a potent central antinociceptive effect [141].



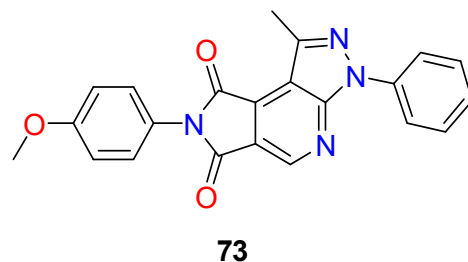
**Figure 30.** Zolpidem and its 1*H*-pyrazolo[3,4-*b*]pyridine analog.

Corticotropin-releasing factor type 1 (CRF(1)) is a novel target for the treatment of depression, anxiety, and stress-related disorders. Pyrazole-based molecule **72** (Figure 31) potently binds the CRF(1) with a  $K_i = 2.9$  nM and inhibits the adrenocorticotrophic hormone (ACTH) release from rat pituitary cell culture with an  $IC_{50}$  of 6.8 nM, which is the key hormone governing stress response. This compound also shows a great ACTH reduction of 84–86% when it is given orally at 30 mg/kg doses [142].



**Figure 31.** 1*H*-Pyrazolo[3,4-*b*]pyridine-inhibiting adrenocorticotrophic hormone (ACTH) release.

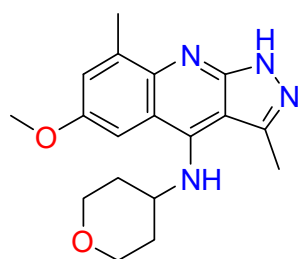
Compound **73** (Figure 32), which displays its CNS action as a muscarinic M1 receptor agonist, is an efficient compound to diminish the locomotor activity in mice at a dose of 10  $\mu$ mol/kg [143].



**Figure 32.** 1*H*-Pyrazolo[3,4-*b*]pyridine active as an M1 receptor agonist.

Pyrazoloquinoline **74** (Figure 33) has been described as a potent, selective, and orally active phosphodiesterase 10A inhibitor (PDE10A) for the potential treatment of schizophrenia. Compound **74** inhibits MK-801-induced hyperactivity at 3 mg/kg with an  $ED_{50}$  of

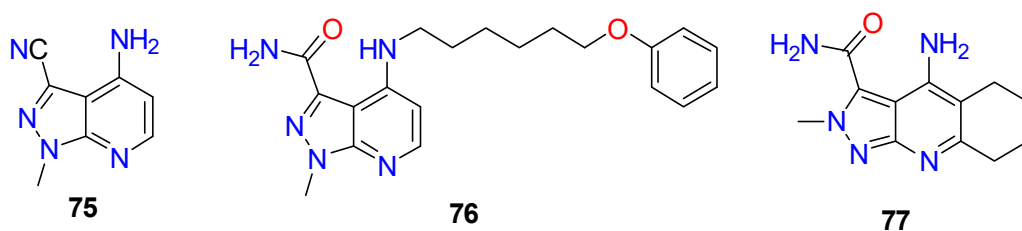
4 mg/kg and exhibits a 6-fold improvement between the ED<sub>50</sub> for inhibition of MK-801-induced hyperactivity and hypolocomotion in rats [144].



74

**Figure 33.** 1*H*-Pyrazolo[3,4-*b*]pyridine active as phosphodiesterase 10A inhibitor (PDE10A).

The latest indicators demonstrate that of the two confirmed methods for measuring amyloid, the decrease in cerebrospinal fluid (CSF) amyloid  $\beta_{1-42}$  ( $A\beta_{1-42}$ ) may be an earlier sign of Alzheimer disease (AD) risk [145]. Compounds **75** and **76** (Figure 34) avoid the decrease in cell viability caused by  $A\beta_{1-42}$ . **76** also prevents the upregulation of AChE induced by  $A\beta_{1-42}$ . It also may act as an antagonist of voltage-sensitive calcium channels. Compound **77** exhibits potential for the treatment of Alzheimer disease [146].



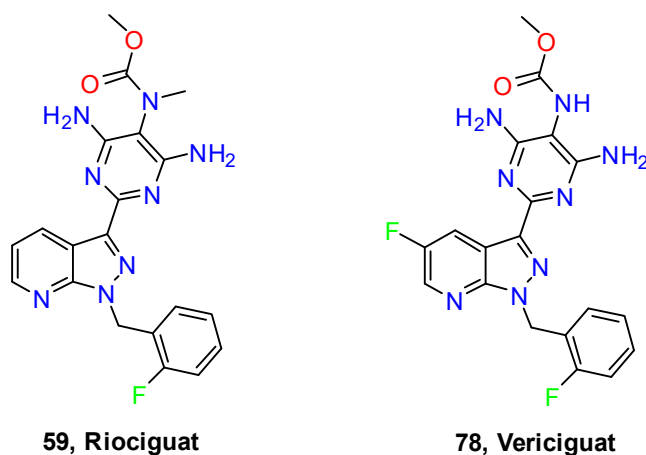
75

76

77

**Figure 34.** 1*H*-Pyrazolo[3,4-*b*]pyridines potentially active against Alzheimer disease.

To close this review, the search carried out in DrugBank (see our Introduction) has allowed us to establish that only two 1*H*-pyrazolo[3,4-*b*]pyridines have already been approved: Riociguat **59**, commercialized by Bayer as Adempas (described above and approved in 2013) and Vericiguat **78** (Figure 35), a stimulator of soluble guanylate cyclase (sGC) approved by the FDA in January 2021 and commercialized by Merck as Verquvo for the treatment of systemic heart failure [147].



59, Riociguat

78, Vericiguat

**Figure 35.** 1*H*-Pyrazolo[3,4-*b*]pyridines approved as treatments for cardiovascular diseases.

## 5. Conclusions

In this paper, we reviewed the substitution patterns of 1*H*-pyrazolo[3,4-*b*]pyridines (**1**), establishing the type of substituents mainly used at positions N1, C3, C4, C5, and C6. Such analysis has established that the 1*H*-isomers (substituted or unsubstituted at N1) predominate in a ratio of 3.6 to 1. Among 1*H*-pyrazolo[3,4-*b*]pyridines (**1**), two substitution patterns also are predominant: 3,4,6-trisubstitution and 3,5-disubstitution, both groups presenting mainly a hydrogen atom or methyl substituent at N1.

The complex landscape of the synthetic methods used for preparing such heterocycles has been analyzed and classified into two main methodologies: (a) formation of a pyridine ring into an existing pyrazole ring, and (b) the formation of the pyrazole ring into a preexisting pyridine ring. Most of the reactions found in the literature are of type (a) and use 3-aminopyrazole (substituted or not at N1) as the starting material, which generally acts as a 1,3-NCC-dinucleophile, reacting, therefore, with a 1,3-CCC-biselectrophile. The different subtypes depend on the nature of the 1,3-CCC-biselectrophile. Most of the type (b) constructions use hydrazine (or substituted hydrazine) onto a 2-chloro substituted pyridine ring bearing an aldehyde, ketone, ester, or cyano group at C3. Such groups determine the nature of the substituent present a C3 of the final 1*H*-pyrazolo[3,4-*b*]pyridine formed.

Finally, we have analyzed the potential biological uses of 1*H*-pyrazolo[3,4-*b*]pyridines **1**, establishing that such types of structures have been used for a wide range of biological targets. In fact, one-half of the molecules described were developed to discover biological activities. The main bioactivity indicators found include antitumor agents, anti-inflammatory agents, and nervous system agents that cover 36% of the overall biomedical applications. The most important biological targets and molecules developed have been summarized, showing the high versatility of these structures. Also, the substitution patterns and types of substituents used for each of the biological activities analyzed have been summarized.

The fact that, from the total number of references included in SciFinder since 1908, more than 50% correspond to the period from 2012 to 2022, showing an almost exponential increase, with half of them being patents, clearly indicates that this type of structure currently plays an important role as a scaffold for the development of drug candidates. The only drawbacks they present are the regioselectivity issues described in the synthetic section of this review and the fact that, in many cases, it is difficult to establish unequivocally the regioisomer formed based on spectroscopic techniques.

**Author Contributions:** Conceptualization: J.I.B.; writing—original draft preparation: A.D.-A., A.M.M. and J.I.B. (these authors contributed equally); validation: R.P.d.I.B., R.E.-T. and J.T.; writing—review and editing: J.I.B. All authors have read and agreed to the published version of the manuscript.

**Funding:** This research was funded by Ministerio de Ciencia, Innovación y Universidades, Proyectos de I + D + I “Retos Investigación” del Programa Estatal de I+D+I orientada a los Retos de la Sociedad, grant number RTI2018-096455-B-I00.

**Institutional Review Board Statement:** Not applicable.

**Informed Consent Statement:** Not applicable.

**Data Availability Statement:** Data sharing is not applicable.

**Conflicts of Interest:** The authors declare no conflict of interest.

**Sample Availability:** Samples of the compounds not available from the authors.

## References

1. Buckley, B.R. Bicyclic 5-6 Systems: Three Heteroatoms 2:1. In *Comprehensive Heterocyclic Chemistry III*; Elsevier: Amsterdam, The Netherlands, 2008; Volume 10, pp. 431–491, ISBN 9780080449920.
2. Ortoleva, G. New Compound Obtained by the Action of Iodine on Benzalphenylhydrazine in Pyridine Solution. *Gazz. Chim. Ital.* **1908**, *37*, 71–82.
3. Bulow, C. Synthesis of Derivatives of 1,2,7-Pyrazopyridine. A New Variety of Homo-(C. C)-Condensed, Bisheterocyclic Compounds. *Ber. Dtsch. Chem. Ges.* **1911**, *43*, 3401.
4. Chemical Abstracts Service. *Scifinder*, Version 2019; Chemical Abstracts Service: Columbus, OH, USA, 2019.

5. Sanghvi, Y.S.; Larson, S.B.; Robins, R.K.; Revankar, G.R. Synthesis of Certain C-4 Substituted Pyrazolo[3,4-*b*]Pyridine Nucleosides Structurally Related to Adenosine and Inosine by the Sodium Salt Glycosylation Procedure. *Nucleosides Nucleotides* **1989**, *8*, 887–890. [CrossRef]
6. Dodiya, D.K.; Trivedi, A.R.; Kataria, V.B.; Shah, V.H. Advances in the Synthesis of Pyrazolo[3,4-*b*]Pyridines. *Curr. Org. Chem.* **2012**, *16*, 400–417. [CrossRef]
7. Rao, R.P. Synthesis of New Pyrazolopyridines and Pyrazolopyrimidines. *Rec. Chem. Prog.* **1968**, *29*, 103.
8. Komarova, E.S.; Makarov, V.A.; Granik, V.G.; Parkanyi, C. Synthesis of Pyrazolo[3,4-*b*]Pyridin-6-Ones. *J. Heterocycl. Chem.* **2012**, *49*, 969–998. [CrossRef]
9. Alkorta, I.; Elguero, J. Theoretical Estimation of the Annular Tautomerism of Indazoles. *J. Phys. Org. Chem.* **2005**, *18*, 719–724. [CrossRef]
10. Aggarwal, R.; Singh, G.; Kumar, S. Molecular Iodine Mediated Transition-Metal-Free Oxidative Dehydrogenation of 4,7-Dihydropyrazolo[3,4-*b*]Pyridines. *Synth. Commun.* **2021**, *51*, 3601–3609. [CrossRef]
11. Lemmers, J.G.H.; Deretey, E.; Klomp, J.P.G.; Cals, J.M.G.; Oubrie, A. Preparation of 4-(4-Phenoxyphenyl)-4,5,6,7-Tetrahydro-2*H*-Pyrazolo[3,4-*b*]Pyridin-6-One Derivatives and Related Compounds as Estrogen-Related Receptor Alpha (ERR $\alpha$ ) Modulators. WO Patent 2021074365A1, 22 April 2021.
12. Bou-Petit, E.; Plans, A.; Rodríguez-Picazo, N.; Torres-Coll, A.; Puigjaner, C.; Font-Bardia, M.; Teixidó, J.; Ramon, Y.; Cajal, S.; Estrada-Tejedor, R.; et al. C4-C5 Fused Pyrazol-3-Amines: When the Degree of Unsaturation and Electronic Characteristics of the Fused Ring Controls Regioselectivity in Ullmann and Acylation Reactions. *Org. Biomol. Chem.* **2020**, *18*, 5145–5156. [CrossRef] [PubMed]
13. Almansa, C.; Virgili, M.; Carceller, E.; Grima-Poveda, P. Versatile Three Component Coupling for the Synthesis of Pyrazolopyridines and Other Pyrido Fused Systems. *Heterocycles* **2008**, *75*, 1695–1709. [CrossRef]
14. Grandberg, I.I. Pyrazoles. XIX. Aminopyrazoles as the Amino Components in the Skraup Reaction. Synthesis of Pyrazolopyridines. *Zhurnal Obs. Khimii* **1961**, *31*, 2307–2310.
15. Bhatt, A.; Singh, R.K.; Kant, R.; Chauhan, P.K. Synthesis, Characterization and Biological Evaluation of Some Novel Pyrazolo[3,4-*b*]Pyridin-3-Amine Derivatives. *Chem. Biol. Interface* **2016**, *6*, 357–365.
16. Patel, J.B.; Malick, J.B.; Salama, A.I.; Goldberg, M.E. Pharmacology of Pyrazolopyridines. *Pharmacol. Biochem. Behav.* **1985**, *23*, 675–680. [CrossRef]
17. Wenglowksy, S. Pyrazolo[3,4-*b*]Pyridine Kinase Inhibitors: A Patent Review (2008–Present). *Expert Opin. Ther. Pat.* **2013**, *23*, 281–298. [CrossRef] [PubMed]
18. Abdel-Latif, E.; Mehdhar, F.S.; Abdel-Ghani, G.E. Synthesis of New Polyheterocyclic Ring Systems Derived from 3-Amino-5-Bromo-4,6-Dimethyl-1*H*-Pyrazolo[3,4-*b*]Pyridine. *Polycycl. Aromat. Compd.* **2021**, *41*, 333–346. [CrossRef]
19. Park, A.; Hwang, J.; Lee, J.Y.; Heo, E.J.; Na, Y.J.; Kang, S.; Jeong, K.S.; Kim, K.Y.; Shin, S.J.; Lee, H. Synthesis of Novel 1*H*-Pyrazolo[3,4-*b*]Pyridine Derivatives as DYRK 1A/1B Inhibitors. *Bioorganic Med. Chem. Lett.* **2021**, *47*, 128226. [CrossRef]
20. Li, Z.; Qin, J.; Sun, X.; Jin, Y.; Su, W. Fast, Solvent-Free, and Highly Efficient Synthesis of Pyrazolo[3,4-*b*]Pyridines Using Microwave Irradiation and K<sub>2</sub>SO<sub>4</sub> as A Reusable Green Catalyst. *Heterocycles* **2019**, *98*, 1408–1422. [CrossRef]
21. Urvashi; Tandon, V.; Das, P.; Kukreti, S. Synthesis of 3,6-Diaryl-1*H*-Pyrazolo[3,4-*b*]Pyridines via One-Pot Sequential Suzuki-Miyaura Coupling. *RSC Adv.* **2018**, *8*, 34883–34894. [CrossRef]
22. Xing, Y.; Zuo, J.; Krogstad, P.; Jung, M.E. Synthesis and Structure-Activity Relationship (SAR) Studies of Novel Pyrazolopyridine Derivatives as Inhibitors of Enterovirus Replication. *J. Med. Chem.* **2018**, *61*, 1688–1703. [CrossRef] [PubMed]
23. Prakash, R.; Shekarrao, K.; Saikia, P.; Gogoi, S.; Boruah, R.C. Palladium Mediated Regioselective Intramolecular Heck Reaction: Synthesis of 1,3,4-Trisubstituted Pyrazolo[3,4-*b*]Pyridines, 3*H*-Pyrazolo[3,4-*c*]Isoquinolines and 3*H*-Pyrazolo[4,3-*f*][1,7]Naphthyridines. *RSC Adv.* **2015**, *5*, 21099–21102. [CrossRef]
24. Hao, S.Y.; Qi, Z.Y.; Wang, S.; Wang, X.R.; Chen, S.W. Synthesis and Bioevaluation of N-(3,4,5-Trimethoxyphenyl)-1*H*-Pyrazolo[3,4-*b*]Pyridin-3-Amines as Tubulin Polymerization Inhibitors with Anti-Angiogenic Effects. *Bioorganic Med. Chem.* **2021**, *31*, 115985. [CrossRef] [PubMed]
25. Merchant, R.R.; Lang, S.B.; Yu, T.; Zhao, S.; Qi, Z.; Suzuki, T.; Bao, J. A General One-Pot Protocol for Hindered N-Alkyl Azaheterocycles from Tertiary Carboxylic Acids. *Org. Lett.* **2020**, *22*, 4180–4184. [CrossRef] [PubMed]
26. Mekky, A.E.M.; Sanad, S.M.H. Synthesis, Characterization, and Antimicrobial Evaluation of Novel Thiohydrazonates and Pyrazolo[3,4-*b*]Pyridines. *Polycycl. Aromat. Compd.* **2021**, *41*, 936–949. [CrossRef]
27. Aggarwal, R.; Kumar, S.; Sadana, R.; Guzman, A.; Kumar, V. Multicomponent Synthesis, in Vitro Cytotoxic Evaluation and Molecular Modelling Studies of Polyfunctionalized Pyrazolo[3,4-*b*]Pyridine Derivatives against Three Human Cancer Cell Lines. *Synth. Commun.* **2021**, *51*, 3308–3324. [CrossRef]
28. Pfaffenrot, B.; Klövekorn, P.; Juchum, M.; Selig, R.; Albrecht, W.; Zender, L.; Laufer, S.A. Design and Synthesis of 1*H*-Pyrazolo[3,4-*b*]Pyridines Targeting Mitogen-Activated Protein Kinase Kinase 4 (MKK4)—A Promising Target for Liver Regeneration. *Eur. J. Med. Chem.* **2021**, *218*, 113371. [CrossRef] [PubMed]
29. Ribeiro, J.L.S.; Soares, J.C.A.V.; Portapilla, G.B.; Providello, M.V.; Lima, C.H.S.; Muri, E.M.F.; de Albuquerque, S.; Dias, L.R.S. Trypanocidal Activity of New 1,6-Diphenyl-1*H*-Pyrazolo[3,4-*b*]Pyridine Derivatives: Synthesis, in Vitro and in Vivo Studies. *Bioorganic Med. Chem.* **2021**, *29*, 115855. [CrossRef]

30. Luo, D.; Guo, Z.; Zhao, X.; Wu, L.; Liu, X.; Zhang, Y.; Zhang, Y.; Deng, Z.; Qu, X.; Cui, S.; et al. Novel 5-Fluorouracil Sensitizers for Colorectal Cancer Therapy: Design and Synthesis of S1P Receptor 2 (S1PR2) Antagonists. *Eur. J. Med. Chem.* **2022**, *227*, 113923. [CrossRef]
31. Miyachi, H.; Yuzuriha, T.; Tabata, R.; Fukuda, S.; Nunomura, K.; Lin, B.; Kobayashi, T.; Ishimoto, K.; Doi, T.; Tachibana, K. Structural Development of 1*H*-Pyrazolo-[3,4-*b*]Pyridine-4-Carboxylic Acid Derivatives as Human Peroxisome Proliferator-Activated Receptor Alpha (PPAR $\alpha$ )-Selective Agonists. *Bioorganic Med. Chem. Lett.* **2019**, *29*, 2124–2128. [CrossRef]
32. Doi, T.; Tachibana, K.; Kobayashi, T.; Yuzuriha, T.; Ishimoto, K.; Miyachi, H. PPAR $\alpha$  Transcriptional Activator Containing Pyrazolopyridine Derivative, and Use Thereof. WO Patent 2017082377A1, 18 May 2017.
33. Pal, A.; Banik, B.K. Microwave-Induced Suzuki-Coupling toward Pyrazoles. *Heterocycl. Lett.* **2021**, *11*, 19–23.
34. Bhukya, B.; Guguloth, H. Synthesis and Anticancer Activity of Novel Oxadiazole Functionalized Pyrazolo[3,4-*b*]Pyridine Derivatives. *Asian J. Chem.* **2021**, *33*, 1331–1335. [CrossRef]
35. Shen, L.-Q.; Tang, Y.; Wu, A.-Q.; Pan, D.; Diao, K.-S. Synthesis, X-ray Crystal Structure, and Computational Study of Novel Pyrazolo[3,4-*b*]Pyridin-3-*Ol* Derivatives. *Phosphorus Sulfur Silicon Relat. Elem.* **2014**, *189*, 674–686. [CrossRef]
36. Chang, Y.; Lu, X.; Shibu, M.A.; Dai, Y.B.; Luo, J.; Zhang, Y.; Li, Y.; Zhao, P.; Zhang, Z.; Xu, Y.; et al. Structure Based Design of N-(3-((1*H*-Pyrazolo[3,4-*b*]Pyridin-5-*Yl*)Ethyly)Benzenesulfonamides as Selective Leucine-Zipper and Sterile- $\alpha$  Motif Kinase (ZAK) Inhibitors. *J. Med. Chem.* **2017**, *60*, 5927–5932. [CrossRef] [PubMed]
37. Sumesh, R.V.; Kumar, R.R.; Almansour, A.I.; Kumar, R.S.; Ashraf, M.K.M. Pyrano[2,3-*f*]Pyrazolo[3,4-*b*]Quinoline-3-Carbonitriles: A Three-Component Synthesis and AChE Inhibitory Studies. *Synth. Commun.* **2021**, *51*, 1058–1065. [CrossRef]
38. Teixeira, F.C.; Lucas, C.; Curto, M.J.M.; André, V.; Duarte, M.T.; Teixeira, A.P.S. Synthesis of Novel Pyrazolo[3,4-*b*]Quinolinebisphosphonic Acids and an Unexpected Intramolecular Cyclization and Phosphonylation Reaction. *Org. Biomol. Chem.* **2021**, *19*, 2533–2545. [CrossRef] [PubMed]
39. Hamza, E.K.; Hamdy, N.A.; Zarie, E.S.; Fakhr, I.M.I.; Elwahy, A.H.M.; Awad, H.M. Synthesis and in Vitro Evaluation of Novel Tetralin-Pyrazolo[3,4-*b*]Pyridine Hybrids as Potential Anticancer Agents. *J. Heterocycl. Chem.* **2020**, *57*, 182–196. [CrossRef]
40. Jadhav, C.; Nipate, A.; Chate, A.; Gill, C. Triethylammonium Hydrogen Sulfate [Et<sub>3</sub>NH][HSO<sub>4</sub>]-Catalyzed Rapid and Efficient Multicomponent Synthesis of Pyrido[2,3-*d*]Pyrimidine and Pyrazolo[3,4-*b*]Pyridine Hybrids. *ACS Omega* **2021**, *6*, 18215–18225. [CrossRef]
41. Patnaik, S.; Basu, D.; Southall, N.; Dehdashti, S.; Wan, K.K.; Zheng, W.; Ferrer, M.; Taylor, M.; Engel, D.A.; Marugan, J.J. Identification, Design and Synthesis of Novel Pyrazolopyridine Influenza Virus Nonstructural Protein 1 Antagonists. *Bioorganic Med. Chem. Lett.* **2019**, *29*, 1113–1119. [CrossRef]
42. Ibrahim, S.A.; Rizk, H.F.; El-Borai, M.A.; Sadek, M.E. Green Routes for the Synthesis of New Pyrazole Bearing Biologically Active Imidiazolyl, Pyridine and Quinoxaline Derivatives as Promising Antimicrobial and Antioxidant Agents. *J. Iran. Chem. Soc.* **2021**, *18*, 1391–1404. [CrossRef]
43. Teleb, M.A.M.; Hassaneen, H.M.; Abdelhamid, I.A.; Saleh, F.M. 5-Aminopyrazole-4-Carbonitriles as Precursors to Novel 4-Aminotetrahydropyrazolo[3,4-*b*]Quinolin-5-Ones and N-(4-Cyanopyrazol-5-*Yl*)Pyridine-3-Carbonitrile. *Synth. Commun.* **2021**, *51*, 2357–2364. [CrossRef]
44. Mohamed, S.S.; Shabaan, S.N.; Abdelghaffar, N.F.; Dauoud, N.T.; Sayed, G.H.; Anwer, K.E. Synthesis and Exploring Novel Annulated 1,3-Diphenylpyrazole Derivatives as Antimicrobial and Anticancer Agents. *J. Basic Environ. Sci.* **2021**, *8*, 124–139.
45. Ramzan, A.; Siddiqui, S.; Irfan, A.; Al-Sehemi, A.G.; Ahmad, A.; Verpoort, F.; Chughtai, A.H.; Khan, M.A.; Munawar, M.A.; Basra, M.A.R. Antiplatelet Activity, Molecular Docking and QSAR Study of Novel *N*'-Arylmethylidene-3-Methyl-1-Phenyl-6-*p*-Chlorophenyl-1*H*-Pyrazolo[3,4-*b*]Pyridine-4-Carbohydrazides. *Med. Chem. Res.* **2018**, *27*, 388–405. [CrossRef]
46. Orlikova, B.; Chaouni, W.; Schumacher, M.; Aadil, M.; Diederich, M.; Kirsch, G. Synthesis and Bioactivity of Novel Amino-Pyrazolopyridines. *Eur. J. Med. Chem.* **2014**, *85*, 450–457. [CrossRef] [PubMed]
47. Arokiaraj, S.R.; Tajuddin, N.B.; Muthusamy, K.; Jayaraj, J.M.; Alagumuthu, M. TRAF2 and NCK-Interacting Kinase Inhibitors for Colorectal Cancer: In Vitro and Theoretical Validations. *ACS Comb. Sci.* **2020**, *22*, 608–616. [CrossRef] [PubMed]
48. Mostinski, Y.; Heynen, G.J.J.E.; Lopez-Alberca, M.P.; Paul, J.; Miksche, S.; Radetzki, S.; Schaller, D.; Shanina, E.; Seyffarth, C.; Kolomeets, Y.; et al. From Pyrazolones to Azaindoles: Evolution of Active-Site SHP2 Inhibitors Based on Scaffold Hopping and Bioisosteric Replacement. *J. Med. Chem.* **2020**, *63*, 14780–14804. [CrossRef] [PubMed]
49. Abdel-Mohsen, S.A.; El-Emary, T.I. New Pyrazolo[3,4-*b*]Pyridines: Synthesis and Antimicrobial Activity. *Pharma Chem.* **2018**, *10*, 44–51.
50. Hu, L.; Li, L.; Chang, Q.; Fu, S.; Qin, J.; Chen, Z.; Li, X.; Liu, Q.; Hu, G.; Li, Q. Discovery of Novel Pyrazolo[3,4-*b*]Pyridine Derivatives with Dual Activities of Vascular Remodeling Inhibition and Vasodilation for the Treatment of Pulmonary Arterial Hypertension. *J. Med. Chem.* **2020**, *63*, 11215–11234. [CrossRef]
51. Adib, M.; Peytam, F. An Efficient Synthesis of Fully Substituted Pyrazolo[3,4-*b*]Pyridin-5-Amines from  $\alpha$ -Azidochalcones. *Tetrahedron* **2018**, *74*, 2414–2420. [CrossRef]
52. Rao, H.S.P.; Adigopula, L.N.; Ramadas, K. One-Pot Synthesis of Densely Substituted Pyrazolo[3,4-*b*]-4,7-Dihydropyridines. *ACS Comb. Sci.* **2017**, *19*, 279–285. [CrossRef]
53. Czodrowski, P.; Mallinger, A.; Wienke, D.; Esdar, C.; Poeschke, O.; Busch, M.; Rohdich, F.; Eccles, S.A.; Ortiz-Ruiz, M.-J.; Schneider, R.; et al. Structure-Based Optimization of Potent, Selective, and Orally Bioavailable CDK8 Inhibitors Discovered by High-Throughput Screening. *J. Med. Chem.* **2016**, *59*, 9337–9349. [CrossRef]

54. Aly, A.A.; El-Emary, T.I.; Mourad, A.-F.E.; Khallaf Alyan, Z.; Brase, S.; Nieger, M. 5-Carbohydrazide and 5-Carbonylazide of Pyrazolo[3,4-*b*]Pyridines as Reactive Intermediates in the Synthesis of Various Heterocyclic Derivatives. *J. Chem. Res.* **2019**, *43*, 219–229. [CrossRef]
55. Alam, R.M.; Keating, J.J. An Expedient Approach to Pyrazolo[3,4-*b*]Pyridine-3-Carboxamides via Palladium-Catalyzed Aminocarbonylation. *Synthesis* **2021**, *53*, 4709–4722. [CrossRef]
56. Chen, X.; Liu, Y.; Zhang, L.; Chen, D.; Dong, Z.; Zhao, C.; Liu, Z.; Xia, Q.; Wu, J.; Chen, Y.; et al. Design, Synthesis, and Biological Evaluation of Indazole Derivatives as Selective and Potent FGFR4 Inhibitors for the Treatment of FGF19-Driven Hepatocellular Cancer. *Eur. J. Med. Chem.* **2021**, *214*, 113219. [CrossRef] [PubMed]
57. Hamajima, T.; Takahashi, F.; Kato, K.; Sugano, Y.; Yamaki, S.; Moritomo, A.; Kubo, S.; Nakamura, K.; Yamagami, K.; Hamakawa, N.; et al. Optimization and in Vivo Evaluation of Pyrazolopyridines as a Potent and Selective PI3K $\delta$  Inhibitor. *Bioorganic Med. Chem.* **2018**, *26*, 3917–3924. [CrossRef] [PubMed]
58. Ravula, S.; Bobbala, R.R.; Kolli, B. Synthesis of Novel Isoxazole Functionalized Pyrazolo[3,4-*b*]Pyridine Derivatives; Their Anticancer Activity. *J. Heterocycl. Chem.* **2020**, *57*, 2535–2538. [CrossRef]
59. Hansen, B.B.; Jepsen, T.H.; Larsen, M.; Sindet, R.; Vifian, T.; Burhardt, M.N.; Larsen, J.; Seitzberg, J.G.; Carnerup, M.A.; Jerre, A.; et al. Fragment-Based Discovery of Pyrazolopyridones as JAK1 Inhibitors with Excellent Subtype Selectivity. *J. Med. Chem.* **2020**, *63*, 7008–7032. [CrossRef]
60. Labhade, K.R.; Jachak, M.N.; Labhade, S.R.; Kale, A.S.; Gaikwad, V.B. Synthesis and in Vitro Antimicrobial Evaluation of Novel Trifluoromethyl Substituted Pyrazolo[3,4-*b*]Pyridine 6-One Derivatives. *Indo Am. J. Pharm. Res.* **2016**, *6*, 6442–6447.
61. Sanad, S.M.H.; Abdel-Fattah, A.M.; Attaby, F.A.; Elneairy, M.A.A. Pyridine-2(1H)-Thiones: Versatile Precursors for Novel Pyrazolo[3,4-*b*]Pyridine, Thieno[2,3-*b*]Pyridines, and Their Fused Azines. *J. Heterocycl. Chem.* **2019**, *56*, 651–662. [CrossRef]
62. Mohamed, L.W.; Shaaban, M.A.; Zaher, A.F.; Alhamaky, S.M.; Elsahar, A.M. Synthesis of New Pyrazoles and Pyrolo[3,4-*b*]Pyridines as Anti-Inflammatory Agents by Inhibition of COX-2 Enzyme. *Bioorganic Chem.* **2019**, *83*, 47–54. [CrossRef]
63. Ghaedi, A.; Bardajee, G.R.; Mirshokrayi, A.; Mahdavi, M.; Shafiee, A.; Akbarzadeh, T. Facile, Novel and Efficient Synthesis of New Pyrazolo[3,4-*b*]Pyridine Products from Condensation of Pyrazole-5-Amine Derivatives and Activated Carbonyl Groups. *RSC Adv.* **2015**, *5*, 89652–89658. [CrossRef]
64. El-borai, M.A.; Rizk, H.F.; Abd-Aal, M.F.; El-Deeb, I.Y. Synthesis of Pyrazolo[3,4-*b*]Pyridines under Microwave Irradiation in Multi-Component Reactions and Their Antitumor and Antimicrobial Activities. Part 1. *Eur. J. Med. Chem.* **2012**, *48*, 92–96. [CrossRef]
65. Volochnyuk, D.M.; Ryabukhin, S.V.; Plaskon, A.S.; Dmytriv, Y.V.; Grygorenko, O.O.; Mykhailiuk, P.K.; Krotko, D.G.; Pushechnikov, A.; Tolmachev, A.A. Approach to the Library of Fused Pyridine-4-Carboxylic Acids by Combes-Type Reaction of Acyl Pyruvates and Electron-Rich Amino Heterocycles. *J. Comb. Chem.* **2010**, *12*, 510–517. [CrossRef]
66. Emelina, E.E.; Petrov, A.A.; Selivanov, S.I.; Filyukov, D.V.  $\alpha$ -Aminoazoles in Synthesis of Heterocycles: III. 4-Trifluoromethylpyrazolo[3,4-*b*]Pyridines: Synthesis and Structure. *Russ. J. Org. Chem.* **2008**, *44*, 251–256. [CrossRef]
67. Wenglowksy, S.; Ren, L.; Ahrendt, K.A.; Laird, E.R.; Aliagas, I.; Alicke, B.; Buckmelter, A.J.; Choo, E.F.; Dinkel, V.; Feng, B.; et al. Pyrazolopyridine Inhibitors of B-RafV600E. Part 1: The Development of Selective, Orally Bioavailable, and Efficacious Inhibitors. *ACS Med. Chem. Lett.* **2011**, *2*, 342–347. [CrossRef]
68. Mityuk, A.P.; Hrebonkin, A.; Lebed, P.S.; Grabchuk, G.P.; Volochnyuk, D.M.; Ryabukhin, S.V. Efficient Route for the Synthesis of Diverse Heteroannulated 5-Cyanopyridines. *Synthesis* **2021**, *53*, 2133–2141. [CrossRef]
69. Jouha, J.; Loubidi, M.; Bouali, J.; Hamri, S.; Hafid, A.; Suzenet, F.; Guillaumet, G.; Dagci, T.; Khouili, M.; Aydın, F.; et al. Synthesis of New Heterocyclic Compounds Based on Pyrazolopyridine Scaffold and Evaluation of Their Neuroprotective Potential in MPP<sup>+</sup>-Induced Neurodegeneration. *Eur. J. Med. Chem.* **2017**, *129*, 41–52. [CrossRef] [PubMed]
70. Iaroshenko, V.O.; Mkrtchyan, S.; Gevorgyan, A.; Vilches-Herrera, M.; Sevenard, D.V.; Villinger, A.; Ghochikyan, T.V.; Saghiyan, A.; Sosnovskikh, V.Y.; Langer, P. Synthesis of Heteroannulated 3-Nitro- and 3-Aminopyridines by Cyclocondensation of Electron-Rich Aminoheterocycles with 3-Nitrochromone. *Tetrahedron* **2012**, *68*, 2532–2543. [CrossRef]
71. Iaroshenko, V.O.; Gevorgyan, A.; Mkrtchyan, S.; Grigoryan, T.; Movsisyan, E.; Villinger, A.; Langer, P. Regioselective Direct Arylation of Fused 3-Nitropyridines and Other Nitro-Substituted Heteroarenes: The Multipurpose Nature of the Nitro Group as a Directing Group. *ChemCatChem* **2015**, *7*, 316–324. [CrossRef]
72. Iaroshenko, V.O.; Mkrtchyan, S.; Gevorgyan, A.; Miliutina, M.; Villinger, A.; Volochnyuk, D.; Sosnovskikh, V.Y.; Langer, P. 2,3-Unsubstituted Chromones and Their Enaminone Precursors as Versatile Reagents for the Synthesis of Fused Pyridines. *Org. Biomol. Chem.* **2012**, *10*, 890–894. [CrossRef]
73. Stepaniuk, O.O.; Stepaniuk, O.O.; Rudenko, T.V.; Rudenko, T.V.; Vashchenko, B.V.; Vashchenko, B.V.; Matvienko, V.O.; Kondratov, I.S.; Kondratov, I.S.; Tolmachev, A.A.; et al. Synthesis of Fused Pyridine Carboxylates by Reaction of  $\beta$ -Alkoxyvinyl Glyoxylates with Amino Heterocycles. *Synthesis* **2020**, *52*, 1915–1926. [CrossRef]
74. Han, Z.G.; Zhang, G.; Jiang, B.; Ning, M.; Shi, F.; Tu, S.J. Diversity Synthesis of Pyrimido[4,5-*E*][1,6]Naphthyridine and Its Derivatives under Microwave Irradiation. *J. Comb. Chem.* **2009**, *11*, 809–812. [CrossRef] [PubMed]
75. Liu, X.C.; Lin, W.; Wang, H.Y.; Huang, Z.B.; Shi, D.Q. Improved and Efficient Synthesis of Chromeno[4,3-*d*]Pyrazolo[3,4-*b*]Pyridin-6(3H)-Ones and Their Fluorescence Properties. *J. Heterocycl. Chem.* **2014**, *51*, 1036–1044. [CrossRef]
76. Liu, M.; Yin, G. ZrCl<sub>4</sub>-Catalysed Synthesis of New 4-(2-Hydroxyphenyl)Pyrazolo[3,4-*b*]Pyridine Derivatives. *J. Chem. Res.* **2015**, *263*, 263–266. [CrossRef]



77. Zou, X.; Tu, S.; Shi, F.; Xu, J. An Efficient Synthesis of Pyrazolo[3,4-*b*]Pyridine Derivatives under Microwave Irradiation. *Gen. Pap. ARKIVOC* **2006**, *2*, 130–135. [CrossRef]
78. Shi, D.Q.; Zhou, Y.; Liu, H. An Efficient Synthesis of Pyrazolo[3,4-*b*]Pyridine Derivatives in Ionic Liquid. *Synth. Commun.* **2010**, *40*, 3660–3668. [CrossRef]
79. Lavrard, H.; Popowycz, F. Harnessing Cascade Suzuki-Cyclization Reactions of Pyrazolo[3,4-*b*]Pyridine for the Synthesis of Tetracyclic Fused Heteroaromatics. *Eur. J. Org. Chem.* **2017**, *2017*, 600–608. [CrossRef]
80. Miah, A.H.; Champigny, A.C.; Graves, R.H.; Hodgson, S.T.; Percy, J.M.; Procopiou, P.A. Identification of Pyrazolopyrimidine Arylsulfonamides as CC-Chemokine Receptor 4 (CCR4) Antagonists. *Bioorganic Med. Chem.* **2017**, *25*, 5327–5340. [CrossRef] [PubMed]
81. Guercio, G.; Castoldi, D.; Giubellina, N.; Lamonica, A.; Ribecai, A.; Stabile, P.; Westerduin, P.; Dams, R.; Nicoletti, A.; Rossi, S.; et al. Overall Synthesis of GSK356278: Quick Delivery of a PDE4 Inhibitor Using a Fit-for-Purpose Approach. *Org. Process. Res. Dev.* **2010**, *14*, 1153–1161. [CrossRef]
82. Azevedo, A.R.; Ferreira, V.F.; de Mello, H.; Leão-Ferreira, L.R.; Jabor, A.V.; Frugulhetti, I.C.P.P.; Pereira, H.S.; Moussatche, N.; Rolim Bernardino, A.M. Synthesis and biological evaluation of 1H-pyrazolo[3,4-*b*]pyridine-5-carboxylic acids against vaccinia virus. *Heterocycl. Commun.* **2002**, *8*, 427–432. [CrossRef]
83. Rimland, J.; Dunne, A.; Hunjan, S.S.; Sasse, R.; Uings, I.; Montanari, D.; Caivano, M.; Shah, P.; Standing, D.; Gray, D.; et al. The Identification a Novel, Selective, Non-Steroidal, Functional Glucocorticoid Receptor Antagonist. *Bioorganic Med. Chem. Lett.* **2010**, *20*, 2340–2343. [CrossRef]
84. Pan, T.; Xie, S.; Zhou, Y.; Hu, J.; Luo, H.; Li, X.; Huang, L. Dual Functional Cholinesterase and PDE4D Inhibitors for the Treatment of Alzheimer's Disease: Design, Synthesis and Evaluation of Tacrine-Pyrazolo[3,4-*b*]Pyridine Hybrids. *Bioorganic Med. Chem. Lett.* **2019**, *29*, 2150–2152. [CrossRef]
85. Ezzati, M.; Khalafy, J.; Marjani, A.P.; Prager, R.H. The Catalyst-Free Syntheses of Pyrazolo[3,4-*b*]Quinolin-5-One and Pyrazolo[4',3':5,6]Pyrido[2,3-*d*]Pyrimidin-5,7-Dione Derivatives by One-Pot, Three-Component Reactions. *Tetrahedron* **2017**, *73*, 6587–6596. [CrossRef]
86. Quiroga, J.; Trilleras, J.; Sánchez, A.I.; Insuasty, B.; Abonía, R.; Noguera, M.; Cobo, J. Regioselective Three-Component Synthesis of Indolylpyrazolo[3,4-*b*]Pyridines Induced by Microwave and under Solvent-Free Conditions. *Lett. Org. Chem.* **2009**, *6*, 381–383. [CrossRef]
87. Huang, Z.; Hu, Y.; Zhou, Y.; Shi, D. Efficient One-Pot Three-Component Synthesis of Fused Pyridine Derivatives in Ionic Liquid. *ACS Comb. Sci.* **2011**, *13*, 45–49. [CrossRef] [PubMed]
88. Rahmati, A.; Khalesi, Z. Catalyst Free Synthesis of Fused Pyrido[2,3-*d*]Pyrimidines and Pyrazolo[3,4-*b*]Pyridines in Water. *Chin. Chem. Lett.* **2012**, *23*, 1149–1152. [CrossRef]
89. Shi, C.L.; Shi, D.Q.; Kim, S.H.; Huang, Z.B.; Ji, S.J.; Ji, M. A Novel and Efficient One-Pot Synthesis of Furo[3',4':5,6]Pyrido[2,3-*c*]Pyrazole Derivatives Using Organocatalysts. *Tetrahedron* **2008**, *64*, 2425–2432. [CrossRef]
90. Shi, D.Q.; Yang, F.; Ni, S.N. A Facile Synthesis of Furo[3,4-*e*]Pyrazolo[3,4-*b*]Pyridine-5(7H)-One Derivatives via Three-Component Reaction in Ionic Liquid without Any Catalyst. *J. Heterocycl. Chem.* **2009**, *46*, 469–476. [CrossRef]
91. Hamama, W.S.; El-Gohary, H.G.; Soliman, M.; Zoorob, H.H. A Versatile Synthesis, PM3-Semiempirical, Antibacterial, and Antitumor Evaluation of Some Bioactive Pyrazoles. *J. Heterocycl. Chem.* **2012**, *49*, 543–554. [CrossRef]
92. Marzouk, M.I.; Sayed, G.H.; Abd ElHalim, M.S.; Mansour, S.Y. Synthesis and Characterization of Novel Pyrazolone Derivatives. *Eur. J. Chem.* **2014**, *5*, 24–32. [CrossRef]
93. Witherington, J.; Bordas, V.; Garland, S.L.; Hickey, D.M.B.; Ife, R.J.; Liddle, J.; Saunders, M.; Smith, D.G.; Ward, R.W. 5-Aryl-Pyrazolo[3,4-*b*]Pyridines: Potent Inhibitors of Glycogen Synthase Kinase-3 (GSK-3). *Bioorganic Med. Chem. Lett.* **2003**, *13*, 1577–1580. [CrossRef]
94. Shi, J.; Xu, G.; Zhu, W.; Ye, H.; Yang, S.; Luo, Y.; Han, J.; Yang, J.; Li, R.; Wei, Y.; et al. Design and Synthesis of 1,4,5,6-Tetrahydropyrrolo[3,4-*c*]Pyrazoles and Pyrazolo[3,4-*b*]Pyridines for Aurora-A Kinase Inhibitors. *Bioorganic Med. Chem. Lett.* **2010**, *20*, 4273–4278. [CrossRef]
95. Ren, X.; Pan, X.; Zhang, Z.; Wang, D.; Lu, X.; Li, Y.; Wen, D.; Long, H.; Luo, J.; Feng, Y.; et al. Identification of GZD824 as an Orally Bioavailable Inhibitor That Targets Phosphorylated and Nonphosphorylated Breakpoint Cluster Region-Abelson (Bcr-Abl) Kinase and Overcomes Clinically Acquired Mutation-Induced Resistance against Imatinib. *J. Med. Chem.* **2013**, *56*, 879–894. [CrossRef] [PubMed]
96. Li, Y.; Cheng, H.; Zhang, Z.; Zhuang, X.; Luo, J.; Long, H.; Zhou, Y.; Xu, Y.; Taghipouran, R.; Li, D.; et al. N-(3-Ethynyl-2,4-Difluorophenyl)Sulfonamide Derivatives as Selective Raf Inhibitors. *ACS Med. Chem. Lett.* **2015**, *6*, 543–547. [CrossRef] [PubMed]
97. Arafa, W.A.A.; Hussein, M.F. Design, Sonosynthesis, Quantum-Chemical Calculations, and Evaluation of New Mono- and Bis-Pyridine Dicarbonitriles as Antiproliferative Agents. *Chin. J. Chem.* **2020**, *38*, 501–508. [CrossRef]
98. Rateb, N.M. Synthesis and Reactions of 4-Trifluoromethyl-3-Cyano Pyridine-2(1H)-Thione/One Derivatives. *J. Sulfur Chem.* **2011**, *32*, 611–622. [CrossRef]
99. Bakhite, E.A.; Abdel-Rahman, A.E.; Al-Taifi, E.A. Fluorine-Containing Heterocycles: Part III. Synthesis of Some New Furo[2,3-*b*]-, Pyrazolo[3,4-*b*]- and Thieno[2,3-*b*]Pyridines with Anticipated Biological Activities. *Arab. J. Chem.* **2014**, *7*, 936–946. [CrossRef]

100. van Linden, O.P.J.; Farenc, C.; Zoutman, W.H.; Hameetman, L.; Wijtmans, M.; Leurs, R.; Tensen, C.P.; Siegal, G.; de Esch, I.J.P. Fragment Based Lead Discovery of Small Molecule Inhibitors for the EPHA4 Receptor Tyrosine Kinase. *Eur. J. Med. Chem.* **2012**, *47*, 493–500. [CrossRef]
101. Mali, J.R.; Pratap, U.R.; Jawale, D.V.; Mane, R.A. Water-Mediated One-Pot Synthetic Route for Pyrazolo[3,4-*b*]Quinolines. *Tetrahedron Lett.* **2010**, *51*, 3980–3982. [CrossRef]
102. Waly, M.A.; El-Hawary, I.I.; Hamama, W.S.; Zoorob, H.H. Synthesis and Antitumor Evaluation of Some New Fused and Binary Pyridines. *J. Heterocycl. Chem.* **2013**, *50*, E12–E17. [CrossRef]
103. Lapa, G.B.; Bekker, O.B.; Mirchink, E.P.; Danilenko, V.N.; Preobrazhenskaya, M.N. Regioselective Acylation of Congeners of 3-Amino-1*H*-Pyrazolo[3,4-*b*] Quinolines, Their Activity on Bacterial Serine/Threonine Protein Kinases and in Vitro Antibacterial (Including Antimycobacterial) Activity. *J. Enzym. Inhib. Med. Chem.* **2013**, *28*, 1088–1093. [CrossRef]
104. Masoud, M.S.; AbouEl-Enein, S.A.; Ali, A.E.; Abd Elhamed, E.H. Chelating Behavior of 3-Amino-4,6-Dimethyl-1*H*-Pyrazolo[3,4-*b*]Pyridine Ligand towards Some Metal Ions, Spectral and Thermal Measurements as Well as Molecular Modeling and Biological Studies. *J. Mol. Struct.* **2020**, *1202*, 127172. [CrossRef]
105. Moir, M.; Lane, S.; Lai, F.; Connor, M.; Hibbs, D.E.; Kassiou, M. Strategies to Develop Selective CB2 Receptor Agonists from Indole Carboxamide Synthetic Cannabinoids. *Eur. J. Med. Chem.* **2019**, *180*, 291–309. [CrossRef] [PubMed]
106. Kim, J.; Lee, D.; Park, C.; So, W.; Jo, M.; Ok, T.; Kwon, J.; Kong, S.; Jo, S.; Kim, Y.; et al. Discovery of Phenylaminopyridine Derivatives as Novel HIV-1 Non-Nucleoside Reverse Transcriptase Inhibitors. *ACS Med. Chem. Lett.* **2012**, *3*, 678–682. [CrossRef] [PubMed]
107. Al-Kaabi, S.S.; Elgemeie, G.E.H. Studies on Fused 2(1*H*)-Pyridenethiones-New Routes for the Synthesis of Fused 1*H*-Pyrazolo[3,4-*b*]Pyridines and Fused Thieno[2,3-*b*]Pyridines. *Chem. Soc. Jpn.* **1992**, *65*, 2241–2245. [CrossRef]
108. Selvi, S.T.; Nadaraj, V.; Mohan, S.; Sasi, R.; Hema, M. Solvent Free Microwave Synthesis and Evaluation of Antimicrobial Activity of Pyrimido[4,5-*b*]- and Pyrazolo[3,4-*b*]Quinolines. *Bioorganic Med. Chem.* **2006**, *14*, 3896–3903. [CrossRef] [PubMed]
109. El-Borai, M.A.; Rizk, H.F.; Beltagy, D.M.; El-Deeb, I.Y. Microwave-Assisted Synthesis of Some New Pyrazolopyridines and Their Antioxidant, Antitumor and Antimicrobial Activities. *Eur. J. Med. Chem.* **2013**, *66*, 415–422. [CrossRef] [PubMed]
110. Kale, A.; Medishetti, N.; Kanugala, S.; Ganesh Kumar, C.; Atmakur, K. Na<sub>2</sub>S<sub>2</sub>O<sub>8</sub>-Promoted Reduction of Azides in Water: Synthesis of Pyrazolopyridines in One Pot and Evaluation of Antimicrobial Activity. *Org. Biomol. Chem.* **2019**, *17*, 3186–3194. [CrossRef] [PubMed]
111. Aly, A.A.; El-Emary, T.I.; Mourad, A.F.E.; Alyan, Z.K.; Bräse, S.; Nieger, M. Synthesis of New Heterocycles from Reactions of 1-Phenyl-1*H*-Pyrazolo[3,4-*b*]Pyridine-5-Carbonyl Azides. *J. Heterocycl. Chem.* **2019**, *56*, 1369–1375. [CrossRef]
112. Ghattas, A.B.A.G.; Khodairy, A.; Abd-Rahman, M.A.; Younes, S. Synthesis of Some New Pyrazolopyridines, Pyrazolothienopyridines, Pyrazolopyridothienopyrimidines and Pyrazolopyridothienotriazines. *Phosphorus Sulfur Silicon Relat. Elem.* **2003**, *178*, 1781–1794. [CrossRef]
113. Girisha, K.S.; Kalluraya, B.; Vidyashree, J.H.S. Synthesis, Characterisation and Antimicrobial Activity of 3-Methyl-6-(Aryl)-1-Phenyl-1*H*-Pyrazolo[3,4-*b*]Pyridine. *Indian J. Chem.* **2012**, *51*, 1767–1770.
114. Castillo, J.C.; Quiroga, J.; Abonia, R.; Rodriguez, J.; Coquerel, Y. The Aryne Aza-Diels-Alder Reaction: Flexible Syntheses of Isoquinolines. *Org. Lett.* **2015**, *17*, 3374–3377. [CrossRef]
115. Xu, H.; Li, L.; Wang, Z.; Xi, J.; Rong, L. A Green Synthesis of 1,7-Dihydrodipyrazolo[3,4-*b*:4',3'-*e*]Pyridin-3(2*H*)-One Derivatives from Deamination Cyclization Reactions in Aqueous Medium. *Res. Chem. Intermed.* **2018**, *44*, 3211–3226. [CrossRef]
116. Cacciari, B.; Spalluto, G. Facile and Versatile Route to the Synthesis of Fused 2-Pyridones: Useful Intermediates for Polycyclic Systems. *Synth. Commun.* **2006**, *36*, 1173–1183. [CrossRef]
117. Witherington, J.; Bordas, V.; Gaiba, A.; Garton, N.S.; Naylor, A.; Rawlings, A.D.; Slingsby, B.P.; Smith, D.G.; Takle, A.K.; Ward, R.W. 6-Aryl-Pyrazolo[3,4-*b*]Pyridines: Potent Inhibitors of Glycogen Synthase Kinase-3 (GSK-3). *Bioorganic Med. Chem. Lett.* **2003**, *13*, 3055–3057. [CrossRef]
118. Misra, R.N.; Xiao, H.Y.; Rawlins, D.B.; Shan, W.; Kellar, K.A.; Mulheron, J.G.; Sack, J.S.; Tokarski, J.S.; Kimball, S.D.; Webster, K.R. 1*H*-Pyrazolo[3,4-*b*]Pyridine Inhibitors of Cyclin-Dependent Kinases: Highly Potent 2,6-Difluorophenacyl Analogues. *Bioorganic Med. Chem. Lett.* **2003**, *13*, 2405–2408. [CrossRef]
119. Huang, S.; Lin, R.; Yu, Y.; Lu, Y.; Connolly, P.J.; Chiu, G.; Li, S.; Emanuel, S.L.; Middleton, S.A. Synthesis of 3-(1*H*-Benzimidazol-2-yl)-5-Isoquinolin-4-ylpyrazolo[1,2-*b*]Pyridine, a Potent Cyclin Dependent Kinase 1 (CDK1) Inhibitor. *Bioorganic Med. Chem. Lett.* **2007**, *17*, 1243–1245. [CrossRef]
120. Jing, L.; Tang, Y.; Xiao, Z. Discovery of Novel CDK Inhibitors via Scaffold Hopping from CAN508. *Bioorganic Med. Chem. Lett.* **2018**, *28*, 1386–1391. [CrossRef] [PubMed]
121. Lin, R.; Connolly, P.J.; Lu, Y.; Chiu, G.; Li, S.; Yu, Y.; Huang, S.; Li, X.; Emanuel, S.L.; Middleton, S.A.; et al. Synthesis and Evaluation of Pyrazolo[3,4-*b*]Pyridine CDK1 Inhibitors as Anti-Tumor Agents. *Bioorganic Med. Chem. Lett.* **2007**, *17*, 4297–4302. [CrossRef]
122. Hoorens, M.W.H.; Ourailidou, M.E.; Rodat, T.; van der Wouden, P.E.; Kobauri, P.; Kriegs, M.; Peifer, C.; Feringa, B.L.; Dekker, F.J.; Szymanski, W. Light-Controlled Inhibition of BRAFV600E Kinase. *Eur. J. Med. Chem.* **2019**, *179*, 133–146. [CrossRef]
123. Li, Y.; Shen, M.; Zhang, Z.; Luo, J.; Pan, X.; Lu, X.; Long, H.; Wen, D.; Zhang, F.; Leng, F.; et al. Design, Synthesis, and Biological Evaluation of 3-(1*H*-1,2,3-Triazol-1-yl) Benzamide Derivatives as Potent Pan Bcr-Abl Inhibitors Including the Threonine315→isoleucine315 Mutant. *J. Med. Chem.* **2012**, *55*, 10033–10046. [CrossRef]

124. Barghash, R.F.; Eldehna, W.M.; Kovalová, M.; Vojáčková, V.; Kryštof, V.; Abdel-Aziz, H.A. One-Pot Three-Component Synthesis of Novel Pyrazolo[3,4-*b*]Pyridines as Potent Antileukemic Agents. *Eur. J. Med. Chem.* **2022**, *227*, 113952. [CrossRef] [PubMed]
125. Zheng, X.; Bair, K.W.; Bauer, P.; Baumeister, T.; Bowman, K.K.; Buckmelter, A.J.; Caligiuri, M.; Clodfelter, K.H.; Feng, Y.; Han, B.; et al. Identification of Amides Derived from 1*H*-Pyrazolo[3,4-*b*]Pyridine-5-Carboxylic Acid as Potent Inhibitors of Human Nicotinamide Phosphoribosyltransferase (NAMPT). *Bioorganic Med. Chem. Lett.* **2013**, *23*, 5488–5497. [CrossRef] [PubMed]
126. Huber, K.V.M.; Salah, E.; Radic, B.; Gridling, M.; Elkins, J.M.; Stukalov, A.; Jemth, A.S.; Göktürk, C.; Sanjiv, K.; Strömberg, K.; et al. Stereospecific Targeting of MTH1 by (S)-Crizotinib as an Anticancer Strategy. *Nature* **2014**, *508*, 222–227. [CrossRef] [PubMed]
127. Zhai, M.; Liu, S.; Gao, M.; Wang, L.; Sun, J.; Du, J.; Guan, Q.; Bao, K.; Zuo, D.; Wu, Y.; et al. 3,5-Diaryl-1*H*-Pyrazolo[3,4-*b*]Pyridines as Potent Tubulin Polymerization Inhibitors: Rational Design, Synthesis and Biological Evaluation. *Eur. J. Med. Chem.* **2019**, *168*, 426–435. [CrossRef] [PubMed]
128. Nam, Y.; Hwang, D.; Kim, N.; Seo, H.S.; Selim, K.B.; Sim, T. Identification of 1*H*-Pyrazolo[3,4-*b*]Pyridine Derivatives as Potent ALK-L1196M Inhibitors. *J. Enzym. Inhib. Med. Chem.* **2019**, *34*, 1426–1438. [CrossRef]
129. Kihara, T.; Yuan, J.; Watabe, T.; Kitajima, K.; Kimura, N.; Ohkouchi, M.; Hashikura, Y.; Ohkubo, S.; Takahashi, T.; Hirota, S. Pimipib Is Effective on Cecal GIST in a Mouse Model of Familial GISTs with KIT-Asp820Tyr Mutation through KIT Signaling Inhibition. *Exp. Mol. Pathol.* **2021**, *123*, 104692. [CrossRef] [PubMed]
130. Huang, Y.; Li, Y.; Dong, G.; Zhang, W.; Liu, N.; Sheng, C. Identification of Pyrazolopyridine Derivatives as Novel Spleen Tyrosine Kinase Inhibitors. *Arch. Pharm.* **2018**, *351*, 1800083. [CrossRef]
131. Goldenberg, N.M.; Rabinovitch, M.; Steinberg, B.E. Inflammatory Basis of Pulmonary Arterial Hypertension Implications for Perioperative and Critical Care Medicine. *Anesthesiology* **2019**, *131*, 898–907. [CrossRef]
132. Mittendorf, J.; Weigand, S.; Alonso-Alija, C.; Bischoff, E.; Feurer, A.; Gerisch, M.; Kern, A.; Knorr, A.; Lang, D.; Muentner, K.; et al. Discovery of Riociguat (BAY 63-2521): A Potent, Oral Stimulator of Soluble Guanylate Cyclase for the Treatment of Pulmonary Hypertension. *ChemMedChem* **2009**, *4*, 853–865. [CrossRef] [PubMed]
133. Bharate, S.B.; Mahajan, T.R.; Gole, Y.R.; Nambiar, M.; Matan, T.T.; Kulkarni-Almeida, A.; Balachandran, S.; Junjappa, H.; Balakrishnan, A.; Vishwakarma, R.A. Synthesis and Evaluation of Pyrazolo[3,4-*b*]Pyridines and Its Structural Analogues as TNF- $\alpha$  and IL-6 Inhibitors. *Bioorganic Med. Chem.* **2008**, *16*, 7167–7176. [CrossRef]
134. Revesz, L.; Blum, E.; di Padova, F.E.; Buhl, T.; Feifel, R.; Gram, H.; Hiestand, P.; Manning, U.; Neumann, U.; Rucklin, G. Pyrazoloheteroaryls: Novel P38 $\alpha$  MAP Kinase Inhibiting Scaffolds with Oral Activity. *Bioorganic Med. Chem. Lett.* **2006**, *16*, 262–266. [CrossRef]
135. Hamdy, N.A.; Gamal-Eldeen, A.M. New Pyridone, Thioxopyridine, Pyrazolopyridine and Pyridine Derivatives That Modulate Inflammatory Mediators in Stimulated RAW 264.7 Murine Macrophage. *Eur. J. Med. Chem.* **2009**, *44*, 4547–4556. [CrossRef] [PubMed]
136. Ochiai, H.; Ishida, A.; Ohtani, T.; Kusumi, K.; Kishikawa, K.; Yamamoto, S.; Takeda, H.; Obata, T.; Nakai, H.; Toda, M. New Orally Active PDE4 Inhibitors with Therapeutic Potential. *Bioorganic Med. Chem.* **2004**, *12*, 4089–4100. [CrossRef] [PubMed]
137. Hamblin, J.N.; Angell, T.D.R.; Ballantine, S.P.; Cook, C.M.; Cooper, A.W.J.; Dawson, J.; Delves, C.J.; Jones, P.S.; Lindvall, M.; Lucas, F.S.; et al. Pyrazolopyridines as a Novel Structural Class of Potent and Selective PDE4 Inhibitors. *Bioorganic Med. Chem. Lett.* **2008**, *18*, 4237–4241. [CrossRef]
138. Mitchell, C.J.; Ballantine, S.P.; Coe, D.M.; Cook, C.M.; Delves, C.J.; Dowle, M.D.; Edlin, C.D.; Hamblin, J.N.; Holman, S.; Johnson, M.R.; et al. Pyrazolopyridines as Potent PDE4B Inhibitors: 5-Heterocycle SAR. *Bioorganic Med. Chem. Lett.* **2010**, *20*, 5803–5806. [CrossRef]
139. Jimenez, J.M.; Boyall, D.; Brenchley, G.; Collier, P.N.; Davis, C.J.; Fraysse, D.; Keily, S.B.; Henderson, J.; Miller, A.; Pierard, F.; et al. Design and Optimization of Selective Protein Kinase C  $\theta$  (PKC $\theta$ ) Inhibitors for the Treatment of Autoimmune Diseases. *J. Med. Chem.* **2013**, *56*, 1799–1810. [CrossRef]
140. Schenone, S.; Bruno, O.; Fossa, P.; Ranise, A.; Menozzi, G.; Mosti, L.; Bondavalli, F.; Martini, C.; Trincavelli, L. Synthesis and Biological Data of 4-Amino-1-(2-Chloro-2-Phenylethyl)-1*H*-Pyrazolo[3,4-*b*]Pyridine-5-Carboxylic Acid Ethyl Esters, a New Series of A 1-Adenosine Receptor (A 1 AR) Ligands. *Bioorganic Med. Chem. Lett.* **2001**, *11*, 2529–2531. [CrossRef]
141. Menegatti, R.; Silva, G.M.S.; Zapata-Sudo, G.; Raimundo, J.M.; Sudo, R.T.; Barreiro, E.J.; Fraga, C.A.M. Design, Synthesis, and Pharmacological Evaluation of New Neuroactive Pyrazolo[3,4-*b*]Pyrrolo[3,4-*d*]Pyridine Derivatives with in Vivo Hypnotic and Analgesic Profile. *Bioorganic Med. Chem.* **2006**, *14*, 632–640. [CrossRef] [PubMed]
142. Dyck, B.; Grigoriadis, D.E.; Gross, R.S.; Guo, Z.; Haddach, M.; Marinkovic, D.; McCarthy, J.R.; Moorjani, M.; Regan, C.F.; Saunders, J.; et al. Potent, Orally Active Corticotropin-Releasing Factor Receptor-1 Antagonists Containing a Tricyclic Pyrrolopyridine or Pyrazolopyridine Core. *J. Med. Chem.* **2005**, *48*, 4100–4110. [CrossRef]
143. Nascimento-Júnior, N.M.; Mendes, T.C.F.; Leal, D.M.; Corrêa, C.M.N.; Sudo, R.T.; Zapata-Sudo, G.; Barreiro, E.J.; Fraga, C.A.M. Microwave-Assisted Synthesis and Structure-Activity Relationships of Neuroactive Pyrazolo[3,4-*b*]Pyrrolo[3,4-*d*]Pyridine Derivatives. *Bioorganic Med. Chem. Lett.* **2010**, *20*, 74–77. [CrossRef] [PubMed]
144. Ho, G.D.; Yang, S.W.; Smotryski, J.; Bercovici, A.; Nechuta, T.; Smith, E.M.; McElroy, W.; Tan, Z.; Tulshian, D.; McKittrick, B.; et al. The Discovery of Potent, Selective, and Orally Active Pyrazoloquinolines as PDE10A Inhibitors for the Treatment of Schizophrenia. *Bioorganic Med. Chem. Lett.* **2012**, *22*, 1019–1022. [CrossRef]

145. Goudey, B.; Fung, B.J.; Schieber, C.; Faux, N.G.; Weiner, M.W.; Aisen, P.; Petersen, R.; Jack, C.R.; Jagust, W.; Trojanowki, J.Q.; et al. A Blood-Based Signature of Cerebrospinal Fluid A $\beta$  1–42 Status. *Sci. Rep.* **2019**, *9*, 4163. [CrossRef] [PubMed]
146. Silva, D.; Chioua, M.; Samadi, A.; Agostinho, P.; Garção, P.; Lajarín-Cuesta, R.; de Los Ríos, C.; Iriepa, I.; Moraleda, I.; Gonzalez-Lafuente, L.; et al. Synthesis, Pharmacological Assessment, and Molecular Modeling of Acetylcholinesterase/Butyrylcholinesterase Inhibitors: Effect against Amyloid- $\beta$ -Induced Neurotoxicity. *ACS Chem. Neurosci.* **2013**, *4*, 547–565. [CrossRef] [PubMed]
147. Markham, A.; Duggan, S. Vericiguat: First Approval. *Drugs* **2021**, *81*, 721–726. [CrossRef] [PubMed]



MDPI  
St. Alban-Anlage 66  
4052 Basel  
Switzerland  
[www.mdpi.com](http://www.mdpi.com)

*Molecules* Editorial Office  
E-mail: [molecules@mdpi.com](mailto:molecules@mdpi.com)  
[www.mdpi.com/journal/molecules](http://www.mdpi.com/journal/molecules)



Disclaimer/Publisher's Note: The statements, opinions and data contained in all publications are solely those of the individual author(s) and contributor(s) and not of MDPI and/or the editor(s). MDPI and/or the editor(s) disclaim responsibility for any injury to people or property resulting from any ideas, methods, instructions or products referred to in the content.





Academic Open  
Access Publishing

[mdpi.com](http://mdpi.com)

ISBN 978-3-0365-8790-5